

EXHIBIT A: List of citations in Declaration of Michael L. Brines, M.D., Ph.D.

Paragraph Brines I	Citation in 10/185,841 (10165-015-999)	Corresponding citation in 10/520,140 (10165-037-999)
1	page 23, lines 16-18	page 25, line 20 to page 25, line 1
7	pages 29-36	pages 30-41
7	Examples 4 and 5 at pages 76-83	Examples 2 and 3 at pages 89-100
7	asialoerythropoietin (Examples 4, 5 and 8)	asialoerythropoietin (Example 2, 3 and 10)
7	phenylglyoxalerythropoietin (Example 4)	phenylglyoxalerythropoietin (Example 3)
7	biotinylated EPO (Example 5)	biotinylated EPO (Example 2)
7	iodoerythropoietin (Example 5)	iodoerythropoietin (Example 2)
7	carbamylated EPO (Example 5)	carbamylated EPO (Example 2)
7	acetylated EPO (Example 5)	acetylated EPO (Example 2)
7	succinylated EPO (Example 5)	succinylated EPO (Example 2)
7	EPO with modified arginine residues (Example 5)	EPO with modified arginine residues (Example 3)
7	EPO with modified tyrosine residues (Example 5)	EPO with modified tyrosine residues (Example 3)
7	EPO with modified glutamic acid and aspartic acid carboxyl groups (Example 5)	EPO with modified glutamic acid and aspartic acid carboxyl groups (Example 3)
7	EPO with modified tryptophan residues (Example 5)	EPO with modified tryptophan residues (Example 3)
7	EPO with amino groups removed (Example 5)	EPO with amino groups removed (Example 3)
7	EPO with disulfide reduction and stabilization (Example 5)	EPO with disulfide reduction and stabilization (Example 3)
7	EPO subjected to limited chemical proteolysis (Example 5)	EPO subjected to limited chemical proteolysis (Example 3)

Paragraph Brines I	Citation in 10/185,841 (10165-015-999)	Corresponding citation in 10/520,140 (10165-037-999)
8	page 80, lines 17-19	page 91, 6-19
13	page 78, lines 14-15	page 29, lines 21-25
15	page 79, lines 14-22	page 95, line 16 to page 95 line 1
17	page 77, lines 7-18	page 90, lines 9-18
19	Example 2 (at pages 74-75)	Example 6 (at pages 102-104)
19	Example 3 (at pages 75-76)	Example 7 (at page 104)
19	Example 4 (at pages 76-78)	Example 2 (at pages 89-97)
19	Example 6 (at pages 84-85)	Example 8 (at pages 104-105)
19	Example 7 (at pages 84-85)	Example 9 (at page 106)
19	Example 8 (at page 85)	Example 10 (at page 196)
22	Example 7 (at pages 84)	Example 9 (at page 106)
36	page 80, lines 17-19	page 91, 6-19
37	page 81, lines 6-8	page 92, lines 1-8
37	page 77, lines 7-18	page 90, lines 9-18
38	page 32, last line to page 33, first line	page 34, lines 7-8
39	page 80, lines 17-19	page 91, 6-19

IN THE UNITED STATES PATENT AND TRADEMARK OFFICE

Application of: Brines *et al.*

Confirmation No.: 4914

Application No.: 10/185,841

Group Art Unit: 1647

Filed: June 26, 2002

Examiner: DeBerry, Regina M.

For: PROTECTION, RESTORATION AND
ENHANCEMENT OF ERYTHROPOIETIN-
RESPONSIVE CELLS, TISSUES AND ORGANS

Attorney Docket No.: 10165-015-999

DECLARATION OF MICHAEL L. BRINES, M.D., PH.D.

Sir:

I, MICHAEL L. BRINES, do hereby declare and state:

1. I am an inventor of the invention described and claimed in the above-identified patent application (hereinafter the "'841 application"). I am presently Chief Scientific Officer at Warren Pharmaceuticals, Inc., licensee of the '841 application.

2. I have over thirty years of experience in biological research and clinical investigation. I am a certified member of the American Board of Internal Medicine. My academic and technical experience and honors, and a list of my publications, are set forth in my curriculum vitae, a copy of which is attached hereto as Appendix A.

3. I have read and am familiar with the '841 application, the pending claims and the outstanding Office Action. I understand that the technology of the '841 application relates to the use of erythropoietin ("EPO") and modified forms of EPO for protecting, maintaining, enhancing or restoring the function or viability of cells, tissues and

organs.¹ Such modified forms of EPO can be EPO molecules that do not increase hemoglobin concentration² but retain their tissue-protective activity. I have been informed and believe that the claims of the '841 application are subject to a rejection based on the contention that the '841 application does not provide sufficient guidance for such uses.

4. I have been asked to evaluate whether a person of ordinary skill in the fields of pharmacology and physiology on or before December 29, 2000 (the "Molecular Physiologist"), using merely ordinary skill and the guidance of the '841 application, would have been able to:

- a. make chemically modified EPOs;
- b. identify chemically modified EPOs that are non-erythropoietic;
- c. identify chemically modified EPOs that are tissue-protective; and
- d. identify EPO-responsive cells, tissues and organs.

I. OVERVIEW

5. The amino acid sequence of the native EPO protein was well-known prior to December 29, 2000. For many years, EPO had been used to treat anemia on account of its erythropoietic activity. Methods for the chemical modification of proteins were also well-established. In particular, chemically modified EPO proteins had been generated and their erythropoietic activities been tested. Assays for testing the tissue-protective activity of proteins were also well-established by December 29, 2000. In view of the guidance in the '841 application that the erythropoietic activity of EPO can be separated from its tissue-protective function, the Molecular Physiologist could have used well-established techniques to (a) generate chemically modified forms of EPO; (b) test their erythropoietic activity; (c)

¹ For ease of reference, I will use the term "tissue-protection" instead of the phrase "protecting, maintaining, enhancing or restoring the function or viability of cells, tissues and organs." Likewise, the ability of a protein to protect, maintain, enhance or restore the function or viability of cells, tissues and organs will be referred to as its "tissue-protective" activity.

² Molecules that do not increase hemoglobin concentration in a mammal will be referred to as non-erythropoietic.

test their tissue-protective activity; and (d) test their tissue-protective activity in different types of cells, tissues, and organs.

II. METHODS FOR MAKING THE CHEMICALLY MODIFIED EPOS

6. The claimed methods of the '841 application involve the use of chemically modified EPOs. The chemical structure of the native EPO molecule was known to Molecular Physiologists, and is described in the '841 application (for example, see page 23, lines 16-18). In particular, the amino acid sequence of EPO has long been known (see, e.g., Jacobs 1985, Nature 313:806-10).³

7. Specific chemically modified forms of EPO are described and referenced, for example, at pages 29-36 and in Examples 4 and 5 at pages 76-83 of the '841 application. These routine methods of chemical modification include, among others, guanidination, amidination, trinitrophenylation, acetylation, succinylation, nitration, and modification of arginine residues and carboxyl groups. Particular chemically modified EPOs and methods for obtaining them are described in the Examples of the '841 application. These EPOs include: asialoerythropoietin (Examples 4, 5 and 8); phenylglyoxalerythropoietin (Example 4); biotinylated EPO (Example 5); iodoerythropoietin (Example 5); carbamylated EPO (Example 5); trinitrophenylated EPO; acetylated EPO (Example 5); succinylated EPO (Example 5); EPO with modified arginine residues (Example 5); EPO with modified tyrosine residues (Example 5); EPO with modified glutamic acid and aspartic acid carboxyl groups (Example 5); EPO with modified tryptophan residues (Example 5); EPO with amino groups removed (Example 5); EPO with disulfide reduction and stabilization (Example 5); and EPO subjected to limited chemical proteolysis (Example 5).

8. Methods for chemical modifications of proteins were well established by December 29, 2000. For example, carbamylation of proteins is a technique that had been well-established for years. See, e.g., Plapp 1971, J. Biol. Chem. 246:939-945. Carbamylation of EPO is also described at p. 80, ll. 17-19 of the '841 application.

³ A list of cited references and copies of the cited references are attached as Appendix B.

9. Additional routine methods of chemically modifying proteins are described, *e.g.*, in *Chemical Reagents for Protein Modification*, R. L. Lundblad (CRC Press: Boca Raton, Florida, 1991). For instance, Lundblad described methods of modifying cysteine residues and cleaving disulfide bonds (Chapters 6 and 7); methods of chemically modifying lysine residues of a protein (Chapter 10); methods of chemically modifying arginine residues of a protein (Chapter 11); and methods of chemically modifying tryptophan residues of a protein (Chapter 12).

10. Moreover, in 1990, Satake described numerous methods of chemically modifying EPO, including guanidination, amidination, carbamylation, trinitrophenylation, acetylation, succinylation, and nitration (Satake 1990, *Biochimica et Biophysica Acta* 1038:125-29).

11. Thus, by following the teachings in the '841 application, and by employing well-established techniques, a Molecular Physiologist would have been capable of modifying the structure of the EPO molecule to obtain the chemically modified EPO molecules.

12. Once the Molecular Physiologist has produced the modified forms of EPO in accordance with the '841 application and standard protocols, the Molecular Physiologist could then use routine, well-established assays to test these EPOs for (i) their erythropoietic activity (see section III.) and (ii) for their tissue-protective activity (see section IV.).

III. EPO WITHOUT ERYTHROPOIETIC ACTIVITY

13. Routine assays for testing erythropoietic activity were well-established by December 29, 2000. The so-called UT-7 assay, which measures the proliferation of human leukemic cells, is an example. See Leveque *et al.* 1996, *Hematol. Oncol.* 14:137-146. Further, failure to bind to the erythrocyte erythropoietin receptor is indicative of lack of erythropoietic activity (p. 78, *II*. 14-15, of the '841 application). In addition, the '841 application refers to Satake as an example of a reference showing the lack of erythropoietic activity of certain chemically modified forms of EPO.

14. Satake illustrates that it would have been routine for a Molecular Physiologist to test the erythropoietic activity of chemically modified EPOs. Specifically, Satake teaches that erythropoietic activity can be measured by determining the incorporation of ⁵⁹Fe into cultured rat bone marrow cells after incubation with particular chemically modified EPOs (p. 126, rt. col.). Satake further teaches that *in vivo* erythropoietic activity can be measured using the exhypoxic polycythemic mouse bioassay (p. 126, rt. col.).

15. The Molecular Physiologist would have been familiar with the effects of particular chemical modifications on EPO's erythropoietic activity. Satake reported that modification of the lysine residues of EPO to neutral or negative charges, using known methods such as carbamylation, trinitrophenylation, acetylation and succinylation, significantly reduced EPO's erythropoietic activity (Appendix B). Other modified forms of EPO, such as guanidinated EPO and amidinated EPO, in which the positive charges are not eliminated, are erythropoietic. In an even earlier study, Wojchowski noted that esterification of carboxylate groups and acylation of amino groups resulted in abrogation of EPO's erythropoietic activity. (Wojchowski 1989, Blood 74:952-58; cited at p. 79, ll. 14-22 of the '841 application; Appendix B). Thus, the Molecular Physiologist could have applied the insight provided by, *e.g.*, Satake and Wojchowski to other chemical modifications.

16. Thus, by following the teachings in the '841 application and by employing routine techniques and know-how, a Molecular Physiologist would have been capable of identifying chemically modified EPO molecules that fail to increase hemoglobin concentration and hematocrit.

IV. EPO WITH TISSUE-PROTECTIVE ACTIVITY AND RESPONSIVE CELLS, TISSUES AND ORGANS

17. The '841 application describes the use of the P19 cell assay to test the tissue-protective activity of a compound (see, *e.g.*, p. 77, ll. 7-18). Upon withdrawal of serum, P19 cells undergo apoptosis. The ability of a compound to prevent this serum-deprivation induced cell death demonstrates the neuroprotective capacity of that compound. Similar assays for other cell types were well-known in the art. For example, NMDA-induced apoptosis in hippocampal neurons provides such an assay system. See, *e.g.*, Prehn 1994, PNAS 91:12599-12603. An assay for determining the effect of oxydative stress in cardiomyocytes was for example taught in Zorov (2000, J. Exp. Med. 192:1001-1014).

18. These *in vitro* assays simulate pathological conditions *in vivo*, and the results obtained in such *in vitro* systems are predictive of tissue-protective effects of a compound *in vivo*. In particular, anti-apoptotic activity in the *in vitro* assays predicts anti-apoptotic activity *in vivo*. Since apoptotic cell death occurs under many different pathological conditions, an anti-apoptotic compound will have many therapeutic benefits.

19. Examples of routine *in vivo* and *ex vivo* assays are also described in the '841 application. For instance, a Molecular Physiologist could follow the *ex vivo* assay described in Example 2 (at pages 74-75) to assess a particular chemically modified EPO for its utility in maintaining the function of a heart prepared for transplantation. A Molecular Physiologist could use the *in vivo* assay described in Example 3 (at pages 75-76) to assess a particular chemically modified EPO for protecting heart function during an ischemic event. A Molecular Physiologist could use the *in vivo* rat focal ischemia model assay in Example 4 (at pages 76-78) to assess the neuroprotective effects of a chemically modified EPO following ischemia. Other *in vivo* assays provided in the '841 application include the *in vivo* assay for cell protection following retinal ischemia (Example 6 at pages 84-85), the *in vivo* assay for restoration of cognitive function following brain injury (Example 7 at pages 84-85), and the *in vivo* kainate model for assessing neurotoxicity (Example 8 at page 85). Using the descriptions of these assays in the '841 application, a Molecular Physiologist could discern which assay is appropriate for testing the suitability of different chemically modified EPOs for the protection of a particular type of tissue from injury.

20. Additional assays useful to a Molecular Physiologist for assessing the tissue-protective effects of a compound in different tissues were well-known. For example, the tissue-protective effect of a compound on kidney cells can be tested in a model system for ischemia/ reperfusion injury (*e.g.*, Ysebaert 2000, Nephrol. Dial. Transplant 15:1562-74). Assays for evaluating the protective effect of a compound on heart tissue *in vivo* and *in vitro* were well-established in the art. See, *e.g.*, Kajstura, Diabetes 50:1414-1424.

21. Lack of oxygen is the cause of tissue-damage in many different pathological conditions. Such ischemic events can be simulated by occlusion of arteries in animal models. For example, the three-vessel-occlusion model is used to recapitulate damage caused by stroke (Brines 2000, PNAS 97:10526-10531 (see MCA occlusion in Materials and Methods)). The ischemic damage can be quantified by measuring the extent of the tissue

injury, *e.g.*, the size of the lesion, and by measuring functional parameters, *e.g.*, learning and memory, motor coordination etc.

22. Other assays to assess the function of the central nervous system include the Morris water maze, which tests spatial memory ('841 application Example 7, at p. 84). Another well-established animal model system for testing the effects of a compound on the function of the nervous system is the "wobbler mouse" (Duchen 1968, J. Neurol. Neurosurg. Psychiat. 31:535-542).

23. Thus, once equipped with the teachings of the '841 application, the Molecular Physiologist, using merely ordinary skill, could identify chemically modified forms of EPO suitable for tissue-protection and enhancement of tissue function.

V. SUCCESSFUL APPLICATION OF THE METHODS OF THE '841 APPLICATION

24. The following discussion shows that different chemically modified forms of EPO are indeed suitable for tissue-protection in a wide range of tissues and injuries.

A. EPO Protects Different Tissues from Different Injuries and Improves Function

25. Fiordaliso showed that non-erythropoietic, carbamylated EPO prevents apoptosis in cardiomyocytes in cell culture (2005, PNAS 102:2046-2051). As predicted by this *in vitro* data, carbamylated EPO has cardioprotective activity during ischemia in the *in vivo* model of myocardial infarction used in Fiordaliso. Fiordaliso demonstrated the cardioprotective effect by measuring functional parameters of the heart. Moon *et al.* demonstrated that carbamylated EPO protects cardiac tissue from toxin-induced and oxidative stress (2005, J. Pharmacol. Exp. Therapeutics 316:999-1005). In particular, on a cellular level, Moon showed the antiapoptotic effect of carbamylated EPO on isolated cardiomyocytes and in the heart tissue of a rat model of myocardial ischemia. In addition, Moon demonstrated the improved function of the heart.

26. Imamura demonstrated that carbamylated EPO protects kidneys in a rat animal model from ischemia reperfusion injury (2006, Biochem Biophys Res Comm, in press). Imamura demonstrated antiapoptotic activity of carbamylated EPO in kidney tissue after ischemia-reperfusion injury. In addition, Imamura demonstrated a greater regenerative effect in kidney tissue after ischemia-reperfusion injury due to treatment with carbamylated

EPO. Similarly, Okada showed that asialoEPO protected kidney function and prevented apoptosis in kidneys of ischemia/reperfusion injury in mice (Transplantation 84(4):504-510). Chong demonstrated that EPO protects endothelial cells from apoptosis caused by total lack of oxygen (2002, Circulation 106:2973-9).

27. Leist demonstrated the neuroprotective effect of carbamylated EPO by showing that carbamylated EPO reduced NMDA-induced apoptosis in cultured hippocampal cells. Leist further demonstrated the carbamylated EPO is tissue protective in a rat stroke model, in a model for spinal cord injury, in a model for multiple sclerosis (EAE), and in a model for diabetic neuropathy (2004, Science 305:239-242). Structural and functional measurements were conducted to assay the protective effect of carbamylated EPO. Lesion volume was measured in the stroke model, motor function for the model for spinal cord injury, motor deficit in the model for multiple sclerosis, and withdrawal latency in the model for diabetic neuropathy.

28. Similarly, Erbayraktar I and Erbayraktar II demonstrated the neuroprotective activity of a asialoEPO or carbamylated EPO, respectively, in animal models of different types of tissue-injury: cerebral ischemia, spinal cord compression, sciatic nerve crush, and radiation-induced necrosis (2003, PNAS 100:6741-6746; and 2006, Molecular Medicine 12:74-80). Schmidt showed that carbamylated EPO protected neurons in an animal model of diabetes from diabetes-induced neuritic dystrophy (2007, Exp. Neurol., doi: 10.1016/j.expneurol.2007.09.018). Wang demonstrated the neuroprotective effect of asialoEPO under hypoxia-ischemia conditions in new-born rats (J. Neurochem., 2004, 91:900-910)

29. Villa demonstrated that carbamylated EPO protects against ischemic damage and improves postischemic neurological function as evaluated by motor function (2007, Journal of Cerebral Blood Flow & Metabolism 27:255-63). Similarly, Bianchi demonstrated that carbamylated EPO preserved the function of neurons in the peripheral nervous system after exposure of these neurons to a neurotoxic drug (2006, Clin. Cancer Res. 12(8):2607-2612).

30. Mahmood demonstrated that administration of carbamylated EPO improved spatial learning in the Morris water maze assay following traumatic brain injury

(2007, J. Neurosurg. 107:392-397). This data shows that chemically modified forms of EPO have a positive effect on the function of the nervous system.

31. Mennini *et al.* demonstrated the beneficial effects of asialo-EPO and carbamylated EPO in the wobbler mouse (2006, Molecular Medicine 12:153-160). Both non-erythropoietic forms of EPO significantly improve the behavioral scores of wobbler mice in difference assays showing that these forms of EPO can restore the function of the nervous system.

32. These data show that chemically modified EPO protects tissues as different as heart tissue, kidney tissue, endothelial tissue, and central nervous system tissue. Similarly, the type of injury from which these chemically modified EPO protect a given tissue range from ischemia, such as stroke and infarction, toxin-induced stress, oxidative stress, reperfusion injury, NMDA-induced apoptosis, spinal cord compression, sciatic nerve crush, and radiation-induced necrosis. Further, the beneficial effect of chemically modified EPO on tissue function has been demonstrated by evaluating motor function, spatial learning, and other behavioral parameters.

B. Different Modified Forms of EPO

33. In the following paragraphs, examples are provided that demonstrate that different chemical modifications of EPO as taught in the '841 application indeed retain their tissue-protective activity.

34. As discussed above, carbamylated EPO, a chemically modified, non-erythropoietic form of EPO has the tissue-protective and enhancing effects that make it suitable for use with the methods of the '841 application.

35. In addition, several other chemically modified forms of EPO were generated in my laboratory and tested for their erythropoietic and tissue-protective effects, respectively.

36. Carbamylated Aranesp®, a hyperglycosylated form of EPO, was generated as described at p. 80, *ll.* 17-19, of the '841 application. We demonstrated that this form of EPO was not erythropoietic by its failure to bind to the EPOR monomer. We also

demonstrated that this form is tissue-protective by virtue of its protection of hippocampal cells in the assay of Prehn 1994 (Figure 1D in Villa 2007).

37. Succinylated EPO was generated as taught in the '841 application at p. 81, *ll.* 6-8. We demonstrated that this form of EPO was not erythropoietic by its failure to bind to the EPOR monomer and that this form is tissue-protective by virtue of its protection of P19 cells in the assay described at p. 77, *ll.* 7-18, of the '841 application.

38. Carboxymethylated EPO was generated by a method well-known by December 29, 2000 (Glomb and Monnier 1995, *J. Biol. Chem.* 270:10017-26 (cited in the '841 application at p. 32, last line, to p. 33, first line). We demonstrated that this form of EPO was not erythropoietic by its failure to bind to the EPOR monomer and that this form is tissue-protective in the three-vessel-occlusion model (Brines 2000, *PNAS* 97:10526-10531 (see MCA occlusion in Materials and Methods)).

39. Carbamylated-monopegylated EPO was generated by carbamylation as described in the '841 application (p. 80, *ll.* 17-19; see also, Plapp). We demonstrated that this form of EPO was not erythropoietic in the UT-7 assay (Leveque 1996). We also showed that this form is tissue-protective by virtue of its protection of hippocampal cells in the assay of Prehn 1994.

40. Thus, different chemical modifications as taught in the '841 application were indeed found to lack erythropoietic activity while maintaining tissue-protective activity.

VI. CONCLUSION

41. The data discussed above demonstrate that forms of EPO that were chemically modified in accordance with the '841 application are indeed non-erythropoietic. The data further demonstrate that these forms of EPO are tissue-protective in different tissues and under different pathological conditions. These data further show that these forms of EPO restore function of tissues. The tests that were employed to verify these activities were well-established by December 29, 2000 and their performance required merely what would have been ordinary skill in the art at that time.

42. It is well-recognized that there are common mechanisms among various diseases impacting the function and viability of cells, tissues and organs. For example, in the case of neurodegeneration, it has been noted that, irrespective of the primary causes of individual neurodegenerative diseases, it is the onset of oxidative stress resulting from free radical mechanisms that results in neuronal cell death and progression of the disease (*see Jenner, 1996, Pathol. Biol. (Paris), 44(1):57-64*). Thus, the anti-apoptotic activity of the chemically modified forms of EPO will be therapeutically efficacious independent from the initial cause of the disorder.

43. As I have discussed above, the methods claimed in the '841 application are supported by (1) the disclosure in the '841 application; together with (2) routine techniques and know-how available to Molecular Physiologists as of December 29, 2000; moreover, the ability of a Molecular Physiologist to practice the claimed methods is clearly illustrated by the successful experiments in the peer-reviewed publications I have described herein. Based on the foregoing, I am confident that a Molecular Physiologist, as of December 29, 2000, could have successfully practiced the methods claimed in the '841 application.

44. I declare further that all statements made in this Declaration of my own knowledge are true, that all statements made on information and belief are believed to be true, and further that these statements are made with the knowledge that willful false statements and the like so made are punishable by fine or imprisonment or both, under Section 1001 of Title 18 of the United States Code and that such willful false statements may jeopardize the validity of the application or any patent issuing thereon.

Respectfully submitted,

December 5, 2007
Date

Michael L. Brines
Michael L. Brines

Attachments:

Appendix A: Curriculum Vitae of Dr. Michael L. Brines, M.D., Ph.D.

Appendix B: Cited References

MICHAEL L. BRINES PhD, MD

1 Wepawaug Road, Woodbridge, CT 06525; office: 914-762-7586; email: mbrines@kswi.org

- 2004- Co-founder, Director and Chief Scientific Officer,
Warren Pharmaceuticals, Inc. Ossining, New York
- 1998- Senior Member,
The Kenneth S. Warren Institute, Ossining, New York
- 1989-98 Assistant & Associate Professor, Endocrinology and Metabolism,
Department of Internal Medicine, Yale University School of Medicine
- 1992-98 Co-Director, Molecular Core, Yale Diabetes and Endocrinology Research
Center
- 1989-98 Co-Director, Yale Pituitary Center
- 1978-82 Research Associate & Assistant Professor,
The Rockefeller University, New York (neuroscience)
- 1975-76 Research Associate, Department of Biology,
City University of New York
- 1970-73 Research Assistant and Teaching Assistant
Departments of Biology and Physics, University of Notre Dame

Education and Training

- 1986-89 Postdoctoral Fellow, Training Program in Endocrinology &
Neuroendocrinology
- 1986-88 Postdoctoral Fellow, Training Program in Clinical Investigation
Department of Internal Medicine, Yale University
- 1984-86 Intern and Resident, Department of Internal Medicine
Yale-New Haven Hospital, New Haven, Connecticut
- 1983 M. D., Yale University, New Haven, Connecticut
- 1978 Ph. D., Neurobiology and Behavioral Science,
The Rockefeller University, New York, New York
- 1973 B. S. (with highest honors), Physics and Biology,
University of Notre Dame, Notre Dame, Indiana

Licensure and Board Certification

1989 American Board of Endocrinology and Metabolism
1988 American Board of Internal Medicine
1985 State of Connecticut, Physician and Surgeon

Professional Associations

1993 The Pituitary Society
1991 The Endocrine Society
1976 American Optical Society
1976 Society for Neuroscience
1973 Sigma Xi

Honors, Awards and Visiting Professorships

2003 11th Richard Stow Visiting Professor, Ohio State University
1991 Andrew Mellon Fellowship Award (Yale University)
1989 Epilepsy Foundation Fellowship
1976 The Albert Cass Traveling Fellowship (Princeton University)
1973 Phi Beta Kappa
1967 Ford Future Scientist of America

Issued U.S. Patents

Tissue protection: 6531121: Protection and enhancement of erythropoietin-responsive cells, tissues and organs.

Novel drug delivery systems: 6569152 & 7090861: Sustained release delivery systems for solutes

Advanced glycosylation endproduct therapeutics: 6713050 & 6777557 & 7022721: Method and composition for rejuvenating cells, tissues, organs, hair and nails.

Primary Manuscripts (* key recent publications)

Villa P, van Beek J, Larsen AK, Gerwien J, Christensen S, Cerami A, Brines M, Leist M, Ghezzi P, Torup L. (2007) Reduced functional deficits, neuroinflammation, and secondary tissue damage after treatment of stroke by nonerythropoietic erythropoietin derivatives. *J Cereb Blood Flow Metab* 27: 552-563.

Mennini T, De Paola M, Bigini P, Mastrotto C, Fumagalli E, Barbera S, Mengozzi M, Viviani B, Corsini E, Marinovich M, Torup L, Van Beek J, Leist M, Brines M, Cerami A, Ghezzi P. (2006) Nonhematopoietic erythropoietin

derivatives prevent motoneuron degeneration in vitro and in vivo. *Mol Med (Cambridge, Mass)* 12: 153-160.

- Fantacci M, Bianciardi P, Caretti A, Coleman TR, Cerami A, **Brines M**, Samaja M. (2006) Carbamylated erythropoietin ameliorates the metabolic stress induced in vivo by severe chronic hypoxia. *Proc Natl Acad Sci U S A* 103: 17531-17536.
- Erbayraktar S, de Lanerolle N, de Lotbiniere A, Knisely JP, Erbayraktar Z, Yilmaz O, Cerami A, Coleman TR, **Brines M**. (2006) Carbamylated erythropoietin reduces radiosurgically-induced brain injury. *Molecular medicine (Cambridge, Mass)* 12: 74-80.
- *Coleman TR, Westenfelder C, Togel FE, Yang Y, Hu Z, Swenson L, Leuvenink HG, Ploeg RJ, d'Uscio LV, Katusic ZS, Ghezzi P, Zanetti A, Kaushansky K, Fox NE, Cerami A, **Brines M**. (2006) Cytoprotective doses of erythropoietin or carbamylated erythropoietin have markedly different procoagulant and vasoactive activities. *Proc Natl Acad Sci U S A* 103: 5965-5970.
- Grasso G, Sfacteria A, Erbayraktar S, Passalacqua M, Meli F, Gokmen N, Yilmaz O, La Torre D, Buemi M, Iacopino DG, Coleman T, Cerami A, **Brines M**, Tomasello F. (2006) Amelioration of spinal cord compressive injury by pharmacological preconditioning with erythropoietin and a nonerythropoietic erythropoietin derivative. *Journal of neurosurgery* 4: 310-318.
- Bianchi R, **Brines M**, Lauria G, Savino C, Gilardini A, Nicolini G, Rodriguez-Menendez V, Oggioni N, Canta A, Penza P, Lombardi R, Minoia C, Ronchi A, Cerami A, Ghezzi P, Cavaletti G. (2006) Protective effect of erythropoietin and its carbamylated derivative in experimental Cisplatin peripheral neurotoxicity. *Clin Cancer Res* 12: 2607-2
- Savino C, Pedotti R, Baggi F, Ubiali F, Gallo B, Nava S, Bigini P, Barbera S, Fumagalli E, Mennini T, Vezzani A, Rizzi M, Coleman T, Cerami A, **Brines M**, Ghezzi P, Bianchi R. (2006) Delayed administration of erythropoietin and its non-erythropoietic derivatives ameliorates chronic murine autoimmune encephalomyelitis. *J Neuroimmunol* 172: 27-37.
- Moon C, Krawczyk M, Paik D, Coleman T, **Brines M**, Juhaszova M, Sollott S, Lakatta EG, Talan MI. (2006) Erythropoietin, modified to not stimulate red blood cell production, retains its cardioprotective properties. *J Pharmacol Exp Ther*: 999-1005.
- Grasso G, Sfacteria A, Passalacqua M, Morabito A, Buemi M, Macri B, **Brines M**, Tomasello F. (2005) Erythropoietin and erythropoietin receptor expression

after experimental spinal cord injury encourages therapy by exogenous erythropoietin. *Neurosurgery* 56: 821-827; discussion 821-827.

Gorio A, Madaschi L, Di Stefano B, Carelli S, Di Giulio AM, De Biasi S, Coleman T, Cerami A, **Brines M**. (2005) Methylprednisolone neutralizes the beneficial effects of erythropoietin in experimental spinal cord injury. *Proc Natl Acad Sci U S A* 102: 16379-16384.

Fiordaliso F, Chimenti S, Staszewsky L, Bai A, Carlo E, Cuccovillo I, Doni M, Mengozzi M, Tonelli R, Ghezzi P, Coleman T, **Brines M**, Cerami A, Latini R. (2005) A nonerythropoietic derivative of erythropoietin protects the myocardium from ischemia-reperfusion injury. *Proc Natl Acad Sci U S A* 102: 2046-2051.

*Leist M, Ghezzi P, Grasso G, Bianchi R, Villa P, Fratelli M, Savino C, Bianchi M, Nielsen J, Gerwien J, Kallunki P, Larsen AK, Helboe L, Christensen S, Pedersen LO, Nielsen M, Torup L, Sager T, Sfacteria A, Erbayraktar S, Erbayraktar Z, Gokmen N, Yilmaz O, Cerami-Hand C, Xie QW, Coleman T, Cerami A, **Brines M**. (2004) Derivatives of erythropoietin that are tissue protective but not erythropoietic. *Science* 305: 239-242.

Grasso G, Sfacteria A, **Brines M**, Tomasello F. (2004) A new computed-assisted technique for experimental sciatic nerve function analysis. *Med Sci Monit* 10: BR1-3.

Eid T, **Brines M**, Cerami A, Spencer DD, Kim JH, Schweitzer JS, Ottersen OP, de Lanerolle NC. (2004) Increased expression of erythropoietin receptor on blood vessels in the human epileptogenic hippocampus with sclerosis. *J Neuropathol Exp Neurol* 63: 73-83.

Ehrenreich H, Degner D, Meller J, **Brines M**, Behe M, Hasselblatt M, Woldt H, Falkai P, Knerlich F, Jacob S, von Ahsen N, Maier W, Bruck W, Ruther E, Cerami A, Becker W, Siren AL. (2004) Erythropoietin: a candidate compound for neuroprotection in schizophrenia. *Mol Psychiatry* 9: 42-54.

***Brines M**, Grasso G, Fiordaliso F, Sfacteria A, Ghezzi P, Fratelli M, Latini R, Xie QW, Smart J, Su-Rick CJ, Pobre E, Diaz D, Gomez D, Hand C, Coleman T, Cerami A. (2004) Erythropoietin mediates tissue protection through an erythropoietin and common beta-subunit heteroreceptor. *Proc Natl Acad Sci U S A* 101: 14907-14912.

Bianchi R, Buyukakilli B, **Brines M**, Savino C, Cavaletti G, Oggioni N, Lauria G, Borgna M, Lombardi R, Cimen B, Comelekoglu U, Kanik A, Tataroglu C, Cerami A, Ghezzi P. (2004) Erythropoietin both protects from and reverses experimental diabetic neuropathy. *Proc Natl Acad Sci U S A* 101: 823-828.

- Villa P, Bigini P, Mennini T, Agnello D, Laragione T, Cagnotto A, Viviani B, Marinovich M, Cerami A, Coleman TR, **Brines M**, Ghezzi P. (2003) Erythropoietin selectively attenuates cytokine production and inflammation in cerebral ischemia by targeting neuronal apoptosis. *J Exp Med* 198: 971-975.
- *Erbayraktar S, Grasso G, Sfacteria A, Xie QW, Coleman T, Kreilgaard M, Torup L, Sager T, Erbayraktar Z, Gokmen N, Yilmaz O, Ghezzi P, Villa P, Fratelli M, Casagrande S, Leist M, Helboe L, Gerwein J, Christensen S, Geist MA, Pedersen LO, Cerami-Hand C, Wuerth JP, Cerami A, **Brines M**. (2003) Asialoerythropoietin is a nonerythropoietic cytokine with broad neuroprotective activity in vivo. *Proc Natl Acad Sci U S A* 100: 6741-6746.
- Calvillo L, Latini R, Kajstura J, Leri A, Anversa P, Ghezzi P, Salio M, Cerami A, **Brines M**. (2003) Recombinant human erythropoietin protects the myocardium from ischemia-reperfusion injury and promotes beneficial remodeling. *Proc Natl Acad Sci U S A* 100: 4802-4806.
- Junk AK, Mammis A, Savitz SI, Singh M, Roth S, Malhotra S, Rosenbaum PS, Cerami A, **Brines M**, Rosenbaum DM. (2002) Erythropoietin administration protects retinal neurons from acute ischemia-reperfusion injury. *Proc Natl Acad Sci U S A* 99: 10659-10664.
- *Gorio A, Gokmen N, Erbayraktar S, Yilmaz O, Madaschi L, Cichetti C, Di Giulio AM, Vardar E, Cerami A, **Brines M**. (2002) Recombinant human erythropoietin counteracts secondary injury and markedly enhances neurological recovery from experimental spinal cord trauma. *Proc Natl Acad Sci U S A* 99: 9450-9455.
- *Ehrenreich H, Hasselblatt M, Dembowski C, Cepek L, Lewczuk P, Stiefel M, Rustenbeck HH, Breiter N, Jacob S, Knerlich F, Bohn M, Poser W, Ruther E, Kochen M, Gefeller O, Gleiter C, Wessel TC, De Ryck M, Itri L, Prange H, Cerami A, **Brines M**, Siren AL. (2002) Erythropoietin therapy for acute stroke is both safe and beneficial. *Mol Med* 8: 495-505.
- Chatterjee O, Nakchbandi IA, Philbrick WM, Dreyer BE, Zhang JP, Kaczmarek LK, **Brines M**, Broadus AE. (2002) Endogenous parathyroid hormone-related protein functions as a neuroprotective agent. *Brain Res* 930: 58-66.
- Celik M, Gokmen N, Erbayraktar S, Akhisaroglu M, Konak S, Ulukus C, Genc S, Genc K, Sagiroglu E, Cerami A, **Brines M**. (2002) Erythropoietin prevents motor neuron apoptosis and neurologic disability in experimental spinal cord ischemic injury. *Proc Natl Acad Sci U S A* 99: 2258-2263.

- Agnello D, Bigini P, Villa P, Mennini T, Cerami A, **Brines M**, Ghezzi P. (2002) Erythropoietin exerts an anti-inflammatory effect on the CNS in a model of experimental autoimmune encephalomyelitis. *Brain Res* 952: 128-134.
- Vaitkevicius PV, Lane M, Spurgeon H, Ingram DK, Roth GS, Egan JJ, Vasan S, Wagle DR, Ulrich P, **Brines M**, Wuerth JP, Cerami A, Lakatta EG. (2001) A cross-link breaker has sustained effects on arterial and ventricular properties in older rhesus monkeys. *Proc Natl Acad Sci U S A* 98: 1171-1175.
- *Siren AL, Fratelli M, **Brines M**, Goemans C, Casagrande S, Lewczuk P, Keenan S, Gleiter C, Pasquali C, Capobianco A, Mennini T, Heumann R, Cerami A, Ehrenreich H, Ghezzi P. (2001) Erythropoietin prevents neuronal apoptosis after cerebral ischemia and metabolic stress. *Proc Natl Acad Sci U S A* 98: 4044-4049.
- ***Brines M**, Ghezzi P, Keenan S, Agnello D, de Lanerolle NC, Cerami C, Itri LM, Cerami A. (2000) Erythropoietin crosses the blood-brain barrier to protect against experimental brain injury. *Proc Natl Acad Sci U S A* 97: 10526-10531.
- Asif M, Egan J, Vasan S, Jyothirmayi GN, Masurekar MR, Lopez S, Williams C, Torres RL, Wagle D, Ulrich P, Cerami A, **Brines M**, Regan TJ. (2000) An advanced glycation endproduct cross-link breaker can reverse age-related increases in myocardial stiffness. *Proc Natl Acad Sci U S A* 97: 2809-2813.
- Brines M**, Ling Z, Broadus AE. (1999) Parathyroid hormone-related protein protects against kainic acid excitotoxicity in rat cerebellar granule cells by regulating L-type channel calcium flux. *Neurosci Lett* 274: 13-16.
- Brines M**, Broadus AE. (1999) Parathyroid hormone-related protein markedly potentiates depolarization-induced catecholamine release in PC12 cells via L-type voltage-sensitive Ca²⁺ channels. *Endocrinology* 140: 646-651.
- Borg MA, Borg WP, Tamborlane WV, **Brines M**, Shulman GI, Sherwin RS. (1999) Chronic hypoglycemia and diabetes impair counterregulation induced by localized 2-deoxy-glucose perfusion of the ventromedial hypothalamus in rats. *Diabetes* 48: 584-587.
- Yavari R, Adida C, Bray-Ward P, **Brines M**, Xu T. (1998) Human metalloprotease-disintegrin Kuzbanian regulates sympathoadrenal cell fate in development and neoplasia. *Hum Mol Genet* 7: 1161-1167.
- Xie H, **Brines M**, de Lanerolle NC. (1998) Transcripts of the transposon mariner are present in epileptic brain. *Epilepsy Res* 32: 140-153.

- de Lanerolle NC, Eid T, von Campe G, Kovacs I, Spencer DD, **Brines M.** (1998) Glutamate receptor subunits GluR1 and GluR2/3 distribution shows reorganization in the human epileptogenic hippocampus. *Eur J Neurosci* 10: 1687-1703.
- de Lanerolle NC, Williamson A, Meredith C, Kim JH, Tabuteau H, Spencer DD, **Brines M.** (1997) Dynorphin and the kappa 1 ligand [3H]U69,593 binding in the human epileptogenic hippocampus. *Epilepsy Res* 28: 189-205.
- Brines M,** Sundaresan S, Spencer DD, de Lanerolle NC. (1997) Quantitative autoradiographic analysis of ionotropic glutamate receptor subtypes in human temporal lobe epilepsy: up-regulation in reorganized epileptogenic hippocampus. *Eur J Neurosci* 9: 2035-2044.
- Holt EH, Broadus AE, **Brines M.** (1996) Parathyroid hormone-related peptide is produced by cultured cerebellar granule cells in response to L-type voltage-sensitive Ca²⁺ channel flux via a Ca²⁺/calmodulin-dependent kinase pathway. *J Biol Chem* 271: 28105-28111.
- de Lanerolle NC, Gunel M, Sundaresan S, Shen MY, **Brines M,** Spencer DD. (1995) Vasoactive intestinal polypeptide and its receptor changes in human temporal lobe epilepsy. *Brain Res* 686: 182-193.
- Brines M,** Tabuteau H, Sundaresan S, Kim J, Spencer DD, de Lanerolle N. (1995) Regional distributions of hippocampal Na⁺,K(+) -ATPase, cytochrome oxidase, and total protein in temporal lobe epilepsy. *Epilepsia* 36: 371-383.
- Brines M,** Dare AO, de Lanerolle NC. (1995) The cardiac glycoside ouabain potentiates excitotoxic injury of adult neurons in rat hippocampus. *Neurosci Lett* 191: 145-148.
- Borg WP, During MJ, Sherwin RS, Borg MA, **Brines M,** Shulman GI. (1994) Ventromedial hypothalamic lesions in rats suppress counterregulatory responses to hypoglycemia. *J Clin Invest* 93: 1677-1682.
- de Lanerolle NC, **Brines M,** Kim JH, Williamson A, Philips MF, Spencer DD. (1993) Neurochemical remodelling of the hippocampus in human temporal lobe epilepsy. In: G. Avanzini et al (eds.) *Molecular Neurobiology of Epilepsy*, pp. 205-220.
- de Lanerolle N, **Brines M,** Williamson A, Kim J, Spencer D. (1993) Neurotransmitters and their receptors in human temporal lobe epilepsy. In: Ribak C, Gall C, Mody I (eds.) *The Dentate Gyrus and its role in Seizures.*, pp. 235-250.

- Brines M, Robbins RJ.** (1993) Cell-type specific expression of Na⁺, K⁺-ATPase catalytic subunits in cultured neurons and glia: evidence for polarized distribution in neurons. *Brain Res* 631: 1-11.
- Brines M, Robbins RJ.** (1993) Glutamate up-regulates alpha 1 and alpha 2 subunits of the sodium pump in astrocytes of mixed telencephalic cultures but not in pure astrocyte cultures. *Brain Res* 631: 12-21.
- Zahler R, Brines M, Kashgarian M, Benz EJ, Jr., Gilmore-Hebert M.** (1992) The cardiac conduction system in the rat expresses the alpha 2 and alpha 3 isoforms of the Na⁺,K⁺-ATPase. *Proc Natl Acad Sci U S A* 89: 99-103.
- Schmauss C, Brines M, Lerner MR.** (1992) The gene encoding the small nuclear ribonucleoprotein-associated protein N is expressed at high levels in neurons. *J Biol Chem* 267: 8521-8529.
- Kolansky DM, Brines M, Gilmore-Hebert M, Benz EJ, Jr.** (1992) The A2 isoform of rat Na⁺,K⁺-adenosine triphosphatase is active and exhibits high ouabain affinity when expressed in transfected fibroblasts. *FEBS Lett* 303: 147-153.
- de Lanerolle NC, Brines M, Kim JH, Williamson A, Philips MF, Spencer DD.** (1992) Neurochemical remodelling of the hippocampus in human temporal lobe epilepsy. *Epilepsy Res Suppl* 9: 205-219; discussion 220.
- de Lanerolle NC, Brines M, Williamson A, Kim JH, Spencer DD.** (1992) Neurotransmitters and their receptors in human temporal lobe epilepsy. *Epilepsy Res Suppl* 7: 235-250.
- Brines M, Robbins RJ.** (1992) Inhibition of alpha 2/alpha 3 sodium pump isoforms potentiates glutamate neurotoxicity. *Brain Res* 591: 94-102.
- Robbins RJ, Brines M, Kim JH, Adrian T, de Lanerolle N, Welsh S, Spencer DD.** (1991) A selective loss of somatostatin in the hippocampus of patients with temporal lobe epilepsy. *Ann Neurol* 29: 325-332.
- Isales CM, Barrett PQ, Brines M, Bollag W, Rasmussen H.** (1991) Parathyroid hormone modulates angiotensin II-induced aldosterone secretion from the adrenal glomerulosa cell. *Endocrinology* 129: 489-495.
- Brines M, Gulanski BI, Gilmore-Hebert M, Greene AL, Benz EJ, Jr., Robbins RJ.** (1991) Cytoarchitectural relationships between [3H]ouabain binding and mRNA for isoforms of the sodium pump catalytic subunit in rat brain. *Brain Res Mol Brain Res* 10: 139-150.

- Weir EC, **Brines M**, Ikeda K, Burtis WJ, Broadus AE, Robbins RJ. (1990) Parathyroid hormone-related peptide gene is expressed in the mammalian central nervous system. *Proc Natl Acad Sci U S A* 87: 108-112.
- Thiede MA, Daifotis AG, Weir EC, **Brines M**, Burtis WJ, Ikeda K, Dreyer BE, Garfield RE, Broadus AE. (1990) Intrauterine occupancy controls expression of the parathyroid hormone-related peptide gene in preterm rat myometrium. *Proc Natl Acad Sci U S A* 87: 6969-6973.
- Orloff JJ, Wu TL, Heath HW, Brady TG, **Brines M**, Stewart AF. (1989) Characterization of canine renal receptors for the parathyroid hormone-like protein associated with humoral hypercalcemia of malignancy. *J Biol Chem* 264: 6097-6103.
- Dworkin B, Miller NE, Dworkin S, Birbaumer N, **Brines M**, Jonas S, Schwentker EP, Graham JJ. (1985) Behavioral method for the treatment of idiopathic scoliosis. *Proc Natl Acad Sci U S A* 82: 2493-2497.
- Brines M**, Gould J. (1982) Skylight polarization patterns and animal orientation. *J. Exp. Biol.* 96: 69-91.
- Gould J, Kirschvink J, Deffeyes K, **Brines M**. (1980) Magnetic field sensitivity: bees do not employ a permanent magnet detector. *J. Exp. Biol.* 86: 1-8.
- Brines M**. (1980) Dynamic patterns of skylight polarization as clock and compass. *J Theor Biol* 86: 507-512.
- Dworkin B, Miller N, **Brines M**. (1979) Visceral learning and homeostasis. *Proceedings of the Joint Automatic Control Conference*.
- Brines M**, Gould J. (1979) Bees have rules. *Science* 206: 571-573.
- Brines M**. (1978) Skylight polarization patterns as cues for honey bee orientation: physical measurements and behavioral experiments. The Rockefeller University, New York, 378 pp.

Invited Reviews

- Brines M**, Cerami A. (2006) Discovering erythropoietin's extra-hematopoietic functions: biology and clinical promise. *Kidney Internat* 70: 246-250.
- Brines M**, Cerami A. (2006) Tissue-protective cytokines in spinal cord injury: Challenges for a novel neuroprotective strategy. In: Hoke A (ed.) *Erythropoietin and the Nervous System: Novel Therapeutic Options for Neuroprotection*. Springer, New York, pp. 147-164.

- Brines M, Cerami A.** (2005) Emerging biological roles for erythropoietin in the nervous system. *Nat Rev Neurosci* **6**: 484-494.
- Grasso G, Sfacteria A, Cerami A, **Brines M.** (2004) Erythropoietin as a tissue-protective cytokine in brain injury: What do we know and where do we go? *The Neuroscientist* **10**: 93-98.
- Grasso G, **Brines M.** (2004) From erythropoiesis to a rational neuroprotective therapeutic strategy and beyond. *J. Supportive Oncol* **2**: 44-45.
- Ghezzi P, **Brines M.** (2004) Erythropoietin as an antiapoptotic, tissue-protective cytokine. *Cell Death Differ* **11 Suppl 1**: S37-44.
- Coleman T, **Brines M.** (2004) Science review: recombinant human erythropoietin in critical illness: a role beyond anemia? *Crit Care* **8**: 337-341.
- Cerami A, **Brines M,** Cerami C. (2004) Epoetin alfa has potential efficacy in central nervous system disorders. *Eur. J. Cancer* **2**: 29-35.
- Erbayraktar S, Yilmaz O, Gokmen N, **Brines M.** (2003) Erythropoietin Is a Multifunctional Tissue-protective Cytokine. *Curr Hematol Rep* **2**: 465-470.
- Eid T, **Brines M.** (2002) Recombinant human erythropoietin for neuroprotection: what is the evidence? *Clin Breast Cancer* **3 Suppl 3**: S109-115.
- Cerami A, **Brines M,** Ghezzi P, Cerami C, Itri LM. (2002) Neuroprotective properties of epoetin alfa. *Nephrol Dial Transplant* **17 Suppl 1**: 8-12.
- Brines M.** (2002) What evidence supports use of erythropoietin as a novel neurotherapeutic? *Oncology (Huntingt)* **16**: 79-89.
- Cerami A, **Brines ML,** Ghezzi P, Cerami CJ. (2001) Effects of epoetin alfa on the central nervous system. *Semin Oncol* **28**: 66-70.
- de Lanerolle NC, Kim JH, **Brines ML.** (1994) Cellular and Molecular Alterations in Partial Epilepsy. *Clin. Neurosci.* **2**: 64-81.
- de Lanerolle N, Magge S, Philips M, Trombley P, Spencer D, **Brines M.** (1994) Adaptive changes of epileptic human temporal lobe tissue: properties of neurons and glia. In: Wolf P (ed.) *Seizures and Syndromes in Epilepsy*. J. Libby and Company Ltd., London, pp. 431-448.

Clinical Publications

- Inzucchi S, **Brines M.** (1997) Pheochromocytoma. In: Gilman S, Goldstein G, Waxman S (eds.) *Neurobase*. Arbor Publishing, La Jolla, CA.
- Inzucchi S, **Brines M.** (1997) Syndrome of Inappropriate Antidiuresis. In: Gilman S, Goldstein G, Waxman S (eds.) *Neurobase*. Arbor Publishing, La Jolla, CA.
- Brines M.** (1997) Diabetes Insipidus. In: Gilman S, Goldstein G, Waxman S (eds.) *Neurobase*. Arbor Publishing, La Jolla, CA.
- Brines M.** (1997) Sheehan's Syndrome. In: Gilman S, Goldstein G, Waxman S (eds.) *Neurobase*. Arbor Publishing, La Jolla, CA.
- Wallace EA, **Brines M**, Kinder BK, de Lotbiniere AC. (1996) Clinical case seminar: Cushing's syndrome in an elderly woman with large thyroid and pituitary masses. *J Clin Endocrinol Metab* 81: 453-456.
- Brines M.** (1995) Pituitary Apoplexy. In: Gilman S, Goldstein G, Waxman S (eds.) *Neurobase*. Arbor Publishing, La Jolla, CA.
- Brines M.** (1995) Hypopituitarism. In: Gilman S, Goldstein G, Waxman S (eds.) *Neurobase*. Arbor Publishing, La Jolla, CA.
- Korn EA, Gaich G, **Brines M**, Carpenter TO. (1994) Thyrotropin-secreting adenoma in an adolescent girl without increased serum thyrotropin-alpha. *Horm Res* 42: 120-123.
- Bohler HC, Jr., Jones EE, **Brines M.** (1994) Marginally elevated prolactin levels require magnetic resonance imaging and evaluation for acromegaly. *Fertil Steril* 61: 1168-1170.

REFERENCE

TAB

Brines 2000, PNAS 97:10526-10531.....	1
Bianchi, et al., Clin Cancer Res 2006; 12: 2607-2612	2
Chemical Reagents for Protein Modification, R. L. Lundblad (CRC Press: Boca Raton, Florida, 1991, Chapters 6, 7, 10, 11 and 12	3
Chong 2002, Circulation 106:2973-9.....	4
Duchen 1968, J. Neurol. Neurosurg. Psychiat. 31:535-542.....	5
Erbayraktar 2003, PNAS 100:6741-6746	6
Erbayraktar 2006, Molecular Medicine 12:74-80	7
Fiordaliso 2005, PNAS 102:2046-2051	8
Glomb and Monnier 1995, J. Biol. Chem. 270:10017-26	9
Imamura et al., 2006, Biochem Biophys Res Comm, in press	10
Jacobs 1985, Nature 313:806-10.....	11
Jenner, 1996, <i>Pathol. Biol. (Paris)</i> , 44(1):57-64	12
Kajstura, Diabetes 50:1414-1424	13
Leist et al., 2004, Science 305:239-242	14
Leveque <i>et al.</i> 1996, Hematol. Oncol. 14:137-146.....	15
Mahmood 2007, J. Neurosurg. 107:392-397	16
Mennini <i>et al.</i> 2006, Molecular Medicine 12:153-160	17
Moon <i>et al.</i> 2005, J. Pharmacol. Exp. Therapeutics 316:999-1005	18
Okada et al. 2007; 84: 504-510.....	19
Plapp 1971, J. Biol. Chem. 246:939-945	20
Prehn 1994, PNAS 91:12599-12603.....	21
Satake 1990, Biochimica et Biophysica Acta 1038:125-29.....	22
Schmidt, et al., 2007, Exp. Neurol., In press	23
Villa et al., 2007, Journal of Cerebral Blood Flow & Metabolism 27:255-63	24
Wang et al., 2004, 91:900-910.....	25
Wojchowski 1989, Blood 74:952-58	26
Ysebaert 2000, Nephrol. Dial. Transplant 15:1562-74.....	27
Zorov 2000, J. Exp. Med. 192:1001-1014.....	28

Erythropoietin crosses the blood–brain barrier to protect against experimental brain injury

Michael L. Brines^{*†}, Pietro Ghezzi^{*‡}, Sonja Keenan^{*}, Davide Agnello[§], Nihal C. de Lanerolle[§], Carla Cerami^{*}, Loretta M. Itri[¶], and Anthony Cerami^{*}

^{*}The Kenneth S. Warren Laboratories, 765 Old Saw Mill River Road, Tarrytown, NY 10591; [†]Laboratory of Neuroimmunology, Mario Negri Institute for Pharmacological Research, Milan, Italy 20157; [‡]Department of Neurosurgery, Yale University School of Medicine, 333 Cedar Street, New Haven, CT 06520; and [§]Ortho Biotech Inc., P.O. Box 670, 700 U.S. Highway, Route 202 South, Raritan, NJ 08869-0602

Contributed by Anthony Cerami, July 25, 2000

Erythropoietin (EPO), recognized for its central role in erythropoiesis, also mediates neuroprotection when the recombinant form (r-Hu-EPO) is directly injected into ischemic rodent brain. We observed abundant expression of the EPO receptor at brain capillaries, which could provide a route for circulating EPO to enter the brain. In confirmation of this hypothesis, systemic administration of r-Hu-EPO before or up to 6 h after focal brain ischemia reduced injury by ~50–75%. R-Hu-EPO also ameliorates the extent of concussive brain injury, the immune damage in experimental autoimmune encephalomyelitis, and the toxicity of kainate. Given r-Hu-EPO's excellent safety profile, clinical trials evaluating systemically administered r-Hu-EPO as a general neuroprotective treatment are warranted.

Erythropoietin (EPO) and its receptor (EPO-R) function as primary mediators of the normal physiologic response to hypoxia. EPO, a glycoprotein that increases red cell mass to improve tissue oxygenation, is produced by the kidney in response to hypoxia. Recombinant human EPO (r-Hu-EPO) is effective and widely used for the treatment of anemia associated with renal failure, HIV infection, cancer, and surgery. However, like other members of the cytokine superfamily to which EPO and its receptor belong, both are expressed by other tissues, including the nervous system. Similar to its regulation in the periphery, EPO within the central nervous system is inducible by hypoxia (1–4). An *in vivo* neuroprotective function for EPO has been demonstrated by the observation that direct intracerebraventricular injection of r-Hu-EPO in advance of hypoxic/ischemic stress offers significant protection of neuronal tissue (5–7). A critical neuroprotective role for endogenous EPO in the central nervous system has been confirmed by the administration of soluble EPO-R, which neutralizes EPO, consequently exacerbating ischemic stress and increasing tissue injury (7).

Hypoxia may not be the only relevant stimulus for brain EPO production, however, as metabolic disturbances, including hypoglycemia and strong neuronal depolarization, generate mitochondrial reactive oxygen species that may increase brain EPO expression through hypoxia inducible factor 1 (8). EPO may thus protect nervous tissue under any condition characterized by a relative deficiency of ATP in the face of increased metabolic demands. EPO has been shown to exhibit classic neurotrophic effects *in vivo* and *in vitro* (2, 9–11). The mechanism of action of EPO in erythropoiesis, neuroprotection, and neurotrophic effects ultimately may involve activation of the bcl-x family of antiapoptotic genes, promoting survival rather than apoptosis (12–14).

Despite the demonstrated benefit of intrathecally administered r-Hu-EPO in preventing ischemic neuronal damage, direct delivery of r-Hu-EPO into the brain is not a practical approach in most clinical contexts. Systemic delivery of r-Hu-EPO has not been evaluated because of the perception that the brain EPO system is parallel and distinct from the control of peripheral hemoglobin levels. However, this concept is based on the untested assumption that the blood–brain barrier (BBB) effectively excludes large glycosylated molecules such as EPO (1, 6, 7, 15, 16). Although in the

classic view the BBB is considered to be impermeable to large molecules, recent study clearly establishes that some large molecules can be specifically transported into the brain across the capillary endothelium (17–19) to affect brain function. Specific vectorial movement of macromolecules into the brain parenchyma begins by binding to receptors present on the luminal surfaces of the endothelial cells. This initiates endocytosis, followed by translocation across the BBB (reviewed in ref. 20). Using immunohistochemistry, we observed that the EPO-R is abundantly expressed at brain capillaries. Thus, we hypothesized that systemically administered r-Hu-EPO would be transported across the BBB, and if so, generally would defend against brain injury. In the present report we describe the ability of systemically administered r-Hu-EPO to function as a neuroprotective agent in animal models of focal brain ischemia, concussive brain injury, experimental autoimmune encephalomyelitis (EAE), and kainate-induced seizures.

Materials and Methods

Reagents. The r-Hu-EPO used is a human 165-aa glycoprotein manufactured by using recombinant DNA technology, which contains the identical amino acid sequence of isolated natural EPO and possesses the same biologic activity (21, 22). R-Hu-EPO is approximately 80% homologous to rodent EPO, and it has been shown to be biologically active in rodents for erythropoietic as well as neurotrophic functions. Although an immune response against human antigens can be elicited in rodents, it requires several weeks to obtain even a weak response (data not shown) and thus is not important in the context of these short-term studies. All experiments were performed by using r-Hu-EPO (Epoetin alfa, Procrit, Ortho Biotech, Raritan, NJ), which is formulated as a sterile, colorless liquid in an isotonic sodium chloride/sodium citrate or a sodium chloride/sodium PBS with added 1.25% human albumin.

EPO Assay. R-Hu-EPO concentrations in mouse serum obtained by serial phlebotomy via the orbital sinus were determined by using a commercially available enzyme-linked immunosorbent assay (Immunobiological Laboratories, Hamburg, Germany) following the manufacturer's protocol. The lower limit of detection was ~2 milliunits/ml.

Biotinylation of R-Hu-EPO. R-Hu-EPO was isolated from the albumin present in the clinical material by using cibacron blue columns (Aff, Gel Blue, Bio-Rad) followed by molecular weight-selective spin columns (Centricon, Millipore). Isolated r-Hu-

Abbreviations: EPO, erythropoietin; r-Hu-EPO, recombinant human EPO; EPO-R, EPO receptor; BBB, blood–brain barrier; EAE, experimental autoimmune encephalomyelitis; MCA, middle cerebral artery; BW, body weight.

[†]To whom reprint requests should be addressed. E-mail: mbrines@kswl.org.

The publication costs of this article were defrayed in part by page charge payment. This article must therefore be hereby marked "advertisement" in accordance with 18 U.S.C. §1734 solely to indicate this fact.

EPO then was biotinylated by using a commercially available kit (Boehringer Mannheim). Briefly, 0.2 mg of a long arm biotin (Vector Laboratories) was dissolved in 100 μ l of DMSO. This solution was added to the concentrated r-Hu-EPO solution and vortexed immediately. The mixture then was incubated at room temperature for 4 h protected from light with aluminum foil, while gently stirring. The unbound biotin was removed from this solution by using a Centricon-10 column. Confirmation of successful biotinylation and separation of r-Hu-EPO was confirmed by visualizing an \approx 34-kDa product after electrophoresis in a 6% agarose gel by using a streptavidin-biotin peroxidase kit (Vectostain, Vector Laboratories).

Immunocytochemistry. Human hippocampal specimens with adjacent white matter and temporal cortex were freshly isolated as 0.5-cm blocks cut from surgical specimens obtained during margin resection for temporal lobe tumors or vascular malformations. These were immediately postfixed by 5% acriline in 0.1 M phosphate buffer, pH 7.4 for 3 h. Sections for histological analyses were cut with a vibrating microtome (Vibratome, Ted Pella, Redding, CA) at 40 μ m thick. We previously have shown that these sections are anatomically normal (23). Immunohistochemical staining was performed as described (24) by using free floating sections and the indirect antibody peroxidase-antiperoxidase method with a 1:500 dilution EPO-R antiserum (Santa Cruz Biotechnology). Tissue controls by antibody omission and antibody specificity controls by use of the appropriate blocking peptide (Santa Cruz Biotechnology) also were carried out to confirm that staining was specific for EPO-R. Endogenous peroxidase activity was quenched by pretreatment of tissue sections with hydrogen peroxide (3% in methanol for 30 min). These antibodies have been previously validated for study of human tissue (2, 25). Cytochemical localization of biotinylated r-Hu-EPO in sections of perfused mouse brain was visualized by methodology similar to the immunocytochemistry, except for elimination of primary and secondary antibodies.

Animal Experimentation. Procedures involving animals and their care were conducted in conformity with the institutional guidelines that are in compliance with Italian and international laws and policies. Specific protocols were approved by the Animal Use and Care Committee of the Kenneth S. Warren Laboratories. All statistics were computed by using the analysis program JMP (SAS Institute, Cary, NC).

Middle Cerebral Artery (MCA) Occlusion. Sprague-Dawley male rats weighing \approx 250 g were anesthetized with pentobarbital [60 mg/kg body weight (BW)]. Body core temperature was thermostatically maintained at 37°C by using a water blanket and a rectal thermistor (Harvard Apparatus) for the duration of the anesthesia. The carotid arteries were visualized, and the right carotid was occluded by two sutures and cut. A burr hole adjacent and rostral to the right orbit allowed visualization of the MCA, which was cauterized distal to the rhinal artery. Animals then were positioned on a stereotaxic frame. To produce a penumbra surrounding this fixed MCA lesion, the contralateral carotid artery was occluded for 1 h by using traction provided by a fine forceps. Saline or r-Hu-EPO (250–5,000 units/kg BW) was administered at time points determined from the onset of the reversible carotid occlusion. To evaluate the extent of injury, the animals were killed after 24 h, the brains were removed, and serial 1-mm thick sections through the entire brain were cut by using a brain matrix device (Harvard Apparatus). Each section subsequently was incubated in a solution of 2% triphenyltetrazolium chloride (wt/vol) in 154 mM NaCl for 30 min at 37°C and stored in 4% paraformaldehyde until analysis. Quantification of the extent of injury was determined by using a computerized image analysis system (MCID, Imaging Research, St. Catharines, ON, Canada). To accomplish this, a digital image of each section was obtained and

the area of injury delineated by outlining the region in which the tetrazolium salt was not reduced, i.e., nonviable tissue. For cases in which the necrosis was so severe that tissue was actually lost and therefore the borders could not be directly assessed, an outline of the contralateral side was used to estimate the volume of injured brain. Total volume of infarct was calculated by reconstruction of the serial 1-mm thick sections. An indirect neuroprotective role for r-Hu-EPO via its effects on the circulating red cell mass was ruled out by the time frame of this experiment, which was shorter than the minimum required to produce a measurable erythropoietic effect (longer than 1 week).

Blunt Trauma. To produce trauma to the temporal and frontal cortices reproducibly, a pneumatic piston was precisely driven by using miniature precision valves (Clippard, Cincinnati, OH) powered by nitrogen. Displacement and velocity of the piston was determined by a digital motion detector (EPD Technologies, Elmsford, NY). Female BALB/c mice were anesthetized with pentobarbital, and their heads were placed securely in a stereotaxic frame. A scalp incision was made to locate the bregma. A 3-mm diameter stainless steel piston then was positioned to deliver the blow 2 mm caudal and 2 mm ventral to the bregma. Once the piston was activated, the velocity and time of impact was noted, as well as the amount of damage to the skull. The scalp incision was closed by using sutures. R-Hu-EPO was administered before, at the time of, or 3 or 6 h after impact and continued daily for a total of 5 days. Ten days after impact, the animals were anesthetized with pentobarbital and their brains were fixed by perfusion of 4% paraformaldehyde. The brains then were embedded in paraffin and 20- μ m sections were cut through the region of injury and stained with hematoxylin/eosin. Quantitative analysis of volume of injury was determined by using the MCID system as described above. Qualitative analysis of degree of inflammatory infiltrate was performed by a blinded observer scoring each slide by using a scale of 0–5, 0 corresponding to no visible inflammation and 5 to the densest infiltrate.

EAE. Female Lewis rats, 6–8 weeks of age, were purchased from Charles River (Calco, Italy). Animals were immunized by injecting 50 μ g of guinea pig myelin basic protein (Sigma) in water, emulsified in equal volumes of complete Freund's adjuvant (CFA; Sigma) into both hind footpads along with an additional 7 mg/ml of heat-killed *Mycobacterium tuberculosis* (H37Ra; Difco) administered under light ether anesthesia. The final volume was 100 μ l. Control mice received CFA alone. Rats were observed in a blinded fashion daily for signs of EAE and scored as follows: 0, no symptoms; 1, flaccid tail; 2, ataxia; and 3, complete hind limb paralysis with urinary incontinence. Statistical significance of experimental results was assessed by using a two-tailed Student's *t* test.

Kainate-Induced Seizures. Female BALB/c mice received r-Hu-EPO (5,000 units/kg i.p.) or saline at different time intervals with respect to administering kainate i.p. (Sigma) at various concentrations. Latency and seizure severity were assessed as described (26) by using a numerical scale of 0 to 5: 0 = no evident seizure activity; 1 = mild, nonsustained activity (e.g., wet dog shakes, immobility); 2 = mild limbic activity (e.g., forelimb clonus, tooth chattering); 3 = brief bursts of sustained seizure activity; 4 = status epilepticus with rearing and loss of balance; and 5 = status epilepticus with inability to stand. End points were time of onset of status epilepticus and time of death. Because seizure activity developed only within 20–30 min in the BALB/c mouse model, these experiments were limited to a maximum of 60 min, at which time surviving animals were killed.

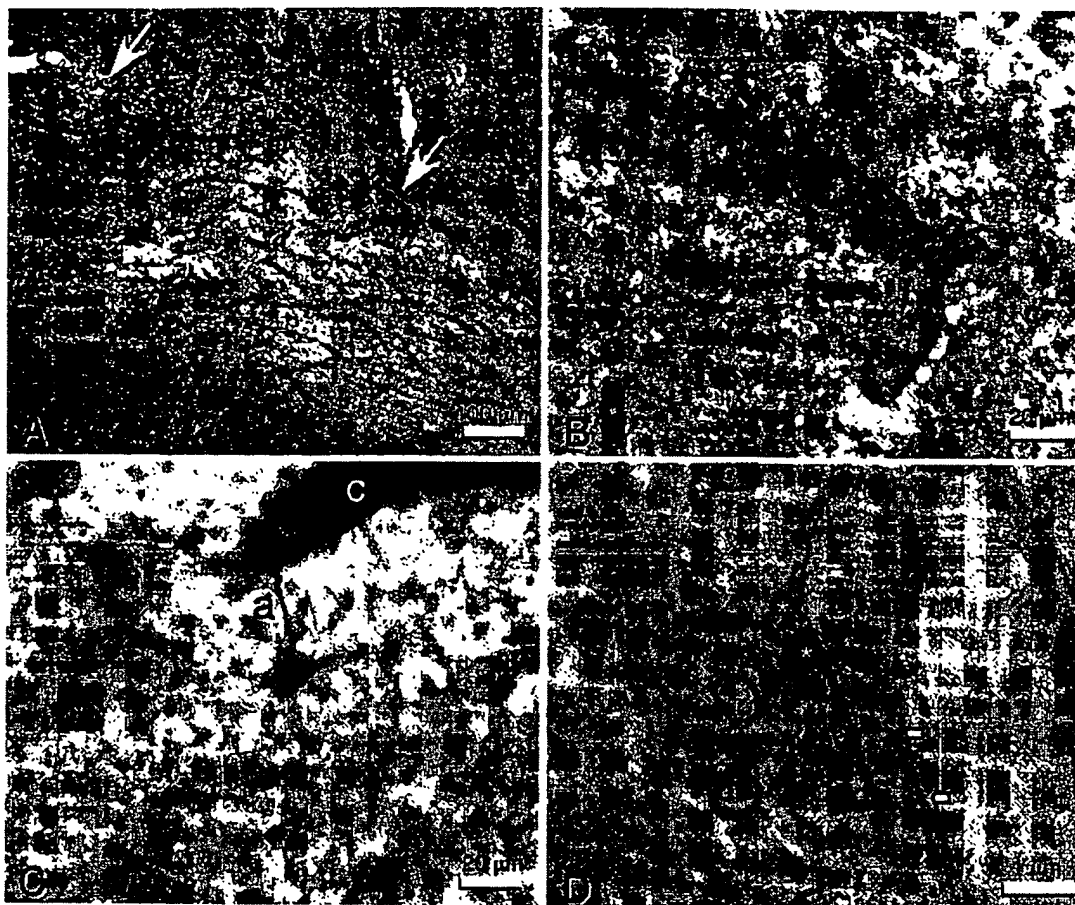


Fig. 1. EPO-R is found within and around human brain capillaries. (A) Anti-EPO-R staining in white matter (human hippocampal fimbria) is primarily localized to capillaries (arrows). (B) High-power view of capillaries illustrates the distinctly fibrous quality of EPO-R immunoreactivity around the capillary wall. (C) This immunoreactivity at the capillary (c) often could be identified as an astrocytic process (a). The entire cytoplasmic volume of such stellate astrocytes contain EPO-R immunoreactivity. (D) Transmission electron microscopy confirms that the predominant EPO-R immunoreactivity is within astrocytic foot processes (*), but it is also present within endothelial cells (arrows).

Results

EPO and EPO-R Are Expressed at Capillaries of the Brain-Periphery Interface. We first determined the expression of EPO and EPO-R in the normal brain by using specific polyclonal antibodies applied to sections of human, rat, and mouse tissue (unpublished work). Similar to many brain regions examined, the frontal cortex and hippocampus exhibited intense immunoreactivity for EPO-R in many medium to large neurons, but in a pattern restricted to the somata and proximal dendrites, and capillaries, particularly within white matter (Fig. 1A, arrows). In contrast, larger vessels and most astroglia were generally unreactive for anti-EPO-R. Under higher magnification, capillaries appeared enveloped by numerous EPO-R immunopositive processes (Fig. 1B) derived from nearby stellate astrocytes (Fig. 1C). Transmission electron microscopy confirmed that the predominance of anti-EPO-R immunoreactivity was located within the astrocytic endfeet surrounding the capillaries (Fig. 1D, *). In addition, substantial EPO-R immunoreactivity was observed within or on the surface of capillary endothelial cells (Fig. 1D, arrows).

Biotinylated r-Hu-EPO Crosses the BBB. These observations derived from immunocytochemical staining clearly suggest an anatomical basis for direct transport of EPO within the systemic circulation into the central nervous system in the absence of any neural insult. To

test this hypothesis, biotinylated r-Hu-EPO was injected i.p. into mice and subsequently visualized in brain sections by using streptavidin-peroxidase methodology. Two time intervals of 5 and 17 h were selected for evaluation, based on the pharmacokinetics of a single 5,000 units/kg BW r-Hu-EPO dose administered i.p. R-Hu-EPO administered in this fashion reaches a peak serum concentration at approximately 4 h ($\approx 25,000$ milliunits/ml; 1 milliunit ≈ 10 ng) and subsequently decays slowly to baseline levels over the next 20–30 h. We selected a 5-h time point for analysis to allow for an adequate exposure of the capillary endothelium to peak concentrations of r-Hu-EPO and compared this to 17 h later, when the serum levels had decreased to $<0.1\%$ of the peak.

Five hours after i.p. administration of biotinylated r-HuEPO (5,000 units/kg BW), peroxidase reaction product was observed surrounding capillaries (Fig. 2A) extending into the brain parenchyma a distance 3–4 times that of the thickness of the capillary wall (Fig. 2B). Simultaneous administration of unlabeled r-Hu-EPO (100-fold excess) with biotinylated r-Hu-EPO resulted in a markedly reduced or absent reaction product around the capillaries (Fig. 2C). Brain sections prepared 17 h after biotinylated r-Hu-EPO administration also lacked pericapillary reaction product. Instead, the label was localized to scattered neurons (data not shown). These anatomical studies provided evidence supportive of an active translocation of

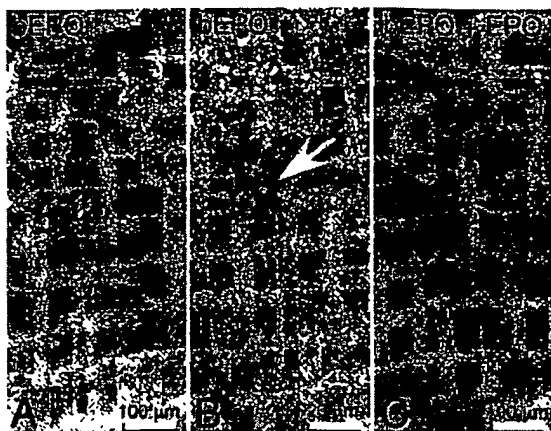


Fig. 2. Systemically administered biotinylated r-Hu-EPO labels capillaries within the mouse brain. (A) Localization of biotinylated r-Hu-EPO (b-EPO) is around capillaries 5 h after i.p. injection into mice but is not observed (C) if given with 100 times excess of unlabeled r-Hu-EPO (bEPO + EPO). Tissue sections are from the striatum. (B) Biotinylated r-Hu-EPO surrounds the lumen of capillaries (arrow) 5 h after administration.

peripheral EPO across the BBB and further suggested that neurons might be one target for EPO. To test this idea further, we administered r-Hu-EPO systemically in a rodent focal stroke model, for which intracerebraventricular r-Hu-EPO administration is known to reduce the infarct volume in the penumbra (6).

R-Hu-EPO Administered Systemically Is Neuroprotective in Focal Ischemic Stroke. Ischemia that recapitulates damage caused by human stroke can be induced in adult male rats by permanently occluding both the right MCA (27) and carotid artery, followed by a reversible 1-h occlusion of the left carotid artery (28). Using this model, a large penumbral region of ischemia was obtained in the right frontal cortex and r-Hu-EPO (5,000 units/kg BW) or vehicle was injected i.p. 24 h before, simultaneously, or 3, 6, or 9 h after MCA occlusion. The volume of brain infarcted 24 h after ischemia, determined by computerized volumetric analysis of triphenyltetrazolium reduction (i.e., to distinguish living from dead tissue) within serial sections, was markedly reduced in animals receiving r-Hu-EPO administered systemically 24 h before or up to 3 h after occlusion (Fig. 3). By 6 h after occlusion this protective effect was partially lost and r-Hu-EPO provided

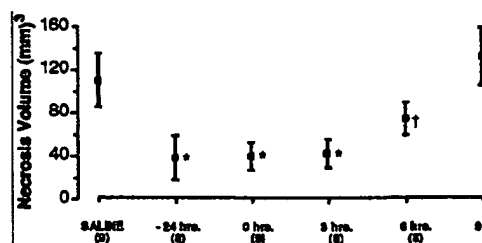


Fig. 3. Systemic administration of r-Hu-EPO reduces infarct volume after cerebral artery occlusion. Animals given r-Hu-EPO (5,000 units/kg BW i.p.) before, during, or 3 h after carotid artery occlusion showed significant ($P < 0.01$) and equivalent reduction of necrosis volume compared with controls. In contrast, animals receiving r-Hu-EPO 6 h after the onset of reversible ischemia exhibited a significant, but substantially smaller, decrease in injury volume compared with animals receiving r-Hu-EPO sooner ($P < 0.05$). High-dose r-Hu-EPO given 9 h after the onset of occlusion was ineffective in reducing the cortical volume of injury. Numbers in parentheses indicate number of animals studied under each condition.

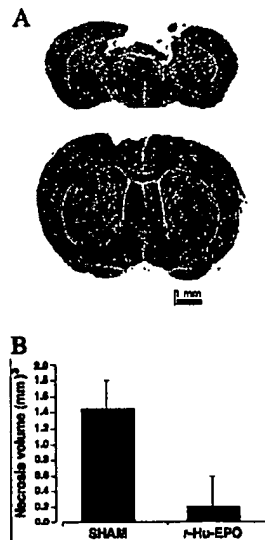


Fig. 4. Systemic administration of r-Hu-EPO attenuates injury after blunt trauma. (A) Mice receiving a nonpenetrating blow to the frontal cortex exhibited extensive cavitory necrosis when examined 10 days after injury if treated with saline (Upper) in contrast to the minimal injury observed if they had received r-Hu-EPO (Lower). Cresyl violet stain of representative brain sections through site of injury. (B) Results of a representative experiment for r-Hu-EPO (5,000 units/kg BW) given 24 h before delivery of the impact. $n = 6$ animals each group; $P < 0.05$. The experiment was repeated four times with similar results.

no apparent protection when given 9 h after occlusion. The minimum effective dose for r-Hu-EPO administered at the same time as vascular occlusion was found to be ≈ 450 units/kg BW (data not shown). Thus in this model of stroke, a window up to 6 h after the onset of ischemia appears open for intervention by using r-Hu-EPO, which can be administered systemically over a dose ranging from 450 units/kg BW to 5,000 units/kg BW.

R-Hu-EPO Administration Reduces Injury by Blunt Trauma. A mechanical insult delivered to the brain elicits elements of ischemic, excitotoxic, and inflammatory injury and, if severe enough, produces a cavitory lesion after 7–10 days (29). To determine whether systemically administered r-Hu-EPO is also protective of such injury, we used a mouse model in which the frontal cortex was subjected to a blow delivered to the intact calvaria by a calibrated pneumatic piston. Under pentobarbital anesthesia, animals received a blow of moderate severity (4 m/s; 2-mm displacement) and received an i.p. injection of r-Hu-EPO (5,000 units/kg BW i.p.) 24 h before or 0, 3, or 6 h after blow delivery. Animals continued to receive r-Hu-EPO once daily for 4 additional days (five doses total). Ten days after injury, each animal was killed, and their brains were perfused, fixed, serially sectioned and stained with hematoxylin and eosin or cresyl violet. Animals not receiving r-Hu-EPO exhibited extensive cavitory injury 10 days after blow delivery, in marked contrast to animals receiving r-Hu-EPO 24 h before, as Fig. 4A illustrates for brain sections obtained from representative animals. Quantitative analysis of injury volume for animals given r-Hu-EPO 24 h in advance of injury (Fig. 4B) illustrates that r-Hu-EPO pretreatment significantly reduced this concussive injury. As observed in the model of focal ischemia, qualitative examination of animals receiving r-Hu-EPO at 0, 3, or 6 h in relationship to trauma revealed a similar protection as pretreatment with r-Hu-EPO (data not shown).

Histologic examination of serial brain sections showed that for animals receiving saline alone the region immediately surrounding the necrotic core was densely populated with mononuclear

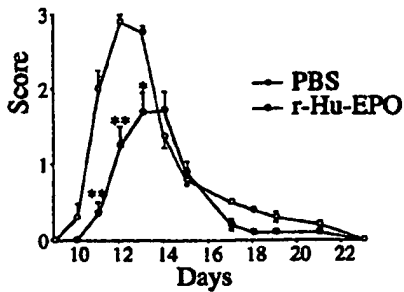


Fig. 5. Systemic administration of r-Hu-EPO ameliorates EAE. Lewis rats receiving r-Hu-EPO (5,000 units/kg BW) beginning at day 3 after immunization with myelin basic protein demonstrate both a delay in onset and a marked reduction of clinical symptoms ($n = 18$ animals in each group, three separate experiments; **, $P < 0.01$; *, $P < 0.05$).

inflammatory cells. In contrast, regions surrounding the necrotic core in r-Hu-EPO-treated animals were characterized by a markedly reduced inflammatory infiltrate (not shown). Thus, as in the experimental model for stroke, the results of these experiments demonstrate the ability of systemically administered r-Hu-EPO to protect brain tissue from blunt trauma.

R-Hu-EPO Reduces the Clinical Severity of EAE. Observations obtained from study of the blunt trauma model were striking in the absence of a prominent mononuclear cell infiltrate at the site of injury. These findings suggested that r-Hu-EPO also might reduce nervous system inflammation caused by other pathological processes. To test this hypothesis, we administered r-Hu-EPO in a rat model of EAE. In these experiments, EAE is induced in female Lewis rats by using guinea pig myelin basic protein and complete Freund's adjuvant. Immunized rats develop clinical symptoms by day 10, which peak with an increasing degree of paralysis by day 12. Daily administration of r-Hu-EPO (5,000 units/kg BW) or saline was initiated on day 3 after receiving myelin basic protein/complete Freund's adjuvant and continued until day 18. As shown in Fig. 5, r-Hu-EPO administration both significantly delayed the onset and reduced the severity of symptoms compared with saline-administered controls. Animals were followed for a total of 3 weeks after discontinuing r-Hu-EPO administration, during which time no "rebound" of symptoms occurred, as is typically observed after discontinuing treatment with glucocorticoids or IFN- β (30).

R-Hu-EPO Ameliorates the Latency and Severity of Seizures Induced by Kainate. Excitotoxicity is a prominent component common to many forms of brain injury (reviewed in refs. 31–33) and could be a target for EPO action. To test for this possibility, we determined whether r-Hu-EPO reduced the toxicity of the glutamate analogue kainic acid, as assessed by latency and severity of seizures. To accomplish this, first the relationship between doses of systemically administered kainate and its toxicity was established by determining the latency and severity of seizures. In mice, death caused by status epilepticus occurred with a latency of ≈ 18 min when kainate was administered alone at the ED₅₀ dose of ≈ 20 mg/kg. Mice were treated with r-Hu-EPO (5,000 units/kg BW) or saline 24 h before receiving kainate. Animals receiving both r-Hu-EPO and 20 mg/kg of kainate exhibited a significant delay of onset of status epilepticus with a markedly reduced motor involvement. The reduction in status epilepticus severity was reflected by the fact that there was a significant reduction in mortality of $\approx 45\%$ compared with controls (Fig. 6A) as well as an increase in mean survival time (25.8 min for r-Hu-EPO treatment compared with 18.2 min for control ($P < 0.0002$; $n = 68$ animals each group). Additionally,

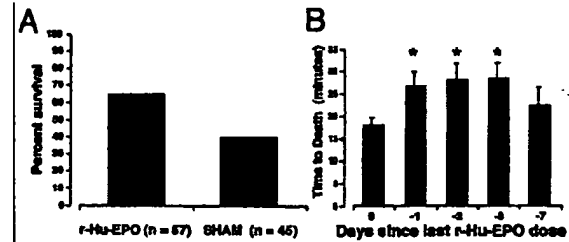


Fig. 6. Systemic administration of r-Hu-EPO delays and lessens kainate-induced seizures. (A) Mortality subsequent to a convulsant dosage of kainate (20 mg/kg BW i.p.) is significantly reduced ($P < 0.01$) by a 24-h pretreatment of mice with r-Hu-EPO (5,000 units/kg BW i.p.). (B) A single dose of r-Hu-EPO (5,000 units/kg BW) administered on day 0, 1, 2, 3, or 7 before testing continues to provide protection from kainate ($n = 18, 36, 17, 8$, or 8 respectively; *, $P < 0.05$ compared with control).

for each dose of kainate studied below the ED₅₀ of 20 mg/kg that did not produce status epilepticus, the behavioral seizure activity was significantly less severe than that observed for the sham-treated controls (data not shown).

In contrast to r-Hu-EPO administered 24 h before kainate, no protection from seizures was afforded by administering r-Hu-EPO 30 min before kainate (Fig. 6B) or after the development of any grade of motor seizure (data not shown). Further, a single exposure to r-Hu-EPO (5,000 units/kg BW) provided protection from kainate for at least 3 days (Fig. 6B). Thus, r-Hu-EPO is clearly not acting in the manner of conventional antiepileptic agents, which can terminate ongoing seizure activity but require a continued presence for efficacy. Presumably, EPO is inducing the expression of an array of genes that continue protection even in the absence of the cytokine.

Discussion

It is now clear that EPO possesses biological activities in addition to the erythropoietic effects that originally provided its name. Diverse cell types have been demonstrated to produce EPO and many cells besides erythroid progenitors express the EPO-R, including in the brain. The discovery that astrocytes produce EPO in response to hypoxia and that the EPO could protect nearby neuronal cells from ischemic injury *in vivo* (7) added further support for the pleiotropic nature of this cytokine. However, these findings also have historically suggested that the brain and peripheral EPO systems are separate. This concept is further reinforced by the known impermeability of the BBB to most plasma proteins. In the present paper, we have provided evidence that cross talk is possible between the peripheral and central EPO systems. Perhaps the most striking effect of these interacting systems is the ability of peripherally injected r-Hu-EPO to protect brain tissue from a variety of insults including ischemia/hypoxia, as well as trauma, immune-mediated inflammation, and excessive neuronal excitation.

A full understanding of how EPO mediates its effects across the BBB has not yet been elucidated, but we report here a plausible manner in which this is accomplished. First, our observation that the EPO-R is present on the capillaries of the brain, including the endothelial cells, but excluded from larger vessels, is consistent with a location at the anatomical locus of the BBB. Second, although previous studies report that small amounts of large proteins such as albumin can cross the BBB (34, 35), the mechanism is not receptor-mediated. At 5 h after systemic injection of biotinylated r-Hu-EPO, we observed biotin label only surrounding the BBB capillaries and not around larger vessels, as would be expected for a nonspecific transport mechanism. Third, movement of the biotin label was eliminated by coinjection of excess amounts of unlabeled r-Hu-EPO, consis-

tent with a specific and saturable transport mechanism. In sum, these observations are consistent with a specific receptor-mediated translocation of EPO into the brain.

The inflammatory response elicited by trauma results in a permeable BBB and thus could "deliver" in a nonspecific way any plasma substance into the site of injury. Although this mechanism certainly could contribute to the site-specific delivery of r-Hu-EPO after an injury, it cannot explain the protective effects of 24-h pretreatment in the MCA occlusion and kainate models, for which the serum r-Hu-EPO levels were low at the time of injury. Further, a minimum effective dose of 450 units/kg BW argues against a nonspecific leakage into the brain, which presumably could take place at much lower dosages as only small amounts of r-Hu-EPO are needed intrathecally (7). Systemic delivery of r-Hu-EPO has the advantage in that it is universally available to the capillary endothelium, and thus potentially present everywhere in the brain, in contrast to intrathecal injection, which is highly localized and not practical in clinical settings.

The quantity of r-Hu-EPO we administered in the MCA occlusion studies is much higher than that needed for erythropoiesis and substantially higher than most conventional clinical dosages. Nonetheless, large doses equivalent to those administered in this study have been tested in preclinical and phase I clinical trials without adverse effects (36) and many cancer patients now receive r-Hu-EPO as a weekly injection of 40,000–60,000 units.¹ We reasoned that a bolus of r-Hu-EPO should be presented to the brain capillaries as quickly as possible to be available for transport across the BBB to provide protection. Using these conditions, we found that systemic administration of r-Hu-EPO in the MCA model extended neuroprotective effects for up to 6 h after the initiating injury. This window of protection may be explained by the ability of exogenous r-Hu-EPO to induce protective genes in potentially viable cells within the ischemic penumbra before they enter into programmed cell death. In acute *in vivo* situations, the endogenous production of EPO by astrocytes is likely not sufficient or fast enough to provide significant protection to adjacent neural tissue.

The manner in which r-Hu-EPO provides this impressive neuroprotection is currently unclear. R-Hu-EPO could rescue cells from death through modulation of apoptosis, a role defined for EPO action in erythropoiesis and later extended to neuronal-like

cells *in vitro* (9, 10, 37), modulation of necrosis, or immune-mediated injury. All three forms of neuronal demise are thought to play a role in a wide variety of brain injury syndromes (reviewed in refs. 31–33). The experiments reported here were not designed to distinguish between these possibilities. Further work is obviously needed to evaluate these complex interactions *in vivo*.

Inflammatory processes play a key role in many forms of brain injury. The reduction in inflammatory infiltrate we observed in the blunt trauma experiments suggests that EPO may play an immunomodulatory role not previously described, but typical of many other cytokines. In the EAE model, both the inflammatory and immune systems are activated, whereas cell death is not thought to be a significant component of the clinical syndrome. The action of r-Hu-EPO in this model is to delay and blunt clinical manifestations in a manner consistent with known anti-inflammatory agents such as glucocorticoids. Whether one or both of these systems is responsible for the neuroprotective effects of EPO remains to be determined. However, our observation that mononuclear cell infiltration is reduced in r-Hu-EPO-treated animals suffering traumatic injury taken with the results of the EAE experiments suggest that both the inflammatory and immune responses are affected. If true, EPO may then exemplify a new therapeutic class.

In addition to an antiapoptotic role for EPO in the brain, one other function is suggested by the kainate experiments: r-Hu-EPO also can modulate neuronal excitability. However, EPO does not appear to have acute activity, clearly implying that its effects are secondary to activation of gene expression. The relevance of this type of neuronal activity to the now amply documented beneficial effects of r-Hu-EPO on quality of life (38) and possible improvement of cognitive function in patients receiving r-Hu-EPO (39) is intriguing.

Over the last decade, r-Hu-EPO has proven to be a safe therapeutic agent with minimal adverse effects. The results of studies presented here constitute a basis for examining the effectiveness of this agent for the treatment of several human maladies that currently are therapeutically underserved. Hopefully, r-Hu-EPO will prove as effective in humans as it appears to be in animals.

Note Added in Proof. In further support of the transport of r-Hu-EPO across the BBB, we have measured EPO in the cerebral spinal fluid of male rats obtained from the cisterna magna. The administration of r-Hu-EPO at 5,000 units/kg BW i.p. is associated with an ~100 milli-units/ml increase in EPO in the spinal fluid within 30 min.

This research was supported in part by Ortho Biotech Inc. and The Kenneth S. Warren Laboratories. D.A. is a fellow of the Alfredo Leonardi Fund and G. L. Pfeiffer Foundation.

Gabrilow, J. L., Einhorn, L. H., Livingston, R. B., Winer, E. & Cleeland, C. S. (1999) *Proc. Am. Soc. Clin. Oncol.* 18, 2216 (abstr.).

- Juul, S. E., Stallings, S. A. & Christensen, R. D. (1999) *Pediatr. Res.* 46, 543–547.
- Juul, S. E., Anderson, D. K., Li, Y. & Christensen, R. D. (1998) *Pediatr. Res.* 43, 40–49.
- Marti, H. H., Wenger, R. H., Rivas, L. A., Straumann, U., Digicaylioglu, M., Henn, V., Yonekawa, Y., Bauer, C. & Gassmann, M. (1996) *Eur. J. Neurosci.* 8, 666–676.
- Masuda, S., Okano, M., Yamagishi, K., Nagao, M., Ueda, M. & Sasaki, R. (1994) *J. Biol. Chem.* 269, 19488–19493.
- Sadamoto, Y., Igase, K., Sakanaka, M., Sato, K., Otsuka, H., Sakaki, S., Masuda, S. & Sasaki, R. (1998) *Biochem. Biophys. Res. Commun.* 253, 26–32.
- Bernaudo, M., Marti, H. H., Roussel, S., Divoux, D., Nouvelot, A., MacKenzie, E. T. & Petit, E. (1999) *J. Cereb. Blood Flow Metab.* 19, 643–651.
- Sakanaka, M., Wen, T. C., Matsuda, S., Masuda, S., Morishita, E., Nagao, M. & Sasaki, R. (1998) *Proc. Natl. Acad. Sci. USA* 95, 4635–4640.
- Chandel, N. S., Maltepe, E., Goldwasser, E., Mathieu, C. E., Simon, M. C. & Schumacker, P. T. (1998) *Proc. Natl. Acad. Sci. USA* 95, 11715–11720.
- Tabira, T., Konishi, Y. & Gaillyas, F., Jr. (1995) *Int. J. Dev. Neurosci.* 13, 241–252.
- Konishi, Y., Chui, D. H., Hirose, H., Kunitaira, T. & Tabira, T. (1993) *Brain Res.* 609, 29–35.
- Campana, W. M., Misasi, R. & O'Brien, J. S. (1998) *Int. J. Mol. Med.* 1, 235–241.
- Silva, M., Grillot, D., Benito, A., Richard, C., Nunez, G. & Fernandez-Luna, J. L. (1996) *Blood* 88, 1576–1582.
- Silva, M., Benito, A., Sanz, C., Prosper, F., Ekhterani, D., Nunez, G. & Fernandez-Luna, J. L. (1999) *J. Biol. Chem.* 274, 22165–22169.
- Gregory, T., Yu, C., Ma, A., Orkin, S. H., Blobel, G. A. & Weiss, M. J. (1999) *Blood* 94, 87–96.
- Buemi, M., Allegra, A., Corica, F., Floccari, F., D'Avella, D., Aloisi, C., Calapai, G., Iacopino, G. & Frisina, N. (2000) *Nephrol. Dial. Transplant.* 15, 422–423.
- Marti, H. H., Gassmann, M., Wenger, R. H., Kvietikova, I., Morganti-Kossmann, M. C., Kossmann, T., Trentz, O. & Bauer, C. (1997) *Kidney Int.* 51, 416–418.
- Pardridge, W. M., Eisenberg, J. & Yang, J. (1987) *Metabolism* 36, 892–895.
- Golden, P. L., Maccagnan, T. J. & Pardridge, W. M. (1997) *J. Clin. Invest.* 99, 14–18.
- Duffy, K. R., Pardridge, W. M. & Rosenfeld, R. G. (1988) *Metabolism* 37, 136–140.
- Pardridge, W. M. (1997) *J. Cereb. Blood Flow* 17, 713–731.
- Egrie, J. C., Strickland, T. W., Lane, J., Aoki, K., Cohen, A. M., Smalling, R., Trail, G., Lin, F. K., Browne, J. K. & Hines, D. K. (1986) *Immunobiology* 172, 213–224.
- Egrie, J. C., Browne, J., Lai, P. & Lin, F. K. (1985) *Prog. Clin. Biol. Res.* 191, 339–350.
- de Lanerolle, N. C., Kim, J. H. & Brines, M. L. (1994) *Clin. Neurosci.* 2, 64–81.
- de Lanerolle, N. C., Kim, J. H., Robbins, R. J. & Spencer, D. D. (1989) *Brain Res.* 495, 387–395.
- Juul, S. E., Yachnis, A. T. & Christensen, R. D. (1998) *Early Hum. Dev.* 52, 235–249.
- Brines, M. L., Dare, A. O. & de Lanerolle, N. C. (1995) *Neurosci. Lett.* 191, 145–148.
- Coyle, P. (1982) *Stroke* 13, 855–859.
- Zimmerman, G. A., Meistrell, M., 3rd, Bloom, O., Cockcroft, K. M., Bianchi, M., Rinauci, D., Broome, J., Farmer, P., Cerami, A., Vlassara, H., et al. (1995) *Proc. Natl. Acad. Sci. USA* 92, 3744–3748.
- Dixon, C. E., Lighthall, J. W. & Anderson, T. E. (1988) *J. Neurotrauma* 5, 91–104.
- van der Meide, P. H., de Labie, M. C., Ruuls, S. R., Groenestein, R. J., Bolman, C. A., Olsson, T. & Dijkstra, C. D. (1998) *J. Neuroimmunol.* 84, 14–23.
- Martin, L. J., Al-Abdulla, N. A., Brambrink, A. M., Kirsch, J. R., Sieber, F. E. & Portera-Cailliau, C. (1998) *Brain Res. Bull.* 46, 281–309.
- Juurink, B. H. & Paterson, P. G. (1998) *J. Spinal Cord Med.* 21, 309–334.
- Dirmagl, U., Iadecola, C. & Moskowitz, M. A. (1999) *Trends Neurosci.* 22, 391–397.
- Broadwell, R. D., Balin, B. J. & Salzman, M. (1988) *Proc. Natl. Acad. Sci. USA* 85, 632–636.
- Poduslo, J. F., Curran, G. L. & Berg, C. T. (1994) *Proc. Natl. Acad. Sci. USA* 91, 5705–5709.
- Cheung, W. K., Goon, B. L., Guilfoyle, M. C. & Washoltz, M. C. (1998) *Clin. Pharmacol. Ther.* 64, 412–423.
- Ling, Z. D., Potter, E. D., Lipton, J. W. & Carvey, P. M. (1998) *Exp. Neurol.* 149, 411–423.
- Demetri, G. D., Kris, M., Wade, J., Degos, L. & Cella, D. (1998) *J. Clin. Oncol.* 16, 3412–3425.
- Pickett, J. L., Theberge, D. C., Brown, W. S., Schweizer, S. U. & Nissenson, A. R. (1999) *Am. J. Kidney Dis.* 33, 1122–1130.

Protective Effect of Erythropoietin and Its Carbamylated Derivative in Experimental Cisplatin Peripheral Neurotoxicity

Roberto Bianchi,¹ Michael Brines,³ Giuseppe Lauria,² Costanza Savino,¹ Alessandra Gilardini,⁴ Gabriella Nicolini,⁴ Virginia Rodriguez-Menendez,⁴ Norberto Oggioni,⁴ Annalisa Canta,⁴ Paola Penza,² Raffaella Lombardi,² Claudio Minoia,⁵ Anna Ronchi,⁵ Anthony Cerami,³ Pietro Ghezzi,^{1,3} and Guido Cavaletti⁴

Abstract **Purpose:** Antineoplastic drugs, such as cisplatin (CDDP), are severely neurotoxic, causing disabling peripheral neuropathies with clinical signs known as chemotherapy-induced peripheral neurotoxicity. Cotreatment with neuroprotective agents and CDDP has been proposed for preventing or reversing the neuropathy. Erythropoietin given systemically has a wide range of neuroprotective actions in animal models of central and peripheral nervous system damage. However, the erythropoietic action is a potential cause of side effects if erythropoietin is used for neuroprotection. We have successfully identified derivatives of erythropoietin, including carbamylated erythropoietin, which do not raise the hematocrit but retain the neuroprotective action exerted by erythropoietin.

Experimental Design: We have developed previously an experimental chemotherapy-induced peripheral neurotoxicity that closely resembles CDDP neurotoxicity in humans. The present study compared the effects of erythropoietin and carbamylated erythropoietin (50 µg/kg/d thrice weekly) on CDDP (2 mg/kg/d i.p. twice weekly for 4 weeks) neurotoxicity *in vivo*.

Results: CDDP given to Wistar rats significantly lowered their growth rate ($P < 0.05$), with slower sensory nerve conduction velocity ($P < 0.001$) and reduced intraepidermal nerve fibers density ($P < 0.001$ versus controls). Coadministration of CDDP and erythropoietin or carbamylated erythropoietin partially but significantly prevented the sensory nerve conduction velocity reduction. Both molecules preserved intraepidermal nerve fiber density, thus confirming their neuroprotective effect at the pathologic level. The protective effects were not associated with any difference in platinum concentration in dorsal root ganglia, sciatic nerve, or kidney specimens.

Conclusions: These results widen the spectrum of possible use of erythropoietin and carbamylated erythropoietin as neuroprotectant drugs, strongly supporting their effectiveness.

Chemotherapy-induced peripheral neurotoxicity (CIPN) is a major clinical problem because it is a dose-limiting side effect of important and effective antineoplastic drugs (1). The incidence, severity, and clinical symptoms and signs of CIPN depend on the drug given and its schedules. Severe neuropathy can occur in 3% to 7% of treated cases with single agents but can increase to 38% with combined regimens (2, 3). Moreover, even when CIPN is not dose-limiting, it may severely affect the

quality of life of cancer patients and cause chronic discomfort. Therefore, effective prevention and/or treatment of CIPN would be a major advance for cancer patients.

Cisplatin (CDDP) and the other platinum-derived drugs are among the most effective antineoplastic agents, but they are severely neurotoxic. The clinical features of CDDP neurotoxicity in humans are mainly ataxia, pain, and sensory impairment secondary to accumulation of CDDP in the dorsal root ganglia (DRG) and subsequent damage, resulting in secondary nerve fiber axonopathy.

We have developed an experimental model of peripheral neurotoxicity induced by CDDP (4–9) that closely resembles CDDP neurotoxicity in humans. It involves the reversible primary involvement of DRG neurons, with secondary sensory axonal neuropathy and sparing of the motoneurons. This model has already been used to investigate the mechanisms of neurotoxic action of CDDP (4, 5, 7, 9) and to test the effect of putative neuroprotective agents (6, 8–13). Among these agents, cotreatment with neurotrophic agents has been proposed as a means of preventing or reversing CIPN (14).

Among the several substances with trophic action on central neurons and peripheral nerves, erythropoietin has a

Authors' Affiliations: ¹"Mario Negri" Institute for Pharmacological Research; ²"Besta" National Neurological Institute, Milan, Italy; ³Kenneth S. Warren Institute, Kitchawan, New York; ⁴University of Milan "Bicocca," Monza, Italy; and ⁵"Maugeri" Foundation, Pavia, Italy

Received 10/5/05; revised 1/16/06; accepted 1/26/06.

Grant support: Fondazione Banca Del Monte di Lombardia (G. Cavaletti).

The costs of publication of this article were defrayed in part by the payment of page charges. This article must therefore be hereby marked *advertisement* in accordance with 18 U.S.C. Section 1734 solely to indicate this fact.

Requests for reprints: Roberto Bianchi, Molecular Biochemistry and Pharmacology, "Mario Negri" Institute for Pharmacological Research, Via Eritrea, 62, Milan 20157, Italy. Phone: 39-239014484; Fax: 39-02-3548277; E-mail: robbia@marionegri.it.

© 2006 American Association for Cancer Research.
doi:10.1158/1078-0432.CCR-05-2177

wide range of neuroprotective effects *in vivo*. Erythropoietin receptors are expressed both in nerve axons and Schwann cells and in DRG neurons and are overexpressed after nerve injury (15–17), presenting a target for pharmacotherapy. In primary neuronal cultures or neuronal cell lines, recombinant human erythropoietin protects from apoptosis (18, 19). *In vivo*, erythropoietin protects neurons from cerebral ischemia and traumatic injury (20) and reduces the severity of experimental autoimmune encephalomyelitis, spinal cord injury, and sciatic nerve compression (21). We recently found that erythropoietin both protects against and lowers the severity of experimental diabetic neuropathy (22). Erythropoietin is also protective against peripheral neuropathy induced by CDDP in rats, evaluated by electrophysiology (compound muscle action potential) and histologic examination of the number of nerve fibers (23).

One major issue in the use of erythropoietin is its erythrodifferentiating action that could be cause of several side effects, including vascular perfusion defects (24). In mice, the increase in hematocrit induced by erythropoietin causes vasoconstriction and cardiac dysfunction due to nitric oxide depletion and endothelin activation (25, 26). In animals and humans, erythropoietin can lead to hypertension (27, 28) or thrombosis (29).

Recently, we have identified derivatives of erythropoietin, including carbamylated erythropoietin (30) and asialo-erythropoietin (21), which are nonerythropoietic but retain neuroprotective action in different animal models, including cerebral ischemia, spinal cord injury, and diabetic neuropathy.

In this study, we investigated the potential role of erythropoietin and carbamylated erythropoietin for neuroprotection against CIPN induced by CDDP.

Because carbamylated erythropoietin does not increase the hematocrit and does not bind the hemopoietic, homodimeric erythropoietin receptor, the present model should enable us to dissociate a peripheral neuroprotective action of erythropoietin from a hemopoietic effect and determine whether neuroprotection can be achieved without the risk associated with the use of erythropoietin in nonanemic patients.

Materials and Methods

Animal husbandry. All the procedures involving animals and their care were conducted in conformity with the institutional guidelines in compliance with national (Law by Decree No. 116, February 18, 1992, *Gazzetta Ufficiale della Repubblica Italiana*, Suppl. 40) and international (European Economic Community Council Directive 86-609, December 12, 1987, in *Official Journal of Law*, p. 358; Guide for the Care and Use of Laboratory Animals, U.S. National Research Council, 1996) laws and policies. The protocols for the investigation were reviewed and approved by the Animal Care and Use Committees of the Istituto di Ricerche Farmacologiche "Mario Negri" (Milan) and the Faculty of Medicine, University of Milano "Bicocca".

A total of 72 female Wistar rats (200–220 g at the beginning of the experiment; Harlan Italia, Correzzana, Italy) were used for the study. They were housed in a limited access animal facility with room temperature and relative humidity $22 \pm 2^\circ\text{C}$ and $55 \pm 10\%$ and unrestricted access to food and water. Artificial lighting provided a 24-hour cycle of 12-hour light/12-hour dark (light 7 a.m.–7 p.m.).

Drugs. CDDP (Platamine) was purchased from Pharmacia Italia (Milan, Italy). Erythropoietin was obtained from Dragon Pharmaceuticals (Vancouver, British Columbia, Canada). Carbamylated erythro-

poietin was prepared as described (30) and was kindly provided by H. Lundbeck (A/S, Valby, Copenhagen, Denmark).

In vivo studies. Two separate experiments were done. In a first experiment, we studied the effects of erythropoietin on CDDP-induced neuropathy. Thirty-two rats were randomly divided into four groups (8 per group): CDDP, CDDP plus erythropoietin, erythropoietin, and untreated controls. CDDP was dissolved in sterile saline and rats were injected with CDDP 2 mg/kg i.p. twice weekly for 8 times using a volume of 4 mL/kg (31, 32). The CDDP plus erythropoietin group was treated with the same dose of CDDP plus erythropoietin (50 $\mu\text{g/kg}$ i.p. thrice weekly). The erythropoietin group received only the drug as above. In a second experiment, we studied the effect of carbamylated erythropoietin (50 $\mu\text{g/kg}$ i.p. thrice weekly) on CDDP-induced neuropathy. Forty rats were randomly divided into five groups (8 per group): CDDP, CDDP plus erythropoietin, CDDP plus carbamylated erythropoietin, carbamylated erythropoietin, and control.

In both experiments, control rats received sham i.p. injections with the CDDP solvent.

Methods of evaluation. General conditions of the animals were recorded daily, and weight was measured at the time of drug administration.

At the end of the treatment, each rat's sensory nerve conduction velocity (SNCV) was determined in the tail using a previously described method (6, 9). Briefly, antidromic SNCV was assessed by stimulating the tail nerve with ring electrodes placed 5 and 10 cm proximally to the recording ring electrodes placed distally in the tail. The latencies of the potentials recorded at the two sites after nerve stimulation were determined (peak-to-peak) and the nerve conduction velocity was calculated accordingly. All the neurophysiologic measurements were done under standard conditions in a temperature-controlled room.

At the end of the experiment, the animals were euthanized under general xylazine/ketamine anesthesia and tissue specimens were obtained.

Peripheral nerve damage was assessed on pathologic grounds by skin biopsy and an estimate of intraepidermal nerve fiber (IENF) density in the hindpaw footpad (33). Briefly, skin specimens were fixed in 2% paraformaldehyde-lysine periodate for 24 hours at 4°C , cryoprotected overnight, and serially cut with a cryostat to obtain 20 μm sections. Three sections were randomly selected and immunostained with polyclonal anti-PGP 9.5 (Biogenesis, Poole, United Kingdom) using a free-floating protocol (33). Three blinded observers counted the total number of IENF in each section under a light microscope at high magnification using a microscope-mounted video camera. Individual fibers were counted as they crossed the dermal-epidermal junction, and secondary branching within the epidermis was excluded. The length of the epidermis was measured using a computerized system (Microscience, Seattle, WA) to obtain the linear density of IENF.

Whole blood was obtained through abdominal aorta puncture, collected into a heparinated tube for hematocrit determination, and centrifuged at 2,500 rpm for 20 minutes at 4°C . Total and erythrocyte capillary tube length was measured and the hematocrit was calculated as a percentage by dividing the particulate by total length and multiplying it by 100.

Sciatic nerves, DRG, and kidneys of rats from all CDDP-treated groups were obtained, snap-frozen in liquid nitrogen, and kept at -80°C until used to determine the platinum concentration by inductively coupled plasma-tandem mass spectrometry according to the previously reported protocol (6).

Statistics. The differences between all experimental groups in body weight, SNCV, IENF density, and tissue platinum concentrations were examined by ANOVA and the Tukey-Kramer post-test.

Results

General toxicity. All the rats completed the studies, with no evidence of severe general toxicity. In each experiment, at

Table 1. Physiologic variables of rats treated with CDDP and/or cotreated with erythropoietin and carbamylated erythropoietin

Group	Experiment 1			Experiment 2		
	Baseline body weight (g)	Final body weight (g)	Hematocrit (%)	Baseline body weight (g)	Final body weight (g)	Hematocrit (%)
Control + vehicle	186 ± 2	221 ± 3	51.9 ± 1.0	184 ± 5	255 ± 9	50.0 ± 1.8
CDDP + vehicle	197 ± 3	199 ± 3*	47.5 ± 1.2	181 ± 3	212 ± 6*	52.3 ± 1.1
Control + erythropoietin	196 ± 2	222 ± 3	82.4 ± 1.5 [†]			
Control + carbamylated erythropoietin				184 ± 3	248 ± 6	56.4 ± 2.3
CDDP + erythropoietin	195 ± 3	209 ± 6	84.3 ± 1.2 [‡]	182 ± 5	229 ± 7	76.2 ± 6.3 [§]
CDDP + carbamylated erythropoietin				180 ± 5	230 ± 5	51.0 ± 1.3

NOTE: Data are mean ± SE (8 per group). Statistics by ANOVA with Tukey-Kramer HSD test for multiple comparisons.

**P* < 0.01 versus control and control + erythropoietin (experiment 1).

[†]*P* < 0.01 versus all the other groups (experiment 2).

[‡]*P* < 0.01 versus control and CDDP (experiment 1).

[§]*P* < 0.01 versus all the other groups (experiment 2).

baseline, there was no difference in body weight between groups. CDDP alone significantly reduced weight gain (Table 1); CDDP-treated rats weighed 10% and 17% less than the control groups in experiments 1 and 2, respectively (*P* < 0.01 in both cases), and the coadministration of erythropoietin or carbamylated erythropoietin reduced the difference by ~50%.

Hematocrit was significantly higher in both erythropoietin-treated groups (*P* < 0.01), whereas carbamylated erythropoietin did not produce any significant change from control rats (Table 1).

Tail nerve neurophysiologic evaluation. In each experiment, baseline SNCV did not differ in the two groups. In the first experiment, tail SNCV studies at the end of the treatment showed that the erythropoietin and control groups were very similar (Fig. 1A). This was confirmed in the second experiment, which, in addition, showed similar results for carbamylated erythropoietin (Fig. 1B). CDDP, however, reduced mean SNVC by 26% and 30% compared with control in experiments 1 and 2, respectively (*P* < 0.001). In both experiments, erythropoietin had a partial, but highly significant, protective effect (Fig. 1A and B) and SNCV compared with the CDDP group, although it remained different from control (mean of experiments 1 and 2, -15.7% and -17.8%, respectively; *P* < 0.001). Similarly, carbamylated erythropoietin partially prevented the decrease in SNVC induced by CDDP (*P* < 0.05; Fig. 1B).

IEFN density. In footpad skin, both the neurotoxic effect of CDDP and the neuroprotective action of erythropoietin and carbamylated erythropoietin were confirmed at the pathologic level. Figure 2 summarizes the results of the two experiments. Erythropoietin and carbamylated erythropoietin coadministered did not affect IEFN density in control rats (data not shown). CDDP significantly reduced the epidermal innervation density (mean 13.1% lower than control) and caused diffuse morphologic changes of nerve fibers, indicating axonal degeneration (Fig. 3). Erythropoietin and carbamylated erythropoietin coadministered significantly (*P* < 0.001) protected against from the loss of IEFN induced by CDDP (Figs. 2 and 3).

Tissue platinum concentration. Platinum in control specimens was below the limit of detection of the inductively coupled plasma-mass spectrometry method (i.e., <0.001 µg/g tissue), but it was detectable in specimens from CDDP-treated rats. No significant differences were observed between CDDP and CDDP plus erythropoietin groups (7.64 ± 0.82 versus 9.11 ± 1.84, 1.86 ± 0.41 versus 1.67 ± 0.23, and

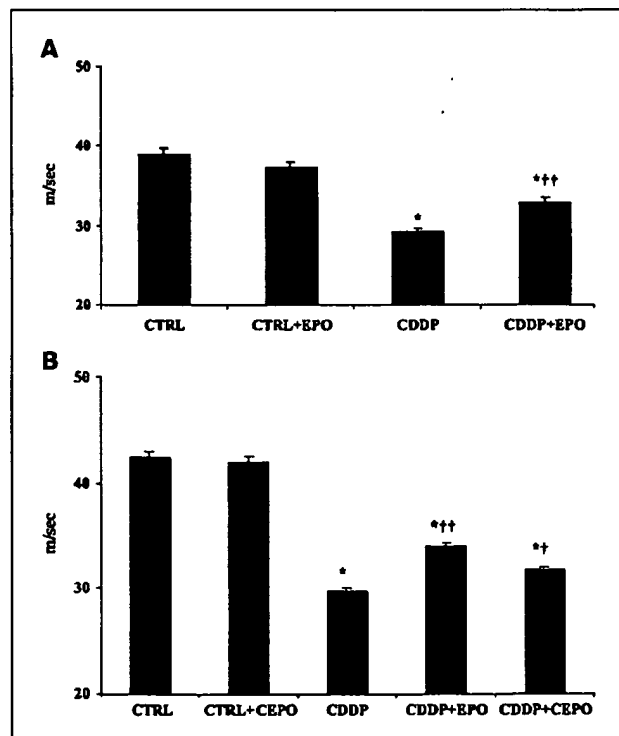


Fig. 1. SNCV at the end of the treatment. Columns, mean (in m/s) of seven to eight per group; bars, SE. A, experiment 1. *, *P* < 0.001 versus control (CTRL) and control + erythropoietin (EPO); ***, *P* < 0.01 versus CDDP. B, experiment 2. *, *P* < 0.001 versus control and control + carbamylated erythropoietin (CEPO); **, *P* < 0.05 versus CDDP; ***, *P* < 0.01 versus CDDP.

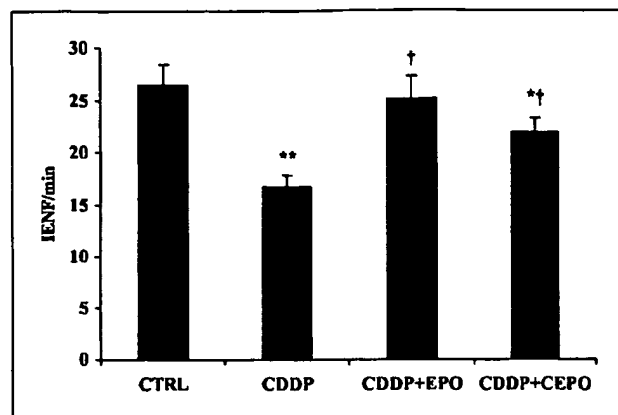


Fig. 2. Erythropoietin restores the loss of intraepidermal fibers in CDDP-treated rats. Skin biopsies were obtained at the end of the treatment. Columns, mean (number of IENF/mm) of seven to eight per group; bars, SE. *, $P < 0.05$ versus control (CTRL); **, $P < 0.001$ versus control; †, $P < 0.001$ versus CDDP.

2.38 versus 3.16 $\mu\text{g/g}$ tissue for kidney, sciatic nerves, and pooled DRG samples, respectively). Hence, the protective effect of erythropoietin was not associated with any difference in platinum concentration in DRG, sciatic nerve, or kidney specimens.

Discussion

CIPN is a major limitation in the current treatment of cancer with platinum drugs, because it frequently requires a dose reduction or even treatment withdrawal, on account of adverse effects. Therefore, effective strategies to prevent or reduce the severity of CIPN are a major goal of preclinical research, with a view to clinical application. *In vitro* studies have been frequently used for screening putative neuroprotective agents, because they are faster and cheaper than *in vivo* testing. However, the latter reproduce the clinical picture in humans more reliably, including the effects of drug metabolism and bioavailability and tissue distribution, with respect to the target organs in particular.

The peripheral neuropathy induced in rats by repeated administration of CDDP is qualitatively similar to that in humans, involving the degeneration of sensory nerve fibers caused by DRG neuronopathy. The model of CIPN used in this study has already been extensively characterized in our laboratory (4–9) and has been used to assess the effectiveness of several putative neuroprotective agents. Some were not effective (9, 31), whereas others had at least a partial effect (6, 8, 10, 12, 13). The usefulness and reliability of the preclinical results were further strengthened when one of these neuroprotectants (reduced glutathione) was evaluated in a randomized, double-blind, placebo-controlled clinical trial in ovarian cancer patients (32), which confirmed its partial protective effect against CDDP neurotoxicity, previously evidenced in the animal model.

The use of neurophysiologic tests to assess the effect of neurotoxic or neuroprotective agents is well established (6–8, 34–36). They are also largely used in clinical practice in human neuropathies. However, pathologic confirmation of the neurophysiologic results is always advisable. In our

CDDP model, we have extensively reported the pathologic features in DRG, sciatic nerves, and tibial nerves (5). In the present study, for the first time, we investigated the effect of CDDP at the pathologic level by quantifying IENF density in the footpad skin using a standardized method (33). This procedure is currently used to assess the degeneration of skin nerve fibers in human peripheral neuropathies (37). Skin biopsy for IENF density quantification is a reliable and minimally invasive technique in patients. It showed both degeneration and regeneration of nerve fibers in experimental and human diabetic neuropathies (22, 38, 39) and it might be proposed as an outcome measure in clinical trials with neurotoxic drugs. SNCV and IENF density studies explore different nerve fiber populations: SNCV evaluation mostly

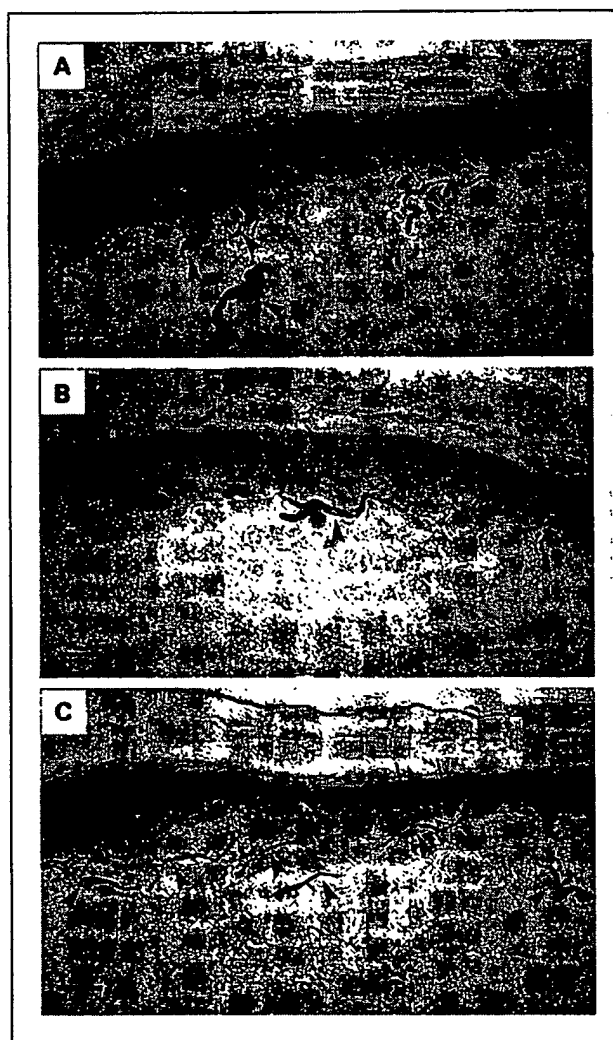


Fig. 3. Microphotographs are skin biopsies from the hindpaw footpad of Wistar rats. Sections were immunostained with the panaxonal marker PGP 9.5. Arrows, IENF; arrowheads, dermal nerve bundles. Bar, 30 μm . A, normal epidermal and dermal innervation density. B, reduced density of IENF and dermal nerve bundles in CDDP-induced neuropathy. IENF show weaker and fragmented PGP 9.5 immunoreactivity indicative of axonal degeneration. C, normal density and morphology of IENF and dermal nerve bundles in a rat cotreated with CDDP and carbamylated erythropoietin.

reflects changes in large myelinated fibers, whereas IENF density is an estimate of small-diameter fibers that are affected early in most peripheral neuropathies.

Erythropoietin, a 165-amino acid sialoglycoprotein, is essential in the regulation of erythropoiesis. Among its several clinical applications, erythropoietin is a very effective, well tolerated, and widely used treatment for anemia in cancer patients undergoing chemotherapy. However, the bone marrow is not the only target tissue of erythropoietin, and the wide expression of functional receptors for erythropoietin explains its nonerythropoietic functions, including its neuroprotective action on the injured nervous system (40). Rat models have been used to test the protective effect of erythropoietin (15, 16, 22), which was recently confirmed in an experimental model of CDDP (23). However, this rat model involved a motor, demyelinating neuropathy that did not reproduce the typical effects of CDDP in humans (i.e., sensory impairment with axonal damage in the peripheral nerves), thus raising some concern about the relevance of the positive results for potential clinical application.

Because, in rats, both DRG and peripheral nerves express the erythropoietin receptor (15, 16), our model of CDDP-induced DRG sensory neuronopathy with secondary axonal neuropathy seems adequate to assess the use of erythropoietin as a neuroprotective agent. The effect of a nonerythropoietic erythropoietin derivative, such as carbamylated erythropoietin, which showed tissue-protecting properties in several animal models of peripheral nerve damage (30), was also evaluated.

Our study shows that erythropoietin or carbamylated erythropoietin alone have no effect on the normal function of the peripheral nerves but had significant and reproducible neuroprotective effects in CDDP-induced neurotoxicity. These results were supported both by the neurophysiologic findings showing the improvement of tail SNCV and at the pathologic level by the higher density of IENF in the footpad skin.

A major concern in the use of neuroprotectant drugs to prevent CIPN is interference with the antineoplastic activity of chemotherapy. Although the effects of erythropoietin on tumor growth is still controversial, Sigounas et al. (41) suggested a synergy between erythropoietin and chemotherapeutic agents in a murine cancer model. We investigated whether erythropoietin or carbamylated erythropoietin affected the tissue distribution of CDDP by measuring the concentration of platinum in the kidney (where it accumulates after CDDP administration and CDDP-DNA adducts are present; 11) and in the peripheral nervous system. We found no difference in platinum tissue concentrations, supporting the opinion that erythropoietin and carbamylated erythropoietin do not interfere with CDDP.

The mechanism of neuroprotection of erythropoietin and carbamylated erythropoietin in our experimental paradigm is still an open issue. Based on current knowledge, a direct protective effect of erythropoietin and carbamylated erythropoietin can be suggested on sensory neurons and/or peripheral nerves through the direct binding to the erythropoietin receptor, which is widely expressed in the peripheral nervous system and overexpressed after nerve injury (16, 17). Carbamylated erythropoietin does not bind to the classic erythropoietin receptors expressed by bone marrow (30). This

affinity for the neural-type erythropoietin receptor shared by erythropoietin and carbamylated erythropoietin suggests that high circulating levels of erythropoietin or carbamylated erythropoietin might have an effect on damage prevention and/or repair. We already reported that erythropoietin reduced the severity of experimental diabetic neuropathy in two different experimental paradigms (22), thus raising the possibility that it has a "nonspecific" neuroprotective effect against different types of injury of the peripheral nervous system as shown recently *in vitro* (17).

The major point of concern in proposing of erythropoietin for neuroprotection in clinical practice is the risk of a marked increase in hematocrit with long-term treatment as observed in our experiment. However, short-term administration of erythropoietin as a neuroprotectant in clinical trials of stroke has not resulted in elevated hematocrit (42) and the optimal schedule (dose and timing) of erythropoietin treatment for the prevention of CIPN still needs to be defined. Recent data suggest that erythropoietin in combination with other growth factors (and possibly with other neuroprotectants) may synergistically activate neuroprotective pathways that allow a lower dose of erythropoietin to be used (43).

A different approach to minimize the erythropoietic effect of erythropoietin is modification of the molecule as has been done with carbamylated erythropoietin. Extensive studies of the relationship between the structure and the activity of the erythropoietin molecule identified regions and amino acids essential for its binding receptor (44) and found that several chemical modifications abolish the hematopoietic bioactivity (45, 46). Previous studies and our results are encouraging because carbamylated erythropoietin maintained its neuroprotective effect without changing the hematocrit (30). These findings open up the possibility of distinguishing between the tissue-protective action of erythropoietin and its potentially detrimental effects (e.g., endothelial activation and platelet reactivity, prothrombotic effects, and excessive erythropoiesis with chronic dosing; refs. 47, 48).

When considering the differences between erythropoietin and carbamylated erythropoietin, it is important to note that these two molecules have very similar pharmacokinetic variables and plasma half-life in particular (30), in contrast to asialo-erythropoietin that has a very short half-life (21). We have shown that, whereas erythropoietin bind the classic homodimeric erythropoietin receptor, carbamylated erythropoietin does not (30), but both molecules require the presence of the β common subunit shared by the granulocyte-macrophage colony-stimulating factor and the interleukin-3 and interleukin-5 receptors, as knockout mice deficient in this transducer do not show protective effects of either carbamylated erythropoietin or erythropoietin (49).

In conclusion, these results we obtained in a model of CIPN that reproduces the clinical features of the effects of CDDP in humans widen the spectrum of possible use of erythropoietin and carbamylated erythropoietin as neuroprotectant drugs, strongly supporting their effectiveness. However, they also indicate the need for further preclinical studies to optimize their effectiveness, to determine the exact mechanism and site of action, and to clarify the issues of long-term tolerability and safety *in vivo*, with the final aim of identifying the best strategy for clinical application.

References

- Quasthoff S, Hartung HP. Chemotherapy-induced peripheral neuropathy. *J Neurol* 2002;249:9–17.
- Connelly E, Markman M, Kennedy A, et al. Paclitaxel delivered as a 3-hr infusion with cisplatin in patients with gynecologic cancers: unexpected incidence of neurotoxicity. *Gynecol Oncol* 1996;62:166–8.
- Rose PG, Blessing JA, Gershenson DM, McGehee R. Paclitaxel and cisplatin as first-line therapy in recurrent or advanced squamous cell carcinoma of the cervix: a Gynecologic Oncology Group study. *J Clin Oncol* 1999;17:2676–80.
- Barajon I, Bersani M, Quartu M, et al. Neuropeptides and morphological changes in cisplatin-induced dorsal root ganglion neuropathy. *Exp Neurol* 1996;138:93–104.
- Cavaletti G, Tredici G, Mamiroti P, et al. Morphometric study of the sensory neuron and peripheral nerve changes induced by chronic cisplatin (DDP) administration in rats. *Acta Neuropathol (Berl)* 1992;84:364–71.
- Cavaletti G, Minoia C, Schieppati M, Tredici G. Protective effects of glutathione on cisplatin neurotoxicity in rats. *Int J Radiat Oncol Biol Phys* 1994;29:771–6.
- Cavaletti G, Tredici G, Mamiroti P, et al. Off-treatment course of cisplatin-induced dorsal root ganglia neuropathy in rats. *In vivo* 1994;8:313–6.
- Tredici G, Cavaletti G, Petruccioli MG, et al. Low-dose glutathione administration in the prevention of cisplatin-induced peripheral neuropathy in rats. *Neurotoxicology* 1994;15:701–4.
- Tredici G, Tredici S, Fabbria D, et al. Experimental cisplatin neuropathy in rats and the effect of retinoic acid administration. *J Neurooncol* 1998;36:31–40.
- Tredici G, Braga M, Nicolini G, et al. Effect of recombinant human nerve growth factor on cisplatin neurotoxicity in rats. *Exp Neurol* 1999;159:551–8.
- Meijer C, DeVries EG, Mamiroti P, et al. Cisplatin-induced DNA-platination in experimental dorsal root ganglia neuropathy. *Neurotoxicology* 1999;20:883–7.
- Pisano C, Pratesi G, Laccabue D, et al. Paclitaxel and Cisplatin-induced neurotoxicity: a protective role of acetyl-L-carnitine. *Clin Cancer Res* 2003;9:5756–67.
- Hausheer F, Cavaletti G, Tredici G, et al. Oral and intravenous BNP7787 protects against platinum neurotoxicity without *in vitro* and *in vivo* tumor protection. Proceedings of the 90th AACR Meeting: Philadelphia, PA; 1999. pp. 398.
- Cavaletti G, Mamiroti P. Chemotherapy-induced peripheral neurotoxicity. *Expert Opin Drug Saf* 2004;3:535–46.
- Campana WM, Myers RR. Erythropoietin and erythropoietin receptors in the peripheral nervous system: changes after nerve injury. *FASEB J* 2001;15:1804–6.
- Campana WM, Myers RR. Exogenous erythropoietin protects against dorsal root ganglion apoptosis and pain following peripheral nerve injury. *Eur J Neurosci* 2003;18:1497–506.
- Keswani SC, Buldanlioglu U, Fischer A, et al. A novel endogenous erythropoietin mediated pathway prevents axonal degeneration. *Ann Neurol* 2004;56:815–26.
- Digicaylioglu M, Lipton SA. Erythropoietin-mediated neuroprotection involves cross-talk between Jak2 and NF- κ B signalling cascades. *Nature* 2001;412:641–7.
- Siran AL, Fratelli M, Brines M, et al. Erythropoietin prevents neuronal apoptosis after cerebral ischemia and metabolic stress. *Proc Natl Acad Sci U S A* 2001;98:4044–9.
- Brines ML, Ghezzi P, Keenan S, et al. Erythropoietin crosses the blood-brain barrier to protect against experimental brain injury. *Proc Natl Acad Sci U S A* 2000;97:10526–31.
- Erbayraktar S, Grasso G, Sfacteria A, et al. Asialoerythropoietin is a nonerythropoietic cytokine with broad neuroprotective activity *in vivo*. *Proc Natl Acad Sci U S A* 2003;100:6741–6.
- Bianchi R, Buyukakilli B, Brines M. Erythropoietin both protects from and reverses experimental diabetic neuropathy. *Proc Natl Acad Sci U S A* 2004;101:823–8.
- Orhan B, Yalcin S, Nurlu G, et al. Erythropoietin against cisplatin-induced peripheral neurotoxicity in rats. *Med Oncol* 2004;21:197–203.
- Natali A, Toschi E, Baldeweg S. Haematocrit, type 2 diabetes, and endothelium-dependent vasodilatation of resistance vessels. *Eur Heart J* 2005;26:464–71.
- Quaschnig T, Ruschitzka F, Stallmach T, et al. Erythropoietin-induced excessive erythrocytosis activates the tissue endothelin system in mice. *FASEB J* 2003;17:259–61.
- Ruschitzka FT, Wenger RH, Stallmach T, et al. Nitric oxide prevents cardiovascular disease and determines survival in polyglobulic mice overexpressing erythropoietin. *Proc Natl Acad Sci U S A* 2000;97:11609–13.
- Lim VS. Recombinant human erythropoietin in predialysis patients. *Am J Kidney Dis* 1991;18:34–7.
- Varet B, Casadevall N, Lacombe C, Naveaux P. Erythropoietin: physiology and clinical experience. *Semin Hematol* 1990;27:25–31.
- Bokemeyer C, Aapro MS, Courdi A, et al. EORTC guidelines for the use of erythropoietic proteins in anaemic patients with cancer. *Eur J Cancer* 2004;40:2201–16.
- Leist M, Ghezzi P, Grasso G, et al. Derivatives of erythropoietin that are tissue protective but not erythropoietic. *Science* 2004;305:239–42.
- Cavaletti G, Braga M, Dondè E, et al. Effect of recombinant human NGF or GDNF on cisplatin neurotoxicity in rats. *Ital J Anat Embryol* 1999;104:85.
- Cascinu S, Cordella L, Del Ferro E, et al. Neuroprotective effect of reduced glutathione on cisplatin-based chemotherapy in advanced gastric cancer: a randomized double-blind placebo-controlled trial. *J Clin Oncol* 1995;13:26–32.
- Lauria G, Lombardi R, Borgna M, et al. Intraepidermal nerve fiber density in rat foodpad: neuropathologic-neurophysiologic correlation. *J Peripher Nerv Syst* 2005;10:199–205.
- Apfel SC, Arezzo JC, Lipson L, Kessler JA. Nerve growth factor prevents experimental cisplatin neuropathy. *Ann Neurol* 1992;31:76–80.
- Apfel SC, Lipton RB, Arezzo JC, Kessler JA. Nerve growth factor prevents toxic neuropathy in mice. *Ann Neurol* 1991;29:87–90.
- Wang MS, Davis AA, Culver DG, et al. Calpain inhibition protects against Taxol-induced sensory neuropathy. *Brain* 2004;127:671–9.
- McArthur JC, Stocks EA, Hauer P, et al. Epidermal nerve fiber density: normative reference range and diagnostic efficiency. *Arch Neurol* 1998;55:1513–20.
- Lauria G, McArthur JC, Hauer PE, et al. Neuropathological alterations in diabetic truncal neuropathy: evaluation by skin biopsy. *J Neurol Neurosurg Psychiatry* 1998;65:762–6.
- Polydefkis M, Hauer P, Sheth S, et al. The time course of epidermal nerve fibre regeneration: studies in normal controls and in people with diabetes, with and without neuropathy. *Brain* 2004;127:1606–15.
- Buemi M, Cavallaro E, Flocari F, et al. The pleiotropic effects of erythropoietin in the central nervous system. *J Neuropathol Exp Neurol* 2003;62:228–36.
- Sigounas G, Sallah S, Sigounas VY. Erythropoietin modulates the anticancer activity of chemotherapeutic drugs in a murine lung cancer model. *Cancer Lett* 2004;214:171–9.
- Ehrenreich H, Hasselblatt M, Dembowski C, et al. Erythropoietin therapy for acute stroke is both safe and beneficial. *Mol Med* 2002;8:495–505.
- Digicaylioglu M, Garden G, Timberlake S, et al. Acute neuroprotective synergy of erythropoietin and insulin-like growth factor I. *Proc Natl Acad Sci U S A* 2004;101:9855–60.
- Grodberg J, Davis KL, Sykowski AJ. Alanine scanning mutagenesis of human erythropoietin identifies four amino acids which are critical for biological activity. *Eur J Biochem* 1993;218:597–601.
- Mun KC, Golper TA. Impaired biological activity of erythropoietin by cyanate carbamylation. *Blood Purif* 2000;18:13–7.
- Satake R, Kozutsumi H, Takeuchi M, Asano K. Chemical modification of erythropoietin: an increase in *in vitro* activity by guanidination. *Biochim Biophys Acta* 1990;1038:125–9.
- Raine AE. Hypertension, blood viscosity, and cardiovascular morbidity in renal failure: implications of erythropoietin therapy. *Lancet* 1988;1:97–100.
- Stohlman PJ, Dzirlo L, Hergovich N, et al. Effects of erythropoietin on platelet reactivity and thrombopoiesis in humans. *Blood* 2000;95:2983–9.
- Brines M, Grasso G, Fiordaliso F, et al. Erythropoietin mediates tissue protection through an erythropoietin and common β -subunit heteroreceptor. *Proc Natl Acad Sci U S A* 2004;101:14907–12.

Chemical Reagents for Protein Modification

2nd Edition

Author

Roger L. Lundblad, Ph.D.
Professor of Pathology and Biochemistry
Dental Research Center
University of North Carolina
Chapel Hill, North Carolina



CRC Press

Boca Raton Ann Arbor Boston London

Property Of

Becton Dickinson
Research Center

...
e
n
e
e
c

f
l
s
f
l
e
s

i

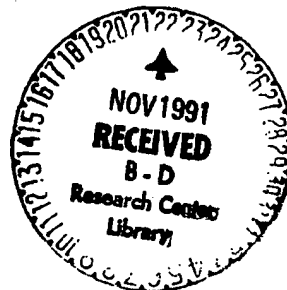
i

QU
55
L9:2c
1991

Ab
rel
co
mc
res
mi

mi
So
at
thi
su
au
M

Di



Library of Congress Cataloging-in-Publication Data

Lundblad, Roger L.

Chemical reagents for protein modification / author, Roger L.

Lundblad. -- 2nd ed.

p. cm.

Includes bibliographical references and index.

ISBN 0-8493-5097-2

1. Proteins--Chemical modification. 2. Chemical tests and reagents. I. Title.

[DNLM: 1. Indicators and Reagents. 2. Proteins--analysis. QU 55 L962c]

QP551.L88 1991

574.19'245--dc20

DNLM/DLC

for Library of Congress

91-19423
CIP

This book represents information obtained from authentic and highly regarded sources. Reprinted material is quoted with permission, and sources are indicated. A wide variety of references are listed. Every reasonable effort has been made to give reliable data and information, but the author and the publisher cannot assume responsibility for the validity of all materials or for the consequences of their use.

All rights reserved. This book, or any parts thereof, may not be reproduced in any form without written consent from the publisher.

Direct all inquiries to CRC Press, Inc., 2000 Corporate Blvd., N.W., Boca Raton, Florida 33431.

© 1991 by CRC Press, Inc.

International Standard Book Number 0-8493-5097-2

Library of Congress Card Number 91-19423

Printed in the United States of America 1 2 3 4 5 6 7 8 9 0

TABLE OF CONTENTS

Chapter 1	
Site-Specific Chemical Modification of Proteins	1
Chapter 2	
Amino Acid Analysis	21
Chapter 3	
Peptide Separation by Reverse-Phase High-Performance Liquid Chromatography	29
Chapter 4	
Methods for Sequence Determination	37
Chapter 5	
Chemical Cleavage of Peptide Bonds	49
Chapter 6	
The Modification of Cysteine	59
Chapter 7	
The Modification of Cysteine — Cleavage of Disulfide Bonds	95
Chapter 8	
The Modification of Methionine	99
Chapter 9	
The Modification of Histidine Residues	105
Chapter 10	
The Modification of Lysine	129
Chapter 11	
The Modification of Arginine	173
Chapter 12	
Chemical Modification of Tryptophan	215
Chapter 13	
The Modification of Tyrosine	239
Chapter 14	
The Modification of Carboxyl Groups	267
Chapter 15	
The Chemical Cross-Linking of Peptide Chains	287
Chapter 16	
Affinity Labeling	305
Index	337

THE MODIFICATION OF CYSTEINE

The sulfhydryl group of cysteine (Figure 1) is potentially the most reactive functional group in a protein. Cysteinyl residues are easily alkylated, acylated, arylated, and oxidized. The reactivity of cysteine is, as with most other functional groups in proteins, a reflection of the nucleophilic nature of the thiol groups. It is impossible to thoroughly discuss the reactions of protein sulfhydryl groups. The reader is directed to the excellent review by Liu¹ on the properties and reactions of sulfhydryl groups for a more extensive discussion of the chemistry of sulfur in proteins. In addition Kenyon and Bruice² review a collection of thiol reagents.

Cysteine is relatively sensitive to oxidation but there is little selectivity in these reactions. Mild oxidizing conditions can result in the formation of disulfide bonds with appropriately aligned cysteinyl residues. Formation of sulfenic acid is generally readily reversible unless stabilized by local conditions³ and more highly oxidized forms such as cysteine-sulfonic acid are more frequently observed. More rigorous conditions such as treatment with performic acid result in the formation of cysteic acid.

Modification of cysteine with sodium tetrathionate (Figure 2)⁴ is similar to oxidation. This reaction has the advantage of ready reversibility by mild reducing agents. Reaction with sodium tetrathionate has been used to study cysteine in chalcone isomerase.⁵ The native enzyme was only slowly inactivated by sodium tetrathionate (pH 5.2 [50 mM MES], $k^2 < 0.005 \text{ M}^{-1} \text{ min}^{-1}$; pH 7.5 [50 mM HEPES], $k^2 = 0.009 \text{ M}^{-1} \text{ min}^{-1}$; pH 9.4 [50 mM CHES], $k^2 = 0.093 \text{ M}^{-1} \text{ min}^{-1}$). In the presence of 6.0 M urea, the enzyme was rapidly inactivated (pH 7.5, $k^2 > 690 \text{ M}^{-1} \text{ min}^{-1}$).

Methyl methanethiosulfonate was introduced by Smith et al.⁶ as reagent for the reversible reaction of sulfhydryl groups (Figure 3). This concept was extended by Bruice and Kenyon as a mechanism for introducing novel substituents⁷ (see Figure 4) into proteins via modification of cysteine sulfhydryl groups. These reagents have subsequently been used for the modification of site-specific mutants of carboxypeptidase Y.⁸

Cysteine is far more reactive as the thiolate anion. The pKa for the formation of the thiolate anion is 10.5 with free cysteine but is considerably reduced with the cysteinyl residue in peptide bond. For example, the pKa for the formation of the thiolate anion *N*-acetylcysteine ethyl ester is 8.5 while with *N*-formyl cysteine, it is 9.5. It is useful to compare these values with pKa values for other functional groups as is done in Table 1.

Haloacetates, the corresponding amides and derivatives have been extremely useful reagents for the specific modification of cysteinyl residues. These reagents react with cysteine via a S_N2 reaction mechanism to give the corresponding carboxymethyl or carboxamidomethyl derivatives (see Figure 5). When a rapid reaction is desired, the iodine-containing compounds are used. For example, the reaction of iodoacetate with cysteine is approximately twice as fast as the reaction of bromoacetate and 20 to 100 times as rapid as chloroacetate. There are situations in which fast reaction rates are not necessarily desirable, such as the studies of Gerwin on streptococcal proteinase.⁹ This particular study was of considerable importance since it emphasized the importance of microenvironmental effects on the reaction of cysteine with α -halo acids and α -halo amides. Chloroacetic acid was far less effective than chloroacetamide. The sulfhydryl group at the active site of streptococcal proteinase has enhanced reactivity in that modification with iodoacetate readily occurred in the presence of 100- to 1000-fold excess of β -mercaptoethanol or cysteine. The enhanced reactivity of the active-site cysteine is also apparent from a comparison of the relative rates of modification of streptococcal proteinase and reduced glutathione. The rate of modification of streptococcal proteinase is 50 to 100 times more rapid than that of glutathione. The unique properties of

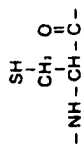


FIGURE 1. The chemical structure of covalently bound cysteine.

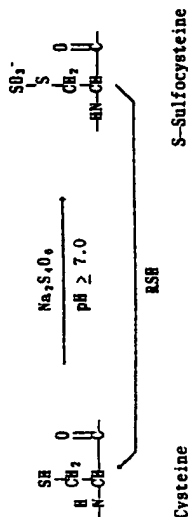


FIGURE 2. Conversion of cysteine to S-sulfocysteine by reaction with sodium tetrathionate and reversal by exogenous thiols.

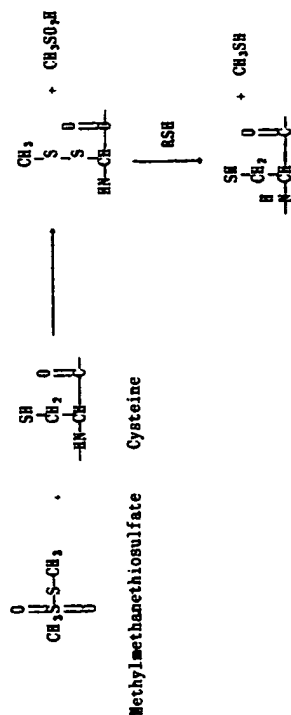


FIGURE 3. The reaction of methyl methanethiosulfate with cysteine and reversal with exogenous thiols.

this cysteine residue can be explained in part by the presence of an adjacent histidyl residue which was demonstrated by an elegant series of studies by Liu.¹⁰ Although histidine residues will react with α -halo acids and amides, the presence of an adjacent cysteine residue precluded the use of this class of reagents to demonstrate the presence of a histidyl residue at the active site of streptococcal proteinase. Liu took advantage of the reversible modification of cysteinyl residues with sodium tetrathionate to modify the active-site histidine.

The reaction of chloroacetic acid and chloroacetamide with papain has also yielded interesting results.^{11,12} In studies with chloroacetamide, the active-site sulphydryl group of papain reacts at a rate more than tenfold faster than free cysteine ($5.78 \text{ M}^{-1} \text{ s}^{-1}$ vs. $0.429 \text{ M}^{-1} \text{ s}^{-1}$).¹¹ As was the situation with streptococcal proteinase, there are dramatic differences in the rate of reaction of papain with chloroacetic acid and chloroacetamide. The reaction with chloroacetic acid has a pH optimum of approximately 7 while the optimum for reaction with chloroacetamide is at a pH greater than 9. A comparison of the effect of pH on the reaction of papain with chloroacetic acid and chloroacetamide is shown in Figure 6. This investigation

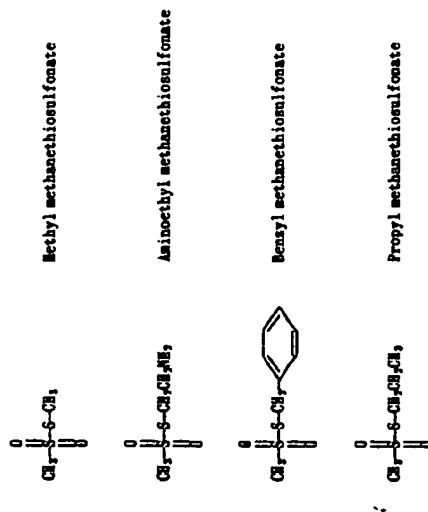


FIGURE 4. Structures of selected alkyl and aryl methanethiosulfonates.

Table 1
ACID DISSOCIATION VALUES FOR
FUNCTIONAL GROUPS IN
PROTEINS

Functional Group	pKa
Carboxyl (Asp, Glu)	4.6
Imidazole (His)	7.0
Alpha-amino	7.8
Sulphydryl (Cys)	8.5
Phenolic hydroxyl (Tyr)	9.6
Side-chain amino (Lys)	10.5

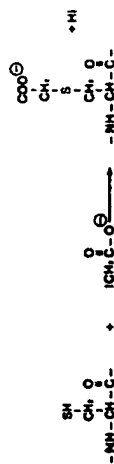


FIGURE 5. The modification of cysteine with iodoacetic acid to form S-carboxymethylcysteine.

notes the influence of the neighboring histidyl residue as has been discussed for streptococcal proteinase. These data further emphasize the importance of neighboring functional group effects on cysteinyl reactivity in proteins as well as the importance of rigorous evaluation of the effect of pH on the rate of the modification reaction.

The α -halo acids decompose in water, with the rate being far more rapid at alkaline pH. In the case of iodoacetic acid, the products are iodide and glycolic acid. We recrystallize the commercially obtained reagents and store over P_2O_5 . The compounds are readily soluble

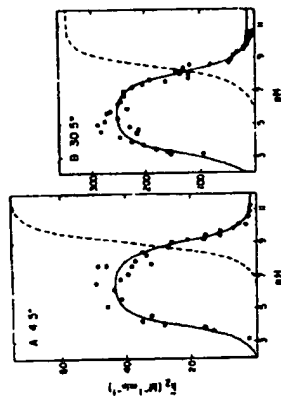


FIGURE 6. The effect of pH on the second-order rate constant for the inactivation of papain by chloroacetic acid at low ionic strength (0.07). The broken lines are the theoretical curves for the reaction of papain with chloroacetamide under the same reaction conditions. (From Chalken, I. M. and Smith, E. L., *J. Biol. Chem.*, 244, 5093, 1969. With permission.)

in water. In the case of the free acid, it is useful to dissolve the compound in base prior to addition to the reaction mixture. In the case of α -haloacetyl derivatives, the resultant S-carboxymethylcysteine is easily quantitated by amino acid analysis.

Jörnvall and co-workers¹¹ have used reaction with iodoacetate to probe differences in structure in wild-type β -galactosidase and various mutant forms of the enzyme. The modification reactions were performed in 0.1 M Tris, pH 8.1 under nitrogen in the dark. (This condition is of considerable importance since the α -halo acids are photolabile.) The reaction was terminated by the addition of excess β -mercaptoethanol. Kalimi and Love¹² have examined the reaction of the hepatic glucocorticoid-receptor with iodoacetamide in 0.010 M Tris, 0.25 M sucrose. Again, this reaction was performed in the dark. Kalis and Holmgren¹³ have examined the differences in reactivity of two sulphydryl groups present at the active site of thioredoxin. The pH dependence of the reaction with iodoacetate suggested that one group had a pKa value of 6.7 while the second was 9.0. Iodoacetamide showed the same pH dependence but the rate of reaction was approximately 20-fold greater than with iodoacetate. For example, at pH 7.2, the second-order rate constant for reaction with iodoacetate was $5.2 \text{ M}^{-1} \text{ s}^{-1}$ while it was $107.8 \text{ M}^{-1} \text{ s}^{-1}$ for iodoacetamide. The results from this study are shown in Figure 7. The low pK of one of the sulphydryl groups was suggested to be a reflection of the presence of an adjacent lysine residue. Mikami and co-workers have examined the inactivation of soybean β -amylase with iodoacetamide and iodoacetate.¹⁶ Inactivation with iodoacetamide occurred approximately 60 times more rapidly than with iodoacetate at pH 8.6. Hempel and Pietruszko¹⁷ have shown that human liver alcohol dehydrogenase is inactivated by iodoacetamide but not by iodoacetic acid. These experiments were performed in 0.030 M sodium phosphate, pH 7.0 containing 0.001 M EDTA.

The reaction of sulphydryl groups with iodoacetate¹⁸ is still extensively used in the preparation of proteins for primary structure analysis, although pyridylethylation^{19,20} is proving to be quite useful (Figure 8).

Dahl and McKinley-McKee²¹ have made a rather detailed study of the reaction of alkyl halides with thiols. It is emphasized that reactivity of alkyl halides not only depends on the halogen but also on the nature of the alkyl groups. These investigators emphasized that the reactivity of an alkyl halide such as iodoacetate depends not only on the leaving potential of the halide substituent ($\text{I} > \text{Br} > \text{Cl}$; 130:90:1) but also on the nature of the alkyl group. The rate of reaction of 2-bromoethanol with the sulphydryl group of L-cysteine (pH 9.0)

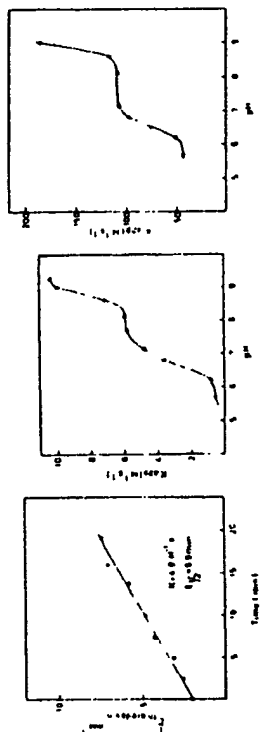


FIGURE 7. The left figure shows a time course for the reaction of thioredoxin and iodoacetic acid at pH 7.2. Analysis of this data yields a single second-order rate constant of $4.8 \text{ M}^{-1} \text{ s}^{-1}$ and a half-life of 6.9 min. The center figure shows the effect of pH on the second-order rate constant for the reaction between iodoacetic acid and thioredoxin. The figure on the right shows the effect of pH on the second-order rate constant for the reaction between iodoacetamide and thioredoxin. (From Kallia, G.-B. and Holmgren, A., *J. Biol. Chem.*, 255, 10261, 1980. With permission.)

ANALYSIS OF DISULFIDE BONDS

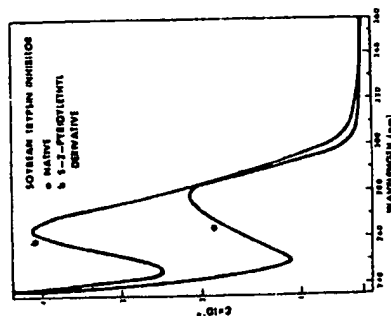


FIGURE 8. The UV absorption spectra of soybean trypsin inhibitor and the 5-pyridylethythyl derivative of soybean trypsin inhibitor at a concentration of 0.5 mg/ml (23 μM) at pH 3.0 in 0.05 M glycine-HCl. (From Friedman, M., Knoll, R. H., and Cavins, J. F., *J. Biol. Chem.*, 245, 3668, 1970. With permission.)

is approximately 1000 times less than that observed with bromoacetic acid. The reactions are extremely pH dependent, emphasizing the importance of the thiolate anion in the reaction.

While haloacetates and haloacetamides continue to be useful,^{22,27} there has been far greater interest in the use of this chemistry as a mechanism for introducing a larger molecule which can serve as structural probe. Examples include 5-iodoacetamido-fluorescein²⁸ (Figure 9), 5-[2-((iodoacetyl)amino)ethyl]naphthalene-1-sulfonic acid (1,5-IAEDANS)^{29,32} (Figure 10) and 4-(2-iodoacetamido)-TEMPO³³ (Figure 11). Iodoacetate has also been used for introducing a biotin probe (Figure 12) in proteins.²³

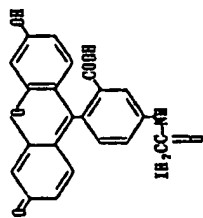


FIGURE 9. Structure of 5-iodoacetamidofluorescein.

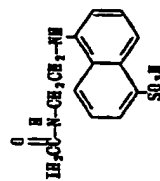


FIGURE 10. Structure of 5-[2-(iodoacetyl)aminoethyl]aminonaphthalene-1-sulfonic acid (1,5-IAE-DANS).

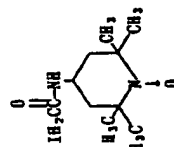


FIGURE 11. Structure of iodoacetamido-TEMPO.

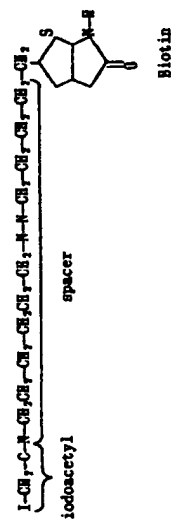
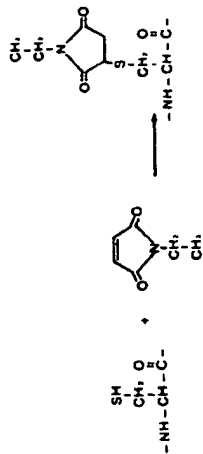
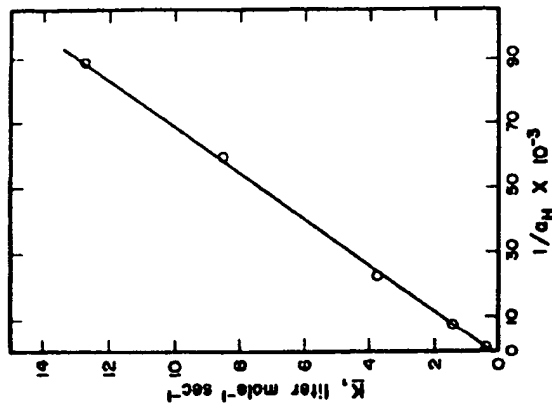


FIGURE 12. Iodoacetyl derivative of biotin for coupling with protein sulphydryl groups.

FIGURE 13. The reaction of *N*-ethylmaleimide with cysteine.FIGURE 14. The pH dependence of the reaction of *N*-ethylmaleimide with cysteine. (From Gorin, G., Martic, P. A., and Dougherty, G., *Arch. Biochem. Biophys.*, 115, 593, 1966. With permission.)

N-Ethylmaleimide reacts with sulphydryl groups (Figure 13) in proteins with considerable specificity.^{33,35} The effect of pH on the reaction of free cysteine and *N*-ethylmaleimide is shown in Figure 14. These determinations were performed in the pH range of 3 to 5 and these investigators estimated that a rate constant of $1.53 \times 10^3 \text{ M}^{-1} \text{ s}^{-1}$ would be obtained at pH 7.0. This reaction can be followed spectrophotometrically by the decrease in absorbance at 300 nm, the absorbance maximum of *N*-ethylmaleimide. The extinction coefficient of *N*-ethylmaleimide is $620 \text{ M}^{-1} \text{ cm}^{-1}$ at 302 nm.³³ This reaction product yields *S*-succinyl cysteine on acid hydrolysis. Although the reagent is reasonably specific for cysteine, reaction with other nucleophiles must be considered.³⁶ The use of reaction with *N*-ethylmaleimide in the identification of selenocysteine has been proposed.³⁷ A "diagonal" procedure for the

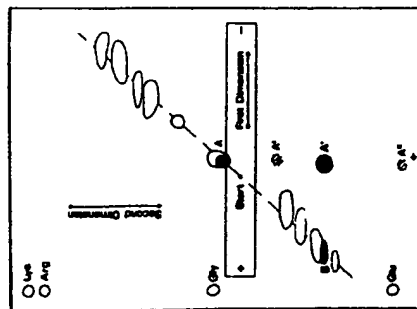


FIGURE 15. A "diagonal" method for the identification of cysteine peptides. A mixture of chymotryptic peptides containing a peptide with a cysteinyl residue alkylated with radiolabeled *N*-ethylmaleimide was subjected to diagonal electrophoresis with intervening exposure to ammonia for 5.5 h at 35°C. The treatment with ammonia results in the hydrolysis of the *N*-ethylsuccinimide to *N*-ethylsuccinic acid thus generating a new negative charge permitting the resolution of the labeled peptides from the unlabeled peptides during the second electrophoresis. (From Gehring, H., and Christen, P., *Anal. Biochem.*, 107, 358, 1980. With permission.)

isolation of cysteine-containing peptides modified with *N*-ethylmaleimide has been reported (Figure 15).³⁸ This procedure is based on the hydrolysis of the reaction product of cysteine and *N*-ethylmaleimide to cysteine-*S*-*N*-ethyl succinamic acid generating a new negative charge.

There has been a considerable amount of interest recently in maleimide derivatives. For example, various derivatives of maleimide provide the basis for the design of cross-linking reagents (see Chapter 15). Brown and Matthews^{39,40} have studied the reaction of lactose repressor protein with *N*-ethylmaleimide, two spin-label derivatives of *N*-ethylmaleimides and a fluorophore derivative. The investigators demonstrated that three sulfhydryl residues present in *Escherichia coli* lactose repressor protein monomer had distinctly different reaction characteristics. These data are presented in Figure 16. (The modification reactions were performed in 0.24 M potassium phosphate, pH 7.0 containing 5% (v/v) glycerol under nitrogen for 1 to 4 h.) The extent of reaction was determined by the reaction of the remaining free sulfhydryl groups with 2-chloromercuri-4-nitrophenol.^{41,42} Modification at a specific cysteinyl residue was determined by reaction of the modified protein with 2-bromoacetamido-4-nitrophenol and quantitation of the three 5-(2-acetamido-4-nitrophenol)-cysteine-containing peptides following enzymatic digestion of the modified protein and gel filtration on G-50 Sephadex (0.1 M NH₄HCO₃ containing 2% (w/v) sodium dodecyl sulfate). The spin-labeled compounds showed the same pattern of reaction with the three cysteinyl residues as seen with *N*-ethylmaleimide. The fluorophore-derivative (*N*-(3-pyrene)maleimide) shows a slightly different reaction pattern. As is the situation for the α -halo acetyl derivatives, there has only been limited use of *N*-ethylmaleimide^{39,43-46} during the past six years. However, the chemistry associated with the modification of sulfhydryl groups with *N*-alkylmaleimides

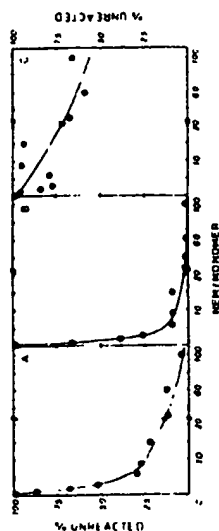


FIGURE 16. The reaction of lactose repressor protein with *N*-ethylmaleimide at specific cysteine residues as a function of *N*-ethylmaleimide concentration. Panel A shows reaction at cysteine-107, panel B shows reaction at cysteine-140, while panel C shows reaction at cysteine-281. (From Brown, R. D. and Matthews, K. S., *J. Biol. Chem.*, 254, 5128, 1979. With permission.)

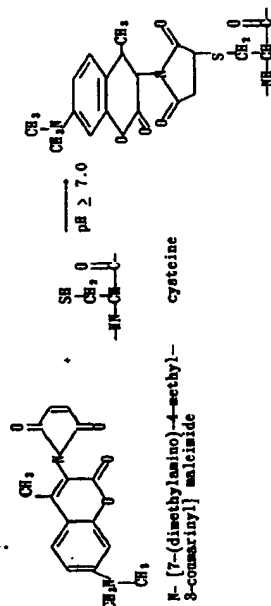


FIGURE 17. Modification of a cysteinyl residue with a maleimido-fluorescent probe.

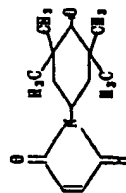


FIGURE 18. The structure of 4-maleimide-2,2,6,6-tetramethyl-1-piperidinyloxy, a spin-label maleimide derivative.

has proved useful for introducing structural probes into proteins (Figure 17). Such probes include 4-maleimide-2,2,6,6-tetramethylpiperidine-1-oxyl⁴⁷ (Figure 18), maleimidoethanemethylrhodamine,⁴⁸ *N*-(1-pyrenyl) maleimide⁴⁹ (Figure 19), 2-(4-maleimidoamino) naphthalene-6-sulfonic acid,⁵⁰ 2,5-dimethoxy-4-sulbenzylmaleimide,⁵¹ rhodamine maleimide,⁵² and eosin-5-maleimide.⁵³ Le-Quoc and colleagues have examined the effect of the nature of the *N*-substituent groups on the rate of sulfhydryl group modification in succinate dehydrogenase.⁵⁴ The derivatives used were *N*-ethylmaleimide, *N*-butylmaleimide, and *N*-benzylmaleimide. The most reactive thiol groups in succinate dehydrogenase are probably located in an apolar environment since the benzyl derivative reacted twice as fast as the

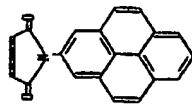


FIGURE 19. The structure of *N*-(1-pyrenyl)maleimide, a hydrophobic fluorescent maleimide-based structural probe.

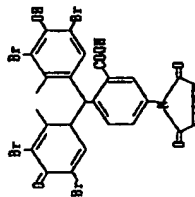


FIGURE 20. The structure of covalin-5-maleimide.

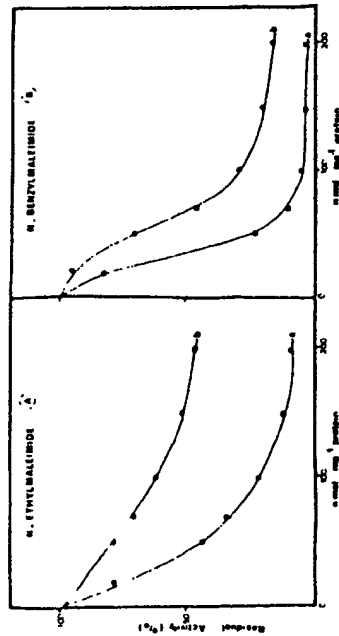


FIGURE 21. The inactivation of succinate dehydrogenase with *N*-ethylmaleimide (panel A) or *N*-benzylmaleimide (panel B) as a function of reagent concentration. Reaction a was performed with enzyme preparations preincubated with 50 mM succinate, 3 mM thienylfluoracetone and 10 μ g rotenone. Reaction b was performed with no additions other than the maleimide derivatives, in 0.05 M sodium phosphate, pH 7.6. (From Le-Quoc, K., Le-Quoc, D., and Guademe, Y., *Biochemistry*, 20, 1705, 1981. With permission.)

ethyl derivative, as shown in Figure 21 (these modification reactions were performed in 0.050 M sodium phosphate, pH 7.6, at 37°C).

A recent study has explored hydrophobic derivatives of *N*-ethylmaleimide (Figure 22) as probes of the environment surrounding a sulfhydryl group in membrane anion channels.⁵² Reaction with *N*-ethylmaleimide, *N*-benzylmaleimide, and *N,N'*-1,2-phenylenedimaleimide

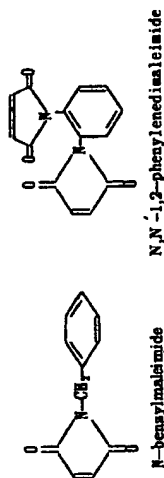


FIGURE 22. The structures of some hydrophobic *N*-alkylmaleimide derivatives, *N*-benzylmaleimide and *N,N'*-1,2-diphenylenedimaleimide.

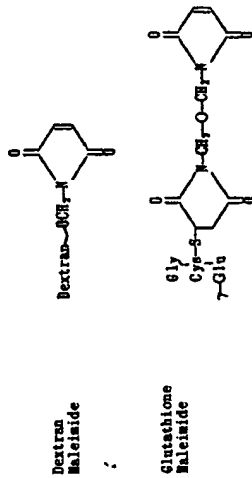


FIGURE 23. Some membrane-impermeant *N*-alkylmaleimide derivatives (from Reference 58).

was evaluated and the reaction rate increased with increasing hydrophobicity. *N*-Phenylmaleimide has been used for the modification of a sulfhydryl group in the acetylcholine receptor.^{53,54} Detergent was required for the modification reaction (10 mM MOPS to 100 mM NaCl to 0.1 mM EDTA with 0.02% sodium azide and 1% cholate). These studies identified cysteine residues potentially important in membrane function. Subsequent studies using site-specific mutagenesis have supported the importance of these cysteinyl residues.⁵⁵

Localization of sulfhydryl groups within membranes has been achieved through the comparison of the reaction with membrane-permeant and membrane-impermeant derivatives (Figure 23).^{44,46,55,57} The use of these reagents can be traced back to the original observations of Abbott and Schacter in 1976.⁵⁸ The basic concept is to provide either a polar derivative or a derivative with steric considerations which preclude passage through or into the membranes (c.f. dextran-maleimide in Figure 23). Maleimide derivatives of glucosamine have been synthesized as affinity labels for the human erythrocyte hexose transport protein.⁵⁹

A particularly novel approach to this problem has been used by Koshland's laboratory to analyze aspartate receptor structure.⁶⁰ In this study, site-specific mutagenesis was used to place cysteinyl residues at six positions in the peptide chain. A new membrane-impermeant reagent (Figure 24) was used to study the reactivity of the individual sulfhydryl residues. From these studies it was possible to "map" the domain structure of the receptor protein. Cysteinyl residues placed in the surface area could be modified by aqueous reagents while transmembrane areas could be excluded by lack of reaction with membrane-impermeant reagents. Finally, spatial proximity of multiple cysteinyl residues could be evaluated by disulfide bond formation.

4,4'-Diisothiocyanostilbene 2,2'-disulfonic acid (Figure 25) has been used to study the importance of specific sulfhydryl groups in anion transport by membrane proteins.^{61,62} Bimanes



FIGURE 24. The structure of *N*-(6-phosphonyl)-4-ethylmaleimide (PHM), a membrane-impermeant *N*-allylmaleimide. (From Falke, J. J., Dermburg, A. F., Stromberg, D. A., Zalkin, N., Milligan, D. L., and Koobland, D. E., Jr., Structure of a bacterial sensory receptor: A site-directed sulphydryl study. *J. Biol. Chem.*, 263, 14,830, 1988. With permission.)

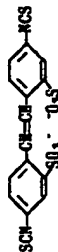


FIGURE 25. The structure of 4,4'-disothiocyanatobenzene-2,2'-disulfonic acid.

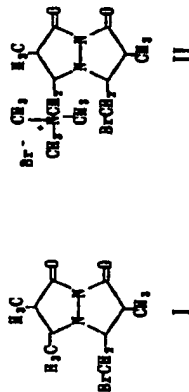


FIGURE 26. Structure of two bismane derivatives which have proved useful in the study of protein sulphydryl groups. (I) Monobromobimane, a relatively hydrophobic derivative; and (II) monobromomethylammonium bismane, a relatively hydrophilic derivative.

have proven to be useful structural probes for proteins. The structures of monobromobimane (I) and monobromomethylammonium bismane (II) are shown in Figure 26. These are two examples of various derivatives available with monobromobimane being considered a non-polar or hydrophobic probe and monobromomethylammonium bismane being considered a polar probe. The reader is directed toward three recent studies on the use of these reagents for the study of sulphydryl group chemistry in proteins.^{22,23,24} Martin et al.²³ have compared the reaction of ATP sulphyrase with various sulphydryl reagents, including bismane derivatives. Hydrophobic reagents were more effective than hydrophilic derivatives (i.e., *N*-phenylmaleimide > *N*-ethylmaleimide; dithionitropyridine > dithionitrobenzoate; monobromobimane > monobromomethylammonium bismane).

The conversion of cysteinyl residues to the *S*-cyanide has also received considerable attention as the modification can be accomplished with a chromogenic reagent such as 2-nitro-5-thiocyanobenzoic acid. Although the formation of the *S*-cyano derivative (Figure 27) is the predominant reaction, Degani and Degani²⁵ have also demonstrated formation of the mixed disulfide with mercaptionitrobenzoate as well. These investigators studied the reaction of rabbit muscle creatine kinase with 2-nitro-5-thiocyanobenzoic acid in 0.02 *M* Tris, pH 7.8 containing 0.25 *mM* EDTA with a 2.5- to 10-fold molar excess of

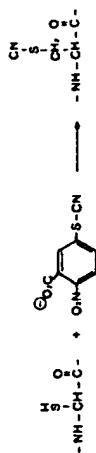


FIGURE 27. The reaction of 2-nitro-5-thiocyanobenzoic acid with sulphydryl groups in proteins.

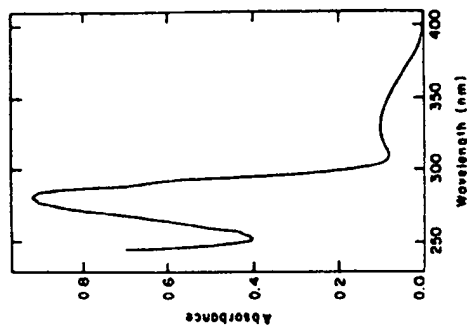


FIGURE 28. The UV absorption spectra of rabbit muscle creatine kinase after modification with 2-nitro-5-thiocyanobenzoic acid (NTCB). The spectra were obtained in 0.02 *M* Tris-acetate, pH 7.0. (From Degani, Y. and Degani, C., *Biochemistry*, 18, 5917, 1979. With permission.)

reagent. The expected reaction was that shown in Figure 27. While reaction of creatine kinase with 5,5'-dithiobis (2-nitrobenzoic acid) resulted in the modification of two sulphydryl groups with greater than 99% loss of activity, reaction with 2-nitro-5-thiocyanobenzoic acid resulted in an equivalent loss of activity with apparent modification only at a single sulphydryl residue as judged by the release of 2-mercapto-5-nitrobenzoic acid. There were not, however, any free sulphydryl groups remaining after the reaction with 2-nitro-5-thiocyanobenzoic acid. Spectral analysis of the modified enzyme (Figure 28) was consistent with the incorporation of 1 mol of reagent per mol of protein ($\epsilon_{280} = 7500$) as would result from the reaction shown in Figure 29. The denatured enzyme showed only the *S*-cyanation reaction. Reaction of the modified protein with cyanate (0.11 *M* potassium cyanate, pH 9.5) resulted in the conversion to the cyanated derivative with the return of 75% of the enzymatic activity of the native enzyme. Reaction of creatine kinase with 5,5'-dithiobis(2-nitrobenzoic acid) resulted in the modification of approximately 2 sulphydryl groups (1.75 to 1.8 mol/mol of enzyme) with an almost complete loss of enzyme activity (greater than 99.5% loss of activity).

The formation of 2-mercapto-5-nitrobenzoic acid, which occurs with the reaction of 2-nitrothiocyanobenzoic acid with thiols to form *S*-cyano derivatives, can be used for the

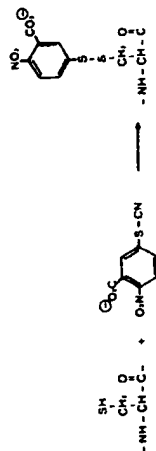


FIGURE 29. The formation of a mixed disulfide between cysteine and 2-nitro-5-thiocyanobenzoic acid.

quantitative determination of sulphydryl groups. 2-Mercapto-5-nitrobenzoic acid has an absorbance maximum at 412 nm with a molar extinction coefficient of $13,600 \text{ M}^{-1} \text{ cm}^{-1}$.⁶⁵ Pecci and co-workers⁶⁶ have characterized the reaction of rhodanese with 2-nitrothiocyanobenzoic acid. These investigators used a 1.3 molar excess of reagent in 0.050 M phosphate buffer, pH 8.0 at 18°C. The reaction was followed spectrophotometrically by the release of 2-mercapto-5-nitrobenzoic acid and was complete after 6 h.

Cleavage at S-cyano-cysteinyl residues was first studied by Vanaman and Stark.⁶⁷ S-Cyanocysteine was first generated from the mixed disulfide of cysteine and 5-thio-2-nitrobenzoic acid by reaction with KCN (0.05 M) at pH 8.2 (0.2 M Tris-acetate with 20 mM EDTA).

Cleavage at S-cyano residues has also been reported by Marshall and Cohen.⁶⁸ In these studies the enzyme was first reacted with 5,5'-dithiobis (2-nitrobenzoic acid) in 0.020 M 4-morpholinopropanesulfonic acid-0.1 M KCl, pH 7.1 for 3 h at 25°C. Conversion to the S-cyano derivative was accomplished by reaction in 0.2 M KCN, pH 8.1. Cleavage was accomplished by incubation at pH 8.0 at 50°C for 24 h. The reaction of 2-nitro-5-thiocyanobenzoic acid with phosphofructokinase has been studied by Ogilvie.⁶⁹ Approximately 1 mol of cysteine is available for modification in the native enzyme with an approximately stoichiometric excess of reagent (1.06 mol 2-nitro-5-thiocyanobenzoic acid per mole enzyme protomer) (Figure 30). The modification with 2-nitro-5-thiocyanobenzoic acid was performed in 0.025 M glycylglycine — 0.025 M sodium phosphate, pH 7.2 (containing 1 mM EDTA, 0.4 mM fructose-6-phosphate, and 0.1 mM ATP) at 24°C. Cleavage at the S-cyanocysteinyl residue is accomplished by incubation of the modified protein in 0.2 M Tris-acetate, pH 8.1 containing 2% sodium dodecyl sulfate at 37°C. Approximately 20% of the total phosphofructokinase was cleaved after 48 h of incubation at 37°C. This would correspond to approximately 40% cleavage of the S-cyanylated protein. Cleavage at S-cyano derivatives of cysteine is covered in detail in Chapter 5.

Kindman and Jencks⁷⁰ have reported interesting observations on the reaction of 2-nitrothiocyanobenzoic acid with succinyl-CoA:3-ketoacid coenzyme A transferase. These investigators conclude that the thiol group which reacts with this reagent to form the S-cyano derivative was not essential to activity. Reaction of the enzyme with 2-nitrothiocyanobenzoic acid was performed in 0.2 M potassium borate, pH 8.1 (Tris buffers as well as other buffers with nucleophilic characteristics should be avoided because of reaction with the reagent). While the reaction to yield the S-cyano derivative had no effect on catalytic activity, the formation of a mixed disulfide with 2-mercapto-5-nitrobenzoic acid via either 5,5'-dithiobis (2-nitrobenzoic acid) or 2-nitrothiocyanobenzoic acid (2-nitro-5-(thiocyanato) benzoic acid) resulted in an inactive enzyme (Figure 31).

One of the most popular reagents for the modification and determination of the sulphydryl group has evolved from the early studies of Ellman^{65,71} on 5,5'-dithiobis(2-nitrobenzoic acid) (Figure 32). Reaction with sulphydryl groups in proteins results in the release of 2-nitro-5-mercaptobenzoic acid (Figure 33), which has a molar extinction coefficient of

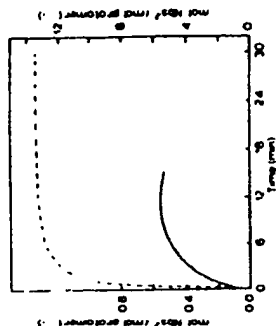


FIGURE 30. The release of 5-mercapto-2-nitrobenzoate dianion (Nbs^{2-}) during the sequential reaction of phosphofructokinase with 2-nitro-5-thiocyanobenzoic acid and 5,5'-dithiobis(2-nitrobenzoic acid) as determined by the increase in absorbance at 412 nm. The solid line (left ordinate) represents the results of the reaction of 2-nitro-5-thiocyanobenzoic acid with phosphofructokinase (1.06 mol/mol protomer) at pH 7.2 resulting in the cyanylation of 0.57 mol/mol of cysteine per mole of protomer. The dashed line (right ordinate) represents the results of the reaction of 5,5'-dithiobis(2-nitrobenzoic acid) (60-fold molar excess with respect to protomer) in 2% sodium dodecyl sulfate (SDS), pH 7.2 with phosphofructokinase containing 0.57 mol of cyanylated cysteine per mole of protomer. (From Ogilvie, J. W., *Biochim. Biophys. Acta*, 622, 277, 1980. With permission.)

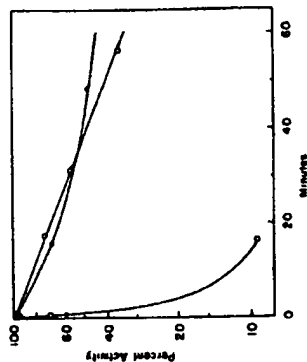


FIGURE 31. 5,5'-dithiobis(2-nitrobenzoic acid) (DTNB) inactivation of succinyl-CoA:3-ketoacid coenzyme A transferase previously modified with 2-nitro-5-(thiocyanato)benzoic acid (NTCB) (Δ). NTCB-modified enzyme separated from reagent by gel filtration (\circ), and NTCB-modified enzyme preincubated with 0.095 M dithiothreitol for 1 h in 0.2 M Tris-sulfate, pH 8.1 prior to gel filtration (\square). (From Kindman, L. A. and Jencks, W. P., *Biochemistry*, 20, 5183, 1981. With permission.)

$13,600 \text{ M}^{-1} \text{ cm}^{-1}$ at 410 nm. Recent examples of the use of this reagent have included studies on *E. coli* citrate synthase⁷² and D-amino acid transaminase⁷³ (0.1 M Tris, 0.002 M EDTA, pH 7.5). The study on the reaction of 5,5'-dithiobis(2-nitrobenzoic acid) with the bacterial citrate synthase is worth considering in greater detail. Figure 34 shows the rate for the reaction of this reagent with citrate synthase. Potassium chloride stimulates the rate

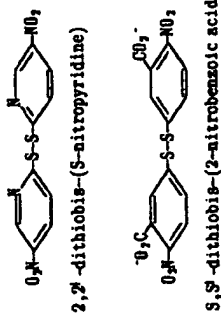


FIGURE 32 The structure of 2,2'-dithiobis(5-nitropyridine) which is relatively hydrophobic compared to 5,5'-dithiobis(2-nitrobenzoic acid).

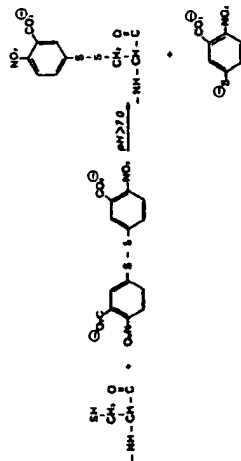


FIGURE 33 The reaction of 5,5'-dithiobis(2-nitrobenzoic acid) with cysteinyl residues in protein.

of reaction apparently by a direct effect on the velocity of the reaction as opposed to a change in the affinity of the protein for the reagent. A maximum increase of 85-fold with KCl is observed in 0.02 M Tris buffer, pH 7.8 (containing 1.0 M EDTA). The effect of salt is not a general effect on the reactivity of sulphydryl groups since 0.1 M KCl decreases the rate of reaction of 5,5'-dithiobis(2-nitrobenzoic acid) with coenzyme A. It is of interest that there is the release of 5-thio-2-nitrobenzoate from the modified enzyme after removal of reagents by gel filtration as shown in Figure 35. This release presumably reflects the formation of a cysteine disulfide in the protein as there are two fewer sulphydryl groups in the modified protein as compared to the control. These investigators also reported on the modification of citrate synthase with 4,4'-dithiodipyridine. This reagent is similar to 5,5'-dithiobis(2-nitrobenzoic acid) in that a mixed disulfide is formed between a cysteinyl residue in the protein and the reagent with the concomitant release of pyridine-4-thione. The reaction of 4,4'-dithiodipyridine with protein sulphydryl groups can be followed by spectroscopy ($\epsilon_{324 \text{ nm}} = 19,800 \text{ M}^{-1} \text{ cm}^{-1}$). The reaction is readily reversed by the addition of a reducing agent such as dithiothreitol. The reaction of citrate synthase and 4,4'-dithiodipyridine in 0.02 M Tris, pH 7.8 at 21°C is shown in Figure 36. Figure 37 shows the effect of prior reaction of citrate synthase with one of the above reagents on subsequent reactivity with the other reagent. Modification of one sulphydryl group with either reagent greatly reduced both the rate and extent of subsequent reaction with the other reagent. The reaction of 5,5'-dithiobis(2-nitrobenzoic acid) with D-amino acid transaminase also provides an illustration of the use of this reagent.¹³ These studies were performed in 0.1 M Tris, pH 7.5; the results are shown in Figure 38. An extinction coefficient of $14,140 \text{ M}^{-1} \text{ cm}^{-1}$ for the 2-nitro-5-thiobenzoate anion was used in these studies. Approximately one half of the sulphydryl

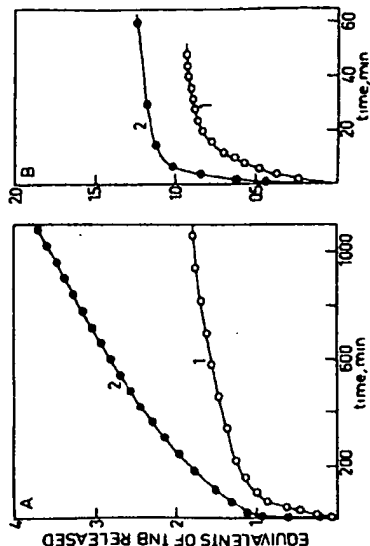


FIGURE 34 The reaction of *Escherichia coli* citrate synthase with 5,5'-dithiobis(2-nitrobenzoic acid) (DTNB). The reaction was performed at pH 7.8. In panel A, KCl was not present; experiment 1 contained 50 μM DTNB and 13.4 μM enzyme and experiment 2 contained 1500 μM DTNB and 132 μM enzyme. In panel B, 0.1 M KCl was present; experiment 1 contained 100 μM DTNB and 30.7 μM enzyme and experiment 2 contained 1100 μM DTNB and 293 μM enzyme. The extent of reaction was monitored by the release of the thiophenolate anion of 5-thio-2-nitrobenzoic acid (TNB). (From Talgoy, M. M., Bell, A. W., and Duckworth, H. W., *Can. J. Biochem.*, 57, 822, 1979. With permission.)

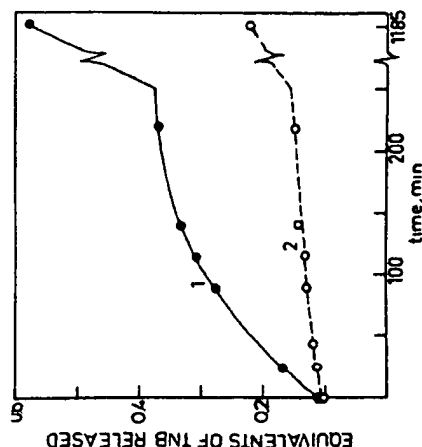


FIGURE 35 The spontaneous release of TNB from DTNB-modified citrate synthase after the removal of reagents by gel filtration. The solvent was 0.02 M Tris-HCl, pH 7.8-1 mM EDTA. In experiment 2 the solvent also contained 0.1 M KCl. The release of TNB was monitored by the increase in absorbance at 412 nm. (From Talgoy, M. M., Bell, A. W., and Duckworth, H. W., *Can. J. Biochem.*, 57, 822, 1979. With permission.)

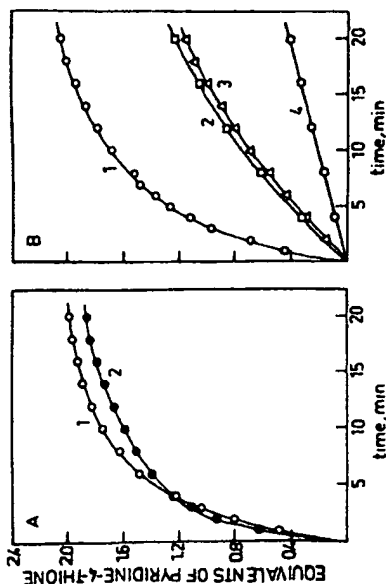


FIGURE 36. The reaction of citrate synthase with 4,4'-dithiodipyridine (4,4'-PDS). The reactions were performed at pH 7.8 in 0.02 M Tris-HCl, 1 mM EDTA. In panel A, KCl was absent in curve 1 and present at a concentration of 0.1 M in curve 2. In panel B, curve 1 contains only the Tris-EDTA buffer, curve 2 contains 1.66 mM 5'-AMP, curve 3 contains 32 μ M NADH, and curve 4 contains 2.94 mM ADP-ribose. The enzyme concentration was 21.8 μ M in all experiments while the concentration of 4,4'-PDS was 50 μ M. (From Taljor, M. M., Bell, A. W., and Duckworth, W., *Can. J. Biochem.*, 57, 822, 1979. With permission.)

groups are available for reaction with this reagent in the native enzyme. Reaction with 5,5'-dithiobis(2-nitrobenzoic acid) does result in the loss of activity and this loss of activity appears to be correlated with the modification of one of the more slowly reacting cysteinyl residues. Other proteins which have been studied with this reagent include rat brain nicotinic-like acetylcholine receptors⁷⁴ (calcium-containing Ringers solution, pH 7.4), lipophilin from human myelin⁷⁵ (0.001 M glycylglycine — 0.0001 M EDTA, pH 8.0), and human hemoglobin.⁷⁶ The latter study followed the changes in absorbance at 450 nm to monitor the release of the 2-nitro-5-mercaptobenzoic acid. The molar extinction coefficients obtained at 450 nm were 5550 $M^{-1} cm^{-1}$ (pH 6.0); 6510 $M^{-1} cm^{-1}$ (pH 7.0); 6810 $M^{-1} cm^{-1}$ (pH 8.0); 6940 $M^{-1} cm^{-1}$ (pH 9.0); and 7010 $M^{-1} cm^{-1}$ (pH 9.5). The synthesis of a selenium analog of this class of reagents, 6,6-diselenobis(3-nitrobenzoic acid), has been reported.⁷⁷ The selenium-containing reagent has the same reaction characteristics as the sulfur-containing compound in terms of specificity of reaction with cysteinyl residues in proteins. The reaction is monitored by spectroscopy following the release of 6-seleno-3-nitrobenzoate which has a maximum at 432 nm (Figure 39). The extinction coefficient for the 6-seleno-3-nitrobenzoate anion varies slightly from 9532 $M^{-1} cm^{-1}$ (with excess reagent) to 10,200 $M^{-1} cm^{-1}$ (with either excess cysteine or excess β -mercaptoethanol).

More recent studies on the use of DTNB to modify sulfhydryl groups in proteins have included the modification of ATP sulfurylase,⁴¹ oncomodulin,⁷⁸ glutathione synthetase,⁷⁹ fibronectin,⁸⁰ and streptococcal NADH peroxidase.⁸¹ In studies on the modification of ATP sulfurylase,⁴¹ it was observed that DTNB was less potent than the more hydrophobic dithionitropyridine derivative (see Figure 32).

The above reagents (5,5'-dithiobis(1-nitrobenzoic acid), 4,4'-dithiodipyridine, etc.) utilize mixed disulfide formation with reagent to obtain modification at cysteinyl residues. There are several other examples of this approach which are worth further consideration.

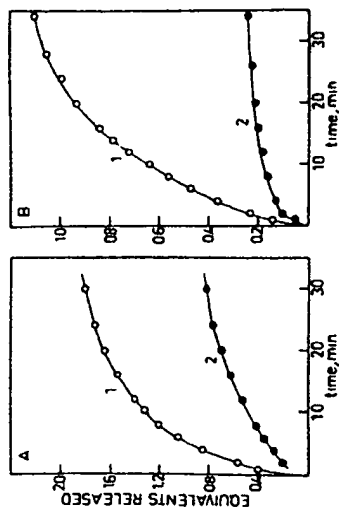


FIGURE 37. The effect of the prior modification of citrate synthase with one sulphydryl reagent upon subsequent reaction with a different reagent. In panel A, curve 1 represents the time course of the modification of citrate synthase with 4,4'-PDS; curve 2 represents a preparation of citrate synthase which was first modified with DTNB in the presence of 0.1 M KCl, subjected to gel filtration and allowed to react with 4,4'-PDS as in curve 1. At 32 min the difference between curve 1 and curve 2 is 0.99 groups per subunit. In panel B, curve 1 represents the time course for the reaction of citrate synthase with DTNB in the presence of 0.1 M KCl; curve 2 represents the time course of reaction of a preparation of citrate synthase previously modified with 4,4'-PDS, subjected to gel filtration and then allowed to react with DTNB under the same conditions as curve 1. At 34 min, the difference between curves 1 and 2 is 0.86 groups per subunit. (From Taljor, M. M., Bell, A. W., and Duckworth, W., *Can. J. Biochem.*, 57, 822, 1979. With permission.)

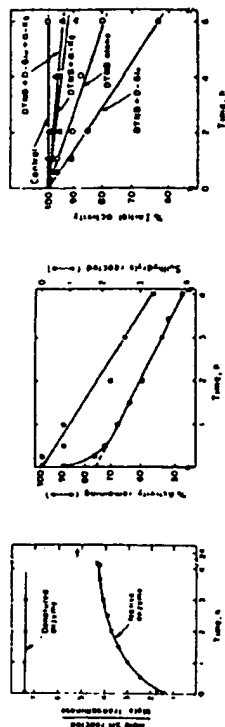


FIGURE 38. The left figure shows the time course for the modification of the sulphydryl groups of D-amino acid transaminase with DTNB in 0.1 M Tris, pH 7.2, 2.0 mM EDTA. The absorbance at 412 nm was followed as a function of time and the number of sulphydryl groups modified was determined using an extinction coefficient of 14,140. The experiment with the denatured enzyme was performed in the presence of 6.4 M guanidine hydrochloride. The center figure represents the temporal correlation between the extent of sulphydryl group modification and loss of D-amino acid transaminase activity. The right-hand figure shows the effect of submerses on the inactivation of D-amino acid transaminase by DTNB. (From Soper, T. S., Jones, W. M., and Manning, J. M., *J. Biol. Chem.*, 245, 10901, 1979. With permission.)

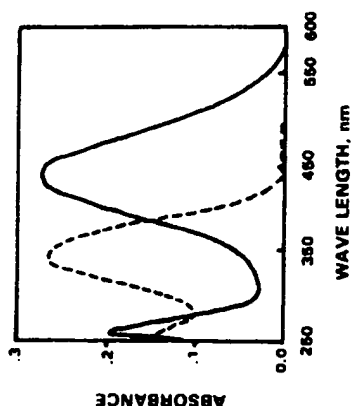


FIGURE 39. The UV absorption spectrum of 6-selenobis(3-nitrobenzoic acid) (SNB^{2-}) (25.9 μM) and 6,6-diselenobis(3-nitrobenzoic acid) (DSNB) (12.9 μM) in 0.2 M Tris-HCl, pH 8.2. 1 mM EDTA (From Lubers, M. P., Duolap, R. B., and Odum, J. D., *Anal. Biochem.*, 117, 94, 1981. With permission.)

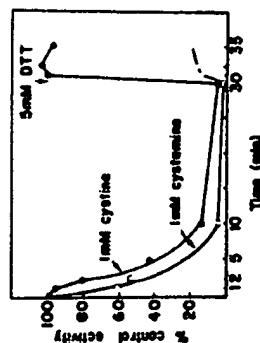


FIGURE 40. The effect of mixed disulfide formation on guanylate cyclase activity. Guanylate cyclase was incubated with either 1 mM cysteine or 1 mM cystamine in 0.02 M Tris-HCl, pH 7.6, 1 mM dithiothreitol, 10% sucrose. After 30 min of incubation, dithiothreitol was added to a final concentration of 5 mM. (From Bradwejn, J., Lewicki, J., and Mural, F., *J. Biol. Chem.*, 256, 2938, 1981. With permission.)

Cysteine or cystamine have proved effective in the modification of guanylate cyclase⁴¹ as shown in Figure 40. Note the ready reversibility of the modification on the addition of dithiothreitol. Kaiser and co-workers⁴² introduced methyl 3-nitro-2-pyridyl disulfide and methyl 2-pyridyl disulfide. Both of these reagents modify sulfhydryl groups forming the thiomethyl derivative. Figure 41 shows the spectra of methyl 3-nitro-2-pyridyl disulfide (NPySSMe) and 3-nitro-2-pyridone (NPySH) with determinations of the latter compared at several different conditions of pH. The spectrum of 3-nitro-2-pyridone is pH dependent. There is an isosbestic point at 310.4 nm which can be used to determine the extent of the

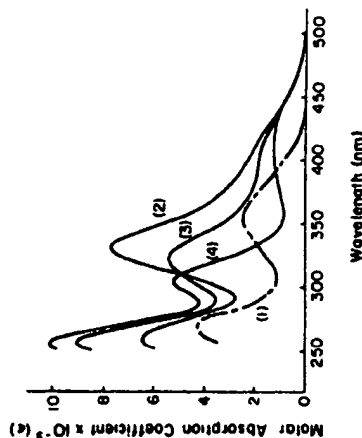


FIGURE 41. The UV absorption spectra of methyl 3-nitro-2-pyridyl disulfide (NPySSMe) and 3-nitro-2-pyridone (NPySH) in 0.050 M sodium phosphate; NPySSMe at pH 4.8 (curve 1), NPySH at pH 4.0, 4.6 (curve 2), pH 6.4 (curve 3), and pH 8.4, 8.8 (curve 4). (From Kinura, T., Matsuda, R., Nakagawa, Y., and Kaiser, E. T., *Anal. Biochem.*, 122, 274, 1982. With permission.)

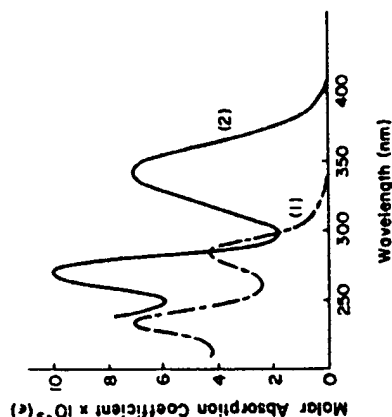


FIGURE 42. The UV absorption spectra of methyl 2-pyridyl disulfide (PySSMe) and 2-thiopyridone (PySH) in 0.050 M sodium phosphate, pH 7.5. Curve 1 is that for PySSMe and curve 2 for PySH. (From Kinura, T., Matsuda, R., Nakagawa, Y., and Kaiser, E. T., *Anal. Biochem.*, 122, 274, 1982. With permission.)

reaction of methyl 3-nitro-2-pyridyl disulfide with sulfhydryl groups. Similar spectral studies for methyl 2-pyridyl disulfide (PySSMe) and 2-thiopyridone (PySH) are shown in Figure 42. The difference in spectrum obtained does not show the pH dependence of the nitropyridyl derivative (see Figure 41). At 343 nm, the change in extinction coefficient is $7,060 \text{ M}^{-1} \text{ cm}^{-1}$. Confirmation of S-methylcysteine and 2-thiopyridone as the reaction products from

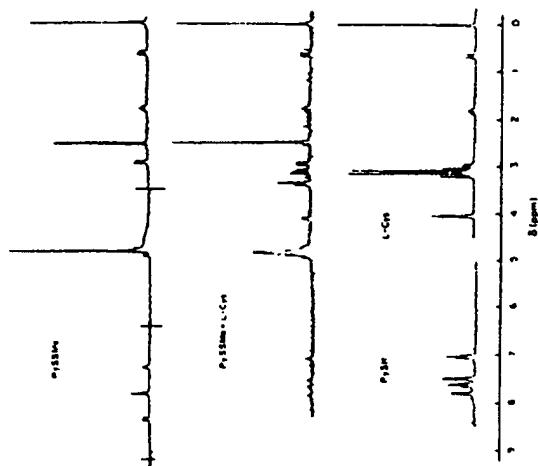


FIGURE 43. The nuclear magnetic resonance spectra of methyl-2-pyridyl disulfide (PySSMe), a mixture of PySSMe and cysteine (L-Cys) and a mixture of 2-thiopyridone (PySH) and cysteine (L-Cys). (From Kimura, T., Matsuda, R., Nakagawa, Y., and Kaiser, E. T., *Anal. Biochem.*, 122, 274, 1982. With permission.)

L-cysteine and methyl-2-pyridyl disulfide was obtained from NMR spectroscopy (Figure 43). The time course for the reaction of methyl-2-pyridyl disulfide with glutathione or papain is shown in Figure 44. Note the differences in the rate of the reaction of methyl-2-pyridyl disulfide with the cysteinyl residue in glutathione and papain.

The reaction of the single cysteinyl residue in albumin with 2,2'-dithiopyridine has been studied by Pederson and Jacobsen.⁴³ The suggested reaction mechanism and the spectra of 2,2'-dithiopyridine and 2-thiopyridone are shown in Figure 45. The extinction coefficient ($7600 \text{ M}^{-1} \text{ cm}^{-1}$) of the 2-thiopyridone at 343 nm is relatively stable from pH 3 to pH 8.0. Above pH 8.0 there is a marked decrease reflecting the loss of a proton. Reaction with the sulphydryl group in the protein clearly proceeds more rapidly at alkaline pH.

In a related study, Drews and Faulstich⁴² prepared 2,4-dinitrophenyl-¹⁴C-cysteinyl disulfide (Figure 46) via a facile synthetic method as a means for introducing radiolabeled cysteine into proteins via disulfide exchange with free thiols. The reaction can be monitored by following the release of 2,4-dinitrophenol at 408 nm ($408 = 12,700 \text{ M}^{-1} \text{ cm}^{-1}$). The specificity of this reagent corresponded to that obtained with DTNB. Reaction with the sulphydryl groups of papain was more rapid than that observed with DTNB. The resulting derivative can be easily reversed with thiols but is stable to cyanogen bromide degradation and peptide purification.

p-Hydroxymercuribenzoate continues to be of use for the modification of sulphydryl groups in proteins. The reagent is obtained as *p*-chloromercuribenzoate but is instantaneously converted to the hydroxy derivative in aqueous solution. This reagent was originally described

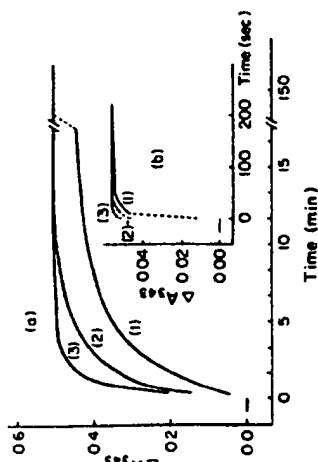


FIGURE 44. Time course studies of the formation of 2-thiopyridone resulting from the reaction of methyl-2-pyridyl disulfide (PySSMe) with glutathione (a) or papain (b). In the experiments with glutathione (a), the concentration of glutathione was $71.7 \mu\text{M}$ and the ratio of PySSMe to glutathione was 1.04 (1), 1.57 (2), and 3.13 (3). In the experiments with papain (b), the concentration of papain was $8.29 \mu\text{M}$ and the ratio of PySSMe to papain was 1.02 (1), 1.70 (2), and 3.41 (3). (From Kimura, T., Matsuda, R., Nakagawa, Y., and Kaiser, E. T., *Anal. Biochem.*, 122, 274, 1982. With permission.)

by Boyer.⁴⁴ The absorbance change at 255 nm upon modification is $6200 \text{ M}^{-1} \text{ cm}^{-1}$ at pH 4.6 and $7600 \text{ M}^{-1} \text{ cm}^{-1}$ at pH 7.0. Bai and Hayashi⁴⁵ have examined the reaction of organic mercurials with yeast carboxypeptidase (carboxypeptidase Y). The titration of the catalytically essential cysteinyl residue in carboxypeptidase Y with *p*-hydroxymercuribenzoate is shown in Figure 47. Treatment of the modified enzyme with millimolar cysteine resulted in virtually complete recovery of catalytic activity. The inactivation of chalcone isomerase by *p*-chloromercuribenzoate and mercuric chloride has been studied by Bednar et al.⁴⁶ The modified protein could be readily reactivated by treatment with either thiols or KCN. The reactivation by KCN is based on the formation of a tight complex between cyanide and either organic or inorganic mercurials. The modification by mercuric chloride can be monitored by the increase in absorbance at 250 nm. Ojcius and Solomon⁴⁷ have examined the inhibition of erythrocyte urea and water transport by *p*-chloromercuribenzoate. Other studies with this reagent have included dissociation of erythrocyte membrane proteins,⁴⁸ NADH peroxidase,⁴⁹ and sulfobromophthalan transport protein.⁴⁵

2-Chloromercuri-4-nitrophenol is a compound related to the organic mercurial described above. It has proved useful as a "reporter" group in the study of microenvironmental changes in the modified protein.^{41,42} An excellent example of this is provided from the studies of Marshall and Cohen⁵⁰ on the properties of ornithine transcarbamylase modified with 2-chloromercuri-4-nitrophenol. The enzyme from *S. faecalis* was modified in 0.1 M MOPS, 0.1 M KCl, pH 7.5 using changes in absorbance at 403 nm to follow the extent of modification. The pH dependence of the spectrum of the modified *S. faecalis* enzyme is shown in Figure 48. The bovine enzyme is carboxamido methylated on a nonessential sulphydryl group before reaction with the organic mercurial. Modification of the bovine enzyme with 2-chloromercuri-4-nitrophenol is performed in 0.020 M MOPS, 0.1 M KCl, pH 7.11 at 25°C. The modification was followed by the change in absorbance at 405 nm. The effect of pH on the spectrum of the modified bovine enzyme is shown in Figure 49. Baines and Brocklehurst⁵¹ have reported the synthesis and characterization of 2-(2'-pyridylmercapto)-mercuri-4-nitrophenol, a reagent which does have certain advantages. In particular, the

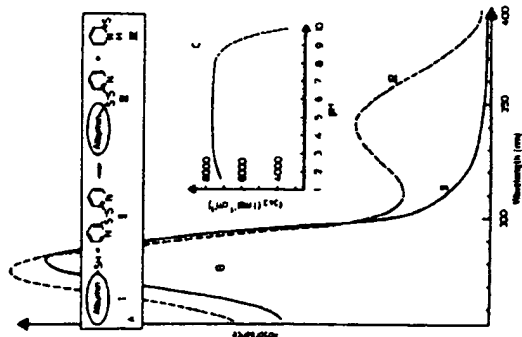


FIGURE 45. (A) A scheme for the reaction of 2,2'-dithiopyridine and mercapalbumin; (B) The UV absorption spectra for 2,2'-dithiopyridine (solid line, II) and 2-thiopyridone (dashed line, IV) in 0.1 M sodium phosphate, pH 7.0; (C) the molar extinction coefficient at 343 nm for 2-thiopyridone as a function of pH. (From Pedersen, A. O. and Jacobsen, J., *Eur. J. Biochem.*, 106, 291, 1980. With permission.)

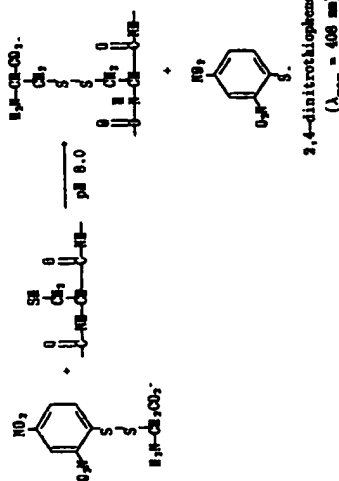


FIGURE 46. The reaction of 2,4-dinitrophenyl cysteinyl disulfide with cysteine in proteins.

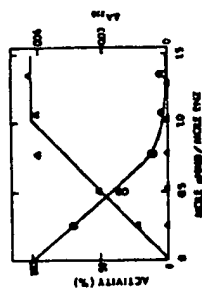


FIGURE 47. The spectrophotometric titration of native and DIP-carboxypeptidase Y with *p*-hydroxymercaptobenzate (*p*-HMB). The reaction with the protein was accomplished in 0.08 M sodium phosphate, pH 7.0. Increments of *p*-HMB were added to the protein preparations and allowed to stand for 20 min at which time absorbance at 250 nm was determined as catalytic activity (Z-Phe-Leu or Ac-Phe-OEt). The open circles indicate activity toward Ac-Phe-OEt, the closed circles indicate activity toward Z-Phe-Leu, the open triangles represent the absorbance at 250 nm of the native carboxypeptidase Y, and the closed triangles represent the absorbance at 250 nm of carboxypeptidase Y previously reacted with diisopropylphosphorofluoridate (DIP-carboxypeptidase Y). (From Bai, Y. and Hayashi, R., *J. Biol. Chem.*, 254, 8473, 1979. With permission.)

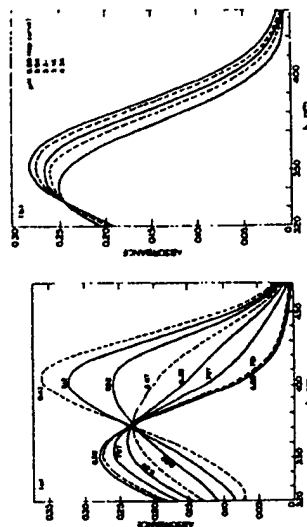


FIGURE 48. The effect of pH on the spectrum of the 2-chloro-mercuri-4-nitrophenyl derivative of ornithine transferase. Panel a represents the results obtained in the pH range of 9.43 to 6.50. Panel b represents the results obtained in the pH range of 6.5 (top curve) to 4.36 (bottom curve). (From Marshall, M. and Cohen, P., *J. Biol. Chem.*, 255, 7296, 1980. With permission.)

spectral changes occurring on modification (Figure 50) permit the more facile *in situ* determination of the extent of reaction.

A number of other modifications of sulfhydryl groups have proved useful. *O*-Methylisourea reacts with cysteinyl residues to form the *S*-methyl derivative (Figure 51).⁹² Cyanate also can modify sulfhydryl groups as shown in Table 2.⁹³ The carbamoyl derivative of cysteine is stable at acid pH but rapidly decomposes at alkaline pH.

4-Chloro-7-nitrobenzo-2-oxa-1,3-diazole (4-chloro-7-nitrobenzofurazan; Nbf-Cl) (Figure 52) is a reagent developed for the modification of amino groups.⁹⁴ It has also found application in the modification of sulfhydryl groups and is useful in that it introduces a fluorescent probe.⁹⁵⁻⁹⁹ Nitta and co-workers⁹⁵ have noted that there are other possible reaction products of Nbf-Cl including the possibility of reaction products with sulfhydryl groups. The

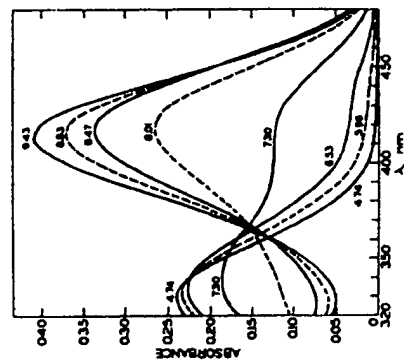


FIGURE 49. The effect of pH on the UV absorption spectrum of the 3-chloromercuri-4-nitrophenol derivative of the mercaptobenzimidazole-bovine liver ornithine transcarbamylase. (From Marshall, M. and Cohen, P. P., *J. Biol. Chem.*, 255, 7296, 1980. With permission.)

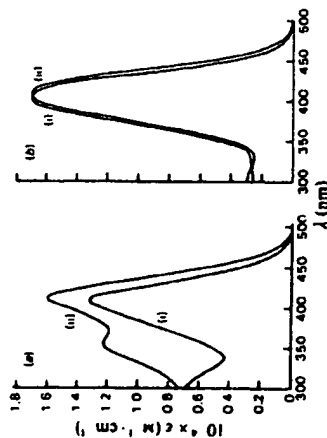


FIGURE 50. The UV absorption spectra of (a) 2-(2'-pyridylmercapto)mercuri-4-nitrophenol and (b) 2-chloromercuri-4-nitrophenol before (i) and after (ii) the addition of an excess of β-mercaptoethanol. The solvent was sodium/potassium phosphate (ionic strength = 0.1) containing 13% (v/v) ethanol. The reaction of the mercurial (concentration = 10 μM) with β-mercaptoethanol (concentration = 45 mM) was complete after 5 min of reaction. (From Baines, B. S. and Brockhurst, K., *Biochem. J.*, 179, 701, 1979. With permission.)



FIGURE 51. The reaction of *O*-methylisourea with cysteine.

Table 2
REACTION OF CYANATE WITH
FUNCTIONAL GROUPS IN PROTEINS

Functional group	pKa	M ⁻¹ min ⁻¹
Alpha amino	7.8-8.2	1.4 × 10 ⁻¹
Epsilon amino	10.5-10.8	2 × 10 ⁻¹
Sulphydryl	8.3-8.5	4.0
Imidazole	7.0-7.2	1.8 × 10 ⁻¹

From Stark, G. R., *Methods Enzymol.*, 11, 590, 1967. With permission.

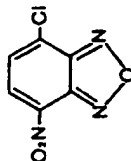


FIGURE 52. The structure of 4-chloro-7-nitrobenzo-2-oxa-1,3-diazole (4-chloro-7-nitrobenzofurazan, Nbf-Cl).

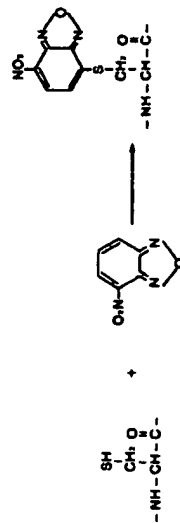


FIGURE 53. The reaction of 4-chloro-7-nitrobenzo-2-oxa-1,3-diazole with cysteine.

modification of the sulphydryl group with concomitant reaction at the 4-position yields a derivative with molar absorption coefficient of 13,000 (Figure 53).¹⁰ The reaction of Nbf-Cl with sulphydryl groups in glutathione reductase and liponamide dehydrogenase has also been reported.¹⁰ Nitta and co-workers¹⁰ have examined the chemistry of the reaction of Nbf-Cl with model sulphydryl compounds in some detail. The spectra of the reagent (Nbf-Cl) and product of reaction with 2-mercaptoethanol (4-(2'-hydroxy-ethylthio)-7-nitrobenzofuran; Nbf-OHEtS) are presented in Figure 54. These data should be compared with that presented in Figure 55. Note the dependence of the different spectra on sulphydryl concentration and pH/solvent species. The data in Figure 55 (f) were obtained in trietha-

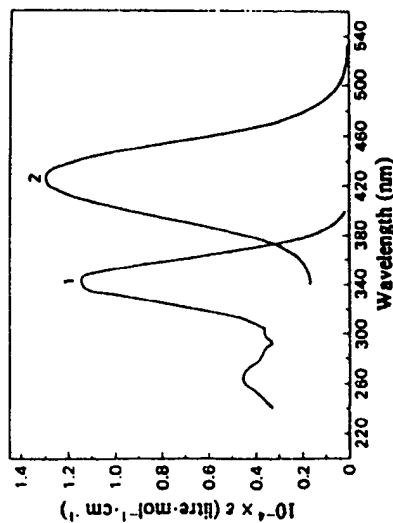


FIGURE 54. The UV absorption spectra of 4-chloro-7-nitrobenzo-2-oxa-1,3-diazole (Nbf-Cl) (curve 1) and the reaction product between Nbf-Cl and β -mercaptoethanol (curve 2). The solvent was water adjusted to pH 7.1. (From Nitta, K., Braucher, S. C., and Kronman, M. J., *Biochem. J.*, 177, 385, 1979. With permission.)

nomaline, pH 7.5 with an approximate 20-fold molar excess of β -mercaptoethanol while that in part II was obtained with an approximate 200-fold molar excess. Experimental series part III was performed with a 20-fold molar excess of β -mercaptoethanol in sodium citrate buffer, pH 5.0. Similar spectral changes are seen with dithiothreitol in Figure 56. The data in experimental series I were obtained at an Nbf-Cl concentration of 0.148 mM and a dithiothreitol concentration of 0.0097 mM while the data in experimental series III were obtained at an Nbf-Cl concentration of 0.0742 mM and a dithiothreitol concentration of 9.38 mM. The variety of potential products in this reaction requires that considerable caution be used in the interpretation of spectra data obtained with this reagent.

Toyo'oka and Imai¹⁰¹ have reported the synthesis of a related compound, 4-(aminosulfonyl-7-fluoro-2,1,3-benzoxadiazole) (Figure 57) which is a fluorogenic reagent for sulphydryl groups. In a subsequent study, Kirby¹⁰² has used this compound to label cysteinyl residues in proteins. Reaction readily occurred at pH 8.0 (100 mM borate-2 mM EDTA with 3% SDS).

The modification of cysteinyl residues in proteins with 2-bromoethane sulfonate has been reported.¹⁰³ This derivatization procedure was developed in response to a need for a strongly hydrophilic substituent in samples for the Edman degradation. The modification time is longer than for the corresponding carboxymethyl derivatives, taking 12 h for lysozyme, 24 h for insulin, and 48 h for glutathione. This derivative has considerable utility since the S-sulfoethylated lysozyme derivative is soluble between pH 5.0 and 10.0 while the S-carboxymethylated derivative is not. This procedure has potential for primary structure analysis.

A derivatization procedure that has proved useful in the primary structure analysis of protein has been the reaction of ethyleneimine (Figure 58) with sulphydryl groups in proteins.¹⁰⁴ This reaction produces S-aminoethyl cysteine which provides an additional point of tryptic cleavage in proteins.¹⁰⁵ With bovine pancreatic ribonuclease A, with a 1/100 ratio of trypsin at pH 8.0, 83% cleavage of arginyl and lysyl bonds was obtained while 56%

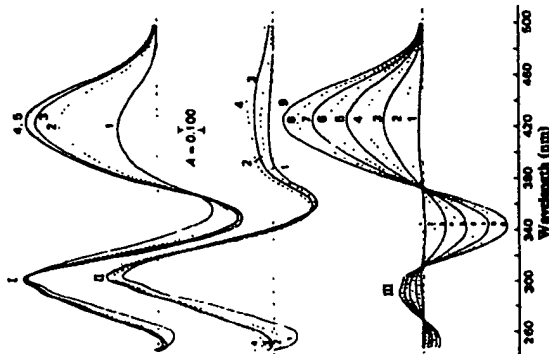


FIGURE 55. Different spectra of mixtures of 4-chloro-7-nitrobenzofurazan (Nbf-Cl) and β -mercaptoethanol at ambient temperature. The spectra were scanned at a rate of 30 nm/min from high to low wavelength. The times given below are for the initial wavelength in the scan. The solution containing the Nbf-Cl + β -mercaptoethanol was in the sample beam. The spectra in set I were obtained in 0.05 M triethanolamine HCl/NaOH, pH 7.5, at an Nbf-Cl concentration of 0.102 mM and a β -mercaptoethanol concentration of 2.28 mM. The times for the individual curves in set I were 2 min (curve 1), 12 min (curve 2), 22 min (curve 3), 42 min (curve 4), and 72 min (curve 5). The spectra in set II were obtained in 0.05 M triethanolamine HCl/NaOH buffer, pH 7.5, at an Nbf-Cl concentration of 0.104 mM and a β -mercaptoethanol concentration of 22.8 mM. The times for the individual curves in set II were 3 min (curve 1), 15 min (curve 2), 35 min (curve 3), and 60 min (curve 4). The spectra in set III were obtained in 0.05 M sodium citrate/tris acid, pH 5.0, at an Nbf-Cl concentration of 0.112 mM. The times for the individual curves of set III were 3 min (curve 1), 27 min (curve 2), 57 min (curve 3), 87 min (curve 4), 117 min (curve 5), 147 min (curve 6), 177 min (curve 7), 207 min (curve 8), and 237 min (curve 9). (From Nitta, K., Braucher, S. C., and Kronman, M. J., *Biochem. J.*, 177, 385, 1979. With permission.)

cleavage was obtained at S-aminoethyl cysteine. This chemistry has been used to introduce a dansyl label into unconjugated protein via modification of a cysteinyl residue with dansylaziridine (Figure 59).⁷⁸ Since the aziridines are photosensitive compounds (see Chapter 16), reaction proceeded in the dark. A 100-fold molar excess of reagent (dissolved in either dimethylformamide or dimethylsulfoxide) at pH 7.5 (Tris or HEPES) was used. The reaction was allowed to proceed for 16 to 20 h with rocking (most of the dansylaziridine is insoluble) and reagent removed by centrifugation.

Mutus et al.¹⁰⁶ have introduced 1-p-chlorophenyl-4,4-dimethyl-5-diethylamino-1-pentene-3-one hydrobromide (Figure 60) as a reagent for the modification of thiol groups. This reagent readily and reversibly reacts with low molecular weight thiols such as cysteine or glutathione with a large decrease in absorbance at 310 nm ($\epsilon = 21,000 \text{ M}^{-1} \text{ cm}^{-1}$). The reaction with larger thiol-containing molecules such as proteins appears to be irreversible.

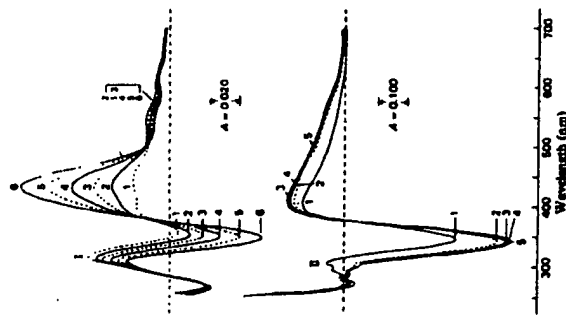


FIGURE 56. Different spectra of mixtures of 4-chloro-7-nitrobenzofurazan (Nbf-Cl) and dihydrotol at ambient temperature. Spectra were scanned at the rate of 30 nm/min from high to low wavelength. The times given below were for the initial wavelength in the scan. The solution of Nbf-Cl + thiol compound was in the sample beam. The buffer used was 0.05 *N* triethanolamine HCl/NaOH (pH 7.5). The spectra of set I were obtained at an Nbf-Cl concentration of 0.148 mM and a dihydrotol concentration of 9.97 μ M at 3 min (curve 1), 13 min (curve 2), 23 min (curve 3), 38 min (curve 4), 58 min (curve 5), and 88 min (curve 6). The spectra in set II were obtained at an Nbf-Cl concentration of 9.389 mM at 2 min (curve 1), 12 min (curve 2), 22 min (curve 3), 42 min (curve 4), and 72 min (curve 5). (From Nitta, K., Bratcher, S. C., and Kromann, M. J., *Biochem. J.*, 177, 385, 1979. With permission.)

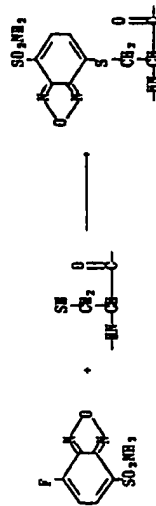


FIGURE 57. The structure of 4-aminosulfonyl-7-fluoro-2,1,3-benzoxadiazole (ABD-F), a fluorogenic reagent for the modification of cysteine residues in proteins.

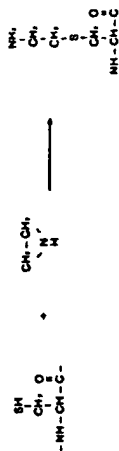


FIGURE 58. The reaction of ethylenimine with cysteine.

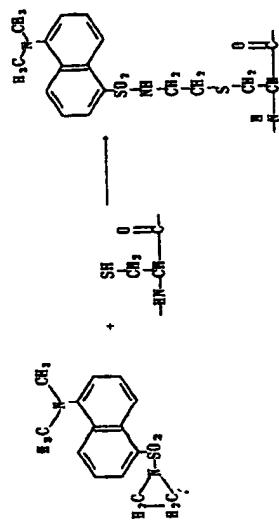
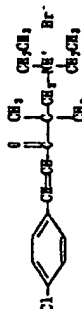


FIGURE 59. The reaction of cysteine with dansyl aziridine.



1-p-chlorophenyl-4,4-dimethyl-5-diethylamino-1-penten-3-one hydrobromide

FIGURE 60. The structure of a novel sulphydryl reagent.

REFERENCES

1. Lin, T.-Y., The role of sulfur in proteins. *The Proteins*, Vol. 3, 3rd ed., Neurath, H. and Hill, R. L., Eds., Academic Press, New York, 1977, 240.
2. Kenyon, G. L. and Bruter, T. W., Novel sulphydryl reagents. *Methods Enzymol.*, 47, 407, 1977.
3. Poole, L. B. and Chisborne, A., The non-flavin redox center of the streptococcal NADH peroxidase. II. Evidence for a stabilized cysteine-sulfenic acid. *J. Biol. Chem.*, 264, 12330, 1989.
4. Phil, A. and Lange, R., The interaction of oxidized glutathione: cystamine monosulfide, and tetraethionate with the -SH groups of rabbit muscle α -glyceraldehyde 3-phosphate dehydrogenase. *J. Biol. Chem.*, 237, 1356, 1962.
5. Bednar, R. A., Fried, W. B., Lock, Y. W., and Pramanik, B., Chemical modification of chalcone isomerase by mercurials and tetraethionate. Evidence for a single cysteine residue in the active site. *J. Biol. Chem.*, 264, 14272, 1989.
6. Smith, D. J., Magglo, E. T., and Kenyon, G. L., Simple alkane thiol groups for temporary blocking of sulphydryl groups of enzymes. *Biochemistry*, 14, 766, 1975.
7. Bruter, T. W. and Kenyon, G. L., Novel alkyl alkanethiolate sulphydryl reagents. Modification of derivatives of L-cysteine. *J. Protein Chem.*, 1, 47, 1982.

8. Beech, L. M., and Brodhead, K., Chemical modification of a cysteinyl residue introduced in the binding site of carboxypeptidase Y by site-directed mutagenesis. *Carlsberg Res. Commun.*, 53, 381, 1988.
9. Gerwin, B. I., Properties of the single sulfhydryl group of streptococcal proteinase: A comparison of the rates of alkylation by chloroacetic acid and chloroacetamide. *J. Biol. Chem.*, 242, 451, 1967.
10. Liu, T. Y., Demonstration of the presence of a histidine residue at the active site of streptococcal proteinase. *J. Biol. Chem.*, 242, 4029, 1967.
11. Chalkins, I. M., and Smith, E. L., Reaction of chloroacetamide with the sulfhydryl group of papain. *J. Biol. Chem.*, 244, 5087, 1969.
12. Chalkins, I. M., and Smith, E. L., Reaction of the sulfhydryl group of papain with chloroacetic acid. *J. Biol. Chem.*, 244, 5095, 1969.
13. Jernvall, H., Fowler, A. V., and Zalkin, I., Probe of β -galactosidase structure with indoxylacetate. Differential reactivity of thiol groups in wild-type and mutant forms of β -galactosidase. *Biochemistry*, 17, 5160, 1978.
14. Kalland, M., and Love, K., Role of chemical reagents in the activation of rat hepatic glucocorticoid-receptor complex. *J. Biol. Chem.*, 255, 4687, 1980.
15. Kalits, G.-B., and Holmgren, A., Differential reactivity of the functional sulfhydryl groups of cysteine-32 and cysteine-35 present in the reduced form of thiodoxin from *Erwinia coli*. *J. Biol. Chem.*, 255, 10261, 1980.
16. Mikami, R., Albarra, S., and Morita, Y., Chemical modification of sulfhydryl groups in soybean β -amylase. *J. Biochem.*, 88, 103, 1980.
17. Hempel, J. D., and Pienkowski, R., Selective chemical modification of human liver aldehyde and dehydrogenases E₁ and E₂ by iodoacetamide. *J. Biol. Chem.*, 256, 10889, 1981.
18. Crestfield, A. M., Moore, S., and Stein, W. H., The preparation and enzymatic hydrolysis of reduced and S-carboxymethylated proteins. *J. Biol. Chem.*, 238, 622, 1963.
19. Friedmann, M., Knoll, L. H., and Cavities, J. P., The chromatographic determination of cysteine and cysteine residues in proteins as S-(4-pyridyl-ethyl) cysteine. *J. Biol. Chem.*, 245, 3868, 1970.
20. Maki, A. S., and Jones, B. L., Application of 5-pyridyl-ethylamine of cysteine to the sequence analysis of proteins. *Anal. Biochem.*, 84, 432, 1978.
21. Dahl, K. S., and McKelvey-McKee, J. S., The reactivity of affinity labels: a kinetic study of the reaction of alkyl halides with thiolate anions — a model reaction for protein alkylation. *Bioorganic Chem.*, 10, 329, 1981.
22. Soper, T. S., Ueno, H., and Manning, J. M., Substrate-induced changes in sulfhydryl reactivity of bacterial d-amino acid transaminase. *Arch. Biochem. Biophys.*, 240, 1, 1985.
23. Kadow, R. R., Schlatterbeck, J. D., Mar, V. L., and Bernette, W. N., Alkylation of cysteine 41, but not cysteine 200, decreases the ADP-ribosyltransferase activity of the S1 subunit of pertussis toxin. *J. Biol. Chem.*, 264, 6386, 1989.
24. Makino, A. L., and Novak, T., A reactive cysteine in avian liver phosphoenolpyruvate carboxylase. *J. Biol. Chem.*, 264, 12148, 1989.
25. Poole, L. B., and Chalkins, A., The non-flavin redox center of the streptococcal NADH peroxidase. I. Thiol reactivity and redox behavior in the presence of urea. *J. Biol. Chem.*, 264, 12322, 1989.
26. Wei, H., Yao, Q.-Z., and Tsou, C.-L., Creatine kinase is modified by 2-chloromercapto-4-nitrophenol at the active site thiols with complete inactivation. *Biochim. Biophys. Acta*, 997, 78, 1989.
27. Wang, Z.-X., Preda, B., and Tsou, C.-L., Kinetics of inactivation of creatine kinase during modification of its thiol groups. *Biochemistry*, 27, 5095, 1988.
28. Selfried, S. E., Wang, Y., and Van Hippel, P. H., Fluorescent modification of the cysteine 202 residue of *Escherichia coli* transcription termination factor rho. *J. Biol. Chem.*, 263, 13511, 1988.
29. Pardo, J. P., and Slayman, C. W., Cysteine 532 and cysteine 545 are the N-ethylmaleimide-reactive residues of the *Neurospora* plasma membrane H⁺ [ATPase]. *J. Biol. Chem.*, 264, 9373, 1989.
30. Miyazaki, T., and Borjdo, J., Differential behavior of two cysteine residues on the myosin head in muscle fibers. *Biochemistry*, 28, 1287, 1989.
31. Bishop, J. E., Squire, T. C., Bigelow, D. J., and Inesi, G., (Iodoacetamido) fluorescein labels a pair of proximal cysteines on the Ca²⁺ [ATPase] of sarcoplasmic reticulum. *Biochemistry*, 27, 5233, 1988.
32. First, E. A., and Taylor, S. S., Selective modification of the catalytic subunit of cAMP-dependent protein kinase with sulfhydryl-specific fluorescent probes. *Biochemistry*, 28, 3598, 1989.
33. Gregory, J. D., The stability of N-ethylmaleimide and its reaction with sulfhydryl groups. *J. Am. Chem. Soc.*, 77, 3922, 1955.
34. Ledlie, J., Spectral shifts in the reaction of N-ethylmaleimide with proteins. *Anal. Biochem.*, 10, 162, 1965.
35. Corlin, G., Marle, P. A., and Doughty, G., Kinetics of the reaction of N-ethylmaleimide with cysteine and some congeners. *Arch. Biochem. Biophys.*, 115, 933, 1966.
36. Smyth, D. G., Blumenthal, O. O., and Knippsberg, W., Reaction of N-ethylmaleimide with peptides and amino acids. *Biochem. J.*, 91, 589, 1964.
37. Portanova, J. P., and Shedd, A., Usefulness of N-ethylmaleimide in the identification of "Se-labeled" selenocysteine. *J. Chromatogr.*, 139, 391, 1977.
38. Gehring, H., and Christen, P., A diagonal procedure for isolating sulfhydryl peptides alkylated with N-ethylmaleimide. *Anal. Biochem.*, 107, 358, 1980.
39. Brown, R. D., and Matthews, K. S., Chemical modification of lactose repressor proteins using N-substituted maleimides. *J. Biol. Chem.*, 254, 5128, 1979.
40. Brown, R. D., and Matthews, K. S., Spectral studies on *Lac* repressor modified with N-substituted maleimide probes. *J. Biol. Chem.*, 254, 5135, 1979.
41. Quecho, F. E., and Thompson, J. W., Substrate binding to an active creatine kinase with a thiol-bound mercurimethyl chromophore probe. *Proc. Natl. Acad. Sci. U.S.A.*, 70, 2838, 1973.
42. Quecho, F. E., and Olson, J. S., The reaction of creatine kinase with 2-chloromercapto-4-nitrophenol. *J. Biol. Chem.*, 249, 3883, 1974.
43. Martin, R. L., Daley, L. A., Lovric, Z., Weiss, L. M., Renosto, F., and Segal, I. H., The "regulatory" sulfhydryl group of *Penicillium chrysogenum* ATP sulfurylase. Cooperative ligand binding after SH modification: chemical and thermodynamic properties. *J. Biol. Chem.*, 264, 11768, 1989.
44. Werner, P. K., Lieberman, D. M., and Kellhammer, R. A. F., Accessibility of the N-ethylmaleimide-unreactive sulfhydryl of human erythrocyte band 3. *Biochim. Biophys. Acta*, 982, 309, 1989.
45. Passamonti, S., and Sotoca, G. L., The role of sulfhydryl groups in sulfolipid metabolism in transport in rat liver plasma membrane vesicles. *Biochim. Biophys. Acta*, 979, 294, 1989.
46. Pfister, K. K., Weger, M. C., Bloom, G. S., and Brady, S. T., Modification of the microtubule-binding and ATPase activities of kinesin by N-ethylmaleimide (NEM) suggests a role for sulfhydryls in fast axonal transport. *Biochemistry*, 28, 9006, 1989.
47. Perussi, J. R., Tiano, M. H., Nacimento, O. R., and Tabak, M., Characterization of protein spin labeling by maleimide: evidence for nitroreduction. *Anal. Biochem.*, 173, 289, 1988.
48. Marques, J., Friets, A., and Martines-Carmona, M., Covalent modification of a critical sulfhydryl group in the acetylcholine receptor: cysteine-222 of the α -subunit. *Biochemistry*, 28, 7433, 1989.
49. Mills, J. S., Walsh, M. P., Nemeth, K., and Johnson, J. D., Biologically active fluorescent derivatives of spinach calmodulin that report calmodulin target protein binding. *Biochemistry*, 27, 991, 1988.
50. Jank, P., and Draboth, Z., Sulfhydryl groups of the uncoupling protein of brown adipose tissue mitochondria — distinction between sulfhydryl groups of the H⁺ T channel and the nucleotide binding site. *Eur. J. Biochem.*, 183, 89, 1989.
51. Le-Quec, K., Le-Quec, D. E., and Gaudemer, Y., Evidence for the existence of two classes of sulfhydryl groups essential for membrane-bound succinate dehydrogenase activity. *Biochemistry*, 20, 1705, 1981.
52. Rial, E., Arredondo, I., Salazar-de-Maza, E., and Nicholls, D. G., Effect of hydrophobic sulfhydryl reagents on the uncoupling protein and inner-membrane anion channel of brown-adipose-tissue mitochondria. *Eur. J. Biochem.*, 182, 187, 1989.
53. Yee, A. S., Corley, D. E., and McNamara, M. G., Thiol-group modification of *Torpedo californica* acetylcholine receptor: subunit localization and effects on function. *Biochemistry*, 25, 2110, 1986.
54. Pradler, L., Yee, A. S., and McNamara, M. G., Use of chemical modifications and site-directed mutagenesis to probe the functional role of thiol groups on the gamma subunit of *Torpedo californica* acetylcholine receptor. *Biochemistry*, 28, 6582, 1989.
55. Abbott, R. E., and Schaeffer, D., Topography and functions of sulfhydryl groups of the human erythrocyte glucose transport mechanism. *Mol. Cell. Biochem.*, 82, 85, 1988.
56. May, J. M., Reaction of an extrinsic sulfhydryl group on the erythrocyte hexose carrier with an impermeant maleimide. Relevance to the mechanism of hexose transport. *J. Biol. Chem.*, 263, 13635, 1988.
57. May, J. M., Interaction of a permeant maleimide derivative of cysteine with the erythrocyte glucose carrier. Differential labelling of an extrinsic carrier thiol group and its role in the transport mechanism. *Biochem. J.*, 263, 875, 1989.
58. Abbott, R. E., and Schaeffer, D., Impermeant maleimides. Oriented probes of erythrocyte membrane proteins. *J. Biol. Chem.*, 251, 1716, 1976.
59. May, J. M., Selective labeling of the erythrocyte hexose carrier with a maleimide derivative of glucosamine: relationship of an extrinsic sulfhydryl to carrier conformation and structure. *Biochemistry*, 28, 1718, 1989.
60. Fialke, J. J., Denenberg, A. F., Sternberg, D. A., Zalkin, N., Milligan, D. L., and Koshland, D. E., Jr., Structure of a bacterial sensory receptor. A site-directed sulfhydryl study. *J. Biol. Chem.*, 263, 14850, 1988.
61. Lepke, S., Fasel, H., Pring, M., and Passow, H., A study of the relationship between inhibition of anion exchange and binding to the red blood cell membrane of 4,4'-dithiocyanosilbene-2,2'-disulfonic acid (DIDS) and its dihydro derivative (H₂DIDS). *J. Membrane Biol.*, 29, 147, 1976.
62. Bettesdorff, L., Wilm, P., and Schaffelds, E., Thiamine triphosphate from *Electrophorus electricus* origin is anion-dependent and irreversibly inhibited by 4,4'-dithiocyanosilbene-2,2'-disulfonic acid. *Biochem. Biophys. Res. Commun.*, 154, 942, 1988.

63. Speth, M. and Schutze, H.-J., On the nature of the interaction between 4,4'-diiodiodicynostilbene 2,2'-disulfonic acid and microsomal glucose-6-phosphatase. Evidence for the involvement of sulphydryl groups of the phosphatase. *Eur. J. Biochem.*, 174, 111, 1988.
64. Degand, Y. and Degani, C., Subunit-selective chemical modifications of creatine kinase. Evidence for asymmetrical association of the subunits. *Biochemistry*, 18, 5917, 1979.
65. Elman, G. L., Tissue sulphydryl groups. *Arch. Biochem. Biophys.*, 82, 70, 1959.
66. Pecci, L., Camella, C., Penna, B., Costa, M., and Cavallini, D., Cysylation of rhodanese by 2-nitro-5-thiocyanobenzoic acid. *Biochim. Biophys. Acta*, 623, 348, 1980.
67. Vasanman, T. C. and Stark, G. C., A study of the sulphydryl groups of the catalytic subunit of *Escherichia coli* aspartate transcarbamylase. The use of enzyme-5-thio-2-nitrobenzoate mixed disulfides as intermediates in modifying enzyme sulphydryl groups. *J. Biol. Chem.*, 245, 3565, 1970.
68. Marshall, M. and Cohen, P. P., Ornithine transcarbamylase: Ordering of 5-cyanopeptides and location of characteristically cysteine residues within the sequence. *J. Biol. Chem.*, 255, 7287, 1980.
69. Ogilvie, J. W., Cleavage of phosphofructokinase at 5-cyanylated cysteine residues. *Biochim. Biophys. Acta*, 622, 277, 1980.
70. Klotman, L. A. and Jencks, W. P., Modification and inactivation of CoA transferase by 2-nitro-5-(thiocyanato) benzoic acid. *Biochemistry*, 20, 5183, 1981.
71. Haber, A. F. S. A., Reaction of protein sulphydryl groups with Ellman's reagent. *Methods Enzymol.*, 25, 457, 1972.
72. Talbot, M. M., Bell, A. W., and Duckworth, R. W., The reactions of *Escherichia coli* citrate synthase with the sulphydryl reagents 5,5'-dithiobis(2-nitrobenzoic acid) and 4,4'-dithiodipyridine. *Can. J. Biochem.*, 57, 822, 1979.
73. Soper, T. S., Jones, W. M., and Manning, J. M., Effects of substrates on the selective modification of the cysteinyl residues of D-amino acid transaminase. *J. Biol. Chem.*, 254, 10901, 1979.
74. Lukas, R. J. and Benaseth, E. L., Chemical modification and reactivity of sulphydryls and disulfides of rat brain nicotinic-like acetylcholine receptors. *J. Biol. Chem.*, 255, 5573, 1980.
75. Cockle, S. A., Rørdam, R. M., Stohary, J. G., and Moazzam, M. A., Nature of the cysteinyl residues in lipophilin from human myelin. *J. Biol. Chem.*, 255, 9182, 1980.
76. Hallaway, B. E., Hedlund, B. E., and Benson, E. S., Studies of the effect of reagent and protein charges on reactivity of the 893 sulphydryl group of human hemoglobin using selected mutations. *Arch. Biochem. Biophys.*, 203, 332, 1980.
77. Luthra, M. P., Dunlap, R. B., and Odell, J. D., Characterization of a new sulphydryl group reagent: 6,6'-diethynylbis(3-nitrobenzoic acid), a selenium analog of Ellman's reagent. *Anal. Biochem.*, 117, 94, 1981.
78. Claybalt, T. M., Taylor, D. F., and Hend, M. T., Reactivity of cysteine 18 in oncomodulin. *J. Biol. Chem.*, 265, 1800, 1990.
79. Kato, H., Tanaka, T., Nishio, T., Kimura, A., and Oda, J., Role of cysteine residues in glutathione synthetase from *Escherichia coli* B. Chemical modification and oligomerization site-directed mutagenesis. *J. Biol. Chem.*, 263, 11646, 1988.
80. Nierstian, C., Lal, C. S., Hsu, A., and McCarthy, J. J., One free sulphydryl group of plasma fibronectin becomes inactivable upon binding of the protein to solid substrates. *Biochemistry*, 27, 4970, 1988.
81. Poole, L. B. and Chaborn, A., Evidence for a single active-site cysteinyl residue in the streptococcal NADH peroxidase. *Biochem. Biophys. Res. Commun.*, 153, 261, 1988.
82. Drees, G. and Frakich, H., 2,4-Dinitrophenyl[¹⁴C]cysteinyl disulfide allows selective radiolabeling of protein thiols under spectrophotometric control. *Anal. Biochem.*, 188, 109, 1990.
83. Brandwisch, R. J., Lewicki, J. A., and Murad, F., Reversible inactivation of guanylate cyclase by mixed disulfide formation. *J. Biol. Chem.*, 256, 2958, 1981.
84. Kimura, T., Matsuda, R., Nakagawa, Y., and Kaiser, E. T., New reagents for the introduction of the thiomethyl group at sulphydryl residues of proteins with concomitant spectrophotometric titration of the sulphydryl: methyl 3-nitro-2-pyridyl disulfide and methyl 2-pyridyl disulfide. *Anal. Biochem.*, 122, 274, 1982.
85. Pedersen, A. O. and Jacobsen, J., Reactivity of the thiol group in human and bovine albumin at pH 3-9, as measured by exchange with 2,2'-dithiodipyridine. *Eur. J. Biochem.*, 106, 291, 1980.
86. Boyer, P. D., Spectrophotometric study of the reaction of protein sulphydryl groups with organic mercurials. *J. Am. Chem. Soc.*, 76, 4331, 1954.
87. Bai, Y. and Hayashi, R., Properties of the single sulphydryl group of carboxypeptidase Y. Effects of alkyl and aromatic mercurials on activities toward various synthetic substrates. *J. Biol. Chem.*, 254, 8473, 1979.
88. Ojcius, D. M. and Solomon, A. K., Sites of p-chloromercuribenzenesulfonate inhibition of red cell urea and water transport. *Biochim. Biophys. Acta*, 942, 73, 1988.
89. Clark, S. J. and Ralston, G. B., The dissociation of peripheral proteins from erythrocyte membranes brought about by p-mercuribenzenesulfonate. *Biochim. Biophys. Acta*, 1021, 141, 1990.
90. Marshall, M. and Cohen, P. P., The essential sulphydryl group of ornithine transcarbamylase-pH dependence of the spectra of its 2-mercuri-4-nitrophenol derivative. *J. Biol. Chem.*, 255, 7296, 1980.
91. Bieles, B. S. and Brodthurn, K., A thiol-labeling reagent and reactivity probe containing electrophilic mercury and a chromophoric leaving group. *Biochem. J.*, 179, 701, 1979.
92. Banks, T. E. and Shaffer, J. A., Inactivation of papain by S-methylation of its cysteinyl residue with O-methylisourea. *Biochemistry*, 11, 110, 1972.
93. Stark, G., Modification of proteins with cyanate. *Methods Enzymol.*, 11, 590, 1967.
94. Ghosh, P. B. and Whitehouse, M. W., 2-Chloro-4-nitrobenzo-2-oxa-1,3-diazole: a new fluorogenic reagent for amino acids and other amines. *Biochem. J.*, 108, 135, 1968.
95. Birckett, D. J., Price, N. D., Radda, G. K., and Salmons, A. G., The reactivity of SH groups with a fluorogenic reagent. *FEBS Lett.*, 6, 346, 1970.
96. Birckett, D. J., Dwek, R. A., Radda, G. K., Richards, R. E., and Salmons, A. G., Probes for the conformational transitions of phosphoribose. Effect of ligands studied by proton relaxation enhancement, fluorescence and chemical reactivities. *Eur. J. Biochem.*, 20, 494, 1971.
97. Lad, P. M., Woffman, N. M., and Hammes, G. G., Properties of rabbit muscle phosphofructokinase modified with 7-chloro-4-nitrobenzo-2-oxa-1,3-diazole. *Biochemistry*, 16, 4802, 1977.
98. Nitta, K., Bretcher, S. C., and Kronman, M. J., Anomalous reaction of 4-chloro-7-nitrobenzofuran with thiol compounds. *Biochem. J.*, 177, 385, 1979.
99. Dwek, R. A., Radda, G. K., Richards, R. E., and Salmons, A. G., Probes for the conformational transitions of phosphoribose. Effect of ligands studied by proton-relaxation enhancement, and chemical reactivities. *Eur. J. Biochem.*, 29, 509, 1972.
100. Carlberg, I. and Manservigi, B., Interaction of 2,4,6-trinitrobenzenesulfonate and 4-chloro-7-nitrobenzo-2-oxa-1,3-diazole with the active sites of glutathione reductase and lipamide dehydrogenase. *Acta Chem. Scand.*, B34, 144, 1980.
101. Toyooka, T. and Inel, K., New fluorogenic reagent having halogenbenzofuran structure for thiols: 4-(aminosulfonyl)-7-fluoro-2,1,3-benzoxadiazole. *Anal. Chem.*, 56, 1984.
102. Kirby, T. L., Reduction and fluorescent labeling of cysteine-containing proteins for subsequent structural analyses. *Anal. Biochem.*, 180, 231, 1989.
103. Niketic, V., Thomsen, J., and Kristiansen, K., Modification of cysteine residues with 2-bromoethanesulfonate. The application of S-sulfoethylated peptides in automatic Edman degradation. *Eur. J. Biochem.*, 46, 547, 1974.
104. Rafferty, M. A. and Cole, R. D., On the aminoethylation of proteins. *J. Biol. Chem.*, 241, 3457, 1966.
105. Plapp, B. V., Rafferty, M. A., and Cole, R. D., The tryptic digestion of S-aminoethylated ribonuclease. *J. Biol. Chem.*, 242, 265, 1967.
106. Matsui, B., Wagner, J. D., Talpes, C. J., Dimmock, J. R., Phillips, O. A., and Reid, R. S., 1-p-Chlorophenyl-4,4-dimethyl-5-diethylamino-1-penten-3-one hydrobromide, a sulphydryl-specific compound which reacts irreversibly with protein thiols but reversibly with small molecular weight thiols. *Anal. Biochem.*, 177, 237, 1989.

Chapter 7

THE MODIFICATION OF CYSTINE — CLEAVAGE OF DISULFIDE BONDS

There are several approaches to the cleavage of disulfide bonds in proteins. The majority of studies involve the cleavage of the disulfide bond of cystine to the free thiol group of cysteine by reduction. Reduction has been generally accomplished with a mild reducing agent such as β -mercaptoethanol or cysteine. Gorin and co-workers¹ have examined the rate of reaction of lysozyme with various thiols. At pH 10.0 (0.025 M borate), the relative rates of reaction were β -mercaptoethanol (2-mercaptoethanol), 0.2; dithiothreitol, 1.0; 3-mercaptopropionate, 0.4; and 2-aminoethanol, 0.01. The results with aminoethanethiol were somewhat surprising since the reaction (disulfide exchange) involves the thiolate anion and 2-aminoethanethiol would be more extensively ionized than the other mercaptans. Dithiothreitol has been a useful reagent in the reduction of disulfide bonds in proteins² as introduced by Cleland. Dithiothreitol and the isomeric form, dithioerythritol, are each capable of the quantitative reduction of disulfide bonds in proteins. Furthermore, the oxidized form of dithiothreitol has an absorbance maximum at 283 nm ($\Delta\epsilon = 273$) which can be used to determine the extent of disulfide bond cleavage.² The UV spectra of dithiothreitol and oxidized dithiothreitol are shown in Figure 1. Insolubilized dihydrolipoic acid has also been proposed for use in the quantitative reduction of disulfide bonds.⁴

Reduction of disulfide bonds can be controlled by various factors. Homandberg and Wai⁵ recently demonstrated that the reduction of urokinase by dithiothreitol in the presence of arginine allows the selective reduction of a disulfide bond joining the catalytically active chain to a nonessential 13 amino acid peptide. A synthetic peptide may then be coupled to the free sulfhydryl group.

In most proteins, the free sulfhydryl groups (cysteine) derived from the reduction of cystine will, at alkaline pH, fairly rapidly undergo reoxidation to form the original disulfide bonds. This process can be accelerated by the sulfhydryl-disulfide interchange enzyme^{6,7} or sulfhydryl oxidase.⁸ Thus, it is necessary to "block" the new sulfhydryl groups by alkylation, arylation or reaction with dithionite (see Chapter 6).

A novel reaction has been developed by Neumann and co-workers¹⁰ which allows for the reduction of disulfide bonds under mild conditions. Phosphorothioate reacts with disulfide bonds to yield the *S*-phosphorothioate derivatives. The reaction proceeds optimally at alkaline pH (pH optimum 9.7) and the reaction product, *S*-phosphorothioate cysteine, has an absorbance maximum at 250 nm ($\epsilon = 631 \text{ M}^{-1} \text{ cm}^{-1}$) as shown in Figure 2. Phosphorothioate does not absorb at this wavelength. This reagent has been used to study the reactivity of disulfide bonds in ribonuclease.¹⁰ In the absence of a denaturing agent (reaction conditions: tenfold molar excess of reagent, pH 9.0, 16 h at 25°C), two specific disulfide bonds (Cys₆₅ - Cys₇₂; Cys₃₈ - Cys₁₁₀) are converted to phosphorothioate derivatives. The resultant derivative of ribonuclease is fully active in hydrolysis of RNA and has increased activity in the hydrolysis of cyclic cytidylic acid. The synthesis of radiolabeled phosphorothioate from either [³²P] or [³⁵S] thiophosphoryl chloride was reported in this study.

Light and co-workers have examined the susceptibility of disulfide bonds in trypsinogen to reduction.¹¹ At pH 9.0 (0.1 M sodium borate), a single disulfide bond (Cys₁₇₉ - Cys₂₀₃) is cleaved in trypsinogen by 0.1 M NaBH₄. The resulting sulfhydryl groups are "blocked" by alkylation. The characterization of the modified protein has been performed by the same group.¹² The disulfide bond which is modified under these conditions is critical in establishing the structure of the primary specificity site in trypsin.

From the above studies, there is little doubt that the various disulfide bonds in a protein show different reactivity toward reducing agents. These differences in reactivity can be explored with various reagents and can be utilized with the aid of partial reduction followed

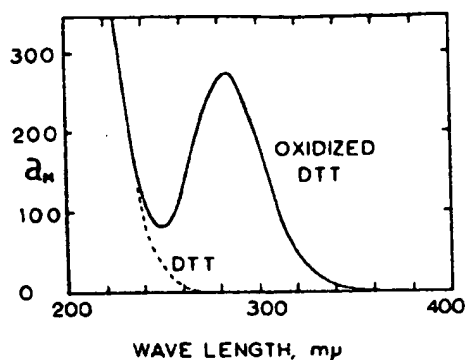


FIGURE 1. The absorption spectra of dithiothreitol (DTT) and oxidized dithiothreitol (oxidized DTT) in aqueous solution. (From Cleland, W. W., *Biochemistry*, 3, 480, 1964. With permission.)

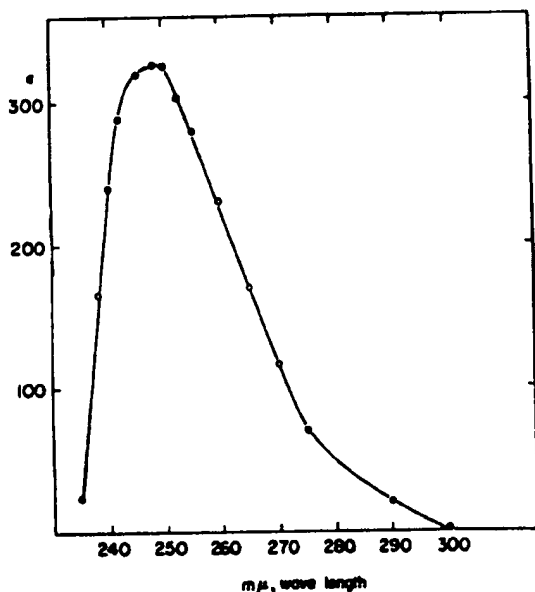


FIGURE 2. The absorption spectrum of the reaction product formed from cystine and phosphorothioate (PS). (From Neumann, H. and Smith, R. L., *Arch. Biochem. Biophys.*, 122, 354, 1967. With permission.)

by alkylation with radiolabeled iodoacetate to determine the position of disulfide bonds in proteins.¹³

Gorin and Godwin¹⁴ have reported that cystine can be quantitatively converted to cysteic acid by reaction with iodate in 0.1 to 1.0 M HCl. This reaction has been applied to insulin. The reaction product was not completely characterized, but given the relationship between iodate consumption and the cystine residues in insulin, the primary reaction is the oxidation

of disulfide reaction,

Disulfide by Donovan with an infrared Florence. in protein intermediates

The electrophoretic investigation reduced size and the reduction

Tri-n-butylperoxide is added to disulfide benzodiazole

Finally shown in proceeds such as cys of all cyst to form cys

This reaction in the absorption spectrum at 0.1 M sodium and 0.4 M

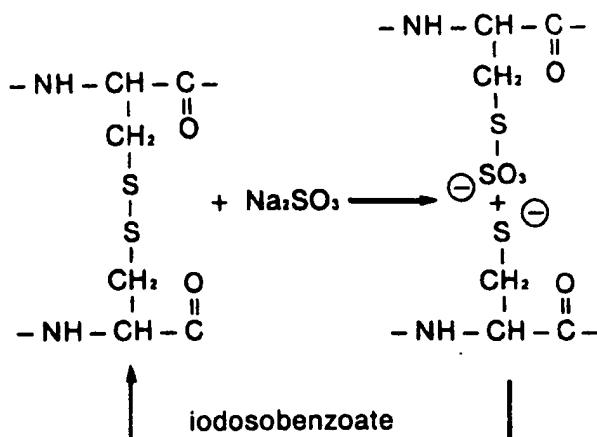


FIGURE 3. The cleavage of disulfide bonds by sodium sulfite to form the *S*-sulfo derivative.

of disulfide bonds. This reaction was complete in 15 to 30 min. After longer periods of reaction, the iodination of tyrosine residues occurred.

Disulfide bonds are somewhat unstable at alkaline pH (pH ≥ 13.0). This has been examined by Donovan in some detail.¹⁵ With protein-bound cystine, there is change in the spectrum with an increase in absorbance at 300 nm. This problem has been more recently studied by Florence.¹⁶ This investigation presented evidence to suggest that cleavage of disulfide bonds in proteins by base proceeds via β -elimination to form dehydroalanine and a persulfide intermediate which can decompose to form several products.

The electrolytic reduction of proteins has been explored by Leach and co-workers.¹⁷ These investigators recognized that although small peptides containing disulfide bonds could be reduced using cathodic reduction, there would likely be problems with proteins because of size and tertiary structure considerations. Therefore, a small thiol was used as a catalyst for the reduction.

Tri-*n*-butylphosphine will reduce disulfide bonds in proteins.¹⁸ The reaction is generally performed under alkaline conditions (pH 8.0, 0.1 *M* Tris or 0.5 *M* bicarbonate). *n*-Propanol is added to dissolve the tri-*n*-butylphosphine. This procedure has recently been used to reduce disulfide bonds in various proteins prior to reaction with 4-(aminosulfonyl)-7-fluoro-2,1,3-benzodiazole.¹⁹

Finally, disulfide bonds can be cleaved by sulfite to form the *S*-sulfonate derivative as shown in Figure 3. The chemistry of this reaction has been reviewed by Cole.²⁰ The reaction proceeds optimally at alkaline pH (pH 9.0). It is necessary to include an oxidizing agent such as cupric ions, or as shown in Figure 3, *o*-iodosobenzoate to ensure effective conversion of all cystine residues to the corresponding *S*-sulfonate derivatives. The reaction is reversible to form cysteine upon treatment with a suitable mercaptan such as β -mercaptoethanol.

This reaction has been adapted to the controlled reduction of disulfide bonds in proteins in the absence of denaturing agents.²¹ In the example presented, the disulfide bonds of bovine serum albumin were cleaved at pH 7.0 (0.1 *M* phosphate) at 40°C in the presence of 0.1 *M* sodium sulfite and simultaneously converted to the *S*-sulfo derivatives with oxygen and 0.4 mM cupric sulfate. The rate of reaction decreased markedly above pH 7.0.

REFERENCES

1. Gorin, G., Fulford, R., and Deonier, R. C., Reaction of lysozyme with dithiothreitol and with other mercaptans, *Experientia*, 24, 26, 1968.
2. Cleland, W. W., Dithiothreitol, a new protective reagent for SH groups, *Biochemistry*, 3, 480, 1964.
3. Iyer, K. S. and Klee, W. A., Direct spectrophotometric measurement of the rate of reduction of disulfide bonds. The reactivity of the disulfide bonds of bovine α -lactalbumin, *J. Biol. Chem.*, 248, 707, 1973.
4. Gorecki, M. and Patchornik, A., Polymer-bound dihydrolipoic acid: a new insoluble reducing agent for disulfides, *Biochim. Biophys. Acta*, 303, 36, 1973.
5. Homandberg, G. A. and Wal, T., Reduction of disulfides in urokinase and insertion of a synthetic peptide, *Biochim. Biophys. Acta*, 1038, 209, 1990.
6. Fuchs, S., DeLorenzo, F., and Anfinsen, C. B., Studies on the mechanism of the enzymic catalysis of disulfide interchange in proteins, *J. Biol. Chem.*, 242, 398, 1967.
7. Creighton, T. E., Hillson, D. A., and Freedman, R. B., Catalysis by protein-disulphide isomerase of the unfolding and refolding of proteins with disulphide bonds, *J. Mol. Biol.*, 142, 43, 1980.
8. Janollino, V. G., Sliwowski, M. Y., Swalsgood, H. F., and Horton, H. R., Catalytic effect of sulfhydryl oxidase on the formation of three-dimensional structure in chymotrypsinogen A, *Arch. Biochem. Biophys.*, 191, 269, 1978.
9. Neumann, H. and Smith, R. L., Cleavage of the disulfide bonds of cystine and oxidized glutathione by phosphorothioate, *Arch. Biochem. Biophys.*, 122, 354, 1967.
10. Neumann, H., Steinberg, J. Z., Brown, J. R., Goldberger, R. F., and Sela, M., On the non-essentiality of two specific disulphide bonds in ribonuclease for its biological activity, *Eur. J. Biochem.*, 3, 171, 1967.
11. Light, A., Hardwick, B. C., Hatfield, L. M., and Sondack, D. L., Modification of a single disulfide bond in trypsinogen and the activation of the carboxymethyl derivative, *J. Biol. Chem.*, 244, 6289, 1969.
12. Knights, R. J. and Light, A., Disulfide bond-modified trypsinogen. Role of disulfide 179-203 on the specificity characteristics of bovine trypsin toward synthetic substrates, *J. Biol. Chem.*, 251, 222, 1976.
13. Mise, T. and Bahl, O. P., Assignment of disulfide bonds in the α -subunit of human chorionic gonadotropin, *J. Biol. Chem.*, 255, 8516, 1980.
14. Gorin, G. and Godwin, W. E., The reaction of iodate with cystine and with insulin, *Biochem. Biophys. Res. Commun.*, 25, 227, 1966.
15. Donovan, J. W., Spectrophotometric observation of the alkaline hydrolysis of protein disulfide bonds, *Biochem. Biophys. Res. Commun.*, 29, 734, 1967.
16. Florence, T. M., Degradation of protein disulphide bonds in dilute alkali, *Biochem. J.*, 189, 507, 1980.
17. Leach, S. J., Meschers, A., and Swanepoel, O. A., The electrolytic reduction of proteins, *Biochemistry*, 4, 23, 1965.
18. Ruegg, U. Th. and Rudinger, J., Reductive cleavage of cystine disulfides with tributylphosphine, *Meth. Enzymol.*, 47, 111, 1977.
19. Kirley, T. L., Reduction and fluorescent labeling of cyst(e)ine-containing proteins for subsequent structural analysis, *Anal. Biochem.*, 180, 231, 1989.
20. Cole, R. D., Sulfitolysis, *Meth. Enzymol.*, 11, 206, 1967.
21. Kella, N. K. D. and Kinsella, J. E., A method for the controlled cleavage of disulfide bonds in proteins in the absence of denaturants, *J. Biochem. Biophys. Meth.*, 11, 251, 1985.

The site what diffi functional carbon se; nucleophil character (Since the specific de been sugg possible a

Oxidati conditions attention i periodate³ thionine v amine T chloramin methionin acids (i.e. of analysi reaction c studied th native en: sulphydry. prior mod methionyl Sakurai a oxidation 0.05 M T both chlor treated sa mosuccin

It is poe thus prov This can l zymatic a shown th: threitol, z was the rr well at co could be the reduc Methio and their amined ir methionir with cyste

39. Burstein, V., Walsh, K. A., and Neurath, H., Evidence of an essential histidine residue in thermolysin. *Biochemistry*, 13, 205, 1974.
40. Roemer, J. L., Reaction of histidine residues in proteins with diethylpyrocarbonate: differential molar absorptivities and reactivities. *Anal. Biochem.*, 88, 314, 1978.
41. Vangyaperte, W., Aepke, C., Kersters-Hilderson, H., and Teng, P., Single active-site histidine in D-xylose isomerase from *Streptomyces Volcanaruber*. Identification by chemical derivatization and peptide mapping. *Biochem. J.*, 263, 195, 1989.
42. Hordis, K., Teager, H., and McCormick, D. B., Evidence for an essential histidyl residue at the active site of pyruvate kinase (pyridoxal-5-phosphate) from rabbit liver. *J. Biol. Chem.*, 254, 6638, 1979.
43. Cordillo, E., Ayala, A., P-Lobato, M., Burstein, V., and Machado, A., Possible involvement of histidine residues in the loss of enzymatic activity of rat liver malic enzyme during aging. *J. Biol. Chem.*, 263, 8053, 1988.
44. Kinnunen, P. M., DeMichele, A., and Lange, L. G., Chemical modification of acyl-CoA:cholesterol O-acyltransferase. I. Identification of acyl-CoA:cholesterol O-acyltransferase subtypes by differential diethyl pyrocarbonate sensitivity. *Biochemistry*, 27, 7344, 1988.
45. Sahaja, A. K., and McFadden, B. A., Modification of histidine at the active site of spinach ribulose biphosphate carboxylase. *Biochem. Biophys. Res. Commun.*, 94, 1091, 1980.
46. Blomham, D. P., The chemical reactivity of the histidine-195 residue in lactate dehydrogenase thiomethylated at the cysteine-165 residue. *Biochem. J.*, 193, 93, 1981.
47. Cronmarty, T. H., Sulfhydryl and histidyl residues in the flavoenzyme alcohol oxidase from *Candida boidini*. *Biochemistry*, 20, 3416, 1981.
48. Bond, M. D., Stetler-Stuebe, D. B., and Van Wart, H. E., Identification of essential amino acid residues in *Clostridium histolyticum* collagenase using chemical modification reactions. *Biochem. Biophys. Res. Commun.*, 102, 243, 1981.
49. Baron, H. H., and Aub, J. L., Inactivation of dihydrofolate reductase from *Lactobacillus casei* by diethyl pyrocarbonate. *Biochemistry*, 21, 737, 1982.
50. Sams, C. F., and Matthews, K. S., Diethyl pyrocarbonate reaction with the lactose repressor protein affects both inducer and DNA binding. *Biochemistry*, 27, 2277, 1988.
51. Wold, F., Bifunctional reagents. *Methods Enzymol.*, 25, 423, 1972.

THE MODIFICATION OF LYSINE

The chemical modification of lysine residues in proteins is based upon the ability of the ϵ -amino group of this residue to react as a nucleophile. Under normal reaction conditions, lysyl residues are the second strongest nucleophiles in a protein molecule; cysteine is the most reactive nucleophile. However, for lysine to function optimally as a nucleophile, the proton usually bound to lysyl residues at physiological pH must be removed. This is shown in Figure 1. The protonated form is essentially unreactive. The pKa of an "average" lysyl residue in a protein is 10 (see Table 2 in Chapter 6). The majority of modification reactions are performed at pH 8.0 to 9.0.

It is somewhat difficult to selectively modify lysyl residues in proteins. A number of the reagents which are used to modify lysyl residues also have the potential to react with the N-terminal amino group(s), with tyrosyl residues and with cysteinyl residues.

Lysine residues can be modified by reaction with α -ketoalkyl halides such as iodoacetic acid.⁶ Acylation can occur at pH greater than 7.0 but the rate of reaction is much slower than reaction with cysteinyl residues. Both the mono- and disubstituted derivatives have been reported. The monosubstituted derivative migrates close to methionine on amino acid analysis while the disubstituted derivative migrates near aspartic acid. It should be noted that reaction with α -ketoalkyl halides is not considered particularly useful for the modification of primary amino groups. This reaction can be a possible side reaction occurring during the reduction and carboxymethylation of proteins. The reactivity of a given lysyl residue is affected by the nature of surrounding amino residues.

Both fluorodinitrobenzene and fluorodinitrobenzene have been of considerable value in protein chemistry since Sanger and Tuppy's work on the structure of insulin.⁷ Carty and Hirs⁸ developed the use of 4-sulfonyl-2-nitrofluorobenzene for the modification of amino groups in pancreatic ribonuclease (Figure 2). This is a particularly useful experiment since it is critical to understand that these investigators actually measured the amount of native protein remaining by chromatographic fractionation. As would be expected, the rate of modification increases with increasing pH. This reagent also is more stable than, for example, fluorodinitrobenzene under alkaline conditions, permitting more accurate measurement at pH greater than 9.0. The lysine residue at position 41 is the site of major substitution which is a reflection of the lower pKa for the ϵ -amino group of this residue. Use of this compound did not present the solubility and reactivity problems posed by the fluorodinitrobenzene compounds. It was possible to qualitatively determine the classes of amino groups in ribonuclease; these were the α -amino group, nine "normal" amino groups and lysine 41. The reactivity of lysine 41 was influenced by neighboring functional groups. This effect was lost at pH greater than 11 or on thermal denaturation of the protein. The reaction of 1-dimethylamino-naphthalene-5-sulfonyl chloride (dansyl chloride) has been useful both in the structural analysis and amino group modification with proteins. In one study,⁹ dansyl chloride (in acetone) is added to a solution of trypsin in 0.1 M phosphate, pH 8.0. The reaction is terminated after 24 h at 25°C by acidification to pH 3.0 with 1.0 M HCl. Insoluble material is removed by centrifugation and the supernatant fraction placed in dialysis. These investigators reported modification of the amino-terminal isoleucine and one lysine residue. The extent of modification was determined by absorbance at 336 nm ($\epsilon_m = 3.4 \times 10^4 M^{-1} cm^{-1}$). Reaction of dansyl chloride with phosphoenolpyruvate carboxylase has been used to introduce a fluorescent probe into this protein.¹⁰ A somewhat specific modification of one of the eight lysine residues was achieved. The extent of modification was determined by spectral analysis at 355 nm using an extinction coefficient of $3400 M^{-1} cm^{-1}$.

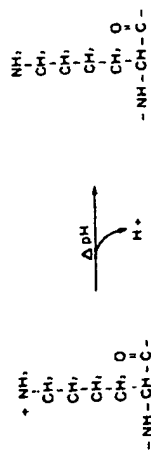


FIGURE 1. The structure of lysine.

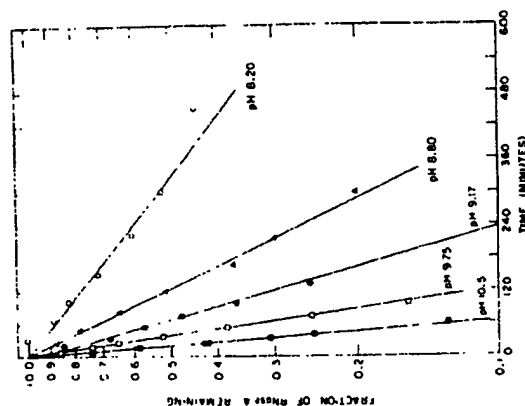


FIGURE 2. The reaction of bovine pancreatic ribonuclease A with 4-sulfonyloxy-2-nitrofluorobenzene (potassium salt) as a function of pH. The pH was maintained by addition of 0.2 *N* NaOH during the course of the reaction at 28°C. The amount of ribonuclease remaining was determined by chromatographic analysis (Averilite® IRC-50). (From Carry, R. P. and Hin, C. H. W., *J. Biol. Chem.*, 243, 5254, 1968. With permission.)

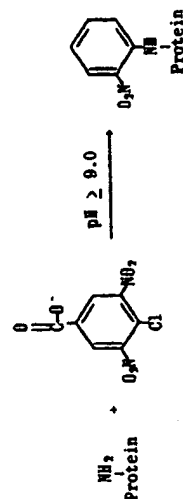


FIGURE 3. The reaction of an amino group with 4-chloro-3,5-dinitrobenzoate.

The reaction of 2-carboxy-4,6-dinitrochlorobenzene with proteins (Figure 3) has been explored.¹⁷ This reagent reacts with amino, sulphydryl, and amino groups. This reagent has recently been used for the modification of specific lysine residues in cytochrome c.¹⁸ The modification reaction (approximately 6-fold molar excess of reagent) was performed in 0.2 *M* sodium bicarbonate, pH 9.0 at ambient temperature for 24 h. The extent of modification was determined as described by Brautigan et al.¹⁸ The absorbance maximum of derivatives formed with various alkylamines was 436 nm with an extinction coefficient of $6.9 \times 10^3 \text{ M}^{-1} \text{ cm}^{-1}$. Chromatographic fractionation of the modified protein (sulfoethylcellulose) yielded six fractions with major lysine group modification. Hirasaka and Uchida¹⁹ examined the reaction of *N*-methyl-2-anilino-6-naphthalenesulfonyl chloride with lysyl residues in cardiac myosin. There was a difference in the nature of the reaction in the presence and absence of divalent cation. *N*-methyl-2-anilino-6-naphthalenesulfonyl chloride has been suggested for use as a fluorescent probe for hydrophobic regions of protein molecules.^{11,12} The extent of incorporation of the *N*-methyl-2-anilino-6-naphthalenesulfonyl moiety into protein can be determined by spectral analysis at 327 nm ($\Delta\epsilon = 2.0 \times 10^4 \text{ M}^{-1} \text{ cm}^{-1}$).^{11,12} Modification of protein amino groups with isothiocyanate derivatives of various dyes has proved to be an effective means of introducing structural probes into proteins at specific sites.¹³ Eosin isothiocyanate has been used to modify the lysyl residues in phosphoenolpyruvate carboxylase.⁵ The reagent was dissolved in dimethylsulfoxide/50 mM HEPES, pH 8.0 (50/50) immediately prior to use and added to the protein (in 50 mM HEPES, pH 8.0). The modified derivatives were used to determine the spatial proximity of the modified lysine residues using resonance energy transfer. Fluorescein isothiocyanate has been used to modify cytochrome P-450 (reaction performed in 30 mM Tris, pH 8.0 containing 0.1% Tween 80; 2 h at 0°C),¹⁴ actin (2 mM borate, pH 8.5; 3 h at ambient temperature then at 4°C for 16 h),¹⁵ and ricin (pH 8.1, 6°C for 4 h).¹⁶ The extent of modification with fluorescein isothiocyanate can be determined by spectroscopy using an extinction coefficient of $80,000 \text{ M}^{-1} \text{ cm}^{-1}$ at 495 nm (1% SDS with 0.1 *M* NaOH)¹⁴ or $74,500 \text{ M}^{-1} \text{ cm}^{-1}$ (0.1 *M* Tris, pH 8.0).¹⁵ Antibodies labeled with fluorescein have been used as targeted phototoxic agents.¹⁷ In this approach, the fluorescein moiety is iodinated resulting in a photodynamic sensitizer.

Welches and Baldwin¹⁸ have recently examined the reaction of bacterial luciferase with 2,4-dinitrofluorobenzene. The fluorescence of *N*-methyl-2-anilino-6-naphthalenesulfonyl derivatives is extremely sensitive to the polarity of the medium.¹⁸ Modification was associated with inactivation at the rate of $157 \text{ M}^{-1} \text{ min}^{-1}$ at pH 7.0 (0.05 *M* phosphate). Both lysyl and cysteinyl residues can be modified under the experimental conditions (0.05 *M* phosphate, pH 7.0 at 25°C) used in these studies. In order to assess the significance of reaction at primary amino groups, the cysteinyl residues were "blocked" with methyl methanethiosulfonate. Reaction of luciferase with methyl methanethiosulfonate resulted in greater than 95% loss of catalytic activity (twofold molar excess of methyl methanethiosulfonate in 0.02 *M* phosphate, pH 7.0 at 25°C). The loss of activity can be completely reversed with β -mercaptoethanol (97 mM). The small amount of residual activity present after treatment with methyl methanethiosulfonate is further reduced on treatment with 2,4-dinitrofluorobenzene and the recovery of activity subsequent to β -mercaptoethanol is greatly reduced (see Figure 4). Quantitative analysis was not performed but qualitative analysis suggested that the modification occurred at the α -amino group of methionine or the α - and/or β -subunits. The effects of pH on the reaction of fluorodinitrobenzene with luciferase is shown in Figure 5. It is of interest to compare the rate of reaction of fluorodinitrobenzene with model compounds and luciferase as has been done by these investigators as shown in Figure 6. Note that the rate of reaction with luciferase is much faster than with any of the model compounds. In a recent study, a combination of site-specific mutagenesis and site-specific chemical modification with 2,4-dinitrofluorobenzene was used to study lysine residues in angiotensin.²⁰

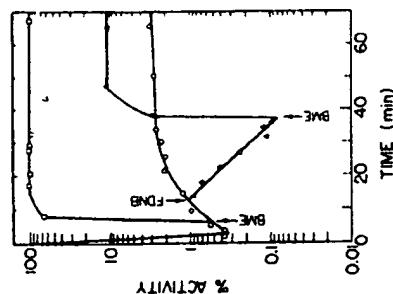


FIGURE 4. Protection of the thiol functional group reactivity with 2,4-dinitrofluorobenzene (FDNB) by prior reaction with methyl methanesulphonate-sulfonate. Three portions of the methyl methanesulphonate-luciferase were studied: the control preparation (O), a second portion treated with 97 mM β -mercaptoethanol (BME) (\square) (indicated by the BME arrow), and a third portion (Δ) which was allowed to react with FDNB (indicated by the FDNB arrow) which was allowed to proceed until 90% of the activity had been lost at which point β -mercaptoethanol (97 mM) was added (indicated by the BME arrow at approximately 40 min). (From Welch, W. R. and Baldwin, T. O., *Biochemistry*, 20, 512, 1981. With permission.)

Acylation of amino groups in proteins by reaction with carboxylic acid anhydrides has been extensively used. Riordan and Valle²¹ have discussed the process of acetylation in some detail. Acetylation is generally carried out with acetic anhydride at alkaline pH in either a pH-stat or in saturated sodium acetate. Performing the modification reaction under these latter conditions (saturated sodium acetate) results in increased specificity since *O*-acetyl tyrosine is unstable in sodium acetate. Acetylation has been used to study calicium²² and a bacterial cytochrome.²³ Acetic and maleic anhydride have been used to study elastase.²⁴ In these studies, the reaction was carried out in a pH-stat to maintain alkaline pH. Reaction occurred at both lysyl and tyrosyl residues. It is relatively easy to differentiate between the two sites of modification since *O*-acetyl tyrosyl residues are unstable at pH ≥ 9.0 . Studies with maleic anhydride showed that the amino terminal valine was not available for modification at pH 8.0 to 9.0 but could be modified at pH 11.0. Modification of this residue could be achieved in the presence of urea at a lower pH.

Competitive labeling (trace labeling) is a technique for determining the ionization state or constant and intrinsic reactivity of individual amino groups in a protein.²⁵ The method is based on the hypothesis that the individual amino groups will compete for a trace amount of radiolabeled reagent (the reagent is selected on the basis of nonselective reactivity with amino groups; with most studies, acetic anhydride has been the reagent of choice). The extent of radiolabel incorporation into the protein at a given site will then be a function of the pKa, microenvironment, and inherent nucleophilicity of that particular amino group.²⁵ After the reaction with the radiolabeled reagent is complete, the protein is denatured and complete modification at each amino group is achieved by the addition of an excess of unlabeled reagent. A reproducible digestion method (i.e., tryptic or chymotryptic hydrolysis) is used to obtain peptides from the completely modified protein. The peptides are separated by a chromatographic technique and the extent of radiolabel at each site determined. The

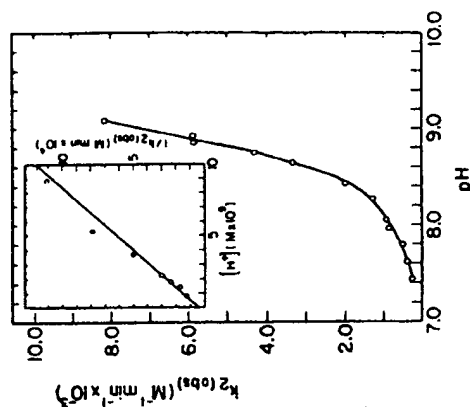


FIGURE 5. The pH dependence for the reaction of FDNB with luciferase. The observed second-order rate constant is plotted as a function of pH (0.05 M pyrophosphate). The inset shows a plot of the reciprocal of the observed second-order rate constant as a function of the hydrogen ion concentration permitting the evaluation of the absolute second-order rate constant for the reaction (k_2) ($2.4 \times 10^7 \text{ M}^{-1} \text{ min}^{-1}$) and an apparent pKa of 9.4. (From Welch, W. R. and Baldwin, T. O., *Biochemistry*, 20, 512, 1981. With permission.)

reagent or protein	functional group	k_2 (obsd) ($\text{M}^{-1} \text{ min}^{-1}$)
2-mercaptoethanol ^a	SH	5.5
<i>N</i> -acetylcysteine ^a	SH	6.3
<i>N</i> -acetyllysine ^a	NH ₂	0.013
methionine ^a	NH ₂	0.070
luciferase	NH ₂	15 ^b

^a Reactions were performed at pH 7.0, 20 °C, in 0.02 M phosphate buffer; the progress of the reaction was monitored spectrophotometrically.

FIGURE 6. The apparent second-order rate constants for the reaction of various functional groups with 2,4-dinitrofluorobenzene at pH 7.0 (0.02 M phosphate, 20 °C). (From Welch, W. R. and Baldwin, T. O., *Biochemistry*, 20, 512, 1981. With permission.)

extent of radiolabel incorporation at a given site is a function of the reactivity of that individual amino group under the reaction conditions used at the radiolabel step. An alternative approach^{36,37} involves a "trace" labeling step with tritiated acetic anhydride followed by complete modification with unlabeled acetic anhydride under denaturing conditions. This modified protein is then mixed with a preparation of the same protein which has been uniformly labeled with the ¹⁴C-labeled acetic anhydride. Digestion and separation of peptide is performed by conventional techniques (see above) and the extent of radiolabeling is determined. The ratio of ³H/¹⁴C in peptides containing amino groups is an indication of functional group reactivity. This method is somewhat more sensitive than the original method. Reductive methylation (see below) has also been used.²⁸

Although this is a laborious technique, the data obtained are excellent and provide considerable insight into the solution structure of proteins. There has been a consistent use of this technique for the study of troponin-T,³⁸ troponin-C,³⁹ troponin-I,³¹ calmodulin,^{32,34} and tropomyosin.³⁵ In particular, studies^{32,33} which have used this technique to assess conformational change in solution have been particularly rewarding.

More recently, trifluoroacetylated derivatives have been of interest in the study of protein structure. In these studies, ethylthiofluoroacetate was used to modify cytochrome c in 0.14 M sodium phosphate, pH 8.0.^{36,37} The pH was maintained at 8.0 using a pH-stat. Singly substituted derivatives of cytochrome c can be separated by chromatography on anion-exchange resin (Bio Rex 70) and carboxymethylcellulose. It is critical to avoid lyophilization during the preparation of the various derivatives. These derivatives have been subjected to further investigation^{38,39} including the use of ¹⁹F-containing derivatives for nuclear magnetic resonance probes.⁴⁰

Succinic anhydride has also proved useful in the modification of lysine.⁴¹ Modification of lysine residues with succinic anhydride results in charge reversal. Reaction with succinic anhydride frequently results in the dissociation of multimeric proteins and has also been used to "solubilize" insoluble proteins. Meighen and co-workers⁴² have produced a "variant" form of bacterial luciferase through reaction with succinic anhydride. The succinylated protein retained the dimeric subunit structure of the native enzyme. By complementation experiments involving the mixing/hybridization of the modified and native enzyme, it was determined that succinylation of bacterial luciferase resulted in the inactivation of the α -subunit without markedly affecting the function of the β -subunit. Shetty and Rao⁴³ studied the reaction of succinic anhydride with arachin. In this study, reaction of the protein was performed in 0.1 M sodium phosphate, pH 7.8, with the pH maintained over the course of the reaction by the addition of 2.0 M NaOH. The extent of modification was determined by reaction of the unmodified primary amino groups on the protein with trinitrobenzenesulfonic acid (see below). With a 200:1 molar excess of succinic anhydride, 82% of the available amino groups were succinylated with concomitant dissociation of the subunits of this protein. The reaction of chymotrypsinogen with succinic anhydride has been studied.⁴⁴ In these experiments, the reaction was performed under ambient conditions in 0.05 M sodium phosphate, pH 7.5. During the course of the reaction the pH was maintained at 7.5 by the addition of 1.0 M NaOH. Chymotrypsinogen (1 g) was dissolved in the sodium phosphate buffer and 50 mg of succinic anhydride was added over a 30-min period. Under these conditions, 8 of the 14 lysine residues were modified. A related reaction involves the trimesylation of amino groups in proteins (see Figure 7).⁴⁵ This reaction involves the modification of the protein with di(trimethylsilyl)trimelic acid. Removal of the blocking groups results in an extremely polar derivative. The procedure is suggested to have value in the solubilization of membrane proteins.

Citraconic anhydride has proved useful since the modification of lysine residues with this reagent is a reversible reaction (Figure 8). Reaction conditions for the modification of lysine residues in proteins are similar to those described above for other carboxylic acid anhydrides. Atassi and Habeeb⁴⁶ have discussed the use of this reagent in some detail. As an example,

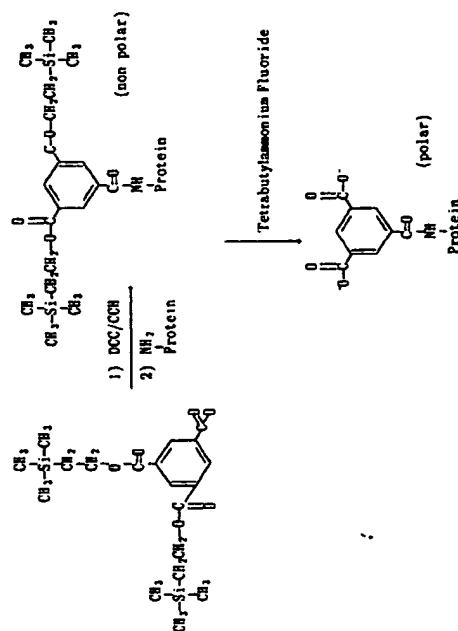


FIGURE 7. A scheme for the reaction of di(trimethylsilyl)trimelic acid with amino groups on protein and subsequent deprotection to produce a polar derivative.

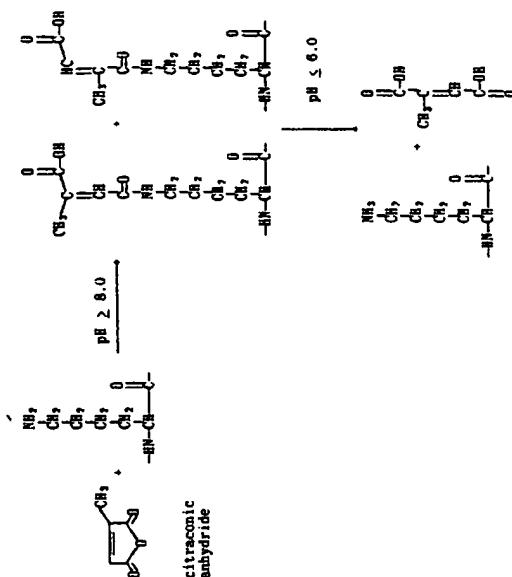


FIGURE 8. A scheme for the reversible reaction of lysine residues with citraconic anhydride.

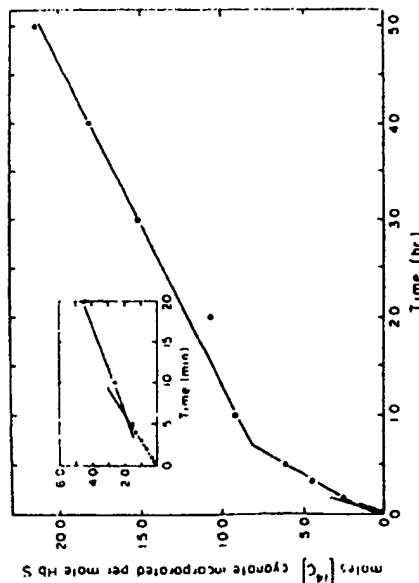


FIGURE 12. The carbamylation of the α - and ϵ -amino groups of oxymyoglobin S (cattle cell hemoglobin) as measured by the incorporation of $[^{14}\text{C}]$ sodium cyanate at pH 7.4 in a pH-stat. Portions were removed at the indicated periods of time, precipitated with cold 5% trichloroacetic acid. The inset describes the early phase of the reaction demonstrating that there are three distinct rates for the reaction. (From Lee, C. K. and Manning, J. M., *J. Biol. Chem.*, 248, 5861, 1973. With permission.)

hemoglobin S by countercurrent distribution. The same laboratory has examined the carbamylation of α -chain and β -chain in some detail.⁵⁰ With the deoxy protein, the ratio of radiolabel from ^{14}C -cyanate on α -chain as compared to the β -chain is 1.7:1.0 while it is 1:1 with the oxy protein. The carbamylation of the amino-terminal valine residues of hemoglobin is approximately 2.5-fold greater in partially deoxygenated media as compared to fully oxygenated media. Thus, it would appear the reactivity of the amino-terminal valine is a sensitive index of conformational change.⁵⁰ It is also of interest that removal of Arg⁴¹ (α) with carboxypeptidase B abolishes the enhancement of carbamylation observed with the removal of oxygen from hemoglobin.

Mahley and co-workers⁵¹ used carbamylation to explore the role of lysyl residues in the binding of plasma lipoprotein to fibroblasts. The reaction was performed in 0.3 M sodium borate, pH 8.0. The extent of modification was determined in two ways. In the first, the modified protein was subjected to acid hydrolysis. The amount of homocitrulline, the product of the reaction of the ϵ -amino group of lysine with cyanate, was considered equivalent to the number of lysine residues modified. However homocitrulline is partially degraded on acid hydrolysis to produce lysine (17 to 30%). In order to obviate this difficulty, these investigators removed a portion of the modified protein and reacted it under denaturing conditions with 2,4-dinitrofluorobenzene, yielding an acid-stable derivative. The number of lysine residues modified was therefore the sum of free lysine and homocitrulline obtained on amino acid analysis following acid hydrolysis.

In an elegant study by Plapp and co-workers,⁵² the modification of lysyl residues in bovine pancreatic deoxyribonuclease A by several different reagents, including cyanate, was examined as shown in Figure 15. The modification with cyanate is performed at 37°C in

Protein	$k \times 10^3 \text{ min}^{-1}$
CO-HbA	2.3
CO-HbS	2.4
Deoxy HbA	4.2
Deoxy HbS	4.0
CO-HMB- α_1	1.9
CO-HMB- α_2	1.8
CO-HMB- β_1	1.9
CO-HMB- β_2	1.6

FIGURE 13. pH dependence of first-order rate constants for the carbamylation of hemoglobin preparations with cyanate at pH 7.4. Carbamoyoxy-hemoglobin solutions (9.6 μM as tetramer) were carbamylated with radiolabeled sodium cyanate. Deoxyhemoglobin solutions were prepared as 7.5 μM as tetramer with approximately 1 mg $\text{Na}_2\text{S}_2\text{O}_4$. After 5 min, NaN^{14}CO (final concentration 20 mM) was added for initiation of the reaction. The rate constants are an average of four determinations for HbA and six determinations for HbS. The carbamoyoxy HMB- α and HMB- β chains of Hb. 30 μM , were incubated with 20 mM NaN^{14}CO . The precision of the kinetic constants is ± 0.50 for the deoxyhemoglobins. (From Lee, C. K. and Manning, J. M., *J. Biol. Chem.*, 248, 5861, 1973. With permission.)

1.0 M triethanolamine hydrochloride, pH 8.0. The extent of modification was determined by analysis for homocitrulline following acid hydrolysis. A time course of hydrolysis was utilized to provide for the accurate determination of homocitrulline since this amino acid slowly decomposes to form lysine during acid hydrolysis (see above). This modification was sensitive to the conformation of the protein since both the extent of modification and loss of catalytic activity depended on the presence or absence of calcium ions as shown in Figures 16 and 17.

Chollet and Anderson⁵³ have examined the modification of lysyl residues with potassium cyanate in the catalytic subunit of tobacco ribulose biphosphate carboxylase. The modification was performed in 0.050 M HEPES, 0.025 M NaCl, pH 7.4. Stoichiometry was not established in this study but it was noted that modification occurred at both the amino terminal and the ϵ -amino groups of lysine.

The reaction of imidoesters with the primary amino groups of proteins has been the subject of considerable investigation in the past 10 to 20 years. The most extensive use of this class of reagents has been the covalent cross-linking of proteins (see Chapter 15). These reagents have the particular advantage that the charge of the lysine residue is maintained during the modification as shown for the reaction of lysine with methyl acetimidate in Figure 18. Ethyl acetimidate has been used to study the role of lysyl residues in thrombin.⁵⁴ The reaction was performed with a 1000-fold molar excess of reagent in 0.02 M sodium borate-0.15 M NaCl, pH 8.5. Amino acid analysis indicated that approximately 80% of the lysyl residues were modified under these conditions. The modification of a glutamine synthetase from *Bacillus stearothermophilus* with ethyl acetimidate has been studied by Sekiguchi and co-workers.⁵⁵ The modification was performed at pH 9.5 with 0.2 M phosphate for 1 h at 35°C and terminated by dialysis at pH 7.2. The extent of modification was determined by titration of the modified protein with trinitrobenzenesulfonic acid. As these investigators suggest, consideration must be given to the possibility of cross-linking occurring with this reagent under the conditions used.⁵⁵ Monneron and d'Alayer⁵⁶ examined the reaction of either methyl acetamidate or dimethyl suberimidate with particulate adenylate cyclase. The

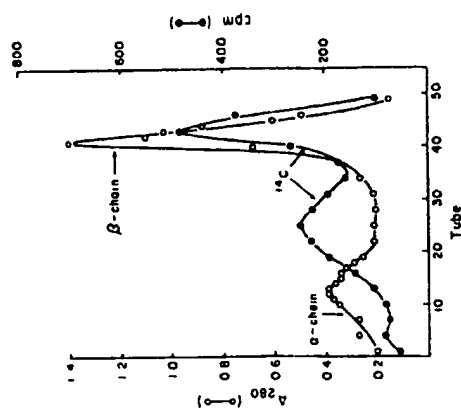


FIGURE 14. Countercurrent distribution patterns for carbamylated HbS (sickle cell hemoglobin). Oxygenated erythrocytes were incubated with 10 mM radiolabeled sodium cyanate for 1 h at 37°C. Globin was prepared from the labeled erythrocytes and subjected to 50 transfers in 1% dichloroacetic acid-2-butanol. (From Lee, C. K. and Manning, J. M., *J. Biol. Chem.*, 248, 5861, 1973. With permission.)

reaction was performed in 0.05 M triethanolamine, 10% (w/v) sucrose, 0.005 M MgCl₂, pH 8.1. Plapp and co-workers⁴¹ examined the reaction of methyl picolinimidate with pancreatic deoxyribonuclease. Methyl picolinimidate is an imidoester which reacts with the primary amino groups in proteins (Figure 19). The reaction was performed in 0.5 M triethanolamine hydrochloride, pH 8.0 containing 1 mM CaCl₂ with 0.1 M methyl picolinimidate for 22 h at 25°C, then with 0.2 M methyl picolinimidate for an additional 8 h. The extent of modification of a protein by methyl picolinimidate can be determined by spectral analysis (see Figure 20). Under these conditions, essentially all of the primary amino groups in deoxyribonuclease (nine lysine and one amino-terminal amino group) were modified but there was no change in biological activity. The work on DNase modification forms a particularly useful paper⁴¹ because of its wealth of experimental detail as well as the comparison of the reaction of deoxyribonuclease with four different reagents which modify primary amino groups: *O*-methylisourea, methyl picolinimidate, cyanate, and trinitrobenzenesulfonic acid. As mentioned above, the reaction of methyl picolinimidate with deoxyribonuclease either in the presence or absence of calcium ions resulted in the modification of essentially all of the primary amino groups without change in biological activity. Reaction of deoxyribonuclease with cyanate in either the presence or absence of calcium ions eventually resulted in the modification of all of the primary amino groups with the complete loss of biological activity (see Figures 16 and 17). Modification of seven to eight amino groups with trinitrobenzenesulfonic acid resulted in the loss of all biological activity (Figure 21), while reaction of a similar number of residues with *O*-methylisourea only resulted in approximately 50% inactivation (see Figure 15). Plapp has also studied the reaction of methyl picolinimidate with horse liver alcohol dehydrogenase.⁴² This study was somewhat unique

Derivative	Substructure	CD ₂₈₅ mdeg	% of native activity
Citabuloline		0	100
Picabuloline		0	100
α -Picabuloline		0	100
Carbamyl		0	100
Thiopyridine		0	100

* Assayed in the absence of Ca⁺⁺

FIGURE 15. The modification of bovine pancreatic DNase I by various reagents specific for the modification of lysine residues. The extent of lysine modification was determined by benzoylamine formation for reaction with *O*-methylisourea (guaranteed), radiolabeled sodium cyanate for carbamylation and spectroscopy for picolinimidation or trinitrobenzenylation. Enzymatic activity is expressed as a percent of that of a control preparation of DNase. (From Plapp, B. V., Moore, S., and Stein, W. H., *J. Biol. Chem.*, 246, 939, 1971. With permission.)

in that modification of the enzyme resulted in enhanced catalytic activity reflecting more rapid dissociation of the enzyme-coenzyme complex. It should be noted that the derivatized lysine reverts to lysine (60% yield) under the normal conditions of acid hydrolysis.

A number of investigators have used pyridoxal-5'-phosphate to modify lysyl residues in proteins. Pyridoxal-5'-phosphate is the cofactor form of vitamin B₆ and plays an important role in biological catalysis.⁴³ Pyridoxal phosphate is useful for the modification of lysine because of selectivity of reaction, spectral properties of the modified residue, reversibility of reaction, and the establishment of stereochemistry by use of radiolabeled sodium borohydride (sodium boronitride) to reduce the Schiff base initially formed on the reaction of pyridoxal phosphate with a primary amine. Pyridoxal phosphate will react with all primary amines (both ϵ -amino groups of lysine and the amino-terminal α -amino function) in a protein (Figure 22). In general, pyridoxal 5'-phosphate is far more reactive than pyridoxal because of intramolecular hemiacetal formation and the neighboring group effect of the phosphate moiety (Figure 23). Horecker and co-workers investigated the reaction of pyridoxal phosphate with rabbit muscle aldolase.⁴⁴ The initial reaction produced a species with an absorbance maximum at 430 nm reflecting the protonated Schiff base form of the pyridoxal phosphate-protein complex. After reduction with sodium borohydride, the absorbance maximum is at 325 nm which is characteristic of the reduced Schiff base. This is a quite useful

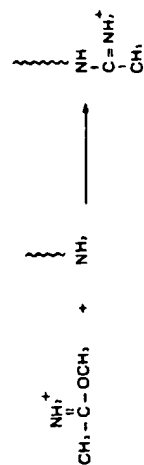


FIGURE 18. The reaction of lysine with methyl acetimidate.

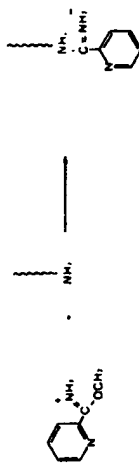


FIGURE 19. The reaction of amino groups with methyl picolinimidate.

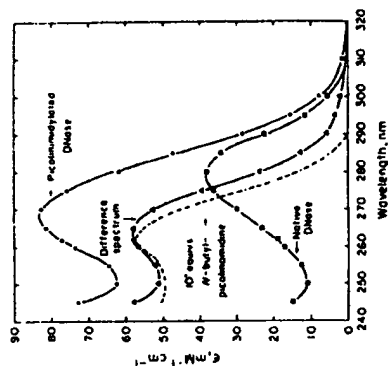


FIGURE 20. The UV spectra of native DNase and the picolinimidylated derivative. The spectra of picolinimidylated DNase (●) and native DNase (■) are presented together with the difference spectrum (Δ). From the absorbance at 262 nm and the extinction coefficient for *N*-butylpicolinamide ($3700 \text{ M}^{-1} \text{ cm}^{-1}$), it was calculated that the modified enzyme contained 10 picolinimidyl groups (the theoretical difference spectrum for this extent of modification is shown by the dashed line.) The products were dissolved in 0.05 M sodium acetate, 1 mM CaCl₂, and clarified by centrifugation prior to analysis. A molecular weight of 31,000 was assumed in the calculations. (From Plapp, B. V., Moore, S., and Stein, W. H., *J. Biol. Chem.*, 246, 939, 1971. With permission.)

142 Chemical Reagents for Protein Modification

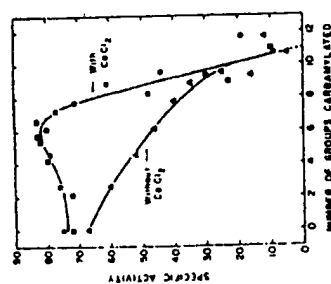


FIGURE 16. The modification of bovine pancreatic DNase I with potassium cyanate in the presence (●) or absence (Δ) of 10 mM CaCl₂. The calcium-free DNase was assayed in the presence (●) or absence (Δ) of 10 mM CaCl₂. (From Plapp, B. V., Moore, S., and Stein, W. H., *J. Biol. Chem.*, 246, 939, 1971. With permission.)

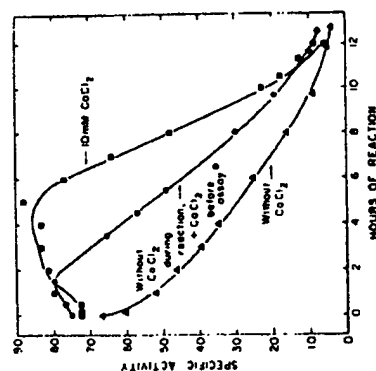


FIGURE 17. The inactivation of bovine pancreatic DNase with cyanate. The reactions were performed at pH 8.0 (1.0 M triethanolamine) in the presence of 1.0 M potassium cyanate at 37°C. In the experiment described with the solid squares, 10 mM CaCl₂ was present during the reaction with potassium cyanate. In the experiment with the solid circles, the enzyme carbamylated in the absence of calcium ions was diluted into 10 mM CaCl₂ 15 min prior to assay as compared to the experiment described with the solid triangles where the DNase was carbamylated and assayed in the absence of CaCl₂. (From Plapp, B. V., Moore, S., and Stein, W. H., *J. Biol. Chem.*, 246, 939, 1971. With permission.)

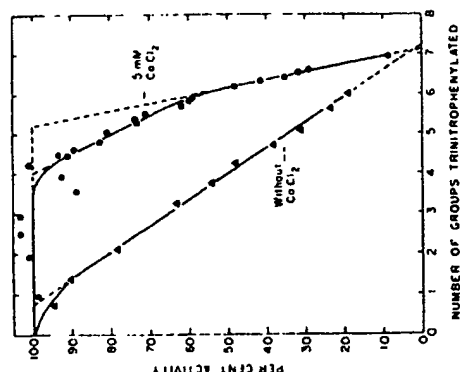


FIGURE 21. The reaction of bovine pancreatic DNase by 2,4,6-trinitrobenzenesulfonic acid. Reaction was accomplished in 0.3 M sodium borate buffer, pH 9.5 in the dark for 3 h in absence of added metal ion (O) or for 23 h in the presence of 5mM CaCl_2 (●). The extent of modification with 2,4,6-trinitrobenzenesulfonic acid was assessed by absorbance at 367 nm. (From Platt, B., V. Moore, S., and Stein, W. H., *J. Biol. Chem.*, 246, 939, 1971. With permission.)

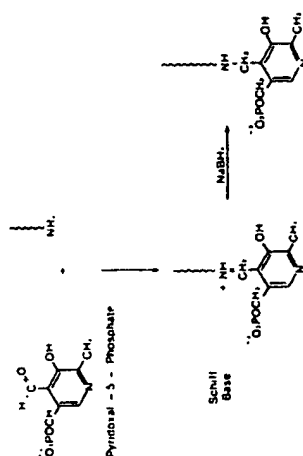


FIGURE 22. The reaction of pyridoxal-5-phosphate with amino groups in proteins.

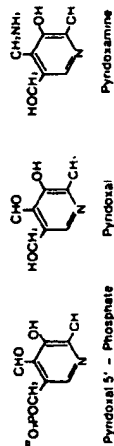


FIGURE 23. The structure of pyridoxal-5-phosphate, pyridoxal, and pyridoxamine.

study in that the difference in reactivity between pyridoxal and pyridoxal-5-phosphate is demonstrated as is the reversible nature of the initial complex. Schnackerz and Noltmann²⁰ compared the reaction of pyridoxal-5-phosphate and other aldehydes in reaction with rabbit muscle phosphoglucose at pH 8.0. Pyridoxal-5-phosphate (0.19 mM) resulted in 82% inactivation while the following results were obtained with other aldehydes: pyridoxal (8.4 mM), 16% inactivation; acetaldehyde (75 mM), 75% inactivation; and acetone (75 mM), 31% inactivation. This last reaction is of interest as many investigators are unaware that acetone can react with amino groups in proteins. The reaction of acetone with primary amino groups has been known for some time²¹ and is discussed in further detail below within the topic of reductive alkylation. The reaction of ribulose 1,5-bisphosphate carboxylase/oxygenase with pyridoxal-5-phosphate has been studied by Paech and Tolbert.²² Pyridoxal-5-phosphate inactivated the enzyme with or without reduction with NaBH_4 . This reaction was performed in 0.1 M Bicine (*N,N*-(2-hydroxyethyl) glycine), 0.010 M MgCl_2 , 0.2 mM EDTA, 0.001 M dithiothreitol. The reaction demonstrated an optimum at pH 8.4. Spectral studies showed the formation of a species absorbing at 432 nm. As is characteristic for the Schiff base derivative, this peak disappears on reduction to yield a species with an optimum at 325 nm ($\Delta\epsilon = 4800 \text{ M}^{-1} \text{ cm}^{-1}$). This supports the suggestion that the loss of activity observed on reaction with pyridoxal-5-phosphate is due to the formation of a Schiff base which can be reduced with NaBH_4 to form a stable derivative, as opposed to the formation of a 2-azolidine ring with a second nucleophile as has been observed by other investigators.²³⁻²⁵ Jones and Priest²⁶ have investigated the modification of apo-serine hydroxymethyltransferase with pyridoxal phosphate and the subsequent use of the enzyme-bound pyridoxal phosphate as a structural probe. Cortijo and co-workers²⁷ have suggested the use of the ratio of absorbance at 415 nm and 335 nm of enzyme-bound pyridoxal phosphate as an indication of the polarity of the medium. Cake and co-workers²⁸ have demonstrated that modification of activated hepatic glucorticoid receptor with pyridoxal-5-phosphate obviated the binding of the receptor to DNA. Greatly reduced inhibition was seen with pyridoxamine-5-phosphate, pyridoxamine, or pyridoxine (see Figure 24). Inhibition could be reversed by gel filtration or treatment with dithiothreitol while treatment with NaBH_4 resulted in irreversible inhibition of DNA binding. These investigators used 0.2 M borate, 0.25 M sucrose, 0.003 M MgCl_2 (pH 8.0) as the solvent for reaction with pyridoxal-5-phosphate. Siebe and Martinez-Carrion²⁹ have introduced the use of phosphopyridoxal trifluoroethyl amine as a probe for pyridoxal phosphate binding sites in enzymes (Figure 25). Nishigori and Tofte³⁰ explored the reaction of pyridoxal-5-phosphate with the avian progesterone receptor. Reaction with pyridoxal-5-phosphate was performed in 0.02 M barbitol, 10% (v/v) glycerol, 0.005 mM dithiothreitol, 0.010 M KCl, pH 8.0. The modification was stabilized by NaBH_4 . It is of interest that these investigators noted that the modification was readily reversed in Tris buffer unless stabilized by NaBH_4 . Sugiyama and Mukohata³¹ observed that modification with pyridoxal-5-phosphate of the lysine residue in chloroplast coupling factor using 0.020 M Tricine, 0.001 M EDTA, 0.010 M MgCl_2 , pH 8.0 resulted in complete inactivation of the ATPase activity. Peters and co-workers³² reported on the inactivation of the ATPase activity in a bacterial coupling factor by reaction with pyridoxal-5-phosphate. The modification was performed in 0.050 M morpholiniosulfonic acid, pH 7.5. The inhibition was

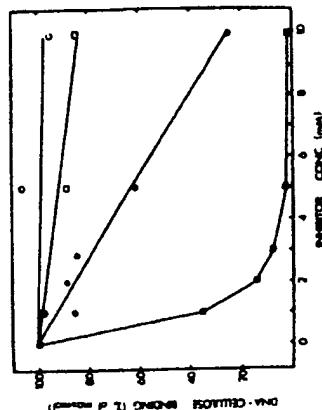


FIGURE 24. The specificity of the effect of pyridoxal-5'-phosphate on the DNA binding site of activated hepatic glucocorticoid receptor. The reactions were performed in 0.2 M boric acid, 0.25 M sucrose, 3 mM NaCl, pH 8.0 at 0°C. The reactions included either pyridoxal-5'-phosphate, 0.15 mM (□), 0.15 mM pyridoxamine-5'-phosphate, 0.15 mM (●), or pyridoxamine (O). In data not shown, pyridoxamine or phosphate ions were without effect in the inhibition of DNA binding by the activated receptor. (From Calk, M. A., DiSorbo, D. M., and Litwack, G., *J. Biol. Chem.*, 253, 4866, 1978. With permission.)

readily reversed by dilution or by 0.01 M lysine and was, as expected, stabilized by NaBH₄. Gould and Engel³³ reported on the reaction of mouse testicular lactate dehydrogenase with pyridoxal-5'-phosphate in 0.050 M sodium pyrophosphate, pH 8.7 at 25°C. This reaction resulted in the inactivation of the dehydrogenase activity. The inactivation was reversed by cysteine (Figure 26) and stabilized by NaBH₄. These investigators reported that the observed absorption coefficient at 325 nm may be decreased as much as 50% with protein-bound pyridoxal phosphate. Thus, estimation of the number of lysine residues modified using the absorption coefficient obtained with model compounds might provide only a minimum value. Ogawa and Fujioka³⁴ studied the reaction of pyridoxal-5'-phosphate with saccharopine dehydrogenase in 0.1 M potassium phosphate, pH 6.8, at ambient temperature in the dark. Both spectral analysis (Figure 27) and tritium incorporation from sodium borohydride reduction (Figure 28) were consistent with the modification of one lysine residue per mol of enzyme being responsible for the loss of enzyme activity. A value of $1 \times 10^4 \text{ M}^{-1} \text{ cm}^{-1}$ for the extinction coefficient at 325 nm³⁵ was used in this study. It is of interest that this study demonstrated that it is possible to establish an equilibrium between the native and modified forms of the enzyme. The reversibility of the modification is shown in Figure 28. Also shown in Figure 28 is a series of experiments designed to determine the equilibrium constant for the reaction using a graphical method where the reciprocal of the concentration of pyridoxal-5-phosphate is plotted vs. the activity at equilibrium (A_{eq}) divided by the value obtained ($A_0 - A_{eq}$) by subtracting the activity at equilibrium (A_{eq}) from the initial activity (A_0). The slope of this graph provides the equilibrium constant (K_{eq}) for the reaction under the experimental conditions (0.1 M potassium phosphate, pH 6.8 at 0°C). A value of $3.3 \times 10^3 \text{ M}^{-1}$ was obtained for the equilibrium constant as shown in Figure 29. Protection is not provided by α -ketoglutarate in the absence of the reduced coenzyme. Pyridoxal was much less effective than pyridoxal-5'-phosphate in the inactivation of saccharopine dehydrogenase. The concentrations of pyridoxal and pyridoxal-5'-phosphate were determined

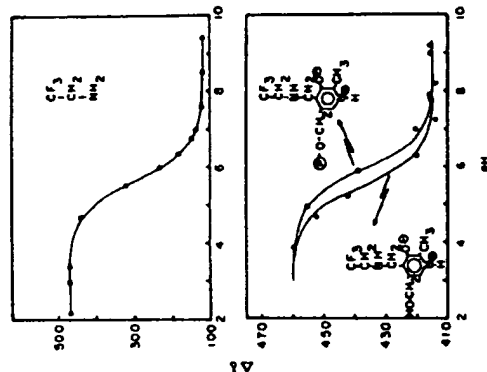


FIGURE 25. The pH dependence of the chemical shift response of ¹⁹F nuclear magnetic resonance with fluorinated compounds in the absence of enzymes. The top panel shows 2,2,2-trifluoroethylamine (100 mM). The solid curve indicates a theoretical titration curve of a simple ionization group for a pKa of 5.65. The bottom panel shows pyridoxal-5-phosphate (10 mM) before (●) and after (○) treatment with alkaline phosphatase. The solid lines show theoretical titration curves for a single ionization with a pKa of 5.90 and 5.30 respectively. (From Siebe, J. C. and Martinez-Carrion, M., *J. Biol. Chem.*, 253, 2093, 1978. With permission.)

spectrophotometrically in 0.1 M NaOH using an extinction coefficient of $5.8 \times 10^3 \text{ M}^{-1} \text{ cm}^{-1}$ at 300 nm and $6.6 \times 10^3 \text{ M}^{-1} \text{ cm}^{-1}$ at 388 nm respectively.³⁶ Amine compounds have the potential to interfere in the reaction of pyridoxal-5'-phosphate with proteins. Molodun and Cidlowski³⁷ demonstrate that 0.1 M Tris, pH 7.4 markedly interfered with the modification of rat uterine estrogen receptor with pyridoxal-5'-phosphate. These investigators also noted that, as in the other studies, 0.05 M lysine would block the modification reaction and could also reverse the modification if the Schiff base had not been reduced. Stock solutions of pyridoxal phosphate were prepared in 0.01 M NaOH to avoid acid decomposition. The importance of local environmental factors in the specificity of modification by pyridoxal phosphate is emphasized by Ohsawa and Gualerzi.³⁸ These investigators examined the modification of *Escherichia coli* initiation factor by pyridoxal phosphate in 0.020 M triethanolamine, 0.03 M KCl, pH 7.8. In the course of the studies, it was observed that pyridoxal phosphate will not react with poly (AUG). These investigators also reported the preparation of N⁶-pyridoxal lysine by reaction of pyridoxal phosphate with polylysine in 0.01 M sodium phosphate, pH 7.2 at 37°C followed by reduction with NaBH₄. The reduction was terminated by the addition of acetic acid. Acid hydrolysis (6 N HCl, 110°C, 22 h) yielded N⁶-pyridoxal-L-lysine. Bürger and Griesch³⁹ reported the inactivation of histidinol dehydrogenase upon reaction with pyridoxal phosphate in 0.02 M Tris, pH 7.6. This modification could be

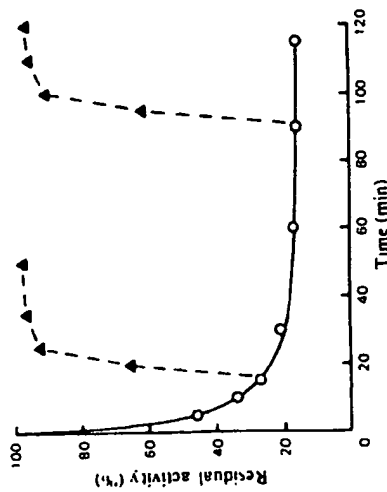


FIGURE 36. The L-cysteine reversal of the inactivation of mouse C_1 lactate dehydrogenase inactivated by pyridoxal-5'-phosphate. Mouse C_1 lactate dehydrogenase was incubated with 1 mM pyridoxal-5'-phosphate in the dark at 25°C in 0.05 M sodium pyrophosphate, pH 8.7 (O). At 15 min and 90 min, 0.2 ml portions of the reaction mixture were removed and mixed with 10 μ l of 1.0 M cysteine and assayed for enzyme activity at the time points indicated (Δ). (From Gould, K. G. and Eigel, P. C., *Biochem. J.*, 191, 365, 1980. With permission.)

reversed by dialysis unless the putative Schiff base was stabilized by reduction with NaH, (*n*-octyl) alcohol added to prevent foaming). These investigators used a $\Delta\epsilon$ for ϵ -amino pyridoxal lysine of $1 \times 10^4 \text{ M}^{-1} \text{ cm}^{-1}$ at 325 nm. Recent applications of pyridoxal-5'-phosphate modification have been used to study hydroxymethylbilane synthetase,⁴⁰ DNA polymerase I,⁴¹ and rabbit glycogen synthase isozymes.⁴² A novel affinity label (pyridoxal-5'-diphospho-5'-adenosine; see Figure 30) utilizing pyridoxal-5'-phosphate chemistry has been used to study the adenine nucleotide binding sites in yeast hexokinase.⁴³

A substantial portion of the specificity of pyridoxal-5'-phosphate in protein modification arises from electrostatic interaction(s) via the phosphate group with positively charged groups (i.e., arginine) on the protein surface. A conceptually related compound is methyl acetyl hydroxybutyrate dehydrogenase.⁴⁴ Manning and co-workers have examined the chemistry of the reaction of methyl acetyl phosphate with hemoglobin in some detail.^{45,46} It appears to be an affinity label for the 2,3-diphosphoglycerate binding site.⁴⁵ More recent work suggests that this reagent may be a useful probe for other anion binding sites in proteins.⁴⁶ The modification of primary amines in proteins by reductive alkylation has proved to be a useful reaction (Figure 32). This reaction has the advantage that the basic charge properties of the modified residue are preserved. The early work on this modification has been reviewed by Means and co-workers.⁴⁷ Both monosubstituted and disubstituted derivatives can be prepared depending upon reaction conditions and the nature of the carbonyl compound.

Rice and co-workers⁴⁸ reported the stabilization of trypsin by reductive methylation. This reaction utilized formaldehyde/sodium borohydride in 0.2 M sodium borate, pH 9.2 in the cold. Unsubstituted amino groups were present after the reaction as demonstrated by titration with trinitrobenzenesulfonic acid. The amino-terminal isoleucine residue was not modified

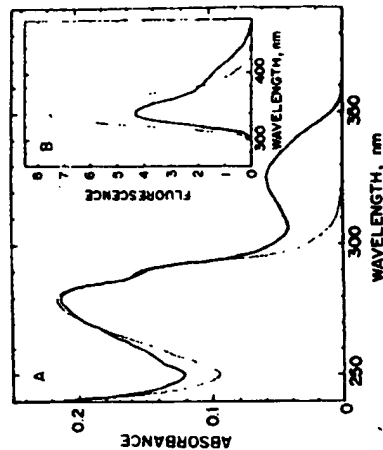


FIGURE 27. The UV spectra and fluorescence spectra of native and pyridoxal-5'-phosphate-treated saccharopine dehydrogenase (L-lysine forming). The enzyme preparation (17.9 nmol) was incubated with 0.5 mM pyridoxal-5'-phosphate in 0.1 M potassium phosphate, pH 6.8 followed by reduction with sodium borohydride and dialysis again with 0.1 M potassium phosphate, pH 6.8 in the dark. Panel A shows the UV absorption spectra for the native (dotted line) and modified enzyme (solid line). Panel B shows the fluorescence emission spectra for the native (dotted line) and the reduced enzyme (solid line). The excitation wavelength in the fluorescence spectrum was 280 nm. The protein concentrations for the native and modified enzyme were identical in these experiments. (From Ogawa, H. and Fujioke, M., *J. Biol. Chem.*, 255, 7420, 1980. With permission.)

under these conditions. Morris and co-workers⁴⁹ investigated the reductive methylation of monellin. The modification was performed in 0.2 M sodium borate, pH 8.0 with 1 mM monellin (11 mM) with respect to primary amino groups in the cold. Sodium borohydride was added to give a final concentration of 0.5 mg/ml, and 1 to 5 μ l of 6 to 8 M formaldehyde was added per ml of solution. Tritiated formaldehyde was used to establish the extent of modification. One of the problems with the use of formaldehyde in this reaction is the presence of paraformaldehyde. Chen and Benoit⁵⁰ obviated this difficulty by the *in situ* generation of formaldehyde from methanol.

The introduction of sodium cyanoborohydride as a reducing agent for this reaction represented a real advance. Sodium cyanoborohydride is stable in aqueous solution at pH 7.0. Unlike sodium borohydride which can reduce aldehydes and disulfide bonds, sodium cyanoborohydride only reduces the Schiff base formed in the initial process of reductive alkylation. The radiolabeling of proteins using ^{14}C -formaldehyde and sodium cyanoborohydride has been reported.⁵¹ The modification was performed in 0.04 M phosphate, pH 7.0 at 25°C. The modification can be performed equally well at 0°C but, as would be expected, takes a longer period of time; there is no effect on the extent of the modification. In this regard, these authors estimated that the same extent of modification obtained in 1 h at 37°C could be achieved in 4 to 6 h at 25°C or 24 h at 0°C. Although the majority of experiments in this study were performed in phosphate buffer at pH 7.0, equivalent results can be obtained in Tris or HEPES (*N*-2-hydroxyethylpiperazine-*N'*-2-ethanesulfonic acid) buffer at pH 7.0. A greater extent of modification was observed with sodium cyanoborohydride at pH 7.0 than with sodium borohydride at pH 9.0.

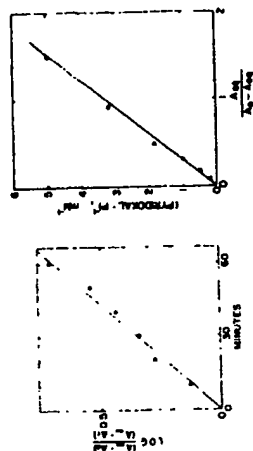


FIGURE 28. Left panel shows recovery of activity of saccharopine dehydrogenase inactivated by pyridoxal-5'-phosphate. The enzyme (2.5 nmol) was inactivated by reaction in 0.2 ml of 0.1 M potassium phosphate buffer, pH 6.8 at 0°C. After 30 min, 10- μ l portions were transferred to 1.7 ml 0.1 M potassium phosphate, pH 6.8 at 0°C. At the indicated times, portions were reduced with sodium borohydride and assayed for enzyme activity. A_t indicates enzyme activity at zero time. A_0 indicates enzyme activity at time 1 while A_t/A_0 indicates enzyme activity at equilibrium. The right panel shows a plot of the reciprocal of pyridoxal-5'-phosphate concentration vs. $A_t/A_0 - A_0$. Saccharopine dehydrogenase (2 nmol) was incubated in 0.1 M potassium phosphate, pH 6.8 and residual enzyme activity determined at 24°C. (From Ogawa, H., and Fujioaka, M., *J. Biol. Chem.*, 255, 7420, 1980. With permission.)

Reductive methylation with 14 C-enriched formaldehyde has been used to introduce an NMR probe for the study of protein conformation.¹⁰² A similar approach has been developed using deuterated acetone.¹⁰³

The effect of carbonyl compounds of different size on the extent of reductive alkylation has been examined by Feecey and co-workers.¹⁰⁴ The extent of modification is more a reflection of the type of alkylating agent and reaction conditions than an intrinsic property of the protein under study. For example, nearly 100% disubstitution can be obtained with formaldehyde and approximately 35% disubstitution with *n*-butanol, while only monosubstitution can be obtained with acetone, cyclopentanone, cyclohexanone, and benzaldehyde. While most of the products of reductive alkylation retained solubility, the reaction products obtained with cyclohexanone and benzaldehyde tended to precipitate. Examination of the reductive alkylation of ovomucoid, lysozyme, and ovotransferrin with different aldehydes suggests that such modification occurs without major conformational change as judged by circular dichroism measurements.¹⁰⁵ The same study also examined the stability of the modified proteins by scanning differential calorimetry. The extensive modification of amino groups decreases thermal stability. The destabilization effect increases with increasing size (and hydrophobicity) of the modifying aldehyde.

In another study, the reversible reductive alkylation of proteins has been examined.¹⁰⁶ Both glycylaldehyde and acetal will react with the primary amino groups in proteins to yield derivatives which can be cleaved with periodate under mild basic condition to yield the free amine. Figure 33 shows the distribution of reaction products of lysine and glycylaldehyde as a function of pH with either sodium borohydride (A) or sodium cyanoborohydride (B) as the reducing agent. It is apparent that sodium cyanoborohydride is much more effective in the range of pH 6.0 to pH 8.0 while sodium borohydride is more effective under more alkaline conditions. Treatment of 30.0 mg lysozyme in 6.0 ml 0.2 M sodium borate, pH 9.0, with 60 mg glycylaldehyde and 10 mg sodium borohydride at ambient temperature

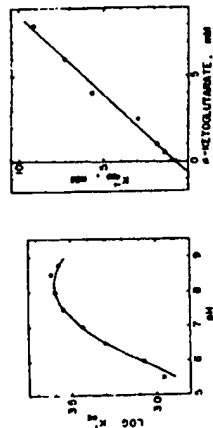


FIGURE 29. The left panel shows the effect of pH on the equilibrium constant for the inactivation of saccharopine dehydrogenase by pyridoxal-5'-phosphate. The enzyme (2.5 nmol) was incubated at 24°C with 0.1 M potassium phosphate at the indicated pH. Values for the equilibrium constant were calculated from the equation

$$K_{eq} = (A_0 - A_{eq})/A_{eq}[P]$$

The points were determined experimentally and the line was calculated from the following equation:

$$\log K_{eq} = \log K + \log \left(1 + \frac{[H^+]}{K_a} \right) + \frac{[H^+P]}{K_{eq}K_a} + \frac{[H^+P]}{K_{eq}K_aK_{eq}} - \log \left(1 + \frac{[H^+]}{K_a} + \frac{[H^+P]}{K_{eq}K_aK_{eq}} \right) - \log \left(1 + \frac{[H^+]}{K_a} \right)$$

The right panel shows a plot of reciprocal apparent equilibrium constant vs. α -ketoglutarate concentration. The enzyme (2 nmol) was incubated with 1.0 mM pyridoxal-5'-phosphate containing 0.2 mM reduced nicotinamide-adenine dinucleotide (NADH) and α -ketoglutarate at the concentrations indicated. The values for the equilibrium constants were calculated using the equation described above. (From Ogawa, H., and Fujioaka, M., *J. Biol. Chem.*, 255, 7420, 1980. With permission.)

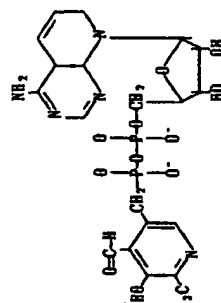


FIGURE 30. The structure of pyridoxal-5'-diphosphate-adenosine, an affinity label based on pyridoxal chemistry.

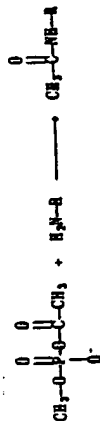


FIGURE 31. The structure of methyl acetyl phosphatate, a site-specific reagent for the modification of lysine residues in proteins.

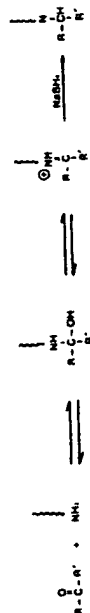


FIGURE 32. The reductive alkylation of amino groups in proteins.

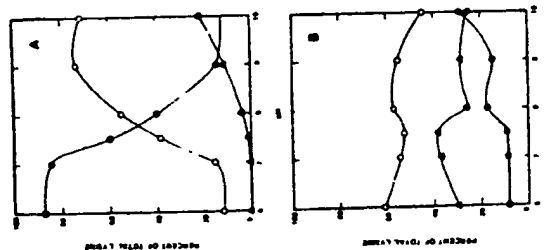


FIGURE 33. The pH dependence of the reductive alkylation of α -L-lysine using two different reducing agents. In panel A sodium borohydride was used as the reducing agent while in panel B sodium cyanoborohydride was used as the reducing agent. The composition of the reaction products was determined after removal of the α -N-acetyl group by acid hydrolysis. The products shown are lysine (●), ϵ -N-(2-hydroxyethyl)lysine (○), and ϵ -N-bis-(2-hydroxyethyl)lysine (▲). (From Goepfert, K. F., Cabacungan, J. C., Dixon, H. R. F., and Feeney, R. E., *Int. J. Peptide Protein Res.*, 17, 345, 1981. With permission.)

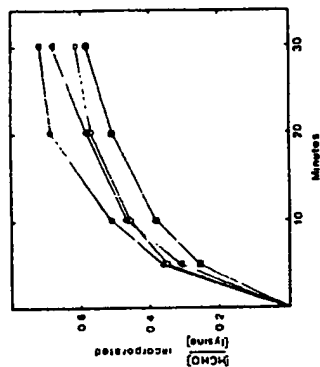


FIGURE 34. The effect of sodium cyanoborohydride concentration on the rate of reductive methylation of albumin. The reaction mixtures contained 1 mg/ml of albumin, 2 mM [^{14}C] formaldehyde in 0.1 M HEPES buffer, pH 7.5. The reaction mixtures were maintained at 22°C and terminated at the indicated points by the addition of trichloroacetic acid and incorporated radiolabel determined. The concentrations of sodium cyanoborohydride used in the experiments were 10 mM (●), 25 mM (▲), 100 mM (○), and 250 mM (○). (From Jenoff, N. and Dearborn, D. G., *J. Biol. Chem.*, 254, 4359, 1979. With permission.)

resulted in 60% 2-hydroxyethylation. Treatment of 20 mg ovomucoid in 2.0 ml 0.2 M sodium borate, pH 9.0 with 10% acetol and 30 mg sodium borohydride (added in portions) resulted in 55% hydroxyisopropylation. In both situations, the reaction was terminated by adjustment of the pH to 5 with glacial acetic acid. The extent of modification was determined either by titration with trinitrobenzenesulfonic acid and/or by amino acid analysis after acid hydrolysis. Periodate oxidation could be accomplished with 0.015 M sodium periodate at pH 7.9 for 30 min at ambient temperature.

The replacement of sodium borohydride with sodium cyanoborohydride appears to represent a significant advance in the stabilization of Schiff bases in proteins after reaction with carbonyl compounds. There are several difficulties associated with the use of sodium borohydride in this reaction including the reduction of aldehydes to alcohols, the dependence of reduction on pH, the reduction of disulfide bonds, and the possible cleavage of peptide bonds. Jenoff and Dearborn have studied the use of sodium cyanoborohydride in some detail.¹⁰⁷ In particular, the preparation of sodium cyanoborohydride is critical and most, if not all, commercial preparations require recrystallization prior to use. This reflects the presence of impurities which limit the extent of the reductive alkylation (see below). Recrystallization is accomplished by dissolving 11 g of sodium cyanoborohydride in 25 ml acetonitrile. Insoluble material is removed by centrifugation. Crystallization is accomplished by the addition of 150 ml methylene chloride and allowing to stand overnight at 4°C. The recrystallized sodium cyanoborohydride is collected by filtration and stored in a vacuum desiccator. A fresh solution of reagent is prepared daily. Using [^{14}C] formaldehyde and sodium cyanoborohydride, the major product is ϵ -methylated lysine, with minor incorporation of radiolabel into arginine and histidine. Figure 34 shows the effect of sodium cyanoborohydride incorporation on the extent of reductive methylation (^{14}C -formaldehyde) in 0.1 M HEPES buffer, pH 7.5. The rate of reductive methylation in this experiment with albumin was not sensitive to cyanoborohydride concentration. The effect of pH on the reaction is

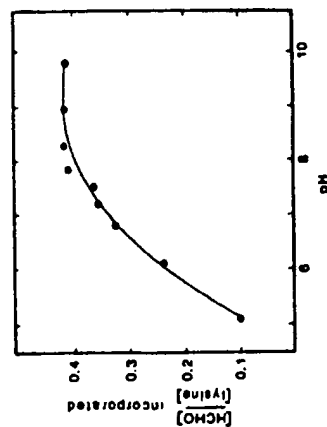


FIGURE 35. The pH dependence for the reductive methylation of lysine residues in albumin. The reaction mixtures contained 0.86 mg/ml of protein, 20 mM sodium cyanoborohydride, and 2 mM [14 C] formaldehyde and were incubated for 10 min at 22°C. The extent of modification was determined by incorporation of radio-label. The buffers used were sodium acetate (pH 5.1), sodium phosphate (pH 6.1 and pH 6.8), HEPES (pH 7.2 and 8.25), and sodium borate (pH 9.0 and 9.8). (From Jenoff, N. and Dearborn, D. G., *J. Biol. Chem.*, 254, 4359, 1979. With permission.)

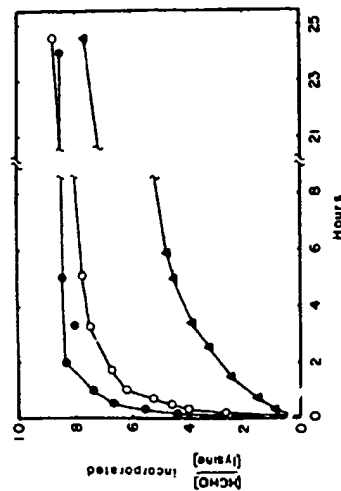


FIGURE 36. The effect of time and temperature on the reductive methylation of albumin. The reaction mixture contained 1.0 mg/ml albumin in 0.2 M HEPES, pH 7.5 in the presence of 20 mM sodium cyanoborohydride, and 2 mM [14 C] formaldehyde. The reactions were incubated at 4°C (Δ), 22°C (\circ), or 37°C (\bullet) for the indicated periods of time. (From Jenoff, N. and Dearborn, D. G., *J. Biol. Chem.*, 254, 4359, 1979. With permission.)

shown in Figure 35. Optimal reductive methylation was obtained at pH values greater than 8.0 during a short-term (10 min) incubation. The effect of pH is much less pronounced at longer periods of incubation (1 to 2 h) with optimal reductive methylation occurring between pH 7.0 and pH 8.0. The effect of temperature on the rate of reaction at pH 7.5 (0.1 M HEPES) is shown in Figure 36. Note that although the reaction is much slower at 4°C, the

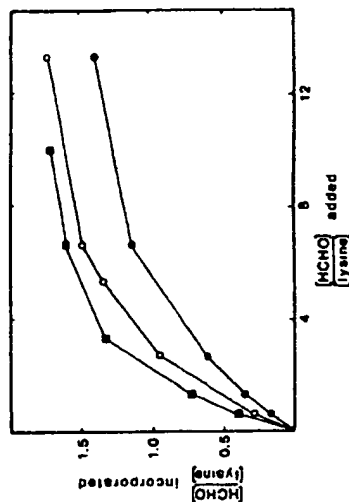


FIGURE 37. The effect of formaldehyde concentration and protein concentration on the reductive methylation of albumin. The reaction mixtures contained 20 mM sodium cyanoborohydride, with varying amounts of formaldehyde and albumin in 0.1 M HEPES buffer, pH 7.5. In (\circ), the reaction mixture contained 0.43 mg/ml albumin, in (\bullet), 1.07 mg/ml albumin and in (\square), 3.41 mg/ml albumin. The reactions were maintained at 22°C for 2 h. The extent of modification was determined by measuring the extent of radiolabel incorporated [14 C] formaldehyde. (From Jenoff, N. and Dearborn, D. G., *J. Biol. Chem.*, 254, 4359, 1979. With permission.)

extent of modification is almost equivalent to that achieved at higher temperature. The effect of formaldehyde concentration and protein concentration on the extent of reductive methylation is shown in Figure 37. An examination of this data suggests that approximately 80% modification can be achieved at a protein (bovine serum albumin) concentration of greater than 1 mg/ml at a formaldehyde/lysine ratio of 8 while virtually quantitative modification was obtained at a ratio of 12. These investigators also noted that Tris, β -mercaptoethanol, dithiothreitol, ammonium ions (as ammonium sulfate), and guanidine (5 M) inhibited the reductive alkylation of albumin by formaldehyde and sodium cyanoborohydride in 0.1 M HEPES, pH 7.5. The use of [14 C] formaldehyde in the reductive alkylation of ribonuclease has been reported.^{10a} In a subsequent study,^{10b} Jenoff and Dearborn characterized the inhibition by cyanide of reductive alkylation with sodium cyanoborohydride (Figure 38). This is of some importance since cyanide is a product of reductive alkylation with sodium cyanoborohydride. Inhibition by cyanide can be blocked by nickel (II) or cobalt (III). The observation that nickel (II) can preclude the inhibition of reductive alkylation by cyanide was shown to obviate the previously observed necessity for recrystallization of the sodium cyanoborohydride. The effect of NiCl₂ or KCN on the time course of the reductive methylation of bovine serum albumin at pH 7.5 (0.030 M HEPES) is shown in Figure 39. Additional studies on the development of reagents alternative to sodium borohydride have been reported from other laboratories. Feeney and co-workers¹⁰ compared sodium cyanoborohydride, dimethylamine borane, and trimethylamine borane (Figure 40) with respect to effectiveness in reductive alkylation. Reduction at disulfide bonds was not observed with any of the three reagents. Dimethylamine borane was only slightly less effective than sodium cyanoborohydride while trimethylamine borane was much less effective (Figure 41). This decrease in effectiveness in reductive alkylation is balanced by the absence of toxic by-products such as cyanide evolving during the reaction. Figure 42 compares dimethylamine borane and trimethylamine borane in the reductive methylation of turkey ovomucoid in

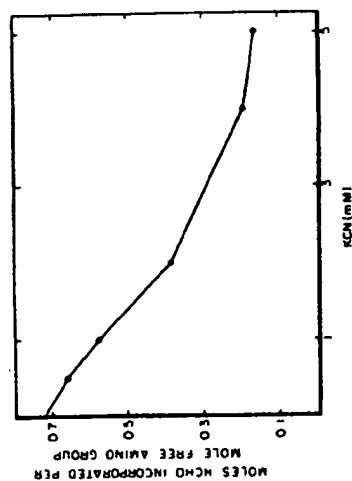


FIGURE 38. The effect of the addition of potassium cyanide (KCN) on the reductive methylation of albumin. Reaction mixtures contained 1.04 mg/ml bovine serum albumin, 2 mM [14 C] formaldehyde, 10 mM sodium cyanoborohydride in 0.05 M HEPES, pH 7.5 with varying amounts of KCN as indicated. The extent of modification was determined by measuring the amount of radiolabel incorporation. (From Jenioff, N. and Dearborn, D. G., *Anal. Biochem.*, 106, 186, 1980. With permission.)

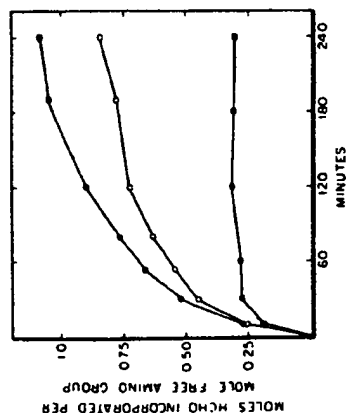


FIGURE 39. The effect of Ni(II) and KCN on the time course of the reductive methylation of albumin. The reactions were performed in 0.05 M HEPES, pH 7.5 with 10 mM sodium cyanoborohydride, and 2 mM [14 C] formaldehyde and incubated in the presence of either 2 mM NiCl $_2$ (●), 2 mM KCN (■), or no addition (O). (From Jenioff, N. and Dearborn, D. G., *Anal. Biochem.*, 106, 186, 1980. With permission.)

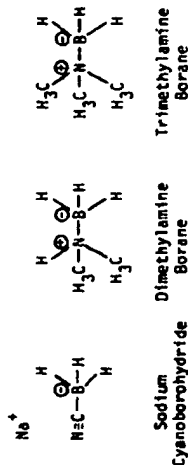


FIGURE 40. The structure of sodium cyanoborohydride, dimethylamine borane, and trimethylamine borane. (From Geopiegan, K. F., Cabocungan, J. C., Dixon, H. B. F., and Feeney, R. E., *Int. J. Peptide Protein Res.*, 17, 345, 1981. With permission.)

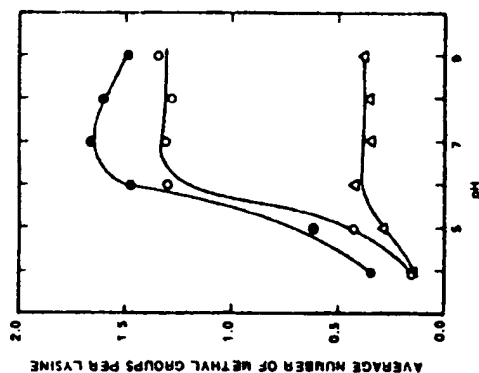


FIGURE 41. The effect of pH on the reductive methylation of turkey ovomucoid in the presence of various reducing agents. The concentration of turkey ovomucoid was 5 mg/ml, the concentration of formaldehyde was 20 mM in the presence of either sodium cyanoborohydride (●), 15 mM, dimethylamine borane (O), 15 mM, or trimethylamine borane (Δ), 15 mM. (From Geopiegan, K. F., Cabocungan, J. C., Dixon, H. B. F., and Feeney, R. E., *Int. J. Peptide Protein Res.*, 17, 345, 1981. With permission.)

0.2 M sodium phosphate, pH 7.0. Quantitative reductive methylation (equal to or greater than one methyl group per lysyl residue) is achieved at 10 mM formaldehyde with dimethylamine borane and at 50 mM formaldehyde with trimethylamine borane. It should be noted that a similar extent of modification is obtained with 5 mM formaldehyde using sodium cyanoborohydride. In a subsequent study¹¹¹ this laboratory reported the successful use of pyridine borane in the reductive alkylation of proteins. Wu and Means¹¹² have used reductive

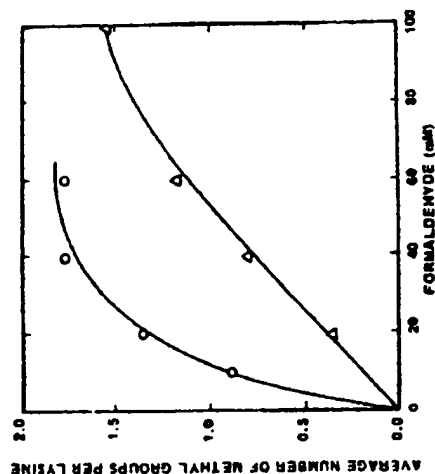


FIGURE 42. The effect of formaldehyde concentration on the reductive methylation of turkey ovomucoid. The reaction was performed in 0.2 M sodium phosphate, pH 7.0 with a turkey ovomucoid concentration of 5 mg/ml. The reducing agents were used at a concentration of 15 mM and included dimethylamine borane (O) and trimethylamine borane (Δ) at 22°C. The reducing agents were dissolved in methanol at a concentration of 150 mM and diluted 1:10 in the reaction mixture such that the final concentration of methanol was 10% (v/v). (From George, K. F., Cabocang, J. C., Dixon, H. B. F., and Feeney, R. E., *Int. J. Peptide Protein Res.*, 17, 345, 1981. With permission.)

alkylation with a nonpolar aldehyde (dodecylaldehyde) to subsequently prepare insoluble proteins by binding of the modified protein to octyl-Sepharose.

The reaction of glyceraldehyde with carbonmonoxymoglobin S has been explored by Acharya and Manning.¹³ This reaction was performed with 0.010 M glyceraldehyde in phosphate-buffered saline, pH 7.4, and the resultant Schiff bases were stabilized by reduction with sodium borohydride. Using radiolabeled glyceraldehyde, these investigators were able to obtain support for the concept that there is selectivity in the reaction of sugar aldehydes with hemoglobin. The reaction product between glyceraldehyde and hemoglobin S did have stability properties without reduction that were not consistent with only Schiff base products. These investigators suggested that the glyceraldehyde-hemoglobin Schiff base could undergo an Amadori rearrangement (Figure 43) to form a stable ketamine adduct which could be reduced with sodium borohydride to form a product identical to that obtained by direct reduction of the Schiff base. In a subsequent study, these investigators did show that the glyceraldehyde-hemoglobin S Schiff base could rearrange to form a ketamine via an Amadori rearrangement.¹⁴ These investigators were able to use reaction with phenylhydrazine to detect the protein-bound ketamine adduct as shown in Figure 44.

Another class of aldehydes that reacts with protein to give interesting products are simple monosaccharides which exist in solution in enol and keto forms (Figure 45). Wilson¹⁵ showed that bovine pancreatic ribonuclease dimer would react with lactose in the presence of sodium cyanoborohydride to yield an active derivative that shows selectivity in uptake by the liver during *in vivo* experiments. The modification of ribonuclease dimer was performed in 0.2 M potassium phosphate, pH 7.4 (phosphate buffer was used to protect lysine-41

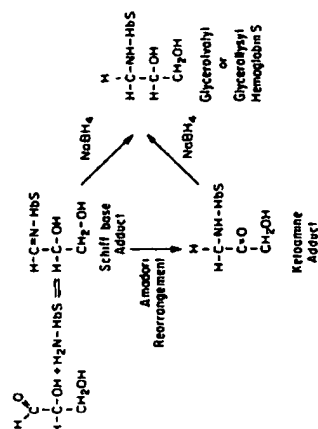


FIGURE 43. Schematic representation of the formation of glycerolaldehyde or glyceraldehyde on the reaction of hemoglobin S with glyceraldehyde. (From Acharya, A. S. and Manning, J. M., *J. Biol. Chem.*, 255, 1406, 1980. With permission.)

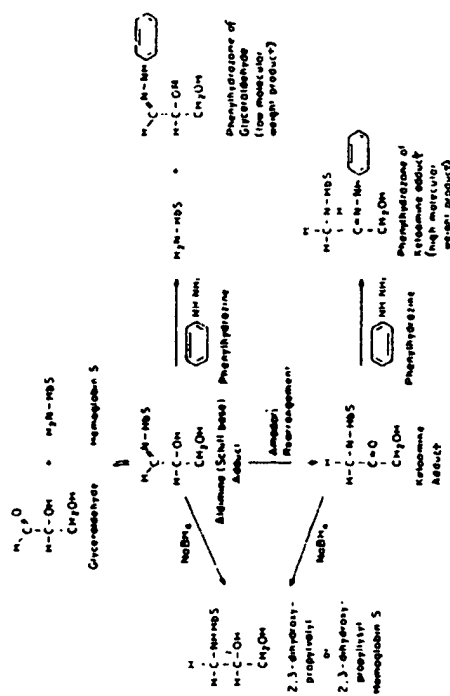


FIGURE 44. The reaction of the glyceraldehyde-hemoglobin adduct with either phenylhydrazine or sodium borohydride. (From Acharya, A. S. and Manning, J. M., *J. Biol. Chem.*, 255, 1406, 1980. With permission.)

from modification) at 37°C for 5 days with lactose and sodium cyanoborohydride. Under these conditions, 80% of the amino groups were modified. Bunn and Higgins¹⁶ have explored the reaction of monosaccharides with protein amino groups in the presence of sodium cyanoborohydride in some detail. These investigators studied the reaction of hemoglobin with various monosaccharides in Krebs-Ringer phosphate buffer, pH 7.3 (Figure 46). The extent of modification was determined using tritiated sodium cyanoborohydride. The rate of modification was demonstrated to be a direct function of the amount of each sugar in the carbonyl (or keto) form (Figure 47). Thus the k_1 ($\times 10^{-3} \text{ mM}^{-1} \text{ h}^{-1}$) for D-glucose is 0.6 with 0.002% in the carbonyl form while the k_1 ($\times 10^{-3} \text{ mM}^{-1} \text{ h}^{-1}$) for D-ribose is 10.0 with 0.05% in the carbonyl form.

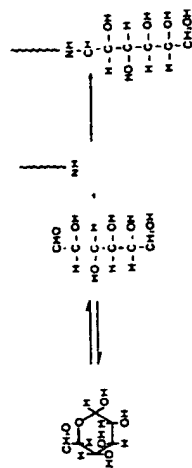


FIGURE 45 A scheme for the reaction of a monosaccharide with a primary amino group.

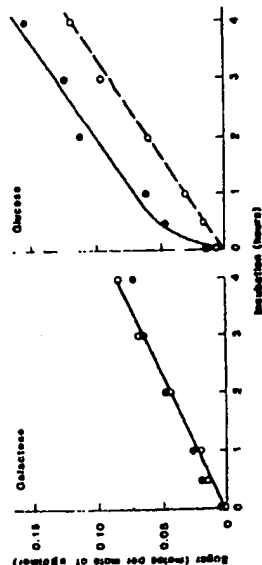


FIGURE 46 The measurement of the rate of condensation of monosaccharides with hemoglobin. The extent of reaction was measured either by incubation with unlabeled sugar followed by reduction of the aldimine linkage with tritiated sodium cyanoborohydride (open circles) or by incubation of the [^{14}C]-labeled sugar with hemoglobin followed by reduction with unlabeled sodium cyanoborohydride (closed circles). The left panel shows the rate of reaction with 42 mM D-galactose ($k_1 = 1.9 \times 10^{-3} \text{ mM}^{-1} \text{ h}^{-1}$). The right panel shows the reaction with 42 mM D-glucose ($k_1 = 0.6 \times 10^{-3} \text{ mM}^{-1} \text{ h}^{-1}$). The initial rapid rate of incorporation of D-[^{14}C] glucose can be explained by the small amount of rapidly reacting impurity remaining in the preparation (From Bunn, H. F. and Higgins, R. J., *Science*, 213, 222, 1981. With permission.)

The reaction of trinitrobenzenesulfonic acid with amino groups has been of value in studying the function and reactivity of the ϵ -amino groups of lysyl residues in proteins.^{117,118} The reaction of trinitrobenzenesulfonic acid with the primary amino groups in proteins is shown in Figure 48. The modification of amino groups with trinitrobenzenesulfonic acid is easy to monitor by spectral analysis. In the presence of an excess of sulfite, absorbance at 420 nm is the most sensitive index, having $\epsilon = 2.0 \times 10^4 \text{ M}^{-1} \text{ cm}^{-1}$. Absorbance at 420 nm is dependent upon the ability of the reaction product to form a complex with sulfite. It has proved convenient in our laboratories to use the fact that the spectrum of a trinitrobenzyl amino compound has an isobestic point at 367 nm with $\epsilon = 1.05 \times 10^4 \text{ M}^{-1} \text{ cm}^{-1}$. As suggested by Fields,¹²⁰ we recrystallize trinitrobenzenesulfonic acid from 2.0 M HCl prior to use. We generally perform the modifications in phosphate buffer (pH 6.0 to 9.0). The derivatives of α -amino groups and ϵ -amino groups have similar spectra with the exception that α -amino derivatives have a slightly higher extinction coefficient at 420 nm ($\epsilon = 2.20 \times 10^4 \text{ M}^{-1} \text{ cm}^{-1}$) than ϵ -amino groups ($\epsilon = 1.92 \times 10^4 \text{ M}^{-1} \text{ cm}^{-1}$). Both of these derivatives have much higher extinction coefficients than the derivative obtained by reaction of trinitrobenzenesulfonic acid with cysteinyl residues ($\epsilon = 2.25 \times 10^3 \text{ M}^{-1} \text{ cm}^{-1}$). The α -amino and ϵ -amino derivatives can be differentiated by their stability to acid or base

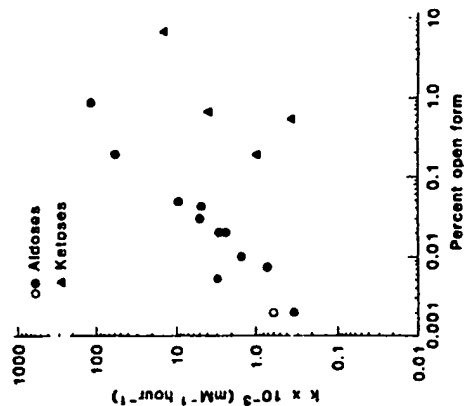


FIGURE 47 The relation between the rate of condensation of monosaccharide with hemoglobin and the equilibrium between the open and ring structures of the monosaccharide (I). The open circle is for glucose ($k_1 = 0.6 \times 10^{-3} \text{ mM}^{-1} \text{ h}^{-1}$). The closed circles represent data for other aldoses and the closed triangles for ketoses. (From Bunn, H. F. and Higgins, R. J., *Science*, 213, 222, 1981. With permission.)

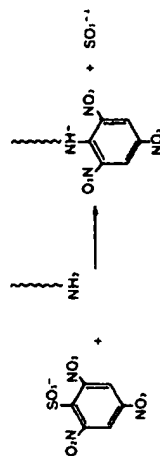


FIGURE 48 The reaction of 2,4,6-trinitrobenzenesulfonic acid with primary amines in proteins.

hydrolysis. The α -amino derivatives are unstable to acid hydrolysis (8 h at 110°C) or base hydrolysis.¹²¹

Frieden and co-workers have explored the reaction of trinitrobenzenesulfonic acid with bovine liver glutamate dehydrogenase.^{122,123} In these studies, the modification was performed in 0.04 M potassium phosphate, pH 8.0. Under these reaction conditions, the cysteinyl residues were not modified. The preparative reactions were terminated by reaction with β -mercaptoethanol. It is of interest that under certain conditions (with reduced coenzyme), glutamate dehydrogenase catalyzed the conversion of trinitrobenzenesulfonic acid to trinitrobenzene.¹²⁴

The reaction of trinitrobenzenesulfonic acid with simple amines and hydroxide ions has been studied in some detail by Means and co-workers.¹²⁵ The reaction of trinitrobenzene-

sulfonic acid with hydroxide is first-order with respect to both trinitrobenzenesulfonate and hydroxide ions. Reaction with amines was considered in some detail. In general, reactivity of trinitrobenzenesulfonate with amines increases with increasing basicity except that secondary amines and α -alkylamines are comparatively unreactive. The specific binding of trinitrobenzenesulfonate to proteins must be considered in the study of the reaction of this compound with proteins. Only amines with a pK_a greater than 8.7 follow a simple rate law. These investigators presented the following considerations regarding the reaction of trinitrobenzenesulfonic acid with proteins. Reactivity is a sensitive measure of the basicity of an amino group. Adjacent charged groups have an influence on the rate of reaction with an increase observed with a positively charged group and a decrease with a negatively charged group. Proximity to surface hydrophobic regions which can bind trinitrobenzenesulfonic acid can increase the observed reactivity of a particular amino group.

Flügge and Heldt have explored the labeling of a specific membrane component with trinitrobenzenesulfonic acid¹²⁶ and pyridoxal-5'-phosphate.¹²⁷ The modification of the phosphate translocation protein in spinach chloroplasts with trinitrobenzenesulfonic acid was performed in 0.050 M HEPES, 0.33 M sorbitol, 0.001 M $MgCl_2$, 0.001 M $MnCl_2$, 0.002 M EDTA, pH 7.6 at 4°C for periods of time up to 15 min at which point trinitrobenzenesulfonic acid was added to both terminate the reaction and radiolabel the trinitrophenyl borohydride.¹²⁸ It is possible to label components on the surface of membranes with trinitrobenzenesulfonic acid as the sulfonate moiety does not permit membrane penetration. The same is true for pyridoxal-5'-phosphate.

On occasion, the modification of an amino acid residue in a protein is associated with an apparent increase in catalytic activity. This was the situation with the modification of 14S and 30S dynein adenosine triphosphatase activities with trinitrobenzenesulfonic acid.¹²⁹ In this study, the reaction was performed in 0.030 M barbitol, pH 8.5 at 25°C. The extent of modification was determined spectrophotometrically at 345 nm ($\epsilon = 1.45 \times 10^4 M^{-1} cm^{-1}$). In studies similar to those obtained with glutamate dehydrogenase as discussed above,¹³⁴ glutathione reductase was demonstrated to reduce trinitrobenzenesulfonate.¹³⁰ Inhibition of glutathione reductase was noted at low concentration (0.05 μM) of trinitrobenzenesulfonate.

The reaction of trinitrobenzenesulfonic acid with ammonium has also been investigated by Whitaker and co-workers.¹³¹ This reaction was performed in tetraborate buffer and 1 μM sulfite. The rate of the reaction was determined by following the increase in absorbance at 420 nm ($\epsilon = 2.02 \times 10^4 M^{-1} cm^{-1}$). The rate of reaction with ammonium ($k = 0.128 min^{-1}$) was slower than that with the average amine in a protein ($k = 0.907 min^{-1}$ for enterotoxin) (Figure 49). The reaction with ammonium does, however, provide a sensitive assay for ammonia (as low as 6 nmol) with a precision of 1 to 2%.

The use of trinitrobenzenesulfonate in the selective modification of membrane surface components has been explored by Salem and co-workers.¹³² This study involved the modification of intact cells with the trinitrobenzenesulfonic acid (dissolved in methyl alcohol) diluted to a 1% methanolic solution. As mentioned above, trinitrobenzenesulfonate does not pass across (or into) membranes, being more hydrophilic than, for example, fluorodinitrobenzene.

Haniu et al.¹³³ have examined the reaction of lysine residues in NAD(P)H:quinone reductase with trinitrobenzenesulfonic acid as compared to the reaction of tyrosine residues with *p*-nitrobenzenesulfonyl fluoride. Isolation and characterization of the peptides containing the modified residues showed that the modified tyrosyl residues are in hydrophobic regions of the protein while the modified lysine residues are in hydrophilic regions. Other recent examples of the use of trinitrobenzenesulfonic acid for the site-specific chemical modification of proteins include placental 17 β -dehydrogenase,¹³⁴ a snake venom phospholipase A_{233} ,¹³⁵ rat liver 6-phosphogluconate dehydrogenase,¹³⁶ luffin-a,¹³⁷ and myosin.¹³⁸ In this latter study,

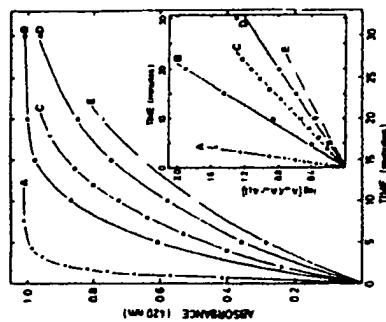


FIGURE 49. The reaction of 2,4,6-trinitrobenzenesulfonic acid (TNBS) with ammonia and the available amino groups of enterotoxin. The basic experimental approach was that described by Fields.¹³⁰ The rate assay involves the addition of TNBS to a reference cuvette containing only reagent and cuvette containing the sample. The difference in the rate of increase in absorbance at 420 nm is recorded (the buffer contains sodium sulfite). In the endpoint method, the reaction is allowed to proceed for a period of time at which point it is terminated by the addition of 0.1 M NaH_2PO_4 containing 1.5 mM sodium sulfite. The absorbance at 420 nm is then determined. Experiment A used the rate assay method with 6.7 μM enterotoxin at 25°C. Curve B used the endpoint method with 50 μM ammonium sulfate at 35°C. Curve C used the rate assay method with 50 μM ammonium sulfate at 25°C. Curve D used the endpoint method with 50 μM ammonium sulfate at 25°C with twice the TNBS concentration in the other experiments. Curve E used the endpoint method with 50 μM ammonium sulfate. The inset is a plot of the rate data according to the first-order rate equation. (From Whitaker, J. R., Granum, P. E., and Aveson, G., *Anal. Biochem.*, 108, 12, 1980. With permission.)

the peptides containing the modified lysine residues were isolated by immunoaffinity chromatography using an anti-trinitrophenyl antibody obtained from rabbits immunized with trinitrophenyl hemocyanin.

Guanidination of proteins is a reaction which is fairly specific for ϵ -amino groups.¹³⁹ This modification involves the reaction of *O*-methylisourea with lysyl residues at basic pH (pH >9) to yield homoarginine (Figure 50). This reaction is fairly slow and generally takes several days to go to completion. Bregman and co-workers¹⁴⁰ examined the modification of the single lysyl residue in glucagon. In this study 3.4 g *O*-methylisourea (*O*-methylisourea hydrogen sulfate) was dissolved in 20 ml H_2O and 6.0 g $Ba(OH)_2$ added followed by filtration or centrifugation to remove the resulting $BaSO_4$. The pH of the solution was adjusted to 11.0 and 200 mg glucagon added. The reaction was allowed to proceed for 8 h at 4°C and was terminated by the addition of glacial acetic acid. The products of the reaction were purified on Sulfopropyl-Sephadex. Guanidination of human recombinant erythropoietin has been accomplished with either *O*-methylisourea (Figure 50) or 1-guanyl-3,5-dimethylpyrazole (Figure 51).¹⁴¹ Seven of the eight lysine residues were modified with *O*-methylisourea while all eight lysine residues were modified with 1-guanyl-3,5-dimethylpyrazole. Both derivatives demonstrated increased biological activity.

With the exception of the Bouillon-Hunter reagent¹⁴² (Figure 52), the use of *N*-hydroxysuccinimide ester derivatives to modify lysine residues has been somewhat restricted to cross-linking reagents as described in Chapter 15. However, the specificity demonstrated by this chemistry provides considerable potential for the introduction of structural probes and other unique functional groups into proteins. Yen et al.¹⁴³ have used *N*-hydroxysuccinimide chem-

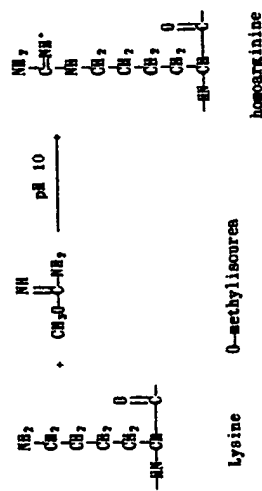


FIGURE 50 A scheme for the guanidination of lysine residues in proteins to produce homoarginine.

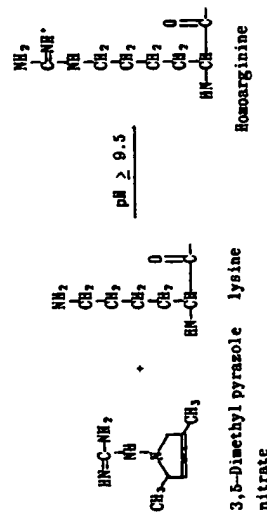


FIGURE 51 A scheme for the reaction of lysine with guanyl-3,5-dimethyl pyrazole to produce homoarginine.

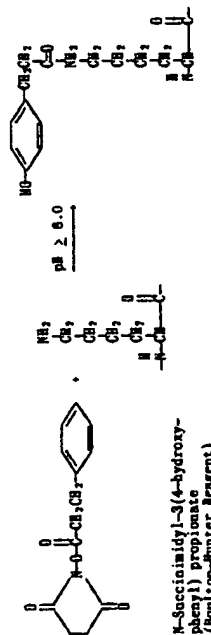


FIGURE 52 The structure of N-succinimidyl-3-(4-hydroxyphenyl) propionate (Boulton-Hunter reagent) and its reaction with lysine residues in proteins.

istry to introduce biotin into recombinant interleukin-1- β (Figure 53). This is a fascinating technology with substantial promise.^{146,145} It is possible to selectively modify the α -amino groups of proteins by chemical transamination with glyoxylate (Figure 54) at slightly acid pH.^{146,147} This modification has been applied to *Escherichia coli* C-552. This reaction was performed in 2.0 M sodium acetate, 0.10 M acetic acid, 0.005 M nickel sulfate, 0.2 M sodium glyoxylate and resulted in the

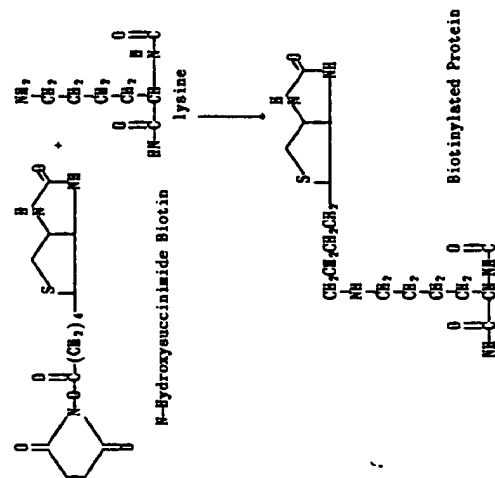


FIGURE 53 Incorporation of biotin into protein via reaction with an N-hydroxy succinimide derivative.

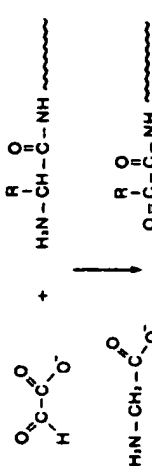


FIGURE 54 The modification of α -amino groups in proteins with glyoxylate.

complete loss of the amino-terminal residue. Snake venom phospholipase A₂ has been subjected to chemical transamination.¹⁴⁷ This reaction was performed in 2.0 M sodium acetate, 0.4 M acetic acid, 0.010 M cupric ions, 0.1 M glyoxylic acid, pH 5.5.

REFERENCES

1. Gund, P. R. N., Carboxymethylation. *Meth. Enzymol.*, 11, 532, 1967.
2. Sanger, F. and Tuppy, H., The amino acid sequence in the phenylalanyl chain of insulin. I. The identification of lower peptides from partial hydrolyses. *Biochem. J.*, 49, 463, 1951.
3. Curry, R. P. and Hirs, C. W., Modification of bovine pancreatic ribonuclease A with 4-sulfonyl-2-nitrofluorobenzene. *J. Biol. Chem.*, 243, 5254, 1968.
4. Franklin, J. G. and Leslie, J., Some enzymatic properties of trypsin after reaction with 1-dimethylamino-naphthalene-5-sulfonyl chloride. *Can. J. Biochem.*, 49, 516, 1971.

5. Wagner, R., Podest, F. E., González, D. H., and Andros, C. S., Proximity between fluorescent probes attached to four essential lysyl residues in phosphoenolpyruvate carboxylase — a resonance energy transfer study. *Eur. J. Biochem.*, 173, 561, 1988.
6. Braestling, D. L., Ferguson-Miller, S., and Margall-Gustash, E., Definition of cytochrome c binding domains by chemical modification. I. Reaction with 4-chloro-3,5-dinitrobenzoate and chromatographic separation of singly substituted derivatives. *J. Biol. Chem.*, 253, 130, 1978.
7. Belles, J., Ujima, H., and Kartha, G., A new arylating agent, 2-carboxy-4,6-dinitrobenzoic acid. Reaction with model compounds and bovine pancreatic ribonuclease. *Int. J. Peptide Protein Res.*, 14, 199, 1979.
8. Hall, J., Zha, X., Yu, L., Yu, C.-A., and Millett, F., Role of specific lysine residues in the reaction of Rhodobacter sphaeroides cytochrome c₁ with the cytochrome b₆ complex. *Biochemistry*, 28, 2568, 1989.
9. Long, J. E., Durham, B., Ohamura, M., and Millett, F., Role of specific lysine residues in binding cytochrome c₁ to the Rhodobacter sphaeroides reaction center in optimal orientation for rapid electron transfer. *Biochemistry*, 28, 6970, 1989.
10. Hiratsuka, T., and Uchida, K., Lysyl residues of cardiac myosin accessible to labeling with a fluorescent reagent, N-methyl-2-amino-6-naphthalenesulfonyl chloride. *J. Biochem.*, 88, 1437, 1980.
11. Ogonowski, M., Shikawa, H., and Takagi, T., Fluorescent probes for antibody active sites. I. Production of antibodies specific to the N-methyl-2-amino-6-naphthalene-6-sulfonate group in rabbits and some fluorescent properties of the hapten bound to the antibodies. *J. Biochem.*, 79, 195, 1976.
12. Cory, R. P., Becker, B. R., Rosenbluth, R., and Isenberg, L., Synthesis and fluorescent properties of some N-methyl-2-amino-6-naphthalenesulfonyl derivatives. *J. Am. Chem. Soc.*, 90, 1643, 1968.
13. Haugland, R. P., *Molecular Probes. Handbook of Fluorescent Probes and Research Chemicals*, Molecular Probes, Inc., Eugene, OR, 1989, 37.
14. Tubb, J. J., Green, L., and Millett, F., Fluorescein isothiocyanate specifically modifies lysine 338 of cytochrome P-450₁ and inhibits adrenodoxin binding. *J. Biol. Chem.*, 264, 16421, 1989.
15. Miki, M., Interaction of Lys-61 labeled actin with myosin subfragment-1 and the regulatory proteins. *J. Biochem. (Tokyo)*, 106, 651, 1989.
16. Beckett, A., Ippolito, R., Brunsell, M., Kam, Z., Benveniste, M., Emswaul, F., Turpin, E., Allen, A., and Percy, J. P., Binding and internalization of ricin labelled with fluorescein isothiocyanate. *Biochem. Biophys. Res. Commun.*, 169, 602, 1990.
17. Derasathanan, S., Dab, T. A., Middea, W. R., and Neckers, D. C., Readily available fluorescein isothiocyanate-conjugated antibodies can be easily converted into targeted phototoxic agents for antibacterial, antiviral, and anticancer therapy. *Proc. Natl. Acad. Sci. U.S.A.*, 87, 2980, 1990.
18. Turner, D. C., and Broad, L., Quantitative estimation of protein binding site polarity. Fluorescence of N-acyliminophthalocyanones. *Biochemistry*, 7, 3381, 1968.
19. Welches, W. R., and Baldwin, T. O., Active center studies on bacterial luciferase: modification of the enzyme with 2,4-dinitrofluorobenzene. *Biochemistry*, 20, 512, 1981.
20. Shapiro, R., Fox, E. A., and Borden, J. F., Role of lysines in human angiotensin: chemical modification and site-directed mutagenesis. *Biochemistry*, 28, 1726, 1989.
21. Riordan, J. F., and Valle, B. L., Acetylation. 11, 565, 1967.
22. Merle, M., Lefevre, G., Stueh, J. F., Rosdals, D., and Milhaud, G., Acylation of porcine and bovine calactinin: effects on hypocalcemic activity in the rat. *Biochem. Biophys. Res. Commun.*, 79, 1071, 1977.
23. Aitman, I., The role of lysines in *Escherichia coli* cytochrome C-552. Chemical modification studies. *Arch. Biochem. Biophys.*, 181, 199, 1977.
24. Karthman, D., Jones, C., Gerber, A., Derrington, K. J., and Hedmann, T., On the reaction of acetic and maleic anhydrides with chitinase. Evidence for a role of the NH₂-terminal valine. *Biochemistry*, 13, 2891, 1974.
25. Kaplan, H., Sreenivas, K. J., and Hartley, B. S., Competitive labeling, a method for determining the reactivity of individual groups in proteins. The amino groups of porcine elastin. *Biochem. J.*, 124, 289, 1971.
26. Bonshard, H. R., Koch, G. L. E., and Harder, B. S., The aminoacyl tRNA synthetase-tRNA complex: detection by differential labeling of lysine residues involved in complex formation. *J. Mol. Biol.*, 119, 125, 1978.
27. Richardson, R. H., and Brew, K., Lactose synthase. An investigation of the interaction site of alpha-lactalbumin for galactosyltransferase by differential kinetic labeling. *J. Biol. Chem.*, 255, 3377, 1980.
28. Bieder, R., and Bonshard, H. R., The cytochrome c oxidase binding site on cytochrome c. Differential chemical modification of lysine residues in free and oxidase-bound cytochrome c. *J. Biol. Chem.*, 253, 6043, 1978.
29. Hitchcock, S. E., Zimmerman, C. J., and Sausley, C., Study of the structure of tropomyosin-T by measuring the relative reactivities of lysines with acetic anhydride. *J. Mol. Biol.*, 147, 125, 1981.

30. Hitchcock, S. E., Study of the structure of tropomyosin-C by measuring the relative reactivities of lysines with acetic anhydride. *J. Mol. Biol.*, 147, 153, 1981.
31. Hitchcock-De Gregori, S. E., Study of the structure of tropomyosin-I by measuring the relative reactivities of lysine with acetic anhydride. *J. Biol. Chem.*, 257, 7172, 1982.
32. Gledhill, D. P., Shiba, S. K., Brew, K., and Poett, D., Differential trace labeling of calmodulin. Investigation of binding sites and conformational states by individual lysine reactivities. Effects of beta-endorphin, trifluoroperazine, and ethylene glycol bis(beta-aminoethyl) ether-N,N'-tetraacetic acid. *J. Biol. Chem.*, 260, 13406, 1985.
33. Wei, Q., Jackson, A. E., Pervasi, K. L., Carrar, K. L., Lee, E. Y. C., Puett, D., and Brew, K., Effects of interactions of with calmodulin of the reactivities of calmodulin lysines. *J. Biol. Chem.*, 263, 1941, 1988.
34. Winkler, M. A., Fried, V. A., Merril, D. L., and Cheung, W. V., Differential reactivities of lysines in calmodulin complexed to phosphatase. *J. Biol. Chem.*, 262, 15466, 1987.
35. Hitchcock-De Gregori, S. E., Lewis, S. F., and Mistrak, M., Lysine reactivities of tropomyosin complexed with tropomyosin. *Arch. Biochem. Biophys.*, 264, 410, 1988.
36. Staudenmayer, N., Smith, M. B., Smith, H. T., Spies, F. K., Jr., and Millett, F., An enzyme kinetics and ¹⁹F nuclear magnetic resonance study of selectively trifluoroacetylated cytochrome c derivatives. *Biochemistry*, 15, 3198, 1976.
37. Smith, M. B., Staudenmayer, J., Ahmed, A. J., Staudenmayer, N., and Millett, F., Use of specific trifluoroacetylation of lysine residues in cytochrome c to study the reaction with cytochrome b₆ cytochrome c₁ and cytochrome oxidase. *Biochim. Biophys. Acta*, 592, 303, 1980.
38. Webb, M., Staudenmayer, J., and Millett, F., The use of specific lysine modifications to locate the reaction site of cytochrome c with sulfite oxidase. *Biochim. Biophys. Acta*, 593, 290, 1980.
39. Ahmed, A. J., and Millett, F., Use of specific lysine modifications to identify the site of reaction between cytochrome c and ferricyanide. *J. Biol. Chem.*, 256, 1611, 1981.
40. Smith, M. B., and Millett, F., A ¹⁹F nuclear magnetic resonance study of the interaction between cytochrome c and cytochrome C peroxidase. *Biochim. Biophys. Acta*, 626, 64, 1980.
41. Klotz, I. M., Succinylation. *Methods. Enzymol.*, 11, 576, 1967.
42. Meighem, E. A., Niedman, M. Z., and Hastings, J. W., Hybridization of bacterial luciferase with a variant produced by chemical modification. *Biochemistry*, 10, 4062, 1971.
43. Shetty, K. J., and Rao, M. S. N., Effect of succinylation on the oligomeric structure of anethin. *Int. J. Peptide Protein Res.*, 11, 305, 1978.
44. Shiao, D. P., Lumry, R., and Rajender, S., Modification of protein properties by change in charge. Succinylated chymotrypsinogen. *Eur. J. Biochem.*, 29, 377, 1972.
45. Morton, R. C., and Gerber, G. E., Water solubilization of membrane proteins. Extensive derivatization with a novel polar derivatizing reagent. *J. Biol. Chem.*, 263, 7989, 1988.
46. Alsadi, M. Z., and Habesh, A. F. S. A., Reaction of protein with citraconic anhydride. *Methods. Enzymol.*, 25, 546, 1972.
47. Habesh, A. F. S. A., and Alsadi, M. Z., Enzymic and immunochemical properties of lysozyme. Evaluation of several amino group reversible blocking reagents. *Biochemistry*, 9, 4939, 1970.
48. Shetty, K. J., and Klose, J. E., Ready separation of protein from nucleoprotein complexes by reversible modification of lysine residues. *Biochem. J.*, 191, 269, 1980.
49. Weisgraber, K. H., Lumsberry, T. L., and Mahley, R. W., Role of the lysine residues of plasma lipoproteins in high affinity binding to cell surface receptors on human fibroblasts. *J. Biol. Chem.*, 253, 9053, 1978.
50. Mahley, R. W., Weisgraber, K. H., Lumsberry, T. L., and Weisgraber, H. G., Accelerated clearance of low-density and high-density lipoproteins and retarded clearance of E. apoprotein-containing lipoproteins from the plasma of rats after modification of lysine residues. *Proc. Natl. Acad. Sci. U.S.A.*, 76, 1746, 1979.
51. Uraibe, I., Yamamoto, M., Yamada, Y., and Okada, H., Effect of hydrophobicity of acyl groups on the activity and stability of acylated thermolysin. *Biochim. Biophys. Acta*, 524, 435, 1978.
52. Howlett, G. J., and Wardrop, A. J., Dissociation and reconstitution of human erythrocyte membrane proteins using 3,4,5,6-tetrachlorophthalic anhydride. *Arch. Biochem. Biophys.*, 188, 429, 1978.
53. Stark, G. R., Stein, W. H., and Moore, S., Reaction of the cytosine present in aqueous urea with amino acids and proteins. *J. Biol. Chem.*, 233, 3177, 1960.
54. Stark, G. R., and Smyth, D. G., The use of cyanate for the determination of NH₂-terminal residues in proteins. *J. Biol. Chem.*, 238, 214, 1963.
55. Stark, G. R., Modification of proteins with cyanate. *Methods. Enzymol.*, 25, 579, 1972.
56. Shaw, D. C., Stals, W. H., and Moore, S., Inactivation of chymotrypsin by cyanate. *J. Biol. Chem.*, 239, 671, 1964.
57. Cermati, A., and Manning, J. M., Potassium cyanate as an inhibitor of the sickling of erythrocytes in vitro. *Proc. Natl. Acad. Sci. U.S.A.*, 68, 1180, 1971.

58. Lee, C. K. and Manning, J. M., Kinetics of the carbamylation of the amino groups of sickle cell hemoglobin by cyanate. *J. Biol. Chem.*, 248, 5861, 1973.
59. Nilkann, N., Jones, W. M., Nigam, A. M., Williams, R. C., Jr., and Manning, J. M., Carbamylation of the chains of hemoglobin S by cyanate in vitro and in vivo. *J. Biol. Chem.*, 248, 8052, 1973.
60. Nigam, A. M., Bass, B. D., and Manning, J. M., Reactivity of cyanate with valine-1 (α) of hemoglobin. A probe of conformational change and anion binding. *J. Biol. Chem.*, 251, 7638, 1976.
61. Papp, B. V., Moore, S., and Stein, W. H., Activity of bovine pancreatic doxycyclase A with modified amino groups. *J. Biol. Chem.*, 246, 939, 1971.
62. Chellat, R. and Anderson, L. L., Cyanate modification of essential lysyl residues in the catalytic subunit of tobacco ribulosebiphosphate carboxylase. *Biochem. Biophys. Acta*, 523, 455, 1978.
63. Kang, E. P., Antifibrinolytic thrombin, preparation and peptide activity. *Thromb. Res.*, 12, 171, 1977.
64. Sekiguchi, T., Oshiro, S., Goto, E. M., and Nishida, Y., Chemical modification of ε-amino groups in glutamine synthetase from *Bacillus licheniformis* with ethyl acetimidate. *J. Biochem.*, 85, 75, 1979.
65. Brown, D. J. and Kent, S. B. H., Formation of non-amidic products in the reaction of primary amines with imido esters. *Biochem. Biophys. Res. Commun.*, 67, 126, 1975.
66. Mountrou, A. and d'Alayer, J., Effects of imido-esters on membrane-bound adenylylase cyclase. *FEBS Lett.*, 122, 241, 1980.
67. Papp, B. V., Enhancement of the activity of horse liver alcohol dehydrogenase by modification of amino groups at the active sites. *J. Biol. Chem.*, 245, 1727, 1970.
68. Desautels, H. C., Stereochemical aspects of pyridoxal phosphate catalysis. In *Adv. Enzymol.*, 35, 79, 1971.
69. Shapiro, S., Esser, M., Pugh, E., and Horvath, B. L., The effect of pyridoxal phosphate on rabbit muscle aldolase. *Arch. Biochem. Biophys.*, 128, 534, 1968.
70. Schnack, K. D. and Nitzman, E. A., Pyridoxal-5'-phosphate as a site-specific protein reagent for a catalytically critical lysine residue in rabbit muscle phosphoglucose isomerase. *Biochemistry*, 10, 4837, 1971.
71. Havran, B. T. and du Vigneaud, V., The structure of acetone-lysine vasopressin as established through its synthesis from the acetone derivative of 5-benzyl-L-cysteinyl-L-tyrosine. *J. Am. Chem. Soc.*, 91, 2606, 1969.
72. Paech, C. and Tolbert, N. E., Active site studies of ribulose-1,5-bisphosphate carboxylase from spinach with pyridoxal-5'-phosphate. *J. Biol. Chem.*, 253, 7864, 1978.
73. Kent, A. B., Krebs, E. G., and Fischer, E. H., Properties of crystalline phosphorylase b. *J. Biol. Chem.*, 232, 549, 1958.
74. Witzner, M. J., Mo, T., Sawyers, D. L., and Harrison, J. B., Biphasic inactivation of porcine heart mitochondrial malate dehydrogenase by pyridoxal-5'-phosphate. *J. Biol. Chem.*, 250, 710, 1975.
75. Biele, D. M., Jamieson, J. L., and Harrison, J. H., Inactivation of porcine heart cytoplasmic malate dehydrogenase by pyridoxal-5'-phosphate. *J. Biol. Chem.*, 251, 6304, 1976.
76. Jones, C. W., III and Pried, D. G., Interaction of pyridoxal-5'-phosphate with apo-serine hydroxymethyltransferase. *Biochim. Biophys. Acta*, 526, 369, 1978.
77. Cortijo, M., Jimenez, J. S., and Llor, J., Criteria to recognize the structure and microlocality of pyridoxal-5'-phosphate binding sites in proteins. *Biochem. J.*, 171, 497, 1978.
78. Calk, M. A., DiSanto, D. M., and Litwack, G., Effect of pyridoxal phosphate on the DNA binding site of activated hepatic glucocorticoid receptor. *J. Biol. Chem.*, 253, 4886, 1978.
79. Schee, J. C. and Martinez-Carmona, M., Selective chemical modification and ³¹P NMR in the assignment of a pK value to the active site lysyl residue in aspartate transaminase. *J. Biol. Chem.*, 253, 2093, 1978.
80. Nishigori, H. and Tuft, D., Chemical modification of the avian progesterone receptor by pyridoxal-5'-phosphate. *J. Biol. Chem.*, 254, 9155, 1979.
81. Sugiyama, Y. and Mekobasa, Y., Modification of one lysine by pyridoxal phosphate completely inactivates chloroplast coupling factor 1 ATPase. *FEBS Lett.*, 98, 276, 1979.
82. Peters, H., Ritz, S., and Dose, K., Evidence for essential primary amino groups in a bacterial coupling factor F₁ATPase. *Biochem. Biophys. Res. Commun.*, 97, 1215, 1980.
83. Gould, K. G. and Engel, P. C., Modification of mouse testicular lactate dehydrogenase by pyridoxal-5'-phosphate. *Biochem. J.*, 191, 365, 1980.
84. Ogawa, H. and Fujikawa, M., The reaction of pyridoxal-5'-phosphate with an essential lysine residue of saccharopine dehydrogenase (L-lysine-forming). *J. Biol. Chem.*, 255, 7420, 1980.
85. Forester, A. W., Olegard, R. B., Nolan, C., and Fischer, E. H., Synthesis and properties of α- and ε-pyridoxyl lysines and their phosphorylated derivatives. *Biochimie*, 53, 269, 1971.
86. Seber, H. A., in *Handbook of Biochemistry*, 2nd ed., The Chemical Rubber Company, Cleveland, Ohio, 1970.
87. Moldova, T. G. and Chikowski, J. A., Specific modifications of rat uterine estrogen receptor by pyridoxal-5'-phosphate. *J. Biol. Chem.*, 255, 3100, 1980.
88. Ohawa, H., and Guaderr, C., Structure-function relationship in *Escherichia coli* inhibition factors. Identification of a lysine residue in the ribosomal binding site of initiation factor by site-specific chemical modification with pyridoxal phosphate. *J. Biol. Chem.*, 256, 4005, 1981.
89. Burger, E. and Gierlich, H., Evidence for an essential lysine at the active site of L-histidinol-NAD⁺ oxidoreductase, a functional dehydrogenase. *Eur. J. Biochem.*, 118, 125, 1981.
90. Miller, A. D., Pechman, L. C., Hart, G. J., Alfonsen, P. R., Abell, C., and Batterbury, A. R., Evidence that pyridoxal phosphate modification of lysine residues (Lys-35 and Lys-59) causes inactivation of hydroxymethylbilane synthase (porphobilinogen desaminase). *Biochem. J.*, 262, 119, 1989.
91. Bass, S., Bass, A., and Modak, M. J., Pyridoxal 5'-phosphate mediated inactivation of *Escherichia coli* DNA polymerase I: identification of lysine-633 as an essential residue for the processive mode of DNA synthesis. *Biochemistry*, 27, 6710, 1988.
92. Madenbach, A. M., Wang, Y., and Roach, P. J., Catalytic site of rabbit glycogen synthase isozymes. Identification of an active site lysine close to the amino terminus of the subunit. *J. Biol. Chem.*, 263, 10561, 1988.
93. Tamura, K., LaDine, J. R., and Cross, R. L., The adenine nucleotide binding site on yeast hexokinase PII. Affinity labeling of Lys-111 by pyridoxal 5'-diphosphate-5'-adenosine. *J. Biol. Chem.*, 263, 7907, 1988.
94. Kager, R., Methyl acetyl phosphate. A small anionic acetylating agent. *J. Org. Chem.*, 45, 2733, 1980.
95. Ueno, H., Pospischil, M. A., Manning, J. M., and Karger, R., Site-specific modification of hemoglobin by methyl acetyl phosphate. *Arch. Biochem. Biophys.*, 244, 795, 1986.
96. Ueno, H., Pospischil, M. A., and Manning, J. M., Methyl acetyl phosphate as a covalent probe for union-binding sites in human and bovine hemoglobins. *J. Biol. Chem.*, 264, 12344, 1989.
97. Maeno, G. E., Reductive alkylation of amino groups. *Meth. Enzymol.*, 47, 469, 1977.
98. Rice, R. H., Means, G. E., and Brown, W. D., Stabilization of bovine trypsin by reductive methylation. *Biochim. Biophys. Acta*, 492, 316, 1977.
99. Morris, R. W., Cagan, R. H., Martenson, R. E., and Deliber, G., Methylation of the lysine residues of myosin. *Proc. Soc. Exp. Biol. Med.*, 157, 194, 1978.
100. Chen, F. M. F. and Bondeson, N. L., Reductive N,N-dimethylation of amino acid and peptide derivatives using methanol as the carbonyl source. *Can. J. Biochem.*, 56, 150, 1978.
101. Dotariv-Martin, D. and Havel, J. M., Radiolabeling of proteins by reductive alkylation with [¹⁴C] formaldehyde and sodium cyanoborohydride. *Anal. Biochem.*, 87, 562, 1978.
102. Deck, L. R., Geraldine, C. F. G., Sherry, A. D., Gray, C. W., and Gray, D. M., ¹³C NMR of methylated lysines of fd phage: evidence for a conformational change involving lysine 24 upon binding of a negatively charged lanthanide chelate. *Biochemistry*, 28, 7896, 1989.
103. Brown, E. M., Pfeiffer, P. E., Kamodeh, T. F., and Greenberg, R., Accessibility and mobility of lysine residues in β-lactoglobulin. *Biochemistry*, 27, 5601, 1988.
104. Fretwell, K., Iwaki, S., and Feeney, R. F., Extensive modification of protein amino groups by reductive addition of different sized substituents. *Int. J. Peptide Protein Res.*, 14, 451, 1979.
105. Fretwell, K., Eshelbacher, B., and Harblitz, O., Effect of alkylation with different size substituents on the conformation of ovomucoid, lysozyme and ovomandarin. *Int. J. Peptide Protein Res.*, 25, 601, 1985.
106. Goughan, K. F., Varna, D. M., and Feeney, R. E., Reversible reductive alkylation of amino groups in proteins. *Biochemistry*, 18, 5392, 1979.
107. Jentoft, N. and Dearborn, D. G., Labeling of proteins by reductive methylation using sodium cyanoborohydride. *J. Biol. Chem.*, 254, 4359, 1979.
108. Jentoft, J. E., Jentoft, N., Gerbacia, T. A., and Dearborn, D. G., ¹³C NMR studies of ribonuclease A methylated with [¹⁴C] formaldehyde. *J. Biol. Chem.*, 254, 4366, 1979.
109. Jentoft, N. and Dearborn, D. G., Protein labeling by reductive methylation with sodium cyanoborohydride. Effect of cyanide and metal ions on the reaction. *Anal. Biochem.*, 106, 186, 1980.
110. Goughan, K. F., Cabecenas, J. C., Olson, H. B. F., and Feeney, R. E., Alternative reducing agent for reductive methylation of amino groups in proteins. *Int. J. Peptide Protein Res.*, 17, 345, 1981.
111. Cabecenas, J. C., Ahmed, A. J., and Feeney, R. E., Amine boranes as alternative reducing agents for reductive alkylation of proteins. *Anal. Biochem.*, 124, 772, 1982.
112. Wu, H.-L. and Means, G. E., Immobilization of proteins by reductive alkylation with hydrophobic aldehydes. *Biochem. Biophys. Res. Commun.*, 23, 855, 1981.
113. Acharya, A. S. and Manning, J. M., Reactivity of the amino groups of carbonmonoxyhemoglobin S with glyceraldehyde. *J. Biol. Chem.*, 255, 1406, 1980.
114. Acharya, A. S. and Manning, J. M., Amadori rearrangement of glyceraldehyde-hemoglobin Schiff base adducts. A new procedure for the determination of ketamine adducts in proteins. *J. Biol. Chem.*, 255, 7218, 1980.
115. Wilson, G. G., Effect of reductive lactosamination on the hepatic uptake of bovine pancreatic ribonuclease A dimer. *J. Biol. Chem.*, 253, 2070, 1978.
116. Banno, H. F. and Higgins, P. J., Reaction of monosaccharides with proteins: possible evolutionary significance. *Science*, 213, 222, 1981.

117. Goldfarb, A. R., A kinetic study of the reactions of amino acids and peptides with trinitrobenzenesulfonic acid. *Biochemistry*, 5, 2570, 1966.
118. Goldfarb, A. R., Heterogeneity of amino groups in proteins. I. Human serum albumin. *Biochemistry*, 5, 2574, 1966.
119. Haberecht, A. F. S. A., Determination of free amino groups in proteins by trinitrobenzenesulfonic acid. *Anal. Biochem.*, 14, 328, 1966.
120. Fields, R., The rapid determination of amino groups with TNBS. *Metb. Enzymol.*, 25, 464, 1972.
121. Kotaki, A. and Satake, K., Acid and alkaline degradation of the TNP-amino acids and peptides. *J. Biochem.*, 56, 299, 1964.
122. Coffee, C. J., Bradshaw, R. A., Goldin, B. R., and Frieden, C., Identification of the sites of modification of bovine liver glutamate dehydrogenase reacted with trinitrobenzenesulfonate. *Biochemistry*, 10, 3516, 1971.
123. Goldin, B. R. and Frieden, C., Effects of trinitrophenylation of specific lysyl residues on the catalytic, regulatory and molecular properties of bovine liver glutamate dehydrogenase. *Biochemistry*, 10, 3527, 1971.
124. Bates, D. J., Goldin, B. R., and Frieden, C., A new reaction of glutamate dehydrogenase: the enzyme-catalyzed formation of trinitrobenzene from TNBS in the presence of reduced coenzyme. *Biochem. Biophys. Res. Commun.*, 39, 502, 1970.
125. Meema, G. E., Congdon, W. I., and Bender, M. L., Reactions of 2,4,6-trinitrobenzenesulfonate ion with amines and hydroxide ion. *Biochemistry*, 11, 3564, 1972.
126. Flügge, U. I. and Hecht, H. W., Specific labelling of the active site of the phosphate translocator in spinach chloroplasts by 2,4,6-trinitrobenzene sulfonate. *Biochem. Biophys. Res. Commun.*, 84, 37, 1978.
127. Flügge, U. I. and Hecht, H. W., Specific labelling of a protein involved in phosphate transport of chloroplasts by pyridoxal-5'-phosphate. *FEBS Lett.*, 82, 29, 1977.
128. Parrott, C. L. and Stauff, S., A spectrophotometric study of the reaction of borohydride with trinitrophenyl derivatives of amino acids and proteins. *Biochim. Biophys. Acta*, 491, 114, 1977.
129. Shimada, T., Enhancement of 14S and 30S dyrenin adenosine triphosphatase activities by modification of amino groups with trinitrobenzenesulfonate. A comparison with modification of SH groups. *J. Biochem.*, 85, 1421, 1979.
130. Carlberg, I. and Maness, B., Interaction of 2,4,6-trinitrobenzene sulfonate and 4-chloro-7-nitrobenzo-2-oxa-1,3-diazole with the active sites of glutathione reductase and liponamide dehydrogenase. *Acta Chem. Scand.*, B34, 144, 1980.
131. Whitaker, J. R., Graziano, P. E., and Aasen, G., Reaction of ammonia with trinitrobenzene sulfonic acid. *Anal. Biochem.*, 108, 72, 1980.
132. Salem, N., Jr., Lester, C. J., and Trausa, E. G., Selective chemical modification of plasma membrane ectoenzymes. *Biochim. Biophys. Acta*, 641, 366, 1981.
133. Handa, M., Yuan, H., Chen, S., Iyanaga, T., Lee, T. D., and Shively, J. E., Structure-function relationship of NAD(P)H:quinone reductase: characterization of NH₂-terminal blocking group and essential lysine and lysine residues. *Biochemistry*, 27, 6877, 1988.
134. Imano, H., Chemical modification of lysine residues at active-site of human placental estradiol 17 β -dehydrogenase. *Biochem. Biophys. Res. Commun.*, 152, 789, 1988.
135. Yang, C.-C. and Chang, L.-S., Studies on the sites of lysine residues in phospholipase A₂ from *Naja naja* (Tawana cobra) snake venom. *Biochem. J.*, 262, 855, 1989.
136. Gordillo, E., Ayala, A., Bautista, J., and Machado, A., Implication of lysine residues in the loss of enzymatic activity in rat liver 6-phosphogluconate dehydrogenase found in aging. *J. Biol. Chem.*, 264, 17024, 1989.
137. Watanabe, K., Sorenson, Y., and Ponskus, G., Identification of lysine residues at or near active site of luffin-4, a ribosome-inactivating protein from seeds of *Luffa cylindrica*. *J. Biochem. (Tokyo)*, 106, 977, 1989.
138. Den-Goor, M., Kessel, M., and Mulholland, A., Anti-TNP antibody localization of the reactive lysine residues in myosin. *Biochim. Biophys. Acta*, 1038, 269, 1990.
139. Klemm, J. R., Guanidination of proteins. *Metb. Enzymol.*, 11, 584, 1967.
140. Bregman, M. D., Trivedi, D., and Rieby, V. J., Glucagon amino groups. Evaluation of modification leading to antagonism and agonism. *J. Biol. Chem.*, 255, 11725, 1980.
141. Saitake, R., Kozsostomi, H., Takerechi, M., and Asano, K., Chemical modification of erythropoietin: an increase in *in vitro* activity by guanidination. *Biochim. Biophys. Acta: Protein Structure and Molecular Enzymology*, 1038 125, 1990.
142. Bostrom, A. E. and Hunter, W. M., The labelling of proteins to high specific radioactivities by conjugation to a 125I-containing acylating agent. *Biochem. J.*, 133, 529, 1973.
143. Yen, A. W., Zacher-Neff, H. A., Richard, K. A., Stuts, N. D., Hebrichsen, B. L., and Deibel, M. R., Jr., Biotinylation of reactive amino groups in native recombinant human interleukin-1 β . *J. Biol. Chem.*, 264, 17691, 1989.
144. Wilschek, M. and Bayer, E., Biotin-containing reagents. *Metb. Enzymol.*, 184, 123, 1990.
145. Bayer, E. and Wilschek, M., Protein Biotinylation. *Metb. Enzymol.*, 184, 148, 1990.
146. Dixon, H. B. F. and Fields, R., Specific modification of NH₂-terminal residues by transemination. *Metb. Enzymol.*, 25, 409, 1972.
147. Verheij, H. M., Egmund, M. R., and de Haas, G. H., Chemical modification of the α -amino group in snake venom phospholipases A₂. A comparison of the interaction of pancreatic and venom phospholipases with lipid-water interfaces. *Biochemistry*, 20, 94, 1981.

Chapter 11

THE MODIFICATION OF ARGININE

Until approximately 20 years ago the specific chemical modification of arginine was relatively difficult to achieve. The high pKa of the guanidine functional group ($pK_a \approx 12$ to 13) necessitated fairly drastic reaction conditions ($pH \geq 12$) to generate an effective nucleophile. Most proteins are not stable to extreme alkaline pH. The modification of arginyl residues was however possible and the early efforts in this area have been previously reviewed.¹

It is reasonable to suggest that the recent advances in the study of the function of arginine residues in proteins stem from the work of Takahashi² on the use of phenylglyoxal as a reagent for the specific modification of arginine although observations on the use of 2,3-butanedione³ and glyoxal⁴ appeared at approximately the same time. The greatly increased interest in the elucidation of functional arginyl residues probably arises from the suggestion of Riordan and co-workers⁵ that arginyl residues function as "general" anion recognition sites in proteins. Pathy and Thész⁶ extended this concept by suggesting that the pKa of arginyl residues at anion binding sites (Figure 1) is lower than that of other arginine residues which would explain the specificity of the dicarbonyl residues which will be discussed below.

This chapter will primarily consider the reaction of arginyl residues in proteins with three different reagents: phenylglyoxal, 2,3-butanedione, and 1,2-cyclohexanedione since the vast majority of reports during the past decade have used these reagents. It is noted that several other reagents have been used for the modification of arginine. The modification of arginyl residues with ninhydrin occurs under relatively mild conditions (pH 8.0, 25°C, 0.1 M N-ethylmorpholine acetate, pH 8.0) as described by Takahashi.⁷ The modification of pancreatic ribonuclease A or ribonuclease T by ninhydrin is shown in Figure 2. The reaction proceeds quite rapidly at pH 8.0 with the modification of both arginyl and lysyl residues. Reducing the pH to 5.5 (0.1 M sodium acetate, pH 5.5) reduced the rate of inactivation but did not increase the specificity of the modification. The UV spectra of ribonuclease T, before and after modification with ninhydrin are presented in Figure 3. Takahashi⁷ achieved specificity of modification by first modifying available lysyl residues with a reagent such as methylenic anhydride (citraconic anhydride) which can subsequently be removed under conditions where the arginine derivative is stable (pH 3.6). The arginine derivative is unstable under basic conditions (1% piperidine, ambient temperature, 34 h) and arginine was regenerated. Under the conditions commonly used for the preparation of protein samples for amino acid analysis (6 N HCl 110°C, 24 h), the ninhydrin-arginine derivative was destroyed with the partial regeneration of free arginine. The structure of the ninhydrin-arginine derivative (Figure 4) is similar to that proposed for the α,α' -dicarbonyl compounds such as phenylglyoxal⁸ or 1,2-cyclohexanedione.⁹ At the same time a report by Chaplin⁹ appeared proposing the use of ninhydrin for the reversible modification of arginine residues in proteins. The study suggested that at pH 9.1 (0.1 M sodium phosphate), 37°C, the rate of reaction at arginine residues is approximately 100-fold more rapid than at lysine residues but reaction at cysteinyl residues is approximately 100-fold more rapid than at arginine. The extent of reaction was determined by measuring the decrease in the absorbance of ninhydrin at 232 nm ($\epsilon = 3.4 \times 10^4 M^{-1} cm^{-1}$). As noted by Takahashi,⁷ the ninhydrin-arginine derivative is unstable under alkaline conditions and can be used for the reversible modification of arginine residues. The fluorescence properties of the reaction product between ninhydrin and guanidino compounds such as arginine have provided the basis for the use of ninhydrin for the detection of guanidine compounds in biological fluids (plasma) following separation by high-performance liquid chromatography.¹⁰

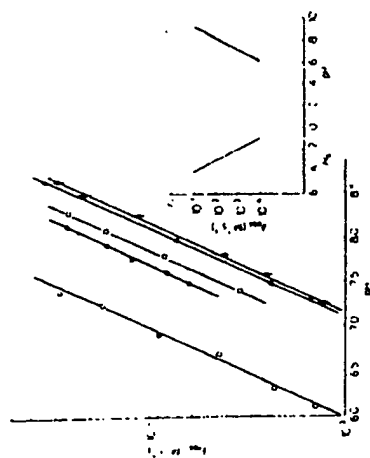


FIGURE 1. Dependence of the reaction of arginine with dicarbonyl compounds on pH. Shown are second-order rate constants for the reaction of phenylglyoxal (O—O), hydroxypyruvaldehyde (O—C), glyoxal (A—A), and 1,2-cyclohexanedione (e—e) with free arginine at 25°C at the indicated pH (the buffers were 0.1 M sodium phosphate for pH 6 to 8; 0.1 M triethanolamine-HCl for pH 7 to 9 and in HCl solutions (H₂A-0). Also included are the rate constants for the reaction of 1,2-cyclohexanedione with albumin determined in 0.1 M triethanolamine-HCl buffers at 25°C (e—e). The inset shows the second-order rate constants for the arginine-glyoxal reaction over a wider pH range. (From Piaty, L. and Thézé, J., *Eur. J. Biochem.*, 105, 387, 1980. With permission.)

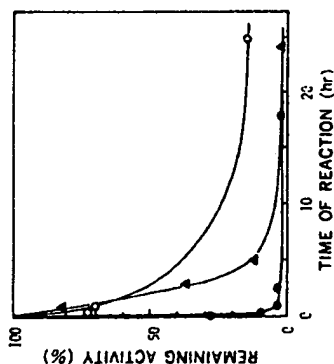


FIGURE 2. Rates of inactivation of ribonucleases A and T₁ by ninhydrin. The reaction was performed at 25°C in the dark either at pH 8.0 in 0.1 M N-ethylmorpholine acetate, or at pH 5.5 in 0.1 M sodium acetate, at a protein concentration of 0.5%, and a ninhydrin concentration of 1.5%. pH 8.0: ○, ribonuclease A; ●, ribonuclease T₁. pH 5.5: ○, ribonuclease A. (From Takahashi, K., *J. Biochem.*, 80, 1173, 1976. With permission.)

The modification of arginyl residues with glyoxal has also been proposed.¹¹ Specificity of reaction is a problem with reaction also at primary amine groups and sulphydryl groups. For example, reaction of glyoxal with bovine serum albumin at pH 9.0 resulted in modification of greater than 80% of the arginine residues with approximately 30% modification of lysine residues.¹¹ Glass and Pelzig¹² have examined the reversible modification of arginyl residues with glyoxal in some detail. Several products are formed from the reaction of glyoxal and arginine at alkaline pH. One of these derivatives is markedly stable in strong

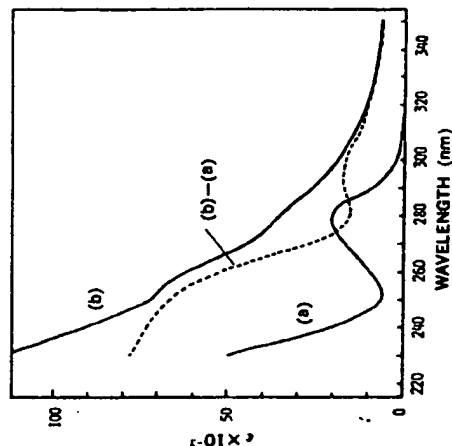


FIGURE 3. Changes in the UV absorption spectrum of ribonuclease T₁ on reaction with ninhydrin. The spectra were measured in 0.01 M ammonium acetate. — (a) native enzyme; (b) ninhydrin-modified enzyme. ---: difference, (b) - (a). (From Takahashi, K., *J. Biochem.*, 80, 1173, 1976. With permission.)

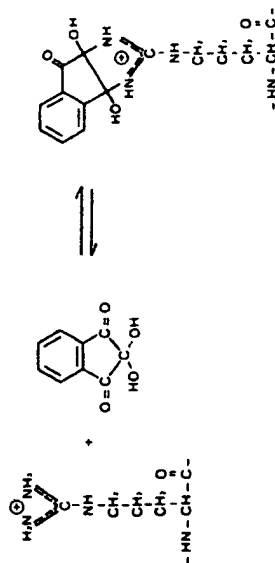


FIGURE 4. A scheme for the reaction of ninhydrin with arginine.

acid (12 M HCl) at ambient temperature but is rapidly degraded to form free arginine in the presence of *O*-phenylenediamine (0.16 M) at pH 8.1 to 8.3. More alkaline conditions resulted in more rapid decomposition of the glyoxal-arginine derivative and ninhydrin-positive compounds other than arginine were formed. Reaction of arginine with glyoxal in borate buffer also yields the product described above. The same research group has reported on the reversible modification of arginine residues with camphorquinone-10-sulfonic acid and derivatives such as camphorquinone-10-sulfonylnorleucine.¹³ The synthesis of the parent compounds and various derivatives is reported. The sulfonic acid function provides a basis for the attachment of a "tag" such as norleucine which can be used for determining the extent of modification.¹⁴ Reaction with arginine occurs in 0.2 M sodium borate, pH 9.0. Under

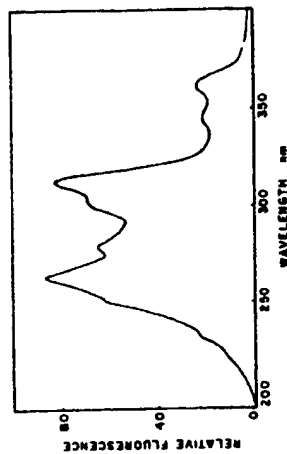


FIGURE 5. The fluorescence excitation spectrum of the condensation product of arginine and 9,10-phenanthrenequinone. Arginine (50 μ M) was reacted with 9,10-phenanthrenequinone (68 μ M) in 70% aqueous ethanol containing 0.2 M NaOH at 30°C for 60 min. The reaction mixture was then diluted with an equal volume of 1.2 M HCl and the spectrum recorded. The spectrum was recorded using an emission wavelength of 400 nm and a 2.5-nm slit width. (From Smith, R. E. and McQuarrie, R., *Anal. Biochem.*, 90, 246, 1978. With permission.)

these conditions, reaction of camphorquinone-sulfonic acid with an amino acid analysis standard showed a greater than 90% loss of arginine and a 25% loss of cystine. Loss of cystine was not observed in the proteins studied (soybean trypsin inhibitor, ribonuclease S-peptide). The arginine derivative is stable for 24 h in trifluoroacetic acid and under other mild acid conditions. The derivative is stable to 0.5 M hydroxylamine, pH 7.0, conditions under which the cyclohexanedione derivative of arginine decomposes⁸ but arginine is regenerated in 0.2 M *o*-phenylenediamine, pH 8.5 (approximately 75% after 4 h; complete after 16 h).

The modification of arginyl residues with hydrazine (aqueous conditions) results in the formation of ornithine but also results in peptide bond cleavage (predominantly at gly-X, X-gly, asn-X, and X-ser peptide bonds).¹³

The determination of the extent of arginine modification is generally determined by amino acid analysis after acid hydrolysis but conditions generally need to be modified to prevent loss of the arginine derivative.¹⁴ This will be discussed for each of the reagents discussed below. The Sakaguchi reaction¹⁵ continues to be useful with recent modifications^{17,18} and has recently been used, after acid hydrolysis, to determine the extent of arginine modification by 2,3-butanedione.¹⁹ The use of ninhydrin as a fluorometric reagent for arginine has been described above.¹⁰ Another fluorometric method for the determination of arginine using 9,10-phenanthrenequinone²⁰ has been described. Figure 5 shows the excitation spectrum for the reaction product of arginine and phenanthrenequinone, while the emission spectrum is shown in Figure 6. The time course for the reaction with free arginine is shown in Figure 7 while the time course for the reaction with arginyl residues in proteins is shown in Figure 8. This method is some 1000-fold more sensitive than the Sakaguchi reaction but some concern remains concerning the absolute accuracy of the reagent for determination of arginine in peptide linkage. This is also true of the other reagents.

The use of phenylglyoxal (Figure 9) was developed by Takahashi² and has since been applied to the study of the role of arginyl residues in proteins as shown in Table 1 and Figure 10. The use of this reagent has been somewhat limited in the last six years but there has been interest in modifying residues involved in ion transport. Unfortunately, many of these studies fail to recognize that phenylglyoxal, like glyoxal, will react with α -amino groups at a significant rate² (Figure 11). The rate of inactivation of ribonuclease A by phenylglyoxal at different values of pH is shown in Figure 12. Polymerization was noted in a sample

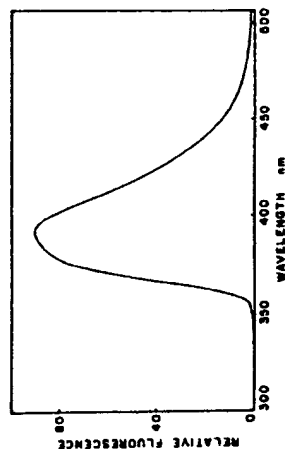


FIGURE 6. The fluorescence emission spectrum of the condensation product of arginine and 9,10-phenanthrenequinone. The reaction conditions are described in Figure 4. The spectrum was recorded using an excitation wavelength of 260 nm and a 2.5-nm slit width. (From Smith, R. E. and McQuarrie, R., *Anal. Biochem.*, 90, 246, 1978. With permission.)

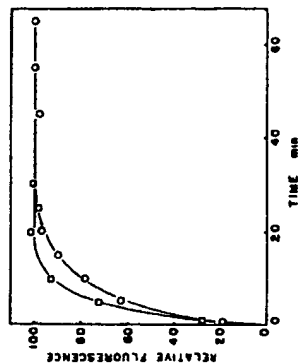


FIGURE 7. The development of fluorescence as a function of the time of reaction of arginine and 9,10-phenanthrenequinone. The reaction was initiated by mixing 1 ml of arginine (8 μ g) in water with 3 ml of 50 μ M 9,10-phenanthrenequinone in ethanol and 0.5 ml of 2 M NaOH at either 30°C (○) or 44°C (●). At the indicated times, portions were withdrawn and mixed with an equal volume of 1.2 N HCl. The fluorescence was recorded using an excitation wavelength of 312 nm and an emission wavelength of 392 nm. A 5-nm slit width was used. (From Smith, R. E. and McQuarrie, R., *Anal. Biochem.*, 90, 246, 1978. With permission.)

incubated for 21 h. The amino-terminal lysine residue was rapidly modified under these conditions. The possible effect of light on the reaction of phenylglyoxal with arginine has been reported for 2,3-butanedione^{21,22} has not been studied. As noted by Takahashi, the stoichiometry of the reaction involves the reaction of 2 mol of phenylglyoxal with 1 mol of arginine (Figure 9). The [¹⁴C]-labeled reagent can be easily prepared.²³ A facile modification reported by Hartman and co-workers.²⁴ Radiolabeled acetophenone was added to an equal amount (on the basis of weight) of selenium dioxide in dioxane-water (30:1). The mixture was refluxed for 3 h after which solvent was removed under a stream of nitrogen. The residue was taken up in boiling water and activated charcoal added. The hot slurry was filtered through Celite. The phenylglyoxal crystallized spontaneously from the filtrate on cooling.

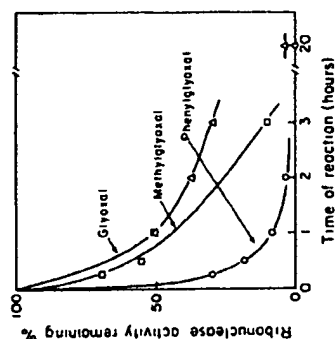


FIGURE 10. The rate of inactivation of ribonuclease A by reaction with phenylglyoxal and related compounds. The reactions were performed in 0.2 M N-ethylmorpholine acetate, pH 8.0, at 25°C. The protein concentration was 0.5% with either 1.5% phenylglyoxal, 1.5% methylglyoxal, or 1.5% glyoxal hydrate as indicated in the figure. (From Takahashi, K., *J. Biol. Chem.*, 243, 6171, 1968. With permission.)

Table 1
REACTION OF PHENYLGLYOXAL WITH ARGINYL RESIDUES IN PEPTIDES AND PROTEINS

Protein	Solvent	Reagent excess ^a	Extent of modification	Ref.
Pancreatic RNase	0.1 M N-ethylmorpholine acetate, pH 8.0	—	2–34 ^a	1
Porcine carboxypeptidase B	0.3 M borate, pH 7.9	200 ^b	1 ^c	2
Aspartate transcarbamylase	0.125 M potassium bicarbonate, pH 8.3 or 0.1 M N-ethylmorpholine, pH 8.3	—	2.7 ^d	3
Pyruvate kinase	0.1 M triethanolamine, pH 7.0	—	3/28.33 ^e	4
Horse liver alcohol dehydrogenase	—	—	—	5, 6
Mitochondrial ATPase	0.097 M sodium borate, 0.097 M EDTA, pH 8.0	—	4 ^f	7
Adenylase kinase	0.1 M triethanolamine-HCl, pH 7.0	—	p	8, 9
<i>Rhodospirillum rubrum</i> chromatophores	0.05 M borate, pH 8.0	—	A	10
Glutamic acid decarboxylase	0.05 M sodium borate ¹	—	—	11
Ribulose biphosphate carboxylase	0.066 M sodium ² bicarbonate, 0.060 M bicline, 0.1 M EDTA, pH 8.0	—	2–3/35 ^g	12
Yeast hexokinase	0.035 M Veronal, pH 7.5	—	1/18 ^h	13
Propionyl CoA carboxylase	0.050 M borate, pH 8.0	—	—	14
β -Methylcrotonyl CoA carboxylase	0.050 M borate, pH 8.0	—	—	14
Superoxide dismutase	0.125 M sodium bicarbonate, pH 8.0	—	1/4 ⁱ	15

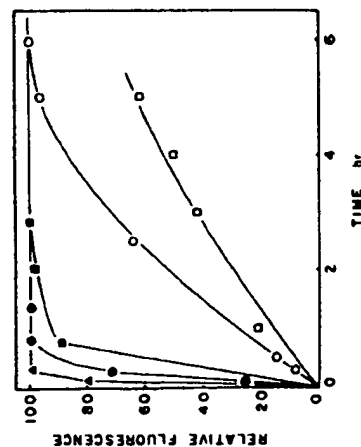


FIGURE 8. The development of fluorescence as a function of time of reaction of proteins with 9,10-phenanthroline. The reaction was initiated by mixing 1 ml of protein (100 μ g) in 50 mM borate, pH 8.5, with 3 ml of 50 μ M 9,10-phenanthroline in ethanol and 0.5 ml of 2 M NaOH. At the indicated times, portions were removed and mixed with an equal volume of 1.2 N HCl. The fluorescence was recorded using an excitation wavelength of 312 nm and an emission wavelength of 392 nm with a 5-nm slit width. The reactions were performed either at 30°C (open symbols) or 60°C (closed symbols). The proteins used were bovine serum albumin (O), lysozyme (□), and the β -chain of insulin (Δ). (From Smith, R. E. and McQuarrie, R., *Anal. Biochem.*, 90, 246, 1978. With permission.)

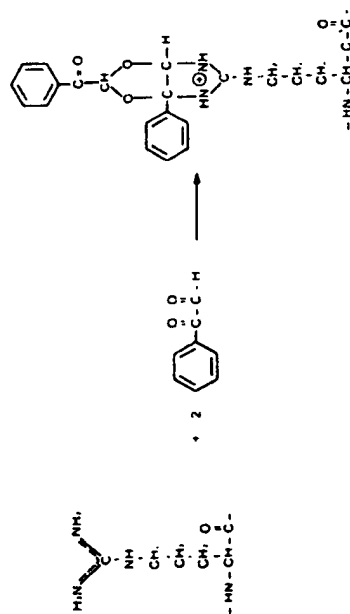


FIGURE 9. A scheme for the reaction of phenylglyoxal with arginine.

The synthesis of phenyl [2-³H] glyoxal²⁷ has been reported. Borders and co-workers²⁷ have reported the synthesis of a chromophoric derivative, 4-hydroxy-3-nitrophenylglyoxal, which should prove quite useful in the study of arginyl residues, *p*-Hydroxyphenylglyoxal²⁸ has also been used as a spectrophotometric reagent for the study of this reaction.

Of particular interest has been the observations of Fonda and Cheung²⁹ that the reaction of arginine with phenylglyoxal is greatly accelerated in bicarbonate-carbonate buffer systems. Figure 13 shows the reaction of phenylglyoxal with *N*-acetylarginine, *N*-acetyllysine and *N*-acetylcysteine in 0.083 M sodium bicarbonate, pH 7.5. Reaction is only seen, for all practical purposes, with the arginine derivative. L-Arginine reacted in the same manner suggesting that modification of the α -amino group did not occur under these conditions. Figure 14

Table 1 (continued)
REACTION OF PHENYLGLYOXAL WITH ARGINYL RESIDUES IN PEPTIDES
AND PROTEINS

Protein	Solvent	Reagent excess ^a	Extent of modification	Ref.
Myosin (subfragment 1)	0.1 M potassium bicarbonate, pH 8.0	—	1.7/35 ^a	16
Thymidylate synthetase	0.125 M bicarbonate, pH 8.0	—	3.6/12	17
Glutamate apocarbonylase	0.125 M sodium bicarbonate, pH 7.5	—	1/23 ^a	18
Adenylate kinase (yeast)	0.025 M HEPES, pH 7.5	—	—	19
Cardiac myosin S-1	0.1 M N-ethylmorpholine acetate, pH 7.6	—	2.8/42 ^a	20
Cystathionase	0.125 M bicarbonate, pH 7.9	—	18/45	21
Fatty acid synthetase	0.1 M sodium phosphate, 0.0005 M dithioerythritol, 0.001 M EDTA, pH 7.6	—	4/106	22
Yeast inorganic pyrophosphatase	0.08 M N-ethylmorpholine acetate, pH 7.0	—	1/6	23
Porcine phospholipase A	0.125 M potassium bicarbonate, pH 8.5	—	1.4/4 ^a	24
Superoxide dismutase ^b	0.100 M sodium bicarbonate, pH 8.3	50—100	0.88/4.0 ^a	25, 26 ^a
p-Hydroxybenzoate hydroxylase	0.050 M potassium phosphate, pH 8.0	250	2—3/24 ^a	27
Thymidylate synthetase	0.200 M N-ethylmorpholine, pH 7.4 ^a	65	2/12 ^a	28
Acetylcholine esterase	0.025 M borate, 0.005 phosphate, 0.080 M NaCl, pH 7.0	—	3/31 ^a	29
γ -Aminobutyrate aminotransferase	0.05 M Tris, pH 8.5	—	—	30
n-B-Hydroxybutyrate dehydrogenase	0.05 M HEPES, pH 7.5	—	— ^a	31
Ornithine transcarboxylase	0.05 M Tricine, 0.1 M KCl, 0.0001 M EDTA, pH 8.05	—	— ^a	32
Coenzyme B ₁₂ -dependent diol dehydratase	0.05 M borate, pH 8.0	—	—	33
Transketolase	0.125 M sodium bicarbonate, pH 7.6	—	4/34 ^a	34
ATP citrate lyase	0.050 M HEPES, pH 8.0	—	8.5/40	36
Malic enzyme	0.037 M borate, pH 7.5	—	—	37
Pyridoxamine-5'-phosphate oxidase	0.1 M potassium phosphate, pH 8.0, containing 5% EtOH	—	6/40	38
Ornithine transcarboxylase	0.125 M potassium bicarbonate, pH 8.3	— ^a	1.5/4 ^a	39
Acetate kinase	0.050 M methanamine, pH 7.6	— ^a	— ^a	40
Pancreatic phospholipase A ₂	0.125 M N-ethylmorpholine, pH 8.0	30	1.0—1.2 ^a	41
Phosphatidylcholine transfer protein	0.1 M sodium bicarbonate, pH 8.0	—	4/10 ^a	42
Aldehyde reductase	0.020 M phosphate, pH 7.0	—	0.6/16 ^a	43
Choline acetyltransferase	0.050 M HEPES, pH 7.8	—	— ^a	44
ADP-glucose synthetase	0.05 M potassium phosphate, 0.00025 M EDTA, pH 7.5	110	1 ^a	45

Table 1 (continued)
REACTION OF PHENYLGLYOXAL WITH ARGINYL RESIDUES IN PEPTIDES
AND PROTEINS

Protein	Solvent	Reagent excess ^a	Extent of modification	Ref.
Pyruvate oxidase	0.1 M sodium phosphate, 0.010 M magnesium chloride, pH 7.8	—	2.5/5 ^a	46
Calcineurin	50 mM Tris, pH 7.5, with 0.1 M EDTA, 0.1 mM NiCl ₂ and 0.3 mM CsCl ₃	10,000 ^a	—	47
Carbon monoxide	20 mM sodium phosphate, pH 8.2 with 4 mM dithiothreitol	—	—	48
Epithelial sodium channel	pH 8.1 ^a	—	—	49
Calcium "pump"	100 mM N-ethylmorpholine-40 mM KCl-6 mM HEPES-0.7 mM MgCl ₂ -0.2 mM EGTA, pH 7.7	—	—	50
Calmodulin-dependent	40 mM HEPES, pH 7.5 with 7% glycerol, 0.1 M EDTA and 0.3 mM CaCl ₂	333 ^a	—	51

- ^a Reagent/protein.
- ^b After 3 h at 25°C.
- ^c Had modification of α -amino group and lysine residues.
- ^d Reagent/arginine.
- ^e After 1 h at 37°C.
- ^f After 3 h at 25°C.
- ^g 1.3/8 In regulatory chain.
- ^h 20 Min at 37°C with 23.8 mM phenylglyoxal, protein 1 mg/ml.
- ⁱ 30 Min of reaction at 30°C; the presence of efrapeptin, a low-molecular weight antibiotic which is a potent inhibitor of oxidative phosphorylation, prevented the modification of one "fast-reacting" arginyl residue.
- ^j A single arginine residue is modified (Arg-97).
- ^k pH Not given; reaction at 23°C. Kinetic evidence for stoichiometric inactivation.
- ^l Solvent made metal-free using BioRad Chelex; reaction performed with and without MgCl₂.
- ^m Analysis of sulphydryl groups after phenylglyoxal modification showed no loss of cysteine. These investigations noted the modification with phenylglyoxal is apparently more specific than 2,3-butanedione.
- ⁿ The authors claim 1:1 stoichiometry of phenylglyoxal with the arginyl residue from analysis of dependence of pseudo first-order rate constant vs. reciprocal of reagent (phenylglyoxal concentration). Partial inactivation of modified enzyme was observed reflecting lability of modified arginine residues. Reaction also shows saturation kinetics reflecting "specific" affinity of reagent for enzyme possibly from hydrophobic interaction. These authors suggest that this phenomenon is observed with the reaction of other hydrophobic reagents with this enzyme. A similar phenomenon has been observed with trinitrobenzenesulfonic acid (see Chapter 10).
- ^o 25°C, 1 h.
- ^p 25°C, 3 mM phenylglyoxal, 3 min.
- ^q Rates of enzyme inactivation were dependent upon buffer: at 5.9 mM phenylglyoxal, the following data were obtained, bicarbonate ($T_{1/2}$ = 6.0 min), MOPS ($T_{1/2}$ = 11.5 min), borate ($T_{1/2}$ = 34.0), and phosphate ($T_{1/2}$ = 48.0 min) at 25°C.
- ^r These investigators noted a significant buffer effect on the reaction which is more thoroughly explored in Reference 29 of Chapter 11. In this study the following second-order rate constants were obtained with the following reagent/solvent conditions (reactions performed at 25°C): 0.69 M⁻¹ min⁻¹ with 2,3-butanedione/0.050 M borate, pH 8.0; 33.78 M⁻¹ min⁻¹ with glyoxal/0.125 M sodium bicarbonate, pH 8.0; 31.00 M⁻¹ min⁻¹ with methylglyoxal/0.125 M sodium bicarbonate, pH 8.0; and 107.68 M⁻¹ min⁻¹ with phenylglyoxal/0.125 M sodium bicarbonate, pH 8.0.
- ^s 300-Fold excess of reagent, 0.083 M sodium bicarbonate, pH 8.1, 7 min, 23°C.
- ^t See more complete discussion of this work in Table 2. 2,3-Butanedione or 1,2-cyclohexanedione appeared to be more effective than phenylglyoxal in this system.

Table 1 (continued)

- 6 Min, 22°C, 50% loss of activity
- Determined at 90% inactivation (25°C) of phospholipase activity (release of fatty acid from egg yolk in water with 3 mM CaCl_2 and 1.4 mM sodium deoxycholate. These investigations see Reference 24, Table 1) did examine the possibility of amino-terminal alanine modification on loss of alanine was observed with 75% inactivation (0.9 mol Arg modified/mol protein) while enzyme samples with a greater extent of inactivation did have some loss of amino-terminal alanine (quantity not given). These investigators did examine the pH dependence of enzyme inactivation by phenylglyoxal (presumably a direct measure of the rate of arginine modification) and reported the following second-order rate constants ($M^{-1} \text{ min}^{-1}$): pH 6.5, 0.3; pH 7.5, 1.5; pH 8.5, 3.3; and pH 9.5, 3.9. These investigators also showed that phenylglyoxal ($I_{50} = 1 \text{ min}$) was more effective than 2,3-butanedione ($I_{50} = 20 \text{ min}$) and 1,2-cyclohexanedione ($I_{50} = 120 \text{ min}$).
- Cu, Zn superoxide dismutase from *Saccharomyces cerevisiae*.
- Determined at 80% loss of enzymatic activity using reaction of the modified enzyme with 9,10-phenanthrenequinone. This value corresponded to that determined by the incorporation of radiolabeled phenylglyoxal assuming 2:1 adduct. Amino acid analysis with samples prepared using normal hydrolytic conditions (6 N HCl, 110°C, 20 h) suggested only approximately 50% of this extent of arginine modification. When thioglycolic acid was included during the hydrolysis, values for the extent of arginine modification approached those determined by the fluorescence technique and radiolabel incorporation.
- The study is an extension of the observation reported in Reference 25 and uses reaction with 4-hydroxy-3-nitrophenylglyoxal, a chromophoric derivative of phenylglyoxal, to identify the specific arginine residue modified. It is of some interest that the rate of reaction with this derivative is approximately sixfold less than that with the parent phenylglyoxal.
- Reaction at 25°C for 60 to 120 min. Loss of lysine residues was not observed under these reaction conditions. Amino acid analysis (hydrolysis in 6 N HCl, 110°C, 24 h) correlated well with radiolabeled phenylglyoxal incorporation assuming 2:1 stoichiometry (i.e., amino acid analysis gave 3.6 mol Arg bound/mol enzyme while 7.54 mol radiolabel was incorporated).
- These investigations (see Reference 28, Table 1) examined the reaction at pH 7.4 (rate of inactivation of 32 $M^{-1} \text{ min}^{-1}$). An approximate 100-fold increase in the rate of inactivation.
- The presence of substrate, 2-deoxyuridylic acid, prevents the modification of 1 mol of arginine per mole of enzyme. It is noted that results differ from those reported in Reference 17. There were differences in solvent conditions. It is not clear why this would account for the differences observed in these two studies. It is noted that the investigation in Reference 17 obtained similar stoichiometry with 2,3-butanedione.
- See more complete discussion of this study under Table 2. For inactivation by phenylglyoxal, a second-order rate constant of 56 $M^{-1} \text{ min}^{-1}$ was obtained at pH 8.04. The reactions were performed in the dark.
- Analysis of Tsou plots²⁶ indicates at least two classes of residues react at different rates.
- Most studies were performed in this solvent at 30°C with a second-order rate constant of 0.33 $M^{-1} \text{ s}^{-1}$. The rate was reduced in potassium phosphate ($k = 0.25 M^{-1} \text{ s}^{-1}$) and borate ($k = 0.078 M^{-1} \text{ s}^{-1}$).
- Under these conditions at 24°C, a second-order rate constant of $k = 7.08 M^{-1} \text{ min}^{-1}$ assuming that the rate of inactivation is directly related to the modification of arginine. With 2,3-butanedione in 0.04M M borate a second-order rate constant of $k = 5.4 M^{-1} \text{ min}^{-1}$ is compared to 1.69 $M^{-1} \text{ min}^{-1}$ with methylglyoxal and 0.032 $M^{-1} \text{ min}^{-1}$ with 2,4-pentanedione.
- The rate of inactivation at 25°C for the apocysteine was determined to be 3.7 $M^{-1} \text{ min}^{-1}$ and 11.1 $M^{-1} \text{ min}^{-1}$ for the holocysteine.
- A second-order rate constant of $k = 4.6 M^{-1} \text{ min}^{-1}$ at 25°C was obtained under these conditions.
- Based on incorporation of radiolabeled phenylglyoxal, 1.5 arginine residues are modified per 35,000 chain after 3 h of reaction. There are likely different classes of reactive arginyl residues where the more reactive group(s) directly associated with catalytic activity.
- Saturation kinetics are observed with phenylglyoxal suggesting the formation of an enzyme-inhibitor complex prior to reaction with an arginine residue(s).
- With 95% loss of catalytic activity there is 94% modification of arginine.
- See Reference 24 for somewhat differing results. This study shows that this level of arginine modification is associated with 80% loss of amino-terminal alanine. It was necessary to protect the α -amino group of the amino-terminal alanine with a t-butyloxycarbonyl group to avoid modification under these reaction conditions. The use of radiolabeled cyclohexanedione established Arg-6 as the primary site of modification.
- 30 Min at 25°C. Extent of modification based on radiolabel incorporation and amino acid analysis.
- For reaction at 30°C, a second-order rate constant of $k = 2.6 M^{-1} \text{ min}^{-1}$ assuming that the loss of activity seen with phenylglyoxal directly reflected the loss of an arginine residue(s).
- Determined from both amino acid analysis and radiolabel incorporation.
- Phenylglyoxal was much more effective than 2,3-butanedione or camptothecin-10-sulfonic acid.
- Assuming 2:1 stoichiometry of phenylglyoxal to arginine; reaction at 25°C. Phenylglyoxal is much more effective than 1,2-cyclohexanedione (twofold molar excess of 1,2-cyclohexanedione had $T_{1/2} = 24 \text{ min}$).

Table 1 (continued)

- From radiolabel incorporation assuming 2:1 stoichiometry. There are clearly at least two classes of reactive arginine residues. When the reaction is performed at pH 6.0, inactivation with phenylglyoxal can be partially reversed on dilution to pH 6.0 buffer.
- Inactivation rate constant of 1.3 $M^{-1} \text{ min}^{-1}$ at pH 7.5/30°C.
- Reaction performed with an undefined quantity of Tris buffer. The inactivation reaction was markedly increased by the presence of sodium ions.
- Inactivation rate constant of 132 $M^{-1} \text{ min}^{-1}$ at pH 7.5

References for Table 1

1. Takahashi, K., The reaction of phenylglyoxal with arginine residues in proteins. *J. Biol. Chem.*, 243, 6171, 1968.
2. Weber, M. M. and Sakonkay, M., Chemical evidence for a functional arginine residue in carboxypeptidase B. *Biochem. Biophys. Res. Commun.*, 48, 384, 1972.
3. Kastrowitz, E. R. and Lipson, W. N., Functionally important arginine residues of aspartate transcarbamylase. *J. Biol. Chem.*, 252, 2873, 1977.
4. Bergmeyer, H. J., Modifizierung von Argininen in pyruvat-kinase. *Hoppe-Seyler's Physiol. Chem.*, 358, 1365, 1977.
5. Lange, L. G., III, Riordan, J. F., and Vallee, B. L., Functional arginyl residues as NADH binding sites of alcohol dehydrogenase. *Biochemistry*, 13, 4361, 1974.
6. Jernvall, H., Lange, L. G., III, Riordan, J. F., and Vallee, B. L., Identification of a reactive arginyl residue in horse liver alcohol dehydrogenase. *Biochem. Biophys. Res. Commun.*, 77, 73, 1977.
7. Kohlbreiter, W. E. and Cross, R. L., Elfrapido prevents modification by phenylglyoxal of an essential arginyl residue in mitochondrial sedolone triphosphatase. *J. Biol. Chem.*, 253, 7609, 1978.
8. Bergmeyer, H. J., A reactive arginine in adenylate kinase. *Biochim. Biophys. Acta*, 577, 370, 1975.
9. Bergmeyer, H. J. and Schirmer, R. H., Properties of adenylate kinase after modification of Arg-97 by phenylglyoxal. *Biochim. Biophys. Acta*, 537, 428, 1978.
10. Vallejos, R. H., Leeson, W. L. M., and Luzzo, H. A., Involvement of an essential arginyl residue in the coupling activity of *Rhodospirillum rubrum* chromophores. *Arch. Biochem. Biophys.*, 190, 578, 1978.
11. Tunncliffe, G. and Ngo, T. T., Functional role of arginine residues in glutamic acid decarboxylase from brain and bacteria. *Experientia*, 34, 989, 1978.
12. Schless, J. V., Norum, I. L., Strager, C. D., and Hartman, F. C., Inactivation of ribulobisphosphate carboxylase by modification of arginyl residues with phenylglyoxal. *Biochemistry*, 17, 3626, 1978.
13. Phillips, M., Pho, D. B., and Friedel, L. A., An essential arginyl residue in yeast hexokinase. *Biochim. Biophys. Acta*, 566, 296, 1979.
14. Wolf, B., Kolesch, F., and Rosenberg, L. E., Essential arginine residues in the active sites of propionyl CoA carboxylase and beta-methylcrotonyl CoA carboxylase. *Enzyme*, 24, 302, 1979.
15. Mullinwald, D. P. and Fridland, I., Chemical modification of arginine at the active site of the bovine erythrocyte superoxide dismutase. *Biochemistry*, 18, 5809, 1979.
16. Merrett, D., Patel, P., Audenard, E., and Kasab, R., Involvement of an arginyl residue in the catalytic activity of myosin heads. *Eur. J. Biochem.*, 100, 421, 1979.
17. Cipolletti, K. L. and Doolittle, R. B., Essential arginyl residues in thymidylate synthetase from *Escherichia coli*. *Biochemistry*, 18, 5537, 1979.
18. Cheung, S.-T. and Fonda, M. L., Kinetics of the inactivation of *Escherichia coli* glutamate aspartate synthase by phenylglyoxal. *Arch. Biochem. Biophys.*, 199, 457, 1980.
19. Variano, K. and Lonsdaleborough, J., Evidence for essential arginine in yeast adenylate cyclase. *FEBS Lett.*, 106, 153, 1979.
20. Morfitt, E., Flahk, I. L., and Bawerjee, S. K., Phenylglyoxal modification of cardiac myosin S-1. Evidence for essential arginine residues at the active site. *J. Biol. Chem.*, 254, 12647, 1979.
21. Portner, C., Perre, Y., Loretto, C., and Chagnier, F., Number of arginine residues in the substrate binding sites of rat liver cytochrome P-450. *FEBS Lett.*, 108, 419, 1979.
22. Poulos, A. J. and Kadamakur, P. E., Presence of one essential arginine that specifically binds the 2'-phosphate of NADPH on each of the tetraacyl reductase and enoyl reductase active sites of fatty acid synthetase. *Arch. Biochem. Biophys.*, 199, 457, 1980.
23. Bond, M. W., Chan, N. Y., and Cooperman, B. S., Identification of an arginine residue important for enzymatic activity within the covalent structure of yeast inorganic pyrophosphatase. *Biochemistry*, 19, 94, 1980.
24. Venek, L. A. and Kastrowitz, E. R., An essential arginine residue in porcine phospholipase A_2 . *J. Biol. Chem.*, 255, 7306, 1980.

References for Table 1 (continued)

25. Borders, C. L., Jr. and Johnson, J. T., Essential arginyl residues in Cu, Zn superoxide dismutase from *Saccharomyces cerevisiae*, *Carlsberg Res. Commun.*, 45, 185, 1980.
26. Borders, C. L., Jr. and Johnson, J. T., Identification of Arg-143 as the essential arginyl residue in yeast Cu, Zn superoxide dismutase by the use of a chromophoric arginine reagent, *Biochem. Biophys. Res. Commun.*, 96, 1071, 1980.
27. Shoun, H., Reppas, T., and Arima, K., An essential arginine residue at the substrate-binding site of *p*-hydroxybenzoate hydroxylase, *J. Biol. Chem.*, 255, 9319, 1980.
28. Belfort, M., Mahy, G. F., and Miley, P., A single functional arginyl residue involved in the catalysis promoted by *Lariboritur casri* thymidine synthetase, *Arch. Biochem. Biophys.*, 204, 340, 1980.
29. Lu, H. S., Talbot, J. M., and Grady, R. W., Chemical modification of critical catalytic residues of lysine, arginine and tyrosine in human glucose phosphatase isomerase, *J. Biol. Chem.*, 256, 785, 1981.
30. Fujikawa, M., and Takata, Y., Role of arginine residue in saccharopine dehydrogenase (L-Lysine Forming) from baker's yeast, *Biochemistry*, 20, 468, 1981.
31. El Kabbaj, M. S., Larruffa, N., and Casademir, Y., Presence of an essential arginine residue in *D*- β -hydroxybutyrate dehydrogenase from mitochondrial inner membrane, *Biochem. Biophys. Res. Commun.*, 96, 1569, 1980.
32. Marshall, M., and Cohen, P. P., Evidence for an exceptionally reactive arginyl residue at the binding site for carbonyl phosphate in bovine ornithine transcarbamylase, *J. Biol. Chem.*, 255, 7201, 1980.
33. Kuno, S., Toraya, T., and Fukui, S., Coenzyme B₁₂-dependent diol dehydrase: chemical modification with 2,3-butanedione and phenylglyoxal, *Arch. Biochem. Biophys.*, 205, 240, 1980.
34. Krenner, A. B., Egan, R. M., and Sabbe, H. Z., The active site of transketolase. Two arginine residues are essential for activity, *J. Biol. Chem.*, 255, 2405, 1980.
35. Tsou, C.-L., Relation between modification of functional groups of proteins and their biological activity. I. A graphical method for the determination of the number and type of essential groups, *Sci. Sin.*, 11, 1535, 1962.
36. Ramakrishna, S., and Benjamin, W. B., Evidence for an essential arginine residue at the active site of ATP citrate lyase from rat liver, *Biochem. J.*, 195, 735, 1981.
37. Chang, G.-G., and Huang, T.-M., Modification of essential arginine residues of pigeon liver malic enzyme, *Biochim. Biophys. Acta*, 660, 341, 1981.
38. Choi, J.-D., and McCormick, D. B., Roles of arginyl residues in pyridoxamine-5'-phosphate oxidase from rabbit liver, *Biochemistry*, 20, 5722, 1981.
39. Fortin, A. F., Hauber, J. M., and Kantrowitz, E. R., Comparison of the essential arginine residue in *Escherichia coli* ornithine and aspartate transcarbamylases, *Biochim. Biophys. Acta*, 662, 8, 1981.
40. Wong, S. S., and Wong, L.-J., Evidence for an essential arginine residue at the active site of *Escherichia coli* acetate kinase, *Biochim. Biophys. Acta*, 660, 142, 1981.
41. Fleer, E. A. M., Pulik, W. C., Shoboom, A. J., and DeHaas, G. H., Modification of arginine residues in porcine pancreatic phospholipase A₂, *Eur. J. Biochem.*, 116, 277, 1981.
42. Alkerdy, R., Lange, L. G., Westerman, J., and Wirtz, K. W. A., Modification of the phosphatidyl-choline-transfer protein from bovine liver with butanedione and phenylglyoxal. Evidence for one essential arginine residue, *Eur. J. Biochem.*, 121, 77, 1981.
43. Braumant, G., Trilsch, D., and Billeman, J.-F., Evidence for the presence of anion-recognition sites in pig-liver aldehyde reductase. Modification by phenylglyoxal and *p*-carboxyphenyl glyoxal of an arginyl residue located close to the substrate-binding site, *Eur. J. Biochem.*, 116, 505, 1981.
44. Masauer, H. G., Palya, A. A., and Merrill, R. E., Evidence for presence of an arginine residue in the coenzyme A binding site of choline acetyltransferase, *Proc. Natl. Acad. Sci. U.S.A.*, 78, 7449, 1981.
45. Carlson, C. A., and Pridis, J., Involvement of arginine residues in the allosteric activation of *Escherichia coli* ADP-glucose synthetase, *Biochemistry*, 21, 1929, 1982.
46. Koland, J. G., O'Brien, T. A., and Camda, R. B., Role of arginine in the binding of thiamin pyrophosphate to *Escherichia coli* pyruvate oxidase, *Biochemistry*, 21, 2655, 1982.
47. King, M. M., and Henry, L. P., Chemical modification of the calmodulin-stimulated phosphatase, calcineurin, by phenylglyoxal, *J. Biol. Chem.*, 262, 10638, 1987.
48. Shanmugasundaram, T., Kumar, G. K., Shenoy, B. C., and Wood, H. G., Chemical modification of the functional arginine residues of carbon monoxide dehydrogenase from *Clastridium thermocellum*, *Biochemistry*, 28, 7112, 1989.
49. Garry, R., Yeager, O., and Asher, C., Sodium-dependent inhibition of the epithelial sodium channel by an arginyl-specific reagent, *J. Biol. Chem.*, 263, 5550, 1988.
50. Misselen, L., Raeymaekers, L., Droogmans, G., Wuyts, F., and Casteels, R., Role of arginine residues in the stimulation of the smooth-muscle plasma-membrane Ca²⁺ (T pump by negatively charged phospholipids, *Biochem. J.*, 264, 609, 1989.
51. King, M. M., Conformation-sensitive modification of the type II calmodulin-dependent protein kinase by phenylglyoxal, *J. Biol. Chem.*, 263, 4754, 1988.

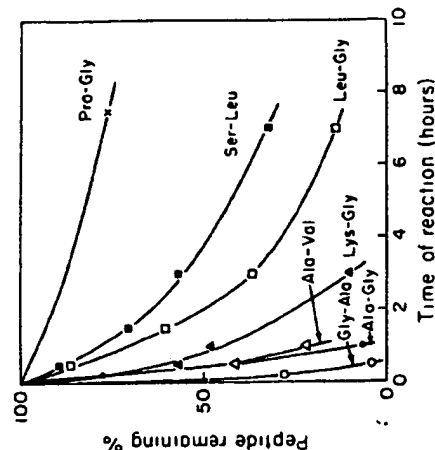


FIGURE 11. The rate of reaction of phenylglyoxal with various dipeptides. The reactions were performed in 0.2 M *N*-ethylmorpholine acetate, pH 8.0, at 25°C. The concentration of peptide was 0.01% and the concentration of phenylglyoxal hydrate was 1.25%. At the indicated times a 50- μ l portion was withdrawn from the reaction mixture, diluted into 1.2 ml sodium citrate, pH 2.2, and stored at -10°C until analysis for residual peptide on the amino acid analyzer and for amino acids after acid hydrolysis. (From Takahashi, K., *J. Biol. Chem.*, 243, 6171, 1968. With permission.)

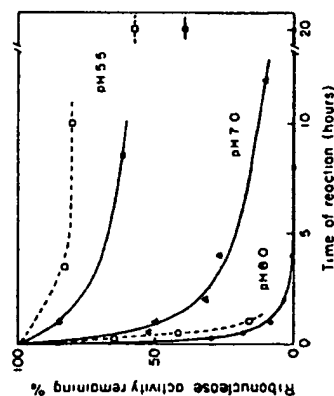


FIGURE 12. The rate of inactivation of bovine pancreatic ribonuclease A by phenylglyoxal as a function of pH. The concentration of protein was 0.5% and the concentration of phenylglyoxal hydrate was 1.5% at 25°C under the following conditions: \circ - - - pH 8.0 (0.1 M *N*-ethylmorpholine acetate); \bullet - - - pH 8.0 (0.1 M *N*-ethylmorpholine acetate with 0.6% 2'-(3'-cytidylic acid); Δ - - - pH 7.0 (0.1 M sodium phosphate); \square - - - pH 5.5 (0.1 M sodium acetate); \blacksquare - - - pH 5.5 (0.1 M sodium acetate with 0.6% 2'-(3'-cytidylic acid). (From Takahashi, K., *J. Biol. Chem.*, 243, 6171, 1968. With permission.)

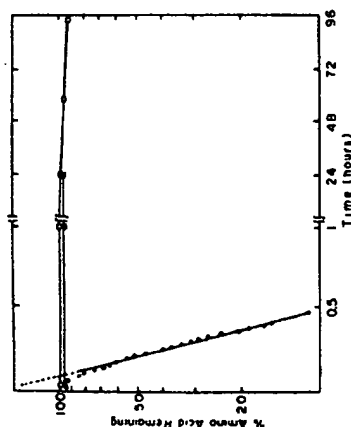


FIGURE 13. The modification of amino acid derivatives with phenylglyoxal in bicarbonate buffer. Shown is the time course for the reaction of *N*-acetylarginine (●), *N*-acetyllysine (○), and *N*-acetylcysteine (Δ) with phenylglyoxal in 83 mM bicarbonate buffer, pH 7.5, at 25°C. The reaction with *N*-acetylarginine was monitored by the increase in absorbance at 340 nm. The amounts of unreacted *N*-acetyllysine and *N*-acetylcysteine were determined by reaction with 2,4,6-trinitrobenzenesulfonic acid. (From Cheung, S.-T. and Fonda, M. L., *Biochem. Biophys. Res. Commun.*, 90, 940, 1979. With permission.)

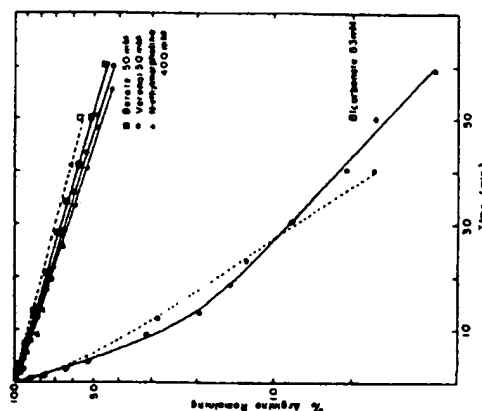


FIGURE 14. The reaction of arginine with phenylglyoxal in various buffers. The reactions mixtures contained 5 mM *L*-arginine and 25 mM phenylglyoxal in the designated buffer at pH 7.5 and 25°C. Portions were removed at the indicated times, and the arginine concentrations were determined by the Sakaguchi test (solid lines and closed symbols) or by amino acid analysis (dashed lines and open symbols). (From Cheung, S.-T. and Fonda, M. L., *Biochem. Biophys. Res. Commun.*, 90, 940, 1979. With permission.)

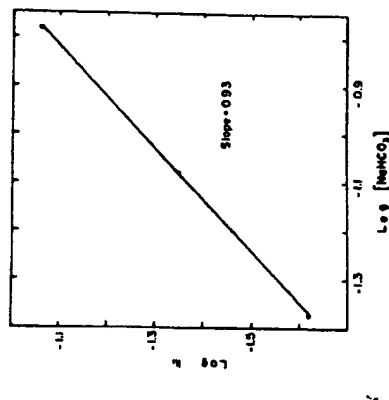


FIGURE 15. The effect of bicarbonate concentration on the rate of reaction of arginine with phenylglyoxal. Shown is a plot of logarithm apparent first-order rate constants vs. logarithm bicarbonate concentrations. The reaction mixtures contained 5 mM *N*-acetylarginine and 25 mM phenylglyoxal in sodium bicarbonate, pH 7.5, at 25°C. The absorbance at 340 nm was recorded, and the rate constants were obtained from the slopes of the plots of $\ln(A-A_\infty)$ vs. time. The slope of the line obtained in this figure is 0.93 suggesting that the reaction is first order with respect to bicarbonate. (From Cheung, S.-T. and Fonda, M. L., *Biochem. Biophys. Res. Commun.*, 90, 940, 1979. With permission.)

compares the rate of reaction of phenylglyoxal with arginine in bicarbonate buffer with that in other buffer systems (borate, Veronal, *N*-ethylmorpholine). The reaction appears to be first order with respect to bicarbonate (Figure 15). The reaction of methylglyoxal with arginine is also enhanced by bicarbonate (Figure 16) while a similar effect is not seen with either glyoxal or 2,3-butanedione. The molecular basis for this specific buffer effect is not clear at this time nor is it known whether reaction with α -amino functional groups occurs at a different rate than with other solvent systems used for this modification of arginine with phenylglyoxal. Petney and co-workers³⁰ reported that *p*-nitrophenylglyoxal (prepared from *p*-nitroacetophenone — see Reference 31) reacts with arginine in 0.17 sodium pyrophosphate — 0.15 *M* sodium ascorbate, pH 9.0 to yield a derivative which absorbs at 475 nm. There is also reaction with histidine (the imidazole ring is critical for this reaction in that the 1-methyl derivative yielded a derivative which absorbed at 475 nm while the 3-methyl derivative did not). Free sulphydryl groups also yielded a product with absorbance at 475 nm, but its absorbance was only 3% of that of the arginine. Branlant and co-workers³² have used *p*-carboxyphenyl glyoxal in bicarbonate buffer at pH 8.0 to modify aldehyde reductase. Saturation kinetics were noted with the use of this reagent.

Eun³³ has examined the effect of borate on the reaction of arginine with phenylglyoxal and *p*-hydroxyphenylglyoxal. The base buffer of these studies was 0.1 *M* sodium pyrophosphate, pH 9.0. Spectroscopy was used to follow the rate of arginine modification. The rate of modification of either free arginine or *N*-acetyl-*L*-arginine with phenylglyoxal was 10 to 15 times faster than that of *p*-hydroxyphenylglyoxal in the base buffer system. The inclusion of sodium borate (10 to 50 mM) markedly increased the rate of the reaction (approximately 20-fold) of *p*-hydroxyphenylglyoxal with either arginine or *N*-acetyl-*L*-arginine while there was only a slight enhancement of the phenylglyoxal reaction. In a related study,³⁴ the effect of phenylglyoxal on sodium-channel gating in frog myelinated nerve was compared with that of *p*-hydroxyphenylglyoxal or *p*-nitrophenylglyoxal. Both *p*-hydroxy-

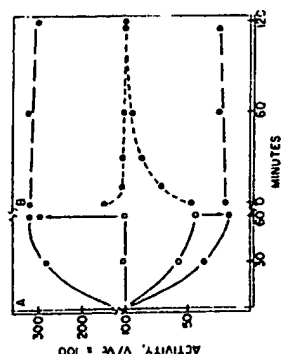


FIGURE 18. The modification of carboxypeptidase A with 2,3-butanedione in borate buffer. (A) Changes in esterase (O, Δ) and peptidase (O, Δ) activities on modification of carboxypeptidase A (0.15 mM) with 2,3-butanedione in 0.05 M borate — 1.0 M NaCl, pH 7.5 (O mM reagent, closed symbols), or in 0.02 M Veronal — 1.0 M NaCl, pH 7.5 (75 mM reagent, open symbols) at 20°C. The changes in the activity immediately on addition of borate after 1 h to the sample reacted in Veronal buffer are indicated by the arrows. (B) Changes in activities of the samples reacted in borate buffer subsequent to gel filtration through Bio-Gel P-4 equilibrated either with 0.05 M borate — 1.0 M NaCl, pH 7.5 (—), or with 0.02 M Veronal — 1.0 M NaCl, pH 7.5 (---). (From Ruedan, J. F., *Biochemistry*, 12, 3915, 1973. With permission.)

the changes in biological activity occurring on the reaction of carboxypeptidase A (0.15 mM) with 2,3-butanedione (freshly distilled). Note that in particular, the enhancement of esterase activity in the presence of butanedione is dependent on the presence of borate buffer as no significant change is seen with butanedione in 0.02 M Veronal, 1.0 M NaCl, pH 7.5. The removal of borate by gel filtration results in the recovery of activity.

The ability of 2,3-butanedione to act as a photosensitizing agent for the destruction of amino acids and proteins in the presence of oxygen was emphasized in work by Fliss and Viswanatha.²¹ Figure 19 shows the destruction of certain amino acids in the presence of 2,3-butanedione and oxygen at pH 6.0 (phosphate) 36°C upon irradiation at 350 to 375 nm ("Blak-Lite" UV-Lamp, 100 W bulb, 20 cm from sample contained in a quartz cuvette). As would be expected from consideration of early photooxidation work, tryptophan and histidine are lost most rapidly with methionine; cysteine and tyrosine are lost at a much slower rate. Loss is not seen on irradiation in the absence of 2,3-butanedione (open symbols). Azide (10 mM), a singlet oxygen scavenger, greatly reduced the rate of loss of amino acids. The absence of oxygen also greatly reduces the rate of loss of sensitive amino acids.

These observations have been confirmed and extended by other laboratories.^{22,23} An examination of recent studies using 2,3-butanedione to modify arginyl residues in proteins is presented in Table 2.

The use of 1,2-cyclohexanedione under very basic conditions to modify arginyl residues was demonstrated in 1967.²⁴ However, it was not until Parthy and Smith⁴ reported on the reaction of 1,2-cyclohexanedione in borate with arginyl residues in proteins that the use of this reagent became practical. These investigators reported that 1,2-cyclohexanedione reacted with arginyl residues in 0.2 M borate, pH 9.0. At alkaline pH, reaction of 1,2-cyclohexanedione with arginine (Figure 20) forms *N*-(4-oxo-1,3-diazaspiro[4.4]non-2-ylidene)-L-ornithine (CHD-arginine), a reaction which cannot be reversed. Between pH 7.0 and pH 9.0 a compound is formed from arginine and 1,2-cyclohexanedione, *N*-(4-oxo-1,2-dihydroxycyclohex-1,2-ylene)-L-arginine (DHCH-arginine). This compound is stabilized by the presence of borate and is unstable in the presence of buffers such as Tris. This compound is readily converted back to free arginine in 0.5 M hydroxylamine, pH 7.0 (Figure 21).

These authors have subsequently used this reagent to identify functional residues in bovine pancreatic ribonuclease A and egg white lysozyme.²⁵ Extent of modification of arginine

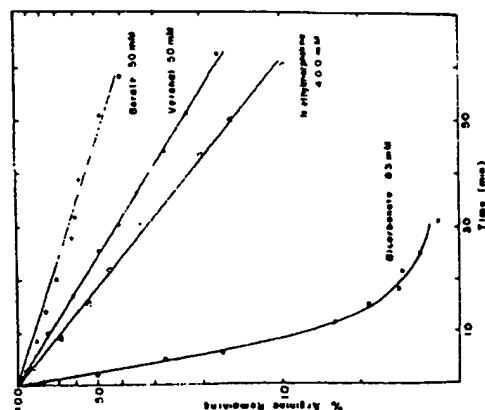


FIGURE 16. The effect of various buffers on the rate of reaction of arginine with methylglyoxal. The reaction mixtures contained 5 mM arginine and 25 mM methylglyoxal in the buffers indicated. Portions were removed at the indicated times for the determination of the amount of arginine remaining by the Sakaguchi test. (From Cheung, S.-T. and Fonda, M. L., *Biochem. Biophys. Res. Commun.*, 90, 940, 1979. With permission.)

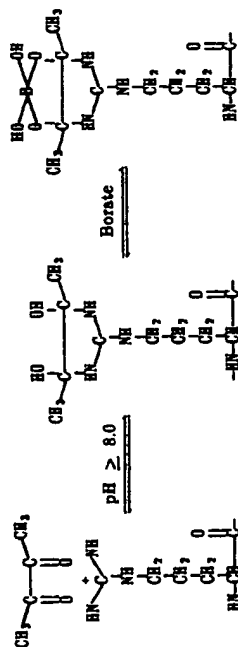


FIGURE 17. A scheme for the reaction of arginine with 2,3-butanedione.

phenylglyoxal and *p*-nitrophenylglyoxal had less effect than phenylglyoxal in reduced sodium current. The results are discussed in terms of the differences in hydrophobicity of the reagents but it is clear that the intrinsic difference in reagent effectiveness described by Eun may be responsible, in part, for the observed differences.

2,3-Butanedione is a second well-characterized reagent for the selective modification of arginyl residues in proteins. Yankelov and co-workers introduced the use of this reagent.^{26,27} There were problems with the specificity of the reaction (c.f. Reference 35) and the time required for modification until the observation of Rioridan²⁸ that borate had a significant effect on the nature of the reaction of 2,3-butanedione with arginyl residues in proteins (Figure 17). Figure 18 shows the effect of borate (0.05 M borate, 1.0 M NaCl, pH 7.5) on

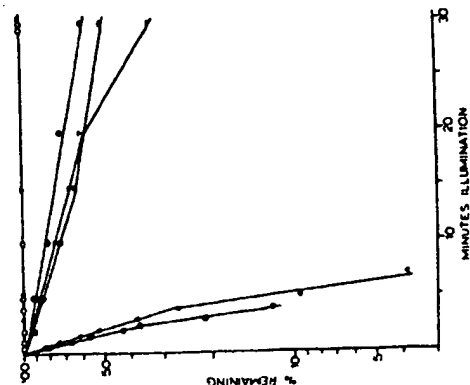


FIGURE 19. 2,3-Butanedione-oxidized destruction of α -amino acids. \circ , tyrosine (99.5 μ M); \square , methionine (1000 μ M); \triangle , histidine (92 μ M); \circ , cysteine (33.3 μ M) in the presence of 2,3-butanedione (9580 μ M) and continuous oxygenation were irradiated at pH 6.0 (irradiation was performed in quartz cuvettes) 20 cm from a "Blak-Lite" UV light source, Canlab catalog No. L6093-1, equipped with a 100 W lamp emitting light almost exclusively in the range of 350 to 375 nm at 36°C. Open symbols represent preparations of amino acids (at the same concentrations as the experiments described above) irradiated in the absence of 2,3-butanedione. The above experiment used freshly distilled monomer preparation of 2,3-butanedione. (From Fliiss, H. and Viswanatha, T., *Can. J. Biochem.*, 57, 1267, 1979. With permission.)

Table 2
USE OF 2,3-BUTANEDIONE TO MODIFY ARGINYL RESIDUES IN PROTEINS

Protein	Solvent	Reagent excess ^a	Stoichiometry	Ref.
Carboxypeptidase A	0.05 M borate, 1.0 M NaCl, pH 7.5	—	2/10	1
Chymotrypsin	0.1 M phosphate, pH 6.0	100 ^b	1/3 ^c	2
Thymidylate synthetase	0.050 M borate, pH 8.0	—	—	3
Prostatic acid phosphatase	0.050 M borate, pH 8.0	—	—	4
Purine nucleoside phosphorylase	0.0165 M borate, pH 8.0	—	—	5
Yeast hexokinase PII	0.050 M borate, pH 8.3	—	4.2/18 ^d	6
Isoctinate dehydrogenase	0.05 M MES, pH 6.2, 20% glycerol, 0.0021 M MnSO_4	—	1.6/13.4 ^e	7
Sterylcoenzyme A desaturase	0.050 M sodium borate, pH 8.1	2500	2/2	8
Superoxide dismutase	0.050 M borate, pH 9.0	—	1.3/4 ^f	9
Energy-independent transhydrogenase	0.050 M sodium ^g borate, pH 7.8	—	—	10
Enolase	0.050 M borate, pH 8.3, 0.001 M Mg (OAc) ₂ , 0.01 mM EDTA	260	3/16 ^h	11
NADPH-dependent aldehyde reductase	0.050 M borate, pH 7.0	—	1/18 ⁱ	12

^a Mole reagent per mole protein unless otherwise indicated.

^b This study demonstrated that, in the presence of borate, there is essentially no difference in the reaction of 2,3-butanedione enolizer and borate-free trimer. It is noted that the commercially available 2,3-butanedione should be distilled immediately prior to use.

^c This study used 2,3-butanedione trimer prepared by allowing 2,3-butanedione (40 ml) to stand with 80 g untreated Permuit under dry air (after shaking to obtain an even dispersion of 2,3-butanedione in Permuit) for 4 to 6 weeks at ambient temperature. The mixture was extracted with anhydrous ether. The ether extract was taken to an oil with dry air. The oil was allowed to stand for 5 to 7 days to permit crystallization of the trimer.

Table 2 (continued)
USE OF 2,3-BUTANEDIONE TO MODIFY ARGINYL RESIDUES IN PROTEINS

Protein	Solvent	Reagent excess ^a	Stoichiometry	Ref.
Argyl sulfatase A	0.050 M NaHCO_3 , pH 8.0	—	—	13
Na^+ , K^+ -ATPase	0.04 M TES, 0.02 M borate, pH 7.4	—	—	14
Carbamate kinase	0.005 M trichloroamine, 0.050 M borate, pH 7.5	20X0	1.2/3.0 ^b	15
Thymidylate synthetase	0.050 M borate, 0.001 M EDTA, pH 8.0	1201	2.1/12 ^c	16
(K^+ + H^+)-ATPase	0.125 M sodium borate, pH 7.0	—	—	17
Cu, Zn superoxide dismutase	0.050 M borate, pH 8.3	— ^d	—	18
Fatty acid synthetase	0.020 M borate, 0.200 M KCl, 0.001 M dithiothreitol, 0.001 mM EDTA, pH 7.6	—	—	19
Acetylcholinesterase ^e	0.005 M phosphate, 0.025 M borate, 0.050 M NaCl, pH 7.0	—	4/31 ^f	20
Coenzyme B ₁₂ -dependent diol dehydrase	0.050 M borate, pH 8.5	—	—	21
Ominibine transcarbamylase	0.05 M bicine, 0.1 mM EDTA, 0.1 M KCl, pH 7.67	—	0.88/11 ^g	22
Glycogen phosphorylase	0.020 M sodium tetraborate, 1 mM EDTA, pH 7.5	—	—	23
Cytochrome c	0.05 M sodium bicarbonate, pH 7.5	9900 ^h	2/2 ⁱ	24
Bacteriorhodopsin	0.100 M borate, pH 8.2	66,700	4/79 ^j	25
α -Ketoglutarate dehydrogenase	0.050 M sodium borate, pH 8.0	— ^k	—	26
Acetate kinase	0.050 M borate, pH 8.6	—	—	27
Malic enzyme	0.045 M borate ^l , pH 7.3	—	—	28
Glucose phosphate isomerase	0.05 M sodium borate, pH 8.7	—	7.8/70 ^m	29
Saccharopine dehydrogenase	0.08 M HEPES, 0.2 M KCl, 0.01 M borate, pH 8.0	— ⁿ	8/38 ^o	30
Testicular hyaluronidase	0.050 M borate, pH 8.3	—	3.6/28	31
Glutathione reductase	0.050 M sodium borate, pH 8.3, 1 mM EDTA	20,000	5.3 ^p	32
<i>E. coli</i> fibrillar adhesins	100 mM sodium borate with 0.9% NaCl, pH 7.5	—	—	34
Inter-alpha trypsin inhibitor	10 mM HEPES-175 mM NaCl, 100 mM sodium borate, pH 7.4	—	—	35
D-Glyceraldehyde-3-phosphate dehydrogenase	100 mM sodium ^q buffer, pH 8.3 with 5 mM EDTA and 2 mM dithiothreitol	—	—	36

Table 2 (continued)
USE OF 2,3-BUTANEDIONE TO MODIFY ARGINYL RESIDUES IN PROTEINS

- The use of isolated "membrane fraction" prevented the establishment of stoichiometry in these studies. Analysis of the dependence of reaction rate on concentration of 2,3-butanedione is consistent with the modification of a single arginine residue. As expected, the stability of modification is dependent upon the presence of borate. Gel filtration into HEPES (0.125 M, pH 7.0) and subsequent inactivation at 37°C resulted in the recovery of a substantial amount of catalytic activity. Similar results were obtained with imidazole and Tris buffers under similar reaction conditions. This reactivation does not occur when the incubation following gel filtration is performed at 0°C instead of 37°C.
- A reaction rate with a second-order constant of $k = 5.2 M^{-1} \text{ min}^{-1}$ is obtained at 25°C. Inactivation is dependent on the presence of borate as inactivation is not observed with use of BICINE buffer. Dialysis vs. 0.025 M phosphate, pH 7.0 for 21 h at 4°C results in an increase in activity of 14 to 85% while complete recovery of activity is achieved after 21 h of dialysis.
- Stoichiometry was not established for the reaction with 2,3-butanedione. As shown in Table 1, reaction with phenylglyoxal modifies approximately 4 of the 106 arginyl residues in each subunit of fatty acid synthase. The loss of the biological activity is determined either by fatty acid synthase activity, ketoreductase activity, or enoylreductase activity was considerably more rapid with phenylglyoxal than with 2,3-butanedione. It is noted that these reactions are performed in borate buffer for the studies with 2,3-butanedione and phosphate buffer for the studies with phenylglyoxal, both buffers at pH 7.6 with the reactions performed at 30°C.
- Reactions were performed at 25°C. The modification of arginyl residues is associated with an approximate 70% loss of enzymatic activity. The presence of *N*-phenylpyridinium-2-aldoxime iodide reduces the extent of arginine modification by approximately 1 mol/mol of enzyme with concomitant protection of enzymatic activity. It should be noted that modification of this enzyme with phenylglyoxal results in the modification of 3 mol of arginine/mol enzyme with 17% loss of enzymatic activity (see Table 1). It is not clear when modification of a particular arginyl residue with the two reagents is a mutually exclusive event.
- Reactions were performed at 25°C. Rigorous evaluation of the stoichiometry of the reaction is not available. Analysis of the dependence of first-order rate constants on reagent concentration (double-logarithmic relationship) is consistent with the modification of a single arginyl residue. The inactivation was reversed by 100-fold dilution into 0.05 M potassium phosphate, pH 8.5, at 25°C.
- The inactivation of ornithine transcarbamylase is readily reversible in this solvent; the presence of borate precludes reactivation observed on dilution of modified enzyme in solvent. A value of $179 M^{-1} \text{ min}^{-1}$ for the second-order rate constant for reaction of 2,3-butanedione with ornithine transcarbamylase under these conditions was recorded.
- Obtained at 88% inactivation.
- Reaction at 22°C.
- Determined by amino acid analysis. The reaction is readily reversible, even in the presence of borate.
- Determined by amino acid analysis. Constructed Scatchard plot shows that two residues were not available for modification with 2,3-butanedione.
- Second-order rate constant, $k = 2.95 M^{-1} \text{ min}^{-1}$ in this solvent, assuming that loss in catalytic activity is a measure of reaction with arginine.
- Stoichiometry was not established. Kinetic analysis suggests that inactivation of catalytic activity results from the modification of a single arginine residue.
- Modification reaction was performed at 24°C. Very little inactivation is observed if the reaction is performed in Tris buffer at the same pH. Reactivation of enzyme modified in borate buffer is observed when the inactivated enzyme is diluted in borate buffer.
- The reaction was performed at 25°C for 4 h. The presence of the competitive inhibitor, 6-phosphogluconate, protected 1 mol of arginine/mol of enzyme from modification suggesting that there is a single arginine residue critical for catalytic activity. A 20-fold increase in inhibitor concentration resulted in the modification of greater than 95% of the total arginine residues.
- Second-order rate constant of $k = 7.5 M^{-1} \text{ min}^{-1}$ at 25°C was obtained from the analysis of reaction rate data. pH dependence study showed optimal rate of inactivation at pH 8.2.
- Determined by amino acid analysis on 95 ± 5% inactivated enzyme. Plotting loss of activity vs. arginine residues modified suggests that inactivation is due to the modification of a single arginine residue. Inactivation occurs with loss of sulphydryl content.
- Second-order rate constant of $k = 13.57 M^{-1} \text{ min}^{-1}$ obtained at 20°C. Inactivation much less rapid in 0.050 M HEPES, pH 8.3 ($T_{50} = 30 \text{ min}$ in borate; 11.5 min in HEPES).
- Reactions performed at 30°C. Modification associated with 80 to 90% inactivation. Reaction with phenylglyoxal (0.050 M sodium phosphate, 1 mM EDTA, pH 7.6) at 200-fold molar excess led to the modification of 2 arginyl residues (at a level of 90% inactivation). The extent of arginine was determined by spectrophotometric analysis (increase in absorbance at 250 nm, $\Delta\epsilon = 11,000 M^{-1} \text{ cm}^{-1}$; see Reference 33).
- Reaction readily reversible, reflecting the absence of borate in the buffer.

Table 2 (continued)
USE OF 2,3-BUTANEDIONE TO MODIFY ARGINYL RESIDUES IN PROTEINS

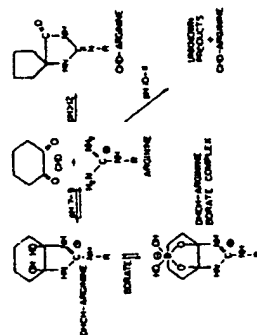
- In the absence of light, also some loss of lysine; no loss of catalytic activity. In the presence of sunlight there was rapid inactivation of the enzyme with loss of lysine, arginine (less than in the dark), and lysine. With the exception of lysine modification, the changes in amino acid composition in the reaction exposed to light were less than those for the dark reaction despite the more significant loss of activity. Study of the wavelength dependence demonstrates that light of 300 nm is most effective. 2,3-Butanedione monomer was not effective in this photoactivation process.
- Stoichiometry of reaction not established. Inactivation was reversed by gel filtration in 0.05 M Tris, 0.010 M β -mercaptoethanol, pH 8.0.
- Ambient temperature. Calf spleen enzyme had 76 Arg modified at 98% loss of activity. Reaction with arginyl residues (as judged by loss of catalytic activity) was 50% as rapid with 2,3-butanedione in borate ($T_{50} = 40.3 \text{ min}$) as with phenylglyoxal in Tris buffer ($T_{50} = 19.2 \text{ min}$).
- Reaction at 25°C. Determined by amino acid analysis after acid hydrolysis (6 N HCl, 110°C, 18 h). MgATP (5 mM) did not protect against either modification or loss of enzymatic activity but MgATP and glucose reduced extent of modification from 3.3 arginine residues per subunit (65% inactivation) to 2.1 residues per subunit (20% inactivation). Inactivation was also observed with phenylglyoxal in 0.050 M BICINE, pH 8.3. Stoichiometry with this modification was not established.
- Determined by amino acid analysis. As indicated, the maximum value obtained is 1.6 residues modified out of an average of 13.4 arginyl residues per subunit.
- The modification was performed at 25°C. The presence of acetyl-CoA greatly decreased the rate and extent of inactivation by 2,3-butanedione. When the modified enzyme is taken into 0.020 Tris (acetate), 0.100 M NaCl, pH 8.1 by gel filtration there is a rapid recovery of activity and the concomitant decrease in the extent of arginine modification. A similar extent of modification and loss of catalytic activity was seen with 1,2-cyclohexanedione in 0.1 M sodium borate, pH 8.1.
- Inactivation occurred at a rate of $10.9 M^{-1} \text{ min}^{-1}$ under these conditions (compared to $4.0 M^{-1} \text{ min}^{-1}$ with phenylglyoxal in bicarbonate/carbonate and $6.6 M^{-1} \text{ min}^{-1}$ with 1,2-cyclohexanedione in 0.050 M borate, pH 9.0). Inactivation with 2,3-butanedione is not observed in 0.05 M bicarbonate/carbonate, pH 9.0 at 25°C; however there is reduced modification of arginine (0.4 residue per subunit as compared to 1.3 residues per subunit with 71% inactivation).
- The majority of arginine modification could be reversed by the removal of reagent and borate solvent by dialysis vs. 0.05 M potassium phosphate, pH 7.8. Enzymatic activity was also recovered as a result of the dialysis procedure. These investigators were able to obtain evidence supporting the selective modification of Arg¹⁰⁰ by either 2,3-butanedione, 1,2-cyclohexanedione or phenylglyoxal.
- The modification was performed at 22°C. These studies were performed with bacterial membrane preparations. Stoichiometry was not established. Analysis of the rates of inactivation suggested that inactivation was due to the modification of a single arginine residue. NADH, which stimulates the transhydrogenation of 3-acetylpyridine-NAD by NADPH, protects the enzyme from inactivation.
- The modification was performed at 25°C. The extent of modification was determined by amino acid analysis after acid hydrolysis. The extent of modification reported was obtained after 75 min of reaction concomitant with 85% loss of activity. The presence of substrate, α -phosphogluconate, reduced the extent of modification to 2 mol arginine per subunit with only 5% loss of catalytic activity.
- A second-order rate constant of $0.0635 M^{-1} \text{ min}^{-1}$ was obtained for the loss of enzymatic activity upon reaction with 2,3-butanedione in 0.030 M borate, pH 7.0 at 25°C. This presumably reflects the modification of a single arginine residue (see Footnote p). The inactivation of the enzyme by 1,2-cyclohexanedione, methylglyoxal, and phenylglyoxal is compared with that by 2,3-butanedione (all at 10 mM in 0.05 M borate, pH 7.0). Butanedione is clearly most effective followed by phenylglyoxal, methylglyoxal, and 1,2-cyclohexanedione. The authors note that the enzyme under study, aldehyde reductase, can utilize methylglyoxal and phenylglyoxal as substrates, precluding their rigorous evaluation in this study.
- Obtained by amino acid analysis after acid hydrolysis (6 N HCl, 110°C, 24 h). The control preparation yielded a value of $17.8 \pm 1 \text{ Arg}$ while the modified enzyme yielded a value of $16.7 \pm 1 \text{ Arg}$. The presence of cofactor yielded a preparation with $17.5 \pm 1 \text{ Arg}$.
- The reactions are reported at 17.5 ± 1 Arg. Borate buffers could not be used since borate is a competitive inhibitor of the enzyme and prevents inactivation in bicarbonate buffer. Reaction with phenylglyoxal in the same solvent. Reaction performed at 25°C. Stoichiometry established by amino acid analysis after acid hydrolysis (6 N HCl, 100°C, 20 h). Arginine is the only amino acid modified under these reaction conditions. These values were obtained at 80% inactivation. The presence of ADP reduced activity loss to 55% with extent of arginine modification reduced to 0.4 to 0.3 residues.
- Reaction performed at 25°C for 90 min. Stoichiometry determined by amino acid analysis after acid hydrolysis (6 N HCl, 110°C, 24 h).

References for Table 2

1. Rjordan, J. F., Functional arginyl residues in carboxypeptidase A. Modification with butanedione. *Biochemistry*, 12, 3915, 1973.
2. Elias, H., Tozer, N. M., and Vivasubash, T., The reaction of ethylenediamine with 2,3-butanedione trimer. *Can. J. Biochem.*, 53, 275, 1975.
3. Cipolletti, K. L., and Dunlap, R. B., Essential arginyl residues in thymidylate synthetase. *Biochem. Biophys. Res. Commun.*, 81, 1139, 1978.
4. McTigue, J. J., and Van Etten, R. L., An essential arginine residue in human prostatic acid phosphatase. *Biochim. Biophys. Acta*, 523, 422, 1978.
5. Jordan, F., and Wu, A., Inactivation of putine nucleotide phosphorylase by modification of arginine residues. *Arch. Biochem. Biophys.*, 190, 690, 1978.
6. Bordas, C. L., Jr., Cipolletti, K. L., and Jurdasch, J. F., Role of arginyl residues in yeast hexokinase. *PNL Biochemistry*, 17, 2654, 1978.
7. Hayman, S., and Collins, R. F., Effect of arginine modification on the catalytic activity and allosteric activation by adenosine diphosphate of the diphosphopyridine nucleotide specific isocitrate dehydrogenase of pig heart. *Biochemistry*, 17, 4161, 1978.
8. Enoch, G. G., and Strittmatter, P., Role of tyrosyl and arginyl residues in rat liver microsomal sterol-coenzyme A desaturase. *Biochemistry*, 17, 4927, 1978.
9. Malinowski, D. P., and Erdreich, L., Chemical modification of arginine at the active site of the bovine cytochrome c oxidase. *Biochemistry*, 18, 5909, 1979.
10. Hoeny, M., and Bregg, P. D., Steady-state kinetics and the inactivation by 2,3-butanedione of the energy-independent transhydrogenase of *Escherichia coli* cell membranes. *Biochim. Biophys. Acta*, 571, 201, 1979.
11. Borders, C. L., Jr., and Zacher, J. A., Rabbit muscle enolase also has essential arginyl residues. *FEBS Lett.*, 108, 415, 1979.
12. Davidson, W. S., and Flynn, T. G., A functional arginine residue in NADPH-dependent aldehyde reductase from pig kidney. *J. Biol. Chem.*, 254, 3724, 1979.
13. James, G. T., Essential arginine residues in human liver aspartate aminotransferase. *Biochem. Biophys.*, 197, 57, 1979.
14. Griebahn, C. M., Characterization of essential arginyl residues in sheep kidney ($\text{Na}^+ + \text{K}^+$)-ATPase. *Biochem. Biophys. Res. Commun.*, 88, 229, 1979.
15. Pitt, R. P., Marshall, M., and Villafraña, J. J., Modification of an essential arginine of carbamate kinase. *Arch. Biochem. Biophys.*, 199, 16, 1980.
16. Cipolletti, K. L., and Dunlap, R. B., Essential arginyl residues in thymidylate synthetase from amphotericin-resistant *Leishmania tarentolae*. *Biochemistry*, 18, 5337, 1979.
17. Schryver, J. J., Layman, W. A. H. M., DePrest, J. J. H. M., and Beetham, S. L., Studies on ($\text{K}^+ + \text{H}^+$)-ATPase. I. Essential arginine residue in its substrate binding center. *Biochim. Biophys. Acta*, 597, 331, 1980.
18. Belburt, M., Males, G. F., and Males, F., A single functional arginyl residue involved in the catalysis promoted by *Leishmania tarentolae* thymidylate synthetase. *Arch. Biochem. Biophys.*, 204, 340, 1980.
19. Paulose, A. J., and Kollatinsky, P. E., Presence of one essential arginine that specifically binds the 2'-phosphate of NADPH on each of the ketoreductase and enoyl reductase active sites of fatty acid synthetase. *Arch. Biochem. Biophys.*, 190, 437, 1980.
20. Moller, H., and Soud, H., Essential arginine residue in acetylcholinesterase from *Torpedo californica*. *FEBS Lett.*, 119, 213, 1980.
21. Kuno, S., Toriye, T., and Fukui, S., Coenzyme B_{12} -dependent diol dehydratase: chemical modification with 2,3-butanedione and phenylglyoxal. *Arch. Biochem. Biophys.*, 205, 240, 1980.
22. Marshall, M., and Cohen, P. F., Evidence for an exceptionally reactive arginyl residue at the binding site for carbonyl phosphate in bovine ornithine transcarbamylase. *J. Biol. Chem.*, 255, 7201, 1980.
23. Dryden, M., Vandenbinder, B., and Bue, H., Mechanism of allosteric activation of glycogen phosphorylase probed by the reactivity of essential arginyl residues. Physicochemical and kinetic studies. *Biochemistry*, 19, 3634, 1980.
24. Paudyal, J., and Meyer, Y. P., The arginines of cytochrome c. The reduction-binding site for 2,3-butanedione and ascorbate. *J. Biol. Chem.*, 255, 11094, 1980.
25. Tristram-Nagle, S., and Peck, L., Effects of arginine modification on the photocycle and proton pumping of bacteriorhodopsin. *Biochem. Int.*, 3, 621, 1981.
26. Gomazova, V. S., Suleeva, and Severin, S. E., The role of arginine residues in the functioning of α -ketoglutarate dehydrogenase from pigeon breast muscle. *Biochem. Int.*, 2, 51, 1981.
27. Wang, S. S., and Wong, L.-J., Evidence for an essential arginine residue at the active site of *Escherichia coli* acetate kinase. *Biochim. Biophys. Acta*, 660, 142, 1981.
28. Chang, G.-G., and Rung, T.-M., Modification of essential arginine residues of pigeon liver malic enzyme. *Biochim. Biophys. Acta*, 660, 341, 1981.

References for Table 2 (continued)

29. Lu, H. S., Takem, J. M., and Gray, R. W., Chemical modification of critical catalytic residues of lysine, arginine and tryptophan in human glucose phosphate isomerase. *J. Biol. Chem.*, 256, 783, 1981.
30. Fujikawa, M., and Takata, Y., Role of arginine residue in ascorbate dehydrogenase (L-Lysine Forming) from baker's yeast. *Biochemistry*, 20, 468, 1981.
31. Gaceta, P., Savitsky, M. J., Dodgson, K. S., and Olavsen, A. H., Modification of functional arginine residues in purified bovine testicular lysyltransferase with butane-2,3-dione. *Biochim. Biophys. Acta*, 661, 205, 1981.
32. Boggaram, V., and Mannervik, B., Essential arginine residues in the pyridine nucleotide binding sites of glutathione reductase. *Biochim. Biophys. Acta*, 701, 119, 1982.
33. Takahashi, K., Further studies on the reactions of phenylglyoxal and related reagents with proteins. *J. Biochem.*, 91, 403, 1977.
34. Jacobs, A. A. C., van Mechelen, J. R., and De Graaf, F. K., Effect of chemical modification on the K99 and K88ab fimbrial adhesins of *Escherichia coli*. *Biochim. Biophys. Acta*, 832, 148, 1983.
35. Swalin, M. W., and Plazo, S. V., Modification of the tandem reactive centres of human inter- γ -trypsin inhibitor with butanedione and *cis*-dichlorodiamminoplatinum (II). *Biochem. J.*, 254, 171, 1988.
36. Aoyama, R. A., Kumbakaya, E. V., Tikhov, V. I., Desubekere, I. V., and Nagardova, N. K., An examination of the role of arginine residues in the functioning of α -glyceroldehyde-3-phosphate dehydrogenase. *Biochim. Biophys. Acta*, 997, 159, 1989.



Scheme 1

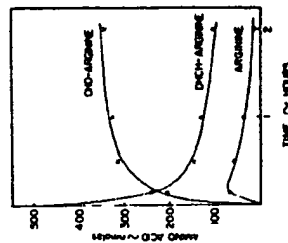


FIGURE 20. The reaction of arginine with 1,2-cyclohexanedione. Scheme 1 shows a representation of the reaction of 1,2-cyclohexanedione with arginine. The figure shows the conversion of DHCH-arginine to CHD-arginine in 0.5 M NaOH. Amino acids were determined on the amino acid analyzer. (From Puthy, L. and Smith, E. L., *J. Biol. Chem.*, 250, 557, 1975. With permission.)

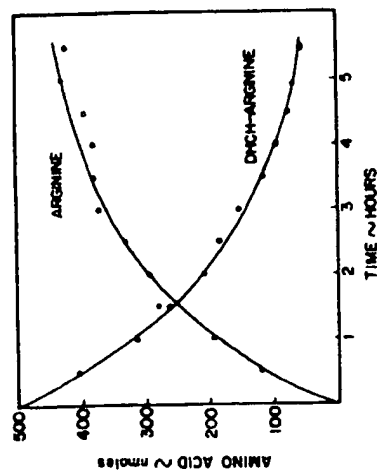


FIGURE 21 Disappearance of DHCH-arginine and formation of arginine on treatment with neutral hydroxylamine. DHCH-arginine (0.1 M) was incubated in 0.3 M hydroxylamine, pH 7.0, at 37°C. The amino acids were determined on the amino acid analyzer. Both sets of data are first order with a half time of 100 min. (From Puthy, L. and Smith, E. L., *J. Biol. Chem.*, 250, 557, 1975. With permission.)

residues in protein by 1,2-cyclohexanedione is generally assessed by amino acid analysis after acid hydrolysis. Under the conditions normally used for acid hydrolysis (6 N HCl, 110°C, 24 h), the borate-stabilized reaction product between arginine and 1,2-cyclohexanedione is unstable and there is partial regeneration of arginine and the formation of unknown degradation products.⁴ Acid hydrolysis in the presence of an excess of mercaptoacetic acid (20 μ M) of hydrolysis prevents the destruction of DHCH-arginine.⁴ Table 3 lists some of the enzymes in which structure-function relationships have been studied by reaction with 1,2-cyclohexanedione and others are discussed below in comparison with phenylglyoxal and/or 2,3-butanedione. It is the purpose of the following section to discuss some selected studies on the use of the reagents discussed above for the modification of arginyl residues in proteins. We have chosen these particular studies *strictly on the basis of the illustration of a specific aspect of the chemistry of a given reagent(s)*. As will be apparent, a number of investigators use several reagents (e.g., phenylglyoxal and/or 2,3-butanedione) with a given protein.

Vallejos and co-workers¹⁹ have examined the modification of a photophosphorylation factor in *Rhodospirillum rubrum* chromatophore with either 2,3-butanedione or phenylglyoxal as shown in Figure 22. The reactions were performed in 0.050 M borate, pH 7.8 (25°C). Stoichiometry is not reported but it is not unreasonable to suggest that the two reagents react at the same site, in which case phenylglyoxal is more effective. These reactions were performed in the dark. When the reaction with 2,3-butanedione is performed in the light there is an approximately 25-fold increase in the rate of inactivation. These investigators discuss this in terms of a conformational change in the chromatophore but do not consider possible photosensitization as described above. Homyk and Bragg²⁰ compared the effect of 2,3-butanedione and phenylglyoxal on the energy-independent transhydrogenase of *Escherichia coli*. The results of these experiments are shown in Figure 23. The reactions were performed in 0.050 M sodium borate, pH 7.8 at 22°C. Phenylglyoxal and 2,3-butanedione were of approximately equal effectiveness in reducing enzymatic activity. The insets show plots of the logarithm of the observed pseudo-first-order rate constants vs. the logarithm of

Table 3
REACTION OF ARGINYL RESIDUES IN PROTEINS WITH 1,2-CYCLOHEXANEDIONE

Protein	Solvent	Reagent excess	Extent of modification	Ref.
Ribonuclease A	0.2 M sodium borate, pH 9.0	50,000	3/4	1
Lysozyme	0.2 M sodium borate, pH 9.0	50,000	11/11	1
Kunitz bovine trypsin inhibitor	0.2 M sodium borate, pH 9.0	—	5.5/6	2
Threonine dehydrogenase	25 μ M Trethanolamine-2S μ M sodium borate with 2.5 μ M 2-mercaptoethanol, pH 7.4	—	—	3
Phosphoenolpyruvate carboxylase	65 mM Tris-Cl, pH 7.4	—	—	4

- Rate of inactivation with 1,2-cyclohexanedione less than that observed with corresponding molar excesses of either phenylglyoxal or 2,3-butanedione.
- Rate constant for inactivation of 0.313 hr^{-1} at pH 7.4/22°C.

References for Table 3

1. Puthy, L. and Smith, E. L., Identification of functional arginine residues in ribonuclease A and lysozyme, *J. Biol. Chem.*, 250, 565, 1975.
2. Meigs, R. E., Ferroni, R., Bessard, C. A., and Rerach, R., Arginine modification in Kunitz bovine trypsin inhibitor through 1,2-cyclohexanedione, *Int. J. Pept. Protein Res.*, 10, 146, 1977.
3. Eggerly, B. B. and Dekker, E. E., Inactivation of *Escherichia coli* L-threonine dehydrogenase by 2,3-butanedione. Evidence for a catalytically essential arginine residue, *J. Biol. Chem.*, 264, 18296, 1989.
4. Cheng, K.-C. and Novak, T., Arginine residues at the active site of avian liver phosphoenolpyruvate carboxylase, *J. Biol. Chem.*, 264, 3317, 1989.

the inhibitor concentration. In this type of analysis a straight line should be obtained with a slope equal to the number of inhibitor molecules reacting with each active site to yield an inactive enzyme.^{41,42} The analysis for phenylglyoxal yielded a slope of 1.1 while that for 2,3-butanedione gave a slope of 0.8. Therefore these experiments are consistent with the loss in catalytic activity resulting from the modification of one arginyl residue per active site of the enzyme. Also shown in Figure 23 is the protection by substrates and substrate analogs on the rate of inactivation by 2,3-butanedione.

The modification of hexokinase⁴³ by phenylglyoxal (Figure 24) is of interest since analysis of the dependence of reaction rate on reagent concentration suggests the formation of a protein-phenylglyoxal complex prior to the modification of arginine. Note also that a stoichiometry of 1:1 is suggested based on [¹⁴C] phenylglyoxal incorporation while the original studies with free arginine² suggested 2:1 stoichiometry. The reaction of phenylglyoxal with arginyl residues in a myosin fragment⁴⁴ (Figures 25 and 26) also suggests "saturation kinetics" with the formation of a reagent-protein complex prior to modification of an arginine residue. The effect of bicarbonate on the reaction of phenylglyoxal with arginine has been discussed above. Fonda and co-workers⁴⁵ have extended these observations to a consideration of the modification of arginyl residues in glutamate decarboxylase. The holoenzyme is resistant to inactivation by a variety of reagents specific for arginine while the apoenzyme is susceptible. Phenylglyoxal was the most effective ($k_2 = 107.68 \text{ M}^{-1} \text{ min}^{-1}$ in 0.125 M bicarbonate, pH 7.5) of the reagents tested. Figure 27 shows the time course of inactivation as a function of pH. The comparison of different buffers for this reaction is shown in Figure 28 while the effect of bicarbonate concentration is shown in Figure 29. As discussed by

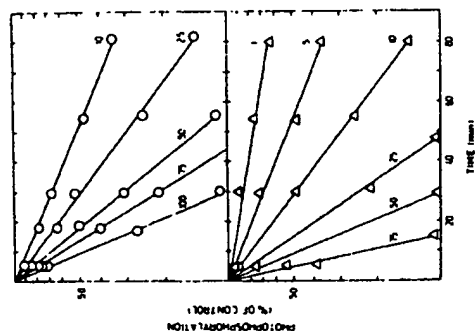


FIGURE 22. Effect of 2,3-butanedione and phenylglyoxal on phosphoribosylation in *Rhodospirillum rubrum* chromatophores. The experiments were performed in 50 mM borate buffer (pH 7.8) at 25°C with either 2,3-butanedione (O—O) or phenylglyoxal (Δ—Δ) at the concentrations indicated in the figure. The reactions were performed in the dark. (From Vallejos, R. H., Lescano, W. I. M., and Lucero, H. A., *Arch. Biochem. Biophys.*, 190, 578, 1978. With permission.)

these investigators, the bicarbonate effect may be a general effect but it is our experience that the modification of arginyl residues in proteins proceeds more rapidly in this buffer system.

The studies of Davidson and Flynn⁴⁶ on the modification of an arginyl residue in an aldehyde reductase provided another evaluation of several different reagents. Figure 30 shows the results of an experiment performed in 0.050 M sodium borate, pH 7.0, at 25°C in which 1,2-cyclohexanedione, methylglyoxal, phenylglyoxal, and 2,3-butanedione are compared. 2,3-Butanedione is the most potent inactivator with phenylglyoxal being somewhat less effective while 1,2-cyclohexanedione is least effective. Another comparison of phenylglyoxal and 2,3-butanedione is provided from the studies of Poulos and Kolamkudy⁴⁷ on the participation of arginyl residues in fatty acid synthetase. Figure 31 contains a comparison of the effect of these two reagents on the various catalytic activities of this multifunctional enzyme. These experiments with phenylglyoxal were performed in 0.1 M sodium phosphate, pH 7.6, containing 1.0 M EDTA and 0.5 mM dithioerythritol, while those with 2,3-butanedione were performed in 0.020 M borate, 0.200 M KCl, pH 7.6, containing 1.0 mM EDTA and 1.0 mM dithioerythritol. Phenylglyoxal was more potent than 2,3-butanedione in the inactivation of the three catalytic activities. Figure 32 provides a further analysis of the reaction of fatty acid synthetase with phenylglyoxal. It is noted that only four arginyl residues out of a total of 106 arginyl residues per subunit are modified under these reaction conditions.

The investigation of the reaction of *Lactobacillus casei* thymidylate synthetase with phenylglyoxal is an interesting example of the use of this reagent.⁴⁸ Figure 33 describes the pH dependence (*N*-ethylmorpholine buffers) for the inactivation. A time-course study for the modification of arginyl residues by phenylglyoxal (350-fold molar excess, 0.200 M

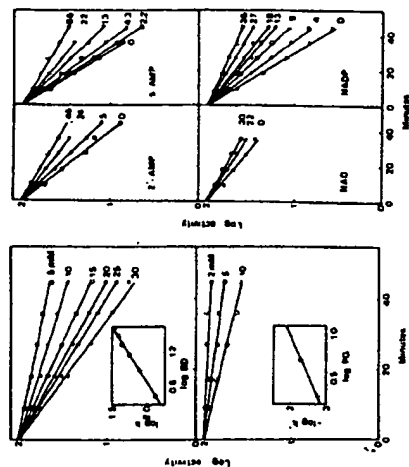


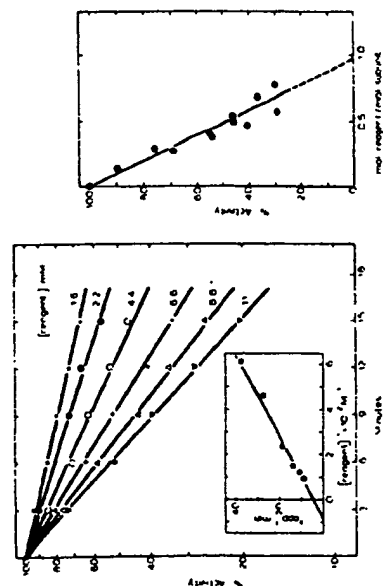
FIGURE 23. Comparison of the modification of an energy-dependent transhydrogenase from *Escherichia coli* cell membranes with 2,3-butanedione and phenylglyoxal. On the left is shown the kinetics of inactivation of the energy-dependent transhydrogenase by 2,3-butanedione (BD) (upper panel) and phenylglyoxal (PG) (lower panel). The membranes were prepared in 50 mM sodium borate, pH 7.8, and incubated at 25°C at a concentration of 1.1 mg and 1.96 mg protein/ml with the indicated concentrations of 2,3-butanedione and phenylglyoxal, respectively. Samples were withdrawn and assayed at timed intervals. Activity is expressed as a percentage of the control activity taken at the onset of incubation. The insets show the relationship between the pseudo-first-order rate constant of inactivation (k , expressed as min^{-1}) and the inhibitor concentration (expressed as mM). The effect of substrate and substrate analogs on the inactivation of the energy-dependent transhydrogenase by 2,3-butanedione is shown on the right. Membranes at a concentration of 1.0 (top panels) and 1.4 (bottom panels) mg protein/ml in 50 mM sodium borate, pH 7.8, were incubated at 25°C with 33.7 mM 2,3-butanedione, in the absence or presence of the indicated millimolar concentrations of substrate and substrate analogs. Samples were withdrawn at timed intervals for assay. Activity is expressed as a percentage of the control activity taken at the onset of incubation. (From Hemyk, M. and Bragg, P. D., *Biochim. Biophys. Acta*, 571, 201, 1979. With permission.)

N-ethylmorpholine, pH 8.2, 25°C) in the presence and absence of a competitive inhibitor (2'-deoxyuridyate) is shown in Figure 34.

Studies from Cooperman's laboratory⁴⁹ on the modification of yeast inorganic pyrophosphatase presented some interesting data on the stability of the reaction product between arginine and phenylglyoxal. Figure 35 shows the change in the UV spectrum of the adduct between 2 molecules of phenylglyoxal and 1 molecule of arginine on incubation in 0.1 M sodium phosphate, pH 8.0. These data are consistent with a model for reaction where there is a rapid dissociation to form free arginine and reagent followed by the formation of a new reaction product with undefined stoichiometry.

Studies⁵⁰ on the modification of arginyl residues in choline acetyltransferase provide a further comparison of 2,3-butanedione and phenylglyoxal as well as a study of camphor-quinone-10-sulfonic acid. Figure 36 compares the rate of inactivation of choline acetyltransferase by the three reagents. Phenylglyoxal is the most effective inactivator but it must be noted that the studies were performed in 0.040 M HEPES, pH 7.8 (25°C) in the absence of borate which is critical⁵¹ for reaction of arginyl residues with 2,3-butanedione.

Hayman and Colman⁵² have studied the modification of arginyl residues in isocitrate dehydrogenase. Figure 37 shows the dependence of first-order rate constant for inactivation of catalytic activity as a function of 2,3-butanedione concentration (0.050 M MES, pH 6.2 containing 20% glycerol and 2.1 mM MnSO_4 , 30°C). A second-order rate constant of



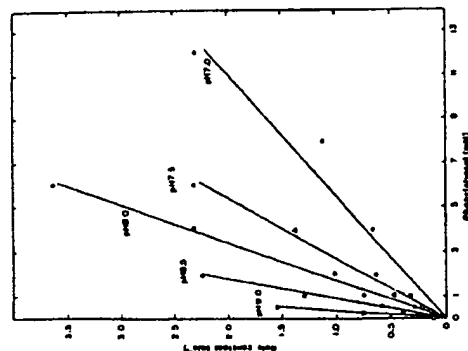


FIGURE 27. The effect of pH on the apparent first-order rate constants of glutamate apodecarboxylase inactivation by phenylglyoxal. Apoenzyme (1.33 μ M) was incubated with varying concentrations of phenylglyoxal in 83 mM bicarbonate buffer. The pH of each solution was determined after the addition of apoenzyme in 10 mM pyridine-Cl, pH 4.6. (From Cheung, S.-T. and Fonda, M. L., *Arch. Biochem. Biophys.*, 198, 541, 1979. With permission.)

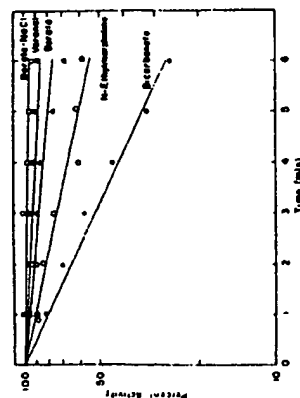


FIGURE 28. The effect of buffer on the inactivation of glutamate apodecarboxylase by phenylglyoxal at pH 7.5. The apoenzyme was incubated with 2 mM phenylglyoxal in 35 mM borate buffer (with or without 1 M NaCl), 50 mM Veronal buffer, 140 mM N-ethylmorpholine-Cl buffer, or 83 mM sodium bicarbonate buffer. (From Cheung, S.-T. and Fonda, M. L., *Arch. Biochem. Biophys.*, 199, 457, 1980. With permission.)

Lanzillo et al.³⁷ have described the reaction of arginine residues in bacterial dipeptidase-4 with either *p*-hydroxyphenylglyoxal or 2,3-butanedione. The inactivation with *p*-hydroxyphenylglyoxal followed pseudo-first-order kinetics (0.2 M N-ethylmorpholine, pH 8.0). The reaction with 2,3-butanedione was biphasic in nature either in the presence or absence of 50 mM sodium borate. It was suggested that the two reagents were reacting with different populations of arginine residues.

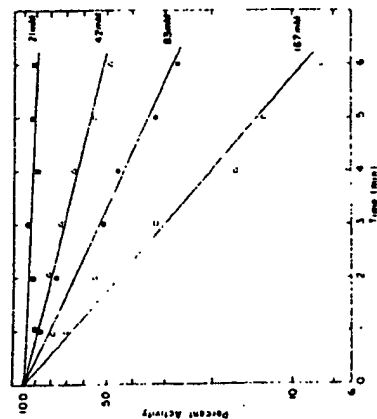


FIGURE 29. The effect of bicarbonate concentration on the inactivation of glutamate apodecarboxylase by 2 mM phenylglyoxal at pH 7.5. The final concentrations of bicarbonate are indicated. (From Cheung, S.-T. and Fonda, M. L., *Arch. Biochem. Biophys.*, 198, 541, 1979. With permission.)

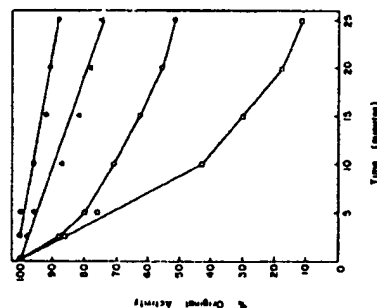


FIGURE 30. Modification of an aldehyde reductase by several reagents specific for reaction with arginine. Shown is the inactivation of pig kidney aldehyde reductase by 10 mM 1,2-cyclohexanedione (O), 10 mM methylglyoxal (Δ), 10 mM phenylglyoxal (O), and 10 mM 2,3-butanedione (O). The enzyme (0.1 mg/ml) was incubated with the various reagents in 50 mM borate buffer, pH 7.0, at 25°C. Portions were removed at the indicated times, diluted into ice cold 0.1 M sodium phosphate, pH 7.0, and assayed for catalytic activity. (From Davidson, W. S. and Pym, T. G., *J. Biol. Chem.*, 254, 3724, 1979. With permission.)

Several additional studies have appeared which compared the relative effectiveness of phenylglyoxal, 1,2-cyclohexanedione, and 2,3-butanedione. Cheng and Nowak³⁸ examined the rate of irreversible inactivation of chicken liver phosphoenol carboxylase by these three reagents. The reactions were performed in 65 mM Tris-Cl, pH 7.5 at 22°C. Phenylglyoxal was the most effective reagent ($3.42 \text{ M}^{-1} \text{ min}^{-1}$) with 2,3-butanedione somewhat

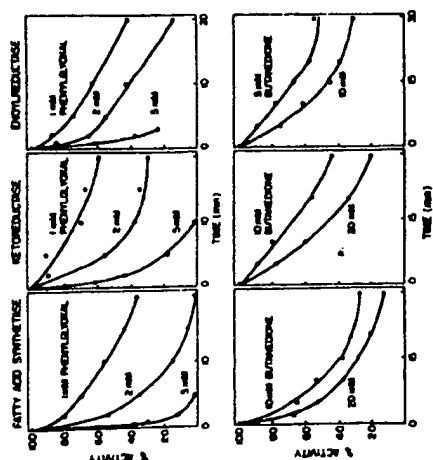


FIGURE 31. Time course of inactivation of ketoreductase, enoyl reductase, and the overall activity of fatty acid synthetase by phenylglyoxal and 2,3-butanediol. Incubation with phenylglyoxal was carried out at a protein concentration of 4.1, 4.3, and 3.3 mg/ml for fatty acid synthetase, ketoreductase, and enoyl reductase, respectively; incubations with 2,3-butanediol were done at 0.33, 0.165, and 1.65 mg/ml, respectively. The modification with phenylglyoxal was performed in 100 mM sodium phosphate, pH 7.6, containing 0.5 mM dithiothreitol and 1.0 mM EDTA at 30°C. The modification with 2,3-butanediol was performed in 20 mM borate containing 200 mM KCl, 1.0 mM dithiothreitol, and 1.0 mM EDTA at pH 7.6 at 30°C. (From Poulou, A. J., and Kolanik, P. E., *Arch. Biochem. Biophys.*, 199, 437, 1980. With permission.)

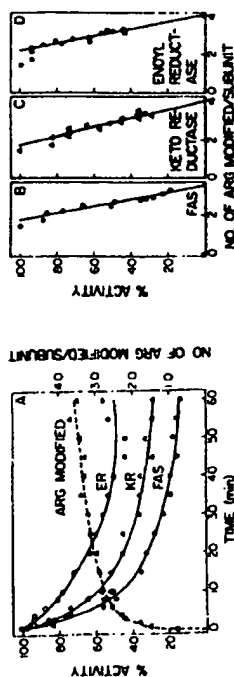


FIGURE 32. Analysis of the modification of arginine residues in fatty acid synthetase by phenylglyoxal. Shown in panel A is the time course of inactivation of the three enzymatic activities and the number of arginine residues modified with 1 mM [2-¹⁴C]phenylglyoxal in 100 mM sodium phosphate buffer (pH 7.0) containing 0.5 mM dithiothreitol and 1.0 mM EDTA. The reactions were performed at a protein concentration of 8.8 mg/ml at 30°C. Panels B to D show the stoichiometry of modification for overall fatty acid synthetase (FAS), ketoreductase, and enoyl reductase. (From Poulou, A. J., and Kolanik, P. E., *Arch. Biochem. Biophys.*, 199, 437, 1980. With permission.)

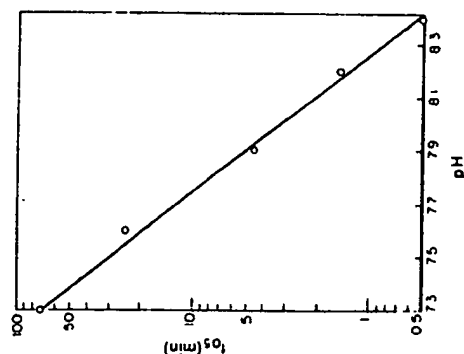


FIGURE 33. pH dependence of inactivation of thymidylate synthetase by phenylglyoxal. Enzyme (7.1 μ M) was incubated under argon at 25°C in 200 mM N-ethylmorpholine at the pH indicated in the presence of 5 mM phenylglyoxal. The $t_{1/2}$ at each of the indicated pH values was determined from a series of semilog plots of inactivation vs. time. (From Belfort, M., Maley, G. F., and Maley, F., *Arch. Biochem. Biophys.*, 204, 340, 1980. With permission.)

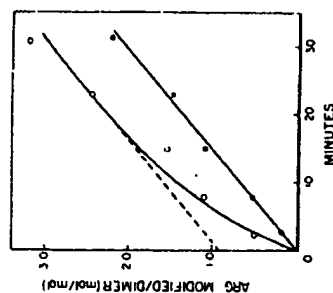


FIGURE 34. The rate of modification of arginine in thymidylate synthetase by phenylglyoxal. Enzyme (14.3 μ M) in 200 mM N-ethylmorpholine (pH 8.2) was preincubated for 30 min at 25°C in the absence (○) and presence (●) of a 200-fold molar excess of decarboxylase (2.86 mM). At 0 min, phenylglyoxal was added to a concentration of 5 mM (350-fold molar excess over enzyme). At the times indicated, 100- μ l portions were added to 1 ml of cold 0.1 N HCl in acetone to halt arginine modification and to precipitate the enzyme. The number of arginine residues modified was calculated by comparison with an unmodified control. (From Belfort, M., Maley, G. F., and Maley, F., *Arch. Biochem. Biophys.*, 204, 340, 1980. With permission.)

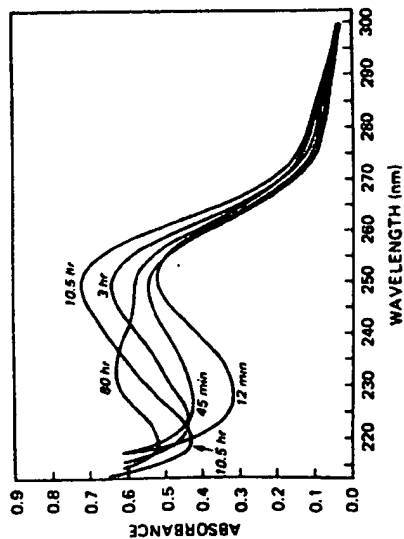


FIGURE 35. Ultraviolet absorption spectral changes on hydrolysis of the reaction product of phenylglyoxal and arginine. Shown are the ultraviolet spectral changes on hydrolysis of N -acetyl-L-(diphenylglyoxal)arginine (N -AcArg(PGAs)) in 0.1 M sodium phosphate buffer, pH 8.0, at 25°C. Spectra were obtained at the times indicated in the figure. (From Bond, M. W., Chu, N. Y., and Cooperman, B. S., *Biochemistry*, 19, 94, 1980. With permission.)

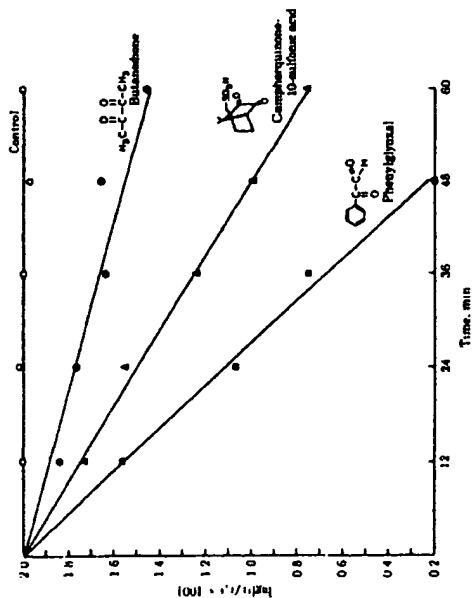


FIGURE 36. The inactivation of choline acetyltransferase (ChATase) by several reagents specific for the modification of arginine. The reagents indicated in the figure were present at a concentration of 10 mM in 50 mM HEPES, pH 7.8, at 25°C; v, initial enzyme activity and enzyme activity at any time point. (From Maunier, H. G., Pakula, A. A., and Merrill, R. E., *Proc. Natl. Acad. Sci. U.S.A.*, 78, 7449, 1981. With permission.)

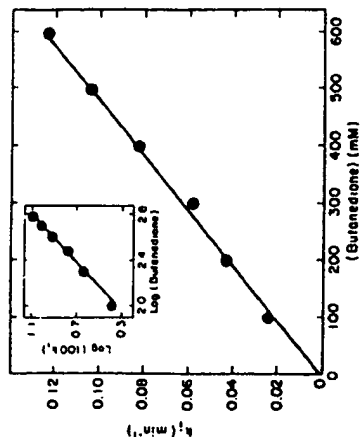


FIGURE 37. The loss of catalytic activity in porcine diphosphopyridine nucleotide-specific isocitrate dehydrogenase on modification with 2,3-butanedione. Shown is the dependence of k_2 (pseudo-first-order rate constant) on reagent concentration. The reactions were 50 mM in MES (pH 6.2), 20% in glycerol, and contained 2.1 mM $MnSO_4$ at 30°C. The 2,3-butanedione concentration is indicated in the figure. The rate constant for each reagent concentration was determined from a semilogarithmic plot of the loss of catalytic activity as a function of time. The second-order rate constant is $0.21 M^{-1} min^{-1}$. The inset shows a plot of $\log k_2$ vs. $\log (2,3\text{-butanedione})$, with a slope of 0.95. (From Hayman, S. and Colman, R. F., *Biochemistry*, 17, 4161, 1978. With permission.)

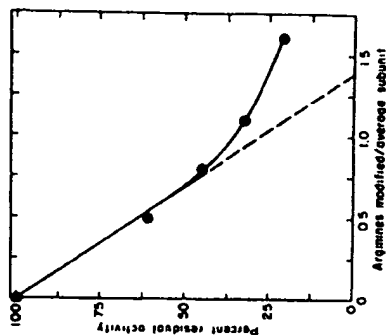


FIGURE 38. Stoichiometry for the modification of DPN-dependent isocitrate dehydrogenase with 2,3-butanedione. The enzyme was incubated for various times up to 73 min at 30°C in 50 mM MES (pH 6.2) containing 2.1 mM $MnSO_4$ and 0.1 M 2,3-butanedione. Portions of the reacted enzyme containing 0.2 mg protein were diluted with an equal volume of 2 N HCl at 0°C to both stop the reaction and prevent the regeneration of free arginine. The modified enzyme was then dialyzed overnight at 4°C against 1 N HCl. The samples were dried *in vacuo* over solid NaOH and subjected to acid hydrolysis. Unmodified enzyme had an arginine content of 13.4 residues per average subunit of 40,000 molecular weight. (From Hayman, S. and Colman, R. F., *Biochemistry*, 17, 4161, 1978. With permission.)

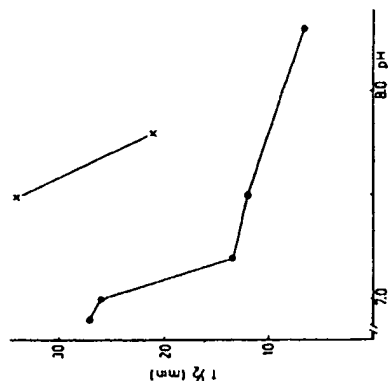


FIGURE 41. pH dependence for the inactivation of adenyl cyclase by 2,3-butanediol in two different buffers. Shown are the half-inactivation times for adenyl cyclase at 30°C with 20 mM 2,3-butanediol in 25 mM borate (●) and 25 mM HEPES (Δ) as a function of pH. Protein concentration during the incubation was 30 mg/ml. (From Varino, K. and Londestorff, S., *FEBS Lett.*, 106, 153, 1979. With permission.)

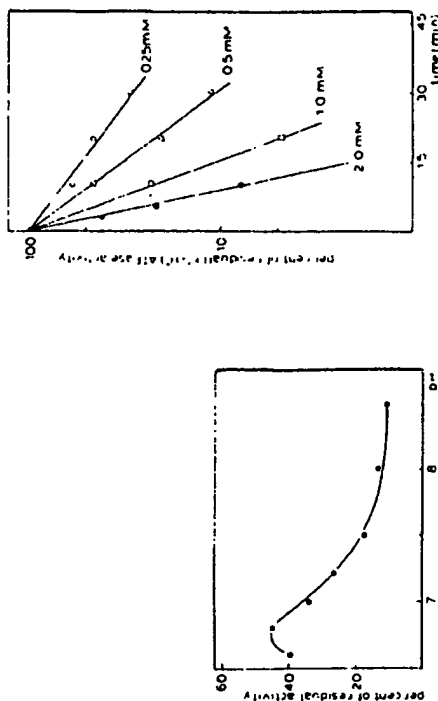


FIGURE 42. The inactivation of $(K^+ + H^+)ATPase$ by 2,3-butanediol. On the left is shown the inactivation by 2,3-butanediol as a function of pH. $(K^+ + H^+)ATPase$ preparation (0.5 mg/ml) was incubated for 20 min at 37°C with 0.5 mM 2,3-butanediol in 125 mM borate buffer containing 5 mM $MgCl_2$, previously brought to the indicated pH values with 5 M NaOH. $(K^+ + H^+)ATPase$ activity is expressed as percent of a control preparation without 2,3-butanediol. On the right is shown the inactivation by 2,3-butanediol as a function of time. $(K^+ + H^+)ATPase$ preparation (0.5 mg protein/ml) was incubated at 37°C with the indicated concentrations of 2,3-butanediol in 125 mM sodium borate (pH 7.0), 5 mM $MgCl_2$. Enzyme activity is expressed as percent of control activity without butanediol. (From Schrijen, J. J., Luyben, W. A. H. M., DePont, J. J. H. M., and Bonting, S. L., *Biochim. Biophys. Acta*, 597, 331, 1980. With permission.)

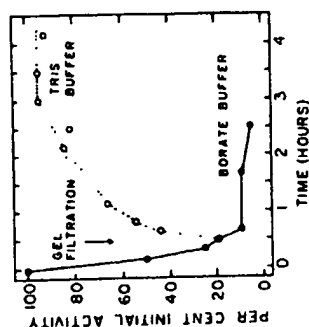


FIGURE 39. The reversal of 2,3-butanediol inactivation of stearylcoenzyme A desaturase. Shown is the reversibility of desaturase inactivation by removal of borate. Desaturase (16 μM , specific activity = 190 units/mg) was treated with 2,3-butanediol (40 mM) in 50 mM sodium borate (pH 8.1); after 30 min at 25°C, 1 ml of this mixture was filtered through Sephadex G-25 (20×1 cm) equilibrated either with the same borate buffer or 20 mM Tris-acetate/100 mM NaCl (pH 8.1). The enzyme, which eluted in the void volume within 3 to 4 min, was incubated at 25°C, and portions were withdrawn at the times indicated for measurement of desaturase activity (●) borate buffer; (○) Tris buffer. (From Enoch, H. G. and Stittman, P., *Biochemistry*, 17, 4927, 1978. With permission.)

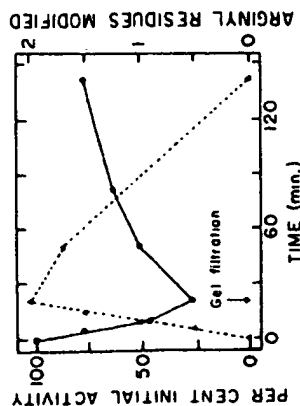


FIGURE 40. The correlation of the reversible modification of stearylcoenzyme A desaturase activity with the modification of arginyl residues. The treatment of desaturase with 2,3-butanediol and the removal of reagent and borate by gel filtration were carried out as described under Figure 39. At various times, samples of the reaction mixture were chilled rapidly to 0°C and used immediately for the measurement of desaturase activity (●) before and (○) after gel filtration, and arginine. (Δ) before and (Δ) after gel filtration. (From Enoch, H. G. and Stittman, P., *Biochemistry*, 17, 4927, 1978. With permission.)

less effective ($3.13 M^{-1} min^{-1}$) while 1,2-cyclohexanedione was much less effective ($0.313 M^{-1} min^{-1}$). In studies with *E. coli* threonine dehydrogenase²⁸ (25 μM triethanolamine-25 μM sodium borate-2.5 μM 2-mercaptoethanol, pH 7.4), 2,3-butanediol and 2,3-pentanedione were the most effective reagents with phenylglyoxal considerably less effective but still markedly better than 1,2-cyclohexanedione.

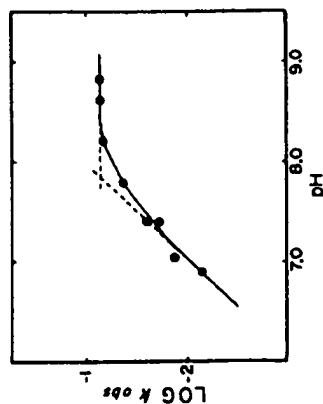


FIGURE 43. The effect of pH on the apparent first-order rate constant for the inactivation of saccharopine dehydrogenase by 2,3-butanedione. The enzyme (0.7 nmol) was incubated with 11.4 mM 2,3-butanedione in 0.1 ml of 0.08 M HEPES buffer at the pH values indicated. The buffers contained 0.2 M KCl and 10 mM borate in addition. Values of the apparent first-order rate constants (k_{obs}) were obtained from the pseudo-first-order kinetic plots. (From Fujioke, M. and Takata, Y., *Biochemistry*, 20, 468, 1981. With permission.)

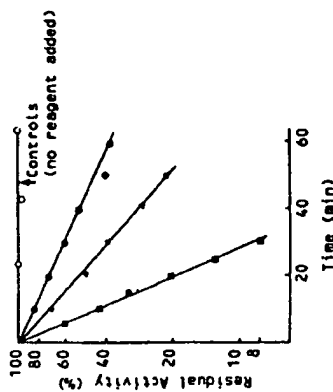


FIGURE 44. The inactivation of phospholipase C by arginine reagents. Enzyme (0.25 mg/ml) incubated with phenylglyoxal (32 mM) in 0.02 M sodium borate buffer (pH 7.0) at 22°C (●). Enzyme (0.22 mg/ml) incubated with 2,3-butanedione (50 mM) in 0.06 M sodium borate buffer (pH 7.5) at 22°C (○). Enzyme incubated with 1,2-cyclohexanedione (85 mM) in 0.2 M sodium borate buffer (pH 8.0) at 37°C (Δ). (From Aurebeck, B. and Little, C., *Int. J. Biochem.*, 8, 757, 1977. With permission.)

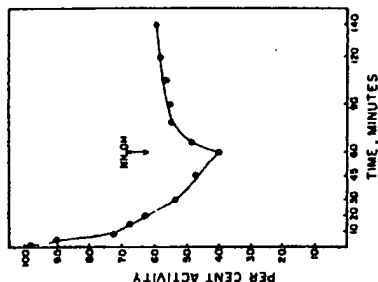


FIGURE 45. Reversibility of the inactivation of an acid phosphatase by 1,2-cyclohexanedione. Acid phosphatase in 50 mM borate buffer (pH 8.1) was modified at 30°C by 50 mM 1,2-cyclohexanedione. At the time indicated by the arrow, neutral hydroxylamine solution was added to a final concentration of 0.2 M. (From McGuire, J. J. and Van Ethen, R. L., *Biochim. Biophys. Acta*, 523, 422, 1978. With permission.)

REFERENCES

1. Yankovsky, J. A., Jr., Modification of arginine by diketones. *Met. Enzymol.*, 25, 566, 1972.
2. Takahashi, K., The reaction of phenylglyoxal with arginine residues in proteins. *J. Biol. Chem.*, 243, 6171, 1968.
3. Yankovsky, J. A., Jr., Mitchell, C. D., and Crawford, T. H., A simple trimerization of 2,3-butanedione yielding a selective reagent for the modification of arginine in proteins. *J. Am. Chem. Soc.*, 90, 1664, 1968.
4. Nakaya, K., Horiuchi, H., and Shibata, K., Sites of amino acid residues in proteins. XIV. Glyoxal as a reagent for discrimination of arginine residues. *J. Biochem.*, 61, 345, 1967.
5. Riordan, J. F., McElwray, K. D., and Borders, C. L., Jr., Arginyl residues: anion recognition sites in enzymes. *Science*, 195, 884, 1977.
6. Parthy, L. and Thöni, J., Origin of the selectivity of α -dicarbonyl reagents for arginyl residues of anion-binding sites. *Eur. J. Biochem.*, 105, 387, 1980.
7. Takahashi, K., Specific modification of arginine residues in proteins with ninhydrin. *J. Biochem.*, 80, 1173, 1976.
8. Parthy, L. and Smith, E. L., Reversible modification of arginine residues. Application to sequence studies by restriction of tryptic hydrolysis to lysine residues. *J. Biol. Chem.*, 250, 557, 1975.
9. Chaplin, M. F., The use of ninhydrin as a reagent for the reversible modification of arginine residues in proteins. *Biochem. J.*, 155, 457, 1976.
10. Ritzke, Y. and Knaus, T., Post-column derivatization of guanidino compounds in high-performance liquid chromatography using ninhydrin. *J. Chromatogr.*, 226, 43, 1981.
11. Jones, A. and Weber, G., Presence of arginine residues at the strong, hydrophobic anion binding sites of bovine serum albumin. *Biochemistry*, 10, 1335, 1971.
12. Glass, J. D. and Pridg, M., Reversible modification of arginine residues with glyoxal. *Biochem. Biophys. Res. Commun.*, 81, 527, 1978.
13. Pardo, C. S., Pridg, M., and Glass, J. D., Camphorquinone-10-sulfonic acid and derivatives: convenient reagents for reversible modification of arginine residues. *Proc. Natl. Acad. Sci. U.S.A.*, 77, 895, 1980.
14. Rajagopalan, T. G., Sita, W. H., and Moore, S., The inactivation of pepsin by diazoacetylornithine methyl ester. *J. Biol. Chem.*, 241, 4295, 1966.
15. Hoeselger, A., Hughes, G. J., and Wilson, K. J., Chemical modification of peptides by hydrazine. *Biochem. J.*, 199, 53, 1981.

16. Sakaguchi, S., A new color reaction of protein and arginine. *J. Biochem.*, 5, 25, 1925.
17. Izumi, Y., New Sakaguchi reaction. *Anal. Biochem.*, 10, 218, 1963.
18. Izumi, Y., New Sakaguchi reaction. II. *Anal. Biochem.*, 12, 1, 1965.
19. Enoch, H. G. and Srinivasan, P., Role of tyrosyl and arginyl residues in rat liver microsomal steryl-coenzyme A desaturase. *Biochemistry*, 17, 4927, 1978.
20. Smith, R. E. and MacQuarrie, R., A sensitive fluorometric method for the determination of arginine using 9,10-phenanthrolinequinone. *Anal. Biochem.*, 90, 246, 1978.
21. Phis, H. and Vivasanatha, T., 2,3-Butanedione as a photoensitizing agent: application to α -amino acids and α -chymotrypsin. *Can. J. Biochem.*, 57, 1267, 1979.
22. Gripen, J.-C. and Holmman, T., Inactivation of aspartyl proteinases by butane-2,3-dione. Modification of tryptophan and tyrosine residues and evidence against reaction of arginine residues. *Biochem. J.*, 193, 55, 1981.
23. Mäkinen, K. K., Mäkinen, P.-L., Wilkes, S. H., Bayliss, M. E., and Prosser, J. M., Photochemical inactivation of *Artemesia* aminopeptidase by 2,3-butanedione. *J. Biol. Chem.*, 257, 1765, 1982.
24. Riley, H. A. and Gray, A. R., Phenylglyoxal. In *Organic Syntheses*, Collective Vol. 2, Blatt, A. H., Ed., John Wiley & Sons, New York, 1943, 309.
25. Schloss, J. V., Norton, I. L., Springer, C. D., and Hartman, F. C., Inactivation of ribulosebiphosphate carboxylase by modification of arginyl residues with phenylglyoxal. *Biochemistry*, 17, 5626, 1978.
26. Augustus, B. W. and Hutchins, D. W., The synthesis of phenyl(2-hydroxyphenyl)glyoxal. *Biochem. J.*, 177, 377, 1979.
27. Borders, C. L., Jr., Pearson, L. J., McLaughlin, A. E., Gustafson, M. E., Vasileff, J. A., An, P. Y., and Morgan, D. J., 4-Hydroxy-3-aminophenylglyoxal. A chromophoric reagent for arginyl residues in proteins. *Biochim. Biophys. Acta*, 568, 491, 1979.
28. Yamasaki, R. B., Vega, A., and Feeley, R. E., Modification of available arginine residues in proteins by *p*-hydroxyphenylglyoxal. *Anal. Biochem.*, 109, 32, 1980.
29. Cheng, S.-T. and Fauda, M. L., Reaction of phenylglyoxal with arginine. The effect of buffers and pH. *Biochem. Biophys. Res. Commun.*, 90, 940, 1979.
30. Yamasaki, R. B., Shiner, D. A., and Feeley, R. E., Colorimetric determination of arginine residues in proteins by *p*-hydroxyphenylglyoxal. *Anal. Biochem.*, 111, 220, 1981.
31. Steinhilber, L. and Becker, E. L., A synthesis for β -aroylacrylic acids substituted with electron-withdrawing groups. *J. Am. Chem. Soc.*, 76, 5808, 1954.
32. Branstetter, G., Triebel, D., and Böhmann, J.-F., Evidence for the presence of anion-recognition sites in pig-liver aldehyde reductase. Modification by phenylglyoxal and *p*-carboxyphenyl glyoxal of an arginyl residue located close to the substrate-binding site. *Eur. J. Biochem.*, 116, 505, 1981.
33. Eum, H.-M., Arginine modification by phenylglyoxal and (*p*-hydroxyphenyl)glyoxal: reaction rates and intermediates. *Biochem. Int.*, 17, 719, 1988.
34. Meves, H., Rübly, N., and Stämpfli, R., The action of arginine-specific reagents on ionic and gating currents in frog myelinated nerve. *Biochim. Biophys. Acta*, 943, 1, 1988.
35. Yankovsky, J. A., Jr., Modification of arginine in proteins by oligomers of 2,3-butanedione. *Biochemistry*, 9, 2433, 1970.
36. Riordan, J. E., Functional arginyl residues in carboxypeptidase A. Modification with butanedione. *Biochemistry*, 12, 3915, 1973.
37. Ted, K., Bynum, E., Norris, E., and Isono, H. A., Studies on the chemical modification of arginine. I. The reaction of 1,2-cyclohexanedione with arginine and arginyl residues of proteins. *J. Biol. Chem.*, 242, 1036, 1967.
38. Pithy, L. and Smith, E. L., Identification of functional arginine residues in ribonuclease A and lysozyme. *J. Biol. Chem.*, 250, 565, 1975.
39. Vallejos, R. H., Lezcano, W. I. M., and Lucero, H. A., Involvement of an essential arginyl residue in the coupling activity of *Rhodospirillum rubrum* chromophores. *Arch. Biochem. Biophys.*, 190, 578, 1978.
40. Homay, M. and Bragg, P. D., Steady-state kinetics and the inactivation by 2,3-butanedione of the energy-independent transhydrogenase of *Escherichia coli* cell membranes. *Biochim. Biophys. Acta*, 57, 201, 1979.
41. Levy, H. M., Leber, P. D., and Ryan, E. M., Inactivation of myosin by 2,4-dinitrophenol and protection by adenosine triphosphate and other phosphate compounds. *J. Biol. Chem.*, 238, 3654, 1963.
42. Bhagwat, A. S. and Ramakrishna, J., Essential histidine residues of ribulosebiphosphate carboxylase indicated by reaction with diethylpyrocarbonate and rose bengal. *Biochim. Biophys. Acta*, 662, 181, 1981.
43. Phillips, M., Pho, D. B., and Pradel, L.-A., An essential arginyl residue in yeast hexokinase. *Biochim. Biophys. Acta*, 566, 296, 1979.
44. Monnet, D., Pustel, P., Audenaert, E., and Karsah, R., Involvement of an arginyl residue in the catalytic activity of myosin heads. *Eur. J. Biochem.*, 100, 421, 1979.
45. Cheng, S.-T. and Fauda, M. L., Kinetics of the inactivation of *Escherichia coli* glutamate aspartate-oxylase by phenylglyoxal. *Arch. Biochem. Biophys.*, 193, 541, 1979.
46. Davidson, W. S. and Flynn, T. G., A functional arginine residue in NADPH-dependent aldehyde reductase from pig kidney. *J. Biol. Chem.*, 254, 3724, 1979.
47. Postone, A. J. and Kolstad, P. E., Presence of one essential arginine that specifically binds the 2'-phosphate of NADPH on each of the tetraacyl reductase and enoyl reductase active sites of fatty acid synthetase. *Arch. Biochem. Biophys.*, 199, 457, 1980.
48. Bond, M. W., Chiu, N. Y., and Cooperman, B. S., Identification of an arginine important for enzymatic activity within the covalent structure of yeast inorganic pyrophosphatase. *Biochemistry*, 19, 94, 1980.
49. Mautner, H. G., Pakula, A. A., and Merrill, R. E., Evidence for presence of an arginine residue in the coenzyme A binding site of choline acetyltransferase. *Proc. Natl. Acad. Sci. U.S.A.*, 78, 7449, 1981.
50. Hayman, S. and Collins, R. F., Effect of arginine modification on the catalytic activity and allosteric activation by adenosine diphosphate of the diphosphopyridine nucleotide specific isocitrate dehydrogenase of pig heart. *Biochemistry*, 17, 4161, 1978.
51. Vartano, K. and Loodesborough, S., Evidence for essential arginine in yeast adenylate cyclase. *FEBS Lett.*, 106, 153, 1979.
52. Malinowski, D. P. and Fridovich, I., Chemical modification of arginine at the active site of the bovine cytochrome c oxidase. *Biochemistry*, 18, 3949, 1979.
53. Schrijen, J. J., Layben, W. A. H. M., DePont, J. J. H. M., and Boudling, S. L., Studies on (K⁺ + H⁺)-ATPase. I. Essential arginine residue in its substrate binding center. *Biochim. Biophys. Acta*, 597, 331, 1980.
54. Fujisaka, M. and Takata, Y., Role of arginine residue in saccharopine dehydrogenase (L-lysine forming) from baker's yeast. *Biochemistry*, 20, 468, 1981.
55. Aurebach, B. and Little, C., Functional arginine in phospholipase C of *Bacillus cereus*. *Int. J. Biochem.*, 8, 757, 1977.
56. McGlynn, J. J. and Van Ekem, R. L., An essential arginine residue in human prostatic acid phosphatase. *Biochim. Biophys. Acta*, 523, 422, 1978.
57. Lanzillo, J. J., Desautels, Y., and Fanberg, B. L., Detection of essential arginine in bacterial penicillin dipeptidase-4: arginine is not the anion binding site. *Biochem. Biophys. Res. Commun.*, 160, 243, 1989.
58. Cheng, K.-C. and Nowak, T., Arginine residues at the active site of avian liver phosphoenolpyruvate carboxylase. *J. Biol. Chem.*, 264, 3317, 1989.
59. Epperly, B. R. and Dekker, E., Inactivation of *Escherichia coli* L-threonine dehydrogenase by 2,3-butanedione. Evidence for a catalytically essential arginine residue. *J. Biol. Chem.*, 264, 18296, 1989.

CHEMICAL MODIFICATION OF TRYPTOPHAN

The specific chemical modification of tryptophan (Figure 1) in protein is one of the more challenging problems in protein chemistry. First, as will be apparent, the solvent conditions for providing specificity of modification are, in general, somewhat harsh. Secondly, there is the considerable possibility of either the concomitant or separate modification of a different amino acid residue. Thirdly, the analysis for the determination of the exact extent of modification requires a rigorous approach combining spectral analysis and amino acid analysis^{1,2} after hydrolysis in a solvent which will not destroy tryptophan.

Treatment of tryptophan with hydrogen peroxide results in the oxidation of the indole ring.^{3,4} Usually the reaction is performed at alkaline pH (1.0 M sodium bicarbonate, pH 8.4) with the H₂O₂ dioxane mixture prepared as described by Hachimori and co-workers.³ The loss of tryptophan is monitored by the change in absorbance at 280 nm.^{3,5,6} The difference in the molar extinction coefficient between tryptophan and the fully oxidized derivative is $3490 \text{ M}^{-1} \text{ cm}^{-1}$.

The reaction of *N*-bromosuccinimide (NBS) with protein has been studied in some detail (Figure 2). This reagent was introduced for use in protein chemistry in 1958.⁷ The early work with this reagent was summarized in 1967.⁸⁻¹⁰

The use of oxidation with *N*-bromosuccinimide to determine the tryptophan content of proteins is of value. One adds small increments of a freshly prepared solution of *N*-bromosuccinimide until there is no further decrease in absorbance at 280 nm. The change in the molar extinction coefficient of tryptophan on conversion to the oxindole derivative is taken to be $4 \times 10^3 \text{ M}^{-1} \text{ cm}^{-1}$.¹¹ It has been our experience that one must either perform the reaction in 8.0 M urea (pH adjusted to 4.0) or with the reduced, carboxymethylated derivative.¹² The spectra must be obtained as soon as possible after the addition of the *N*-bromosuccinimide since, unless the excess reagent and low molecular weight products of the reaction are rapidly removed, there is a reversal of the decrease in absorbance.¹³ This is not a trivial consideration since there is at least one study¹⁴ where there is a real difference in the extent of modification as determined by spectroscopy or amino acid analysis. The rigorous evaluation¹⁵ of the reaction of *N*-bromosuccinimide with model tryptophanyl and tyrosyl compounds reported from Keiuro Hiromi's laboratory provides considerable insight into the problems to be encountered with the study of intact proteins. Figure 3 shows the changes in the UV spectrum of *N*-acetyltryptophan ethyl ester (ATEE) upon reaction with *N*-bromosuccinimide. These spectra were obtained within 5 min after the initiation of the reaction. At ratios of *N*-bromosuccinimide to *N*-acetyltryptophan ethyl ester of greater than 2 there is an apparent reversal of the decrease in absorbance at 280 nm as shown in Figure 4. Figure 5 shows the spectral changes occurring upon the reaction of *N*-bromosuccinimide with *N*-acetyltryptophan ethyl ester as a function of time and molar excess of *N*-bromosuccinimide. The maximal decrease in absorbance occurs at a ratio of *N*-bromosuccinimide to tryptophan of 2. If the data are obtained by stopped-flow spectroscopy, the molar excess of *N*-bromosuccinimide does not have an effect on the maximum decrease observed, but when the spectrum is obtained 5 min after the initiation of the reaction, there is a decrease in the observed magnitude of change in absorbance at 280 nm. The evaluation of spectral changes in a protein is further complicated by the reaction of *N*-bromosuccinimide with tyrosine. This is demonstrated in Figure 6 which shows the spectral changes occurring as a result of reaction of *N*-bromosuccinimide with *N*-acetyltyrosine ethyl ester. Here an increase in absorbance at 280 nm can be observed. Figure 7 shows that the increase in absorbance of *N*-acetyltyrosine ethyl ester on reaction with *N*-bromosuccinimide is dependent on the molar excess of *N*-bromosuccinimide. The use of this procedure for the analysis of tryptophan

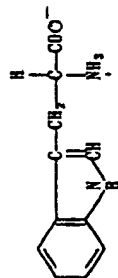
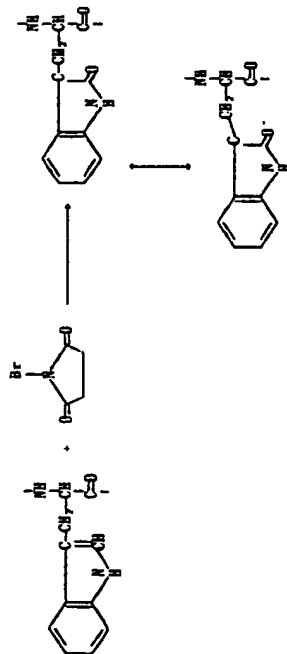


FIGURE 1. The structure of tryptophan.

FIGURE 2 The reaction of tryptophan with *N*-bromosuccinimide.

content in proteins has been largely supplanted by ion-exchange analysis following modified hydrolytic procedures.^{12,14}

The primary use of the *N*-bromosuccinimide modification of proteins during the past decade has been in studies on the effect of such modification on biological (catalytic) activity. In general, the modification reaction is performed in 0.1 *M* sodium acetate, pH 4 to 5. The *N*-bromosuccinimide should be recrystallized from water before use. The presence of halides such as chloride or bromide in the solvent must be avoided since the addition of *N*-bromosuccinimide will oxidize these ions to the elemental form with disastrous and irreparable effects on the proteins under study. In general, a twofold molar excess of *N*-bromosuccinimide per mole of tryptophan is necessary to achieve modification. Daniel and Trowbridge¹⁵ found that (at pH 4.0) the reaction of *N*-bromosuccinimide with acetyl-L-tryptophan ethyl ester required 1.5 mol of *N*-bromosuccinimide per mole of the acetyl-L-tryptophan ethyl ester, while trypsin required 2.0 to 2.3 mol *N*-bromosuccinimide per mole of tryptophan oxidized. An interesting phenomenon was reported by Freisheim and Huennkens.¹⁶ At pH 4.0, only tryptophan in dihydrofolate reductase reacts with NBS while at pH 6.0, a sulfhydryl group apparently is preferentially oxidized by the reagent prior to the reaction of tryptophan. This observation was pursued in greater detail by Freisheim et al.¹⁷ Figure 8 shows the relationship between the decrease in absorbance at 280 nm and the catalytic activity of dihydrofolate reductase as a function of the molar excess of *N*-bromosuccinimide at pH 6.5 (0.1 *M* phosphate). The initial increase in activity reflects oxidation of a cysteinyl residue while the decrease in activity seen at a higher molar excess of reagent appears to be related to the oxidation of tryptophanyl residues in the protein (Figure 9). Poulos and Price have reported on the reaction of a tryptophanyl residue in bovine pancreatic DNase with *N*-bromosuccinimide.¹⁸ Prior reaction of the DNase with another "tryptophan" reagent, 2-hydroxy-5-nitrobenzyl bromide, modified a different residue from the one modified by *N*-bromosuccinimide. These investigators used spectral analysis to determine the

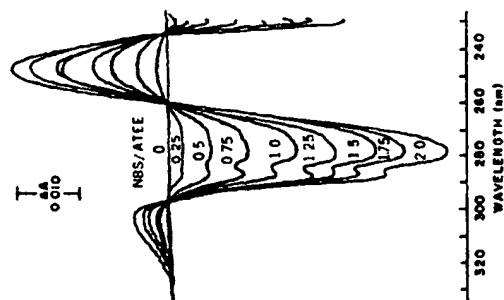


FIGURE 3. Difference UV absorption spectra of *N*-acetyltryptophan ethyl ester caused by reaction with *N*-bromosuccinimide. *N*-acetyltryptophan ethyl ester, 19 μ M. Numbers indicate the molar ratios of *N*-bromosuccinimide to *N*-acetyltryptophan ethyl ester. The reactions were performed in 0.1 *M* acetate buffer, pH 4.5 at 25°C. The difference spectra were obtained within 3 min of the start of the reaction. (From Ohnishi, M., Kawagishi, T., Abe, T., and Hirose, K., *J. Biochem.*, 87, 273, 1980. With permission.)

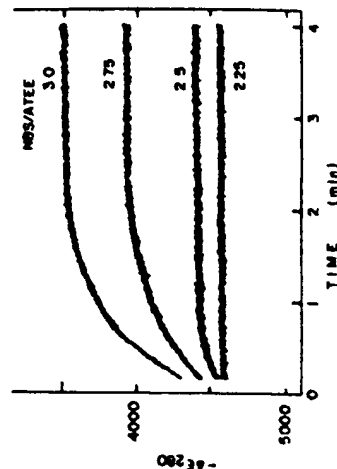


FIGURE 4. Time course of the difference absorbance change of *N*-acetyltryptophan ethyl ester at 280 nm caused by *N*-bromosuccinimide. *N*-acetyltryptophan ethyl ester, 49 μ M; 0.1 *M* acetate buffer, pH 4.5; 25°C. The numbers in the figure indicate the molar ratios of *N*-bromosuccinimide to *N*-acetyltryptophan ethyl ester. (From Ohnishi, M., Kawagishi, T., Abe, T., and Hirose, K., *J. Biochem.*, 87, 273, 1980. With permission.)

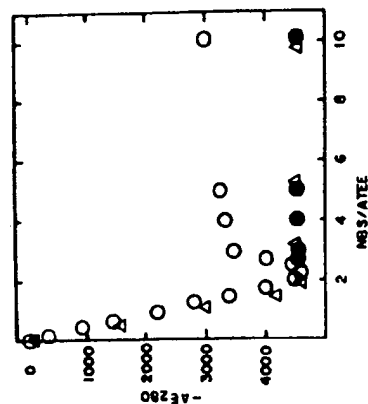


FIGURE 5. Dependence of the difference UV absorption change (decrease) at 280 nm of *N*-acetyltryptophan ethyl ester (ATEE) on time and molar excess of *N*-bromosuccinimide (NBS). The open circles show the difference at 5 min after the addition of *N*-bromosuccinimide and the closed circles the change at 0 min (obtained by extrapolation of the time curves). The triangles represent data obtained by the stopped-flow method. The concentration of *N*-acetyltryptophan ethyl ester was 49 μ M in 0.1 *M* acetate buffer, pH 4.5, at 25°C. (From Ohnishi, M., Kawagishi, T., Abe, T., and Hiroimi, K., *J. Biochem.*, 87, 273, 1980. With permission.)

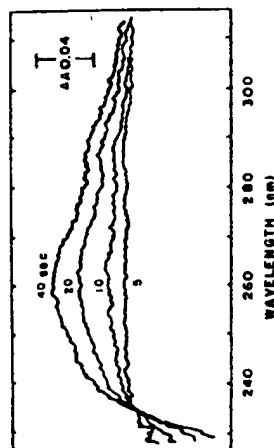


FIGURE 6. The difference UV absorption spectra of *N*-acetyltryptophan ethyl ester on reaction with *N*-bromosuccinimide. *N*-acetyltryptophan ethyl ester, 25 μ M; *N*-bromosuccinimide, 100 μ M; 0.1 *M* acetate buffer, pH 4.5; 25°C. The data were obtained with a stopped-flow spectrophotometer in a rapid scanning mode. The spectra were recorded at 5, 10, 20, and 40 s after the start of the reaction. A spectrum was obtained within 10 msec (scan speed). (From Ohnishi, M., Kawagishi, T., Abe, T., and Hiroimi, K., *J. Biochem.*, 87, 273, 1980. With permission.)

extent of tryptophan modification. Subsequent studies from another laboratory¹⁴ on the modification of DNase with *N*-bromosuccinimide suggested that apparently 2 mol of tryptophan are modified per mole of enzyme at 100% inactivation with a sixfold molar excess of *N*-bromosuccinimide in 0.01 *M* CaCl₂ at pH 4.0. Using amino acid analysis (after hydrolysis in 6 *N* HCl containing mercaptoacetic acid, phenol, and 3-(2-aminoethyl) indole for 24 h at 110°C), these investigators showed that all three tryptophanyl residues are modified under the above experimental conditions. The study on the modification of tryptophan in galactose oxidase¹⁵ is worth comment in that these investigators report the amino acid composition of the modified protein after hydrolysis in 3 *N* *p*-toluenesulfonic acid. There

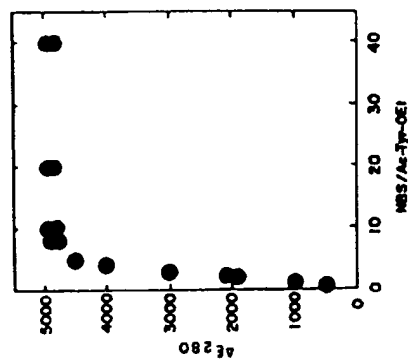


FIGURE 7. Dependence of the difference UV absorption change (increase) of *N*-acetyltryptophan ethyl ester (Ac-Tyr-OEt) caused by reaction with *N*-bromosuccinimide on the *N*-bromosuccinimide (NBS)/*N*-acetyltryptophan ethyl ester ratio. *N*-acetyltryptophan ethyl ester, 25 μ M; 0.1 *M* acetate, pH 4.5; 25°C. The spectra were obtained 5 min after the start of the reaction. (From Ohnishi, M., Kawagishi, T., Abe, T., and Hiroimi, K., *J. Biochem.*, 87, 273, 1980. With permission.)

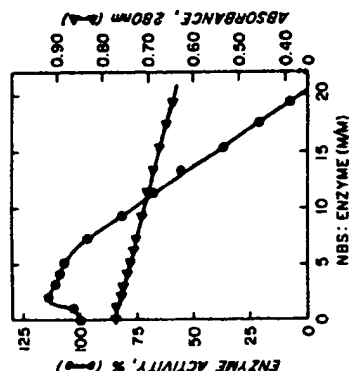


FIGURE 8. Activity and UV absorbance changes of dihydrofolate reductase as a function of the molar excess of *N*-bromosuccinimide. The enzyme concentration was 9.8 μ M in 0.05 *M* potassium phosphate, pH 6.5, at 25°C. The maximum changes in enzyme activity or absorbance at 280 nm occurred in the first 2 to 3 min following the addition of *N*-bromosuccinimide. Enzyme activity is expressed as a percent of an untreated control. (From Warwick, P. E., D'Souza, L., and Friedberg, J. H., *Biochemistry*, 11, 3775, 1972. With permission.)

was excellent agreement between the extent of tryptophan modification as judged by direct amino acid analysis and the value observed by spectral analyses. This study shows one of the consequences of the conversion of tryptophan from the indole to the oxindole. Tryptophan is responsible for the majority of the innate fluorescence of proteins and oxidation by *N*-bromosuccinimide obviates this property as shown in Figure 10. Although the reaction

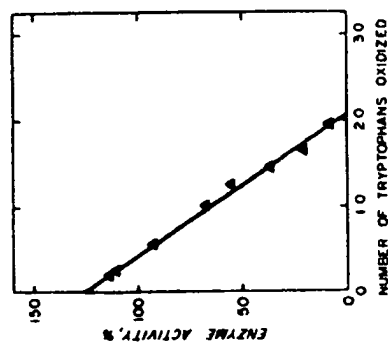


FIGURE 9. Stoichiometry for the inactivation of dihydrofolate reductase by *N*-bromosuccinimide. Shown is the activity of dihydrofolate reductase as a function of the number of tryptophanyl residues oxidized. The experimental conditions were as described in Figure 8. (From Warwick, P. E., D'Souza, L., and Freilich, J. H., *Biochemistry*, 11, 3775, 1972. With permission.)

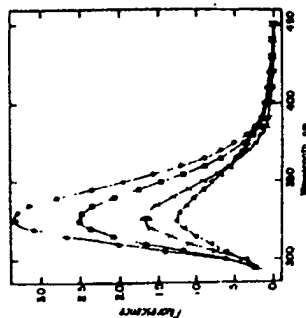


FIGURE 10. Corrected fluorescence emission spectra of deoxyguanosine solutions of galactose oxidase: unmodified (○), with 0.85 oxidized tryptophans (△), with 2.0 oxidized tryptophans (×), and with 3.0 oxidized tryptophans (□). The spectra were recorded in 100 mM sodium acetate, pH 4.15, after the modification with *N*-bromosuccinimide was performed in 5 mM sodium acetate, pH 4.15. The protein concentration was 0.14 mg/ml. The error bars represent the standard deviation of line-averaged recordings. (From Kosman, D. J., Eisinger, M. J., Brennan, R. D., and Giordano, R. S., *Biochemistry*, 16, 1597, 1977. With permission.)

between *N*-bromosuccinimide and tryptophan residues in protein is quite rapid, Fujimori and co-workers,²⁰ using stopped-flow kinetics, were able to determine kinetically different tryptophanyl residues in *Bacillus subtilis* α -amylase. Figure 11 shows the change in the absorbance spectrum of the protein on reaction with *N*-bromosuccinimide, obtained 5 min after the addition of reagent. Figure 12 compares the extent of reaction after 5 min with that obtained using stopped-flow techniques. Four of the eleven tryptophan residues were mod-

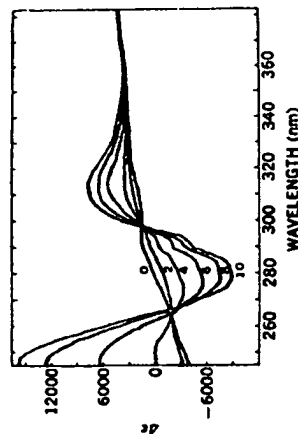


FIGURE 11. Changes in the UV absorption spectrum of *Bacillus subtilis* α -amylase on reaction with *N*-bromosuccinimide. Shown are the difference spectra of the enzyme caused by modification with *N*-bromosuccinimide at pH 7.0 (0.01 M phosphate buffer) at 25°C. The numbers in the figure indicate the molar ratio of *N*-bromosuccinimide to the enzyme (0, base line; no reagent added). The spectra were taken at 5 min after mixing. The enzyme concentration was 2.8 μ M. $\Delta\epsilon$, Difference absorbance per mole of the enzyme. (From Fujimori, H., Ohnishi, M., and Hirose, K., *J. Biochem.*, 83, 1503, 1978. With permission.)

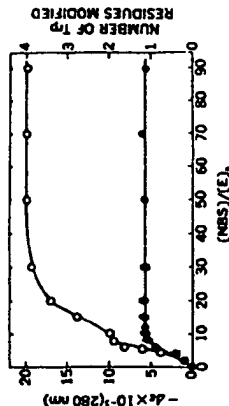


FIGURE 12. Spectrophotometric titration of *Bacillus subtilis* α -amylase with *N*-bromosuccinimide (NBS) at pH 7.0. The enzyme concentration was fixed at 2.8 μ M. (○). The value of $-\Delta\epsilon_{280}$ was measured with a spectrophotometer at 5 min after mixing the enzyme and *N*-bromosuccinimide solutions in a quartz cuvette. (●). The most rapid decrease in absorbance at 280 nm observed by the stopped-flow method within 0.3 s. The number of modified tryptophan residues was calculated from $\Delta\epsilon_{280}$ using a molar difference absorbance per mol of tryptophan residue at 280 nm ($\Delta\epsilon_{280}^{\text{trp}}$) of 5,000 cm^{-1} . (From Fujimori, H., Ohnishi, M., and Hirose, K., *J. Biochem.*, 83, 1503, 1978. With permission.)

ified at the maximum extent of reaction but one of these clearly reacted more rapidly than the other residues. Similar results were obtained when changes in the intrinsic fluorescence of the protein were used to monitor the reaction as shown in Figure 13. These investigators were able to determine a second-order rate constant of $3.5 \times 10^5 \text{ M}^{-1} \text{ s}^{-1}$ for the tryptophanyl residue reacting most rapidly.

There are several other facets of the use of *N*-bromosuccinimide for the modification of tryptophanyl residue in proteins which should be considered. The use of the reagent at mildly acidic pH has been mentioned above. Not only does increasing pH decrease specificity in terms of reaction with amino acid residues other than tryptophan but there is a decrease in the modification of tryptophan. This is shown by the studies²¹ on the modification of a glucosylase from *Aspergillus saitoi*. As shown in Figure 14 there is a modest decrease in modification as the pH is increased from 4.0 to 6.0 with a dramatic decrease at pH 7.0. At

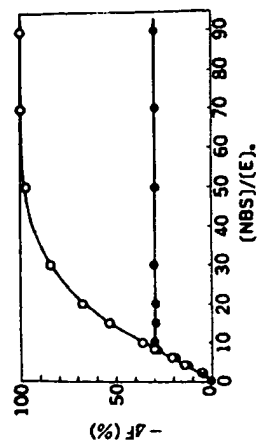


FIGURE 13. The fluorescence titration curve of *Bacillus subtilis* α -amylase with *N*-bromosuccinimide (NBS) at pH 7.0. The enzyme concentration was fixed at $2.8 \mu\text{M}$ in 0.01 M sodium phosphate, pH 7.0. The decrease in fluorescence intensity at 340 nm ($\sim 15^\circ$) of the enzyme excited at 280 nm caused by the addition of *N*-bromosuccinimide is expressed in terms of the percentage fluorescence intensity change with respect to the fluorescence intensity of the native enzyme and plotted against the molar ratio of *N*-bromosuccinimide to the enzyme, (O). The value most rapid decrease in fluorescence intensity observed by the stopped-flow method within 0.3 s . (O). The value obtained with a spectrofluorometer at 5 min after mixing. (From Fujimori, H., Ohnishi, M., and Hiroshi, K., *J. Biochem.*, 83, 1303, 1978. With permission.)

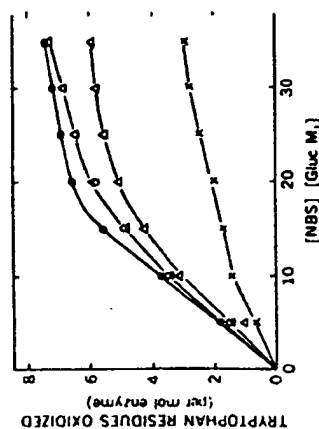


FIGURE 14. *N*-bromosuccinimide oxidation of a glycoamylase (Gluc M_1) as a function of pH. *N*-bromosuccinimide (6.6 mM) was added in 1 to $10\text{-}\mu\text{l}$ portions at 5 min intervals to 1 ml of $6.67 \mu\text{M}$ Gluc M_1 in 0.1 M acetate buffer at pH 4.0 (O), pH 5.0 (Δ), pH 6.0 (\square), and pH 7.0 (\times). The decrease in absorbance at 280 nm was measured after each addition of *N*-bromosuccinimide at 25°C . The amount of tryptophan residues oxidized was calculated according to the method of Spande and Wittkop. (From Inokuchi, N., Takahashi, T., Yoshimoto, A., and Irie, M., *J. Biochem.*, 91, 1661, 1982. With permission.)

pH values close to neutrality there is the increased possibility of modification of amino residues other than tryptophan. The pH dependence of *N*-bromosuccinimide tryptophan modification may well reflect local conformational effects rather than intrinsic chemistry. Stopped-flow studies²² of the *N*-bromosuccinimide modification of tryptophan-62 in lysozyme shows a marked pH dependence with an observed pK_a of 6.2 while there is no pH dependence (3.5 to 8.5) for the modification of *N*-acetyltryptophan ethyl ester. In studies²³ on the reaction on *Escherichia coli* lac repressor protein with *N*-bromosuccinimide at pH 7.8 (1.0 M Tris), cysteine was modified as readily as tryptophan with lesser modification of methionine and tyrosine (Figure 15). Although the great majority of *N*-bromosuccinimide modifications of proteins are performed at pH values less than 5.0 to avoid modification of

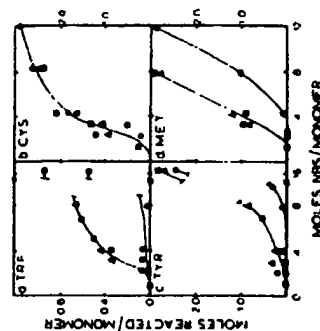


FIGURE 15. The modification of *Escherichia coli* lac repressor protein with *N*-bromosuccinimide. Shown are the moles of amino acid reacted with *N*-bromosuccinimide per monomer of repressor protein. The modification was performed in 1.0 M TrisCl, pH 7.8, for 15 min at ambient temperature in the dark. The reactions were terminated by the addition of dithiothreitol and the modified protein preparations dialyzed vs. water for subsequent analysis. The amount of tryptophan, tyrosine, and methionine were determined by amino acid analysis after hydrolysis in methanesulfonic acid. Cysteine was determined by titration with 2-chloromercuri-4-nitrophenol in 8 M urea. \square — \square , Repressor reacted with *N*-bromosuccinimide alone; \bullet — \bullet , repressor reacted with *N*-bromosuccinimide in the presence of isopropylthio- β -D-glucoside; Δ — Δ , repressor reacted with *N*-bromosuccinimide in the presence of α -nitrophenyl- β -D-thioacetate. (From O'Gorman, R. B. and Matthews, K. S., *J. Biol. Chem.*, 252, 3565, 1977. With permission.)

other functional groups, success can be achieved under less acidic conditions. Kumar et al.²⁴ modified tryptophanyl residues in transcarboxylase in 0.25 M potassium phosphate, pH 6.5, containing 0.1 M dithiothreitol and 0.1 mM phenylmethylsulfonyl fluoride. These investigators also demonstrated that the loss of activity upon modification was not a reflection of gross conformational change by examination of the quenching of intrinsic fluorescence and changes in the susceptibility to tryptic cleavage. In general, modification should occur at a 4 to 6 molar excess (with respect to total tryptophan) of *N*-bromosuccinimide. Under most reaction conditions, the modification of tryptophanyl residues with *N*-bromosuccinimide is quite rapid. Time-dependent reactions have, however, been observed such as that reported for xylanase.²⁵ Reaction with 2-hydroxy-5-nitrobenzyl bromide was also time dependent under these reaction conditions. The use of *N*-bromosuccinimide in the study of proteins is summarized in Table 1.

The reaction of *N*-bromosuccinimide with proteins can also result in the cleavage of peptide bonds at tryptophan, tyrosine, and histidine.²⁶ Thus, the careful investigator will also evaluate the integrity of the polypeptide chain(s) of the protein of interest. Whereas peptide bond cleavage is usually an unwanted side reaction, Feldhoff and Peters²⁷ have devised a procedure which has enhanced specificity for tryptophan. Their procedure uses 8.0 M urea, 2.0 M acetic acid as the solvent with a 20-fold molar excess of *N*-bromosuccinimide. Their approach offers at least two advantages; first, the protein is denatured so that all residues should be equally available and, second, the *N*-bromosuccinimide reacts with urea to yield *N*-bromourea, a less severe oxidizing agent which should have increased specificity for tryptophanyl residues. The use of *N*-chlorosuccinimide for peptide bond cleavage of tryptophanyl residues is considered a superior approach²⁸ (see Chapter 5). A direct comparison of *N*-bromosuccinimide and *N*-chlorosuccinimide in the modification of the single tryptophanyl residue in *Clostridium perfringens* epsilon toxin has been performed.²⁹ Modification with *N*-bromosuccinimide (50 mM sodium acetate, pH 5.0) resulted in the total loss of tryptophan and marked reduction in tyrosine (71% decrease) and methionine

Table 1
EXAMPLES OF THE MODIFICATION OF PROTEINS WITH
N-BROMOSUCCINIMIDE

Protein	Solvent	Molar excess ^a	Extent of modification	Ref.
Tryptophan	pH 7.0 ^b	1-4	1-2	1
Tyrosine	pH 4.0 ^c	1-4	1-2	1
Dihydrofolate reductase	0.1 M sodium phosphate, pH 6.0	15	2.0	2
	0.1 M sodium acetate, pH 6.0	15	2.7	2
	0.1 M sodium acetate, pH 4.0	12	3.8	2
Bovine pancreatic DNAse	0.13 M sodium acetate for male, 5.3 M urea, pH 4.0	6	1.0	3
	0.1 M sodium acetate, pH 4.0 containing 0.033 M CaCl ₂			
Bovine pancreatic DNAse	pH 4.0, 0.010 M CaCl ₂	1-6	3 ^d	4 ^e
Dihydrofolate reductase	0.05 M potassium phosphate, pH 6.5	20	2.0	5
Pyrocathechol (B. <i>Ascarum</i>) ^f	0.1 M phosphate, pH 7.0	—	2	6
Relaxin	0.2 M sodium acetate, pH 4.7	—		7
Rhodopsin	0.1 M Tris acetate, pH 7.4 containing 1% erubipogone	50	6	8
	0.1 M sodium acetate, pH 5.0-1.0 M urea	100	9	8
Pig kidney amino acylase	0.005 M sodium acetate, pH 4.15	7	2	10
Galactose oxidase	0.1 sodium acetate, pH 4.0	1	0.5	11
Bovine thrombin	0.05 M sodium acetate, pH 4.75	2	1.1	11
Papain ^g	1.0 M Tris HCl, pH 7.8	8	1.4	12
Lac repressor protein	1.0 M sodium acetate, pH 4.0	35	10	13
α -Mannosidase (P. <i>vilgaria</i>)	0.01 M sodium phosphate, pH 7.0	8	2	14
α -Amylase (B. <i>subtilis</i>)	0.015 M bis Tris HCl, pH 6.5	50	4	15
Dihydrofolate reductase	0.5 M KCl	4	1.2	16
Xylanase	50 mM NaOAc, pH 4.5	—	— ^h	17
Transcarboxylase	250 mM potassium phosphate, pH 6.9	—	10/90 ⁱ	18
Cellulase	50 mM NaOAc, pH 5.0	30	8/12	19
Winged bean	0.1 M sodium citrate, pH 6.0	10	2/4	20

- ^a Reagent to protein.
- ^b pH maintained at 4.0 by addition of KOH.
- ^c Spectral analysis suggested 2 mol tryptophan oxidized while amino acid analysis demonstrates that all three tryptophan residues modified.
- ^d Thiophenylated apoenzyme (apoenzyme modified with 5,5'-dithiobis (2-nitrobenzoic acid)).
- ^e Not activated
- ^f Also modified tyrosine at this concentration.
- ^g Also had substantial modification of tyrosine, cysteine, and methionine.
- ^h There is an apparent time-dependent reaction with both N-bromosuccinimide and 2-hydroxy-5-nitrobenzyl bromide.

Table 1 (continued)
EXAMPLES OF THE MODIFICATION OF PROTEINS WITH
N-BROMOSUCCINIMIDE

- ⁱ Containing 0.1 mM dihydroethanol and 0.1 M phenylmethylsulfonyl fluoride. The reaction was terminated by the addition of a 10-fold molar excess of N-acetyltryptophanamide.
- ^j At maximum inactivation. A total of 40 tryptophanyl residues were available for oxidation in the native state.

References for Table 1

1. Daniel, V. W., III and Trowbridge, C. G., The effect of N-bromosuccinimide upon tryptophan activation and tryptophan catalysis. *Arch. Biochem. Biophys.* 134, 506, 1969.
2. Friedheim, J. H. and Hoenesken, F. M., Effect of N-bromosuccinimide on dihydrofolate reductase. *Biochemistry* 8, 2271, 1969.
3. Poole, T. L. and Price, P. A., The identification of a tryptophan residue essential to the catalytic activity of bovine pancreatic deoxyribonuclease. *J. Biol. Chem.* 246, 4041, 1971.
4. Sartin, J. L., Hugel, T. E., and Liao, T.-H., Reactivity of the tryptophan residues in bovine pancreatic deoxyribonuclease with N-bromosuccinimide. *J. Biol. Chem.* 255, 8633, 1980.
5. Warwick, P. E., D'Souza, L., and Friedheim, J. H., Role of tryptophan in dihydrofolate reductase. *Biochemistry* 11, 3775, 1972.
6. Nagami, K., The participation of a tryptophan residue in the binding of ferric iron to pyrocatecholase. *Biochem. Biophys. Res. Commun.* 51, 364, 1973.
7. Schwabe, C. and Braden, S. A., Evidence for the essential tryptophan residue at the active site of relaxin. *Biochem. Biophys. Res. Commun.* 68, 1126, 1976.
8. Cooper, A. and Hogan, M. E., Reactivity of tryptophans in rhodopsin. *Biochem. Biophys. Res. Commun.* 68, 178, 1976.
9. Kordel, W. and Schneider, F., Chemical modification of two tryptophan residues abolishes the catalytic activity of aminocyclase. *Hoppe Seyler's Z. Physiol. Chem.* 357, 1109, 1976.
10. Kossman, D. J., Eitzinger, M. J., Berensan, R. D., and Giordano, R. S., Role of tryptophan in the spectral and catalytic properties of the copper enzyme, galactose oxidase. *Biochemistry* 16, 1597, 1977.
11. Uberg, L. C. and Lundblad, R. L., The modification of tryptophan in bovine thrombin. *Biochim. Biophys. Acta* 491, 551, 1977.
12. Glick, B. R. and Brubacher, L. S., The chemical and kinetic consequences of the modification of papain by N-bromosuccinimide. *Can. J. Biochem.* 55, 424, 1977.
13. O'Garra, R. B. and Maribawa, K. S., N-bromosuccinimide modification of lac repressor protein. *J. Biol. Chem.* 252, 3563, 1977.
14. Paus, R., The chemical modification of tryptophan residues of α -mannosidase from *Phascolarctus vulgaris*. *Biochim. Biophys. Acta* 533, 446, 1978.
15. Fujimori, H., Onatidis, M., and Hironaka, K., Tryptophan residues of saccharifying α -amylase from *Bacillus subtilis*. A kinetic discrimination of states of tryptophan residues using N-bromosuccinimide. *J. Biochem.* 83, 1503, 1978.
16. Thomson, J. W., Roberts, G. C. K., and Burgess, A. S. V., The effects of modification with N-bromosuccinimide on the binding of ligands to dihydrofolate reductase. *Biochem. J.* 187, 501, 1980.
17. Keckler, S. S., Srinivasan, M. C., and Deshpande, V. V., Chemical modification of a xylanase from a thermotolerant *Streptomyces*. Evidence for essential tryptophan and cysteine residues at the active site. *Biochem. J.* 261, 49, 1989.
18. Kumar, G. K., Beggs, H., and Wood, H. G., Involvement of tryptophans at the catalytic and subunit-binding domain of transcarboxylase. *Biochemistry* 27, 5972, 1988.
19. Clarke, A. J., Essential tryptophan residues in the function of cellulase from *Schizophyllum commune*. *Biochim. Biophys. Acta* 912, 424, 1987.
20. Higuchi, M., Inoue, K., and Iwai, K., A tryptophan residue is essential to the sugar-binding site of winged bean bean lectin. *Biochim. Biophys. Acta* 829, 51, 1983.

(79% decrease). Reaction with N-chlorosuccinimide (50 mM Tris, pH 8.5) resulted in the total loss of both tryptophan and methionine but no significant change in tyrosine. Reaction with chloramine T (50 mM Tris, pH 8.5) resulted only in the loss of methionine. Activity was lost only with the modification of tryptophan. Peptide bond cleavage was not observed under these reaction conditions.

The conversion of tryptophanyl residues to 1-formyltryptophanyl residues has been re-

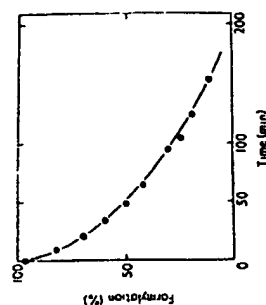


FIGURE 18. Deformylation of tryptophanyl residues in tryptain by incubation at alkaline pH. Shown is the hydrolysis of 1-formyltryptophan in tryptain during incubation at pH 9.3, as measured spectrophotometrically at 298 nm ($\epsilon = 4880$) at 20°C. The solution of formylated tryptain after incubation at pH 8.0 was allowed to stand in the reaction chamber of a pH stat at pH 9.3, 25°C and maintained at this value by the addition of 0.1 M NaOH. (From Colletti-Previero, M.-A., Previero, A., and Zuckerkandl, E., *J. Mol. Biol.*, 39, 493, 1969. With permission.)

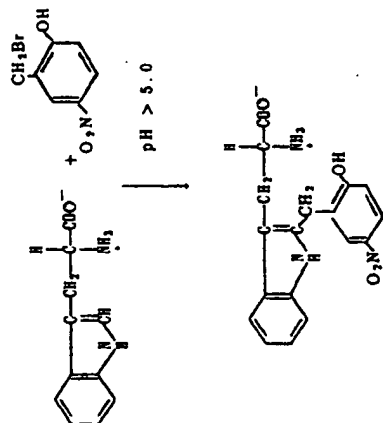


FIGURE 19. A scheme for the reaction of 2-hydroxy-5-nitrobenzyl bromide with tryptophan.

involves the use of 2-hydroxy-5-nitrobenzyl bromide and its various derivatives (Figure 19). 2-Hydroxy-5-nitrobenzyl bromide, frequently referred to as Koshland's reagent, was introduced by Koshland and co-workers.^{33,36} Barman and Koshland³⁷ have reported the use of 2-hydroxy-5-nitrobenzyl bromide for the quantitative determination of tryptophanyl residues in proteins. Although this approach to the quantitative determination of tryptophanyl residues in proteins has been largely replaced by the development of new methods for the hydrolysis of proteins, it can still be useful in certain instances. For this procedure the sample is incubated for 16 to 20 h at 37°C in 1.0 ml 10 M urea (the urea should be recrystallized (EtOH/H₂O) prior to use), pH 2.7 (pH adjusted with concentrated HCl). This solution is cooled to ambient temperature and approximately 5.0 mg of 2-hydroxy-5-nitrobenzyl bromide (in 0.1 ml acetone) is added followed by vigorous stirring (we have found the Pierce Reacti-Vials® very useful for this purpose). Occasionally a precipitate of 2-hydroxy-5-nitrobenzyl alcohol (the hydrolytic product of 2-hydroxy-5-nitrobenzyl bromide) forms which can be

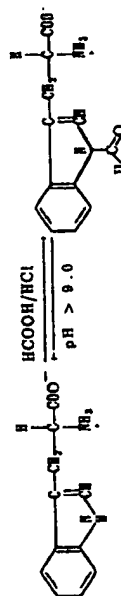


FIGURE 16. A scheme for the reversible formylation of tryptophan residues.

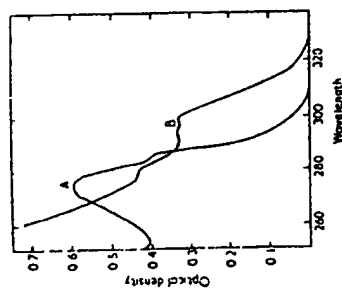


FIGURE 17. Changes in the UV absorption spectrum of tryptain occurring as a result of formylation of tryptophan residues. Shown is the spectrum of tryptain (18 μ M in 8.0 M urea, pH 4.0) before (curve A) and after (curve B) 1-formylation of tryptophanyl residues. Formylation of tryptain was accomplished by dissolving tryptain in formic acid saturated with gaseous HCl at 20°C (2.5 mg/ml). At suitable time intervals, 0.4 ml samples of the solution were diluted with 2 ml of 8 M urea, pH 4.0 for recording the UV spectra. When the maximum increase in absorbance at 298 nm was reached (about 60 min), the solvent was partially removed under vacuum over KOH pellets for 15 min in order to eliminate most of the HCl and the sample was subsequently lyophilized. (From Colletti-Previero, M.-A., Previero, A., and Zuckerkandl, E., *J. Mol. Biol.*, 39, 493, 1969. With permission.)

ported. The reaction conditions are somewhat harsh, but the procedure is reversible (Figure 16) and should prove quite useful for small peptides and has been applied to several proteins. Colletti-Previero and co-workers³⁰ have successfully applied this procedure to bovine pancreatic trypsin. Tryptain was dissolved in formic acid saturated with HCl at a concentration of 2.5 mg/ml at 20°C. The formylation reaction is associated with an increase in absorbance at 298 nm³¹ (Figure 17). It therefore is possible to follow the reaction spectrophotometrically. The reaction is judged complete when there is no further increase in absorbance at 298 nm. The above reaction with tryptain was complete after an incubation period of 1 h. The solvent was partially removed *in vacuo* over KOH pellets followed by lyophilization. The formyl-tryptophan derivative is unstable at alkaline pH. At pH 9.5 (pH-stat), conversion back to tryptophan is complete after 200 min incubation at 20°C as shown in Figure 18. Holmgren has successfully applied this procedure to thionexin.³² A procedure for the acylation of the carbon at position 2 on the indole ring has also been reported.³³ A more recent study on *N*-formylation of tryptophanyl residues in proteins involved the study of epitopes in horse heart cytochrome c.³⁴ The single tryptophanyl residue was formylated with formic acid saturated with HCl. The modified protein had markedly reduced affinity for a monoclonal antibody resulting from local conformational change.

One of the most useful modification procedures for tryptophanyl residues in proteins

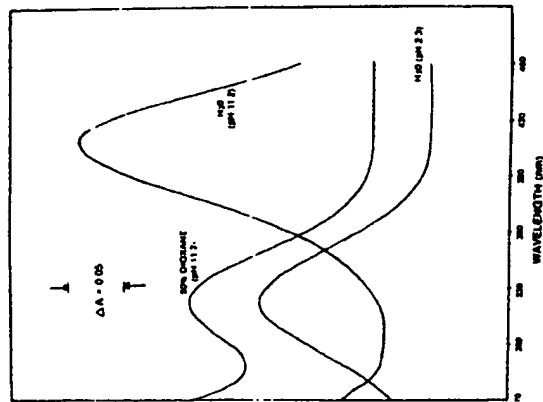


FIGURE 20. The UV absorption spectra of 2-hydroxy-5-nitrobenzyl alcohol (HNB-OH) in different solvents. The concentration of HNB-OH was 33.2 μ M. (From Clemmer, J. D., Carr, J., Knaff, D. B., and Holwerda, R. A., *FEBS Lett.*, 91, 346, 1978. With permission.)

removed by centrifugation. The labeled protein is obtained free of reagent by gel filtration. This step is generally performed under acidic condition (e.g., 0.18 M acetic acid, 10% acetic acid, or 10% formic acid).¹⁸ Depending upon the protein under study, it might be necessary to perform this step in 10 M urea (pH 2.7) to maintain the solubility of the modified protein. A portion of the modified protein is taken to a pH greater than 12 with NaOH. The extent of incorporation is determined at 410 nm using an extinction coefficient of 18,000 $M^{-1}cm^{-1}$. It is necessary to determine the concentration of protein by a technique other than absorbance at 280 nm because of the modification of tryptophan. We have found it convenient to either use amino acid analysis after acid hydrolysis or the ninhydrin reaction¹⁹ after alkaline hydrolysis.²⁰

The most frequent use of 2-hydroxy-5-nitrobenzyl bromide has been in the specific modification of tryptophan in peptides and proteins. Under appropriate reaction conditions (pH 4.0 or below), the reagent is highly specific for reaction with tryptophan. We have, on occasion, seen the modification of methionine residues under these conditions. This reagent also has the advantage of being a "reporter" group in the sense that the spectrum of the hydroxynitrobenzyl derivative is sensitive to changes in the microenvironment as shown in Figure 20. This decrease observed in absorbance at 410 nm associated with an increase in

¹⁸ Despite its wide use as a solvent for peptides and proteins, the use of formic acid is not recommended because of the potential of side reactions at amino functional groups; see Shively, J. E., Hawke, D., and Jones, B. N., *Microsequence analysis of peptides and protein. III. Artifacts and effects of impurities on analysis*, *Anal. Biochem.*, 120, 312, 1982.

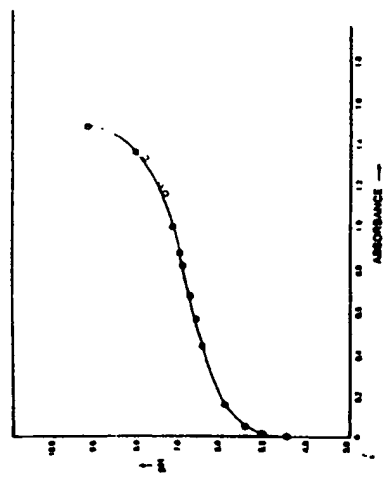


FIGURE 21. Spectrophotometric titration curve for 2-hydroxy-5-nitrobenzyl alcohol (HNB-OH). Shown is the absorbance of HNB-OH (76.4 μ M) at 410 nm as a function of pH (phosphate buffers). (From Clemmer, J. D., Carr, J., Knaff, D. B., and Holwerda, R. A., *FEBS Lett.*, 91, 346, 1978. With permission.)

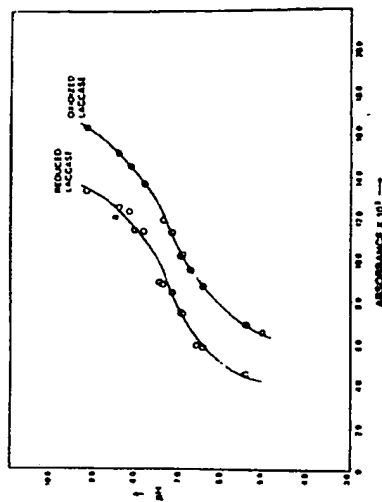


FIGURE 22. Effect of pH on the absorbance (410 nm) of two forms of lactase modified with 2-hydroxy-5-nitrobenzyl bromide (HNB-lactase). Shown are spectrophotometric titration curves for oxidized and reduced HNB-lactase (2.5 μ M; 0.38 mol HNB/mol lactase). The absorbance at 410 nm is shown as a function of pH (phosphate buffers). (From Clemmer, J. D., Carr, J., Knaff, D. B., and Holwerda, R. A., *FEBS Lett.*, 91, 346, 1978. With permission.)

absorbance at 320 nm upon the addition of dioxane is similar to that seen with acidification and reflects the increase in the pK_a of the phenolic hydroxyl group. The spectrophotometric titration curve for 2-hydroxy-5-nitrobenzyl alcohol is shown in Figure 21. Titration curves of oxidized and reduced lactase²¹ which had been modified with 2-hydroxy-5-nitrobenzyl bromide are shown in Figure 22. From this experiment it was concluded that the tryptophanyl

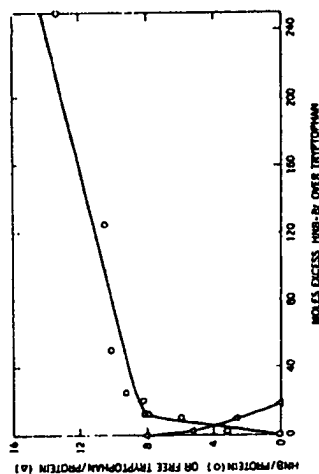


FIGURE 23. The titration of the tryptophanyl residues of carboxymethyl chymotrypsinogen with 2-hydroxy-5-nitrobenzyl bromide. Carboxymethyl chymotrypsinogen (reduced and S-carboxymethylated with iodoacetic acid) was incubated in 10 M urea, pH 2.7, for 16 to 18 h at which point 1-ml portions (5 mg of protein) were reacted with increasing amounts of 2-hydroxy-5-nitrobenzyl bromide dissolved in 0.1 ml acetone. The modified protein was separated from excess reagent by gel filtration (G-25 Sephadex) and subsequently analyzed for tryptophan (amino acid analysis after alkaline hydrolysis) and for the incorporation of the 2-hydroxy-5-nitrobenzyl group. (From Barman, T. E. and Koshland, D. E., Jr., *J. Biol. Chem.*, 242, 5771, 1967. With permission.)

residues in laccase modified with 2-hydroxy-5-nitrobenzyl bromide are in an essentially aqueous microenvironment. The chemistry of the reaction of 2-hydroxy-5-nitrobenzyl bromide with tryptophan has been studied in some detail.⁴¹ Disubstitution on the indole ring is a possibility and is usually seen as a sudden "break" in the plot of extent of modification vs. reagent excess (see Figure 23).

In our hands, the following procedure has been found useful. The protein or peptide to be modified is taken into 0.1 to 0.2 M sodium acetate buffer, pH 4 to 5. Reaction with other nucleophilic centers on the protein will become more of a problem as one approaches neutral pH. A 100-fold molar excess of 2-hydroxy-5-nitrobenzyl bromide (dissolved in a suitable water-miscible organic solvent such as acetone or dimethyl sulfoxide) is added in the dark. After 5 min (this time period was arbitrarily selected; the reaction can be considered to be essentially instantaneous to either modify tryptophan or undergo hydrolysis) the reaction mixture is taken by gel filtration into a solvent suitable for subsequent analysis. The extent of modification is determined under basic conditions as described above for the use of this reagent in the quantitative determination of tryptophan.

The use of 2-hydroxy-5-nitrobenzyl bromide does present problems in that the reagent is extremely sensitive to hydrolysis and is not very soluble under aqueous conditions. These difficulties are avoided and the characteristics of the reaction preserved by the use of the dimethyl sulfonium salt obtained from the reaction of 2-hydroxy-5-nitrobenzyl bromide with dimethyl sulfide.⁴² This compound is easily synthesized or can be obtained from various commercial sources. This water-soluble sulfonium salt derivative has recently been used to modify a tryptophanyl residue in rabbit skeletal myosin subfragment-1.⁴⁴ Purification of peptide-containing modified tryptophanyl residues was achieved by immunodiffusion chromatography using rabbit antibody to bovine serum albumin previously modified with dimethyl(2-hydroxy-5-nitrobenzyl) sulfonium bromide.

Horton and Koshland⁴⁵ have also developed a clever approach for modification of hydrolytic enzymes such as the serine proteases which catalyze the reaction shown in Figure 24. If 2-hydroxy-5-nitrobenzyl bromide is substituted at the phenolic hydroxyl, it is essentially unreactive as originally shown for the methoxy derivative. Horton and Young⁴⁶ prepared



FIGURE 24. The hydrolysis of an ester catalyzed by a serine protease.

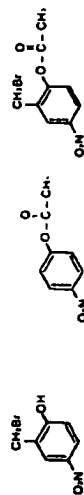


FIGURE 25. The structures of 2-hydroxy-5-nitrobenzyl bromide (left), *p*-nitrophenyl acetate (center), and 2-acetoxy-5-nitrobenzyl bromide.

2-acetoxy-5-nitrobenzyl bromide. This derivative, like the methoxy derivative, is essentially unreactive. There is considerable structural identity between 2-acetoxy-5-nitrobenzyl bromide and *p*-nitrophenyl acetate, which is a nonspecific substrate for chymotrypsin (Figure 25). α -Chymotrypsin removes the acetyl group from 2-acetoxy-5-nitrobenzyl bromide, thus generating 2-hydroxy-5-nitrobenzyl bromide at the active site which then either rapidly reacts with a neighboring nucleophile or undergoes hydrolysis. Uhlig and Lundblad⁴⁷ have used both the acetoxy and butyloxy derivatives in the study of thrombin. A similar approach has been used in the study of papain with 2-chloromethyl-4-nitrophenyl *N*-carbobenzoxycarboxylate.⁴⁸ It has been subsequently shown that this modification occurs at a specific tryptophan residue in papain.⁴⁹

2-Hydroxy-5-nitrobenzyl bromide has been proved to be of use in the study of the functional role of tryptophan in the enzymes, as shown in Table 2.

Reagents with reaction characteristics similar to 2-hydroxy-5-nitrobenzyl bromide are the *o*-nitrophenylsulfenyl derivatives.⁵⁰ The reaction product resulting from the sulfonylation of lysozyme⁵¹ in *o*-nitrobenzenesulfenyl chloride (2-nitrophenylsulfenyl chloride) (40-fold molar excess) pH 3.5 (0.1 M sodium acetate) has spectral characteristics which can be used to determine the extent of reagent incorporation (at 365 nm $\epsilon = 4 \times 10^{-4} \text{ M}^{-1} \text{ cm}^{-1}$) (Figure 26). These reagents show considerable specificity for the modification of tryptophan at pH ≤ 4.0 (Figure 27). Possible side reactions with other nucleophiles such as amino groups need to be considered. In the case of human chorionic somatomammotropin and human pituitary growth hormone,⁵² reaction with *o*-nitrophenylsulfenyl chloride (2-nitrophenylsulfenyl chloride) was achieved in 50% acetic acid but not in 0.1 sodium acetate, pH 4.0. Wilchek and Miron⁵³ have reported on the reaction of 2,4-dinitrophenylsulfenyl chloride with tryptophan in peptides and protein and subsequent conversion of the modified tryptophan to 2-thiotryptophan by reaction with β -mercaptoethanol at pH 8.0 (see Figure 28). The thiolysis of the modified tryptophan is responsible for changes in the spectral properties of the derivative (Figure 29). The characteristics of the modified tryptophan have resulted in the development of a facile purification scheme for peptides containing the modified tryptophan residues.^{54,55} Mollier et al.⁵⁶ examined the reaction of *o*-nitrophenylsulfenyl chloride (2-nitrophenylsulfenyl chloride) with notexin (a phospholipase obtained from *Notexis scutellatus* venom which contains two tryptophanyl residues). Reaction with 2-nitrophenylsulfenyl chloride (2-fold molar excess) in 50% (v/v) acetic acid resulted in two derivative proteins on HPLC analysis. One derivative contained two modified tryptophanyl residues (20 and 110) while the other derivative was modified only at position 20.

Table 2
EXAMPLES OF THE MODIFICATION OF PROTEINS WITH 2-HYDROXY-5-NITROBENZYL BROMIDE

Protein	Solvent	Molar excess	Residues modified	Ref.
Pepsin	0.1 M NaCl ^a	300	2/4	1
Streptococcal proteinase	0.46 M sodium phosphate, pH 3.1	200	1.8/4	2
Pancreatic deoxyribonuclease	0.050 M CaCl ₂ ^b	100	1/3	3
Carbonic anhydrase	0.1 M phosphate, pH 6.8	100	—	4
Trypsin	0.1 M NaCl, 0.02 M CaCl ₂ ^c	ca. 100	1/4	5
Human chorionic somatomotropin	pH 4.2 (pH-stat)	—	—	6
<i>Naja naja</i> neurotoxin	0.05 M glycine, pH 2.8	40	—	7
Glyceraldehyde-3-phosphate dehydrogenase	0.2 M acetic acid ^d	30 ^e	1/3	8
α -Mannosidase (<i>Phascolarctos vulgaris</i>)	0.1 M sodium acetate, pH 3.7	100	5/28	9
Thrombin	0.2 M acetate, pH 4.0	100	1/8	10
Laccase	pH 6.95	50	0.30/6	11
	pH 4.00	50	0.58/6	11
	pH 3.30	110	2.39/6	11
Human serum albumin	10 M urea, pH 4.4	1000	1.1/1 ^f	12
Xylanase	50 mM NaOAc, pH 5.0	—	0.9/4	13
Winged bean	0.1 M sodium citrate, pH 3.1	100	0.9/4	14
		200	1.7/4	
		400	1.8/4	

- ^a pH Adjusted with 50% acetic acid.
- ^b pH Remained between 4.0 and 4.5 without need for buffer.
- ^c Variation with respect to enzyme source.
- ^d pH Maintained at 4.2 by addition of NaOH (pH Stat).
- ^e pH 2.7.
- ^f Polymerization occurred.
- ^g pH Maintained at 6.75 by the addition of 0.1 M NaOH.
- ^h Dimethyl (2-hydroxy-5-nitrobenzyl) sulfonium bromide was used in the experiments. Prior to reaction, the active site sulphydryl was blocked by reaction with 5,5'-dithiobis(2-nitrobenzoate).
- ⁱ Unbuffered, pH maintained by titration with NaOH.
- ^j Incorporation determined at pH 7.4 after the following relationship: μ moles 2-hydroxy-5-nitrobenzyl bromide per mole albumin = $(A_{410} \times 49,000 \times 0.493) / (A_{280} - 0.167) \times A_{410}$.
- ^k A time-dependent inactivation reaction was observed.

References for Table 2

1. Dayhilde, T. A. A. and Jones, W. M., Studies on the tryptophan residues in porcine pepsin. *J. Biol. Chem.*, 243, 3906, 1968.
2. Robinson, G. W., Reaction of a specific tryptophan residue in streptococcal proteinase with 2-hydroxy-5-nitrobenzyl bromide. *J. Biol. Chem.*, 245, 4832, 1970.
3. Poole, T. L. and Piles, P. A., The identification of a tryptophan residue essential to the catalytic activity of bovine pancreatic deoxyribonuclease. *J. Biol. Chem.*, 246, 4041, 1971.
4. Lindeberg, S. and Nilsson, A., The location of tryptophanyl groups in human and bovine carbonic anhydrases. Ultraviolet difference spectra and chemical modification. *Biochim. Biophys. Acta*, 295, 117, 1973.
5. Imhoff, J. M., Kati-Dioska, V., and Kati, B., Functional changes in bovine α - and β -tryptins caused by the substitution of tryptophan-199. *Biochimie*, 55, 521, 1973.
6. Neri, P., Arzuffi, C., Betti, R., Cecchi, F., and Turti, P., Modification of the tryptophanyl residue and its effect on the immunological and biological activity of human chorionic somatomotropin. *Biochim. Biophys. Acta*, 322, 88, 1973.

References for Table 2 (continued)

7. Karlsson, E., Eaker, D., and Drevel, H., Modification of the invariant tryptophan residue of two *Naja naja* neurotoxins. *Biochim. Biophys. Acta*, 328, 510, 1973.
8. Hellman, H. D. and Phelderer, G., On the role of tryptophan residues in the mechanism of action of glyceraldehyde-3-phosphate dehydrogenase as tested by specific modification. *Biochim. Biophys. Acta*, 304, 331, 1975.
9. Pies, E., The chemical modification of tryptophan residues of α -mannosidase from *Phascolarctos vulgaris*. *Biochim. Biophys. Acta*, 533, 446, 1978.
10. Uhdeg, L. C. and Lundblad, R. L., The modification of tryptophan in bovine thrombin. *Biochem. Biophys. Acta*, 491, 551, 1977.
11. Chremers, J. D., Carr, J., Kust, D. B., and Holwerda, R. A., Modification of lactose tryptophan residues with 2-hydroxy-5-nitrobenzyl bromide. *FEBS Lett.*, 91, 346, 1978.
12. Fésák, K. J., Möller, W. E., and Weller, U., The modification of the lone tryptophan residue in human serum albumin by 2-hydroxy-5-nitrobenzyl bromide. Characterization of the modified protein and the binding of L-tryptophan and benzodiazepines to the tryptophan-modified albumin. *Hoppe-Seyler's Z. Physiol. Chem.*, 359, 709, 1978.
13. Kaskar, S. S., Srinivasan, M. C., and Deshpande, V. V., Chemical modification of a xylanase from a thermotolerant *Streptomyces*. Evidence for essential tryptophan and cysteine residues at the active site. *Biochem. J.*, 261, 49, 1989.
14. Higuchi, M., Inoue, K., and Iwai, K., A tryptophan residue is essential to the sugar-binding site of winged bean lectin. *Biochim. Biophys. Acta*, 829, 51, 1983.

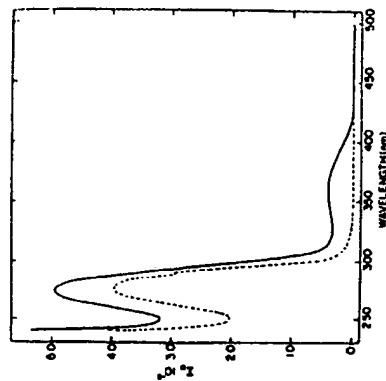


FIGURE 26 The UV absorbance spectrum of egg white lysozyme after modification of tryptophan-62 with 2-nitrophenylsulfenyl chloride (o-nitrobenzenesulfenyl chloride). Shown is the UV absorption spectrum of 1-NPS-lysozyme (—), and native lysozyme (---). The measurements were performed in water at pH 7.0

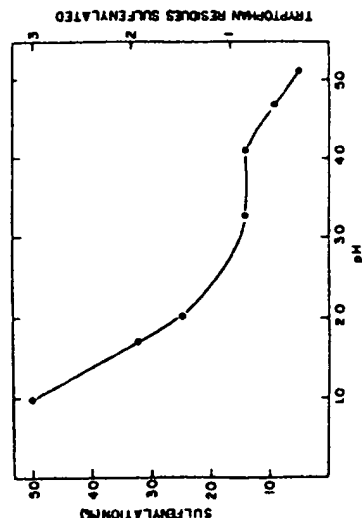


FIGURE 27 The extent of sulfenylation of tryptophan residues in egg white lysozyme by 2-nitrophenylsulfonyl chloride as a function of the pH. Sulfenylation was carried out at protein concentration of 0.5 μ mol in 1 ml of 0.1 M buffered solutions (HCl-KCl) at pH 1 to 2; sodium acetate at pH 3 to 5) with 20 μ mol of 2-nitrophenylsulfonyl chloride for 5 h. (From Schechter, Y., Burstein, Y., and Pascher, A., *Biochemistry*, 11, 653, 1972. With permission.)

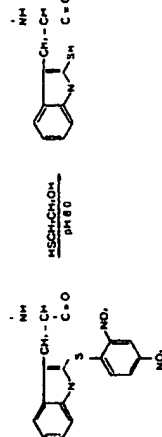


FIGURE 28 Thiolysis of the tryptophan derivative formed on reaction with 2,4-dinitrophenylsulfonyl chloride.

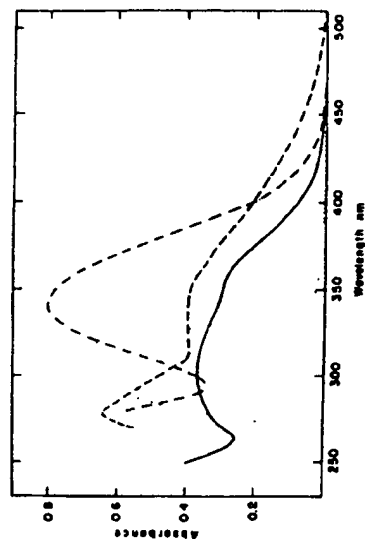


FIGURE 29 UV absorption spectra of the derivatives formed by the thiolysis of 2,4-dinitrophenylsulfonyl tryptophan. Shown are the UV absorption spectra of 2,4-dinitrophenylsulfonyltryptophan (---), 2-nitrotryptophan (—), 2,4-dinitrophenyl-2-disulfide (—), and 2,4-dinitrophenyl-2-mercaptosuccinate (---). The spectral studies were performed in 0.1 M ammonium bicarbonate. (From Wüchek, M., and Miron, T., *Biochem. Biophys. Res. Commun.*, 47, 1015, 1972. With permission.)

REFERENCES

1. Liu, T.-Y., and Chang, Y. H., Hydrolysis of proteins with *p*-toluenesulfonic acid. Determination of tryptophan. *J. Biol. Chem.*, 246, 2042, 1971.
2. Srinivasan, R. J., Neuberg, M. R., and Liu, T.-Y., Complete amino acid analysis of proteins from a single hydrolysis. *J. Biol. Chem.*, 251, 1936, 1976.
3. Hachisaka, Y., Horikawa, H., Kurthara, K., and Shibata, K., Sites of amino residues in proteins. V. Different reactivities with H_2O_2 of tryptophan residues in lysozyme, proteinase and synaptob, *Biochim. Biophys. Acta*, 93, 346, 1984.
4. Kozuka, I., Matsushima, A., Bando, M., and Inada, Y., Tyrosine and tryptophan residues and amino groups in thrombin related to enzymic activities. *Biochim. Biophys. Acta*, 214, 490, 1970.
5. Sando, A., and Irie, M., Chemical modification of tryptophan residues in ribonuclease from a *Rhizopus* sp., *J. Biochem.*, 87, 1079, 1980.
6. Matsushima, A., Takahashi, H., Saito, Y., and Inada, Y., Significance of tryptophan residues in the D-domain of the fibrin molecule in fibrin polymer formation. *Biochim. Biophys. Acta*, 625, 230, 1980.
7. Pascher, A., Lawson, W. R., and Witkop, B., Selective cleavage of peptide bonds. I. Mechanism of oxidation of β -substituted imides with *N*-bromosuccinimide. *J. Am. Chem. Soc.*, 81, 4747, 1959.
8. Spande, T. F., and Witkop, B., Determination of the tryptophan content of protein with *N*-bromosuccinimide. *Methods Enzymol.*, 11, 498, 1967.
9. Spande, T. F., and Witkop, B., Tryptophan involvement in the function of enzymes and protein hormones as determined by selective oxidation with *N*-bromosuccinimide. *Methods Enzymol.*, 11, 506, 1967.
10. Spande, T. F., and Witkop, B., Tryptophan involvement in binding sites of proteins and in enzymic inhibitor complexes as determined by oxidation with *N*-bromosuccinimide. *Methods Enzymol.*, 11, 522, 1967.
11. Green, N. M., Avidin. 3. The nature of the biotin binding site. *Biochem. J.*, 89, 599, 1963.
12. Crestfield, A. M., Moore, S., and Steals, W. H., The preparation and enzymatic hydrolysis of reduced and S-carboxymethylated proteins. *J. Biol. Chem.*, 238, 622, 1963.
13. Ohtsuki, M., Kawagishi, T., Abe, T., and Hirai, K., Stopped-flow studies on the chemical modification with *N*-bromosuccinimide of model compounds of tryptophan residues. *J. Biochem.*, 87, 273, 1980.
14. Sarda, J. L., Hagi, T. E., and Liao, T.-M., Reactivity of the tryptophan residues in bovine pancreatic deoxyribonuclease with *N*-bromosuccinimide. *J. Biol. Chem.*, 255, 8633, 1980.

15. David, W. W., III and Trowbridge, C. G., The effect of *N*-bromosuccinimide upon trypsinogen activation and trypsin catalysis. *Arch. Biochem. Biophys.* 134, 506, 1969.
16. Friedheim, J. H. and Huesmann, F. M., Effect of *N*-bromosuccinimide on dihydrofolate reductase. *Biochemistry* 8, 2271, 1969.
17. Warwick, P. R., D'Souza, L., and Friedheim, J. H., Role of tryptophan in dihydrofolate reductase. *Biochemistry* 11, 3775, 1972.
18. Poulsen, T. L. and Price, P. A., The identification of a tryptophan residue essential to the catalytic activity of bovine pancreatic deoxyribonuclease. *J. Biol. Chem.* 246, 4041, 1971.
19. Komman, D. J., Edinger, M. J., Bereman, R. D., and Giordano, R. S., Role of tryptophan in the spectral and catalytic properties of the copper enzyme, galactose oxidase. *Biochemistry* 16, 1597, 1977.
20. Fujimori, H., Ohtsuki, M., and Hirotsu, K., Tryptophan residues of saccharifying α -amylase from *Bacillus subtilis*. A kinetic discrimination of sites of tryptophan residues using *N*-bromosuccinimide. *J. Biochem.* 83, 1503, 1978.
21. Isobeuchi, N., Takahashi, T., Yoshimoto, A., and Irie, M., *N*-Bromosuccinimide oxidation of a glutamylase from *Aspergillus niger*. *J. Biochem.* 91, 1661, 1982.
22. Ohtsuki, M., Kawaguchi, T., and Hirotsu, K., Stopped-flow chemical modification with *N*-bromosuccinimide: a good probe for changes in the microenvironment of the Trp 62 residue of chicken egg white lysozyme. *Arch. Biochem. Biophys.* 272, 46, 1989.
23. O'Garra, R. B. and Matthews, K. S., *N*-Bromosuccinimide modification of lac repressor protein. *J. Biol. Chem.* 252, 3365, 1977.
24. Kumar, C. K., Beggs, H., and Wood, H. G., Involvement of tryptophans at the catalytic and substrate-binding domains of transcarboxylase. *Biochemistry* 27, 5972, 1988.
25. Keisler, S. S., Srinivasan, M. C., and Deshpande, V. V., Chemical modification of a xylanase from a thermotolerant *Streptomyces*. Evidence for essential tryptophan and cysteine residues at the active site. *Biochem. J.* 261, 49, 1989.
26. Ramakrishnan, L. K. and Wilkop, B., *N*-Bromosuccinimide cleavage of peptides. *Methods Enzymol.* 11, 283, 1967.
27. Feldhoff, R. C. and Peters, T., Jr., Determination of the number and relative position of tryptophan residues in various albumins. *Biochem. J.* 159, 579, 1976.
28. Schechter, Y., Patchornik, A., and Barsteln, Y., Selective chemical cleavage of tryptophanyl peptide bonds by oxidative chlorination with *N*-chlorosuccinimide. *Biochemistry* 15, 5071, 1976.
29. Sakurai, J. and Nagasawa, M., Role of one tryptophan residue in the latent activity of Clostridium perfringens epsilon toxin. *Biochem. Biophys. Res. Commun.* 128, 760, 1985.
30. Colletti-Previero, M. A., Previero, A., and Zuckerkandl, E., Separation of the proteolytic and esteratic activities of trypsin by reversible structural modifications. *J. Mol. Biol.* 39, 493, 1969.
31. Previero, A., Colletti-Previero, M. A., and Cavallero, J. C., A reversible chemical modification of the tryptophan residue. *Biochim. Biophys. Acta* 147, 453, 1967.
32. Halgren, A., Reversible chemical modification of the tryptophan residues of ribonuclease from *Escherichia coli* B. *Eur. J. Biochem.* 26, 528, 1972.
33. Previero, A., Prota, G., and Colletti-Previero, M. A., C-Acylation of the tryptophan indole ring and its usefulness in protein chemistry. *Biochim. Biophys. Acta* 235, 269, 1972.
34. Cooper, H. M., Jenkinson, R., Hunt, D. P., Griffin, P. R., Yates, J. R., III, Shabanowitz, J., Zhu, N.-Z., and Patterson, Y., Site-directed chemical modification of horse cytochrome c results in changes in antigenicity due to local and long-range conformation perturbations. *J. Biol. Chem.* 262, 11591, 1987.
35. Koelsland, D. E., Jr., Karthaus, Y. D., and Latham, H. G., An environmentally-sensitive reagent with selectivity for the tryptophan residue in proteins. *J. Am. Chem. Soc.* 86, 1448, 1964.
36. Horton, H. R. and Koelsland, D. E., Jr., A highly reactive colored reagent with selectivity for the tryptophanyl residue in proteins. 2-Hydroxy-5-nitrobenzyl bromide. *J. Am. Chem. Soc.* 87, 1126, 1965.
37. Barman, T. E. and Koelsland, D. E., Jr., A colorimetric procedure for the quantitative determination of tryptophan residues in proteins. *J. Biol. Chem.* 242, 5771, 1967.
38. Moore, S., Amino acid analysis: aqueous dimethyl sulfoxide as solvent for the ninhydrin reaction. *J. Biol. Chem.* 243, 6281, 1968.
39. Fractier, R. G. and Crestfield, A. M., Preparation and properties of two active forms of ribonuclease dimer. *J. Biol. Chem.* 240, 3668, 1965.
40. Chennier, J. D., Carr, J., Knoff, D. B., and Hochwerda, R. A., Modification of lactase tryptophan residues with 2-hydroxy-5-nitrobenzyl bromide. *FEBS Lett.* 91, 346, 1978.
41. London, G. M. and Koelsland, D. E., Jr., The chemistry of a reporter group: 2-hydroxy-5-nitrobenzyl bromide. *J. Biol. Chem.* 245, 2247, 1970.
42. Lenzblad, R. L. and Noyes, C. M., Observations on the reaction of 2-hydroxy-5-nitrobenzyl bromide with a peptide-bound tryptophanyl residue. *Anal. Biochem.* 136, 93, 1984.
43. Horton, H. R. and Teckler, W. P., Dimethyl (2-hydroxy-5-nitrobenzyl) sulfonium salts. Water-soluble environmentally sensitive protein reagents. *J. Biol. Chem.* 245, 3397, 1970.
44. Peyser, Y. M., Muhlrad, A., and Werber, M. M., Tryptophan-130 is the most reactive tryptophan residue in rabbit skeletal myosin subfragment-1. *FEBS Lett.* 259, 346, 1990.
45. Horton, H. R. and Koelsland, D. E., Jr., Reactions with reactive alkyl halides. *Methods Enzymol.* 11, 556, 1967.
46. Horton, H. R. and Young, G., 2-Acetoxy-5-nitrobenzyl chloride. A reagent designed to introduce a reporter group near the active site of chymotrypsin. *Biochim. Biophys. Acta* 194, 272, 1969.
47. Utting, L. C. and Lundblad, R. L., The modification of tryptophan in bovine thrombin. *Biochim. Biophys. Acta* 491, 551, 1977.
48. Mink, J. E. and Horton, H. R., A kinetic analysis of the enhanced catalytic efficiency of papain modified by 2-hydroxy-5-nitrobenzyl bromide. *Biochemistry* 12, 5285, 1973.
49. Chang, S.-M. T. and Horton, H. R., Structure of papain modified by reaction with 2-chloromethyl-4-nitrophenyl *N*-carboxymethylglycinate. *Biochemistry* 18, 1559, 1979.
50. Fontana, A. and Scofield, E., Sulfenyl halides as modifying reagents for polypeptides and proteins. *Methods Enzymol.* 25, 482, 1972.
51. Schechter, Y., Barsteln, Y., and Patchornik, A., Sulfenylation of tryptophan-62 in hen egg-white lysozyme. *Biochemistry* 11, 653, 1972.
52. Bewley, T. A., Kawachi, H., and Li, C. H., Comparative studies of the single tryptophan residue in human chorionic gonadotropin and human pituitary growth hormone. *Biochemistry* 11, 4170, 1972.
53. Witwicki, M. and Miron, T., The conversion of tryptophan to 2-thioltryptophan in peptides and proteins. *Biochem. Biophys. Res. Commun.* 47, 1015, 1972.
54. Cherr, A. and Zhao, B., Isolation of tryptophan-containing peptides by absorption chromatography. *Anal. Biochem.* 73, 471, 1976.
55. Rubinstein, M., Schechter, Y., and Patchornik, A., Covalent chromatography — the isolation of tryptophanyl containing peptides by novel polymeric reagents. *Biochem. Biophys. Res. Commun.* 70, 1257, 1976.
56. Moller, P., Chvetzoff, S., Bous, F., Harvey, A. L., and Menez, A., Tryptophan 110, a residue involved in the toxic activity but not in the enzymatic activity of noxalin. *Eur. J. Biochem.* 185, 263, 1989.

Circulation

JOURNAL OF THE AMERICAN HEART ASSOCIATION



Erythropoietin Is a Novel Vascular Protectant Through Activation of Akt1 and Mitochondrial Modulation of Cysteine Proteases

Zhao Zhong Chong, Jing-Qiong Kang and Kenneth Maiese

Circulation 2002;106:2973-2979; originally published online Nov 11, 2002;

DOI: 10.1161/01.CIR.0000039103.58920.1F

Circulation is published by the American Heart Association, 7272 Greenville Avenue, Dallas, TX 75214

Copyright © 2002 American Heart Association. All rights reserved. Print ISSN: 0009-7322. Online ISSN: 1524-4539

The online version of this article, along with updated information and services, is located on the World Wide Web at:
<http://circ.ahajournals.org/cgi/content/full/106/23/2973>

Subscriptions: Information about subscribing to *Circulation* is online at
<http://circ.ahajournals.org/subscriptions/>

Permissions: Permissions & Rights Desk, Lippincott Williams & Wilkins, a division of Wolters Kluwer Health, 351 West Camden Street, Baltimore, MD 21202-2436. Phone: 410-528-4050. Fax: 410-528-8550. E-mail:
journalpermissions@lww.com

Reprints: Information about reprints can be found online at
<http://www.lww.com/reprints>

Erythropoietin Is a Novel Vascular Protectant Through Activation of Akt1 and Mitochondrial Modulation of Cysteine Proteases

Zhao Zhong Chong, MD, PhD; Jing-Qiong Kang, MD, PhD; Kenneth Maiese, MD

Background—Erythropoietin (EPO) is a critical regulator for the proliferation of immature erythroid precursors, but its role as a potential cytoprotectant in the cerebrovasculature system has not been defined.

Methods and Results—We examined the ability of EPO to regulate a cascade of apoptotic death-related cellular pathways during anoxia-induced vascular injury in endothelial cells (ECs). EC injury was evaluated by trypan blue, DNA fragmentation, membrane phosphatidylserine (PS) exposure, protein kinase B activity, mitochondrial membrane potential, and cysteine protease induction. Exposure to anoxia alone rapidly increased genomic DNA fragmentation from $2 \pm 1\%$ to $40 \pm 5\%$ and membrane PS exposure from $3 \pm 2\%$ to $56 \pm 5\%$ over 24 hours. Administration of a cytoprotective concentration of EPO (10 ng/mL) prevented DNA destruction and PS exposure. Cytoprotection by EPO was completely abolished by cotreatment with anti-EPO neutralizing antibody, which suggests that EPO was necessary and sufficient for the prevention of apoptosis. Protection by EPO was intimately dependent on the activation of protein kinase B (Akt1) and the maintenance of mitochondrial membrane potential. Subsequently, EPO inhibited caspase 8-, caspase 1-, and caspase 3-like activities that were linked to mitochondrial cytochrome *c* release.

Conclusions—The present work serves to illustrate that EPO can offer novel cytoprotection during ischemic vascular injury through direct modulation of Akt1 phosphorylation, mitochondrial membrane potential, and cysteine protease activity. (*Circulation*. 2002;106:2973-2979.)

Key Words: apoptosis ■ cytochrome *c* ■ cysteine endopeptidases ■ proteins, mitochondrial ■ proteins, proto-oncogene

To foster new therapeutic approaches for cerebral vascular disease, it becomes critical to dissect the underlying subcellular pathways used by potential cytoprotectants. In this regard, erythropoietin (EPO) has become especially attractive as a potential vascular protectant. Recent work has extended the traditional role of EPO from a mediator of erythroid maturation to one that offers protection against toxic stimuli in the nervous system.^{1,2} Yet, knowledge concerning the ability of EPO to function as a specific vascular protectant, especially in the nervous system, is virtually nonexistent and requires further definition.

The potential for EPO to be an efficacious cytoprotectant in the nervous system may weigh heavily on its ability to foster the survival of cerebral microvascular endothelial cells (ECs) and prevent programmed cell death. Ischemic injury in ECs can lead to the active destruction of the endothelium and can mediate vascular degeneration that may ultimately impair cortical function.^{3,4} Cerebral EC injury is composed of 2 independent apoptotic pathways that consist of nuclear DNA degradation and the exposure of membrane phosphatidylser-

ine (PS) residues.^{5,6} Although DNA degradation in ECs may lead to the acute loss of cerebral microvascular integrity, the exposure of membrane PS residues in ECs may play a more formidable role that involves the precipitation of a procoagulant environment⁷ and cellular inflammation.⁸

Several downstream signal transduction pathways may ultimately determine both the scope and capacity of the protective role of EPO. In particular, the serine/threonine kinase protein kinase B (Akt1), a key determinant of cell survival, appears to be necessary for EPO to prevent apoptosis of erythroid progenitors.⁹ In addition, both the independent preservation of mitochondrial membrane integrity and the modulation of cysteine protease activity through cytochrome *c* release may influence the protective role of Akt1.¹⁰ As a result, mitochondrial membrane depolarization, cytochrome *c* release, and the subsequent activation of a family of executioner cysteine proteases (caspases) that include caspase 8, caspase 1, and caspase 3 may be relevant for EPO to increase vascular cell survival during injury.^{11,12} In light of the strong potential of EPO to provide protection against

Received June 26, 2002; revision received August 22, 2002; accepted August 23, 2002.

From the Division of Cellular and Molecular Cerebral Ischemia (Z.Z.C., J.-Q.K., K.M.), Departments of Neurology (Z.Z.C., J.-Q.K., K.M.) and Anatomy and Cell Biology (K.M.), Center for Molecular Medicine and Genetics (K.M.), Institute of Environmental Health Sciences (K.M.), Wayne State University School of Medicine, Detroit, Mich.

Correspondence to Kenneth Maiese, MD, Department of Neurology, 8C-1 UHC, Wayne State University School of Medicine, 4201 St Antoine, Detroit, MI 48201. E-mail kmaiese@med.wayne.edu

© 2002 American Heart Association, Inc.

Circulation is available at <http://www.circulationaha.org>

DOI: 10.1161/01.CIR.0000039103.58920.1F

Downloaded from circ.ahajournals.org by on October 8, 2007

cerebral vascular disease, we investigated the underlying cellular mechanisms that may determine protection by EPO to gain greater insight into potential therapeutic targets for EC injury.

Methods

Cerebral Microvascular EC Cultures

Vascular ECs were isolated from Sprague-Dawley adult rat brain cerebra by a modified collagenase/dispase-based digestion protocol.¹² Briefly, ECs were cultured in endothelial growth media consisting of M199E with 20% heat-inactivated fetal bovine serum, 2 mmol/L L-glutamine, 90 μ g/mL heparin, and 20 μ g/mL EC growth supplement (ICN Biomedicals). Cells from the third passage were identified by positive direct immunocytochemistry for factor VIII-related antigen.¹³

Experimental Treatments

To induce anoxia, EC cultures were deprived of oxygen by placing them into an anoxic (95% N₂ and 5% CO₂) chamber system (Sheldon) at 37°C for 12 hours.¹⁴ For treatments applied 1 hour before anoxia, application of EPO, EPO antibody (R&D Systems), or the phosphatidylinositol-3-kinase (PI3K) inhibitors wortmannin or LY294002 (Tocris) was continuous.

Assessment of Cell Survival and Injury

EC injury was determined by bright-field microscopy with a 0.4% trypan blue dye exclusion method 24 hours after anoxia per our previous protocols.¹⁴ Mean survival was determined by counting 8 randomly selected nonoverlapping fields with each containing ~10 to 20 cells (viable and nonviable) in each 24-well plate.

Assessment of DNA Fragmentation

Genomic DNA fragmentation was determined by the terminal deoxynucleotidyl transferase nick end labeling (TUNEL) assay.^{12,14} Briefly, ECs were fixed in 4% paraformaldehyde/0.2% picric acid/0.05% glutaraldehyde, and the 3'-hydroxy ends of cut DNA were labeled with biotinylated dUTP with the enzyme terminal deoxynucleotidyl transferase (Promega) followed by streptavidin-peroxidase and visualized with 3,3'-diaminobenzidine (Vector Laboratories).

Assessment of Membrane PS Residue Externalization

Per our prior protocols,^{5,6} a 30 μ g/mL stock solution of annexin V conjugated to phycoerythrin (R&D Systems) was diluted to 3 μ g/mL in warmed calcium containing binding buffer (10 mmol/L HEPES, pH 7.5, 150 mmol/L NaCl, 5 mmol/L KCl, 1 mmol/L MgCl₂, 1.8 mmol/L CaCl₂). Plates were incubated with 500 μ L of diluted annexin V for 10 minutes. Images were acquired by "blinded" assessment with a Leitz DMIRB microscope (Leica) and a Fuji/Nikon Super CCD (6.1 megapixels) that used transmitted light and fluorescent single-excitation light at 490 nm and detected emission at 585 nm.

Assessment of Mitochondrial Membrane Potential

The fluorescent probe JC-1 (Molecular Probes), a cationic membrane potential indicator, was used to assess mitochondrial membrane potential. EC monolayers in 35-mm² Petri dishes were incubated with 2 μ g/mL JC-1 in growth medium at 37°C for 30 minutes. ECs were then analyzed immediately under a Leitz DMIRB microscope with a dual-emission fluorescence filter with 515 to 545 nm for green fluorescence and emission at 585 to 615 nm for red fluorescence.

Western Blot Analysis for Akt1 Phosphorylation and Cytochrome c Release

Cells were homogenized, and after protein determination, each sample (50 μ g/lane) was then subjected to 7.5% SDS-PAGE. Membranes were incubated with a mouse monoclonal antibody against phospho-Akt1 (p-Akt1; 1:1000; Active-Motif). After being

washed, membranes were incubated with a horseradish peroxidase-conjugated secondary antibody (goat anti-mouse IgG, 1:2000; Pierce). The antibody-reactive bands were revealed by chemiluminescence (Amersham Pharmacia Biotech).

Preparation of Mitochondria for Analysis of Cytochrome c Release

Briefly, cells were harvested and homogenized, and the harvested supernatants were centrifuged at 10 000g for 10 minutes at 4°C. Mitochondrial proteins were then separated by 12.5% SDS-PAGE. The Western blot for cytochrome c was performed with primary mouse polyclonal antibody against cytochrome c (1:2000; Pharmin-gen) and revealed by enhanced chemiluminescence.

Assessment of Caspase Activity

At 12 hours after anoxia exposure, cysteine protease activities were determined as described previously.^{5,12} Cell suspensions were prepared, and an aliquot of supernatant containing 30 μ g protein was incubated with a 250 μ mol/L colorimetric substrate for caspase 8 (Ac-IETD-pNA), caspase 1 (Ac-YVAD-pNA), or caspase 3 (Ac-DEVD-pNA; Calbiochem). Absorbance was measured at 405 nm and substrate cleavage reported in micromoles per minute per gram of protein (μ mol \cdot min⁻¹ \cdot g⁻¹) against standard *p*-nitroaniline solutions.

Modulation of Caspase Activity

Modulation of cysteine protease activity in ECs was performed with the irreversible and cell-permeable caspase inhibitors (50 μ mol/L 1 hour before anoxia) Z-IETD-FMK for caspase 8 (IETD), Z-YVAD-FMK (YVAD) for caspase 1, and Z-DEVD-FMK (DEVD) for caspase 3 obtained from Pharmingen Inc.

Statistical Analysis

For each experiment that involved assessment of EC survival, DNA degradation, membrane PS exposure, and caspase activity, the mean and standard error were determined from 4 to 6 replicate experiments. Statistical differences between groups were assessed by means of ANOVA.

Results

EPO Prevents EC Injury During Anoxia

No significant toxicity during normoxia over a 24-hour period was present in the cultures exposed to EPO alone in the concentrations of 0.01 to 1000 ng/mL compared with EC survival in untreated control cultures (95 \pm 3%; data not shown). As shown in Figure 1A, EC survival was significantly reduced to 45 \pm 5% after exposure to anoxia alone compared with untreated control cultures (97 \pm 1%, *P*<0.01). In contrast, application of EPO of 10 ng/mL achieved maximal EC survival (86 \pm 3%), but concentrations lower than 0.1 ng/mL or higher than 10 ng/mL did not improve EC survival during anoxia.

EPO Is Necessary and Sufficient for EC Protection During Anoxia

Administration of EPO antibody in a series of concentrations of 0.01 to 2.00 μ g/mL did not significantly alter EC survival compared with untreated control cultures (data not shown). In the presence of anoxia, application of the EPO antibody (0.01 to 1.00 μ g/mL) also did not alter EC survival compared with cultures treated with anoxia alone (Figure 1B). In the presence of the EPO antibody, concentrations of EPO antibody of 0.10, 0.50, and 1.00 μ g/mL significantly decreased the protective capacity of EPO, yielding EC survival rates of

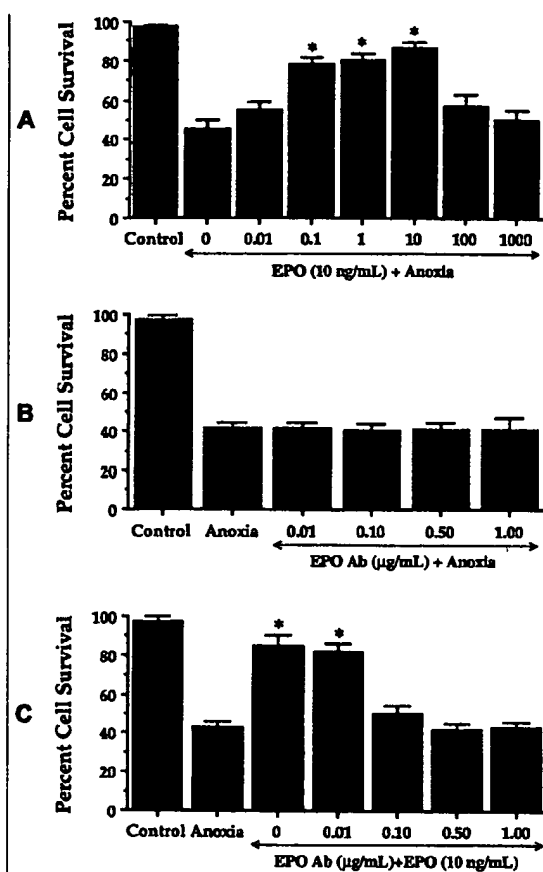


Figure 1. EPO is necessary and sufficient for EC protection during anoxia. **A**, ECs were pretreated with EPO (0.01 to 1000 ng/mL) 1 hour before exposure to anoxia, and cell survival was assessed 24 hours later (* $P < 0.01$ vs anoxia). **B**, EPO antibody (Ab; 0.01 to 1.00 $\mu\text{g/mL}$) was applied 1 hour before anoxia, and EC viability was not altered. **C**, Increasing concentrations of EPO Ab (0.01 to 1.00 $\mu\text{g/mL}$) were applied to ECs in conjunction with EPO (10 ng/mL) for 1 hour before anoxia (* $P < 0.01$ vs anoxia). In all cases, control indicates untreated ECs.

50 \pm 4% ($P < 0.01$), 42 \pm 3% ($P < 0.01$), and 43 \pm 5% ($P < 0.01$), respectively (Figure 1C).

EPO Prevents DNA Fragmentation in ECs During Anoxia

ECs were demonstrated to undergo apoptosis manifested by chromatin condensation and nuclear fragmentation 24 hours after anoxia (Figure 2A). In contrast, ECs pretreated with EPO (10 ng/mL) 1 hour before anoxia were without nuclear fragmentation. As shown in Figure 2a, anoxia resulted in a significant increase in percent DNA fragmentation (40 \pm 5%) compared with untreated control cultures (2 \pm 1%). DNA fragmentation was reduced to 12 \pm 2% in EC cultures during application of EPO over a 24-hour period.

EPO Maintains Membrane PS Asymmetry During Anoxia

In Figure 2B, exposure to anoxia resulted in the marked induction of membrane PS exposure that is present throughout the membrane of ECs. Administration of EPO (10 ng/mL)

1 hour before anoxia prevented the externalization of membrane PS residues in ECs. In Figure 2b, a significant increase in membrane PS residue exposure was observed in EC cultures at 24 hours after anoxia (56 \pm 5%) compared with untreated control cultures (3 \pm 2%). Application of EPO (10 ng/mL) 1 hour before anoxia significantly inhibited externalization of membrane PS residues to 11 \pm 3%.

EC Protection by EPO Is Dependent on Increased Activity of Akt1

Western blot assay was performed for p-Akt1 (the activated form of Akt1) 12 hours after anoxia. In Figure 3A, EPO and anoxia independently (as well as combined) significantly increased the expression of p-Akt1. This increased expression of p-Akt1 was blocked by the agents wortmannin (500 nmol/L) and LY294002 (25 $\mu\text{mol/L}$), which are inhibitors of Akt1 phosphorylation. In Figure 3B, application of EPO (10 ng/mL) 1 hour before anoxia significantly increased EC survival to 78 \pm 2%. Yet, coapplication of wortmannin (500 nmol/L) or LY294002 (25 $\mu\text{mol/L}$) at concentrations that block activation of p-Akt1 during anoxia (Figure 3A) with EPO (10 ng/mL) significantly reduced the ability of EPO to protect ECs against anoxia, which suggests that EPO required some level of Akt1 activation to offer protection.

EPO Modulates Mitochondrial Membrane Depolarization and Release of Cytochrome *c* During Anoxia

Compared with untreated control cultures, exposure to anoxia produced a significant decrease in the red/green fluorescence intensity ratio when the cationic membrane potential indicator JC-1 was used within 3 hours (Figures 4A and 4B), which suggests that anoxia results in mitochondrial membrane depolarization. Application of EPO (10 ng/mL) 1 hour before anoxia significantly increased the red/green fluorescence intensity of the ECs, which indicates that mitochondrial permeability transition pore membrane potential was restored to baseline (Figures 4A and 4B). Administration of EPO (10 ng/mL) 1 hour before anoxia maintained mitochondrial permeability transition pore membrane function and prevented mitochondrial cytochrome *c* release as demonstrated by Western blot analysis (Figure 4C).

EPO Decreases Caspase 8-, Caspase 1-, and Caspase 3-Like Activities During Anoxia

In Figure 5, EPO (10 ng/mL) was applied to the EC cultures 1 hour before anoxia, and data for caspase 8, caspase 1, and caspase 3 activities were obtained 12 hours after anoxia, because this time period represented the peak activities for these cysteine proteases.^{3,14} Administration of EPO significantly decreased caspase 8-like activity to 0.09 \pm 0.04 $\mu\text{mol} \cdot \text{min}^{-1} \cdot \text{g}^{-1}$ ($P < 0.01$; Figure 5A). Similarly, EPO pretreatment significantly reduced the activity of caspase 1-like activity (0.12 \pm 0.03 $\mu\text{mol} \cdot \text{min}^{-1} \cdot \text{g}^{-1}$) and caspase 3-like activity (0.19 \pm 0.07 $\mu\text{mol} \cdot \text{min}^{-1} \cdot \text{g}^{-1}$) compared with cultures treated with anoxia alone (0.42 \pm 0.08 and 0.48 \pm 0.07 $\mu\text{mol} \cdot \text{min}^{-1} \cdot \text{g}^{-1}$, respectively; Figures 5B and 5C).

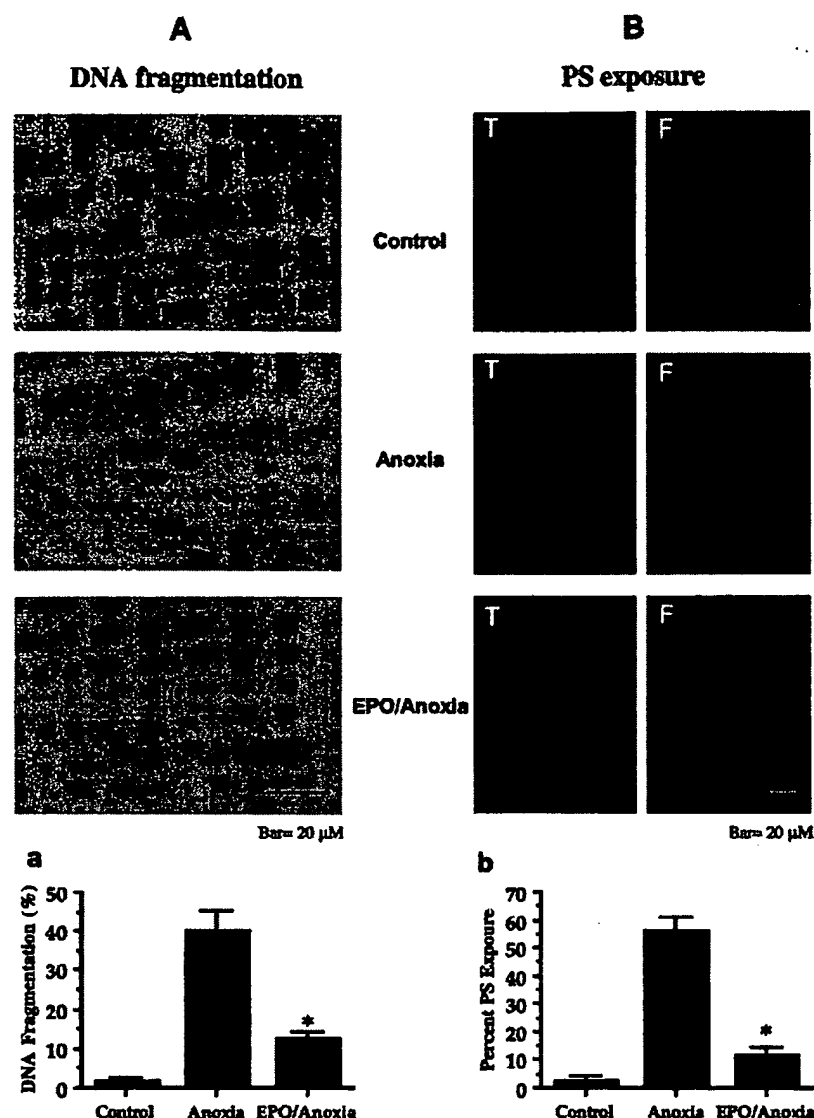


Figure 2. EPO prevents DNA fragmentation and externalization of membrane PS residues in ECs. **A**, ECs were exposed to anoxia, and DNA fragmentation was determined 24 hours later by TUNEL assay. **a**, Pretreatment with EPO (10 ng/mL) decreased DNA fragmentation significantly during anoxia exposure (* P <0.01 vs anoxia). **B**, ECs were labeled with annexin V phycoerythrin to visualize PS exposure 24 hours after anoxia and were imaged with transmitted (T) light and corresponding fluorescence (F) images of same microscopy field. **b**, Pretreatment with EPO (10 ng/mL) 1 hour before anoxia significantly prevented membrane PS externalization (* P <0.01 vs anoxia). In all cases, control indicates untreated ECs.

EPO Protects ECs From Injury Through Modulation of Caspase 8-, Caspase 1-, and Caspase 3-Like Activities

As shown in Figure 6A, pretreatment of ECs with 50 μ mol/L of IETD, YVAD, and DEVD to inhibit caspase 8-, caspase 1-, and caspase 3-like activities significantly increased EC survival to $\approx 83 \pm 3\%$, $80 \pm 4\%$, and $85 \pm 2\%$, respectively. In Figure 6B, coapplication of EPO with the caspase 8 inhibitor (IETD, 50 μ mol/L), caspase 1 inhibitor (YVAD, 50 μ mol/L), or caspase 3 inhibitor (DEVD, 50 μ mol/L) did not provide a synergistic level of protection against anoxic injury, which suggests that cytoprotection by EPO requires the modulation of caspase 8-, caspase 1-, and caspase 3-like activities.

Discussion

We identified several key characteristics of the cytoprotectant EPO that were critical for protection against EC injury and apoptosis. First, although administration of EPO was not toxic in relation to EC survival or programmed cell death,

protection with EPO was achieved only in a limited concentration range. Concentrations of EPO <0.1 ng/mL or >100 ng/mL did not enhance EC survival during anoxia. Similar to the present work, other studies also illustrated a tight therapeutic concentration range for EPO with corresponding extracellular concentrations of ≈ 10 ng/mL.¹⁵ Continuous infusion of EPO at 5 to 25 U/d for 7 days reduced infarct size in models of cerebral ischemia, but this protection was lost when administration of EPO was increased above 50 U/d.¹⁶ Second, administration of EPO is both necessary and sufficient to protect ECs from anoxia. In the presence of anoxia, application of the EPO antibody alone, which can bind to EPO and block its biological activity,¹⁷ did not alter EC survival. Yet, protection by EPO is prevented only with coapplication of the EPO antibody. These results illustrate that EPO provides necessary and sufficient protection against EC injury. Third, EPO maintains EC survival during anoxia through prevention of DNA fragmentation and maintenance of cellular membrane asymmetry. The present studies with

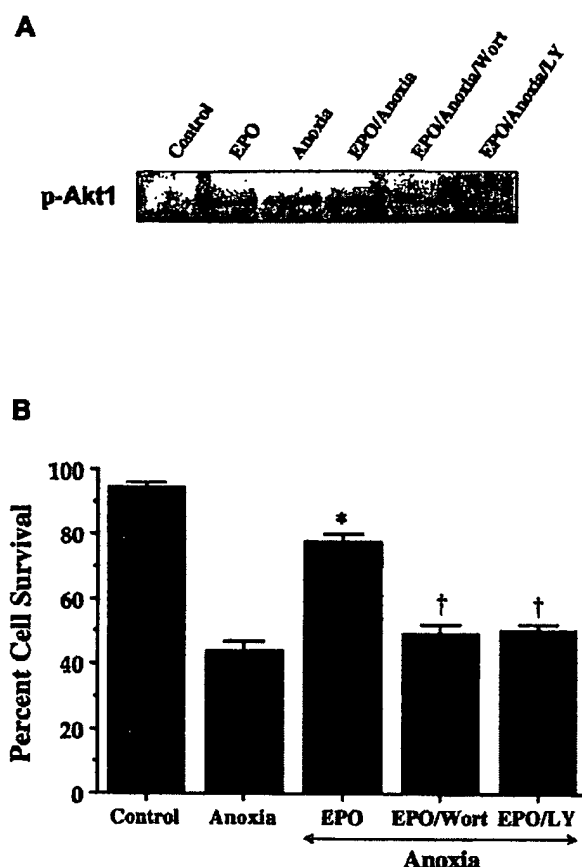


Figure 3. Cytoprotection by EPO in ECs is mediated in part by activation of Akt1. **A**, Equal amounts of EC protein extracts (50 μ g/lane) were immunoblotted with anti-p-Akt1 (active Akt1) antibody. Exposure to EPO (10 ng/mL) or anoxia significantly increased p-Akt1 expression. Application of Akt1 phosphorylation inhibitor wortmannin (Wort; 500 nmol/L) or LY294002 (LY; 25 μ mol/L) was sufficient to block expression of active p-Akt1 in presence of EPO during anoxia. **B**, At concentration that blocks activation of p-Akt1 during anoxia, wortmannin (Wort; 500 nmol/L) or LY294002 (LY; 25 μ mol/L) applied 1 hour before anoxia significantly reduced protective capacity of EPO (10 ng/mL) during anoxia (* P <0.01 vs anoxia; † P <0.01 vs EPO). In all cases, control indicates untreated ECs.

EPO complement prior work that illustrates a separate biological role for DNA degradation that is distinct from the inversion of membrane PS residues.^{6,12} Intact cellular function is afforded by EPO through the maintenance of genomic DNA in ECs. Long-term protection results through the inhibition of membrane PS residue exposure, because PS externalization marks cells for phagocytic elimination,⁶ leads to the propagation of a procoagulant surface,^{7,8} and can promote cellular inflammation.⁸

Several cellular signal transduction pathways may mediate the protection of EPO. EPO can increase the activity of Akt1, and inhibition of Akt1 activation can impair the protective capacity of EPO, which suggests that EPO is dependent on the activation of Akt1 for its cellular protection in ECs. Interestingly, blockade of Akt1 activation can account only partially for the loss of protection by EPO in ECs during

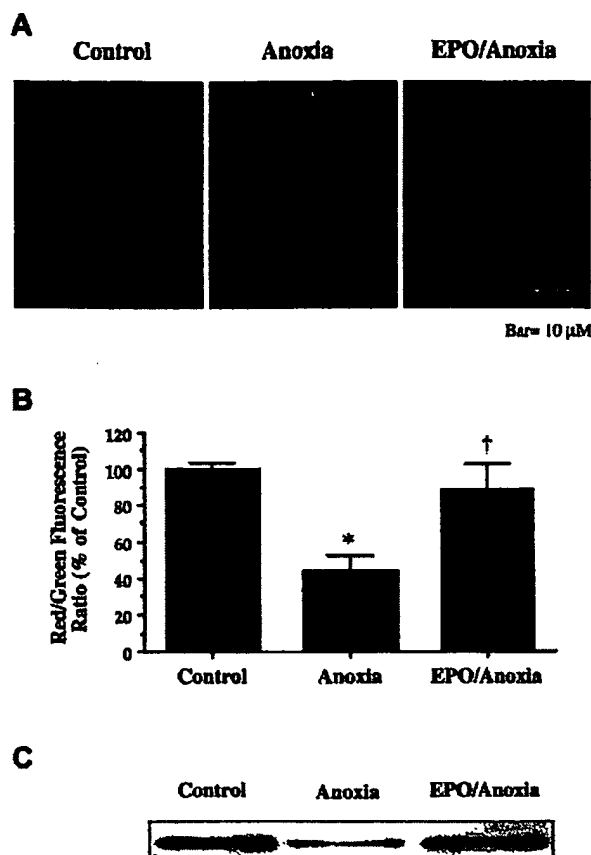


Figure 4. EPO prevents mitochondrial membrane depolarization and cytochrome c release. **A**, EPO (10 ng/mL) was applied directly to ECs 1 hour before anoxia, and mitochondrial staining with membrane potential indicator (JC-1, 2 μ g/mL, 30 minutes) was performed 3 hours later. Application of EPO (10 ng/mL) prevented mitochondrial depolarization. **B**, Relative ratio of red/green fluorescent intensity of mitochondrial staining was measured in 4 independent experiments with analysis performed with public domain NIH Image program (developed at National Institutes of Health and available on the Internet at <http://rsb.info.nih.gov/nih-image/>). * P ≤0.01 vs control; † P <0.01 vs anoxia. **C**, Representative Western blot with equal amounts of mitochondrial protein extracts (50 μ g/lane) were immunoblotted, which demonstrated that application of EPO (10 ng/mL) significantly prevented cytochrome c release from mitochondria during anoxia. In all cases, control indicates untreated ECs.

anoxic injury. The present work suggests that alternate cellular pathways are responsible for the mediation of EC protection by EPO. One particular pathway that is closely associated with Akt1 activation is the modulation of mitochondrial membrane potential.¹⁰ Mitochondrial mediated apoptosis can result in the cytoplasmic release of cytochrome c.¹⁸ In the present studies, we demonstrate that anoxia leads to depolarization of the mitochondrial membrane, with subsequent release of cytochrome c. Consistent with earlier clinical studies that demonstrate preserved mitochondrial function as a result of EPO administration,¹⁹ the present studies illustrate that EPO directly maintains mitochondrial membrane potential and prevents the release of cytochrome c.

In response to mitochondrial membrane depolarization and cytochrome c release, induction of caspase activation occurs.

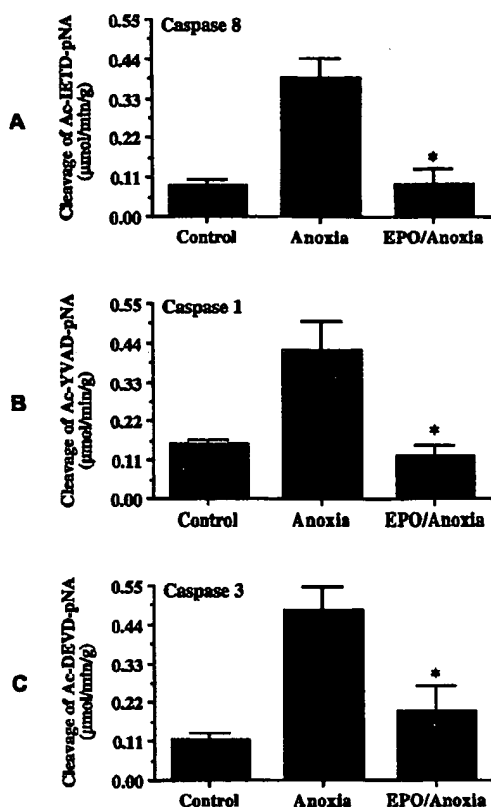


Figure 5. EPO prevents increase in caspase 8-, caspase 1-, and caspase 3-like activities after anoxia. ECs were exposed to anoxia, and caspase 8- (A), caspase 1- (B), and caspase 3- (C)-like activities were assessed 12 hours later through their respective colorimetric substrates. Pretreatment with EPO (10 ng/mL) 1 hour before anoxia significantly inhibited increase in activity of caspase 8 (A), caspase 1 (B), and caspase 3 (C) induced by anoxia (* $P < 0.01$ vs anoxia). In all cases, control indicates untreated ECs.

Anoxia can directly stimulate caspase 1- and caspase 3-like activities after mitochondrial release of cytochrome *c* to precipitate DNA fragmentation and membrane PS exposure.^{14,20} Caspase 8 serves as the upstream initiator of executioner caspases, such as caspase 1 and caspase 3, and also leads to the release of cytochrome *c*.²¹ Previous studies suggested that prevention of apoptosis in erythroid progenitor cells may be associated with modulation of caspase activity by EPO.²² The present work demonstrates that EPO prevents the induction of caspase 8-, caspase 1-, and caspase 3-like activities during anoxia. In addition, experiments that examined the combined application of cysteine protease inhibitors with EPO during anoxia demonstrated no synergistic increase in EC survival, which suggests that EPO directly inhibits caspase 8-, caspase 1-, and caspase 3-like activities to provide EC protection. The ability of EPO to prevent cysteine protease activity appears to occur at the level of downstream cellular pathways, such as through the prevention of mitochondrial membrane depolarization and the release of cytochrome *c*.

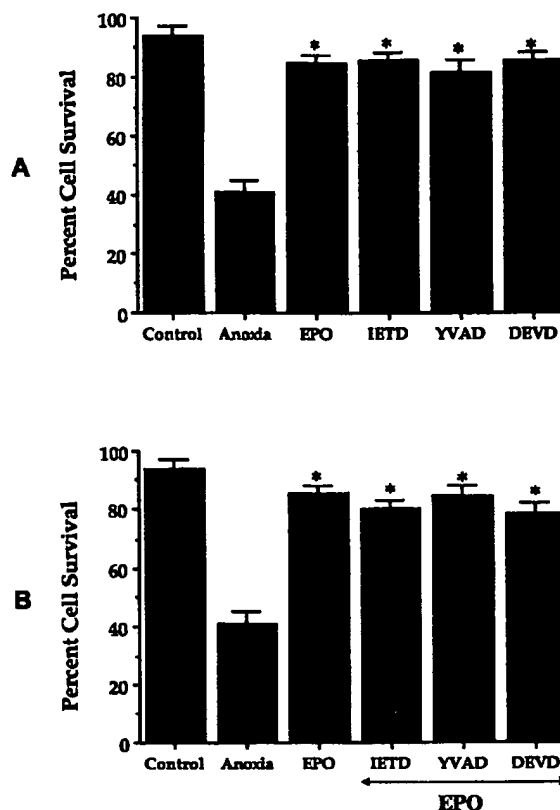


Figure 6. EPO protects ECs from injury through modulation of caspase 8-, caspase 1-, and caspase 3-like activities. A, ECs were pretreated with caspase 8 inhibitor (IETD, 50 μ M/L), caspase 1 inhibitor (YVAD, 50 μ M/L), or caspase 3 inhibitor (DEVD, 50 μ M/L) 1 hour before anoxia, and survival was determined 24 hours after anoxia (* $P < 0.01$ vs anoxia). B, ECs were pretreated with EPO (10 ng/mL) alone or in combination with IETD (50 μ M/L), YVAD (50 μ M/L), or DEVD (50 μ M/L). No enhanced or synergistic protection was observed during application of each caspase inhibitor combined with EPO compared with cultures exposed to EPO and anoxia alone. In all cases, control indicates untreated ECs.

Acknowledgments

This research was supported by the following grants (to Dr Maiese): American Heart Association (national office), Janssen Neuroscience Award, Johnson and Johnson Focused Investigator Award, LEARN Foundation Award, MI Life Sciences Challenge Award, and NIH NIEHS (P30 ES06639).

References

- Chong ZZ, Kang JQ, Maiese K. Hematopoietic factor erythropoietin fosters neuroprotection through novel signal transduction cascades. *J Cereb Blood Flow Metab*. 2002;22:503–514.
- Bernaudo M, Bellail A, Marti HH, et al. Neurons and astrocytes express EPO mRNA: oxygen-sensing mechanisms that involve the redox-state of the brain. *Glia*. 2000;30:271–278.
- Zhang J, Tan Z, Tran ND. Chemical hypoxia-ischemia induces apoptosis in cerebrovascular endothelial cells. *Brain Res*. 2000;877:134–140.
- de la Monte SM, Neely TR, Cannon J, et al. Oxidative stress and hypoxia-like injury cause Alzheimer-type molecular abnormalities in central nervous system neurons. *Cell Mol Life Sci*. 2000;57:1471–1481.
- Lin SH, Vincent A, Shaw T, et al. Prevention of nitric oxide-induced neuronal injury through the modulation of independent pathways of programmed cell death. *J Cereb Blood Flow Metab*. 2000;20:1380–1391.

6. Maiese K, Vincent AM. Membrane asymmetry and DNA degradation: functionally distinct determinants of neuronal programmed cell death. *J Neurosci Res*. 2000;59:568–580.
7. Bombeli T, Karsan A, Tait JP, et al. Apoptotic vascular endothelial cells become procoagulant. *Blood*. 1997;89:2429–2442.
8. Dombroski D, Balasubramanian K, Schroit AJ. Phosphatidylserine expression on cell surfaces promotes antibody-dependent aggregation and thrombosis in beta2-glycoprotein I-immune mice. *J Autoimmun*. 2000;14:221–229.
9. Uddin S, Kottegoda S, Stigger D, et al. Activation of the Akt/FKHRL1 pathway mediates the antiapoptotic effects of erythropoietin in primary human erythroid progenitors. *Biochem Biophys Res Commun*. 2000;275:16–19.
10. Kennedy SG, Kandel ES, Cross TK, et al. Akt/protein kinase B inhibits cell death by preventing the release of cytochrome c from mitochondria. *Mol Cell Biol*. 1999;19:5800–5810.
11. Mitra D, Kim J, MacLow C, et al. Role of caspases 1 and 3 and Bcl-2-related molecules in endothelial cell apoptosis associated with thrombotic microangiopathies. *Am J Hematol*. 1998;59:279–287.
12. Chong ZZ, Lin SH, Maiese K. Nicotinamide modulates mitochondrial membrane potential and cysteine protease activity during cerebral vascular endothelial cell injury. *J Vasc Res*. 2002;39:131–147.
13. Antonov AS, Nikolaeva MA, Klueva TS, et al. Primary culture of endothelial cells from atherosclerotic human aorta, part 1: identification, morphological and ultrastructural characteristics of two endothelial cell subpopulations. *Atherosclerosis*. 1986;59:1–19.
14. Lin SH, Maiese K. The metabotropic glutamate receptor system protects against ischemic free radical programmed cell death in rat brain endothelial cells. *J Cereb Blood Flow Metab*. 2001;21:262–275.
15. Alafaci C, Salpietro F, Grasso G, et al. Effect of recombinant human erythropoietin on cerebral ischemia following experimental subarachnoid hemorrhage. *Eur J Pharmacol*. 2000;406:219–225.
16. Sakanaka M, Wen TC, Matsuda S, et al. In vivo evidence that erythropoietin protects neurons from ischemic damage. *Proc Natl Acad Sci U S A*. 1998;95:4635–4640.
17. Koshimura K, Murakami Y, Sohmiya M, et al. Effects of erythropoietin on neuronal activity. *J Neurochem*. 1999;72:2565–2572.
18. Harfouche R, Hassessian HM, Guo Y, et al. Mechanisms which mediate the antiapoptotic effects of angiopoietin-1 on endothelial cells. *Microvasc Res*. 2002;64:135–147.
19. Miro O, Marrades RM, Roca J, et al. Skeletal muscle mitochondrial function is preserved in young patients with chronic renal failure. *Am J Kidney Dis*. 2002;39:1025–1031.
20. Matsushita H, Morishita R, Nata T, et al. Hypoxia-induced endothelial apoptosis through nuclear factor-kappaB (NF-kappaB)-mediated bcl-2 suppression: in vivo evidence of the importance of NF-kappaB in endothelial cell regulation. *Circ Res*. 2000;86:974–981.
21. Tang D, Lahti JM, Kidd VJ. Caspase-8 activation and bid cleavage contribute to MCF7 cellular execution in a caspase-3-dependent manner during staurosporine-mediated apoptosis. *J Biol Chem*. 2000;275:9303–9307.
22. Gregoli PA, Bondurant MC. Function of caspases in regulating apoptosis caused by erythropoietin deprivation in erythroid progenitors. *J Cell Physiol*. 1999;178:133–143.

An hereditary motor neurone disease with progressive denervation of muscle in the mouse: the mutant 'wobbler'

L. W. DUCHEN AND SABINA J. STRICH (With an Appendix by D. S. FALCONER)

*From the Department of Neuropathology, Institute of Psychiatry,
The Maudsley Hospital, London S.E.5, and the Institute of Animal Genetics, Edinburgh*

More than one hundred hereditary neurological diseases of mice are now on record (Grüneberg, 1952, 1956; Sidman, Green, and Appel, 1965). For many of these conditions only clinical descriptions and genetic data are available and few pathological investigations have been made. This paper describes the clinical and pathological studies of an hereditary disease in mice in which the primary abnormality appears to be located in the perikaryon of motor neurones. The disease arose as the result of a spontaneous mutation in the C57 BL/Fa strain of mice at the Institute of Animal Genetics, Edinburgh. The mutant, which was named 'wobbler' (Falconer, 1956) is transmitted by an autosomal recessive gene *wr* (see Appendix). The clinical and pathological characteristics of this mutant were briefly described in a preliminary communication (Duchen, Falconer, and Strich, 1966).

THE CLINICAL SYNDROME

These observations are based on a study of more than 50 affected animals aged from 19 days to more than one year. Mice which are heterozygous for the gene *wr* are clinically normal, but about 25% of their offspring may be expected to be homozygous 'wobblers' (*wr/wr*). The homozygous mice show no clinical abnormality during the first three weeks after birth, but by the fourth week they are smaller than their littermates and always remain so. They have a high-stepping, slightly unsteady gait and a fine tremor of the head. Over the next few weeks there is progressive unsteadiness associated with a wobbling type of gait with the head and front part of the trunk held lower than normally. Weakness of muscles becomes apparent by the fourth or fifth week and is most obvious in the forelimbs, the grip of the forepaws being particularly affected. From the fourth to about the twelfth week there is progressive weakness and wasting especially of the muscles of the

head, neck and forelimbs, while the hindlimbs are less affected. The unsteady wobbling gait becomes more obvious and the mouse becomes unable to extend the forepaws at the wrist, so that it ultimately walks on the dorsum of the paws (Fig. 1). In advanced stages of the disease the mouse has great difficulty in using the forelimbs for climbing (Fig. 2) or walking, and pushes itself along with the hindlimbs which are usually less severely affected. The facial muscles are atrophied, giving the snout a pointed appearance and the ears tend to lie back. As in other neurological diseases in mice, the hindlimbs become flexed and adducted instead of extended when the animal is lifted by the tail.

The course of the disease varies somewhat in different mice. Usually after a period of rapid deterioration up to the third or fourth month of age, the progress of the disease seems to slow down and it may even become 'burnt out'. Some affected mice have lived for more than a year in spite of muscle weakness and wasting. In other cases the disease causes more extensive and severe muscle weakness and is fatal by the third or fourth month. There is no clinical evidence of any abnormality in any of the sensory systems. It has proved impossible to breed from affected males or females.

MATERIAL AND METHODS

Histological studies were made of 40 clinically affected mice ranging in age from 5 weeks to 13 months. Unaffected littermates, some of which may have been heterozygous for the gene *wr*, and normal mice of other strains were used as controls. In order to determine whether there were histological changes before the onset of clinical abnormalities two entire litters, aged 19 and 22 days respectively, derived from known heterozygous parents, were examined. In each litter one mouse showed histological abnormalities.

The mice were killed with chloroform, the thoracic and abdominal cavities opened and the skin over the skull and



FIG. 1. A 'wobbler' mouse 10 weeks old. Note the abnormal posture. The animal cannot extend the forepaws. The face is thinner than that of a normal mouse.



FIG. 2. A 'wobbler' mouse 6 months old climbing on a vertical wire grid. The mouse does not grip with the forepaws but uses the forelimb like a hook. The ears do not stand up because of paralysis of the levator auris longus.

spinal column reflected. The mouse was then immersed in fixative which was either formol-alcohol (10% formalin in 60% alcohol) or formol-calcium (10% formalin with 1% calcium acetate). After fixation whole mice were decalcified in formic-citrate solution (65 parts 20% sodium citrate and 35 parts 90% formic acid) and blocks of tissue were embedded in paraffin wax or in gelatin for frozen sections. Paraffin sections were made of brain and brain-stem in sagittal or coronal planes and of the trunk and limbs in transverse or longitudinal planes. Much use was made of the 'serial block' method of Beesley and

Daniel (1956) in which consecutive transverse segments of tissue are embedded in one block of wax. With the use of this method the entire brain and spinal cord of several animals of different ages were examined in serial sections. Staining methods used on paraffin sections included haematoxylin and eosin, iron haematoxylin, and van Gieson's mixture; Mallory's phosphotungstic acid-haematoxylin; periodic acid-Schiff; Holzer's method for astrocytes; cresyl violet (Nissl's method) alone or combined with luxol-fast blue (Klüver and Barrera, 1953) to demonstrate myelin; Gallyas's method (1963) for microglia; and Palmgren's (1948) silver method for nerve fibres. Frozen sections of central and peripheral nervous systems were stained for fat with oil-red-O, and nerve fibres were demonstrated in thick (60 μ) serial sections of whole limbs by Schofield's (1960) method.

HISTOLOGICAL OBSERVATIONS

The most characteristic abnormality found in all the affected mice was a degeneration of nerve cells of the motor system in the brain-stem and spinal cord, but not in basal ganglia or cerebral cortex. There was progressive denervation of skeletal muscle.

In all animals examined, motor nerve cells in various stages of degeneration were seen side by side with normal-looking cells (Fig. 3). In what appeared to be an early stage, the nerve cell was enlarged, sometimes became rounded, and the Nissl substance of the perikaryon stained poorly (Fig. 4). The nucleus with its prominent nucleolus was central in position as in the normal cell. At a later stage in the degeneration the cell body was filled or partially filled with vacuoles which appeared empty with all the stains used. In some cells the nucleus was eccentric in position (Fig. 3). In the last stages of degeneration the nerve cells were almost unrecognizable. In these cells the nucleus was surrounded by an ill-defined mass of vacuoles (Fig. 5). No glial or microglial reaction was observed around any of the abnormal cells, nor were glial nodules found in the later stages of the disease. Cells in all stages of degeneration could usually be found in the same animal. Nerve cells showing these changes have never been found in any clinically normal littermates of 'wobbler' mice, nor in mice of any of the other strains which have been studied in this laboratory.

The early changes in skeletal muscle consisted of enlargement of sarcolemmal nuclei and their migration to the centre of the muscle fibre (Fig. 6). Later there was a decrease in the diameter of muscle fibres, first singly, then in groups and eventually involving whole bundles (Fig. 7). This was followed by the appearance of fat between atrophied fibres (Fig. 8).

The pattern of motor innervation of skeletal muscles became abnormal. In the early stages there was sprouting from preterminal axons, and single

nerve fibres innervated several muscle fibres (Figs. 9 and 10). (In the mouse, as in other mammals, each preterminal nerve fibre normally supplies one muscle fibre.) In later stages there was a marked reduction in the number of motor nerve fibres in the affected muscles. These changes in muscle and nerve fibres are characteristic of progressive motor denervation.

No abnormalities were found in the sensory innervation of structures such as skin, mucosae, teeth, or Pacinian corpuscles. Muscle spindles appeared normal and had normal spiral endings in young 'wobblers'. In old animals some muscle spindles were atrophied and had thickened capsules, but only in regions where denervation atrophy of extrafusal fibres was very severe. The innervation of the muscle spindles was not studied in detail.

PRECLINICAL STAGE In the 19- and 22-day-old mice many abnormal nerve cells were found in the brain-stem, in the ventral magnocellular reticular nucleus (Fig. 3), and in the motor nuclei of cranial nerves V and VII. A few abnormal cells were found in the red

nucleus, substantia nigra, anterior and posterior colliculi, and in the deep cerebellar nuclei. No abnormalities were seen in the cerebral cortex. In the spinal cord many abnormal cells were present in the ventral horns of the cervical region, but fewer in thoracic and lumbar levels.

In paraffin sections of skeletal muscle a few fibres with centrally placed nuclei were seen but no atrophied fibres were present. In the frozen silver-impregnated sections of the limb muscles, however, abnormalities were present in the nerve fibres. Fragmented axons were seen in some intramuscular nerve trunks and some motor fibres ended in bizarre club-shaped swellings instead of the fine terminal arborization normally seen. Many preterminal axons showed fine sprouting and innervated more than one muscle fibre.

YOUNG 'WOBBLER' MICE In these mice clinical abnormalities were clearly present. Nerve cells in various stages of degeneration were present in the brain-stem and spinal cord. They appeared to be more numerous in the ventral horn of cervical spinal cord than in brain-stem or thoracic and lumbar cord, though cell counts were not done. Silver impregna-

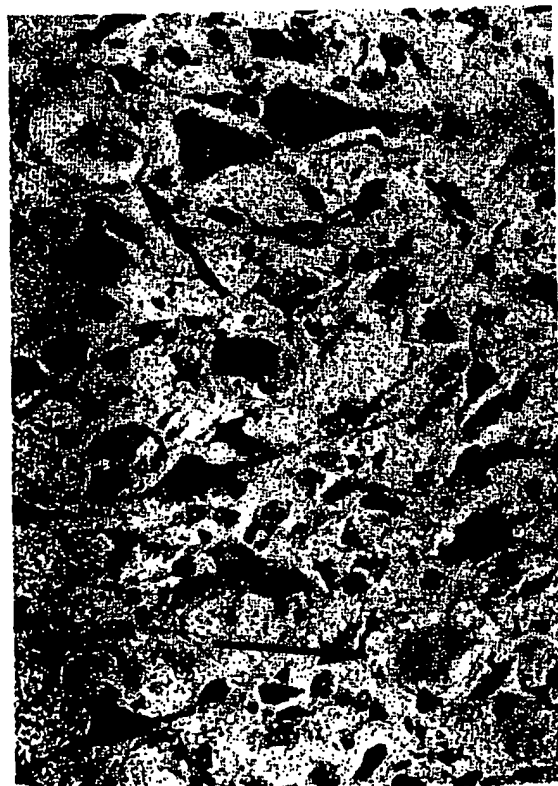


FIG. 3. Swollen and vacuolated nerve cells (arrows) in the magnocellular reticular nucleus of the medulla of a 19-day-old mouse killed before the onset of clinical signs. (Cresyl violet, $\times 250$.)

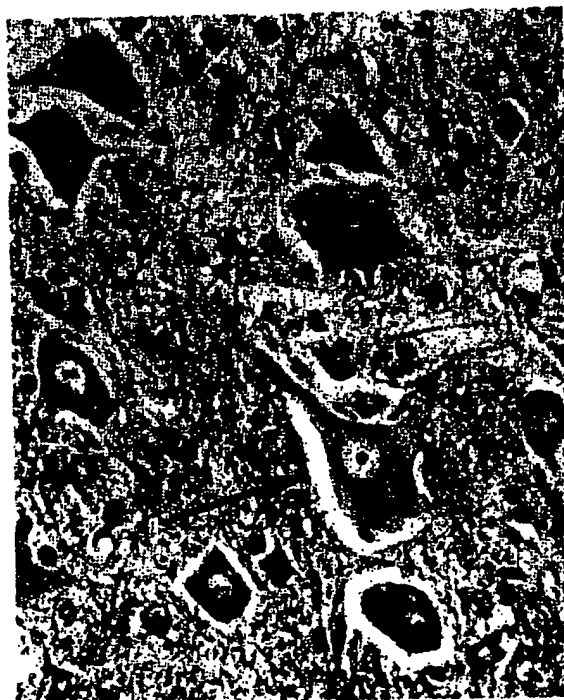


FIG. 4. Ventral horn cells of the cervical spinal cord of a 'wobbler' mouse 8 weeks old. One cell (arrow) shows early degenerative change. It is enlarged and has no stainable Nissl bodies. (Luxol-fast-blue/cresyl violet, $\times 400$.)

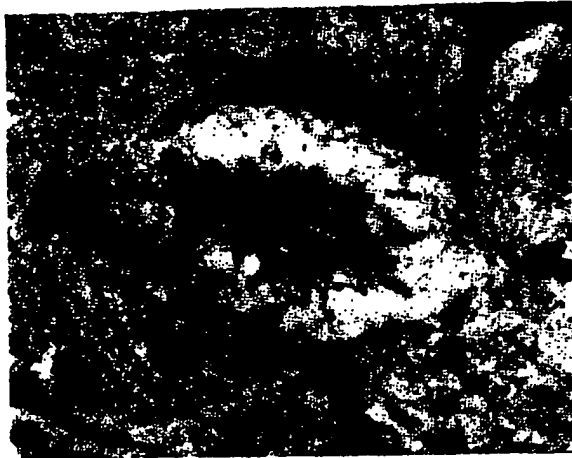


FIG. 5. Ventral horn cell in an advanced state of degeneration. The nucleus is surrounded by a mass of vacuoles. (Luxol-fast-blue/cresyl violet, $\times 800$.)

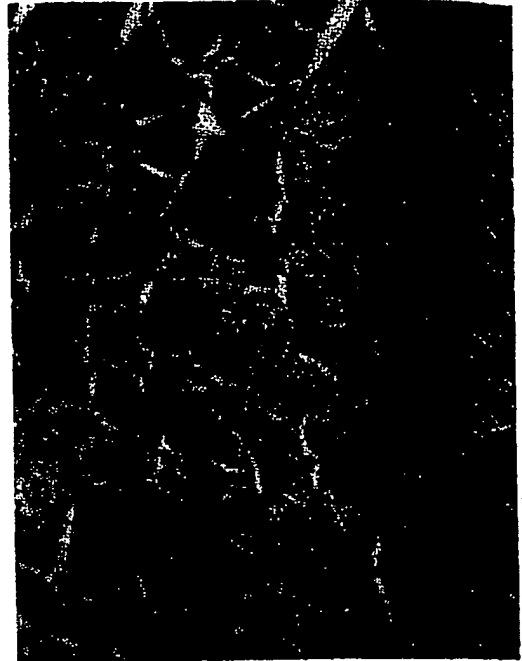


FIG. 6. Foreleg muscle of a 'wobbler' mouse 36 days old. Early denervation changes are present. Many muscle fibres (arrows to two) have centrally-placed nuclei and are smaller than normal. (H and E, $\times 400$.)

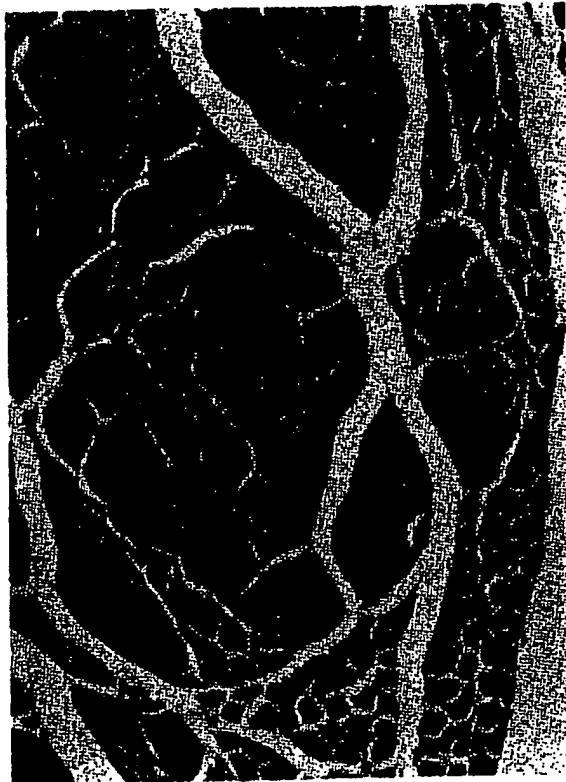


FIG. 7. Facial muscles of a 5-month-old 'wobbler' mouse. There is atrophy of some fascicles whilst others are normal, a pattern typical of partial motor denervation. (H and E, $\times 400$.)



FIG. 8. Forelimb muscle showing advanced denervation atrophy. There is fat between severely atrophied muscle fibres. A bundle of normal-sized fibres is present. (H and E, $\times 400$.)

tion of frozen sections of limb muscles now showed marked collateral sprouting of axons and many of the fine nerve fibres were beaded. The preterminal axons innervated several muscle fibres and some nerve endings were small and unbranched. The nerve sprouting occurred mainly from the myelinated part of the axon and not from the terminal arborization. Abnormalities in skeletal muscle fibres were now readily seen. Sarcolemmal nuclei were enlarged with prominent nucleoli and many muscle fibres contained centrally placed nuclei (Fig. 6). Atrophied muscle fibres were first seen in 6-7-week-old mice—that is, two weeks after the onset of clinical weakness—and were situated at the periphery of the muscle bundles. Later there was atrophy of groups of muscle fibres (Fig. 7). These denervation changes were found in muscles of the head, neck, shoulder girdle, and forelimb more than in the hindlimb.



FIG. 9. Silver impregnation of muscle of a 4-month-old 'wobbler'. A single preterminal axon (arrow) branches repeatedly and innervates several muscle fibres. (Schofield, $\times 265$.)

OLDER 'WOBBLER' MICE Degenerating nerve cells were seen and were still most numerous in cervical spinal cord. Grey and white matter of the spinal cord was smaller than in littermate controls, but the size of the spinal cord was not obviously out of proportion to the size of the animal. The pyramidal tracts appeared normal. In the ventral horn there seemed to be a reduction in the number of motor nerve cells. No astrocytic gliosis or microglial proliferation was seen in the spinal cord. The ventral roots were not fibrosed.

The skeletal muscles which were affected became more atrophied. Muscle fibres became progressively smaller in diameter and some muscles were largely replaced by fat. No muscle fibre necrosis and no 'target' fibres were seen at any stage of the disease. Studies of the innervation of the severely atrophied muscles showed a marked reduction in the number of motor nerve fibres, while many of the axons which were present showed collateral sprouting (Figs. 9 and 10). Thin beaded nerve fibres apparently ending in fatty tissue and not on muscle fibres were present. In mice which survived for more than a year occasional degenerating nerve cells were present in the ventral horns of the spinal cord. Evidence of early denervation was usually present in some muscles while in others the atrophy was advanced.

DISTRIBUTION OF DENERVATION ATROPHY The distribution of the skeletal muscles which showed denervation atrophy was remarkably similar in all the animals studied. Not every muscle was affected, but those which did show atrophy were affected on both sides of the body. For example, of the facial muscles, the platysma—innervated by the VIIth cranial nerve—was always severely and symmetrically affected while the masseters—innervated by the Vth cranial nerve—were at least partially preserved even in the longest survivors. The muscles



FIG. 10. Silver impregnation of muscle of a 'wobbler' showing one long nerve fibre with many sprouts. This is characteristic of partial motor denervation. (Schofield, $\times 340$.)

of the neck and shoulder region were severely affected, while the forelimbs showed more severe atrophy proximally than distally. Trunk muscles and diaphragm were relatively spared and hindlimb muscles were less involved than those of the forelimb. In the hindlimb, proximal muscles were more atrophied than distal ones, and in some animals the only muscles below the knee to show denervation atrophy were the gastrocnemii.

DISCUSSION

The abnormalities which have been observed in the brain-stem and spinal cord of the 'wobbler' mouse indicate that this disease primarily affects motor nerve cells. The first abnormality seen in the motor neurones was swelling of the cell body and disappearance of Nissl substance. Later the cytoplasm became vacuolated. Andrews and Maxwell (1967) have studied the ventral horn cells of the 'wobbler' mouse with the electron microscope and observed that the perikaryon was filled with many small vesicles in some cells, while in other nerve cells the vesicles were large and almost replaced the cell. These abnormalities can be correlated well with the light microscopic changes described in the nerve cells in the present paper. The pathological findings suggest a primary degeneration of the nerve cell body and are not like the changes in the perikaryon secondary to axonal degeneration. It has been shown (Torvik and Heding, 1967) that the reaction to axonal injury in motor nerve cells of the nucleus of the facial nerve in the mouse is characterized by increased basophilia of the perikaryon and reduction in size of Nissl granules.

In the skeletal muscles the atrophy of muscle fibres occurred in groups and fascicles, a pattern characteristic of motor denervation. Sprouting and branching of preterminal motor nerve fibres, of the pattern seen in the skeletal muscles of these mice, are like those described as a response to partial motor denervation (Tello, 1907; Edds, 1950; Wohlfart and Hoffman, 1956). No necrosis of muscle fibres was seen at any stage of the disease and there was no evidence to suggest that this disease process primarily affects muscle fibres. The rapid accumulation of fat in the atrophied muscles of the 'wobbler' mouse is also seen in other forms of motor denervation in the mouse (atrophy after local injection of botulinum toxin: Duchen and Strich, 1968; atrophy after nerve section: authors' unpublished observations).

Nerve cell degeneration was seen in 3-week-old mice killed before the onset of detectable muscle weakness. In these animals there was already abundant sprouting from intramuscular axons. Clinical muscle weakness was detectable at about 4 weeks of

age and atrophy of muscle fibres was first seen at 6 weeks. It seems likely, therefore, that re-innervation by collateral sprouting of intramuscular nerve fibres was able to compensate for the loss of motor neurones for some weeks.

In all the mice studied histologically the distribution of atrophied skeletal muscles was very similar. Some muscles were always relatively spared. The manner in which an hereditary defect can affect some nerve cells but spare others of the same system is not clear. A relatively constant distribution of muscle weakness is also found in some hereditary neuromuscular diseases in man, such as peroneal muscular atrophy, the juvenile form of muscular atrophy (Kugelberg and Welander, 1956) and in muscular dystrophies. In the infantile form of motor neurone disease (Werdnig-Hoffmann disease) weakness is first seen in the trunk muscles, but in the fully developed disease abnormal motor nerve cells are seen throughout brain-stem and spinal cord (Conel, 1938, 1940).

Sporadic or inherited cases of spinal motor neurone degeneration have occasionally been described in various animals (Innes and Saunders, 1962). The 'wobbler' mouse provides an example of an hereditary disease of motor nerve cells in a small laboratory animal. Although the underlying causes of the disease may differ from those in human diseases this mutant is a useful model for the study of many aspects of neuromuscular disorders.

SUMMARY

The clinical and pathological findings in an hereditary neuromuscular disorder in mice are described. This disease, known as 'wobbler', arose by spontaneous mutation and is transmitted by a single autosomal recessive gene *wr*. The condition is characterized by progressive muscular weakness and wasting. Degenerating motor nerve cells were found in the brain-stem and spinal cord and there was progressive motor denervation of skeletal muscle. The pathological findings indicate that in this hereditary disease there is a primary abnormality in the perikaryon of motor nerve cells.

We should like to thank Mr. A. R. Salliss, Mr. A. J. Davey, and Mr. I. J. Stiff for the technical work, and Mr. P. M. Taylor for the photographs. This work was supported by grants from the Research Fund of the Bethlem Royal and Maudsley Hospitals and from the Muscular Dystrophy Associations of America, Inc.

REFERENCES

- Andrews, J. M., and Maxwell, D. S. (1967). Ultrastructural features of anterior horn cell degeneration in the wobbler (*wr*) mouse. *Anat. Rec.*, 157, 206.
- Beasley, R. A., and Daniel, P. M. (1956). A simple method for preparing serial blocks of tissue. *J. clin. Path.*, 9, 267-268.

- Coel, J. L. (1938). Distribution of affected nerve cells in a case of amyotonia congenita. *Arch. Neurol. Psychiat. (Chic.)*, 40, 337-351.
- (1940). Distribution of affected nerve cells in amyotonia congenita (second case). *Arch. Path.*, 30, 153-164.
- Duchen, L. W., Falconer, D. S., and Strich, S. J. (1966). Hereditary progressive neurogenic muscular atrophy in the mouse. *J. Physiol. (Lond.)*, 183, 53-55P.
- , and Strich, S. J. (1968). The effects of botulinum toxin on the pattern of innervation of skeletal muscle in the mouse. *Quart. J. exp. Physiol.*, 53, 84-89.
- Edds, M. V. Jr. (1950). Collateral regeneration of residual motor axons in partially denervated muscles. *J. exp. Zool.*, 113, 317-352.
- Falconer, D. S. (1956). *Mouse News Lett.*, 15, 23.
- Gallyas, F. (1963). Silver impregnation method for microglia. *Acta Neuropath.*, 3, 206-209.
- Grüneberg, H. (1952). *The Genetics of the Mouse*, 2nd ed., Martinus Nijhoff, The Hague.
- (1956). *An Annotated Catalogue of the Mutant Genes of the House Mouse*. (M.R.C. Mem. No. 33.) H.M.S.O., London.
- Jones, J. R. M., and Saunders, L. Z. (1962). *Comparative Neuropathology*. Academic Press, New York.
- Klüver, H., and Barrera, E. (1953). A method for the combined staining of cells and fibers in the nervous system. *J. Neuropath. exp. Neurol.*, 12, 400-403.
- Kugelberg, E., and Welander, L. (1956). Heredofamilial juvenile muscular atrophy simulating muscular dystrophy. *Arch. Neurol. Psychiat. (Chic.)*, 75, 300-309.
- Palmgren, A. (1948). A rapid method for selective silver staining of nerve fibres and nerve endings in mounted paraffin sections. *Acta zool. (Stockh.)*, 29, 377-392.
- Schofield, G. C. (1960). Experimental studies on the innervation of the mucous membrane of the gut. *Brain*, 83, 490-514.
- Sidman, R. L., Green, M. C., and Appel, S. H. (1965). *Catalog of the Neurological Mutants of the Mouse*, Harvard Univ. Press, Cambridge, Mass.
- Tello, F. (1907). Dégénération et régénération des plaques motrices après la section des nerfs. *Trab. Lab. Invest. Biol. (Madrid)*, 5, 117-149.
- Torvik, A., and Hedning, Anna. (1967). Histological studies on the effect of Actinomycin D on retrograde nerve cell reaction in the facial nucleus of mice. *Acta Neuropath.*, 9, 146-157.
- Wohlfart, G., and Hoffman, H. (1956). Reinnervation of muscle fibers in partially denervated muscles in Theiler's encephalomyelitis of mice (mouse poliomyelitis). *Acta psychiat. scand.*, 31, 345-365.

APPENDIX

D. S. Falconer

The gene wobbler (*wr*) arose by spontaneous mutation in the C57BL/Fa inbred strain, and was first detected in the progeny of one pair in 1955. It was maintained on the C57BL background for eight years, awaiting possible investigation. In order to facilitate the maintenance it was transferred to a non-inbred background in 1963.

Two proved heterozygotes when outcrossed produced a total of 21 female and 14 male offspring, all of which were normal. This proved the gene to be recessive. The segregation from proved heterozygous pairs is given in the Table. On the C57BL background there was a significant deficiency of *wr/wr* homozygotes, when tested against the expectation of 25%. The deficiency was greater in females than males, though not significantly so. The non-inbred matings showed a smaller and non-significant deficiency which, in this case, was less in females than in males. The two types of mating are, however, not significantly heterogeneous with respect to the

ratios obtained, even when only the females are compared. Thus, there were undoubtedly fewer than the expected number of classified homozygotes in the C57BL families and possibly also in the non-inbred families.

The cause of the deficiency of *wr/wr* homozygotes was not identified. It seems unlikely to have been due to differential mortality between birth and classification, because the proportion of offspring that died—given also in the Table—was not higher where the deficiency was greater. Since classification cannot be made with certainty until a week or more after the mice are weaned at about 3 weeks of age, there was a possibility that some litters might have been prematurely discarded with some individuals erroneously classified as normal. This, however, does not seem to be the explanation because the deficiency was equally evident in litters that had been classified at two months or more. In the absence of identified postnatal causes, the deficiency must presumably be

TABLE
PHENOTYPES OF OFFSPRING FROM +*wr* × +*wr* MATINGS

	Matings (no.)	Sex	<i>wr</i>	+	Total	% <i>wr</i>	Dead before classification (no.) (%)
Inbred	28	Females	45	234	279	16.1	16 (5.4)
		Males	67	264	331	20.2	24 (6.8)
		Unknown	—	—	—	—	6 —
		Total	112	498	610	18.2	46 (7.5)
Outbred	9	Females	22	73	95	23.2	10 (9.5)
		Males	26	97	123	21.1	8 (6.1)
		Unknown	—	—	—	—	5 —
		Total	48	170	218	22.0	23 (10.1)

+ *wr* = heterozygotes; *wr* = 'wobbler' mice; + = non 'wobbler' mice.

ascribed to increased prenatal mortality. In this case the differential mortality of homozygotes in the C57BL families was 32%.

If this greatly increased prenatal mortality is real, it will have an interesting bearing on the search for the primary genetic lesion. The clinical signs of disease do not appear until 3 weeks after birth, but

even if the motor neurone degeneration started before birth, it is hard to believe that this would seriously reduce the viability of embryos. The primary genetic lesion may, therefore, be a more generalized metabolic defect of which the nerve cell degeneration is a later consequence.

Carbamylated Erythropoietin Reduces Radiosurgically-Induced Brain Injury

Serhat Erbayraktar,¹ Nihal de Lanerolle,² Alain de Lotbinière,² Jonathan PS Knisely,³ Zubeyde Erbayraktar,¹ Osman Yilmaz,¹ Anthony Cerami,⁴ Thomas R Coleman,⁴ and Michael Brines^{4†}

¹Dokuz Eylül School of Medicine, Izmir, Turkey; ²Neurosurgery and ³Therapeutic Radiology, Yale School of Medicine, New Haven, CT, USA; ⁴The Kenneth S. Warren Institute and Warren Pharmaceuticals, Ossining, NY, USA

Gamma knife radiosurgery is an attractive noninvasive treatment of brain tumors and vascular malformations that minimizes collateral tissue damage. However, exposure of normal tissue to even low-dose radiation triggers a cascade of acute and chronic injury and potentially significant morbidity and mortality. Because many irradiated patients now survive for years, identifying methods to prevent radiotherapy-induced collateral tissue damage is a major focus of current research. Erythropoietin (EPO), a cytokine produced locally by many tissues in response to injury, antagonizes apoptosis, reduces inflammation, and promotes healing. Systemic administration of recombinant EPO, widely used for treatment of anemia, provides robust protection from numerous insults in a variety of tissues, including the brain. Although irradiation injury is likely sensitive to EPO, the hematopoietic activity of EPO is undesirable in this setting, increasing erythrocyte number and predisposing to thrombosis. To avoid these potential adverse effects, we developed carbamylated EPO (CEPO) which does not stimulate the bone marrow. In this study, we show that CEPO (50 $\mu\text{g kg}^{-1}$ intraperitoneally) improves functional outcome when administered to adult rats just before, and then once daily for 10 d after, a necrotizing dose of radiation (100 Gy) to the right striatum. Immediately following irradiation, use and reflex movements of the contralateral forelimb to vibrissae stimulation were abnormal but rapidly improved in animals receiving CEPO. Moreover, histological examination revealed that the extent of brain necrosis after 90 days was reduced by ~ 50%. These findings further extend the kinds of injury for which administration of a tissue-protective cytokine provides benefit.

Online address: <http://www.molmed.org>

doi: 10.2119/2006-00042.Erbayraktar

INTRODUCTION

Historically, radiation-induced brain injury was thought to exhibit a delayed response (requiring months to years to become evident) as affected cells die. It is now clear, however, that the nervous system responds to radiation in both acute and chronic ways. For example, recent data show that radiation damage is a dynamic process, involving many cell types, similar to other forms of tissue injury (1,2). Moreover, radiation technology that delivers much higher doses in a single treatment (i.e., stereotactic radiosurgery) produces a pronounced acute injury consisting of edema and inflammation and can lead

to the rapid development of necrosis of surrounding normal brain tissue. The presence of a structural lesion may further predispose surrounding tissue to injury by physical distortion, inflammation and the development of fibrosis (2). For example, radiosurgery performed for arteriovenous malformations is associated with an incidence of life-threatening brain necrosis of up to 10% to 20% in treated patients (3,4). Although protracted courses of glucocorticoids and rheological agents such as warfarin, acetylsalicylic acid, and heparin are frequently used as treatment for postradiosurgery injury, these interventions are not primary treatments

and their true efficacy is anecdotal and largely unknown (5-7). Further, incidental damage producing long-term disabilities may occur to important structures such as cranial nerves adjacent to the radiosurgical target, as is frequently seen with the radiosurgical treatment of skull-base tumors such as vestibular schwannomas and meningiomas. With many ongoing improvements in health care, cancer patients and others undergoing radiotherapeutic treatments survive long enough for these effects to become clinically significant and adversely affect quality of life. Therefore, the development of any adjuvant therapy that reduces radiation-related side effects is clearly desirable.

For many years it was unclear how the centrifugal spread of tissue injury away from a damaged region is terminated. Recently, it has been recognized that the cytokine erythropoietin (EPO) is

Address correspondence and reprint requests to Michael Brines, The Kenneth S. Warren Institute, 712 Kitchawan Road, Ossining, NY 10562. Phone: 914-762-7586; fax: 914-762-4000; e-mail: mbrines@kswi.org.

Submitted June 12, 2006; accepted for publication July 10, 2006.

produced locally and limits injury in a multifunctional manner by antagonizing the action of proinflammatory cytokines and by preventing apoptosis, reducing edema, maintaining vascular autoregulation, and mobilizing stem cells (reviewed in ref. 8). However, EPO does not appear to directly attenuate necrosis, the primary manner by which radiated lesions are thought to involute following radiosurgical treatment. These characteristics suggest that EPO could limit damage to tissue occurring around the target of a necrotizing dose of radiation, while at the same time not causing radioresistance within the targeted lesion. Because EPO has long been appreciated for its hormonal role in maintaining adequate numbers of erythrocytes—for which recombinant human EPO (rhEPO) is widely used clinically—this molecule has received much interest for use as a general tissue-protective agent (8). The widespread availability of rhEPO has opened up the possibility of exogenous administration for therapy of tissue injuries, including before potential iatrogenic injury, for example, radiosurgery. The beneficial effects of rhEPO have been especially well documented in experimental models of brain and spinal cord injury in which large therapeutic time windows (hours to days) have been documented (8). In preclinical models, however, tissue protection using rhEPO typically requires doses that are higher than those employed in treatment of anemia, especially for nervous tissue. Unfortunately, rhEPO given at a high dose has potential adverse effects, particularly via an interaction between the vascular endothelium and platelets, strongly promoting thrombosis (9). Notably, several cancer clinical trials evaluating rhEPO administration at relatively high doses have encountered serious adverse effects, including increased mortality in the rhEPO treatment arm (10,11). Because radiotherapy is itself well known to be thrombogenic (12), synergistic adverse effects of high-dose rhEPO treatment could negate any beneficial tissue-protective effects.

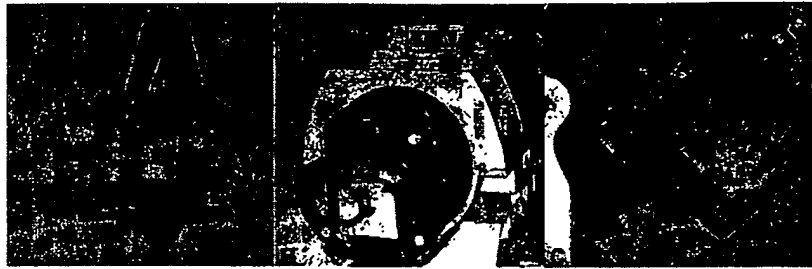


Figure 1. The experimental setup included a modified stereotactic frame to hold and orient the rat (A). This device allowed positioning within the GE Signa MRI scanner (B) and Leskell γ Knife (C) used in this study.

The receptor for EPO expressed by the bone marrow consists of a homodimer [EPOR:EPOR; (EPOR)₂] that until recently was believed to function in both the hematopoietic and tissue-protective pathways. The receptor for EPO expressed by nonhematopoietic tissues [for example, the nervous system (13)], however, possesses a lower binding affinity for EPO than does the hematopoietic receptor and, further, is associated with different proteins, consistent with a distinct receptor isoform. We have recently proposed that the tissue protective receptor is a heteromer comprising the EPOR in association with the common β receptor (β c, also known as CD131) used by the cytokines GM-CSF, IL-3, and IL-5 (14). The binding sites of EPO for the homodimeric receptor are well known, and we have shown how specific chemical or mutational modification of amino acid residues within the binding site produces molecules that do not have affinity for (EPOR)₂, yet are equipotent with EPO for tissue protection (15). For example, carbamylated EPO (CEPO) does not bind to (EPOR)₂ and, therefore, lacks hematopoietic activity yet mediates potent tissue protection through the EPOR: β c receptor (14).

Herein, we demonstrate that CEPO given before and for a short time after necrotizing γ irradiation significantly reduces both the acute behavioral abnormalities and the ultimate extent of necrosis following high-dose radiation injury.

MATERIALS AND METHODS

The animal protocols followed in this study were approved by the Animal Use and Care Committee of the Kenneth S. Warren Institute in accordance with the directives of the Guide for the Care and Use of Laboratory Animals of the National Research Council. Male Sprague-Dawley rats weighing 250 to 275 g were anesthetized using ketamine and immobilized in a MRI-compatible stereotactic device (Figure 1A) as per Kondziolka et al. (16). Noncontrast volumetric imaging using a 1.5 T GE Signa MRI scanner (GE Healthcare Technologies, Waukesha, WI, USA) (Figure 1B) was used to identify a radiosurgical target in the right striatum. A Leskell γ Knife Model B (Elekta, Stockholm, Sweden) and a 4-mm collimator helmet (Figure 1C) were used to stereotactically deliver 100 Gy to the maximal dose point in the right striatum (Figure 2). This dose and site were selected based on a previous study showing that this dose reliably produces necrosis in rat brain by 90 days (16). Before delivery of the γ radiation, the experimental animals were randomized into 2 groups of 6 animals receiving either normal saline or 50 μ g kg⁻¹ intraperitoneal CEPO 24 h before radiation, immediately after, and for an additional 9 days. Researchers were blinded as to which arm of the study the experimental animals were assigned. Follow-up evaluation consisted of 3 neurological tests of motor function performed on the dosing day, day 17, and day 25, as well as histopathological eval-

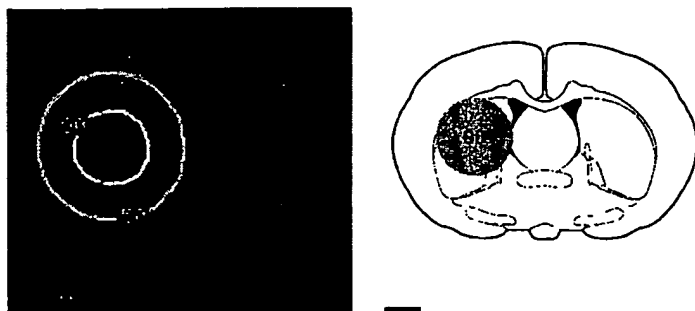


Figure 2. (Left) Concentric circles indicate tissue receiving 90% and 50% of the 100-Gy dose within the targeted region of the right striatum of animal visualized by MRI. (Right) The coronal section indicates the intended target for the 90-Gy dose. Scale bar, 2 mm.

uation of the lesion at 30 days (2 animals each group) and 90 days following injury.

Neurological Testing

Neurological testing included forelimb use asymmetry, vibrissae-elicited limb placement, and forelimb akinesia. To reduce the contribution of learning and adaptation to the behavioral analysis, the animals were habituated to the testing protocols before receiving radiation.

Limb use asymmetry test. Forelimb use in exploratory behavior was assessed according to the protocol of Schallert et al. (17). Briefly, animals were videotaped for 5 min within a transparent cylinder (20 cm diameter, 30 cm height) using a camera capable of single-frame display. A mirror was placed behind the cylinder to permit recording of forelimb movements whenever the animal turned away from the camera. After recording, a single investigator blinded to the treatment evaluated forelimb usage as follows.

(A) A wall exploration score was derived by enumerating: (1) the independent use of the left or right forelimb for initial contact on the wall; (2) use of either forelimb to initiate a weight-shifting movement; (3) use of the left or right forelimb to regain the center of gravity while moving laterally in a vertical posture; and (4) simultaneous use of both forelimbs for contacting the wall or lateral stepping movements along the wall.

(B) A landing score was determined by noting (1) independent use of the left or right forelimb to land after a rearing movement and (2) simultaneous use of both the left and right forelimb for landing after a rearing movement. If the rater could not clearly determine whether a limb was being used independently or simultaneously, that movement was not scored. Additional criteria for exclusion included movements along the ground after landing (stepping) and instances in which an animal performed < 5 landings and < 10 wall movements during a testing session. Additional details for scoring can be found in Schallert et al. (17).

Data analysis of limb asymmetry. Wall exploration and landing scores were determined separately, and each was expressed in terms of (1) the percentage of use of the nonimpaired forelimb relative to the total number of limb-use movements, (2) the percentage of use of the impaired forelimb relative to the total number of limb-use movements, and (3) the percentage of bilateral use of both limbs relative to the total number of limb-use movements. The percentage of use of the impaired forelimb was then subtracted from the percentage of use of the nonimpaired forelimb for exploration and landing. These 2 scores (wall and landing) were averaged together for a single limb-use asymmetry score that corrected for

variability in the number of wall versus landing movements.

Vibrissae-elicited forelimb placement. Following the protocol of Woodlee et al. (18), animals were held by their torso facing the edge of a table, allowing forelimbs to hang free. Independent testing of each forelimb was induced by gently brushing the respective vibrissae on the edge of a tabletop for a total of 10 trials. In this test, normal animals place the forelimb of both sides quickly onto the countertop. Rats with unilateral damage show varying degrees of impaired limb-placing ability, while still placing the unimpaired limb reliably. The percentage of successful placing responses was determined by counting the number of bilateral limb placements divided by the number of trials.

Forelimb akinesia. Movement initiation for each limb was assessed using a forelimb akinesia test. The hindquarters of the animal were suspended while the animal supported its weight on a forelimb. The animal was allowed to initiate stepping movements in a 10-s period for one forelimb and then the other in a balanced order. Normal animals did not initiate any limb stepping during the 10-s test interval.

Evaluation of brain necrosis

The neuropathological consequences of γ knife irradiation were evaluated at 30 and 90 days after delivery of radiation. The animals were killed by exsanguination under barbiturate anesthesia, and the brains were perfused and fixed with 4% formaldehyde in 0.1 M phosphate buffer, pH 7.4. The brains were then embedded in paraffin, and serial sections were obtained every 5 μ m through the target area and stained with hematoxylin and eosin (H&E). The stained sections were examined microscopically for pathological changes, and the extent of injury was traced using a camera lucida in every 40th section (every 200 μ m) from the beginning of the region of injury by an observer blinded to the experimental group. The images were then digitized, the area of necrosis

was determined by digital planimetry, and the lesion volume was mathematically derived.

Statistical methods

Behavioral data were evaluated by repeated-measures ANOVA. Lesion volume between the groups was assessed using unpaired Student's *t* test.

RESULTS

Both experimental groups successfully underwent delivery of a necrotizing dose of γ irradiation without incident. The day after radiation, animals from both groups exhibited abnormal neurological function, as assessed by the vibrissae and forelimb akinesia tests. These tests, performed serially, also showed large and significant differences between the treatment groups, with a smaller decline and more rapid recovery exhibited by the CEPO group. In contrast, the limb asymmetry test exhibited a significant deterioration much later (> 10 days).

The vibrissae test (Figure 3) exhibited an initial decline from normal for both

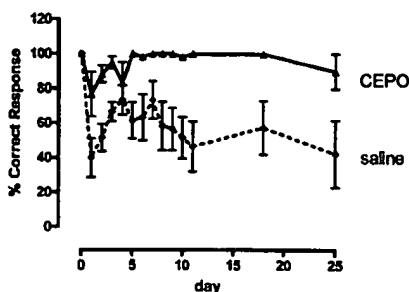


Figure 3. Vibrissae-stimulated limb placing test results indicate that both CEPO- and saline-treated animals exhibited an acute decline in correct responses (both forelimbs extending to table edge after ipsilateral or contralateral vibrissae stimulation) immediately after irradiation. Saline-administered animals recovered only partially, reaching a plateau and then declining. In contrast, this reflex normalized in animals that received CEPO. $P < 0.05$ between groups; 6 animals per group.

experimental groups, but more so for those receiving saline (60% of the time the affected limb was not reflexively extended to the table edge). By the second day, some recovery occurred, reaching a plateau on days 4 to 6 and then falling again after day 7 (Figure 3). Performance on day 25, the last day examined, was at a mean value of only $\sim 50\%$ correct. In contrast, the CEPO group exhibited a transient decrease for 4 days after radiation, with full recovery for the remaining time period (Figure 3).

A similar pattern was observed in the forelimb akinesia test. In this test, recovery was characterized by an acute decline after injury in the saline group, followed by partial nonsustained recovery to day 7, and then a progressive decline through the last data point at day 25 (Figure 4). In contrast, CEPO-treated animals exhibited a smaller acute decline, followed by complete recovery beyond day 5 (Figure 4).

The limb use asymmetry test exhibited a longer latency in onset of abnormal responses (Figure 5). Notably, both groups exhibited a bias for the unaffected limb by day 25, the last time point evaluated. The saline group, however, favored the unaffected forelimb with significantly higher frequency at most time points evaluated.

Thirty days after irradiation, histological examination of H&E-stained sections did not show any discernible differences between the irradiated and nonirradiated basal ganglia (data not shown), even though profound functional deficits were documented. In contrast, 90 days after irradiation, H&E-stained serial brain sections revealed striking differences between treatment groups. As illustrated in Figure 6A, both treatment groups exhibited necrosis within the 90- to 100-Gy target region (inner circle). The group receiving CEPO exhibited extensive tissue salvage within the 50- to 90-Gy region (region between inner and outer circle), distinctly different from the saline group. Upon quantification, the volume of necrotic tissue within the group receiving CEPO was about half that observed

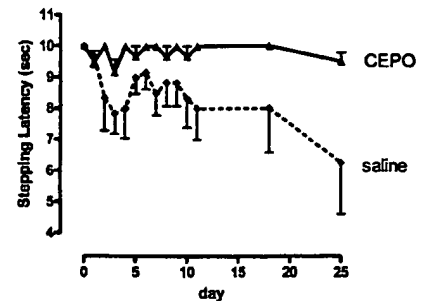


Figure 4. Forelimb akinesia is increased in the saline group, characterized by an acute decline, then partial, nonsustained recovery. The CEPO group differed significantly from the saline group ($P < 0.05$).

in the saline-treated rats (Figure 6B). The periphery surrounding the irradiated region in both treatment groups showed proliferation of reactive glial cells and areas of loose tissue with vacuolation. The central parts of the irradiated region showed varying numbers of necrotic foci with secondary calcification. The necrotic core of saline-treated animals typically contained large masses of calcified granules, in striking contrast to the CEPO group (Figure 6C).

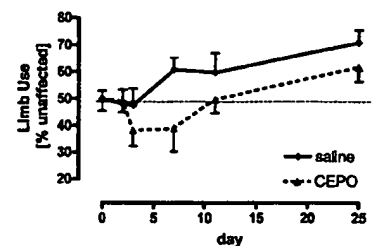


Figure 5. Forelimb use asymmetry test demonstrates a significant difference between saline- and CEPO-treated animals. Saline-treated animals favored the unaffected limb by day 7 after injury. In contrast, CEPO-treated animals deteriorated more slowly, preferentially using the unaffected limb only on the final observation day (25). Points above dashed line indicate favoring the right (unaffected) limb. CEPO significantly differs from saline ($P < 0.05$).

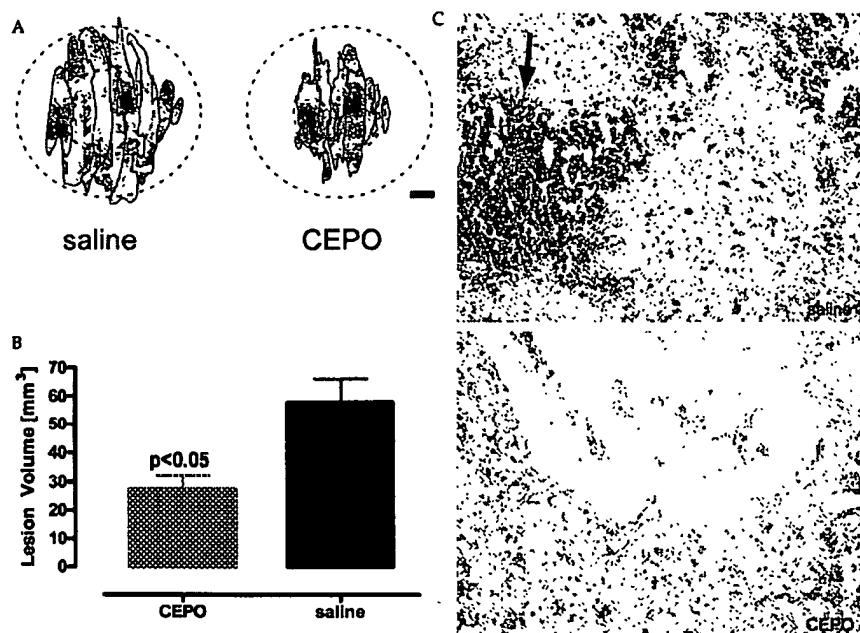


Figure 6. CEPO-treated animals have significantly less necrosis within the targeted brain volume. (A) Lesion size at the center of the necrosis volume in representative animals from the saline and CEPO groups 90 days after the delivery of radiation. Inner dashed circle indicates the delivery of 90 to 100 Gy. Difference between outer and inner circles indicates a region receiving between 50 and 90 Gy. Note that CEPO treatment was associated with a marked reduction in injury within the lower dose range. Distances between slices is 200 μ m; scale bar, 1 mm. (B) Mean volume of necrosis in the CEPO-treated group was half of that observed for the saline treatment group. (C) Representative photomicrographs comparing lesions of the 2 treatment groups. Animals that received saline generally possessed dense calcification (arrow) in contrast to the less affected CEPO group. Original magnification $\times 40$.

DISCUSSION

The observation of more nearly-normal motor function associated with less necrosis at 90 days in the CEPO-treated group supports a potential therapeutic role for nonerythropoietic tissue-protective cytokines in limiting radiation-induced neurological injury. Although the rat brain is well known to be relatively radioresistant compared with that of humans, previous studies have shown that it is a good model for assessing the effects of radiation injury (16,19). However, prior work has focused primarily upon a histological assessment of damage to estimate the severity of injury. Specifically, within hours of a therapeutic dose of γ radiation (6–20 Gy) in a rat model, glia

within the target area became activated and began to proliferate (20). By 14 days, tissue edema was clearly present (16), whereas necrosis of neurons and other cells occurred much later, 30 days or more after injury (20). These effects are directly proportional to the dose employed for a given beam diameter (16,19,20).

In the present study, high-dose radiation (100 Gy) to the striatum produced acute neurological defects as determined by vibrissae and proprioceptive testing of the forelimbs, with a delayed effect on the pattern of use of the forelimbs. Three months after radiation, substantial necrosis was observed in both groups within the 100- to 90-Gy

target region (Figure 6B). The deterioration noted for bilateral limb usage in both groups is presumably secondary to the frank pathological lesion present by 90 days. Of note, a limited histological examination of irradiated brains after 1 month did not show any evidence of injury. Thus the acute behavioral effects following radiation exposure appear to be a sensitive method by which to evaluate the degree of injury in the acute and subacute periods, not requiring the months needed for frank necrosis to occur.

The central nervous system exhibits a large capacity for repair following mild radiation injury [reviewed in Andrasschke et al. (21)]. The mechanisms responsible have not been extensively delineated, but appear to be similar to the underlying responses to other forms of brain injury (1) for which locally produced (endogenous) EPO has been implicated as a key cytoprotective agent.

Stem cell mobilization is thought to be of major importance in the healing phase of radiation-induced injury, and EPO has been shown to recruit stem cells within the brain (22), particularly after ischemic injury (23). However, Fukuda et al. (24) have reported that radiation preferentially damages progenitor cells within the immature rat brain and, further, that this injury could not be attenuated by exogenous rhEPO.

This observation is surprising, as neural progenitor cells have been shown to specifically express receptors for EPO and, further, EPO critically modulates apoptosis within this population during brain development (25). Additionally, progenitor cells have been found to generate reactive oxygen species (ROS) and undergo apoptosis after irradiation, cellular responses that can be greatly inhibited by rhEPO in other model systems (8). Notably, Fukuda et al. (24) employed very high doses of rhEPO ($\sim 10,000$ U/kg⁻¹ intraperitoneally), which could be problematic, as numerous investigators have shown that EPO protection generally follows an inverted U-shaped curve in vivo and in vitro, in

part potentially owing to ROS generated by high-dose rhEPO (26). On the other hand, caspase inhibition was ineffective in the study by Fukuda et al. (24), suggesting that in this model, injury may be closer to a purely necrotic process that is not sensitive to EPO. Finally, it should be noted that the immature brain is especially sensitive to radiation, which in addition to direct effects on progenitor cells, also alters the microenvironment (27) in ways that potentiate tissue injury. These effects may not occur to the same extent in adult brain.

The clinical presentation of radiation injury can be divided into immediate, subacute, or delayed phenotypes (6). Acute injury is likely mediated by radiation-induced vascular leakiness and the development of vasogenic edema. Potential effects secondary to neuronal dysfunction are certainly possible but have not been specifically demonstrated. One of EPO's prominent tissue-protective effects is on the permeability of the vascular endothelium of the blood-brain barrier. In this role, EPO increases the tightness of the barrier and reduces leakiness in both in vitro (28) and in vivo (29,30) models. Late effects of radiation injury are associated with necrosis, mainly arising from vascular dropout. In a time- and radiation dose-dependent fashion, the endothelium swells, the basement membrane thickens, the microvessels undergo hypertrophy, and ultimately the tissue cellular density diminishes (31). White matter necrosis is especially prominent and depends on oligodendrocyte apoptosis and ischemia-reperfusion injury secondary to perivascular edema (6). The smaller necrosis volume observed in the CEPO group could be explained by a primary effect on protecting the microvascular circulation. If so, the efficacy of CEPO administered for 10 d following injury implies that the evolving pathological processes can be terminated by a brief exposure to tissue-protective cytokines. It is unknown whether other, delayed effects might also respond favorably to longer exposure to CEPO.

The tissue-protective properties of CEPO we have observed in the brain in this report likely also apply for other radiosensitive tissues with microvascular injury as a pathological mechanism. To our knowledge, the only other study evaluating the effects of rhEPO on radiation injury outside of the CNS focused on the adult kidney (21). Curiously, in that study, EPO at 2 doses (500 or 2000 U kg⁻¹) given subcutaneously in 3 doses before and just after irradiation was associated with diminished renal function between 5 and 9 months after exposure. This unexpected finding might be explained by the EPO-mediated acute reduction in renal blood flow that occurs after high doses of EPO (9). The reduced perfusion is similar to that occurring after activation of an organ-specific renin-angiotensin system that has also been hypothesized to play a role in radiation-induced tissue injury [reviewed in Robbins and Diz (32)]. We have recently shown (9) that CEPO, in contrast, increases renal blood flow (both cortical and total). It will be important, therefore, to determine whether lower doses of EPO or use of CEPO will be nephroprotective in the setting of irradiation.

Other interventions with the potential for preservation of normal tissue surrounding the radiated site are currently under investigation and could act synergistically with a tissue-protective cytokine. For example, inhibition of the renin-angiotensin system, growth factors (for example, TGF β), COX-2 inhibitors, and antioxidants, among others (33), have shown some promise, and it will be interesting to evaluate these for possible synergistic effects with tissue-protective cytokines.

The striking improvements in both behavioral and pathological outcomes following short-term CEPO treatment indicate the need for further study. Because both radiotherapy and rhEPO treatment can elicit thrombotic events, we believe that the results observed in this preclinical model foreshadow the promise for nonerythropoietic tissue protection in patients.

ACKNOWLEDGMENTS

Supported in part by the Kenneth S. Warren Institute and Elekta AB to N.d.L. and A.d.L. We thank Dr. Jung Kim for his expert neuropathological assessments, as well as Deborah Diaz and Daniel Gomez for technical support.

REFERENCES

- Denham JW, Hauer-Jensen M. (2002) The radiotherapeutic injury: a complex 'wound.' *Radiother. Oncol.* 63:129-45.
- Stone HB, Coleman CN, Anscher MS, McBride WH. (2003) Effects of radiation on normal tissue: consequences and mechanisms. *Lancet Oncol* 4:529-36.
- Flickinger JC et al. (1999) A multi-institutional analysis of complication outcomes after arteriovenous malformation radiosurgery. *Int. J. Radiat. Oncol. Biol. Phys.* 44:67-74.
- Miyawaki L et al. (1999) Five year results of LINAC radiosurgery for arteriovenous malformations: outcome for large AVMS. *Int. J. Radiat. Oncol. Biol. Phys.* 44:1089-106.
- Chuba PJ et al. (1997) Hyperbaric oxygen therapy for radiation-induced brain injury in children. *Cancer* 80:2005-12.
- Giglio P, Gilbert MR. (2003) Cerebral radiation necrosis. *Neurologist* 9:180-8.
- Koehler PJ, Jager J, Verbiest H, Vecht CJ. (1995) Anticoagulation for radiation injury. *Neurology* 45:1786.
- Brines M, Cerami A. (2005) Emerging biological roles for erythropoietin in the nervous system. *Nat. Rev. Neurosci.* 6:484-94.
- Coleman TR et al. (2006) Cytoprotective doses of erythropoietin or carbamylated erythropoietin have markedly different procoagulant and vasoactive activities. *Proc. Natl. Acad. Sci. U. S. A.* 103: 5965-5970.
- Leyland-Jones B. (2003) Breast cancer trial with erythropoietin terminated unexpectedly. *Lancet. Oncol.* 4:459-60.
- Rosenzweig MQ, Bender CM, Lucke JP, Yasko JM, Brufsky AM. (2004) The decision to prematurely terminate a trial of R-HuEPO due to thrombotic events. *J. Pain Symptom Manage.* 27:185-90.
- Hoegler D. (1997) Radiotherapy for palliation of symptoms in incurable cancer. *Curr. Probl. Cancer* 21:129-83.
- Masuda S et al. (1993) Functional erythropoietin receptor of the cells with neural characteristics: comparison with receptor properties of erythroid cells. *J. Biol. Chem.* 268:11208-16.
- Brines M et al. (2004) Erythropoietin mediates tissue protection through an erythropoietin and common beta-subunit heteroreceptor. *Proc. Natl. Acad. Sci. U. S. A.* 101:14907-12.
- Leist M et al. (2004) Derivatives of erythropoietin that are tissue protective but not erythropoietic. *Science* 305:239-42.

16. Kondziolka D, Lunsford LD, Claassen D, Maiz AH, Flickinger JC. (1992) Radiobiology of radiosurgery: Part I. The normal rat brain model. *Neurosurgery* 31:271-9.
17. Schallert T, Fleming SM, Leasure JL, Tillerson JL, Bland ST. (2000) CNS plasticity and assessment of forelimb sensorimotor outcome in unilateral rat models of stroke, cortical ablation, parkinsonism and spinal cord injury. *Neuropharmacology* 39:777-87.
18. Woodlee MT, Asseo-Garcia AM, Zhao X, Liu SJ, Jones TA, Schallert T. (2005) Testing forelimb placing "across the midline" reveals distinct, lesion-dependent patterns of recovery in rats. *Exp. Neurol.* 191:310-7.
19. Munter MW et al. (2001) [Late radiation changes after small volume radiosurgery of the rat brain. Measuring local cerebral blood flow and histopathological studies]. *Strahlenther. Onkol.* 177:354-61. (German)
20. Yang T, Wu SL, Liang JC, Rao ZR, Ju G. (2000) Time-dependent astroglial changes after gamma knife radiosurgery in the rat forebrain. *Neurosurgery* 47:407-15.
21. Andrasschke N et al. (2006) Preclinical evaluation of erythropoietin administration in a model of radiation-induced kidney dysfunction. *Int. J. Radiat. Oncol. Biol. Phys.* 64:1513-8.
22. Shingo T, Sorokan ST, Shimazaki T, Weiss S. (2001) Erythropoietin regulates the in vitro and in vivo production of neuronal progenitors by mammalian forebrain neural stem cells. *J. Neurosci.* 21:9733-43.
23. Tsai PT et al. (2006) A critical role of erythropoietin receptor in neurogenesis and post-stroke recovery. *J. Neurosci.* 26:1269-74.
24. Fukuda H et al. (2004) Irradiation-induced progenitor cell death in the developing brain is resistant to erythropoietin treatment and caspase inhibition. *Cell Death Differ.* 11:1166-78.
25. Yu X et al. (2002) Erythropoietin receptor signaling is required for normal brain development. *Development* 129:505-16.
26. Diaz Z, Assaraf MI, Miller WH, Jr., Schipper HM. (2005) Astroglial cytoprotection by erythropoietin pre-conditioning: implications for ischemic and degenerative CNS disorders. *J. Neurochem.* 93:392-402.
27. Fukuda A et al. (2005) Age-dependent sensitivity of the developing brain to irradiation is correlated with the number and vulnerability of progenitor cells. *J. Neurochem.* 92:569-84.
28. Martinez-Estrada OM, Rodriguez-Millan E, Gonzalez-De Vicente E, Reina M, Vilaro S, Fabre M. (2003) Erythropoietin protects the in vitro blood-brain barrier against VEGF-induced permeability. *Eur. J. Neurosci.* 18:2538-44.
29. Li W, Maeda Y, Yuan RR, Elkabes S, Cook S, Dowling P. (2004) Beneficial effect of erythropoietin on experimental allergic encephalomyelitis. *Ann. Neurol.* 56:767-77.
30. Uzum G, Sarper Diler A, Bahcekapili N, Ziya Ziyen Y. (2005) Erythropoietin prevents the increase in blood-brain barrier permeability during pentylentetrazol induced seizures. *Life Sci.* 22:2571-2576.
31. Kamiryo T, Lopes MB, Kassell NF, Steiner L, Lee KS. (2001) Radiosurgery-induced microvascular alterations precede necrosis of the brain neuropil. *Neurosurgery* 49:409-14.
32. Robbins ME, Diz DL (2006) Pathogenic role of the renin-angiotensin system in modulating radiation-induced late effects. *Int. J. Radiat. Oncol. Biol. Phys.* 64:6-12.
33. Coleman CN et al. (2003) Molecular and cellular biology of moderate-dose (1-10 Gy) radiation and potential mechanisms of radiation protection: report of a workshop at Bethesda, Maryland, December 17-18, 2001. *Radiat. Res.* 159:812-34.

Asialoerythropoietin is a nonerythropoietic cytokine with broad neuroprotective activity *in vivo*

Serhat Erbayraktar^{***}, Giovanni Grasso^{**§}, Alessandra Sfacteria^{**§}, Qiao-wen Xie^{*}, Thomas Coleman^{*}, Mads Kreilgaard[¶], Lars Torup[¶], Thomas Sager[¶], Zubeyde Erbayraktar^{*†}, Necati Gokmen[¶], Osman Yilmaz[¶], Pietro Ghezzi^{***}, Pia Villa^{***††}, Maddalena Fratelli^{**}, Simona Casagrande^{**}, Marcel Leist[¶], Lone Helboe[¶], Jens Gerwein[¶], Søren Christensen[¶], Marie Aavang Geist[¶], Lars Østergaard Pedersen[¶], Carla Cerami-Hand^{*}, Jean-Paul Wuerth^{*}, Anthony Cerami^{*}, and Michael Brines^{***}

^{*}The Kenneth S. Warren Institute, Kitchawan, NY 10562; [¶]H. Lundbeck A/S, 2500 Valby, Denmark; [†]Dokuz Eylül University School of Medicine, Izmir 35340, Turkey; ^{**}Mario Negri Institute of Pharmacological Research, 20157 Milan, Italy; and ^{††}Consiglio Nazionale delle Ricerche, Institute of Neuroscience, Cellular and Molecular Pharmacology Section, 20129 Milan, Italy

Contributed by Anthony Cerami, March 26, 2003

Erythropoietin (EPO) is a tissue-protective cytokine preventing vascular spasm, apoptosis, and inflammatory responses. Although best known for its role in hematopoietic lineages, EPO also affects other tissues, including those of the nervous system. Enthusiasm for recombinant human erythropoietin (rhEPO) as a potential neuroprotective therapeutic must be tempered, however, by the knowledge it also enlarges circulating red cell mass and increases platelet aggregability. Here we examined whether erythropoietic and tissue-protective activities of rhEPO might be dissociated by a variation of the molecule. We demonstrate that asialoerythropoietin (asialoEPO), generated by total enzymatic desialylation of rhEPO, possesses a very short plasma half-life and is fully neuroprotective. In marked contrast with rhEPO, this molecule at doses and frequencies at which rhEPO exhibited erythropoiesis, did not increase the hematocrit of mice or rats. AsialoEPO appeared promptly within the cerebrospinal fluid after i.v. administration; intravenously administered radiolabeled asialoEPO bound to neurons within the hippocampus and cortex in a pattern corresponding to the distribution of the EPO receptor. Most importantly, asialoEPO exhibits a broad spectrum of neuroprotective activities, as demonstrated in models of cerebral ischemia, spinal cord compression, and sciatic nerve crush. These data suggest that nonerythropoietic variants of rhEPO can cross the blood-brain barrier and provide neuroprotection.

The widespread and highly efficacious use of recombinant human erythropoietin (rhEPO) for the treatment of EPO-deficient anemias reflects a triumph of biotechnology. As a typical member of the cytokine superfamily, EPO also performs other functions. Recently, EPO has been identified as an important endogenous mediator of the adaptive responses of tissues to metabolic stress, primarily by limiting the extent of injury. For example, EPO synthesized by hypoxic astrocytes may mediate the protective phenomenon of preconditioning in the nervous system in which exposure to a brief, nontoxic episode of ischemia dramatically increases the resistance of neurons to subsequent insults (1–3).

Given the large size of rhEPO, it was initially surprising to discover that rhEPO administered peripherally readily penetrates the blood-brain barrier and effectively reduces brain injury after insults (4). Additional evidence has also shown widespread efficacy of rhEPO in injury models of the spinal cord (5, 6), retina (7), and the heart (8). Mechanistically, EPO acts in a coordinated fashion at multiple levels, including limiting the production of tissue-injuring molecules [e.g., reactive oxygen species and glutamate (9–11)], reversal of vasospasm (12, 13), attenuation of apoptosis (5, 10, 14, 15), modulation of inflammation (4, 16), and recruitment of stem cells (17). A recent clinical trial supports the relevance of these animal models for human disease by demonstrating significant improvement in

outcome of stroke patients who were administered rhEPO intravenously within 8 h of the onset of symptoms (18).

Animal models have demonstrated that single doses of rhEPO are remarkably effective for the treatment of acute injury (4–6, 19). Many clinical situations, however, will likely require multiple doses of rhEPO, which will lead to potentially harmful increases in the red cell mass. For example, animal models clearly show that EPO-dependent increases in hematocrit can cause and amplify brain injury (20). Pharmacological doses of rhEPO also stimulate the production of hyperreactive platelets (21) that can predispose to thrombosis (22), especially in the setting of injury. This potential complication of rhEPO therapy is relevant for humans as well (23, 24), because thrombotic events have been observed in the setting of “blood doping” by athletes (25). These considerations temper enthusiasm for rhEPO as a tissue-protective agent. Clearly, molecules retaining the beneficial tissue-protective actions of EPO, but not stimulating the bone marrow, are desirable.

One distinguishing feature between erythropoiesis and neuroprotection is that effective production of red cells requires the continuous presence of EPO, whereas a brief exposure is sufficient for neuroprotection *in vitro* (26). We reasoned that if neuroprotection is activated after a brief exposure to EPO, then a short-lived EPO could be translocated into tissue beds to initiate neuroprotection through EPO receptor (EPO-R) activation, but yet not survive long enough within the circulation to stimulate erythropoiesis. To produce a short-lived EPO, we completely removed the sialic acids that delay clearance *in vivo* (27, 28). In this article, we show that systemically administered asialoerythropoietin (asialoEPO) does not increase erythrocyte mass, yet is fully protective in animal models of stroke, spinal cord injury, and peripheral neuropathy.

Materials and Methods

Preparation and Characterization of AsialoEPO. The sialic acid of rhEPO (Dragon Pharmaceuticals, Vancouver) was removed by digestion with neuraminidase isolated from *Streptococcus* sp. 6646K (Seikagaku America, Rockville, MD, no. 120050). The reaction was performed at 37°C, pH 6.8, for 3 h using 0.05 units of enzyme per mg of rhEPO. The product (asialoEPO) was purified by anion-exchange chromatography and the homogeneity was confirmed by isoelectric focusing gel analysis. The final

Abbreviations: EPO, erythropoietin; rhEPO, recombinant human EPO; EPO-R, EPO receptor; CSF, cerebrospinal fluid; bw, body weight; CMAP, compound muscle action potential.

[†]Present address: Dokuz Eylül University School of Medicine, Izmir 35340, Turkey.

[§]S.E., G.G., and A.S. contributed equally to this work.

[¶]Present address: Department of Neurosurgery, University of Messina, 98122 Messina, Italy.

^{***}To whom correspondence should be addressed at: The Kenneth S. Warren Institute, 712 Kitchawan Road, Kitchawan, NY 10562. E-mail: mbrines@kswi.org.

Table 1. Comparison of the affinity, potency, and predominating plasma half-life of asialoEPO and rhEPO

	IC ₅₀ for sFc-EPO-R* binding, pM	EC ₅₀ for proliferation of UT-7, pM	Percent protection		Plasma half-life, h*		
			P-19	PC12	i.v.	i.p.	s.c.
rhEPO	10	20 ± 10	51	31 ± 7	5.6	7.0	5.4
asialoEPO	14	20 ± 10	43	34 ± 4	0.023	0.5	2.5

*Soluble Fc-EPO-R fusion construct.

*Plasma half-lives are terminal phase except for i.v. asialoEPO, which is initial phase.

sialic acid content was determined according to the European Pharmacopoeia (51) method and acid hydrolysis followed by high-performance anion-exchange chromatography with pulsed amperometric detection (Dionex).

For practical reasons, rhEPO and asialoEPO were considered to be of equivalent mass for dosing, as the sialic acid content accounted for ≤8% of the total weight of this ~34,000-Da protein. Concentrations are expressed as molarity instead of units, as asialoEPO exhibits no erythropoietic activity *in vivo*. One international unit of erythropoietic activity is equal to ~8 ng of rhEPO protein.

For binding assays, asialoEPO and rhEPO were radiolabeled according to a standard protocol by using chloramine T as described (29). The radioligand activity corresponded to ~50 µCi/µg (1 Ci = 37 GBq) with 50% bindability. Soluble Fc-EpoR fusion constructs (5 pM; R & D Systems), 4 pM radioligand, and graded concentrations (0–10,000 pM) of unlabeled EPO or asialoEPO were incubated for 30 min at 22°C in 100 µl of PBS before the addition of 100 µl of PBS with a 0.25-mg scintillation proximity assay (SPA) polyvinyl toluene protein A reagent (Amersham Pharmacia Biosciences, Amersham, U.K.). This reaction was incubated for an additional 2 h before luminescence recording by a scintillation counter.

Erythroleukemic UT-7 cells (30) were obtained from Deutsche Sammlung von Mikroorganismen und Zellkulturen (Braunschweig, Germany, no. ACC137). The assay of EPO derivatives was performed as described (31) over a 48-h period, and using WST-1 reduction (Roche Diagnostics, no. 1 644 807) to quantitate living cells. Signal-to-noise ratio of the assay was 8:15, and the half-maximal effective concentration of EPO variants was determined by a four-parameter-fit from concentration-response curves by using at least six drug concentrations. The P-19 survival assay was performed exactly as described (15). PC-12 cells were differentiated in the presence of nerve growth factor (NGF) and cell death was triggered by NGF withdrawal. EPO variants were used in this assay as described (32) and were present 24 h before and during the withdrawal period. For viability assessment the reduction of thiozole salts was used.

Animal Protocols. All procedures involving animals were approved by the animal research committees at each respective Institution and conducted in compliance with international laws and policies (33–36).

Pharmacokinetic Determination of Plasma and Cerebrospinal Fluid (CSF) Concentrations. CSF samples were obtained from male Sprague–Dawley rats by a needle placed into the cisterna magna using the methodology of Frankmann (37). Plasma half-life was determined from blood samples drawn serially from a catheter implanted in the carotid artery in awake Sprague–Dawley rats. After i.v., i.p., or s.c. administration of 44 µg/kg of body weight (bw) of asialoEPO/rhEPO, timed blood samples were collected with an Accusampler (Dilab, Lund, Sweden) over a 20-h period. AsialoEPO concentrations were determined by enzyme-linked immunoassay kits (R & D Systems and Immuno-Biological Laboratories, Hamburg, Germany). Extensive evaluation confirmed that the antibodies used in these kits identified

asialoEPO and rhEPO with equal sensitivity. The lower limit of quantification was 1.0 pM.

In Vivo Autoradiography. NMRI mice were injected i.v. with 100 µg/kg radioiodinated asialoEPO, and after 4 h the animals were perfused with PBS/heparin. The brains were removed, frozen on dry ice, and cryosectioned (20 µm). For cellular localization of radiolabel, slides were dipped in photographic emulsion and were exposed for 5 weeks before development.

Hemoglobin Responses to Repeated Doses of AsialoEPO *in Vivo*. The response of the bone marrow to asialoEPO versus rhEPO was assessed by repeated parenteral administration of equal doses of asialoEPO or rhEPO to BALB/c or C3H/hen female mice. Serum hemoglobin concentrations were determined by a hemoglobinometer using blood (<50 µl) withdrawn from the orbital sinus once weekly under isoflurane anesthesia. Animals were not iron supplemented.

Focal Ischemia Model. Ischemic stroke within the distribution of the middle cerebral artery (MCA) was produced as described (4). Briefly, under isoflurane anesthesia the ipsilateral carotid was ligated and the MCA was permanently occluded just distal to the bifurcation of the MCA into the rhinal artery. To produce a reversible ischemic event, the contralateral carotid was non-traumatically occluded for 90 min and then released. AsialoEPO was given intravenously with respect to the time of reperfusion at the dosages indicated in the text. The core temperature was maintained at 35–37°C until full recovery from anesthesia. Infarct volume was determined 24 h later by quantitative image analysis of tetrazolium salt-stained 1-mm slices of brain as described (4).

Spinal Cord Compression. Spinal cord compression was performed under controlled core temperature (35–37°C) using an aneurysm clip (53-g closing force) applied for 1 min at thoracic level 3, avoiding compression of the paravertebral arteries as described (6). Animals subsequently received either three daily doses of asialoEPO, rhEPO (both at 10 µg/kg of bw i.v.) or saline, and biweekly doses thereafter. Motor function of lesioned animals was evaluated in a blinded fashion by using the methodology of Basso and colleagues (38, 39). Three days after injury, five animals from each group were killed and the spinal cords were removed and fixed in formalin for histological analysis. Paraffin embedded tissue was sectioned (6 µm) to determine the extent of injury at the following five distinct levels: the lesion epicenter, 1 cm above and 1 cm below the epicenter, and the cervical and lumbar enlargements. Specimens were stained by using anti-NeuN (Chemicon, Temecula, CA), an indicator of living neurons (40). Surviving neurons within gray matter (i.e., histological characteristics of normal structures and presenting clear immunoreactivity for NeuN) were counted in each section. The results of neuronal counting in five randomly selected sections were averaged.

Sciatic Nerve Compression. Sprague–Dawley rats (250–350 g) were anesthetized by using isoflurane and their core temperature was

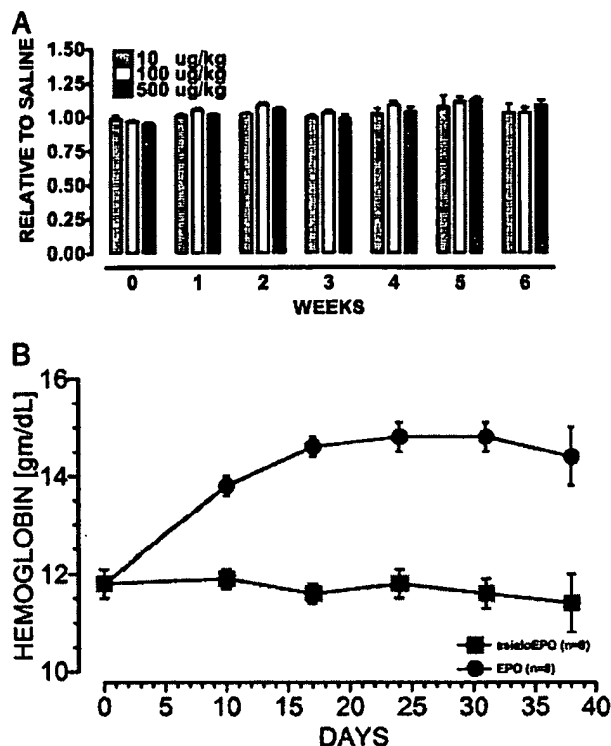


Fig. 1. (A) Biweekly i.v. injections of asialoEPO over a wide dosage range do not change hemoglobin concentration in mice ($n = 8$ for each group; $50 \mu\text{g/kg}$ of bw and $200 \mu\text{g/kg}$ of bw omitted for clarity). (B) Biweekly i.p. administration of asialoEPO at a neuroprotective dose ($100 \mu\text{g/kg}$ of bw) does not change the hemoglobin concentration. In contrast, an equal dose of rhEPO raises the hemoglobin concentration.

maintained at $35\text{--}37^\circ\text{C}$. Electrophysiological function of the sciatic nerve was assessed by recording compound muscle action potentials (CMAPs) at supramaximal stimulation (3 Hz, duration of 0.1 msec) delivered by means of stainless steel electrodes at midthigh. Two gold-plated balls (2-mm diameter) 1 cm apart were used for recording with the anode at the belly of the gastrocnemius muscle and the cathode at midtendon 6 mm from the calcaneus. CMAPs were acquired over 64 stimulations and were then averaged for five independent placements of the recording electrode.

After recording of baseline CMAP, the left sciatic nerve was exposed at midthigh and an aneurysm clip (53-g compression) was placed around the sciatic nerve for 2 min. Either 24 h or 15 min before (pretreatment) or immediately after the release of compression (posttreatment), a single dose of asialoEPO, rhEPO (both at $50 \mu\text{g/kg}$ of bw), or saline was administered intravenously and the surgical incision was closed. After drug administration, the CMAP was redetermined and, thereafter, was obtained successively over the next several weeks.

Neurological function was performed in a blinded fashion by averaging three determinations of rear foot toe splaying (the sciatic static index) according to the methodology of Bervar (41). In this assay, 0 is normal and negative scores indicate motor weakness.

Data Analysis. Statistical analysis was performed using ANOVA or by Student's t test where appropriate. Comparison of motor function over time was accomplished by a repeated measures analysis. Counts of surviving neurons in the spinal cord sections were compared by the Kruskal–Wallis one-way ANOVA by

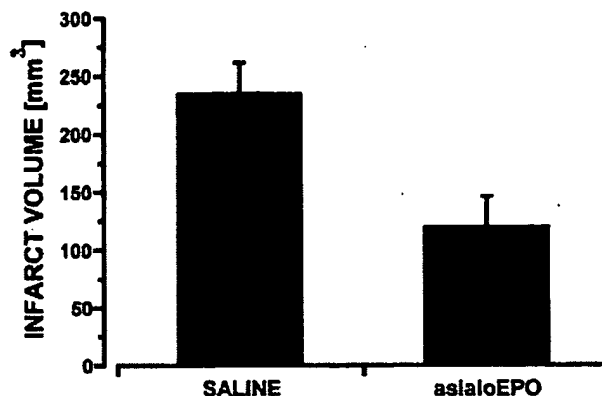


Fig. 2. AsialoEPO administered i.v. versus saline reduces infarct size in a rat reperfusion model of focal stroke ($n = 6$ for each group; $P < 0.01$).

ranks. *In vitro* experiments were repeated in at least three independent preparations with essentially similar results.

Results

In Vitro Characterization of AsialoEPO. The asialoEPO obtained by enzymatic conversion of rhEPO with sialidase contained <0.02 sialic acids per molecule and migrated as one homogeneous band at $pI \approx 8.5$. In contrast, the isoforms of rhEPO migrated at pI 3.3–4.5 (sialic acid content typically 10–14 per molecule; data not shown). Bioactivity of the final reaction product was verified by proliferation assays in TF-1 (data not shown) and UT-7 cells (Table 1) where the compound was found to be equipotent with rhEPO. The binding affinity to pure EpoR-Fc constructs was also in a similar range as that of rhEPO (Table 1). Bioactivity in neuronal-like cells was assessed by using P19 and PC-12 cells, in which asialoEPO protected from serum (P19) or NGF (PC-12) withdrawal to a similar extent (Table 1).

Pharmacokinetics. Intravenously injected asialoEPO exhibited a predominant plasma half-life of 1.4 min (Table 1) and was below the lower limit of quantification in the systemic circulation within 1–2 h, in contrast to rhEPO with a plasma half-life of ≈ 5.6 h. Administration of asialoEPO by i.p. or s.c. routes gave rise to effective plasma half-lives of 0.5 and 2.5 h, respectively. AsialoEPO appeared promptly in CSF after i.v. or i.p. injection and concentrations sufficient to bind appreciably to the EpoR

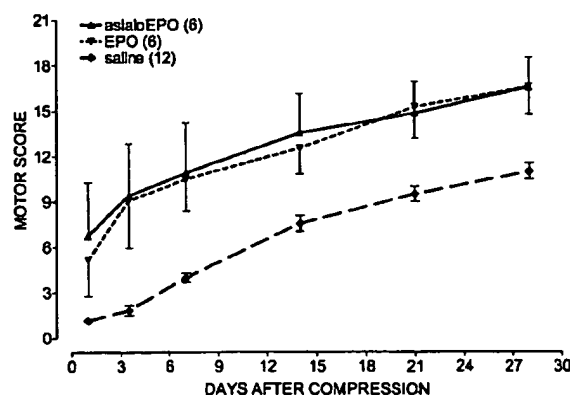


Fig. 3. AsialoEPO is as effective as rhEPO in restoring motor function after spinal cord compression. Agents were administered i.v. ($10 \mu\text{g/kg}$ of bw) once daily for 3 days after compression and biweekly thereafter.

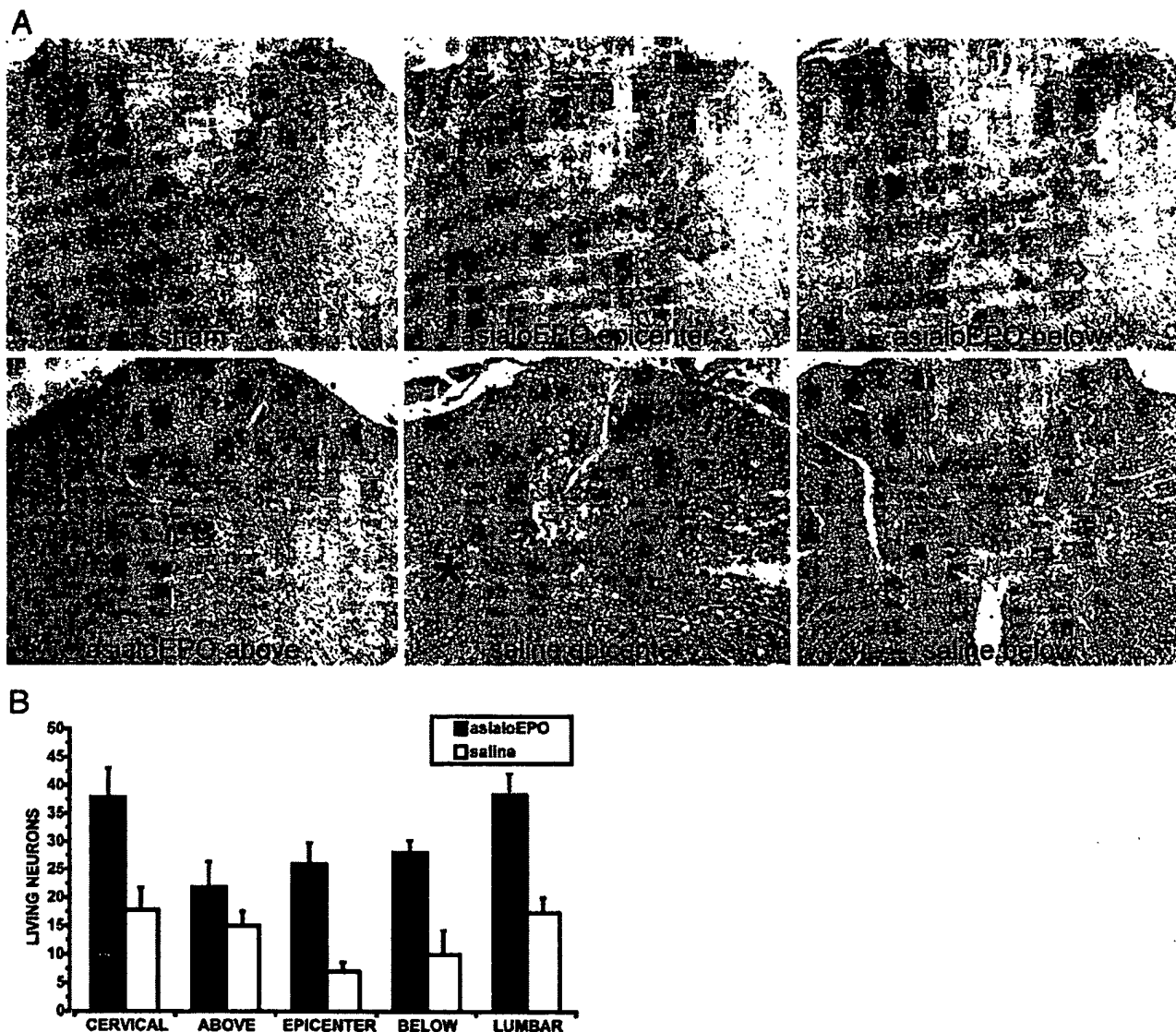


Fig. 4. (A) Spinal cord histology 3 days after a 2-min compressive injury. NeuN immunohistochemistry identifies living neurons after asialoEPO (10 µg/kg i.v.) or saline administration immediately after injury. Sections were obtained at the lesion epicenter, 1 cm above, and 1 cm below. Note the extensive disruption of the central gray in the saline-treated cord (Lower Center). White matter (*) is also disrupted and edematous compared with animals receiving asialoEPO. Shown are representative sections obtained from five animals in each group. (B) Summary of the mean living neurons number in the five levels investigated after asialoEPO, or saline treatment. Animals treated with asialoEPO presented with a significantly high number of living neurons compared with the saline group ($P < 0.05$ at all levels).

(0.5–30 pM range) were reached. The maximum CSF concentrations followed the plasma peak with a delay of 30–60 min, depending on the plasma kinetics profile of different routes of administration (data not shown). Brain tissue penetration of asialoEPO was followed by using radiolabeled compound. Histological localization of the radiolabel after injection of ^{125}I -asialoEPO showed a specific neuronal pattern, e.g., in the hippocampus (see Fig. 6, which is published as supporting information on the PNAS web site, www.pnas.org), similar to the one observed with ^{125}I -rhEpo (data not shown) or by immunohistochemical localization of the EpoR (14, 42, 43).

Effect of AsialoEPO on the Serum Hemoglobin Concentration. A wide range of asialoEPO dosage regimens was explored, none of which affected hemoglobin concentrations. For example, i.v.

injection of asialoEPO from 10 to 500 µg/kg of bw every 3 days was equivalent to saline (Fig. 1A). In contrast, rhEPO exhibited a pronounced dose-dependent effect (data not shown). Because asialoEPO persists longer in the plasma when given i.p., this regimen was also tested for changes in hematocrit. Administration of asialoEPO (50 µg/kg of bw i.p.) twice weekly did not effect hemoglobin concentration (Fig. 1B). In contrast, equivalent doses of rhEPO raised the hemoglobin concentration as expected.

Focal Ischemia. In pilot experiments, asialoEPO administered as a single dose i.p. was equipotent with rhEPO in reducing damage in a MCAO model of cerebral ischemia in the range of 5–50 µg/kg of bw (data not shown). In further experiments, asialoEPO was then tested after i.v. administration, i.e., the protocol

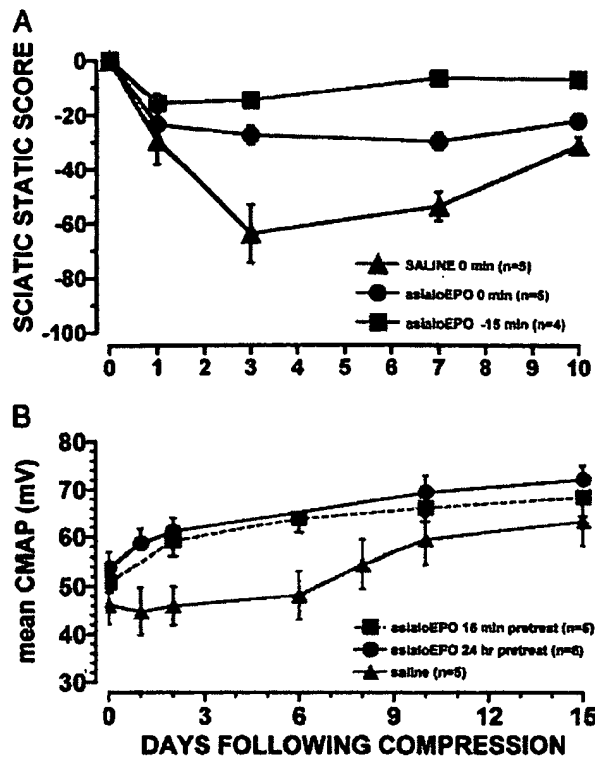


Fig. 5. (A) Motor function after compressive injury of the sciatic nerve in the rat. AsialoEPO (50 μ g/kg of bw i.v.) is more efficacious when administered 15 min before compression ($P < 0.01$; repeated measures analysis). (B) Average maximum CMAPs illustrate that 24-h or 15-min pretreatment with asialoEPO (50 μ g/kg of bw i.v.) attenuates injury to an equivalent extent.

resulting in the shortest possible plasma half-life. AsialoEPO given as an i.v. bolus (44 μ g/kg of bw) at the restoration of blood flow (i.e., 90 min after occlusion) reduced infarct volume by $\sim 50\%$ ($P < 0.01$) at 24 h (Fig. 2), similar to rhEPO (data not shown). Thus, the presence of EPO-like activity in plasma for only a few minutes can elicit neuroprotection.

Spinal Cord Compression. Both asialoEPO and rhEPO administered (10 μ g/kg of bw i.v.) for the first 3 days after spinal cord compression, and biweekly thereafter, were associated with an immediate and equivalent improvement of motor function in contrast to saline (Fig. 3; $P < 0.001$). The histological finding after 3 days differed strikingly between the groups. Notably, asialoEPO administration was associated with a restriction of injury to the epicenter alone, with nearly normal architecture both above and below (Fig. 4A). In contrast, the saline-treated group exhibited extensive cytoarchitectural disruption and edema (Fig. 4A) throughout the cord. The histological appearance of the white matter remained normal in asialoEPO-treated animals, consistent with their superior motor scores. Finally, the number of surviving (NeuN-positive) neurons was significantly higher in the asialoEPO-treated rats ($P < 0.05$) compared with the saline group (Fig. 4B).

Sciatic Nerve Crush Model. Saline administration after sciatic nerve compression was associated with decreased motor function as assessed by the sciatic static index and CMAP amplitude, reaching a nadir 2–4 days after injury (Fig. 5) and normalizing by 3–4 weeks. AsialoEPO administered 15 min before or immediately after the release of compression reduced the degree

of injury compared with saline control. ($P < 0.01$; Fig. 5A). Additional study was undertaken to define better the onset of neuroprotection. In one experiment, a single dose (50 μ g/kg of bw) of asialoEPO or saline was administered 24 h or 15 min before nerve compression. The immediate postcompression CMAPs (day 0, Fig. 5B) recorded exhibited less functional loss ($P < 0.05$) for asialoEPO pretreatment (Fig. 5B). Similar observations were obtained with motor score testing, with the asialoEPO animals exhibiting significant improvement at the earliest time points evaluated (data not shown).

Discussion

Fully desialated rhEPO was prepared, and as reported (27, 28), disappeared very rapidly from the systemic circulation after i.v. injection. As anticipated, the affinity for EPO-R was similar to that of rhEPO when examined by using a variety of *in vitro* systems. Despite its short plasma half-life, asialoEPO appeared promptly within the CSF at concentrations within the *in vitro* neuroprotective range. *In vivo* autoradiography, performed by using sections obtained 4 h after administration of radioiodinated asialoEPO, confirmed that i.v.-administered drug actually reaches hippocampal and cortical neurons, typical cells expressing EPO-R in the normal brain. The anatomical pathway from the circulation across the blood-brain barrier to the labeled neurons visualized has not been established, but could involve the specialized glial cells that ensheath the capillaries (4).

Because of a short plasma survival of asialoEPO only a small proportion of the erythrocyte precursors are committed to enter the erythrocyte pool. Administration of asialoEPO, therefore, never increased hemoglobin concentration. Although it is inevitable that some erythrocyte precursors are recruited into the circulating pool, modulation of endogenous EPO concentrations (i.e., transient suppression) will tend to maintain red cell mass at the systemic set point. Although not directly assessed, similar kinetics for thrombocyte maturation (44–46) imply that asialoEPO would not appreciably increase the fraction of reactive platelets within the circulation.

Based on the observed transfer of asialoEPO into the brain, it is no surprise that asialoEPO is effective in the treatment of a variety of neurological injuries. The very brief duration of its action supports the concept of a triggering of neuroprotection, as has been suggested by *in vitro* models (26). The similar efficacy of asialoEPO and rhEPO observed in the stroke model confirm that only a very brief exposure is required to initiate a gene expression program (e.g., antiapoptosis) *in vivo* as well.

Longer followup periods of the stroke model will be necessary to determine whether late differences (i.e., other than effects on early apoptosis) exist and can be effected by additional exposure to asialoEPO. However, three consecutive daily doses of asialoEPO are as efficacious as rhEPO in the spinal cord compression model, because spinal cord injury occurs in distinct temporal phases that span several weeks (47, 48). The first is acute in onset (hours) and represents the immediate reaction to direct tissue injury, including cellular necrosis, hemorrhage, ischemia, and free radical formation. Histological evaluation shows that asialoEPO markedly attenuates this phase. Secondary injury occurs later (8–14 days) during which time axonal dysfunction becomes permanent because of the programmed cell death of oligodendrocytes. The observations reported here favor a model wherein primary and secondary injury are causally related. Thus, modulation of the primary injury phase profoundly affects the secondary phase, without need for additional therapy. Further experiments will be necessary to determine whether a later administration of asialoEPO (such as in a multiple dosing regimen) further improves motor recovery, such as might happen if asialoEPO is also effective at preventing the delayed oligodendrocyte apoptosis.

The sciatic nerve model also supports the relevance of a triggering mechanism by EPO. However, the immediate protective effect of treatment in the sciatic neuropathy model shown by the 15-min pretreatment protocol cannot be explained by an effect on gene expression, but may reflect maintenance of vascular autoregulation, as has been reported for experimental subarachnoid hemorrhage (40, 49). Further, an immediate difference in function for asialoEPO-treated animals despite disruption of axoplasm suggests that secondary causes, such as edema formation, are also likely reduced. Further study is needed to evaluate these possibilities. It has been reported that the sciatic nerve expresses very high levels of EPO-R (50). Since EPO-R expression is up-regulated after injury (50), postinjury treatment paradigms may yield additional interesting results.

Identification of a tissue-protective erythropoietin derivative with a brief plasma half-life potentially offers important advantages over rhEPO and would allow for multiple or chronic dosing strategies in neurodegenerative and other diseases. Another approach is to develop molecules that differ in mediating classical erythropoietic functions as compared with tissue-protective actions. Efforts to produce and validate candidate drugs that would constitute initial members of such a class of tissue-protective therapeutics may yield interesting results.

We thank Deborah Diaz and Daniel Gomez for providing invaluable technical assistance in the performance of these studies.

- Ruscher, K., Freyer, D., Karsch, M., Isaev, N., Megow, D., Sawitzki, B., Priller, J., Dirnagl, U. & Meisel, A. (2002) *J. Neurosci.* **22**, 10291–10301.
- Grimm, C., Wenzel, A., Groszer, M., Mayser, H., Seeliger, M., Samardzija, M., Bauer, C., Gassmann, M. & Reme, C. E. (2002) *Nat. Med.* **8**, 718–724.
- Dawson, T. M. (2002) *Lancet* **359**, 96–97.
- Brines, M. L., Ghezzi, P., Keenan, S., Agnello, D., de Lanerolle, N. C., Cerami, C., Itri, L. M. & Cerami, A. (2000) *Proc. Natl. Acad. Sci. USA* **97**, 10526–10531.
- Celik, M., Gokmen, N., Erbayraktar, S., Akhisaroglu, M., Konak, S., Ulukus, C., Genc, S., Genc, K., Sagiroglu, E., Cerami, A. & Brines, M. (2002) *Proc. Natl. Acad. Sci. USA* **99**, 2258–2263.
- Gorio, A., Gokmen, N., Erbayraktar, S., Yilmaz, O., Madaschi, L., Cichetti, C., Di Giulio, A. M., Vardar, E., Cerami, A. & Brines, M. (2002) *Proc. Natl. Acad. Sci. USA* **99**, 9450–9455.
- Junk, A., Mammis, A., Savitz, S. I., Singh, M., Roth, S., Malhotra, S., Rosenbaum, P., Cerami, A., Brines, M. & Rosenbaum, D. (2002) *Proc. Natl. Acad. Sci. USA* **99**, 10659–10664.
- Calvillo, L., Latini, R., Kajstura, J., Leri, A., Anversa, P., Ghezzi, P., Cerami, A. & Brines, M. (2003) *Proc. Natl. Acad. Sci. USA* **100**, 4802–4806.
- Kawakami, M., Sekiguchi, M., Sato, K., Kozaki, S. & Takahashi, M. (2001) *J. Biol. Chem.* **276**, 39469–39475.
- Digicaylioglu, M. & Lipton, S. A. (2001) *Nature* **412**, 641–647.
- Calapai, G., Marciano, M. C., Corica, F., Allegra, A., Parisi, A., Frisina, N., Caputi, A. P. & Buemi, M. (2000) *Eur. J. Pharmacol.* **401**, 349–356.
- Squadrito, F., Altavilla, D., Squadrito, G., Campo, G. M., Arlotta, M., Quartarone, C., Saitta, A. & Caputi, A. P. (1999) *Br. J. Pharmacol.* **127**, 482–488.
- Grasso, G. (2001) *J. Neurosurg. Sci.* **45**, 7–14.
- Juul, S. E., Anderson, D. K., Li, Y. & Christensen, R. D. (1998) *Pediatr. Res.* **43**, 40–49.
- Siren, A. L., Fratelli, M., Brines, M., Goemans, C., Casagrande, S., Lewczuk, P., Keenan, S., Gleiter, C., Pasquali, C., Capobianco, A., et al. (2001) *Proc. Natl. Acad. Sci. USA* **98**, 4044–4049.
- Agnello, D., Bigini, P., Villa, P., Mennini, T., Cerami, A., Brines, M. & Ghezzi, P. (2002) *Brain Res.* **952**, 128–134.
- Shingo, T., Sorokan, S. T., Shimazaki, T. & Weiss, S. (2001) *J. Neurosci.* **21**, 9733–9743.
- Ehrenreich, H., Hasselblatt, M., Dembowski, C., Cepek, L., Lewczuk, P., Stiefel, M., Rustenbeck, H. H., Breiter, N., Jacob, S., Knerlich, F., et al. (2002) *Mol. Med.* **8**, 495–505.
- Bernaudo, M., Marti, H. H., Roussel, S., Divoux, D., Nouvelot, A., MacKenzie, E. T. & Petit, E. (1999) *J. Cereb. Blood Flow Metab.* **19**, 643–651.
- Wiessner, C., Allegrini, P. R., Ekotodramis, D., Jewell, U. R., Stallmach, T. & Gassmann, M. (2001) *J. Cereb. Blood Flow Metab.* **21**, 857–864.
- Wolf, R. F., Peng, J., Friese, P., Gilmore, L. S., Burstein, S. A. & Dale, G. L. (1997) *Thromb. Haemostasis* **78**, 1505–1509.
- Wolf, R. F., Gilmore, L. S., Friese, P., Downs, T., Burstein, S. A. & Dale, G. L. (1997) *Thromb. Haemostasis* **77**, 1020–1024.
- Stohlawetz, P. J., Dzirio, L., Hergovich, N., Lackner, E., Mensik, C., Eichler, H. G., Kabrna, E., Geissler, K. & Jilma, B. (2000) *Blood* **95**, 2983–2989.
- Begu, Y. (1999) *Haematologica* **84**, 541–547.
- Fisher, J. W. (2003) *Exp. Biol. Med. (Maywood)* **228**, 1–14.
- Morishita, E., Masuda, S., Nagao, M., Yasuda, Y. & Sasaki, R. (1997) *Neuroscience* **76**, 105–116.
- Fukuda, M. N., Sasaki, H., Lopez, L. & Fukuda, M. (1989) *Blood* **73**, 84–89.
- Imai, N., Higuchi, M., Kawamura, A., Tomonoh, K., Oh-Eda, M., Fujiwara, M., Shimonaka, Y. & Ochi, N. (1990) *Eur. J. Biochem.* **194**, 457–462.
- Pedersen, L. O., Stryhn, A., Holter, T. L., Etzerodt, M., Gerwien, J., Nissen, M. H., Thogersen, H. C. & Buus, S. (1995) *Eur. J. Immunol.* **25**, 1609–1616.
- Komatsu, N., Nakauchi, H., Miwa, A., Ishihara, T., Eguchi, M., Moroi, M., Okada, M., Sato, Y., Wada, H., Yawata, Y., et al. (1991) *Cancer Res.* **51**, 341–348.
- Leveque, E., Nagel, M. D. & Haye, B. (1996) *Hematol. Oncol.* **14**, 137–146.
- Koshimura, K., Murakami, Y., Sohmiya, M., Tanaka, J. & Kato, Y. (1999) *J. Neurochem.* **72**, 2565–2572.
- European Economic Council Directive 86/609 (December 12, 1987) in *Official Journal of Law*, p. 358.
- Law by Decree No. 116 (February 18, 1992) *Gazzetta Ufficiale della Repubblica Italiana*, Suppl. 40.
- Law by Circular No. 8 (July 14, 1994) *Gazzetta Ufficiale della Repubblica Italiana*, Suppl. 40.
- Committee on Care and Use of Laboratory Animals (1996) *Guide for the Care and Use of Laboratory Animals* (Natl. Acad. Press, Washington, DC).
- Frankmann, S. P. (1986) *Physiol. Behav.* **37**, 489–493.
- Basso, D. M., Beattie, M. S. & Bresnahan, J. C. (1996) *Exp. Neurol.* **139**, 244–256.
- Basso, D. M., Beattie, M. S. & Bresnahan, J. C. (1995) *J. Neurotrauma* **12**, 1–21.
- Grasso, G., Buemi, M., Alafaci, C., Sfacteria, A., Passalacqua, M., Sturiale, A., Calapai, G., De Vico, G., Piedimonte, G., Salpietro, F. M. & Tomasello, F. (2002) *Proc. Natl. Acad. Sci. USA* **99**, 5627–5631.
- Bervar, M. (2000) *J. Neurosci. Methods* **102**, 109–116.
- Nagai, A., Nakagawa, E., Choi, H. B., Hatori, K., Kobayashi, S. & Kim, S. U. (2001) *J. Neuropathol. Exp. Neurol.* **60**, 386–392.
- Siren, A. L., Knerlich, F., Poser, W., Gleiter, C. H., Bruck, W. & Ehrenreich, H. (2001) *Acta Neuropathol.* **101**, 271–276.
- Tange, T. & Miyazaki, H. (1996) *Pathol. Int.* **46**, 968–976.
- Eaton, D. L. & de Sauvage, F. J. (1995) *Curr. Opin. Hematol.* **2**, 167–171.
- Li, J. & Kuter, D. J. (2001) *Int. J. Hematol.* **74**, 365–374.
- Liu, X. Z., Xu, X. M., Hu, R., Du, C., Zhang, S. X., McDonald, J. W., Dong, H. X., Wu, Y. J., Fan, G. S., Jacquin, M. F., et al. (1997) *J. Neurosci.* **17**, 5395–5406.
- Bethea, J. R., Castro, M., Keane, R. W., Lee, T. T., Dietrich, W. D. & Yezierski, R. P. (1998) *J. Neurosci.* **18**, 3251–3260.
- Springborg, J. B., Ma, X., Rochat, P., Knudsen, G. M., Amtorp, O., Paulson, O. B., Juhler, M. & Olsen, N. V. (2002) *Br. J. Pharmacol.* **135**, 823–829.
- Campana, W. M. & Myers, R. R. (2001) *FASEB J.* **15**, 1804–1806.
- European Pharmacopoeia (2000) in *2001 Supplement* (Council of Europe, Strasbourg, France), pp. 277–281.

A nonerythropoietic derivative of erythropoietin protects the myocardium from ischemia–reperfusion injury

Fabio Fiordaliso^{*†}, Stefano Chimentì^{*†}, Lidia Staszewsky^{*}, Antonio Bai^{*}, Eleonora Carlo^{*}, Ivan Cuccovillo^{*}, Mirko Doni^{*}, Manuela Mengozzi^{*}, Rossella Tonelli^{*}, Pietro Ghezzi^{**}, Thomas Coleman[‡], Michael Brines[‡], Anthony Cerami^{*§}, and Roberto Latini^{*¶}

^{*}Mario Negri Institute for Pharmacological Research, Milan 20157, Italy; ^{**}Kenneth S. Warren Institute, Ossining, NY 10562; and [‡]Department of Medicine, New York Medical College, Valhalla, NY 10595

Contributed by Anthony Cerami, December 16, 2004

The cytokine erythropoietin (EPO) protects the heart from ischemic injury, in part by preventing apoptosis. However, EPO administration can also raise the hemoglobin concentration, which, by increasing oxygen delivery, confounds assignment of cause and effect. The availability of EPO analogs that do not bind to the dimeric EPO receptor and lack erythropoietic activity, e.g., carbamylated EPO (CEPO), provides an opportunity to determine whether EPO possesses direct cardioprotective activity. *In vivo*, cardiomyocyte loss after experimental myocardial infarction (MI) of rats (40 min of occlusion with reperfusion) was reduced from ~57% in MI-control to ~45% in animals that were administered CEPO daily for 1 week (50 µg/kg of body weight s.c.) with the first dose administered intravenously 5 min before reperfusion. CEPO did not increase the hematocrit, yet it prevented increases in left ventricular (LV) end-diastolic pressure, reduced LV wall stress in systole and diastole, and improved LV response to dobutamine infusion compared with vehicle-treated animals. In agreement with the cardioprotective effect observed *in vivo*, staurosporine-induced apoptosis of adult rat or mouse cardiomyocytes *in vitro* was also significantly attenuated (~35%) by CEPO, which is comparable with the effect of EPO. These data indicate that prevention of cardiomyocyte apoptosis, in the absence of an increase in hemoglobin concentration, explains EPO's cardioprotection. Nonerythropoietic derivatives such as CEPO, devoid of the undesirable effects of EPO, e.g., thrombogenesis, could represent safer and more effective alternatives for treatment of cardiovascular diseases, such as MI and heart failure. Furthermore, these findings expand the activity spectrum of CEPO to tissues outside the nervous system.

apoptosis | cardioprotection | cytokine | tissue injury

Erythropoietin (EPO) protects the brain and the spinal cord from ischemic and traumatic injury (1, 2), the peripheral nerve from diabetic damage (3), the kidney from ischemic (4, 5) or toxic insults (6), and the heart from acute ischemia, either permanent (7–9) or with reperfusion (10). Current data suggest that the observed protective effects of EPO depend on an antiapoptotic effect of this cytokine (7, 10). In the brain, EPO also greatly reduces the inflammatory response after ischemia–reperfusion (11). It is notable that in several acute models, e.g., brain ischemia, a single dose of EPO that does not increase the Hb concentration nevertheless confers neuroprotection. However, in other *in vivo* injury models, including cardiac ischemia with reperfusion and diabetic neuropathy, injury develops gradually, and multiple doses of EPO appear superior but also increase the Hb concentration. The possibility that part of the benefit obtained with EPO in these models may depend on the increased oxygen-carrying capacity of the blood cannot be excluded. However, cardiac protection has clearly been demonstrated after only a single dose (8, 10) when evaluated 1–3 days after infarction before any increase in hematocrit was measur-

able. Furthermore, the fact that EPO is cytoprotective for cardiomyocytes *in vitro* (7) indicates that it has some direct cardioprotective effects independent of changes in Hb concentration.

Recently, a second receptor for EPO that mediates EPO's tissue protection has been identified as consisting of the EPO receptor and β -common (CD131) receptor, which is present in the myocardium (12). The EPO molecule can be modified, such as by carbamylation [carbamylated EPO (CEPO)], so that it signals only through this receptor and not the homodimeric EPO receptor yet is neuroprotective (13). By using CEPO, a definitive proof of concept that cardiac protection by EPO does not depend on, increases in red blood cell number can now be accomplished.

In the current study, we determined whether CEPO protects cardiac myocytes from ischemia–reperfusion injury-related apoptosis *in vivo* and *in vitro*. A CEPO-mediated reduced cell loss was observed *in vitro*, as expected, and was also obtained *in vivo*. Furthermore, a favorable outcome [left ventricular (LV) function, basal and under stress] occurred *in vivo* after 1 week of daily dosing, which did not affect Hb concentration. Taken together, these data confirm a direct effect of EPO/CEPO on the myocardium.

Materials and Methods

All experiments were performed in a blinded fashion and in accordance with all laws and regulations pertaining to animal research.

Cardiomyocytes in Primary Culture. LV myocytes were isolated from adult Sprague–Dawley rats and C57/BL6 mice as described (14). Briefly, hearts were perfused through the aorta with collagenase buffer (Selected Type II, Worthington Biochemical) and gassed in an atmosphere of 85% O₂ and 15% N₂ at 37°C. LV myocytes were then isolated by mechanical dissociation, separated by differential centrifugation, and plated on 35-mm laminin-coated polystyrene tissue culture dishes in MEM supplemented with Hanks' salts and L-glutamine (GIBCO). After 1 h of plating, the medium was changed, and CEPO [100 ng/ml, prepared as described (13)] was added to the myocytes 30 min before induction of apoptosis by staurosporine (2 µM, Sigma-Aldrich). After 16 h of incubation, cardiomyocytes were fixed and processed for the assessment of apoptosis. Identification of apoptotic cell death was determined by the presence of double-stranded DNA cleavage, using a terminal deoxynucleotidyltrans-

Abbreviations: EPO, erythropoietin; rhEPO, recombinant human EPO; CEPO, carbamylated EPO; MI, myocardial infarction; LV, left ventricular; SF, shortening fraction; TdT, terminal deoxynucleotidyltransferase.

[†]F.F. and S.C. contributed equally to this work.

[§]To whom correspondence should be addressed. E-mail: acerami@kswi.org.

© 2005 by The National Academy of Sciences of the USA

ferase (TdT) assay, and confirmed by evaluation using interference contrast microscopy of myocyte morphological features characteristic of apoptosis.

In Vivo Experimental Protocol. Male Sprague-Dawley rats (253 ± 4 g) were anesthetized with isoflurane 3% (O_2 , 0.25 liters/min; N_2 , 0.4 liters/min) and were ventilated (70 breaths per min, tidal volume of 1.2 ml per 100 g of body weight) through an endotracheal cannula. The left anterior descending coronary artery was ligated with a 7-0 silk suture after exteriorization of the heart through a 15-mm opening at the fourth-intercostal space. An overhand knot was tied over two pieces of suture to arrest blood flow and was removed after 40 min to initiate reperfusion. Ischemia was confirmed by the appearance of ventricular ectopy and blanching of the myocardium. The chest was then closed under negative pressure, and the rat was weaned from mechanical ventilation under continuous electrocardiographic monitoring. Successful reperfusion was indicated by a restoration of normal cardiac rubor. Sham-operated rats underwent identical surgical procedures, but without coronary artery ligation. CEPO dissolved in saline was administered a dose of $50 \mu\text{g/kg}$ of body weight i.v. 5 min before reperfusion, then $50 \mu\text{g/kg}$ of body weight s.c. every day for 6 days. Hematocrit was assessed in duplicate from tail blood on day 7. Blood was collected 3–4 and 24 h after the last CEPO administration. CEPO in plasma was measured with an ELISA by using CEPO as a standard, a monoclonal anti-rhEPO (MAB287, R & D Systems) as capture antibody, and a polyclonal anti-rhEPO (AB-286-NA, R & D Systems), biotinylated according to standard procedures, as detection antibody. The sensitivity of the assay was 0.5 ng/ml.

Echocardiography. Rats surviving a 40-min left anterior descending coronary artery occlusion underwent transthoracic echocardiography (Aloka SSD-5500, Aloka, Tokyo) on day 14 under light sedation (diazepam and xylazine i.p.) by using a 13-MHz linear transducer at high frame rate imaging (57 Hz). Short- and long-axis 2D views and M-mode at the level of infarction were analyzed in real-time and recorded on a magnetooptic disk for off-line analysis by a sonographer who was blinded to study treatments. Anterior and posterior end-diastolic and end-systolic wall thicknesses and LV internal dimensions were measured, as recommended by the American Society of Echocardiography (15, 16). Shortening fraction (SF) was calculated from the composite LV internal, diastolic (LVIDd) and LV internal, systolic (LVIDs) dimensions as

$$\text{SF} = [(LVIDd - LVIDs)/LVIDd] \times 100$$

from M-mode short-axis views. LV end-diastolic volume, LV end-systolic volume, and LV ejection fraction were calculated by modified Simpson's single-plane rule from a long-axis view. The 2D echocardiographic images were divided into 16 segments that were counted as abnormal at any degree of wall motion abnormality, e.g., akinesis, dyskinesis, and hypokinesis. LV wall dys-synergy (akinetic, dyskinetic, and severely hypokinetic segments) was considered as an *in vivo* index of the extent of damage caused by infarction to the ventricular wall. Systolic and diastolic wall stress was calculated from LV systolic and diastolic pressure measured with a Millar catheter (see below) and echocardiographic dimensions by the formula

$$WS = P \cdot a^3 \cdot (1 + b^3) / 2R^3 \cdot (b^3 - a^3),$$

where P = intraventricular pressure, R = LV radial coordinate, a = LV inner radius, and b = LV outer radius (17, 18). After echocardiographic examination at rest, stepwise i.v. (22-gauge heparin lock percutaneously inserted into the tail vein) infusion

of dobutamine (echo stress) was performed to evaluate myocardial viability and recovery of global LV function (19, 20).

Hemodynamics. At least 24 h after completion of echocardiographic exams (i.e., day 15), a microtip pressure transducer (SPC-320, Millar Instruments, Houston) was inserted into the right carotid artery to measure systolic and diastolic blood pressure and heart rate (Windowgraph, Gould Electronics, Valley View, OH) under pentobarbital anesthesia (50 mg/kg i.p.). The pressure transducer was then advanced into the LV to measure systolic and end-diastolic pressure, the first derivatives (positive and negative) of LV pressure over time.

Histomorphometry. Upon completion of hemodynamic measurements, the heart was arrested in diastole by i.v. injection of a 2.5-M solution of KCl, quickly removed from the chest, blotted dry, and weighted. The atria were trimmed, and the free right ventricle wall and LV inclusive of the septum were weighed individually. LV internal length was measured by use of a probe. Two slices just below the arterial ligation, basal and apical, were fixed in formaldehyde. Two 5- μm sections from each paraffin-embedded slice (i.e., basal and apical) were obtained (one just below the ligature and the other from the basal side of the apical part of LV) and were stained with hematoxylin/eosin. Scar and spared myocardium area were assessed by counting the number of intersection points of an ocular grid with 121 points overlying scar (infarct) or spared myocardium of the LV. Infarct area was calculated as the ratio between scar area and the area of the whole-LV section and expressed in percentages. The cardiomyocyte cross-sectional area was measured by manually tracing the cell contour on images acquired on the IMAGE ANALYZER IBAS 2.0 (Kontron-Zeiss image analysis system) at $\times 400$ magnification and averaged >50 cardiomyocytes in each section (21). The total number and volume of myocytes were determined by quantitative morphometric methods on hematoxylin/eosin-stained 5- μm sections (22). Measurements obtained in the two representative sections of each heart were averaged.

In Situ TdT Assay for Detection of Apoptosis. Myocytes obtained by isolation from different rat or mouse hearts of each experimental groups were incubated with TdT (23). Positive controls (myocytes treated with DNase I) and negative controls (omission of biotin-16-dUTP or TdT) were also included. Nuclei were visualized with propidium iodide, and interference contrast microscopy was used to exclude apoptotic nuclei of non-cardiomyocyte origin. The number of TdT-labeled cells was determined by two different operators blinded to the experimental groups by counting an average of >450 isolated myocytes in each culture dish. Immunofluorescent images were obtained by using an Olympus FV500 laser-scanning confocal microscope.

Calculations and Statistical Analysis. All data are presented as mean \pm SEM. Mean changes versus baseline in echocardiographic variables during dobutamine infusion were calculated by area under effect versus dose-response curve truncated at $15 \mu\text{g}$ of dobutamine (i.e., the plateau) and used to estimate inotropic reserve. Maximal values of heart rate and SF on dobutamine were also calculated. Experimental groups were compared by one-way ANOVA, followed by post hoc Dunnett's test, using myocardial infarction (MI)-control as reference group (PRISM 4.0 for Windows).

Results

In Vitro Study. In contrast to cells cultured in serum-free medium for 16 h (Fig. 5 A and B, which is published as supporting information on the PNAS web site), myocytes in the presence of staurosporine showed cytoplasm shrinkage, nuclear condensation, and fragmentation (Fig. 5 C and D) associated with 3'-OH



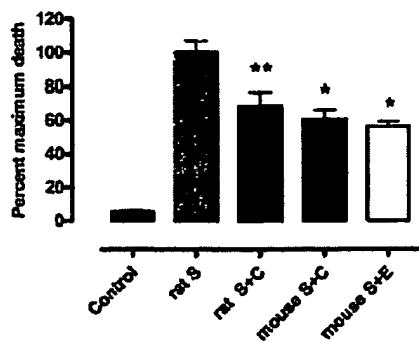


Fig. 1. Mean percentage of myocytes positive for TdT assay counted on 450 cells in each dish obtained by isolation from different rat or mouse hearts. Shown are data for rat control ($n = 9$), S (Staurosporine, $n = 10$), rat S plus C (S plus CEPO, $n = 10$), mouse S plus C ($n = 4$), and mouse S plus E (S plus EPO; $n = 4$). *, $P < 0.05$; **, $P < 0.01$ versus staurosporine.

DNA ends identified by TdT assay (Fig. 5D). Only nuclei of myocytes that retained the typical rod-shape morphology of uninjured cells were negative for the TdT staining (Fig. 5B–D). After 16 h of culture in the absence of staurosporine, rat myocytes exhibited a low basal percentage of TdT-labeled nuclei ($3.0 \pm 0.5\%$) that markedly increased 18.3-fold ($55.0 \pm 3.7\%$; $P < 0.01$, Fig. 1) after staurosporine incubation (S, $2 \mu\text{M}$) to the medium. The presence of CEPO (S plus C) was associated with a significant reduction of staurosporine-induced apoptosis to $37.5 \pm 4.8\%$ ($P < 0.01$), confirming a direct effect of CEPO on survival. A similar degree of protection was observed for EPO (S plus E). Cells from either rats or mice behaved similarly.

In Vivo Study. A total of 38 male CD rats underwent surgery, and 8 rats (21%) died within 6 h after surgery. There were no

differences in the distribution of perioperative mortality between the MI groups. Postmortem examination revealed extensive MIs. Ten infarcted rats received CEPO in saline 0.9% (MI-CEPO group), 13 rats used as controls received saline 0.9% (MI-control group), and 8 rats served as Sham-operated controls (Sham group). All were included in final analysis, except for three MI-control rats who died during followup. CEPO was measurable in all treated rats, at both 3–4 h and 24 h after s.c. administration; concentrations averaged $55.5 \pm 8.7 \text{ ng/ml}$ and $15.2 \pm 1.4 \text{ ng/ml}$, respectively. CEPO was always below the detection limit in untreated rats. As anticipated, CEPO did not affect the hematocrit on day 7 after surgery: MI-CEPO, $43.6 \pm 1.7\%$; MI-control, $41.6 \pm 2.0\%$ ($P = \text{not significant}$).

Histomorphometric Analysis. Infarct size, calculated as the fractional area of the scar, was smaller in MI-CEPO group than in the MI-control group: 17% versus 23% (Fig. 2A; $P = 0.065$). Calculated number of cardiac myocyte nuclei in the whole LV was decreased significantly in both MI groups (Fig. 2B). Cardiac myocyte volume per nucleus was smaller in CEPO-treated animals (Fig. 2C; $P < 0.05$). Consistent with this result, myocyte cross-sectional area in MI-CEPO group was 14% lower than in the MI-control group (Fig. 2D; $P < 0.05$).

Echocardiography. Cardiac anatomical and functional variables (LV wall thickness, internal chamber diameter, SF, LV volumes, and ejection fraction, and LV wall motion) measured at rest showed a dilated and dysfunctional left ventricle in infarcted animals when compared with Sham-operated animals (Table 1). CEPO treatment was associated with a nonsignificant improvement in other variables except for LV wall stress in diastole. Although LV wall stress increased in both systole and diastole for infarcted animals, CEPO treatment significantly reduced the deterioration compared with vehicle-treated controls (Fig. 3). After dobutamine infusions from 0 to $40 \mu\text{g/kg}$ per min, Inotropic reserve (Fig. 4A) and peak (maximum) SF were

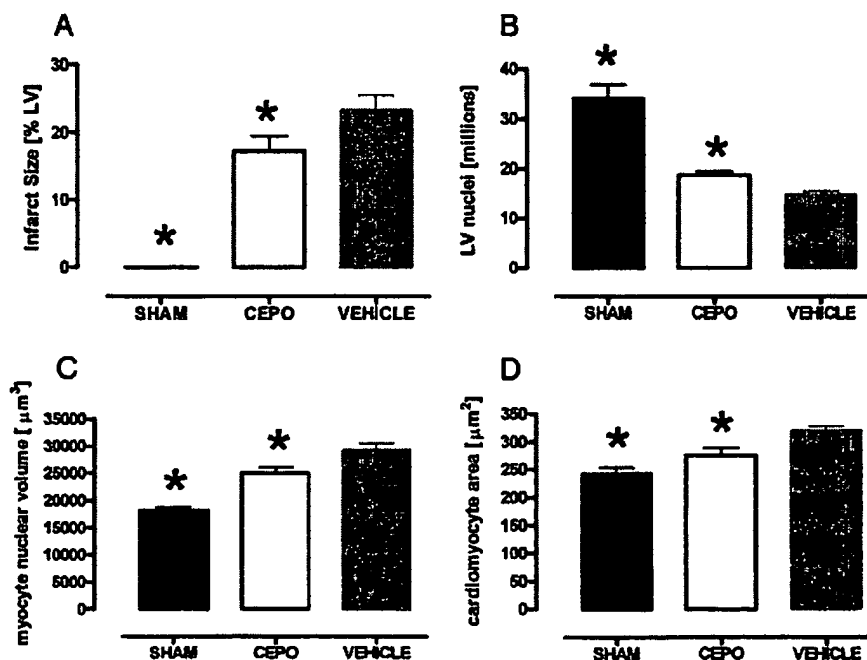


Fig. 2. Histomorphometric evaluation of infarct size (A), number of cardiac myocyte nuclei in left ventricle (B), cardiac myocyte volume per nucleus (C), and cross-sectional area of cardiac myocytes in the spared left ventricle of Sham-operated rats and in coronary-ligated rats untreated or treated with CEPO (D). MI-control group; CEPO, MI-CEPO group. *, $P < 0.01$ versus vehicle.

Table 1. Baseline echocardiographic variables measured 14 days after ischemia and reperfusion in rats Sham-operated, with infarction treated with CEPO or untreated (VEH)

	CEPO (n = 10)	VEH (n = 10)	Sham (n = 7)
Heart rate, bpm	403 ± 20	346 ± 18	354 ± 25
LVIDd, mm	7.52 ± 0.30	7.79 ± 0.31	6.31 ± 0.10*
LVIDs, mm	4.65 ± 0.41	5.34 ± 0.43	2.83 ± 0.32*
SE, %	39.1 ± 3.7	31.8 ± 3.8	49.1 ± 2.2*
IVSThd, mm	1.97 ± 0.05	1.91 ± 0.05	1.99 ± 0.04
AWThd, mm	1.22 ± 0.08	1.16 ± 0.12	1.94 ± 0.03*
EDV, ml	0.35 ± 0.03	0.41 ± 0.03	0.30 ± 0.03
ESV, ml	0.15 ± 0.02	0.19 ± 0.02	0.06 ± 0.03*
EF, %	54.7 ± 4.7	51.1 ± 12.1	81.1 ± 2.0*
A/D/H extension, %	22.80 ± 1.87	26.67 ± 1.67	—

Dunnett comparison with the VEH group (reference group). *, $P < 0.01$. LVIDd, LV internal diastolic diameter; LVIDs, LV internal systolic diameter; IVSThd, diastolic interventricular septum thickness; AWThd, diastolic anterior wall thickness; EDV, end-diastolic volume; ESV, end-systolic volume; A/D/H, akinesis/dyskinesis/hypokinesis.

greater in Sham-operated rats than in infarcted rats ($P < 0.01$), MI-CEPO rats responded to dobutamine better ($P < 0.05$) than did MI-control rats (Fig. 4 A and B). These effects on SF were observed in the absence of differences in peak heart rate (Fig. 4C).

Hemodynamics. Systemic arterial and LV pressures, their derivative and heart rate, did not show significant changes attributable to MI, except for LV end-diastolic pressure that was significantly increased: 2.1 ± 0.5 mmHg in Sham versus 7.1 ± 1.0 mmHg in MI-control ($P < 0.01$). CEPO attenuated the increase in LV end-diastolic pressure observed in MI-controls: MI-CEPO, 4.3 ± 0.6 mmHg; MI-control, 7.1 ± 1.0 mmHg ($P = 0.023$).

Discussion

The results obtained from the isolated adult rat ventricular cardiomyocytes show that CEPO, a nonerythropoietic derivative

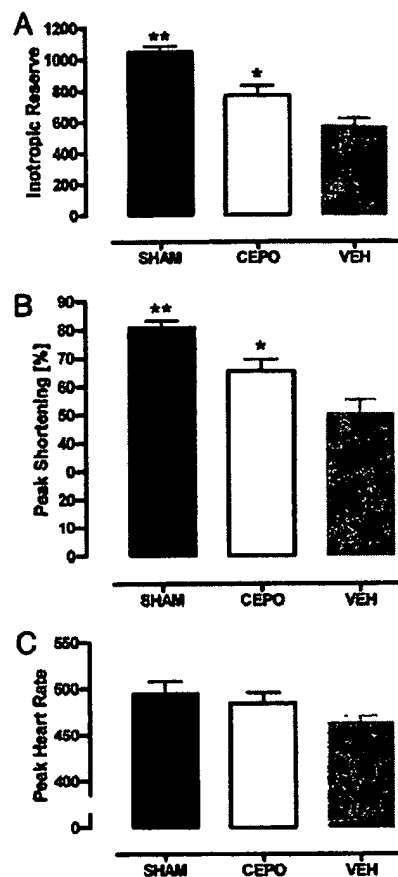


Fig. 4. Echo dobutamine stress test for the assessment of myocardial viability in lightly sedated rats. Inotropic reserve (A), Maximum (peak) SF (B), and maximum heart rate (C) on dobutamine in Sham-operated rats and in coronary ligated rats untreated or treated with CEPO are shown. VEH, MI-control group; CEPO, MI-CEPO group. *, $P < 0.05$; **, $P < 0.01$ versus VEH group.

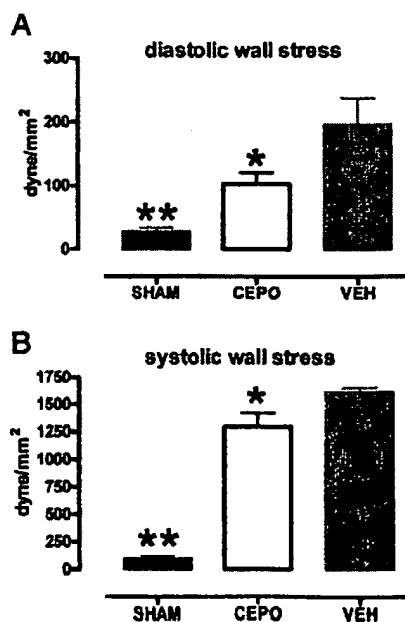


Fig. 3. CEPO administration prevents full increase in LV wall stress in diastole (A) and in systole (B). *, $P < 0.05$ or **, $P < 0.01$ versus MI-control (VEH).

of EPO, possesses the same antiapoptotic effect as previously observed for EPO (7). Positive results obtained by using cells from two species (rat and mouse) confirm that the findings are general in nature. Because CEPO has no affinity for the classical EPO receptor (i.e., the erythropoietic dimeric form), cytoprotection by CEPO is mediated by another receptor type. Prior study has shown that this tissue protective receptor uses the β -receptor common to IL-3, IL-5, and granulocyte-macrophage colony-stimulating factor (12). Extension of the protective effects of CEPO from the nervous system to the heart supports the concept of EPO and CEPO as general tissue-protective molecules.

In the cardiomyocyte model, exposure to staurosporine induced the majority of myocytes to undergo apoptosis similar to that observed for previous studies using 12–24 h of hypoxia (7, 8). Staurosporine, an inhibitor of protein kinase C, has been shown to induce apoptosis in a wide variety of cell types, including cardiomyocytes (24). An advantage of using staurosporine to induce apoptosis is that the morphological and molecular characteristics of staurosporine-induced injury, such as cytoplasm shrinkage, nuclear condensation (Fig. 5) and fragmentation, loss of mitochondrial transmembrane potential, Bax translocation, cytochrome *c* release, and caspase-3 activation (25), closely mimic apoptotic processes during hypoxia and reoxygenation of isolated adult cardiomyocytes (26).

The positive results obtained *in vitro* encouraged testing cardiac protection *in vivo* by using a rat model of myocardial

infarction with reperfusion. Treatment with CEPO, beginning just before the release of coronary occlusion, and then continued once daily for 6 additional days, resulted in an attenuated loss of cardiac myocytes and prevented compensatory hypertrophy, as assessed on day 15 after infarction. These findings, similar to those observed for EPO (7), can be explained by the antiapoptotic action observed for both EPO (7) and CEPO, particularly as expected for in the LV free wall (27, 28) and the region adjacent to the infarcted LV free wall (29, 30). Although assessment of MI size on day 15 by calculation of fractional area of the scar is potentially complicated by scar shrinkage and compensatory hypertrophy of spared myocardium, a trend toward smaller scars in CEPO-treated rats was observed, which is consistent with the observed 21% reduction in cardiomyocyte loss. The attenuation of cell loss and hypertrophy by CEPO was also accompanied by other evidence of more favorable changes in LV function under both basal and stressed conditions. Specifically, the small but significant increase in LV end-diastolic pressure observed in MI-control was normalized by CEPO. This effect, together with the strong trend for smaller LV volumes in the CEPO group, explains the significant reduction in LV diastolic wall stress by 47%. Wall stress is a major determinant of the LV progressive dilatation and the associated hemodynamic deterioration that begins in the first days after MI, and it becomes more evident over the following months.

Because 40 min of ischemia followed by reperfusion led to a mild-to-moderate structural and functional impairment over a period of 15 days, we reasoned that LV functional reserves, as assessed by dobutamine infusion, might amplify differences attributable to treatment with CEPO (19, 20). Indeed, although the SF under baseline conditions was comparable at $39 \pm 4\%$ in the CEPO group and $32 \pm 4\%$ in the MI-control group ($P = \text{NS}$), the CEPO-treated group showed a better response than vehicle to dobutamine (Fig. 4A), with a greater peak SF, without significant differences in the maximum heart rate (Fig. 4B and C).

Cardioprotection by EPO has been shown to involve both acute and delayed components, which is consistent with a pharmacological form of preconditioning (reviewed by Bogoyevitch in ref. 31). In our experiments, we administered CEPO at the time of reperfusion in a manner consistent with timing for many clinical interventions, e.g., percutaneous angioplasty. This procedure likely provides both acute and delayed effects. However, it is currently unknown what schedule of dosing will result in maximum tissue salvage. In a recent limited time-window study using EPO, administration at the time of cardiac reperfusion was associated with a better outcome than when given 2 h before (32). However, given the prolonged time course of ventricular remodeling and development of heart

failure and its association with continued cardiomyocyte apoptosis (reviewed in refs. 30 and 33), it is most likely that multiple doses of tissue-protective cytokines will be required to produce maximum protection. Another critical but unexplored question concerning intervention with tissue protective cytokines in myocardial ischemia is information on the optimum dose. This issue is especially critical because EPO has been shown to exhibit an inverted U-shaped dose-response curve in a number of experimental systems, e.g., EPO-mediated endothelial cell nitric oxide (NO) production (34), such that high doses of EPO lose biological activity. Furthermore, because EPO has been shown in the nervous system to require only a brief presence to trigger protective functions (2), further study will be needed to determine whether peak serum concentrations or area under the concentration curve is the important variable.

The larger fraction of myocardium recruitable for contraction in the CEPO group and the structural and functional benefits obtained with CEPO definitively demonstrate that cardioprotection can be separated from the erythropoietic action of EPO. The dissociation of myocardial protection from erythropoiesis is highly desirable from the perspective of a therapeutic use of CEPO. Notably, in mice, EPO-mediated increases in hematocrit causes vasoconstriction and cardiac dysfunction through NO depletion and endothelin activation (35, 36). Furthermore, in humans, recombinant human EPO (rhEPO) administration can lead to hypertension (37–39). It is also well known that EPO can cause thrombosis and therefore tissue injury (40). Even a single exposure of normal humans to EPO causes a dose-dependent increase in E-selectin within 2 days, which is consistent with significant endothelial cell activation (41). Similar responses have also been documented for other markers associated with thrombosis, e.g., P-selectin, and *in vitro* studies confirm direct and rapid prothrombotic effects of EPO on the endothelium (42). Clearly, an increased potential for thrombosis is not desirable in vascular occlusive myocardial disease.

These considerations suggest that the possible beneficial effects of rhEPO therapy might be masked or even reversed by these adverse effects of EPO. The availability of nonerythropoietic derivatives such as CEPO, retaining tissue protection but without the undesired effects of rhEPO, could be safer and more effective therapeutics for cardiovascular diseases such as myocardial infarction and heart failure. Finally, we expect that the protective effects of molecules like CEPO will extend to other tissues and organs for which EPO has been shown in experimental models to provide protection from injury.

We thank Ingrid Seinen (Aloka, Assago, Italy) for setting up echocardiography for the dobutamine stress test. This work was partially supported by a grant from Fondazione CARIPLO Bando 2003 and European Genomic Network Contract LSHM-CT-2003 503254.

- Brines, M. L., Ghezzi, P., Keenan, S., Agnello, D., de Lanerolle, N. C., Cerami, C., Itri, L. M. & Cerami, A. (2000) *Proc. Natl. Acad. Sci. USA* 97, 10526–10531.
- Erbayraktar, S., Grasso, G., Sfacteria, A., Xie, Q. W., Coleman, T., Kreilgaard, M., Torup, L., Sager, T., Erbayraktar, Z., Gokmen, N., et al. (2003) *Proc. Natl. Acad. Sci. USA* 100, 6741–6746.
- Bianchi, R., Buyukakilli, B., Brines, M., Savino, C., Cavaletti, G., Oggioni, N., Lauria, G., Borgna, M., Lombardi, R., Cimen, B., et al. (2004) *Proc. Natl. Acad. Sci. USA* 101, 823–828.
- Gong, H., Wang, W., Kwon, T. H., Jonassen, T., Li, C., Ring, T., Froki, A. J. & Nielsen, S. (2004) *Kidney Int.* 66, 683–695.
- Yang, C. W., Li, C., Jung, J. Y., Shin, S. J., Choi, B. S., Lim, S. W., Sun, B. K., Kim, Y. S., Kim, J., Chang, Y. S. & Bang, B. K. (2003) *FASEB J.* 17, 1754–1755.
- Yalcin, S., Muftuoglu, S., Cetin, E., Sarer, B., Yildirim, B. A., Zeybek, D. & Orhan, B. (2003) *Med. Oncol.* 20, 169–174.
- Calvillo, L., Latini, R., Kajstura, J., Leri, A., Anversa, P., Ghezzi, P., Salio, M., Cerami, A. & Brines, M. (2003) *Proc. Natl. Acad. Sci. USA* 100, 4802–4806.
- Parsa, C. J., Matsumoto, A., Kim, J., Riel, R. U., Pascal, L. S., Walton, G. B., Thompson, R. B., Petrofski, J. A., Annex, B. H., Stamler, J. S. & Koch, W. J. (2003) *J. Clin. Invest.* 112, 999–1007.
- Parsa, C. J., Kim, J., Riel, R. U., Pascal, L. S., Thompson, R. B., Petrofski, J. A., Matsumoto, A., Stamler, J. S. & Koch, W. J. (2004) *J. Biol. Chem.* 279, 20655–20662.
- Moon, C., Krawczyk, M., Ahn, D., Ahmet, I., Paik, D., Lakatta, E. G. & Talan, M. I. (2003) *Proc. Natl. Acad. Sci. USA* 100, 11612–11617.
- Villa, P., Bigini, P., Mennini, T., Agnello, D., Laragione, T., Cagnotto, A., Viviani, B., Marinovich, M., Cerami, A., Coleman, T. R., et al. (2003) *J. Exp. Med.* 198, 971–975.
- Brines, M., Grasso, G., Fiordaliso, F., Sfacteria, A., Ghezzi, P., Fratelli, M., Latini, R., Xie, Q. W., Smart, J., Su-Rick, C. J., et al. (2004) *Proc. Natl. Acad. Sci. USA* 101, 14907–14912.
- Leist, M., Ghezzi, P., Grasso, G., Bianchi, R., Villa, P., Fratelli, M., Savino, C., Bianchi, M., Nielsen, J., Gerwien, J., et al. (2004) *Science* 305, 239–242.
- Kajstura, J., Fiordaliso, F., Andreoli, A. M., Li, B., Chimenti, S., Medow, M. S., Limana, F., Nadal-Ginard, B., Leri, A. & Anversa, P. (2001) *Diabetes* 50, 1414–1424.
- Sahn, D. J., DeMaria, A., Kisslo, J. & Weyman, A. (1978) *Circulation* 58, 1072–1083.

16. Schiller, N. B., Shah, P. M., Crawford, M., DeMaria, A., Devereux, R., Feigenbaum, H., Gutgesell, H., Reichek, N., Sahn, D., Schnittger, I., *et al.* (1989) *J. Am. Soc. Echocardiogr.* 2, 358–367.
17. Mirsky, I. (1969) *Biophys. J.* 9, 189–208.
18. Anversa, P., Li, P., Malhotra, A., Zhang, X., Herman, M. V. & Capasso, J. M. (1993) *Am. J. Physiol.* 265, H713–H724.
19. Taylor, A. L., Kieso, R. A., Melton, J., Hite, P., Pandian, N. G. & Kerber, R. E. (1985) *Circulation* 71, 1292–1300.
20. Geleijnse, M. L., Fioretti, P. M. & Roelandt, J. R. (1997) *J. Am. Coll. Cardiol.* 30, 595–606.
21. Masson, S., Arosio, B., Luvara, G., Gagliano, N., Fiordaliso, F., Santambrogio, D., Vergani, C., Latini, R. & Annoni, G. (1998) *J. Mol. Cell. Cardiol.* 30, 1505–1514.
22. Anversa, P., Beghi, C., Kikkawa, Y. & Olivetti, G. (1985) *Am. J. Pathol.* 118, 484–492.
23. Fiordaliso, F., Leri, A., Cesselli, D., Limana, F., Safai, B., Nadal-Ginard, B., Anversa, P. & Kajstura, J. (2001) *Diabetes* 50, 2363–2375.
24. Yue, T. L., Wang, C., Romanic, A. M., Kikly, K., Keller, P., DeWolf, W. E., Jr., Hart, T. K., Thomas, H. C., Storer, B., Gu, J. L., *et al.* (1998) *J. Mol. Cell. Cardiol.* 30, 495–507.
25. Shiraiishi, J., Tatsumi, T., Keira, N., Akashi, K., Mano, A., Yamanaka, S., Matoba, S., Asayama, J., Yaoi, T., Fushiki, S., *et al.* (2001) *Am. J. Physiol.* 281, H1637–H1647.
26. Kang, P. M., Haunstetter, A., Aoki, H., Usheva, A. & Izumo, S. (2000) *Circ. Res.* 87, 118–125.
27. Gottlieb, R. A., Burleson, K. O., Kloner, R. A., Babior, B. M. & Engler, R. L. (1994) *J. Clin. Invest.* 94, 1621–1628.
28. Kajstura, J., Cheng, W., Reiss, K., Clark, W. A., Sonnenblick, E. H., Krajewski, S., Reed, J. C., Olivetti, G. & Anversa, P. (1996) *Lab. Invest.* 74, 86–107.
29. Cheng, W., Kajstura, J., Nitahara, J. A., Li, B., Reiss, K., Liu, Y., Clark, W. A., Krajewski, S., Reed, J. C., Olivetti, G. & Anversa, P. (1996) *Exp. Cell Res.* 226, 316–327.
30. Anversa, P., Cheng, W., Liu, Y., Leri, A., Redaelli, G. & Kajstura, J. (1998) *Basic Res. Cardiol.* 93, Suppl. 3, 8–12.
31. Bogoyevitch, M. A. (2004) *Cardiovasc. Res.* 63, 208–216.
32. Lipsic, E., van der Meer, P., Henning, R. H., Suurmeijer, A. J., Boddeus, K. M., van Veldhuisen, D. J., van Gilst, W. H. & Schoemaker, R. G. (2004) *J. Cardiovasc. Pharmacol.* 44, 473–479.
33. Takemura, G. & Fujiwara, H. (2004) *Pharmacol. Ther.* 104, 1–16.
34. Beleslin-Cokic, B. B., Cokic, V. P., Yu, X., Weksler, B. B., Schechter, A. N. & Noguchi, C. T. (2004) *Blood* 104, 2073–2080.
35. Quaschnig, T., Ruschitzka, F., Stallmach, T., Shaw, S., Morawietz, H., Goettsch, W., Hermann, M., Slowinski, T., Theuring, F., Hoher, B., Luscher, T. F. & Gassmann, M. (2003) *FASEB J.* 17, 259–261.
36. Ruschitzka, F. T., Wenger, R. H., Stallmach, T., Quaschnig, T., de Wit, C., Wagner, K., Labugger, R., Kelm, M., Noll, G., Rulicke, T., *et al.* (2000) *Proc. Natl. Acad. Sci. USA* 97, 11609–11613.
37. Anonymous (1991) *Am. J. Kidney Dis.* 18, 50–59.
38. Lim, V. S. (1991) *Am. J. Kidney Dis.* 18, 34–37.
39. Varet, B., Casadevall, N., Lacombe, C. & Nayeaux, P. (1990) *Semin. Hematol.* 27, 25–31.
40. Wagner, K. F., Katschinski, D. M., Hasegawa, J., Schumacher, D., Meller, B., Gembruch, U., Schramm, U., Jelkmann, W., Gassmann, M. & Fandrey, J. (2001) *Blood* 97, 536–542.
41. Stohlawetz, P. J., Dzirlo, L., Hergovich, N., Lackner, E., Mensik, C., Eichler, H. G., Kabrna, E., Geissler, K. & Jilma, B. (2000) *Blood* 95, 2983–2989.
42. Fuste, B., Serradell, M., Escolar, G., Cases, A., Mazzara, R., Castillo, R., Ordinas, A. & Diaz-Ricart, M. (2002) *Thromb. Haemostasis* 88, 678–685.

Mechanism of Protein Modification by Glyoxal and Glycolaldehyde, Reactive Intermediates of the Maillard Reaction*

(Received for publication, September 9, 1994, and in revised form, February 6, 1995)

Marcus A. Glomb† and Vincent M. Monnier

From the Institute of Pathology, Case Western Reserve University, Cleveland, Ohio 44106

The role of glyoxal and glycolaldehyde in protein cross-linking and *N*^ε-(carboxymethyl)lysine (CML) formation during Maillard reaction under physiological conditions was investigated. Incubation of bovine serum albumin with these reagents lead to rapid formation of C-2-imine cross-links and CML. Initial CML formation rate from glyoxal was not dependent on oxidation, suggesting an intramolecular Cannizzaro reaction. CML formation from glucose/lysine or Amadori product of both was strongly dependent on oxidation. Blocking of Amadori product by borate acid totally suppressed CML formation from Amadori product, but only by 37% in the glucose/lysine system. Trapping of glyoxal with aminoguanidine hardly suppressed CML formation from Amadori product, whereas it blocked 50% of CML production in the glucose/lysine system. While these results would support a significant role for glucose autooxidation in CML formation, the addition of lysine to a glucose/aminoguanidine incubation system catalyzed glyoxal-triazine formation 7-fold, thereby strongly suggesting that glucose autooxidation is not a factor for glyoxal-mediated CML formation. Based on these results, it can be estimated that approximately 50% of the CML forming in a glucose/lysine system originates from oxidation of Amadori product, and 40–50% originates from a pre-Amadori stage largely independent from glucose autooxidation. This step may be related to the so-called Namiki pathway of the Maillard reaction.

The reaction between reducing sugars and amino structures in amino acids or proteins (also called Maillard reaction) has been shown to proceed in living systems and to correlate with age and severity of diabetes (1). Unlike organic syntheses, it does not result in one or few well defined products but proceeds through complex reaction pathways resulting in a large number of structures (2). After the initial formation of a Schiff base adduct between the carbonyl and the amine moiety, the aldime rearranges to a more stable ketoamine or Amadori product. Enolization, dehydration, cyclization, fragmentation, and oxidation reactions form reactive intermediates that ultimately lead to stable end products.

Although enormous effort was devoted to elucidate the nature of these protein modifications, so far only two structures besides the Amadori product have been successfully estab-

lished *in vivo*, pentosidine and *N*^ε-carboxymethyllysine (CML)¹ (3, 4). A third structure, pyrrole, was found in tissue matrix by immunochemical and chromatographic methods (5–7), but its existence *in vivo* is controversial (8).

The slow progress in elucidating the structure of the major Maillard cross-link in proteins together with the finding of a C-2-glucose fragmentation product in form of CML, suggested to us that the pathway proposed by Namiki (9) may play an important role in CML formation and cross-linking. In this pathway, glyoxal and glycolaldehyde were detected as Maillard fragmentation products in heated model systems of sugars and alkylamines (10, 11). According to Namiki, the Schiff base adduct 1 undergoes retro aldol condensation at C-2–C-3 to yield fragment 2 (Fig. 1). Compound 2 is the Schiff base adduct of the amine with glycolaldehyde, which on one hand could hydrolyze to release glycolaldehyde or rearrange to form aldamine 3. Condensation with a second molecule 3 was proposed to result in pyrazine 4, which has been shown to be easily oxidized and fragmented to give, for example, di-Schiff base adduct 5 or to release glyoxal (12). Condensation with a second amine compound would yield imine 7. Thus, the formation of glyoxal and glycolaldehyde in this pathway are linked together, and both, upon reaction with amines, would result in common structures. Both molecules are highly reactive intermediates and have been reported to modify and cross-link proteins, although structures were only proposed (13–15).

Based on these preliminary observations and the finding that carboxymethylation of amino acids can occur with glyoxal in heated reaction mixtures (16, 17), we hypothesize that a mechanism involving glyoxal/glycolaldehyde could contribute to CML formation and protein cross-linking under physiological conditions. This hypothesis departs from the previous notion that CML originates only from the Amadori product (18, 19).

In the first part of this study, we investigated the relationship between glyoxal/glycolaldehyde and presumed C-2-imine cross-links 5/7 in proteins incubated with these carbonyl compounds and various sugars. In the second part, we studied the mechanism of CML formation from these reagents. In addition, we evaluated the contribution of glyoxal *versus* oxidative cleavage of the Amadori product on CML formation and the relative importance of the "Namiki pathway" during incubations with reducing sugars.

EXPERIMENTAL PROCEDURES

Reagents

Reagents of highest quality available were obtained from Sigma, Fisher, and Aldrich, unless otherwise indicated.

* This work was supported by grants from the National Eye Institute (EY 07099) and the National Institute on Aging (AG 05801). The costs of publication of this article were defrayed in part by the payment of page charges. This article must therefore be hereby marked "advertisement" in accordance with 18 U.S.C. Section 1734 solely to indicate this fact.

† Recipient of a Fellowship of the Deutsche Forschungsgemeinschaft, Germany. To whom correspondence should be addressed: Inst. of Pathology, Case Western Reserve University, 2085 Adelbert Rd., Cleveland, Ohio 44106. Tel.: 216-368-6613; Fax: 216-844-1810.

¹ The abbreviations used are: CML, *N*^ε-(carboxymethyl)lysine; GC/MS, coupled gas chromatography-mass spectrometry; HPLC, high performance liquid chromatography; BSA, bovine serum albumin; *N*^ε-(glutitolyl)lysine, reduced Amadori product of glucose and lysine; TLC, thin-layer chromatography; *t*-Boc, *t*-butoxycarbonyl.

Spectra

^1H and ^{13}C nuclear magnetic resonance (NMR) spectra ($\text{Me}_2\text{Si}(\text{CDCl}_3)_3$, 3-(trimethylsilyl)propionic-2,2,3,3- d_4 -acid (D_2O) as internal standards) were recorded with a Varian 300 MHz spectrometer Gemini-300 (Varian Associates, Inc. Palo Alto, CA). High resolution fast atom bombardment mass spectral data were obtained at Michigan State University Mass Spectrometry Facility, and high resolution mass spectra were obtained with a Kratos MS 25 RFA dual beam, double focussing, magnetic sector mass spectrometer (direct probe insertion, EI 20 eV).

High Performance Liquid Chromatography

HPLC was performed on a Waters gradient system (Waters Chromatography Division, Milford, MA) equipped with two model 510 pumps and a model 470 fluorescence detector. Amino acids were derivatized postcolumn with *o*-phthalaldehyde (Aldrich) (20). System 1 for detection of CML consisted of water (eluent A) and 70% methanol in water (eluent B), both with 0.01 M heptafluorobutyric acid (Aldrich), C18 column (0.4×25 cm, 5 μm , VYDAC 218TP54, Hesperia, CA), flow rate 1 ml/min, gradient 2% B for 20 min and then in 5 min to 100% B. System 2 for detection of CML and glucitolyl-lysine was as follows: column as system 1, with 5% propanol (eluent A) and 60% propanol in water (eluent B), both with 3 g of SDS (Fluka)/liter, 1 g of monobasic sodium phosphate monohydrate/liter, and adjusted to pH 2.8 with phosphoric acid, gradient 15% B \rightarrow 22% B in 30 min \rightarrow 40% B in 20 min \rightarrow 100% B in 5 min and flow rate 1 ml/min. System 3 for detection of 8 was as follows: column, flow and eluents like system 1, gradient 15% B \rightarrow 40% B in 25 min \rightarrow 50% B in 22 min \rightarrow 100% B in 3 min. System 4 for detection of 6 was as follows: column and flow like system 2, eluent A 5% propanol and eluent B 60% propanol in water, both with 3 g of SDS/liter, 1.5 g of monobasic sodium phosphate monohydrate/liter and adjusted to pH 7 with potassium hydroxide, gradient 15% B \rightarrow 25% B in 30 min \rightarrow 35% B in 5 min \rightarrow 100% B in 5 min. System 5 for preparative isolation of 6 was as follows: eluents like system 1, C18 column (2.2×25 cm, 10 μm , VYDAC 218TP1022), gradient 15% B \rightarrow 50% B in 50 min \rightarrow 100% B in 25 min and flow 8 ml/min. System 6 for preparative isolation of CML and 9 was as follows: eluents, column and flow like system 5, gradient 2% B for 40 min then to 100% B in 5 min. System 7 for detection of 9 was as follows: column, flow, and eluents like system 2, gradient 20% B \rightarrow 28% B in 40 min \rightarrow 100% B in 5 min.

Coupled Gas Chromatography-Mass Spectrometry

GC/MS was performed on a Hewlett Packard 5890 series II chromatograph (Wilmington, DE), quartz capillary column (25 m, inner diameter 0.2 mm, Ultra 5 (Hewlett Packard), 0.33 μm , He, 12 psi, 26.26 cm/s, constant flow program on), injection port 270 $^\circ\text{C}$, interface 280 $^\circ\text{C}$, temperature program 100 $^\circ\text{C}$ \rightarrow 200 $^\circ\text{C}$ /5 $^\circ\text{C}\cdot\text{min}^{-1}$ to 200 $^\circ\text{C}$ \rightarrow 270 $^\circ\text{C}$ /10 $^\circ\text{C}\cdot\text{min}^{-1}$ to 10 min isothermal 270 $^\circ\text{C}$; connected to Hewlett Packard 5971 series mass selective detector, EI and positive $\text{CH}_4\text{-CI}$ mode.

Chromatography

Silica gel 60 F₂₅₄ Merck 5554 (EM Separations, Gibbstown, NJ) was used for thin-layer chromatography (TLC) and silica gel (63–200 μm) (Alltech, Deerfield, IL) was used for column chromatography. Chromatography solvents were all ACS grade. From the individual chromatographic fractions, solvents were evaporated under reduced pressure.

Synthetic Procedures

Ethylenedihexylamine—A solution of 0.5 g (4.2 mmol) of 2,3-dihydroxy-1,4-dioxane (Fluka) and 1.25 g (12.5 mmol) of hexylamine (Fisher) in 5 ml of anhydrous methanol was stirred at 25 $^\circ\text{C}$ for 30 min, 380 mg of sodium borohydride (Fluka) was added, and after 15 min of stirring, the solvents were evaporated to dryness. The residue was taken up in 1 N NaOH and extracted with ethyl acetate. The combined organic layers were dried over anhydrous sodium sulfate and the solvents were evaporated. The residue was dissolved in 10 ml of anhydrous pyridine, and 5 ml of trifluoroacetic anhydride (Aldrich) were slowly added at 0 $^\circ\text{C}$. The solution was stirred for 5 min at 0 $^\circ\text{C}$ and then for 55 min at ambient temperature. The solvents were evaporated to dryness, and the resulting brown oil was purified by column chromatography (eluent CH_2Cl_2). Fractions containing *N,N'*-di-(trifluoroacetyl)ethylenedihexylamine (R_f 0.56, TLC (same solvent)) were combined and evaporated to dryness (300 mg (17%), colorless oil, GC t_R 23.21 min). CI-GC/MS, m/z 421 ($M + 1$; 100) 307(10) 224(13) 210(3) 198(6) 154(5). To remove the trifluoroacetyl groups, 300 mg of *N,N'*-di-(trifluoroacetyl)ethylenedihexylamine was dissolved in 0.5% potassium hydroxide solution in methanol and stirred for 45 min at 80 $^\circ\text{C}$. TLC (solvent as above) showed complete absence of trifluoroacetyl derivative. Solvents

were evaporated and the residue was taken up in 1 N NaOH and extracted with diethylether. The combined organic layers were dried over anhydrous sodium sulfate, and solvents were evaporated to yield ethylenedihexylamine (150 mg (overall 16%) of colorless oil, TLC R_f 0.49 (solvent butanol/water/acetic acid, 25:5:3), GC t_R 19.02 min). CI-GC/MS, m/z 229 ($M + 1$; 100) 227(91) 157(40) 128(51) 114(53). ^1H NMR(CDCl_3), δ (ppm) 0.88 (t, 6H, $J = 6.9$ Hz) 1.28 (m, 12H) 1.48 (m, 4H) 2.59 (t, 4H, $J = 7.5$ Hz) 2.71 (s, 4H).

2,15-Diamino-7,10-diaza-hexadecane-1,16-dioic acid 6—A suspension of 0.25 g (2.1 mmol) of 2,3-dihydroxy-1,4-dioxane, 1.28 g (5.2 mmol) of *N*-(4-Boc-lysine) (Bachem, Torrance, CA) and three potassium hydroxide pellets in 5 ml of anhydrous methanol was stirred for 1 h at room temperature. Following addition of 190 mg (5 mmol) of sodium borohydride, the solution was stirred for another 15 min, and the pH was then adjusted to 7 with 1 N HCl. TLC (solvent butanol/water/acetic acid, 25:5:3) revealed a new spot at R_f 0.10. Eluents were evaporated to dryness, protecting groups were removed by treatment with 3 N HCl for 30 min, and the solution was then freeze dried. The lyophilisate was taken up in water and subjected to preparative HPLC system 5. Fractions containing 6 were collected and freeze dried (65 mg (10%), colorless amorphous hygroscopic powder, HPLC system 5, t_R 63 min; system 3, t_R 47.5 min; system 4, t_R 30.3 min; GC (6 as its trifluoroacetyl-methyl ester derivative) t_R 32.81 min). EI(70 eV)-GC/MS, m/z 378 ($M^+ - 35$; 24) 356(9) 319(13) 309(35) 305(54) 184(29) 180(100) 178(48) 152(15) 140(98) 126(19) 114(9) 96(10) 84(10) 67(40). ^1H NMR(D_2O), δ (ppm) 1.38 (m, 4H), 1.62 (p, 4H, $J = 7.7$ Hz) 1.80 (m, 4H), 2.99 (t, 4H, $J = 7.7$ Hz), 3.28 (s, 4H), 3.81 (t, 2H, $J = 6.3$ Hz). ^{13}C NMR(D_2O), δ (ppm) 23.85, 27.56, 31.85, 45.39, 50.17, 55.68, 175.26. High resolution fast atom bombardment mass spectrometry, 319.4217 calculated 319.4233 for $\text{C}_{14}\text{H}_{31}\text{N}_4\text{O}_4$. Elementary analysis showed that material obtained was the 6-4 heptafluorobutyrate salt.

***N*-(Carboxymethyl)lysine—246 mg (1 mmol) of *N*-(4-Boc-lysine) and 186 mg (1 mmol) of iodoacetic acid (Aldrich) were dissolved in 10 ml of phosphate buffer, pH 10, and stirred overnight at ambient temperature. The solution was freeze dried and purified by column chromatography (solvent methanol/ethyl acetate, 2:1). Fractions containing material with R_f 0.69 (TLC/solvent methanol) were evaporated, taken up in 3 N HCl, and stirred for 60 min at room temperature. Solvents were removed by freeze drying, and the lyophilisate was subjected to preparative HPLC system 6. Fractions containing CML were combined and freeze dried (45 mg (22%), colorless amorphous powder, HPLC system 6, t_R 22.1 min, system 1 t_R 9.4 min, system 2 t_R 26.3 min, GC (CML as its trifluoroacetyl-methyl ester derivative) t_R 22.03 min, spectroscopic data compliant with the literature (4), elementary analysis showed that the material obtained was the CML-2 heptafluorobutyrate salt).**

***N*-(Glucitolyl)lysine (reduced Amadori product of glucose and lysine)**—A solution of 0.6 g (3.3 mmol) of glucose (Sigma), 0.82 g (3.3 mmol) of *N*-(4-Boc-lysine), and 0.21 g (3.3 mmol) of sodium cyanoborohydride (Aldrich) in 8.5 ml of anhydrous methanol was stirred overnight, 2 g of silica gel was added, solvents were evaporated, and the resulting powder was fractionated by column chromatography (eluent methanol/ethyl acetate, 1:2). Fractions containing *N*-(4-Boc-*N*-(glucitolyl)lysine (R_f 0.12, TLC, eluent butanol/water/acetic acid, 25:5:3) were evaporated. The residue was taken up in 3 N HCl, stirred for 60 min at room temperature, and freeze dried. *N*-(glucitolyl)lysine was obtained as colorless crystals (125 mg (12%), HPLC system 2 t_R 39.1 min, spectroscopic data compliant with the literature (21)).

***N*-(2-Hydroxyethyl)lysine 9**—273 mg (1.1 mmol) of *N*-(4-Boc-lysine), 66 mg (1.1 mmol) of glycolaldehyde, and 69 mg (1.1 mmol) of sodium cyanoborohydride were dissolved in 7 ml of anhydrous methanol and stirred overnight. Solvents were evaporated, and the resulting oil was applied to column chromatography (eluent methanol/ethyl acetate, 1.75:1) to remove inorganic salts. Fractions containing material with R_f 0.37 (TLC solvent *n*-butyl alcohol/water/acetic acid, 25:5:3) were combined, eluents were removed, and the residue was taken up in 3 N HCl and stirred for 60 min at room temperature. Solvents were removed by freeze drying, and the lyophilisate was subjected to preparative HPLC system 6. Fractions with 9 were combined and freeze dried. (75 mg (35%), colorless amorphous powder, HPLC system 6 t_R 37 min, system 1 t_R 15.5 min, system 7 t_R 37.1 min, GC (9 as its trifluoroacetyl-methyl ester derivative) t_R 20.31 min, elementary analysis showed that the material obtained was the HEL-2 heptafluorobutyrate salt). EI(70 eV)-GC/MS, m/z 460 ($M^+ - 32$; 14) 433(6) 395(6) 379(9) 346(12) 319(50) 266(35) 180(59) 141(100) 69(50). High resolution mass spectrometry, m/z 492.0948 (M^+), calculated 492.0943 for $\text{C}_{15}\text{H}_{21}\text{F}_9\text{N}_5\text{O}_6$, m/z 480.0636, calculated 460.0591 for $\text{C}_{14}\text{H}_{13}\text{F}_9\text{N}_5\text{O}_6$, m/z 266.0254, calculated 266.0256 for $\text{C}_7\text{H}_9\text{F}_9\text{N}_1\text{O}_5$.

***N*-(2-Hydroxy-1-*D*-ethyl) (9') and *N*-(2-hydroxy-1,2-*d}_2*-ethyl)lysine**

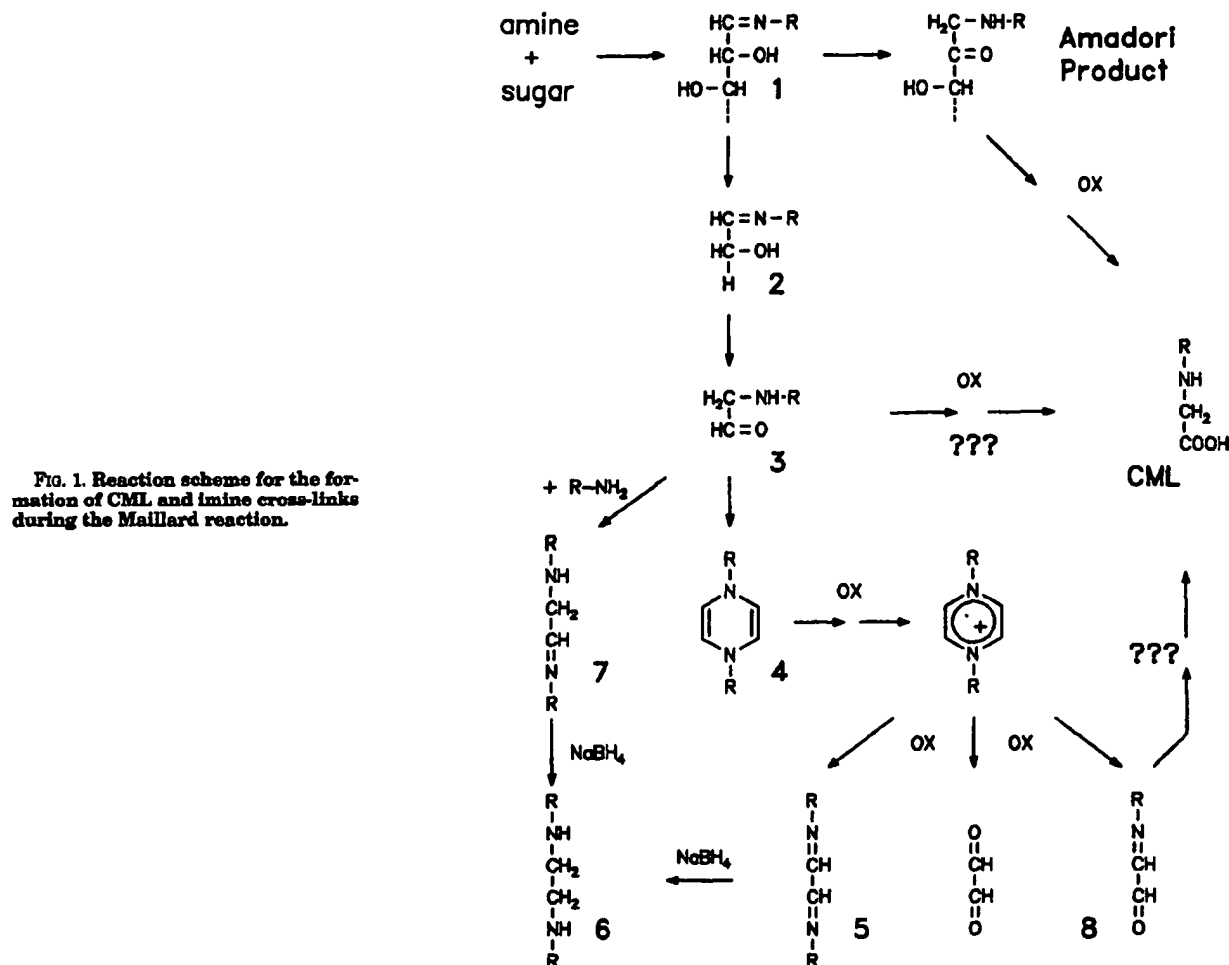


FIG. 1. Reaction scheme for the formation of CML and imine cross-links during the Maillard reaction.

(9') were synthesized like nonlabeled 9 but with the use of sodium cyanoborodeuteride (9') or sodium cyanoborodeuteride (Aldrich) and glyoxal (9'). EI(70 eV)-GC/MS, 9' (trifluoroacetylmethyl ester derivative), m/z 461 ($M^+-32;14$) 434(6) 396(5) 380(8) 347(9) 320(59) 287(45) 180(63) 142(100) 69(71). EI(70 eV)-GC/MS 9' (trifluoroacetylmethyl ester derivative), m/z 462 ($M^+-32;11$) 435(4) 397(5) 381(6) 348(10) 321(48) 268(31) 180(47) 143(100) 69(51).

Radioactive Labeled *N*-(1-Deoxyfructos-1-yl)propylamine—Unlabeled glucose was added to 250 μCi of 1- C^{14} - and 6- C^{14} -labeled glucose (Amersham Corp.) to adjust the specific activity to 10.8 mCi/mmol . After complete removal of water, the residue was taken up in 50 μl of anhydrous methanol and 150 μl of a solution of 4.2 μl of propylamine/100 μl of methanol, and the solution was heated for 45 min at 65 $^\circ\text{C}$ in a closed system. Solvents were evaporated, 100 μl of a solution of 2.94 mg of oxalic acid- $2\text{H}_2\text{O}/100 \mu\text{l}$ of methanol were added, and the mixture was heated for 15 min at 65 $^\circ\text{C}$ in a closed system. The methanol was removed, 0.5 ml of 1 N NaOH was added, and the solution was extracted 5 times with methylenechloride. After neutralization with 1 N HCl, the aqueous layer was freeze dried, and the lyophilisate was taken up in 400 μl of water and applied to column chromatography (Dowex 50W-X4-400, Aldrich, 3 cm height in Pasteur pipette). To remove unreacted glucose, the column was first washed with 6 ml of water; the Amadori product was then eluted with 0.2 N pyridine formate, pH 5.5, and proper fractions were combined (control by TLC (eluent *n*-butyl alcohol/water/acetic acid, 25:5:3, R_f 0.16) and radioactivity TLC scanner (Berthold, Germany)) and freeze dried.

***N*-(1-*Boc*-*N*-(1-deoxyfructos-1-yl)lysine and *N*-(1-*Boc*-*N*-(1-deoxyribulos-1-yl)lysine** were synthesized mainly according to Ref. 22. *N*-(1-Deoxyfructos-1-yl)propylamine and 3-amino-1,2,4-triazine (GC t_R 8.40 min (triazine as its trimethylsilyl derivative)) according to Refs. 23 and 24, respectively.

Incubations

All incubations were conducted at 37 $^\circ\text{C}$ in a shaker incubator after sterile filtration (0.2- μm filter, Gelman Science, Ann Arbor, MI), followed by reduction prior to hydrolysis. Deaerated conditions were achieved by the presence of 1 mM phytic acid (Sigma), 1 mM diethylenetriaminepentaacetic acid (Sigma), and gassing for 3 min with argon. Phosphate-buffered saline (pH 7.4, unless otherwise indicated) was used in all glyoxal/glycolaldehyde experiments; in all other cases, 0.2 M phosphate buffer, pH 7.4, was used. Samples were reduced for 1 h at room temperature in the presence of a 1.25-fold (glyoxal/glycolaldehyde) and a 5.8-fold (all other) molar excess of sodium borohydride to the carbonyl compounds used. In protein incubations, BSA (Sigma) concentration was 0.1 mM. After reduction, the protein was precipitated and washed twice with trichloroacetic acid (Sigma) (10, 5, and 5%). The resulting precipitate was dried and subjected to acid hydrolysis (6 N HCl) for 20 h at 110 $^\circ\text{C}$ under argon. For incubations with radioactive labeled sugars (specific activity, 10.8 mCi/mmol) concentrations of 77.3 $\mu\text{Ci}/500 \mu\text{l}$ were used.

Analytical Procedures

Imines 5 and 7 were monitored as their common reduction product 6. For HPLC analysis, hydrolysates were evaporated in a Savant Speed-Vac concentrator (Hicksville, NY) and taken up in water. 9 was determined with HPLC system 7 after material had been collected from HPLC system 1 (t_R 13.5–18.0 min) without postcolumn derivatization. CML from incubations with radioactive labeled sugars was first collected from HPLC system 1 without postcolumn detection (t_R 6–11.6 min) and then quantified on HPLC system 2 by counting the radioactivity of proper fractions (LS6000, Beckman, Fullerton, CA) or postcolumn derivatization.

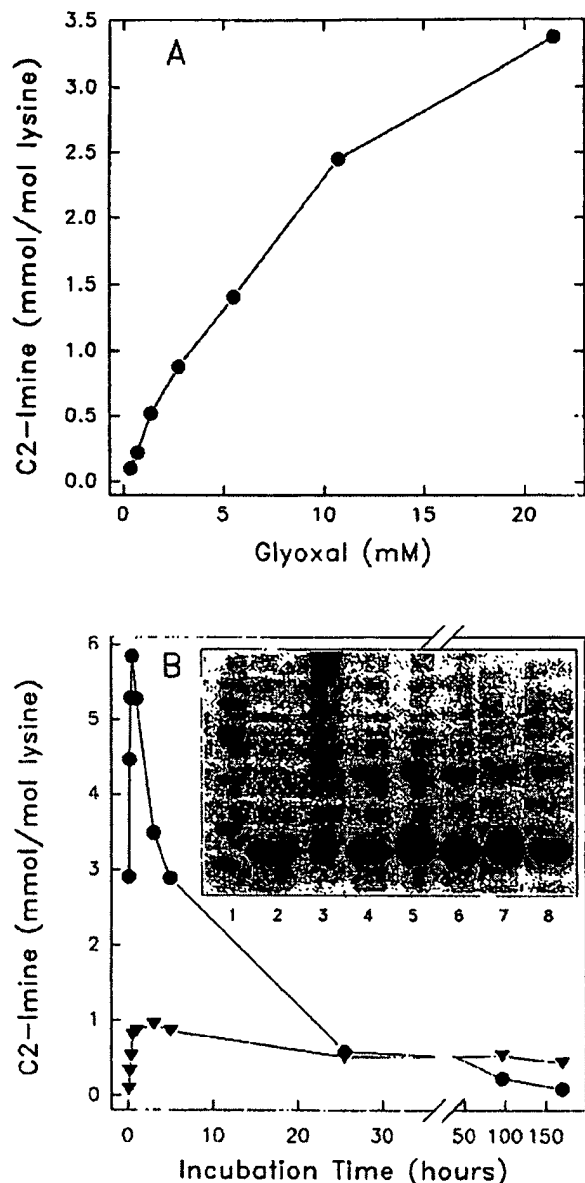


FIG. 2. A, effect of glyoxal concentration on the formation of C-2-imine 5 in BSA incubations. B, time-dependent formation of C-2-imines 5 and 7 in BSA incubations with 20 mM glyoxal (●) and 20 mM glycolaldehyde (▼). B, inset, formation of polymers during incubation of RNase with 20 mM glyoxal (8/5 h, 7/170 h), 200 mM glyoxal (6/5 h, 5/170 h), and 20 mM glycolaldehyde (4/5 h, 3/170 h), monitored by SDS-polyacrylamide gel electrophoresis. Lane 1 shows low molecular mass standard (14.4–97.4 kDa), and lane 2 shows control incubation (170 h) without carbonyl compounds added.

For GC/MS analysis of amino acids, proper fractions were collected from HPLC without postcolumn derivatization (HPLC system 5 for 6, HPLC system 6 for CML and 9, 9', 9''), solvents were removed to absolute dryness, and material obtained was derivatized as trifluoroacetylmethyl ester derivatives. First, up to 10 mg of material was dissolved in 1 ml of 0.1 M thionylchloride (Fluka) solution in anhydrous methanol and heated for 1 h at 110 °C. Solvents were evaporated to absolute dryness. The residue was taken up in 300 μ l of pyridine and 100 μ l of trifluoroacetic anhydride (Aldrich), and the reaction mixture was heated for 10 min at 65 °C. After complete removal of solvents, the residue was dissolved in ethyl acetate and passed over a short silica gel column (eluent ethyl acetate). Proper fractions were combined and subjected to GC/MS.

TABLE I
C-2-imine/CML formed in various sugar-BSA incubations

Sugar	Concentration mM	C-2-imine		CML	
		5 h	170 h	5 h	170 h
D-Glucose	200			0.3	1.4
D-Ribose	200	0.09	0.15	1.4	103.7
L-Threose	200	0.21	0.66	3.9	16.8
Glyceraldehyde	200	0.41	0.79	11.8	44.9
Ascorbic acid	200	0.10	0.32	0.9	42.1
Glyoxal	20	2.89	0.09	8.2	40.4
Glycolaldehyde	20	0.85	0.44	3.3	29.2

3-Amino-1,2,4-triazine was extracted from incubations containing aminoguanidine with ethyl acetate. Solvents were evaporated after drying the combined organic layers over anhydrous sodium sulfate. The residue was derivatized using a 1:1 (v/v) ratio of pyridine and *N,O*-bistrimethyl silylacetamide (Fluka), and the reaction mixture was analyzed with GC/MS.

Amadori product concentration in incubations with *N*^ε-t-Boc-lysine was determined prior to acid hydrolysis after reduction and removal of the protecting groups by 3 N HCl as *N*^ε-(glucitolyl)lysine. Solvents were removed in a Savant Speed-Vac concentrator, and the residue was taken up in water and subjected to HPLC system 2.

SDS-Polyacrylamide Gel Electrophoresis

For estimation of the extent of cross-linking mediated by glyoxal/glycolaldehyde at various time points, RNase (0.5 mM, Sigma) incubations were reduced, dialyzed overnight at 4 °C against phosphate-buffered saline, pH 7.4, and analyzed by SDS-gel electrophoresis on a 12% acrylamide gel. The amounts of RNase loaded onto the gel was 20 μ g in each lane. The gel was stained with Coomassie Blue for 1 h and destained in a mixture of 40% methanol and 10% acetic acid in water.

RESULTS

Because of the instability of the C-2-imines 5 and 7 (Fig. 1) during acid hydrolysis, their common reduced form 6, 2,15-diamino-7,10-diaza-hexadecane-1,16-dioic acid, was synthesized from *N*^ε-t-Boc-lysine and 2,3-dihydroxy-1,4-dioxane and purified by preparative HPLC. The structure was unequivocally established from its spectroscopic data as described under "Experimental Procedures." To optimize conditions, the synthesis of the hexylamine derivative of 6 was studied first. Best conditions were obtained using 2,3-dihydroxy-1,4-dioxane as a water-free glyoxal substitute (25), strong alkaline reaction conditions, and subsequent reduction with sodium borohydride rather than the use of commercially available glyoxal/water solutions under neutral conditions in the presence of sodium cyanoborohydride. Product formation was assessed by coupled GC/MS.

Structure 6 was found to be stable under the conditions used for acid hydrolysis of proteins. To confirm the nature of 6 in hydrolysates, two different HPLC systems with *o*-phthalaldehyde-postcolumn derivatization and fluorescence detection were developed, and the absence of the corresponding peak in nonreduced samples was confirmed throughout all investigations. Additionally, in selected cases, the material was collected by HPLC, derivatized, and applied to GC/MS.

In BSA incubations, the formation of diimine 5 monitored after reduction to 6 was dependent on the glyoxal concentration and began to level off above 10–20 mM (Fig. 2A). We chose 20 mM to investigate cross-link structures 5 and 7 in BSA incubated with glyoxal or glycolaldehyde, respectively. Time course experiments ranging from 5 min to 170 h showed that the formation quickly reached a maximum at about 0.5 h followed by degradation (Fig. 2B). Remarkably, in the case of glycolaldehyde, the initial peak was much smaller, but the steady level reached later was higher than with glyoxal. These findings were correlated with the rate of cross-linking using SDS-polyacrylamide gel electrophoresis after dialysis of the reduced and unreduced reaction mixtures (Fig. 2B, inset). Reduced and un-

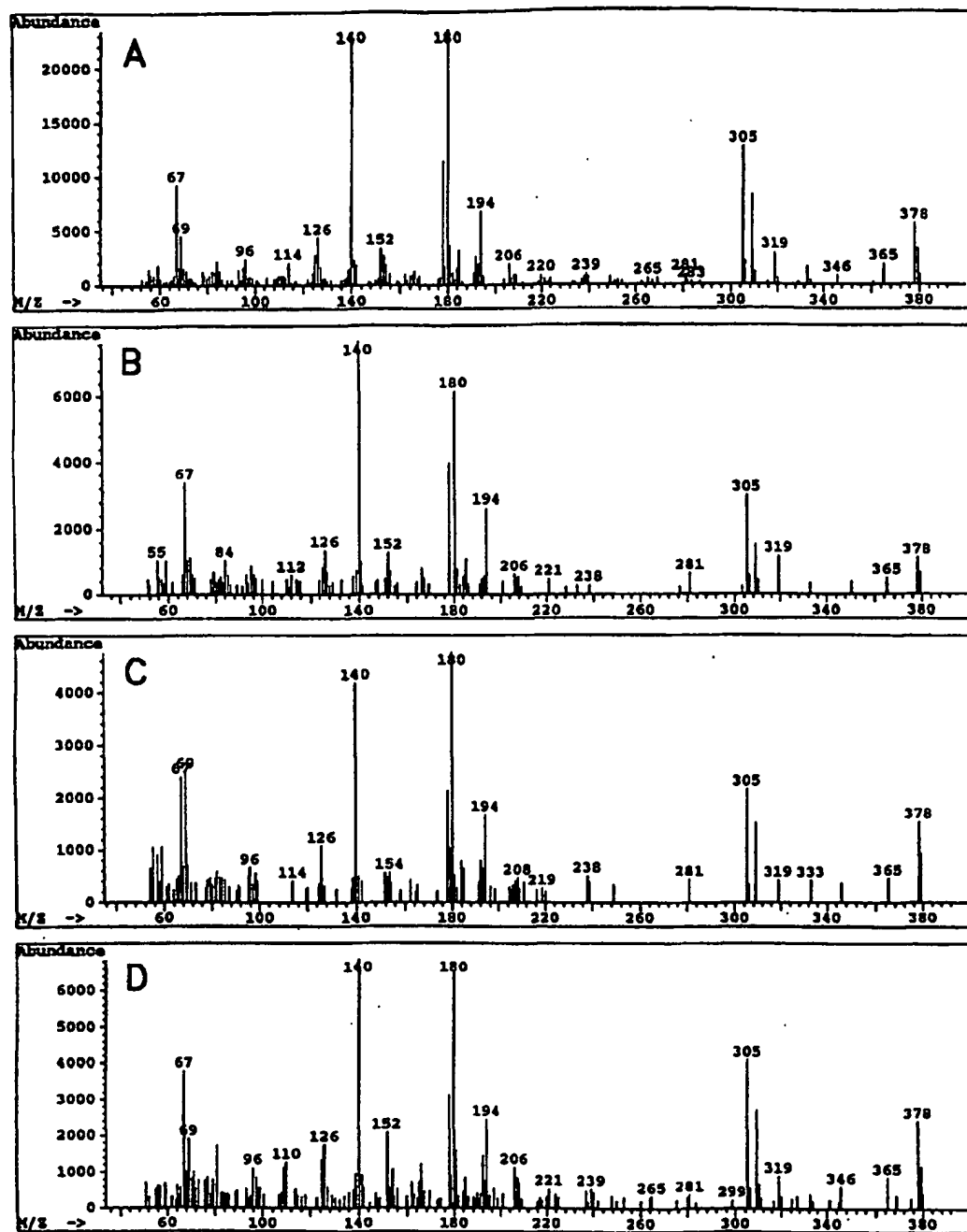


FIG. 3. Identification of C-2-imines 5 and 7 as their reduction product 6 in BSA incubations with 20 mM glyoxal (B), 20 mM glycolaldehyde (C) and 200 mM ribose (D). Mass spectra obtained after derivatization are identical to the one of synthesized authentic amino acid 6 (A).

reduced samples showed no visible difference (data not shown). Cross-linking increased with time. With glyoxal, the trimer became faintly visible at 20 mM, and more intramolecular modifications could be observed in contrast to glycolaldehyde that had significant intermolecular reactions.

C-2-imines 5/7 were also detected in other sugar-BSA incubations (Table I). The rate of formation was time-dependent and roughly followed the reactivity of the sugar. Glucose protein mixtures showed no cross-link formation under the same conditions (detection limit of this experiment, 0.1 mmol/mol of

lysine). In a detailed time course experiment, the cross-links formed progressively during incubation with ribose until a peak was reached at about 120 h with 0.28 mmol/mol of lysine followed by degradation. Retention times and mass spectra of derivatized collected HPLC material from glyoxal/glycolaldehyde/ribose incubation mixtures were identical to the data of the synthesized authentic product 6 (Fig. 3).

The data presented so far suggested that a significant amount of 5 and 7 was further degraded into one or several more stable products. One known product, which contains a

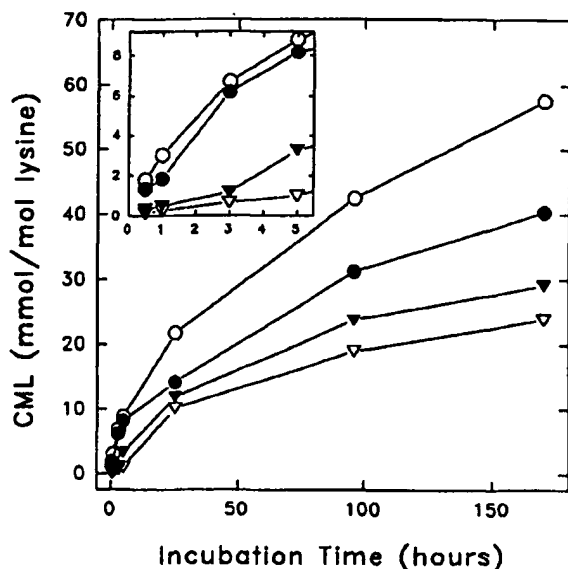


FIG. 4. Time-dependent formation of CML in BSA incubations with (●) 20 mM glyoxal and (▼) 20 mM glycolaldehyde. Full symbols indicate aerated conditions; open symbols indicate deaerated conditions. Inset shows same experiment up to 5 h.

C-2 fragment of the original sugar, is CML. Incubations of BSA with both glyoxal and glycolaldehyde revealed indeed large quantities of CML formed (Fig. 4). The identity of CML detected by HPLC was confirmed after collection and derivatization by GC/MS (Fig. 5). For comparison, authentic CML was synthesized. Deaerated conditions and presence of transition metal ion chelator altered the rate of formation from both carbonyl compounds.

However, the role of oxidation in CML formation from glyoxal and glycolaldehyde is complex since the initial formation rate of CML from glyoxal is not dependent on oxygen, whereas it is totally suppressed under anaerobic conditions for glycolaldehyde (Fig. 4, inset). This suggests that CML formation from glyoxal can occur through an intramolecular Cannizzaro reaction without oxidation (Fig. 6, intermediate 8). In support of this possibility, pH studies showed that CML synthesis from glyoxal was favored by alkaline conditions, pH 9, but totally suppressed at pH 5 (data not shown).

Whereas oxidation of Amadori-rearranged glycolaldehyde adduct 3 (Fig. 6) is a necessary step for initial CML formation, the finding that CML formation during long term incubation of BSA with glycolaldehyde progresses in spite of deaerated conditions suggests a possible intermolecular Cannizzaro reaction of aldamine 3 into acid CML and alcohol *N*-(2-hydroxyethyl)-lysine 9. In order to clarify the significance of this pathway, authentic 9 was synthesized and detected in high levels upon trapping the Schiff base 2 with sodium cyanoborohydride. On the other hand, only small levels were recovered without reducing reagent (i.e. 4.5 compared with 29.2 mmol/mol of lysine of CML at 170 h). Since even lower levels were detected under deaerated conditions (2.0 mmol/mol of lysine), intermolecular Cannizzaro reaction is excluded as a significant source of CML from glycolaldehyde.

Additional experiments with 5 mM aminoguanidine as a trapping reagent specific for α -dicarbonyl compounds (24) showed that whereas only 1.16% (aeration) and 0.95% (deaeration) of glycolaldehyde was transformed into glyoxal, as measured as by the corresponding triazine, as much as 37% CML formation was suppressed. The formation of an aromatic ring

structure represents such gain of stability that not only free glyoxal will react, but hidden glyoxal in Schiff bases like 8 or aminals (26) will also react. Thus, detection of the glyoxal-triazine and significant inhibition of CML formation suggests glyoxal or glyoxal derivatives 8 as major intermediates for CML synthesis in glycolaldehyde incubations.

The data so far implicate unequivocally glyoxal and glycolaldehyde in CML formation and raise the question of the mechanisms by which CML forms from higher sugars, as demonstrated in Table I and by others (19, 27). In our own experiments (Table I), CML formation rates in BSA incubations generally followed the anomerization rates of the sugar except for D-ribose, which was a potent generator of CML.

The key question concerning CML synthesis from higher sugars is whether formation rates are primarily dependent on sugar autooxidation or Schiff base fragmentation as proposed by Wolff (28) and Namiki (10), respectively, or whether the major source stems from oxidative breakdown of the Amadori product of the sugar (19). Clarification of this question is problematic since all molecules are simultaneously present in sugar-amine incubation systems.

As previously reported (18), CML formation from glucose and *N*^ε-*t*-Boc-lysine was strongly dependent on presence of oxygen and free metals (Fig. 7). Aminoguanidine and boric acid were used as tools to dissect the relative importance of Amadori product versus glucose as a precursor of CML in incubations with *N*^ε-*t*-Boc-lysine. Only when the reaction was started from glucose itself did aminoguanidine have an important impact, as evidenced by almost 50% reduction in CML formation. In presence of Amadori product, incubations with aminoguanidine showed almost no effect up to 100 h, although the absolute amount of inhibition after 170 h was larger compared with glucose experiments. Formation of the triazine derived from glyoxal and aminoguanidine measured by GC/MS was strictly dependent on oxidation (Table II). After 170 h, the Amadori product produced about 4 times more glyoxal than the sugar. In addition, 7-fold catalytic effect of *N*^ε-*t*-Boc-lysine on glyoxal formation as the amine component in glucose systems is evident. In contrast to aminoguanidine, 10 times excess boric acid completely inhibit CML formation from the Amadori compound, but only by about 37% when the reaction was initiated by glucose. This suggests an additional mechanism, which is not dependent on the Amadori product. Indeed, whereas in presence of Amadori product, only as much as 40% degradation within 170 h yielded 2.8 mmol of glyoxal triazine/mol of lysine (Table II), only 0.7% Amadori product were actually detected in the glucose/*N*^ε-*t*-Boc-lysine system after the same time (100% refers to the initial Amadori concentration in Amadori product only incubations).

Two different approaches were utilized to establish the formation of glyoxal and glycolaldehyde in incubations of higher sugars without the use of trapping reagent. First, the formation of *N*-(2-hydroxyethyl)lysine 9 in reduced incubations of glucose and ribose was confirmed reaching concentrations of 0.1 and 7.5 mmol/mol of lysine, respectively, after 170 h. In the case of ribose, the nature of the original C-2 carbonyl intermediates could be elucidated by reducing with sodium borodeuterate. Isotopic distribution of characteristic fragments in the mass spectrum, as 461 for *N*-(2-hydroxy-1-*d*-ethyl)lysine 9' and 462 for *N*-(2-hydroxy-1, 2-*d*₂-ethyl)lysine 9'', revealed a ratio of 4:5 of 9' to 9'' through comparison with the spectra of authentic synthesized compounds 9, 9', and 9''. Signals at 461 and 462 represent loss of methanol, which is a common fragmentation pattern for methylesters. Second, in incubations of the Amadori product (0.5 mM) of glucose and propylamine with *N*^ε-*t*-Boc-lysine (42 mM), the formation of CML was confirmed and

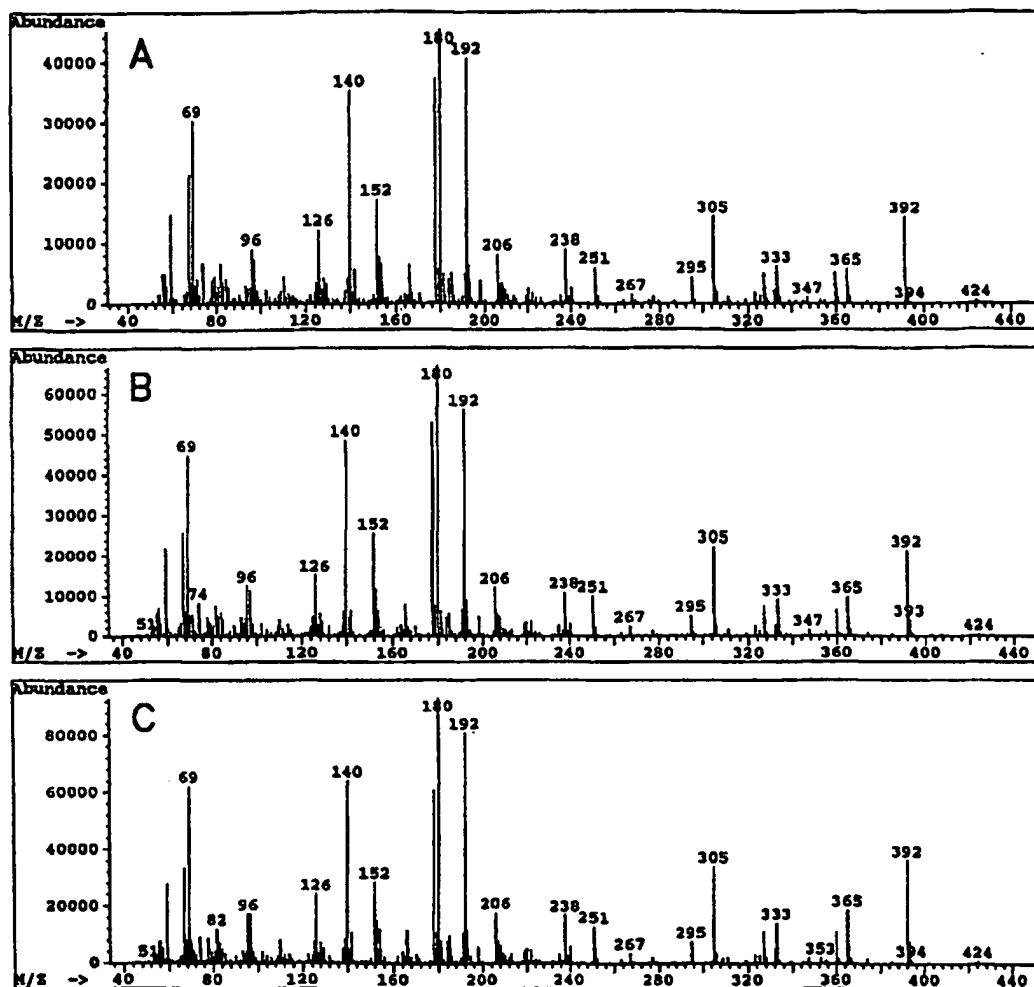


FIG. 5. Identification of CML formed in BSA incubations with 20 mM glyoxal (B) and 20 mM glycolaldehyde (C) by GC/MS. Mass spectra obtained after derivatization are identical to the one of authentic CML (A).

found to increase with time (0.47 mmol/mol of lysine at 170 h).

Investigations into the origin of carbon atoms involved in CML formation utilizing C-1 and C-6 radiolabeled sugars revealed surprising findings. By comparison of CML measured by HPLC using radioactivity with total CML using postcolumn derivatization 74% (5 days)/68% (10 days) of CML was attributed to the C-1 and 29%/31% to the C-6 portion of *N*-(1-deoxyfructos-1-yl)propylamine. Starting the incubation with glucose only 38% (5 days)/32% (10 days) for the C-1 and 22%/36% for the C-6 region were recovered, suggesting thereby that about 30% of CML is stemming from the C-2–C-5 region of the original carbon backbone.

DISCUSSION

The purpose of this study was to clarify the mechanism of formation of structures incorporating a C-2 fragment of the original sugar during the Maillard reaction of reducing sugars and proteins *in vivo*. Clarification of this question is important because the major advanced Maillard product found *in vivo* so far is CML. Its levels increase with age in human skin (29) and in the presence of diabetes, and the levels can be correlated with severity of diabetic complications (30). In addition, CML was detected in human lens, where it is thought to originate from ascorbate (4, 27). Previous mechanistic studies by Dunn *et al.* (19)

suggested that CML forms from the Amadori product of glucose or threose through metal-catalyzed oxidative fragmentation.

The data in this study show unequivocally that, under physiological conditions at 37 °C and pH 7.4, glyoxal and glycolaldehyde are immediate precursors in the formation of CML and that they are involved in formation of C-2-imine cross-link 5,7 (Fig. 1) and other more important, but yet unknown, structures. Formation of CML and 5/7 during Maillard reaction from higher sugars like glucose is much more complex because all three potential sources, i.e. the free sugar, the Schiff base adduct, and the Amadori product, are present together as soon as the reaction proceeds. Additionally, our findings raise questions of the importance of glyoxal and glycolaldehyde in the reaction pathways leading to CML and cross-linking.

When the reaction was initiated from the Amadori product of glucose, very large quantities of CML were formed that were almost totally stalled by deaerated conditions (Fig. 7B). The fact, that aminoguanidine had no suppressive effect until 100 h strongly favors a mechanism involving direct oxidative cleavage of the Amadori product. In contrast, when starting the reaction from glucose in the presence of *N*^ε-*t*-Boc-lysine, 50% inhibition of CML formation by aminoguanidine indicates approximately a 50% participation of the C-2 intermediates glyoxal/glycolaldehyde and 50% of CML originating from the Ama-

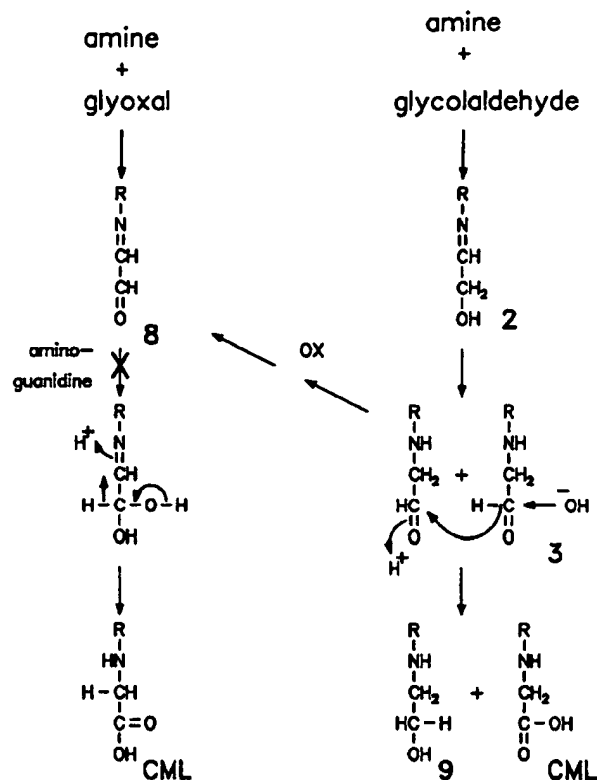


FIG. 6. Proposed mechanism for formation of CML from glyoxal and glycolaldehyde.

dori product via oxidative cleavage, which is not influenced by aminoguanidine.

The key question therefore is what is the major source of glyoxal/glycolaldehyde production leading to CML. Fig. 7B shows at 170 h that only 15% of total CML formation from the Amadori product can be attributed to C-2 intermediates. Indeed, the amount of glyoxal-triazine generated in the presence of 42 mM Amadori product was only 2.8 mmol/mol of initial sugar concentration. Thus, less than 0.3% of the original Amadori product was transformed into glyoxal (Table II). As the Amadori product concentration in a glucose/*N*^ε-*t*-Boc-lysine system reaches only 0.7% of 42 mM, this source contributes only minor quantities CML by C-2 intermediates. Based on Fig. 7B, it can be estimated at approximately 7%. This leaves 43% of total CML originating from other sources via glyoxal/glycolaldehyde (Fig. 8).

Utilizing the data on 3-amino-1,2,4-triazine formation, glucose autooxidation, as proposed by Wolff *et al.* (28), can be excluded as a significant source of glyoxal generation (Table II). We recovered small quantities of the triazine from glucose incubated in absence of amine. However, about 7 times higher levels were formed when the identical experiment was carried out in the presence of *N*^ε-*t*-Boc-lysine.

Thus, in an incubation system starting from glucose in the presence of amines, the major pathway leading to glyoxal is not autooxidation of glucose or degradation of the Amadori product but degradation of an amine-assisted oxidative step prior to formation of the Amadori product, presumably the Schiff base adduct (Fig. 8).

Incubations conducted in the presence of boric acid support the findings with aminoguanidine. Boric acid forms a stable chelating complex with the coplanar cis diol groups of the

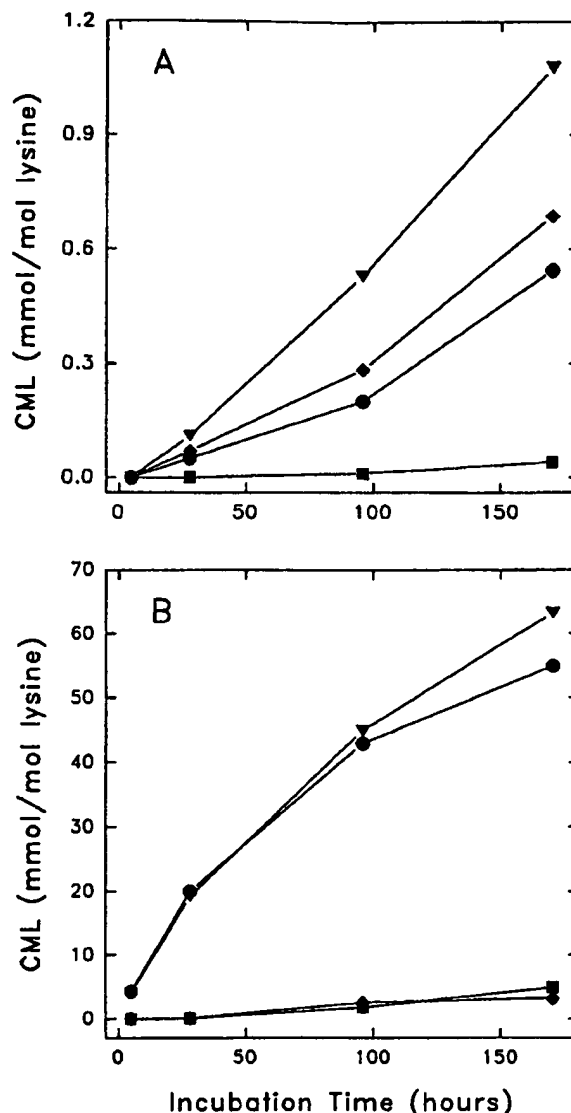


FIG. 7. Time dependent formation of CML in incubations of (A) glucose (42.2 mM) and *N*^ε-*t*-Boc-lysine (42.2 mM) (B) Amadori product of glucose and *N*^ε-*t*-Boc-lysine. Incubations were conducted under (▼) aerated, aerated in presence of aminoguanidine (5 mM, ●), and in the presence of boric acid (420 mM, ◆), and (■) deaerated conditions.

TABLE II
3-Amino-1,2,4-triazine formed after 170 h in various sugar/amine incubations (all 42.2 mM) in the presence of 5 mM aminoguanidine

Sugar	Triazine	
	Aerated	Deaerated
mmol / mol initial sugar concentration		
Glucose	0.11	0
Glucose/ <i>t</i> -Boc-lysine	0.73	0.01
Amadori product	2.80	0.02

furanoic structure of 1-deoxyfructos-1-yl-amines (31) and thus totally blocks CML formation from Amadori products via oxidative cleavage and glyoxal/glycolaldehyde (Fig. 7B). Based on the experiments with aminoguanidine, this should result in a decrease of 57% CML synthesis in glucoseamine systems. The actual decrease of 37% was found to be smaller and is probably due to accelerated CML synthesis linked to increased salt

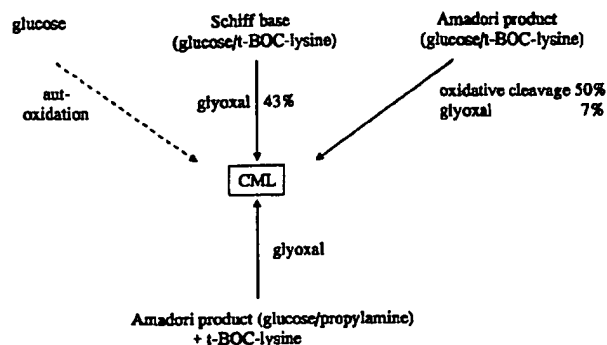


FIG. 8. Formation of CML from various sugars during the Maillard reaction. Contribution of oxidative cleavage versus glyoxal is calculated on data in Fig. 7.

concentrations (18).

Since aminoguanidine itself is an amine compound, it could compete with the target amine of the system used and contribute to the generation of reactive intermediates. The possibility of generating glyoxal/glycolaldehyde solely by this reaction pathway was discounted based on the detection of CML in incubations of the Amadori product of propylamine and glucose with *N*^ε-*t*-Boc-lysine. The Amadori product will primarily form carboxymethylated propylamine via oxidative cleavage and glyoxal generation, but part of the glyoxal will also react with lysine to give carboxymethylated lysine or CML (Fig. 8).

Other independent evidence for glyoxal and glycolaldehyde generation from higher sugars was gained from the abundance of imine-intermediates 2 and 3 as glycolaldehyde and 8 as glyoxal derivatives (Figs. 1 and 6) in incubation mixtures with proteins. After reduction, 9 as their common product was detected in incubations with glucose and in much higher levels also with ribose. Use of a deuterated reduction reagent made it possible to distinguish between the *N*^ε-(2-hydroxy-1-*d*-ethyl)-lysine 9' for reduced 2 and 3 and *N*^ε-(2-hydroxy-1, 2-*d*₂-ethyl)-lysine 9'' for reduced 8 in ribose incubations. This experiment unequivocally proves the existence of glycolaldehyde and glyoxal as their imine derivatives in incubations under physiological conditions and therefore emphasizes their role as potential contributors of CML formation from higher sugars.

Based on these considerations, and the finding that Amadori products are present in significant concentrations in tissues, the source of CML formation *in vivo* is expected to follow the sequence of precursor reactivity: Amadori product (via oxidative cleavage) > Schiff base adduct (via glyoxal/glycolaldehyde) >>> glucose (via autooxidation). Indeed, when using the data of CML and glyoxal-triazine formation to calculate the contribution for CML formation under severe diabetic conditions, i.e. 30 mM glucose and 2 mM Amadori product (32), most would originate from the Amadori product via oxidative cleavage, but glyoxal from Amadori product and glucose-amine interaction would also account for 17% (Table III).

The fact that addition of a heterologous Amadori product to *N*^ε-*t*-Boc-lysine induced CML formation led to investigations about the origin of the C-2 fragments with radiolabeled sugars. Incubating glucose with protein, about 30% of total CML incorporate the C-1 and about 30% incorporate the C-6 region, representing a C-2-C-3 and C-4-C-5 split of the sugar backbone. This indicates that significant amounts of C-2 fragments originate in between C-1 and C-6 and are therefore not accounted for by radioactivity. About 70% originate from the C-1 and about 30% from the C-6 part, when CML was induced by labeled Amadori product of glucose and propylamine. In this case, only glyoxal/glycolaldehyde transfer to the ε-amino lysine

TABLE III
Calculated CML and glyoxal formation after 170 h of incubation mimicking severe diabetic conditions, based on results presented in Table II and Fig. 7

	Total CML	CML from Glyoxal
	mmol/mol lysine	mmol/mol lysine
Glucose/ <i>t</i> -Boc-lysine (30 mM)	0.77	0.52
Amadori product (2 mM)	3.00	0.13
Total	3.77	0.65

residues can generate CML. Thus, other reaction pathways in addition to the one proposed by Namiki contribute to CML formation. These may not be in contradiction with the importance of the Schiff base as a major contributor to C-2 fragmentation as evidenced above, because activation of the sugar by the imine bond may result in enolization through the whole molecule and facilitated fragmentation in multiple sites (2).

Hayashi *et al.* (10) reported the formation of glyoxalalkyldiimines in heated reaction systems. The data shown in this paper establish the formation of analogue lysine derivative diimine 5 and also imine 7 (Fig. 1) under physiological conditions. Both structures could be detected in protein incubations with their immediate precursors glyoxal and glycolaldehyde, as well as from various sugars. Although the C-2-imine cross-links are formed *in vitro*, they are not stable and, as such, of minor importance as permanent cross-links. For this reason, no attempt was made to distinguish between 5 and 7. The concentrations formed were very small compared with other modifications like CML and were strictly dependent on the amount of glyoxal and glycolaldehyde present in the system. Since the expected steady-state levels of both carbonyl compounds formed in living systems are extremely low, and neither 5 nor 7 accumulate, this cross-link may therefore be present only in trace amounts *in vivo* and not contribute to protein cross-linking during aging or diabetes. Thus, it is not surprising that preliminary analysis of human skin and aorta tissue and serum samples showed no evidence for the formation of 5 and 7.

In summary, the generation of glyoxal and glycolaldehyde from higher sugars under physiological conditions and the tight relationship between these carbonyl compounds and CML formation became apparent in this study. In addition the *in vitro* data of protein cross-linking by us and others (33) provide new insights in the possible nature and mechanisms of sugar-mediated protein modification *in vivo*. Mechanistic studies *in vivo* are now necessary to probe the significance of the proposed pathway for CML formation and cross-linking. It is conceivable that some answers may come from *in vivo* determination of the type of triazines formed during the aminoguanidine therapy (34).

Acknowledgments—We thank Dr. Douglas Gage at the Michigan State University Mass Spectrometry Facility for performing high resolution fast atom bombardment spectral analysis. This facility is supported, in part, by a grant (DRR-00480) from the Biotechnology Resources Branch, Division of Research Resources, National Institutes of Health.

REFERENCES

- Baynes, J. V., and Monnier, V. M. (1989) *Prog. Clin. Biol. Res.* 304, 1-410
- Lodi, F., and Schleicher, E. (1990) *Angew. Chem. Int. Ed. Engl.* 29, 565-594
- Sell, D. R., Nagaraj, R. H., Grandhee, S. K., Odetti, F., Lapolla, A., Fogarty, J., and Monnier, V. M. (1991) *Diabetes Metab. Rev.* 7, 239-251
- Dunn, J. A., Patrick, J. S., Thorpe, S. R., and Baynes, J. W. (1989) *Biochemistry* 28, 9464-9468
- Miyata, S., and Monnier, V. M. (1992) *J. Clin. Invest.* 89, 1102-1112
- Marion, M. S., and Carlson, E. C. (1994) *Biochim. Biophys. Acta* 1191, 33-42
- Portero-Otin, M., Rammanakoppa, H. N., Monnier, V. M. (1995) *Biochim. Biophys. Acta*, in press
- Smith, P. R., Somani, H. H., Thornelly, P. J., Benn, J., and Sonksen, P. H. (1983) *Clin. Sci.* 84, 87-93
- Hayashi, T., and Namiki, M. (1986) in *Amino-Carbonyl Reaction in Food and Biological Systems* (Fujimaki, M., Namiki, M., and Kato, H., eds) pp. 29-38,

- Elsevier, Amsterdam
10. Hayashi, T., Sasako, M., and Namiki, M. (1985) *Agric. Biol. Chem.* **49**, 3131-3137
 11. Nedvidek, W., Ledl, F., and Fischer, P. (1992) *Z. Lebensm. Untera. Forsch.* **194**, 222-228
 12. Hayashi, T., Ohta, Y., and Namiki, M. (1977) *Agric. Food Chem.* **25**, 1282-1287
 13. Bowes, J. H., and Cater, C. W. (1968) *Biochim. Biophys. Acta* **168**, 341-352
 14. Acharya, A. S., and Manning, J. M. (1983) *Proc. Natl. Acad. Sci. U. S. A.* **80**, 3590-3594
 15. Cho, R. K., Okitani, A., and Kato, H. (1986) *Agric. Biol. Chem.* **50**, 1373-1380
 16. Chuyen, N. V., Kurata, T., and Fujimaki, M. (1973) *Agric. Biol. Chem.* **37**, 2209-2209
 17. Velisek, J., Davidek, T., Davidek, J., Traka, P., Kvasnicka, F., and Velcova, K. (1989) *J. Food Sci.* **54**, 1544-1546
 18. Ahmad, M. U., Thorpe, S. R., and Baynes, J. W. (1986) *J. Biol. Chem.* **261**, 4889-4894
 19. Dunn, J. A., Ahmed, M. U., Murtiashaw, M. H., Richardson, J. M., Walla, M. D., Thorpe, S. R., and Baynes, J. W. (1990) *Biochemistry* **29**, 10964-10970
 20. Benson, J. R., and Hare, P. E. (1975) *Proc. Natl. Acad. Sci. U. S. A.* **72**, 619-622
 21. Schwartz, B. A., and Gray, G. R. (1977) *Arch. Biochem. Biophys.* **181**, 542-549
 22. Grandhee, S. K., and Monnier, V. M. (1991) *J. Biol. Chem.* **266**, 11649-11653
 23. Michael, F., and Hagemann, G. (1959) *Chem. Ber.* **92**, 2836
 24. Erikson, J. G. (1952) *J. Am. Chem. Soc.* **74**, 4706
 25. Venuti, M. C. (1982) *Synthesis* 61-63
 26. Glass, J. P., and Felsig, M. (1978) *Biochem. Biophys. Res. Commun.* **81**, 527-531
 27. Slight, S. H., Prabhakaram, M., Shin, D. B., Feather, M. S., and Orwerth, B. J. (1992) *Biochim. Biophys. Acta* **1117**, 199-206
 28. Wolff, S. P., Jiang, Z. Y., and Hunt, J. V. (1991) *Free. Rad. Biol. Med.* **10**, 339-352
 29. Dunn, J. A., McCance, D. R., Thorpe, S. R., Lyons, T. J., and Baynes, J. W. (1991) *Biochemistry* **30**, 1205-1210
 30. McCance, D. R., Dyer, D. G., Dunn, J. A., Bailie, K. E., Thorpe, S. R., Baynes, J. W., and Lyons, T. J. (1993) *J. Clin. Invest.* **91**, 2470-2478
 31. Brownlee, M., Vlassara, H., Cerami, A. (1980) *Diabetes* **29**, 1044-1047
 32. Johnson, R. N., Metcalf, P. A., and Baker, J. R. (1982) *Clin. Chim. Acta* **127**, 87-85
 33. Fu, M.-X., Knecht, K. J., Thorpe, S. R., and Baynes J. W. (1992) *Diabetes* **41**, 42-48
 34. Brownlee, M., Vlassara, H., Kooney, A., Ulrich, P., and Cerami, A. (1988) *Science* **233**, 1629-1632



Carbamylated erythropoietin protects the kidneys from ischemia-reperfusion injury without stimulating erythropoiesis

Ryoichi Imamura ^a, Yoshitaka Isaka ^{b,*}, Naotsugu Ichimaru ^a,
Shiro Takahara ^b, Akihiko Okuyama ^a

^a Department of Urology, Osaka University Graduate School of Medicine, Suita, Japan

^b Department of Advanced Technology for Transplantation, Osaka University Graduate School of Medicine, Suita, Japan

Received 8 December 2006

Abstract

Several studies have shown that erythropoietin (EPO) can protect the kidneys from ischemia-reperfusion injury and can raise the hemoglobin (Hb) concentration. Recently, the EPO molecule modified by carbamylation (CEPO) has been identified and was demonstrated to be able to protect several organs without increasing the Hb concentration. We hypothesized that treatment with CEPO would protect the kidneys from tubular apoptosis and inhibit subsequent tubulointerstitial injury without erythropoiesis. The therapeutic effect of CEPO was evaluated using a rat ischemia-reperfusion injury model. Saline-treated kidneys exhibited increased tubular apoptosis with interstitial expression of α -smooth muscle actin (α -SMA), while EPO treatment inhibited tubular apoptosis and α -SMA expression to some extent. On the other hand, CEPO-treated kidneys showed minimal tubular apoptosis with limited expression of α -SMA. Moreover, CEPO significantly promoted tubular epithelial cell proliferation without erythropoiesis. In conclusion, we identified a new therapeutic approach using CEPO to protect kidneys from ischemia-reperfusion injury.

© 2006 Elsevier Inc. All rights reserved.

Keywords: Apoptosis; Carbamylated erythropoietin; Ischemia-reperfusion injury; Kidney; Cell proliferation

Renal ischemia-reperfusion (I/R) injury, which is unavoidable in renal transplantation and is frequently associated with shock or surgery, is a major cause of acute renal failure [1]. Despite decades of laboratory and clinical investigations and the advent of renal replacement therapy, the overall mortality rate due to acute tubular necrosis has changed little. Recently, a broader concept of erythropoietin (EPO) as a tissue-protective molecule has emerged. EPO has been found to protect the brain and the spinal cord from ischemic injury [2,3], the peripheral nerve from diabetic damage [4,5], the kidney from ischemic [6,7] or toxic insults [8], and the heart from acute I/R injury [9,10].

The initial understanding of the biology of EPO-mediated tissue protection largely developed from the study of

the nervous system, which is susceptible to ischemic injury due to its high basal metabolic rate. The findings derived from the nervous system studies are applicable to the kidney. The normal kidney, like the nervous system, is characterized by regions in which energy substrates are limited. Commonly, chronic renal hypoxia with subsequent tubulointerstitial injury leads to end-stage renal failure [11]. In contrast, early treatment with EPO slows the progression of renal failure [12].

In the kidney, a potential role for the non-hematopoietic activities of EPO was first suggested by the identification of the EPO receptor (EPO-R) protein that is expressed throughout the kidney, including both proximal and distal tubular cells [13]. However, the affinity of these receptors (~ 1 nM) is well below the normal plasma EPO concentration (1–10 pM). Therefore, EPO's cytoprotective effect may require higher doses than those used to treat anemia.

* Corresponding author. Fax: +81 6 6879 3749.

E-mail address: isaka@att.med.osaka-u.ac.jp (Y. Isaka).

However, recent clinical trials have suggested that higher doses of EPO are likely to be associated with adverse effects [14]. Furthermore, recent report demonstrated that high-hemoglobin level in chronic kidney disease was associated with increased risk and no incremental improvement in the quality of life [15].

Recently, a second receptor for EPO that mediates EPO's tissue protection has been identified as consisting of the EPO-R and the β -common (CD131) receptor (C β -R). The EPO modified by carbamylation [carbamylation EPO (CEPO)] is reported to signal only through this receptor and not through the homodimeric EPO-R [16]. It has been shown that CEPO does not stimulate erythropoiesis, but that it prevents tissue injury in spinal cord neurons [16,17] and cardiomyocytes [18,19]. In this study, we examined whether treatment with CEPO could protect the kidney from tubular apoptosis that occurs after ischemia-reperfusion injury and, thereby, inhibit subsequent tubulointerstitial fibrosis.

Materials and methods

Experimental design. Forty-two male Sprague–Dawley rats weighing 220–280 g were purchased from Japan SLC Inc. (Shizuoka, Japan) and were maintained under standard conditions until the experiments were done. All studies were performed in accordance with the principles of the Guideline on Animal Experimentation of Osaka University. The rats were randomly allocated into three groups: (1) the saline-treatment group (control group; $n = 15$); (2) the EPO-treatment group (EPO group; $n = 15$); and (3) the CEPO-treatment group (CEPO group; $n = 12$). Prior to I/R injury, control, EPO, and CEPO group rats received subcutaneous injections of 1 ml of saline, 100 IU/kg recombinant human EPO (Kirin Corp., Tokyo, Japan), and 100 IU/kg CEPO [16] every 2 days for 2 weeks (a total of six injections), respectively, because pre-treatment with EPO is clinically established in kidney transplantation. One day after the last injections, the rats were subjected to renal I/R injury. All rats were anesthetized with an intraperitoneal injection of sodium thiopentone (30 mg/kg). The animals were allowed to stabilize for 30 min (min) before they were subjected to 45 min of bilateral renal occlusion using artery clips to clamp the renal pedicles. Occlusion was confirmed visually by a change in the color of the kidneys to a paler shade. Reperfusion was initiated with the removal of the artery clips and was confirmed visually by noting a blush. The rats were sacrificed 24 hour (h), 72 h, and 1 week (wk) after reperfusion. Before the ischemic period and 24 h after reperfusion, 1 ml blood samples were collected from the anesthetized rats via their tail veins to measure hemoglobin and serum creatinine levels.

Antibodies. To identify myofibroblasts, we used anti-human α -smooth muscle actin (α -SMA) antibody (EPOS System; Dako, Hamburg, Germany). To detect the pathways that protect the kidneys, we used the following antibodies for immunohistochemical testing: polyclonal Ki-67 antibody (1:200, Abcam, Cambridge, UK), monoclonal phosphatidylinositol-3 kinase (PI3K) p85 α antibody (1:1000, Santa Cruz), polyclonal phospho-Akt (Ser473) antibody (1:1000, Cell Signaling Technology, Beverly, MA), polyclonal Akt antibody (1:1000, Cell Signaling), and polyclonal Ets-1 antibody (1:1000, Santa Cruz). We normalized protein levels with polyclonal β -actin antibody (1:1000, Cell Signaling).

Morphology and immunohistochemical staining. Tissue samples were fixed in 4% (wt/vol) of buffered paraformaldehyde (PFA) for 16 h and then embedded in paraffin. Four micrometers of tissue sections were mounted on silane (2% 3-aminopropyltriethoxysilane)-coated slides (Muto Pure Chemicals, Tokyo, Japan) and deparaffinized with xylene.

Immunohistochemical staining was done using the Envision system (Dako), according to the manufacturer's instructions. Endogenous peroxidase activities were blocked with 3% H₂O₂ for 10 min. The first anti-

bodies were diluted in 1% bovine serum albumin (BSA) in phosphate-buffered saline (PBS) with 0.1% Tween 20 (PBS-T) at specific concentrations as described above, and then incubated for 24 h at 4 °C. This was followed by incubation with suitable secondary antibodies. Antigen retrieval was performed for 10 min in preheated 10 mmol/L sodium citrate (pH 7), using an autoclave. All incubations were performed in a humidified chamber. Chromogenic color was developed with 3,3'-diaminobenzidine tetrahydrochloride (DAB; Dako). Negative controls, omitting the first antibodies, were carefully examined for each reaction. The nuclei were counterstained with hematoxylin. All histological slides were examined by light microscopy using a Nikon Eclipse 80 i (Nikon, Tokyo, Japan); pictures were taken with the Nikon ACT-1 ver. 2.63.

The α -SMA-positive area relative to the total area of the field was calculated as a percentage by a computer-aided manipulator. Glomeruli and large vessels were not included in the microscope fields for image analysis. The scores of 10 fields per kidney were averaged, and the mean scores for each group were then averaged. For Ki-67 staining, the number of positive cell nuclei and the total numbers of cell nuclei stained with hematoxylin were counted in 10 random areas, and the percentages of the numbers of positive nuclei to the numbers of total cell nuclei were then compared.

Terminal deoxynucleotidyltransferase-mediated dUTP nick end-labeling (TUNEL) staining. TUNEL staining was performed using the *in situ* Apoptosis Detection Kit (Takara Bio, Otsu, Japan), according to the manufacturer's instructions. Briefly, the sections were deparaffinized and treated with antigen retrieval in preheated 10 mmol/L sodium citrate (pH 7), using a steamer for 40 min. They were then incubated with 3% H₂O₂ for 10 min, which was followed by incubation with TdT enzyme solution for 90 min at 37 °C. The reaction was terminated by incubation in a stop/wash buffer for 30 min at 37 °C. The number of TUNEL-positive cell nuclei and the total numbers of cell nuclei stained with hematoxylin were counted in 10 random areas, and the percentages of the numbers of TUNEL-positive nuclei to the numbers of total cell nuclei were then calculated.

Western blot Analysis. Kidney tissue was homogenized in a radioimmunoprecipitation (RIPA) Lysis Buffer with phenylmethylsulfonylfluoride (PMSF) solution, sodium orthovanadate solution, and protease inhibitor (Santa Cruz). Homogenates were centrifuged (12,000g for 10 min at 4 °C), and the supernatant total protein was measured by the Lowry protein assay (Bio-Rad, Hercules, CA). Total protein lysate (15 μ g) containing 1:1 denaturing sample buffer was boiled for 3 min and resolved on 5.0–10.0% SDS-polyacrylamide gels and electrophoretically transferred onto an immobilized PVDF membrane (Millipore, Bedford, MA). The filter was blocked with 5% (wt/vol) nonfat milk or 1% BSA in 10 mM Tris-buffered saline with 0.1% Tween 20 (TBS-T), followed by overnight incubation at 4 °C with diluted primary antibodies in TBS-T or blocking buffer. After washing five times in TBS-T, the filter was incubated with secondary antibody (1:1000) (Cell Signaling) in TBS-T for 45 min at room temperature and developed to detect specific protein bands using ECL reagents (Amersham Bioscience Corp., Piscataway, NJ). The band density was analyzed by NIH image software.

Statistical analysis. Data are expressed as means \pm SD. Statistical significance, defined as $p < 0.01$ or < 0.05 , was evaluated using ANOVA.

Results

Effect on erythropoiesis and renal function

When compared to saline-treated rats, EPO-treatment (100 IU/kg \times 3/wk \times 2wk) significantly increased Hb concentration (saline, 13.5 ± 0.9 g/dl vs. EPO, 14.9 ± 1.0 g/dl; $p < 0.01$). On the other hand, CEPO-treatment neither enhanced nor reduced Hb concentration (13.1 ± 0.2 g/dl; $p = 0.73$), suggesting that CEPO, unlike EPO, does not stimulate erythropoiesis. Saline-treated rats demonstrated

the increment of serum creatinine (1.54 ± 0.68 mg/dl) 24 h after I/R injury, and EPO-treatment showed the tendency to suppress the increase of creatinine (1.25 ± 0.80 mg/dl; $p = 0.096$ vs. saline group), while CEPO-treatment significantly suppressed (0.53 ± 0.20 mg/dl; $p < 0.05$ vs. saline group).

Effects on tubular apoptosis and proliferation in the I/R injury kidney

To elucidate the protective mechanisms by which EPO or CEPO administration ameliorated tubular injury, we did TUNEL immunostaining to quantify the number of apoptotic cells. In the saline-treated I/R injury model rats, TUNEL-positive, apoptotic cells increased among the tubular epithelial cells at 24 h (TUNEL-positive cell number per field, 64.3 ± 10.8) (Fig. 1a), while TUNEL-positive, apoptotic cells were significantly decreased by EPO-treatment (5.28 ± 1.16) (Fig. 1b). Moreover, CEPO-treatment decreased the number of apoptotic cells (2.14 ± 0.23) significantly more than EPO-treatment, suggesting that CEPO has a greater anti-apoptotic role than EPO (Fig. 1c and d).

Ki-67 antigen is a large nuclear protein that is preferentially expressed during the active phase of the cell cycle (G_1 , S , G_2 , and M phases), but is absent in resting cells (G_0). To assess the regeneration of tubular epithelial cells, cortical Ki-67-positive tubular cells were counted at 400 \times magnification in a minimum of 10 fields. There were few Ki-67-positive cells in saline-treated kidneys ($2.2 \pm 0.64\%$ of

tubular cells at 24 h and $2.6 \pm 0.48\%$ at 1 wk) (Fig. 2a and d). On the other hand, there were significantly more Ki-67 cells in EPO-treated rats at 24 h ($16 \pm 2.7\%$ of tubular cells at 24 h and $4.0 \pm 1.2\%$ at 1 wk; $p < 0.01$ vs. saline-treatment at 24 h) (Fig. 2b and e). CEPO-treatment further increased the Ki-67-positive cells ($63 \pm 13\%$ of tubular cells at 24 h and $23 \pm 6.5\%$ at 1 wk; $p < 0.01$ vs. saline or EPO-treatment) (Fig. 2c and f). This suggests that CEPO is more likely to have a greater regenerative effect on tubular epithelial cells than EPO.

Effect on cell signaling and *Ets-1* expression

To elucidate the intracellular erythropoietin signaling implicated in tubular protection, we examined the expression of PI3K and the activation of Akt (Fig. 3a–c). Western blot analysis demonstrated that treatment with EPO-significantly increased PI3K at 1 wk ($p < 0.05$ vs. saline group), but not at 24 h. However, treatment with CEPO induced marked expression of PI3K at 24 h ($p < 0.01$ vs. saline and EPO group), and this expression remained until 1 wk after I/R injury (Fig. 3a and b).

Phosphorylation of Akt is dependent on PI3K expression and was markedly up-regulated in CEPO-treated kidneys 24 h after I/R injury ($p < 0.01$ vs. saline and EPO group); it remained activated until 1 wk after I/R injury. However, activation of Akt was weak in EPO-treated kidneys, confirming that CEPO up-regulated the cytoprotective signaling more strongly than EPO (Fig. 3a and c).

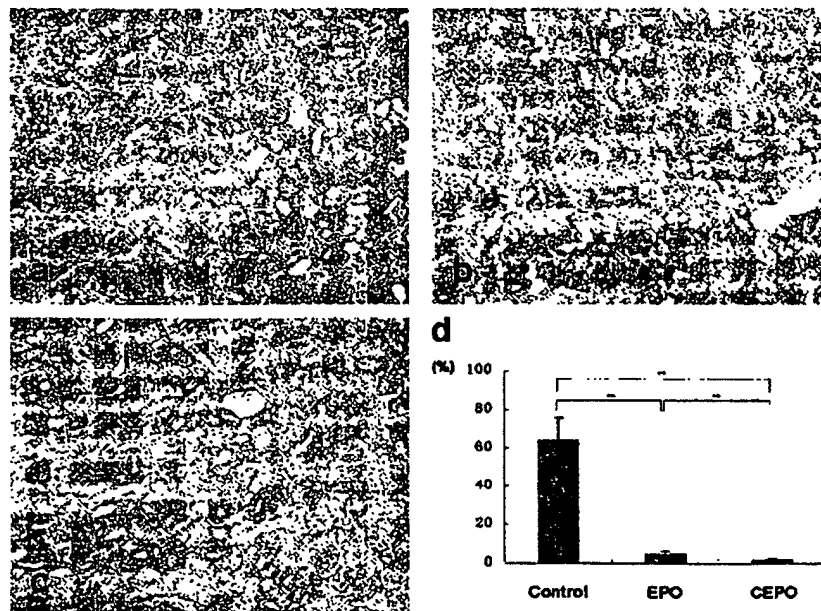


Fig. 1. Effects of EPO and CEPO on apoptosis at 24 h (400 \times). The dark brown dots correspond to representative TUNEL-positive nuclei. (a) control group, (b) EPO group, and (c) CEPO group. (d) Quantification (%) of TUNEL-positive cells in the kidney sections. Data shown are means \pm SD for 10 independently performed experiments. ** $p < 0.01$.

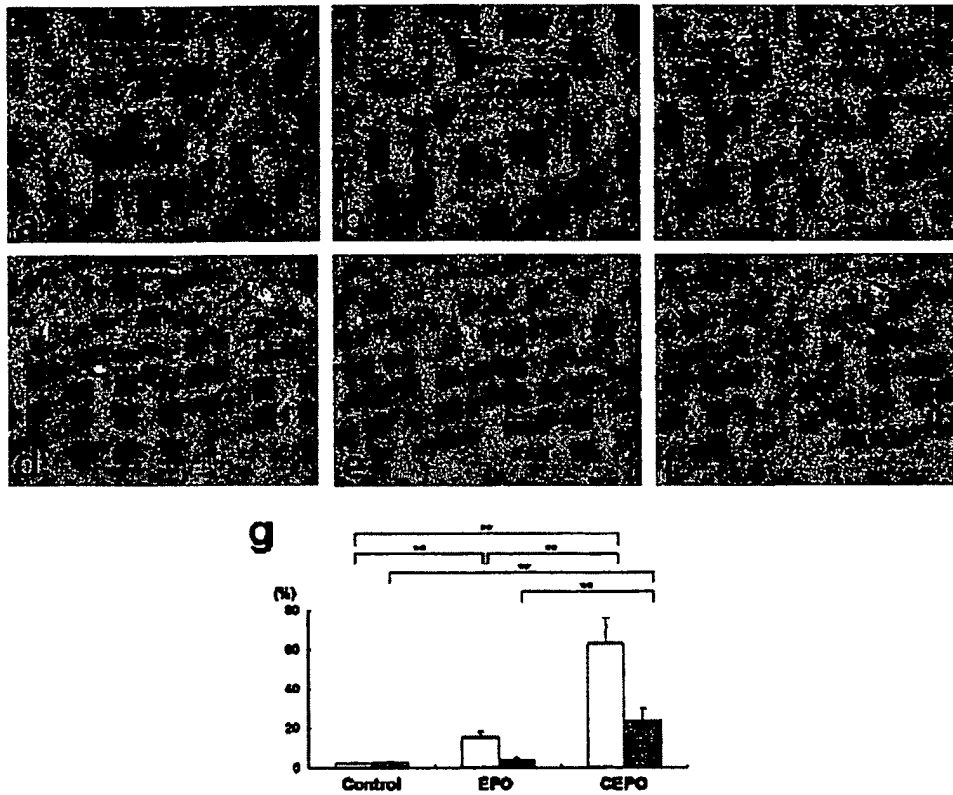


Fig. 2. Immunohistochemical staining of Ki67 (400 \times). Control group (a,d), EPO group (b,e), CEPO group (c,f) at 24 h (a–c) and 1 wk (d–f). (g) Quantification (%) of Ki-67-positive cells in the kidney sections. White bars indicate 24 h after I/R injury and dark bars indicate 1 wk after I/R injury. Data shown are means \pm SD for 10 independently performed experiments. ** p < 0.01.

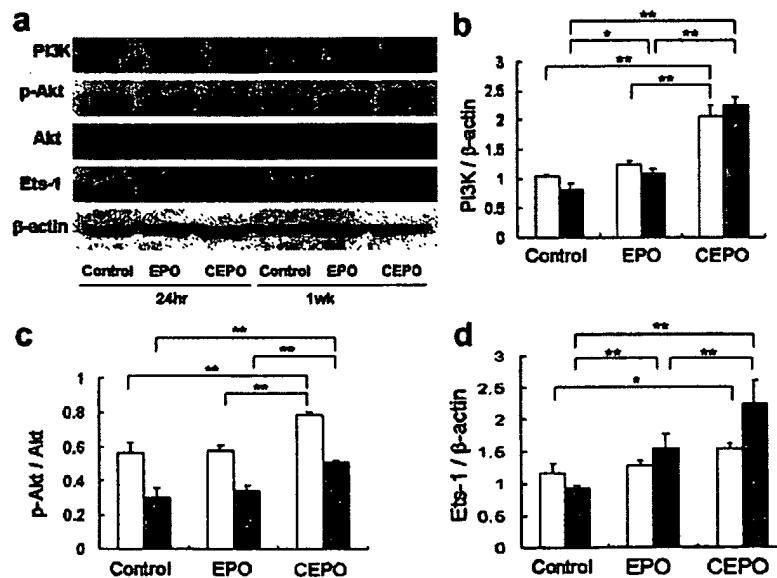


Fig. 3. Western blot analysis of the pathway of cell proliferation. (a) To elucidate the intracellular erythropoietin signaling implicated in tubular protection, we examined the expression of PI3K, Akt, and Ets-1 24 h and 1 wk after I/R injury. Relative protein levels of PI3K (b), p-Akt (c), and Ets-1 (d) were measured using NIH image. White bars indicate 24 h after I/R injury and dark bars indicate 1 wk after I/R injury. Data represent means \pm SD. ** p < 0.01, * p < 0.05.

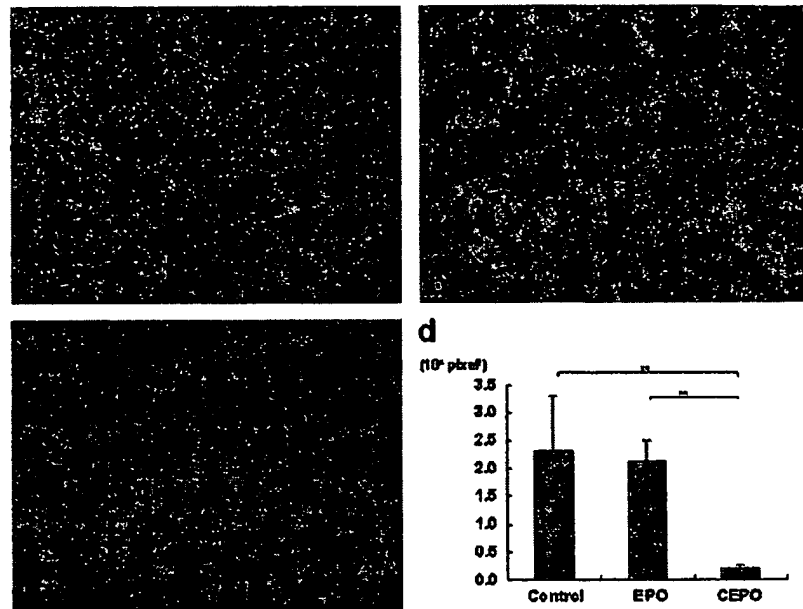


Fig. 4. Effect on phenotypic changes at 1 wk. Interstitial phenotypic changes are assessed by immunohistochemical staining of α -SMA in the control (a), EPO (b), and CEPO (c) groups. (d) Quantification (%) of the α -SMA-positive fields in the kidney sections. Data shown are means \pm SD for 10 independently performed experiments. ** $p < 0.01$.

Given that Ets-1, which is transiently up-regulated after I/R injury, has been reported to induce tubular regeneration [20], we also examined the expression of Ets-1 by Western blot analysis. Western blot analysis demonstrated that the administration of EPO slightly increased Ets-1 protein expression at 24 h, and dramatically up-regulated Ets-1 protein expression 1 wk after I/R injury ($p < 0.01$ vs. saline group). Consistent with the activation of Akt, CEPO induced Ets-1 expression at 24 h ($p < 0.05$ vs. saline group), and the up-regulation was sustained 1 wk after I/R injury ($p < 0.01$ vs. saline and EPO group) (Fig. 3a and d).

Effects on interstitial phenotypic changes in the I/R injury kidney

To detect interstitial myofibroblasts, which are associated with interstitial damage and fibrosis, the expression of α -SMA was examined immunohistochemically. The interstitial expression of α -SMA increased 1 wk after I/R injury in the saline-treated rats (Fig. 4a), while EPO-treatment significantly suppressed interstitial expression of α -SMA (Fig. 4b). CEPO-treatment suppressed interstitial expression of α -SMA even further so that the expression of α -SMA was limited to the blood vessels (Fig. 4c).

Discussion

In this paper, we examined whether EPO or CEPO may have therapeutic effects on tubulointerstitial injury in a rat model of I/R injury. Untreated kidneys exhibited increased tubular apoptosis and interstitial α -SMA expression, while

EPO-treatment inhibited tubular apoptosis and α -SMA expression to some extent. On the other hand, CEPO-treated kidneys showed minimal tubular apoptosis and limited α -SMA expression. In addition, CEPO administration did not increase the Hb concentration, while EPO-treatment increased the Hb concentration.

Based on our results, both EPO and CEPO appear to have a protective function against I/R injury; however, CEPO has more protective effects against I/R injury to tubular epithelial cells than EPO. Several key findings support this conclusion. (1) There were fewer TUNEL-positive, apoptotic cells among the tubular epithelial cells in CEPO-treated kidneys than in EPO-treated kidneys. (2) Compared to EPO, CEPO significantly promoted tubular epithelial cell proliferation assessed by Ki-67 staining. (3) While EPO-treatment significantly suppressed the interstitial phenotypic alteration assessed by α -SMA expression, CEPO-treatment suppressed this even further, so that interstitial α -SMA expression was not observed. (4) CEPO-treatment significantly suppressed the increase of serum creatinine 24 h after I/R injury. These observations suggest that CEPO has a greater therapeutic value in I/R injury than EPO.

We demonstrated that CEPO-treatment markedly suppressed I/R injury-induced tubular epithelial apoptosis compared to EPO-treatment. Furthermore, though EPO-treatment significantly suppressed the interstitial phenotypic alteration assessed by α -SMA expression, CEPO-treatment further suppressed α -SMA expression, so that there was no interstitial expression of α -SMA. One possible signal transduction pathway by which tubular

apoptosis, as well as later interstitial phenotypic changes, could be suppressed may involve the activation of PI3K. In fact, on Western blot analysis, we found that EPO-treatment increased PI3K at 1 wk, but not at 24 h. However, CEPO-treatment induced marked expression of PI3K at 24 h, which continued until 1 wk after I/R injury. Thus, phosphorylation of Akt was markedly up-regulated in CEPO-treated kidneys 24 h after I/R injury and remained activated until 1 wk. However, activation of Akt was weak in EPO-treated kidneys. Kashii et al. [21] reported that PI3K is activated by EPO in the EPO-dependent UT-7 leukemia cell line, where it recruits Akt. The PI3K-Akt pathway also leads to the up-regulation of Bcl-xL and the inhibition of apoptosis in Baf-3 cells [22]. Furthermore, using the EPO-dependent human erythroid progenitor cell line, Silva et al. [23] showed that EPO-treatment maintained the cells' viability by repressing apoptosis through up-regulation of Bcl-xL, an antiapoptotic gene of the Bcl-2 family. These results suggest that the earlier up-regulation of PI3K-Akt pathway in CEPO-treated kidneys suppressed tubular epithelial apoptosis, likely due to the induction of the anti-apoptotic genes of the Bcl-2 family.

As well, CEPO was found to significantly increase the number of proliferating tubular epithelial cells as assessed by Ki-67 expression. Tanaka et al. [20] reported that Ets-1 expression is up-regulated in the early phase of ischemic acute renal failure; Ets-1 expression was localized exclusively in the PCNA-positive regenerative proximal tubules, suggesting that Ets-1 protein may induce the transformation of regenerative renal tubular cells. In our study, compared to EPO-treatment, CEPO-treatment significantly increased the number of Ets-1-positive tubular epithelial cells. In fact, CEPO-treatment was found to further increase the number of Ki-67-positive regenerative tubular epithelial cells more than EPO-treatment. In a recent paper, Oikawa et al. [24] reported that hypoxia induced Ets-1 *via* the activity of HIF-1 α . In their study, the Ets-1 promoter contained a hypoxia-responsive element-like sequence, and HIF-1 α bound to it under hypoxic conditions. Given that we have documented the up-regulation of HIF-1 α by EPO or CEPO treatment (unpublished data), it is likely that EPO or CEPO induced Ets-1 in tubular epithelial cells and, thus, promoted tubular proliferation *via* HIF-1 α expression.

In conclusion, CEPO can protect the kidneys from ischemia-reperfusion injury; thus, the therapeutic use of CEPO warrants further attention and preclinical studies.

References

- [1] F. Gueler, W. Gwinner, A. Schwarz, H. Haller, Long-term effects of acute ischemia and reperfusion injury, *Kidney Int.* 66 (2004) 523–527.
- [2] M. Sakanaka, T.C. Wen, S. Matsuda, S. Masuda, E. Morishita, M. Nagao, R. Sasaki, In vivo evidence that erythropoietin protects neurons from ischemic damage, *Proc. Natl. Acad. Sci. USA* 95 (1998) 4635–4640.
- [3] A.L. Siren, M. Fratelli, M. Brines, C. Goemans, S. Casagrande, P. Lewczuk, S. Keenan, C. Gleiter, C. Pasquali, A. Capobianco, T. Mennini, R. Heumann, A. Cerami, H. Ehrenreich, P. Ghezzi, Erythropoietin prevents neuronal apoptosis after cerebral ischemia and metabolic stress, *Proc. Natl. Acad. Sci. USA* 98 (2001) 4044–4049.
- [4] S.A. Lipton, Erythropoietin for neurologic protection and diabetic neuropathy, *N. Engl. J. Med.* 350 (2004) 2516–2517.
- [5] R. Bianchi, B. Buyukakilli, M. Brines, C. Savino, G. Cavaletti, N. Oggioni, G. Lauria, M. Borgna, R. Lombardi, B. Cimen, U. Comelekoglu, A. Kanik, C. Tataroglu, A. Cerami, P. Ghezzi, Erythropoietin both protects from and reverses experimental diabetic neuropathy, *Proc. Natl. Acad. Sci. USA* 101 (2004) 823–828.
- [6] E.J. Sharples, N. Patel, P. Brown, K. Stewart, H. Mota-Philipe, M. Sheaff, J. Kieswich, D. Allen, S. Harwood, M. Raftery, C. Thiemermann, M.M. Yaqoob, Erythropoietin protects the kidney against the injury and dysfunction caused by ischemia-reperfusion, *J. Am. Soc. Nephrol.* 15 (2004) 2115–2124.
- [7] C.W. Yang, C. Li, J.Y. Jung, S.J. Shin, B.S. Choi, S.W. Lim, B.K. Sun, Y.S. Kim, J. Kim, Y.S. Chang, B.K. Bang, Preconditioning with erythropoietin protects against subsequent ischemia-reperfusion injury in rat kidney, *FASEB J.* 17 (2003) 1754–1755.
- [8] N.D. Vaziri, X.J. Zhou, S.Y. Liao, Erythropoietin enhances recovery from cisplatin-induced acute renal failure, *Am. J. Physiol.* 266 (1994) F360–F366.
- [9] C.J. Parsa, J. Kim, R.U. Riel, L.S. Pascal, R.B. Thompson, J.A. Petrofski, A. Matsumoto, J.S. Stamler, W.J. Koch, Cardioprotective effects of erythropoietin in the reperfused ischemic heart: a potential role for cardiac fibroblasts, *J. Biol. Chem.* 279 (2004) 20655–20662.
- [10] C.J. Parsa, A. Matsumoto, J. Kim, R.U. Riel, L.S. Pascal, G.B. Walton, R.B. Thompson, J.A. Petrofski, B.H. Annex, J.S. Stamler, W.J. Koch, A novel protective effect of erythropoietin in the infarcted heart, *J. Clin. Invest.* 112 (2003) 999–1007.
- [11] M. Nangaku, Chronic hypoxia and tubulointerstitial injury: a final common pathway to end-stage renal failure, *J. Am. Soc. Nephrol.* 17 (2006) 17–25.
- [12] J. Rossert, M. Froissart, C. Jacquot, Anemia management and chronic renal failure progression, *Kidney Int. Suppl.* (2005) S76–S81.
- [13] M. Brines, A. Cerami, Discovering erythropoietin's extra-hematopoietic functions: biology and clinical promise, *Kidney Int.* 70 (2006) 246–250.
- [14] M. Henke, R. Laszig, C. Rube, U. Schafer, K.D. Haase, B. Schilcher, S. Mose, K.T. Beer, U. Burger, C. Dougherty, H. Frommhold, Erythropoietin to treat head and neck cancer patients with anaemia undergoing radiotherapy: randomised, double-blind, placebo-controlled trial, *Lancet* 362 (2003) 1255–1260.
- [15] A.K. Singh, L. Szczec, K.L. Tang, H. Barnhart, S. Sapp, M. Wolfson, D. Reddan, Correction of anemia with epoetin alfa in chronic kidney disease, *N. Engl. J. Med.* 355 (2006) 2085–2098.
- [16] M. Leist, P. Ghezzi, G. Grasso, R. Bianchi, P. Villa, M. Fratelli, C. Savino, M. Bianchi, J. Nielsen, J. Gerwien, P. Kallunki, A.K. Larsen, L. Helboe, S. Christensen, L.O. Pedersen, M. Nielsen, L. Torup, T. Sager, A. Sfacteria, S. Erbayraktar, Z. Erbayraktar, N. Gokmen, O. Yilmaz, C. Cerami-Hand, Q.W. Xie, T. Coleman, A. Cerami, M. Brines, Derivatives of erythropoietin that are tissue protective but not erythropoietic, *Science* 305 (2004) 239–242.
- [17] C. Savino, R. Pedotti, F. Baggi, F. Ubiali, B. Gallo, S. Nava, P. Bigini, S. Barbera, E. Fumagalli, T. Mennini, A. Vezzani, M. Rizzi, T. Coleman, A. Cerami, M. Brines, P. Ghezzi, R. Bianchi, Delayed administration of erythropoietin and its non-erythropoietic derivatives ameliorates chronic murine autoimmune encephalomyelitis, *J. Neuroimmunol.* 172 (2006) 27–37.
- [18] M. Brines, G. Grasso, F. Fiordaliso, A. Sfacteria, P. Ghezzi, M. Fratelli, R. Latini, Q.W. Xie, J. Smart, C.J. Su-Rick, E. Pobre, D. Diaz, D. Gomez, C. Hand, T. Coleman, A. Cerami, Erythropoietin mediates tissue protection through an erythropoietin and common beta-subunit heteroreceptor, *Proc. Natl. Acad. Sci. USA* 101 (2004) 14907–14912.
- [19] F. Fiordaliso, S. Chimenti, L. Staszewsky, A. Bai, E. Carlo, I. Cuccovillo, M. Doni, M. Mengozzi, R. Tonelli, P. Ghezzi, T. Coleman, M. Brines, A. Cerami, R. Latini, A nonerythropoietic

- derivative of erythropoietin protects the myocardium from ischemia-reperfusion injury, *Proc. Natl. Acad. Sci. USA* 102 (2005) 2046–2051.
- [20] H. Tanaka, Y. Terada, T. Kobayashi, T. Okado, S. Inoshita, M. Kuwahara, A. Seth, Y. Sato, S. Sasaki, Expression and function of Ets-1 during experimental acute renal failure in rats, *J. Am. Soc. Nephrol.* 15 (2004) 3083–3092.
- [21] Y. Kashii, M. Uchida, K. Kirito, M. Tanaka, K. Nishijima, M. Toshima, T. Ando, K. Koizumi, T. Endoh, K. Sawada, M. Momoi, Y. Miura, K. Ozawa, N. Komatsu, A member of Forkhead family transcription factor, FKHL1, is one of the downstream molecules of phosphatidylinositol 3-kinase-Akt activation pathway in erythropoietin signal transduction, *Blood* 96 (2000) 941–949.
- [22] T. Chavakis, S.M. Kanse, F. Lupu, H.P. Hammes, W. Muller-Esterl, R.A. Pixley, R.W. Colman, K.T. Preissner, Different mechanisms define the antiadhesive function of high molecular weight kininogen in integrin- and urokinase receptor-dependent interactions, *Blood* 96 (2000) 514–522.
- [23] M. Silva, D. Grillot, A. Benito, C. Richard, G. Nunez, J.L. Fernandez-Luna, Erythropoietin can promote erythroid progenitor survival by repressing apoptosis through Bcl-XL and Bcl-2, *Blood* 88 (1996) 1576–1582.
- [24] M. Oikawa, M. Abe, H. Kurosawa, W. Hida, K. Shirato, Y. Sato, Hypoxia induces transcription factor ETS-1 via the activity of hypoxia-inducible factor-1, *Biochem. Biophys. Res. Commun.* 289 (2001) 39–43.

Received 12 October; accepted 12 December 1984.

1. Carswell, E. A. *et al. Proc. natn. Acad. Sci. U.S.A.* **72**, 3666-3670 (1975).
2. Matthews, N. & Watkins, J. F. *Br. J. Cancer* **38**, 302-309 (1978).
3. Zacharchuk, C. M., Drysdale, B.-E., Mayer, M. M. & Shin, H. S. *Proc. natn. Acad. Sci. U.S.A.* **80**, 6341-6345 (1983).
4. Hayashi, H., Kiyota, T., Sohmura, Y. & Haranaka, K. *Proc. 43rd Japan. Cancer Assoc. No.* **1132**, 314 (1984).
5. Hori, K., Hayashi, H., Sohmura, Y. & Haranaka, K. *Proc. 43rd Japan. Cancer Assoc. No.* **1130**, 314 (1984).
6. Matthews, N. *Immunology* **44**, 135-142 (1981).
7. Matthews, N. *Immunology* **48**, 321-327 (1983).
8. Williamson, B. D., Carswell, E. A., Rubin, B. Y., Prendergast, J. S. & Old, L. J. *Proc. natn. Acad. Sci. U.S.A.* **80**, 5397-5401 (1983).
9. Blattner, F. R. *et al. Science* **196**, 161-169 (1977).
10. Lawn, R. M., Fritsch, E. F., Parker, R. C., Blake, G. & Maniatis, T. *Cell* **15**, 1157-1174 (1978).
11. Maniatis, T., Jeffrey, A. & Kleid, D. G. *Proc. natn. Acad. Sci. U.S.A.* **72**, 1184-1188 (1975).
12. Rigby, P. W. J., Dieckmann, M., Rhodes, C. & Berg, P. *J. molec. Biol.* **113**, 237-251 (1977).
13. Thomas, M. & Davis, R. W. *J. molec. Biol.* **91**, 315-328 (1975).
14. Davis, R. W., Botstein, D. & Roth, J. R. (eds) *Advanced Bacterial Genetics*, 106-107 (Cold Spring Harbor, New York, 1980).
15. Messing, J. *Meth. Enzym.* **101**, 20-78 (1983).
16. Maxam, A. M. & Gilbert, W. *Proc. natn. Acad. Sci. U.S.A.* **74**, 560-564 (1977).
17. Winkler, R. J. in *Hormonal Proteins and Peptides* (ed. Li, C. H.) 1-5 (Academic, New York, 1973).
18. Amann, E., Brosius, J. & Ptashne, M. *Gene* **25**, 167-178 (1983).
19. Corbett, T. H., Griswold, D. P., Roberts, B. J., Peckham, J. C. & Schabel, F. M. *Cancer Chemother. Rep. (Pt. 2)* **5**, 169-186 (1975).
20. Corbett, T. H., Griswold, D. P., Roberts, B. J., Peckham, J. C. & Schabel, F. M. *Cancer* **40**, 2660-2680 (1977).
21. Clark, I. A., Virlizier, J.-L., Carswell, E. A. & Wood, P. R. *Infect. Immun.* **32**, 1058-1066 (1981).
22. Taverne, J., Dockrell, H. M. & Playfair, J. H. L. *Infect. Immun.* **33**, 83-89 (1981).
23. Taverne, J., Deptide, P. & Playfair, J. H. L. *Infect. Immun.* **37**, 927-934 (1982).
24. Playfair, J. H. L., Taverne, J. & Matthews, N. *Immun. Today* **5**, 165-166 (1984).
25. Vieira, J. & Messing, J. *Gene* **19**, 259-268 (1982).
26. Ito, H., Ito, Y., Ikuta, S. & Itakura, K. *Nucleic Acids Res.* **10**, 1755-1769 (1982).
27. Ruff, M. R. & Gifford, G. E. *J. Immun.* **125**, 1671-1677 (1980).
28. Laemmli, U. K. *Nature* **227**, 680-685 (1970).
29. *Isoelectric Focussing: Principles and Methods (User's manual)* (Pharmacia Fine Chemicals, Sweden, 1982).

Isolation and characterization of genomic and cDNA clones of human erythropoietin

Kenneth Jacobs, Charles Shoemaker, Richard Rudersdorf, Suzanne D. Neill, Randal J. Kaufman, Allan Mufson, Jasbir Seehra, Simon S. Jones, Rodney Hewick, Edward F. Fritsch, Makoto Kawakita*, Tomoe Shimizu† & Takaji Miyake†

Genetics Institute, Inc., 225 Longwood Avenue, Boston, Massachusetts 02115, USA

* Kumamoto University, 39-1 Kurokami 2-Chome, Kumamoto-shi, 860 Japan

† Wright State University, Dayton, Ohio 45439, USA

The glycoprotein hormone erythropoietin regulates the level of oxygen in the blood by modulating the number of circulating erythrocytes, and is produced in the kidney¹⁻⁴ or liver^{5,6} of adult and the liver^{7,8} of fetal or neonatal mammals. Neither the precise cell types that produce erythropoietin nor the mechanisms by which the same or different cells measure the circulating oxygen concentration and consequently regulate erythropoietin production (for review see ref. 9) are known. Cells responsive to erythropoietin have been identified in the adult bone marrow¹⁰, fetal liver¹¹ or adult spleen¹². In cultures of erythropoietic progenitors, erythropoietin stimulates proliferation and differentiation to more mature red blood cells. Detailed molecular studies have been hampered, however, by the impurity and heterogeneity of target cell populations and the difficulty of obtaining significant quantities of the purified hormone. Highly purified erythropoietin may be useful in the treatment of various forms of anaemia, particularly in chronic renal failure¹³⁻¹⁵. Here we describe the cloning of the human erythropoietin gene and the expression of an erythropoietin cDNA clone in a transient mammalian expression system to yield a secreted product with biological activity.

Fig. 1 Northern analysis of human fetal liver mRNA. Human fetal liver (5 µg) and adult liver mRNA (5 µg) were electrophoresed in a 0.8% agarose/formaldehyde gel and transferred to nitrocellulose as described previously⁴¹. An erythropoietin-specific single-stranded probe was prepared from an M13 template containing the 87-bp exon of the human erythropoietin gene; the primer was a 20 mer derived from the same tryptic fragment as the original 17 mer probe. The ³²P-labelled probe was prepared as described previously⁴² except that after digestion with *Sma*I, the small fragment was purified from the M13 template by chromatography on a Sepharose CL4b column in 0.1 M NaOH/0.2 M NaCl. The filter was hybridized to ~5 × 10⁶ c.p.m. of this probe for 12 h at 68 °C, washed in 2 × SSC at 68 °C and exposed for 6 days with an intensifying screen. Marker mRNAs of ~2,200 and 1,000 nucleotides (indicated by arrows) were run in an adjacent lane.

Methods. Erythropoietin was purified as described previously²⁷ except that the phenol treatment was eliminated and replaced by heat treatment at 80 °C for 5 min to inactivate neuraminidase and the final step in the purification was fractionation on a C-4 Vydac reverse-phase HPLC column (Separations Group) using a 0-95% acetonitrile gradient in 0.1% trifluoroacetic acid (TFA) over 100 min. The position of erythropoietin in the gradient was determined by gel electrophoresis and N-terminal amino-acid sequence analysis¹⁶ of the major peaks and comparing sequences obtained with those previously reported for erythropoietin²¹⁻²³. Using this approach, erythropoietin was shown to elute at ~53% acetonitrile and represented 40% of the total eluted protein. Fractions containing erythropoietin were evaporated to ~100 µL, adjusted to pH 7 with 1 M ammonium bicarbonate and digested to completion with TPCK-treated trypsin (Worthington) (2% w/w enzyme/substrate) for 18 h at 37 °C. The tryptic digest was then subjected to reverse-phase HPLC using the conditions described above and the absorbance at both 280 and 214 nm monitored. Well-separated peaks were evaporated to near dryness and subjected directly to N-terminal sequence analysis¹⁶ using an Applied Biosystems Model 470A gas phase sequencer. The sequences obtained are underlined in Fig. 2. Two of these tryptic fragments were chosen for synthesis of oligonucleotide probes. From the sequence Val-Asn-Phe-Tyr-Ala-Trp-Lys a 17 mer of 32-fold degeneracy (5'd(TTCANGCG⁺AG⁺AAG⁺TT); pool I) and a partially overlapping 18 mer of 128-fold degeneracy (5'd(CCANGCG⁺AG⁺AAG⁺TTNAC); pool II) were prepared on an Applied Biosystems Model 380A DNA synthesizer. From the sequence Val-Tyr-Ser-Asn-Phe-Leu-Arg, two pools of 14 mers, each 48-fold degenerate (5'd(TAC⁺A⁺G⁺ET⁺AAAT⁺CTT⁺CT); pool III) and 5'd(TAC⁺A⁺G⁺ET⁺AAAT⁺CTT⁺CT); pool IV), which differ at the first position of the leucine codon, were prepared. The oligonucleotides were labelled at the 5' end using polynucleotide kinase (New England Biolabs) and [γ -³²P]ATP (NEN). The specific activity of the oligonucleotides varied between 1,000 and 3,000 Ci mmol⁻¹ oligonucleotide. A human genomic DNA library in bacteriophage λ ⁴³ was screened using a modification of the *in situ* amplification procedure described originally by Woo *et al.*⁴⁴ and using tetramethylammonium chloride as the hybridization salt (see also refs 45-47; K.J. *et al.*, in preparation). Two independent phage (designated λ HEPO1 and λ HEPO2) hybridized to all three probes. DNA from λ HEPO1 was digested to completion with *Sau*3A and subcloned into M13 for DNA sequence analysis using the dideoxy chain termination method⁴⁷. Analysis of this DNA sequence revealed an open reading frame which precisely codes for the tryptic fragment used to deduce pool I. This open reading frame was contained in an 87-bp exon, bounded by potential splice acceptor and donor sites. Confirmation that λ HEPO1 and λ HEPO2 contain portions of the erythropoietin was obtained by identification, through further DNA sequencing of additional exons encoding amino-acid sequences corresponding to previously determined sequences of tryptic fragments of purified erythropoietin (see Figs 2, 3).



5' 3'

27aa leader 166aa mature product

200 400 600 800 1000 1200 1400 bp

AAAAAAAA

ccctggagcc gaccgagacc caccgagccc gctctgctcc acaccggccc

ccctggagcc cgcctctctc ctccagagccc gtggggctgg cctgacaccg ccgagcttcc cggagtgagg cccccggatg

gtaccacccc cgcgccccag gtctgtgagg gaccccgccc agc-cggagc

-27
MET ATG GLY VAL HIS GLU CYS PRO
ATG GCG GTC CAC GAA TGT CTT

ALA TRP LEU TRP LEU LEU LEU SER LEU LEU SER LEU PRO LEU GLY LEU PRO LEU GLY
GCC TGC CTC TGC CTT CTC CTC CTC TCC CTC CTC TCC CTC OCT CTC GGC CTC CCA GTC CTC GTC GGC

1 20
ALA Pro Pro Arg Leu Ile SH Cys Asp Ser Arg Val Leu Glu Ala 20
GCC CCA CCA CCG CTC ATC TGT TAT GAC AGC GGA GTC CTC CTC CAG AGG TAC CTC TTT GAG GGC CCG Lys
AAG

*
Glu Ala Glu Asp Ile Thr SH 30
GAG CCC GAG AAT ATC ACC ACC GGC Cys TGT GCT GAA His Cys Ser Leu Asn Glu Asn Ile Thr
ACT

SH 30
Val Pro Asp Thr Lys Val Asn Phe Tyr Ala Trp Lys Arg Met Glu Val Gly Gln Gln Ala
GTC CCA CAC ACC AAA CTT AAT TTC TAT GGC TCG AAG AGC ATG CAG GTC CCG CAG CAG CAG CAG CCG

60
Val Glu Val Trp Gln Gly Leu Ala Leu Ser Glu Ala Val Leu Arg Gly Gln Ala Leu
GTA GAA GTC TGC CAG GGC CTC CTC GGC CTT GCG GCT GTC GTC CCG GGC CAG GGC CCG CTT

80
Leu Val Asn Ser Ser Gln Pro Trp Glu Pro Leu Gln Leu His Val Asn Lys Ala Val Ser
TTG GTC AAC TCT TCC CAG CCG TCC GAG CCG CTC CAG CTC CAT GTC GAT AAA GGC GTC GTC

100
Gly Leu Arg Ser Leu Thr Thr Leu Leu Arg Ala Leu Gly Ala Cln Lys Glu Ala Ile Ser
GCC CTT CCG ACC CTC ACC ACT CTC CTT CCG GCT GTC GCG GGC CAG AAG CAG GAA GGC ATC TCC

120
Pro Pro Asp Ala Ala Ser Ala Ala Pro Leu Arg Thr Ile Thr Ala Asp Thr Phe Arg
CCT CCA CAG CCG GCC TCA OCT CCT CCA CTC CCA ACA ATC ACT GCT GAC ACT TTC CCG CCG Lys
AAA

140
Leu Phe Arg Val Trp Ser Asn Phe Leu Arg Gly Lys Leu Lys Leu Tyr Thr Gly Glu Ala
CTC TTC CCA GTC TCC TCC AAT TTC CTC CCG GGA AAC CTC AAG CTC TAC ACA GCG GAG CCG CCG

160
SH
TGC ACC CCA CCA Gly Cys Arg Arg TCA ccagatg tgcacactg ggcatactc ccaactccct ccccaactt

gcctgtgctc caccctcccc cgcactctct gacccctctc gaggagctct cagcttcagc ccagctctgt

ccatggacac tccagtgcca gcatgacact ctccaggccc agaggaaact tccagagagt aactctgaga

tccagagatg tccagaggcc aacttgaggg cccagagcag gacgattcca gagacagct ttaactcag

gacagagccc atgtctggaa gacgcttgag ctactctgac accctgcana attgatgcc aggacacgt

ttggagcga ttacactgtt ttcgacacta ccatcaggga caggatgacc tggagaactt aggtggcag

ctgtgacttc tccaggtctc aaggagctg gcactccctt ggtgcagaga gcccccctga ccccgaggt

gtggagacca tgaagacagg atggagctg gcctctgctt ctactggagt ccaagctttg tgtattcttc

aactcatga aacaaactc aaacaccca aaacaccca

The erythropoietin genomic clones were then used to determine whether human fetal liver is a potential source of messenger RNA for complementary DNA cloning, because erythropoietin is released from mouse¹⁷, sheep¹⁸ and human¹⁹ fetal liver. Human fetal (20-week-old) and adult liver mRNAs were analysed by Northern blotting using as a probe a 95-nucleotide single-stranded fragment containing the 87-base pair (bp) exon described in Fig. 1. A strong signal was detected in fetal liver mRNA corresponding to an mRNA ~1,600 nucleotides in length (Fig. 1). An mRNA of identical size was detected weakly in adult liver mRNA and transcripts of ~2,000 nucleotides were detected weakly in both fetal and adult mRNA. The same probe was then used to isolate cDNA clones from a bacteriophage λ cDNA library constructed from the fetal liver mRNA²⁰.

To demonstrate that biologically active erythropoietin could be expressed from the cloned cDNA, we performed transient expression experiments in COS cells²⁴. The vector (p91023B) contains the adenovirus major late promoter, a simian virus 40 (SV40) polyadenylation sequence, an SV40 enhancer and origin of replication and the adenovirus virus-associated (VA) gene^{25,26}. Erythropoietin cDNA was inserted into the p91023B vector downstream of the adenovirus major late promoter (Fig.

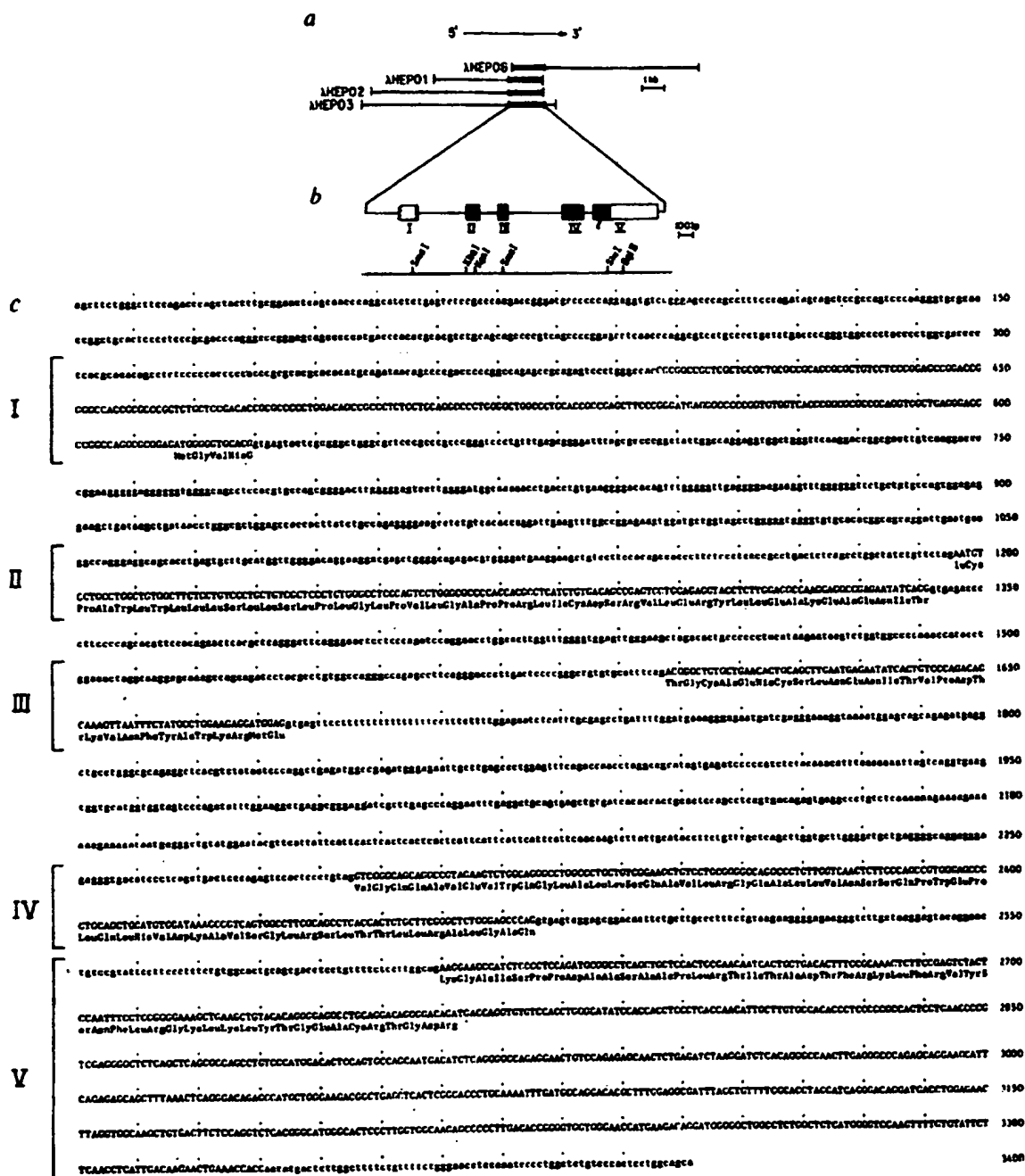


Fig. 3 Structure of the erythropoietin gene. The relative sizes and positions of four independent genomic clones (λ HEPO1, 2, 3, and 6) described in the text are illustrated by the overlapping lines in *a*. The thickened line indicates the position of the erythropoietin gene. The region containing the gene was sequenced completely from both strands using an exonuclease III generated series of deletions (C.S., unpublished observations) through this region. *b*, A schematic representation of five exons coding for erythropoietin mRNA. The precise 5' boundary of exon I is unknown (indicated by the broken box). The 5' boundary of exon I shown here is derived from λ HEPOFL8, which has a 5'untranslated region 39 nucleotides longer than that of λ HEPOFL13. The protein coding portion of the exons are darkened. *c*, Complete nucleotide sequences of the region. Exon sequences are given in capital letters; intron sequence in lower case letters. The location of exons I-V are indicated by the bars with numerals on the left. Because of difficulties in interpreting sequencing gel data from the very G+C-rich regions of exon I, the level of certainty for exon I sequence is reduced slightly.

2). After transfection of this construct into COS-1 cells, erythropoietin activity was detected by assays of the culture supernatant (Table 1).

Thus, the protein originally purified by Miyake *et al.*²⁷ and containing the N-terminus Ala-Pro-Pro-Arg... is erythropoietin (refs 21, 23; Fig. 2). Western blotting (using a polyclonal anti-erythropoietin antibody) indicates that erythropoietin produced in COS cells has a mobility on SDS-polyacrylamide gels identical to that of the native hormone prepared from human urine (data not shown).

As well as the clones described above (λ HEPO1 and λ HEPO2), two other genomic clones (λ HEPO3 and λ HEPO6) were isolated in subsequent screens of the human genomic library (Fig. 3a). Hybridization analysis of the cloned DNAs with oligonucleotide probes and with probes prepared from the erythropoietin cDNA clones positioned the erythropoietin gene in the 3.3-kilobase (kb) region in Fig. 3a. Complete sequence analysis of this region and comparison with the cDNA clones gave the map of intron and exon structure of the erythropoietin gene (Fig. 3b, c); the erythropoietin mRNA is encoded by at

Table 1 Assay for detection of erythropoietin activity

Assay method	Activity
<i>In vitro</i> CFU-E	$2.0 \pm 0.5 \text{ U ml}^{-1}$
<i>In vitro</i> ^3H -thymidine	$3.1 \pm 1.8 \text{ U ml}^{-1}$
<i>In vivo</i> exhypoxic mouse	1 U ml^{-1}
<i>In vivo</i> , starved rat	2.4 U ml^{-1}

The cDNA insert from λ HEOPOFL13 was inserted into the vector p91023B (ref. 25) described in the text. Purified DNA (8 μg) was then used to transfect 5×10^6 M6 COS cells³⁷ using the DEAE-dextran method²⁵; 12 h after transfection the cells were washed and exposed to media containing 10% fetal calf serum for 24 h. Cells were then changed to 4 ml serum-free media and collected 48 h later. *In vitro* biologically active erythropoietin was measured using either a colony-forming assay with mouse fetal liver cells as a source of erythroid colony-forming units (CFU-E)³⁸ or a ^3H -thymidine uptake assay using spleen cells from phenylhydrazine-injected mice¹². Activities are expressed in units ml^{-1} , using a commercial, quantified erythropoietin (Toyobo, Inc.) as a standard. The sensitivities of the assays are $\sim 25 \text{ mU ml}^{-1}$. *In vivo* biologically active erythropoietin was measured using either the hypoxic mouse³⁹ or the starved rat⁴⁰ method. The sensitivities of these assays are $\sim 100 \text{ mU ml}^{-1}$. No activity was detected in either assay from mock-conditioned media. In subsequent experiments with the same vector, expression levels as high as $25 \pm 3 \text{ U ml}^{-1}$ (^3H -thymidine assay method) have been observed.

least five exons. Exons II, III, IV and parts of I and V contain the protein coding information, whereas the rest of exons I and V encode the 5' and 3'-untranslated sequences, respectively. Exon I is 80% G+C and is surrounded by sequences equally G+C-rich. The CpG dinucleotide frequency in this region ($\sim 10\%$) is not significantly under-represented as it is in the remainder of the gene ($\sim 2\%$) and thus suggests a region of high methylation. The location of the actual cap site and the promoter region are not yet known.

The 166-amino-acid sequence deduced from the cDNA clones agrees precisely with our 102 amino acids of partial sequence of human urinary erythropoietin, including 25 residues at the N-terminus and 77 residues in 9 internal tryptic fragments. The sequence differs at four positions from the N-terminal sequences previously published²¹⁻²³, probably because of errors in interpretation or assignments in the original sequencing. The extent of identity between native human erythropoietin and the gene isolated here and the fact that we can detect only a single gene by genomic blotting with erythropoietin cDNA probes (data not shown) implies that the gene we have isolated is not a pseudogene or a closely related variant of the erythropoietin gene. If a second gene exists, it must be highly homologous over many kilobases to the gene described here.

We have assigned the N-terminus of the mature protein based on the N-terminus of the protein released into urine of individuals with aplastic anaemia, consistent with the hypothesis that the preceding 27 highly hydrophobic amino acids constitute a secretory leader peptide. One or more of the amino acids preceding the presumed mature terminus may be normally secreted with the remaining protein as a pro-form of erythropoietin, later processed to the native N-terminus. Amino-acid sequence analysis of tryptic fragments of urinary erythropoietin has not yet identified the fragment containing the C-terminal four amino acids (Thr-Gly-Asp-Arg; see Fig. 2). Thus, processing of erythropoietin may occur at the C-terminus and some or all of the final four amino acids encoded in the cDNA may be removed in this way. C-terminal sequencing of native erythropoietin or identification of the fragment will be necessary to answer this question.

There are four cysteines in the 166 amino acids of mature erythropoietin. Based on the sensitivity of the biological activity of erythropoietin to reducing agents (ref. 28 and T. Shimizu, personal communication), at least two of these residues must be involved in a disulphide bond.

In the mature protein there are three predicted sites of N-linked glycosylation (residues 24, 38 and 83) based on the consensus glycosylation site Asn-X-Ser/Thr²⁹. Amino-acid

sequence analysis suggests that the asparagines at residues 24 and 83 are glycosylated (data not shown) (residue 38 has not been examined). Native erythropoietin is highly glycosylated, displaying a complex, probably poly-antennary sugar structure³⁰. The relative molecular mass (M_r) of the protein backbone deduced from the primary sequence is 18,398. As the reported M_r s for native erythropoietin determined by SDS gel electrophoresis are in the range 34,000–39,000 (refs 27, 31), nearly one-half of the apparent M_r of erythropoietin must be contributed by the sugar side chains. Whether any of the glycosylation is the result of O-linked glycosylation is unknown. The terminal sialic acid residue(s) of native erythropoietin is required for full *in vivo* biological activity but is not necessary for *in vitro* activity³². This effect may result from enhanced clearance of asialylated erythropoietin from the circulation by the liver³³. The biological activity of a completely unglycosylated erythropoietin may now be assessable using a recombinant system.

Lee-Huang³⁴ recently reported the isolation of an erythropoietin cDNA clone from mRNA of a human kidney carcinoma. As no sequence information was provided, we are unable to compare the erythropoietin clones described here with the cDNA clone of Lee-Huang³⁴. Fyhrquist *et al.*³⁵ have suggested that renin substrate (angiotensinogen) may be the erythropoietin precursor. Our results argue against a large precursor and comparison of the human erythropoietin amino-acid sequence with the rat angiotensinogen protein sequence³⁶ reveals no regions of homology and further argues against any relationship between the two polypeptides. Finally, extensive comparison of the erythropoietin amino-acid and cDNA sequence with sequences contained in both the National Biomedical Research Foundation and Genbank data bases has revealed no significant homology with any published sequence.

We thank Dr Judith Sherwood for the anti-erythropoietin antibody, Dr John Tooze for the fetal liver cDNA library, Drs Peter Dukes and Masayoshi Ono for the *in vivo* biological assays, Dr Eugene L. Brown for helpful discussions on the selection of oligonucleotide probes, John Brown, Tatjana Loh, Chris Bassler, Pat Murtha, Louise Wasley, Richard Wright, Evan Beckman, Ann Leary, Tom Gesner, Jane Aghajanian and Lisa Mitsock for technical support, Elizabeth Orr for help with the computer analysis, Joyce Lauer for improvements to the manuscript, Marybeth Erker for typing the manuscript and Dr Robert Kamen and Gabriel Schmergel for their support and encouragement. This project was supported by Chugai Pharmaceuticals, Japan.

Received 17 December 1984; accepted 30 January 1985.

- Sherwood, J. B. & Goldwasser, E. *Endocrinology* 103, 866–870 (1978).
- Hammond, D. & Winnick, D. *Ann. N.Y. Acad. Sci.* 230, 219–227 (1974).
- Jacobson, L. O., Goldwasser, E., Fried, W. & Fizak, L. F. *Trans. Am. Phys.* 10, 305–317 (1957).
- Krantz, S. B. & Jacobson, L. O. thesis, Univ. Chicago (1970).
- Fried, W. *Blood* 40, 671–677 (1972).
- Naughton, B. A. *et al.*, *Science* 196, 301–302 (1977).
- Lucarelli, G. P., Howard, D. & Stohman, F. Jr *J. clin. Invest.* 43, 2195–2203 (1964).
- Zanjani, E. D., Poster, J., Burlington, H., Mann, L. I. & Wasserman, L. R. *J. Lab. clin. Med.* 89, 640–644 (1977).
- Fisher, J. *Proc. Soc. exp. Biol. Med.* 173, 289–305 (1983).
- Krantz, S. B., Gallien-Lartigue, O. & Goldwasser, E. *J. biol. Chem.* 238, 4085–4090 (1963).
- Dunn, C. D., Jarvis, J. H. & Greenman, J. M. *Expt. Hemat.* 3, 65–78 (1975).
- Krystal, G. *Expt. Hemat.* 11, 649–660 (1983).
- Krane, N. *Henry Ford Hosp. Med. J.* 31, 177–181 (1983).
- Anagnostou, A., Barone, J., Vodo, A. & Fried, W. *Br. J. Hemat.* 37, 85–91 (1977).
- Eschbach, J., Mladenovic, J., Garcia, J., Wahl, P. & Adamson, J. *J. clin. Invest.* 74, 434–441 (1984).
- Hewick, R. M., Hunkapiller, M. E., Hood, L. E. & Dreyer, W. J. *J. biol. Chem.* 256, 7990–7997 (1981).
- Zanjani, E. D., Ascensao, J. L., McGlave, P. B., Banisadre, M. & Ash, R. C. *J. clin. Invest.* 67, 1183–1188 (1981).
- Gruber, D. F., Zucali, J. R. & Mirand, E. A. *Expt. Hemat.* 5, 392–398 (1977).
- Congote, L. F. *J. Steroid Biochem.* 8, 423–428 (1977).
- Toole, J. J. *et al.* *Nature* 312, 342–347 (1984).
- Goldwasser, E. *Blood* 58, Suppl. 1, 13 (abstr.) (1981).
- Sae, J. M. and Sytkowski, A. *J. Proc. natn. Acad. Sci. U.S.A.* 80, 3651–3655 (1983).
- Yanagawa, S. *et al.* *J. biol. Chem.* 259, 2707–2710 (1984).
- Gluzman, Y. *Cell* 23, 175–182 (1981).
- Wong, G. C. *et al.* *Science* (in the press).
- Kaufman, Proc. natn. Acad. Sci. U.S.A. (in the press).
- Miyake, T., Kung, C. & Goldwasser, E. *J. biol. Chem.* 252, 5558–5564 (1977).
- Sytkowski, A. *Biochem. biophys. Res. Commun.* 96, 143–149 (1980).
- Wagh, P. V. & Bahl, O. P. *CRC crit. Rev. Biochem.* 307–377 (1981).
- Murphy, M. & Miyake, T. *Acta Haemat. Jap.* 46, 1380–1396 (1983).
- Wang, F. F., Kung, C. K.-H. & Goldwasser, E. *Fedn Proc.* 42, 1872 (abstr.) (1983).

32. Lowy, P., Keighley, G. & Borosok, H. *Nature* **285**, 102-103 (1980).
33. VanLenten, L. & Ashwell, G. *J. Biol. Chem.* **247**, 4633-4640 (1972).
34. Leo-Huang, S. *Proc. natn. Acad. Sci. U.S.A.* **81**, 2708-2712 (1984).
35. Fyrquist, F., Rosenlof, K., Gronhagen-Riska, C., Hortling, L. & Tikkanen, I. *Nature* **308**, 649-652 (1984).
36. Ohkubo, H. *et al. Proc. natn. Acad. Sci. U.S.A.* **80**, 2196-2200 (1983).
37. Horowitz, M., Cepko, C. & Sharp, P. A. *J. molec. appl. Genet.* **2**, 147-149 (1983).
38. Bensch, N. & Ooldo, D. W. In *In Vitro Aspects of Erythropoiesis* (Murphy, M. J.) 252-253 (Springer, New York, 1978).
39. Cote, P. M. & Bangham, D. R. *Nature* **191**, 1065-1068 (1961).
40. Goldwasser, E. & Gross, M. *Meth. Enzym.* **37**, 109-121 (1975).
41. Derman, E. *et al. Cell* **23**, 731-739 (1981).
42. Anderson, S. & Kingston, I. B. *Proc. natn. Acad. Sci. U.S.A.* **80**, 6836-6842 (1983).
43. Lawn, R. M., Fritsch, E. F., Parker, R. C., Blake, G. & Maniatis, T. *Cell* **15**, 1157-1174 (1978).
44. Woo, S. L. C. *et al. Proc. natn. Acad. Sci. U.S.A.* **75**, 3688-3691 (1978).
45. Melchior, W. B. & von Hippel, P. H. *Proc. natn. Acad. Sci. U.S.A.* **70**, 298-302 (1973).
46. Gross, J. M. & Wetmar, J. G. *Biopolymers* **16**, 1183-1199 (1977).
47. Sanger, F., Nicklen, S. & Coulson, A. R. *Proc. natn. Acad. Sci. U.S.A.* **74**, 5463-5467 (1977).
48. Benton, W. D. & Davis, R. W. *Science* **196**, 180-182 (1977).

Identification of DNA sequences required for activity of the cauliflower mosaic virus 35S promoter

Joan T. Odell, Ferenc Nagy & Nam-Hai Chua

Laboratory of Plant Molecular Biology, The Rockefeller University, 1230 York Avenue, New York, New York 10021-6399, USA

Although promoter regions for many plant nuclear genes have been sequenced, identification of the active promoter sequence has been carried out only for the octopine synthase promoter¹. That analysis was of callus tissue and made use of an enzyme assay. We have analysed the effects of 5' deletions in a plant viral promoter in tobacco callus as well as in regenerated plants, including different plant tissues. We assayed the RNA transcription product which allows a more direct assessment of deletion effects. The cauliflower mosaic virus (CaMV) 35S promoter provides a model plant nuclear promoter system, as its double-strand DNA genome is transcribed by host nuclear RNA polymerase II from a CaMV minichromosome². Sequences extending to -46 were sufficient for accurate transcription initiation whereas the region between -46 and -105 increased greatly the level of transcription. The 35S promoter showed no tissue-specificity of expression.

The 35S promoter region was isolated as a *Bgl*II fragment extending from -941 to +208 with respect to the transcription start site mapped for the 35S RNA found in CaMV-infected turnip leaves³. The polyadenylation site for the 19S and 35S CaMV transcripts located at +180 (ref. 3) was deleted, as described in Fig. 1 legend, to eliminate any possible processing signals in the promoter fragment. A 3' deleted promoter fragment extending to +9 was deleted at its 5' end (see Fig. 1) and fragments extending to -343, -168, -105 and -46 were chosen for analysis.

An abbreviated human growth hormone gene (*hgh*)⁴ was added as a test gene downstream to the 35S promoter deletion fragments. Information on plant cell recognition of animal gene splice and 3' polyadenylation signals obtained from analysis of *hgh* RNA transcribed in transformed plant cells will be presented elsewhere (A. Hunt, N. Chu, J.T.O., F.N. and N.-H.C., in preparation). The 35S promoter-*hgh* chimaeric gene was inserted in the pMON178 tumour-inducing (Ti)-plasmid vector, a derivative of pMON120 (ref. 5). Included in this vector is the nopaline synthase (NOS) promoter placed 5' to the neomycin phosphotransferase-II (*npt-II*) coding region (NOS promoter-*npt-II* gene), which is co-transferred with the 35S promoter-*hgh* gene into the tobacco genome and provides an internal standard for comparison of the activities from different 35S promoter deletion fragments.

Following tri-parental matings^{5,6}, *Agrobacterium tumefaciens* containing both chimaeric genes was used to infect SR1 *Nicotiana tabacum* cells by wounding⁵ and co-cultivation^{5,7}.

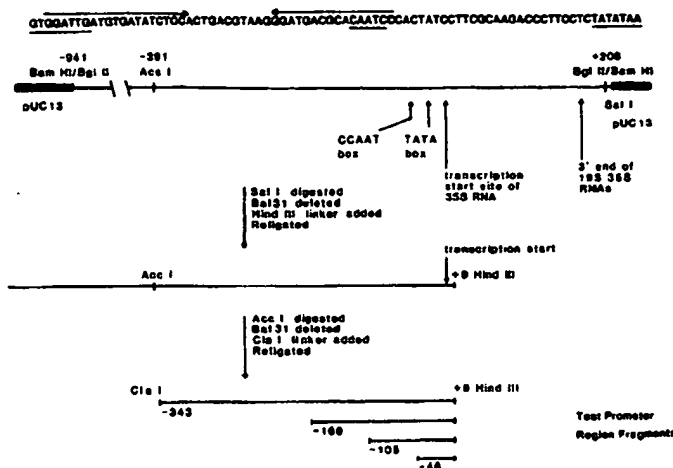


Fig. 1 Construction of 35S promoter region fragments. A 1.15-kb *Bgl*II fragment was subcloned from pCS101, a clone containing the entire Cabb-S CaMV genome³, into the *Bam*HI site of pUC13. The resulting plasmid was linearized at the *Sal*I site in the pUC13 polylinker next to the 3' end of the promoter fragment, digested with *Bal*31 exonuclease¹¹, ligated to *Hind*III linkers and recircularized. Clones were analysed for the extent of 3' deletion by polyacrylamide gel sizing of the *Acc*I/*Hind*III fragments and finally by dideoxy sequencing¹² of subclones in pUC using the universal primer. The plasmid containing a 3' deletion fragment with the *Hind*III linker at +9 was linearized with *Acc*I (site at -391), digested with *Bal*31 exonuclease, ligated to *Cla*I linkers and recircularized. Clones were analysed for the extent of 5' deletion by polyacrylamide gel sizing of the *Cla*I/*Hind*III fragment, followed by dideoxy sequencing of subclones in pUC using either the universal primer or primer generation by exonuclease III digestion¹³. Above is the sequence of the -105 to -25 region of the 35S promoter¹⁴ with TATA-box, CAAT-box, inverted repeat and core enhancer sequence regions marked.

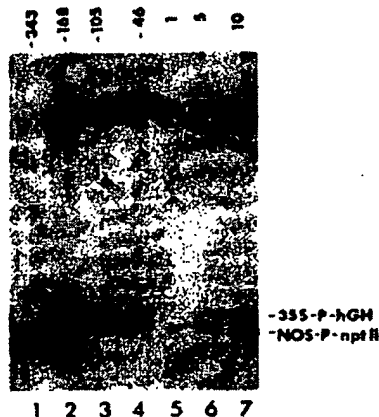


Fig. 2 Southern blot analysis of DNA from transformed tobacco calli. DNA was prepared, digested with *Eco*RI, electrophoresed on a 0.7% agarose gel and blotted onto a nitrocellulose filter¹⁵. A plasmid constructed to serve as the hybridization probe contains a *Bam*HI/*Sma*I *hgh* gene fragment and a *Bam*HI/*Bgl*II *npt-II* gene fragment cloned into pUC12 (GH-Neo24). The plasmid was nick translated¹⁶ and hybridized to the Southern blot by the method of Thomashow *et al.*¹⁷. The following samples contain 15 µg of calli DNA transformed with: lane 1, -343 35S promoter-*hgh*; lane 2, -168 35S promoter-*hgh*; lane 3, -105, 35S promoter-*hgh*; lane 4, -46 35S promoter-*hgh*. Reconstructions of the NOS promoter-*npt-II* gene and 35S promoter-*hgh* gene copy numbers contain 15 µg of control untransformed plant DNA mixed with different amounts of the pMON178 plasmid containing the -105 35S promoter-*hgh* gene: lane 5, 17 pg = 1 copy; lane 6, 85 pg = 5 copies; lane 7, 170 pg = 10 copies. The bands near the top of the filter in lanes 1-4 result from hybridization of the pBR322 sequences in the GH-Neo24 probe plasmid to pBR322 sequences in the integrated pMON178 Ti vector. In lanes 5-7 the upper bands are derived from other regions of the pMON178 plasmid.

1: Pathol Biol (Paris) 1996 Jan;44(1):57-64

Oxidative stress in Parkinson's disease and other neurodegenerative disorders.

Jenner P.

Biomedical Sciences Division, King's College London, UK.

The cause of cell death in neurodegenerative diseases remains unknown but the formation of free radicals and the occurrence of oxidative stress may be a common component of many, if not all, such disorders. For example, in substantia nigra in Parkinson's disease key alterations occur, in iron handling, mitochondrial function and antioxidant defences, particularly reduced glutathione. These indices of oxidative stress are accompanied by evidence of free radical mediated damage in the form of increased lipid peroxidation and oxidation of DNA bases. The alterations in oxidative stress occurring in Parkinson's disease appear not be related to the administration of L-DOPA. Some alterations of oxidative stress are found in other basal ganglia in degenerative disorders (multiple system atrophy, progressive supranuclear palsy, Huntington's disease) but these have not been investigated to the same extent. Similarly, examination of biochemical changes occurring in Alzheimer's disease, motor neurone disease and diabetic neuropathy also suggest the involvement of free radical mediated mechanisms as a component of neurodegeneration. It is probable that irrespective of the primary cause of individual neurodegenerative disorder, the onset of oxidative stress is a common mechanism by which neuronal death occurs and which contributes to disease progression. Clearly, therapeutic strategies aimed at limiting free radical production and oxidative stress and/or damage may slow the advance of neurodegenerative disease.

Publication Types:

Review

Review, Tutorial

PMID: 8734302 [PubMed - indexed for MEDLINE]

IGF-1 Overexpression Inhibits the Development of Diabetic Cardiomyopathy and Angiotensin II–Mediated Oxidative Stress

Jan Kajstura,¹ Fabio Fiordaliso,^{1,3} Anna Maria Andreoli,¹ Baosheng Li,¹ Stefano Chimenti,¹ Marvin S. Medow,² Federica Limana,¹ Bernardo Nadal-Ginard,¹ Annarosa Leri,¹ and Piero Anversa¹

Stimulation of the local renin-angiotensin system and apoptosis characterize the diabetic heart. Because IGF-1 reduces angiotensin (Ang) II and apoptosis, we tested whether streptozotocin-induced diabetic cardiomyopathy was attenuated in IGF-1 transgenic mice (TGM). Diabetes progressively depressed ventricular performance in wild-type mice (WTM) but had no hemodynamic effect on TGM. Myocyte apoptosis measured at 7 and 30 days after the onset of diabetes was twofold higher in WTM than in TGM. Myocyte necrosis was apparent only at 30 days and was more severe in WTM. Diabetic nontransgenic mice lost 24% of their ventricular myocytes and showed a 28% myocyte hypertrophy; both phenomena were prevented by IGF-1. In diabetic WTM, p53 was increased in myocytes, and this activation of p53 was characterized by upregulation of Bax, angiotensinogen, Ang type 1 (AT₁) receptors, and Ang II. IGF-1 overexpression decreased these biochemical responses. In vivo accumulation of the reactive O₂ product nitrotyrosine and the in vitro formation of H₂O₂·OH in myocytes were higher in diabetic WTM than TGM. Apoptosis in vitro was detected in myocytes exhibiting high H₂O₂·OH fluorescence, and apoptosis in vivo was linked to the presence of nitrotyrosine. H₂O₂·OH generation and myocyte apoptosis in vitro were inhibited by the AT₁ blocker losartan and the O₂ scavenger Tiron. In conclusion, IGF-1 interferes with the development of diabetic myopathy by attenuating p53 function and Ang II production and thus AT₁ activation. This latter event might be responsible for the decrease in oxidative stress and myocyte death by IGF-1. *Diabetes* 50:1414–1424, 2001

Diabetes alters the structure and function of the human heart, but the mechanisms involved are unknown (1). Type 1 insulin-dependent diabetes is characterized experimentally by cardiac myopathy, in which cell death by apoptosis predominates (2). Hyperglycemia activates the local renin-angiotensin system (RAS), resulting in the formation of angiotensin (Ang) II and stimulation of the endogenous cell death pathway (2). These observations raise the possibility that IGF-1 may protect the myocardium from the consequences of diabetes. This growth factor interferes with the myocyte RAS and the synthesis and secretion of Ang II (3). IGF-1 enhances the expression of MDM2, which in turn forms MDM2-p53 complexes inhibiting p53 DNA binding (3). Downregulation of p53 function decreases transcription of angiotensinogen (Aogen), which is the limiting factor in the synthesis of Ang II in myocytes (4). Therefore, IGF-1 may exert a therapeutic effect on ventricular dysfunction (5) and diabetic cardiomyopathy by attenuating the cellular RAS. This hypothesis is supported by the observation that ACE inhibition reduces cardiovascular events, improving the morbidity and mortality of diabetic patients (6,7).

Diabetes is associated with an exponential increase in oxidative damage (8). In various cell systems, a direct link has been found between Ang II and reactive O₂ (9–11). However, it is unknown whether the generation of reactive oxygen species (ROS) constitutes the intermediate event in the transmission of death signals to myocytes by Ang II. Alternatively, cooperation between Ang II and ROS may be required for cell death to occur in the diabetic heart. In the absence of ROS-induced DNA damage, Ang II may not be able to execute the death process. We hypothesized that IGF-1 overexpression may protect the myocardium from diabetes by depressing the synthesis of Ang II and thus the formation of ROS and cellular damage. To address these issues, diabetes was induced in mice homozygous for the IGF-1 transgene (12). In vivo determinations were performed in control and diabetic animals to identify the effects of IGF-1 on p53 function, p53-dependent genes, activation of the local RAS, accumulation of oxidative stress products, myocyte death, and cardiac hemodynamics. In vitro studies analyzed both the impact of diabetes on ROS formation and the efficacy of Ang type 1 (AT₁) blockade and reactive O₂ scavenger on oxidative challenge and myocyte death. Transgenic mice (TGM) with targeted

From the Departments of ¹Medicine and ²Pediatrics, New York Medical College, Valhalla, New York; and the ³Istituto Di Ricerche Farmacologiche Mario Negri, Milan, Italy.

Address correspondence and reprint requests to Jan Kajstura, Department of Medicine, New York Medical College, Vossburgh Pavilion, Room 302A, Valhalla, New York. E-mail: jan_kajstura@nymc.edu.

Received for publication 27 October 2000 and accepted in revised form 15 March 2001.

Ang, angiotensin; Aogen, angiotensinogen; AT₁, Ang receptor type 1; CM-H₂DCFDA, 5-(6-chloromethyl-2',7'-dichlorodihydrofluorescein diacetate; LVEDP, left ventricular end-diastolic pressure; LVSP, left ventricular systolic pressure; OD, optical density; PI, propidium iodide; RAS, renin-Ang system; ROS, reactive oxygen species; STZ, streptozotocin; TdT, terminal deoxynucleotidyl transferase; TGM, transgenic mice; WTM, wild-type mice.

expression of IGF-1 in myocytes were preferred over non-transgenic animals with chronic administration of growth factor, because our objective was to characterize the impact of IGF-1 on the development of diabetic cardiomyopathy. Systemic injection of IGF-1 would have influenced other organs, complicating the interpretation of the results in the heart.

RESEARCH DESIGN AND METHODS

Diabetes. A total of 31 male wild-type mice (WTM) and 31 homozygous IGF-1 TGM at 6 months of age were injected into the tail vein with streptozotocin (STZ) (200 mg/kg body wt) dissolved in a citrate-saline solution (pH 4.5) (2). Control mice, 23 in each group, were injected with the diluent and fed a restricted diet to match the decrease in body weight with diabetes. This was done to avoid the influence of calorie loss (caused by glycosuria) on body weight. Mice were killed at 7 and 30 days. Blood glucose was measured at the time of killing. Serum levels of IGF-1 were obtained at 7 days by Nichols Advantage chemiluminescence immunoassay. All protocols used were in accordance with institutional guidelines.

Cardiac function. Just before death, animals were anesthetized with tribromoethanol (1.2%, 0.2 ml i.p.). The carotid artery was cannulated with a microtip pressure transducer (SPR-671, Millar Instruments) connected to an electrostatic chart recorder. The transducer was advanced into the left ventricle for the evaluation of ventricular pressures and the rate of pressure rise (+dP/dt) and decay (-dP/dt). Rectal temperature was maintained at 36–38°C (2–4).

Tissue fixation and sampling. The heart was arrested in diastole with 0.15 M cadmium chloride (100 mmol/l), and the myocardium was perfused through the aorta with 10% formalin (13,14). The heart was excised, cardiac weights were recorded, and three slices of the left ventricle were embedded in paraffin; 48 animals were studied (6 in each group) at 7 and 30 days after STZ or diluent injection. Sections were stained with hematoxylin-eosin, and 60 fields in each heart were examined at $\times 400$ with a reticle containing 42 points to yield the volume percentage of myocytes and interstitium. Ventricular volume was multiplied by the volume fraction of myocytes to compute the aggregate volume of myocytes in the ventricle (13–16).

Myocyte death. This terminal analysis was performed in 48 animals. Myocyte apoptosis was determined by deoxynucleotidyl transferase (TdT) and hairpin probe with single-base 3' overhangs, and myocyte necrosis was determined by hairpin probe with blunt ends. Apoptosis-necrosis was evaluated by TdT and hairpin probe with blunt ends (16). These techniques have been described previously (2,13–18). Myocyte cytoplasm and nuclei were stained by α -sarcomeric actin antibody and propidium iodide (PI), respectively (2,13–18).

Sections from the base, mid-region, and apical portion of each left ventricle were examined by confocal microscopy, and the numbers of myocyte nuclei that were labeled by TdT, hairpin probes, and by TdT and hairpin probe with blunt ends were recorded by analyzing a minimum of 13.5 mm² to a maximum of 44.8 mm² of tissue. The total number of myocyte nuclei sampled for TdT at 7 days of diabetes was 78,393, 51,643, 72,255, and 69,486 in control and diabetic nontransgenic mice and control and diabetic TGM, respectively. Corresponding values for hairpin probe with single-base 3' overhangs were 77,827, 74,764, 101,469, and 81,027. Values with hairpin probe with blunt ends were 81,252, 77,464, 111,660, and 105,912. In a comparable manner, the total number of myocyte nuclei sampled for TdT at 30 days of diabetes was 81,613, 80,849, 77,796, and 81,282 in control and diabetic nontransgenic mice and control and diabetic TGM, respectively. Corresponding values for hairpin probe with single base 3' overhangs were 82,994, 86,658, 90,559, and 77,796. Values with hairpin probe with blunt ends were 92,117, 80,849, 83,687, and 81,282. Values for TdT and hairpin probe with blunt ends are not indicated because this simultaneous association was never found. The density of myocyte nuclei was obtained by counting (per unit area of tissue) the number of nuclei in α -sarcomeric actin-positive cells. The number of apoptotic and necrotic myocytes per 10⁶ cells was then calculated.

Nitrotyrosine labeling. This analysis was performed in 24 animals (6 in each group) at 30 days of diabetes. Sections were incubated overnight with rabbit anti-nitrotyrosine antibody (Upstate Biotechnology, Lake Placid, NY) diluted 1:40 in phosphate-buffered saline (19). Fluorescein isothiocyanate-labeled goat anti-rabbit IgG was used as a secondary antibody. Simultaneous presence of cell death and nitrotyrosine was evaluated with a secondary antibody labeled with tetramethyl rhodamine isothiocyanate. Sections treated with 10% peroxynitrite were used as a positive control. The percentage of myocytes containing nitrotyrosine was obtained by confocal microscopy; 300 myocyte profiles were examined in each animal.

Myocyte size and number. Myocyte cell volume was obtained by three-dimensional section reconstruction of enzymatically dissociated cells. In each left ventricle, 150–200 myocytes were measured. The total number of ventricular myocytes was computed by dividing the aggregate volume of myocytes by the average cell volume. This methodology has been described previously (12,19).

Myocyte isolation. This was performed in 44 mice, 6 in each group, at 7 days after diabetes and in 5 at 30 days after diabetes. Left ventricular myocytes were enzymatically dissociated following a protocol well established in our laboratory (3,12–14). Myocyte yields were $2.1 \pm 0.4 \times 10^6$ in control WTM, $1.4 \pm 0.5 \times 10^6$ in diabetic WTM, $2.9 \pm 0.8 \times 10^6$ in control TGM, and $2.6 \pm 0.7 \times 10^6$ in diabetic TGM. Contamination from nonmyocytes ranged from 1 to 3% in all cases.

Band shift. Oligonucleotides corresponding to the p53 binding site in the Bax, Aogen, and AT₁ promoters were used in mobility shift assays (3,4,17). As a negative control, nuclear extracts were exposed to a p53 antibody (Pab 240; Santa Cruz Biotechnology) before the binding assay. Unlabeled Aogen, AT₁, and Bax probes were used as competitors, and unlabeled mutated Aogen, AT₁, and Bax were used as noncompetitors (4,17).

Western blot. A total of 50 μ g of myocyte proteins were separated by 12% SDS-PAGE. Proteins were transferred to nitrocellulose and exposed to anti-human p53 (Pab 240; Santa Cruz Biotechnology), anti-human Bax (P19; Santa Cruz Biotechnology), anti-rat Aogen (Swant), anti-rat renin (Swant), anti-human AT₁ (306; Santa Cruz Biotechnology), and anti-human AT₂ (C-18; Santa Cruz Biotechnology) antibodies (3,4,17).

Ang II labeling. This was performed in 24 animals (6 in each group) at 7 days after diabetes. Sections were incubated with Ang II antiserum (2,3). Specificity was determined by preabsorption of antibody with antigen and by staining with nonimmune rabbit serum. Ang II-labeled myocytes and Ang II sites per millimeter squared of myocytes were determined (2,3). A total of 200 myocyte profiles were analyzed in each animal.

Reactive O₂. This analysis included five separate myocyte isolations in each group of mice at 7 days of diabetes, using a total of 20 animals. Isolated myocytes were attached to laminin-coated petri dishes, and cells were loaded with 5-(6-chloromethyl-2',7'-dichlorodihydrofluorescein diacetate (CM-H₂DCFDA) (Molecular Probes, Eugene, OR) for 30 min. Fluorescence intensity from individual cells was measured using an excitation wavelength of 485 nm and an emission wavelength of 530 nm (20,21); 100–140 cells were sampled at random in each preparation using an Olympus IX70 inverted microscope equipped with a digital cooled CCD-IEEE camera (Optronics, Goleta, CA) and ImagePro image analysis software (Media Cybernetics, Silver Spring, MD). To avoid changes in fluorescence intensity, only a single measurement per field was collected. Fluorescence was calibrated with InSpec microsphere (Molecular Probes). Calibration curves were generated and cell brightness was measured. Probe fluorescence was established and this background was subtracted from all determinations. Preliminary experiments were also performed to assess the uptake of CM-H₂DCFDA with time. Maximum fluorescence was reached between 20 and 30 min. Therefore, a 30-min interval was used. The volume of each analyzed myocyte was measured by confocal microscopy (9,10), and fluorescence intensity per cell was divided by its volume to correct for differences in cell size. After the completion of the measurements of ROS, cells were fixed and stained for apoptosis.

Ang II, ROS and apoptosis. The effects of 30 min of exposure to Ang II (10^{-9} mol/l) on ROS formation were detected as described above. Freshly isolated myocytes were cultured in laminin-coated petri dishes and serum-free medium for 1 h before the addition of Ang II. Identical cultures were exposed to losartan (10^{-7} mol/l) and to losartan plus Ang II, and ROS generation was measured. Five separate myocyte isolations were used in each condition. For the evaluation of apoptosis, myocytes were cultured in the presence of Ang II for 24 h. Additionally, the effect of losartan or the superoxide anion scavenger Tiron (0.1 mmol/l) on Ang II-mediated apoptosis was determined. In these experiments, losartan or Tiron were added to the culture 30 min before Ang II. Again, six myocyte isolations were used in each protocol.

Statistics. All tissue samples were coded, and the code was broken at the end of the study. Results are presented as the mean \pm SD. Statistical significance between two measurements was determined by the two-tailed unpaired Student's *t* test, and among groups it was determined by the Bonferroni's method (22). Probability values of *P* < 0.05 were considered significant.

RESULTS

Ventricular function. Blood glucose in WTM increased from 11.4 ± 2.1 to 27.5 ± 3.3 and 36.5 ± 3.6 mmol/l at 7 and 30 days after STZ administration, respectively. Comparable changes in blood glucose were detected in TGM: for control, diabetic TGM at 7 days, and diabetic TGM at 30

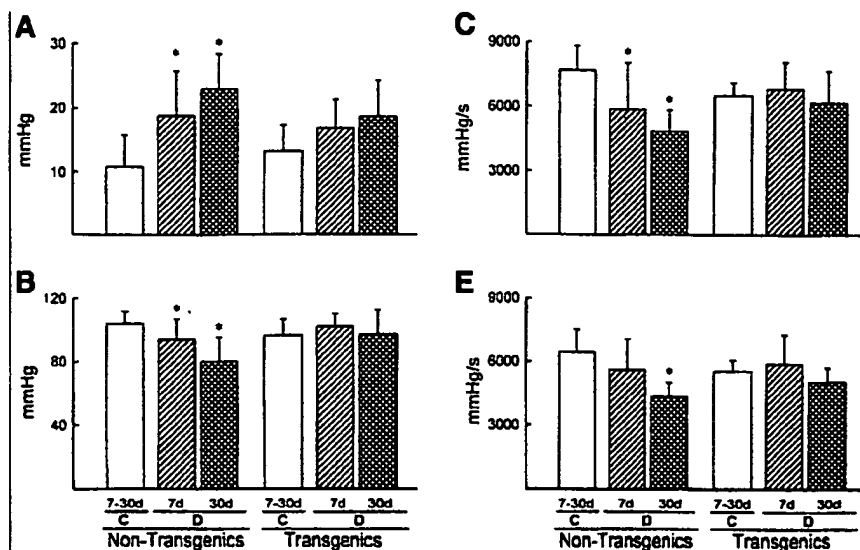


FIG. 1. Effects of diabetes on LVEDP (A), LVSP (B), LV + dP/dt (C), and LV - dP/dt (D) in non-transgenic mice and TGM. Results are means \pm SD. d, Days; C, control; D, diabetic. * $P < 0.05$ vs. C.

days the values were 11.8 ± 1.5 , 28.9 ± 4.0 , and 37.2 ± 4.5 mmol/l, respectively. As indicated by the small standard deviations, all animals in each group developed stable hyperglycemia. At 7 days, diabetes in WTM was characterized by an increase in left ventricular end-diastolic pressure (LVEDP) and a decrease in left ventricular systolic pressure (LVSP) and +dP/dt. Cardiac function was further depressed at 30 days (Fig. 1). In contrast, diabetes at 7 and 30 days did not affect ventricular performance in TGM. Because of pair-feeding, diabetic and nondiabetic mice had comparable body and cardiac weights. Heart weight-to-body weight ratios remained constant in control WTM (3.5 ± 0.2 and 3.6 ± 0.3 mg/g at 7 and 30 days, respectively) and in diabetic WTM (3.7 ± 0.3 and 3.9 ± 0.5). Similarly, control TGM (4.4 ± 0.3 and 4.5 ± 0.4) did not differ from diabetic TGM (4.3 ± 0.5 and 4.7 ± 0.6). Control and diabetic TGM had higher heart weight-to-body weight ratios ($P < 0.01$ to $P < 0.001$) than corresponding WTM (12).

It should be noted that the serum level of IGF-1 was <3 ng/ml in nondiabetic and diabetic WTM. Conversely, IGF-1 was 5.7 ± 1.2 ng/ml in nondiabetic and diabetic TGM, respectively. It cannot be excluded, therefore, that the higher circulating level of IGF-1 in TGM may have had an additional effect on the response of the heart to diabetes in this group.

Myocyte loss. Cell death values at 7 and 30 days were similar in control WTM and control TGM and thus were combined. Diabetes was associated with an increase in myocyte apoptosis, which was higher at 7 days than it was at 30 days in both WTM and TGM (Fig. 2A and B). However, at either interval, cell death was twofold greater in diabetic WTM than in TGM. The extent of apoptosis did not differ when measured by TdT or hairpin probe with single-base 3' overhangs. Myocyte necrosis, evaluated by a hairpin probe with blunt ends, was not increased in diabetic WTM and TGM at 7 days. Conversely, myocyte necrosis with diabetes at 30 days increased 2.9-fold and 1.8-fold in diabetic WTM and TGM, respectively (Fig. 2C). The 1.7-fold difference between the two groups of diabetic mice was significant. Cells dying by both apoptosis and necrosis were never found. In comparison with control WTM, a 24% reduction in the total number of left ventric-

ular myocytes was found in diabetic WTM at 30 days (Fig. 2D). Cell loss in these animals was accompanied by a 28% myocyte hypertrophy (Fig. 2E), which resulted in preservation of ventricular mass (Fig. 2F). The 24% loss of cells in the ventricle reflected an absolute dropout of 1.1×10^6 myocytes. In contrast, diabetes did not change the number, size, and aggregate myocyte volume in TGM (Fig. 2D-F).

p53 DNA binding and myocyte RAS. p53 Function and expression of the p53-dependent and regulated genes (Bax, Aogen, and AT₁) and p53-independent genes (renin and AT₂ receptor) were measured in myocytes isolated from control and diabetic WTM and TGM (Fig. 3A). These determinations were restricted to 7 days because apoptosis with diabetes was greater at this interval. p53 Binding to its cognate DNA sequence on the promoter of Bax (5'-AGCTTGCTCACAAGTTAGAGACAAGCCTGGGC-GTGGCTATATTGA-3'), Aogen (5'-AGCCTCTGTACAGAGTAGCCTGGGAATAGATCCATCTTC-3'), and AT₁ (5'-GCTGAGCTTGGATCTGGAAGGCGACACTGGG-3') was increased in myocytes of diabetic WTM (Fig. 3B-D). The optical density (OD) of the p53-shifted band for each of these three genes was significantly higher than in diabetic TGM (OD data not shown). These differences were coupled with larger quantities of p53 (Fig. 3E) and Bax (Fig. 3F) proteins in WTM myocytes with diabetes. Similarly, Aogen (Fig. 3G), renin (Fig. 3H), and AT₁ (Fig. 3H) increased more in diabetic WTM than in diabetic TGM. AT₂ protein did not change in diabetic mice (Fig. 3J).

The quantitative analysis of Ang II localization in the myocardium (Fig. 4A-D) showed labeling in $51 \pm 7\%$ ($n = 6$) and $31 \pm 6\%$ ($n = 6$, $P < 0.001$) of the myocytes in nondiabetic WTM and TGM, respectively. Diabetes increased the fraction of Ang II-positive myocytes to $77 \pm 9\%$ ($n = 6$, $P < 0.001$) in WTM and to $50 \pm 8\%$ ($n = 6$, $P < 0.01$) in TGM. The number of Ang II sites per millimeter squared of myocytes was twofold ($P < 0.001$) higher in nondiabetic WTM ($14,000 \pm 3,500$ per mm^2) than in TGM ($7,000 \pm 2,100$). With diabetes, these values increased 2.3-fold ($P < 0.001$) in WTM ($32,100 \pm 8,300$) and 1.7-fold ($P < 0.001$) in TGM ($12,000 \pm 3,400$). Thus, Ang II sites in

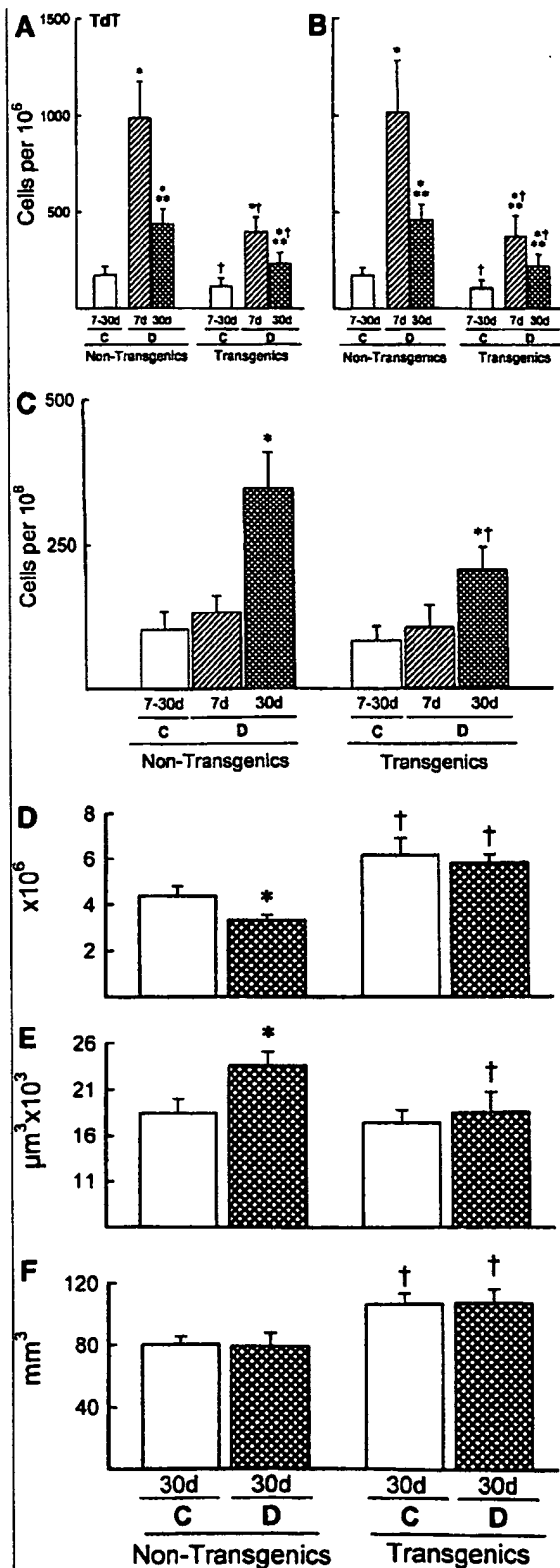


FIG. 2. Effects of diabetes on myocyte apoptosis evaluated with TdT (A) and Hairpin probe (B), and the effects of diabetes on necrosis (C), myocyte number (D), myocyte cell volume (E), and aggregate myocyte mass in the left ventricle (F). See legend to Fig. 1 for symbols. * $P < 0.05$ vs. C; ** $P < 0.05$ vs. D 7 days; and † $P < 0.05$ vs. nontransgenic mice. A–C: C 7–30 days, $n = 12$; D 7 days, $n = 6$; D 30 days, $n = 6$. D–F: $n = 5$.

myocytes were 2.7-fold ($P < 0.001$) more numerous in diabetic WTM than in TGM.

Nitrotyrosine localization. Nitrotyrosine is formed by the interaction of peroxynitrite with cytoplasmic proteins (23). This modified amino acid is a product of oxidative stress that can be detected in the myocardium using a nitrotyrosine-specific antibody (Fig. 5A and B). Its association with myocyte apoptosis can be identified as well (Fig. 5C and D). The analysis of nitrotyrosine localization in myocytes was performed at 30 days of diabetes to allow its accumulation with time. The percentage of myocytes expressing nitrotyrosine was $28 \pm 6\%$ ($n = 6$) and $14 \pm 4\%$ ($n = 6$; $P < 0.05$) in nondiabetic WTM and TGM, respectively. Diabetes increased the fraction of nitrotyrosine-positive myocytes to $71 \pm 16\%$ ($n = 6$, $P < 0.001$) in WTM; this parameter did not change in diabetic TGM, which had a value of $16 \pm 5\%$ ($n = 6$, NS). The presence of nitrotyrosine does not permit the examination of all nuclei of positive cells; nuclei are often not included in the section plane (Fig. 5A and B). Moreover, nitrotyrosine labeling exceeds by several orders of magnitude the extent of cell death. A total of 63 apoptotic myocytes were examined in diabetic WTM to detect the potential implication of nitrotyrosine in apoptosis; in all cases, apoptosis was accompanied by nitrotyrosine labeling (Fig. 5C and D). To confirm the role of oxidative stress in cell death, 38, 26, and 18 apoptotic myocytes were analyzed in diabetic TGM and nondiabetic WTM and TGM, respectively; nitrotyrosine was present in every cell undergoing apoptosis.

ROS formation. The increase in nitrotyrosine in myocytes with diabetes suggested that a causative link existed between oxidative stress and this disease. Additionally, IGF-1 attenuated the effects of oxidative stress on nitrotyrosine accumulation in the diabetic heart. To establish whether a relationship was present between diabetes and Ang II formation and between ROS production and cell death, in vitro studies were performed after 7 days of diabetes. This interval was selected because Ang II labeling of myocytes was obtained at this time and apoptosis in vivo was higher than at 30 days (see above). Myocytes were isolated from nondiabetic and diabetic WTM, and TGM and ROS generation was measured using a fluorescent probe detecting H_2O_2 and $^{\bullet}OH$ in living cells (Fig. 6A and B). In each cell, fluorescence intensity (f) was normalized by the corresponding myocyte cell volume (V). ROS production was 44% ($P < 0.01$) higher in myocytes from nondiabetic WTM ($n = 5$, $1.34 \pm 0.11 f/V$) than in cells from nondiabetic TGM ($n = 5$, 0.93 ± 0.08). Diabetes increased the formation of H_2O_2 - $^{\bullet}OH$ in myocytes of WTM ($n = 5$, $2.40 \pm 0.29 f/V$) and TGM ($n = 5$, 1.23 ± 0.12) 1.8-fold ($P < 0.001$) and 1.3-fold ($P < 0.05$), respectively. Using 0.2- f/V increments, the frequency distribution of fluorescence intensity of myocytes was plotted (Fig. 6C–F). In comparison with WTM, IGF-1 overexpression in nondiabetic and diabetic hearts was characterized by a shift to the left of the reactive O_2 signal. In nondiabetic WTM and TGM and diabetic WTM and TGM, respectively, a total of 563, 585, 601, and 643 myocytes were examined and 1, 0, 7, and 2 apoptotic cells were found. All dying myocytes had high levels of H_2O_2 - $^{\bullet}OH$; f/V values ranged from 3 to 5. The frequency of apoptotic myocytes found in vitro were higher than in vivo. This is a consistent phe-

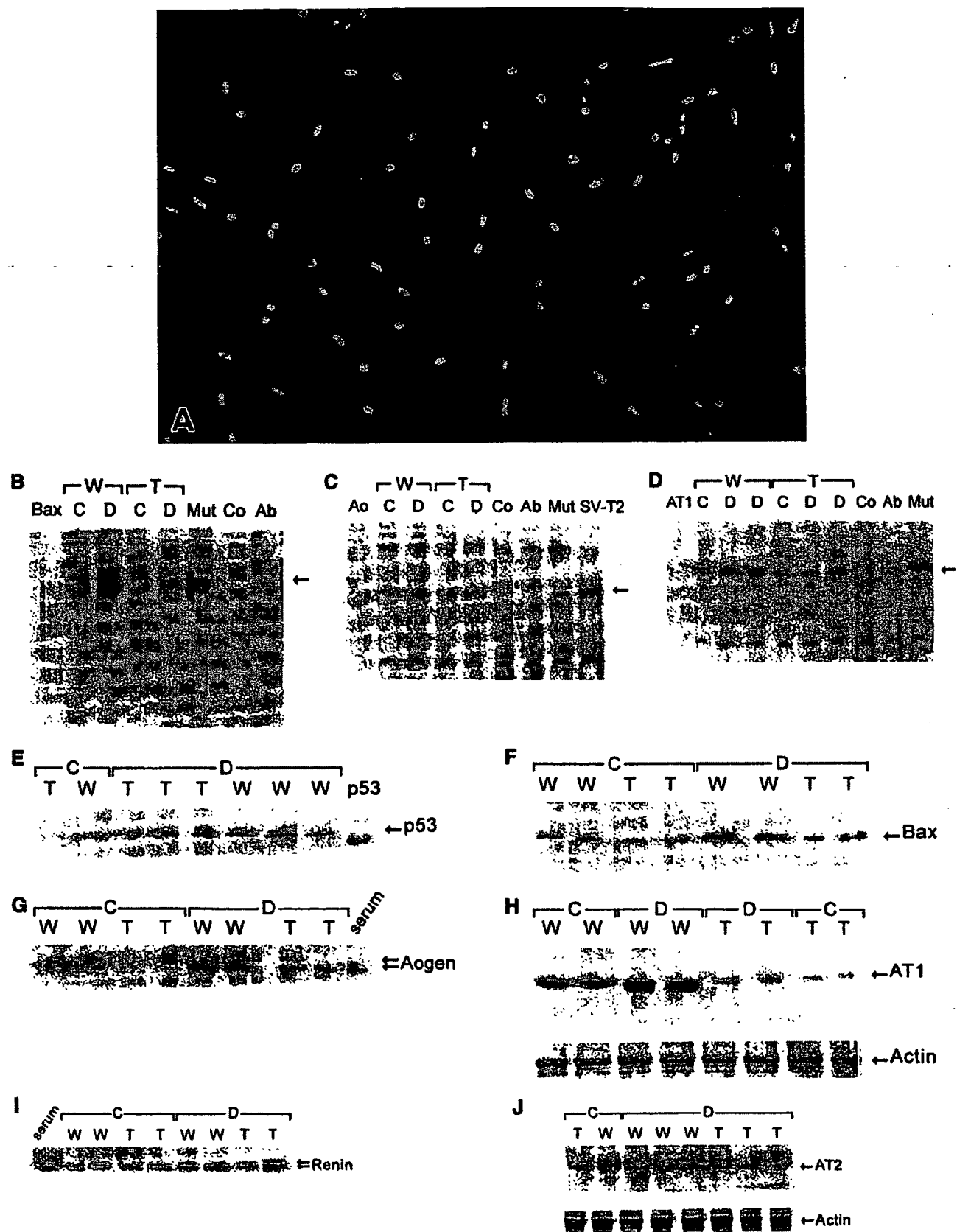


FIG. 3

nomenon associated with cell isolation and culture conditions (4,17).

To identify whether the cellular release of Ang II was responsible for the induction of $\text{H}_2\text{O}_2\cdot\text{OH}$ at baseline and with diabetes or whether oxidative stress was independent from AT_1 receptor activation, myocytes were exposed for 30 min, respectively, to the AT_1 antagonist losartan (10^{-7} mol/l) or the intracellular reactive O_2 scavenger Tiron (0.1 mmol/l). $\text{H}_2\text{O}_2\cdot\text{OH}$ fluorescence was reduced by losartan (Fig. 6G–J) in myocytes obtained from diabetic WTM (from 2.40 ± 0.29 to 1.53 ± 0.13 f/V; 582 cells, two apoptosis) and TGM (0.91 \pm 0.14; 610, one). Values in losartan-treated nondiabetic WTM and TGM were, respectively, 1.26 ± 0.18 f/V (541 cells, one apoptosis) and 0.85 ± 0.09 f/V (572 cells, no apoptosis). Similarly, Tiron-attenuated oxidative stress mimicked the effects of losartan at a more distal level: WTM = 1.12 ± 0.17 f/V (551 cells, no apoptosis), TGM = 0.78 ± 0.11 (539, none), diabetic WTM = 1.29 ± 0.21 (680, one), and diabetic TGM = 0.91 ± 0.14 (554, none).

Ang II, ROS formation and apoptosis. Myocytes from control WTM were exposed to Ang II, and the $\text{H}_2\text{O}_2\cdot\text{OH}$ signal was measured (Fig. 7A). Fluorescence intensity per cell nearly doubled with Ang II. In contrast, pretreatment of cells with losartan prevented the effects of Ang II on ROS production. Myocyte apoptosis markedly increased 24 h after the addition of Ang II. Importantly, Tiron or losartan inhibited the apoptotic signal transmitted by Ang II (Fig. 7B). Thus, Ang II activated apoptosis via the AT_1 receptor by enhancing oxidative stress.

DISCUSSION

IGF-1 overexpression protects from diabetic cardiomyopathy. Whether diabetes per se—in the absence of coronary artery disease and hypertension—leads to cardiac myopathy in humans has been a controversial question (1). Animal models of diabetes have not resolved this issue. Biochemical, mechanical, structural, and electrophysiological alterations have been identified in combination with modest abnormalities in the diastolic properties of the heart (2,24,25). However, indexes of severe ventricular dysfunction and failure have not been observed (1,2). Results presented here document for the first time that in a mouse model of type 1 insulin-dependent diabetes, cardiac performance is impaired soon after the onset of the disease and deteriorates chronically. Myocyte loss and hypertrophy of the remaining cells characterize the diabetic decompensated heart, mimicking cardiac myopathies in humans and animals (26).

Clinical and experimental studies aiming at the identification of a therapeutic role for exogenously administered IGF-1 or growth hormone in pathologic states of the heart have not provided a consistent answer. Positive observations (5,27) have been contrasted by negative results (28,

29). IGF-1 overexpression in TGM has previously been shown to inhibit both myocyte apoptosis in the surviving myocardium after infarction (13) and myocyte necrosis after nonocclusive coronary artery constriction (14). Interference with cell death improved cardiac anatomy and decreased diastolic wall stress in both situations. However, these beneficial effects were not accompanied by a corresponding amelioration in ventricular hemodynamics, possibly due to the presence of large infarcts and restriction in coronary perfusion, respectively. Therefore, the therapeutic impact of IGF-1 on the diseased heart remains unclear. The current findings demonstrate unequivocally that IGF-1 overexpression affected the level of activation of myocyte death with diabetes and preserved ventricular performance. Myocyte death has been questioned as an etiological factor capable of inducing functional alterations. Cell death has been claimed to be an epiphenomenon that has little influence on the onset and evolution of cardiac failure (30). Current data in diabetic nontransgenic mice and TGM challenge this contention.

IGF-1 overexpression inhibits Ang II synthesis and ROS formation. Recent observations in diabetic patients (7) and in rats after STZ administration (2) have demonstrated that the systemic and local RAS are activated with diabetes, exerting a detrimental effect on the course of the disease. Formation of Ang II in the myocardium and stimulation of AT_1 receptors cause myocyte apoptosis and cardiac remodeling (2). The *in vivo* results obtained here are consistent with the concept that upregulation of p53 leads to enhanced expression of the p53-regulated gene (Aogen) responsible for the increased levels of Ang II in myocytes with diabetes. Aogen is the limiting factor in the formation of Ang II in cardiac muscle cells (4,17,31), and inactivation of p53 inhibits generation of the octapeptide (4). IGF-1 attenuates p53 transcriptional activity and thereby downregulates Aogen and the synthesis of Ang II. This negative modulation of RAS by IGF-1 is mediated by MDM2 and the generation of MDM2-p53 inactive complexes (3,32). Ang II leads to oxidative stress in several cell systems through NADH/NADPH oxidase (9). This enzyme is the major source of superoxide; p22^{phox} is critical for the transfer of electrons from NADH or NADPH to O_2 and the production of reactive O_2 (33).

Ang II increases the formation of ROS in neonatal myocytes (34), endothelial cells (11), and smooth muscle cells (9) *in vitro* by activating AT_1 receptors (11). However, a link between ROS and apoptosis has not been established. It is technically impossible to measure the generation of ROS in cardiac myocytes *in vivo*. Therefore, the localization of nitrotyrosine in myocytes was evaluated. Superoxide anion interacts with nitric oxide, forming peroxynitrite (ONOO^-) (23). ONOO^- induces oxidative damage to proteins, leading to the production of a modi-

FIG. 3. Left ventricular myocytes from a diabetic nontransgenic mouse at 7 days (A); α -sarcomeric actin staining of the cytoplasm (red fluorescence and PI labeling of nuclei (yellow fluorescence)), $\times 300$. B–D: Gel mobility assays of p53 binding to its consensus sequence in the promoter of bax (B), Aogen (C), and AT_1 (D). Bax, Ao, and AT_1 ; probes in the absence of nuclear extracts. Co, competition with an excess of unlabeled self-oligonucleotide; Ab, competition with monoclonal p53 antibody; Mut, preincubation with unlabeled mutated form of oligonucleotides; SV-T2, nuclear extracts from SV-T2 cells; C, control; D, diabetic; W, nontransgenics; T, transgenics. OD values of the shifted bands are not listed. E–J: Western blots of p53 (E), Bax (F), Aogen (G), AT_1 (H), renin (I), and AT_2 (J). ODs for p53: WC = 1.9 ± 0.31 , WD = 6.7 ± 1.5 ($P < 0.001$); TC = 0.56 ± 0.16 , TD = 2.1 ± 0.48 ($P < 0.05$). ODs for Bax: WC = 1.4 ± 0.26 , WD = 5.7 ± 0.81 ($P < 0.001$); TC = 0.50 ± 0.15 , TD = 0.78 ± 0.25 ($P < 0.05$). ODs for Aogen: WC = 6.2 ± 1.3 , WD = 19 ± 4 ($P < 0.001$); TC = 1.3 ± 0.44 , TD = 2.4 ± 0.64 ($P < 0.01$). ODs for AT_1 : WC = 3.7 ± 1.0 , WD = 13 ± 3 ($P < 0.001$); TC = 0.99 ± 0.29 , TD = 1.8 ± 0.64 ($P < 0.01$). ODs for renin: WC = 0.88 ± 0.29 , WD = 2.1 ± 0.64 ($P < 0.001$); TC = 0.71 ± 0.19 , TD = 1.1 ± 0.28 (NS). ODs for AT_2 : WC = 0.93 ± 0.39 , WD = 0.91 ± 0.24 (NS); TC = 0.85 ± 0.26 , TD = 0.82 ± 0.27 (NS). $n = 6$ in all cases.

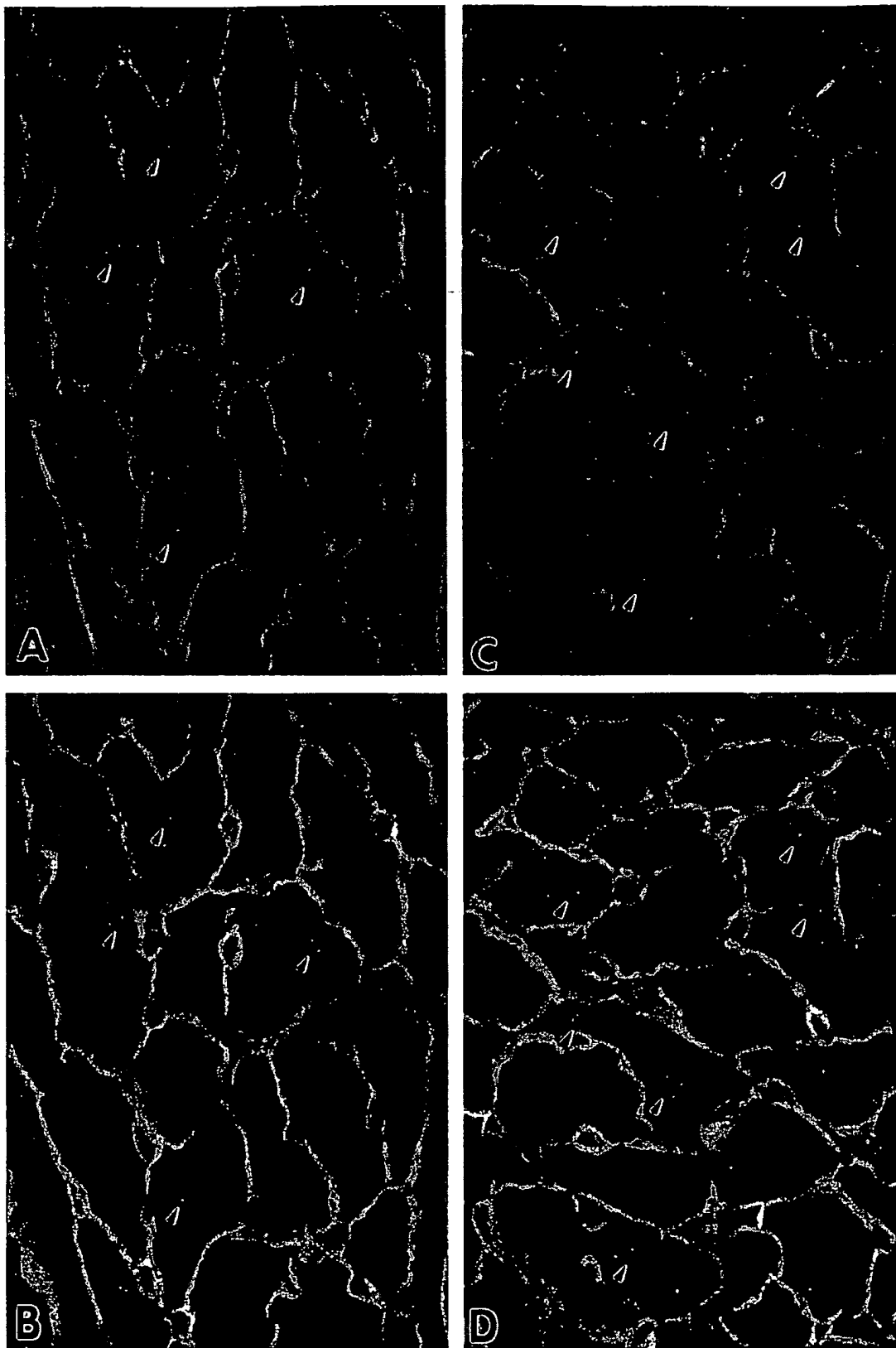


FIG. 4. Myocardium of nondiabetic (*A* and *B*) and diabetic (*C* and *D*) WTM. Green fluorescence (*A* and *C*) and yellow fluorescence (*B* and *D*) reflect Ang II labeling (arrows) and laminin staining of the interstitium. Red fluorescence shows α -sarcomeric actin staining of the cytoplasm (*B* and *D*), and blue fluorescence shows PI labeling of nuclei (*B* and *D*). Magnification: $\times 1,200$.

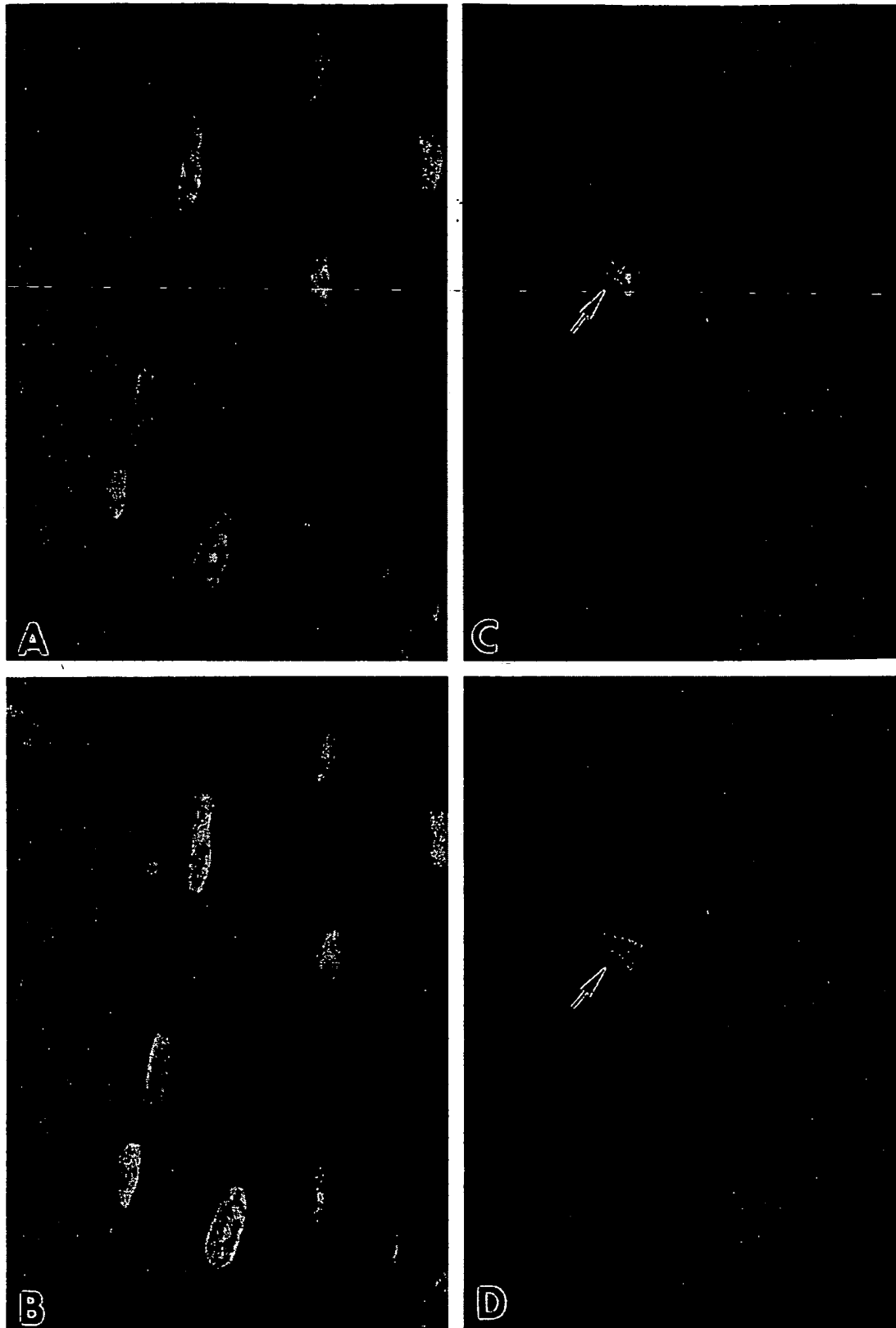


FIG. 5. Nitrotyrosine localization in the myocardium of a diabetic WTM at 30 days (*A* and *B*), shown by blue fluorescence (*A*) and pink fluorescence (*B*). α -Sarcomeric actin staining of the cytoplasm is shown by red fluorescence (*B*) and PI-labeling of nuclei (green-yellow fluorescence, *A* and *B*). *C* and *D* from the same heart show an apoptotic nucleus (green-yellow fluorescence, arrow) detected by hairpin probe with single-base 3' overhangs. Stainings for nitrotyrosine and myocyte cytoplasm are the same as those in *A* and *B*. Magnification: $\times 1,200$.

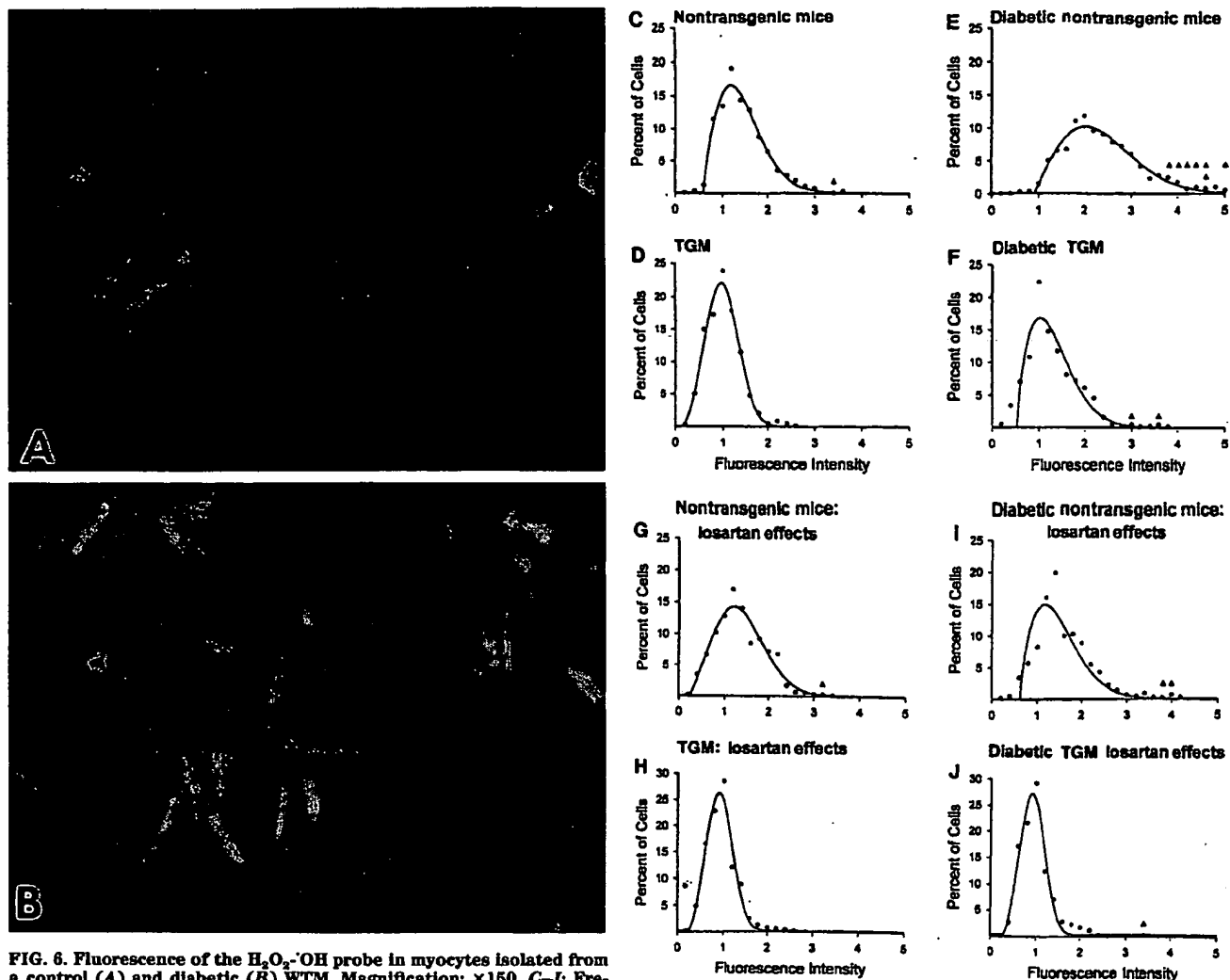


FIG. 6. Fluorescence of the $H_2O_2 \cdot OH$ probe in myocytes isolated from a control (A) and diabetic (B) WTM. Magnification: $\times 150$. C–J: Frequency distribution of $H_2O_2 \cdot OH$ signals in myocytes from nondiabetic and diabetic mice in the absence (C–F) and presence of losartan (G–J). Fluorescence increments of 0.2 fV were used to construct these curves. Regression lines were fitted using Weibull's equation. Solid circles correspond to groups of myocytes within 0.2 fV. Solid triangles correspond to apoptosis of individual myocytes.

fied amino acid (nitrotyrosine). The increased frequency of nitrotyrosine-positive myocytes in diabetic nontransgenic mice pointed to an oxidative challenge in vivo. This cellular response was prevented in diabetic IGF-1 TGM, correlating with the lower level of Ang II in the myocardium. However, these in vivo results did not prove whether Ang II was the trigger for the induction of ROS or whether IGF-1 reduced oxidative stress by interfering only with the synthesis of Ang II. IGF-1 could have affected the activity of NADH/NADPH oxidase, limiting superoxide formation (23). Importantly, AT_1 blockade in myocytes from diabetic WTM and TGM decreased the $H_2O_2 \cdot OH$ signals. Although the levels of $H_2O_2 \cdot OH$ varied in the presence and absence of IGF-1 overexpression, inhibition of Ang II binding markedly depressed the generation of ROS in either myocyte population. Similar results were obtained with the reactive O_2 scavenger Tiron. Thus, Ang II was the mediator of reactive O_2 , and IGF-1 attenuated oxidative stress by reduc-

ing the local synthesis of Ang II in the myocardium with diabetes.

IGF-1 overexpression attenuates myocyte death with diabetes. Myocyte apoptosis and necrosis are both involved in the development of diabetic cardiomyopathy. Necrosis temporally follows apoptosis, contributing to the chronic loss of ventricular myocytes with diabetes. The strict association between nitrotyrosine and apoptosis suggests that oxidative damage is causally implicated in the activation of this form of cell death. Although a similar link was not investigated for myocyte necrosis, different levels of reactive O_2 trigger apoptosis or necrosis; high quantities induce necrosis and low amounts promote apoptosis (35). IGF-1 attenuated necrosis and apoptosis but did not prevent cell death completely. However, myocyte apoptosis and necrosis in TGM did not affect the aggregate number of ventricular myocytes 1 month after STZ administration. This apparent inconsistency may be explained by myocyte regeneration, which could have occurred with IGF-1 overexpression (12).

In conclusion, the positive correlation between the extent of oxidative challenge and myocyte apoptosis in vitro

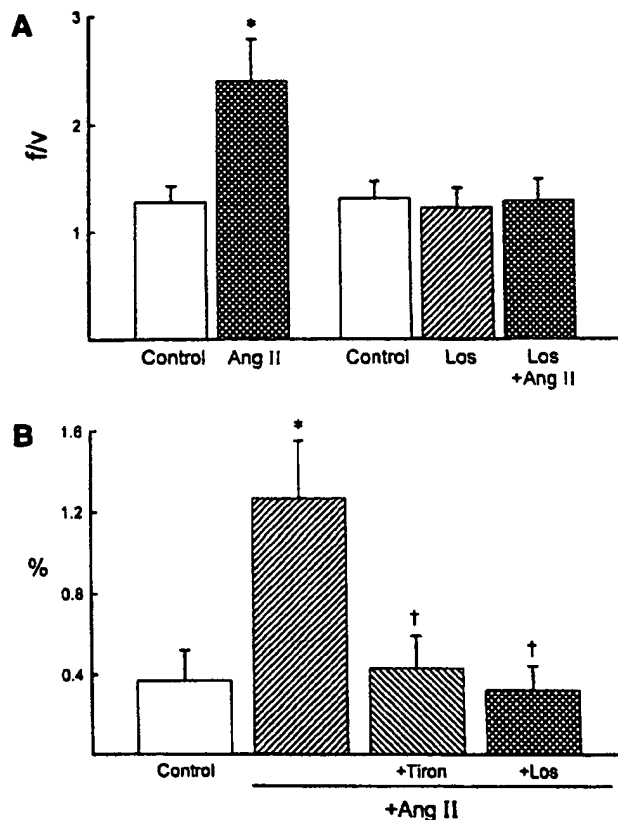


FIG. 7. Effects of Ang II on ROS formation (A) and myocyte apoptosis (B) in cultured myocytes obtained from nondiabetic nontransgenic mice. Results are means \pm SD. Los, losartan. * $P < 0.05$ vs. control; † $P < 0.05$ vs. Ang II alone. $n = 6$ in all cases.

and between nitrotyrosine localization and myocyte apoptosis in vivo strongly suggest that oxygen toxicity may constitute an important cell death signal responsible for cell dropout in the diabetic heart. Diabetic cardiomyopathy may be viewed as a ROS-dependent myopathy in which cell loss initially produces moderate ventricular dysfunction and chronically leads to a severely decompensated heart. IGF-1 protects the myocardium from the detrimental effects of diabetes by attenuating Ang II synthesis and thus reactive O_2 damage and, ultimately, cell death. Whether the protective role of IGF-1 in diabetes persists over long time periods remains an important unanswered question.

ACKNOWLEDGMENTS

This work was supported by National Institutes of Health grants HL-38132, HL-39902, HL-43023, AG-15756, HL-66923, AG-17042, and HL-65577 and by JDF grant 1-2000-62. The initial helpful suggestions of Dr. Ashwani Malhotra are acknowledged.

REFERENCES

- Rodrigues B, McNeill JH: The diabetic heart: metabolic causes for the development of a cardiomyopathy. *Cardiovasc Res* 26:913-922, 1992
- Fiordaliso F, Li B, Latini R, Sonnenblick EH, Anversa P, Leri A, Kajstura J: Myocyte death in streptozotocin-induced diabetes in rats is angiotensin II dependent. *Lab Invest* 80:513-527, 2000
- Leri A, Liu Y, Wang X, Kajstura J, Malhotra A, Meggs LG, Anversa P: Overexpression of IGF-1 attenuates the myocyte renin-angiotensin system in transgenic mice. *Circ Res* 84:752-762, 1999
- Leri A, Fiordaliso F, Setoguchi M, Limana F, Bishopric NH, Kajstura J, Webster K, Anversa P: Inhibition of p53 function prevents renin-angiotensin system activation and stretch-mediated myocyte apoptosis. *Am J Pathol* 157:843-857, 2000
- Duerr RL, McKimman MD, Gim RD, Clark RG, Chien KR, Ross J: Cardiovascular effects of insulin-like growth factor-1 and growth hormone in chronic left ventricular failure in rat. *Circulation* 93:2188-2196, 1996
- Zuanetti G, Latini R, Maggioni AP, Franzosi MG, Santoro L, Tognoni G: Effect of the ACE inhibitor lisinopril on mortality in diabetic patients with acute myocardial infarction. *Circulation* 98:4239-4245, 1997
- Heart Outcomes Prevention Evaluation (HOPE) Study Investigators: Effects of ramipril on cardiovascular and microvascular outcomes in people with diabetes mellitus: results of the HOPE study and MICRO-Hope substudy. *Lancet* 355:253-259, 2000
- Dandona P, Thushu K, Cook S, Snyder B, Makowski J, Armstrong D, Nicotera T: Oxidative damage to DNA in diabetes mellitus. *Lancet* 347:444-445, 1996
- Rajagopalan S, Kurz S, Münzel T, Tarpey M, Freeman BA, Griending KK, Harrison DG: Angiotensin II-mediated hypertension in the rat increases vascular superoxide production via membrane NADH/NADPH oxidase activation: contribution to alterations of vasomotor tone. *J Clin Invest* 97:1916-1923, 1996
- Fukui T, Siegfried MR, Ushio-Fukai M, Griending KK, Harrison DG: Modulation of extracellular superoxide dismutase expression by angiotensin II and hypertension. *Circ Res* 85:23-28, 1999
- Berry C, Hamilton CA, Brosnan MJ, Magill FG, Berg GA, McMurray JJV, Dominiczak AF: Investigation into the sources of superoxide in human blood vessels: angiotensin II increases superoxide production in human internal mammary arteries. *Circulation* 101:2206-2212, 2000
- Reiss K, Cheng W, Ferber A, Kajstura J, Li P, Olivetti G, Homcy CJ, Baserga R, Anversa P: Overexpression of insulin-like growth factor-1 in the heart is coupled with myocyte proliferation in transgenic mice. *Proc Natl Acad Sci U S A* 93:8630-8635, 1996
- Li Q, Li B, Wang X, Leri A, Jana KP, Liu Y, Kajstura J, Baserga R, Anversa P: Overexpression of insulin-like growth factor-1 in mice protects from myocyte death after infarction, attenuating ventricular dilation, wall stress, and cardiac hypertrophy. *J Clin Invest* 100:1991-1999, 1997
- Li B, Setoguchi M, Wang X, Andreoli A-M, Leri A, Malhotra A, Kajstura J, Anversa P: IGF-1 attenuates the detrimental impact of nonocclusive coronary artery constriction on the heart. *Circ Res* 84:1007-1019, 1999
- Li B, Li Q, Wang X, Jana KP, Redaelli G, Kajstura J, Anversa P: Coronary constriction impairs cardiac function and induces myocardial damage and ventricular remodeling in mice. *Am J Physiol* 273:H2508-H2519, 1997
- Didenko VV, Tunstead JR, Hornsby PJ: Biotin-labeled hairpin oligonucleotides: probes to detect double-strand breaks in DNA in apoptotic cells. *Am J Pathol* 152:897-902, 1998
- Leri A, Claudio PP, Li Q, Wang X, Reiss K, Wang S, Malhotra A, Kajstura J, Anversa P: Stretch-mediated release of angiotensin II induces myocyte apoptosis by activating p53 that enhances the local renin-angiotensin system and decreases the Bcl-2-to-Bax protein ratio in the cell. *J Clin Invest* 101:1326-1342, 1998
- Guerra S, Leri A, Wang X, Finato N, Di Loreto C, Beltrami CA, Kajstura J, Anversa P: Myocyte death in the failing human heart is gender dependent. *Circ Res* 85:856-866, 1999
- Kajstura J, Zhang X, Liu Y, Szoke E, Cheng W, Olivetti G, Hintze TH, Anversa P: The cellular basis of pacing-induced dilated cardiomyopathy: myocyte cell loss and myocyte cellular reactive hypertrophy. *Circulation* 92:2306-2317, 1995
- Bass DA, Parce JW, Dechatelet LR, Szejda P, Seeds MC, Thomas M: Flow cytometric studies of oxidative product formation by neutrophils: a grade response to membrane stimulation. *J Immunol* 130:1910-1917, 1983
- Zhu H, Bannenberg GL, Moldeus P, Schertzer HG: Oxidation pathways for the intracellular probe 2',7'-dichlorofluorescein. *Arch Toxicol* 68:582-587, 1994
- Wallenstein S, Zucker CL, Fleiss JL: Some statistical methods useful in circulation research. *Circ Res* 47:1-9, 1980
- Vinten-Johansen J: Physiological effects of peroxynitrite: potential products of the environment. *Circ Res* 87:170-172, 2000
- Malhotra A, Reich D, Reich D, Nakouzi A, Sanghi V, Geenen DL, Buttrick PM: Experimental diabetes is associated with functional activation of protein kinase C- α and phosphorylation of troponin I in the heart, which are prevented by angiotensin II receptor blockade. *Circ Res* 81:1027-1033, 1997
- Schaffer SW, Mozaffari M: Abnormal mechanical function in diabetes: relation to myocardial calcium handling. *Coron Artery Dis* 7:109-115, 1996

26. Anversa P, Leri A, Beltrami CA, Guerra S, Kajstura J: Myocyte death and growth in the failing heart. *Lab Invest* 78:767-786, 1998
27. Fazio S, Sabatini D, Capaldo B, Vigorito C, Giordano A, Guida R, Pardo F, Biondi B, Sacca L: A preliminary study of growth hormone in the treatment of dilated cardiomyopathy. *N Engl J Med* 334:809-814, 1996
28. Shen YT, Wiedmann RT, Lynch JJ, Grossman W, Johnson RG: GH replacement fails to improve ventricular function in hyposectomized rats with myocardial infarction. *Am J Physiol* 271:H1721-H1727, 1996
29. Osterziel KJ, Strohm O, Schiler J, Friedrich M, Hanlein D, Willenbrock R, Anker SD, Poole-Wilson PA, Ranke MB, Dietz R: Randomised, double-blind, placebo-controlled trial of human recombinant growth hormone in patients with chronic heart failure due to dilated cardiomyopathy. *Lancet* 351:1233-1237, 1998
30. Schaper J, Elsässer A, Kostin S: The role of cell death in heart failure. *Circ Res* 85:867-869, 1999
31. Pierzchalski P, Reiss K, Cheng W, Cirielli C, Kajstura J, Nitahara JA, Rizk M, Capogrossi MC, Anversa P: p53 Induces myocytes apoptosis via the activation of the renin-angiotensin system. *Exp Cell Res* 234:57-65, 1997
32. Leri A, Liu Y, Claudio PP, Kajstura J, Wang X, Wang S, Kang P, Malhotra A, Anversa P: IGF-1 induces Mdm2 and downregulates p53, attenuating the myocyte renin-angiotensin system (RAS) and stretch-mediated apoptosis. *Am J Pathol* 154:587-590, 1999
33. Ushio-Fukai M, Zafari AM, Fukui T, Ishizaka N, Griendling KK: p22^{phox} is a critical component of the superoxide-generating NADH/NADPH oxidase system and regulates angiotensin II-induced hypertrophy in vascular smooth muscle cells. *J Biol Chem* 271:23317-23321, 1996
34. von Harsdorf R, Li PF, Dietz R: Signaling pathways in reactive-oxygen species-induced cardiomyocyte apoptosis. *Circulation* 99:2934-2941, 1999
35. Fiers W, Beyaert R, Declercq W, Vandenabeele P: More than one way to die: apoptosis, necrosis, and reactive oxygen damage. *Oncogene* 18:7719-7730, 1999

formation of the region (31) to be comparable with or larger than the rates of deformation associated with faults bounding western Tibet.

References and Notes

1. Z. K. Shen *et al.*, *J. Geophys. Res.* **106**, 30607 (2001).
2. P. Tapponnier, G. Peltzer, R. Armijo, A.-Y. Le Dain, P. Cobbold, *Geology* **10**, 611 (1982).
3. G. Peltzer, P. Tapponnier, *J. Geophys. Res.* **93**, 15085 (1988).
4. J.-P. Avouac, P. Tapponnier, *Geophys. Res. Lett.* **20**, 895 (1993).
5. P. Tapponnier *et al.*, *Science* **294**, 1671 (2001).
6. P. Bird, K. Piper, *Phys. Earth Planet. Inter.* **21**, 158 (1980).
7. P. England, D. McKenzie, *Geophys. J. R. Astron. Soc.* **70**, 295 (1982).
8. G. Houseman, P. England, *J. Geophys. Res.* **91**, 3651 (1986).
9. G. Houseman, P. England, *J. Geophys. Res.* **98**, 12233 (1993).
10. P. England, P. Molnar, *Nature* **344**, 140 (1990).
11. Q. Liu, thesis, Université Paris (1993).
12. E. T. Brown *et al.*, *J. Geophys. Res.* **107**, 2192 (2002).
13. M. Searle, R. F. Weinberg, W. J. Dunlap, *Continental Transpressional and Transensional Tectonics*, R. Holdsworth, R. Strachan, J. F. Dewey, Eds., *Geol. Soc. Spec. Pub.* **135**, 307 (1998).
14. S. Jade *et al.*, *Geol. Soc. Am. Bull.*, in press.
15. P. Banerjee, R. Borgegna, *Geophys. Res. Lett.* **29**, 30 (2002).
16. G. Peltzer, P. Tapponnier, R. Armijo, *Science* **246**, 1285 (1989).
17. R. Bendick, R. Bilham, J. Freymueller, K. Larson, G. Yin, *Nature* **404**, 69 (2000).
18. Z. Chen *et al.*, *J. Geophys. Res.* **105**, 16215 (2000).
19. A. Gillespie, P. Molnar, *Rev. Geophys.* **33**, 311 (1995).
20. T. J. Wright, B. E. Parsons, E. J. Fielding, *Geophys. Res. Lett.* **28**, 2117 (2001).
21. G. Peltzer, F. Crampé, S. Hensley, P. Rosen, *Geology* **29**, 975 (2001).
22. T. Farr, M. Kobrick, *Eos* **81**, 583 (2000).
23. R. Hanssen, *Radar Interferometry: Data Interpretation and Error Analysis* (Kluwer Academic, Dordrecht, Netherlands, 2001).
24. J.-P. Avouac, G. Peltzer, *J. Geophys. Res.* **98**, 21773 (1993).
25. J. Savage, R. Burford, *J. Geophys. Res.* **78**, 832 (1973).
26. G. Peltzer, F. Crampé, G. King, *Science* **286**, 272 (1999).
27. J. Masek, B. Isacks, E. Fielding, *Tectonics* **13**, 659 (1994).
28. T. J. Wright, Z. Lu, C. Wicks, *Geophys. Res. Lett.* **30**, 1974 (2003).
29. A.-S. Meriaux *et al.*, *Geophys. Res. Abstr.* **5**, 08062 (2003).
30. Z. Chen *et al.*, *J. Geophys. Res.* **109**, B01403 (2004).
31. R. Armijo, P. Tapponnier, J. Mercier, T. Han, *J. Geophys. Res.* **91**, 13803 (1986).
32. Q. Wang *et al.*, *Science* **294**, 574 (2001).
33. Supported by the Natural Environment Research Council through the Centre for Observation and Modelling of Earthquakes and Tectonics as well as a research fellowship to T.J.W. We are grateful to the European Space Agency for providing the ERS SAR data used, and to NASA for the SRTM topography. Part of this research was performed at the Jet Propulsion Laboratory (JPL) under contract with NASA. We thank JPL/Caltech for the use of the ROI.pac software to generate our interferograms and S. Lamb, R. Phillips, J. Jackson, and two anonymous reviewers for comments that have improved the manuscript. Some figures were prepared using the public-domain GMT software.

Supporting Online Material

www.sciencemag.org/cgi/content/full/305/5681/236/DC1
SOM Text
Figs. S1 to S5
References

3 February 2004; accepted 10 June 2004

Derivatives of Erythropoietin That Are Tissue Protective But Not Erythropoietic

Marcel Leist,^{1*} Pietro Ghezzi,^{2,3*} Giovanni Grasso,^{3,4} Roberto Bianchi,² Pia Villa,^{2,5} Maddalena Fratelli,² Costanza Savino,² Marina Bianchi,² Jacob Nielsen,¹ Jens Gerwien,¹ Pekka Kallunki,¹ Anna Kirstine Larsen,¹ Lone Helboe,¹ Søren Christensen,¹ Lars O. Pedersen,¹ Mette Nielsen,¹ Lars Torup,¹ Thomas Sager,¹ Alessandra Sfacteria,^{3,4} Serhat Erbayraktar,^{3,6} Zubeyde Erbayraktar,^{3,6} Necati Gokmen,⁶ Osman Yilmaz,^{3,6} Carla Cerami-Hand,^{3,7} Qiao-wen Xie,^{3,7} Thomas Coleman,^{3,7} Anthony Cerami,^{3,7†} Michael Brines^{3,7}

Erythropoietin (EPO) is both hematopoietic and tissue protective, putatively through interaction with different receptors. We generated receptor subtype-selective ligands allowing the separation of EPO's bioactivities at the cellular level and in animals. Carbamylated EPO (CEPO) or certain EPO mutants did not bind to the classical EPO receptor (EPOR) and did not show any hematopoietic activity in human cell signaling assays or upon chronic dosing in different animal species. Nevertheless, CEPO and various nonhematopoietic mutants were cytoprotective in vitro and conferred neuroprotection against stroke, spinal cord compression, diabetic neuropathy, and experimental autoimmune encephalomyelitis at a potency and efficacy comparable to EPO.

Erythropoietin (EPO) is a pleiotropic cytokine originally identified for its role in erythropoiesis (1). Its hematopoietic effects on the bone marrow are mediated by the homodimeric erythropoietin receptor ((EPOR)₂), a class I cytokine receptor. Sasaki and others identified the production of EPO in the central nervous system and, later, its neuroprotective function (1–7). Eventually, a proof-of-concept for neuroprotection by peripherally dosed EPO was obtained in a phase II clinical trial in cerebral ischemia (8).

Desialylated EPO (asialoEPO) has the same (EPOR)₂ affinity and neuroprotective properties as EPO, but an extremely short plasma half-life. Both molecules share the capacity of crossing an intact blood-brain barrier when dosed peripherally (3, 8–10), but bear also the risk of unwanted effects linked to the chronic overstimulation of (EPOR)₂, for example, on the bone marrow.

Extensive structure-activity relationship (SAR) studies of EPO have identified regions and amino acids essential for binding to

(EPOR)₂ (11), and many chemical modifications that abolish EPO's hematopoietic bioactivity are known (12, 13). However, the receptor complex mediating the neuroprotective effects of EPO differs from the hematopoietic receptor with respect to apparent affinity for EPO, apparent molecular weight, and associated proteins (2). The EPO receptor has been reported to associate functionally with other cytokine receptors such as CD131 (14, 15), and a region of EPO not within the (EPOR)₂ binding domains has been associated with neuroprotective effects (16). On the basis of these observations, we postulated that molecular changes to erythropoietin that neutralize erythropoiesis would not necessarily alter tissue-protective potency. One known modification silencing erythropoiesis is the carbamylation of lysines, a process well recognized to profoundly alter protein conformation and function. Surprisingly, we found that carbamylated EPO is neuroprotective and therefore introduces a new class of neuroprotective cytokines that lack erythropoietic activity yet engage a tissue-protective receptor.

All lysines in EPO were transformed to homocitrulline by carbamylation (17) (fig. S1A). CEPO, the resultant product, completely lacked bioactivity in the in vitro UT7 hematopoiesis bioassay (Table 1) and failed to bind to EPOR on these cells (Fig. 1A). However,

¹H. Lundbeck A/S, 2500 Valby, Denmark. ²Mario Negri Institute of Pharmacological Research, 20157 Milano, Italy. ³The Kenneth S. Warren Institute, Ossining, NY 10562, USA. ⁴University of Messina, 98122 Messina, Italy. ⁵Consiglio Nazionale delle Ricerche, Institute of Neuroscience, 20129 Milano, Italy. ⁶Dokuz Eylül University School of Medicine, Izmir 35340, Turkey. ⁷Warren Pharmaceuticals, Inc., Ossining, NY 10562, USA.

*These authors contributed equally to this study. †To whom correspondence should be addressed. E-mail: acerami@kswi.org

REPORTS

CEPO protected P19 cells from apoptosis (Table 1) and prevented *N*-methyl-D-aspartate (NMDA)-induced apoptosis of hippocampal cells with a potency (IC_{50} of 6 to 10 pM) and efficacy (50 to 80% specific protection) similar to EPO (Fig. 1B). Thus, CEPO represents the prototype for a family of designer cytokines with a novel activity spectrum.

We further explored the new principle that erythropoietic bioactivity and cytoprotection followed different SARs, generating mutants of EPO known to disrupt erythropoietic activity, but not conformation (18, 19). Some mutants, such as EPO-S100E or EPO-R103E, retained a high cytoprotective efficacy despite drastically reduced (EPOR)₂ affinity (Table 1). Thus, the tissue-protective potential of EPO could be separated from (EPOR)₂ interaction by multiple approaches affecting the protein backbone of

EPO, whereas changes in sialylation had no effect on the receptor affinities and in vitro bioactivities of the different types of ligands (Table 1). We further characterized the binding of CEPO to live cells (CHO, BaF/3) overexpressing (EPOR)₂ (17). In several of these experiments, asialoCEPO was used to exclude any binding effects of sialic acid-specific lectins previously described for neural cells (20). Depending on the cellular context and receptor species (apparent affinity of human EPO for huEPOR was about three times as high as that for rodent EPOR), EPO bound at 10 to 200 pM, while CEPO or asialoCEPO did not bind at concentrations up to 10,000 pM (fig. S2, A and B, and Fig. 1A).

In contrast to the above hematopoiesis model systems, we found that EPO and asialoCEPO had similar binding affinities for living PC-12 cells as representative of a neural cell type (Fig.

2A). These data suggest that while CEPO does not interact with the classical (EPOR)₂ to a degree detectable by radioligand binding assays, EPO and CEPO appear to compete for a common binding site on some (neural) cell types. We assessed potential interaction of CEPO with the (EPOR)₂ by measuring the phosphorylation of the transcription factor STAT-5 or of Jak2, a downstream kinase directly activated upon ligand binding to the EPOR. In BaF/3-EPOR cells, EPO concentrations > 0.5 nM stimulated the phosphorylation of signaling molecules. In contrast, CEPO concentrations up to 50 nM showed only minimal activity (Fig. 2B).

In clinical applications of neuroprotection, the ability of the engineered cytokines to cross the blood-brain barrier is critical. We found that CEPO distributed at least as well into the cerebrospinal fluid (CSF) as did EPO. For example, after intravenous (iv) bolus CEPO injection (rat, 44 μ g/kg; n = 6), pM concentrations (15 ± 6 pM CEPO versus 7 ± 2 pM EPO) were detected in CSF after 4 hours, and after 24 hours the CSF CEPO concentrations were still significantly elevated above baseline (4 ± 2 pM). The plasma pharmacokinetic parameters for CEPO were also in the same range as those for EPO. The plasma elimination half-life (rat, 44 μ g/kg iv; n = 4) was 3.3 hours. Peak concentrations of 150 pM were reached 14 hours after subcutaneous injection (rat, 44 μ g/kg; n = 4), and the plasma concentrations remained significantly elevated above 2 pM (the erythropoietic threshold for EPO) for >20 hours (17).

CEPO circulates long enough in vivo to potentially trigger hematopoiesis independently of a classical (EPOR)₂ interaction. Hence, we examined this possibility in several systems. Biweekly injections of up to 500 μ g/kg CEPO did not increase the hematocrit in mice (not iron supplemented), in contrast with identically dosed 5 μ g/kg EPO (Fig. 2C). Even five times weekly injections of CEPO administered subcutaneously did not increase the hematocrit. Moreover, CEPO was tested on rats in which an 8-week daily dosing of 50 μ g/kg had no augmenting effect on hemoglobin levels or hematocrit. Finally, mice were dosed subcutaneously daily for 4 weeks with CEPO at 10, 50, or 200 μ g/kg. Whereas the control group receiving EPO (10 μ g/kg) showed a 1.7-fold hematocrit increase, none of the CEPO groups showed any increase after 4 weeks or after a recovery period of an additional 2 weeks (<3% increase in any group). Thus, CEPO is not erythropoietic even when continuously present at high concentrations in plasma.

We also determined whether the modified EPOs might function as antagonists to the (EPOR)₂. The new variants were completely devoid of competitive effects, even at concentrations up to 300 times as high as those of EPO (Table 1 and fig. S2C).

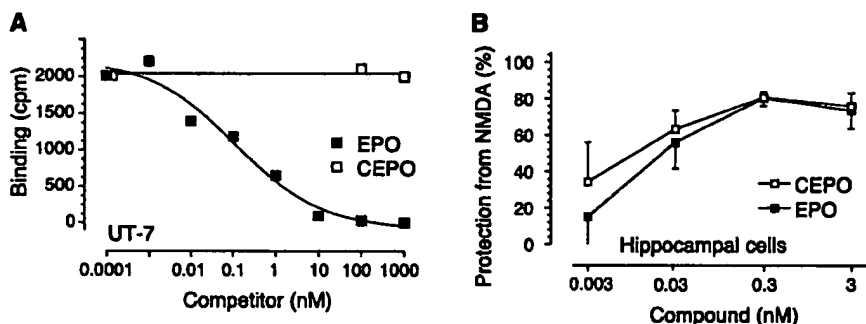


Fig. 1. CEPO is neuroprotective without binding to EPO-R. (A) Binding competition with iodinated EPO was determined for UT-7 cells. Cells were incubated with radiotracer and graded doses of unlabeled EPO or CEPO and analyzed for radiotracer binding. (B) CEPO/EPO was added to hippocampal neurons 24 hours before challenge with NMDA, and toxicity was evaluated 24 hours later by counting apoptotic neurons.

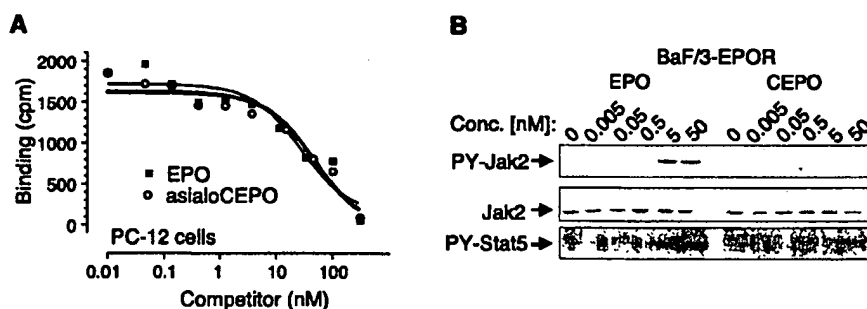


Fig. 2. Differential binding and erythropoietic signaling of EPO, CEPO, and asialoCEPO. (A) PC-12 (neural-type) cells were incubated with radiotracer (EPO) and graded doses of unlabeled EPO or asialoCEPO and analyzed for radiotracer binding. Data are in counts per minute (cpm) for quadruplicate samples. (B) BaF/3-EPOR cells were stimulated for 10 min with CEPO or EPO. Activation was analyzed by Western blotting of cell lysates with phosphorylation site-specific antibodies (PY-Jak2; Stat5). Equal loading was confirmed by reprobing of membranes against nonphosphorylated Jak2. (C) CEPO was intravenously injected (i.v.) biweekly to mice (n = 8). Injection days are marked by triangles. Data are expressed as percentage of saline-treated animals [control hemoglobin (Hb) = 15 ± 3 mg/100 ml]. One group of mice was injected with 5 μ g/kg EPO, and Hb levels were determined after 5 weeks as positive control.

In a cerebral infarct model, CEPO showed the same degree of tissue protection as reported for EPO and was effective over the same dose range (5 to 50 $\mu\text{g/kg}$). Delayed administration of CEPO by up to 4 hours after occlusion of the middle cerebral artery still conferred protection (Fig. 3A). This broad therapeutic time window has also been reported for EPO (9, 10) and distinguishes CEPO as a potential stroke therapeutic different from many other compounds that failed in clinical trials. Moreover, tissue protection by CEPO in the stroke model correlated well with a reduced inflammatory response in the ipsilateral hemisphere: Interleukin-6 levels were significantly ($P < 0.05$) reduced from 11,000 U/g in the control group to 5600 U/g in the CEPO group, and monocyte chemoattractant protein-1 levels from 3150 pg/g to 1720 pg/g ($P = 0.03$). In addition, we evaluated CEPO's effects on loss of function resulting from retinal ischemia (not shown) or sciatic nerve compression (Fig. 3B) and, again, observed a protective effect to the same degree as that described for EPO (9, 10).

Next, CEPO was tested in an established model of spinal cord injury (9). Neurological function after injury was significantly improved in the animals treated over 6 weeks with CEPO compared with the saline or EPO groups (Fig. 3C). A delay of 24 hours in treatment resulted in nearly identical recovery as that observed for animals receiving CEPO immediately after injury (Fig. 3D). Even when the first dose was given with a delay of 48 hours (not shown) or 72 hours after injury, we still observed a significant beneficial effect on the neurological function (Fig. 3D).

EPO is beneficial in another subchronic disease model, experimental autoimmune encephalomyelitis (EAE) (3). The neurological deficits in mice that had been immunized with myelin oligodendrocyte glycoprotein (MOG) to induce EAE were improved by CEPO over a prolonged observation period (Fig. 3E). In a modified setup of the model, first a stable disease state was triggered in the animals. Even 4 weeks after the robust plateau of neurological dysfunction was reached, a three-times-per-week treatment with CEPO significantly improved neurological function (Fig. 3E). Finally, we observed that CEPO reproduced the recently discovered beneficial effects of EPO (21) on diabetic peripheral neuropathy (Fig. 3F) (17).

We have presented the rationale, synthesis, and characterization of CEPO, an engineered cytokine with an activity spectrum preferentially targeting tissues outside the bone marrow. The findings have implications both for the biology of EPO and for the design of new tissue-protective therapies. Unlike other modified cytokines entering the clinic, the new class of compounds is not based on alterations of stability, plasma half-life, or antigenicity with an otherwise similar bioactivity spectrum as the parent cytokine. On the contrary, the phar-

macokinetic properties of CEPO are similar to EPO's, while the pharmacodynamics exhibit an unprecedented profile. CEPO exhibits a new mode of action, best explained by engaging an alternative receptor signaling tissue protection. In this respect, CEPO differs strikingly from asialoEPO, which behaves on the molecular level exactly as EPO (9).

Various sets of experiments with cells, membranes, and EPO receptor constructs show that the classical homodimeric (EPOR)₂ is not the transducer of the tissue-protective effects of CEPO. However, the data do not exclude the possibility of heteromeric receptor complexes containing at least one EPO receptor chain (e.g., with CD131). This would be in agreement with

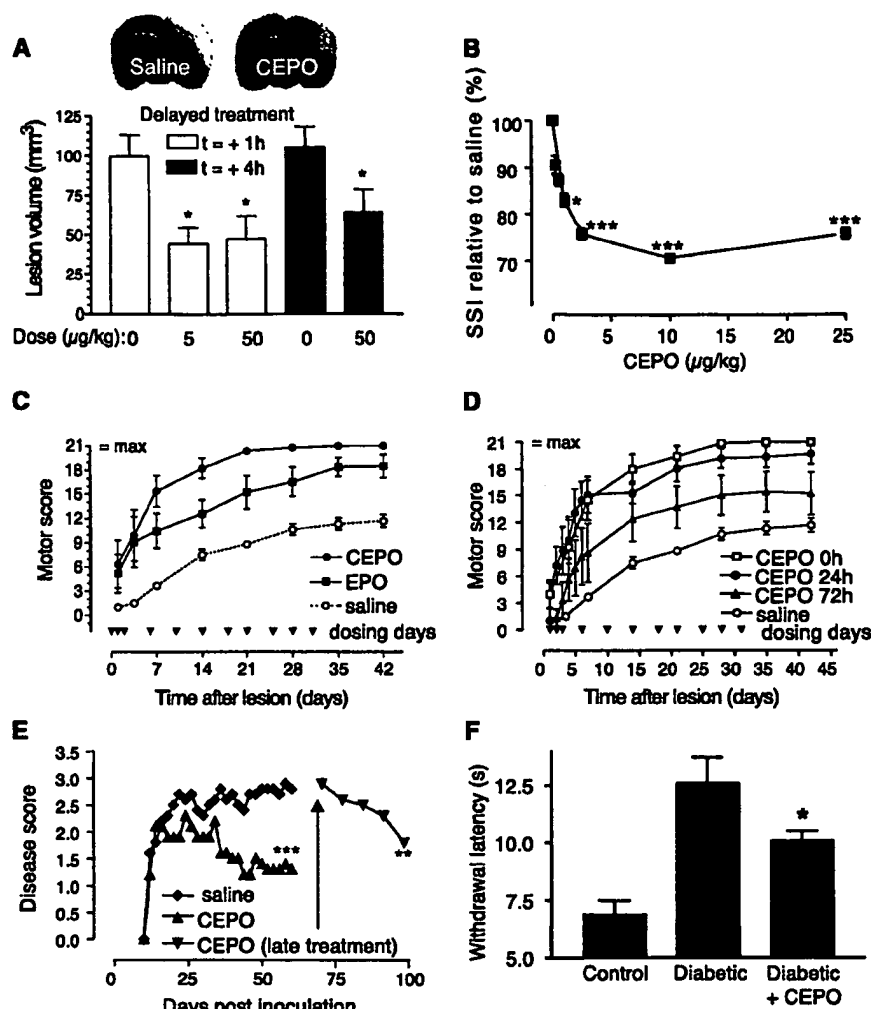


Fig. 3. Neuroprotection by CEPO. (A) Single intravenous injections of CEPO were given 1 hour or 4 hours after occlusion in a rat model of focal ischemia. Reperfusion was initiated after 60 min, and the infarct volume was measured after 24 hours. Data are means \pm SD; $n = 8$. (Insert) Representative images of tetraphenyl tetrazolium chloride-stained sections (at 2 mm caudal to bregma) showing infarct size. (B) The sciatic nerve of rats ($n = 6$) was compressed for 1 min and CEPO or vehicle was dosed immediately after the crush as a single intravenous bolus. The static sciatic index (SSI) is an indicator of motor function after sciatic nerve injury, and data are expressed as percentage versus saline-treated animals. (C) EPO, CEPO, or saline was injected intravenously immediately after surgical induction of spinal cord injury and over a period of 6 weeks, as indicated by triangles. Motor function of all animals was evaluated for 42 days, and data are presented as means \pm SEM; $n = 6$. (D) The experiment was performed as in (C), but the dosing of CEPO (10 $\mu\text{g/kg}$) was delayed by 0, 24, or 72 hours after the spinal cord compression. Injection days are marked by triangles. Data are means \pm SEM; $n = 6$. (E) Chronic EAE was induced by MOG; $n = 8$. The motor deficit was scored on a scale of 0 to 5. Animals were treated for 8 weeks with CEPO (50 $\mu\text{g/kg}$; three times weekly) versus saline. Alternatively, they were left untreated for 10 weeks and then dosed for 4 weeks with CEPO as above. (F) Neuropathy in streptozotocin-treated rats. Four weeks after induction of the diabetic state, the thermal nociceptive threshold was quantified by measurement of the time to paw withdrawal in a "hot plate" test. CEPO (50 $\mu\text{g/kg}$) was injected subcutaneously three times per week for four weeks. * $P < 0.05$; ** $P < 0.01$; *** $P < 0.001$.

REPORTS

Table 1. Comparison of EPOR binding, as well as hematopoietic and neuroprotective properties of different variants of EPO. EPOR binding experiments were performed on dimerized Fc-fusion proteins and measured as inhibition of EPO binding. Block of UT7 proliferation was measured in the presence of 50 pM EPO and 0.3 to 30 nM compound. No, less than 10% block; n.d., not determined; neurons, rat hippocampal neurons exposed to NMDA; P19, murine teratocarcinoma cells stressed by serum withdrawal.

Modification	EPOR IC ₅₀ (pM)	UT7 EC ₅₀ (pM)	UT7 block	Neurons (% protection ± SD at 300 pM)	P19
Wild-type EPO	10	10–30	n.d.	78 ± 13	49 ± 12
AsialoEPO	14	10–30	n.d.	71 ± 15	n.d.
CEPO	>10,000	>10,000	No	70 ± 9	49 ± 10
AsialoCEPO	>10,000	>10,000	No	69 ± 16	n.d.
S100E-EPO	100	>10,000	No	66 ± 9	55 ± 15
R103E-EPO	>10,000	>10,000	No	55 ± 13	n.d.

observations that EPO receptor expression in tissues correlates with the protective effect of EPO (10, 22). Such heteromeric receptors would likely present new binding sites and therefore new pharmacological characteristics.

Although the precise means by which tissue-protective cytokines signal remain to be clarified, the availability of compounds such as CEPO that do not trigger (EPOR)₂ also opens possibilities to distinguish experimentally between EPO's tissue-protective effects (e.g., antiapoptosis) and its potentially detrimental effects [e.g., procoagulant and prothrombotic effects (23) within the microvasculature] and excessive erythropoiesis upon chronic dosing. With these compounds, it is now possible to trigger EPO-mediated

tissue-protective pathways without cross-talk with the hematopoietic system.

References and Notes

1. R. Sasaki, *Intern. Med.* **42**, 142 (2003).
2. S. Masuda et al., *J. Biol. Chem.* **268**, 11208 (1993).
3. M. L. Brines et al., *Proc. Natl. Acad. Sci. U.S.A.* **97**, 10526 (2000).
4. Y. Konishi, D. H. Chui, H. Hirose, T. Kunishita, T. Tabira, *Brain Res.* **609**, 29 (1993).
5. M. Sakanaka et al., *Proc. Natl. Acad. Sci. U.S.A.* **95**, 4635 (1998).
6. M. Digicaylliloglu, S. A. Lipton, *Nature* **412**, 641 (2001).
7. A. L. Siren et al., *Proc. Natl. Acad. Sci. U.S.A.* **98**, 4044 (2001).
8. H. Ehrenreich et al., *Mol. Med.* **8**, 495 (2002).
9. S. Erbayraktar et al., *Proc. Natl. Acad. Sci. U.S.A.* **100**, 6741 (2003).
10. H. Ehrenreich et al., *Mol. Psychiatry* **9**, 42 (2004).
11. J. Grodberg, K. L. Davis, A. J. Sykowski, *Eur. J. Biochem.* **218**, 597 (1993).
12. K. C. Mun, T. A. Golper, *Blood Purif.* **18**, 13 (2000).
13. R. Satake, H. Kozutsumi, M. Takeuchi, K. Asano, *Biochim. Biophys. Acta* **1038**, 125 (1990).
14. Y. Hanazono, K. Sasaki, H. Nitta, Y. Yazaki, H. Hirai, *Biochem. Biophys. Res. Commun.* **208**, 1060 (1995).
15. P. T. Jublinsky, O. I. Krijanovski, D. G. Nathan, J. Tavernier, C. A. Sieff, *Blood* **90**, 1867 (1997).
16. W. M. Campana, R. Misasi, J. S. O'Brien, *Int. J. Mol. Med.* **1**, 235 (1998).
17. Materials and methods are available as supporting material on Science Online.
18. J. Grodberg, K. L. Davis, A. J. Sykowski, *Arch. Biochem. Biophys.* **333**, 427 (1996).
19. J. P. Boissel, W. R. Lee, S. R. Presnell, F. E. Cohen, H. F. Bunn, *J. Biol. Chem.* **268**, 15983 (1993).
20. G. M. Yousef, M. H. Ordon, G. Foussias, E. P. Diamandis, *Biochem. Biophys. Res. Commun.* **284**, 900 (2001).
21. R. Bianchi et al., *Proc. Natl. Acad. Sci. U.S.A.* **101**, 823 (2004).
22. T. Eld, M. Brines, *Clin. Breast Cancer* **3** (suppl. 3), S109 (2002).
23. P. J. Stohlawetz et al., *Blood* **95**, 2983 (2000).
24. This work would not have been possible without substantial and excellent technical assistance, which is gratefully acknowledged. This work is partially supported by grant RBAU01ARSJ and by Fondo Integrativo Speciale per la Ricerca-Neurobiotecologie from the Ministero dell'Istruzione, Università e Ricerca, Rome, Italy (to P.G.). Cerami-Hand, Cerami, and Brines are officers and minority stockholders of Warren Pharmaceuticals. The following patents have been applied for concerning this work: PCT/US03/20964, PCT/US01/49479, and US 10/188,905.

Supporting Online Material

www.sciencemag.org/cgi/content/full/305/5681/239/DC1
Materials and Methods
SOM Text
Figs. S1 and S2
References

25 March 2004; accepted 24 May 2004

Frataxin Acts as an Iron Chaperone Protein to Modulate Mitochondrial Aconitase Activity

Anne-Laure Bulteau,¹ Heather A. O'Neill,² Mary Claire Kennedy,³ Masao Ikeda-Saito,⁴ Grazia Isaya,² Luke I. Szewda^{1*}

Numerous degenerative disorders are associated with elevated levels of pro-oxidants and declines in mitochondrial aconitase activity. Deficiency in the mitochondrial iron-binding protein frataxin results in diminished activity of various mitochondrial iron-sulfur proteins including aconitase. We found that aconitase can undergo reversible citrate-dependent modulation in activity in response to pro-oxidants. Frataxin interacted with aconitase in a citrate-dependent fashion, reduced the level of oxidant-induced inactivation, and converted inactive [3Fe-4S]¹⁺ enzyme to the active [4Fe-4S]²⁺ form of the protein. Thus, frataxin is an iron chaperone protein that protects the aconitase [4Fe-4S]²⁺ cluster from disassembly and promotes enzyme reactivation.

Aconitase, a Krebs-cycle enzyme that converts citrate to isocitrate, belongs to the family of iron-sulfur-containing dehydratases whose activities depend on an intact cubane [4Fe-4S]²⁺ cluster (1, 2). The purified enzyme is highly susceptible to oxidant-induced inactivation due to release of the solvent-exposed Fe-α and formation of a [3Fe-4S]¹⁺

cluster (3, 4). Loss of mitochondrial aconitase activity is an intracellular indicator of superoxide generation and of oxidative damage in a variety of degenerative diseases and aging (5, 6). Nevertheless, aconitase is rapidly inactivated and subsequently reactivated when isolated rat cardiac mitochondria are treated with H₂O₂, suggesting that aconitase

may be an intramitochondrial sensor of redox status (7). The presence of the enzyme's substrate citrate diminishes Fe-α release, cluster disassembly, and enzyme inactivation, and it is required for enzyme reactivation (7). However, the physiological mechanisms responsible for preventing full cluster disassembly and for reduction of the [3Fe-4S]¹⁺ center and reinsertion of Fe(II) are unclear (1).

The mitochondrial matrix protein frataxin and its yeast homolog Yfh1p are thought to play a role in the storage of iron within mitochondria (8–12) and to promote Fe(II) availability (10, 13, 14) as one of the components involved in the maturation of cellular iron-sulfur-containing and heme-containing proteins (13–19). Friedreich's ataxia, a neurodegenerative and cardiac disorder, is char-

¹Department of Physiology and Biophysics, Case Western Reserve University, Cleveland, OH, USA.

²Departments of Pediatric and Adolescent Medicine and Biochemistry and Molecular Biology, Mayo Clinic College of Medicine, Rochester, MN, USA. ³Department of Chemistry, Gannon University, Erie, PA, USA.

⁴Institute of Multidisciplinary Research for Advanced Materials, Tohoku University, Katahira, Aoba-ku, Sendai 980-8577, Japan.

*To whom correspondence should be addressed. E-mail: lszewda@po.cwru.edu

HEMATOLOGICAL ONCOLOGY
(*Hematol. Oncol.*)

CONTENTS

VOLUME 14, ISSUE No. 3

September 1996

Improved Outcome in Solitary Bone Plasmacytomata with Combined Therapy: A. Avilés, J. Huerta-Guzmán, S. Delgado, A. Fernández and J. C. Díaz-Maqueo	111
Alpha-Interferon and Pregnancy in a Patient with CML: J. H. Lipton, C. M. Derzko and J. Curtis	119
Classical Hodgkin and Reed-Sternberg Cells Demonstrate a Non-Clonal Immature B Lymphoid Lineage: Evidence from a Single Cell Assay and <i>In Situ</i> Hybridization: K. Ohshima, J. Suzumiya, Y. Mukai, K. Tashiro, T. Shibata, T. Tanaka, A. Kato and M. Kikuchi	123
Effect of the Interaction between Transforming Growth Factor and Erythropoietin on the Proliferation of Normal Erythroid Progenitors and Leukemic UT-7 Cells: Action of Transforming Growth Factor β on the Erythropoietin Receptor: E. Leveque, M. D. Nagel and B. Haye	137
All-Trans Retinoic Acid (ATRA) in the Treatment of Acute Promyelocytic Leukemia (APL): C. S. Chim, Y. L. Kwong, R. Liang, Y. C. Chu, C. H. Chan, L. C. Chan, K. F. Wong and T. K. Chan	147
BOOK REVIEWS	155
FORTHCOMING MEETINGS	158

Indexed or abstracted by 'BIOMED Database (Institute for Scientific Information ISI)', 'BIOSIS', Cambridge Scientific Abstracts, 'Chemical Abstract Service', 'Current Awareness in Bio. Sci.', Current Contents-Life Sciences, 'CD of Leprosy Literature 1913-1991', 'Excerpta Medica', 'Index Medicus', 'NIOHTIC database', 'Reference Update', Research Alert (ISI), 'Science Citation Index (ISI)', 'SCISEARCH Database (ISI)' and 'Telegen Reporter'.

HAONDL 14 (3) 111-158 (1996)
ISSN 0278-0232

EFFECT OF THE INTERACTION BETWEEN TRANSFORMING GROWTH FACTOR β AND ERYTHROPOIETIN ON THE PROLIFERATION OF NORMAL ERYTHROID PROGENITORS AND LEUKEMIC UT-7 CELLS: ACTION OF TRANSFORMING GROWTH FACTOR β ON THE ERYTHROPOIETIN RECEPTOR

B. LEVEQUE*, M. D. NAGEL† AND B. HAYE*

*Unité de Recherche sur le Mode d'Action Hormonale (URMAH), *Laboratoire de Biochimie, EP CNRS 89,*

†Laboratoire de Physiologie Animale, UFR Sciences Exactes et Naturelles, Université de Reims, France

SUMMARY

The actions of transforming growth factor β (TGF β) and erythropoietin (Epo) were studied using normal erythroid progenitors from fetal rat liver and spleen at 18, 19 and 20 days. rhTGF β 1 inhibited the growth of late BFUe colonies significantly at each age and in both organs in methylcellulose cultures containing 2 U/ml rhEpo. There was no significant inhibition of CFUe proliferation, except for spleen CFUe at 18 days, suggesting different CFUe sensitivities to growth factors at a given fetal age, 18 days, in liver and spleen. The colorimetric MTT assay was used to examine the inhibition of the growth of human leukemic UT-7 cells by TGF β 1. TGF β 1 inhibited the proliferation of UT-7 cells in cultures without Epo at 24 h and in cultures with Epo at 24 and 72 h. The specific binding of [¹²⁵I]Epo to UT-7 surface was decreased by TGF β 1 without any change in non-specific binding. TGF β 1 also inhibited the expression of Epo-receptors on UT-7 cells, without changing receptor affinity. The inhibition of hematopoietic progenitor cell growth by TGF β could involve altering the cell surface expression of growth factor receptors.

KEY WORDS TGF β 1; erythropoietin; BFUe; CFUe; UT-7; Epo-receptor

INTRODUCTION

Erythropoiesis is a multistep process involving the sequential differentiation of multipotential stem cells into at least two subpopulations of erythroid progenitors, erythroid burst-forming units (BFUe) and erythroid colony-forming units (CFUe). BFUe generally require erythropoietin (Epo), interleukin 3 (IL3), granulocyte-macrophage colony-stimulating factor (GM-CSF)¹ and interleukin 9 (IL9)² in order to develop in semi-solid cultures. In contrast, CFUe colony formation depends on Epo alone.^{3,4} The proliferation and differentiation of hematopoietic progenitor cells can be modulated by transforming growth factor β (TGF β). TGF β 1 inhibits cultures of both fresh progenitor cells and growth factor-dependent hematopoietic cell lines.⁵ TGF β may inhibit the entry of cells into the S phase by a mechanism that involves

Addresssee for correspondence: E. Leveque, URMAH, EP CNRS 89, Laboratoire de Biochimie, UFR Sciences Exactes et Naturelles, BP 1039, 51687 REIMS Cedex 2, France, Tél: (33) 03 26 05 32 70, fax: (33) 03 26 05 31 68.

CCC 0278-0232/96/030137-10
© 1996 by John Wiley & Sons, Ltd

Received 24 April 1996
Accepted 30 September 1996

retinoblastoma suppressor gene products,^{6,7} or by perturbing the expression of growth promoting factor receptors.⁸⁻¹⁰ Nevertheless, in spite of the fact that Epo is one of the most well-studied cytokines, no modulation of its receptor density or activity by TGF β has ever been reported to our knowledge.

Keller *et al.*¹¹ found that TGF β had a greater inhibitory effect on immature colonies (CFU-GM, CFU-GEMM, BFUe) than on more mature colonies (CFUg, CFUm, CFUe), and that murine leukemia cell lines with an immature phenotype were more sensitive to TGF β than more mature ones. While most authors seem to agree that TGF β inhibits murine and human BFUe formation,¹¹⁻¹⁷ the findings for its effect on CFUe vary considerably: some observed inhibition in humans,¹³⁻¹⁵ and others none in the mouse.^{11,12} Rich and Kubanek,¹⁸ Kanamaru *et al.*¹⁹ and Rich²⁰ all obtained evidence for a change in the sensitivity of CFUe to erythropoietin during the ontogeny of erythropoiesis in the mouse. We have also observed such differences in CFUe sensitivity towards glucocorticoids and protein fractions extracted from spleen and liver hematopoietic cells at 20 days in the rat.²¹⁻²³

This study therefore examines the action of TGF β 1 on the proliferation of normal erythroid progenitors using late BFUe and CFUe from liver and spleen hematopoietic cells in rat fetuses aged 18, 19 and 20 days. The objective was to identify differences in the sensitivity of erythroid progenitors to TGF β 1 as a function of age within the same organ and in different organs (the liver, with decreasing erythropoietic potential and the spleen, with increasing erythropoietic potential) at the same age. We have also investigated the sensitivity of the human leukemic cell line UT-7 to TGF β 1. UT-7 is a megakaryoblastic cell line established from a patient with M-7 leukemia.²⁴ Its growth is dependent on IL-3 or GM-CSF, and it also responds to Epo.²⁵ The cells are usually grown with GM-CSF, but were deprived of the growth factor for 18 h and incubated with or without Epo or TGF β 1 for 24 or 72 h. The antiproliferative effect of TGF β 1 was estimated by the colorimetric MTT method and Scatchard plots were used to investigate the effect of TGF β 1 on the expression of Epo-receptors.

MATERIALS AND METHODS

Animals

Wistar rats (CF strain from the CNRS) were housed in a constant-temperature room with a 12-h day/12-h night cycle. They had free access to water and food (UAR commercial rat food). Coitus was assessed by the presence of spermatozoa in the morning vaginal smear. In this strain of rat, delivery generally occurs during the night between days 21 and 22 of pregnancy or in the morning of day 22.

Growth factors

Recombinant human Epo (rhEpo) and GM-CSF (rhGM-CSF) were purchased from Amersham (Les Ulis, France) and recombinant human TGF β 1 (rhTGF β 1) was from GIBCO-BRL (Eragny, France). RhEpo was used at a final concentration of 2 U/ml, rhGM-CSF at 2.5 ng/ml and rhTGF β 1 at 2 ng/ml and 10 ng/ml.

Erythroid colony assays

Cell suspensions

Pregnant rats were killed by decapitation. A total of 12-16 of the younger fetuses (18 and 19 days), from three litters, were used for each experiment, and 6-8 older fetuses (20 days), from

two litters, were used per experiment. Fetal spleens and livers were removed aseptically, placed in sterile ice-cold alpha medium (Gibco Bio-Cult Ltd) and gently disrupted in a Potter-Elvehjem homogenizer with a loose-fitting plastic pestel. The suspension was then filtered through a stainless steel sieve (50 μ m mesh) which retained particles, connective tissue and parenchyma cells. The exact volume was measured and the concentration of hematopoietic cells in the filtrate was determined after a five-fold dilution in 2.86 per cent acetic acid solution to remove anucleate red blood cells.

Erythroid colony cultures

Erythroid progenitors were cultured on methylcellulose by the technique of Iscove *et al.*²⁶ as modified by Urabe and Murphy.²⁷ The culture medium was 1.25 ml 2 per cent methylcellulose (A4 M premium, Dow Chemical Corp. Colorcon Ltd, England) in alpha medium containing rhEpo, 0.25 ml 10 per cent bovine serum albumin (BSA, grade V, Sigma Chemical Co., St Louis, MO) in alpha medium, 25 μ l 200 mM L-glutamine in water, 25 μ l kanamycine (Kanamycine solution \times 100, Gibco), 25 μ l penicillin and fungizone (antibiotic antimycotic solution \times 100, Gibco), 0.75 ml heat-inactivated fetal calf serum (FCS) (batch 147 982 02, Boehringer-Mannheim, Meylan, France), 50 μ l 7.5 per cent sodium bicarbonate in water, 25 μ l β -mercaptoethanol (type I, Sigma Chemical Co., St. Louis, MO). The BSA was prepared and deionized according to Murphy and Sullivan.²⁸ The final concentration of cells was 10^5 /ml. The suspensions were mixed carefully, and 0.2 ml samples were distributed in the wells of microtitre plates (Falcon Plastics, Oxnard CA, U.S.A.) and incubated at 37°C in an humidified atmosphere containing 5 per cent CO₂.

Erythroid colonies

Two-day erythroid colonies. The number of erythroid colonies containing eight or more cells after 2 days in culture in each well were counted without staining, as described by Iscove and Sieber.²⁹ These colonies were considered to be CFUe.

Seven-day erythroid colonies. Some colonies developed in hematopoietic liver and spleen cell cultures between days 4 and 7. They gave medium-to-large well-hemoglobinized colonies intermediate between BFUe and CFUe. Colonies of over 64 cells were therefore counted and designated mature or late BFUe.

UT-7-cell cultures

UT-7 cells were usually grown at 37°C in a MEM (ICN Biomedicals, Inc. Costa Mesa, CA, U.S.A.) containing 10 per cent (v/v) FCS and 2.5 ng/ml rhGM-CSF in a water-saturated atmosphere of 5 per cent CO₂ in air. Cells were passaged every 3–4 days.

UT-7 proliferation assays

Cells used in proliferation assays were washed three times with a MEM and incubated for 24 h in a MEM 10 per cent FCS without GM-CSF. They were plated into 96-well microtitre plates at a density of 5×10^3 cells in 100 μ l a MEM containing 10 per cent FCS. Growth factors were added and cultures were incubating for 24 h or 72 h at 37°C and 5 per cent CO₂ in air. Proliferation was then assessed by a modified version of the colorimetric MTT assay of Mosmann.³⁰ Briefly, 25- μ l aliquots of sterilized MTT (3-(4,5-dimethylthiazol-2-yl)-2,5-diphenyl tetrazolium bromide; Sigma Chemical Co, St. Louis, MO) (5 mg/ml buffer/medium) were added to each culture-well containing 100 μ l of cell suspension at the completion of culture and the

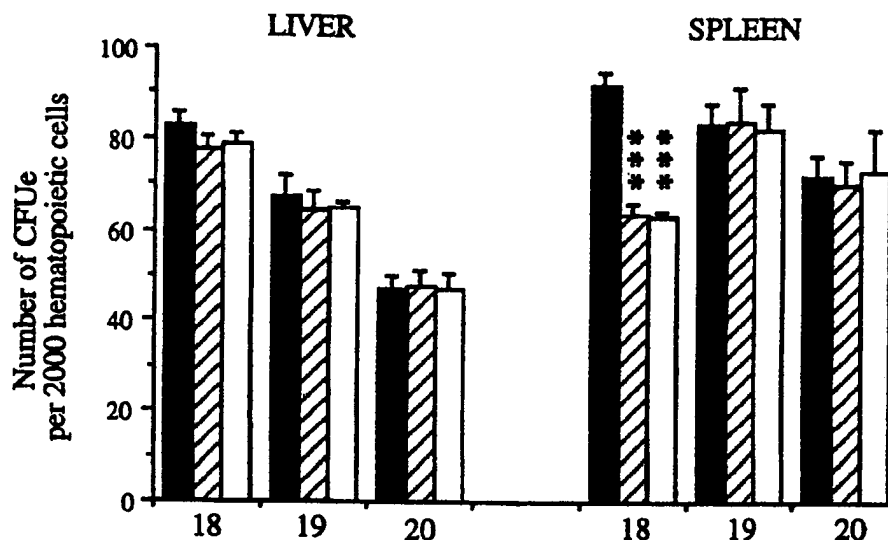


Figure 1. The effect of TGFβ1 on fetal rat liver and spleen CFUe colony formation in 18–20-day rat fetuses. Hematopoietic cells ($1 \times 10^5/\text{ml}$) were cultured for 2 days with 2 U/ml rhEpo in methylcellulose. Experimental assay media were supplemented with 2 or 10 ng/ml rhTGFβ1. The numbers of colonies/2000 hematopoietic cells are means \pm SEM of three different experiments in quadruplicate. Black bars, controls (without TGFβ1); hatched bars, with 2 ng/ml TGFβ1; open bars, with 10 ng/ml TGFβ1.

*** $p < 0.001$

plates were incubated for 5 h at 37°C. Of 10 per cent sodium dodecyl sulfate (SDS), 100 μl were then added to each well, mixed thoroughly and incubated for 12 h at 37°C. Plates were read in a microplate reader (model $\Sigma 960$, Metertech Inc., Bioblock Scientific, Illkirch, France) at 570–630 nm.

[^{125}I]-Epo binding assays

The characteristics of the Epo-receptor were studied by Scatchard analyses³¹ using iodinated ligand. Epo was iodinated to a specific activity of 500–2000 Ci/mmol using Iodogen.³² Cells (10^6) were incubated for 30 min at 37°C with various concentrations of [^{125}I]-Epo in 100 μl Iscove's modified Dulbecco medium containing 5 per cent FCS and 0.1 per cent sodium azide. The cells were then centrifuged and aliquots of the supernatants were used to determine the free hormone concentrations. The cells were washed three times with ice-cold phosphate-buffered saline (PBS) and the radioactivity bound to the cells was measured. Non-specific binding was determined by incubating the cells with a 100-fold excess of unlabelled ligand. Specific binding was determined by subtracting the non-specific from the total binding. Equilibrium binding data were analysed by the Scatchard method.

Statistical analysis

Student's *t*-test was used for statistical analysis.

RESULTS

Inhibition by rhTGFβ1 of CFUe and BFUe colonies in methylcellulose cultures of hematopoietic liver and spleen cells from rat fetuses aged 18, 19 and 20 days

The effect of rhTGFβ1 on normal erythroid progenitors from rat fetus liver and spleen was assessed. Hematopoietic progenitor cultures were grown at 37°C with an optimal concentration

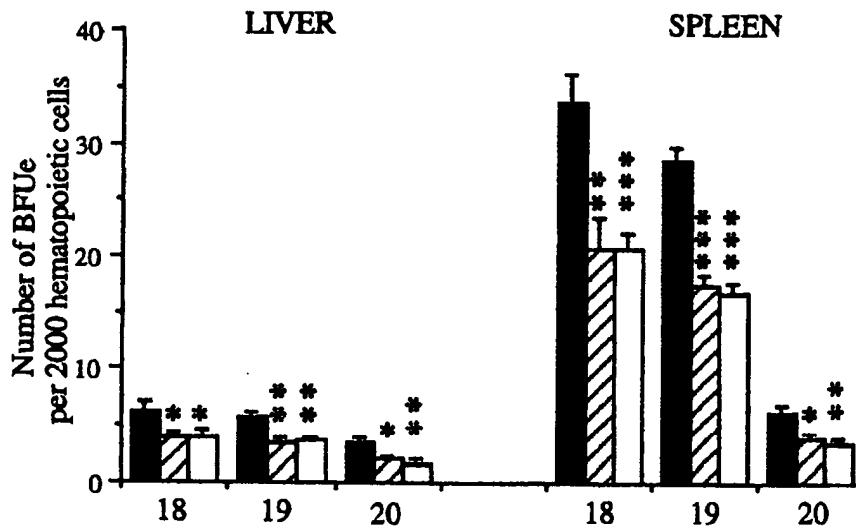


Figure 2. The effect of TGF β 1 on fetal rat liver and spleen late BFUe colony formation in 18–20-day rat fetuses. Hematopoietic cells (1×10^5 /ml) were cultured for 7 days with 2 U/ml rhEpo in methylcellulose. Experimental assay media were supplemented with 2 or 10 ng/ml rhTGF β 1. The numbers of colonies/2000 hematopoietic cells are means \pm SEM of three different experiments in quadruplicate. Black bars, controls (without TGF β 1); hatched bars, with 2 ng/ml TGF β 1; open bars, with 10 ng/ml TGF β 1. * p <0.05; ** p <0.01; *** p <0.001

of rhEpo (2 U/ml). The effect of rhTGF β 1 concentration (0, 0.1, 1, 1.5, 2, 10 and 20 ng/ml rhTGF β 1) on the response was measured in quadruplicate on liver and spleen BFUe at 18 days. Optimal inhibition of 18-day liver and spleen BFUe colony formation was obtained with 1 ng/ml or more rhTGF β 1 (data not shown). Experimental cultures thereafter contained 2 or 10 ng/ml rhTGF β 1. The number of CFUe colonies in controls (without TGF β 1) and in experimental cultures (with TGF β 1) are shown in Figure 1. The formation of CFUe from 18-day spleens was inhibited (30.4 per cent with 2 ng/ml rhTGF β 1 and 30.0 per cent with 10 ng/ml rhTGF β 1). The proliferation of CFUe colonies from the spleens of 19- and 20-day-old rat fetuses and from the rats livers were not significantly inhibited, and 2 ng/ml and 10 ng/ml rhTGF β 1 have the same inhibitory effect.

In contrast, the proliferation of all the BFUe decreased significantly when incubated with rhTGF β 1 (37.4–51.5 per cent inhibition) at all the ages tested and for both liver and spleen cultures (Figure 2). As for CFUe, all the concentrations of TGF β 1 used produced similar degrees of inhibition.

Actions of rhEpo and rhTGF β 1 on the proliferation of the human leukemia cell line UT-7

UT-7 cells were usually grown with GM-CSF and placed in a MEM plus 10 per cent FCS without any growth factor for 18 h. No significant cell death resulted from this period of deprivation and a CFUe assay indicated that the FCS had no erythropoietin activity (data not shown). The UT-7 cell control cultures were distributed in microtitre plates: 100 μ l cell suspension in a MEM plus 10 per cent FCS containing 5×10^3 cells with or without 2 U/ml rhEpo. The experimental wells also contained 2 or 10 ng/ml rhTGF β 1, which were found to be optimal doses.

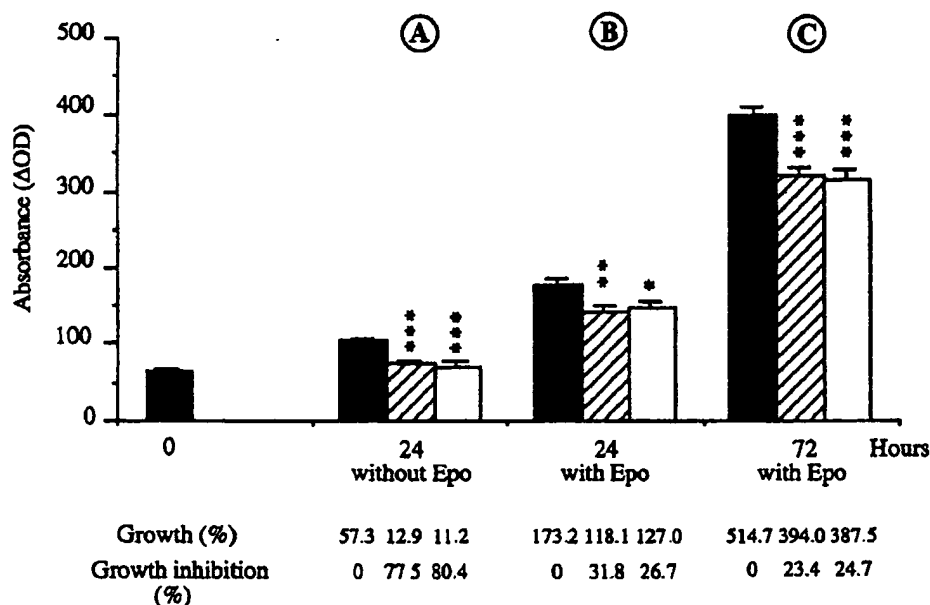


Figure 3. The effect of TGF β 1 on the growth of UT-7 cells. UT-7 cells ($5 \times 10^3/100 \mu\text{l}$) were cultured in a MEM plus 10 per cent FCS with or without 2 U/ml rhEpo in 96-well microtitre plates. Experimental assay media were supplemented with 2 or 10 ng/ml rhTGF β 1. Proliferation was measured after growth for 24 or 72 h by the colorimetric MTT method (absorbance at 570–630 nm). Data (ΔOD) are expressed as means \pm SEM of three or four experiments in quadruplicate. Black bars, controls (without TGF β 1); hatched bars, with 2 ng/ml TGF β 1; open bars, with 10 ng/ml TGF β 1.

* $p < 0.05$; ** $p < 0.01$; *** $p < 0.001$

The control level was estimated at 0 h and proliferation was measured for 24 and 72 h; the cells were then treated with MTT. UT-7 cells incubated for 24 h without Epo had grown moderately (Figure 3a) and their proliferation was stimulated by Epo (Figure 3b). TGF β 1 inhibited the proliferation of UT-7 cells in cultures with or without Epo. Both 2 ng/ml and 10 ng/ml rhTGF β 1 produced similar degrees of inhibition. However, TGF β 1 had a greater effect at 24 h in cultures without Epo than in cultures with Epo. The growth of UT-7 cells after 72 h with Epo (Figure 3c) was dramatically increased, and TGF β 1 had roughly the same degree of inhibition as for cells cultured with Epo for 24 h (Figure 3b). Therefore, the interaction of Epo with TGF β 1 partially inhibited proliferation, as compared to the action of TGF β 1 alone.

For comparison, the effect of TGF β 1 (2 ng/ml) was assayed on UT-7 cells grown in GM-CSF experiments. Growth was inhibited by 2.7 ± 0.7 per cent at 24 h, 27.4 ± 0.2 per cent at 48 h and 34.1 ± 0.5 per cent at 72 h.

Action of rhTGF β 1 on the expression of Epo-receptors in UT-7 cells

The binding of [^{125}I]Epo to UT-7 cells with and without TGF β 1 is shown in Figure 4. More [^{125}I]Epo was specifically bound to cells deprived of GM-CSF than to the negative control. TGF β 1 inhibited specific [^{125}I]Epo-binding significantly, without any effect on non-specific binding. The UT-7 cells bound Epo specifically and binding reached equilibrium by 30 min (data not shown). The equilibrium constants of Epo binding to UT-7 were determined by Scatchard

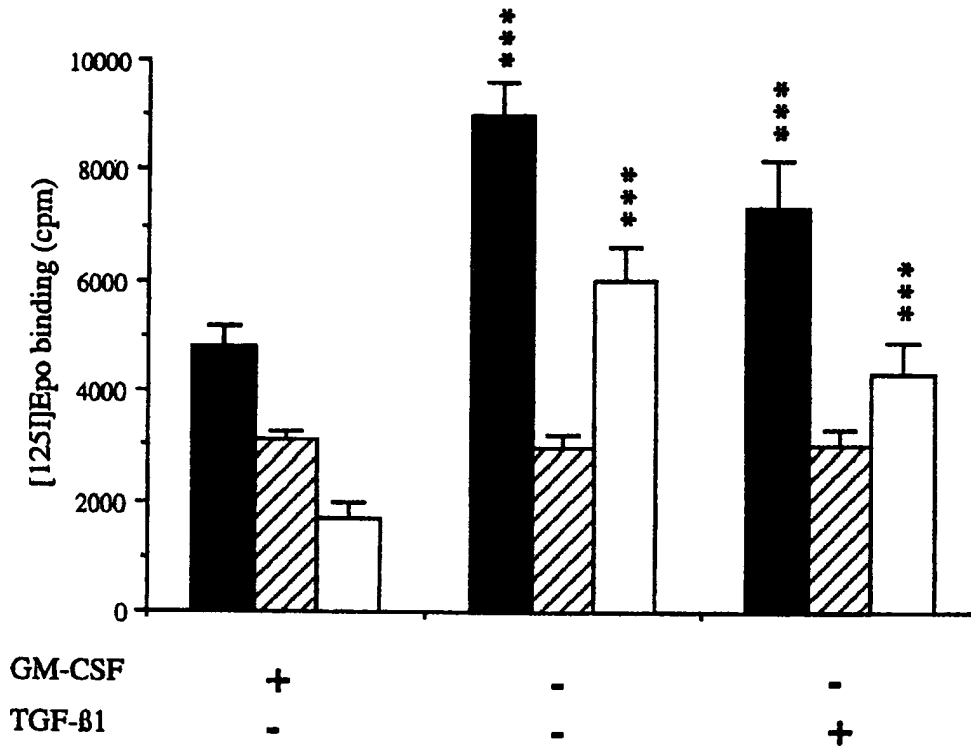


Figure 4. The effects of TGF β 1 on Epo binding to UT-7 cells. UT-7 cells were incubated for 18 h without GM-CSF, in the presence or absence of TGF β 1 (4 ng/ml), and treated as described in Materials and Methods. Cells incubated with GM-CSF are negative controls of Epo-receptor expression. Data are means \pm SEM of three independent experiments in triplicate. Black bars, total binding; hatched bars, non-specific binding; open bars, specific binding.

*** $p < 0.001$

analysis. UT-7 cells grown with GM-CSF gave a straight-line Scatchard plot, indicating a single class of high-affinity binding sites. There were 1265 ± 300 receptors per cell with a dissociation constant of 160 ± 20 pmol/l (Figure 5). UT-7 cells deprived of GM-CSF for 18 h had significantly more sites per cell (4790 ± 30), but the dissociation constant was unchanged (169 ± 13 pmol/l) (Figure 5). These results are in agreement with previous observations.²⁵ Incubation with TGF β 1 (4 ng/ml) for 18 h (Figure 5) reduced the average number of Epo-receptors to 2544 ± 286 /cell, without significantly affecting the receptor affinity (dissociation constant: 179 ± 46 pmol/l).

DISCUSSION

The BFUe, which are less mature progenitors than CFUe, are present in the liver and spleen of rats at the end of intrauterine life and are sensitive to rhTGF β 1. In contrast, CFUe from the same fetuses do not seem to react to rhTGF β 1, except for spleen cultures from 18-day fetuses. This suggests that there are different CFUe populations, having different sensitivities towards growth factors, depending on the age of the fetus and the particular organ. This is in agreement

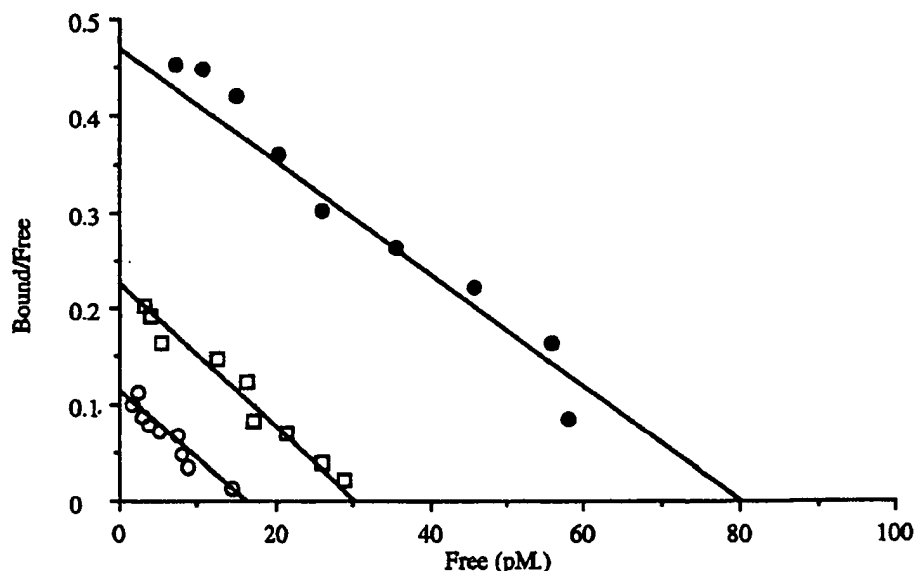


Figure 5. Scatchard analysis of TGF β 1-induced down-regulation of Epo-receptors on UT-7 cells. UT-7 cells usually grown with 2.5 ng/ml GM-CSF (○) were incubated at 37°C for 18 h without any growth factor (●), or with 4 ng/ml rhTGF- β 1 (□). Increasing concentrations of radioiodinated Epo were added to 1×10^6 cells in 100 μ l binding medium, and specific Epo binding was determined as described in Materials and Methods. Equilibrium binding data were analysed by Scatchard's method. Data are representative of three separate experiments

with reports of different CFUe sensitivities toward Epo,¹⁸⁻²⁰ glucocorticoids and protein fractions extracted from hematopoietic cells²¹⁻²³ in the fetus. The effects of TGF β are pleiotropic and may depend in particular on the stage of differentiation, the immediate environment, cell lineage and the presence of other cytokines.³³ Dydebal and Jacobsen³⁴ demonstrated recently that TGF β directly inhibits murine erythroid colonies and that several erythroid stimulators counteract its inhibition of BFUe.

TGF β 1 also significantly inhibits the Epo-induced proliferation of UT-7 cells as early as 24 h, but the inhibition is not much greater at 72 h. For comparison, the GM-CSF-induced proliferation of UT-7 cells is not significantly inhibited before 48 h, but TGF β 1 inhibits Epo and GM-CSF-induced proliferation to about the same degree. TGF β 1 (2 ng/ml or 10 ng/ml) inhibits UT-7 proliferation in the same way as normal hematopoietic progenitors. This inhibitory effect was reduced in the presence of Epo (2 U/ml), indicating that there is an interaction between TGF β 1 and Epo in UT-7 cells. Since TGF β 1 is a selective inhibitor of primitive hematopoietic cells,^{11,15,35} UT-7 may be more a multipotential progenitor factor-dependent cell line rather than a committed cell line.

The antiproliferative effect of TGF β on hematopoietic progenitor cells could be due to a change in the number of CSF receptors and/or their affinity. The expressions of GM-CSF, IL3, G-CSF, IL1 and SCF receptors all appear to be altered by TGF β 1.⁸⁻¹⁰ Scatchard plots were used to study the action of TGF β 1 on the number of Epo-receptors on UT-7 cells. TGF β 1 inhibits only the specific binding of Epo to UT-7 cells. And TGF β 1 seems to reduce the number of Epo-receptors on the UT-7 cell surface without affecting the receptor affinity. TGF β 1 had a

similar action on the Epo-receptors at the surface of UT-7 cells as it does on other cytokine receptors.³⁵⁻³⁷ This action on CSF-receptor expression could be due to a general inhibitory effect of TGF β , because the modulation of CSF receptor expression is closely correlated with its effects on cell proliferation, but the regulation of progenitor cell growth by TGF β need not alter the number of CSF receptors.³⁵ Further studies will undoubtedly provide a better understanding of the way TGF β 1 operates.

ACKNOWLEDGEMENTS

The authors thank Dr P. Mayeux and Dr C. Lacombe (INSERM U.152) for providing the UT-7 cells, Mme M. L. Sowa for technical assistance, Mlle C. Dauphin for help in preparing the manuscript and Dr O. Parkes for checking the English text. This work was supported by grants from the Ministère de l'Enseignement Supérieur et de la Recherche and from the Centre National de la Recherche Scientifique.

REFERENCES

1. Emerson, S. G., Young, Y. C., Clark, S. C., Long, M. W. Human recombinant granulocyte-macrophage colony stimulating factor and interleukin 3 have overlapping but distinct hematopoietic activities. *J. Clin. Invest.* 1988, **82**, 1282-1287.
2. Donahue, R. E., Young, Y. C., Clark, S. C. Human P40 T-cell growth factor (interleukin 9) supports erythroid colony formation. *Blood* 1990, **75**, 2271-2275.
3. Iscove, N. N. The role of erythropoietin in regulation of population size and cell cycling of early and late erythroid precursors in mouse bone marrow. *Cell Tissue Kinet.* 1977, **10**, 323-334.
4. Gregory, C. J., Eaves, A. C. Three stages of erythropoietic progenitor cell differentiation distinguished by a number of physical and biologic properties. *Blood* 1978, **51**, 527-537.
5. Hooper, W. C. The role of transforming growth factor-beta in hematopoiesis. A review *Leukemia Res.* 1991, **15**, 179-184.
6. Massagué, J., Cheifetz, S., Laiho, M., Ralph, D. A., Weis, F. M. B., Zentella, A. Transforming growth factor- β . *Cancer Surveys* 1992, **12**, 81-103.
7. Derynck, R. TGF- β -receptor-mediated signaling. *TIBS* 1994, **19**, 548-553.
8. Dubois, C. M., Ruscetti, F. W., Palaszynski, E. W., Falk, I. A., Oppenheim, J. J., Keller, J. R. Transforming growth factor β is a potent inhibitor of interleukin 1 (IL-1) receptor expression: proposed mechanism of inhibition of IL-1 action. *J. Exp. Med.* 1990, **172**, 737-744.
9. Dubois, C. M., Ruscetti, F. W., Stankova, J., Keller, J. R. Transforming growth factor- β regulates c-kit message stability and cell-surface protein expression in hematopoietic progenitors. *Blood* 1994, **83**, 3138-3145.
10. Jacobsen, S. E. W., Ruscetti, F. W., Dubois, C. M., Lee, J., Boone, T. C., Keller, J. R. Transforming growth factor- β trans-modulates the expression of colony-stimulating factor receptors on murine hematopoietic progenitor cell lines. *Blood* 1991, **77**, 1706-1716.
11. Keller, J. R., Sing, G. K., Ellingsworth, L. R., Ruscetti, F. W. Transforming growth factor β : possible roles in the regulation of normal and leukemic hematopoietic cell growth. *J. Cell. Biochem.* 1989, **39**, 175-184.
12. Hino, M., Tojo, A., Miyazono, K., Urabe, A., Takaku, F. Effects of β transforming growth factors on haematopoietic cells. *Br. J. Haematol.* 1988, **70**, 143-147.
13. Mitjavila, M. T., Vinci, G., Villaval, J. L., et al. Human platelet α granules contain a nonspecific inhibitor of megakaryocyte colony formation: its relationship to type β transforming growth factor (TGF β). *J. Cell. Physiol.* 1988, **134**, 93-100.
14. Ottmann, O. G., Pelus, L. M. Differential proliferative effects of transforming growth factor β on human hematopoietic progenitor cells. *J. Immunol.* 1988, **140**, 2661-2665.
15. Sing, G. K., Keller, J. R., Ellingsworth, L. R., Ruscetti, F. Transforming growth factor β selectively inhibits normal and leukemic human bone marrow cell growth *in vitro*. *Blood* 1988, **72**, 1504-1511.
16. Aglietta, M., Stacchini, A., Severino, A., Sanavio, F., Ferrando, M. L., Piacibello, W. Interaction of transforming growth factor- β 1 with hemopoietic growth factors in the regulation of human normal and leukemic myelopoiesis. *Exp. Hematol.* 1989, **17**, 296-299.

17. Strife, A., Lambek, C., Perez, A., *et al.* The effects of transforming growth factor $\beta 3$ on the growth of highly enriched hematopoietic progenitor cells derived from normal human bone marrow and peripheral blood. *Cancer Res.* 1991, **51**, 4828-4836.
18. Rich, I. N., Kubanek, B. The ontogeny of erythropoiesis in the mouse detected by the erythroid colony-forming technique. II. Transition in erythropoietin sensitivity during development. *J. Embryol. Exp. Morphol.* 1980, **58**, 143-155.
19. Kanamaru, A., Okamoto, T., Hara, H., Nagai, K. Developmental changes in erythropoietin responsiveness of late erythroid precursors in mouse hematopoietic organs. *Dev. Biol.* 1982, **92**, 221-226.
20. Rich, I. N. The developmental biology of hemopoiesis: effect of growth factors on the colony formation by embryonic cells. *Exp. Hematol.* 1992, **20**, 368-370.
21. Nagel, M. D., Nagel, J. Development of erythroid colony-forming cells in rat fetal spleen: apparent lack of sensitivity to *in vivo* corticosteroid excess as compared to fetal liver. *Development* 1987, **99**, 239-246.
22. Nagel, M. D., Nagel, J. Erythroid colony formation by fetal rat liver and spleen cells *in vitro*: inhibition by a low relative molecular mass component of fetal spleen. *Development* 1992, **114**, 213-219.
23. Nagel, M. D. A 29 000 molecular weight fraction from fetal rat liver adhering cells that cooperates with erythropoietin in stimulating the growth of erythroid progenitors. *In Vitro Cell. Dev. Biol.* 1993, **29A**, 782-788.
24. Komatsu, N., Nakauchi, H., Miwa, A., *et al.* Establishment and characterization of a human leukemic cell line with megakaryocytic features: dependency on granulocyte-macrophage colony-stimulating factor, interleukin 3 or erythropoietin for growth and survival. *Cancer Res.* 1991, **51**, 341-348.
25. Hermine, O., Mayeux, P., Titeux, M., *et al.* Granulocyte-macrophage colony-stimulating factor and erythropoietin act competitively to induce two different programs of differentiation in the human pluripotent cell line UT-7. *Blood* 1992, **80**, 3060-3069.
26. Iscove, N. N., Sieber, F., Winterhalter, K. H. Erythroid colony formation in cultures of mouse and human bone marrow, analysis of the requirement for erythropoietin by gel filtration and affinity chromatography on agarose concanavalin A. *J. Cell Physiol.* 1974, **83**, 309-320.
27. Urabe, A., Murphy, M. J. *Miniaturization of Methylcellulose Erythroid Colony Assay*. In *Vitro Aspects of Erythropoiesis*. New York: Springer Verlag, 1978, 28-30.
28. Murphy, M. J., Sullivan, M. E. *Culture of Erythroid Stem Cells from Murine and Human Marrow and Blood*. In *Vitro Aspects of Erythropoiesis*. New York: Springer Verlag, 1978, 262-265.
29. Iscove, N. N., Sieber, F. Erythroid progenitors in mouse bone marrow detected by microscopic colony formation in culture. *Exp. Hematol.* 1975, **3**, 32-43.
30. Mosmann, T. Rapid colorimetric assay for cellular growth and survival: application to proliferation and cytotoxicity assays. *J. Immunol. Methods* 1983, **65**, 55-63.
31. Scatchard, G. The attraction of proteins for small molecules and ions. *Ann. N.Y. Acad. Sci.* 1949, **51**, 660.
32. Mayeux, P., Billat, C., Jacquot, R. The erythropoietin receptor of rat erythroid progenitor cells. Characterization and affinity cross-linkage. *J. Biol. Chem.* 1987, **269**, 13985-13990.
33. Hooper, C. The role of Transforming Growth Factor-beta in hematopoiesis. A review. *Leukemia Res.* 1991, **15**, 179-184.
34. Dydebal, I., Jacobsen, F. E. W. Transforming Growth Factor β (TGF- β), a potent inhibitor of erythropoiesis: neutralizing TGF- β antibodies show erythropoietin as a potent stimulator of murine Burst-Forming Unit Erythroid colony formation in the absence of a Burst-Promoting activity. *Blood* 1995, **86**, 949-957.
35. Jacobsen, S. E. N., Ruscetti, F. W., Roberts, A. B., *et al.* TGF β is a bidirectional modulator of cytokine receptor expression on murine bone marrow cells. *J. Immunol.* 1993, **151**, 4534-4544.
36. Keller, J. R., Jacobsen, S. E. W., Dubois, C. M., Hestdal, K., Ruscetti, F. W. Transforming growth factor- β : a bidirectional regulator of hematopoietic cell growth. *Int. J. Cell Cloning* 1992, **10**, 2-11.
37. Keller, J. R., McNiece, I. K., Sill, K. T., *et al.* Transforming growth factor β directly regulates primitive murine hematopoietic cell proliferation. *Blood* 1990, **75**, 596-602.

Treatment of traumatic brain injury in rats with erythropoietin and carbamylated erythropoietin

ASIM MAHMOOD, M.D.,¹ DUNYUE LU, M.D., PH.D.,² CHANGSHENG QU, M.D.,²
ANTON GOUSSEV, M.D.,² ZHENG GANG ZHANG, M.D., PH.D.,³ CHANG LU,³
AND MICHAEL CHOPP, PH.D.³

Departments of ¹Neurosurgery, ²Neurosurgery Research, and ³Neurology Research, Henry Ford Health System, Detroit, Michigan

Object. This study was designed to investigate the neuroprotective properties of recombinant erythropoietin (EPO) and carbamylated erythropoietin (CEPO) administered following traumatic brain injury (TBI) in rats.

Methods. Sixty adult male Wistar rats were injured with controlled cortical impact, and then EPO, CEPO, or a placebo (phosphate-buffered saline) was injected intraperitoneally. These injections were performed either 6 or 24 hours after TBI. To label newly regenerating cells, bromodeoxyuridine was injected intraperitoneally for 14 days after TBI. Blood samples were obtained on Days 1, 2, 3, 7, 14, and 35 to measure hematocrit. Spatial learning was tested using the Morris water maze. All rats were killed 35 days after TBI. Brain sections were immunostained as well as processed for the enzyme-linked immunosorbent assay to measure brain-derived neurotrophic factor (BDNF).

Results. A statistically significant improvement in spatial learning was seen in rats treated with either EPO or CEPO 6 or 24 hours after TBI ($p < 0.05$); there was no difference in the effects of EPO and CEPO. Also, these drugs were equally effective in increasing the number of newly proliferating cells within the dentate gyrus at both time points. A statistically significant increase in BDNF expression was seen in animals treated with both EPO derivatives at 6 or 24 hours after TBI. Systemic hematocrit was significantly increased at 48 hours and 1 and 2 weeks after treatment with EPO but not with CEPO.

Conclusions. These data demonstrate that at the doses used, EPO and CEPO are equally effective in enhancing spatial learning and promoting neural plasticity after TBI. (DOI: 10.3171/JNS-07/08/0392)

KEY WORDS • carbamylated erythropoietin • erythropoietin • hematocrit • rat • traumatic brain injury

TRAUMATIC brain injury remains a major health problem, and despite all the research, no effective therapy is available to repair biostructural damage following this type of injury. The incidence of patients with closed head injuries admitted annually to hospitals is 200 per 100,000.²⁰

To develop an effective therapy for TBI, extensive research is being conducted, and the recent focus has been to enhance endogenous neuroplasticity by using cell therapy or pharmacotherapy.^{3,13,15,26} Agents that have shown promise in treating neural injury include EPO and its derivatives.²⁴ A cytokine that is produced by the kidney, EPO has hormonal action to increase red cell mass in response to tissue hypoxia. However, recent research has shown that in addition to being hematopoietic, EPO is also tissue protec-

tive, through interaction with different receptors. In particular, EPO is neuroprotective after a variety of neurological insults.^{1,2,9,10,19,23,24} Nevertheless, with continuous dosing the hematopoietic effect of EPO can be potentially deleterious when used clinically due to induction of polycythemia. This has led to development of chemical derivatives of EPO such as CEPO, which is neuroprotective but not hematopoietic.¹¹

The hematopoietic effects of EPO are mediated by the homodimeric erythropoietic receptor EPOR₂, which is a Class I cytokine receptor.¹¹ Nevertheless, the receptor complex mediating EPO's neuroprotective action is different and is functionally related to other cytokine receptors such as CD131. The CEPO molecule does not bind with the homodimeric erythropoietic receptor and lacks hematopoietic properties, but CEPO has been shown to be neuroprotective against stroke, spinal cord compression, diabetic neuropathy, and experimental autoimmune encephalomyelitis. Its efficacy against TBI, however, has not been investigated. In fact, there are limited data on the use of the entire family of erythropoietic agents for treatment of TBI.^{2,16}

Our study was designed to investigate the functional, his-

Abbreviations used in this paper: BDNF = brain-derived neurotrophic factor; BrdU = bromodeoxyuridine; CEPO = carbamylated erythropoietin; ELISA = enzyme-linked immunosorbent assay; EPO = erythropoietin; PBS = phosphate-buffered saline; TBI = traumatic brain injury.

Erythropoietin derivatives for traumatic brain injury

tological, and molecular effects of EPO and CEPO administration after TBI in rats. The effects of EPO and CEPO were compared with each other as well as with control.

Materials and Methods

All procedures were approved by Henry Ford Hospital's Institutional Animal Care and Use Committee.

Recombinant EPO and CEPO

For this study we used recombinant EPO (Epoitin Alfa, PRO-CRIT; 5000 U/kg) provided by Ortho Biotech, Inc., and CEPO (50 µg/kg) prepared according to published protocols by Centocor, Inc. These compounds were injected intraperitoneally into rats. Doses were selected based on our prior studies with EPO¹⁶ as well as studies in stroke.²⁴

Animal Model and Injection of Recombinant EPO and CEPO

A controlled cortical impact model in rats was used.⁷ Sixty male Wistar rats were anesthetized with 10% chloral hydrate administered intraperitoneally. Rectal temperature was controlled at 37°C with a feedback-regulated water-heating pad. A controlled cortical impact device was used to induce the injury, as has been described previously. Briefly, the rats were placed in a stereotactic frame, and two 10-mm-diameter craniotomies were performed adjacent to the central suture, midway between lambda and bregma. The contralateral craniotomy allowed for movement of cortical tissue laterally.²¹ The dura mater was kept intact over the cortex. Injury was induced by impacting the left (ipsilateral) cortex with a pneumatic piston containing a 6-mm-diameter tip at the rate of 4 m/second and 2.5 mm of compression. Velocity was measured with a linear velocity displacement transducer.

At 6 or 24 hours after TBI, the rats were reanesthetized for drug administration. The drug was slowly injected intraperitoneally with a 1-ml syringe. Control animals received an injection of PBS only. Two different drugs were used and the 60 animals were divided into six groups of 10 each, as follows: Group 1, TBI with EPO injection at 6 hours; Group 2, TBI with CEPO injection at 6 hours; Group 3, TBI with PBS injection at 6 hours; Group 4, TBI with EPO injection at 24 hours; Group 5, TBI with CEPO injection at 24 hours; and Group 6, TBI with PBS injection at 24 hours. All animals received BrdU injections for 14 days after TBI, and all rats were killed 35 days postinjury.

Hematocrit Measurement

Blood samples were taken on Days 1, 2, 3, 7, 14, and 35. Hematocrit was measured in all animals.

Morris Water Maze Test

The rats' spatial learning was tested using the Morris water maze, which is a modification of the previously described test.⁴³ The experimental apparatus consisted of a circular water tank that was 140 cm in diameter and 45 cm high. An invisible platform 15 cm in diameter and 35 cm high was placed 1.5 cm below the surface of the water, which was maintained at a temperature of 30°C. The pool was located in a large testing room where there were many clues external to the maze (for example, pictures, lamps, and so forth); these clues were visible from the pool and were presumably used by the rats for spatial orientation. The position of the clues remained unchanged throughout the test. Data collection was automated using the HVS Image 2020 Plus Tracking System (US HVS Image). For descriptive data collection, the pool was subdivided into four equal quadrants formed by imaging lines.

Spatial learning was tested toward the end of the study (Days 31–35) because the neurorestorative processes of neurogenesis, angiogenesis, and synaptogenesis require certain time periods to be clinically evident.^{14,17} Four trials were performed each day with each rat. At the start of each trial, the rat was placed randomly at one of four fixed starting points, randomly facing either toward the wall or

the center of the pool (designated North, South, East, and West) and allowed to swim for 90 seconds or until it found the platform. The platform was placed in a randomly changing position within the northeast quadrant throughout the test period (for example, equidistant from the center and edge of the pool, against the wall, near the center of the pool, or at the edges of the northeast quadrant). Thus the animal learns to search extensively in the correct quadrant, because the platform is located somewhere within the northeast quadrant, although its precise location cannot be predicted.

Given the fixed placement of the platform, once they learn the location, the rats do not need to spend much time searching the quadrant, and when the platform is removed for the occasional brief probe trial, the animal quickly discovers its absence and may spend only a small amount of time searching for it again in that location. Moreover, the maladaptive preservative performance can increase the percentage of time an animal spends in the vicinity of the location from which a fixed-location platform has been removed during a probe trial.

During this test, if the animal found the platform, it was allowed to remain there for 15 seconds before being returned to its cage. If the animal was unable to find the platform within 90 seconds, the training was terminated and a maximal score of 90 seconds was assigned. The percentage of time traveled within the northeast (correct) quadrant was calculated relative to the total amount of time spent swimming before reaching the platform.

Brain Sample Preparation

Brain tissues obtained in five of the rats from each group were processed for preparation of paraffin-embedded sections, which were used for the histological evaluation and immunostaining analysis procedures, and the brain tissues of the remaining five rats were frozen for ELISA evaluations.

Immunohistochemical Studies

Immunohistochemical staining was performed on coronal cerebral samples. Brain sections were immunostained with diaminobenzidine to detect BrdU-positive cells in the dentate gyrus. Briefly, 6-µm-thick sections from the EPO-, CEPO-, and PBS-treated groups were deparaffinized and placed in PBS. For identification of BrdU-positive cells, the sections were placed in 50% formamide in 2 × standard saline citrate at 65°C for 30 minutes. The sections were then treated with 2 N HCl at 37°C for 10 minutes, and then with 0.1 M boric acid at room temperature for 3 minutes. After blocking in normal serum, sections were treated with primary antibody (BrdU, DAKO) at 4°C overnight. After sequential incubation with biotinylated anti-mouse antibody at room temperature for 30 minutes, sections were treated with an avidin-biotin-peroxidase complex kit (Vector Laboratories, Inc.). The diaminobenzidine was then used as a sensitive chromogen for light microscopy.

Estimates of Positive Cell Numbers

The brains were cut in a craniocaudal direction into seven blocks labeled A through G, and three sections from each animal were studied. The BrdU-positive cells were identified in the brains of rats receiving EPO, CEPO, or PBS treatment by using light microscopy. This cellular analysis was performed on block E or F, both of which contain dentate gyrus. Total numbers of BrdU-sensitive chromogen-positive cells in the rat brain sections were identified with a × 40 objective lens under light microscopy.

Enzyme-Linked Immunosorbent Assay

Brain tissues obtained in five animals from each group were used for BDNF analysis. For this the ipsilateral hemisphere was removed and processed for the ELISA according to the procedure specified in the ELISA kits (Quantikine—BDNF, R&D Systems, Inc.). These kits have the sensitivity to detect a factor concentration as low as 1 pg/ml. The brain tissue was homogenized in Iscove modified Dulbecco medium and centrifuged at 1000 rpm at 4°C. The supernatant was harvested for the quantitative analysis of BDNF. The ELISA was performed using the Titertek Multiskan MCC/340 equipment (Labsystems, Finland).

Statistical Analysis

Data were analyzed using analysis of variance for multiple comparisons. Paired t-tests were used to test the difference in the cell counts and BDNF levels among different groups.

Results

Enhanced Restoration of Spatial Learning

The percentage of time spent in the correct quadrant during the water maze test was significantly higher in both EPO- and CEPO-treated animals than in PBS-treated control animals (Fig. 1). This effect was apparent regardless of whether the treatment was administered 6 or 24 hours after TBI, and there was no difference between the effects of EPO and CEPO. These data demonstrate that EPO and CEPO administration reduces the dysfunction of spatial learning caused by the brain damage in this model.

Increased Number of BrdU-Labeled Cells in the Brain

The BrdU-positive cells, which are an index of new cellular proliferation, were counted in the dentate gyrus (Fig. 2). Treatment with EPO and CEPO significantly enhances this cellular proliferation in the dentate gyrus (Fig. 3). The number of BrdU-positive cells was slightly greater when the treatment was administered 6 hours after injury than when it was administered 24 hours after TBI; however, the difference was not statistically significant. Also, there was no significant difference between the effects of EPO and CEPO.

Increase in Hematocrit After EPO but not CEPO Treatment

Rats injected with EPO at 6 or 24 hours after TBI showed an increase in hematocrit at 48 hours, 1 week, and 2 weeks after treatment (Fig. 4). However, this effect was no longer apparent at 5 weeks after treatment. On the other hand, CEPO had no effect on hematocrit.

Enhanced BDNF Expression

Treatment with EPO as well as CEPO administered 6 or 24 hours after TBI increased the expression of BDNF (Fig. 5); however, there was no significant difference between the effects of EPO and CEPO.

Discussion

The results of this study demonstrate that EPO and CEPO are equally effective in improving spatial learning, in stimulating endogenous cellular proliferation, and inducing BDNF expression after TBI in rats. To study the therapeutic window, treatments were administered at two time points, 6 and 24 hours after TBI. Our results showed no functional, histological, or molecular differences between 6- and 24-hour treatments, indicating that treatment can be administered at least 24 hours after TBI.

Erythropoietin is known to be produced either in the fetal liver or adult kidney in response to tissue hypoxia. However, Tan and colleagues²⁵ have shown that it is produced in many other organs besides the liver and kidney, such as the lung, spleen, testis, heart, and brain. Subsequent

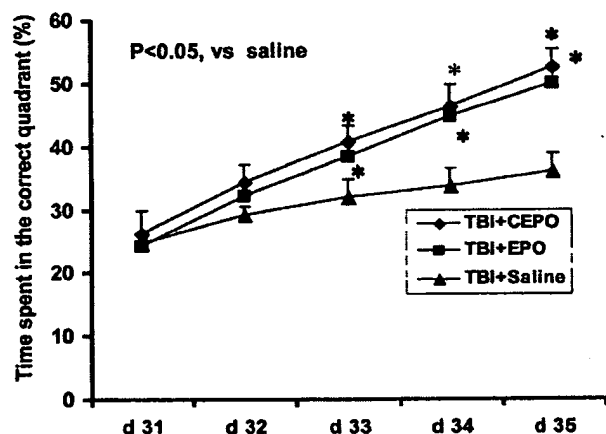
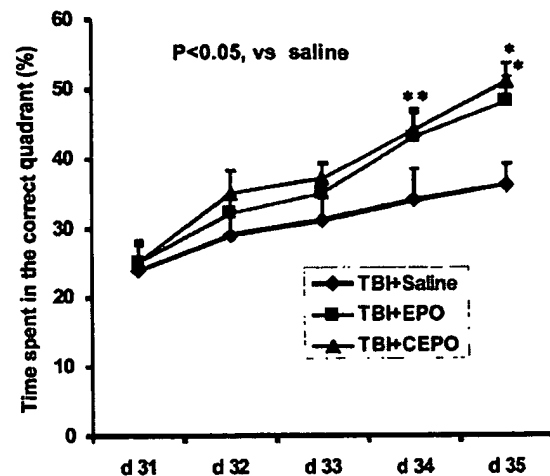


FIG. 1. Plots showing the temporal profile of the percentage of time spent (mean \pm standard deviation) in the correct quadrant of the water maze in rats with EPO and CEPO treatment at 6 (upper) and 24 hours (lower) after TBI. The percentage of time spent in the correct quadrant was significantly higher ($p < 0.05$) in the animals that received either EPO or CEPO compared with the controls. Asterisks denote significant probability values for EPO- or CEPO-treated groups compared with the saline-treated group. d = day.

research showed that EPO receptors are expressed in many areas of the brain,⁶ including the cortex, hippocampus, mid-brain, and endothelial cells. It also became evident that ischemia increased EPO expression in the brain,^{1,22} suggesting a physiological role for this molecule.

With the identification of neuroprotective properties of EPO,^{2,18} attempts were made to develop synthetic derivatives of this agent that possess its tissue-protective properties but are devoid of its hematopoietic effects.¹¹ This led to the development of CEPO. The plasma pharmacokinetic parameters for CEPO are in the same range as EPO, and its distribution into cerebrospinal fluid is equivalent to that of EPO. Our data demonstrate that EPO and CEPO have comparable efficacy in improving spatial memory after TBI. We also found that EPO and CEPO have comparable effi-



FIG. 2. Photomicrographs showing the fluorescent staining for BrdU to identify the newly generated cells (arrows) in the dentate gyrus of the ipsilateral hemispheres of the saline-treated (a), EPO-treated (b), and CEPO-treated (c) rats 24 hours after TBI. Bar = 50 μ .

cacy in promoting endogenous cellular proliferation in the dentate gyrus. We selected dentate gyrus for cellular analysis because of the important role it plays in spatial learning, and because EPO has been shown to induce cellular proliferation in this tissue.¹⁶ These effects on cellular proliferation may well be responsible for enhancement of spatial learning. We also investigated the effect of EPO and CEPO on the expression of BDNF. Neurotrophic factors are essential for neural regeneration and repair after a host of neurological insults.¹⁴ Studies of cerebral ischemia have shown induction of BDNF after EPO treatment.²⁸ Our data show that both EPO and CEPO increase the production of BDNF in the injured brain.

In addition to promoting regeneration of new cells, EPO derivatives can also exert a neuroprotective effect by more than one mechanism, and thereby enhance the survival of existing neurons. Because EPO has a well-known antiapoptotic action on the erythroid precursors in the bone marrow, it is intuitive to hypothesize that it has similar effects on the neurons.¹⁸ Investigations have been conducted in ischemia studies to evaluate whether the apoptotic effect of EPO is mediated via the BCL-2 family of antiapoptotic proteins. This agent has been shown to upregulate BCL-XL mRNA and protein expression in cultured neurons,⁸ and in vivo infusion of EPO in ischemic gerbils caused increased expression of BCL-XL mRNA and protein in the hippocampus.²⁹

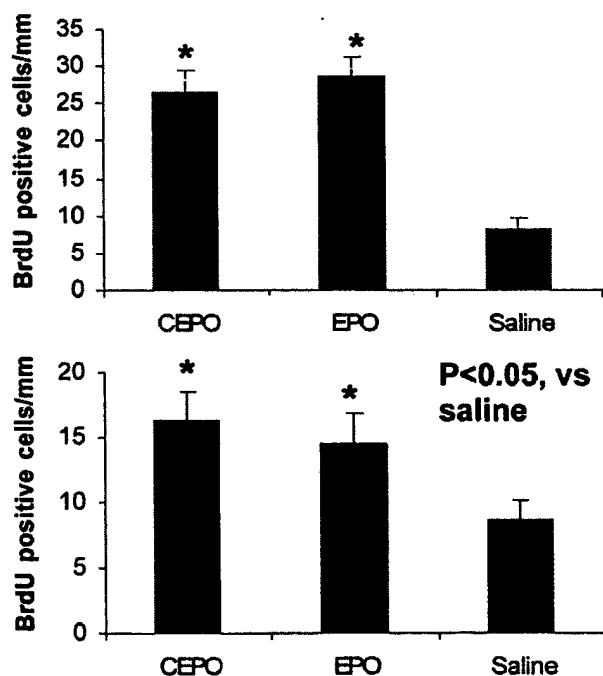


FIG. 3. Bar graphs showing the density of BrdU-labeled cells in the dentate gyrus of rats with EPO and CEPO treatment administered at 6 (upper) and 24 (lower) hours after TBI. Asterisks denote significant probability values for EPO- and CEPO-treated groups compared with the saline-treated group.

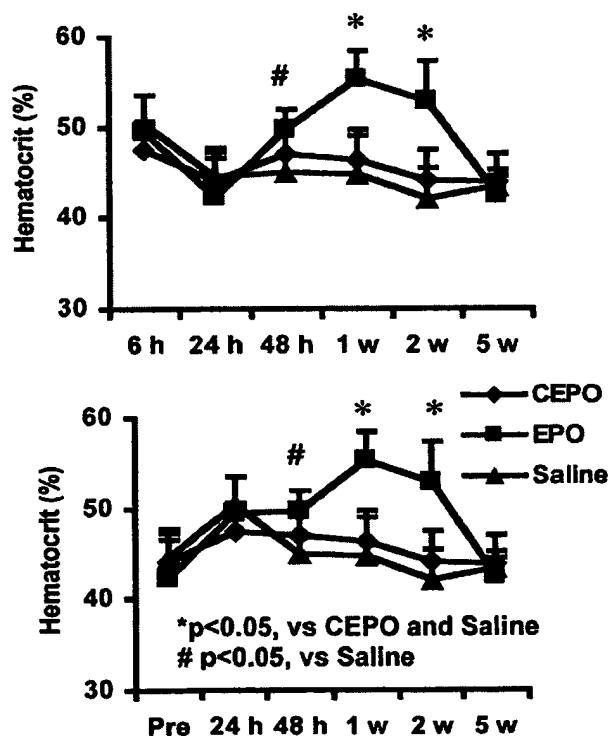


FIG. 4. Plots showing the temporal profile of systemic hematocrit in rats with EPO and CEPO treatment administered at 6 (upper) and 24 (lower) hours after TBI. See lower panel for explanation of symbols. h = hours; pre = pretreatment; w = weeks.

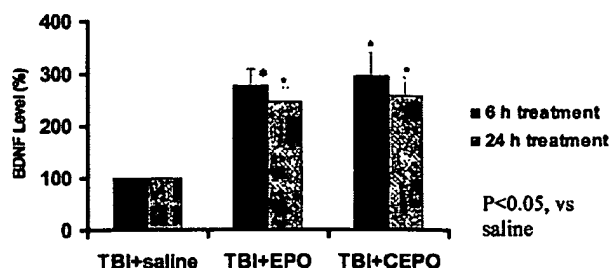


FIG. 5. Bar graph showing the BDNF levels in the ipsilateral hemisphere in rats with EPO and CEPO treatment administered at 6 and 24 hours after TBI. Asterisks denote significant probability values for EPO- and CEPO-treated groups compared with the saline-treated group.

It is also known that EPO increases intracellular calcium in neuronal cells,¹⁸ which in turn leads to a sustained increase in neuronal nitric oxide production. Nitric oxide inhibits caspase functions, which are mediators of apoptosis.¹² This increase in intracellular calcium may also block glutamate-induced neurotoxicity.¹⁹ Erythropoietin may also upregulate enzymes that scavenge oxygen radicals as well as downregulate enzymes that consume large amounts of adenosine triphosphate; for example, polyadenosine ribose polymerase.^{12,18} In addition to reducing neuronal loss by inhibiting apoptosis, EPO provides neuroprotection by reducing the inflammatory response following brain injury.²⁷ (The inflammatory response following brain injury significantly augments the neuronal damage.) In the focal cerebral ischemia model in rats, exogenous administration of EPO markedly reduced the influx of inflammatory cells into the injury zone, thereby attenuating the production of proinflammatory cytokines, subsequently resulting in a much smaller volume of injury.

Conclusions

Although the detailed mechanisms by which EPO and its derivative molecules promote neural recovery remain to be fully defined, molecules that retain the neuroprotective properties of EPO but separate the hematopoietic effects may be desirable as potential therapies for TBI. Nevertheless, the designation of a preferred agent must await the outcome of clinical studies aimed at defining the optimal dose as well as investigating the efficacy and safety of these molecules in the targeted patient populations.

References

- Bernaudo M, Marti HH, Roussel S, Divoux D, Nouvelot A, MacKenzie ET, et al: A potential role for erythropoietin in focal permanent cerebral ischemia in mice. *J Cereb Blood Flow Metab* 19:643–651, 1999
- Brines ML, Ghezzi P, Keenan S, Agnello D, de Lanerolle N, Ceram C, et al: Erythropoietin crosses the blood-brain barrier to protect against experimental brain injury. *Proc Natl Acad Sci U S A* 97:10526–10531, 2000
- Brustle O, Jones KN, Learish RD, Karram K, Choudhary K, Wiestler OD, et al: Embryonic stem cell-derived glial precursors: a source of myelinating transplants. *Science* 285:754–756, 1999
- Day LB, Schallert T: Anticholinergic effects on acquisition of place learning in the Morris water task: spatial mapping deficit or inability to inhibit nonplace strategies? *Behav Neurosci* 110:998–1005, 1996
- Day LB, Weisand M, Sutherland RJ, Schallert T: The hippocampus is not necessary for a place response but may be necessary for place learning. *Behav Neurosci* 113:914–924, 1999
- Digicaylioglu M, Bichet S, Marti HH, Wenger RH, Rivas LA, Bauer C, et al: Localization of specific erythropoietin binding sites in defined areas of the mouse brain. *Proc Natl Acad Sci U S A* 92:3717–3720, 1995
- Dixon CE, Clifton GL, Lighthall JW, Yaghmai AA, Hayes RL: A controlled cortical impact model of traumatic brain injury in the rat. *J Neurosci Methods* 39:253–262, 1991
- Jumbe NL: Erythropoietic agents as neurotherapeutic agents: what barriers exist? *Oncology* 16 (9 Suppl):91–107, 2002
- Konishi Y, Chui DH, Hirose H, Kunishita T, Tabira T: Trophic effect of erythropoietin and other hematopoietic factors on central cholinergic neurons in vitro and in vivo. *Brain Res* 609:29–35, 1993
- Koshimura K, Murakami Y, Sohmiya M, Tanaka J, Kato Y: Effects of erythropoietin on neuronal activity. *J Neurochem* 72:2565–2572, 1999
- Leist M, Ghezzi P, Grasso G, Bianchi R, Villa P, Fratelli M, et al: Derivatives of erythropoietin that are tissue protective but not erythropoietic. *Science* 305:239–242, 2004
- Lipton P: Ischemic cell death in brain neurons. *Physiol Rev* 79:1431–1568, 1999
- Lu D, Goussev A, Chen J, Pannu P, Li Y, Mahmood A, et al: Atorvastatin reduces neurological deficit and increases synaptogenesis, angiogenesis and neuronal survival in rats subjected to traumatic brain injury. *J Neurotrauma* 21:21–32, 2004
- Lu D, Mahmood A, Chopp M: Biological transplantation and neurotrophin-induced neuroplasticity after traumatic brain injury. *J Head Trauma Rehabil* 18:357–376, 2003
- Lu D, Mahmood A, Goussev A, Schallert T, Qu C, Zhang ZG, et al: Atorvastatin reduction of intravascular thrombosis, increase in cerebral microvascular patency and integrity, and enhancement of spatial learning in rats subjected to traumatic brain injury. *J Neurosurg* 101:813–821, 2004
- Lu D, Mahmood A, Qu C, Goussev A, Schallert T, Chopp M: Erythropoietin enhances neurogenesis and restores spatial memory in rats after traumatic brain injury. *J Neurotrauma* 22:1011–1017, 2005
- Mahmood A, Lu D, Qu C, Goussev A, Chopp M: Treatment of traumatic brain injury with a combination therapy of marrow stromal cells and atorvastatin in rats. *Neurosurgery* 60:546–554, 2007
- Marti HH, Bernaudin M, Petit E, Bauer C: Neuroprotection and angiogenesis: Dual role of erythropoietin in brain ischemia. *News Physiol Sci* 15:225–229, 2000
- Morishita E, Masuda S, Nagao M, Yasuda Y, Sasaki R: Erythropoietin receptor is expressed in rat hippocampal and cerebral cortical neurons, and erythropoietin prevents in vitro glutamate-induced neuronal death. *Neuroscience* 76:105–116, 1997
- Narayan RK, Michel ME, Ansell B, Baethmann A, Biegon A, Bracken MB, et al: Clinical trials in head injury. *J Neurotrauma* 19:503–557, 2002
- Postmantur R, Kampfl A, Siman R, Liu J, Zhao X, Clifton GL, et al: A calpain inhibitor attenuates cortical cytoskeletal protein loss after experimental traumatic brain injury in the rat. *Neuroscience* 77:875–888, 1997
- Sadamoto Y, Igase K, Sakanaka M, Sato K, Otsuka H, Sakaki S, et al: Erythropoietin prevents place navigation disability and cortical infarction in rats with permanent occlusion of the middle cerebral artery. *Biochem Biophys Res Commun* 253:26–32, 1998
- Sakanaka M, Wen TC, Matsuda S, Masuda S, Morishita E, Nagao M, et al: In vivo evidence that erythropoietin protects neu-

Erythropoietin derivatives for traumatic brain injury

- rons from ischemic damage. *Proc Natl Acad Sci U S A* 95: 4635–4640, 1998
24. Sasaki R, Masuda S, Nagao M: Pleiotropic functions and tissue-specific expression of erythropoietin. *News Physiol Sci* 16: 110–113, 2001
25. Tan CC, Eckardt KU, Firth JD, Ratcliffe PJ: Feedback modulation of renal and hepatic erythropoietin mRNA in response to graded anemia and hypoxia. *Am J Physiol* 263:F474–F481, 1992
26. Vescovi AL, Gritti A, Galli R, Parati EA: Isolation and intracerebral grafting of nontransformed multipotential embryonic human CNS stem cells. *J Neurotrauma* 16:689–693, 1999
27. Villa P, Bigini P, Mennini T, Agnello D, Laragione T, Cagnotto A, et al: Erythropoietin selectively attenuates cytokine production and inflammation in cerebral ischemia by targeting neuronal apoptosis. *J Exp Med* 198:971–975, 2003
28. Wang L, Zhang Z, Wang Y, Zhang R, Chopp M: Treatment of stroke with erythropoietin enhances neurogenesis and angiogenesis and improves neurological function in rats. *Stroke* 35: 1732–1737, 2004
29. Wen TC, Sadamoto Y, Tanaka J, Zhu PX, Nakata K, Ma YJ, et al: Erythropoietin protects neurons against chemical hypoxia and cerebral ischemic injury by up-regulating Bcl-xL expression. *J Neurosci Res* 67:795–803, 2002

Manuscript submitted September 1, 2006.

Accepted January 26, 2007.

This work was supported by National Institutes of Health R01 Grant No. NS042259 and PO1 Grant No. NS042345.

Address reprint requests to: Asim Mahmood, M.D., Department of Neurosurgery, Henry Ford Hospital, 2799 West Grand Boulevard, Detroit, Michigan 48202. email: nsaam@neuro.hfh.edu.

Nonhematopoietic Erythropoietin Derivatives Prevent Motoneuron Degeneration In Vitro and In Vivo

Tiziana Mennini,¹ Massimiliano De Paola,¹ Paolo Bigini,¹ Cristina Mastrotto,¹ Elena Fumagalli,¹ Sara Barbera,¹ Manuela Mengozzi,¹ Barbara Viviani,² Emanuela Corsini,² Marina Marinovich,² Lars Torup,³ Johan Van Beek,⁴ Marcel Leist,⁵ Michael Brines,⁶ Antony Cerami,⁶ and Pietro Ghezzi^{1,6}

¹Department of Molecular Biochemistry and Pharmacology, "Mario Negri" Institute for Pharmacological Research, Milan, Italy;

²Laboratory of Toxicology and Centre of Excellence of Neurodegenerative Diseases, Department of Pharmacological Sciences, University of Milan, Italy; ³Department of Neuropharmacology and ⁴Department of Disease Biology, H. Lundbeck A/S, Valby-Copenhagen, Denmark;

⁵Faculty of Biology, University of Konstanz, Germany; ⁶The Kenneth S. Warren Institute, Kitchawan, NY, USA.

Chronic treatment with asialo erythropoietin (ASIALO-EPO) or carbamylated erythropoietin (CEPO) improved motor behavior and reduced motoneuron loss and astrocyte and microglia activation in the cervical spinal cord of wobbler mice, an animal model of amyotrophic lateral sclerosis, but had no effect on hematocrit values. ASIALO-EPO and CEPO, like the parent compound EPO, protected primary motoneuron cultures from kainate-induced death in vitro. Both EPO receptor and the common CD131 β chain were expressed in cultured motoneurons and in the anterior horn of wobbler mice spinal cord. Our results strongly support a role for the common β chain CD131 in the protective effect of EPO derivatives on motoneuron degeneration. Thus CEPO, which does not bind to the classical homodimeric EPO receptor and is devoid of hematopoietic activity, could be effective in chronic treatment aimed at reducing motoneuron degeneration.

Online address: <http://www.molmed.org>

doi: 10.2119/2006-00045.Mennini

INTRODUCTION

Amyotrophic lateral sclerosis (ALS) is a degenerative disease of the upper and lower motoneurons leading to progressive motor dysfunction and death within 3 to 5 years from diagnosis (1). At present, the only drug approved by U.S. Federal Drug Administration for treatment of ALS patients is riluzole, which slightly prolongs patients' survival without clear effects on neurological symptoms (2,3). Thus the search for new therapeutic agents is greatly encouraged.

Erythropoietin (EPO), a hematopoietic growth factor, is neuroprotective in different models of neurodegenerative disease, including experimental autoimmune encephalomyelitis (EAE) (4,5), cerebral ischemia (6), and diabetic neuropathy (7). Its mechanism of action is not completely understood: in addition

to its anti-apoptotic effect (6) EPO inhibits CNS inflammation (4,8), enhances neurogenesis in animal models of stroke and EAE (9,10), and augments BDNF expression in vivo and in vitro (9,11).

We have previously reported that in vitro EPO protects cultured motoneurons from serum-BDNF deprivation or long-term kainate exposure (6). The latter is a model of chronic excitotoxicity, used for in vitro studies because motoneurons are selectively vulnerable to activation of the AMPA receptor (12).

Because chronic administration of EPO results in an increase of the hematocrit—which could have undesirable effects, for instance by increasing the risk of thrombosis—different nonerythropoietic molecules derived from EPO have been designed that retain the neuroprotective activities of EPO. One of these molecules,

carbamylated EPO (CEPO), has proven effective in animal models of stroke, EAE, spinal cord injury, and diabetic neuropathy (13). Unlike EPO, CEPO does not bind the classical homodimeric EPO receptor (EPOR) (13), and its neuroprotective action appears to require the common β chain of IL-3/IL-5/GM-CSF receptor (also known as CD131) (14), which can functionally associate with EPOR (15). Another nonerythropoietic EPO derivative is asialo erythropoietin (ASIALO-EPO), which, although it binds to the classic homodimeric EPOR, has a short half-life in vivo and does not increase the hematocrit (an activity that requires persistent circulating levels of EPO) but also retains neuroprotective activities in vivo (16).

In the present study, we extended the in vitro studies on motoneuron cultures to ASIALO-EPO and CEPO, and tested the effect of treatment in an animal model of ALS, the wobbler mouse (17). The wobbler mouse carries a mutation of *Vps54* (18), a gene encoding for a vacuolar-vesicular protein-sorting fac-

Address correspondence and reprint requests to Tiziana Mennini, Mario Negri Institute for Pharmacological Research, Via Eritrea 62, 20157 Milan, Italy. Phone: +390239014402; fax: +39023546277; e-mail: tiziana@marionegri.it

Submitted June 16, 2006; accepted for publication July 13, 2006.

tor involved in vesicular trafficking, and is sensitive to treatments with riluzole (19) or neurotrophins such as BDNF (20), and thus is a useful animal model to test the effect of EPO analogs. The results suggest the possible *in vivo* relevance of the protective effect of EPO derivatives in preventing motoneuron degeneration.

MATERIALS AND METHODS

Materials

Brain-derived neurotrophic factor (BDNF) was a kind gift of Amgen (Thousand Oaks, CA, USA). Neurobasal medium, B27 supplement, and horse serum were obtained from Life Technologies, Gibco (Milan, Italy); glutamine from Seromed (Milan, Italy); and trypsin, bovine serum albumin, and poly-DL-ornithine from Sigma (Milan, Italy). Anti-nonphosphorylated neurofilament monoclonal antibody (SMI 32) was obtained from Sternberger Monoclonals (MD, USA); anti-IL-3/R β (sc 679) polyclonal antibody (raised against a peptide mapping at the N-terminus of the mouse IL-3 receptor β chain), anti-EPOR polyclonal antibody (sc-5624, against the N-terminus residue of human EPOR), and the sc-679 blocking peptide were obtained from Santa Cruz Biotechnology (CA, USA). Kainate was obtained from Tocris (Milan, Italy), and DPX mountant from BDH Laboratory. Vectastain ABC kit was obtained from Vector Laboratories (Burlingame, CA, USA). Recombinant human (rh) EPO was obtained from Ortho Biotech (Raritan, NJ, USA); rhCEPO and rhASIALO-EPO were synthesized as described earlier (13,16).

Animal Experiments

Procedures involving animals were conducted in conformity with the institutional guidelines that comply with national (D.L. no. 116) and international (EEC Council Directive 86/609; NIH Guide for the Care and Use of Laboratory Animals) laws and policies.

Homozygous wobbler mice and healthy littermates (NFR/wr strain; NIH,

Animal Resources, Bethesda, MD, USA) were bred at Charles River Italia (Calco, Lecco, Italy). At arrival, the animals were housed in group cages containing 2 to 3 wobbler and 2 to 3 control mice under standard conditions ($22 \pm 1^\circ\text{C}$, 60% relative humidity, 12-h light/dark schedule) had free access to food (Altromin, MT, Rieper) and water. Mice with heavy motor impairment had food available on the bottom of the cage and water bottles with long drinking spouts. After clear diagnosis of disease at 3 weeks of age based on phenotype analysis, wobbler mice and healthy littermates (control mice) were randomly assigned to the experimental groups, and treated intraperitoneally with EPO, ASIALO-EPO, CEPO (32 $\mu\text{g/kg}$) or vehicle (6.4 mL/kg) 3 times a week, until 12 weeks of age.

To evaluate the clinical worsening of wobbler mice, the following behavioral evaluations were done weekly by an operator that was blinded to treatments:

1. Paw and walking abnormality: Both the paw abnormality and the walking abnormality tests are observational. The operator assigns a score to these parameters, scaled from 0 to 4, on the basis of the severity of abnormalities. The paw position is graded as follows: 0, normal; 1, retracted digits; 2, curled digits; 3, curled wrists; 4, forelimb flexed to body. The walking pattern is graded as follows: 0, normal; 1, trembling (tremor without gait disturbance); 2, wobbling (gait disturbance); 3, curled-paw walking; 4, jaw walking (no use of front paw).
- 2) Running speed: Mice run over an inclined platform (75 cm long ramp inclined at one end to a height of 13 cm) stimulated with a gentle pressure on the tail (adverse stimulus). The running time is defined as the shorter time to reach the top of the platform from the bottom. Healthy mice rapidly improve their performances on the test until they reach the top of the platform in few seconds (1 to 3 s). On the contrary, wobbler mice need a longer time to reach the top of the platform. More-

over, these animals show a marked worsening of their performances due to the progressive muscular atrophy in the forelegs.

- 3) Grip strength: Mice are lifted by the tail and allowed to grasp with both forelegs to a horizontal bar, which is connected to a mechano-electric transducer (Basile). The grip strength of the front paws is measured at the point when the mouse releases the horizontal bar as a result of a gentle traction applied by the operator. Healthy mice can record values higher than 100 g, whereas values recorded by wobbler mice are very low (< 20 g) and drastically reduced during symptom progression. When animals are no longer able to grip the bar, grip strength is recorded as 0 g. Values of grip strength were normalized by dividing each value by body weight to control for weight differences between wobbler and healthy mice.

Because wobbler mice develop early and severe atrophy of forelegs without a clear impairment of hindleg muscles, the classical rota-rod test cannot be considered a reliable tool to evaluate the clinical progression in these mice.

At the end of treatment, 3 days after the last injection, half of the mice for each experimental group were killed by transcardiac perfusion with 4% paraformaldehyde in PBS, under deep anesthesia with chloral hydrate (intraperitoneal). Immediately after perfusion, biceps muscles, brain, and spinal cord were rapidly dissected and post-fixed for 4 h in the same fixative (4°C). All the tissues were dehydrated and cryoprotected with serial steps in 10%, 20%, and 30% sucrose in PBS 0.1 M, pH 7.4, at 4°C until they sank, frozen in *n*-pentane at -45°C , and stored at -80°C until analysis.

The other mice were killed by decapitation. Brain and cervical spinal cord were rapidly dissected, frozen on dry ice, and stored at -80°C until analysis.

A few drops of blood were collected for hematocrit determination. For each

sample, triplicate values were recorded and the mean value used for statistical analysis.

Nissl Staining

For Nissl staining, cryostatic sections of cervical spinal cord (C2 to C6) were serially cut (30 μ m thickness) and placed on gelatin-coated glass slides. Every third section was stained with 0.5% Cresyl violet, dehydrated through graded alcohols (70%, 95%, 100%, twice), placed in xylene, and coverslipped with DPX mountant (BDH Laboratory, Poole, UK) for light microscopy analysis. Motoneurons were identified based on their localization in lamina IX of the ventral horns and their large cell body size (> 30 μ m). For all experimental groups, at least 50 sections of cervical spinal cord were evaluated for each animal; healthy motoneurons were counted in 1 side of each section. The mean of motoneuron number was calculated for each animal, and the values obtained were used for statistical analysis. The counting of Nissl-stained motoneurons was carried out by the same operator in a blinded fashion.

Immunohistochemistry for GFAP and CD11b

Sections were stained based on the avidin-biotin-peroxidase technique. Specimens were incubated in 0.3% hydrogen peroxide for 30 min to block endogenous peroxidase. Sections were then exposed to primary antibodies diluted in blocking solution overnight at 4 °C, incubated with an appropriate biotinylated secondary antibody, processed with a Vectastain ABC kit, and developed using DAB. In all immunohistochemistry protocols, negative controls were performed by omitting the primary antibody, and this always resulted in minimal detected signal. The following antibodies were used: rabbit anti-bovine GFAP (1:4000; #Z 0334; Dako) and rat anti-mouse CD11b (1:10; clone 5C6; #MCA711; Serotec).

Motoneuron Cultures

Dissociated anterior horn cultures were obtained from the ventral horn of

spinal cord of 15-day Sprague-Dawley rat embryos (Charles River, Calco, Italy) as previously described (6,21). Cell death was induced on the 6th day of culture by incubation for 48 h with kainate (5 μ M). EPO or other cytokines (2.5 pmol/mL) or vehicle were added to the cultures 72 h before induction of cell death, and treatment continued for the 48-h exposure to glutamate agonists. After incubation with excitotoxins, the medium was discarded and the motoneurons were stained for nonphosphorylated neurofilaments (SMI 32) to assess their survival. Only the cells that were SMI 32 positive, with a good morphology, large somata, and well conserved axons, were counted across 4 sides of the coverslip.

Immunocytochemistry

Cells were fixed with paraformaldehyde 4% (wt/vol) in PBS for 40 min, permeabilized with Triton X-100 (0.2%) for 30 min, and blocked with FCS 10% (vol/vol) in PBS.

The incubation with primary antibodies (SMI 32, 1:9000; EPOR, 1:500) was carried out overnight in blocking solution at 4 °C.

Cells were washed; appropriate biotinylated secondary antibody (1:200), avidin, and biotinylated horseradish peroxidase macromolecular complex were added; and diaminobenzidine and H₂O₂ (6 mL/10 mL) were used to visualize the positive cells.

RT-PCR

To measure EPO and EPOR expression in mouse cervical spinal cords, 2 μ g total RNA, extracted by Trizol (Invitrogen, Carlsbad, CA, USA), were reverse transcribed using the M-MLV reverse transcriptase enzyme (Invitrogen), and aliquots corresponding to 1/25 of the cDNA obtained were amplified by real-time PCR using the TaqMan gene expression assays for mouse EPO and EPOR and mouse β actin as housekeeping gene (Applied Biosystems, Foster City, CA, USA). All procedures were performed on the ABI PRISM 5700 Sequence Detection System (Applied Biosystems).

RESULTS

Studies In Vitro on Motoneuron Cultures

Figure 1 shows the effect of EPO (2.5 pmol/mL) on SMI 32-positive motoneurons in mixed neuron/glia cultures. Under basal conditions, 5-day treatment with EPO produced a clear neurotrophic effect, increasing the neurite outgrowth and the number and differentiation of motoneurons (Figure 1B). A similar effect was obtained in purified motoneurons (6) and was related to a decrease in spontaneous apoptosis, as judged from the reduction of the percentage of apoptotic nuclei and of the number of activated caspase 3- and 9-positive cells below control values (data not shown).

Under the same experimental schedule (3 days of pre-incubation followed by 48-h coincubation with kainate), EPO was also neuroprotective against kainate (5 μ M) (Figure 1D). The effect of EPO was dose related between 0.25 and 2.5 pmol/mL (the dose that provided full protection), with ED₅₀ about 1.25 pmol/mL.

The viability of motoneurons in mixed neuron/glia cultures was reduced by about 50% after treatment with 5 μ M kainate and returned to control values (101 \pm 35) in cells treated with 2.5 pmol/mL EPO (Figure 2A). The basal survival was increased above control values (128 \pm 38), confirming the neurotrophic effect of EPO (Figure 2A). The same EPO concentration protected motoneurons from kainate toxicity even if added simultaneously with kainate (without preincubation) (Figure 2C) or if present only during the 72-h pretreatment (Figure 2B). However, the maximum protective effect was obtained when EPO was present both in pretreatment and during kainate exposure.

We tested different nonerythropoietic derivatives, including ASIALO-EPO, which has high affinity for the EPORs, and CEPO, which does not bind to the classical homodimeric EPOR. Table 1 shows that both ASIALO-EPO and CEPO, tested at equimolar concentra-

tions under the same treatment schedule used for EPO, were active in preventing kainate-induced motoneuron death.

Immunoreactive EPORs were present in all cell populations of mixed neuron/glia cultures (Figure 3A) and in purified motoneurons (Figure 3C, D) and were not modified after treatment with kainate (not shown). The staining was present on cell bodies and arborizations, and seemed to be located both in the membrane and in the cytosol. To assess if repeated EPO treatments modify the expression or the distribution of EPORs on motoneurons, purified cultures were treated with EPO (2.5 pmol/mL) for 5 days. The staining revealed no difference in the intensity and distribution of EPORs in EPO-treated cells compared with vehicle-treated cells (not shown), indicating that EPO, in the experimental conditions tested, did not down- or up-regulate EPOR.

The common β receptor (CD 131) showed similar localization.

Studies In Vivo In Wobbler Mice

In a preliminary experiment, EPO, given to wobbler mice intraperitoneally at 32 μ g/kg 3 times a wk for 6 weeks, markedly increased hematocrit ($67 \pm 4\%$ and $46 \pm 2.5\%$ in EPO and vehicle, respectively, $P < 0.01$). This effect could worsen health conditions in the mice, thus interfering with the correct evaluation of motor behavior in treated mice. Thus, a pilot experiment was done to test the possibility that treatment with EPO analogs could be effective in wobbler disease. Four wobbler and 4 control mice were treated with CEPO, and their behavior was recorded as described in Materials and Methods section. The evaluation of the results (ANOVA) indicated a significant effect of treatment ($P < 0.001$) on all the behavioral tests, although the

post-hoc tests did not reach statistical significance due to the low number of animals. On the basis of these results, we planned the second experiment using 10 animals in each experimental group.

Figure 4 shows that CEPO treatment significantly improves motor behavior, in particular in the grip strength and the running time tests, in wobbler mice over the time of observation. The behavioral effect was consistent with the reduction

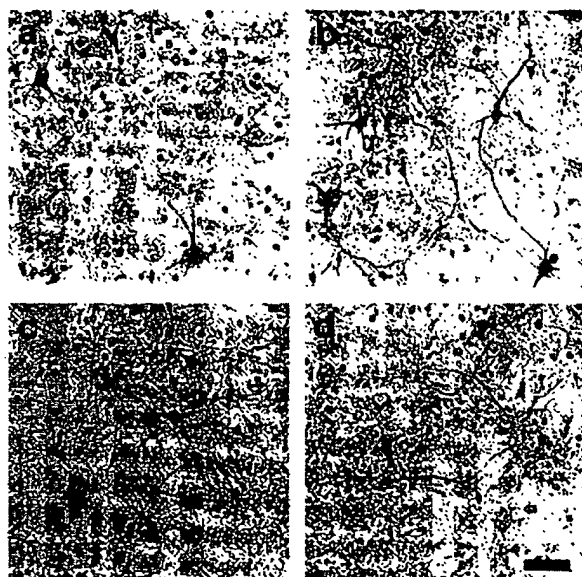


Figure 1. Neurotrophic and neuroprotective effect of EPO on SMI 32-positive motoneurons in mixed neuron/glia cultures. (A) Motoneurons in control cultures, well defined morphologically. (B) Control cultures 5 days after administration of EPO (2.5 pmol/mL) alone: large cell bodies with long axons and an increase of cell number can be seen. (C) Cultures treated for 48 h with 5 μ M kainate. (D) Effect of EPO (added 3 days before and during kainate exposure) on cultures treated with kainate. Motoneurons were stained using an anti-nonphosphorylated neurofilament monoclonal antibody (SMI 32) as described in Materials and Methods. Scale bar = 100 μ m.

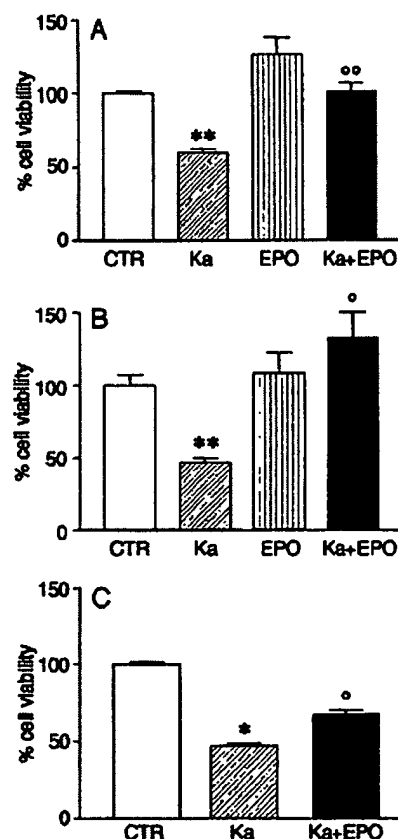


Figure 2. Effects of EPO against toxicity induced by kainate. Viability of SMI 32-positive motoneurons in mixed neuron/glia cultures after 48-h incubation with kainate (5 μ M). When present, EPO (2.5 pmol/mL) was added simultaneously with the glutamate agonists (B), 3 days before treatment (C), or both (A). Data represent mean \pm SD of 12 replications. * $P < 0.05$, ** $P < 0.01$, different from controls; ° $P < 0.05$, different from kainate + EPO.

Table 1. Effect of kainate treatment on motoneuron viability in the absence or presence of EPO derivatives.

Motoneuron survival (% of controls)		
(No. replicates)	Without cytokine	With cytokine
ASIALO-EPO (12)	58 ± 11	91 ± 12 ^a
CEPO (15)	42 ± 12	67 ± 19 ^b

Viability of SMI 32-positive motoneurons in mixed neuron/glia cultures after 48-h incubation with kainate (5 μ M). When present, cytokines (100 ng/mL) were added to motoneuron cultures 3 days before treatment and re-added with the glutamate agonist. Data represent mean \pm SD. For both ASIALO-EPO and CEPO, *flint* $P < 0.001$. ^a $P < 0.001$, ^b $P > 0.01$, different from control motoneurons, 2-way ANOVA and Tukey's test.

in motoneuron loss in the wobbler mice treated with CEPO compared with vehicle (Table 2).

Wobbler mice treated with ASIALO-EPO also performed better than control mice in behavioral tests (Figure 4), particularly in the first part of the treatment, because the effect decreased over time. No significant effect of ASIALO-EPO was found on motoneuron loss (Table 2): only 2 of the 5 animals tested for Nissl staining had motoneuron number higher than 5 (the highest mean of vehicle-treated wobbler mice). These 2 mice also had the highest scores in behavioral tests, compared with the other 3 mice of the ASIALO-EPO group, thus confirming the correlation between motoneuron number and behavior.

CEPO and ASIALO-EPO did not increase hematocrit in treated mice; on the contrary, mice became anemic after 5 to 6 weeks of treatment, possibly owing to the production of antibodies against the EPO induced by the human recombinant proteins (hematocrit measured after 8 weeks of treatment: vehicle: $47 \pm 5\%$; CEPO: $19 \pm 3\%$; ASIALO-EPO: $21 \pm 5\%$, both $P < 0.01$). However, the mice, although anemic, did not lose body weight

and did not appear to suffer during the treatment, at least within the period covered by this experiment (8 weeks); more important, this effect is not likely to occur in humans.

Astroglia and microglia were activated in the cervical spinal cord of wobbler mice compared with controls. Treatment with CEPO or ASIALO-EPO reduced both astroglial and microglial activation in cervical spinal cord of wobbler mice (Figure 5). This reduced inflammation might be important in the neuroprotective effects and neurological benefits observed after CEPO and ASIALO-EPO treatment in wobbler mice.

The levels of endogenous EPO and EPOR, measured in cervical spinal cord of wobbler mice at the age of 6, 10, and 12 weeks, were not different from those found in healthy littermates (not shown).

The pattern of EPOR staining in the cervical region of healthy mice (Figure 6A) reveals a high immunoreactivity in the large-sized neurons of the anterior horn of spinal cord, mainly localized in neuronal cell bodies. Chronic treatment with EPO or its derivatives did not modify the pattern and intensity of staining (not

shown). In contrast, cervical sections from wobbler mice (Figure 6B) showed a reduced number of neurons having a strong immunoreactivity for EPOR and a parallel increase of staining in thin structures close to the ventral area. This may be due to the loss of motoneurons and the marked reactive gliosis occurring in the affected tissues.

Representative photographs showing immunostaining of the common β chain in the cervical spinal cord sections of healthy mice (Figure 6C) and wobbler mice (Figure 6D) show that the immunoreactivity is selective for neuronal cells, that almost all neurons are immunoreactive, and that the staining is more intense in the large-sized neurons of anterior horns. The selective expression of the common β chain in the cervical neurons is confirmed by the evidence that its loss of staining correlates with the marked loss of motoneurons, and the opposite effect of astrocyte and microglia proliferation observed in wobbler mice does not produce a parallel increase in immunoreactivity. No differences were observed after chronic treatment with EPO or its derivatives (not shown).

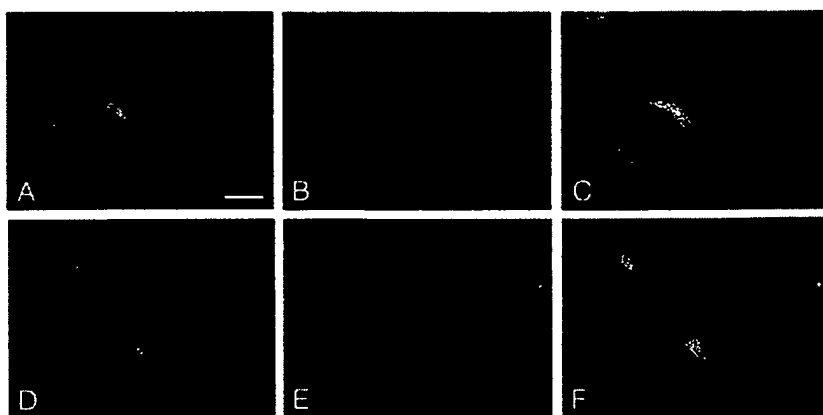


Figure 3. Motoneurons express EPO and CD131 receptors. Mixed neuron/glia cultures were double-stained with SMI32 (green, A, D) and with a specific antibody against EPOR (B) or the β chain common to IL-3, IL-5, and GM-CSF receptors (E). C and F represent the merged pictures. Coincubation with an excess of respective blocking peptides completely abolished the specific stain of anti-EPOR and anti-IL-3R β antibodies (not shown). Scale bar: 20 μ m.

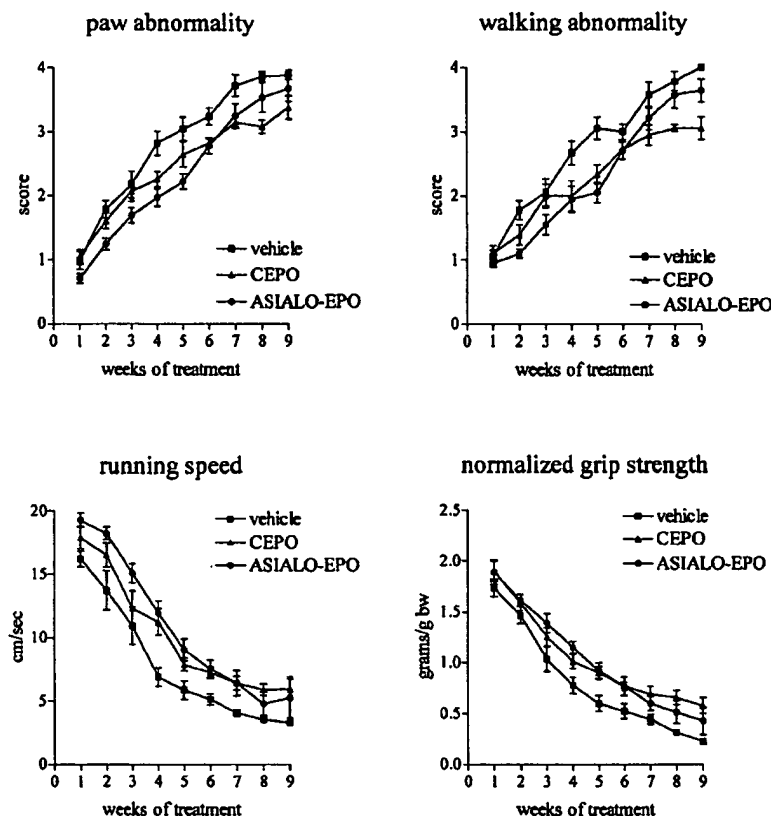


Figure 4. Behavioral scores of ASIALO-EPO and CEPO in wobbler mice. Drugs (32 μ g/kg) were given intraperitoneally 3 times a week starting from 4 weeks of age. ■, vehicle; ●, ASIALO-EPO; △, CEPO. Each point represents the mean \pm SD of 10 animals per group. Statistical analysis was done by 2-way ANOVA and showed significant effect of treatments ($P < 0.001$) for all the considered tests. CEPO and ASIALO-EPO effects were statistically different ($P < 0.05$) in the running time and grip strength tests.

DISCUSSION

The wobbler mouse, carrying a mutation of *Vps54* (18), is considered one of the most useful models for human motoneuron degenerative diseases, such as ALS and infantile spinal muscular atrophy (ISMA); unlike the transgenic mice carrying the human mutated form of *SOD1*, disease in the wobbler mouse is unrelated to the mutation responsible for a small proportion of the familial cases (22). An advantage of wobbler mice over the transgenic *SOD1* mice is that, in the wobbler mice, the disease has an early onset and rapid progression (17), thus allowing shorter treatments that can minimize the production of antibodies using

human recombinant proteins (like those tested in this study).

A preliminary experiment with 5-week EPO treatment in wobbler mice significantly increased the hematocrit. Because sustained high hematocrit causes endothelial damage and could increase susceptibility to vascular disease in mouse brain (23), in this study we tested the effect of 2 nonerythropoietic EPO analogs in wobbler motoneuron degeneration. Although not directly determined in this experiment, the hematocrit decrease observed in the 2 treatment groups likely arises from the formation of neutralizing antibodies that antagonize the effect of endogenous EPO. In other studies, we

have consistently observed this phenomenon, which appears after 3 to 4 weeks of dosing, and we have definitively proven the formation of neutralizing antibodies produced against the human proteins administered (unpublished data).

CEPO has pharmacokinetic features (half-life, peak concentration, CSF distribution) similar to those of EPO but does not bind to the classical homodimeric EPOR, and is therefore devoid of hematopoietic activity (13). A major advantage of CEPO over EPO is the possibility of subchronic and chronic dosing without affecting hematocrit; protective effects of CEPO have already been described for spinal cord compression, diabetic neuropathy, and experimental autoimmune encephalomyelitis (13). Consistent with these assumptions, we show here that wobbler mice treated with CEPO have improved motor behavior and reduced loss of motoneurons in their cervical spinal cord. CEPO treatment also reduced markers of astrocyte and microglia activation. The improved behavioral scores, particularly the running speed, are even more impressive considering the grossly reduced hematocrits in the 2 treatment groups.

Chronic treatment with ASIALO-EPO was also effective in improving motor behavior in wobbler mice, although the effect of ASIALO-EPO in reducing motoneuron loss was not significant when the total number of treated mice was considered, but shows a clear correlation within motoneuron number and behavior for each mouse.

Table 2. Motoneuron number in the cervical spinal cord of wobbler mice.

	Control mice (n=3)	Wobbler mice (n=5)
Vehicle	16.5 \pm 0.13	4.0 \pm 0.77
CEPO	16.3 \pm 0.05	7.8 \pm 0.23 ^a
ASIALO-EPO	16.3 \pm 0.10	4.95 \pm 1.37

Data are means \pm SD. ^a $P < 0.001$ vs. vehicle and ASIALO-EPO, ANOVA and Tukey's test.

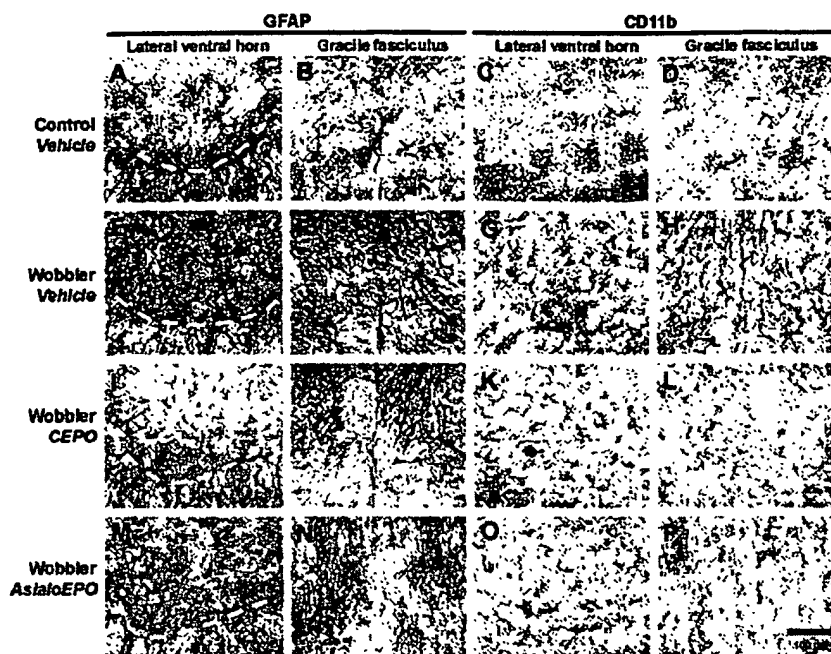


Figure 5. ASIALO-EPO and CEPO treatments both reduce the astroglial (GFAP) and microglial (CD11b) activation in cervical spinal cord of wobbler mice. Representative picture of GFAP and CD11b immunostaining in the cervical region of 12-week-old control (A-D) and wobbler (E-P) mice. Wobbler mice were treated with CEPO (I-L) or ASIALO-EPO (M-P) (32 μ g/kg intraperitoneally 3 times a week) or vehicle (E-H) starting from 4 weeks of age. Scale bar: 100 μ m.

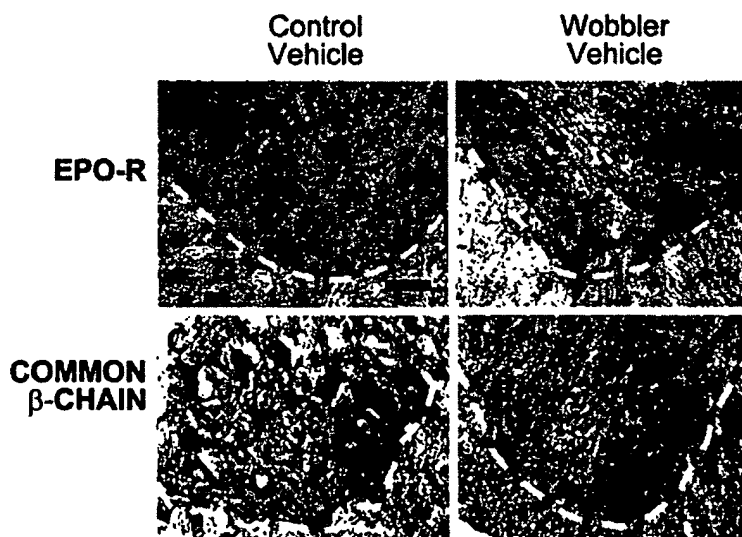


Figure 6. Motoneurons in spinal cord sections express EPO and CD131 receptors. Representative picture of EPO (A,B) and CD131 receptor (common β chain) (C,D) immunostaining in the cervical region of 12-week-old healthy (A,C) and wobbler (B,D) mice. Scale bar: 50 μ m.

When tested *in vitro*, CEPO, ASIALO-EPO, and EPO were equipotent in protecting primary cultured motoneurons from death induced by stimulation of AMPA receptors with kainate, suggesting that the differences observed after chronic *in vivo* treatment were possibly related to the short half-life of ASIALO-EPO.

The effect of ASIALO-EPO and CEPO on wobbler mice cannot be related to a decrease in endogenous EPO expression in affected mice, because wobbler mice have expression of EPO comparable to that of healthy mice. Also, the expression of EPOR in wobbler mice is not different from that in healthy mice and not modified by chronic treatment with EPO analogs.

EPO has been shown to induce mRNA expression and production of biologically active BDNF in primary hippocampal neurons *in vitro*, leading to neuroprotection (11), and *in vivo* in mouse models of EAE (10) and stroke (9). BDNF expression is significantly increased in the ventral spinal cord of wobbler mice, at both early and advanced stages of the disease (24), possibly related to a compensatory mechanism activated to counteract cell processes that were involved in motoneuron neurodegeneration. Treatment with exogenous BDNF (20), or enhancement of endogenous BDNF induced by riluzole treatment (19), significantly slowed neuronal degeneration and impairment of motor function in wobbler mice. However, no significant increase of BDNF mRNA was evident in ASIALO-EPO- and CEPO-injected mice (data not shown).

The neuroprotective effect of ASIALO-EPO and CEPO in the wobbler mice was accompanied by a reduction of reactive gliosis, as evaluated by GFAP and CD11b immunostaining. Thus it is possible that a decrease in inflammation, which is present in the degenerating tissue, contributes to the effect of the EPO analogs, as was suggested for cerebral ischemia (5) and EAE (2).

If protection of motoneurons can be obtained *in vitro* and *in vivo* with CEPO,

the neuroprotective effects we observed with EPO and ASIALO EPO should not be related only to the classic homodimeric EPO receptor.

We found that both EPOR and CD131 were expressed in cultured motoneurons, implicating CD131 in the specific cytoprotective signal transduction of EPO/CEPO. In wobbler mice, the expression and the localization of EPOR and CD131 were not different from those of healthy mice and were not modified by the treatment; thus, they could mediate the neuroprotective effect of administered EPO derivatives.

In conclusion, our study suggests that CEPO, and, to a lesser extent, ASIALO-EPO, could exert neuroprotective effects in a model of chronic motoneuron degeneration and reduce inflammation in the anterior horn of the spinal cord without increasing hematocrit levels. The mechanism by which these compounds act is still not fully clarified. The results indicate that these molecules could offer a potentially important therapeutic approach for ALS.

REFERENCES

- Rowland LP. (1998) Diagnosis of amyotrophic lateral sclerosis. *J. Neurol. Sci.* 160 Suppl 1:S6-24.
- Gordon PH. (2005) Advances in clinical trials for amyotrophic lateral sclerosis. *Curr. Neurol. Neurosci. Rep.* 5:48-54.
- Müller RC, Mitchell JD, Lyon M, Moore DH. (2003) Riluzole for amyotrophic lateral sclerosis (ALS)/motor neuron disease (MND). *Amyotroph. Lateral Scler. Other Motor Neuron Disord.* 4:191-206.
- Agnello D et al. (2002) Erythropoietin exerts an anti-inflammatory effect on the CNS in a model of experimental autoimmune encephalomyelitis. *Brain Res.* 952:128-34.
- Savino C et al. (2006) Delayed administration of erythropoietin and its non-erythropoietic derivatives ameliorates chronic murine autoimmune encephalomyelitis. *J. Neuroimmunol.* 172:27-37.
- Siren AL et al. (2001) Erythropoietin prevents neuronal apoptosis after cerebral ischemia and metabolic stress. *Proc. Natl. Acad. Sci. U. S. A.* 98:4044-9.
- Bianchi R et al. (2004) Erythropoietin both protects from and reverses experimental diabetic neuropathy. *Proc. Natl. Acad. Sci. U. S. A.* 101:823-8.
- Villa P et al. (2003) Erythropoietin selectively attenuates cytokine production and inflammation in cerebral ischemia by targeting neuronal apoptosis. *J. Exp. Med.* 198:971-5.
- Wang L, Zhang Z, Wang Y, Zhang R, Chopp M. (2004) Treatment of stroke with erythropoietin enhances neurogenesis and angiogenesis and improves neurological function in rats. *Stroke* 35:1732-7.
- Zhang J et al. (2005) Erythropoietin treatment improves neurological functional recovery in EAE mice. *Brain Res.* 1034:34-9.
- Viviani B et al. (2005) Erythropoietin protects primary hippocampal neurons increasing the expression of brain-derived neurotrophic factor. *J. Neurochem.* 93:412-21.
- Carriedo SG, Yin HZ, Weiss JH. (1996) Motor neurons are selectively vulnerable to AMPA/kainate receptor-mediated injury in vitro. *J. Neurosci.* 16:4069-79.
- Leist M et al. (2004) Derivatives of erythropoietin that are tissue protective but not erythropoietic. *Science* 305:239-42.
- Brines M et al. (2004) Erythropoietin mediates tissue protection through an erythropoietin and common beta-subunit heteroreceptor. *Proc. Natl. Acad. Sci. U. S. A.* 101:14907-12.
- Jubinsky PT, Krijanovski OI, Nathan DG, Tavernier J, Sieff CA. (1997) The beta chain of the interleukin-3 receptor functionally associates with the erythropoietin receptor. *Blood* 90:1867-73.
- Erbayraktar S et al. (2003) Asialoerythropoietin is a nonerythropoietic cytokine with broad neuroprotective activity in vivo. *Proc. Natl. Acad. Sci. U. S. A.* 100:6741-6.
- Duchen LW, Strich SJ. (1968) An hereditary motor neurone disease with progressive denervation of muscle in the mouse: the mutant 'wobbler.' *J. Neurol. Neurosurg. Psychiatr.* 31:535-42.
- Schmitt-John T et al. (2005) Mutation of Vps54 causes motor neuron disease and defective spermiogenesis in the wobbler mouse. *Nat. Genet.* 37:1213-5.
- Fumagalli E, Bigini P, Barbera S, De Paola M, Mennini T. (2006) Riluzole, unlike the AMPA antagonist RPR119990, reduces motor impairment and partially prevents motoneuron death in the wobbler mouse, a model of neurodegenerative disease. *Exp. Neurol.* 198:114-28.
- Ikeda K et al. (1995) Effects of brain-derived neurotrophic factor on motor dysfunction in wobbler mouse motor neuron disease. *Ann. Neurol.* 37:505-11.
- Comoletti D, Muzio V, Capobianco A, Ravizza T, Mennini T. (2001) Nitric oxide produced by non-motoneuron cells enhances rat embryonic motoneuron sensitivity to excitotoxins: comparison in mixed neuron/glia or purified cultures. *J. Neurol. Sci.* 192:61-9.
- Rosen DR et al. (1993) Mutations in Cu/Zn superoxide dismutase gene are associated with familial amyotrophic lateral sclerosis. *Nature* 362:59-62.
- Ogunshola OO, Djonov V, Staudt R, Vogel J, Gassmann M. (2006) Chronic excessive erythrocytosis induces endothelial activation and damage in mouse brain. *Am. J. Physiol. Regul. Integr. Comp. Physiol.* 290:R678-84.
- Tsuzaka K, Ishiyama T, Pioro EP, Mitsumoto H. (2001) Role of brain-derived neurotrophic factor in wobbler mouse motor neuron disease. *Muscle Nerve* 24:474-80.

Erythropoietin, Modified to Not Stimulate Red Blood Cell Production, Retains Its Cardioprotective Properties

Chanil Moon, Melissa Krawczyk, Doojin Paik, Thomas Coleman, Michael Brines, Magdalena Juhaszova, Steven J. Sollott, Edward G. Lakatta, and Mark I. Talan

Laboratory of Cardiovascular Sciences, Gerontology Research Center, National Institute on Aging, Baltimore, Maryland (C.M., M.K., M.J., S.J.S., E.G.L., M.I.T.); Department of Anatomy and Cell Biology, Hanyang University, Seoul, Korea (D.P.); and Kenneth S. Warren Institute and Warren Pharmaceuticals, Ossining, New York (T.C., M.B.)

Received August 29, 2005; accepted November 21, 2005

ABSTRACT

Erythropoietin (EPO), a hematopoietic cytokine, possesses strong antiapoptotic, tissue-protective properties. For clinical applications, it is desirable to separate the hematopoietic and tissue-protective properties. Recently introduced carbamylated erythropoietin (CEPO) does not stimulate the erythropoiesis but retains the antiapoptotic and neuroprotective effects. We tested the ability of CEPO to protect cardiac tissue from toxin-induced and oxidative stress in vitro and ischemic damage in vivo and compared these effects with the effects of EPO. CEPO reduced by 50% the extent of staurosporine-induced apoptosis in isolated rats' cardiomyocytes and increased by 25% the reactive oxygen species threshold for induction of the mitochondrial permeability transition. In an experimental model of myocardial infarction induced by permanent ligation of a coronary artery in rats, similarly to EPO, a single bolus injection of 30

$\mu\text{g/kg}$ b.wt. of CEPO immediately after coronary ligation reduced apoptosis in the myocardial area at risk, examined 24 h later, by 50%. Left ventricular remodeling (ventricular dilation) and functional decline (fall in ejection fraction) assessed by repeated echocardiography were significantly and similarly attenuated in CEPO- and EPO-treated rats. Four weeks after coronary ligation, the myocardial infarction (MI) size in CEPO- and EPO-treated rats was half of that in untreated coronary-ligated animals. Unlike EPO, CEPO had no effect on hematocrit. The antiapoptotic cardioprotective effects of CEPO, shown by its ability to limit both post-MI left ventricular remodeling and the extent of the myocardial scar in the model of permanent coronary artery ligation in rats, demonstrate comparable potency to that of native (nonmodified) EPO.

Erythropoietin (EPO) is a well known hematopoietic cytokine produced by the kidney in response to hypoxia (Yousoufian et al., 1993). Recombinant human EPO (rhEPO) is widely used to treat the anemia related to surgery, cancer, and kidney failure (Jelkmann, 1994). However, EPO possesses much broader salutary effects than merely stimulation of red blood cell production. EPO receptors, originally thought to be confined only to hematopoietic tissue in adults, were also found in other tissues, for example, neural tissue (for review, see Masuda et al., 1999). Many recent studies have demonstrated the neuroprotective effects of rhEPO in different animal models (Sadamoto et al., 1998; Bernaudin et

al., 1999; Brines et al., 2000) and in a phase II clinical trial in cerebral ischemia (Ehrenreich et al., 2002).

In several recent studies, the effects of systemic administration of rhEPO have been extended to include cardioprotection from ischemia. The antiapoptotic effects of rhEPO on cardiomyocytes have been reported in tissue culture and in vivo animal models of ischemia-reperfusion injury (for review, see Smith et al., 2003; Bogoyevitch, 2004). The recent discovery of EPO receptors in cardiomyocytes of adult rat solidified these findings (Wright et al., 2004).

In a rat model of myocardial ischemia using permanent ligation of a coronary artery, we have shown that in comparison with untreated animals, a single systemic injection of 30 $\mu\text{g/kg}$ b.wt. of rhEPO immediately after coronary artery ligation reduced apoptosis in the myocardial area at risk 24 h later by 50%. Left ventricular remodeling was suppressed in rhEPO-treated rats, and 8 weeks after coronary ligation, the

This research was supported by the Intramural Research Program of the National Institutes of Health, National Institute on Aging.

Article, publication date, and citation information can be found at <http://jpet.aspetjournals.org>.
doi:10.1124/jpet.105.094854.

ABBREVIATIONS: EPO, erythropoietin; rhEPO, recombinant human erythropoietin; MI, myocardial infarction; STAT, signal transducer and activator of transcription; PI3K, phosphatidylinositol 3 kinase; MPT, mitochondrial permeability transition; CEPO, carbamylated erythropoietin; LV, left ventricle; ROS, reactive oxygen species; TMRM, tetramethylrhodamine methyl ester; SH, sham (S); EDV, end-diastolic volume; ESV, end-systolic volume; EF, ejection fraction; TUNEL, terminal deoxynucleotidyltransferase-mediated dUTP nick-end labeling; ANOVA, analysis of variance.

myocardial infarct (MI) scar was 4-fold smaller than in untreated coronary artery-ligated animals (Moon et al., 2003).

A number of signaling pathways reportedly have been involved in the mechanism of EPO-induced cardioprotection. Jak-2/STAT signaling was implicated as well as PI3K signaling (Parsa et al., 2003), protein kinase C, p38, and p42/44 mitogen-activated protein kinase activation, affecting sarcolemmal and mitochondrial potassium channels, K_{ATP} (Shi et al., 2004), and Akt signaling (Calvillo et al., 2003; Parsa et al., 2003). We have recently reported that the end effector of cardioprotection by rhEPO is the permeability transition pore complex: rhEPO limits the induction of mitochondrial permeability transition (MPT) in cardiomyocytes and, thus, promotes their survival during adverse conditions (Juhászova et al., 2004).

Thus, a number of convincing preclinical experiments suggest that systemic administration of rhEPO presents a new therapeutic approach to limit myocardial damage and subsequent heart remodeling after ischemia (Maiese et al., 2005). However, the classic property of EPO to activate production of red blood cells and thrombocytes is the weakness of such therapy, limiting it to a single application and, even as such, might be contraindicated in some patients. The attendant elevation of hematocrit associated with repeated rhEPO treatment may have an adverse effect on the outcome of MI (Spiess, 1999).

A modification of EPO by subjecting it to carbamylation has recently been introduced for tissue protection (Leist et al., 2004). This carbamylated EPO (CEPO) completely lacks bioactivity in hematopoiesis bioassays and in vivo animal testing with repeated high-dose injection but effectively protects isolated neural cells from induced apoptosis. Moreover, in in vivo experiments, CEPO does not bind to EPO receptors (Leist et al., 2004). Further experiments established that CEPO's pharmacodynamic parameters are similar to that of rhEPO, and it mimics rhEPO efficacy in experimental models of brain ischemia, spinal cord and nerve damage, and autoimmune encephalomyelitis (Leist et al., 2004). In a temporary coronary ligation (ischemia-reperfusion model) in the rat (Fiordaliso et al., 2005), CEPO was shown to be cardioprotective in preventing increases in LV end-diastolic pressure, LV wall stress in systole and diastole, and improving the LV response to dobutamine. Protection against staurosporine-induced cardiomyocyte apoptosis in vitro was also observed.

The objective of this study is to establish the relationship between the efficacy of CEPO as a cardioprotective compound in vitro and in vivo and the mechanism of protection operating through induction of the MPT independently of its effects on hematopoiesis. We hypothesized that CEPO would demonstrate antiapoptotic properties in isolated cardiomyocytes undergoing hypoxia/reoxygenation stress and enhance their survival by limiting induction of the MPT. We also hypothesized that similar to EPO, systemic administration of a single dose of CEPO immediately after coronary ligation in rats would 1) reduce apoptosis in the area of myocardium at risk [area at risk (AAR)] 24 h later, 2) would attenuate the ensuing left ventricular remodeling and functional decline in the following weeks, and 3) would result in a smaller MI size at the end of 4 weeks of observation.

Materials and Methods

Materials

CEPO was produced by Warren Pharmaceuticals, Inc. (Ossining, NY) by subjecting rhEPO (Dragon Pharmaceutical, Vancouver, BC, Canada) to carbamylation—the process by which all lysines were transformed to homocitrulline (Leist et al., 2004). The dosages of CEPO used in the in vivo experiments were equivalent to EPO in terms of weight; i.e., 3000 IU/kg b.wt. EPO and 30 μ g/kg b.wt. CEPO.

In Vitro Protocols

Left Ventricular Myocytes Isolation for Experiments on Cell Culture. Left ventricular cardiomyocytes were isolated from adult Sprague-Dawley rats (250–300 g; Taconic Farms, Germantown, NY) in a perfusion chamber using Adumyts (Cellutron, Highland Park, NJ) proprietary buffers. Twenty minutes before sacrifice, animals were given 5000 U/kg heparin (Sigma-Aldrich, St. Louis, MO). Hearts were isolated rapidly, perfused through the aorta, and gassed with 85% O_2 and 15% N_2 at 37°C. Myocytes were then isolated by mechanical dissociation, separated by differential centrifugation, and plated on laminin (Sigma-Aldrich)-coated dishes (Calvillo et al., 2003). After 1 h, the medium was changed, and CEPO or EPO (100 ng/ml) or control buffer was added to the myocytes 30 min before induction of apoptosis by staurosporine (0.1 μ M; Sigma-Aldrich). After 16-h incubation, myocytes were washed with ice-cold Hanks' solution (Invitrogen, Carlsbad, CA), fixed for 20 min in 10% MeOH-free formaldehyde (Polysciences, Warrington, PA) at 4°C, washed in ice-cold Hanks' solution, stored in –20°C 70% EtOH overnight, and processed for in situ terminal deoxynucleotidyl transferase assay (Roche, Minneapolis, MN) for detection of apoptosis.

Left Ventricular Myocytes Isolation for Mitochondrial Permeability Transition Experiments. Single ventricular myocytes were isolated via a previously described technique with minor modifications (Capogrossi et al., 1986). Briefly, 2- to 4-month-old Sprague-Dawley rats were anesthetized with sodium pentobarbital, and hearts were rapidly excised and perfused with 40 ml of nominally Ca^{2+} -free bicarbonate buffer gassed with 95% O_2 to 5% CO_2 at 37°C. The composition of buffer was the following: 116.4 mM NaCl, 5.4 mM KCl, 1.2 mM $MgSO_4$, 1.2 mM NaH_2PO_4 , 5.6 mM glucose, and 26.2 mM $NaHCO_3$, pH 7.4. Hearts were continuously perfused with bicarbonate buffer containing 0.1% collagenase type B, 0.04 mg/ml protease XVI, and 0.1% bovine serum albumin type V for 4 min, and 50 μ M Ca^{2+} was added. After 10-min perfusion, the left ventricle was minced and incubated in bicarbonate buffer containing 100 μ M Ca^{2+} for 10 min at 37°C. Myocytes were then resuspended in HEPES buffer with gradually increasing Ca^{2+} concentration up to 1 mM and kept at room temperature until use. The composition of the HEPES buffer was the following: 137 mM NaCl, 4.9 mM KCl, 1.2 mM $MgSO_4$, 1.2 mM NaH_2PO_4 , 15 mM glucose, 20 mM HEPES, and 1.0 mM $CaCl_2$ (adjusted pH to 7.4). Cardiac myocytes viability was typically 70 to 80%.

Confocal Microscopy and Determination of MPT-ROS Threshold. Experiments were conducted as described previously (Juhászova et al., 2004), using a method to quantify the ROS susceptibility for the induction of MPT in individual mitochondria within cardiac myocytes (Zorov et al., 2000). Briefly, isolated cardiac myocytes were exposed in vitro to conditions that mimic oxidative stress by repetitive laser scanning of a row of mitochondria in a myocyte loaded with tetramethylrhodamine methyl ester (TMRM; see Fig. 2). This results in incremental, additive exposure of only the laser-exposed area to the photodynamic production of ROS and consequent MPT induction. The occurrence of MPT is clearly identified by the immediate dissipation of $\Delta\Psi$. Myocytes were loaded with 125 nM TMRM for at least 1 h at room temperature and imaged with an LSM-510 inverted confocal microscope (Carl Zeiss Inc., Jena, Germany) (Fig. 2A). Line scan images at 2 Hz were recorded from mitochondria arrayed along individual myofibrils with excitation at

568 nm and collecting emission at >560 nm, using a Zeiss Plan-Apochromat 63×/1.4 numerical aperture oil immersion objective, and the confocal pinhole was set to obtain spatial resolutions of 0.4 μ m in the horizontal plane and 1 μ m in the axial dimension. Images were processed by MetaMorph software (Universal Imaging, Downingtown, PA). The ROS threshold for MPT induction (t_{MPT}) was measured as the average time necessary to induce MPT in a row consisting of ~25 mitochondria (Fig. 2B). Experiments were carried out at 23°C. The cardioprotective action of insulin, which normally results in an enhancement of the MPT-ROS threshold by ~35 to 40% (Juhászova et al., 2004), was used as a positive control in the present experiments. In parallel experiments, cells were exposed to CEPO (10, 100, or 250 ng/ml for 20 min prior to t_{MPT} measurements). Wortmannin (50 μ M) was also applied in certain protocols.

II. In Vivo Experiments

Animals and Experimental Design. Eighty male Sprague-Dawley rats, 2 months of age, were housed and studied in conformance with the National Institutes of Health Guide for the Care and Use of Laboratory Animals, Manual 3040-2 (1999), with institutional Animal Care and Use Committee approval. After baseline echocardiography, animals were randomly divided into coronary artery-ligated (MI; $n = 54$) or sham (SH; $n = 16$) groups and, under inhalation anesthesia by isoflurane, subjected to ligation of the left anterior descending coronary artery to induce myocardial infarction (MI) or to a sham operation, as previously described (Moon et al., 2003). Animals in the MI group were either treated with a single systemic injection of CEPO ($n = 18$) or EPO ($n = 18$) or remained untreated ($n = 18$). Both CEPO and EPO, 30 μ g/kg b.wt., were given i.v. in 0.3 ml of saline immediately (<5 min) after surgery. Untreated animals received a single i.v. injection of 0.3 ml of saline at the same time. SH animals were either injected with CEPO ($n = 8$), or with saline ($n = 8$) in a dose and manner similar to MI animals. Therefore, the experimental design consisted of five groups of rats: sham, not treated (SH-SALINE); sham, treated with CEPO (SH-CEPO); MI, not treated (MI-SALINE); and MI, treated with CEPO (MI-CEPO), and MI, treated with EPO (MI-EPO). Six animals from each of the MI-CEPO, MI-EPO, and the MI-SALINE groups were killed 24 h after surgery, and their hearts were harvested for appropriate immunohistochemical staining to assess the early effect of CEPO treatment on the extent of post-MI apoptosis. In the remainder of the operated animals, LV function was assessed by echocardiography 1 and 4 weeks after surgery, at which time all animals were killed using a bolus injection of 4 ml of 0.5 M KCl under general anesthesia with sodium pentobarbital (50 mg/kg b.wt., i.p.), and their hearts were harvested for histological analyses.

Echocardiography. Cardiac function was assessed by echocardiography (HP Sonos 5500 equipped with a 12-MHz phase array linear transducer, S12, allowing a 150-mm/s maximal sweep rate; Hewlett Packard, Palo Alto, CA) under general anesthesia with pentobarbital sodium (30 mg/kg b.wt., i.p.) as described previously (Moon et al., 2003). Briefly, parasternal long-axis views were obtained and recorded, ensuring that the mitral and aortic valves and the apex were visualized. Endocardial area tracings using the leading-edge method were performed in the two-dimensional mode (short- and long-axis views) from digital images captured on cine-loop. LV end-diastolic volume (EDV) and LV end-systolic volume (ESV) were calculated by a modified Simpson's method from the long-axis view. LV ejection fraction (EF %) was derived as $EF = (EDV - ESV)/EDV \times 100$. All measurements were made by one observer who was blinded with respect to the identity of the tracings. All measurements were averaged over three to five consecutive cardiac cycles. The reproducibility of measurements was assessed at baselines by two sets of measurements in 10 randomly selected rats. The repeated measure variability did not exceed $\pm 5\%$.

Infarct Size Measurement. Hearts were excised and placed in 10% phosphate-buffered formalin. The fixed tissue was then embedded in paraffin and serially cut from the apex to the level just below

the coronary artery ligation site; transverse 6- μ m-thick sections were cut at 600- μ m distances such that 10 to 12 sections were obtained from each heart. Sections were stained with hematoxylin/eosin and azan, and morphological analysis was performed by computerized video imaging using an Axioplan microscope (Zeiss) and NIH IMAGE software (Bethesda, MD). The myocardial infarct size of each section was calculated as the ratio of infarction area to the area of total LV section (area method) and as the average of ratios of the outer infarction length to the outer LV circumference and the inner infarction length to the inner LV circumference (perimeter method). The infarct size of all sections for both area and perimeter methods was averaged and expressed as the percentage of LV for each heart.

LV Posterior Wall Thickness Measurement. The thickness of LV posterior wall was measured and averaged in each LV section where the myocardial infarct size was measured.

Assessment of Apoptosis in Hearts. Twenty-four hours after coronary artery ligation or sham operation, under general anesthesia with pentobarbital sodium (50 mg/kg b.wt., i.p.), 2 ml of 5% Evans blue was injected into the right ventricular chamber via the right jugular vein. The rats were killed immediately by a bolus injection of 4 ml of 0.5 M KCl, and the hearts were removed, rapidly rinsed in phosphate-buffered saline, and snap-frozen in liquid nitrogen. Serial, 6- μ m-thick cryostat sections were prepared. Processing of subsequent sections alternated between tetrazolium chloride and terminal deoxynucleotidyltransferase-mediated dUTP nick-end labeling (TUNEL) staining. The parts unstained by Evans blue containing a combination of dead tissue and underperfused but viable myocardium (AAR) were incubated for 20 min in tetrazolium chloride and then transferred into 4% paraformaldehyde. In all resulting sections, the AAR of myocardial tissue was stained in red, whereas dead tissue remained white (Bialik et al., 1997). The AAR on every other section was further subjected to TUNEL staining for detection of apoptotic cells by the nick-end labeling method using a commercially available kit (Roche) as directed by the manufacturer. Slides were examined by light microscopy. In each section, the number of cardiomyocytes and the number of TUNEL-positive cardiomyocyte nuclei were counted and totaled in 10 randomly selected fields of the AAR at $\times 400$ amplification. Only nuclei that were clearly located in cardiomyocytes were counted.

Statistical Analyses. Sonographic indices of morphometric and functional assessment at each time point were expressed as a percentage of change from the baseline (measurements taken before surgery). All values were corrected for body mass. Statistical significance of differences among groups with regard to changes of these indices over time was determined using ANOVA for repeated measurements, specifically noting group \times time interactions. A post hoc pair comparison between MI-SALINE, MI-CEPO, and MI-EPO groups was conducted for the 4th-week data. Statistical significance of differences between groups with regard to infarct size and apoptosis was determined using a one-way ANOVA following by a post hoc pair comparison. The same approach was used in vitro experiments. Statistical significance was assumed at $p < 0.05$.

Results

In Vitro Experiments

Apoptosis in Isolated Cardiomyocytes. After 16 h of staurosporine exposure, 78% of untreated myocytes were apoptotic. In the presence of 100 ng/ml rhEPO or CEPO, the number of apoptotic myocytes was reduced by 77 and 87%, respectively (Fig. 1).

Assessment of MPT-ROS Threshold. Figure 2C presents the cardioprotective effects of CEPO in isolated cardiac myocytes as indexed by the ROS threshold for MPT induction (t_{MPT}). CEPO exposure at 10, 100, and 250 ng/ml resulted in increased MPT-ROS threshold by 20 to 25% above the un-

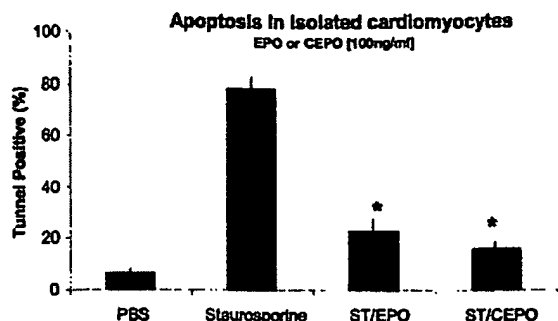


Fig. 1. The antiapoptotic effect of rhEPO and CEPO on isolated rat cardiomyocytes. After a 30-min in vitro exposure of isolated rat ventricular cardiomyocytes to 100 ng/ml CEPO or EPO, apoptosis was induced by staurosporine. After 16-h incubation, myocytes were processed for in situ terminal deoxynucleotidyl transferase assay for detection of apoptosis. PBS, phosphate-buffered saline. *, $p < 0.05$ versus staurosporine (post hoc comparison).

treated control. This protective effect was completely blocked by 50 nM wortmannin. For comparison, insulin, used as a positive control, increased t_{MPT} by 35%.

In Vivo Experiments

Mortality and Final Number of Animals. Three animals died among coronary artery-ligated CEPO-treated animals, four among coronary artery-ligated EPO-treated animals, and two among untreated rats. One animal died in the sham-operated group. No mortality was registered after the first 24 h. Thus, the final number of animals per group in 24-h study was: MI-SALINE, six; MI-CEPO, six; and MI-EPO, six. The final number of animals per group in 4-week study was SH-SALINE, seven; SH-CEPO, eight; MI-SALINE, 10; MI-CEPO, nine; and MI-EPO, eight.

The Effect of CEPO and EPO on Hematocrit. One week after MI induction, the hematocrit values increased on

average by 5.1% in EPO-treated rats ($p < 0.05$) but did not change in CEPO-treated animals (-0.7% , $p > 0.05$).

Echocardiography. At baseline, before coronary artery ligation or sham operation, echocardiographic indices of LV volumes and EF are presented in Table 1. There were no statistical differences at baseline among coronary artery-ligated or sham-operated animals untreated or treated with CEPO or EPO in EDV, ESV, or EF. Average changes of these parameters from baseline during 4 weeks of observation are illustrated in Fig. 3. Treatment of sham-operated animals with CEPO (S-CEPO) did not affect the direction or magnitude of changes during the 4 weeks after surgery relative to untreated animals (S-SALINE). In nontreated ligated animals (MI-SALINE), there was a gradual enlargement of LV over time; by week 4, this averaged a 26% and approximately 140% increase of baseline LV volumes at end-diastole and end-systole, respectively. The EF in MI-SALINE animals fell by more than 50% by week 4. The magnitude and pattern of changes of all indices in MI-SALINE group were significantly different from those of both sham-operated groups (the ANOVA-derived group \times time interaction, $p < 0.05$).

The pattern and magnitude of changes reflecting the extent of LV remodeling and functional decline were less pronounced in both the MI-CEPO and MI-EPO groups than in MI-SALINE group. In fact, contrary to the MI-SALINE group, the evaluation of LV remodeling (ANOVA-derived group \times time interaction) showed that there were no statistical differences between MI-CEPO or MI-EPO and sham groups for all three presented indices. Moreover, EF and ESV were significantly different between either MI-CEPO or MI-EPO and MI-SALINE. Post hoc paired comparisons also revealed that both MI-CEPO and MI-EPO groups statistically differed at week 4 from MI-SALINE group with respect to EF and ESV: ESV at week 4 was significantly smaller and EF was significantly higher in both MI-CEPO and MI-EPO

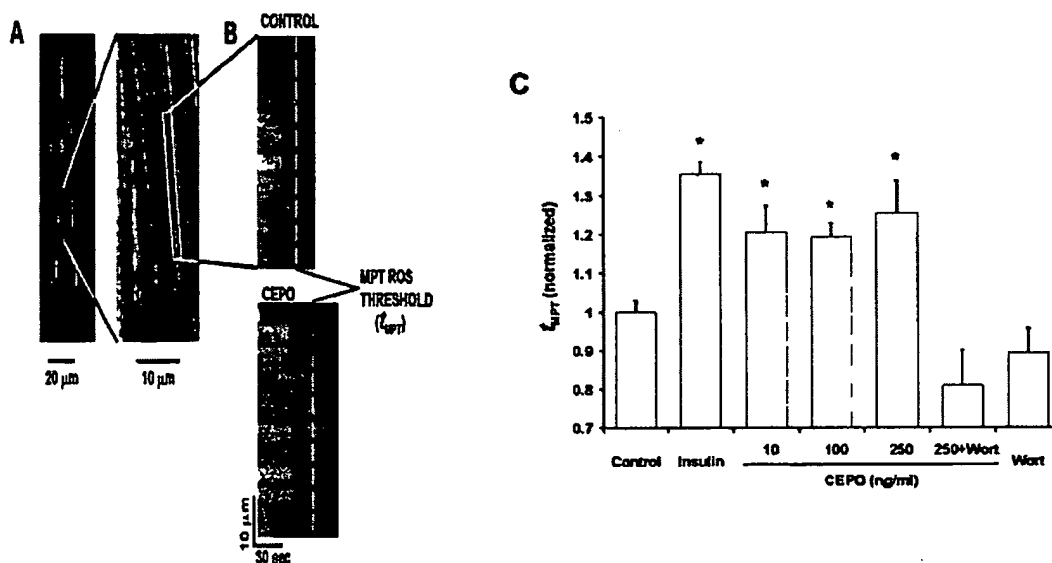


Fig. 2. Cellular mechanism of cardioprotection. A and B, methodology used to determine the ROS threshold of MPT induction, the index of cardioprotection. Mitochondria in isolated rat cardiac myocytes stained with TMRM (A) were laser line-scanned until MPT induction (B). The average time required for the standardized photoproduction of ROS to cause MPT induction (t_{MPT}) is taken as the index of the ROS threshold in that cell (see text and references, Zorov et al., 2000; Juhaszova et al., 2004). C, CEPO reduces the MPT susceptibility to ROS (t_{MPT}) via PI3K-dependent signaling in cardiac myocytes. Isolated cells were exposed to 30 nM insulin (as the positive control) or to 10, 100, or 250 ng/ml CEPO for 20 min prior to t_{MPT} measurement (see text). Wortmannin (50 nM) was used to inhibit PI3K. *, $p < 0.01$ versus control.

TABLE 1
Baseline (week 0) echocardiographic indices of LV volumes and EF (mean \pm S.E.)

	SH-SALINE (n = 7)	SH-CEPO (n = 8)	MI-SALINE (n = 10)	MI-CEPO (n = 9)	MI-EPO (n = 8)
EDV (ml)	0.35 \pm 0.02	0.34 \pm 0.01	0.35 \pm 0.01	0.33 \pm 0.01	0.33 \pm 0.01
ESV (ml)	0.14 \pm 0.004	0.14 \pm 0.008	0.14 \pm 0.005	0.13 \pm 0.004	0.13 \pm 0.005
EF (%)	59.5 \pm 0.9	58.5 \pm 1.2	60.5 \pm 0.8	61.4 \pm 0.4	60.0 \pm 1.3

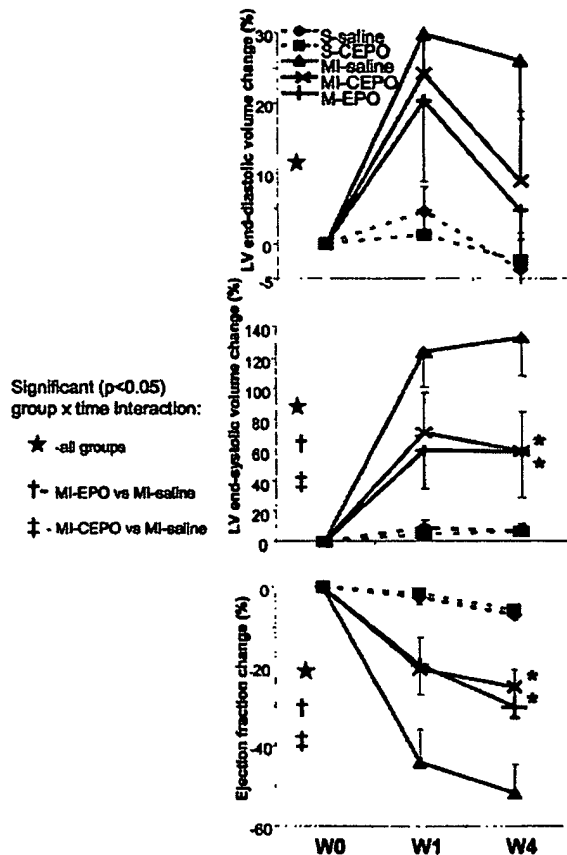


Fig. 3. Changes in echocardiographic indices of LV volume and function (ejection fraction) during 4 weeks after coronary artery ligation (MI) or sham (S) operation in CEPO-, EPO-, and saline-treated (SALINE) rats. All indices are derived from images obtained from the long-axis view in two-dimensional mode echo, adjusted for body mass, and expressed as the percentage of change from the baseline values (see Table 1). Statistically significant ($p < 0.05$) group \times time interactions (ANOVA for repeated measurements) are indicated by the following: *, among all groups; †, MI-SALINE versus MI-CEPO; and ‡, MI-SALINE versus MI-EPO. *, significantly different ($p < 0.05$) in post hoc comparison between MI-SALINE and MI-CEPO (or MI-EPO) groups at week 4.

groups in comparison with MI-SALINE. In any of presented indices, the MI-CEPO and MI-EPO groups did not differ from each other either in the pattern of changes over time or at any specific time point.

Infarct Size. The average infarct size, expressed as a percentage of LV, in MI-SALINE, MI-CEPO, and MI-EPO group is presented in Fig. 4. Regardless of the technique used to estimate the MI size, perimeter, or area calculation, the average MI size in either MI-CEPO or MI-EPO groups was half of that in MI-SALINE group ($p < 0.05$).

Posterior Wall Thickness. The thickness of LV posterior wall measured histologically at the same sections the MI size was measured was similar in MI-EPO and MI-CEPO groups

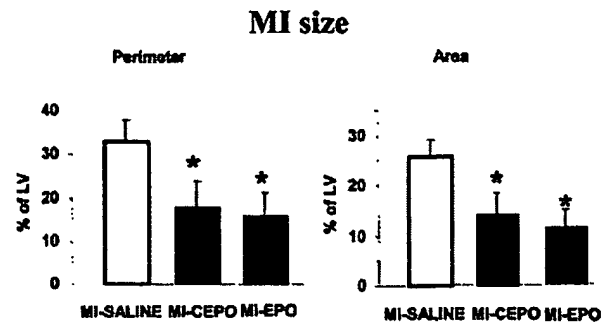


Fig. 4. MI size 4 weeks after ligation of a coronary artery in untreated rats and rats treated with CEPO or EPO. *, $p < 0.05$ post hoc comparison.

(0.89 ± 0.03 mm) and not different from that in MI-SALINE group (0.84 ± 0.02 mm, $p > 0.05$).

Determination of Extent of Apoptosis within the Area at Risk. Figure 5, A and B, illustrates the TUNEL staining at 24 h after coronary artery ligation in representative histological slides of comparable AARs in hearts from MI-SALINE and MI-CEPO groups, respectively. More apoptotic nuclei are clearly observed in the untreated heart (Fig. 5A). Figure 5C shows the average number of apoptotic nuclei in comparison with a total number of counted nuclei in the AAR of untreated hearts and hearts treated with EPO or CEPO. Only $17 \pm 1.2\%$ of nuclei were TUNEL-positive in the MI-CEPO group and $15.3 \pm 1.2\%$ in the MI-EPO group, compared with $33.6 \pm 0.8\%$ in MI-SALINE group ($p < 0.01$) (Fig. 5D).

Discussion

CEPO is a recently introduced, engineered cytokine that was designed to retain the tissue-protective (antiapoptotic) characteristics of EPO but not trigger erythropoiesis (Leist et al., 2004). CEPO's pharmacokinetic parameters are very similar to those of EPO, but even injected daily for 4 weeks in doses as high as $200 \mu\text{g/kg}$ b.wt. it fails to increase hematocrit in mice (Leist et al., 2004). However, CEPO's pharmacodynamics is remarkably different from that of EPO, because CEPO does not signal the classic EPO receptor (Leist et al., 2004). Nevertheless, extensive testing demonstrated strong neuroprotective properties of CEPO that are comparable with that of EPO. Antiapoptotic effects of CEPO have been shown in vitro on isolated neural cells and in vivo in cerebral infarct and spinal injury models in rats (Leist et al., 2004). Similar tissue protective properties of EPO and CEPO and the lack of hemopoietic properties of CEPO led to the recent suggestion that the tissue protection by EPO is mediated through a heteroreceptor complex comprising both the EPO receptor and a common β receptor subunit, also known as CD131 (Brines et al., 2004).

We (Moon et al., 2003) and others (see review in Bogoyevitch, 2004) have reported the cardioprotective properties of EPO in different experimental models of myocardial

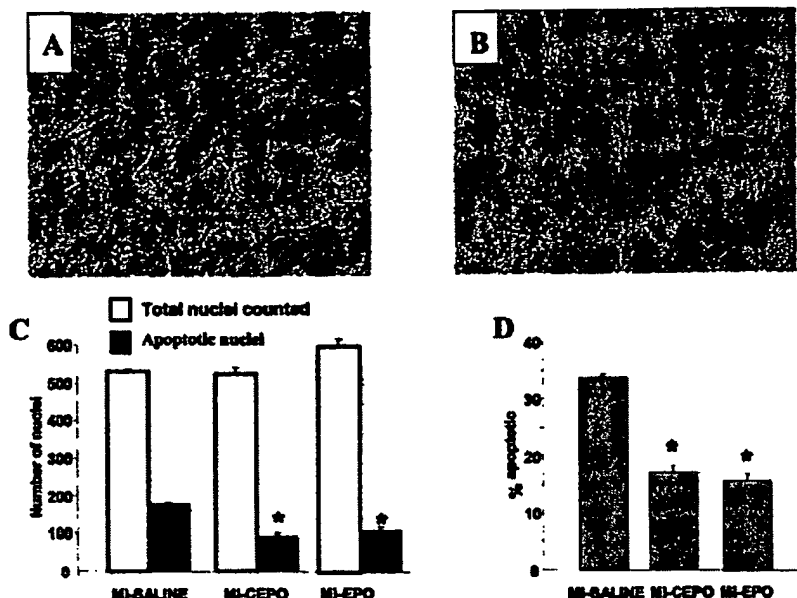


Fig. 5. Representative examples of TUNEL staining in the AAR of myocardium 24 h after coronary artery ligation in untreated rats (A) and in rats treated with CEPO (B) (magnification $\times 400$). C, the average number of counted and TUNEL-positive nuclei in the area at risk in untreated MI rats and rats treated with CEPO or EPO. D, the percentage of TUNEL-positive nuclei in the AAR of the hearts from coronary-ligated rats. *, $p < 0.05$ versus MI-SALINE.

ischemia. Our experiments have shown that a single 3000 IU/kg systemic injection of EPO after permanent ligation of a coronary artery in rat resulted 24 h later in a 50% reduction of apoptosis in the myocardial area at risk. LV remodeling at 8 weeks was significantly attenuated in treated animals, and the MI size was only 15 to 25% of that in untreated animals (Moon et al., 2003). Recently, using a temporary ligation model of myocardial ischemia, cardioprotection using CEPO was also demonstrated (Fiordaliso et al., 2005). In the present study, we showed in a permanent ligation model that, as in an experiment with EPO (Moon et al., 2003), a single dose of CEPO (30 $\mu\text{g/kg}$ b.wt. i.v.) immediately after permanent coronary artery ligation in rat reduced the apoptosis in the AAR 24 h later by 50%. During 4 weeks of post-MI observation, the LV remodeling and functional decline were similarly and significantly attenuated in both CEPO- and EPO-treated animals. The MI scar at the end of 4 weeks was significantly smaller in EPO- or CEPO-treated rats than in untreated animals. The LV posterior wall thickness was not different from that of untreated animals. However, with such a significant LV dilation and obvious posterior wall thinning in untreated animals, and with such a remarkable reduction in LV and MI size in treated animals, one would expect the posterior wall would be significantly thicker in treated animals. The lack of such thickness either suggests the possibility that both EPO and CEPO therapy suppress the myocardial hypertrophy or that 4-week observation is not sufficient to reveal the difference in posterior wall thickness.

The results of in vitro experiments on the culture of isolated cardiomyocytes also were similar for CEPO and EPO: CEPO added to culture protected the myocytes from apoptosis induced by staurosporine, and the effect was comparable with the effect of EPO. This experiment confirms a direct effect of CEPO on cardiomyocytes rather than an indirect effect, which could not be ruled out in the in vivo experiments. The remarkable similarities of outcomes of experiments in which permanent coronary ligation in rats followed by a single injection of EPO or CEPO suggest that both

compounds probably engage the same mechanism of cardioprotection, which is, at least in part, antiapoptotic. This conclusion is supported by experiments with TUNEL staining in cardiomyocyte cultures or in myocardial tissue 24 h after coronary ligation as well as by experiments measuring the MRT-ROS threshold of single cardiomyocytes—a final common pathway for antiapoptotic signaling. The particular signaling pathway involved in EPO-CEPO-induced cardioprotection remains less certain. In different studies of EPO effects, many possible antiapoptotic signaling pathways have been reported: Jak-2/STAT, PI3K, protein kinase C, p38, p42/44 mitogen-activated protein kinase activation, K_{ATP} , and Akt (Brines et al., 2000; Calvillo et al., 2003; Parsa et al., 2003; Ghezzi and Brines, 2004; Shi et al., 2004). Introduction of CEPO allowed us to narrow the possibilities. Because CEPO does not bind to classic EPO receptors (Leist et al., 2004) its effects would not necessarily involve transcription factors STAT-5 or Jak2, a downstream kinase directly activated upon ligand binding to EPO receptors. On the other hand, the finding that the PI3-kinase inhibitor wortmannin completely blocked the beneficial effect of CEPO on MPT-ROS threshold suggests that the PI3-kinase signaling pathway is definitely involved in CEPO-mediated protection against ischemia, similar to that observed with rhEPO (Juhászova et al., 2004). The very effect of CEPO on MPT-ROS threshold gives additional weight to the idea that both EPO and CEPO exert their tissue-protective properties not through affinity to classic homodimeric EPO receptors but rather to heteromeric receptor complexes containing at least one EPO receptor subunit (Brines et al., 2004; Leist et al., 2004).

In summary, the demonstration of strong antiapoptotic effects of CEPO on ischemic myocardium, comparable with that of EPO, in conjunction with CEPO's lack of hematopoietic activity suggests the possibility of its use in treatment of myocardial infarction or myocardial ischemia in situations when repeated dosing is clinically desirable or the use of EPO is prohibitive due to its procoagulant and prothrombotic effects (Stohlawetz et al., 2000). Moreover, since death of car-

diac myocytes due to apoptosis is now considered a major causative factor in evolution of chronic heart failure to end-stage dilated cardiomyopathy (Wencker et al., 2003), CEPO might be suitable for a long-term treatment of the late LV remodeling.

References

- Bernaudo M, Marti HH, Roussel S, Divoux D, Nouvelot A, MacKenzie ET, and Petit E (1999) A potential role for erythropoietin in focal permanent cerebral ischemia in mice. *J Cereb Blood Flow Metab* 19:643–651.
- Bialik S, Geenen DL, Sasson IE, Cheng R, Horner JW, Evans SM, Lord EM, Koch CJ, and Kitsis RN (1997) Myocyte apoptosis during acute myocardial infarction in the mouse localizes to hypoxic regions but occurs independently of p53. *J Clin Invest* 100:1363–1372.
- Brines ML, Ghezzi P, Keenan S, Agnello D, de Lanerolle NC, Cerami C, Itri LM, and Cerami A (2000) Erythropoietin crosses the blood-brain barrier to protect against experimental brain injury. *Proc Natl Acad Sci USA* 97:10526–10531.
- Brines M, Grasso G, Fiordaliso F, Sfacteria A, Ghezzi P, Fratelli M, Latini R, Xie QW, Smart J, Su-Rick CJ, et al. (2004) Erythropoietin mediates tissue protection through an erythropoietin and common beta-subunit heteroreceptor. *Proc Natl Acad Sci USA* 101:14907–14912.
- Bogoyevitch MA (2004) An update on the cardiac effects of erythropoietin cardioprotection by erythropoietin and the lessons learnt from studies in neuroprotection. *Cardiovasc Res* 63:208–216.
- Calvillo L, Latini R, Kajstura J, Leri A, Anversa P, Ghezzi P, Salio M, Cerami A, and Brines M (2003) Recombinant human erythropoietin protects the myocardium from ischemia-reperfusion injury and promotes beneficial remodeling. *Proc Natl Acad Sci USA* 100:4802–4816.
- Capogrossi MC, Kort AA, Spurgeon HA, and Lakatta EG (1986) Single adult rabbit and rat cardiac myocytes retain the Ca²⁺- and species-dependent systolic and diastolic contractile properties of intact muscle. *J Gen Physiol* 88:589–613.
- Ehrenreich H, Hasselblatt M, Dembowski C, Cepek L, Lewczuk P, Stiefel M, Rustenbeck HH, Breiter N, Jacob S, Knerlich F, et al. (2002) Erythropoietin therapy for acute stroke is both safe and beneficial. *Mol Med* 8:495–505.
- Fiordaliso F, Chimenti S, Staszewsky L, Bai A, Carlo E, Cuccovillo I, Doni M, Mengozzi M, Tonelli R, Ghezzi P, et al. (2005) A nonerythropoietic derivative of erythropoietin protects the myocardium from ischemia-reperfusion injury. *Proc Natl Acad Sci USA* 102:2046–2051.
- Ghezzi P and Brines M (2004) Erythropoietin as an antiapoptotic, tissue-protective cytokine. *Cell Death Differ* 11 (Suppl 1):S37–S44.
- Jelkmann W (1994) Biology of erythropoietin. *Clin Invest* 72:53–510.
- Juhaszova M, Zorov DB, Kim SH, Pepe S, Fu Q, Fishbein KW, Ziman BD, Wang S, Ytrehus K, Antos CL, et al. (2004) Glycogen synthase kinase-3 β mediates convergence of protection signaling to inhibit the mitochondrial permeability transition pore. *J Clin Invest* 113:1535–1549.
- Leist M, Ghezzi P, Grasso G, Bianchi R, Villa P, Fratelli M, Savino C, Bianchi M, Nielsen J, Gerwien J, et al. (2004) Derivatives of erythropoietin that are tissue protective but not erythropoietic. *Science (Wash DC)* 305:239–242.
- Maiese K, Li F, and Chong ZZ (2005) New avenues of exploration for erythropoietin. *J Am Med Assoc* 293:90–95.
- Masuda S, Nagao M, and Sasaki R (1999) Erythropoietic, neurotrophic and angiogenic functions of erythropoietin and regulation of erythropoietin production. *Int J Hematol* 70:1–6.
- Moon C, Krawczyk M, Ahn D, Ahmet I, Paik D, Lakatta EG, and Talan MI (2003) Erythropoietin reduces myocardial infarction and left ventricular functional decline after coronary artery ligation in rats. *Proc Natl Acad Sci USA* 100:11612–11617.
- Paras CJ, Matsumoto A, Kim J, Riel RU, Pascal LS, Walton GB, Thompson RB, Petrofski JA, Annex BH, Stamler JS, and Koch WJ (2003) A novel protective effect of erythropoietin in the infarcted heart. *J Clin Invest* 112:999–1007.
- Sadamoto Y, Igase K, Sakanaka M, Sato K, Otsuka H, Sakaki S, Masuda S, and Sasaki R (1998) Erythropoietin prevents place navigation disability and cortical infarction in rats with permanent occlusion of the middle cerebral artery. *Biochem Biophys Res Commun* 253:26–32.
- Shi Y, Rafiee P, Su J, Pritchard KA Jr, Tweddell JS, and Baker JE (2004) Acute cardioprotective effects of erythropoietin in infant rabbits are mediated by activation of protein kinases and potassium channels. *Basic Res Cardiol* 99:173–182.
- Smith KJ, Bleyer AJ, Little WC, and Sane DC (2003) The cardiovascular effects of erythropoietin. *Cardiovasc Res* 58:538–548.
- Spless BD (1999) Is a high hematocrit value an independent risk factor for adverse outcome after coronary artery bypass grafting? *J Thorac Cardiovasc Surg* 118:765–766.
- Stohlawetz PJ, Dzirlo L, Hergovich N, Lackner E, Mensik C, Eichler HG, Kabrna E, Geissler K, and Jilma B (2000) Effects of erythropoietin on platelet reactivity and thrombopoiesis in humans. *Blood* 95:2983–2989.
- Wencker D, Chandra M, Nguyen K, Miao W, Garantzotlis S, Factor SM, Shirani J, Armstrong RC, and Kitsis RN (2003) A mechanistic role for cardiac myocyte apoptosis in heart failure. *J Clin Invest* 111:1497–1504.
- Wright GL, Hanlon P, Amin K, Steenbergen C, Murphy E, and Arcasoy MO (2004) Erythropoietin receptor expression in adult rat cardiomyocytes is associated with an acute cardioprotective effect for recombinant erythropoietin during ischemia-reperfusion injury. *FASEB J* 18:1031–1033.
- Yousoufian H, Lonmae G, Neumann D, Yoshimura A, and Lodish HF (1993) Structure, function and activation of the erythropoietin receptor. *Blood* 81:2223–2236.
- Zorov DB, Filburn CR, Klotz LO, Zweier JL, and Sollott SJ (2000) Reactive oxygen species (ROS)-induced ROS release: a new phenomenon accompanying induction of the mitochondrial permeability transition in cardiac myocytes. *J Exp Med* 192:1001–1014.

Address correspondence to: Dr. Mark Talan, Senior Investigator, Head, Cardiovascular Gene Therapy Unit, Laboratory of Cardiovascular Sciences, Intramural Research Program, National Institute on Aging, 5600 Nathan Shock Drive, Baltimore, MD 21224-6825. E-mail: talanm@grc.nia.nih.gov

Asialoerythropoietin Has Strong Renoprotective Effects Against Ischemia-Reperfusion Injury in a Murine Model

Toshie Okada, Tokihiko Sawada, and Keiichi Kubota

Background. The renoprotective effect of erythropoietin (EPO) and the nonhematopoietic EPO, asialoEPO was investigated in a murine ischemia-reperfusion injury (I/R) model.

Methods. I/R was created by clamping the right renal pedicle for 60 min after left nephrectomy. Balb/c mice were divided into four groups (n=15 in each group): sham operation (Sham), vehicle treatment (Vehicle), EPO treatment (EPO), and asialoEPO treatment (AsialoEPO). EPO and asialoEPO were given at a dose of 500 IU/kg 30 min before I/R. Plasma creatinine (Cr), survival, and the number of apoptotic cells were analyzed. Protein expression was analyzed by Western blotting.

Results. Plasma Cr level was not significantly different at 6 hr after I/R. At 24 hr after I/R, the Cr (mg/dL) levels in Sham, Vehicle, EPO, and asialoEPO were 0.13 ± 0.01 , 1.24 ± 0.70 , 0.24 ± 0.08 , and 0.25 ± 0.13 , respectively ($P < 0.05$). The numbers of apoptotic cells in these groups were 0.1 ± 0.1 , 98.9 ± 42.6 , 3.3 ± 0.7 , and 2.9 ± 1.6 , respectively ($P < 0.05$). Western blotting revealed that in kidney tissue of mice treated with EPO and asialoEPO, p38-MAPK and the proapoptotic molecule Bad was decreased, and the antiapoptotic molecules Bcl-xL and XIAP were increased. Survival rates at 7 days after I/R injury in the Sham, Vehicle, EPO, and AsialoEPO groups were 100%, 21.4%, 23.1%, and 53.8%, respectively ($P = 0.05$).

Conclusion. EPO and asialoEPO attenuated renal dysfunction caused by I/R in mouse kidney at the same level, but only asialoEPO improved survival.

Keywords: Ischemia, Reperfusion, Kidney, Erythropoietin, Asialoerythropoietin.

(*Transplantation* 2007;84: 504–510)

Ischemia-reperfusion (I/R) injury is a major factor responsible for acute renal failure (ARF). ARF is a common clinical morbidity, which can occur as a primary condition, or in association with shock, sepsis, and postoperative complications, and is also a risk factor in renal transplantation. ARF mortality rates range from 7% to 80% (1, 2). Therefore, agents that can attenuate I/R injury have been sought and studied.

Recently, the extrahematopoietic effects of erythropoietin (EPO) have been extensively investigated. These include antiapoptotic effects in the nervous system (3, 4), heart (5, 6), kidney (7, 8), and endothelium (9). In particular, there is a large body of evidence to suggest that EPO protects the kidney from I/R injury in rodent ARF models (10–12). However, chronic administration of EPO at an extremely high dose to achieve tissue protection is hampered by the main effect of

EPO, which is hematopoiesis, because the resulting increase of red blood cells may cause thrombotic events (13, 14). To avoid this situation, nonhematopoietic EPO derivatives are a promising avenue of investigation.

Asialoerythropoietin (asialoEPO) is a desialated form of EPO that is nonhematopoietic but retains the extrahematopoietic effects of EPO (15, 16). In this study, the renoprotective effect of asialoEPO was investigated for the first time in a murine I/R injury model. It was found that asialoEPO attenuated I/R injury to the same degree as EPO, but unlike EPO, improved the survival of mice with I/R injury.

MATERIALS AND METHODS

This study was approved by the Ethics Committee for Animal Experimentation at Dokkyo University School of Medicine.

EPO and AsialoEPO

EPO and asialoEPO were obtained from Chugai Co. Ltd. (Tokyo, Japan). Both were dissolved in a vehicle consisting of phosphate-buffered saline.

Mice and Renal Ischemia-Reperfusion Model

Female Balb/c mice were purchased from SLC (Chiba, Japan) and housed under pathogen-free conditions. The

Second Department of Surgery, Dokkyo University School of Medicine, Tochigi, Japan.

Address correspondence to: Tokihiko Sawada, M.D., Ph.D., Second Department of Surgery, Dokkyo University School of Medicine, Kitakobayashi 880, Mibu, Shimotsuga 880, Tochigi 321-0293, Japan.

E-mail: tsawada@dokkyomed.ac.jp

Received 23 February 2007. Revision requested 5 April 2007.

Accepted 9 May 2007.

Copyright © 2007 by Lippincott Williams & Wilkins

ISSN 0041-1337/07/8404-504

DOI: 10.1097/01.tp.0000277672.02783.33

model of renal I/R injury was created as described elsewhere (11). Mice were anesthetized with pentobarbital. A small incision was made in the left flank, the left kidney was exposed extracorporeally, and its pedicle was ligated with 4-0 silk suture, and then the kidney was removed. Next, a small incision was made in the right flank, and the pedicle of the right kidney was clamped with an atraumatic arterial clamp for 60 min.

Mice were randomly divided into four groups: 1) sham operation (Sham; $n=15$); 2) control group with I/R injury, treated with phosphate-buffered saline vehicle (Vehicle; $n=15$); 3) EPO group with I/R injury, treated with EPO (EPO; $n=15$); 4) asialoEPO group with I/R injury, treated with asialoEPO (asialoEPO; $n=15$). EPO and asialoEPO were injected subcutaneously at a dose of 500 units/kg, 30 min before clamping the renal pedicle. In previous studies, various doses of EPO, ranging from 100 units/kg to 3000 units/kg were employed (10–12, 17). In a dose-setting experiment, we examined doses of 1,000 units/kg ($n=5$), 500 units/kg ($n=5$), and 100 units/kg ($n=5$) for both EPO and asialoEPO, and decided to employ 500 units/kg because this was the minimum dose that attenuated renal I/R injury in our model. Also, a single injection of EPO or asialoEPO at a dose of 500 units/kg did not increase hematopoiesis in any of the experimental mice ($n=15$, in each group).

Blood samples were collected at 6 hours, 24 hours, and 7 days after reperfusion, and the plasma concentrations of blood urea nitrogen (BUN) and creatinine (Cr) were measured (SRL, Tokyo, Japan).

To evaluate the effect of EPO and asialoEPO on mouse survival, deaths of mice in all four groups ($n=15$ in each group) were recorded for 7 days.

Immunohistochemistry

The kidneys were removed at 24 hr after reperfusion and fixed in 10% buffered formalin, embedded in paraffin, and cut into 5- μ m-thick sections. The sections were evaluated quantitatively for apoptotic nuclei by TUNEL assay, performed using an ApopTag Plus Peroxidase In Situ Apoptosis Kit (Millipore/Chemicon International, Billerica, MA) in accordance with the manufacturer's recommendations. Briefly, paraffin sections were deparaffinized, permeabilized with proteinase K, and incubated with a mixture of nucleotides and TdT enzyme for 60 min at 37°C. The signals were detected by incubation with streptavidin-horseradish peroxidase conjugate followed by the substrate diaminobenzidine (DAB). As a negative control, sections were incubated in the absence of TdT enzyme. The number of TUNEL-positive cells was counted in 5 nonoverlapping fields per section at $\times 400$ magnification.

Western Blotting

To elucidate the mechanism of the renoprotective effect by EPO and asialoEPO, protein expression in I/R kidney was evaluated by Western blotting. Previous reports have suggested that EPO exerts its effects through MAPK modification (10). Anti-phospho-p38 MAPK (Thr180/ Tyr182) antibody, anti-phospho-SAPK/JNK (Thr183/Tyr185), anti-Bcl-xL antibody, anti-phospho Bad (ser 112) antibody, anti-Bax antibody, and anti-XIAP antibody were purchased from Cell Signaling Technology (Beverly, MA).

Kidney samples were taken at 6 and 24 hr after I/R injury, and 0.10 g net weight of kidney tissue was homogenized. The supernatant was adjusted by dilution so as to contain a constant amount of protein, confirmed using a BCA Protein Assay Kit (Pierce, Rockford, IL). Samples (20 μ g protein) were run on 12.5% (w/v) SDS-PAGE with 10% gel and electroblotted onto polyvinylidene fluoride (PVDF) membranes. The blots were blocked for 1 hr with 5% (w/v) nonfat milk powder and 0.1% (v/v) Tween 20 in Tris-NaCl, then exposed to the primary antibody at 1000-fold dilution for 24 hr at 4°C. After extensive washing, the blots were incubated with the secondary horseradish-peroxidase-conjugated antibody (1:2000) for 2 hr at 37°C. Immunoreactive bands were visualized using an enhanced chemiluminescence detection system (Amersham Life Science, Arlington Heights, IL). The levels of protein expression were estimated quantitatively by densitometric scanning using a Molecular Imager FX (Bio-Rad Laboratories, Hercules, CA). Relative intensity was calculated using the formula: relative intensity = density of vehicle-, EPO-, or asialoEPO-treated kidney / density of sham-treated kidney.

Statistics

Comparisons between two groups were analyzed by *t* test (two-sided). One-factor analysis of variance (ANOVA) was used for comparisons between the vehicle-, EPO-, and asialoEPO-treated groups. Survival of the mice was compared by log-rank test. A probability value of $P<0.05$ was considered to indicate statistical significance.

RESULTS

Figure 1 shows the levels of plasma BUN and Cr at 6 hr after I/R injury. The BUN levels in mice of the Sham, Vehicle, EPO, and AsialoEPO groups were 16.1 ± 0.1 mg/dL, 51.0 ± 6.1 mg/dL, 56.4 ± 13.1 mg/dL, and 53.9 ± 16.4 mg/dL, respectively. There were no significant differences between any of the four groups ($P=0.87$). The corresponding Cr levels were 0.15 ± 0.02 mg/dL, 0.58 ± 0.08 mg/dL, 0.63 ± 0.17 mg/dL, and 0.52 ± 0.25 mg/dL, respectively, and again there were no significant intergroup differences ($P=0.76$).

Figure 2 shows the levels of plasma BUN and Cr at 24 hr after I/R injury. The BUN levels in the Sham, Vehicle, EPO, and AsialoEPO groups were 15.5 ± 0.1 mg/dL, 179.5 ± 76.0 mg/dL, 44.0 ± 19.1 mg/dL, and 44.8 ± 13.8 mg/dL, respectively. The BUN level in the Vehicle group was significantly higher than that in the Sham, EPO and AsialoEPO groups (one-factor ANOVA; $P<0.05$). The Cr levels in mice of the Sham, Vehicle, EPO, and AsialoEPO groups were 0.13 ± 0.01 mg/dL, 1.24 ± 0.70 mg/dL, 0.24 ± 0.08 mg/dL, and 0.25 ± 0.13 mg/dL, respectively. The plasma Cr level in the Vehicle group was significantly higher than that in the Sham, EPO, and AsialoEPO groups (one-factor ANOVA; $P<0.05$). There were no significant differences in BUN (*t* test; $P=0.54$) and Cr (*t* test; $P=1.73$) levels between the EPO and AsialoEPO groups. At 7 days after I/R injury, the BUN levels in the Sham, Vehicle, EPO, and AsialoEPO groups were 15.1 ± 0.1 mg/dL, 41.2 ± 9.7 mg/dL, 31.0 ± 6.2 mg/dL, and 29.2 ± 5.2 mg/dL, respectively (one-factor ANOVA; $P>0.05$). The Cr levels in mice of the Sham, Vehicle, EPO, and AsialoEPO groups were 0.15 ± 0.01 mg/dL, 0.31 ± 0.03 mg/dL, 0.20 ± 0.01 mg/dL, and 0.21 ± 0.02 mg/dL, respectively (one-factor ANOVA; $P>0.05$; Fig. 3).

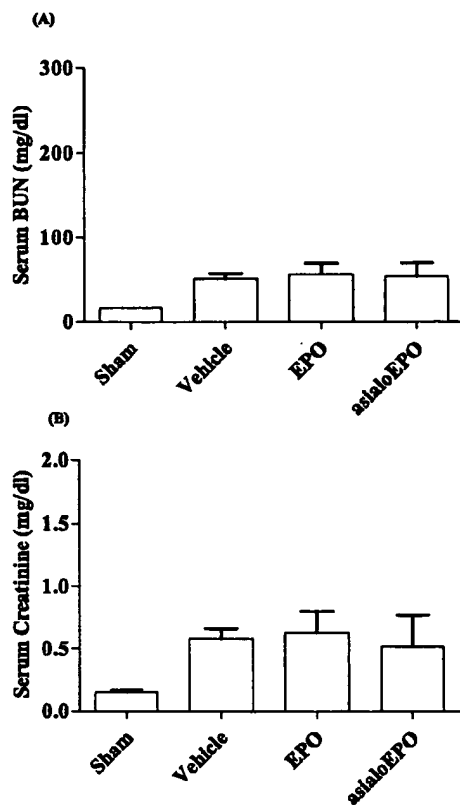


FIGURE 1. Plasma BUN and Cr levels at 6 hr after I/R injury. At 6 hr after I/R injury, there were no significant differences in plasma BUN (A) and Cr (B) levels in the Vehicle, EPO, and AsialoEPO groups.

To evaluate whether EPO and asialoEPO abrogated I/R-induced apoptotic cell death, kidneys 24 hr after I/R injury were stained by the TUNEL method (Fig. 4). In the Vehicle group, apoptotic cells were abundant, being present mainly at the cortico-medullary junction (Fig. 4C and D). On the other hand, apoptotic cells were decreased in the EPO and AsialoEPO groups (Fig. 4E–H). The numbers of apoptotic cells in the Sham, Vehicle, EPO, and AsialoEPO groups were 0.1 ± 0.1 , 98.9 ± 42.6 , 3.3 ± 0.7 , and 2.9 ± 1.6 , respectively (Fig. 4I). The number of apoptotic cells was significantly higher in the Vehicle group than in the other three groups (one-factor ANOVA; $P < 0.05$). There was no significant difference in the number of apoptotic cells between the EPO and AsialoEPO groups (t test; $P = 1.74$). Apoptotic cell death induced by I/R injury was significantly ameliorated by EPO and asialoEPO.

The results of Western blotting are summarized in Figure 5. No change in the expression of p38 was observed at 6 hr after I/R injury. However after 24 hr, EPO and asialoEPO suppressed the expression of p38. The relative intensities in the Vehicle, EPO, and asialoEPO groups were 89.3, 7.2, and 1.6, respectively (one-factor ANOVA; $P < 0.05$), and asialoEPO inhibited the expression of p38 significantly more potently than did EPO (t test; $P = 0.04$).

As TUNEL staining showed that EPO and asialoEPO inhibited I/R injury-induced apoptosis, pro- and anti-apoptotic

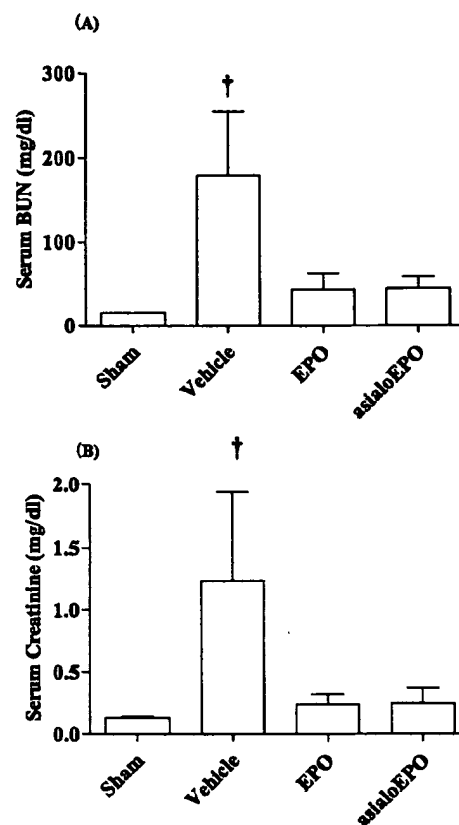


FIGURE 2. Plasma BUN and Cr levels at 24 hr after I/R injury. At 24 hr after I/R injury, the plasma BUN (A) and Cr (B) levels in the Vehicle group were significantly higher than those in the Sham, EPO and AsialoEPO groups. [†]Statistically significant.

molecules were then evaluated. Expression of the proapoptotic molecule Bad was increased 24 hr after I/R injury in the Vehicle group, whereas EPO and asialoEPO suppressed the expression of Bad. The relative intensities of Bad in the Vehicle, EPO, and asialoEPO groups at 24 hr after I/R injury were 43.1, 18.7, and 14.2, respectively, and the degree of inhibition by EPO differed significantly from that by asialoEPO (t test; $P = 0.04$). Expression of the antiapoptotic molecules Bcl-xL and XIAP was suppressed in the Vehicle group, but conversely increased in the EPO and AsialoEPO groups at 6 and 24 hr after I/R injury. The relative intensities of Bcl-xL in the Vehicle, EPO, and asialoEPO groups were 9.5, 20.3, and 19.0 at 6 hr, respectively (one-factor ANOVA; $P < 0.05$), and 5.5, 11.4, and 14.4 at 24 hr, respectively (one-factor ANOVA; $P < 0.05$). The relative intensities of XIAP in the Vehicle, EPO, and asialoEPO were 9.2, 17.3, and 9.2 at 6 hr, respectively (one-factor ANOVA; $P < 0.05$), and 6.8, 14.3, and 18.9 at 24 hr, respectively (one-factor ANOVA; $P < 0.05$). The expression of Bcl-xL and XIAP in the asialoEPO group was greater than that in the EPO group (t test; $P < 0.05$).

We examined whether the protective effect of EPO and asialoEPO against I/R injury would result in improved survival. The survival rates at 7 days after I/R injury in the Sham, Vehicle, EPO, and AsialoEPO groups were 100%, 21.4%,

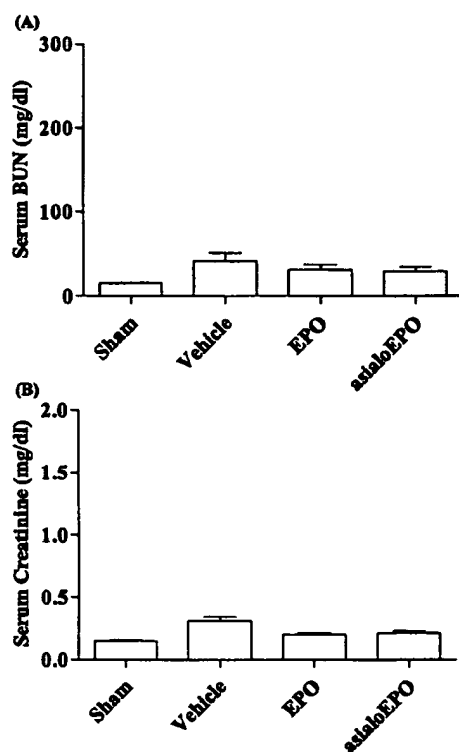


FIGURE 3. Plasma BUN and Cr levels at 7 days after I/R injury. At 7 days after I/R injury, there were no significant differences in plasma BUN (A) and Cr (B) levels between the Vehicle, EPO, and AsialoEPO groups.

23.1%, and 53.8%, respectively (Fig. 6). The survival rate in the AsialoEPO group was significantly higher than that in the Vehicle and EPO groups ($P=0.05$).

DISCUSSION

Previous studies have shown that EPO exerts protective effects in murine and rat models of acute kidney injury. In the study by Patel et al., I/R consisted of 30 min of ischemia, and EPO was given at a dose of 1000 IU/kg for 3 days before, and upon reperfusion. After 24 hr of reperfusion, EPO attenuated renal dysfunction as judged from the serum Cr level and histological studies, but the effect on survival was not reported (18). Many studies have investigated the effect of EPO in rats with acute renal failure. Yang et al. administered EPO (3,000 IU/kg) 24 hr before I/R injury, and reported that it significantly reduced the increase in the serum Cr level and apoptosis of proximal tubule epithelial cells (10). In another study, bolus injection of EPO at a low dose (300 IU/kg) protected the kidney from I/R injury (19). However, the effect of EPO on survival after I/R injury in rodent model was limited.

AsialoEPO, a fully desialated form of EPO, has several unique characteristics, including a shorter plasma half-life, more rapid elimination from the systemic circulation, and higher affinity for the EPO receptor (EPOR) in comparison with EPO (20). In the kidney, EPOR is expressed in proximal and distal tubule cells (21). Also, it has been shown that capillary endothelial cells express EPOR, including renal capillaries (22). Hypoxia activates molecules of the

hypoxia-inducible factor (HIF) family, including EPO (23), and thus the EPO-EPOR pathway is likely to be facilitated in I/R kidney.

It has been reported that the organ- and tissue-protective effects of EPO and its derivatives are exerted not only through the homodimer of classical EPOR, but also through a heterodimer of EPOR and the common β -subunit (CD131). The common β -subunit is expressed in various organs, such as the kidney and liver. Thus, the renoprotective effect of asialoEPO may be due to activation of EPOR and the common β -subunit heterodimer (24).

The intracellular signaling pathway utilized by EPO in kidney I/R injury is not fully understood. EPO binds to EPOR, and subsequently phosphorylates Janus kinase 2 (Jak2). Activation of Jak2 then leads to activation of a number of signaling pathways, such as those involving signaling transducer and activator of transcription 5 (STAT5), phosphoinositol 3 kinase (PI3K)/Akt, and mitogen-activated protein kinase (MAPK) (7).

MAPKs are serine/threonine kinases, consisting of at least three major groups: activation of extracellular signal-regulated kinase (ERK), p38-MAPK, and c-jun NH2-terminal kinase (JNK). MAPKs are activated by dual phosphorylation of tyrosine and threonine residues within their molecule. The ERK pathway is activated mainly by mitogens, and JNK and p38 are activated mainly by cellular stress. Activation of the JNK and p38 pathway leads to various biological events, such as apoptosis and inflammation. In a rat renal I/R model, activation of JNK reportedly triggered cell apoptosis (25). In other studies, activation of p38-MAPK exacerbated I/R injury in the heart (26, 27) and small intestine (28). Yang et al. reported that in a rat model of renal I/R injury, EPO administration inhibited the activation of JNK, and attenuated renal dysfunction (10). In the present study, EPO and asialoEPO did not inhibit the expression of JNK at 6 and 24 hr after I/R injury (data not shown). On the other hand, expression of p38-MAPK was strongly suppressed by EPO and asialoEPO at 24 hr after I/R injury. Thus, EPO and asialoEPO may exert their antiapoptotic effect by inhibiting the p38-MAPK signaling pathway in this mouse renal I/R model.

The mechanism responsible for the antiapoptotic effects of EPO remains unclear. Johnson et al. reported that in a rat acute renal failure model, EPO and darbepoietin decreased the expression of Bax, and did not affect the expression of Bcl-2 and Bcl-xL (29). On the other hand, Sharples et al. reported that EPO increased the expression of Bcl-xL and XIAP in vitro (19). The present study demonstrated that EPO and asialoEPO inhibited the expression of the proapoptotic molecule Bad, and increased the expression of the antiapoptotic molecules Bcl-xL and XIAP.

Our study showed that both EPO and asialoEPO improved the plasma BUN and Cr levels at 24 hr after I/R injury. The plasma levels of BUN and Cr in EPO- and asialoEPO-treated mice were not significantly different. Furthermore, TUNEL staining revealed that apoptosis was significantly inhibited in EPO- and asialoEPO-treated mice, but that the number of apoptotic cells did not differ significantly between the two groups. However, when survival rates were compared with that of vehicle-treated mice, it was found that whereas EPO had no effect on survival, asialoEPO improved survival significantly. The precise mechanism responsible for the bet-

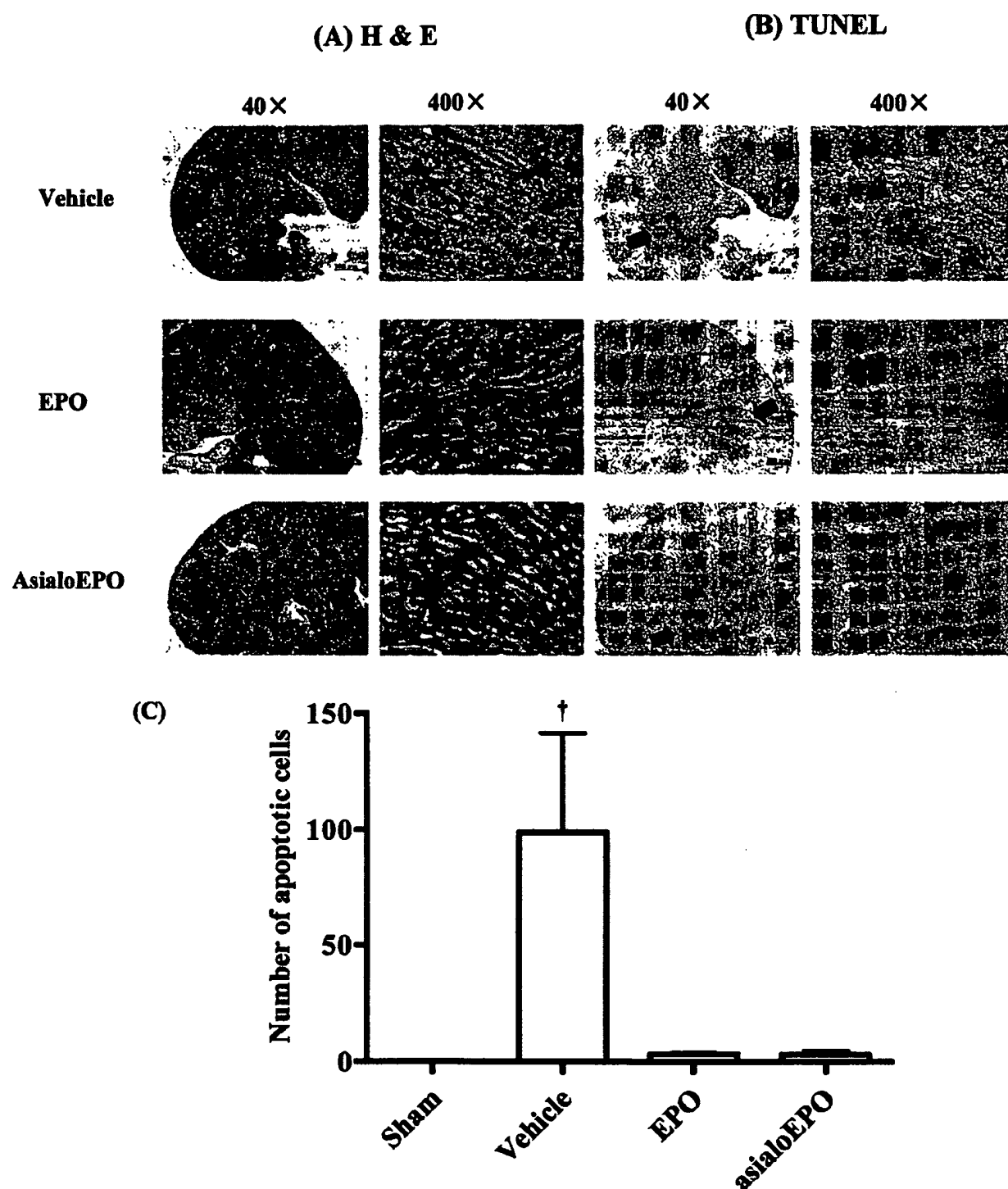


FIGURE 4. Apoptotic cells in the kidney after I/R injury in the Vehicle, EPO, and AsialoEPO groups. In each case, the right kidney was removed 24 hr after I/R injury and stained with hematoxylin and eosin (A) and by the TUNEL method (B). Apoptotic cells appear brown after TUNEL staining and are observed mainly at the corticomedullary junction. (C) Actual numbers of apoptotic cells were counted. The number of apoptotic cells was significantly higher in the Vehicle group than in the other three groups.

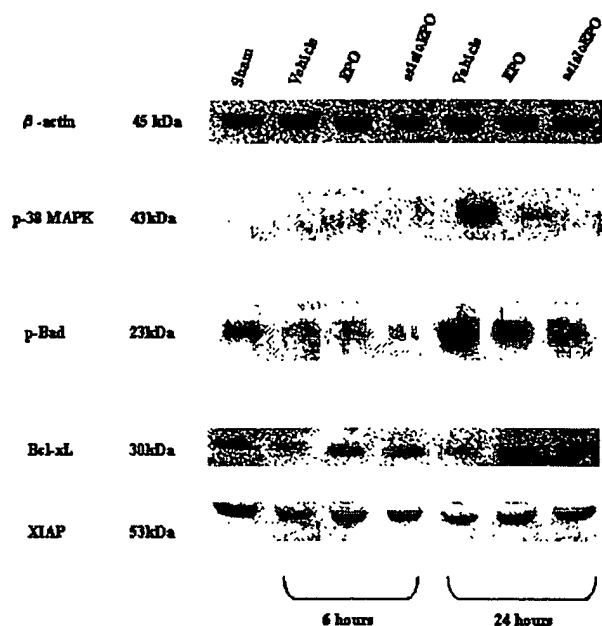


FIGURE 5. Protein expression in the kidney after I/R injury. EPO and asialoEPO inhibited the expression of p38-MAPK at 24 hr after I/R injury. EPO and asialoEPO also inhibited the expression of the pro-apoptotic molecule Bad, and stimulated the expression of the anti-apoptotic molecules Bcl-xL and XIAP at 24 hr after I/R injury. B-actin was used as an endogenous control.

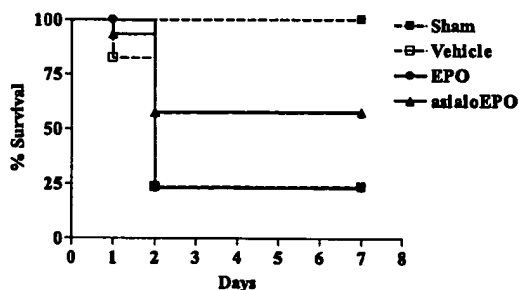


FIGURE 6. Survival after I/R injury. The survival rate at 7 days after I/R injury in the AsialoEPO group was significantly higher than that in the Vehicle and EPO groups.

ter survival of AsialoEPO-treated mice in comparison with EPO-treated mice remains to be elucidated. The higher affinity of AsialoEPO than that of EPO for the EPOR may result in a stronger intracellular cell survival signal by inhibiting apoptosis. In fact, densitometry of Western blots revealed a weaker Bad signal, and stronger Bcl-xL and XIAP signals at 24 hr after I/R injury.

The other possibility is that asialoEPO may exert a more systemic effect than EPO, and the extra-renal effect of asialoEPO may have contributed to the improved survival. In fact, the neuroprotective effect of asialoEPO has been extensively studied, and is reported to be more potent than that of EPO (30, 31). Furthermore, it has been reported that p38-MAPK has broad systemic effects. Inhibition of p38-MAPK activation reduces myocardial injury (32), and inhibits pro-

inflammatory cytokines such as IL-1 and TNF- α (33). In the present study, the more potent inhibitory effect of asialoEPO on p38-MAPK than that of EPO might have contributed to the improved survival. In addition, there was no significant difference in the number of apoptotic cells between the EPO and AsialoEPO groups (Fig. 4). However, asialoEPO may have inhibited tubule necrosis more potently than EPO by inhibition of p38-MAPK (25).

Although the cause of death in the experimental mice was unclear, our model, consisting of 60 min of ischemia in heminephrectomized mice, was more severe than previously reported models (10–13). Even in the asialoEPO-treated group, 46.2% of the mice died within 48 hr of I/R injury, and it is possible that some may have died due to causes other than renal dysfunction.

In conclusion, asialoEPO attenuates renal I/R injury to the same degree as EPO. The renoprotective effect of EPO and asialoEPO may be due to suppression of p-38-MAPK, inhibition of the pro-apoptotic molecule Bad, and activation of the anti-apoptotic molecules Bcl-xL and XIAP. These modulations of intracellular signaling are more potent for asialoEPO than for EPO. Further studies will be needed to clarify precisely why asialoEPO, but not EPO, improves the survival of mice with renal I/R injury.

ACKNOWLEDGMENTS

This work was partly supported by grant from The Kidney Foundation, Japan (JFKB07-34).

REFERENCES

- Nash K, Hafeez A, Hou S. Hospital-acquired renal insufficiency. *Am J Kidney Dis* 2002; 39: 930.
- Thakar CV, Liangos O, Yared JP, et al. ARF after open-heart surgery: influence of gender and race. *Am J Kidney Dis* 2003; 41: 742.
- Brines M, Cerami A. Emerging biological roles for erythropoietin in the nervous system. *Nat Rev Neurosci* 2005; 6: 484.
- Santhanam AV, Katusic ZS. Erythropoietin and cerebral vascular protection: role of nitric oxide. *Acta Pharmacol Sin* 2006; 27: 1389.
- Schneider C, Jaquet K, Malisius R, et al. Attenuation of cardiac remodeling by endocardial injection of erythropoietin: Ultrasonic strain-rate imaging in a model of hibernating myocardium. *Eur Heart J* 2007; 28: 499.
- Lipsic E, Schoemaker RG, van der Meer P, et al. Protective effects of erythropoietin in cardiac ischemia: From bench to bedside. *J Am Coll Cardiol* 2006; 48: 2161.
- Sharples E, Thiemeermann C, Yaqoob MM. Mechanism of disease: cell death in acute renal failure and emerging evidence for a protective role of erythropoietin. *Nat Clin Practice* 2006; 1: 87.
- Johnson DW, Forman C, Vesey DA. Novel renoprotective actions of erythropoietin: New use for an old hormone. *Nephrol* 2006; 11: 306.
- Bahlmann FB, DeGroot K, Duckert T, et al. Endothelial progenitor cell proliferation and differentiation is regulated by erythropoietin. *Kidney Int* 2003; 64: 1648.
- Yang CW, Li C, Jung JY, et al. Preconditioning with erythropoietin protects against subsequent ischemia-reperfusion injury in rat kidney. *FASEB J* 2003; 17: 1754.
- Ates E, Yalcin U, Yilmaz S, et al. Protective effect of erythropoietin on renal ischemia and reperfusion injury. *ANZ J Surg* 2005; 75: 1100.
- Sharples EJ, Yaqoob MM. Erythropoietin in experimental acute renal failure. *Nephrol* 2006; 104: e83.
- Minamino T, Kitakaze M. New therapeutic application of erythropoietin against ischemic heart diseases. *J Pharmacol Sci* 2006; 101: 179.
- Ehrenreich H, Hasselblatt M, Dembowski C, et al. Erythropoietin therapy for acute stroke is safe and beneficial. *Mol Med* 2002; 8: 495.

15. Higuchi M, Oh-eda M, Kuboniwa H, et al. Role of sugar chain in the expression of the biological activity of human erythropoietin. *J Biol Chem* 1992; 267: 7703.
16. Mennini T, De Paolo M, Bigini P, et al. Nonhematopoietic erythropoietin derivatives prevent motoneuron degeneration in vitro and in vivo. *Mol Med* 2006; 12: 153.
17. Vaziri ND, Zhou XJ, Liao SY. Erythropoietin enhances recovery from cisplatin-induced acute renal failure. *Am J Physiol* 1994; 266: F360.
18. Patel NS, Sharples EJ, Cuzzocrea S, et al. Pretreatment with EPO reduces the injury and dysfunction caused by ischemia/reperfusion in the mouse kidney. *Kidney Int* 2004; 66: 983.
19. Sharples E, Patel N, Brown P, et al. Erythropoietin protects the kidney against the injury and dysfunction caused by ischemia-reperfusion. *J Am Soc Nephrol* 2004; 15: 2115.
20. Imai N, Kawamura A, Tomonoh K, et al. Physicochemical and biological characterization of asialoerythropoietin. *Eur J Biochem* 1990; 194: 457.
21. Westenfelder C, Biddle DL, Baranowski RL. Human, rat, and mouse kidney cells express functional erythropoietin receptors. *Kidney Int* 1999; 55: 808.
22. Anagnostou A, Lee ES, Kessimian N, et al. Erythropoietin has a mitogenic and positive chemotactic effect on endothelial cells. *Proc Natl Acad Sci USA* 1990; 87: 5978.
23. Maxwell P. HIF-1: An oxygen response system with special relevance to the kidney. *J Am Soc Nephrol* 2003; 14: 2712.
24. Brines M, Grasso G, Fiordaliso F, et al. Erythropoietin mediates tissue protection through an erythropoietin and common β -subunit heteroreceptor. *Proc Natl Acad Sci USA* 2004; 41: 14907.
25. Kunduzova O, Bianchi P, Pizzinat N, et al. Regulation of JNK/ERK activation, cell apoptosis, and tissue regeneration by monoamine oxidases after renal ischemia-reperfusion. *FASEB J* 2002; 16: 1129.
26. Engelbrecht AM, Niesler C, Page C, et al. p38 and JNK have distinct regulatory functions on the development of apoptosis during simulated ischemia and reperfusion in neonatal cardiomyocytes. *Basic Res Cardiol* 2004; 99: 338.
27. Li Z, Ma Y, Kerr I, et al. Selective inhibition of p38 α MAPK improves cardiac function and reduces myocardial apoptosis in rat model of myocardial injury. *Am J Physiol Heart Circ Physiol* 2006; 291: H1972.
28. Murayama T, Tanabe M, Matsuda S, et al. JNK (c-jun terminal kinase) and p38 during ischemia reperfusion injury in the small intestine. *Transplantation* 2006; 81: 1325.
29. Johnson DW, Pat B, Vesey DA, et al. Delayed administration of darbepoietin or erythropoietin protects against ischemic acute renal injury and failure. *Kidney Int* 2006; 69: 1806.
30. Erbayraktar S, Grasso G, Sfacteria A, et al. Asialoerythropoietin is a nonerythropoietic cytokine with broad neuroprotective activity in vivo. *Proc Natl Acad Sci USA* 2003; 100: 6741.
31. Wang X, Zhu C, Wang X, et al. The nonerythropoietic asialoerythropoietin protects against neonatal hypoxia-ischemia as potentially as erythropoietin. *J Neurochem* 2004; 91: 900.
32. Li Z, Ma Y, Kerr I, et al. selective inhibition of p38 α MAPK improves cardiac function and reduces myocardial apoptosis in rat model of myocardial injury. *Am J Physiol Heart Circ Physiol* 2006; 291: H1972.
33. Lee JC, Kassis S, Kumar S, et al. p38 mitogen-activated protein kinase inhibitors-mechanism and therapeutic potentials. *Pharmacol Ther* 1999; 82: 389.

Activity of Bovine Pancreatic Deoxyribonuclease A with Modified Amino Groups*

(Received for publication, July 31, 1970)

BRYCE V. PLAPP†, STANFORD MOORE, AND WILLIAM H. STEIN

From The Rockefeller University, New York, New York 10021

SUMMARY

Guanidination of the nine ϵ -amino groups or picolinimidylation of the α - and ϵ -amino groups yielded active derivatives of DNase. Since modification of the enzyme with these large substituents, which have delocalized positive charges, should have inactivated the protein if amino groups were involved in the catalytic reaction, none of the primary amino groups of DNase can be essential for catalysis.

When positive charges on the enzyme were removed by carbamylation of the α -amino group and about seven ϵ -amino groups, the protein had about half of its original activity. But the Ca^{++} complex of this derivative was almost fully active. Carbamylation of the remaining two amino groups inactivated DNase and Ca^{++} did not restore activity; therefore, the positive charges on these groups probably help to maintain the active structure of the enzyme. It is not likely that the two amino groups are involved in binding Mn^{++} -DNA, since they do not seem to be freely available for reaction with cyanate.

Trinitrophenylation gave results similar to those of carbamylation, but only one amino group of Ca^{++} -free DNase or four to five groups of Ca^{++} -DNase could be trinitrophenylated without inactivation. The neutral, hydrophobic trinitrophenyl groups probably distort the enzyme more than carbamyl groups do. Two to three amino groups resisted trinitrophenylation, which may also indicate that these groups have structural roles.

Simplified procedures are described for the chromatographic determination of homocitrulline and for the spectrophotometric titration of free amino groups with 2,4,6-trinitrobenzenesulfonic acid.

The α -picolinimidyl, ϵ -guanidino derivative of DNase A was active, and its metal-chelating picolinimidyl group could facilitate the preparation of isomorphous derivatives for x-ray studies.

glycoproteins (1-3) with molecular weights of about 31,000 (4), each consisting of a single polypeptide chain (1, 2). Divalent metal ions are required for activity on DNA (5-7), for stability in the presence of proteases (2), and for re-formation of the disulfide bonds of reduced DNase A (8). Carboxymethylation of 1 histidine residue of DNase A in the presence of Cu^{++} or Mn^{++} inactivates the enzyme (9).

In order to determine whether the one α -amino and the nine ϵ -amino groups of DNase have a role in the mechanism of action of the enzyme or in maintaining its structure, we have modified the amino groups with several reagents. The activities of the derivatives and the effects of metal ions on them have been determined.

EXPERIMENTAL PROCEDURE¹

Materials—DNase, DP grade, was purchased from Worthington and purified by chromatography on phosphocellulose (1) after treatment with DFP² (2). A column (2 × 40 cm) with a sintered glass disc at the bottom was used and 500 mg of DNase were applied; the resolution was the same as on the longer column (1). The A form of DNase (1) was used for the following studies. DNase A, RNase A, and calf thymus DNA were also purchased from Worthington.

DFP and *O*-methylisourea hydrogen sulfate were obtained from Aldrich. Methyl picolinimidate was prepared and used as described previously (10). KNCO was recrystallized (11) and ¹⁴C-KNCO came from New England Nuclear. *N*-Ethylmorpholine was a product of Matheson Coleman and Bell, East Rutherford, New Jersey, and was redistilled over ninhydrin (12). Ultra Pure guanidinium chloride was obtained from Mann. Glycylglycine was supplied by Cyclo Chemical Company and ϵ -aminocaproic acid by K and K Laboratories, Plainview, New York; both had the correct elemental compositions. Other chemicals were reagent grade. Glass-distilled water was used for all solutions.

Dialysis tubing, from Union Carbide, New York, New York, was washed successively in hot 0.1 M Na_2CO_3 ,³ 20 mM sodium acetate and 1 mM EDTA buffer at pH 4.7, 10 mM acetic acid, and water, and stored in 95% ethanol at 4°.

Assay for DNase—DNase activity was determined by a modification of the hyperchromicity assay of Kunitz (13) as described

Bovine pancreatic deoxyribonuclease (deoxyribonuclease oligonucleotidohydrolase, EC 3.1.4.5) is a mixture of very similar

* This study was supported in part by a grant from the United States Public Health Service.

† Present address, Department of Biochemistry, The University of Iowa, Iowa City, Iowa 52240.

¹ The abbreviations used are: DFP, diisopropyl phosphorofluoridate; TNBS, 2,4,6-trinitrobenzenesulfonic acid.

² Throughout this work, the molarities of the buffers refer to the total concentrations of the species that buffer at the indicated pH.

by Price *et al.* (2). One unit of activity gives an increase in absorbance at 260 nm of 1.0 per min in a 1-cm cell of a solution of 40 μ g of calf thymus DNA per ml of 0.1 M sodium acetate and 5 mM MnCl_2 buffer, pH 5.0, at 25°. For one experiment, ZnCl_2 was used in place of the MnCl_2 .

Protein Analyses—The concentration of native DNase was determined spectrophotometrically by use of $A_{260\text{nm}}^{1\text{cm}} = 1.23$ for 1 mg per ml (1, 4). The concentration of derivatives of DNase A could be determined by amino acid analysis on the basis that the enzyme contains 6 histidine, 12 arginine, 33 aspartic acid, 20 glutamic acid, and 22 alanine residues (2). Alternatively, the amount of protein could be estimated (to $\pm 15\%$) by alkaline hydrolysis and ninhydrin analysis (14, 15) with the experimentally determined color yield equivalent to 5.7 μ moles of leucine per mg of protein.

Proteins were hydrolyzed (16) and analyzed for amino acids (17) with accelerated systems (18) on columns of Beckman-Spinco AA-15 (0.9×65 cm) and AA-27 (0.9×11 or 0.6×10 cm) or M-82 (0.9×54 cm) and PA-35 (0.9×6 cm) resins. Homoarginine eluted just after arginine and was assumed to have the same color value as arginine. Picolinimidyllysine was determined as previously described (10). The amino acid compositions, except for lysine, of all of the derivatives were the same as native DNase.

The extent of modification of the NH_2 -terminal leucine residues (1) was determined with the cyanate method (19). Carbamylated DNase (native or modified) gave significant, but variable, amounts of threonine, serine, glutamic acid, and glycine. However, blank determinations on uncarbamylated DNase gave similar amounts, indicating that these amino acids were not NH_2 -terminal.

Determination of Homocitrulline by Amino Acid Analysis—Homocitrulline was eluted between cystine and valine on a column (0.9×64 cm) of Beckman-Spinco resin AA-15 developed at 50 ml per hour with 0.2 N sodium (citrate) buffer, pH 3.30, i.e. 0.05 pH unit higher than usual (17), at 56° (2° higher than usual). The higher pH shifts the cystine peak forward so that it largely overlaps the alanine peak (20). The higher temperature shifts the homocitrulline peak forward so that it is resolved from the valine peak. These modifications permit one to determine homocitrulline on the same column used for routine analysis, rather than on a 150-cm column (21). A separate analysis of the same sample with the usual conditions is required for the determination of alanine and cystine. The color value for an analytically pure sample of homocitrulline was found to be $118 \pm 3\%$ of the average of the values for glycine and valine. Since homocitrulline is slowly hydrolyzed to lysine (19), carbamylated DNase was hydrolyzed for 22 and 46 hours, and the values for homocitrulline were extrapolated with first order kinetics to zero time. The sum of the lysine and homocitrulline residues found was slightly less than the number of lysine residues in native DNase in some samples.

Determination of Number of Free Amino Groups with 2,4,6-Trinitrobenzenesulfonic Acid—The TNBS reaction (22) was carried out under modified conditions (23). In a 1-cm cuvette, 200 μ l of 0.6 M sodium borate buffer, pH 9.5, was mixed with 200 μ l of a solution of DNase or a derivative of DNase (2 to 4 mg per ml) in 0.05 or 0.10 M sodium acetate buffer, pH 4.7, with or without 1 to 5 mM CaCl_2 . After 50 μ l of 0.2 M NaOH were added, the reaction was initiated by the addition of 50 μ l of a

freshly prepared solution of 7.2 mg of TNBS¹ per ml of water. The reaction mixtures were kept at 25° in the cuvette holder in the spectrophotometer and were not exposed to light except when the absorbance at 367 nm was measured against a control mixture with the same composition as the reaction mixture except that the solution of protein was replaced with the buffer against which the protein was dialyzed. The wave length was chosen because it is at the isosbestic point for ϵ -trinitrophenyl- α -acetyllysine and its sulfite complex and thus the extinction coefficient (at 367 nm, $1.1 \times 10^4 \text{ M}^{-1} \text{ cm}^{-1}$ (25)) does not change with the extent of reaction. Hence it is not necessary to acidify the solution before each reading (23). An advantage of the method described here as compared to the method with one time of reaction (23) is that the continuous method may reveal classes of amino groups with different reactivities (26, 27). Furthermore, it is possible to follow the reaction to completion, or at least until a class of groups has fully reacted.

Glycylglycine and ϵ -aminocaproic acid reacted with TNBS giving maximum absorbance ($\epsilon = 1.1 \times 10^4 \pm 10\% \text{ M}^{-1} \text{ cm}^{-1}$ at 367 nm) in 20 and 60 min, respectively (second order rate constants 100 and $40 \text{ M}^{-1} \text{ min}^{-1}$). Similarly, 9.9 of the 11 amino groups of RNase A (phosphate-free) reacted in 60 min. Eight of the ten amino groups of Ca^{++} -free DNase reacted with TNBS (with pseudo first order kinetics) in 1.5 to 3 hours. In the presence of 5 mM CaCl_2 , 7.3 amino groups reacted in 3 hours. Based on these studies, we have assumed that any free amino groups (of the seven to eight groups that can react with TNBS in native DNase) of a derivative of DNase react with TNBS in 1 to 4 hours. (With some derivatives, the A_{367} continued to increase after 4 hours, but the reaction was very slow and probably not with primary amino groups.) Independent analyses of the free α - and ϵ -amino groups of various derivatives were consistent with this assumption. We used this procedure principally to support the chemical analyses or to allow us to determine quickly how many amino groups were free. For instance, we found more free groups in some derivatives than were expected, and we used this as presumptive evidence that proteases had exposed additional α -amino groups; treatment of DNase with DFP before derivatization prevented the appearance of extra amino groups.

RESULTS

Guanidination of DNase—DNase A, 100 mg, was dissolved in 4 ml of 0.25 M sodium acetate buffer,² pH 4.7, containing 20 μ l of DFP and allowed to stand 2 hours at room temperature.⁴

¹ TNBS was prepared from picryl chloride and sodium bisulfite (24), and recrystallized from 5 M HCl; the white crystals were dried over P_2O_5 in a vacuum (water pump): 82° sintered, m.p. 189–192°. To determine the formula weight of the TNBS, which has variable water content, we determined the elemental composition with a Perkin-Elmer 240 Elemental Analyzer: found C 19.86, H 2.45, N 10.02. From the percentage C, we calculated a weight of 360 (3.7 H_2O): theoretical C 20.01, H 2.90, N 11.67. Although the percentage N was low, we believe the analyzer gives incorrect results with trinitrophenyl compounds. The sodium salt of TNBS, which is dihydrated, gave correct percentages for C and H, but low N also.

² DFP treatment at pH 4.7 inactivated traces of proteases in the purified DNase A. At pH 10.6, DFP inactivated DNase, and three diisopropylphosphoryl groups were incorporated into DNase that had 15% residual activity after treatment with 60 mM DFP at pH 10.6 and 25° for 1 hour. At pH 8 or 4.7, DNase was not inactivated by DFP, and, at pH 4.7 (2), diisopropylphosphoryl groups were not incorporated into DNase.

The solution of DNase was dialyzed against 10 mM CaCl_2 at 4° and mixed with an equal volume of 1.0 M *O*-methylisourea at pH 10.6 (adjusted with NaOH). The reaction was allowed to proceed 4 days at 4° (28) and was stopped by dialysis against 0.1 M sodium acetate and 5 mM CaCl_2 buffer, pH 4.7, at 4°. A small amount of insoluble protein was removed by centrifugation. The specific activity of the derivative was 55 units per mg, or 75% of the initial activity. Amino acid analyses showed that all of the 9 lysine residues had been converted to homo-arginine residues. Analysis showed 0.8 ± 0.2 residue of NH_2 -terminal leucine, indicating that the α -amino group was not modified. In confirmation of these analyses, the TNBS reaction (220 min) showed 0.8 free amino group per molecule of guanidino-DNase. The ultraviolet spectrum of guanidinated DNase was very similar to that of native DNase.

If DNase was guanidinated in the absence of CaCl_2 , without the DFP treatment, the derivative had all of its ϵ -amino groups guanidinated and its α -amino group free, but it was only 40% as active as native DNase.

Picolinimidylation of DNase—The conditions for this modification reaction were adapted from Benisek and Richards (29). DNase, 10 mg per ml, in 0.5 M triethanolamine-HCl buffer, pH 8.0, containing 1 mM CaCl_2 , was treated with 0.1 M methyl picolinimidate for 22 hours at 25°, and then with 0.2 M reagent for an additional 8 hours. The picolinimidylated DNase was freed of reagent by dialysis against a 0.05 M sodium acetate and 1 mM CaCl_2 buffer, pH 4.7, at 4°. A small amount of insoluble protein was removed by centrifugation. The derivative had the same specific activity as the starting material. As shown in Fig. 1, about ten picolinimidyl groups were incorporated into the derivative. The red shift in the difference spectrum as compared to the theoretical spectrum was apparent also if the spectrum of picolinimidylated DNase was measured in the absence of CaCl_2 or in the presence of 4.8 M guanidinium chloride. Amino acid analyses showed the presence of about nine picolinimidyllysines, and there was only 0.3 eq of NH_2 -terminal leucine. (Reaction of DNase with 0.1 M methyl picolinimidate for 24 hours resulted in the modification of the nine lysines but only about half of the NH_2 -terminal leucine residues.) Determination of the free amino groups of the derivative with TNBS showed 0.6 of a residue. Thus, most of the amino groups were picolinimidylated.

When DNase was picolinimidylated in the absence of CaCl_2 (and dialyzed against sodium acetate buffer without CaCl_2), its activity was essentially unchanged and about 9.5 picolinimidyl groups were incorporated (as determined by spectral analyses at pH 4.7 with or without 4.8 M guanidinium chloride). Amino acid analyses gave about nine picolinimidyllysines. However, the TNBS reaction showed 2.6 amino groups that reacted in 2 hours. These amino groups probably arose from proteolysis, to which DNase is much more susceptible in the absence of Ca^{++} (2).

α -Picolinimidyl, ϵ -Guanidino-DNase—Since the nine ϵ -amino groups could be guanidinated without modifying the α -amino group or inactivating DNase and the ϵ - and α -amino groups can be picolinimidylated without inactivating DNase, it seemed feasible to prepare an active derivative of DNase with one picolinimidyl group per molecule. Following the approach used by Benisek and Richards (29), we picolinimidylated the guanidinated protein.

The guanidino-DNase was prepared as described in a preced-

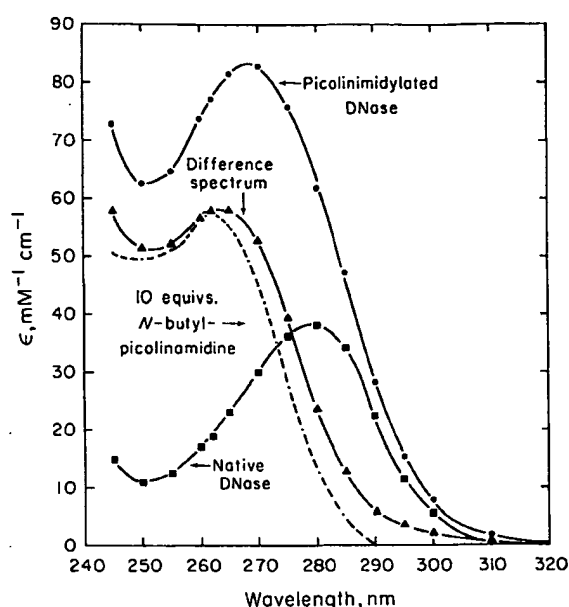


FIG. 1. Spectral characterization of picolinimidylated DNase. The spectra of picolinimidylated DNase (●—●) and native DNase (■—■) and the difference spectrum (▲—▲) are presented. From the absorption at 262 nm and the extinction coefficient for *N*-butylpicolinimidine ($5700 \text{ M}^{-1} \text{ cm}^{-1}$ (29)), we calculated that the derivative had about 10 picolinimidyl groups for which the theoretical difference spectrum is given (---). The proteins were dissolved in 0.05 M sodium acetate and 1 mM CaCl_2 , pH 4.7, and clarified by centrifugation. The spectra were read with a Zeiss PMQ II spectrophotometer. The concentration of DNase was determined from the absorption at 280 nm and the concentration of picolinimidylated DNase was determined by amino acid analysis. A molecular weight of 31,000 (4) was assumed in the calculations.

ing section and was dissolved in 0.1 M sodium acetate and 5 mM CaCl_2 buffer, pH 4.7. A one-third volume of 2 M triethanolamine-HCl and 5 mM CaCl_2 buffer, pH 8, was added, bringing the pH of the solution to 8. We added 1 drop of DFP (about 10 μl) per 4 ml of solution to inactivate proteases. Then 50 μl of methyl picolinimidate were added to each 4 ml of solution (making the solution 0.1 M in reagent) and the reaction was allowed to proceed for 12 hours at 25°, at which time an additional 50 μl of methyl picolinimidate per 4 ml were added. After 12 more hours, the reaction was terminated by dialysis of the solution against 0.1 M sodium acetate and 5 mM CaCl_2 buffer, pH 4.7, at 4°. A small amount of precipitate was removed by centrifugation; the over-all yield of soluble protein was about 70%. The derivative had a specific activity of about 47 units per mg, which is about 65% the activity of the native DNase (dissolved in 0.1 M sodium acetate and 10 mM CaCl_2 buffer, pH 4.7, before assay).

About 1.5 (± 0.4) picolinimidyl groups were incorporated into the derivative as determined from the difference spectra between the derivative and the guanidino-DNase in the presence or absence of 4.8 M guanidinium chloride. The difference spectra were similar to the theoretical spectrum for *N*-butylpicolinimidine, except that the protein derivative had more absorption at 295 nm (as in Fig. 1). This absorption could be due to metals complexing the picolinimidyl groups; however, the addition of EDTA to the solution without guanidinium chloride did not

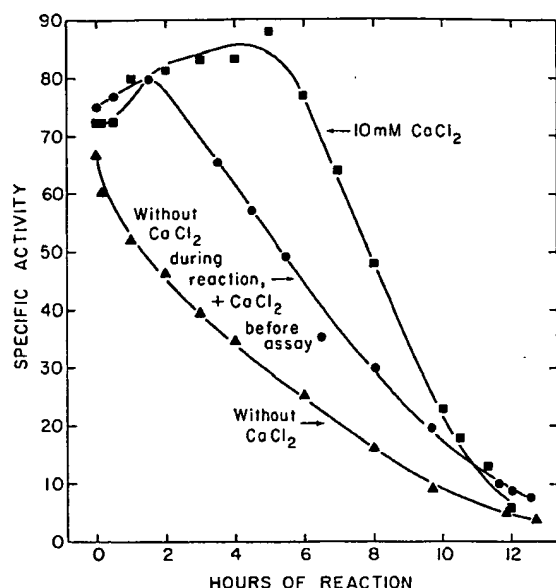


FIG. 2. Inactivation of DNase by cyanate. DNase A, 10 mg per ml, in 1.0 M triethanolamine-HCl buffer, pH 8.0, was treated with 1.0 M KNCO at 37°. The effect of CaCl_2 on the inactivation was tested in two different ways: 10 mM CaCl_2 was present during the carbamylation (■—■), or the enzyme was carbamylated in the absence of CaCl_2 , and then diluted into 10 mM CaCl_2 , 15 min before assay (●—●). For comparison, DNase was carbamylated and assayed in the absence of CaCl_2 (▲—▲). For the enzyme assays an aliquot (0.2 ml) of the reaction mixtures was added to 0.8 ml of 1 M glycylglycine, pH 7. Some of the sample was diluted further (4-fold) into 1 M Tris-HCl buffer, pH 8, with or without 10 mM CaCl_2 . Alternatively, a sample of the reaction mixture was diluted 20-fold into 1 M Tris-HCl buffer, pH 8, with or without 10 mM CaCl_2 . For all assays, 10 μl of the diluted reaction mixture were added to the 1-ml assay mixture.

significantly change the difference spectrum. Perhaps an α -picolinimidyl group does not have the same spectrum as *N*-butylpicolinamidine.

The modified DNase had 0.07 residue of NH_2 -terminal leucine. Since the guanidino-DNase had 0.8 ± 0.2 NH_2 -terminal leucine, picolinimidylation of the α -amino group was almost complete. Amino acid analysis showed a trace of ϵ -picolinimidyllysine, corresponding to about 0.3 residue per molecule. These data indicate that the major product was the desired derivative, but that some molecules of DNase have been picolinimidylated on both α - and ϵ -amino groups and some enzyme with a free α -amino group was present. The TNBS reaction showed that 1.3 groups were free to react within 2 hours; although ϵ -picolinamidines apparently do not react rapidly with TNBS (see previous section), α -picolinamidines may react, which would account for this observation.

We studied the structural stability of the derivative by reducing its disulfide bonds and then allowing them to re-form in the presence of Ca^{++} (8). The enzyme was reduced with 50 mM mercaptoethanol in 50 mM Tris-HCl, pH 7.2, and 5 mM EDTA at 25°. The derivative and DNase lost activity at the same rate. After 60 min of reaction both enzymes were essentially inactive (on Zn^{++} -DNA), but the addition of CaCl_2 (20 mM) at that time initiated the regain of activity. Although DNase and the derivative both regained about 60% of their original activity, the derivative regained activity at about one-half of

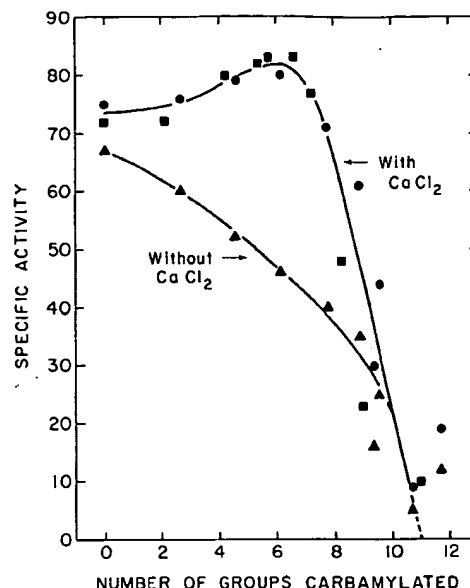


FIG. 3. Incorporation of cyanate into DNase during inactivation. DNase was treated with ^{14}C -KNCO and assayed for enzymic activity as described in Fig. 2. The number of groups carbamylated in Ca^{++} -DNase (■—■), Ca^{++} -free DNase assayed in the presence of Ca^{++} (●—●), or Ca^{++} -free DNase (▲—▲) was determined as follows. Aliquots of the reaction mixtures were taken at 10 min, and 1, 2, 3, 4, 6, 8, 10, and 12 hours and diluted into 1 M glycylglycine (brought to pH 7 with 1 M Tris) as a means of stopping the carbamylation. These samples were dialyzed at 4° against 0.1 M Tris-HCl buffer, pH 8, and then 0.1 M *N*-ethylmorpholine-HCl buffer, pH 8.0, until the radioactivity (10) of the outer dialysate approximated the radioactivity of the background. Samples of the inner dialysate were taken for the determination of the radioactivity (collecting at least 10,000 counts above background) and protein concentration. Samples of the original reaction mixture were counted for the determination of the specific radioactivity of the cyanate. The reaction carried out in the presence of 10 mM CaCl_2 (■—■) had 16 μCi per mmole of cyanate; the reaction without CaCl_2 (●—●, ▲—▲) had 9.3 μCi per mmole of cyanate.

the rate of native DNase. Apparently the structure was not markedly affected by modification of all of the amino groups.

Reaction of DNase and Cyanate—Since substitution of the ϵ -amino groups with positively charged groups did not inactivate DNase, the carbamylation of DNase, which leads to uncharged groups, was studied. At pH 8, cyanate forms stable derivatives with α - and ϵ -amino groups, but not with other functional groups of proteins (11). As shown in Fig. 2, carbamylation of DNase in the presence of 10 mM CaCl_2 slightly increased the activity of DNase. After about 6 hours of reaction, cyanate began to inactivate DNase. If CaCl_2 was not present during the reaction, but if the carbamylated enzyme was diluted into 10 mM CaCl_2 15 min before assay, it was 2 hours before inactivation became apparent. If CaCl_2 was never added, cyanate inactivated DNase without a lag and with pseudo first order kinetics (calculated as a second order rate constant, $k = 2.7 \times 10^{-3} \text{ M}^{-1} \text{ min}^{-1}$) over at least the first 8 hours of reaction.

The activity of DNase as a function of the incorporation of cyanate is presented in Fig. 3. When DNase was carbamylated in the presence or absence of CaCl_2 but assayed after dilution into 10 mM CaCl_2 , 7 to 8 molecules of cyanate could be incorporated

per molecule of DNase without a significant loss of enzymic activity. Incorporation of 3 to 4 more molecules of cyanate led to almost complete inactivation. (Cyanate was incorporated faster into Ca^{++} -free DNase than into the Ca^{++} complex of DNase, thereby shifting the relative positions of the curves from that seen in Fig. 2.) In contrast, the incorporation of up to about 8 molecules of cyanate into Ca^{++} -free DNase was accompanied by partial inactivation of the enzyme. Almost complete inactivation was again obtained with the incorporation of about 11 eq of cyanate. (The extrapolation to 11 is only approximate because of the few points and the inaccuracies of the determinations of radioactivity and protein concentration. We assume that the actual number is 10 (2).)

From NH_2 -terminal analysis and analysis for homocitrulline we determined the number of amino groups modified in DNase that was treated with cyanate in the presence of 10 mM CaCl_2 (as in Fig. 2) for 6 or 24 hours, dialyzed against water, and lyophilized. With the usual procedures of the cyanate method (19), carbamylated NH_2 -terminal residues were cleaved from the protein by cyclization to the hydantoins, and the hydantoins were isolated and hydrolyzed to the free amino acids. One residue of leucine per molecule was obtained for each preparation, indicating that the α -amino group was completely modified. From the rate of reaction of KNCO with α -amino groups (11), only about 15 min should be required to carbamylate completely the α -amino group. On the other hand, ϵ -amino groups are modified about 100 times more slowly (11). From amino acid analyses, the sample carbamylated for 6 hours had 6.9 residues of homocitrulline and the sample carbamylated 24 hours had 8.5 residues.

Trinitrophenylation of DNase—As with carbamylation, trinitrophenylation of amino groups leads to uncharged derivatives, but the trinitrophenyl group is larger than the carbamyl group and is hydrophobic.

DNase reacted readily with TNBS and was inactivated. In the absence of added metal ions, the inactivation began after only about one amino group had reacted, and thereafter the activity remaining was proportional to the number of trinitrophenyl groups incorporated (Fig. 4). Extrapolation of the data to zero activity indicated that reaction of seven amino groups occurred during complete inactivation. If the reaction mixture contained 5 mM CaCl_2 , about four groups could react without causing loss of activity, but, again, when seven groups had reacted, the activity was completely lost.

The stabilizing effect of CaCl_2 was also apparent from the kinetics of trinitrophenylation of the DNase in the two experiments. Without CaCl_2 , the inactivation was pseudo first order (after a 30-min lag) with a calculated second order rate constant of about $60 \text{ M}^{-1} \text{ min}^{-1}$. The rate of incorporation of trinitrophenyl groups was pseudo first order throughout the course of 150 min of reaction, with a second order rate constant of about $50 \text{ M}^{-1} \text{ min}^{-1}$. In the presence of CaCl_2 the rate of inactivation was also pseudo first order (after a 120-min lag) with a second order rate constant of $7 \text{ M}^{-1} \text{ min}^{-1}$. The incorporation data, however, revealed two classes of amino groups (26): three reacting with the rate constant of about $68 \text{ M}^{-1} \text{ min}^{-1}$ and four with a rate of about $12 \text{ M}^{-1} \text{ min}^{-1}$.

If 50 mM MgCl_2 was present during the reaction, instead of 5 mM CaCl_2 , the activity *versus* incorporation curve resembled the curve with CaCl_2 , except that only about three groups could be modified without loss of activity. Thus Mg^{++} can also

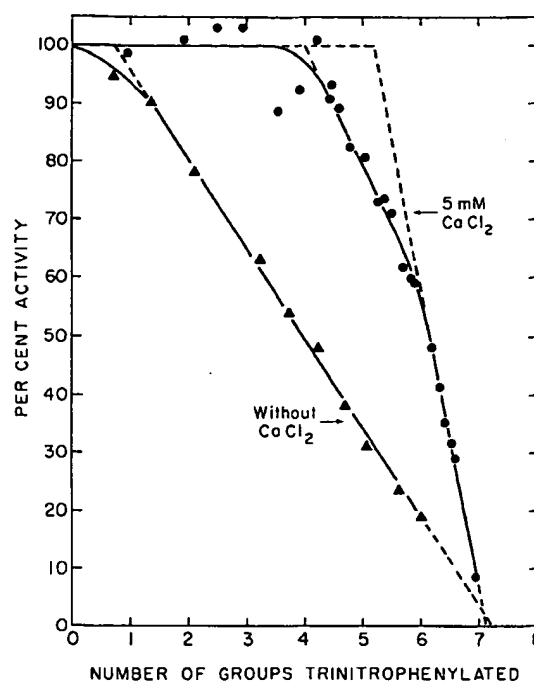


FIG. 4. Inactivation of DNase by the incorporation of trinitrophenyl groups. DNase A, about 0.5 mg per ml, in 0.3 M sodium borate buffer, pH 9.5, was treated with 0.29 mM TNBS in the dark at 25° for 5 hours in the absence of metal ions (Δ — Δ) or for 23 hours in the presence of 5 mM CaCl_2 (\bullet — \bullet). The absorption at 367 nm was measured against a control reaction containing TNBS but no DNase. At appropriate times 10 μ l of the reaction mixture were taken for assay of the enzyme activity. DNase lost no activity if TNBS was not present.

stabilize trinitrophenylated DNase. Adding CaCl_2 to DNase that was partially carbamylated in the absence of CaCl_2 increased the enzymic activity and counteracted to some extent the modification of amino groups (Fig. 2). Therefore we determined whether Mg^{++} could increase the activity of DNase trinitrophenylated in the absence of metal ions. During the reaction, the enzyme was assayed before and after dilution into 50 mM MgCl_2 in 0.3 M sodium borate, pH 9.5. Although Mg^{++} increased the activity observed (by 25% initially), the plots of the percentage of activity against incorporation were the same.

As shown in Fig. 4, the activity *versus* incorporation curves extrapolate to about seven groups incorporated at zero activity. However, the number of groups incorporated at maximum reaction (A_{367} at observed or calculated maximum) was 7.6 to 7.9 without CaCl_2 , 6.9 with 5 mM CaCl_2 , and 7.6 with 50 mM MgCl_2 . Determination of the number of free amino groups with 2 mM TNBS (as described under "Experimental Procedure") gave 8.0 ± 0.1 groups, with or without 50 mM MgCl_2 , but only 7.3 in the presence of 5 mM CaCl_2 . Since DNase has ten amino groups, apparently two to three do not react with TNBS.

DISCUSSION

The derivatives of DNase prepared in this work, the numbers of amino groups modified in each, and their activities are summarized in Table I. Since the guanidino and picolinimidyl derivatives are active we conclude that none of the primary amino groups of DNase is essential for catalysis of the hydrolysis of Mn^{++} -DNA. Although the guanidino and picolinimidyl

groups are positively charged at the pH of the assay (5.0) the charges are delocalized by resonance and the substituents are larger than the amino group. Thus we would expect the derivatives to be inactive if any amino group were essential for catalysis. Guanidination (30) or acetimidylation (31) of the amino groups of RNase A inactivates that enzyme, without causing gross structural changes (31), presumably by modifying the ϵ -amino group of lysine 41, which is at the active site (32, 33).

Carbamylation of the α -amino group and about seven of the ϵ -amino groups of Ca^{++} -free DNase markedly reduces the activity of the enzyme, but Ca^{++} can reverse this apparent inhibition. Thus removal of the positive charges on the amino groups probably alters the structure of DNase. It has been shown that Ca^{++} stabilizes the enzyme (2, 8); the present results show that Ca^{++} also counteracts the effects of carbamylation of eight amino groups.

Completely carbamylated DNase is inactive and Ca^{++} cannot restore its activity. One might conclude from this result that two amino groups are essential for activity; they could be

involved in the binding of DNA, for instance. But these amino groups do not appear to be freely available for such interactions since they are the last groups to react with cyanate. We think it is more likely that the two amino groups participate in maintaining the three-dimensional structure by ionic or hydrogen bonding. Once these groups are modified the enzyme may change into an inactive conformation. In any case, it is clear that removal of the positive charges on these critical groups inactivates DNase. Guanidination or picolinimidylation of these amino groups does not interfere with the normal roles of these groups in determining the active conformation of the molecule; apparently the positively charged substituents can be accommodated by the protein structure. Such modified amino groups could participate in ionic or hydrogen bonding with only slightly less effectiveness than primary amino groups.

We did not study the guanidination and picolinimidylation as a function of the time of reaction, so we do not know whether two amino groups are also less accessible in these reactions. Furthermore, we do not know whether the 2 eq of amino groups that react last with cyanate are on 2 specific lysine residues or distributed among several lysines. Cyanate also inactivates RNase, but it is the carbamylation of the first amino groups to react that leads to inactivation (21).

The results with trinitrophenylation of DNase were similar to those with carbamylation, but fewer groups could be trinitrophenylated without loss of activity. The hydrophobic trinitrophenyl groups could interact with hydrophobic regions of the enzyme, thereby altering the structure of the protein considerably. With RNase A, dinitrophenylation of the especially reactive ϵ -amino group of lysine 41 inactivates the enzyme, apparently with a concomitant conformational change (34); dinitrophenylation of the α -amino group, which is not near the active site (32, 33), reduces the activity of RNase 40% (34). Two to three amino groups of DNase apparently cannot react with TNBS; perhaps these are the same groups that react last with cyanate.

The α -picolinimidyl, ϵ -guanidino derivative is active and might be useful for x-ray crystallography. The picolinimidyl group chelates various heavy metal ions and the preparation of isomorphous derivatives could be facilitated. Benisek and Richards (29) found that the corresponding derivative of lysozyme is fully active and can be crystallized.

Acknowledgments—We are grateful to Mrs. Rita Blanchard for her expert technical assistance, to Dr. William F. Benisek for his helpful discussions about picolinimidylation, and to Mr. S. Theodore Bella for the elemental analyses.

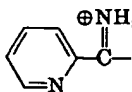
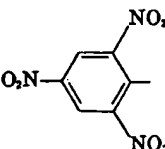
REFERENCES

1. SALNIKOW, J., MOORE, S., AND STEIN, W. H., *J. Biol. Chem.*, **245**, 5685 (1970).
2. PRICE, P. A., LIU, T.-Y., STEIN, W. H., AND MOORE, S., *J. Biol. Chem.*, **244**, 917 (1969).
3. CATLEY, B. J., MOORE, S., AND STEIN, W. H., *J. Biol. Chem.*, **244**, 933 (1969).
4. LINDBERG, U., *Biochemistry*, **6**, 335 (1967).
5. LASKOWSKI, M., SR., in P. D. BOYER, H. LARDY, AND K. MYRBÄCK (Editors), *The enzymes*, Vol. 5B, Academic Press, New York, 1961, p. 123.
6. SHACK, J., AND BYNUM, B. S., *J. Biol. Chem.*, **239**, 3843 (1964).
7. MELGAR, E., AND GOLDTHWAIT, D. A., *J. Biol. Chem.*, **243**, 4409 (1968).
8. PRICE, P. A., STEIN, W. H., AND MOORE, S., *J. Biol. Chem.*, **244**, 929 (1969).

TABLE I

Derivatives of DNase A and their activities

The number of amino groups modified was determined by the various methods described in the text. The activity is relative to native DNase assayed in the same way; the derivative was in a solution containing CaCl_2 before assay unless otherwise indicated. The activities for the carbamyl and trinitrophenyl derivatives are taken from Figs. 3 and 4.

Derivative	Substituent	CaCl_2 used in preparation	No. of amino groups modified	Activity
		mM		%
Guanidino	$\oplus\text{NH}_2$	0	8.8 ϵ , 0.1 α	40
	$\text{H}_2\text{N}-\text{C}=\text{NH}$	5	8.9 ϵ , 0.2 α	75
Picolinimidyl	$\oplus\text{NH}_2$	0	9.5 ($\epsilon + \alpha$)	100
		1	9 ϵ , 0.7 α	100
α -Picolinimidyl, ϵ -guanidino		5	9.0 ϵ , 0.9 α	65
Carbamyl	O	0	7 ϵ , 1 α	55 ^a
	$\text{H}_2\text{N}-\text{C}=\text{O}$	0 or 10	7 ϵ , 1 α	90
		0 or 10	9 ϵ , 1 α	0
Trinitrophenyl		0	1	95 ^a
		0	7-8	0 ^a
		5	4-5	100
		5	7	0

^a Assayed in the absence of Ca^{++} .

9. PRICE, P. A., MOORE, S., AND STEIN, W. H., *J. Biol. Chem.*, **244**, 924 (1969).
10. PLAPP, B. V., *J. Biol. Chem.*, **245**, 1727 (1970).
11. STARK, G. R., in C. H. W. HIRS (Editor), *Methods in enzymology*, Vol. XI, Academic Press, New York, 1967, p. 590.
12. HILL, R. L., AND DELANEY, R., in C. H. W. HIRS (Editor), *Methods in enzymology*, Vol. XI, Academic Press, New York, 1967, p. 339.
13. KUNITZ, M., *J. Gen. Physiol.*, **33**, 349 (1950).
14. FRUCHTER, R. G., AND CRESTFIELD, A. M., *J. Biol. Chem.*, **240**, 3868 (1965).
15. MOORE, S., *J. Biol. Chem.*, **243**, 6281 (1968).
16. MOORE, S., AND STEIN, W. H., in S. P. COLOWICK AND N. O. KAPLAN (Editors), *Methods in enzymology*, Vol. VI, Academic Press, New York, 1963, p. 819.
17. SPACKMAN, D. H., STEIN, W. H., AND MOORE, S., *Anal. Chem.*, **30**, 1190 (1958).
18. SPACKMAN, D. H., in C. H. W. HIRS (Editor), *Methods in enzymology*, Vol. XI, Academic Press, New York, 1967, p. 3.
19. STARK, G. R., AND SMYTH, D. G., *J. Biol. Chem.*, **238**, 214 (1963).
20. MOORE, S., AND STEIN, W. H., *J. Biol. Chem.*, **192**, 663 (1951).
21. STARK, G. R., STEIN, W. H., AND MOORE, S., *J. Biol. Chem.*, **235**, 3177 (1960).
22. SATAKE, K., OKUYAMA, T., OHASHI, M., AND SHINODA, T., *J. Biochem. (Tokyo)*, **47**, 654 (1960).
23. LOVERDE, A., AND STRITTMATTER, P., *J. Biol. Chem.*, **243**, 5779 (1968).
24. WILLGERODT, C., *J. Prakt. Chem.*, **32**, 117 (1885).
25. GOLDFARB, A. R., *Biochemistry*, **5**, 2570 (1966).
26. GOLDFARB, A. R., *Biochemistry*, **5**, 2574 (1966).
27. FREEDMAN, R. B., AND RADDA, G. K., *Biochem. J.*, **108**, 383 (1968).
28. KIMMEL, J. R., in C. H. W. HIRS (Editor), *Methods in enzymology*, Vol. XI, Academic Press, New York, 1967, p. 584.
29. BENISEK, W. F., AND RICHARDS, F. M., *J. Biol. Chem.*, **243**, 4267 (1968).
30. KLEE, W. A., AND RICHARDS, F. M., *J. Biol. Chem.*, **229**, 489 (1957).
31. REYNOLDS, J. H., *Biochemistry*, **7**, 3131 (1968).
32. WYCKOFF, H. W., TSEBNOGLOU, D., HANSON, A. W., KNOX, J. R., LEE, B., AND RICHARDS, F. M., *J. Biol. Chem.*, **245**, 305 (1970).
33. KARTHA, G., BELLO, J., AND HARKER, D., *Nature*, **213**, 862 (1967).
34. HIRS, C. H. W., HALMANN, M., AND KYCIA, J. H., *Arch. Biochem. Biophys.*, **111**, 209 (1965).

Regulation of neuronal Bcl2 protein expression and calcium homeostasis by transforming growth factor type β confers wide-ranging protection on rat hippocampal neurons

(excitotoxicity/apoptosis/necrosis/growth factor)

JOCHEN H. M. PREHN*, VYTAUTAS P. BINDOKAS*, CHARLES J. MARCUCCILLI*, STANISLAW KRAJEWSKI†, JOHN C. REED†, AND RICHARD J. MILLER*‡

*Department of Pharmacological and Physiological Sciences, University of Chicago, 947 East 58th Street, Chicago, IL 60637; and †La Jolla Cancer Research Foundation, Cancer Research Center, 10901 North Torrey Pines Road, La Jolla, CA 92037

Communicated by L. L. Iversen, August 15, 1994 (received for review June 9, 1994)

ABSTRACT Excessive activation of glutamate receptors accompanied by Ca^{2+} overloading is thought to be responsible for the death of neurons in various conditions including stroke and epilepsy. Neurons also die if deprived of important growth factors and trophic influences, conditions sensitive to certain oncogene products such as the Bcl2 protein. We now demonstrate that transforming growth factor type β (TGF- β) prevents neuronal Ca^{2+} overloading of rat hippocampal neurons in response to the glutamatergic agonist *N*-methyl-D-aspartate or the Ca^{2+} ionophore 4-Br-A23187 and, in addition, leads to a substantial increase in neuronal Bcl2 protein expression. Parallel cytotoxicity experiments demonstrate that treatment with TGF- β protects rat hippocampal neurons from death induced by excitotoxicity, trophic factor removal, and oxidative injury. Thus, TGF- β may protect against a wide range of toxic insults by regulating two factors with great importance for neuronal viability.

Inappropriate activation of glutamate receptors is thought to be responsible for the death of neurons following brain insults such as ischemia, epilepsy, and trauma (1). It is widely believed that the deleterious effects of glutamate receptor overactivation (excitotoxicity) are mainly due to massive Ca^{2+} influx through *N*-methyl-D-aspartate (NMDA) receptors, leading to toxic Ca^{2+} overloading and its sequelae (1). On the other hand, it is known that under some circumstances neurons can die due to activation of a process known as programmed cell death. Under these circumstances, death is frequently associated with apoptosis (2). In the central nervous system, this type of neuronal death commonly occurs during development (3). Pathophysiologically, apoptotic cell death may be involved in Alzheimer β -amyloid peptide toxicity (4), in the death of certain neuronal populations in response to cerebral ischemia (5), as well as in free radical-mediated neuronal damage (6). Programmed cell death is also under the control of a set of genes that have either positive or negative effects (7). One of these is the *Bcl2* gene (8, 9), which is expressed in large amounts in the central nervous system (10).

Growth factors and cytokines are promising agents for treatment of a wide variety of neurodegenerative diseases for which little or no alternative treatments exist. Although neurotrophic/neuroprotective effects of these peptides against both excitotoxic and apoptotic cell injury have been reported from numerous *in vitro* and *in vivo* studies, little is known about their potential mechanisms of action. In the present study, we demonstrate that the neuroprotective cytokine transforming growth factor type β (TGF- β ; ref. 11)

is able to acutely stabilize neuronal Ca^{2+} homeostasis under conditions of pathophysiological Ca^{2+} overloading and also produces a rapid induction of the Bcl2 oncoprotein.

MATERIALS AND METHODS

Cell Culture. Primary hippocampal neurons were dissociated from embryonic day 17 Holtzman rat embryos and plated onto poly(L-lysine)-coated glass coverslips. The cells were maintained in serum-free medium [Dulbecco's modified Eagle's medium with modified N2 supplements (N2-DMEM)] above a layer of secondary astrocytes (12). For biochemistry, hippocampal neurons were plated on 35-mm tissue culture dishes with perforated plastic coverslips containing astrocytes directly opposing the neurons. Cells used in this study were between 10 and 16 days *in vitro*. Animal care followed university guidelines.

Induction of Neuronal Injury. Excitotoxic injury was induced by washing the coverslips in Hepes saline (146 mM NaCl/10 mM Hepes/2 mM CaCl_2 /1 mM MgCl_2 /5 mM KCl/10 mM D-glucose, pH 7.4 and 312 mosM) and exposing them subsequently to the glutamatergic agonist NMDA (100 μM) in Mg-free Hepes saline supplemented with 0.1 mM glycine. After 20 min, coverslips were washed in saline and returned to conditioned culture medium. Controls were exposed to Hepes saline only. Mortality was assayed 24 h later by fluorescein diacetate/propidium iodide double staining and trypan blue exclusion. A total of 400–500 neurons were counted per coverslip.

Apoptosis was induced by deprivation of trophic influences. For this purpose, coverslips with neurons were removed from the astrocyte layer, washed once in Hepes saline, and maintained in Hepes saline for a period of 24 h. Osmolarity of the saline was set to that of the culture medium. Cell viability was determined after 24 h of deprivation by morphological criteria. Viable neurons were identified having round to oval, smooth soma and intact neurites. Apoptotic death was verified morphologically and by using terminal deoxynucleotidyltransferase-based immunodetection of DNA fragmentation (Oncor) in conjunction with the diamidinobenzidine staining method.

Free radical-mediated neuronal injury was induced by a 24-h exposure to 0.1–10 μM $\text{Fe}_2(\text{NH}_4)_2(\text{SO}_4)_2$ in N2-DMEM. Viability was determined by morphological criteria. TGF- β (recombinant human; R & D Systems) stocks (1 $\mu\text{g}/\text{ml}$) were made in saline containing 1 mg of ovalbumin per ml and 4 mM HCl. Controls were treated with vehicle.

Abbreviations: $[\text{Ca}^{2+}]_i$, internal free calcium concentration; FCCP, carbonylcyanide *p*-trifluoromethoxyphenylhydrazone; NMDA, *N*-methyl-D-aspartate; R-123, rhodamine 123; TGF- β , transforming growth factor type β .

‡To whom reprint requests should be addressed.

The publication costs of this article were defrayed in part by page charge payment. This article must therefore be hereby marked "advertisement" in accordance with 18 U.S.C. §1734 solely to indicate this fact.

Fluorimetric Measurements. Intracellular free calcium concentration ($[Ca^{2+}]_i$) was calculated by digital video microfluorimetry (13). Cells were loaded with fura-2 acetoxymethyl ester (3 μ M) for 15 min at 37°C and were allowed at least 30 min of wash for dye deesterification. Intracellular free sodium concentration ($[Na^+]_i$) was determined by the dye sodium-binding benzofuran isophthalate (SBFI; Molecular Probes) and fura-2 imaging methods (14, 15). Cultures were loaded with 10 μ M SBFI plus 12.25% pluronic F-127 for 1 h at 37°C and washed 30 min. Mitochondrial potential was monitored by measuring rhodamine 123 (R-123) fluorescence by digital imaging microfluorimetry and methods similar to those described (16). Cells were incubated for 2 min in saline containing 10 μ M R-123 (Molecular Probes), and fluorescence intensity monitoring began after 2 min of wash. Mitochondrial potential was dissipated by 2-min applications of 1 μ M carbonylcyanide *p*-trifluoromethoxyphenylhydrazone (FCCP) to the bath. Experiments were performed at 22–24°C.

Protein Gel Electrophoresis. For biochemistry, plastic coverslips containing the astrocytes were removed from the cultures after treatments; protein samples were quantitated (BCA protein assay; Pierce) and analyzed by SDS/12.5% PAGE. After electrophoresis, the proteins were transferred to nitrocellulose and probed with a polyclonal antibody (1:1000) specific for Bcl2 (17). Detection of the signal was performed with an enhanced chemiluminescence detection kit (Amersham). Densitometric measurements were performed by means of an Ultrascan XL enhanced laser densitometer.

Statistics. Statistical comparisons were made by *t* test or ANOVA followed by the Student–Newman–Keuls test. Non-parametric data were analyzed by the Mann–Whitney U test or the Kruskal–Wallis H test followed by Dunn's test.

RESULTS

TGF- β 1 Protects Against Excitotoxic Injury and Death Induced by Deprivation of Trophic Influences. Injury to cultured rat hippocampal neurons induced by a 20-min exposure to the glutamatergic agonist NMDA was characterized by the appearance of a rough, darkened soma with pyknotic nuclei (Fig. 1A, arrows) and loss of phase brightness. Fragmentation of neurites was preceded by swelling and formation of phase-dark blebs (Fig. 1A Right). A 2-h pretreatment of cultures with TGF- β 1 at concentrations between 1 and 10 ng/ml produced dose-dependent protection from neuronal death with complete protection occurring at 10 ng/ml (Fig. 1B). TGF- β 1 also prevented neuronal death when added simultaneously with NMDA and even conferred a degree of protection when added 1 h after the NMDA exposure (Fig. 1C). Protection against NMDA-induced injury was also obtained with a 2-h pretreatment using TGF- β 3 (10 ng/ml), whereas a variety of other growth factors including fibroblast growth factor 2 (50 ng/ml), brain-derived neurotrophic factor (50 ng/ml), and epidermal growth factor (20 ng/ml) were without an effect in this paradigm (data not shown).

Neuronal injury produced by depriving cells of trophic influences showed distinct morphological changes. After 24 h, these changes were characterized by roughening of the plasma membrane, blebbing, and occasionally large translucent swellings. In many cases, the nucleus moved to one side of the neuronal soma (Fig. 2A). DNA fragmentation was detectable 12 h after trophic factor withdrawal with more widespread and intense staining after 18 h (Fig. 2A Right). Pretreatment of the cultures with TGF- β 1 (0.1–10 ng/ml) for 24 h afforded significant protection against death caused by trophic factor removal (Fig. 2B). While addition of TGF- β 1 2 h before the insult still afforded significant protection, addition of TGF- β 1 at the time of astrocyte removal produced no effect (Fig. 2C).

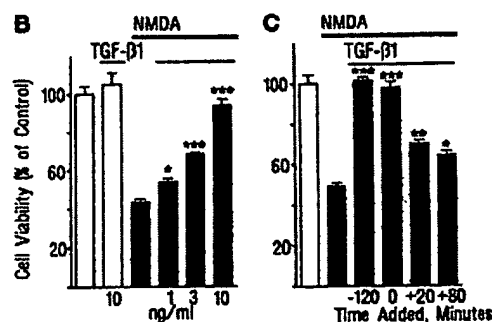
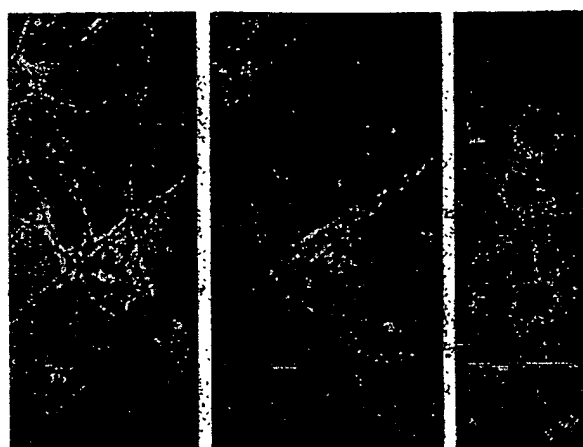


Fig. 1. TGF- β 1 protects cultured rat hippocampal neurons from NMDA-mediated excitotoxicity. (A) (Center) Morphological changes caused by toxic exposure to NMDA typified by rough, darkened soma with pyknotic nuclei (arrows), loss of phase brightness, and fragmentation of neurites. (Left) Neuron before NMDA exposure. (Right) Fragmentation of neurites was preceded by formation of phase-dark blebs. (Bars = 15 μ m). (B) Survival of neurons treated with 100 μ M NMDA for 20 min was significantly enhanced by a 2-h pretreatment with TGF- β 1. Toxicity data are given as means \pm SEM from four or five coverslips. Triplicate experiments gave similar results. (C) Significant protection was obtained with 2-h TGF- β 1 pretreatment (10 ng/ml), when coapplied with NMDA, when applied after the 20-min NMDA treatment, or even 1 h after NMDA exposure. Data are means \pm SEM from four or five coverslips. Duplicate experiments gave similar results. *, $P < 0.05$; **, $P < 0.01$; ***, $P < 0.001$.

TGF- β 1 Prevents Pathophysiological Ca^{2+} Overloading. Fig. 3 shows the effect of NMDA on $[Ca^{2+}]_i$ in an experimental paradigm identical to that used for the toxicity experiments. NMDA produced sustained increases in $[Ca^{2+}]_i$ that often reached high plateaus and persisted even after agonist washout. Many cells also showed secondary increases in $[Ca^{2+}]_i$ after agonist removal, probably an indication of impending death (Fig. 3A). Cells pretreated with TGF- β 1 for 2 h exhibited greatly reduced $[Ca^{2+}]_i$ responses to NMDA (Fig. 3B and C) and returned rapidly to control levels after removal of the agonist. Secondary $[Ca^{2+}]_i$ increases and plateaus were rarely observed. TGF- β 1 also had the capacity to lower NMDA-induced $[Ca^{2+}]_i$ increases when given acutely. Treatment with TGF- β 1 (10 ng/ml) for 10 min reduced the peak increases caused by 10-sec application of 30 μ M NMDA by $24.4 \pm 4.6\%$ compared to vehicle-perfused controls. These changes were specific for $[Ca^{2+}]_i$ since NMDA-induced increases in $[Na^+]_i$ were not altered by acute treatment with TGF- β 1 (Fig. 3D). Using the whole-cell patch clamp technique, we found that NMDA-induced currents

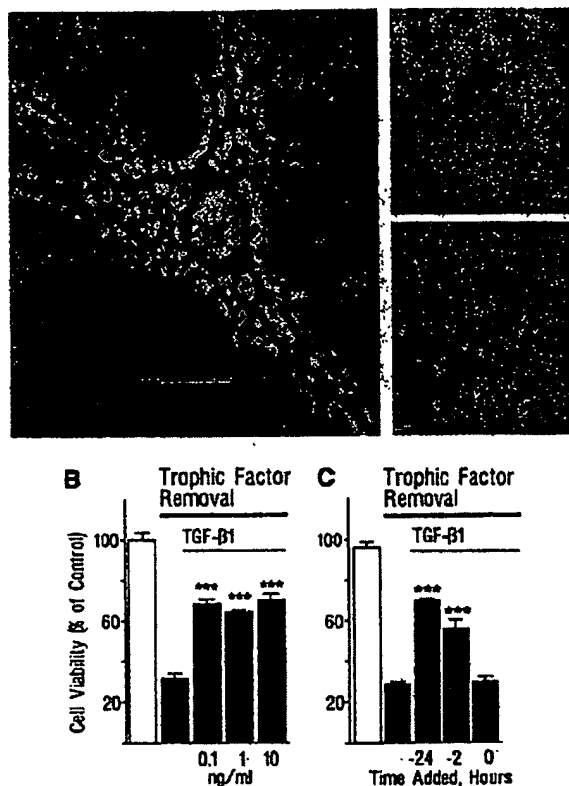


FIG. 2. TGF- β 1 protects cultured rat hippocampal neurons from death induced by deprivation of trophic influences. (A) Morphology of neurons undergoing death induced by trophic factor removal was characterized by roughening of the plasma membrane, blebbing, and large translucent swellings. Note that the nucleus moved to one side of the neuronal soma (Left). DNA fragmentation was detectable after 18 h of deprivation (Lower Right), whereas control cultures showed no staining (Upper Right). (Bar = 15 μ m.) (B) Deprivation of trophic influences resulted in 70% mortality at 24 h in untreated cultures. Significant protection resulted from a 24-h pretreatment with 0.1–10 ng of TGF- β 1 per ml. Data are means \pm SEM from four or five coverslips. Triplicate experiments gave similar results. (C) Highest protection was observed with 24-h pretreatment (time, -24 h) with TGF- β 1 (10 ng/ml), less protection occurred with 2-h pretreatment (time, -2 h), and mortality was not altered if TGF- β 1 was added only at the onset (time, 0) of trophic factor removal. Means \pm SEM from four or five coverslips. Duplicate experiments gave similar results. ***, $P < 0.001$.

also appeared unaltered in cells perfused with TGF- β 1 (data not shown).

The ability of TGF- β 1 to enhance Ca^{2+} buffering during glutamate receptor overactivation is a likely protective mechanism. To test this possibility further, we found that cells treated with TGF- β 1 showed greatly reduced increases in $[\text{Ca}^{2+}]_i$ due to Ca^{2+} ionophore (4-Br-A23187) exposure. Fig. 4A demonstrates that 4-Br-A23187 produced a dose-dependent increase in neuronal $[\text{Ca}^{2+}]_i$. TGF- β 1-treated cells exhibited greatly reduced increases in $[\text{Ca}^{2+}]_i$ after 4-Br-A23187 treatment (Fig. 4B and C). At the highest ionophore concentrations used, $[\text{Ca}^{2+}]_i$ reached very high levels (plateaus), outlasting ionophore application. Despite increasing to high levels during application of 8 μ M 4-Br-A23187, $[\text{Ca}^{2+}]_i$ frequently returned rapidly to baseline in TGF- β 1-treated cells after washout of the ionophore, a result rarely observed in control neurons. Furthermore, smaller maximum slopes for $[\text{Ca}^{2+}]_i$ increases were typical in TGF- β 1-treated cells (Fig. 4D).

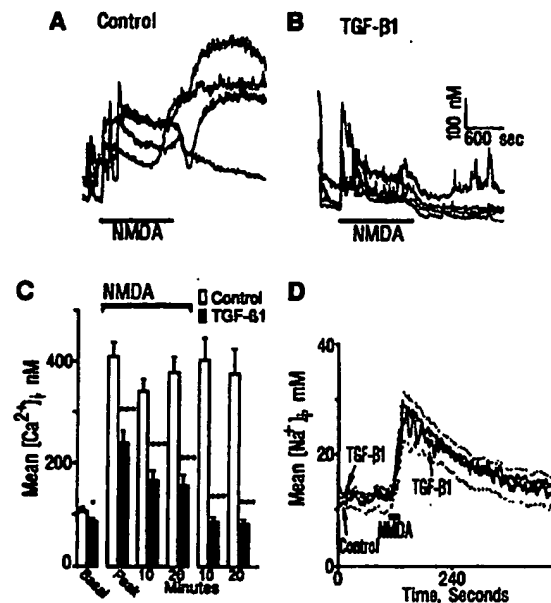


FIG. 3. TGF- β 1 enhances $[\text{Ca}^{2+}]_i$ buffering in hippocampal neurons exposed to NMDA. (A) Baseline fluctuations in $[\text{Ca}^{2+}]_i$ represent ongoing network activity at excitatory synapses established between cultured neurons (12). Four representative neurons are shown. Application of NMDA (100 μ M; 20 min) produced sustained elevations in $[\text{Ca}^{2+}]_i$ in most neurons that outlasted application. Note secondary increases in three of four neurons shown. (B) A 2-h pretreatment with 10 ng of TGF- β 1 per ml reduced peak $[\text{Ca}^{2+}]_i$ and plateau level during NMDA application. TGF- β 1 was present during NMDA exposure. Rapid recovery was evident in all four representative neurons. (C) Average $[\text{Ca}^{2+}]_i$ was significantly lower in TGF- β 1-treated neurons at all time points measured, including basal $[\text{Ca}^{2+}]_i$. Data are from 25 control and 18 TGF- β 1-treated neurons. Experiment was performed four times with similar results. (D) Peak increases and recovery time constants for $[\text{Na}^+]_i$ elevations induced by NMDA (30 μ M; 10 sec) were not significantly altered ($P > 0.1$). Data are means \pm SEM (dotted line) from $n = 27$ controls and $n = 28$ TGF- β 1-treated neurons. Experiments performed in duplicate with similar results. *, $P < 0.05$; ***, $P < 0.001$.

To determine whether the Ca^{2+} -stabilizing effect of TGF- β 1 may be associated with improved cellular energetics, mitochondrial potential was analyzed by using the mitochondrial dye R-123 (16). Mitochondrial staining with R-123 was significantly more intense in neurons pretreated for 24 h with TGF- β 1 than in control neurons (initial intensity: TGF- β 1 = 93.8 ± 6 ; control = 73.2 ± 3.9 intensity units; $P < 0.001$) (Fig. 5). The change in fluorescence produced by the mitochondrial uncoupler FCCP was significantly greater in TGF- β 1-treated cells (for first FCCP application: TGF- β 1, $\Delta = +35.2 \pm 5.4$; control, $\Delta = +15.5 \pm 2.6$ intensity units; $P < 0.01$), indicating a greater mitochondrial potential. Mitochondrial potential in TGF- β -treated cells also recovered more quickly after washout of FCCP, resulting in faster recovery time constants (TGF- β 1 = 13.6 ± 2.0 sec; control = 51.2 ± 8.0 sec; $P < 0.001$) and greater retention of R-123.

TGF- β 1 Induces Neuronal Expression of the Bcl2 Oncoprotein. Unlike NMDA toxicity, the protective effects of TGF- β 1 on cell death caused by deprivation of trophic influences were manifest only after a period of pretreatment (Fig. 2C). It has been demonstrated that the 26-kDa product of the *Bcl2* gene can protect a variety of cells against certain types of cell death, often associated with withdrawal of important trophic factors (8, 9). Although Bcl2 is expressed in the mammalian brain (10), details of its regulation remain undetermined. We observed that neurons treated with

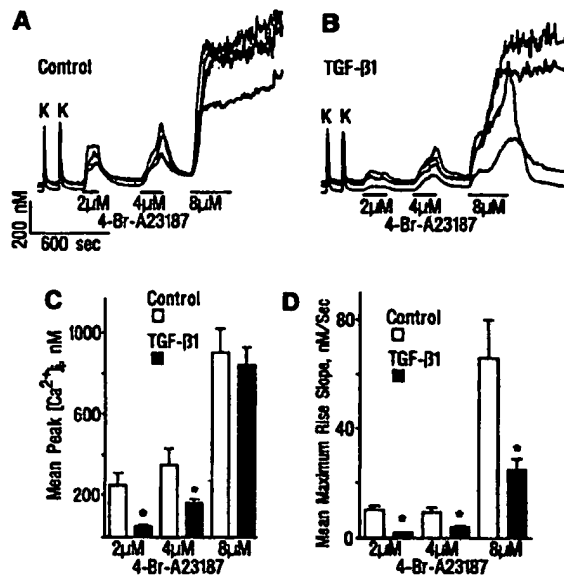


FIG. 4. TGF- β 1 treatment enhances the ability of hippocampal neurons to buffer $[Ca^{2+}]_i$ during treatment with the Ca^{2+} ionophore 4-Br-A23187. (A) Representative records from four control neurons exposed to two 5-sec 50 mM KCl applications and applications of 2, 4, and 8 μ M 4-Br-A23187. (B) Representative records from four neurons pretreated for 2 h with 10 ng of TGF- β 1 per ml. (C) Peak increase in $[Ca^{2+}]_i$ was higher in control neurons, significantly ($P < 0.01$) at 2 and 4 μ M ionophore concentrations ($n = 18$ controls and $n = 20$ TGF- β 1-treated neurons). (D) Maximum slopes attained during increases to peak $[Ca^{2+}]_i$ were significantly faster in controls, even where peak $[Ca^{2+}]_i$ was not different (8 μ M 4-Br-A23187). Reductions in $[Ca^{2+}]_i$ plateaus and/or significantly smaller maximum slopes were observed in seven of eight experiments. *, $P < 0.05$.

TGF- β 1 or - β 3 showed a greatly enhanced expression of the Bcl2 oncoprotein (Fig. 6A). Significant enhancement occurred after 2 h of TGF- β 1 (10 ng/ml) treatment, with even larger effects after 24 h (increase of $239\% \pm 61\%$ and $595\% \pm 176\%$, respectively; $n = 4$ experiments). Bcl2 protein induction occurred at low TGF- β 1 concentrations with clear

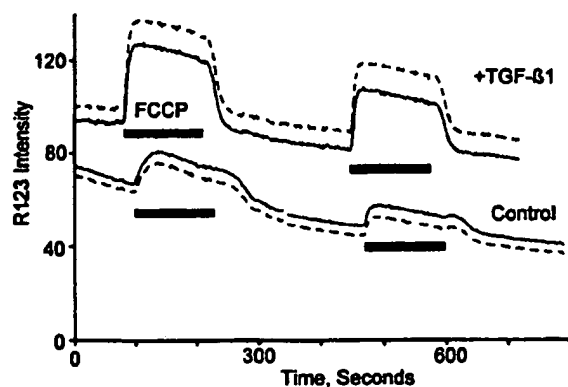


FIG. 5. TGF- β 1 treatment improves mitochondrial energetics. Neurons were stained with R-123 2 min prior to time 0. Upper solid trace represents mean R-123 fluorescence intensity of 15 neurons after a 24-h pretreatment with 10 ng of TGF- β 1 per ml; dashed trace is mean + SEM. Lower trace pairs correspond to control mean ($n = 25$) and mean - SEM. FCCP (1 μ M) released more fluorescence in TGF- β -treated cells, indicating that those mitochondria were initially more polarized than those in control cells. After washout of FCCP, R-123 was resequenced faster and retained better in TGF- β -treated cells. Data are representative of four experiments.

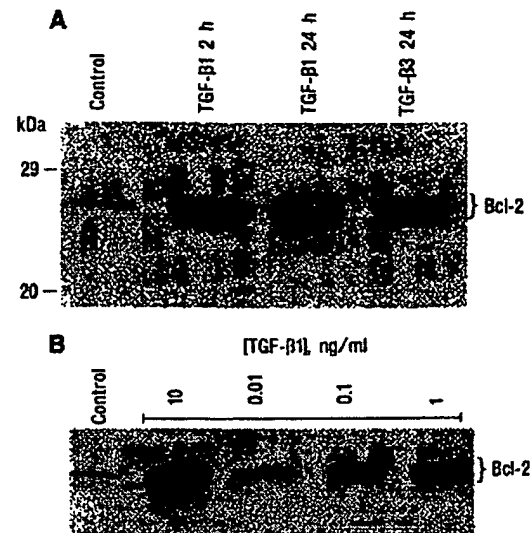


FIG. 6. TGF- β 1 treatments induce expression of Bcl2 oncoprotein. (A) Western blots showing Bcl2 expression in untreated cultures and induction of Bcl2 oncoprotein after 2- and 24-h pretreatment with 10 ng of TGF- β 1 per ml or 24-h pretreatment with 10 ng of TGF- β 3 per ml. (B) Concentration dependence of Bcl2 induction by TGF- β 1 for 24-h pretreatment. First two lanes are vehicle-treated and TGF- β 1-treated (10 ng/ml) cells, followed by treatments with 0.01, 0.1, and 1 ng/ml. Triplicate experiments yielded similar results.

effects after addition of 0.1 ng/ml (Fig. 6B). Thus, the time course and concentration dependence of Bcl2 induction were similar to that observed for the protective effects of TGF- β 1 after deprivation of trophic influences.

TGF- β 1 Protects Against Free Radical-Mediated Neuronal Injury. While the mechanism of Bcl2 action is not yet fully elucidated, recent reports suggest that Bcl2 protects cells by inhibiting the generation or effects of reactive oxygen species (18, 19). We therefore evaluated whether TGF- β 1 might also protect neurons against oxidative neuronal injury. For this purpose, the hippocampal cultures were exposed to ferrous ions that catalyze the formation of oxygen radicals (20). Exposure to iron resulted in a dose-dependent increase in neuronal mortality that was significantly reduced in TGF- β 1 pretreated cells (Fig. 7).

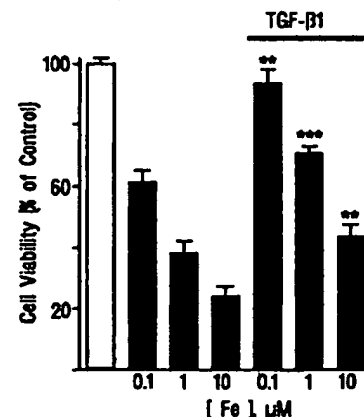


FIG. 7. Pretreatment with TGF- β 1 (10 ng/ml) for 24 h protects against iron-induced oxidative injury. Cultures were exposed to iron as described. Data are means \pm SEM from four coverslips. Experiment was performed in duplicate. **, $P < 0.01$; ***, $P < 0.001$.

DISCUSSION

The present study demonstrates that TGF- β s have the capacity to regulate two factors with great importance for neuronal viability and to protect neurons against a wide range of toxic insults. We suggest that the TGF- β s play an important role both in maintenance of neuronal viability in the unlesioned brain (21) and in limiting the destructive consequences of metabolic and traumatic insults to the central nervous system (22).

Treatment of rat hippocampal neurons with TGF- β 1 protected against NMDA receptor-mediated excitotoxic injury and against injury induced by depriving the cells from trophic factors. While the death induced by deprivation of trophic factors showed many of the characteristics of apoptosis (ref. 2; Fig. 2), excitotoxic injury exhibited morphological changes that are typical of necrotic injury, including dendritotoxic swelling and an early loss of membrane integrity (refs. 1 and 2; Fig. 1). These processes are normally accompanied by failure of the cell to regulate ion homeostasis (refs. 1 and 2; Fig. 3A). In particular, overloading with Ca^{2+} is thought to play a key role in glutamate- and NMDA-induced neuronal injury (1, 23). We demonstrate here that treatment of hippocampal neurons with TGF- β 1 leads to improved Ca^{2+} homeostasis in response to the glutamatergic agonist NMDA or the Ca^{2+} ionophore 4-Br-A23187, an effect that may well be related to the protective effects against NMDA-mediated injury.

TGF- β 1 appears to influence the interaction between $[\text{Ca}^{2+}]_i$ and mitochondrial energetics. In support of this idea, we have found that mitochondria appear to be more hyperpolarized and are more able to maintain their membrane potential after TGF- β treatment (Fig. 5). This implies that mitochondrial function and, as a consequence, Ca^{2+} buffering and extrusion are enhanced. In turn, greater buffering of $[\text{Ca}^{2+}]_i$ during prolonged NMDA or calcium ionophore exposures implies that TGF- β -treated neurons would experience less Ca^{2+} -mediated mitochondrial uncoupling (16, 24). It is interesting to note that a previous study has demonstrated that TGF- β 1 is localized to mitochondria in different cell types (25), but the significance of this remains unknown.

Treatment with TGF- β also produced a rapid and pronounced induction of the Bcl2 oncoprotein in neurons (Fig. 5). Microinjection of Bcl2 expression plasmids has been shown to protect neurons against certain types of apoptotic cell death (9). We now give evidence that this may also occur physiologically—in response to TGF- β 1. Although it seems highly likely that the increased expression of Bcl2 may contribute to the protective effect against trophic factor withdrawal, we cannot exclude that effects of TGF- β 1 other than, or in conjunction with, those on Bcl2 expression may be involved in the protective effect of this cytokine.

It is currently believed that the death of neurons and other cells can be categorized as necrosis or apoptosis according to several criteria (2). Nevertheless, many of the same factors might be involved in both phenomena. This would include a

role for Ca^{2+} and also toxic free radicals (1, 2, 7, 18, 19). It seems that TGF- β s may be able to modulate the viability of neurons in a variety of situations by simultaneously orchestrating different key protective elements in the cell.

This work was supported by Public Health Service Grants DA-02121, MH-40165, and DA-02575. J.H.M.P. was supported by Deutsche Forschungsgemeinschaft Grant Pr338/2-1. C.J.M. holds a M.D./Ph.D. training grant (HD07009) at the University of Chicago.

- Choi, D. W. (1992) *J. Neurobiol.* 23, 1261–1276.
- Wyllie, A. H., Kerr, J. F. R. & Currie, A. R. (1980) *Int. Rev. Cytol.* 68, 251–306.
- Raff, M. C., Barres, B. A., Burne, J. F., Coles, H. S., Ishizaki, Y. & Jacobson, M. D. (1993) *Science* 262, 695–700.
- Loo, D. T., Copani, A., Pike, C. J., Whittemore, E. R., Walencewicz, A. J. & Cotman, C. W. (1993) *Proc. Natl. Acad. Sci. USA* 90, 7951–7955.
- Heron, A., Pollard, H., Dessi, F., Moreau, J., Lasbennes, F., Ben-Ari, Y. & Charriaud-Marlange, C. (1993) *J. Neurochem.* 61, 1973–1976.
- Ratan, R. R., Murphy, T. H. & Baraban, J. M. (1994) *J. Neurochem.* 62, 376–379.
- Reed, J. C. (1994) *J. Cell Biol.* 124, 1–6.
- Hockenberry, D., Nufiez, G., Millman, C., Schreiber, R. D. & Korsmeyer, S. J. (1990) *Nature (London)* 348, 334–336.
- Garcia, I., Martinou, I., Tsujimoto, Y. & Martinou, J.-C. (1992) *Science* 258, 302–304.
- Negrini, M., Silini, E., Kozak, C., Tsujimoto, Y. & Croce, C. M. (1987) *Cell* 49, 455–463.
- Prehn, J. H. M., Backhaus, C. & Kriegstein, J. (1993) *J. Cerebr. Blood Flow Metab.* 13, 521–525.
- Abele, A. E., Scholz, K. P., Scholz, W. & Miller, R. J. (1990) *Neuron* 2, 413–419.
- Bindokas, V. P., Brorson, J. R. & Miller, R. J. (1993) *Neuropharmacology* 32, 1213–1220.
- Minta, A. & Tsien, R. Y. (1989) *J. Biol. Chem.* 264, 19449–19457.
- Negulescu, P. A., Harootunian, A., Tsien, R. Y. & Machen, T. E. (1990) *Cell Regul.* 1, 259–268.
- Duchen, M. R. (1992) *Biochem. J.* 283, 41–50.
- Krajewski, S., Tanaka, S., Takayama, S., Schibler, M. J., Fenton, W. & Reed, J. C. (1993) *Cancer Res.* 53, 4701–4714.
- Hockenberry, D., Oltvai, Z. N., Yin, X.-M., Millman, C. L. & Korsmeyer, S. (1993) *Cell* 75, 241–251.
- Kane, D. J., Sarafian, T. A., Anton, R., Hahn, H., Butler, Gralla, E., Selverstone Valentine, J., Ord, T. & Bredesen, D. E. (1993) *Science* 262, 1274–1277.
- Halliwell, B. & Gutteridge, J. M. C. (1986) *Arch. Biochem. Biophys.* 246, 4501–4514.
- Unsicker, K., Flanders, K. C., Cissel, D. S., Lafyatis, R. & Sporn, M. B. (1991) *Neuroscience* 44, 613–625.
- Logan, A. & Berry, M. (1993) *Trends Neurosci.* 14, 337–343.
- Hartley, D. M., Kurth, M. C., Bjerkness, L., Weiss, J. H. & Choi, D. W. (1993) *J. Neurosci.* 13, 1993–2000.
- Nicholls, D. & Åkerman, K. (1982) *Biochim. Biophys. Acta* 683, 57–88.
- Heine, U. I., Burmester, J. K., Flanders, K. C., Danielpour, D., Munoz, E. F., Roberts, A. B. & Sporn, M. B. (1991) *Cell Regul.* 2, 467–477.

Chemical modification of erythropoietin: an increase in in vitro activity by guanidination

Rika Satake, Hiroyuki Kozutsumi, Makoto Takeuchi and Katsuhiko Asano

Pharmaceutical Laboratory, Kirin Brewery Co., Maebashi, Gunma (Japan)

(Received 16 August 1989)

Key words: Erythropoietin; Chemical modification; Guanidination

Human recombinant erythropoietin (rHuEPO) was chemically modified with several group-specific reagents in order to study the role of each kind of amino-acid residue in its biological activity. Guanidination of the amino groups of the lysine residues yielded derivatives that showed higher activities in vitro than native rHuEPO, whereas amidination had no effect on the activity. By contrast, modification of the positive charges of the lysine residues to neutral or negative charges, such as in carbamylation, trinitrophenylation, acetylation or succinylation, caused a significant loss of rHuEPO activity. Chemical modification of other amino-acid residues, such as arginine and tyrosine residues or carboxyl groups, also led to loss of activity.

Introduction

Erythropoietin is a glycoprotein hormone which regulates the number of peripheral erythrocytes [1,2]. Recently, recombinant human erythropoietin (rHuEPO) was successfully produced in Chinese hamster ovary (CHO) cells [3], and is now available for clinical use. Over the last few years, the biological [4-6] and pharmacological [7,8] properties of rHuEPO have been extensively studied, and its clinical value has been clearly demonstrated [9,10]. However, little is known about the molecular mechanisms of the biological activity of rHuEPO.

To identify the functional domains of rHuEPO, Sytkowski and Donahue [11] used anti-peptide antiserum against erythropoietin (EPO) and pointed out the importance of the region corresponding to the amino-acid residues 99-129, while Wang et al. [12] suggested the crucial role of the disulfide bridge between Cys-29 and Cys-31.

We have previously tried to determine the active domain of rHuEPO by partial proteolysis of the molecule, but no active peptide fragment has so far been found (Satake et al., unpublished data). In this report, we show that the activity of rHuEPO is sensitive to chemical modification of lysine, arginine and tyrosine residues, as well as carboxyl groups, and discuss the influence of these modifications, particularly changes in the net charge of the molecule, on the biological activity.

Materials and Methods

Materials

rHuEPO was highly purified to homogeneity from the conditioned media of the CHO cell line expressing the human erythropoietin gene by ion-exchange, reverse-phase and gel chromatography. The purity was more than 99% by SDS-PAGE and in vivo specific activity was measured at 200 000 IU/mg protein. *o*-Methylisourea hydrogen sulfate, aminoguanidine nitrate, 2,3-butanedione, phenylglyoxal and 1,2-cyclohexanone were purchased from Aldrich (Belgium). Potassium cyanate and tetranitromethane were obtained from Sigma (U.S.A.). 2,4-pentadione, ethylacetamide hydrochloride, 2,4,6-trinitrobenzenesulfonic acid (TNBS) and 1-ethyl-3-(3'-dimethylaminopropyl) carbodiimide hydrochloride (EDC) were obtained from Wako Pure Chemical (Japan). 1-Guanyl-3,5-dimethylpyrazole (GDMP) was synthesized by the method of Bannard et al. [13] from aminoguanidine and 2,4-pentadione.

Abbreviations: rHuEPO, recombinant human erythropoietin; CHO, Chinese hamster ovary; TNBS, 2,4,6-trinitrobenzenesulfonic acid; EDC, 1-ethyl-3-(3'-dimethylaminopropyl)carbodiimide; GDMP, 1-guanyl-3,5-dimethylpyrazole; SDS-PAGE, SDS-polyacrylamide gel electrophoresis.

Correspondence: Katsuhiko Asano, Pharmaceutical Laboratory, Kirin Brewery Co., Ltd., 1-2-2, Souja-machi, Maebashi, Gunma, 371, Japan.

0167-4838/90/\$03.50 © 1990 Elsevier Science Publishers B.V. (Biomedical Division)

Chemical modification

Guanidination. rHuEPO was guanidinated with *o*-methylisourea [14] or GDMP [15]. The solution of rHuEPO (10 mg/ml) was mixed with an equal volume of 1.0 M *o*-methylisourea (pH adjusted to 10.5 with NaOH). The reaction was allowed to proceed for 6 days at 4°C, and at appropriate time intervals aliquots were removed and dialyzed against 1 mM HCl to stop the reaction. rHuEPO was added at the concentration of 3 mg/ml in 0.7 M GDMP (pH adjusted to 9.9 with NaOH). The mixture was left for 5 days at 4°C and the reaction was subsequently stopped by adding HCl to a pH of 3.0, and the excess reagent was removed by dialysis against 1 mM HCl.

Amidation. rHuEPO was amidated by a modified method of Zollock et al. [16]. rHuEPO (2 mg/ml) in 0.25 M borate buffer (pH 10.0) was mixed with an equal volume of 0.4 M ethylacetimide in the same buffer. The reaction was allowed to proceed at room temperature for 4 h and was stopped by dialysis against water.

Carbamylation. rHuEPO (1 mg/ml) was carbamylated with potassium cyanate by the method of Plapp et al. [14].

Trinitrophenylation. rHuEPO (1 mg/ml) was trinitrophenylated with TNBS by the method of Plapp et al. [14].

Acetylation. rHuEPO (2 mg/ml) in 0.3 M phosphate buffer (pH 7.2) was incubated with an equal amount of acetic anhydride at 0°C for 1 h and the reaction was stopped by dialysis against water [17].

Succinylation. rHuEPO (2 mg/ml) in 0.5 M NaHCO₃ (pH 8.0) containing 0.2 M NaCl, was incubated with a 15-fold molar excess of succinic anhydride at 15°C for 1 h and the reaction was stopped by dialysis against water [18].

Modification of arginine residues. Arginine residues of rHuEPO were modified with 2,3-butanedione [19], 1,2-cyclohexanone [20] or phenylglyoxal [21], as described previously.

Nitration. Tyrosine residues of rHuEPO were modified with tetranitromethane [22].

Modification of carboxyl groups. rHuEPO (1 mg/ml, pH adjusted to 4.5 with HCl) was modified at room temperature by 0.02 M EDC employing 1.0 M glycnamide [23]. Over a period of 60 min, aliquots were removed at appropriate time intervals and the reaction was stopped by the addition of 2.5 vol of 1.0 M sodium acetate (pH 4.75).

Analysis

The number of modified amino-acid residues was determined principally by amino-acid analysis, using an Hitachi 835 amino-acid analyzer, after hydrolysis of the samples in 6 M HCl in sealed evacuated tubes at 110°C for 24 or 48 h [14]. The number of free amino groups was determined with TNBS [24].

In vitro biological activity was measured by determining the incorporation of ⁵⁹Fe into cultured rat bone marrow cells after incubation with samples [25] and in vivo biological activity was determined by the exhypoxic polycythemic mouse bioassay. [26].

The amount of sialylated oligosaccharides was determined by paper electrophoresis of oligosaccharides released from derivatives by hydrazinolysis [27].

The digestion of the derivatives (1 mg/ml) with pepsin (2.5 µg/ml) in 0.1 M acetate buffer (pH 4.5) was performed at 37°C for 2 h. At appropriate time intervals, aliquots were analyzed by SDS-PAGE, as described by Laemmli [28], using a 12.5% polyacrylamide gel. The derivatives (0.4 mg/ml) were also digested with plasmin (0.1 U/ml) in 0.01 M phosphate buffer (pH 7.0) containing 0.155 M NaCl at 37°C for 5 h.

Results

Derivatives of rHuEPO and their activities

The derivatives of rHuEPO obtained in this study, the numbers of amino acids modified in each derivative, and their activities, are summarized in Table I. Guanidination of the lysine residues significantly increased the activity of rHuEPO in vitro. About seven

TABLE I
Derivatives of rHuEPO and their activities

Amino acid	Derivative or reagent	Total No. of residues	No. of modified residues	Activity % ^a	
				in vitro	in vivo
Lys	guanidino	8	7.3 ^b	260	50
			8.0 ^c	240	56
	amidino		6.9	100	n.d.
	carbamyl		6.4	<1	n.d.
	trinitrophenyl		4.8	<1	n.d.
Arg	acetyl		6.8	<10	n.d.
	succinyl		4.8	<1	n.d.
	butanedione	12	2.0	<20	n.d.
	cyclohexanone		5.0	<10	n.d.
Tyr	nitro	4	1.0	20	n.d.
			2.0	<10	n.d.
Glu	amido	18	4.0	60	n.d.
			7.0	<10	n.d.

^a Relative to native rHuEPO taken as 100, calculated by the ratio of specific activities ($2.2 \cdot 10^5$ IU/mg protein in vitro, $2.0 \cdot 10^5$ IU/mg protein in vivo).

^b Modified with *o*-methylisourea.

^c Modified with GDMP.

n.d., not done.

out of eight lysine residues were guanidinated with *o*-methylisourea, while all eight lysine residues were modified with GDMP. However, the extent of increased activity was almost the same for both derivatives. Amino-acid analysis showed that no other modification occurred in either of the guanidinated rHuEPO derivatives.

Amidation of amino groups in rHuEPO led to derivatives containing about seven amidinated ϵ -amino groups of lysine, as determined by amino-acid analysis. The derivatives retained the positive charges of the amino groups as did guanidinated derivatives, but the activity remained unchanged.

To understand the role of the positive charges of lysine residues in the activity of rHuEPO, the positive charges were neutralized by carbamylation, trinitrophenylation and acetylation, or were changed to negative charges by succinylation. About six ϵ -amino groups of the lysine residues were carbamylated according to the detection of homocitrulline by amino-acid analysis. Trinitrophenylation and acetylation also led to derivatives containing five to seven modified ϵ -amino groups, respectively. As shown in Table I, the in vitro activities of all these derivatives were either lost or were less than 10% of that of native rHuEPO. Succinylation of free ϵ -amino groups also caused complete loss of in vitro activity. These results suggest that the positive charges of the lysine residues, though not fully identified, are important for the in vitro activity of rHuEPO.

Neutralization of the positive charges of arginine residues of rHuEPO with 2,3-butanedione, 1,2-cyclohexanone or phenylglyoxal also caused a significant loss of in vitro activity, but no particular arginine residue essential for the activity of rHuEPO was identified in the molecule. rHuEPO was also inactivated by both the nitration of two tyrosine residues and the modification of seven carboxyl groups, whereas 60% of the activity remained after the modification of four carboxyl groups.

Characterization of guanidinated rHuEPO

The synthesis of a guanidinated rHuEPO with a higher in vitro activity than native rHuEPO led us to characterize this derivative further. Fig. 1 shows that the activity of the derivative in vitro increased with an increase in the number of guanidinated lysine residues. No significant difference was detected in the effect of guanidination reagents such as *o*-methylisourea and GDMP on the increased activity of rHuEPO. These results suggest that there is no single guanidinated lysine residue specifically involved in the activation of rHuEPO. On the other hand, a peptide-mapping study of both guanidinated derivatives suggests that the guanidination of Lys-152 is not important for the activation of rHuEPO (data not shown), because only Lys-152 was not guanidinated by *o*-methylisourea, whereas all of the lysine residues were guanidinated by

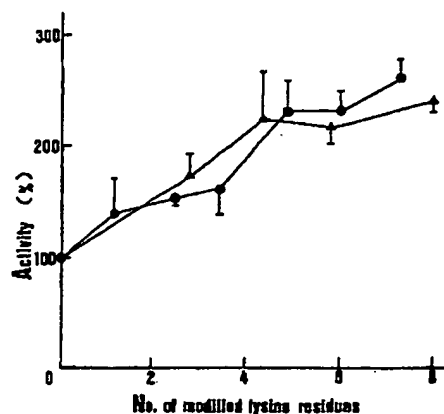


Fig. 1. Effect of guanidination on the activity of rHuEPO. rHuEPO was incubated with *o*-methylisourea (●) or GDMP (Δ). Aliquots were removed at indicated times to measure the number of lysine residues guanidinated, and their in vitro activities were measured as described in Materials and Methods. In vitro activities (%) are calculated by the ratio of specific activities and given as a percent of the control. Each point is the mean \pm S.E. for three determinations.

GDMP, and both these derivatives showed the same increase in activity.

Fig. 2 shows the dose-response curves of guanidinated and native rHuEPO for in vitro activity. ^{59}Fe incorporation into bone marrow cells was enhanced by exposure of the cells ($6.25 \cdot 10^5$ cells) to rHuEPO at concentrations from 1.0 to $100 \cdot 10^{-15}$ mol/ml. Although enhancement was also elicited by guanidinated rHuEPO, its potency was 2- to 3-fold that of native rHuEPO. In addition, there was a significant difference in the slope of the dose-response curves between guanidinated and native rHuEPO. Bone marrow cells showed higher sensitivity to guanidinated rHuEPO than to native rHuEPO. On the other hand, the guanidinated deriva-

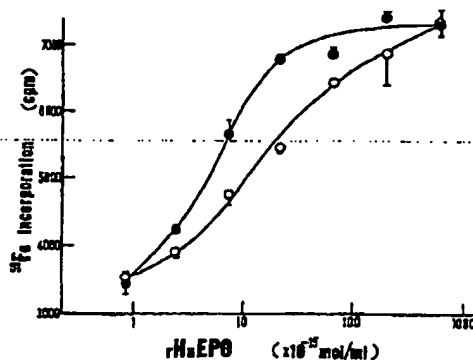


Fig. 2. Dose-response curve of guanidinated and native rHuEPO. $6.25 \cdot 10^5$ bone marrow cells were incubated with rHuEPO guanidinated with GDMP (●), containing all eight lysine residues modified, or native rHuEPO (○). After 24 h culture, ^{59}Fe -incorporation into the cells was measured. Each point is the mean \pm S.E. for three determinations.

TABLE II

Amount of sialylated oligosaccharides obtained from guanidinated and native rHuEPO

The amount of sialylated oligosaccharides was analyzed by paper electrophoresis as described in Materials and Methods. N, neutral; A₁, mono-sialylated; A₂, di-sialylated; A₃, tri-sialylated; A₄, tetra-sialylated; and A_{total}, A₁ + A₂ + A₃ + A₄.

	Fraction					
	N	A ₁	A ₂	A ₃	A ₄	A _{total}
Native rHuEPO	1.96	13.3	10.3	31.1	43.4	98.0
Guanidinated rHuEPO ^a	6.97	17.3	12.9	32.8	30.1	93.0
Guanidinated rHuEPO ^b	1.86	14.4	8.72	31.3	43.7	98.1

^a Guanidinated with *o*-methylisourea.

^b Guanidinated with GDMP.

tive showed only half the biological activity in vivo compared with native rHuEPO, as shown in Table I. This discrepancy in the in vitro and in vivo activities might have occurred because the conditions used in this assay were most suitable for the measurement of in vivo biological activity of both rHuEPO and human urinary EPO [29], but were not optimized for these derivatives. These derivatives may have different in vivo properties such as dose-response curves and speed of effect from native rHuEPO.

It is well-known that the oligosaccharide chains of HuEPO are important for biological activity in vivo [30–33]. When terminal oligosaccharide chains of HuEPO are modified, the activity of HuEPO is abolished completely in vivo, but enhanced by 2- or 3-fold in vitro [31]. To check whether guanidination affects the terminal sialic acids of rHuEPO, N-linked oligosaccharide chains of guanidinated rHuEPO were removed by hydrazinolysis at 100°C for 16 h, and their charge distri-

bution was analyzed by paper electrophoresis as described previously [27]. As shown in Table II, N-linked oligosaccharide chains of rHuEPO were separated into five fractions (N, A₁–A₄). The percentage of neutral sugar chains (N), as well as the ratio among acidic chains (A₁–A₄), was essentially the same between guanidinated and native rHuEPO. This result clearly indicated that guanidination did not alter the charge distribution of the sugar chains of rHuEPO. Therefore, the discrepancy in the in vivo and in vitro activities is not due to the removal of the terminal sialic acids of rHuEPO during guanidination.

To investigate the possibility that guanidinated rHuEPO was more susceptible than native rHuEPO, in vivo, to plasma proteinases such as plasmin, guanidinated rHuEPO was digested with plasmin under the conditions described in Materials and Methods. Fig. 3, however, shows that guanidinated rHuEPO was more resistant to plasmin than native rHuEPO. Guanidinated rHuEPO was also resistant to other proteinases, such as pepsin (data not shown).

Discussion

In the present study we showed that the activity of rHuEPO was sensitive to chemical modifications of the lysine, arginine and tyrosine residues, as well as carboxyl groups. Among these, modification of the lysine residues with various lysine specific reagents resulted in a wide range of changes in the activity of modified rHuEPO. Modifications that changed the positive charges of the lysine residues to neutral or negative charges, such as carbamylation, trinitrophenylation, acetylation or succinylation, caused a substantial loss in the in vitro activity, whereas amidination which left the total number of positive charges of lysine unchanged did not effect the activity. It is clear that the positive charges of the lysine residues are essential for the activity of rHuEPO in vitro. A most noteworthy finding in this study is the marked increase in the activity of guanidinated rHuEPO in vitro. The dose-response curve of guanidinated rHuEPO (Fig. 2) shows the possibility that there is a difference in the affinity to the receptor between guanidinated and native rHuEPO. A major difference between guanidinated and native rHuEPO is the size of the side chain at the lysine residue, suggesting that the larger side chain of the lysine residue is favorable for approach to its receptor. However, this is unlikely because amidinated rHuEPO, which has the same number of positive charges and almost the same size of side chains at the lysine residue as guanidinated rHuEPO, showed essentially the same activity as native rHuEPO. Therefore, it seems probable that the guanidino groups, together with their positive charges, play an important role in the interaction between the receptors and rHuEPO.

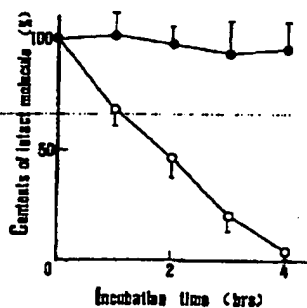


Fig. 3. Digestion of guanidinated and native rHuEPO by proteinase. rHuEPO guanidinated with GDMP (●) and native rHuEPO (○) were incubated with plasmin at 37°C and aliquots were removed at indicated times and analyzed for intact molecule content. The content of intact molecules is measured by densitometry on the gel as compared to the undigested control and given as a % of the control. Each point is the mean ± S.E. for three determinations.

Acknowledgements

The authors wish to thank M. Kubota, M. Wada and Dr. N. Nagano for in vivo bioassay. Y. Inagaki is also thanked for the synthesis of GDMP.

References

- 1 Graber, S.E. and Krantz, S.B. (1978) *Annu. Rev. Med.* 29, 51-66.
- 2 Spivak, J.L. and Graber, S.E. (1980) *Johns Hopkins Med. J.* 146, 311-320.
- 3 Lin, F.-K., Suggs, S., Lin, C.-H., Browne, J.K., Smalling, R., Egrie, J.C., Chen, K.K., Fox, G.M., Martin, F., Stabinsky, Z., Badrawi, S.M., Lai, P.-H. and Goldwasser, E. (1985) *Proc. Natl. Acad. Sci. U.S.A.* 82, 7580-7584.
- 4 Egrie, J.C., Strickland, T.W., Lane, J., Aoki, K., Cohen, A.M., Smalling, R., Trail, G., Lin, F.-K., Browne, J.K. and Hines, D.K. (1986) *Immunobiology* 172, 213-224.
- 5 Browne, J.K., Cohen, A.M., Egrie, J.C., Lai, P.H., Lin, F.-K., Strickland, T., Watson, E. and Stebbing, N. (1986) in *Cold Spring Harbor Symposium on Quantitative Biology* 51 (Harris, R.G., eds), pp. 693-702, Cold Spring Harbor, New York.
- 6 Dessypris, E.N., Gleason, J.H. and Armstrong, D.L. (1987) *Br. J. Haematol.* 65, 265-269.
- 7 Masunaga, H., Goto, K. and Ueda, M. (1987) *Acta Haematol. Jpn.* 50, 1119-1125.
- 8 Misago, M., Chiba, S., Tsukada, J., Kikuchi, M. and Eto, S. (1988) *Acta Haematol. Jpn.* 51, 967-974.
- 9 Eschback, J.W., Egrie, J.C., Downing, M.R., Browne, K.J. and Adamson, J.W. (1987) *N. Engl. J. Med.* 316, 73-78.
- 10 Winears, C.G., Oliver, D.O., Pippard, M.J., Reid, C., Downing, M. and Cotes, P.M. (1986) *Lancet* ii, 1175-1178.
- 11 Sytkowski, A.J. and Donahue, A. (1987) *J. Biol. Chem.* 262, 1161-1165.
- 12 Wang, F.F., Kung, C.K.-H. and Goldwasser, E. (1985) *Endocrinology* 116, 2286-2292.
- 13 Bannard, R.A.B., Cassleman, A.A., Cockburn, W.F. and Brown, G.M. (1958) *Can. J. Chem.* 36, 1541-1549.
- 14 Plapp, B.V., Moore, S. and Stein, W.H. (1971) *J. Biol. Chem.* 246, 939-945.
- 15 Robinson, N.C., Neurath, H. and Walsh, K.A. (1973) *Biochemistry* 12, 414-420.
- 16 Zollock, D.T. and Niehaus, W.G., Jr. (1975) *J. Biol. Chem.* 250, 3080-3088.
- 17 Riordan, J.F. and Vallee, B.L. (1972) *Methods Enzymol.* 25, 494-499.
- 18 Habeeb, A.F.S.A., Cassidy, H.G. and Singer, S.J. (1958) *Biochim. Biophys. Acta* 29, 587-593.
- 19 Riordan, J.F. (1973) *Biochemistry* 12, 3915-3923.
- 20 Patthy, L. and Smith, E.L. (1975) *J. Biol. Chem.* 250, 565-569.
- 21 Werber, M.M., Moldovan, M. and Sokolovsky, M. (1975) *Eur. J. Biochem.* 53, 207-216.
- 22 Nestler, J.E., Chanko, G.K. and Strauss, J.F. (1985) *J. Biol. Chem.* 260, 7316-7321.
- 23 Carraway, K.L. and Koshland, D.E., Jr. (1972) *Methods Enzymol.* 25, 616-623.
- 24 Fields, R. (1971) *Biochem. J.* 124, 581-590.
- 25 Goldwasser, E., Ellason, J.E. and Sikkema, D. (1975) *Endocrinology* 97, 315-323.
- 26 Cotes, P.M. and Bangham, D.R. (1961) *Nature* 191, 1065-1067.
- 27 Takeuchi, M., Takasaki, S., Miyazaki, H., Kato, T., Hoshi, S., Kochibe, N. and Kobata, A. (1987) *J. Biol. Chem.* 263, 3657-3663.
- 28 Lammli, U.K. (1970) *Nature* 227, 680-685.
- 29 Hammond, D., Shore, N. and Movassaghi, N. (1968) *Ann. NY Acad. Sci.* 68, 516-527.
- 30 McMullen, A.L. (1960) *Nature* 185, 102-103.
- 31 Dordal, M.S., Wang, F.P. and Goldwasser, E. (1985) *Endocrinology* 116, 2293-2299.
- 32 Goto, M., Akai, K., Murakami, A., Hashimoto, C., Tsuda, E., Ueda, M., Kawanishi, G., Takahashi, N., Ishimoto, A., Chiba, H. and Sasaki, R. (1988) *Biotechnology* 6, 67-71.
- 33 Takeuchi, M., Inoue, N., Strickland, T.W., Kubota, M., Wada, M., Shimizu, R., Kozutsumi, H., Takasaki, S. and Kobata, A. (1989) *Proc. Natl. Acad. Sci. USA* 86, 7819-7822.



Erythropoietin and its carbamylated derivative prevent the development of experimental diabetic autonomic neuropathy in STZ-induced diabetic NOD-SCID mice

Robert E. Schmidt^{a,*}, Karen G. Green^a, Dongyan Feng^a, Denise A. Dorsey^a,
Curtis A. Parvin^b, Jin-Moo Lee^c, Qinlgi Xiao^c, Michael Brines^d

^a Department of Pathology and Immunology, Division of Neuropathology, Washington University School of Medicine, Saint Louis, MO, USA

^b Department of Pathology and Immunology, Division of Laboratory Medicine, Washington University School of Medicine, Saint Louis, MO, USA

^c Department of Neurology, Washington University School of Medicine, Saint Louis, MO, USA

^d Warren Pharmaceuticals, Inc., Ossining, NY, USA

Received 10 August 2007; revised 9 September 2007; accepted 12 September 2007

Abstract

Autonomic neuropathy is a significant diabetic complication resulting in increased morbidity and mortality. Studies of autopsied diabetic patients and several rodent models demonstrate that the neuropathologic hallmark of diabetic sympathetic autonomic neuropathy in prevertebral ganglia is the occurrence of synaptic pathology resulting in distinctive dystrophic neurites (“neuritic dystrophy”). Our prior studies show that neuritic dystrophy is reversed by exogenous IGF-I administration without altering the metabolic severity of diabetes, i.e. functioning as a neurotrophic substance. The description of erythropoietin (EPO) synergy with IGF-I function and the recent discovery of EPO’s multifaceted neuroprotective role suggested it might substitute for IGF-I in treatment of diabetic autonomic neuropathy. Our current studies demonstrate EPO receptor (EPO-R) mRNA in a cDNA set prepared from NGF-maintained rat sympathetic neuron cultures which decreased with NGF deprivation, a result which demonstrates clearly that sympathetic neurons express EPO-R, a result confirmed by immunohistochemistry. Treatment of STZ-diabetic NOD-SCID mice have demonstrated a dramatic preventative effect of EPO and carbamylated EPO (CEPO, which is neuroprotective but not hematopoietic) on the development of neuritic dystrophy. Neither EPO nor CEPO had a demonstrable effect on the metabolic severity of diabetes. Our results coupled with reported salutary effects of EPO on postural hypotension in a few clinical studies of EPO-treated anemic diabetic and non-diabetic patients may reflect a primary neurotrophic effect of EPO on the sympathetic autonomic nervous system, rather than a primary hematopoietic effect. These findings may represent a major clinical advance since EPO has been widely and safely used in anemic patients due to a variety of clinical conditions.

© 2007 Elsevier Inc. All rights reserved.

Keywords: Diabetes; Autonomic neuropathy; Sympathetic; Neuropathology; Ganglia; Neuroaxonal dystrophy; Synapse

Introduction

Autonomic neuropathy is a significant clinical complication of diabetes which disturbs cardiovascular, alimentary and genitourinary function and results in increased patient morbidity and mortality (Ewing et al., 1980; Hosking et al., 1978; Rundles,

1945; Sampson et al., 1990; Vinik et al., 2003). Several series of autopsied diabetic patients (Duchen et al., 1980; Schmidt et al., 1993; Schmidt and Plurad, 1986) have established the reproducible development of markedly enlarged dystrophic axons and nerve terminals in diabetic prevertebral superior mesenteric (SMG) and celiac sympathetic ganglia (CG) in the absence of substantial loss of principal sympathetic neurons, a pattern similar to sympathetic ganglionic pathology which develops in aged patients (Schmidt et al., 1993).

The regular occurrence of degenerating, regenerating, and pathologically distinctive dystrophic axons and, to a lesser

* Corresponding author. Department of Pathology and Immunology (Box 8118), Washington University School of Medicine, 660 South Euclid Avenue Saint Louis, MO 63110, USA. Fax: +1 314 362 4096.

E-mail address: reschmidt@wustl.edu (R.E. Schmidt).

degree abnormal dendrites, in the absence of neuron loss has also been demonstrated in prevertebral sympathetic ganglia of streptozotocin (STZ)- and genetically-diabetic rodents, closely corresponding to human disease [reviewed in (Schmidt, 2002)]. Our previous studies have shown the striking improvement in the severity of diabetic autonomic neuropathy in rats treated with exogenous rhIGF-I in the absence of an effect on the severity of hyperglycemia (Schmidt et al., 1999), a result thought to reflect a neurotrophic role for IGF-I. The demonstration of endogenous IGF-I deficiency in the serum and sympathetic ganglia of diabetic rats (Schmidt et al., unpublished data), the known function of IGF-I as a sympathetic neurotrophic substance *in vitro* (Recio-Pinto et al., 1986) and differences in the development of sympathetic ganglionic dystrophy in types I and II diabetic rat and mouse models, i.e. animals deficient in or with increased levels of circulating IGF-I, respectively (Schmidt et al., 2004) suggest that loss of a neurotrophic effect of IGF-I might underlie the development of diabetic autonomic neuropathy.

Although the administration of IGF-I in a variety of human diseases has been accomplished, there has been concern that IGF-I may promote the development or progression of malignancies (Clark, 2004). As a result, substances with IGF-I like effects lacking its side effects have been sought. Interestingly, it has been noted that within the nervous system astrocytes respond to IGF-I by synthesizing EPO (Masuda et al., 1997). Further, a synergy has been observed between EPO and IGF-I (Digicaylioglu et al., 2004). These observations raised the question of whether EPO might substitute for IGF-I in treatment of diabetic neuropathy.

It is known that EPO receptors are located on peripheral dorsal root ganglia neurons, axons and Schwann cells and activate the PI3K/Akt signaling pathway, using receptors and early pathway intermediates distinct from IGF-I. Although EPO does not directly activate IGF-I or insulin receptors, EPO receptor activation results in stimulation of the PI-3Kinase/Akt signaling pathway which it shares with IGF-I and insulin signaling pathways.

Initially discovered as a mediator of erythropoiesis, for some time EPO has been recognized to have salutary effects on a variety of animal models of neurodegenerative processes including ischemic brain damage (Zhang et al., 2006), experimental allergic encephalomyelitis (Savino et al., 2006) and amyotrophic lateral sclerosis (Koh et al., 2007). Similarly, EPO is protective of peripheral nervous system insults (Hoke, 2006) including acrylamide and cisplatin toxic neuropathies (Bianchi et al., 2007; Keswani et al., 2004a; Melli et al., 2006), HIV sensory neuropathy (Keswani et al., 2004b) and, significantly, experimental diabetic somatic neuropathy (Bianchi et al., 2004; Tam et al., 2006). Therefore, to identify a possible role of EPO in the treatment of diabetic autonomic neuropathy, in this study we have demonstrated the presence of sympathetic neuronal EPO receptors (EPO-R) and examined the effect of exogenous administration of rhEPO on the frequency of neuritic dystrophy in our experimental mouse model of diabetic sympathetic autonomic neuropathy. Since EPO treatment of patients without anemia may possibly produce side effects of erythrocytosis or

effect tumor growth, we have also examined the effect of the carbamylated derivative of EPO (CEPO) which has been shown to possess tissue protective activities but no erythropoietic potency (Leist et al., 2004; Montero et al., 2007; Savino et al., 2006).

Materials and methods

Animals

Male Non-Obese Diabetic-Severe Combined Immune Deficient (NOD-SCID) mice were purchased from the Jackson Laboratory (Bar Harbor, ME) and were kept in pathogen-free conditions at Washington University. NOD-SCID mice are the result of breeding of the SCID mutation to the NOD background for many generations, such that the NOD-SCID mouse is genetically identical to the NOD mouse save for the absence of DNA-dependent protein kinase, a DNA repair enzyme (Blunt et al., 1996) resulting in loss of B and T cell function. Our previous studies (Schmidt et al., 2003) showed that NOD-SCID mice treated with streptozotocin rapidly become severely diabetic and develop dramatic autonomic neuropathy within 3–5 weeks. All animals were housed and cared for in accordance with the guidelines of the Washington University Committee for the Humane Care of Laboratory Animals and with National Institutes of Health guidelines on laboratory animal welfare. All mice were allowed standard mouse chow and water *ad libitum* and maintained on a 12/12 h light/dark cycle. A few male 4-month-old Sprague–Dawley (Charles River Laboratories, Wilmington, Massachusetts) were also used in this study. Rats were fed Purina rodent chow *ad libitum* and were housed in small groups with a 0700–1900 light cycle.

Induction of diabetes and treatment protocol

Mice were made diabetic by i.p. injection of freshly made streptozotocin (STZ [Sigma, St. Louis, MO], 50 mg/kg in citrate–saline buffer, pH 4.5) on four consecutive days under ketamine/xylazine anesthesia. Control animals received a comparable volume of citrate–saline buffer. The day following the last injection of STZ mice were bled and significantly hyperglycemic animals (plasma glucose >250 mg%) were considered diabetic. The effect of treatment with EPO and CEPO was examined in two separate experiments. Treatment with recombinant human erythropoietin (rhEPO, Dragon Pharmaceuticals, Vancouver, Canada) or carbamylated EPO (rhCEPO, Warren Pharmaceuticals) at a dose of 10 µg/kg (i.e. equivalent to ~1000 IU/kg of EPO) in saline × 3 injections/week for 4 weeks was begun the day after the last STZ injection. Control and diabetic animals not receiving EPO or CEPO received injections of saline.

Tissue preparation

After 4 weeks of treatment animals were anesthetized with ketamine/xylazine and perfused with 50 ml of heparinized saline followed by 100–200 ml of 3% glutaraldehyde in 0.1 M

phosphate buffer, pH 7.3, containing 0.45 mM Ca^{2+} . The superior mesenteric–celiac ganglia (SMG–CG) were dissected as a single block, cleaned of extraneous tissue while maintaining the superior mesenteric artery with the ganglionic block, and fixation continued overnight at 4 °C in the same buffer. Tissue samples were postfixed in phosphate-buffered 2% OsO_4 , dehydrated in graded concentrations of ethanol and embedded in EMBED-812 (Electron Microscopy Sciences, Hatfield, PA) with propylene oxide as an intermediary solvent. One-micron-thick plastic sections were examined by light microscopy after staining with toluidine blue. Ultrathin sections of individual SMG–CG were cut onto formvar coated slot grids, which permits visualization of entire ganglionic cross sections. Tissues were subsequently stained with uranyl acetate and lead citrate and examined with a JEOL 1200 electron microscope.

Quantitative histologic methods

Dystrophic elements are typically intimately related to neuronal perikarya and, therefore, we routinely express their frequency as the ratio of numbers of lesions to nucleated neuronal cell bodies. This method, used in our previous studies (Schmidt et al., 2003), substantively reduced the variance in assessments of intraganglionic lesion frequency. In addition, its simplicity permits the quantitative ultrastructural examination of relatively large numbers of ganglia. In our current animal studies an entire cross section of the SMG–CG was scanned at 12,000 \times magnification and the number of dystrophic neurites and synapses was determined by an investigator blinded to the identity of individual animals. Dystrophic neurites consist of swollen axons, synapses, dendritic spines or dendrites containing a variety of organelles including tubulovesicular aggregates, admixed normal and degenerating subcellular organelles, multivesicular and dense bodies, neurofilaments, and pure aggregates of minute mitochondria. The number of nucleated neurons (range: 50–200 neurons examined in each ganglionic cross section) was then determined by recounting at 6000 \times magnification. The frequency of ganglionic neuritic dystrophy was expressed as the ratio of number of dystrophic neurites to the number of nucleated neurons in the same cross section.

PCR demonstration of EPO-R in sympathetic ganglionic neuron cultures in vitro

Primary rat sympathetic ganglia cultures (25,000 neurons/dish) were maintained in the presence of NGF for 6 d and then deprived of NGF for 24 h as described previously (Estus et al., 1994). Total RNA was extracted from NGF maintained and NGF-deprived cultured neurons using TRI reagent (Molecular Research Center) following the manufacturer's instructions. Two hundred nanograms of total RNA were reverse transcribed and amplified using Titan One Step RT-PCR kit (Roche). The primer sequences for amplification of erythropoietin receptor were 5'-CTA TGG CTG TTG CAA CGC GA-3' (forward) and 5'-CCG AGG GCA CAG GAG CTT AG-3' (reverse). RT reactions were performed at 55 °C for 45 min. PCR conditions

were denaturing at 94 °C for 3 min followed by 30 cycles of denaturing at 94 °C for 30 s, annealing at 56 °C for 45 s and extension at 68 °C for 1 min, and ended by 7 min extension at 68 °C. The PCR products were analyzed by 1.5% agarose gel electrophoresis.

Immunohistochemistry

Rats were fixed by perfusion with freshly made 4% buffered paraformaldehyde at 0–4 °C and processed routinely for paraffin embedding. Paraffin embedded sections 5–8 μm thick were deparaffinized in xylene and rehydrated in a series of ethanol dilutions. Sections were preincubated for 20 min at room temperature in phosphate-buffered saline containing 2% BSA and 0.3% Triton X-100. Rabbit anti-EPO receptor antibody (1:100–1:200, Santa Cruz, sc-697) was next added and the slides incubated overnight at 4 °C, washed and a secondary biotinylated goat anti-rabbit IgG (1:500) was applied, washed and, in some experiments, followed by tyramide signal amplification using successive incubation with streptavidin HRP and cyanine-3 tyramide (Perkin-Elmer Life Science Products, Boston, MA).

Statistical analysis

All results are expressed as means \pm S.E.M. Analysis of variance (ANOVA) was performed using the SAS general linear models procedure.

Results

EPO receptors are present on rat sympathetic neurons

To determine if EPO receptors are expressed on sympathetic neurons, we asked if the EPO receptor mRNA was expressed in sympathetic cultures enriched in neurons. A previously extensively examined and validated set of cDNAs from NGF-maintained (lane 1, Fig. 1) and NGF-deprived rat sympathetic neurons (lane 2, Fig. 1) were examined by semi-quantitative

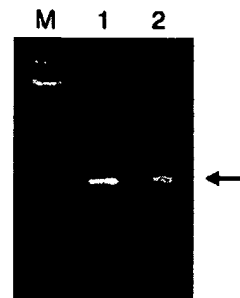


Fig. 1. Effect of NGF-deprivation on EPO-R in rat sympathetic ganglionic neurons in vitro. A validated set of cDNAs prepared from NGF-maintained (lane 1) and 24 h NGF-deprived rat sympathetic neurons (lane 2) were examined by semi-quantitative RT-PCR using a 402 bp product corresponding to the EPO receptor. Consistent with a neuronal localization, 24 h of NGF-deprivation in culture, which kills most of the neurons but not non-neuronal cells, greatly reduced the amount of EPO receptor in the cultures.

RT-PCR using a 402 bp product corresponding to EPO receptor. Consistent with a neuronal localization, 24 h of NGF-deprivation in culture, which kills most of the neurons but not non-neuronal cells, greatly reduced the amount of receptor in the cultures (lane 2, Fig. 1).

Immunolocalization of EPO receptors was performed on the sympathetic ganglia of control and diabetic rats. We found strong perikaryal staining in control rat SCG (Fig. 2A) and celiac ganglia (Fig. 2B) and those of diabetic rats (data not shown), confirming our results using cultured sympathetic neurons.

Metabolic and hematologic parameters in STZ-treated NOD-SCID mice

NOD-SCID mice became diabetic (blood glucose readings of >250 mg%) within a few days of induction of diabetes (data not shown) and were markedly hyperglycemic and weighed less at the time of sacrifice (Tables 1 and 2). Treatment with EPO (Table 1) or CEPO (Table 2) did not significantly affect the body weight or degree of hyperglycemia in diabetic mice. Age-matched saline, EPO- or CEPO-treated control NOD-SCID mice were consistently normoglycemic.

The hematocrit of diabetic animals was mildly increased compared to controls in both experiments which may reflect a mild degree of dehydration on the day of sacrifice. EPO increased the hematocrit of treated controls compared to saline-treated controls but had little effect on diabetic mice (Table 1).

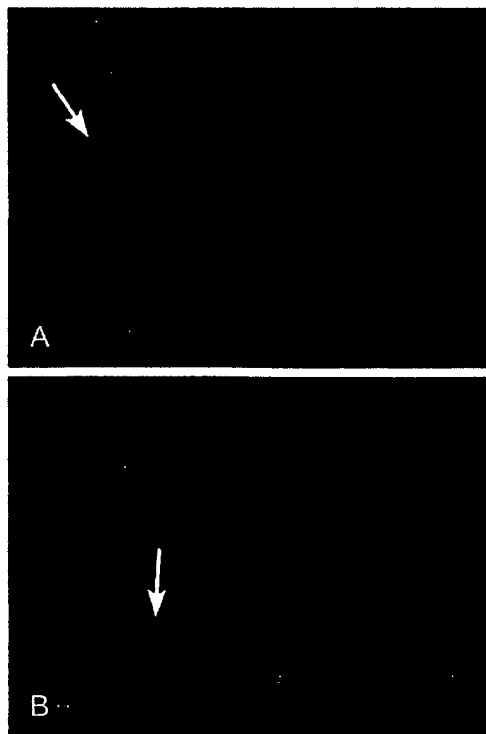


Fig. 2. Immunolocalization of EPO-receptor to sympathetic neurons. EPO-R is present in sympathetic neuronal cell bodies (arrows) in rat SCG (A) and celiac (B) sympathetic ganglia (original magnification 400 \times).

Table 1
Effects of EPO on diabetic NOD-SCID mice

Rx	n	SMG–CG neuritic dystrophy (#lesions/#neurons)	Glucose (mg%)	Weight (g)	Hematocrit (%)
DM+EPO	8	0.30 \pm 0.07*	>600	25.1 \pm 0.8	64 \pm 1.8
DM+SALINE	7	0.97 \pm 0.14	>600	23.9 \pm 1.0	61 \pm 0.4
C+EPO	4	0.06 \pm 0.04* (3)	100 \pm 5	27 \pm 1.2 [#]	72 \pm 3.8 ^{#,^}
C+SALINE	5	0.20 \pm 0.03* (3)	125 \pm 5	29.4 \pm 1.2 [#]	55 \pm 1.1 [#]

C=control, DM=diabetic, Values=mean \pm S.E.M. of *n* mice.

*= $p \leq 0.001$, #= $p \leq 0.01$ vs. saline-treated diabetic; ^= $p \leq 0.01$ vs. saline-treated control.

As expected, CEPO failed to have a hematologic effect on controls or diabetics (Table 2).

Neuropathology of SMG–CG

Examination of 1- μ m-thick plastic sections of SMG–CG in 4 week saline-treated diabetics in both experiments showed a well preserved complement of principal sympathetic neurons (Fig. 3) surrounded by neuropil composed of an admixture of axons and dendritic elements. There was no evidence of active neuronal degeneration (specifically, no apoptosis), nodules of Nageotte (tombstones of prior neuron loss) or chromatolysis. None of the diabetic ganglia contained an inflammatory infiltrate or an association of individual lymphocytes or macrophages with neuronal perikarya.

Large swollen neurites were prominent in light microscopic examination of 1- μ m-thick toluidine-blue stained plastic sections (arrows, Figs. 3A, B) of the SMG–CG of NOD-SCID mice diabetic for 4 weeks in comparison to saline-treated controls (Fig. 3C) and EPO-treated diabetics (Fig. 3D) or CEPO-treated diabetics (not shown), although dystrophic neurites were found in all groups of treated and untreated diabetics and controls, differing only in number (Tables 1 and 2). Dystrophic neurites were typically located immediately adjacent to neuronal cell bodies within their satellite cell sheaths (Figs. 3A, B), which resulted in the displacement and distortion of perikaryal contours of targeted neurons, as well as within the ganglionic neuropil. Dystrophic neurites ranged from swollen processes with pale cytoplasm (arrows, Fig. 3A) to those staining strongly with toluidine blue (arrows, Fig. 3B) and corresponding ultrastructurally to collections of mitochondria.

Table 2
Effects of CEPO on diabetic NOD-SCID mice

Rx	n	SMG–CG neuritic dystrophy (#lesions/#neurons)	Glucose (mg%)	Weight (g)	Hematocrit (%)
DM+CEPO	11	0.34 \pm 0.09*	563 \pm 14	22.1 \pm 0.2	50.6 \pm 1.8 [@]
DM+SALINE	6	1.09 \pm 0.08	526 \pm 26	24.4 \pm 0.7	48.0 \pm 1.0 (5)
C+CEPO	3	0.27 \pm 0.07*	115 \pm 5	28.7 \pm 0.7 [#]	43.6 \pm 0.3
C+SALINE	7	0.26 \pm 0.05*	128 \pm 5	29.9 \pm 0.6*	44.0 \pm 1.4

C=control, DM=diabetic, Values=mean \pm S.E.M. of *n* mice.

*= $p \leq 0.001$, #= $p \leq 0.01$, vs. saline-treated diabetic; @= $p \leq 0.05$ vs. saline-treated control.

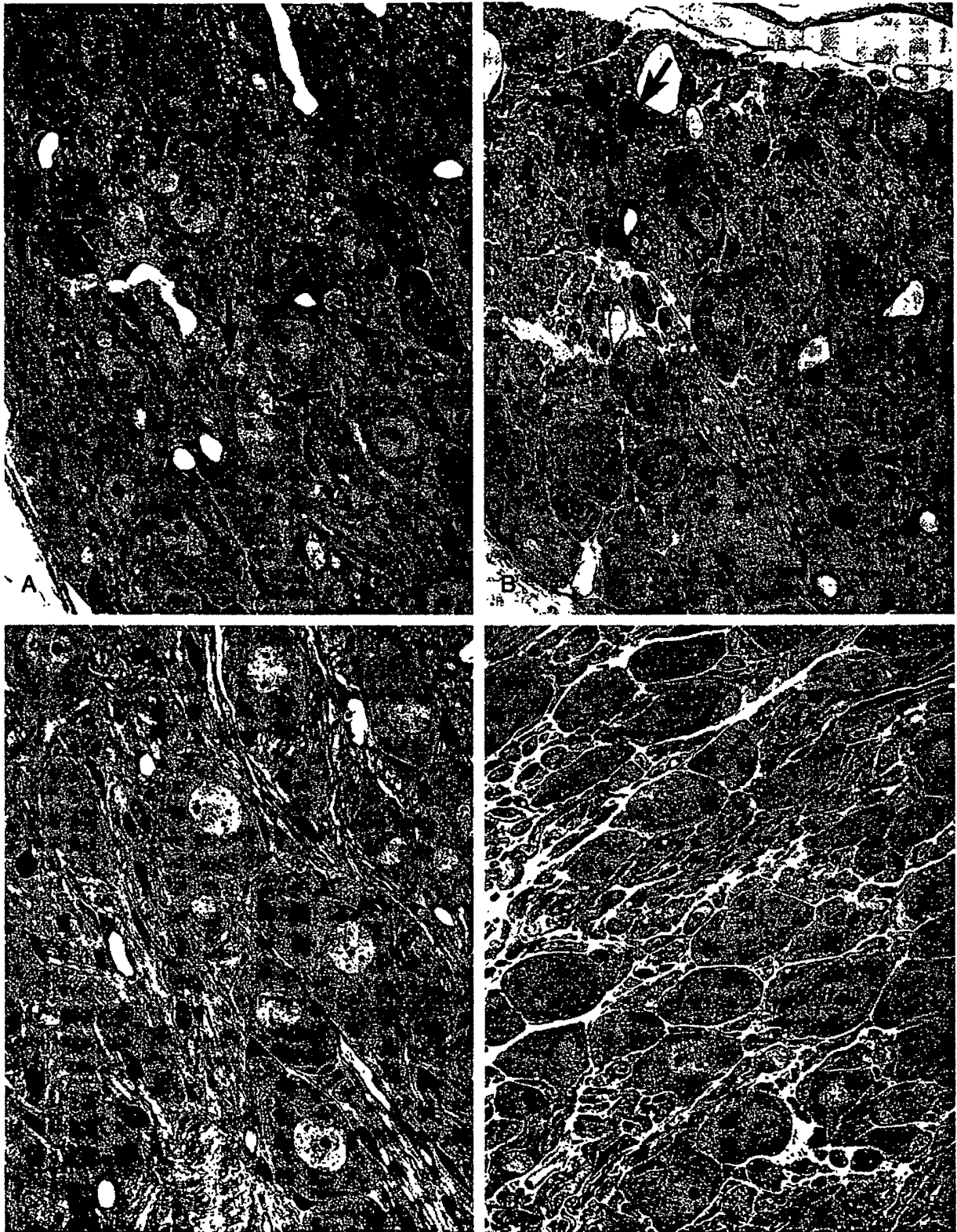
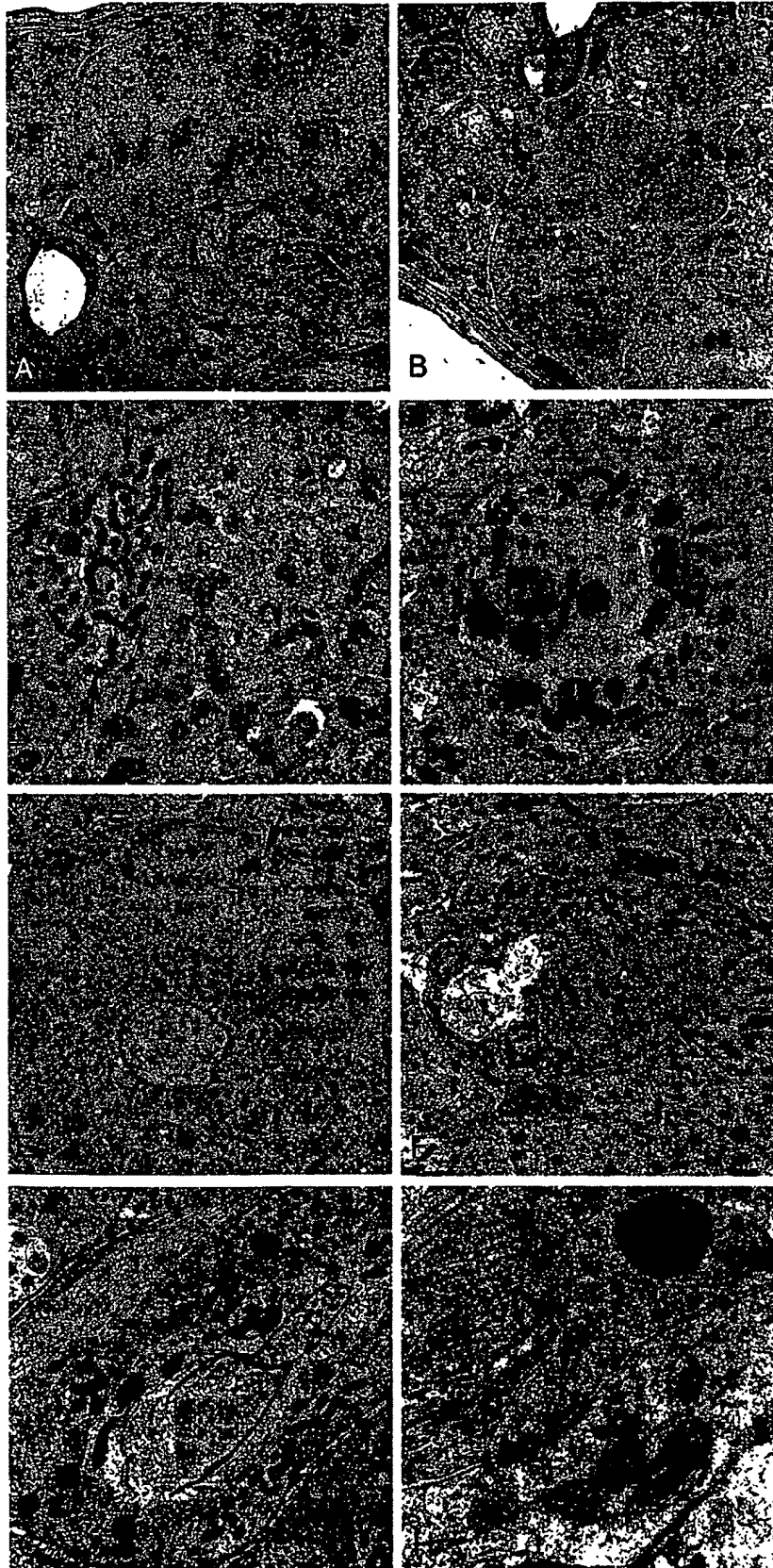


Fig. 3. Light microscopic appearance of 1- μ m-thick toluidine blue stained plastic sections of the SMG-CG of 4 week diabetic NOD-SCID mouse (A, B) in comparison to saline-treated controls (C) and EPO-treated diabetics (D). Dystrophic neurites, which range from swollen processes with pale cytoplasm (arrows, A) to those staining strongly with toluidine blue (arrows, B), distort the contours of otherwise normal appearing neuronal perikarya in NOD-SCID diabetic mice (original magnification: A–D—300 \times).



Ultrastructural examination confirmed the light microscopic appearance, demonstrating that swollen dystrophic elements were numerous in SMG–CG of saline-treated diabetic NOD-SCID mice and less frequent in EPO- or CEPO-treated diabetics and treated and untreated non-diabetic age-matched controls. Dystrophic elements exhibited a variety of ultrastructural patterns based on differences in their content of subcellular organelles (Fig. 4), as we have previously described (Schmidt et al., 2003). The most typical appearance (Figs. 4A, B) consisted of neuritic swellings containing large numbers of mitochondria which were tightly aggregated, usually without a significant amount of intervening axoplasm, and were significantly smaller than mitochondria within adjacent neuronal perikarya (Fig. 4C). Less frequently, neurites contained mixed collections of organelles (mitochondria, autophagosomes, neurofilaments and multivesicular bodies, Fig. 4D). Others were composed of numerous tubulovesicular elements ranging from small numbers within a pale unstructured cytoplasm (arrow, Fig. 4E) to compact aggregates (arrow, Fig. 4F). Occasional elements were identified as dendrites by their content of ribosomes, lipopigment or as postsynaptic elements (arrows, Figs. 4G, H). Dystrophic neurites were typically completely enclosed within the cytoplasm of Schwann or satellite cells and were often separated from adjacent perikarya by interposed satellite cell processes. In many cases it was difficult to confidently identify dystrophic elements as either axons or dendrites and, thus, we have referred to dystrophic processes simply as involving neuritic elements and the process as neuritic dystrophy. Neuritic dystrophy in the current experiments is comparable to that we have previously described in spontaneously diabetic NOD mice, STZ-treated NOD-SCID mice and various STZ-treated mouse strains (Schmidt et al., 2003).

Since dystrophic neurites were present in all groups of mice, differing only in numbers, it was necessary to apply an ultrastructural quantitative method to accurately compare their relative numbers. The numbers of dystrophic neurites were counted and expressed as a ratio (numbers of dystrophic elements/numbers of nucleated neurons). This analysis established that dystrophic neurites were increased 4–5-fold in 4 week diabetic NOD mouse SMG–CG compared to age-matched non-diabetic siblings (Table 1). The frequency of neuritic dystrophy in EPO (Table 1) and CEPO (Table 2) treated diabetic mice was not significantly different from saline-treated controls.

Discussion

The results of the current studies demonstrate a clear effect of EPO and CEPO given in a preventative paradigm on the deve-

lopment of experimental murine diabetic autonomic neuropathy. Our studies are consistent with recent studies which have shown that EPO produces a salutary effect on altered mechanical and thermal nociception, biochemistry and electrophysiology in diabetic rat somatic nerves (Bianchi et al., 2004; Roesler et al., 2004). Similarly, CEPO has demonstrated neuroprotective physiologic and structural effects in diabetic sensory neuropathy (Bianchi et al., 2004; Leist et al., 2004). EPO has been proposed to be synergistic with IGF-I in the activation of the PI3K/Akt pathway, which is diminished in somatic and vagus nerves of rats with STZ-diabetes (Cai and Helke, 2003; Huang et al., 2005). Interestingly, at least within the brain, IGF-I directly stimulates EPO production (Masuda et al., 1997) so that EPO/IGF-I synergy may exist physiologically in the nervous system. It is known that EPO and IGF-I downstream signaling pathways are also shared with insulin. Topical insulin application to diabetic rat sciatic nerve has been shown to have salutary neurotrophic effects on diabetic somatic neuropathy (Singhal et al., 1997) in the absence of improvement of systemic glucose levels. However, although treatment with insulin at doses resulting in partial blood glucose normalization do correct neuroaxonal dystrophy in STZ-rat diabetic mesenteric nerves (Schmidt and Plurad, 1983), subglycemic systemic doses of insulin used to mimic the transient hypoglycemic effect of IGF-I injection do not (Schmidt et al., 1999).

Neuroprotection by EPO is mediated through a heteroreceptor complex comprising both the EPO receptor and a common β -receptor subunit, also known as CD131 (Brines et al., 2004; reviewed by Brines and Cerami, 2005). Activation of EPO receptors on neurons and Schwann cells triggers neuroprotective pathways involving the PI3K/Akt cascade (Sirén et al., 2001; Lipton, 2004) and protects from excitotoxic, apoptotic and oxidative stress (Brines et al., 2000). In response to experimental axonal injury, nitric oxide is thought to stimulate periaxonal Schwann cells to release EPO which binds to neuronal EPO receptors and prevents axonal degeneration (Keswani et al., 2004a). Our experiments clearly establish that prevertebral sympathetic neurons also contain EPO-receptors and preliminary studies (Schmidt et al., unpublished results) show an EPO dose-dependent increase in phosphoAkt/total Akt ratio of sympathetic neurons in culture. A peptide sequence in EPO has been shown to induce differentiation and prevent cell death in neuroblastoma cell lines in the absence of an effect on erythropoietic cell lines or mouse primary spleen cells (Campana et al., 1998).

EPO has been used in the treatment of chemotherapy-associated and other refractory anemias. Anemia in diabetes (reviewed in McGill and Bell, 2006) may be multifactorial but is

Fig. 4. Ultrastructural appearance of neuritic dystrophy in NOD-SCID mouse SMG–CG. (A–C) Markedly enlarged neurites containing nearly pure collections of mitochondria represent the major category of neuritic dystrophy. The accumulated mitochondria in neuritic processes (arrows, C) are typically smaller than those of adjacent perikarya (arrowhead, C) (saline-treated diabetic, original magnification: A, B—3000 \times ; C—25,000 \times). (D) Dystrophic neurites may also contain a variety of admixed organelles including mitochondria, tubulovesicular elements, dense bodies and neurofilaments (saline-treated control, original magnification: D—25,000 \times). (E, F) A common ultrastructural appearance of dystrophic neurites consists of dilatations containing tubulovesicular elements which may be delicate or coarse. The contours of the sympathetic neuron cell body adjacent to the large dystrophic element (E) are distorted but the neuron appears otherwise normal (saline-treated diabetic, original magnification: E—4000 \times ; F—15,000 \times). (G, H) Synaptic specializations (arrow, G), seen at higher magnification (H), are occasionally found upon dystrophic neurites (saline-treated diabetic, original magnification: G—20,000 \times ; H—60,000 \times).

particularly common in diabetic patients with kidney disease even before the demonstrable loss of glomerular filtration capacity (Craig et al., 2005; McGill and Bell, 2006). One potential cause of anemia in diabetes is EPO deficiency or ineffectiveness (Bosman et al., 2001, 2002). A number of investigators have described the association of autonomic neuropathy in diabetic patients with anemia (Cotroneo et al., 2000; McGill and Bell, 2006; Ricerca et al., 1999; Saito et al., 2007; Spallone et al., 2004; Winkler et al., 1999). Since denervation of the kidney or use of beta adrenergic blocking agents are known to decrease kidney EPO production in experimental animals (Beynon, 1977; Fink and Fisher, 1976, it has been thought that loss of autonomic innervation of the kidney secondarily resulted in decreased EPO production. Serum EPO levels are decreased in type 1 diabetic patients with postural hypotension in comparison to age- and duration-matched type 1 diabetics free of complications as well as non-anemic, non-diabetic controls and patients with iron deficiency anemia (Winkler et al., 1999). A blunted EPO response to severe anemia has also been described as a result of autonomic neuropathy in studies of patients with both types 1 and 2 diabetes (Cotroneo et al., 2000; Ricerca et al., 1999; Saito et al., 2007; Spallone et al., 2004).

An effect of exogenous EPO on clinical autonomic neuropathy has been observed (Hoeldtke and Streeten, 1993). In one study, 6–10 weeks of EPO treatment of 8 patients with symptomatic orthostatic hypotension, anemia and decreased red cell mass in the clinical settings of type 1 diabetes, primary autonomic failure or sympathotonic orthostatic hypotension was reported to improve both postural hypotension and anemia (Hoeldtke and Streeten, 1993). Similarly, a 7-month trial of EPO in the treatment of postural hypotension in anemic type 1 diabetic patients also showed improvement in both anemia and postural hypotension (Winkler et al., 2001). Salutory effects of EPO on postural hypotension and anemia have also been described in patients with familial amyloidotic polyneuropathy (Ando et al., 1996), primary autonomic failure (Biaggioni et al., 1994; Perera et al., 1995) and multiple system atrophy with sympathetic failure (Winkler et al., 2002).

The mechanism of EPO's salutary effect on autonomic neuropathy is unknown and may be multifactorial. Although initially the effect of EPO was thought to reflect an increase in red cell mass or direct effects on the vasculature in the absence of hypervolemia (Hoeldtke and Streeten, 1993), it is not clear that uncomplicated anemia produces orthostatic hypotension. Indeed, one report describes improvement of severe orthostatic hypotension in the absence of improved anemia (Kawakami et al., 2003). Increased levels of serum norepinephrine, binding of nitric oxide to an increased hemoglobin concentration with resultant loss of NO-induced vasodilatation, change in viscosity of blood, increased vascular sensitivity to angiotensin II or other direct effects on smooth muscle cells have been proposed to explain EPO-induced improvement in postural hypotension (Rao and Stamler, 2002; Winkler et al., 2001). However, based on the results reported in our current investigation and these clinical studies, it is possible that the reported clinical effects of EPO on red cell mass and autonomic dysfunction may reflect

separate erythropoietic and neurotrophic effects. In future experiments, it will be possible to separate an effect of increased red cell mass from a neurotrophic effect in patients with autonomic neuropathy uncomplicated by anemia by treatment with CEPO or another non-erythropoietic EPO derivative.

Although experience with EPO is extensive with apparent safety (Sowade et al., 1998), there are reported side effects of EPO administration including accelerated hypertension and risk of thrombosis (Drueke et al., 2006; Rao and Stamler, 2002; Singh et al., 2006; Spivak, 2001). Recently, caution in the use of EPO has been proposed in light of the suggestion that it may exert a possible effect on tumor growth, particularly at higher doses (Crawford, 2007; Henke et al., 2006; Steensma and Loprinzi, 2005), prompting the FDA to issue a warning for the use of erythropoiesis stimulating agents in oncology patients. Additionally, the prothrombotic effects of EPO in the setting of injury are well known. A recent study has demonstrated neuroprotection from cisplatin-induced peripheral neuropathy in the absence of an effect on tumor growth (Bianchi et al., 2007). Although these issues are currently unresolved, it may prove that agents such as carbamylated EPO may well provide the salutary effects of EPO without triggering adverse effects such as pathological thrombosis or promoting growth of tumors.

Acknowledgment

The authors would like to thank Eugene M. Johnson for critical reading of the manuscript.

References

- Ando, Y., Asahara, K., Obayashi, K., Suhr, O., Yonemitsu, M., Yamashita, T., Tashima, K., Uchino, M., Ando, M., 1996. Autonomic dysfunction and anemia in neurologic disorders. *J. Auton. Nerv. Syst.* 61, 145–148.
- Beynon, G., 1977. The influence of the autonomic nervous system in the control of erythropoietin secretion in the hypoxic rat. *J. Physiol.* 266, 347–360.
- Biaggioni, I., Robertson, D., Krantz, S., Jones, M., Haile, V., 1994. The anemia of primary autonomic failure and its reversal with recombinant erythropoietin. *Ann. Intern. Med.* 121, 181–186.
- Bianchi, R., Buyukakilli, B., Brines, M., Savino, C., Cavaletti, G., Oggioni, N., Lauria, G., Borgna, M., Lombardi, R., Cimen, B., Comelekoglu, U., Kanik, A., Tataroglu, C., Cerami, A., Ghezzi, P., 2004. Erythropoietin both protects from and reverses experimental diabetic neuropathy. *Proc. Natl. Acad. Sci. U. S. A.* 101, 823–828.
- Bianchi, R., Gilardini, A., Rodriguez-Menendez, V., Oggioni, N., Canta, A., Colombo, T., Michele, G.D., Martone, S., Sfacteria, A., Piedemonte, G., Grasso, G., Beccaglia, P., Ghezzi, P., D'Incalci, M., Lauria, G., Cavaletti, G., 2007. Cisplatin-induced peripheral neuropathy: neuroprotection by erythropoietin without affecting tumour growth. *Eur. J. Cancer* 43, 710–717.
- Blunt, T., Gell, D., Fox, M., Taccioli, G.E., Lehmann, A.R., Jackson, S.P., Jeggo, P.A., 1996. Identification of a nonsense mutation in the carboxyl-terminal region of DNA-dependent protein kinase catalytic subunit in the acid mouse. *Proc. Natl. Acad. Sci. U. S. A.* 93, 10285–10290.
- Bosman, D.R., Winkler, A.S., Marsden, J.T., Macdougall, I.C., Watkins, P.J., 2001. Anemia with erythropoietin deficiency occurs early in diabetic nephropathy. *Diabetes Care* 24, 495–499.
- Bosman, D.R., Osborne, C.A., Marsden, J.T., Macdougall, I.C., Gardner, W.N., Watkins, P.J., 2002. Erythropoietin response to hypoxia in patients with diabetic autonomic neuropathy and non-diabetic chronic renal failure. *Diabet. Med.* 19, 65–69.

- Brines, M.L., Cerami, A., 2005. Emerging biological roles for erythropoietin in the nervous system. *Nat. Rev., Neurosci.* 6, 484–494.
- Brines, M.L., Ghezzi, P., Keenan, S., Agnello, D., de Lanerolle, N.C., Cerami, C., Itri, L.M., Cerami, A., 2000. Erythropoietin crosses the blood–brain barrier to protect against experimental brain injury. *Proc. Natl. Acad. Sci. U. S. A.* 97, 10526–10531.
- Brines, M.L., Grasso, G., Fiordaliso, F., Sfacteria, A., Ghezzi, P., Fratelli, M., Latini, R., Xie, Q.-W., Smart, J., Su-Rick, C.-J., Pobre, E., Diaz, D., Gomez, D., Hand, C., Coleman, T., Cerami, A., 2004. Erythropoietin mediates tissue protection through an erythropoietin and common beta-subunit heteroreceptor. *Proc. Natl. Acad. Sci. U. S. A.* 101, 14907–14912.
- Cai, F., Helke, C.J., 2003. Abnormal PI3 kinase/Akt signal pathway in vagal afferent neurons and vagus nerve of streptozotocin-diabetic rats. *Brain Res. Mol. Brain Res.* 110, 234–244.
- Campana, W.M., Misasi, R., O'Brien, J.S., 1998. Identification of a neurotrophic sequence in erythropoietin. *Int. J. Mol. Med.* 1, 235–241.
- Clark, R.G., 2004. Recombinant human insulin-like growth factor I (IGF-I): risks and benefits of normalizing blood IGF-I concentrations. *Horm. Res.* 62 (Suppl 1), 93–100.
- Cotroneo, P., Maria Ricerca, B., Todaro, L., Pitocco, D., Manto, A., Ruotolo, V., Storti, S., Damiani, P., Caputo, S., Ghirlanda, G., 2000. Blunted erythropoietin response to anemia in patients with Type 1 diabetes. *Diabetes Metab. Res. Rev.* 16, 172–176.
- Craig, K.J., Williams, J.D., Riley, S.G., Smith, H., Owens, D.R., Worthing, D., Cavill, I., Phillips, A.O., 2005. Anemia and diabetes in the absence of nephropathy. *Diabetes Care* 28, 1118–1123.
- Crawford, J., 2007. Erythropoietin: high profile, high scrutiny. *J. Clin. Oncol.* 25, 1021–1023.
- Digicaylioglu, M., Garden, G., Timberlake, S., Fletcher, L., Lipton, S.A., 2004. Acute neuroprotective synergy of erythropoietin and insulin-like growth factor I. *Proc. Natl. Acad. Sci. U. S. A.* 101, 9855–9860.
- Drueke, T.B., Locatelli, F., Clyne, N., Eckardt, K.U., Macdougall, I.C., Tsakiris, D., Burger, H.U., Scherhag, A., 2006. Normalization of hemoglobin level in patients with chronic kidney disease and anemia. *N. Engl. J. Med.* 355, 2071–2084.
- Duchen, L.W., Anjorin, A., Watkins, P.J., Mackay, J.D., 1980. Pathology of autonomic neuropathy in diabetes mellitus. *Ann. Intern. Med.* 92, 301–303.
- Estus, S., Zaks, W.J., Freeman, R.S., Gruda, M., Bravo, R., Johnson Jr., E.M., 1994. Altered gene expression in neurons during programmed cell death: identification of *c-jun* as necessary for neuronal apoptosis. *J. Cell Biol.* 127, 1717–1727.
- Ewing, D.J., Campbell, I.W., Clarke, B.F., 1980. The natural history of diabetic autonomic neuropathy. *Q. J. Med.* 49, 95–108.
- Fink, G.D., Fisher, J.W., 1976. Erythropoietin production after renal denervation or beta-adrenergic blockade. *Am. J. Physiol.* 230, 508–513.
- Henke, M., Matter, D., Pepe, M., Bezay, C., Weissenberger, C., Werner, M., Pajonk, F., 2006. Do erythropoietin receptors on cancer cells explain unexpected clinical findings? *J. Clin. Oncol.* 24, 4708–4713.
- Hoeldtke, R.D., Streeten, D.H., 1993. Treatment of orthostatic hypotension with erythropoietin. *N. Engl. J. Med.* 329, 611–615.
- Hoke, A., 2006. Neuroprotection in the peripheral nervous system: rationale for more effective therapies. *Arch. Neurol.* 63, 1681–1685.
- Hosking, D.J., Bennett, T., Hampton, J.R., 1978. Diabetic autonomic neuropathy. *Diabetes* 27, 1043–1055.
- Huang, T.J., Verkhatsky, A., Fernyhough, P., 2005. Insulin enhances mitochondrial inner membrane potential and increases ATP levels through phosphoinositide 3-kinase in adult sensory neurons. *Mol. Cell. Neurosci.* 28, 42–54.
- Kawakami, K., Abe, H., Harayama, N., Nakashima, Y., 2003. Successful treatment of severe orthostatic hypotension with erythropoietin. *Pacing Clin. Electrophysiol.* 26, 105–107.
- Keswani, S.C., Buldanlioglu, U., Fischer, A., Reed, N., Polley, M., Liang, H., Zhou, C., Jack, C., Leitz, G.J., Hoke, A., 2004a. A novel endogenous erythropoietin mediated pathway prevents axonal degeneration. *Ann. Neurol.* 56, 815–826.
- Keswani, S.C., Leitz, G.J., Hoke, A., 2004b. Erythropoietin is neuroprotective in models of HIV sensory neuropathy. *Neurosci. Lett.* 371, 102–105.
- Koh, S.H., Kim, Y., Kim, H.Y., Won Cho, G., Kim, K.S., Kim, S.H., 2007. Recombinant human erythropoietin suppresses symptom onset and progression of G93A-SOD1 mouse model of ALS by preventing motor neuron death and inflammation. *Eur. J. Neurosci.* 25, 1923–1930.
- Leist, M., Ghezzi, P., Grasso, G., Bianchi, R., Villa, P., Fratelli, M., Savino, C., Bianchi, M., Nielsen, J., Gerwien, J., Kallunki, P., Larsen, A.K., Helboe, L., Christensen, S., Pedersen, L.O., Nielsen, M., Torup, L., Sager, T., Sfacteria, A., Erbayraktar, S., Erbayraktar, Z., Gokmen, N., Yilmaz, O., Cerami-Hand, C., Xie, Q.W., Coleman, T., Cerami, A., Brines, M., 2004. Derivatives of erythropoietin that are tissue protective but not erythropoietic. *Science* 305, 239–242.
- Lipton, S.A., 2004. Erythropoietin for neurologic protection and diabetic neuropathy. *N. Engl. J. Med.* 350, 2516–2517.
- Masuda, S., Chikuma, M., Sasaki, R., 1997. Insulin-like growth factors and insulin stimulate erythropoietin production in primary cultured astrocytes. *Brain Res.* 746, 63–70.
- McGill, J.B., Bell, D.S., 2006. Anemia and the role of erythropoietin in diabetes. *J. Diabetes Its Complicat.* 20, 262–272.
- Melli, G., Jack, C., Lambrinos, G.L., Ringkamp, M., Hoke, A., 2006. Erythropoietin protects sensory axons against paclitaxel-induced distal degeneration. *Neurobiol. Dis.* 24, 525–530.
- Montero, M., Poulsen, F.R., Norberg, J., Kirkeby, A., van Beek, J., Leist, M., Zimmer, J., 2007. Comparison of neuroprotective effects of erythropoietin (EPO) and carbamylerythropoietin (CEPO) against ischemia-like oxygen-glucose deprivation (OGD) and NMDA excitotoxicity in mouse hippocampal slice cultures. *Exp. Neurol.* 204, 106–117.
- Perera, R., Isola, L., Kaufmann, H., 1995. Effect of recombinant erythropoietin on anemia and orthostatic hypotension in primary autonomic failure. *Clin. Auton. Res.* 5, 211–213.
- Rao, S.V., Stamler, J.S., 2002. Erythropoietin, anemia, and orthostatic hypotension: the evidence mounts. *Clin. Auton. Res.* 12, 141–143.
- Recio-Pinto, E., Rechler, M.M., Ishii, D.N., 1986. Effects of insulin, insulin-like growth factor-II, and nerve growth factor on neurite formation and survival in cultured sympathetic and sensory neurons. *J. Neurosci.* 6, 1211–1219.
- Ricerca, B.M., Todaro, L., Caputo, S., Cotroneo, P., Damiani, P., Manto, A., Pitocco, D., Storti, S., Ghirlanda, G., 1999. Blunted erythropoietin response to anemia in type 1 diabetic patients. *Diabetes Care* 22, 647.
- Roesler, R., Quevedo, J., Schroder, N., 2004. Erythropoietin, glutamate, and neuroprotection. *N. Engl. J. Med.* 351, 1465–1466 (author).
- Rundles, R., 1945. Diabetic neuropathy. General review with report of 125 cases. *Medicine* 24, 111–160.
- Saito, T., Tojo, K., Nishimura, R., Kageyama, S., Tajima, N., 2007. Coefficient of variation of R-R intervals in electrocardiogram is a sensitive marker of anemia induced by autonomic neuropathy in type 1 diabetes. *Diabetes Res. Clin. Pract.* 78, 60–64.
- Sampson, M.J., Wilson, S., Karagiannis, P., Edmonds, M., Watkins, P.J., 1990. Progression of diabetic autonomic neuropathy over a decade in insulin-dependent diabetics. *Q. J. Med.* 75, 635–646.
- Savino, C., Pedotti, R., Baggi, F., Ubiali, F., Gallo, B., Nava, S., Bigini, P., Barbera, S., Fumagalli, E., Mennini, T., Vezzani, A., Rizzi, M., Coleman, T., Cerami, A., Brines, M., Ghezzi, P., Bianchi, R., 2006. Delayed administration of erythropoietin and its non-erythropoietic derivatives ameliorates chronic murine autoimmune encephalomyelitis. *J. Neuroimmunol.* 172, 27–37.
- Schmidt, R., 2002. Neuropathology and pathogenesis of diabetic autonomic neuropathy. In: Tomlinson, D.R. (Ed.), *Neurobiology of Diabetic Neuropathy*. Academic Press, Amsterdam, pp. 267–292.
- Schmidt, R.E., Plurad, S.B., 1986. Ultrastructural and biochemical characterization of autonomic neuropathy in rats with chronic streptozotocin diabetes. *J. Neuropathol. Exp. Neurol.* 45, 525–544.
- Schmidt, R.E., Plurad, S.B., 1983. The effect of pancreatic islet transplantation and insulin therapy on experimental diabetic autonomic neuropathy. *Diabetes* 32, 532–540.
- Schmidt, R.E., Plurad, S.B., Parvin, C.A., Roth, K.A., 1993. Effect of diabetes and aging on human sympathetic autonomic ganglia. *Am. J. Pathol.* 143, 143–153.
- Schmidt, R.E., Dorsey, D.A., Beaudet, L.N., Plurad, S.B., Parvin, C.A., Miller, M.S., 1999. Insulin-like growth factor I reverses experimental diabetic autonomic neuropathy. *Am. J. Pathol.* 155, 1651–1660.

- Schmidt, R.E., Dorsey, D.A., Beaudet, L.N., Frederick, K.E., Parvin, C.A., Plurad, S.B., Levisetti, M.G., 2003. Non-obese diabetic mice rapidly develop dramatic sympathetic neuritic dystrophy: a new experimental model of diabetic autonomic neuropathy. *Am. J. Pathol.* 163, 2077–2091.
- Schmidt, R.E., Dorsey, D.A., Beaudet, L.N., Parvin, C.A., Zhang, W., Sima, A.A., 2004. Experimental rat models of types 1 and 2 diabetes differ in sympathetic neuroaxonal dystrophy. *J. Neuropathol. Exp. Neurol.* 63, 450–460.
- Singh, A.K., Szczech, L., Tang, K.L., Barnhart, H., Sapp, S., Wolfson, M., Reddan, D., 2006. Correction of anemia with epoetin alfa in chronic kidney disease. *N. Engl. J. Med.* 355, 2085–2098.
- Singhal, A., Cheng, C., Sun, H., Zochodne, D.W., 1997. Near nerve local insulin prevents conduction slowing in experimental diabetes. *Brain Res.* 763, 209–214.
- Sirén, A.-L., Fratelli, M., Brines, M., Goemans, C., Casagrande, S., Lewczuk, P., Keenan, S., Gleiter, C., Pasquali, C., Capobianco, A., Mennini, T., Heumann, R., Cerami, A., Ehrenreich, H., Ghezzi, P., 2001. Erythropoietin prevents neuronal apoptosis after cerebral ischemia and metabolic stress. *Proc. Natl. Acad. Sci. U. S. A.* 98, 4044–4049.
- Sowade, B., Sowade, O., Mocks, J., Franke, W., Warnke, H., 1998. The safety of treatment with recombinant human erythropoietin in clinical use: a review of controlled studies. *Int. J. Mol. Med.* 1, 303–314.
- Spallone, V., Maiello, M.R., Kurukulasuriya, N., Barini, A., Lovecchio, M., Tartaglione, R., Mennuni, G., Menzinger, G., 2004. Does autonomic neuropathy play a role in erythropoietin regulation in non-proteinuric Type 2 diabetic patients? *Diabet. Med.* 21, 1174–1180.
- Spivak, J.L., 2001. Erythropoietin use and abuse: when physiology and pharmacology collide. *Adv. Exp. Med. Biol.* 502, 207–224.
- Steensma, D.P., Loprinzi, C.L., 2005. Erythropoietin use in cancer patients: a matter of life and death? *J. Clin. Oncol.* 23, 5865–5868.
- Tam, J., Diamond, J., Maysinger, D., 2006. Dual-action peptides: a new strategy in the treatment of diabetes-associated neuropathy. *Drug Discov. Today* 11, 254–260.
- Vinik, A.I., Maser, R.E., Mitchell, B.D., Freeman, R., 2003. Diabetic autonomic neuropathy. *Diabetes Care* 26, 1553–1579.
- Winkler, A.S., Marsden, J., Chaudhuri, K.R., Hambley, H., Watkins, P.J., 1999. Erythropoietin depletion and anaemia in diabetes mellitus. *Diabet. Med.* 16, 813–819.
- Winkler, A.S., Landau, S., Watkins, P.J., 2001. Erythropoietin treatment of postural hypotension in anemic type 1 diabetic patients with autonomic neuropathy: a case study of four patients. *Diabetes Care* 24, 1121–1123.
- Winkler, A.S., Landau, S., Watkins, P., Chaudhuri, K.R., 2002. Observations on haematological and cardiovascular effects of erythropoietin treatment in multiple system atrophy with sympathetic failure. *Clin. Auton. Res.* 12, 203–206.
- Zhang, F., Signore, A.P., Zhou, Z., Wang, S., Cao, G., Chen, J., 2006. Erythropoietin protects CA1 neurons against global cerebral ischemia in rat: potential signaling mechanisms. *J. Neurosci. Res.* 83, 1241–1251.

Reduced functional deficits, neuroinflammation, and secondary tissue damage after treatment of stroke by nonerythropoietic erythropoietin derivatives

Pia Villa^{1,2,*}, Johan van Beek^{3,*}, Anna Kirstine Larsen³, Jens Gerwien³, Søren Christensen³, Anthony Cerami⁴, Michael Brines⁴, Marcel Leist^{3,†}, Pietro Ghezzi¹ and Lars Torup³

¹Mario Negri Institute of Pharmacological Research, Milan, Italy; ²CNR, Institute of Neuroscience, Cellular and Molecular Pharmacology Section, Milan, Italy; ³H Lundbeck A/S, Valby-Copenhagen, Denmark; ⁴Kenneth S. Warren Institute, Ossining, New York, USA

Carbamylerthropoietin (CEPO) does not bind to the classical erythropoietin (EPO) receptor. Nevertheless, similarly to EPO, CEPO promotes neuroprotection on the histologic level in short-term stroke models. In the present study, we investigated whether CEPO and other nonerythropoietic EPO analogs could enhance functional recovery and promote long-term histologic protection after experimental focal cerebral ischemia. Rats were treated with the compounds after focal cerebral ischemia. Animals survived 1, 7, or 60 days and underwent behavioral testing (sensorimotor and foot-fault tests). Brain sections were stained and analyzed for Iba-1, myeloperoxidase, Tau-1, CD68 (ED1), glial fibrillary acidic protein (GFAP), Fluoro-Jade B staining, and overall infarct volumes. Treatment with CEPO reduced perifocal microglial activation ($P < 0.05$), polymorphonuclear cell infiltration ($P < 0.05$), and white matter damage ($P < 0.01$) at 1 day after occlusion. Carbamylerthropoietin-treated rats showed better functional recovery relative to vehicle-treated animals as assessed 1, 7, 14, 28, and 50 days after stroke. Both GFAP and CD68 were decreased within the ipsilateral thalamus of CEPO-treated animals 60 days postoperatively ($P < 0.01$ and $P < 0.05$, respectively). Furthermore, behavioral analysis showed efficacy of CEPO treatment even if administered 24 h after the stroke. Other nonerythropoietic derivatives such as carbamylated darbepoetin alfa and the mutant EPO-S100E were also found to protect against ischemic damage and to improve postischemic neurologic function. In conclusion, these results show that postischemic intravenous treatment with nonerythropoietic EPO derivatives leads to improved functional recovery, which may be linked to their long-term effects against neuroinflammation and secondary tissue damage.

Journal of Cerebral Blood Flow & Metabolism (2007) 27, 552–563. doi:10.1038/sj.jcbfm.9600370; published online 12 July 2006

Keywords: erythropoietin; focal ischemia; functional recovery; inflammation; neuroprotection

Introduction

Recombinant human erythropoietin (EPO) has shown widespread efficacy in animal models of

stroke (Sakanaka *et al*, 1998; Brines *et al*, 2000; Calapai *et al*, 2000; Siren *et al*, 2001; Brines and Cerami, 2005). Despite its large size, recombinant human EPO administered peripherally crosses the blood–brain barrier to protect against brain injury (Brines *et al*, 2000). Erythropoietin may act against ischemic damage at multiple levels including attenuation of apoptosis (Siren *et al*, 2001; Villa *et al*, 2003), and reduction of brain inflammation (Villa *et al*, 2003). More recently, EPO treatment was shown to improve functional recovery, and enhance neurogenesis and angiogenesis after focal ischemia, suggesting a beneficial effect of EPO treatment on brain repair after stroke (Wang *et al*, 2004a). Translation of these research findings into therapeutic application looks promising because the use

Correspondence: Dr L. Torup, H. Lundbeck A/S, Department of Neuropharmacology (805), Ottiliavej 9, Valby-Copenhagen 2500, Denmark.

E-mail: LTO@lundbeck.com

*These two authors contributed equally to this work.

†Current address: Faculty of Biology, University of Konstanz, Konstanz, Germany.

This work was partly supported by the Fondazione Cariplo, Milan, Italy (to PG) and by the Ministero della Sanità-Ricerca Finalizzata (to PG).

Received 20 December 2005; revised 1 June 2006; accepted 3 June 2006; published online 12 July 2006

of erythropoietin in a small clinical trial in patients suffering from stroke improved neurologic scores and functionality (Ehrenreich *et al*, 2002).

In clinical situations that are likely to require multiple doses of EPO, a major limitation of the compound is that it would trigger unwanted overstimulation of the bone marrow, raise the hematocrit and induce a procoagulant state. For instance, a high hematocrit in transgenic mice overexpressing human EPO is associated with increased susceptibility to ischemic damage (Wiessner *et al*, 2001). To circumvent this side effect issue, various strategies to dissociate erythropoietic and tissue-protective activities of EPO have been developed. For instance, asialoerythropoietin, an EPO derivative with a very short half-life generated by enzymatic desialylation of EPO, is neuroprotective in models of focal ischemia (Erbayraktar *et al*, 2003) and neonatal hypoxia-ischemia (Wang *et al*, 2004b) without increasing the hematocrit. More recently, we have described chemically modified forms of EPO such as carbamylerythropoietin (CEPO) or EPO mutants that do not bind to the classical EPO receptor (EPOR). These retain their tissue-protective properties without effects on the bone marrow and hematocrit (Leist *et al*, 2004). Carbamylerythropoietin treatment reduced brain infarction after focal ischemia to the same degree as reported for EPO and with a broad therapeutic window (4 h) (Leist *et al*, 2004).

In the present study, we further explored the effects of CEPO and other nonerythropoietic derivatives of EPO on poststroke functional recovery, secondary tissue damage, and inflammation.

Materials and methods

Focal Ischemia Model

All experimental procedures were performed in accordance with the directives of the European Communities Council Directive #86/609 for care of laboratory animals and in agreement with national regulations on animal research in Italy and Denmark. Surgery was performed on male Crl:CD (SD)BR rats weighing 250 to 285 g (Charles River, Calco, Italy). Focal ischemic stroke within the distribution of the middle cerebral artery (MCA) was produced as described previously (Brines *et al*, 2000). Briefly, the right common carotid artery (CCA) was occluded by two sutures and cut. A burr hole adjacent and rostral to the right orbit allowed visualization of the MCA, which was cauterized distal to the rhinal artery. Animals were then positioned on a stereotaxic frame and the contralateral CCA was occluded for 1 h by using traction with a fine forceps. Body core temperature was thermostatically maintained at 37°C by using a heating pad and a rectal thermistor (Letica, Barcelona, Spain) for the duration of the anesthesia.

Reagents

Carbamylerythropoietin was synthesized from rhEPO (Dragon Pharmaceuticals, Vancouver, Canada) as described

earlier (Leist *et al*, 2004). Carbamylated darbepoetin alfa (Caranesp) was synthesized from Aranesp (darbepoetin alfa; Amgen, Thousand Oaks, CA, USA) using the same protocol. Carbamylation of EPO and darbepoetin alfa transformed all lysines to homocitrulline resulting in products lacking bioactivity in the *in vitro* UT7 hemato-poiesis assay and failing to bind to EPOR on these cells. Generation of mutant EPO-S100E was described previously (Leist *et al*, 2004).

Drug Treatments

The drug doses (CEPO, 50 µg/kg; Caranesp, 50 µg/kg; EPO-S100E, 50 µg/kg) were all equivalent with respect to the mass relation to approximately 5,000 IU/kg of EPO. Doses of nonerythropoietic derivatives were chosen based on the observation that equivalent doses of EPO and nonerythropoietic variants are required for neuroprotective effects (Erbayraktar *et al*, 2003; Leist *et al*, 2004; Wang *et al*, 2004b). Drugs or vehicle (0.05% human serum albumin in phosphate-buffered saline) were administered intravenously at different time points after MCA occlusion as described in the text and figures.

Neurologic Deficits

Animals were evaluated for neurologic deficits using the limb placing and the foot-fault tests at different times after occlusion. The limb-placing test developed by De Ryck *et al* (1989) evaluates sensorimotor integration in limb-placing responses to visual, vibrissae, tactile, and proprioceptive stimuli. For each test, limb placing scores were 0, no placing; 1, incomplete and/or delayed (> 2 secs) placing; or 2, immediate and complete placing. Each test was repeated for each paw up to 10 times and for each body side; the maximum limb placing score was 16. The foot-fault test developed by Hernandez and Schallert (1988) measures the ability of the animal to integrate motor responses. The rats were placed on a grid with 2 cm spaces between 0.3 cm diameter metal rods and were observed for 2 mins. With each weight-bearing step, the paw may fall or slip between the wires and this is recorded as foot-fault. The number of foot-faults for the paws contralateral and ipsilateral to the infarction was recorded with the number of successful steps and the foot-fault index was calculated as the percentage of contralateral limb foot-faults per limb step minus the percentage of ipsilateral limb foot-faults per limb step. Baseline foot-fault index as acquired in nontreated nonoperated rats was usually <5 (data not shown).

Infarct Assessment

Infarct volumes were determined 24 h after MCA occlusion by quantitative image analysis of triphenyl tetrazolium chloride-stained 1-mm brain sections using a computerized image analysis system (AIS version 3.0 software, Imaging Research, St Catherine's, ON, Canada) as described previously (Brines *et al*, 2000). Alternatively,

infarct volumes were measured at day 7 after occlusion. Sections selected from predetermined coronal planes (+5.2 to -7.4 mm from bregma) were stained with toluidine blue. Images of brain sections were captured and measurements of hemispheric damage to cortical neuronal perikarya was determined by summation of cortical infarct volumes measured in each brain slice using CAST software (Olympus, Denmark). Alternatively, the infarct volume was calculated as the percentage of infarct volume to the volume of the contralateral hemisphere (indirect volume calculation) as described previously (Zhang *et al*, 1997).

Immunohistochemistry and Fluoro-Jade B Staining

Animals were anesthetized with chloral hydrate and perfused transcardially with phosphate-buffered saline followed by 4% phosphate-buffered paraformaldehyde for 15 mins. Brains were cryoprotected in 30% sucrose, and sectioned into 20- μ m coronal cryosections. Cryosections were processed as free-floating sections using the protocol based on the avidin-biotin-peroxidase technique as described previously (van Beek *et al*, 2000). Alternatively, triphenyl tetrazolium chloride-stained slices were post-fixed in 4% paraformaldehyde fixative in phosphate buffer and paraffin-embedded. Four micron coronal sections were cut on a microtome and processed for immunohistochemistry using the same protocol as described above supplemented with antigen retrieval by microwaving in a citric acid buffer (10 mmol/L; pH 6). In all immunohistochemistry protocols, negative controls were performed by omitting the primary antibody, and this resulted in minimal detected signal in all cases. The following antibodies were used: goat anti-human Iba-1 (1:4,000; Abcam, Cambridge, UK; #Ab5076), mouse anti-rat CD68 (clone ED1; 1:50; Serotec, Oxford, UK), rabbit anti-human myeloperoxidase (1:4,000; DAKO, Glostrup, Denmark; #A 0398), mouse anti-cow Tau-1 (clone PC1C6; 1:5,000; Chemicon International, Temecula, CA, USA; #MAB3420), and rabbit anti-cow glial fibrillary acidic protein (GFAP) (1:4,000; DAKO; #Z 0334). Fluoro-Jade B staining was performed as described previously (Schmued *et al*, 1997).

Staining Quantification

Images were captured with a JenOptik ProgRes digital camera and image analysis was performed on an Openlab imaging station (Improvision, Coventry, UK). Images from brain areas were captured as follows: perifocal cortex for Iba1 and GFAP (1.00 mm relative to bregma), infarcted core for myeloperoxidase and CD68 (1.00 mm relative to bregma), ipsilateral internal capsule and corpus callosum for Tau1 (-3.14 mm relative to bregma). For examination of Fluoro-Jade B staining, images from whole ipsilateral striatum were captured (1.00 mm relative to bregma). For quantification of thalamic GFAP and CD68 staining, images from whole ipsilateral thalamus were captured (-3.14 mm relative to bregma). Density slicing of regions

of interest under standardized conditions was used to detect the area of staining (Staining Index).

In Vitro Neuroprotection

Primary neuronal cultures were prepared from new born rat hippocampi by trypsinization, and cultured as described (Leist *et al*, 2004). On day 14, the cultures were challenged with 300 μ mol/L *N*-methyl-D-aspartate for 5 mins at room temperature. After the excitotoxic insult, preconditioned medium was returned to the cultures for 24 h. Cells were fixed in 4% paraformaldehyde, stained with Hoechst 33342 (Molecular Probes, Eugene, OR, USA) and condensed apoptotic nuclei were counted. Approximately 300 neurons were counted per condition in at least three separate wells and the experiments were repeated at least twice.

Hematopoietic Bioactivity

To test the hematopoietic bioactivity in a proliferation assay, the EPO-dependent human leukemia cell line UT7 was obtained from Deutsche Sammlung von Mikroorganismen und Zellkulturen (Braunschweig, Germany). The assay was performed as described previously (Erbayraktar *et al*, 2003) over 48 h. Compounds were tested at 0.2 pmol/L to 20 nmol/L and proliferation was quantified using WST-1 reduction (Roche Applied Science, Indianapolis, IN, USA).

Statistical Analysis

Data are presented as mean values \pm s.e.m. Cortical infarct distribution data at 7 days after occlusion were analyzed using repeated-measures analysis of variance followed by Bonferroni tests. For histopathologic data and comparison between vehicle- and CEPO-treated animals, a Student's *t*-test was used. The nonparametric Mann-Whitney and Kruskal-Wallis tests were used to determine significant differences in neurologic scores when two or more groups were compared, respectively.

Results

Protection Against Ischemic Damage *In Vivo* and Excitotoxic Injury *In Vitro* by Caranesp

Cortical infarct areas were significantly reduced by treatment with Caranesp and CEPO compared with vehicle in the 1-day survival group (31% and 28% reduction from control, respectively; $P < 0.05$; Figures 1A and 1B). A significant ($P < 0.01$) improvement in sensorimotor function was observed in Caranesp- and CEPO-treated animals compared with vehicle-treated rats (Figure 1C). Caranesp prevented *N*-methyl-D-aspartate-induced apoptosis of primary hippocampal cells ($P < 0.001$; Figure 1D) but completely lacked bioactivity in the *in vitro* UT7 hematopoiesis assay (Figure 1E).

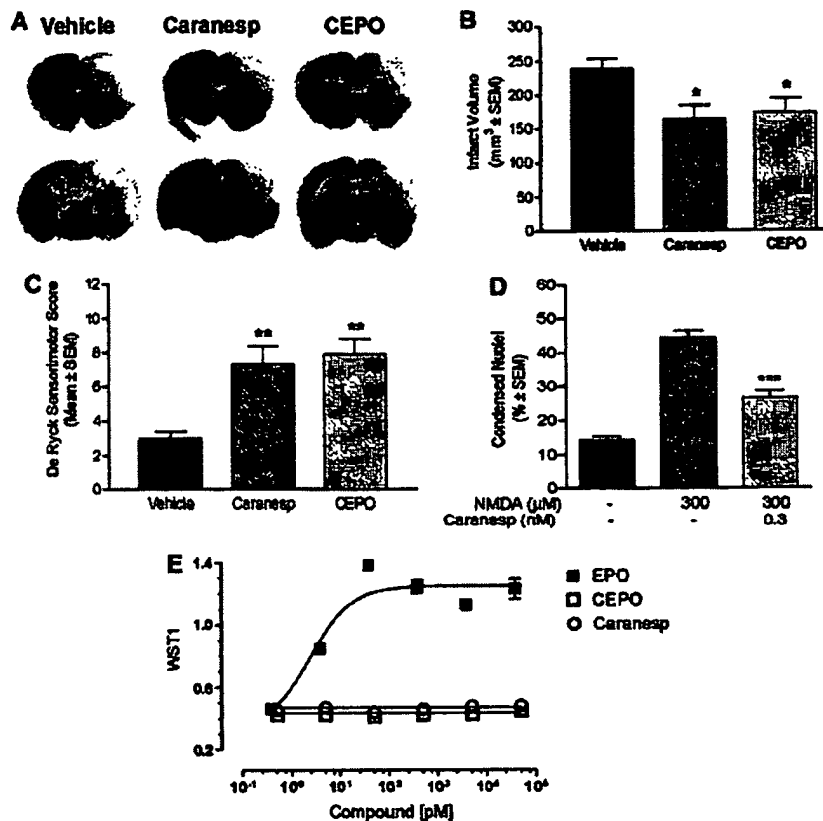


Figure 1 Neuroprotective properties of CEPO and Caranesp. (A) representative images of tetraphenyl tetrazolium chloride-stained sections 24 h after occlusion. (B) Total infarct volume as measured at 24 h after occlusion. Vehicle, Caranesp, or CEPO were administered intravenously 1 h after occlusion. Cortical infarct volume was significantly reduced by CEPO and Caranesp treatment ($n = 8$ and 9 , respectively) compared with vehicle group ($n = 9$). $*P < 0.05$ compared with vehicle group; Student's t -test. (C) De Ryck sensorimotor test. The impairment in the sensorimotor test was significantly reduced by CEPO and Caranesp treatment. $**P < 0.01$ compared with vehicle group; Kruskal-Wallis. Note that Caranesp protected against ischemic injury and restores sensorimotor function to a similar extent as CEPO. (D) Effect of Caranesp on N -methyl-D-aspartate-induced toxicity in primary hippocampal neurons. Caranesp protects neurons against excitotoxicity. $***P < 0.001$ compared with N -methyl-D-aspartate-treated primary cortical neurons; Student's t -test. (E) Hematopoietic bioactivity of CEPO and Caranesp in the UT7 EPO-dependent human leukemia cell line proliferation assay.

Attenuation of Postischemic Perifocal Microglial Activation and Polymorphonuclear Leukocyte Infiltration by Carbamylerythropoietin Treatment

Triphenyl tetrazolium chloride-stained slices from vehicle- and CEPO-treated rats (1-day survival groups) were further processed for immunostaining for inflammatory markers including GFAP, Iba-1, and myeloperoxidase. At 1 day after occlusion, GFAP expression in the perifocal area was not significantly ($P > 0.05$) increased compared with contralateral control area (data not shown). Glial fibrillary acidic protein expression was not affected by CEPO treatment (data not shown). Iba-1-positive microglia were observed in regions surrounding the ischemic core (Figure 2A) and numerous polymorphonuclear leukocytes stained for myeloperoxidase were seen in the ischemic core (Figure 2B). Very few CD68-positive macrophages were observed within

the infarcted core (data not shown). Carbamylerythropoietin treatment was found to reduce perifocal microglial activation ($P < 0.05$; Figure 2A) as well as polymorphonuclear leukocyte infiltration within the ischemic core ($P < 0.05$; Figure 2B).

Reduction of Ischemic White Matter Ischemic Damage by Carbamylerythropoietin Treatment

Ischemic insult to oligodendrocytes was assessed by Tau-1 immunostaining as described previously (Valeriani et al, 2000). After 24 h occlusion, cells positive for Tau-1 with the characteristic morphology of oligodendrocytes, featuring a thin rim of cytoplasm and small soma, were present throughout ipsilateral gray and white matter, as described previously (Dewar and Dawson, 1995; Valeriani et al, 2000). In particular, Tau-1-positive oligodendrocytes

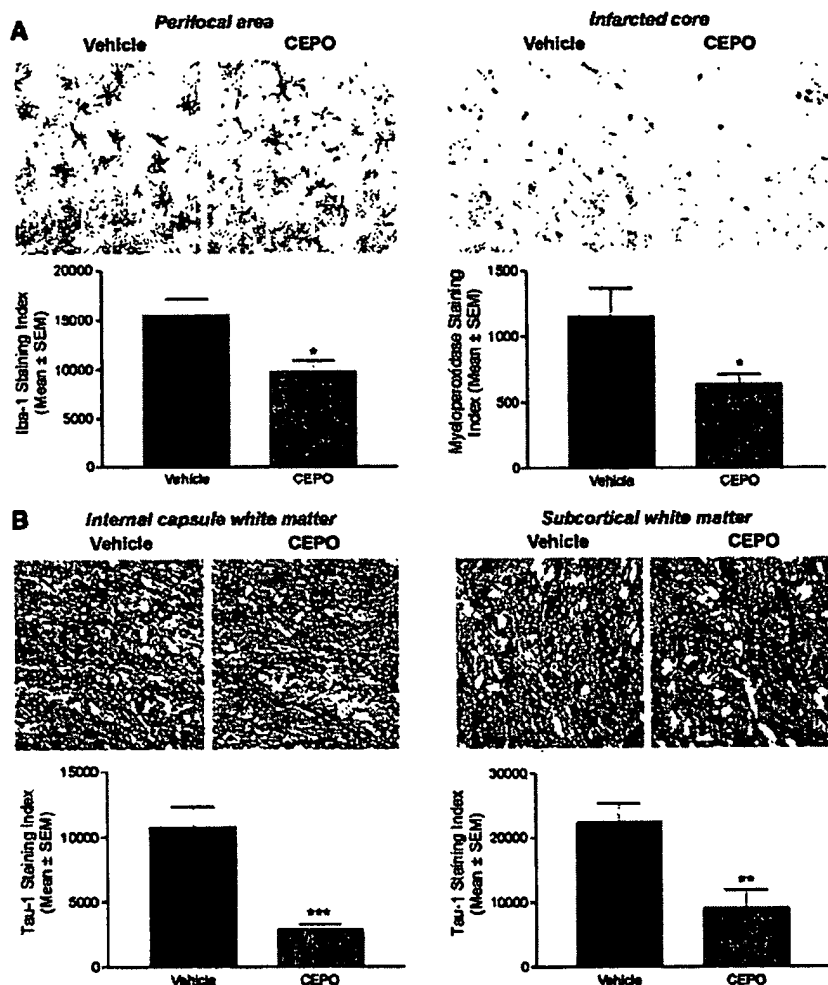


Figure 2 Reduction of postischemic microglial activation and polymorphonuclear leukocyte infiltration by CEPO. (A) Representative photomicrographs and quantification of perifocal microglial activation assessed with Iba-1 immunoreactivity. (B) Representative photomicrographs and quantification of myeloperoxidase (polymorphonuclear leukocytes) staining within the ischemic core. (C and D) Representative photomicrographs and quantification of Iba-1 (white matter damage) immunoreactivity in the ipsilateral internal capsule (C) and subcortical white matter (D). Rats were treated intravenously with vehicle ($n = 9$) or CEPO ($n = 8$) 1 h after occlusion and killed 24 h after occlusion. * $P < 0.05$, ** $P < 0.01$, and *** $P < 0.001$ compared with vehicle-treated animals; Student's t -test.

were consistently observed in the ipsilateral internal capsule (Figure 2C) and subcortical white matter (Figure 2D). The extent of oligodendrocyte pathology in the internal capsule (Figure 2C) and subcortical white matter (Figure 2D) ipsilateral to the occluded MCA was significantly ($P < 0.001$ and $P < 0.01$, respectively) reduced in the CEPO-treated group compared with the vehicle-treated group.

Reduced Striatal Damage by Carbamylerythropoietin Treatment 7 Days After Occlusion

Fluoro-Jade B staining revealed extensive neurodegeneration in the ipsilateral but not the contralateral striatum, as assessed at 7 days postoperatively

(Figure 3A). Intravenous treatment with CEPO (50 $\mu\text{g}/\text{kg}$) administered 3, 24, and 48 h after occlusion significantly ($P < 0.01$) attenuated striatal (subcortical) damage (86% reduction from control; Figure 3B). Nevertheless, cortical infarct volume, as assessed by either direct (Figure 3C) or indirect (data not shown) calculation methods, was not significantly ($P > 0.05$) reduced in rats treated with CEPO administered 3 h or 3, 24, and 48 h after occlusion compared with the vehicle group (Figure 3C).

Improvement of Neurologic Outcome After Erythropoietin Treatment 7 Days After Occlusion

We further assessed the effect of EPO treatment on cortical infarct volume and behavioral outcome.

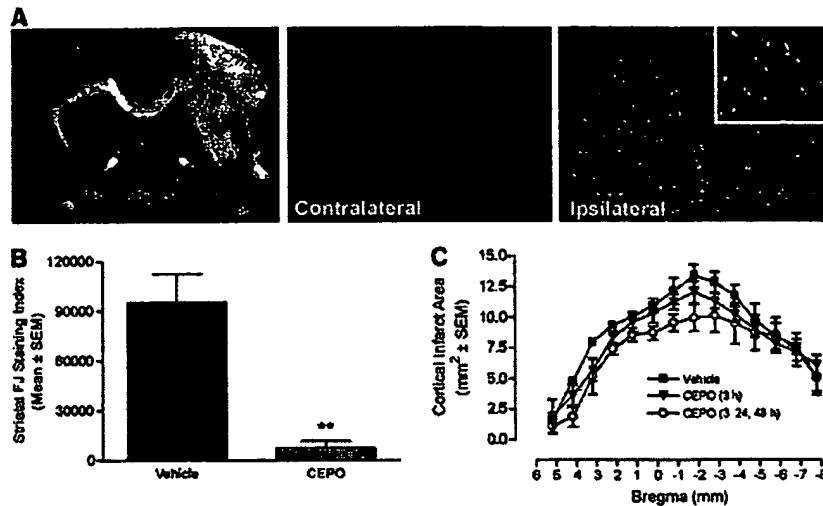


Figure 3 Protection against delayed striatal injury by CEPO. (A) Fluoro-Jade B staining shows extensive neuronal damage in the cortex and the striatum at day 7 after occlusion in a vehicle-treated animal. (B) Quantitative analysis of Fluoro-Jade B staining within the ipsilateral striatum. Carbamylerythropoietin treatment (3, 24, and 48 h after occlusion; $n = 5$) protects the ipsilateral striatum against ischemic damage. $**P < 0.01$ compared with vehicle group; Student's t -test. (C) Rostrocaudal distribution of cortical areas of infarction 7 days after MCA occlusion at 14 coronal levels as assessed using toluidine blue staining. Carbamylerythropoietin treatment administered 3 h ($n = 7$) or 3, 24, and 48 h ($n = 5$) after occlusion has no effect on cortical infarct volume when compared with vehicle-treated rats ($n = 5$) as assessed by toluidine blue staining. Data were analyzed using repeated-measures analysis of variance followed by Bonferroni tests.

Cortical infarct volume was not significantly ($P > 0.05$) reduced in rats treated with EPO, as assessed by either direct (Figure 4A) or indirect (data not shown) calculation methods. Animals subjected to ischemia showed an increase in contralateral (left) limb placing deficits on the De Ryck sensorimotor test (Figure 4B) as well as in contralateral forelimb foot-faults on the Hernandez-Schallert foot-fault test (Figure 4C). No deficits in ipsilateral limb placing in animals with cerebral ischemia were observed (data not shown). Sham-operated animals had no impairment in limb behavior at any time periods and their score was 16 (data not shown). Treatment with EPO significantly improved neurologic outcome on the De Ryck (Figure 4B) and the foot-fault (Figure 4C) tests at days 1 and 7 after stroke.

Rescue of Neurologic Function by Carbamylerythropoietin Treatment

Carbamylerythropoietin-treated rats showed a significant ($P < 0.05$) enhancement in recovery of contralateral limbs at 28 and 50 days after occlusion (Figure 5A). Moreover, CEPO-treated rats had a significantly ($P < 0.05$) better contralateral forelimb performance on the Hernandez-Schallert foot-fault test than the vehicle-treated animals within 7 days of treatment. This effect was sustained at every observational point throughout the survival period (Figure 5B). The two dosing regimes used (3 h versus

3, 24, and 48 h after occlusion) provided identical beneficial effects on functional deficits (Figures 5A and 5B).

Reduction of Delayed Postischemic Thalamic Gliosis by Carbamylerythropoietin

In addition to changes in the cortical infarct region, a dense homogeneous astrogliosis occurred in fiber tracts connecting cortex and thalamus and in the corresponding thalamic nuclei at 60 days after occlusion as assessed by GFAP immunostaining (Figure 5C). The extent of thalamic GFAP immunostaining significantly ($P < 0.05$) correlated to behavioral impairment in the foot-fault test at day 50 after stroke, whereas the correlation analysis did not reach significance for the De Ryck sensorimotor test (data not shown). Carbamylerythropoietin treatment significantly ($P < 0.01$) reduced GFAP density in the thalamic nuclei ipsilateral to the ischemic insult (Figures 5C and 5D). Glial fibrillary acidic protein-positive astrocytic cell bodies and processes in the ipsilateral thalamus were consistently thicker in vehicle-treated animals compared with CEPO-treated rats (Figure 5C). Microglia/macrophage activation was prominent within the ipsilateral thalamus, as assessed by CD68 immunostaining (Figure 5E). Microglia/macrophage activation significantly ($P < 0.001$) correlated with functional deficit as measured in the foot-fault test 50 days after stroke. In contrast, the outcome of the De Ryck sensorimotor

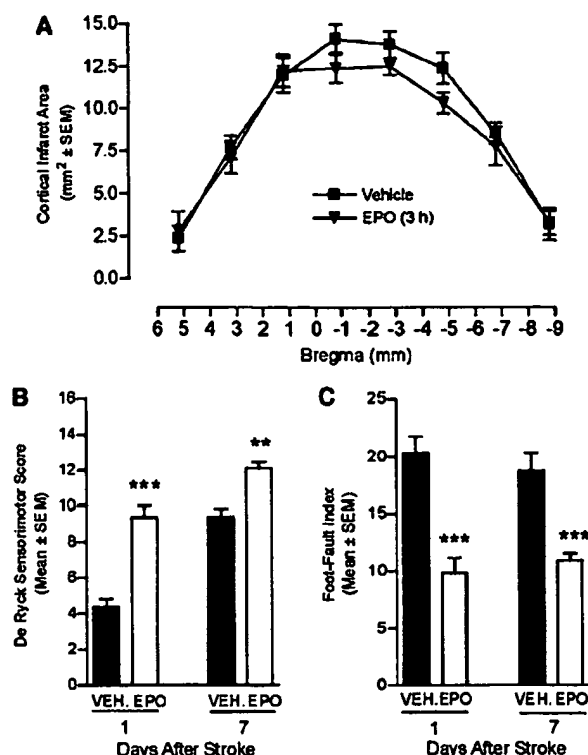


Figure 4 Rescue of neurologic function by EPO treatment. (A) Rostrocaudal distribution of cortical areas of infarction 7 days after MCA occlusion at eight coronal levels as assessed using toluidine blue staining. Erythropoietin treatment administered 3 h after occlusion ($n = 7$) has no effect on cortical infarct volume when compared with vehicle-treated rats ($n = 7$) as assessed by toluidine blue staining. Data were analyzed using repeated-measures analysis of variance followed by Bonferroni tests. (B) De Ryck sensorimotor test. Erythropoietin treatment improved sensorimotor function 1 and 7 days after occlusion. (C) Foot-fault test. Erythropoietin-treated rats had a better contralateral forelimb performance on the Hernandez–Schallert foot-fault test than the vehicle-treated animals 1 and 7 days after stroke. ** $P < 0.01$ and *** $P < 0.001$ compared with vehicle group; Kruskal–Wallis test.

test did not significantly ($P > 0.05$) correlate to microglia/macrophage activation. Carbamylerythropoietin treatment significantly ($P < 0.01$) reduced CD68 immunostaining (Figures 5E and 5F), with CEPO-treated animals showing less retracted and thinner CD68-positive microglia/macrophages (Figure 5E).

Efficacy of Carbamylerythropoietin Treatment with Extended Time-to-Treatment Window

We further assessed whether animals treated with CEPO at a later time point after stroke, that is, 1 day, would exhibit improved functional recovery. Animals were administered CEPO intravenously at 1 and 2 days after occlusion. A significant ($P < 0.01$) recovery of sensorimotor function was observed at

7 days after occlusion in CEPO-treated animals compared with vehicle-treated rats (Figure 6A). The effect was sustained at 14, 21, and 28 days postoperatively ($P < 0.01$; Figure 6A). Additionally, CEPO-treated rats exhibited better contralateral forelimb performance on the Hernandez–Schallert foot-fault test than the vehicle-treated animals 7 ($P < 0.01$) and 28 days ($P < 0.05$) after stroke (Figure 6B).

Improvement of Functional Motor Recovery by Treatment with the Nonhematopoietic Mutant Erythropoietin S100E

Some mutants generated by site-directed mutagenesis of the human EPO encoding sequence lack affinity for the EPOR homodimer, but retain their tissue-protective property (Leist *et al*, 2004). We further tested the ability of the mutant EPO-S100E to improve neurologic function after stroke. When administered 3 h after ischemia, EPO-S100E significantly improved the sensorimotor score in the De Ryck test at 1 ($P < 0.01$) and 14 days ($P < 0.05$) postoperatively (Figure 7A). Moreover, EPO-S100E treatment resulted in reduced foot-faults compared with vehicle treatment at days 7 ($P < 0.05$) and 14 ($P < 0.05$) after stroke (Figure 7B). Erythropoietin-S100E had no hematopoietic bioactivity as measured in the UT7 EPO-dependent human leukemia cell line proliferation assay (Figure 7C).

Discussion

Our results show that postischemic intravenous treatment with CEPO elicits histologic protection and promotes recovery. CEPO treatment inhibited microglia activation and neutrophil infiltration, protected against ischemic white matter injury, reduced delayed striatal injury and thalamic glial activation, and ameliorated sensorimotor function. The time-to-treatment window with CEPO was extended to 24 h after stroke. Moreover, other nonerythropoietic derivatives such as Caranesp and the mutant EPO-S100E were also found to protect against ischemic damage and to improve postischemic neurologic function.

Carbamylerythropoietin has been described previously to decrease postischemic cortical infarct volume 1 day after occlusion (Leist *et al*, 2004). We further assessed whether the neuroprotective effect of CEPO was sustained 7 days after occlusion. We found that CEPO treatment had no effect on the apparent cortical infarct volume at 7 days postoperatively as assessed by toluidine blue staining. One potential explanation is that infarct volume measurements in rodents become inexact and influenced by many confounding factors (tissue shrinkage, glial scarring, cell infiltrates) at periods of more than 3 days after the ischemic insult. These effects may have obscured a potential tissue

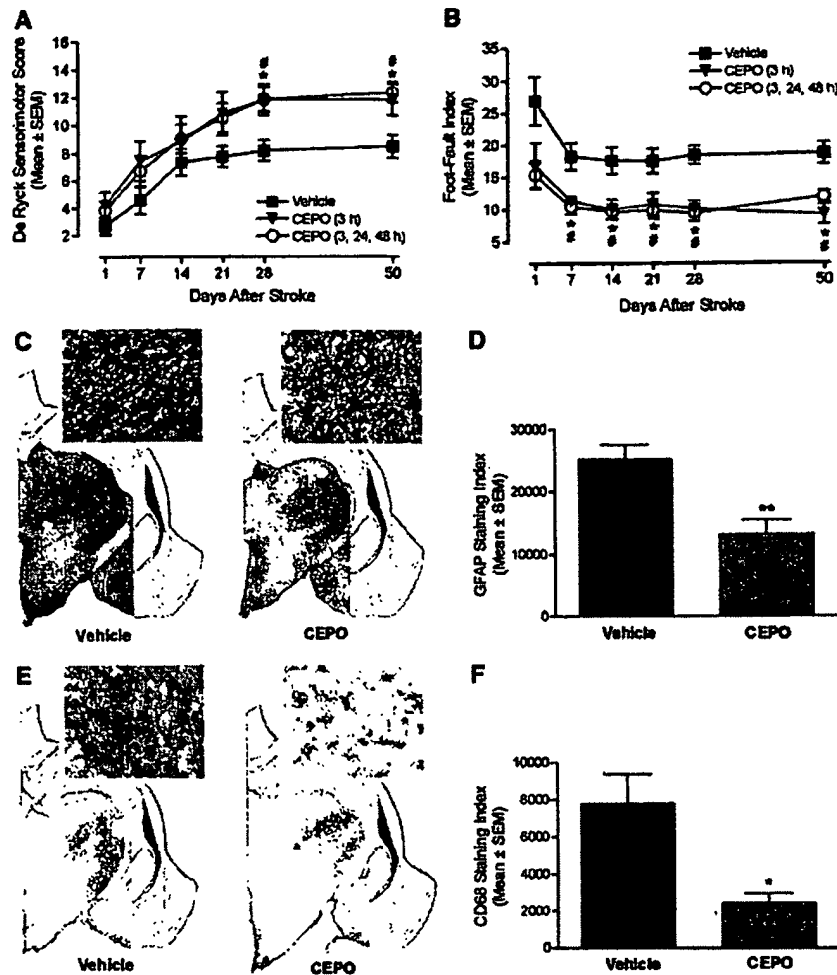


Figure 5 Facilitation of long-term recovery and attenuation of delayed thalamic glial activation by CEPO. (A) De Ryck sensorimotor test. Animals were administered vehicle ($n = 7$), CEPO 3 h after occlusion ($n = 5$), or CEPO 3, 24, and 48 h after occlusion ($n = 6$). Carbamylerythropoietin-treated animals show significantly improved recovery of contralateral limbs at 21 and 50 days after occlusion. (B) Foot-fault test. Impairment in this test was significantly reduced by CEPO treatment starting from the first week after stroke and thereafter. Note that the two dosing regimens had similar effect on the improvement of clinical deficit. Behavioral differences were statistically different between CEPO-treated rats (3 h after occlusion; $n = 5$) and vehicle-treated animals ($n = 7$) ($*P < 0.05$; Kruskal–Wallis test) and between CEPO (3, 24, 48 h after occlusion; $n = 6$)-treated rats and vehicle-treated animals ($*P < 0.05$; Kruskal–Wallis test). (C) Representative reconstructed photomicrographs of GFAP immunostaining within the ipsilateral thalamus. (D) Carbamylerythropoietin treatment (3, 24, and 48 h after occlusion) reduces thalamic astrogliosis (GFAP) at day 60 after occlusion. (E) Thalamic CD68 immunostaining in vehicle- and CEPO-treated rats. (F) Effect of CEPO treatment (3, 24, and 48 h after occlusion) on thalamic macrophage activation (CD68) in vehicle- and CEPO-treated rats 60 days postoperatively. Immunostaining differences were statistically different between CEPO- and vehicle-treated animals ($*P < 0.05$ and $**P < 0.01$; Student's t -test).

protective effect, and the issue needs to be addressed in the future by a longitudinal study based on magnetic resonance imaging technology. Another potential explanation is that this might reflect differential effects of CEPO on acute and delayed infarct expansion, as observed for other compounds (Tateishi *et al*, 2002). In our stroke model, the temporary occlusion of the contralateral CCA produces a penumbra surrounding the fixed MCA lesion (Zimmerman *et al*, 1995) and a wide ischemic

penumbra is a prerequisite for the occurrence of a delayed infarct expansion (Hossmann, 1994). It can thus not be refuted that CEPO treatment might delay cortical infarct expansion without affecting final cortical infarct volume. In line with this view, we further observed that cortical infarct volume at day 7 after occlusion was not affected in rats treated with EPO. The separation between behavioral outcome and infarct size after EPO treatment has been described before (Renzi *et al*, 2003; Wang *et al*,

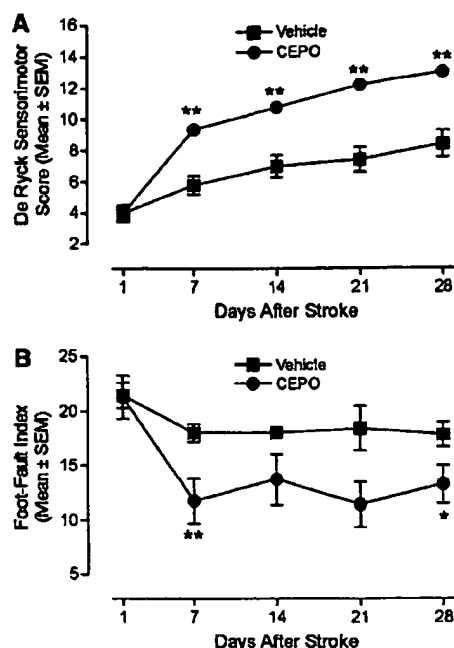


Figure 6 Improvement of postischemic motor function by CEPO with extended time-to-treatment window. (A) De Ryck sensorimotor test. Animals were administered vehicle ($n = 5$) or CEPO ($n = 5$) intravenously 1 and 2 days after MCA occlusion. Delayed treatment with CEPO elicits recovery of contralateral limbs at day 7 after occlusion and up to 50 days after ischemia. (B) Foot-fault test. Delayed CEPO treatment ameliorates neurologic function in the Hernandez-Schallert foot-fault test 7 and 28 days postoperatively. * $P < 0.05$ and ** $P < 0.01$ compared with vehicle-treated group; Mann-Whitney test.

2004a), indicating that dosing regimen may be critical for long-term histologic effect of EPO and EPO derivatives. Nevertheless, EPO, CEPO, and related analogs all elicited robust and long-lasting improved functional recovery, suggesting a poor correlation between final cortical infarct volume and behavioral outcome in our model, as described before in other models. For instance, intravenous administration of a subneuroprotective dose of brain-derived neurotrophic factor was found to improve functional outcome without affecting final infarct size (Schabitz *et al*, 2004). Because infarct volume correlates only moderately with clinical outcome of stroke patients, it was suggested to constrain the use of infarct volume as a surrogate (or auxiliary) end point in ischemic stroke clinical trials (Saver *et al*, 1999).

Cerebral infarction induced by tandem permanent occlusion of the right MCA and ipsilateral CCA followed by temporary occlusion of the contralateral CCA has been shown to be confined to the cortical zone (Zimmerman *et al*, 1995). However, using Fluoro-Jade B, a polyanionic fluorescein derivative which sensitively and specifically binds to degenerating neurons (Schmued *et al*, 1997), we were able

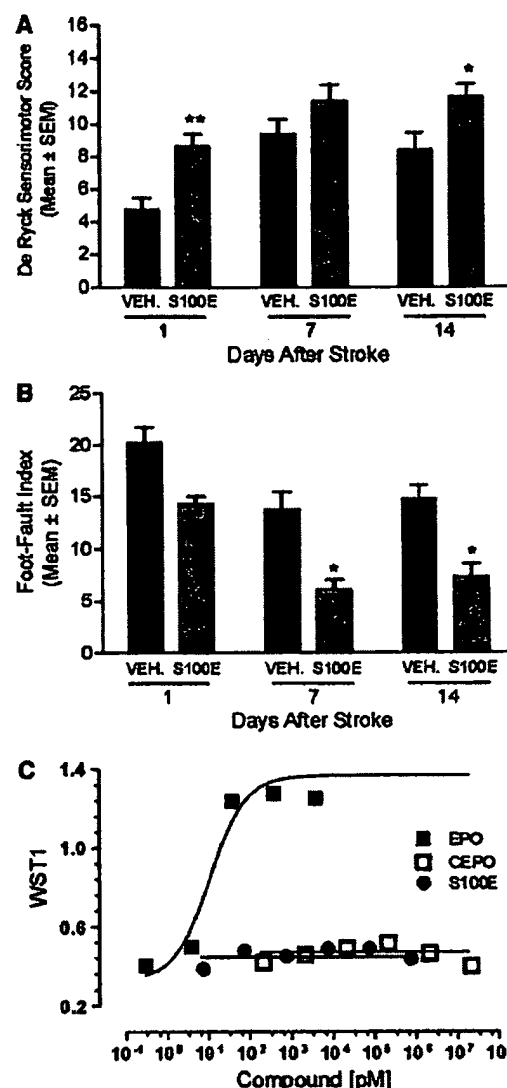


Figure 7 Improvement of motor function after stroke by the nonhematopoietic mutant EPO-S100E. (A) De Ryck sensorimotor test. Vehicle ($n = 8$) or EPO-S100E (S100E; $n = 8$) was administered intravenously 3 h after occlusion. S100E treatment improved sensorimotor function 1 and 14 days after occlusion. (B) Foot-fault test. S100E-treated rats had a better contralateral forelimb performance on the Hernandez-Schallert foot-fault test than the vehicle-treated animals 7 and 14 days after stroke. * $P < 0.05$ and ** $P < 0.01$ compared with vehicle group; Kruskal-Wallis test. (C) Hematopoietic bioactivity of S100E in the UT7 EPO-dependent human leukemia cell line proliferation assay.

to show extensive neuronal degeneration in the ipsilateral but not the contralateral striatum 7 days after occlusion. Furthermore, we found that CEPO dramatically protected animals against postischemic delayed striatal damage. Delayed degeneration of fiber tracts in the striatum after focal ischemia, as evidenced using Fluoro-Jade staining has been

documented before (Butler *et al*, 2002). Fluoro-Jade was proposed as a useful alternative to tedious (e.g., suppressed silver staining) or nonspecific staining methods (e.g., toluidine blue) for the evaluation of postischemic damage. Moreover, because Fluoro-Jade labelling is not specific to a particular mechanism of injury or type of cell death, the method broadens the opportunities to assess neuroprotective effect of compounds.

Recently, Belayev *et al* (2005) reported that treatment of experimental focal stroke with darboetin alfa, a novel EPO-derived protein, resulted in behavioral and histologic neuroprotection. Our observation that Caranesp is neuroprotective *in vitro* and *in vivo* (same degree as observed with CEPO) broadens the proof-of-concept for carbamylation of other EPO-derived erythropoiesis-stimulating agents. The carbamylation of EPO-derived agents thus may have potential utility in treating stroke in the clinical setting.

Focal ischemia elicits a profound inflammation response that is believed to contribute to cell death (Dirnagl *et al*, 1999). Although clinical trials undertaken with compounds inhibiting cellular inflammation have not shown efficacy so far, further development of strategies to modulate postischemic inflammatory events remain attractive (Legos and Barone, 2003; Dirnagl, 2004). In addition to its neuroprotective effect, EPO administration is also associated with decreased production of proinflammatory cytokines within the ischemic tissue after focal stroke (Villa *et al*, 2003). Similarly, tissue protection by CEPO has been correlated with reduced inflammatory mediators (interleukin-6 and membrane cofactor protein-1 levels) in ischemic tissue (Leist *et al*, 2004). We herein further show that CEPO inhibits perifocal microglial activation and reduces polymorphonuclear leukocyte infiltration within the ischemic core, possibly leading to decreased damage. However, the exact mechanisms underlying the antiinflammatory properties of CEPO treatment after stroke remain to be elucidated.

Few compounds have been examined for their ability to protect against ischemic white matter damage in preclinical models before reaching clinical trials. Nevertheless, functional recovery after an ischemic insult will be improved not only by protection of cortical gray matter but also protection of associated white matter (Dewar *et al*, 1999). A reason why stroke clinical trials have, so far, proved disappointing might reside in the inability of the tested drugs to protect white matter, specifically axons and oligodendrocytes, against ischemic damage (Dewar *et al*, 1999). Accordingly, ability of drugs to protect white matter damage was recently proposed as an additional read-out to the STAIR recommendations for preclinical evaluation of compounds before progression to clinical trials (Green *et al*, 2003). Our current observation that white matter damage, as reflected by Tau-1 immunostaining index, was reduced by CEPO treatment thus may have important clinical implications.

The present study further shows that CEPO is not only a neuroprotectant but also mediates functional recovery after stroke. The administration of CEPO 3 h after stroke improved functional neurobehavior, as assessed by sensorimotor and foot-fault placing tests. This beneficial effect was maximal within the first week after treatment and persisted throughout the 50-day survival period. The mutant EPO-S100E, which lacks affinity for the EPOR homodimer but retains its neuroprotective activity *in vitro* (Leist *et al*, 2004), improved postischemic behavioral outcome to a similar extent to that observed with CEPO treatment. This interesting observation further supports the existence of a second cognate receptor mediating neuroprotective activities of EPO. Several studies using various models of ischemic stroke have reported beneficial effect of EPO on postischemic behavioral outcome (Sadamoto *et al*, 1998; Wang *et al*, 2004a; Chang *et al*, 2005; Spandou *et al*, 2005). We herein provide further evidence that CEPO treatment ameliorates the functional recovery even if administered 24 h after stroke. Similarly, delayed administration of CEPO by up to 48 or 72 h after spinal cord injury resulted in enhanced functional recovery (Leist *et al*, 2004). This information is critical from the clinical point of view when treating patients in subacute or even long-term dosing regimes and distinguishes CEPO as a potential treatment of stroke from many other drugs that failed in clinical trials.

Functional improvement elicited by CEPO treatment after stroke could be caused by modulation of long-term tissue inflammation. The outcome of behavioral impairment in the foot-fault test significantly correlated with the extent of both microglia/macrophage and astrocyte activation in the ipsilateral thalamus. Moreover, we found that the beneficial effect of CEPO treatment on neurobehavioral effect is associated with reduced thalamic glial inflammation. Increased astrocytic and microglial reactivity is a common feature of neurologic disorders, but whether beneficial or adverse effect on neuronal function predominate is unclear. Recent studies have suggested that reactive astrocytes secrete neurotrophic factors at the lesion site in response to injury (Clarke *et al*, 2001), providing a permissive substrate for axonal regrowth (Ridet *et al*, 1997). However, at later stages, scar-type astrocytes may be an obstacle to axonal regrowth (Fawcett and Asher, 1999). Our observation that reduced glial activation at late stage (e.g., 2 months after stroke) after CEPO treatment is associated with diminished behavioral impairment corroborates recent findings by Badan *et al* (2003) demonstrating that increased postischemic glial reactivity in aged rats correlates with reduced functional recovery.

In the time frame of 60 days after stroke, long-term neurorestorative effects of CEPO may also be considered, such as angiogenesis and neurogenesis. Erythropoietin, in addition to a direct protective effect on neuronal cells during cerebral ischemia,

has been reported to promote brain vessel growth *in vivo* and *in vitro* (Marti et al, 2000). Recently, Wang et al (2004a) showed that treatment with EPO significantly improved poststroke functional recovery along with increased density of cerebral microvessels and number of neuroblasts in the perifocal area. Erythropoietin receptor conditional knock-down were further found to lead to deficit in poststroke neurogenesis through impaired migration of neuroblasts to the peri-infarct cortex, suggesting that both EPO and EPOR are essential for migration of regenerating neurons during postinjury recovery (Tsai et al, 2006). Studies to evaluate the effect of CEPO and other nonerythropoietic EPO derivatives on postischemic angiogenesis and neurogenesis are warranted.

In conclusion, our present findings add to the accumulating evidence that engineered derivatives of EPO that are tissue protective without stimulating erythropoiesis could have significant clinical application for the treatment of stroke.

Acknowledgements

The authors thank the excellent technical assistance of Kirsten Jørgensen, Pia Carstensen, and Bo Albrechtslund. Jacob Nielsen, Pekka Kallunki, Lone Helboe, and Thomas Sager are acknowledged for valuable discussion.

References

- Badan I, Buchhold B, Hamm A, Gratz M, Walker LC, Platt D, Kessler C, Poppa-Wagner A (2003) Accelerated glial reactivity to stroke in aged rats correlates with reduced functional recovery. *J Cereb Blood Flow Metab* 23:845–54
- Belayev L, Khoutorova L, Zhao W, Vigdorchik A, Belayev A, Busto R, Magal E, Ginsberg MD (2005) Neuroprotective effect of darbepoietin alfa, a novel recombinant erythropoietic protein, in focal cerebral ischemia in rats. *Stroke* 36:1071–6
- Brines M, Cerami A (2005) Emerging biological roles for erythropoietin in the nervous system. *Nat Rev Neurosci* 6:484–94
- Brines ML, Ghezzi P, Keenan S, Agnello D, de Lanerolle NC, Cerami C, Itri LM, Cerami A (2000) Erythropoietin crosses the blood–brain barrier to protect against experimental brain injury. *Proc Natl Acad Sci USA* 97:10526–31
- Butler TL, Kassed CA, Sanberg PR, Willing AE, Penny-packer KR (2002) Neurodegeneration in the rat hippocampus and striatum after middle cerebral artery occlusion. *Brain Res* 929:252–60
- Calapai G, Marciano MC, Corica F, Allegra A, Parisi A, Frisina N, Caputi AP, Buemi M (2000) Erythropoietin protects against brain ischemic injury by inhibition of nitric oxide formation. *Eur J Pharmacol* 401:349–56
- Chang YS, Mu D, Wendland M, Sheldon RA, Vexler ZS, McQuillen PS, Ferriero DM (2005) Erythropoietin improves functional and histological outcome in neonatal stroke. *Pediatr Res* 58:106–11
- Clarke WE, Berry M, Smith C, Kent A, Logan A (2001) Coordination of fibroblast growth factor receptor 1 (FGFR1) and fibroblast growth factor-2 (FGF-2) trafficking to nuclei of reactive astrocytes around cerebral lesions in adult rats. *Mol Cell Neurosci* 17:17–30
- De Ryck M, Van Reempts J, Borgers M, Wauquier A, Janssen PA (1989) Photochemical stroke model: flunarizine prevents sensorimotor deficits after neocortical infarcts in rats. *Stroke* 20:1383–90
- Dewar D, Dawson D (1995) Tau protein is altered by focal cerebral ischaemia in the rat: an immunohistochemical and immunoblotting study. *Brain Res* 684:70–8
- Dewar D, Yam P, McCulloch J (1999) Drug development for stroke: importance of protecting cerebral white matter. *Eur J Pharmacol* 375:41–50
- Dirnagl U (2004) Inflammation in stroke: the good, the bad, and the unknown. *Ernst Schering Res Found Workshop* 87–99
- Dirnagl U, Iadecola C, Moskowitz MA (1999) Pathobiology of ischaemic stroke: an integrated view. *Trends Neurosci* 22:391–7
- Ehrenreich H, Hasselblatt M, Dembowski C, Cepek L, Lewczuk P, Stiefel M, Rustenbeck HH, Breiter N, Jacob S, Knerlich F, Bohn M, Poser W, Ruther E, Kochen M, Gefeller O, Gleiter C, Wessel TC, De Ryck M, Itri L, Prange H, Cerami A, Brines M, Siren AL (2002) Erythropoietin therapy for acute stroke is both safe and beneficial. *Mol Med* 8:495–505
- Erbayraktar S, Grasso G, Sfacteria A, Xie QW, Coleman T, Kreilgaard M, Torup L, Sager T, Erbayraktar Z, Gokmen N, Yilmaz O, Ghezzi P, Villa P, Fratelli M, Casagrande S, Leist M, Helboe L, Gerwein J, Christensen S, Geist MA, Pedersen LO, Cerami-Hand C, Wuerth JP, Cerami A, Brines M (2003) Asialoerythropoietin is a nonerythropoietic cytokine with broad neuroprotective activity *in vivo*. *Proc Natl Acad Sci USA* 100:6741–6
- Fawcett JW, Asher RA (1999) The glial scar and central nervous system repair. *Brain Res Bull* 49:377–91
- Green RA, Odergren T, Ashwood T (2003) Animal models of stroke: do they have value for discovering neuroprotective agents? *Trends Pharmacol Sci* 24:402–8
- Hernandez TD, Schallert T (1988) Seizures and recovery from experimental brain damage. *Exp Neurol* 102:318–24
- Hossmann KA (1994) Viability thresholds and the penumbra of focal ischemia. *Ann Neurol* 36:557–65
- Legos JJ, Barone FC (2003) Update on pharmacological strategies for stroke: prevention, acute intervention and regeneration. *Curr Opin Investig Drugs* 4:847–58
- Leist M, Ghezzi P, Grasso G, Bianchi R, Villa P, Fratelli M, Savino C, Bianchi M, Nielsen J, Gerwein J, Kallunki P, Larsen AK, Helboe L, Christensen S, Pedersen LO, Nielsen M, Torup L, Sager T, Sfacteria A, Erbayraktar S, Erbayraktar Z, Gokmen N, Yilmaz O, Cerami-Hand C, Xie QW, Coleman T, Cerami A, Brines M (2004) Derivatives of erythropoietin that are tissue protective but not erythropoietic. *Science* 305:239–42
- Marti HH, Bernaudin M, Petit E, Bauer C (2000) Neuroprotection and angiogenesis: dual role of erythropoietin in brain ischemia. *News Physiol Sci* 15:225–9
- Renzi MJ, Wang-Fischer Y, Gold M, Thirumalai N, Jolliffe LK, Farrell FX (2003) An expanded window of opportunity for erythropoietin in stroke: separation of behavioral outcome from infarct size. Abstract No. 741.8. Society for Neuroscience, Washington, DC

- Ridet JL, Malhotra SK, Privat A, Gage FH (1997) Reactive astrocytes: cellular and molecular cues to biological function. *Trends Neurosci* 20:570-7
- Sadamoto Y, Igase K, Sakanaka M, Sato K, Otsuka H, Sakaki S, Masuda S, Sasaki R (1998) Erythropoietin prevents place navigation disability and cortical infarction in rats with permanent occlusion of the middle cerebral artery. *Biochem Biophys Res Commun* 253:26-32
- Sakanaka M, Wen TC, Matsuda S, Masuda S, Morishita E, Nagao M, Sasaki R (1998) *In vivo* evidence that erythropoietin protects neurons from ischemic damage. *Proc Natl Acad Sci USA* 95:4635-40
- Saver JL, Johnston KC, Homer D, Wityk R, Koroshetz W, Truskowski LL, Haley EC (1999) Infarct volume as a surrogate or auxiliary outcome measure in ischemic stroke clinical trials. The RANTTAS Investigators. *Stroke* 30:293-8
- Schabitz WR, Berger C, Kollmar R, Seitz M, Tanay E, Kiessling M, Schwab S, Sommer C (2004) Effect of brain-derived neurotrophic factor treatment and forced arm use on functional motor recovery after small cortical ischemia. *Stroke* 35:992-7
- Schmued LC, Albertson C, Slikker W, Jr (1997) Fluoro-Jade: a novel fluorochrome for the sensitive and reliable histochemical localization of neuronal degeneration. *Brain Res* 751:37-46
- Siren AL, Fratelli M, Brines M, Goemans C, Casagrande S, Lewczuk P, Keenan S, Gleiter C, Pasquali C, Capobianco A, Mennini T, Heumann R, Cerami A, Ehrenreich H, Ghezzi P (2001) Erythropoietin prevents neuronal apoptosis after cerebral ischemia and metabolic stress. *Proc Natl Acad Sci USA* 98:4044-9
- Spandou E, Papadopoulou Z, Soubasi V, Karkavelas G, Simeonidou C, Pazaiti A, Guiba-Tziampiri O (2005) Erythropoietin prevents long-term sensorimotor deficits and brain injury following neonatal hypoxia-ischemia in rats. *Brain Res* 1045:22-30
- Tateishi N, Mori T, Kagamiishi Y, Satoh S, Katsube N, Morikawa E, Morimoto T, Matsui T, Asano T (2002) Astrocytic activation and delayed infarct expansion after permanent focal ischemia in rats. Part II: suppression of astrocytic activation by a novel agent (R)-(-)-2-propyloctanoic acid (ONO-2506) leads to mitigation of delayed infarct expansion and early improvement of neurologic deficits. *J Cereb Blood Flow Metab* 22: 723-34
- Tsai PT, Ohab JJ, Kertesz N, Groszer M, Matter C, Gao J, Liu X, Wu H, Carmichael ST (2006) A critical role of erythropoietin receptor in neurogenesis and post-stroke recovery. *J Neurosci* 26:1269-74
- Valeriani V, Dewar D, McCulloch J (2000) Quantitative assessment of ischemic pathology in axons, oligodendrocytes, and neurons: attenuation of damage after transient ischemia. *J Cereb Blood Flow Metab* 20: 765-71
- van Beek J, Chan P, Bernaudin M, Petit E, MacKenzie ET, Fontaine M (2000) Glial responses, clusterin, and complement in permanent focal cerebral ischemia in the mouse. *Glia* 31:39-50
- Villa P, Bigini P, Mennini T, Agnello D, Laragione T, Cagnotto A, Viviani B, Marinovich M, Cerami A, Coleman TR, Brines M, Ghezzi P (2003) Erythropoietin selectively attenuates cytokine production and inflammation in cerebral ischemia by targeting neuronal apoptosis. *J Exp Med* 198:971-5
- Wang L, Zhang Z, Wang Y, Zhang R, Chopp M (2004a) Treatment of stroke with erythropoietin enhances neurogenesis and angiogenesis and improves neurological function in rats. *Stroke* 35:1732-7
- Wang X, Zhu C, Wang X, Gerwien JG, Schrattenholz A, Sandberg M, Leist M, Blomgren K (2004b) The nonerythropoietic asialoerythropoietin protects against neonatal hypoxia-ischemia as potently as erythropoietin. *J Neurochem* 91:900-10
- Wiessner C, Allegrini PR, Ekatothramis D, Jewell UR, Stallmach T, Gassmann M (2001) Increased cerebral infarct volumes in polyglobulic mice overexpressing erythropoietin. *J Cereb Blood Flow Metab* 21:857-64
- Zhang RL, Chopp M, Zhang ZG, Jiang Q, Ewing JR (1997) A rat model of focal embolic cerebral ischemia. *Brain Res* 766:83-92
- Zimmerman GA, Meistrell M, III, Bloom O, Cockcroft KM, Bianchi M, Risucci D, Broome J, Farmer P, Cerami A, Vlassara H (1995) Neurotoxicity of advanced glycation endproducts during focal stroke and neuroprotective effects of aminoguanidine. *Proc Natl Acad Sci USA* 92: 3744-8

The nonerythropoietic asialoerythropoietin protects against neonatal hypoxia-ischemia as potently as erythropoietin

Xiaoyang Wang,*† Changlian Zhu,*† Xinhua Wang,*† Jens Gammeltoft Gerwien,‡
Andre Schrattenholz,§ Mats Sandberg,¶ Marcel Leist‡ and Klas Blomgren***

*Perinatal Center, Department of Physiology, Göteborg University, Göteborg, Sweden

†Department of Pediatrics, The Third Affiliated Hospital of Zhengzhou University, Zhengzhou, China

‡Disease Biology, H. Lundbeck A/S, Valby, Denmark

§ProteoSys AG, Mainz, Germany

¶Department of Medical Biophysics, Göteborg University, Göteborg, Sweden

***Department of Pediatrics, The Queen Silvia Children's Hospital, Göteborg, Sweden

Abstract

Recently, erythropoietin (EPO) and the nonerythropoietic derivative asialoEPO have been linked to tissue protection in the nervous system. In this study, we tested their effects in a model of neonatal hypoxia-ischemia (HI) in 7-day-old rats (unilateral carotid ligation and exposure to 7.7% O₂ for 50 min). EPO (10 U/g body weight = 80 ng/g; *n* = 24), asialoEPO (80 ng/g; *n* = 23) or vehicle (phosphate-buffered saline with 0.1% human serum albumin; *n* = 24) was injected intraperitoneally 4 h before HI. Both drugs were protective, as judged by measuring the infarct volumes, neuropathological score and gross morphological score. The infarct volumes were significantly reduced by both EPO (52%) and asialoEPO (55%) treatment, even though the plasma levels of asialoEPO had dropped below the detection limit (1 pM) at the onset of HI,

while those of EPO were in the nanomolar range. Thus, a brief trigger by asialoEPO before the insult appears to be sufficient for protection. Proteomics analysis after asialoEPO treatment alone (no HI) revealed at least one differentially up-regulated protein, synaptosome-associated protein of 25 kDa (SNAP-25). Activation (phosphorylation) of ERK was significantly reduced in asialoEPO-treated animals after HI. EPO and the nonerythropoietic asialoEPO both provided significant and equal neuroprotection when administered 4 h prior to HI in 7-day-old rats. The protection might be related to reduced ERK activation and up-regulation of SNAP-25.

Keywords: asialoerythropoietin, erythropoietin, hypoxia, ischemia, neonatal, neuroprotection.

J. Neurochem. (2004) **91**, 900–910.

Hypoxic-ischemic brain injury (HI) is one of the major causes of subsequent neurological, life-long disability in both preterm and term infants. The injury develops over hours to days after the insult, and several mechanisms of injury have been identified; however, so far no treatment strategies have been found reliable in mitigating the neurological injury or resulting impairments (Hagberg *et al.* 2001). The neuropathology of brain injury after HI includes focal ischemic infarction, selective neuronal necrosis, inflammation and apoptosis (Hagberg 1992; Volpe 2001; Hagberg *et al.* 2002). During normal development more than half of the neurons are lost through apoptosis in certain brain regions (Raff *et al.* 1993). The immature brain has been suggested to retain this developmental cell death program to some extent, and apoptosis-related mechanisms may play a more important

role after HI in the immature than in the adult brain (Ni *et al.* 1998; Hu *et al.* 2000; Blomgren *et al.* 2001; Gill *et al.* 2002). Many key elements of apoptosis have been demonstrated to be activated and even up-regulated in the immature

Received February 2, 2004; revised manuscript received May 30, 2004; accepted July 23, 2004.

Address correspondence and reprint requests to Xiaoyang Wang, Perinatal Center, Department of Physiology, Göteborg University, Box 432, SE 405 30 Göteborg, Sweden.

E-mail: xiaoyang.wang@fysiologi.gu.se

Abbreviations used: asialoEPO, asialoerythropoietin; EPO, erythropoietin; EPOR, erythropoietin receptor; ERK, extracellular signal-related kinase; HI, hypoxia-ischemia; i.c.v., intracerebroventricular; i.p., intraperitoneal; i.v., intravenous; MAP2, microtubule associated protein 2; PBS, phosphate-buffered saline; SNAP-25, synaptosomal-associated protein-25 kDa.

brain, such as caspase-3 (Cheng *et al.* 1998; Blomgren *et al.* 2001; Wang *et al.* 2001), AIF (Zhu *et al.* 2003), APAF-1 (Ota *et al.* 2002), Bcl-2 (Merry *et al.* 1994) and Bax (Vekrellis *et al.* 1997).

Human erythropoietin is a sialoglycoprotein (molecular weight c. 30 kDa) containing a 165 amino acid residue backbone (Jelkmann 1992). This cytokine has been associated mainly with the formation of new erythrocytes by protecting erythroid progenitors in the bone marrow against apoptosis, and the clinical applications of recombinant human EPO (rhEPO) have so far been focused mainly on the treatment of anemias. EPO mRNA was shown to be up-regulated in several tissues after hypoxia, including the brain (Tan *et al.* 1992), and astrocytes have been suggested to mediate hypoxic preconditioning by producing EPO, thereby increasing the resistance of neurons to subsequent insults (Grimm *et al.* 2002; Ruscher *et al.* 2002). Both EPO and its receptor (EPOR) have been identified in the brain of several mammals (Digicaylioglu *et al.* 1995; Marti *et al.* 1996), including humans (Juul *et al.* 1999b). It appears that EPO acts on several different levels, such as attenuation of apoptosis (Juul *et al.* 1998; Digicaylioglu and Lipton 2001; Siren *et al.* 2001; Celik *et al.* 2002), excitotoxicity (Kawakami *et al.* 2001), oxygen-free radicals (Calapai *et al.* 2000; Digicaylioglu and Lipton 2001) and inflammation (Brines *et al.* 2000). Interestingly, despite its size, EPO did readily cross the blood-brain barrier, reach hippocampal and cortical neurons (Erbayraktar *et al.* 2003), or mediate protection against focal ischemia in adult rats (Brines *et al.* 2000). The concentrations of EPO in plasma and CSF were higher in asphyxiated infants than in controls, but this was not the case after meningitis (Juul *et al.* 1999a), indicating that EPO was selectively increased in the CSF by hypoxia. Neuroprotective concentrations of rhEPO were detected in the cerebrospinal fluid after a single intravenous (i.v.) or intraperitoneal (i.p.) injection in fetal sheep and non-human primates (Juul *et al.* 2004). In adult rodents, EPO treatment has provided neuroprotection when administered intracerebroventricular (i.c.v.) before (Bemaudin *et al.* 1999) and after (Sakanaka *et al.* 1998; Wen *et al.* 2002) the insult, but also systemic (i.p.) administration before (Siren *et al.* 2001) and after (Brines *et al.* 2000; Erbayraktar *et al.* 2003) an ischemic insult was effective. In all these settings, EPO was present at high plasma concentrations during the development of tissue damage. Recent reports indicate that EPO treatment is protective also in the neonatal setting, both after i.c.v. (Aydin *et al.* 2003) and i.p. administration in 7-day-old rats (Kumral *et al.* 2003) and mice (Matsushita *et al.* 2003). The mechanisms mediating this protection *in vivo* have not been elucidated. EPO treatment is attractive because it has been in clinical use for years, and is also considered safe for pediatric purposes. However, multiple dosing may cause potentially harmful increases in hematocrit that augment brain injury (Wiessner *et al.* 2001). EPO devoid of sialic acid has been

demonstrated to retain the neuroprotective properties of EPO without affecting hematocrit (Erbayraktar *et al.* 2003). It has been suggested that EPO or asialoEPO trigger neuroprotective signaling cascades that are memorized by cells. Due to its extremely short plasma half-life, asialoEPO is an ideal tool for studies addressing the cellular changes triggered by EPO and relevant for delayed tissue protection, but this type of EPO derivative has not been tried in the immature brain. The present study was undertaken to compare the effects of EPO and the nonerythropoietic asialoEPO in a model of perinatal HI.

Materials and methods

Induction of hypoxia-ischemia and drug administration

Unilateral hypoxia-ischemia was induced in 7-day-old Wistar rat pups (from Charles River, Sulzfeld, Germany) of either sex using the Rice-Vannucci model (Rice *et al.* 1981). Animals were anesthetized with halothane (5% for induction, 1.5–3.5% for maintenance) in a mixture of nitrous oxide and oxygen (1 : 1), and the duration of anesthesia was < 5 min. The left common carotid artery was cut between double ligatures of prolene sutures (6–0). After the surgical procedure the wounds were infiltrated with a local anesthetic, and the pups were allowed to recover for 1 h. The litters were placed in a chamber perfused with a humidified gas mixture (7.7% oxygen in nitrogen) for 50 min. The temperature in the incubator, and the temperature of the water used to humidify the gas mixture, was kept at 36°C. After hypoxic exposure the pups were returned to their dams and allowed to recover for up to 5 days. Control pups were neither subjected to ligation nor hypoxia. Animals were injected i.p. with EPO (10 U/g body weight, equivalent to 80 ng/g) (Dragon Pharmaceuticals, Vancouver, Canada), asialoEPO (80 ng/g body weight), produced at Lundbeck as described earlier (Erbayraktar *et al.* 2003), or vehicle [phosphate-buffered saline (PBS) with 0.1% human serum albumin] 4 h before the insult. In a separate series, animals were injected i.p. twice, at 24 h and 4 h before the insult, with EPO (5 U/g body weight, equivalent to 40 ng/g), asialoEPO (40 ng/g body weight) or vehicle (PBS with 0.1% human serum albumin). All animal experimentation was approved by the Ethical committee of Göteborg (204–2001 and 288–2002).

Assessment of brain damage

Infarct volume measurement

Five-day post-HI pups were deeply anesthetized and perfusion-fixed with 5% formaldehyde in 0.1 M PBS. The brains were rapidly removed and immersion-fixed in 5% formaldehyde at 4°C for 24 h. After dehydration with graded ethanol and xylene, the brains were paraffin-embedded and cut into 5-µm frontal sections. Every 100th section was stained for microtubule-associated protein 2 (MAP2). The areas in the cortex, striatum, thalamus and hypothalamus displaying loss of MAP2 staining were measured using Micro Image (Olympus, Tokyo, Japan) and the volumes calculated according to the Cavalieri Principle using the following formula: $V = \Sigma A \times p \times T$, where V = total volume, ΣA is the sum of the areas measured, p = the inverse of the sections sampling fraction, and T

is the section thickness. The investigator measuring the MAP2-negative areas and calculating the volumes was blinded to the treatment of the animals. Total tissue loss was calculated by subtracting the MAP2-positive volume of the ipsilateral hemisphere from the contralateral hemisphere.

Neuropathology score

Brain injury in different regions was evaluated using a semiquantitative neuropathological scoring system as described previously (Hedtj  m *et al.* 2002). Briefly, sections were stained with thionin/acid fuchsin and scored by an observer blinded to the treatment of the animals. The cortical injury was graded from 0 to 4, 0 being no observable injury and 4 confluent infarction encompassing most of the hemisphere. The damage in hippocampus, striatum and thalamus was assessed both with respect to hypotrophy (shrinkage) (0–3) and observable cell injury/infarction (0–3) resulting in a neuropathological score for each brain region (0–6). The total score (0–22) was the sum for all four regions.

Gross morphology score

Gross morphology scoring was performed according to a method modified from Yager *et al.* (1992). After dissecting out the brain, the degree of injury was evaluated by inspection of the brain surface. Grade 0, normal, equal size of the two hemispheres and no visible white lesion; grade 1, a small white lesion plaque; grade 2, hypotrophy and large cysts in the ipsilateral hemisphere; grade 3, only parasagittal viable tissue left in the whole midline; and grade 4, total loss of the ipsilateral hemisphere.

CA1 neuronal count

The number of neurons in one visual field of CA1 5 days post-HI was counted by an observer blinded to the treatment of the animals (400 \times magnification, one visual field = 0.196 mm²). One section per animal was counted in the vehicle-treated ($n = 24$), EPO-treated ($n = 24$) and asialoEPO-treated ($n = 23$) animals and the average was compared between groups.

Pharmacokinetics

EPO or asialoEPO were administered i.p. (80 ng/g body weight) to 7-day-old rats and blood was sampled at 4 min, 10 min, 1 h and 4 h ($n = 3$ per time point) after the injection. Heparinized blood was centrifuged at 3200 \times g for 10 min at 4 $^{\circ}$ C and the plasma samples thus obtained were analyzed for EPO and asialoEPO using a validated ELISA at Lundbeck (Valby, Denmark), as described earlier (Erbayraktar *et al.* 2003).

Immunoblotting

Animals treated with asialoEPO or vehicle as above were killed by decapitation 3 h after HI ($n = 6$ per time point). Littermates treated with asialoEPO but not subjected to HI were killed at the same time as those subjected to HI (7 h after the injection). The brains were rapidly dissected out on a bed of ice. The parietal cortex (including the hippocampus) and diencephalon (including the thalamus, hypothalamus and striatum) were snap frozen in liquid nitrogen and stored at -80° C. Tissue samples were homogenized by sonication in ice-cold isolation buffer [15 mM Tris-HCl, pH 7.6, 320 mM sucrose, 1 mM dithiothreitol, 1 mM MgCl₂, 3 mM EDTA-K, 0.5% protease inhibitor cocktail (P8340; Sigma) and 50 mg/mL

cyclosporine A], aliquoted and stored at -80° C. The protein concentration was determined according to Whitaker and Granum (1980), adapted for micro plates. Samples were mixed with an equal volume of concentrated (3 \times) sodium dodecyl sulfate–polyacrylamide gel electrophoresis (SDS–PAGE) buffer and heated (96 $^{\circ}$ C) for 5 min. Individual samples were run on 4–20% Tris-glycine gels (Novex, San Diego, CA, USA) and transferred to reinforced nitrocellulose (Schleicher & Schuell, Dassel, Germany) membranes. After blocking with 30 mM Tris-HCl (pH 7.5), 100 mM NaCl and 0.1% Tween 20 (TBS-T) containing 5% fat-free milk powder for 1 h at room temperature, the membranes were incubated with primary antibodies: anti-p-ERK (#9101, 1 : 1000, Cell Signaling Technology, Inc. Beverly, MA, USA), anti-ERK (#9102, 1 : 1000, Cell Signaling), anti-SNAP-25 (sc-7538, 1 : 500, Santa Cruz Biotechnology, Inc, Santa Cruz, CA, USA), anti-nitrotyrosine (1 μ g/mL, HM12, Biomol, Plymouth Meeting, PA, USA), anti-EPOR (M-20, sc-697, Santa Cruz Biotechnology, Santa Cruz, USA and MAB307, R & D Systems, Minneapolis, MN, USA) or anti-actin (A2066, 1 : 200, Sigma, Stockholm, Sweden) at room temperature for 1 h followed by an appropriate peroxidase-labeled, secondary antibody for 30 min at room temperature (horse anti-mouse 1 : 2000, horse anti-goat 1 : 2000, or goat anti-rabbit, 1 : 500, Vector, Burlingame, CA, USA). Immunoreactive species were visualized using the Super Signal Western Dura substrate (Pierce, Rockford, IL, USA) and a LAS 1000-cooled CCD camera (Fujifilm, Tokyo, Japan). Immunoreactive bands were quantified using the Image Gauge software (Fujifilm, Tokyo, Japan). Every sample was quantified 1–3 times on different membranes, and the average value was used as $n = 1$.

Immunohistochemistry

Antigen recovery was performed by heating the sections in 10 mM boiling sodium citrate buffer (pH 6.0) for 10 min. Nonspecific binding was blocked for 30 min with 4% horse serum in PBS. Anti-MAP2 (clone HM-2, 1 : 2000; Sigma) incubated for 1 h at room temperature, followed by a biotinylated horse anti-mouse secondary antibody for 1 h (1 : 200, Vector, Burlingame, CA, USA). Endogenous peroxidase activity was blocked with 3% H₂O₂ for 5 min. Visualization was performed using Vectastain ABC Elite with 0.5 mg/mL 3,3'-diaminobenzidine (DAB) enhanced with 15 mg/mL ammonium nickel sulfate, 2 mg/mL beta-D-glucose, 0.4 mg/mL ammonium chloride and 0.01 mg/mL beta-glucose oxidase (Sigma).

Proteomics analysis

The proteomics analysis was performed at ProteoSys AG (Mainz, Germany). Seven-day-old Wistar rats of either sex were injected i.p. with vehicle or asialoEPO (80 ng/g body weight) ($n = 24$ per group). Animals were randomized to proteomics analysis or HI. Half of the animals ($n = 12$ per group) were subjected to HI, killed 5 days later and evaluated by gross morphological scoring to verify the protective effect of asialoEPO. The other half of the animals ($n = 12$ per group) were killed 4 h after the injection and the parietal cortex (including the hippocampus) was dissected out on ice from each hemisphere, snap frozen in liquid nitrogen and stored at -80° C. Triplicate samples of the total proteome and the phosphoproteome were analyzed. Briefly, the brains from the same group (vehicle or asialoEPO) were combined and pulverized under liquid nitrogen. For total proteome analysis about 100 mg of ground tissue

was homogenized in 1 mL alkylation buffer (0.1 M Tris (pH 8.8), 2% (SDS). For phosphoproteome enrichment, about 1 g of ground tissue was extracted in extraction buffer (50 mM MOPS (pH 6.8), 4% Zwittergent 3-12, 2% Triton X-100, 5 mM NaF, 5 mM sodium glycerophosphate, 1 mM activated sodium orthovanadate, 5 mM Na-EDTA, 1 × Complete® Protease-Inhibitor) yielding about 60 mg of protein. Ni-NTA columns were activated by washing four times with two bed volumes regeneration buffer (2% Triton X-100, 50 mM Tris-HCl (pH 7.4), 0.5 M NaCl, 0.1 M EDTA-Na₄), followed by eight bed volumes MilliQ water and four bed volumes of activation buffer (100 mM FeCl₃). After activation the column was washed with eight bed volumes MilliQ water and eight bed volumes binding buffer (50 mM bis-(hydroxyethyl)piperazine (pH 3.4), 4% zwittergent 3-10, 2% Triton X-100). Protein solutions after DNA removal were submitted to a gel filtration column (NAP-10 or NAP-25) to exchange the buffer against the binding buffer [50 mM bis-(hydroxyethyl)piperazine (pH 3.4), 4% Zwittergent 3-10, 2% Triton X-100]. The extract was subsequently loaded onto an activated Fe-NTA-Agarose column (maximum 2 mg per 0.5 mL settled bed volume). The column was then washed three times with two bed volumes of binding buffer and eluted with two bed volumes elution buffer (50 mM bis-(hydroxyethyl)piperazine (pH 3.4), 4% Zwittergent 3-10, 2% Triton X-100, 50 mM NaH₂PO₄). Flow through, wash and elution fractions were collected. The eluate was TCA-precipitated, the pellet appropriately washed and recovered in alkylation buffer (0.1 M Tris (pH 8.8), 2% (SDS). Alkylation and sample treatment were performed exactly as described (Vuong *et al.* 2000; Cahill *et al.* 2003).

The differential and quantitative protein expression analysis was performed using the ProteoTope method (Cahill *et al.* 2003) which is based on radioiodination, 2D-PAGE and high sensitivity radio-imaging. In brief, small amounts of each sample were labeled with ¹²⁵I and ¹³¹I for differential pattern control. The signals from these two isotopes were distinguished in one 2D-PAGE gel to generate a quantitative multicolor differential display of proteins. A direct comparison of integrated spot intensities for the samples run on one gel was used for further analysis. In parallel, silver-stained gels were produced for spot picking and protein identification and for complementary quantification. In general, a spot was selected for further analysis if the *t*-test probability was higher than 95% and the expression ratio higher than 1.5. At that point the image quality was checked to assure that the spot was consistently detected on all images. Protein identification was based on different mass spectrometric methods. Briefly, gel plugs of selected protein spots were excised and the proteins contained in the gel plugs digested using trypsin. The resulting solution was analyzed first with a high throughput peptide mass fingerprint procedure based on MALDI-TOF-MS. For those spots where no unambiguous identification was achieved a fragment ion analysis based on LC-ESI-IonTrap-MS/MS was added (Cahill *et al.* 2003). For the identification of the proteins the peptide masses extracted from the mass spectra were searched against the NCBI non-redundant protein database (<http://www.ncbi.nlm.nih.gov>) using MASCOT software version 1.9 (Matrix Science, London).

Statistics

ANOVA followed by Fischer's PLSD *post hoc* test was used for comparing the results from infarct volume measurements, gross

morphology score, neuropathology score, CA1 neuron counting, and p-ERK and SNAP 25 immunoblot quantification. Simple linear regression analysis was used for the comparison of gross morphology score, infarct volume measurement, total tissue loss and neuropathology score. Unpaired *t*-test was used to assess statistical significance of the differences between the spot intensities on control and sample gel in proteomics analysis.

Results

Evaluation of brain damage

Brain damage was evaluated using three independent methods, infarct volume measurement, neuropathology score and gross morphology score. The total infarct volume (mean ± SEM) in the ipsilateral hemisphere in vehicle-treated rats was 31.5 ± 6.3 mm³ (*n* = 24), 15.0 ± 2.9 mm³ in EPO-treated rats (*n* = 24) (51.7% reduction, *p* = 0.0146), and 13.5 ± 4.1 mm³ in asialoEPO-treated rats (*n* = 23) (54.7% reduction, *p* = 0.0085) (Fig. 1a,b). There was considerable variation in different brain regions. The changes were most pronounced in the cortex (53.7% reduction in EPO-treated animals and 56.2% in asialoEPO-treated animals, *p* = 0.0136 and 0.0083, respectively) and least in thalamus (14.9% in EPO-treated animals and 28.6% in asialoEPO-treated animals, non-significant) (Fig. 1c). The protective effect was confirmed using gross morphology scoring (Fig. 2a) and neuropathology score (Table 1). Interestingly, when the drugs were administered twice, at 24 h and 4 h prior to the insult (5 U/g or 40 ng/g each, i.e. the same total dose of 10 U/g or 80 ng/g), no protection was observed as judged by gross morphology score (Fig. 2b). The presence or absence of human serum albumin in the vehicle did not make any difference in this respect (data not shown).

In histological sections, the CA1 region of vehicle-treated rats displayed a marked decline in viable neurons when compared with the CA1 of EPO- or asialoEPO-treated rats (Fig. 3a). The number of neurons per visual field per section in the CA1 was 19 ± 3 (mean ± SEM) in vehicle-treated rats compared to 25 ± 2 in EPO-treated and 30 ± 3 for asialoEPO-treated rats, i.e. a 50% increase in the asialoEPO-treated animals, *p* = 0.0036 (Fig. 3b).

Pharmacokinetics

As neonatal animals may differ significantly from adult rodents we repeated pharmacokinetic studies for the relevant time span. The plasma concentration profiles of EPO and asialoEPO during the first four hours after an i.p. injection were strikingly similar to those observed in adults (Erbayraktar *et al.* 2003) (Fig. 4). Basal EPO concentrations were < 1 pM, i.e. below the detection limit. After injection, the plasma EPO concentrations increased from 50 to 90 pM at 4–10 min to values of about 2000 pM after 60–240 min.

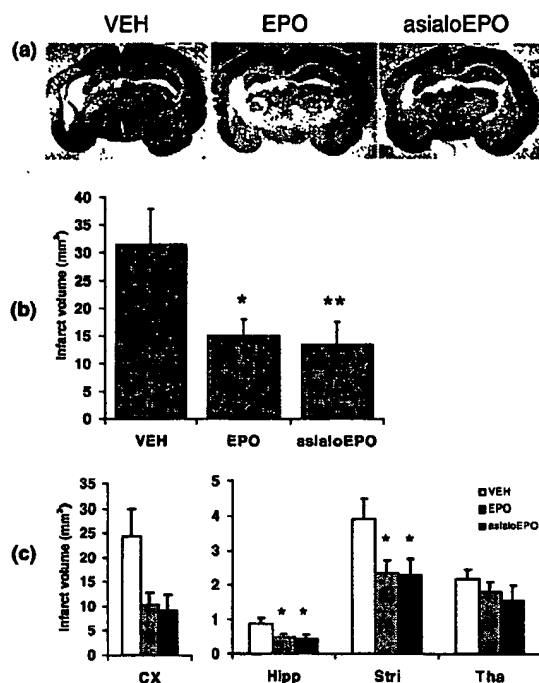


Fig. 1 Infarct volumes after EPO and asialoEPO treatment. The infarct volumes (MAP2-negative volumes) were quantified 5 days post-HI. (a) Representative pictures of MAP2 staining from animals treated with vehicle (VEH), erythropoietin (EPO) or asialoerythropoietin (asialoEPO). (b) The average total infarct volume \pm SEM is indicated for the vehicle- ($n = 24$), EPO- ($n = 24$) and asialoEPO-treated ($n = 23$) animals. (c) The regional differences are depicted, showing the average infarct volumes \pm SEM in the cortex (CX), hippocampus (Hipp), striatum (Stri) and thalamus (Tha). * $p < 0.05$, ** $p < 0.01$, using ANOVA and Fischer's *post hoc* test.

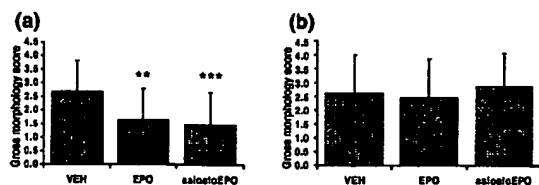


Fig. 2 Assessment of brain injury using gross morphology score after EPO and asialoEPO treatment. Gross morphology scoring was performed 5 days post-HI. (a) Treatment with vehicle (VEH) ($n = 24$), EPO ($n = 24$), and asialoEPO ($n = 23$) once 4 h prior to HI. Dose: 80 ng/g body weight for EPO and asialoEPO. (b) Treatment with vehicle (VEH) ($n = 31$), EPO ($n = 29$) and asialoEPO ($n = 32$) twice at 24 and 4 h prior to HI. Dose: 40 ng/g body weight per injection for EPO and asialoEPO. ** $p < 0.01$, *** $p < 0.001$, using ANOVA and Fischer's *post hoc* test.

Also asialoEPO was above the detection limit already after 4 min, rose to a plateau of about 50 pM between 10 and 60 min and dropped below the detection limit at 4 h (Fig. 4), the time point when HI was performed. Thus, effects of

Table 1 Assessment of brain injury using neuropathology score after EPO and asialoEPO treatment

Brain regions	VEH	EPO	p	AsialoEPO	p
Cortex	2.70 ± 1.08	1.88 ± 0.95	0.075	1.73 ± 0.88	0.001
Hippocampus	3.74 ± 1.52	2.89 ± 1.12	0.032	2.79 ± 0.84	0.011
Striatum	3.55 ± 1.37	2.44 ± 0.75	0.001	2.46 ± 0.92	0.002
Thalamus	2.99 ± 1.32	2.27 ± 0.53	0.016	1.93 ± 1.13	0.005
Total score	12.99 ± 4.89	9.48 ± 2.69	0.003	8.91 ± 3.10	0.001

Neuropathology scores for the different brain regions indicated, as well as the total score, in animals treated with vehicle (VEH) ($n = 23$), EPO ($n = 24$) or asialoEPO ($n = 24$).

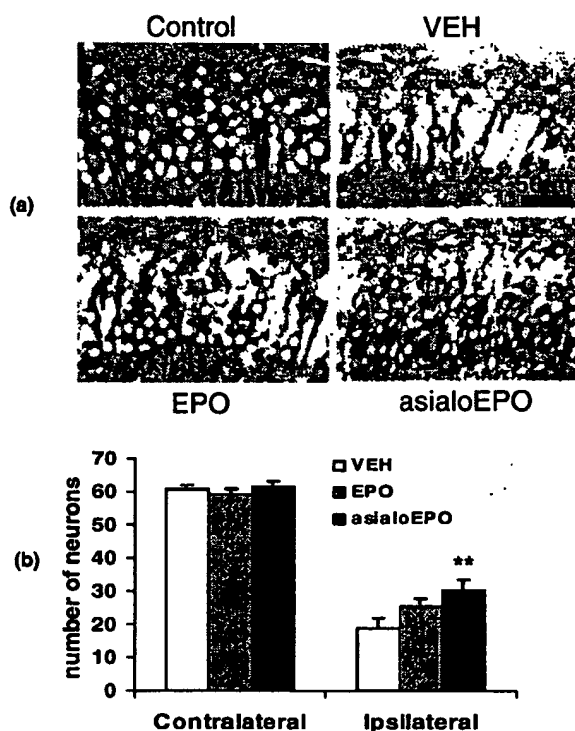


Fig. 3 Neuronal loss in the CA1. (a) Representative MAP2 stainings of the CA1 area 5 days after the insult in control animals not subjected to HI (control) and animals treated with vehicle (VEH), erythropoietin (EPO), or asialoerythropoietin (asialoEPO). The black or dark MAP2 staining is apparent in the cytosol of CA1 neurons, whereas the nuclei remain unstained and virtually white. (b) The average total number of neurons in the CA1 \pm SEM in the contralateral and ipsilateral hemispheres in the three groups. * $p < 0.05$, ** $p < 0.01$, using ANOVA and Fischer's *post hoc* test.

asialoEPO cannot be attributed to the opening of the blood-brain barrier during HI, and any signal observed at 4 h in brain was likely triggered earlier by asialoEPO and memorized. The ventricular system in neonatal rat brains is too small to allow sampling of cerebrospinal fluid, so we attempted analyzing brain tissue extracts at the same time

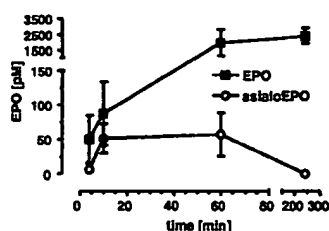


Fig. 4 The plasma concentrations of EPO and asialoEPO after a single injection. EPO or asialoEPO were injected i.p. at a dose of 80 ng/g. The concentrations in blood plasma were measured over a 4-h period, sampled from three animals per data point. Data are displayed as means \pm SD.

points as the plasma measurements. The results merely reflected the plasma concentrations, but at a much lower level, in the case of asialoEPO even close to detection level because of different immunoreactivity (data not shown). This makes major accumulation of EPO or asialoEPO in the brain unlikely.

Proteomics analysis

We compared total protein extracts from asialoEPO-treated versus vehicle-treated cortices 4 h after injection, the time point when HI would have been induced. Based on our selection criteria of a significant ($p < 0.05$) up-regulation of $> 50\%$, three differential protein spots were identified on 2D-gel patterns. However, these proteins could not be identified by mass spectrometry. One identified protein, NADH dehydrogenase (ubiquinone) Fe-S protein 1, was significantly down-regulated. Other proteins remained entirely unaffected. Phosphoprotein enrichment focuses the molecular analysis on a functionally important negatively charged subset of approximately 15% of total proteins. Quantification by radioactive differential display revealed one significantly up-regulated protein when comparing samples from animals treated with asialoEPO versus control. The protein, later identified by MALDI-MS as synaptosome-associated protein of 25 kDa (SNAP-25), was low abundant in the phosphoproteome, but was identified both in silver stained (Fig. 5) and in radioactive quantitative gels ($p < 0.01$). SNAP-25 displayed a 50–60% up-regulation using either method. Three further protein spots were significantly increased, but could not be identified. The bulk of other proteins remained unaffected.

We used immunoblotting to check for SNAP-25 up-regulation, but we were not able to detect changes in the overall levels of SNAP-25. Animals treated with EPO or asialoEPO alone (no HI) did not display significant differences in the levels of SNAP-25 4 h after the injection, neither in homogenates, nor in a synaptosomal fraction (where SNAP-25 would conceivably be enriched; data not shown). Animals treated with asialoEPO and 4 h later subjected to HI did not display significant differences in the levels of SNAP-25 3 or 24 h (not shown) after the insult.

SNAP-25 was up-regulated in the phosphoproteome, not in the total proteome, but there was no antibody available specific for phosphorylated SNAP-25. This presumably explains the negative Western blotting data.

Signal transduction mechanisms

A number of signal transduction proteins previously implied in EPO signaling were investigated using immunoblotting and immunohistochemistry. The levels of phosphorylated Akt (p-AKT), extracellular signal-related kinase (p-ERK), GSK-3 beta (p-GSK-3 beta), nitrotyrosine, as well as X-linked inhibitor of apoptosis protein (XIAP) and EPO receptor (EPOR) were measured using immunoblotting 4 h after EPO or asialoEPO treatment alone (no HI), the time point when HI would have been induced. None of these proteins were found to be differentially regulated after treatment (data not shown). However, when asialoEPO treatment was combined with HI, a significant difference could be detected in the levels of p-ERK (Fig. 6). As described earlier, the levels of p-ERK increased after HI (Wang *et al.* 2003), but in the asialoEPO-treated animals this increase was significantly reduced by more than 30% when measured 3 h after HI (7 h after treatment), compared with vehicle-treated rats (Fig. 6). The tendency was the same for the basal levels of p-ERK (without HI), but the difference was not significant (Fig. 6). Total ERK (Fig. 6), as well as the other signal transduction proteins investigated, p-AKT, p-GSK-3 beta, nitrotyrosine, XIAP and EPOR, were not differentially regulated after asialoEPO combined with HI using western blotting and/or immunohistochemistry (data not shown).

Discussion

Tissue protection

Neuroprotection using different EPO treatment regimes has been demonstrated in both the adult (Sadamoto *et al.* 1998; Bernaudin *et al.* 1999; Brines *et al.* 2000; Siren *et al.* 2001; Wen *et al.* 2002; Erbayraktar *et al.* 2003) and neonatal (Aydin *et al.* 2003; Kumral *et al.* 2003; Matsushita *et al.* 2003; Sun *et al.* 2004) brain. We found that both EPO and the nonerythropoietic asialoEPO provided neuroprotection in a model of neonatal HI when administered as a single, i.p. injection 4 h prior to HI. The protection was confirmed using three independent methods of brain damage assessment. This is the first report demonstrating that the nonerythropoietic asialoEPO protects against neonatal HI brain damage. The dosage and timing appear to be critical when using EPO and its derivatives. Even though significant protection was observed using 80 ng/g asialoEPO or using 10 U/g EPO (yielding 40 times higher plasma concentrations than asialoEPO) 4 h prior to HI, the same total dose of EPO or asialoEPO (10 U/g or 80 ng/g) was ineffective when administered using

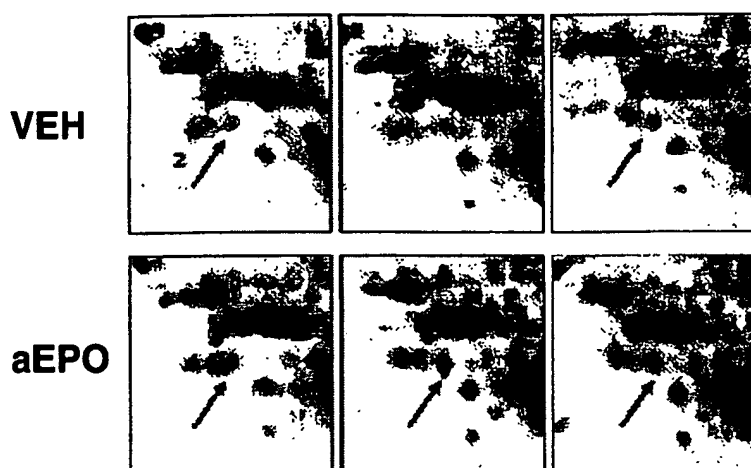


Fig. 5 Identification and differential regulation of SNAP-25 in the phosphoproteome after asialoEPO administration. Silver stained gels showing the SNAP-25 spots. These six figures show triplicate silver stained gels from vehicle- (VEH) and asialoEPO- (aEPO) treated animals, with detailed views of the SNAP-25 protein spot (arrow). The spot was subsequently identified using MALDI.

two injections at 24 h and 4 h prior to HI (5 U/g or 40 ng/g on each occasion). This was repeated twice, using two different types of vehicle (with or without human serum albumin), but the results were identical (data not shown). This was probably not due to an insufficient dose, because 5 U/g is a commonly used dose in other paradigms, including neonatal HI (Matsushita *et al.* 2003). It is conceivable that the 24-h pretreatment in our model may have down-regulated the EPO receptor or other effector mechanisms so that the effect of the second dose was diminished.

When systematically comparing the three independent methods of assessing brain damage, infarct volume measurement (and the related total tissue loss), gross morphology score, and neuropathological score using simple linear regression analysis, there was a significant positive linear correlation between all these three (or four) evaluation methods (Fig. 7). This strongly suggests that gross morphology score, which is the simplest and quickest way to assess brain injury, can be used at least for the initial evaluation of possible protective effects.

Pharmacokinetics

The rapid clearance of asialoEPO from the circulation is the reason why it does not affect the erythropoiesis (Erbayraktar *et al.* 2003). Even though asialoEPO was no longer detectable in plasma at the onset of HI, it still provided the same, or an even better (in the case of CA1 neuronal counts) degree of protection. This indicates that the protective mechanisms were activated and remained for a period of time, similar to the concept of preconditioning. Also, it has been demonstrated that even a short-lasting exposure (5 min) to EPO was sufficient to increase the resistance of neurons to glutamate toxicity *in vitro* (Morishita *et al.* 1997). In clinical settings, it may be an advantage that asialoEPO does not stimulate the erythropoiesis, particularly in a situation where multiple

dosing is required. An increased number of red blood cells may aggravate brain injury (Wiessner *et al.* 2001) or stimulate the formation of hyperactive platelets (Wolf *et al.* 1997a) and predispose to thrombosis (Wolf *et al.* 1997b), effects to be avoided when treating an asphyxiated infant or a stroke patient.

Proteomics

A proteomics approach was undertaken to detect differentially regulated proteins in the total proteome as well as the phosphoproteome of the cerebral cortex 4 h after a single injection of asialoEPO. There were three significantly increased protein spots matching the selection criteria in the total proteome and four in the phosphoproteome, but only one of these could be identified, SNAP-25 in the phosphoproteome. In general, the concentration changes detected were subtle and most proteins remained unaffected. It is possible that the changes observed were diluted by unrelated cell populations or compartments. SNAP-25 was quite low abundant in the phosphoproteome, but was consistently up-regulated as judged by two independent methods, silver stain and ProteoTope gels. SNAP-25 is a neuronal, soluble *N*-ethylmaleimide-sensitive factor attachment protein receptor (SNARE) syntaxin involved in vesicle trafficking. It belongs to a family of evolutionarily conserved proteins whose members are essential for exocytosis and has been exclusively detected in neuronal tissues (Bark *et al.* 1995). It has been reported that SNAP-23, an isoform of SNAP-25, was induced 2 h after stimulation by various cytokines, including EPO, in the erythroid cell line SKT6 (Morikawa *et al.* 1998). The functional role of SNAP-25 in asialoEPO-mediated neuroprotection, if any, might be related to synaptic transmission. The results from the phosphoproteome could not be confirmed on immunoblots, neither following EPO or asialoEPO treatment alone, nor after asialoEPO followed by

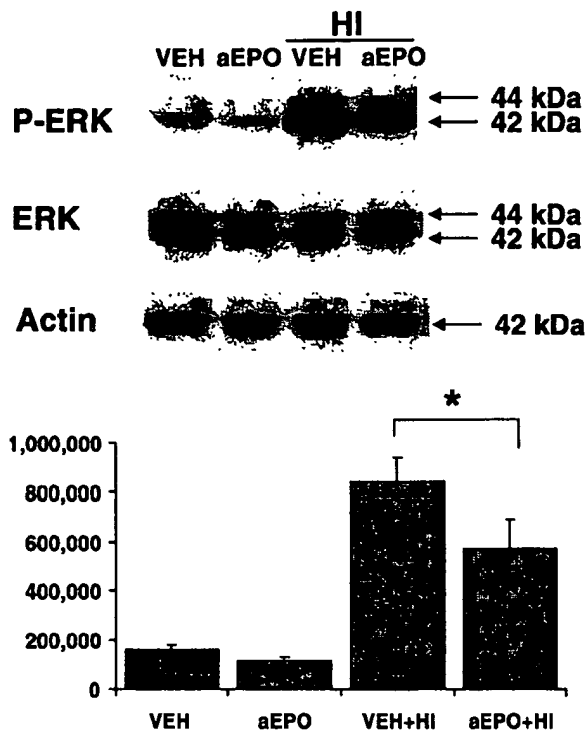


Fig. 6 The immunoreactivity of activated ERK was decreased in asialoEPO-treated animals after hypoxia-ischemia. All rats were injected i.p. with either asialoEPO (aEPO) or vehicle 4 h before HI and killed 3 h after the insult. Rats not subjected to HI were killed at the same time, i.e. 7 h after the injection. The upper panel shows representative immunoblots of phosphorylated ERK (p-ERK), total ERK (ERK) and actin (as a control for equal loading), demonstrating low levels of p-ERK in control animals, and a substantial increase of p-ERK immunoreactivity in the ipsilateral hemisphere 3 h after HI, less pronounced after asialoEPO treatment. The lower panel shows the average p-ERK immunoreactivity \pm SEM after densitometric quantification of individual samples ($n = 6$ in each group). * $p < 0.05$ using Student's *t*-test.

HI and evaluated either 3 or 24 h after the insult. The reason for this is probably that the antibody used detected total SNAP-25, while the phosphoproteome analysis detected changes in the phosphorylated form of SNAP-25, or that multiple isoforms exist. To elucidate this, a phospho-specific antibody against SNAP-25 would be required. A recent study showed that PKA-induced phosphorylation of SNAP-25 regulated the size of the releasable vesicle pool (Nagy *et al.* 2004).

Signaling mechanisms

Several mechanisms mediating the protective effects of EPO have been suggested: decreased glutamate toxicity (Morishita *et al.* 1997; Kawakami *et al.* 2001); neuronal anti-apoptotic

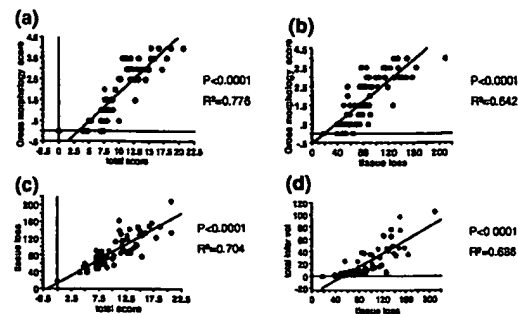


Fig. 7 Correlation between different methods for assessment of brain damage. Simple linear regression analysis showed that the gross morphology score, neuropathology score, infarct volume and total tissue loss all show a positive, significant correlation. (a) Correlation between the gross morphology score and neuropathology score (total score), $R^2 = 0.776$. (b) Correlation between the gross morphology score and total tissue loss, $R^2 = 0.642$. (c) Correlation between the total tissue loss and neuropathology score, $R^2 = 0.704$. (d) Correlation between the total infarct volume and total tissue loss, $R^2 = 0.686$. The p -value was < 0.0001 in all four analyses.

mechanisms (Juul *et al.* 1998; Renzi *et al.* 2002); reduced inflammation (Brines *et al.* 2000); up-regulation of HSP-27 (Sun *et al.* 2004); decreased nitric oxide-mediated injury (Digicaylioglu and Lipton 2001); direct antioxidant effects and indirect effects on endothelial cell growth (Hayashi *et al.* 1998). (For current reviews, see Juul 2000; Marti *et al.* 2000; Buemi *et al.* 2002; Chong *et al.* 2002). An interesting feature of EPO signaling is that it may act as a preconditioning factor, i.e. change a cell's sensitivity towards injury without being continuously present. This is difficult to examine using a molecule with a half-life of several hours, but such experimental designs are possible using asialoEPO, which has a half-life of merely a few minutes in plasma. Even though p-AKT, p-GSK-3 beta, p-ERK, NO signaling, XIAP and EPOR have all been implicated in the signal transduction mechanisms mediating EPO protection, we were unable to detect any changes in the levels of these proteins (or NO-mediated formation of nitrotyrosine) using immunoblotting or immunohistochemistry 4 h after a single injection. This may indicate that they are not involved in this paradigm; alternatively the changes may have been too small to be detected using immunoblotting of samples from the entire cortex, or the protective mechanisms do not require changes in the total levels to be effective. It is possible that the priming effects of an insult, such as hypoxia or HI, are required for the mechanisms to be activated. This is supported by studies where hypoxia-induced EPOR expression in cultured neuronal cells (Chin *et al.* 2000; Yu *et al.* 2002). When we combined asialoEPO treatment with HI, we did find significantly decreased levels of p-ERK 3 h post insult, but no effects on p-AKT, p-GSK-3 beta, XIAP, nitrotyrosine or EPOR at 3 or 24 h after HI. Previous studies

have described an increase in EPOR expression upon EPO treatment (Ruscher *et al.* 2002; Sun *et al.* 2004), and asialoEPO has been shown to bind to EPOR with a similar affinity as EPO (Erbayraktar *et al.* 2003), but we were unable to find any changes of EPOR under any conditions. Sun *et al.* (2004) found enhanced EPOR expression 24, 72 h and 7 days after (repeated) EPO treatment, while we sampled brain tissue 4 h after the treatment, when HI would have been induced.

The effect on p-ERK is consistent with our previous findings, where p-ERK was detected in injured neurons for at least 8 h after HI, as judged by double labeling with markers of injury (Wang *et al.* 2003). Involvement of ERK in EPO-mediated signaling has also been demonstrated by others (Shan *et al.* 1999; Siren *et al.* 2001; Mori *et al.* 2003). Surprisingly, we did not find any effect on the levels of caspase-3-, -8- or -9-like activity, measured using fluorogenic peptide substrates 24 h after the insult (data not shown), the time point when caspase activities peak in this model (Blomgren *et al.* 2001; Wang *et al.* 2001; Zhu *et al.* 2003), despite the fact that we observed tissue protection. We expected the extent of tissue damage and caspase activity to show a positive correlation, regardless of whether there is a causal or indirect relation between them. Possibly, non-caspase-dependent types of cell death (Leist and Jäättelä 2001) may play a major role in this model (Zhu *et al.* 2003), and EPO might affect tissue protection more via these pathways than through direct caspase inhibition. Another issue related to insult priming is the permeability of the blood-brain barrier (BBB) to EPO and asialoEPO. On the one hand there are reports showing that EPO administered to preterm and term infants (Juul *et al.* 1997) or normal neonatal rats (Dame *et al.* 2001) did not lead to elevated levels in the CSF in the absence of brain injury. On the other hand there are reports showing that a single EPO dose of 5 U/g i.p. did lead to increased concentrations in the CSF in adult rodents (Brines 2002) as well as in neonatal sheep, non-human primates (Juul *et al.* 2004), and humans (Ehrenreich *et al.* 2004). Furthermore, tissue sections obtained 4 h after i.v. administration of radio-iodinated asialoEPO displayed labeling in hippocampal and cortical neurons, cells which also express EPOR in the normal adult rat brain (Erbayraktar *et al.* 2003). Furthermore, the fact that we find tissue protection after asialoEPO treatment, which is no longer present at time points when the BBB may be opened by the HI damage, supports the hypothesis that EPO protection is mediated through a priming mechanism and that it may pass the BBB without prior permeabilization.

In summary, EPO and the nonerythropoietic asialoEPO both provided significant neuroprotection when administered 4 h prior to hypoxia-ischemia in 7-day-old rats. The protective effect might be related to a reduction of ERK activation and SNAP-25 up-regulation. Further work is

needed to further elucidate the signaling mechanisms and the optimal treatment regimes, but it is clear that these drugs, particularly asialoEPO, may provide powerful and safe tools in the management of asphyxiated neonates to treat and prevent brain injury.

Acknowledgements

This work was supported by the Swedish Research Council (to MS and KB), the Swedish Child Cancer Foundation (Barncancerfonden) (to KB), the National Institute of Health (to MS, GM 44842), the Göteborg Medical Society, the Åhlén Foundation, the Swedish Society of Medicine, the Wilhelm and Martina Lundgren Foundation, the Sven Jerring Foundation, the Frimurare Barnhus Foundation, the Magnus Bergvall Foundation, the National Natural Science Foundation of China (to CZ), the Bureau of Science and Technology of Henan Province (to CZ) and the Department of Education of Henan Province (to CZ).

References

- Aydin A., Genc K., Akhisaroglu M., Yorukoglu K., Gokmen N. and Gonullu E. (2003) Erythropoietin exerts neuroprotective effect in neonatal rat model of hypoxic-ischemic brain injury. *Brain Dev.* **25**, 494–498.
- Bark I. C., Hahn K. M., Ryabinin A. E. and Wilson M. C. (1995) Differential expression of SNAP-25 protein isoforms during divergent vesicle fusion events of neural development. *Proc. Natl Acad. Sci. USA* **92**, 1510–1514.
- Bernardin M., Marti H. H., Roussel S., Divoux D., Nouvelot A., MacKenzie E. T. and Petit E. (1999) A potential role for erythropoietin in focal permanent cerebral ischemia in mice. *J. Cereb. Blood Flow Metab.* **19**, 643–651.
- Blomgren K., Zhu C., Wang X., Karlsson J. O., Leverin A. L., Bahr B. A., Mallard C. and Hagberg H. (2001) Synergistic activation of caspase-3 by m-calpain after neonatal hypoxia-ischemia: a mechanism of 'pathological apoptosis'? *J. Biol. Chem.* **276**, 10 191–10 198.
- Brines M. (2002) What evidence supports use of erythropoietin as a novel neurotherapeutic? *Oncology (Huntingt.)* **16**, 79–89.
- Brines M. L., Ghezzi P., Keenan S., Agnello D., de Lanerolle N. C., Cerami C., Itri L. M. and Cerami A. (2000) Erythropoietin crosses the blood-brain barrier to protect against experimental brain injury. *Proc. Natl Acad. Sci. USA* **97**, 10 526–10 531.
- Buemi M., Aloisi C., Cavallaro E., Corica F., Floccari F., Grasso G., Lasco A., Pettinato G., Ruello A., Sturiale A. and Frisina N. (2002) Recombinant human erythropoietin (rHuEPO): more than just the correction of uremic anemia. *J. Nephrol.* **15**, 97–103.
- Cahill M. A., Wozny W., Schwall G. *et al.* (2003) Analysis of relative isotopologue abundances for quantitative profiling of complex protein mixtures labelled with the acrylamide/D3-acrylamide alkylation tag system. *Rapid Commun. Mass Spectrom.* **17**, 1283–1290.
- Calapai G., Marciano M. C., Corica F., Allegra A., Parisi A., Frisina N., Caputi A. P. and Buemi M. (2000) Erythropoietin protects against brain ischemic injury by inhibition of nitric oxide formation. *Eur. J. Pharmacol.* **401**, 349–356.
- Celik M., Gokmen N., Erbayraktar S., Akhisaroglu M., Konak S., Ulukus C., Genc S., Genc K., Sagiroglu E., Cerami A. and Brines M. (2002) Erythropoietin prevents motor neuron apoptosis and

- neurologic disability in experimental spinal cord ischemic injury. *Proc. Natl Acad. Sci. USA* 99, 2258–2263.
- Cheng Y., Deshmukh M., D'Costa A., Demaro J. A., Gidday J. M., Shah A., Sun Y., Jacquin M. F., Johnson E. M. and Holtzman D. M. (1998) Caspase inhibitor affords neuroprotection with delayed administration in a rat model of neonatal hypoxic-ischemic brain injury. *J. Clin. Invest.* 101, 1992–1999.
- Chin K. YuX., Beleslin-Cokic B., Liu C., Shen K., Mohrenweiser H. W. and Noguchi C. T. (2000) Production and processing of erythropoietin receptor transcripts in brain. *Brain Res. Mol. Brain Res.* 81, 29–42.
- Chong Z. Z., Kang J. Q. and Maiese K. (2002) Hematopoietic factor erythropoietin fosters neuroprotection through novel signal transduction cascades. *J. Cereb. Blood Flow Metab.* 22, 503–514.
- Dame C., Juul S. E. and Christensen R. D. (2001) The biology of erythropoietin in the central nervous system and its neurotrophic and neuroprotective potential. *Biol. Neonate* 79, 228–235.
- Digicaylioglu M. and Lipton S. A. (2001) Erythropoietin-mediated neuroprotection involves cross-talk between Jak2 and NF-kappaB signalling cascades. *Nature* 412, 641–647.
- Digicaylioglu M., Bichet S., Marti H. H., Wenger R. H., Rivas L. A., Bauer C. and Gassmann M. (1995) Localization of specific erythropoietin binding sites in defined areas of the mouse brain. *Proc. Natl Acad. Sci. USA* 92, 3717–3720.
- Ehrenreich H., Degner D., Meller J. et al. (2004) Erythropoietin: a candidate compound for neuroprotection in schizophrenia. *Mol. Psychiatry* 9, 42–54.
- Erbayraktar S., Grasso G., Sfacteria A. et al. (2003) Asialoerythropoietin is a nonerythropoietic cytokine with broad neuroprotective activity in vivo. *Proc. Natl Acad. Sci. USA* 100, 6741–6746.
- Gill R., Soriano M., Blomgren K. et al. (2002) Role of caspase-3 activation in cerebral ischemia-induced neurodegeneration in adult and neonatal brain. *J. Cereb. Blood Flow Metab.* 22, 420–430.
- Grimm C., Wenzel A., Groszer M., Mayser H., Seeliger M., Samardzija M., Bauer C., Gassmann M. and Reme C. E. (2002) HIF-1-induced erythropoietin in the hypoxic retina protects against light-induced retinal degeneration. *Nat. Med.* 8, 718–724.
- Hagberg H. (1992) Hypoxic-ischemic damage in the neonatal brain: excitatory amino acids. *Dev. Pharmacol. Ther.* 18, 139–144.
- Hagberg H., Mallard C. and Blomgren K. (2001) Neuroprotection of the fetal and neonatal brain, in *Fetal and Neonatal Neurology and Neurosurgery*, 3rd edn. (Levene, M. I., Chervenak, F. A. and Whittle, M. J., eds), pp. 505–520. Churchill Livingstone, London.
- Hagberg H., Ichord R., Palmer C., Yager J. Y. and Vannucci S. J. (2002) Animal models of developmental brain injury: relevance to human disease. A summary of the panel discussion from the Third Hershey Conference on Developmental Cerebral Blood Flow and Metabolism. *Dev. Neurosci.* 24, 364–366.
- Hayashi T., Abe K. and Itoyama Y. (1998) Reduction of ischemic damage by application of vascular endothelial growth factor in rat brain after transient ischemia. *J. Cereb. Blood Flow Metab.* 18, 887–895.
- Hedtj rn M., Leverin A. L., Eriksson K., Blomgren K., Mallard C. and Hagberg H. (2002) Interleukin-18 involvement in hypoxic-ischemic brain injury. *J. Neurosci.* 22, 5910–5919.
- Hu B. R., Liu C. L., Ouyang Y., Blomgren K. and Siesjo B. K. (2000) Involvement of caspase-3 in cell death after hypoxia-ischemia declines during brain maturation. *J. Cereb. Blood Flow Metab.* 20, 1294–1300.
- Jelkmann W. (1992) Erythropoietin: structure, control of production, and function. *Physiol. Rev.* 72, 449–489.
- Juul S. E. (2000) Nonerythropoietic roles of erythropoietin in the fetus and neonate. *Clin. Perinatol.* 27, 527–541.
- Juul S. E., Harcum J., Li Y. and Christensen R. D. (1997) Erythropoietin is present in the cerebrospinal fluid of neonates. *J. Pediatr.* 130, 428–430.
- Juul S. E., Anderson D. K., Li Y. and Christensen R. D. (1998) Erythropoietin and erythropoietin receptor in the developing human central nervous system. *Pediatr. Res.* 43, 40–49.
- Juul S. E., Stallings S. A. and Christensen R. D. (1999a) Erythropoietin in the cerebrospinal fluid of neonates who sustained CNS injury. *Pediatr. Res.* 46, 543–547.
- Juul S. E., Yachnis A. T., Rojiani A. M. and Christensen R. D. (1999b) Immunohistochemical localization of erythropoietin and its receptor in the developing human brain. *Pediatr. Dev. Pathol.* 2, 148–158.
- Juul S. E., McPherson R. J., Farrell F. X., Jolliffe L., Ness D. J. and Gleason C. A. (2004) Erythropoietin concentrations in cerebrospinal fluid of nonhuman primates and fetal sheep following high-dose recombinant erythropoietin. *Biol. Neonate* 85, 138–144.
- Kawakami M., Sekiguchi M., Sato K., Kozaki S. and Takahashi M. (2001) Erythropoietin receptor-mediated inhibition of exocytotic glutamate release confers neuroprotection during chemical ischemia. *J. Biol. Chem.* 276, 39 469–39 475.
- Kumral A., Ozer E., Yilmaz O., Akhisaroglu M., Gokmen N., Duman N., Ulukus C., Genc S. and Ozkan H. (2003) Neuroprotective effect of erythropoietin on hypoxic-ischemic brain injury in neonatal rats. *Biol. Neonate* 83, 224–228.
- Leist M. and J  ttel  M. (2001) Four deaths and a funeral: from caspases to alternative mechanisms. *Nat. Rev. Mol. Cell Biol.* 2, 589–598.
- Marti H. H., Wenger R. H., Rivas L. A., Straumann U., Digicaylioglu M., Henn V., Yonekawa Y., Bauer C. and Gassmann M. (1996) Erythropoietin gene expression in human, monkey and murine brain. *Eur. J. Neurosci.* 8, 666–676.
- Marti H. H., Bernaudin M., Petit E. and Bauer C. (2000) Neuroprotection and angiogenesis: dual role of erythropoietin in brain ischemia. *News Physiol. Sci.* 15, 225–229.
- Matsushita H., Johnston M. V., Lange M. S. and Wilson M. A. (2003) Protective effect of erythropoietin in neonatal hypoxic ischemia in mice. *Neuroreport* 14, 1757–1761.
- Merry D. E., Veis D. J., Hickey W. F. and Korsmeyer S. J. (1994) bcl-2 protein expression is widespread in the developing nervous system and retained in the adult PNS. *Development* 120, 301–311.
- Mori M., Uchida M., Watanabe T., Kirito K., Hatake K., Ozawa K. and Komatsu N. (2003) Activation of extracellular signal-regulated kinases ERK1 and ERK2 induces Bcl-xL up-regulation via inhibition of caspase activities in erythropoietin signaling. *J. Cell Physiol.* 195, 290–297.
- Morikawa Y., Nishida H., Misawa K., Nosaka T., Miyajima A., Senba E. and Kitamura T. (1998) Induction of synaptosomal-associated protein-23 kD (SNAP-23) by various cytokines. *Blood* 92, 129–135.
- Morishita E., Masuda S., Nagao M., Yasuda Y. and Sasaki R. (1997) Erythropoietin receptor is expressed in rat hippocampal and cerebral cortical neurons, and erythropoietin prevents *in vitro* glutamate-induced neuronal death. *Neuroscience* 76, 105–116.
- Nagy G., Reim K., Matti U., Brose N., Binz T., Rettig J., Neher E. and Sorensen J. B. (2004) Regulation of releasable vesicle pool sizes by protein kinase A-dependent phosphorylation of SNAP-25. *Neuron* 41, 417–429.
- Ni B., Wu X., Su Y., Stephenson D., Smalstig E. B., Clemens J. and Paul S. M. (1998) Transient global forebrain ischemia induces a prolonged expression of the caspase-3 mRNA in rat hippocampal CA1 pyramidal neurons. *J. Cereb. Blood Flow Metab.* 18, 248–256.
- Ota K., Yakovlev A. G., Itaya A., Kameoka M., Tanaka Y. and Yoshihara K. (2002) Alteration of apoptotic protease-activating factor-1 (APAF-1)-dependent apoptotic pathway during development of rat brain and liver. *J. Biochem. (Tokyo)* 131, 131–135.

- Raff M. C., Barres B. A., Burne J. F., Coles H. S., Ishizaki Y. and Jacobson M. D. (1993) Programmed cell death and the control of cell survival: lessons from the nervous system. *Science* **262**, 695–700.
- Renzi M. J., Farrell F. X., Bittner A., Galindo J. E., Morton M., Trinh H. and Jolliffe L. K. (2002) Erythropoietin induces changes in gene expression in PC-12 cells. *Brain Res. Mol. Brain Res.* **104**, 86–95.
- Rice J. E., Vannucci R. C. and Brierley J. B. (1981) The influence of immaturity on hypoxic-ischemic brain damage in the rat. *Ann. Neurol.* **9**, 131–141.
- Ruscher K., Freyer D., Karsch M., Isaev N., Megow D., Sawitzki B., Priller J., Dimagl U. and Meisel A. (2002) Erythropoietin is a paracrine mediator of ischemic tolerance in the brain: evidence from an *in vitro* model. *J. Neurosci.* **22**, 10 291–10 301.
- Sadamoto Y., Igase K., Sakanaka M., Sato K., Otsuka H., Sakaki S., Masuda S. and Sasaki R. (1998) Erythropoietin prevents place navigation disability and cortical infarction in rats with permanent occlusion of the middle cerebral artery. *Biochem. Biophys. Res. Commun.* **253**, 26–32.
- Sakanaka M., Wen T. C., Matsuda S., Masuda S., Morishita E., Nagao M. and Sasaki R. (1998) *In vivo* evidence that erythropoietin protects neurons from ischemic damage. *Proc. Natl Acad. Sci. USA* **95**, 4635–4640.
- Shan R., Price J. O., Gaarde W. A., Monia B. P., Krantz S. B. and Zhao Z. J. (1999) Distinct roles of JNKs/p38 MAP kinase and ERKs in apoptosis and survival of HCD-57 cells induced by withdrawal or addition of erythropoietin. *Blood* **94**, 4067–4076.
- Siren A. L., Fratelli M., Brines M. *et al.* (2001) Erythropoietin prevents neuronal apoptosis after cerebral ischemia and metabolic stress. *Proc. Natl Acad. Sci. USA* **98**, 4044–4049.
- Sun Y., Zhou C., Polk P., Nanda A. and Zhang J. H. (2004) Mechanisms of erythropoietin-induced brain protection in neonatal hypoxia-ischemia rat model. *J. Cereb. Blood Flow Metab.* **24**, 259–270.
- Tan C. C., Eckardt K. U., Firth J. D. and Ratcliffe P. J. (1992) Feedback modulation of renal and hepatic erythropoietin mRNA in response to graded anemia and hypoxia. *Am. J. Physiol.* **263**, F474–F481.
- Vekrellis K., McCarthy M. J., Watson A., Whitfield J., Rubin L. L. and Ham J. (1997) Bax promotes neuronal cell death and is down-regulated during the development of the nervous system. *Development* **124**, 1239–1249.
- Volpe J. J. (2001) *Neurology of the Newborn*, 4th edn, p. 995. Saunders, Philadelphia.
- Vuong G. L., Weiss S. M., Kammer W., Priemer M., Vingron M., Nordheim A. and Cahill M. A. (2000) Improved sensitivity proteomics by postharvest alkylation and radioactive labelling of proteins. *Electrophoresis* **21**, 2594–2605.
- Wang X., Karlsson J. O., Zhu C., Bahr B. A., Hagberg H. and Blomgren K. (2001) Caspase-3 activation after neonatal rat cerebral hypoxia-ischemia. *Biol. Neonate* **79**, 172–179.
- Wang X., Zhu C., Qiu L., Hagberg H., Sandberg M. and Blomgren K. (2003) Activation of ERK1/2 after neonatal rat cerebral hypoxia-ischaemia. *J. Neurochem.* **86**, 351–362.
- Wen T. C., Sadamoto Y., Tanaka J., Zhu P. X., Nakata K., Ma Y. J., Hata R. and Sakanaka M. (2002) Erythropoietin protects neurons against chemical hypoxia and cerebral ischemic injury by up-regulating Bcl-xL expression. *J. Neurosci. Res.* **67**, 795–803.
- Whitaker J. R. and Granum P. E. (1980) An absolute method for protein determination based on difference in absorbance at 235 and 280 nm. *Anal. Biochem.* **109**, 156–159.
- Wiessner C., Allegrini P. R., Ekatodramis D., Jewell U. R., Stallmach T. and Gassmann M. (2001) Increased cerebral infarct volumes in polyglobulic mice overexpressing erythropoietin. *J. Cereb. Blood Flow Metab.* **21**, 857–864.
- Wolf R. F., Gilmore L. S., Friese P., Downs T., Burstein S. A. and Dale G. L. (1997b) Erythropoietin potentiates thrombus development in a canine arterio-venous shunt model. *Thromb. Haemost.* **77**, 1020–1024.
- Wolf R. F., Peng J., Friese P., Gilmore L. S., Burstein S. A. and Dale G. L. (1997a) Erythropoietin administration increases production and reactivity of platelets in dogs. *Thromb. Haemost.* **78**, 1505–1509.
- Yager J. Y., Heitjan D. F., Towfighi J. and Vannucci R. C. (1992) Effect of insulin-induced and fasting hypoglycemia on perinatal hypoxic-ischemic brain damage. *Pediatr. Res.* **31**, 138–142.
- Yu X., Shacka J. J., Eells J. B. *et al.* (2002) Erythropoietin receptor signalling is required for normal brain development. *Development* **129**, 505–516.
- Zhu C., Qiu L., Wang X., Hallin U., Cande C., Kroemer G., Hagberg H. and Blomgren K. (2003) Involvement of apoptosis-inducing factor in neuronal death after hypoxia-ischemia in the neonatal rat brain. *J. Neurochem.* **86**, 306–317.

Biotinylated Recombinant Human Erythropoietins: Bioactivity and Utility as Receptor Ligand

By Don M. Wojchowski and Laurie Caslake

Recombinant human erythropoietin labeled covalently with biotin at sialic acid moieties has been prepared, and has been shown to possess high biological activity plus utility as a receptor ligand. Initially, the effects on biological activity of covalently attaching biotin to erythropoietin alternatively at carboxylate, amino, or sialic acid groups were compared. Biotinylation of erythropoietin at carboxylate groups using biotin-amidocaproyl hydrazide plus 1-ethyl-3-(3-dimethylaminopropyl) carbodiimide led to substantial biological inactivation, although biotinylated molecules retained detectable activity when prepared at low stoichiometries. Biotinylation at amino groups using sulfo-succinimidyl 6-(biotinamido) hexanoate resulted in a high level of biological inactivation with little, if any, retention of biological activity, regardless of labeling stoichiometries. Biotinylation at sialic acid moieties using periodate and biotinamidocaproyl hydrazide proceeded efficiently (> 85% and 80% labeling efficiencies for human urinary

and recombinant erythropoietin, respectively) and yielded stably biotinylated erythropoietin molecules possessing comparably high biological activity (i.e., 45% of the activity of unmodified hormone). Utility of recombinant biotin-(sialyl)-erythropoietin (in combination with ¹²⁵I-streptavidin) in the assay of cell surface receptors was demonstrated using two distinct murine erythroleukemia cell lines, Friend 745 and Rauscher Red 1. The densities and affinities of specific hormone binding sites were 116 ± 4 sites, 3.3 ± 0.4 nmol/L K_d and 164 ± 5 sites, 2.7 ± 0.4 nmol/L K_d, respectively. It is predicted that the present development of biotin-(sialyl)-erythropoietin as a chemically and biologically stable, bioactive ligand will assist in advancing an understanding of the regulated expression and physicochemistry of the human and murine erythropoietin receptors.

© 1989 by Grune & Stratton, Inc.

THE PRODUCTION of erythrocytes in mammals and in birds requires the exposure of committed progenitor cells to the glycoprotein growth factor, erythropoietin.¹ Specifically, erythropoietin promotes the rapid growth of erythroid progenitors in marrow,² spleen,³ and fetal liver,⁴ and is essential for their subsequent terminal differentiation to circulating red cells.⁵ Thus, the interaction between erythropoietin and its cell surface receptor comprises a pivotal event in erythropoiesis. A recent advance toward understanding the nature of this interaction is given by the isolation of the human erythropoietin gene^{6,7} and cDNA^{8,9} plus the expression and purification of active, recombinant factor in our laboratory, and others.¹⁰⁻¹⁴ In an effort to provide a biologically and chemically stable labeled ligand for receptor studies, we presently have prepared recombinant human erythropoietins biotinylated alternatively at carboxyl, amino, and sialic acid groups. Among these biotinylated adducts, biotin-(sialyl)-erythropoietin is shown to possess high biological activity. Further, the utility of this bioactive, biotinylated ligand in the assay of erythropoietin receptors on specified murine erythroleukemia cell lines is established.

MATERIALS AND METHODS

Chemicals. Chemicals used in the present experiments were obtained from the following sources: biotinamidocaproyl hydrazide, Calbiochem; d-biotin, sulfosuccinimidyl 6-(biotinamido) hexanoate, peroxidase-labeled streptavidin, fetuin, and asialofetuin (Sigma, St. Louis); sodium meta-periodate and sodium cyanoborohydride (Baker Chemicals, Phillipsburg, NJ); immobilized streptavidin and 1-ethyl-3-(3-dimethylaminopropyl) carbodiimide (Pierce Chemical, Rockford, IL); ¹²⁵I-streptavidin (30 µCi/µg) (Amersham, Arlington Heights, IL).

Cells. Friend murine erythroleukemia cells¹⁵ (ATCC, clone 745) and Rauscher murine erythroleukemia cells¹⁶ (clone Red 1, Dr. Nico DeBoth, Erasmus University) were maintained at 37°C, 7.5% CO₂ in Dulbecco's modified Eagle's medium (DMEM) supplemented with 10% fetal calf serum plus 1 × 10⁻³ mol/L 2-mercaptoethanol.

Biotinylation of erythropoietin. Biotinylation at carboxylate groups was accomplished by incubating recombinant human erythropoietin (10,000 U/mL, 50,000 U/mg) in 20 mmol/L pyridine-HCl, pH 4.8, for 12 hours at 23°C, with 1-ethyl-3-(3-dimethylaminopropyl) carbodiimide at 0, 0.05, 0.25, and 1.25 mg/mL, plus biotinamidocaproyl hydrazide at 10 mg/mL. Biotinylated reaction products were isolated by exhaustive dialysis against phosphate buffered saline (PBS), 0.02% Tween-20. Biotinylation of erythropoietin at amino groups was accomplished by incubating hormone for 30 minutes at 37°C in 50 mmol/L sodium borate pH 8.0 with sulfo-succinimidyl 6-(biotin-Amido) hexanoate at 0, 0.05, 0.25, and 1.25 mg/mL. Following the addition of glycine (100-fold molar excess), reaction products were recovered by dialysis as above. Biotinylation of human urinary erythropoietin (10,000 U/mL, 10,000 U/mg) and human recombinant erythropoietin (40,000 U/mL, 150,000 U/mg.) at sialic acid moieties was accomplished by initially incubating hormone at 0°C in 12.5 mmol/L sodium meta-periodate, 0.1 mol/L NaCl, 0.1 mol/L sodium acetate, pH 5.8, for varying intervals. Following dialysis against 80 mmol/L Na₂HPO₄, 20 mmol/L NaH₂PO₄, pH 7.5, at 0°C, oxidized hormone then was incubated for 120 minutes at 37°C with biotinamidocaproyl hydrazide at 10 mg/mL, plus 20 mmol/L NaCNBH₃, and subsequently dialyzed exhaustively against PBS, 0.02% Tween-20 at 4°C. In each instance, that portion of erythropoietin molecules which was biotinylated and, in addition, retained hormonal activity was estimated by

From the Department of Molecular and Cell Biology, The Pennsylvania State University, University Park, PA.

Submitted November 28, 1988; accepted April 27, 1989.

Supported in part by National Institutes of Health Grant No. DK40242.

Address reprint requests to Don M. Wojchowski, PhD, Pennsylvania State University, Department of Molecular & Cell Biology, College of Science, 408 S Frear Laboratory, University Park, PA 16802.

The publication costs of this article were defrayed in part by page charge payment. This article must therefore be hereby marked "advertisement" in accordance with 18 U.S.C. section 1734 solely to indicate this fact.

© 1989 by Grune & Stratton, Inc.
0006-4971/89/7403-0035\$3.00/0

incubating products (25 μ L aliquots) in the presence of PBS, 0.1% bovine serum albumin (BSA), 0.02% Tween-20 (100 μ L) with 50 μ L of streptavidin agarose for two hours at 37°C and subjecting gel supernatants (i.e., unadsorbed hormone) to biological assay (see below). As a control, products also were incubated in parallel with aliquots of streptavidin agarose, which previously had been incubated with soluble biotin at 0.25 mg/mL for one hour at 37°C. Reaction products also were subjected to bioassay directly.

Binding analyses. Analyses of the binding of biotin-(sialyl)-erythropoietin to various cell lines (1×10^5 cells per assay at 2×10^5 cells/mL) were performed in PBS, 0.1% BSA, at 4°C. Information regarding the incubation intervals and concentrations of hormone used is provided below. Levels of nonspecific binding were assessed by coinubation with a 50-fold molar excess of purified, unmodified recombinant erythropoietin. Bound biotin-(sialyl)-erythropoietin was detected using 125 I-streptavidin. Briefly, following incubation with hormone, cells were washed in ice-cold PBS, 0.1% BSA, and were incubated at 4°C for 15 minutes with 200,000 cpm of 125 I-streptavidin. Cells then were again rapidly washed at 0°C, and subjected to gamma radiation counting. Equilibrium binding data were analyzed by iterative nonlinear regression using Feldman's model¹⁷ and the least squares method of Marquardt.¹⁸

Biological assay of erythropoietin. Erythropoietic activities of various erythropoietin preparations and reaction products were assayed essentially as described by Krystal.³ Although the specificity of this assay for erythropoietin previously has been established,¹⁹ specificity was confirmed further by experiments in which antiserum to purified human recombinant erythropoietin was shown to neutralize the bioactivity of the above preparations.

Electrophoresis. Sodium dodecyl sulfate polyacrylamide gel electrophoresis was performed under nonreducing conditions in 12.5% separation gels.²⁰ Western blot analyses were performed as described by Towbin et al.²¹

RESULTS

Preparation and assessment of the biologic activities of biotinylated erythropoietins. In initial experiments, the effect on hormonal activity of covalently attaching biotin to erythropoietin at three chemically distinct sites was assessed. Specifically, (a) 1-ethyl-3-(3-dimethylaminopropyl) carbodiimide plus biotinamidocaproyl hydrazide, (b) sulfosuccinimidyl 6-(biotinamido)hexanoate, and (c) periodate plus biotinamidocaproyl hydrazide were used to biotinylate erythropoietin at carboxylate groups, amino groups, and sialic acid moieties, respectively. In each instance, the following experimental design was used to assess the extent of hormonal inactivation incurred upon modification. First, each distinct biotin-erythropoietin adduct was prepared at varying stoichiometries of labeling and the total biological activity of each reaction product was determined directly. Subsequently, that portion of total biological activity associated with biotinylated erythropoietin molecules was estimated by incubating aliquots of each reaction product with streptavidin agarose in order to allow for the selective adsorption (i.e., removal) of biotinylated product. The residual quantity of any unlabeled, unadsorbed erythropoietin molecules contained in streptavidin agarose gel supernatants then was quantified by bioassay. As a control, equivalent aliquots of various reaction products were incubated in parallel with streptavidin agarose which had been preincubated with d-biotin, and the resulting gel supernatants

were subjected to bioassay. Thus, by comparing the activities of control v selectively adsorbed preparations, the portion of total bioactivity possessed by biotinylated erythropoietin molecules was determined.

Use of carbodiimide plus biotinamidocaproyl hydrazide to biotinylate erythropoietin at carboxylate groups resulted in substantial hormonal inactivation. Specifically, based on the estimated relative concentrations of various reaction products required to elicit a 50% maximal biological response (i.e., erythropoietin-dependent incorporation of [3 H]thymidine into erythroid splenocytes), losses in activity of approximately 52%, 92%, and >95% resulted from the use of carbodiimide at concentrations of 150, 750, and 3,750-fold molar excess, respectively (Fig 1a). Further, it was shown that biotinylated erythropoietin molecules derived only from the use of carbodiimide at a 750-fold molar excess retained measurable bioactivity. As described above, this was established by bioassay following the selective adsorption of biotinylated hormone molecules to streptavidin agarose (Fig 1b; closed symbols, activity of gel supernatants) v controls (open symbols, activity of biotin-blocked gel supernatants). An estimated 40% of the residual erythropoietic activity contained in this specified product was selectively adsorbed to immobilized streptavidin (Fig 1b; closed v open squares), and thus corresponds to biotinylated erythropoietin. This result was reproducible, and was obtained in three separate labeling experiments. The apparent absence of active biotinylated erythropoietin molecules in products prepared at lower labeling stoichiometries is attributed to a correspondingly low frequency of biotinylation.

The use of sulfosuccinimidyl 6-(biotinamido)hexanoate to label recombinant human erythropoietin at amino groups at increasing stoichiometries also led to substantial hormonal inactivation (Fig 1c). Only the least modified reaction product (triangles) possessed activity approximating that of unmodified erythropoietin (i.e., 29% loss in activity) while little if any bioactivity was retained by the most highly biotinylated product (inverted triangles, >95% loss in activity). Using the above described streptavidin agarose gel adsorption procedure, the portion of total bioactivity possessed by biotinylated erythropoietin molecules per se was estimated for each product. Incubation with streptavidin agarose resulted in little, if any, specific adsorption of bioactive hormone from biotin-(amino)-erythropoietin preparations regardless of labeling stoichiometry (Fig 1d; closed symbols, activity of streptavidin agarose gel supernatants v open symbols, activity of biotinblocked streptavidin agarose gel supernatants), thus indicating that biotinylation of erythropoietin at amino groups, even at minimum levels, leads to a high level of biological inactivation.

Biotinylation of human urinary erythropoietin at sialic acid moieties using periodate plus biotinamidocaproyl hydrazide led to a comparably limited loss in biological activity (Fig 1e). Specifically, oxidation with periodate for three, nine, and 27 minutes, followed by incubations with biotinamidocaproyl hydrazide, resulted in estimated losses in activity of 56%, 82%, and 85%, respectively. That this diminution in activity was associated with biotinylation per se was indi-

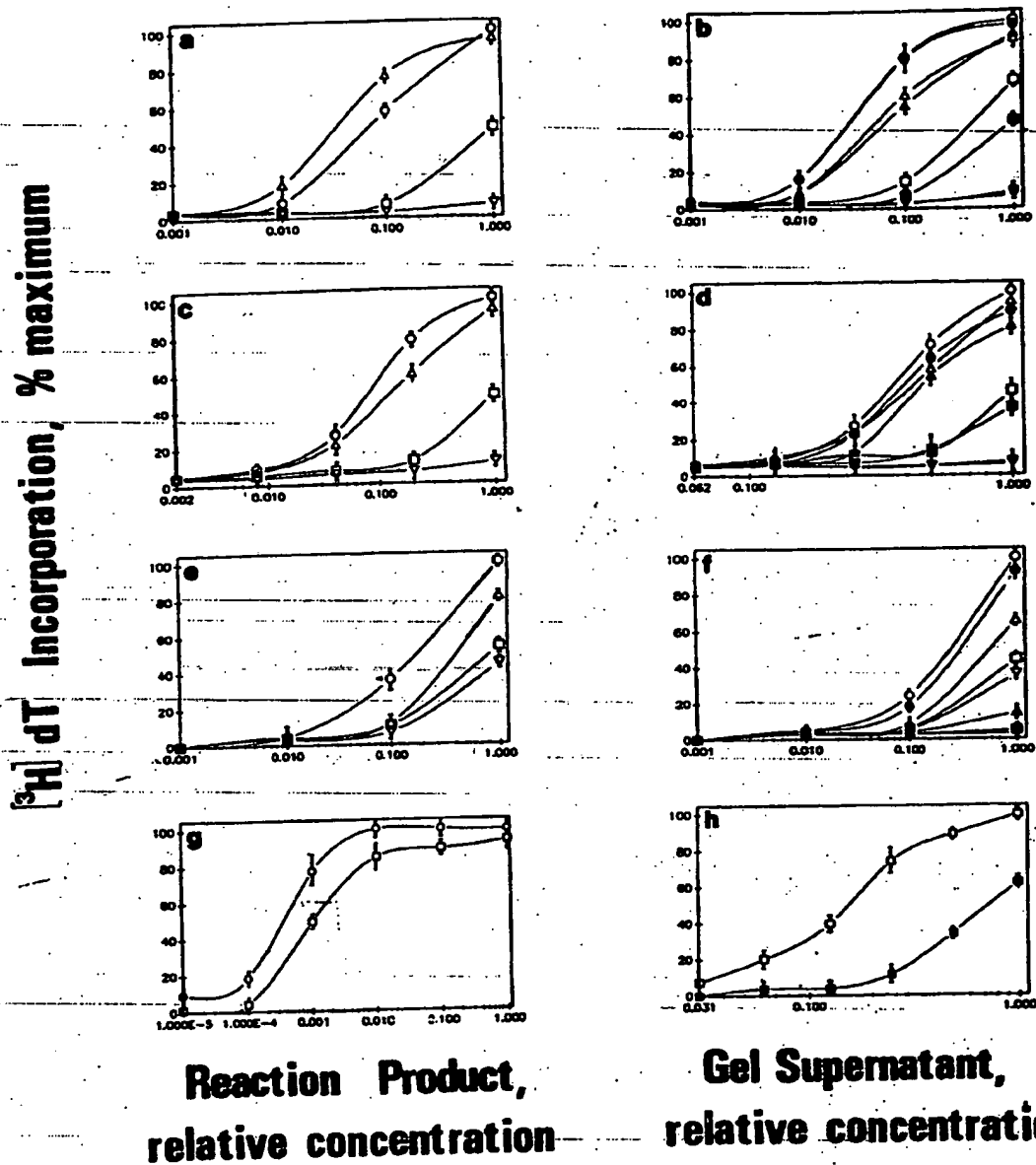


Fig 1. Effect on biological activity of covalently attaching biotin to human erythropoietin at carboxylate, amino, or steric acid residues. Biotinylation of erythropoietin at carboxylate (a, b), amino (c, d), and steric acid groups (e-h) at varying stoichiometries was accomplished using carbodiimide plus biotin hydrazide, sulfosuccinimidyl 6-(biotinamido)-hexanoate, and periodate plus biotin hydrazide, respectively. The total biological activity of each distinct reaction product was determined directly through assay at increasing dilutions (a, human recombinant biotin-(COOH)-erythropoietin derived from reaction with carbodiimide at 0 (O), 0.05 (Δ), 0.25 (\square), and 1.25 mg/ml (∇); c, human recombinant biotin-(amino)-erythropoietin derived from reaction with sulfosuccinimidyl 6-(biotinamido)hexanoate at 0 (O), 0.05 (Δ), 0.25 (\square), and 1.25 mg/ml (∇); e, human urinary biotin-(alanyl)-erythropoietin derived from exposure to periodate for 0 (O), 3 (Δ), 9 (\square), and 27 minutes (∇); g, human recombinant biotin-(alanyl)-erythropoietin. Subsequently, that portion of active product comprised by biotinylated erythropoietin molecules was determined by comparing the activities of products following adsorption with streptavidin agarose (activity of gel supernatants, closed symbols, b, d, f, h) v biotin-blocked streptavidin agarose as a control (activity of gel supernatants, open symbols, a, c, e, g, h).

cated by experiments in which incubations of erythropoietin with periodate (12.5 mmol/L, 0°C) for periods as long as 30 minutes plus subsequent incubation with borohydride to reduce aldehyde groups were shown to have little, if any, effect on hormonal activity. It is especially noteworthy that essentially all bioactive erythropoietin molecules derived from all reaction conditions used to label sialic acid moieties, in fact, were biotinylated. This was shown by the essentially complete and specific adsorption of active products to streptavidin agarose (Fig 1f; closed symbols, activity of gel supernatants) as compared with controls (open symbols, activity of biotin-blocked streptavidin agarose gel supernatants). The initial use of human urinary erythropoietin was directed by reported differences in the sialic acid content of recombinant human erythropoietins produced in various heterologous mammalian cell lines.¹⁴ In subsequent experiments, the efficiency of the above labeling procedure in preparing bioactive, human recombinant biotin-(sialyl)-erythropoietin was assessed.

Results of trial experiments indicated that the efficient biotinylation of recombinant human erythropoietin at sialic acid moieties required the exposure of hormone to periodate for periods of ten minutes, or greater, plus subsequent incubation with biotinamidocaproyl hydrazide. Overall, a loss in activity of approximately 55% resulted from this procedure (Fig 1g). As above, the extent of biotinylation of bioactive erythropoietin molecules was estimated by comparing the activities of product following incubations with streptavidin agarose (Fig 1h; closed squares, activity of gel supernatants) v biotin-blocked streptavidin agarose as a control (open squares activity of biotin-blocked gel supernatants). Eighty percent of the total activity of this product was adsorbed selectively, and thus corresponds to biotinylated

erythropoietin. In order to confirm the efficiency of this adsorption procedure, streptavidin agarose gel supernatants also were analyzed by Western blotting using a peroxidase-streptavidin conjugate. These analyses showed that the adsorption of biotinylated erythropoietin molecules was highly efficient, with virtually no detectable amounts of biotinylated erythropoietin remaining in streptavidin agarose gel supernatants (Fig 2, - lane). This adsorption also was highly selective, and was blocked efficiently by the preincubation of streptavidin agarose gels with biotin (Fig 2, + lane, i.e., (+) biotin). The major, molecular weight (mol wt) 33,000 biotinylated component corresponds to monomeric biotin-(sialyl)-erythropoietin. The minor, stained mol wt 66,000 product corresponds to a comparably small amount of biotinylated dimeric aggregate derived from exposure to periodate as demonstrated by staining with antibodies prepared against purified recombinant human erythropoietin (not shown). Western blotting with peroxidase-streptavidin conjugate also was used to confirm that the chemistry of labeling used, in fact, provided for biotinylation selectively at sialic acid moieties. In this experiment, fetuin, a sialoglycoprotein,²¹ and asialofetuin were used as labeling substrates. When co-reacted at equimolar concentrations under the above-prescribed reaction conditions, fetuin was readily biotinylated, while no levels of biotinylation of asialofetuin were detectable (data not shown).

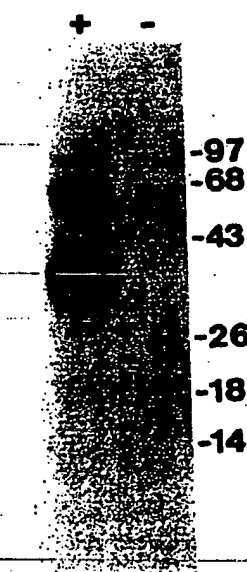


Fig 2. Efficiency of the adsorption of biotinylated erythropoietin molecules to streptavidin agarose as demonstrated by Western blotting. Gel supernatants derived from the incubation of recombinant human biotin-(sialyl)-erythropoietin with either streptavidin agarose (lane -) or biotin-blocked streptavidin agarose (lane +, i.e., plus biotin) were electrophoresed under denaturing conditions, transferred to nitrocellulose, and stained using a horseradish peroxidase-streptavidin conjugate. Molecular weights of co-electrophoresed standards are specified in the right margin.

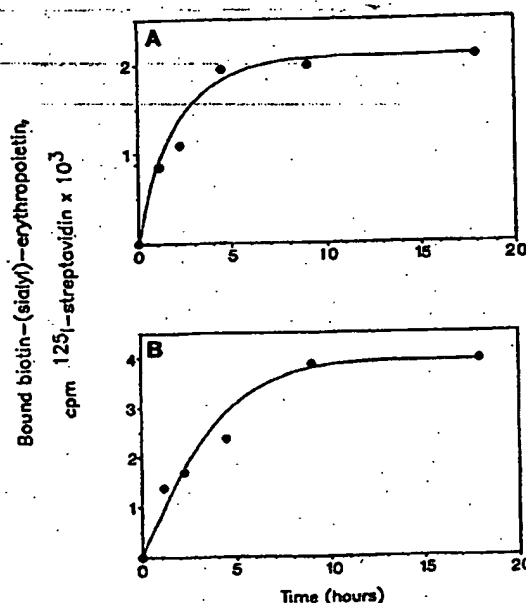


Fig 3. Kinetics of the association between biotin-(sialyl)-erythropoietin and Friend or Rauscher murine erythroleukemia cells. Biotin-(sialyl)-erythropoietin (20 nmol/L) was incubated with Friend 745 (A) or Rauscher Red 1 cells (B) at 4°C, and at the time intervals indicated, quantities of bound hormone were determined using ¹²⁵I-streptavidin.

Human recombinant biotin-(sialyl)-erythropoietin as a receptor ligand. The utility of biotin-(sialyl)-erythropoietin in receptor studies was demonstrated through analyses of specific binding sites on the murine erythroleukemic cell lines Friend 745 and Rauscher Red 1. In order to establish conditions for binding at equilibrium, cells were incubated at 4°C with biotin-(sialyl)-erythropoietin (20 nmol/L) and at timed intervals, the amount of hormone bound to cells was determined using 125 I-streptavidin. As shown in Fig 3 an apparent equilibrium was achieved for each cell by approximately eight hours of incubation. Subsequently, binding of biotin-(sialyl)-erythropoietin at equilibrium was examined. Binding isotherms for specific hormone binding sites are shown in Fig 4 and indicate that, for each cell line, saturation

essentially was achieved with one-half maximal binding occurring at nanomolar concentrations of erythropoietin. Quantitative estimates for specific binding affinities and densities were calculated via iterative non-linear regression analysis. Site densities and affinities of 116 ± 4 sites, 3.3 ± 0.4 nmol/L and 164 ± 5 sites, 2.7 ± 0.4 nmol/L were observed for Friend 745 and Rauscher Red 1 cells, respectively. These estimates assume that on the average, one molecule of 125 I-streptavidin binds per each receptor-bound molecule of biotin-(sialyl)-erythropoietin.

DISCUSSION

Recombinant human erythropoietin biotinylated selectively at sialic acid moieties presently is shown to retain high

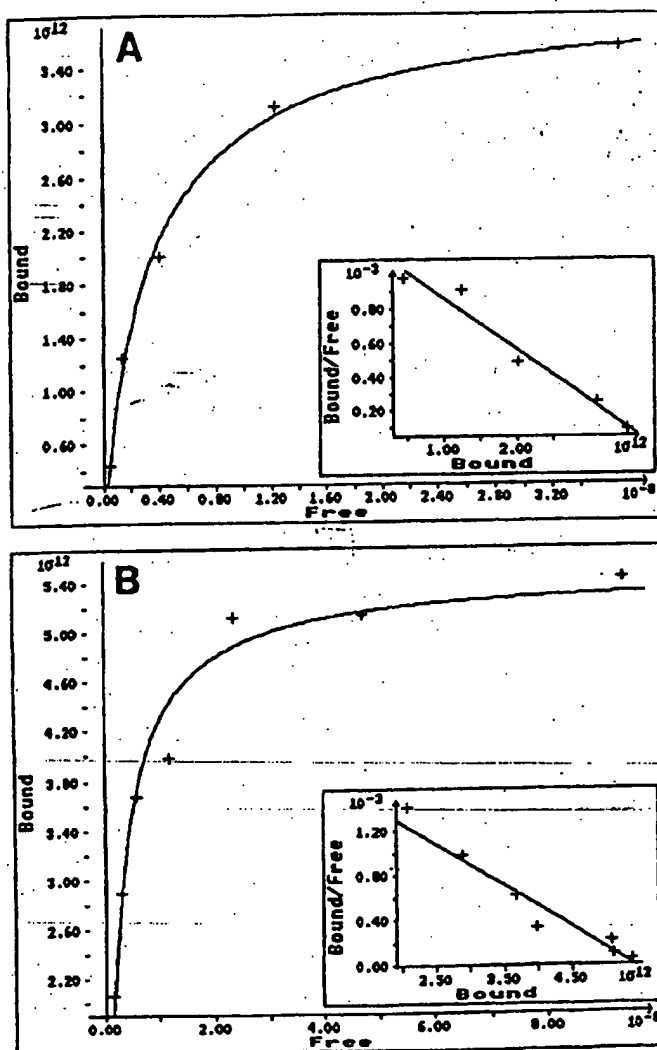


Fig 4. Analysis of the binding of biotin-(sialyl)-erythropoietin to Friend and Rauscher murine erythroleukemia cells at equilibrium. (A) Friend 745 cells; (B) Rauscher Red 1 cells.

biological activity, and comprise a useful ligand for studies of its cell surface receptor. Also, it is shown that comparably large losses in hormonal activity result from the covalent attachment of biotin to erythropoietin at alternative sites, including carboxylate and amino groups. Although the chemistries of these biotinylated adducts are distinct, these findings are consistent with the results of earlier studies involving the direct chemical modification of human erythropoietin. Abrogation of erythropoietic activity previously has been shown to result from the esterification of carboxylate groups using thionyl chloride plus methanol,²³ as well as from the acylation of amino groups using radioiodinated N-succinimidyl-3-(4-hydroxyphenyl) propionate.²⁴ These studies, along with our results, indicate that carboxylate and amino groups of erythropoietin are important for biological activity. In contrast, no similar role for sialic acid residues in mediating interaction between erythropoietin and its receptor is indicated, since removal of these residues using neuraminidase reportedly has little, or no effect on hormonal activity.²⁵ Consistent with this finding, the covalent attachment of biotin to sialic acid residues of erythropoietin presently is shown to proceed efficiently and to yield product possessing substantial bioactivity (Fig 1, c-h). Based on its capacity to interact productively with receptor, biotin-(sialyl)-erythropoietin comprises a highly suitable ligand for use in receptor analyses. Analyses of the specific binding of biotin-(sialyl)-erythropoietin to Friend 745 and Rauscher Red 1 cells served to confirm this conclusion.

Regarding Friend 745 cells, the saturability and high-affinity of binding sites for biotin-(sialyl)-erythropoietin, indicate that these sites correspond to the murine erythropoietin receptor. Previously, saturable and specific sites for ¹²⁵I-erythropoietin binding on Friend erythroleukemia cells have been identified.^{26,27} Estimates of the affinity of these sites vary from 0.15 nmol/L²⁶ to 1.3 nmol/L kd,²⁷ while estimates of binding site density vary from 113²⁷ to 760 sites per cell.²⁶ Variation in these estimates possibly is attributable to the consideration that varying amounts of biological inactivation may result from chloroamide-mediated radioiodination of erythropoietin, possibly including complete inactivation.^{11,24,28-32} This inactivation apparently derives from iodination, and not from exposure to oxidants per se, since exposure of erythropoietin to either Chloramine-T or 1,3,4,6-tetrachloro-3,6-diphenylglycouril in the absence of iodide reportedly does not alter activity.³⁴ As a result, ¹²⁵I-erythropoietins used in binding analyses typically have been prepared at stoichiometries of less than one atom of ¹²⁵I-iodide per hormone molecule.^{26,27} Obviously, this circumstance (ie, nonstoichiometric labeling) complicates detection by bioassay of possible inactivation of modified erythropoietin molecules. Unfortunately, no attempt to purify and directly assay iodinated hormone molecules has been

reported. Additionally, it has been reported that biological activity which is retained in preparations of ¹²⁵I-erythropoietin may be unstable and possess a short half-life (ie, <10 days).¹¹ A single class of high affinity receptors for biotin-(sialyl)-erythropoietin also was identified on Rauscher erythroleukemia cells (clone Red 1; 164 ± 5 sites per cell, 2.7 ± 0.4 nmol/L kd; Fig 4B). Although this clone has not been studied previously, high affinity receptors for ¹²⁵I-erythropoietin (0.44 to 0.55 nmol/L kd) have been reported for an alternate Rauscher cell clone, Red 5.³² Binding site density on an isolated erythropoietin-responsive subclone, Red 5-1.5, was estimated at 1,690 sites per cell.

Biotin-(sialyl)-erythropoietin as presently developed as an alternative ligand for receptor studies is advantageous in several regards. First, this labeled adduct is shown to possess high biological activity (Fig 1, c-h). Second, biotin-(sialyl)-erythropoietin is biologically stable, and retains ≥90% of its biological activity for minimally 1 month when stored at 4°C. Third, biotin-(sialyl)-erythropoietin is chemically stable, and no significant decrease in the proportion of active, biotinylated molecules is detectable during minimally 1 month of storage. Fourth, as assessed using a 50-fold excess of purified, unmodified recombinant erythropoietin as competitor, the binding of biotin-(sialyl)-erythropoietin to putative receptors on two distinct erythroid cell lines is shown to occur with high specificity. Finally, the chemical nature of biotin as a label is advantageous in that extended utility derives from its use combined with various covalently modified forms of streptavidin. For example, avidin attached covalently to agarose has been used successfully in combination with biotinylated forms of insulin,³³ growth hormone,³⁴ estrogen,³⁵ and parathyroid hormone³⁶ to purify their respective receptors by ligand affinity chromatography. An alternative example of extended utility is given by the recent use of biotinylated interleukin-6 in the isolation of a cDNA encoding its receptor.³⁷ In this application, expression cloning was accomplished using biotinylated hormone in combination with fluorescein-labeled avidin and fluorescent-activated cell sorting. Based on these reports, it is anticipated that biotin-(sialyl)-erythropoietin as presently developed will figure advantageously not only in studies of the regulated expression of erythropoietin receptors on intact cells, but also in facilitating receptor isolation through either direct, or genetic means.

ACKNOWLEDGMENT

The expert technical assistance of Rebecca Burkert is gratefully acknowledged. Purified recombinant human erythropoietin (150,000 U/mg) as produced in cultured Chinese hamster ovary cells was generously provided by Ortho Pharmaceutical Corp, Raritan, NJ.

REFERENCES

1. Jelkman W: Renal erythropoietin: Properties and production. *Rev Physiol Biochem Pharmacol* 104:139, 1986
2. Krantz SB, Gallien-Lartigue O, Goldwasser E: The effect of erythropoietin upon heme synthesis by marrow cells in vitro. *J Biol Chem* 238:4085, 1963
3. Krystal G: A simple microassay for erythropoietin based on ³H-thymidine incorporation into spleen cells from phenylhydrazine-treated mice. *Exp Hematol* 11:649, 1983
4. Dunn CD, Jarvis JH, Greenman JM: A quantitative bioassay

- for erythropoietin using mouse fetal liver cells. *Exp Hematol* 3:65, 1975
5. Nigon V, Godet J: Genetic and morphogenetic factors in hemoglobin synthesis during higher vertebrate development: An approach to cell differentiation mechanisms. Bourne GH, Danielli JF, Jeon KW (eds): *International Review of Cytology*, vol 46. San Diego, Academic, 1976, p 79
6. Jacobs K, Shoemaker C, Rudersdorf R, Neill SD, Kaufman RJ, Mufson A, Soehra J, Jones SS, Hewick R, Fritsch EF, Kawakita M, Shimizu T, Miyake T: Isolation and characterization of genomic and cDNA clones of human erythropoietin. *Nature* 313:806, 1985
7. Lin F-K, Suggs S, Lin C-H, Brown JK, Smalling R, Egrie JC, Chen KK, Fox GM, Martin F, Stabinsky Z, Badrawi SM, Lai P-H, Goldwasser E: Cloning and expression of the human erythropoietin gene. *Proc Natl Acad Sci USA* 82:7580, 1985
8. Powell JS, Berkner KL, Lebo RV, Adamson JW: Human erythropoietin gene: High level expression in stably transfected mammalian cells and chromosome localization. *Proc Natl Acad Sci USA* 83:6465, 1986
9. Wojchowski DM, Sue JM, Sytkowski AJ: Site-specific antibodies to human erythropoietin: Immunoaffinity purification of urinary and recombinant hormone. *Biochim Biophys Acta* 913:170, 1987
10. Wojchowski DM, Orkin SH, Sytkowski AJ: Active human erythropoietin expressed in insect cells using a baculovirus vector: A role for N-linked oligosaccharide. *Biochim Biophys Acta* 910:224, 1987
11. Miyake T, Kung CK-H, Goldwasser E: Purification of human erythropoietin. *J Biol Chem* 252:5558, 1977
12. Sasaki H, Bothner B, Dell A, Fukuda M: Carbohydrate structure of erythropoietin expressed in Chinese hamster ovary cells by a human erythropoietin cDNA. *J Biol Chem* 262:12059, 1987
13. Recny MA, Scobie HA, Kim Y: Structural characterization of natural human urinary and recombinant DNA-derived erythropoietin. *J Biol Chem* 262:17156, 1987
14. Goto M, Akai K, Murakami A, Hashimoto C, Tsuda E, Ueda M, Kawaniishi G, Takahashi N, Ishimoto A, Chiba H, Sasaki R: Production of recombinant human erythropoietin in mammalian cells: Host-cell dependency of the biological activity of the cloned glycoprotein. *BioTechnology* 6:67, 1988
15. Chesebro B, Wehrly K, Chesebro K, Portis J: Characterization of Ia8 antigen, Thy-1.2 antigen, complement receptors, and virus production in a group of murine virus-induced leukemia cell lines. *J Immunol* 117:1267, 1976
16. de Both NJ, Vermey M, van't Hull E, Klootwijk-van Dijke E, van Griensven LJD, Mol JNM, Stoof TJ: A new erythroid cell line induced by Rauscher murine leukaemia virus. *Nature* 272:626, 1978
17. Feldman HA: Mathematical theory of complex ligand binding systems at equilibrium. *Analyt Biochem* 48:317, 1972
18. Marquardt D: An algorithm for least squares estimation of non-linear parameters. *J Soc Indust Appl Math* 11:2, 1963
19. Lappin TRJ, Rich I, Goldwasser E: The effect of erythropoietin and other factors on DNA synthesis by mouse spleen cells. *Exp Hematol* 11:661, 1983
20. Laemmli UK: Cleavage of structural proteins during the assembly of the head of bacteriophage T4. *Nature* 227:680, 1970
21. Towbin H, Staehelin T, Gordon J: Electrophoretic transfer of proteins from polyacrylamide gels to nitrocellulose sheets: Procedure and some applications. *Proc Natl Acad Sci* 76:4350, 1979
22. Spiro RG: Studies on fetuin, a glycoprotein of fetal serum. *J Biol Chem* 235:2860, 1960
23. Krantz S, Jacobson LO: Erythropoietin and the Regulation of Erythropoiesis. Goldwasser E (ed). New York, Liss, 1975, p 53
24. Goldwasser E: Erythropoietin and red cell differentiation, in Cunningham D, Goldwasser E, Watson J, Fox FC (eds): *Control of Cellular Division and Development (part A)*. New York, Liss, 1981, p 487
25. Goldwasser E, Kung CK-H, Eliason J: On the mechanism of erythropoietin-induced differentiation. *J Biol Chem* 249:4202, 1974
26. Todokoro K, Kanazawa S, Amanuma H, Iizawa Y: Specific binding of erythropoietin to its receptor on responsive mouse erythroleukemia cells. *Proc Natl Acad Sci USA* 84:4126, 1987
27. Sasaki R, Yanagawa S-I, Hitomi K, Chiba H: Characterization of erythropoietin receptor of murine erythroid cells. *Eur J Biochem* 168:43, 1987
28. Sawyer ST, Krantz SB, Goldwasser E: Binding and receptor-mediated endocytosis of erythropoietin in Friend virus-infected erythroid cells. *J Biol Chem* 262:5554, 1987
29. Fraser JK, Lin F-K, Berridge MV: Expression and modulation of specific high affinity binding sites for erythropoietin on the human erythroleukemia cell line, K562. *Blood* 71:104, 1988
30. Tsai C-J, Tojo A, Pakamachi H, Kitamura T, Saito T, Uraha A, Takaku F: Expression of the functional erythropoietin receptors on interleukin-3 dependent murine cell lines. *J Immunol* 140:89-93, 1988
31. Sakaguchi M, Koishihara Y, Tsuda H, Fujimoto K, Shibuya K, Kawakita M, Takatsuki K: The expression of functional erythropoietin receptors on an interleukin-3-dependent cell line. *Biochem Biophys Res Commun* 146:7, 1987
32. Broudy VC, Lin N, Egrie J, de Haen C, Weiss T, Papayannopoulou T, Adamson JW: Identification of the receptor for erythropoietin on human and murine erythroleukemia cells and modulation by phorbol ester and dimethyl sulfoxide. *Proc Natl Acad Sci USA* 85:6513, 1988
33. Finn FM, Titus G, Hofmann K: Ligands for insulin receptor isolation. *Biochemistry* 23:2554, 1984
34. Haeuptle MT, Aubert ML, Djiane J, Krachenbuhl J-P: Binding sites for lactogenic and somatogenic hormones from rabbit mammary gland and liver. *J Biol Chem* 258:305, 1983
35. Rodeuilh G, Secco C, Baulieu E-E: The use of the biotinyl estradiol-avidin system for the purification of "nontransformed" estrogen receptor by biohormonal affinity chromatography. *J Biol Chem* 260:3996, 1985
36. Brennan DP, Levine MA: Characterization of soluble and particulate parathyroid hormone receptors using a biotinylated bioactive hormone analogue. *J Biol Chem* 262:14795, 1987
37. Yamasaki K, Taga T, Hirata Y, Yawata H, Yoshikawa K, Seed B, Taniguchi T, Hirano T, Kishimoto T: Cloning and expression of the human interleukin-6 (BSF-2/IFN β 2) receptor. *Science* 241:825, 1988

Original Article

Identification and kinetics of leukocytes after severe ischaemia/reperfusion renal injury

Dirk K. Ysebaert¹, Kathleen E. De Greef¹, Sven R. Vercauteren¹, Manuela Ghielli², Gert A. Verpooten², Erik J. Eyskens¹ and Marc E. De Broe²

Departments of ¹Experimental Surgery, and ²Nephrology, University of Antwerp, Belgium

Abstract

Background. Leukocyte adhesion/infiltration in response to renal ischaemia/reperfusion (I/R) injury is a well-known but poorly understood phenomenon. The identification, kinetics, and exact role of these inflammatory cells in I/R injury and regeneration are still matters of debate.

Methods. Uninephrectomized rats were submitted to 60 min renal ischaemia by clamping of renal vessels.

Results. Severe acute renal failure was observed, with maximum functional impairment on day 2. By 12 h after the ischaemic event, up to 80% of proximal tubular cells in the outer stripe of outer medulla (OSOM) were already severely damaged. Proliferation (proliferating cell nuclear antigen (PCNA) staining) started after 24 h, reaching maximum activity on day 3. Regeneration of tubular morphology started on the 3rd day, and after 10 days 50% of tubules had regenerated completely. Interstitial leukocytes (OX-1 immunohistochemical staining) were already prominent at day 1, thereafter gradually increasing with time. The so-called neutrophil-specific identification methods (myeloperoxidase (MPO), chloroacetate esterase, mAb HIS-48) proved to be non-specific, since they also stained for macrophages, as demonstrated by flow cytometry and the combination of these stainings with the macrophage-specific ED-1 staining. MPO activity was already significantly increased at 1 h post-I/R ($439 \pm 34\%$, $P < 0.005$), reaching its maximum activity after 12 h of I/R ($1159 \pm 138\%$, $P < 0.0005$), declining thereafter. On the other hand, neutrophil presence investigated by H&E staining revealed only a few neutrophils in glomeruli, medullary rays, and OSOM at 24 h after the ischaemic event (4.7 ± 4.2 cells/mm² vs controls = 2.3 ± 2.0 cells/mm² (n.s.)), and remained unchanged over the next 10 days. In contrast, significant monocyte/macrophage adhesion/infiltration (ED-1 staining) occurred at the OSOM at 24 h post-ischaemia (at 24 h, 120 ± 46 cells/mm² vs sham = 18 ± 4 cells/mm²

($P < 0.05$)), became prominent at day 5 (1034 ± 161 cells/mm² vs sham = 18 ± 18 cells/mm² ($P < 0.05$)), and almost disappeared after 10 days. CD4⁺ cells (W3/25) gradually increased from day 5, reaching a maximum at day 10. A few CD8⁺ cells (OX-8) were apparent from days 3 until 10, but no B-cells (OX-33) were observed.

Conclusions. After severe warm I/R renal injury, a pronounced acute tubular necrosis occurs during the first 12–24 h in the absence of a marked cellular infiltrate, but with an important renal MPO activity, reflecting the activation of the adhering inflammatory cells (polymorphonuclear cells (PMNs) and mainly monocytes/macrophages). Only later at the time and site (OSOM) of regeneration a sequential accumulation of monocytes/macrophages and T cells becomes prominent, in contrast with the low number of neutrophils found in the kidney during the 10-day post-ischaemic period. The non-specificity of the so-called neutrophil-specific identification methods (MPO activity, naphthol AS-D chloroacetate esterase, or mAb HIS-48 staining), cross-reacting with monocytes/macrophages, explains the controversy in literature concerning the number of PMNs in post-ischaemic injury.

Keywords: damage; kidney; macrophages; myeloperoxidase; neutrophils; rat; regeneration

Introduction

Ischaemia/reperfusion (I/R) injury is a common clinical event, still associated with high mortality and morbidity [1], and lacking a specific therapy. Post-ischaemic acute tubular necrosis (ATN) is observed most frequently in patients after major surgery (cardiac and aortic operations), trauma, severe hypovolaemia, burns, and others [2]. In addition, delayed graft function of renal allografts is mainly caused by post-ischaemic ATN, with significant long-term graft survival [3]. Despite decades of laboratory and clinical investigation, the pathophysiology of I/R injury is still incompletely understood [1].

Correspondence and offprint requests to: Marc E. De Broe MD PhD, University of Antwerp, Department of Nephrology-Hypertension, p/a University Hospital Antwerp, Wilrijkstraat 10, B-2650 Edegem/Antwerpen, Belgium.

Renal injury after ischaemia appears to be a consequence of tissue hypoxia from interrupted blood supply but also from the process of reperfusion, leading to an active inflammatory response [4]. Sublethal or even lethal injured proximal tubular and endothelial cells trigger this process through the release of cytokines and chemokines that will promote cellular infiltration. Leukocytes may play an important role in the mechanism of parenchymal injury after I/R as well as in the regeneration process, but their exact role is far from clear. Polymorphonuclear cells (PMNs) recruited during reperfusion have long been implicated as critical mediators of the early renal parenchymal injury in ischaemic ARF, as recently reviewed [5]. These assumptions were supported by morphological criteria (H&E stain [6]), enzymatic criteria (myeloperoxidase [7–9], chloroacetate esterase [10–13], mAb HIS-48 [14]) and labelling techniques (e.g. ^{111}In labelling [15]), in most cases suggesting robust PMN recruitment in the post-ischaemic kidney [1]. These PMNs may contribute by potentiating an inflammatory response that leads to the generation of vasoconstrictor agents, cytokines, and toxic mediators such as reactive oxygen species and proteases [16,17]. I/R in rat myocardium [18], liver [19], and brain [20] has been correlated with the number of granulocytes adherent at the capillary walls. Also in the kidney, PMNs have been put forward as inducing or amplifying additional damage in post-ischaemic renal injury [7–9,12,13,15,21]. Several investigators, however, found that infiltration of the renal parenchyma by PMNs was not a prominent feature of experimental or human post-ischaemic ARF when PMNs in renal sections were counted using routine histology (H&E) [1].

The first step in unravelling this controversy consists in the careful analysis of the identification of these adhering/infiltrating cells and their kinetics and distribution, related to the course of tubular injury and repair after severe warm I/R.

Subjects and methods

Animals and experimental groups

After overnight fasting, the surgical procedures were carried out under anaesthesia with sodium pentobarbitone (60 mg/kg) in inbred male LEW rats (220–260 g). A midline abdominal incision was made and heparin (50 IU, i.p.) was administered. To help to maintain thermoregulation during ischaemia, the abdomen contents were replaced and covered with a wet dressing. No specific heating pad was used. Animals were randomly assigned to two groups: (i) left renal ischaemia, performed by cross-clamping the left renal pedicle for 60 min with a microvascular clamp, followed by right nephrectomy at the end of the ischaemia period ($n=40$); (ii) right nephrectomy alone, without ischaemia ($n=40$). In these control animals the left renal pedicle was dissected, but not clamped. Careful dissection was carried out to preserve the blood supply to the adrenal glands. The kidneys were inspected for ischaemia as well for good reperfusion for 2 min. This uninephrectomized model was chosen for analogy with

the situation of renal transplantation; moreover, prior investigations have shown that contralateral nephrectomy enhances the functional and morphological recovery of the post-ischaemic kidney [22,23].

Post-operative animals were allowed to recover, each in a separate cage, at constant temperature (18°C) and humidity (45%) on a 12-h light/dark cycle. They received free tap water *ad libitum*, and standard laboratory rat pellets by the paired-feeding method. In this way non-ischaemic animals received the same protein and salt intake as post-ischaemic animals, which show greater post-operative anorexia. Animals were weighed and inspected daily. Sacrifice of 4 animals per experimental time point was done at hours 1, 2, 6 and 12 and on days 1, 2, 3, 5, 7, and 10. Blood samples were taken by heart puncture. All procedures were carried out in accordance with the NIH Guide for the Care and Use of Laboratory Animals No. 85–23 (1985), and with approval of the Ethical Committee of the University of Antwerp.

Biochemical determinations:

Blood samples were allowed to clot and were centrifuged at high speed for 15 min. Serum was obtained and stored at -20°C until use. Serum creatinine values were determined in duplicate using a colorimetric method as modified by Jaffé (Creatinine Merckotest, Diagnostica Merck, Germany).

Tissue collection and fixation:

Immediately after sacrifice, tissue for analysis was collected from the left kidney. After dissection of the capsular fat, the kidney was weighed. Five sagittal tissue sections (1 mm thick) were made and fixed in formalin calcium, methacarn and Dubosq Brazil fixative. Two sections were stored in liquid nitrogen.

Morphological analysis of tubular injury, regeneration and cell proliferation:

The degree of injury in different tubular compartments was established on periodic acid-Schiff reagent (PAS)-haematoxylin-PCNA stained sections of methacarn-fixed and paraffin-embedded renal tissue. Proliferation was determined by immunohistochemical staining for the PCNA using the PC10 monoclonal antibody (Dako, Denmark). Sections were counterstained with PAS. Nuclei were stained with methyl green. Histological damage of the kidney was scored semi-quantitatively: 50 tubules in the outer stripe of the outer medulla (most sensitive zone for ischaemic injury) were assigned using a score-system ranging from 0 to 6 (score 0, normal tubule; score 1, (limited to) loss of brush border; score 2, <50% tubular damage, meaning less than 50% of naked basal membrane; score 3, >50% tubular damage; score 4, total destruction of all epithelial cells, naked basement membrane; score 5, small rim of cytoplasm with large dark nuclei (PCNA+); score 6, increase in cytoplasm volume; evolution to score 1, uncompleted brush border and score 0, complete regenerated brush border). The proliferation was measured by counting the number of PCNA-immunoreactive nuclei in 25 circular-shaped proximal tubules.

Renal adhesion/infiltration—leukocyte cell markers:

Sections (4 μm) were mounted on poly-L-lysine-coated microscope slides and treated for 5 min with 0.003% trypsin III (Sigma Chemical Co., St Louis, USA) in 10 mmol/l Tris-HCl

buffer pH 7.3. After washing in Tris saline buffer (TSB, 0.01 mol/l Tris-HCl pH 7.6 in 0.9% NaCl) and treatment with normal horse serum (1/5), the sections were incubated overnight with the primary antibody OX-1 (1/6000). This OX-1 mAb recognizes the rat leukocyte common antigen CD45, which is present on all marrow-derived leukocytes [24]. Positive cells were counted in 20 fields of 0.16 mm² and data were expressed as leukocytes/mm². Immunohistochemical detection of monocytes/macrophages was performed on methacarn-fixed, paraffin-embedded renal-tissue sections using the ED1 monoclonal antibody (Serotec, UK). This antibody is directed to a cytoplasmic antigen of tissue macrophages and monocytes [25]. As control, a peripheral blood smear and a spleen section of the rat were stained. T-lymphocytes (Helper T-cells: W3/25, suppressor T-cells: OX-8), and B-lymphocytes (OX-33) were demonstrated on 5 µm renal tissue cryosections prefixed in 4% formaldehyde (BDH Chemical Ltd, Poole, UK) buffered with 0.1 mol/l Na-cacodylate pH 7.4 containing 1% CaCl₂. Sections were incubated overnight with W3/25 (1/800), OX-8 (1/400) or OX-33 (1/100) (Serotec, Oxford, UK). Appropriate antibody dilutions were determined in preliminary experiments. The W3/25 monoclonal antibody recognizes the rat CD4-equivalent present on T-helper cells [26], and, in lower density, on some macrophages [27]. The OX-8 monoclonal antibody reacts with T-suppressor/cytotoxic and natural killer cells, and is directed to the rat CD8-equivalent [28]. The OX-33 monoclonal antibody reacts with only peripheral B-cells [29]. Positively stained cells were quantified in 10 randomly chosen OSOM microscope fields (magnification 125) in each animal and expressed as positive cells per square millimetre. Endogenous tissue peroxidase activity was inhibited by immersion in methanol for 15 min, followed by 30 min incubation with 0.03% H₂O₂ in TSB. After washing, subsequent incubations were performed with the avidin-biotin peroxidase complex (Vectastain, Vector Laboratories Inc., Burlingame, USA) and 9-amino-ethylcarbazole as the chromogen supplemented with the H₂O₂ as substrate. As controls, a spleen section of the rat was also stained. Nuclei were counterstained with methyl green.

Myeloperoxidase (MPO) assessment of rat post-ischaemic kidney

This colorimetric method measures the activity of MPO found in the azurophilic granules present in PMNs [30]. Normal and post-ischaemic kidney at 1, 2, 6, 12, and 24 h post-reperfusion was homogenized in 5 mmol/l potassium phosphate buffer first and then centrifuged at 30 000 g for 30 min at 4°C prior to extraction. To avoid interference with supernatants from control and post-ischaemic kidney the pellets were washed twice [31]. The resulting pellets expressed MPO activity after suspending them in 50 mmol/l phosphate buffer containing 0.5% hexadecyltrimethyl ammonium bromide (HTAB). The pellets were centrifuged at 40 000 g for 15 min; 0.2 ml specimen was added to 0.8 ml 50 mmol/l potassium phosphate buffer (pH 6.0) containing 0.167 mg/ml O-dianisidine dihydrochloride and 0.0005% H₂O₂. Absorbency was measured at 460 nm for 2 min, and assay linearity was confirmed. MPO activity, normalized to protein content of the supernatant, was expressed as the percentage of levels in kidneys subjected to sham surgery.

Identification/quantification methods of PMNs

H&E staining

Histochemical detection of polymorphonuclear cells was performed on methacarn-fixed, paraffin-embedded renal-

tissue sections. The H&E staining was used to identify and to quantify the infiltration of polymorphonuclear cells, based upon the localization of the cell and morphology of the nucleus of the cell. Positively stained cells were quantified in 75 randomly chosen microscope fields (magnification 1000) in cortex, outer stripe of outer medulla (+ medullary rays), and inner medulla, expressed as positive cells per square millimetre.

ED-1 staining on cryosections in combination with MPO staining

In brief, after incubation with the mAb ED-1 against macrophages (step 1), MPO was stained using the chromogen benzidine dihydrochloride (step 2). Thereafter, MPO was inactivated (step 3) and the ED-1 staining itself was developed (step 4) (Figure 1). More in detail, 5 µm renal tissue cryosections were used, prefixed in formalin calcium (4% formaldehyde (BDH Chemical Ltd., Poole, UK)) buffered with 0.1 M Na-cacodylate pH 7.4 containing 1% CaCl₂. In a first step, the sections were mounted on poly-L-lysine coated microscope slides and treated for 5 min with 0.003% trypsin III (Sigma Chemical Co., St Louis, USA) in 10 mmol/l Tris-HCl buffer pH 7.3. After washing in TSB with 1% bovine serum albumin and treatment with normal horse serum (1/5), the sections were incubated overnight with the primary mouse anti-rat antibody ED-1 (1/15 000). This very specific antibody is directed to a cytoplasmic antigen of tissue macrophages, monocytes and dendritic cells [25]. Sections were then incubated for 30 min with biotinylated horse anti-mouse IgG. As second step, staining for the MPO was performed, using the chromogen benzidine dihydrochloride (30% ethanol, containing 1.5 g benzidine, pH 6.0) and hydrogen peroxide 0.03% as substrate. This shows the yellow-coloured intra-cytoplasmic granules. The sections were mounted with gelatine and photographed with a Leica microscope using the program KS 400 v. 2.0. In a third step, the sections were demounted to further develop the ED-1 mAb: after inhibition of endogenous peroxidase using methanol for 15 min and H₂O₂ 0.03% in TSB for 30 min, sections were incubated with avidin-biotin labelled with peroxidase (Vectastain, Vector Laboratories Inc., Burlingame, USA) and developed with 9-amino-ethylcarbazole as chromogen and H₂O₂ as substrate, which finally shows the ED-1 positive red-brownish-coloured cytoplasm of the macrophage. The sections were mounted with gelatine/glycerine and photographed again.

As part of control experiments the specific ED-1 staining was tested in peripheral blood. Rat blood samples were taken at moment of sacrifice. A peripheral blood smear was performed and fixed for 30 s in formalin calcium. Then the ED-1 staining (without MPO staining) was performed as described previously. A counterstaining with haematoxylin was performed.

ED-1 staining on cryosections in combination with naphthol AS-D chloroacetate esterase staining

In brief, after incubation with the mAb ED-1 against macrophages, the naphthol AS-D chloroacetate esterase reaction was performed. Thereafter, the ED-1 staining itself was developed. More in detail, ED-1 positive cells were demonstrated as described above; 4 µm renal tissue cryosections were used, prefixed in formalin calcium (4% formaldehyde (BDH Chemical Ltd, Poole, UK) buffered with 0.1 M Na-cacodylate pH 7.4 containing 1% CaCl₂). In a first step, the sections were mounted on poly-L-lysine coated

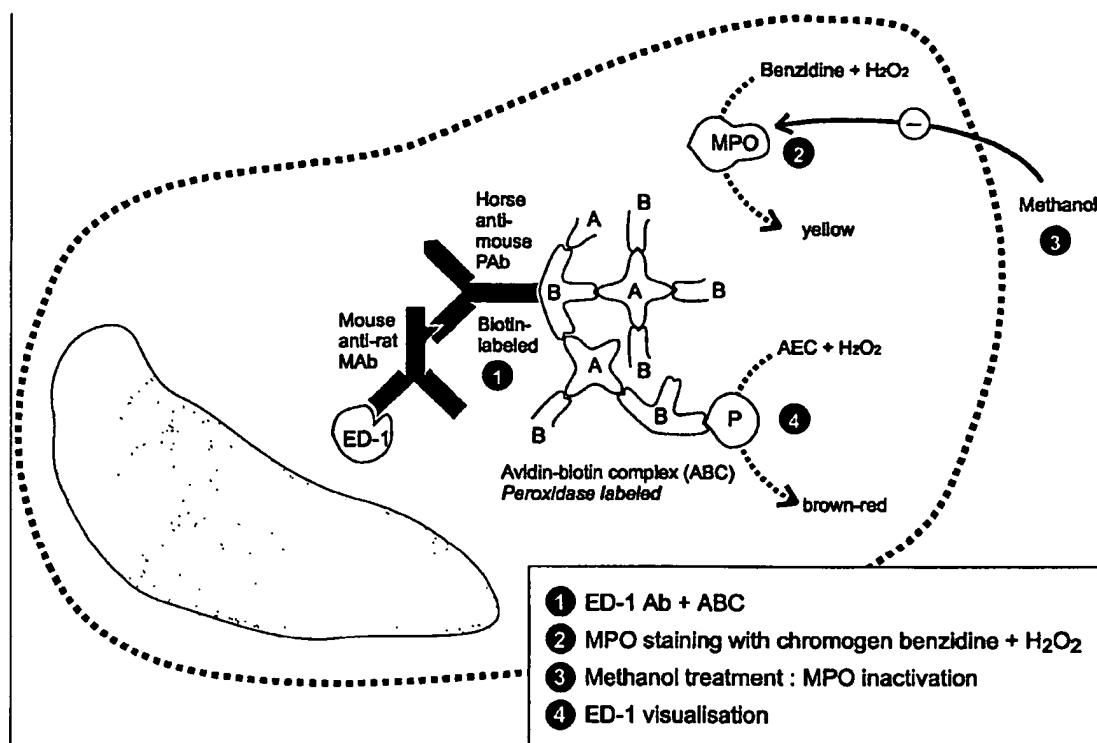


Fig. 1. Method of combined ED-1/MPO staining on cryosections. For further explanation of different steps, see text.

microscope slides and treated for 5 min with 0.003% trypsin III (Sigma Chemical Co., St Louis, USA) in 10 mM Tris-HCl buffer pH 7.3. After washing in TSB with 1% bovine serum albumin and treatment with normal horse serum (1/5), the sections were incubated overnight with the primary mouse anti-rat antibody ED-1 (1/15 000). Sections were then incubated with biotinylated horse anti-mouse IgG. After 30 min incubation, as a second step, the chloroacetate staining was performed as described by Leder [32]: slides were incubated with naphthol AS-D chloroacetate esterase in 4% pararosaniline and 4% sodium nitrate in 0.1 M acetate buffer for 30 min. The sections were mounted with gelatine and photographed: cells containing red-brownish granules were regarded as positive. In a third step, the sections were demounted. After inhibition of endogenous peroxidase using methanol for 15 min and H₂O₂ 0.03% in TSB for 30 min, sections were incubated with avidin-biotin horseradish peroxidase (Vectastain, Vector Laboratories Inc., Burlingame, USA) and developed as described above, to show the ED-1-positive cells. Control stainings were similar as described for MPO (see above).

HIS-48 (granulocytes) in combination with ED-1

In brief, first the primary antibody HIS-48 was demonstrated, photographs were taken, decoloured, and thereafter ED-1 staining was performed. More in detail, 5-µm renal tissue cryosections were prefixed and mounted as described above, and incubated overnight with HIS-48 (1/10) (monoclonal antibody against polymorphonuclear cells) [14]. As controls sections were also incubated with the primary mAb ED-1

(1/150 000) and mAb against α -smooth muscle actin (α -SMA) (1/30 000). After inhibition of endogenous peroxidase using methanol for 15 min and H₂O₂ 0.03% in TSB for 30 min, sections were incubated with biotinylated horse anti-mouse IgG for 30 min. Sections were then incubated with avidin-biotin horseradish peroxidase (Vectastain, Vector Laboratories Inc., Burlingame, USA) and developed with 9-amino-ethylcarbazole as chromogen and H₂O₂ as substrate. The sections were mounted with gelatine/glycerine and photographed. The sections were demounted, decoloured with isopropanol and again photographed. Then the sections were heated in a microwave [14] for 10 min in order to destroy the horse anti-mouse binding on HIS-48 and were allowed to cool down. The sections were blocked with polyclonal rabbit antiserum for 20 min and then incubated overnight with ED-1, which was a FITC (fluoresceine isothiocyanate)-labelled antibody. Then the sections were incubated with a rabbit polyclonal anti-FITC antibody, which was peroxidase labelled and thereafter, developed with 9-amino-ethylcarbazole as chromogen and H₂O₂ as substrate.

This rabbit anti-ED-1 FITC-labelled antibody was used in order to exclude aspecific staining with the previous secondary polyclonal horse anti-mouse antibody and avidin-biotin complexes. In another control experiment aspecific binding of ED-1 with the horse anti-mouse antibody, used during first staining step, was excluded using α -SMA in the first staining.

Labelling of rat peripheral blood cells with mAb HIS48

Erythrocytes from 20 µl of heparinized blood were lysed (hypotonic buffer, 10 min, 20°C) and leukocytes were then

incubated (30 min, 4°C) with mAb HIS-48. A second incubation step (30 min, 4°C) with FITC-conjugated rabbit-anti-mouse IgG (RAM-FITC) followed washing of the cells (PBS + 0.1% BSA + 0.05% NaN₃). Cells were resuspended in washing buffer prior to analysis on a FACStar plus (Becton & Dickinson, Immunocytometry Systems). To identify positive cells, these were sorted onto poly-L-Lysine-coated glass slides and stained by May-Grünwald-Giemsa standard procedure.

Statistics

Data are presented as means \pm standard deviation. They were compared with an one-way ANOVA analysis, and a Student-Newman-Keuls test was used to prove qualitative differences by using the software package SPSS. Significant differences were anticipated when $P < 0.05$.

Results

Animals (Figure 2 A-B)

During surgery, animals cooled from 38 to 28°C, as no specific heating pad was used. Post-ischaemic animals sustained a severe acute renal failure with a mortality of 15%, observed at days 3–4, while non-ischaemic animals all survived the right nephrectomy. Due to the paired feeding, all animals had comparative post-operative weight loss, which had not recovered during the 10-day study period. At sacrifice, the post-ischaemic kidneys showed a weight gain of 45% at day 5, which persisted, reflecting oedema and infiltration.

Kidney function (Figure 2C)

Unilateral nephrectomy, without any ischaemia, caused a slight increase in the serum creatinine (S-crea) levels on day 2 (S-crea_{nephrectomy day 0} = 0.75 mg/dl \pm 0.05 vs S-crea_{nephrectomy day 2} = 1.22 mg/dl \pm 0.13; $P < 0.05$), and returned to normal on day 3. A period of 60 min of warm ischaemia caused a severe acute renal failure on the second day (S-crea_{ischaemia day 0} = 0.75 mg/dl \pm 0.05 vs S-crea_{ischaemia day 2} = 4.0 mg/dl \pm 1.9; $P < 0.05$). Functional recovery of the kidney started after day 2 and was almost complete at day 7 (S-crea_{ischaemia day 7} = 1.06 mg/dl \pm 0.11; not significant).

Damage and regeneration/PCNA positivity (Figures 3, 4)

The zones of most severe injury (PAS staining) and proliferation (PCNA staining), which are the OSOM and medullary rays, are exactly the same zones of most important leukocyte infiltration (OX-1 pan leukocyte staining) (Figure 3). The evolution of damage and regeneration of the kidney tubules was scored semi-quantitatively (Figure 4). In cases of a unilateral neph-

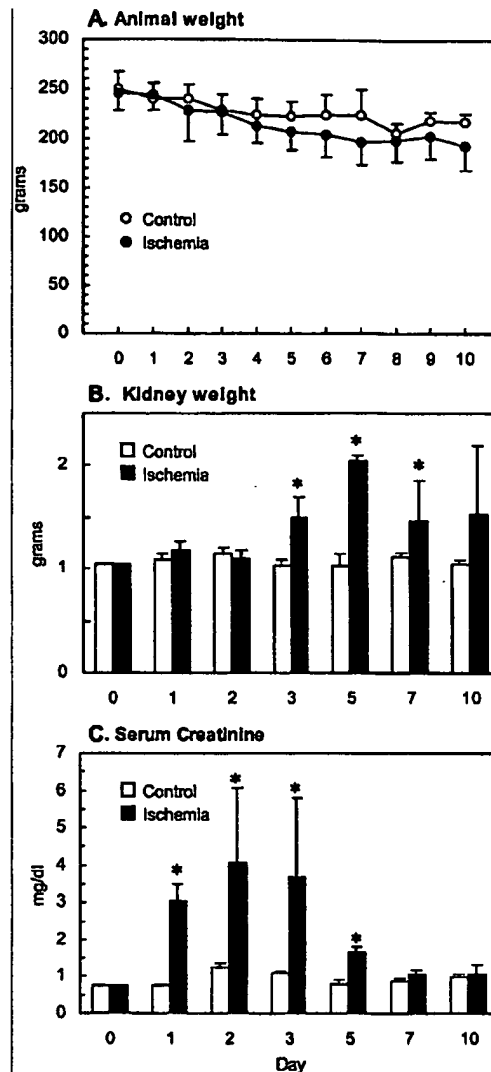


Fig. 2. (A) Post-ischaemic animal weight loss. (B) Evolution of weight of the post-ischaemic kidney. (C) Kidney function, serum creatinine. Dark bars and circles, post-ischaemic animals, after 60 min warm ischaemia on remaining left kidney. Light bars and circles, controls without ischaemia. (* $P < 0.05$).

rectomy without ischaemia of the unique kidney, no signs of damage or regeneration were seen in the remaining kidney during the study period of 10 days. No PCNA positivity or infiltrating leukocytes was noticed. In contrast to the non-ischaemic groups, 60 min of warm ischaemia resulted in remarkable damage of the proximal S3 segment and the thick ascending limb of the nephron in the OSOM and medullary rays. The first day after the ischaemia, almost half of the tubules showed a complete detachment (score 4) of their epithelial cells from their basement membrane. On day 2, the first signs of

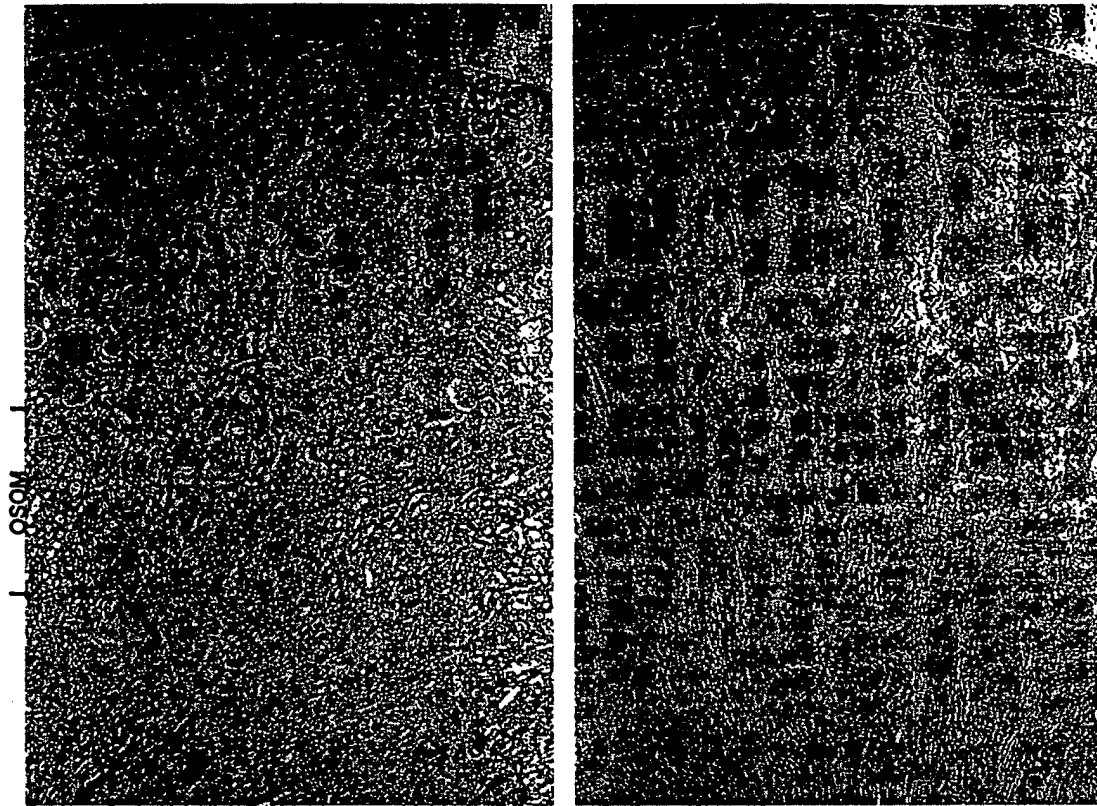


Fig. 3. Morphological damage and cellular infiltration at S3-nephron segment. Left, outer stripe of outer medulla (OSOM) and medullary rays are the zones of most severe injury (PAS staining) and proliferation (PCNA staining) (at day 2 post-I/R). Right, OSOM and medullary rays are also the zones of most important leukocyte infiltration (OX-1 pan leukocyte staining) (at day 10 post I/R). (Arrow, medullary rays).

regeneration appeared and they reached a maximum at day 3, together with a maximum of PCNA positivity. The characteristics of this early regeneration consisted of small non-differentiated cells with strong PCNA-positive nuclei, localized on the basement membrane of the proximal tubule and the thick ascending limbs (score 5). The following days, the volume of the cytoplasm of these cells increased (score 6), until finally the brush border recovered (back to score 0). The amount of PCNA-positive cells decreased in time and returned to baseline from the 5th day onwards. At the end of the investigated period (day 10), half of the proximal tubules were regenerated completely.

Interstitial leukocytes (Figure 5)

In the non-ischaemic group, no increase in number of interstitial leukocytes (OX-1 staining) could be seen within the study period of 10 days. Ischaemia of a unique kidney resulted in a gradually increasing interstitial leukocyte infiltrate in the OSOM during the 10 days investigation period. At day 10, the interstitial infiltrate was quite prominent ($\text{OX-1}_{\text{ischaemia}} = 1733 \pm 10 \text{ cells/mm}^2$).

ED-1 staining (monocytes/macrophages)

As early as 24 h after I/R injury, an increased number of monocytes (ED-1 positive cells) was found in the renal interstitium ($119 \pm 46 \text{ cells/mm}^2$ vs controls = $20.9 \pm 7.3 \text{ cells/mm}^2$ ($P < 0.05$)). Five days after the ischaemic event, a peak of ED-1 positive cells occurred ($1034 \pm 161 \text{ cells/mm}^2$ vs controls = $18.4 \pm 18.4 \text{ cells/mm}^2$ ($P < 0.05$)).

W3/25 staining (CD4^+ molecule)

A lymphocytic infiltration occurred from day 5 on in the ischaemic group, and persisted after 10 days.

OX-8 staining (CD8^+ molecule)

The outer stripe of the outer medulla contained only a small but significant number of CD8^+ cells, entering the ischaemic kidney at the 3rd day ($35 \pm 6.76 \text{ cells/mm}^2$ vs controls = $6.8 \pm 8.05 \text{ cells/mm}^2$ ($P < 0.05$)) and persisting until day 10.

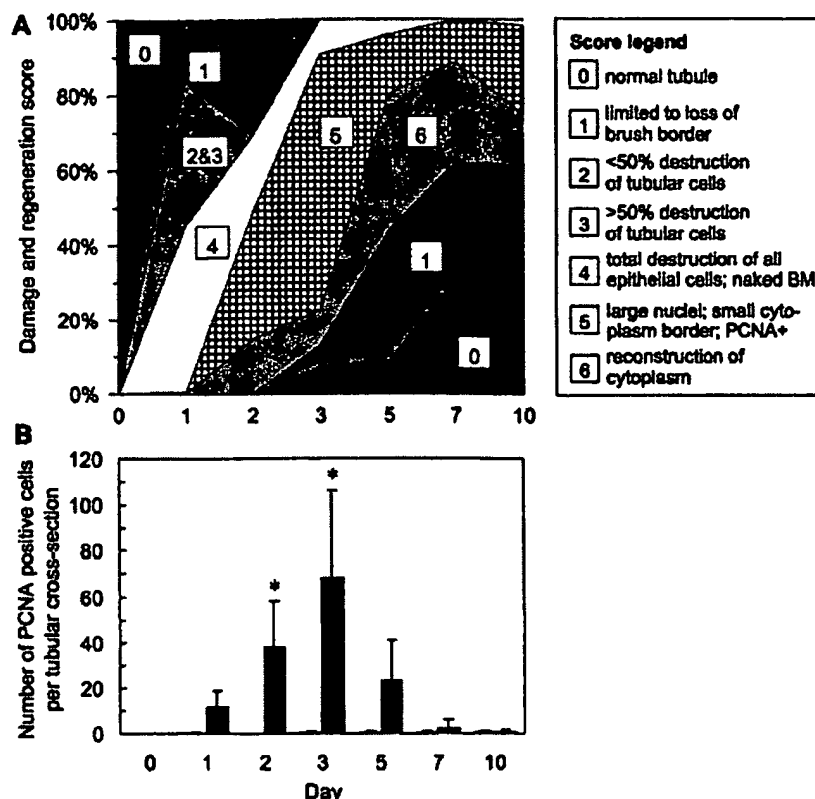


Fig. 4. (A) Renal damage and regeneration. semiquantitative score of damage (score 1–3) and regeneration (score 4–6). (B) Number of PCNA-positive cells (per circular-shaped tubular cross-section) (* $P < 0.05$).

OX-33 staining (B-cells)

The spleen section was clearly positive for B-cells. Neither the control kidney nor the ischaemic kidney contained B-cells.

Early staining of PMNs vs monocytes/macrophages: analysis of 0–24 h (Figure 6)

In all segments only scarce neutrophils (H&E staining) could be noticed at the early phase after the I/R injury, not significantly different from controls (OSOM, 8.37 ± 7.68 cells/mm² vs controls = 2.41 ± 2.84 cells/mm²; medullary rays, 2.50 ± 2.02 cells/mm² vs controls = 2.47 ± 2.16 cells/mm²; cortex, 4.73 ± 1.90 cells/mm² vs controls = 2.91 ± 2.34 cells/mm²). The few neutrophils that were noted were mainly located in the peritubular capillaries. As mentioned above, the number of monocytes/macrophages increased steadily with time, mainly in OSOM, and after 24 h was 12 times higher than the number of neutrophils present.

MPO assessment of rat post-ischaemic kidney during the first 24 h post-I/R (Figure 6)

MPO activity was expressed as the percentage of levels in kidneys subjected to sham surgery (=100%). MPO activity is already significantly increased after 1 h post-I/R ($439 \pm 34\%$, $P < 0.005$), reaching its maximum activity after 12 h of I/R ($1159 \pm 138\%$, $P < 0.0005$). However, kidney function, measured by S-creatinine, starts to be impaired after 6 h.

Identification of infiltrating cells (Figure 7)

ED-1 staining on peripheral blood smear and kidney sections

The ED-1 staining of peripheral blood monocytes showed ED-1-positive granules in the cytoplasm, whereas neutrophils and lymphocytes are negative for ED-1. Haematoxylin staining on a kidney section of a pyelonephritis kidney showed massive presence of intratubular PMNs, negative for ED-1 staining (data not shown).

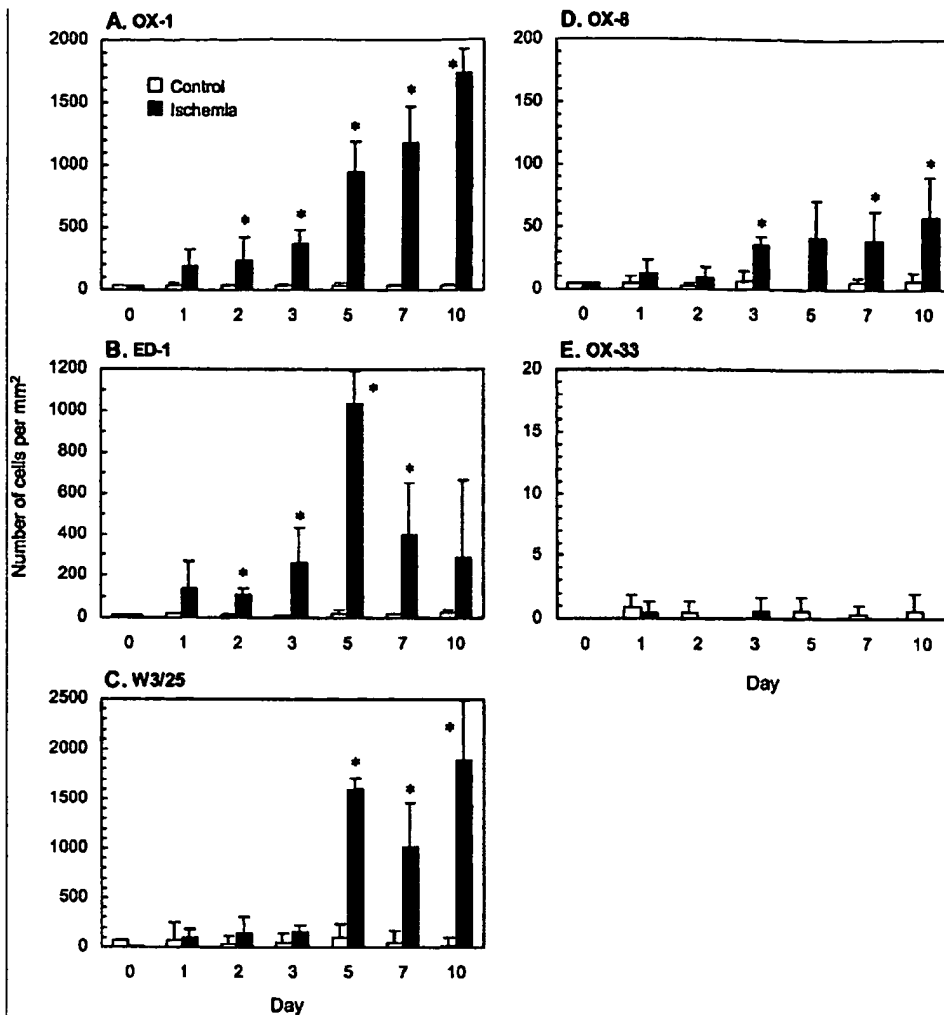


Fig. 5. Renal interstitial infiltrate, expressed as number/mm². OX-1, pan-leukocytes; ED-1, macrophages; W3/25, CD4⁺ helper T-cells; OX-8, suppressor/cytotoxic T-cells; OX-33, B-cells. Dark bars, post-ischaemic animals, after 60 min warm ischaemia on remaining left kidney. Light bars, controls without ischaemia (* $P < 0.05$).

ED-1 staining on cryosections in combination with MPO-staining

Figure 7A shows MPO staining of ED-1-positive cells, indicating that macrophages, like neutrophils, stain for MPO. By performing the staining procedure as described above but without incubation with the primary ED-1 mAb, no positive staining was observed, indicating no aspecific binding of the secondary mAbs and the avidin-biotin complexes, or residual MPO activity.

ED-1 staining on cryosections in combination with chloroacetate staining

Figure 7B shows naphthol AS-D chloroacetate esterase staining of ED-1-positive cells, which shows that

macrophages, like neutrophils, stain with chloroacetate. By performing the staining procedure as described above but without incubation with the primary ED-1 mAb, no positive staining was observed, indicating no aspecific binding of the secondary mAbs and the avidin-biotin complexes, no residual activity of the endogenous peroxidase activity.

HIS-48 (granulocytes) in combination with ED-1

Figure 7C shows that ED-1-positive cells (macrophages) also stain for HIS-48. Different control experiments were performed (data not shown): first, by performing the double-staining procedure as described above but without incubation with the anti-ED-1 FITC mAb, no positivity was observed, indicating no

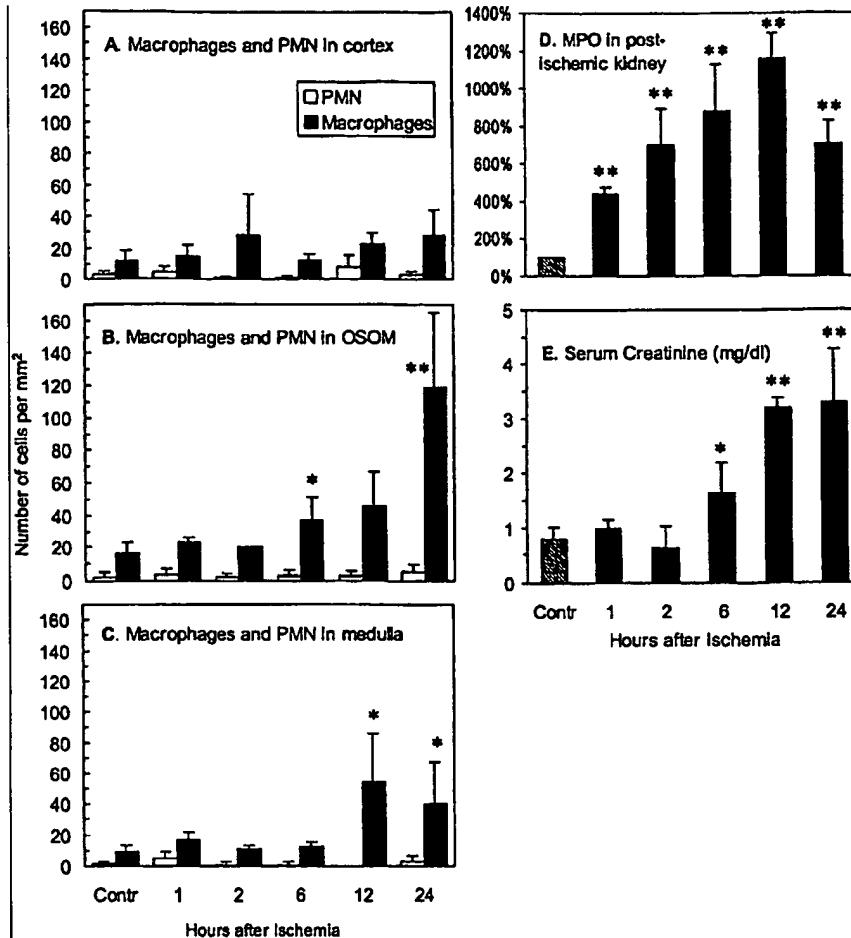


Fig. 6. Relationship of monocytes/macrophage and neutrophils adhesion/infiltration in cortex, OSOM and medulla, in relation to whole kidney MPO-activity and renal function (S-creatinine) during the first 24 h post-I/R. Left, Dark bars, number of monocytes/macrophages/mm². Light bars, number of PMNs/mm². Right, MPO activity in post-ischaemic kidney (dark bars), normalized to protein content of the supernatant, expressed as the percentage of levels in kidneys subjected to sham surgery (striped bar). Serum creatinine (mg/dl) of post-ischaemic animals (dark bars), vs controls without ischaemia (striped bar) (** $P < 0.01$; * $P < 0.05$).

aspecific binding of the second staining procedure. However, the ED-1 itself might bind with parts of the primary staining procedure. Therefore, a second control staining was performed by a double-immunohistochemical staining combining mAb against α -SMA in the first staining with ED-1 FITC in the second staining. The typical pattern of peritubular and periglomerular α -SMA staining and also that in the walls of large blood vessels is different from the typical interstitial pattern of macrophage staining. If in our control staining ED-1 should bind non-specifically to the secondary biotinylated horse anti-mouse antibody of the first staining, the ED-1 staining would have had the staining pattern of α -SMA, which was not the case. Hence the secondary staining for ED-1 was specific for the monocyte/macrophage cell type. In order to exclude aspecificity or decreased activity of a FITC-

labelled antibody, a control staining was performed by combining the ED-1 in the first staining with the ED-1 FITC-labelled antibody in the second staining. Not surprisingly, although less intensive, all cells positive for ED-1 were also positive for the FITC-labelled antibody.

Labelling of rat peripheral blood cells with mAb HIS48 (Figure 8)

The HIS-48-labelled subsets were sorted according to a selection procedure based on fluorescence intensity in a negative, a weakly positive, and a strongly positive subpopulation. In these weakly and strongly HIS-48-labelled subsets the nuclear morphology was analysed and the distribution of lymphocytes,

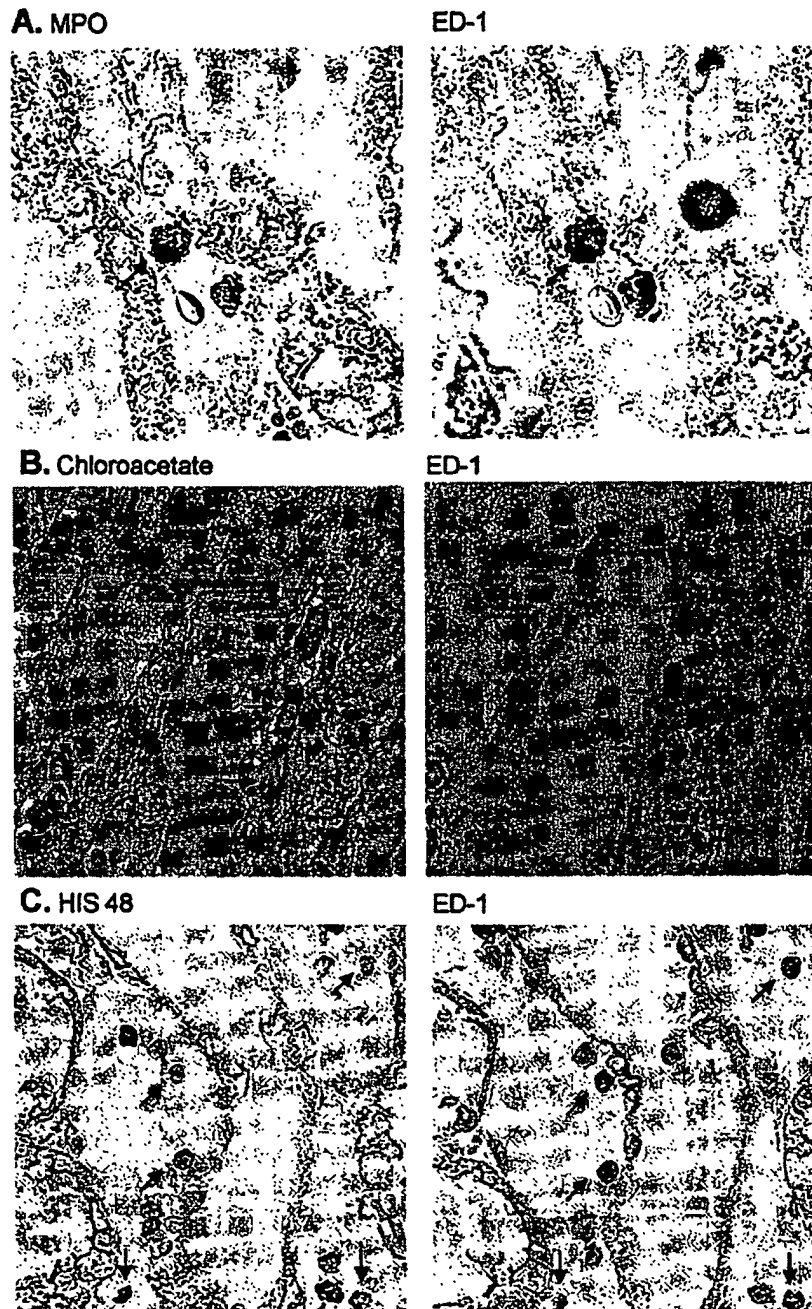


Fig. 7. MPO, chloroacetate and HIS-48 reactivity of macrophages. (A) *ED-1* staining on cryosections in combination with MPO staining. MPO staining of ED-1 positive cells, showing that macrophages are also able to produce MPO (like PMNs). (B) *ED-1* staining on cryosections in combination with chloroacetate staining. Chloroacetate staining of ED-1-positive cells, showing that macrophages are able to produce chloroacetate (like PMNs). (C) *HIS-48* in combination with *ED-1*. ED-1-positive cells (macrophages) also stain for HIS-48.

monocytes, and PMNs was counted. The most strongly HIS-48-labelled cells were identified as monocytes/macrophages, while the weakly labelled cells were identified as PMNs.

Discussion

Renal ischaemia/reperfusion injury is a major cause of ARF in the native as well as in the transplanted organ,

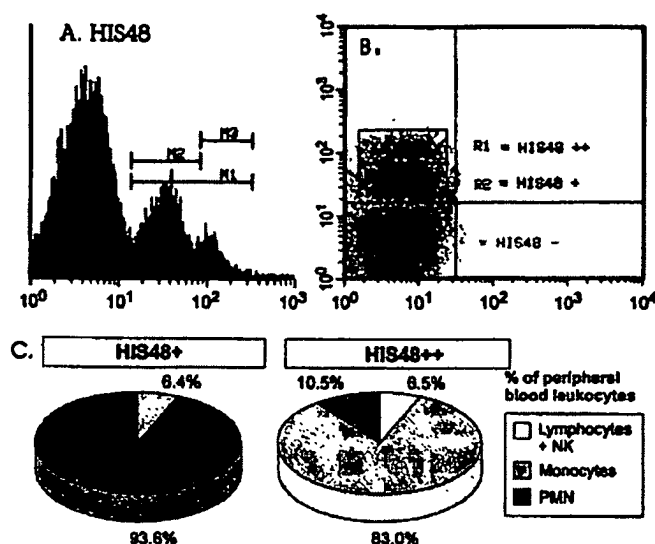


Fig. 8. Labelling of rat peripheral blood cells with mAb HIS-48. (A) Flow cytometric labelling of peripheral blood cells with mAb HIS-48 shows cell in a wide intensity range (M1) but especially a weakly and a strongly (M3) labelled cell subset. (B) These labelled subsets were sorted according to a selection procedure based on fluorescence intensity. (C) Analysis of nuclear morphology reveals a majority of PMNs in the weakly HIS-48 labelled subset and a majority of monocytes in the strongly HIS-48 labelled subset.

and is associated with a high mortality and morbidity. There is no specific treatment for this devastating clinical syndrome, reflecting, in part, the relatively poor understanding of the disease pathophysiology [1]. Leukocyte adhesion/infiltration and *in situ* proliferation in response to I/R injury is a well-known but ill-defined phenomenon. Sublethal damaged epithelial cells in proximal tubules and thick ascending limbs have the capacity of liberating chemotactic substances [33] which, through upregulation of adhesion molecules at the site of endothelial cells, may facilitate a leukocyte adhesion/infiltration, the role of which in injury or in the regeneration process after I/R is still not clarified.

The presence of these leukocytes, particularly of neutrophils, is generally considered as a damaging event, exacerbating I/R damage [17]. Recent experiments that interfere with leukocyte activation and adhesion/infiltration (mAbs to ICAM-1 and/or LFA-1, ICAM-1 antisense oligonucleotides, etc.) have shown that the kidney can be functionally protected against post-I/R injury [7,34]. On the other hand, phagocytes are also regarded as important scavengers of apoptotic cells or necrotic debris, and their presence in the kidney following I/R injury could alternatively represent a repair process [1]. Yet these infiltrating inflammatory cells may be a source of growth-stimulating substances [35], implying a role in the repair process after ARF [36–38].

Although many data are available concerning the overall cellular infiltrate after injury, only scarce information is available on the careful identification and time course of the different subsets of these adhering/infiltrating and proliferating leukocytes [5]. Recently, a mixed mononuclear cell (macrophage and

CD4⁺ cell) infiltration of the kidney, within a few days after I/R, was described after 45 min warm ischaemia [39] and after experimental cold ischaemia [40], with limited information, however, as to its exact topographical localization and kinetics. In the latter and many other studies, no important neutrophilic infiltration was mentioned, while even very recently, others, using enzymatic tests and membrane markers described mainly neutrophilic adhesion/infiltration [12,13,21,34]. These findings underscore discussion in the literature concerning the number and role of neutrophils after renal I/R. Our results contribute to the unravelling of this controversy.

First, during the first 24–48 h the detailed identification and quantification of the interstitial leukocytes in the rat kidney after severe warm I/R injury showed a pronounced acute tubular necrosis, with only a moderate monocyte/macrophage infiltration and proliferation. It is important to stress that the decrease in body temperature from 37°C to 28°C during anaesthesia and surgery might change kinetics and other properties of the cellular infiltrate, especially at early time points after ischaemia. Despite there being no significant increase of PMNs (identified by routine H&E staining) and the slightly increased monocytes/macrophages (ED-1 staining) during the first 12 h, the MPO activity, generally related to presence of PMNs [7,9,30,31], was significantly increased in the first hours post-ischaemia. This early (1 h) to maximal (12 h) MPO activity of the post-ischaemic kidney remains to be explained in the absence of significant increased number of inflammatory cells. It could be argued that PMNs and monocytes/macrophages do not infiltrate early after reperfusion but only adhere long enough to the activ-

ated endothelium to release their enzymes (like MPO) and to interfere with microcirculation with blockage of the vascular flow in the capillary network ('no reflow') [41,42], followed by re-entry to the circulation ('hit-and-run' phenomenon). In this respect, MPO activity reflects in fact more the activation of the adhering inflammatory cells and eventual of residential interstitial macrophages, resulting from post-ischaemic chemotactic and other cytokine activation, rather than infiltration itself. After this first critical period of 24 h, the number monocytes/macrophages was 12–25 times higher than the scarcely present PMNs, which remained comparable to control values. This indicates that firm adhesion and diapedesis has taken place, generating the classical infiltration and proliferation observed in many conditions (ischaemia, HgCl_2 , obstruction, etc.). It could be suggested therefore that the immediate beneficial functional effect of anti-adhesion therapy with for example antibodies to ICAM-1 and LFA-1, has to be explained at the level of early intravascular (microcirculation) leukocyte activation, and adhesion, but not at the level of the interstitial infiltration, which appears slightly later, at a time when the functional recovery is already operational.

Secondly, we could demonstrate that MPO activity is not a specific measure of PMN presence, since MPO content of post-ischaemic tissue reflects not only presence of PMNs but at least also of monocytes/macrophages and/or of activated residential interstitial macrophages [30,43,44]. In addition, by combined histochemical and immunohistochemical methods, we could demonstrate naphthol AS-D chloroacetate esterase activity in macrophages, present in the renal interstitium after I/R. Again, the latter staining is extensively used as specific for PMNs [10,12,21]. Finally, staining of ED-1 (specific for macrophages) followed by HIS-48, a monoclonal antibody considered to be specific for polymorphonuclear cells, showed that macrophages also react with mAb HIS-48. Flow cytometric analysis of circulating white blood cells demonstrating the high affinity of macrophages for the anti-HIS-48 antibody, supported this result. Hence, none of the so-called cell-specific stainings for PMNs have proved to be specific for this particular cell type, and cross-react with monocytes/macrophages. The H&E staining (morphology of cell nucleus) remains the gold standard for identification of PMNs. MPO assays or chloroacetate esterase stainings should be regarded as tools to quantitate both PMNs and monocytes/macrophages. These observations explain the long lasting and frequently observed dissociation between the use of H&E staining vs enzymatic and/or membrane markers in the identification in the number of neutrophils [1,45].

Three days post-I/R, functional recovery starts, at the moment of maximum tubular cell proliferation. Only later, after 5–10 days, the mononuclear infiltrate becomes quite prominent, consisting of a sequential accumulation and proliferation of monocytes/macrophages and helper T-cells, a few suppressor/cytotoxic T-cells and no B-cells. These cells are most prominent at the site of maximal damage/regeneration, which is

the OSOM and medullary rays. The total number of adhering/infiltrating PMNs in the different nephron segments remained unchanged up to 10 days post-I/R, their absolute number in the interstitium remaining far beyond that of other inflammatory cells.

In conclusion, the non-specificity of the so-called neutrophil-specific identification methods (MPO-activity, naphthol AS-D chloroacetate esterase or mAb HIS-48 staining), cross-reacting with monocytes/macrophages, explains the controversy in the literature concerning the number of PMNs in post-ischaemic injury. The only reliable method to quantitate PMNs remains H&E staining. Twelve to 24 h after severe warm I/R renal injury, a pronounced acute tubular necrosis occurs in the absence of a marked cellular infiltrate, along with a striking increase of MPO activity. This important MPO activity in this very early critical post-ischaemia period most probably reflects the activation of the adhering inflammatory cells (PMNs and monocytes/macrophages). Only at the later time of regeneration a sequential infiltration/proliferation of monocytes/macrophages and T-cells becomes prominent. The total number of PMNs remained low during the first 10 days post-I/R. These observations underscore an early effect of the few activated neutrophils, associated with the higher number of activated monocytes/macrophages.

Acknowledgements. Our appreciation goes to Simonne Dauwe for excellent morphological slide preparation, Marleen Nysten for technical assistance with the animal experiments, Dirk De Weerd for the excellent illustrations, and K. Achten for his excellent operative skills. Also the critical appraisal of the morphology by N. Buysens is greatly appreciated. Part of this work was supported by a grant of the Fund for Scientific Research (FWO No 15.045.96N).

References

1. Rabb H, O'Meara YM, Maderna P, Coleman P, Brady HR. Leukocytes, cell adhesion molecules and ischemic acute renal failure. *Kidney Int* 1997; 51: 1463–1468
2. Brady H, Singer G. Acute renal failure. *Lancet* 1995; 346: 1533–1540
3. Shoskes DA, Halloran PF. Delayed graft function in renal transplantation: etiology, management and long-term significance. *J Urol* 1996; 155: 1831–1840
4. Bonventre JV. Mechanisms of ischemic acute renal failure. *Kidney Int* 1993; 43: 1160–1178
5. De Greef K, Ysebaert D, Ghielli M *et al*. Neutrophils and ischemia reperfusion injury. a review. *J Nephrol* 1998; 11, 3: 2–13
6. Thornton MA, Winn R, Alpers CE, Zhager RA. An evaluation of the neutrophil as the mediator of *in vivo* renal ischemia-reperfusion injury. *Am J Pathol* 1988; 135: 509–515
7. Kelly KJ, Williams WW, Colvin RB, Bonventre JV. Antibody to intercellular adhesion molecule 1 protects the kidney against ischemic injury. *Proc Natl Acad Sci USA* 1994; 91: 812–816
8. Klausner JM, Paterson IA, Goldman G *et al*. Postischemic renal injury is mediated by neutrophils and leukotrienes. *Am J Physiol* 1989; 256: F794–802
9. Kelly KJ, Williams WW, Colvin RB *et al*. Intercellular adhesion molecule-1-deficient mice are protected against ischemic renal injury. *J Clin Invest* 1996; 97: 1056–1063
10. Willinger CC, Schramek H, Pfaller K, Pfaller W. Tissue distribution of neutrophils in postischemic acute renal failure. *Virchows Arch B Cell Pathol* 1992; 62: 237–243
11. Paller MS. Effect of PMN depletion on ischemic renal injury. *J Lab Clin Invest* 1989; 133: 379–386

12. Chiao H, Kohda Y, McLeroy P, Craig L, Housini I, Star RA. α -Melanocyte-stimulating hormone protects against renal injury after ischemia in mice and rats. *J Clin Invest* 1997; 99: 1165-1172
13. Vukicevic S, Basic V, Rogic D *et al*. Osteogenic protein-1 reduces severity of injury after ischemic acute renal failure in rat. *J Clin Invest* 1998; 102: 202-214
14. VanGoor H, Fidler V, Weening J, Grond J. Determinants of focal and segmental glomerulosclerosis in rat after renal ablation. *Lab Invest* 1991; 64: 754-765
15. Linas SL, Wittenburg D, Parsons PE, Repine JE. Ischemia increases neutrophil retention and worsens acute renal failure: Role of oxygen metabolites and ICAM-1. *Kidney Int* 1995; 48: 1584-1591
16. Wellbourn CR, Goldman G, Paterson IS, Valeri CR, Shepro D, Hectman HB. Pathophysiology of ischemia reperfusion: central role of the neutrophil. *Br J Surg* 1991; 78: 651-655
17. Heinzlmann M, Mercer-Jones MA, Passmore JC. Neutrophils and renal failure. *Am J Kidney Dis* 1999; 34: 384-399
18. Lucchesia BR. Modulation of leukocyte-mediated myocardial reperfusion injury. *Annu Rev Physiol* 1990; 52: 561-576
19. Vollmar B, Menger MD, Glasz J, Leiderer R, Messmer K. Impact of leukocyte-endothelial cell interaction in hepatic ischemia-reperfusion injury. *Am J Physiol* 1994; G786-793
20. Hallenbeck JM *et al*. Polymorphonuclear leukocyte accumulation in brain regions with low blood flow during the early postischemic period. *Stroke* 1986; 17: 246-253
21. Chiao H, Kohda Y, McLeroy P, Craig L, Lina S, Star RA. α -Melanocyte-stimulating hormone inhibits renal injury in the absence of neutrophils. *Kidney Int* 1998; 54: 765-774
22. Finn WF, Fernandez-Repollet E, Goldfarb D, Iana A, Eliahou E. Attenuation of injury due to unilateral renal ischemia: delayed effects of contralateral nephrectomy. *J Clin Lab Med* 1984; 103: 193-203
23. Fried TA, Hishida A, Barnes JL, Stein JH. Ischemic acute renal failure in the rat: protective effect of uninephrectomy. *Am J Physiol* 1984; 247: F568-574
24. Sunderland CA, McMaster CR, Williams AF. Purification with monoclonal antibody of a predominant leukocyte-common antigen and glycoprotein from rat thymocytes. *Eur J Immunol* 1979; 9: 155-159
25. Dijkstra CD, Dopp EA, Joling P, Kraal G. The heterogeneity of mononuclear phagocytes in lymphoid organs. distinct macrophage subpopulations in the rat recognized by monoclonal antibodies ED1, ED2 and ED3. *Immunology* 1985; 54: 589
26. Bredieu RJ *et al*. Two subsets of rat T lymphocytes defined with monoclonal antibodies. *Eur J Immunol* 1980; 10: 609-615
27. Jefferies WA, Green JR, Williams AF. Authentic T helper CD4 (W3/25) antigen on rat peritoneal macrophages. *J Exp Med* 1985; 162: 117-127
28. Green JR. Generation of cytotoxic T-cells in the rat mixed lymphocyte reaction is blocked by monoclonal antibody MRC OX-8. *Immunology* 1984; 52: 253-260
29. Woollet GR, Barclay AN, Puklavec M, Williams AF. Molecular and antigenic heterogeneity of the rat leukocyte-common antigen and glycoprotein from rat thymocytes. *Eur J Immunol* 1985; 9: 168-173
30. Bradley PP, Priebe DA, Christensen RD, Rothstein G. Measurement of cutaneous inflammation: estimation of neutrophil content with enzyme marker. *J Invest Dermatol* 1982; 78: 206-209
31. Hillegass L, Griswold D, Brickson B, Albrightson-Winslow C. Assessment of myeloperoxidase activity in whole rat kidney. *J Pharmacol Methods* 1990; 24: 285-295
32. Leder LD. The chloroacetate esterase reaction. *Am J Dermatopathol* 1979; 1: 39-42
33. Luster AD. Chemokines—chemotactic cytokines that mediate inflammation. *N Engl J Med* 1998; 338: 436-445
34. Haller H, Dragun D, Miethke A *et al*. Antisense oligonucleotides for ICAM-1 attenuate reperfusion injury and renal failure in the rat. *Kidney Int* 1996; 50: 473-480
35. Humes H. Potential molecular therapy for acute renal failure. *Cleve Clin J Med* 1993; 60: 166-168
36. Safirstein E. Renal stress response and acute renal failure. *Adv Ren Replace Ther* 1997; 4: 38-42
37. Lieberthal W. Biology of ischemic and toxic renal tubular cell injury. role of nitric oxide and the inflammatory response. *Curr Opin Nephrol Hypertens* 1998; 7: 289-295
38. Fine LG, Ong AC, Norman TJ. Mechanisms of tubulointerstitial injury in progressive renal diseases. *Eur J Clin Invest* 1993; 23: 259-265
39. Takada M, Nadeau KC, Shaw GD, Marquette KA, Tilney NL. The cytokine-adhesion molecule cascade in ischemia/reperfusion injury of the rat kidney. Inhibition by a soluble P-selectin ligand. *J Clin Invest* 1997; 99: 2682-2690
40. Azuma H, Nadeau K, Takada M, Mackenzie HS, Tilney NL. Cellular and molecular predictors of chronic renal dysfunction after initial ischemia/reperfusion injury of a single kidney. *Transplantation* 1997; 64: 190-197
41. Yin M, Kurvers HAJM, Tangelde GJ, Booster MH, Buurman WA, Kootstra G. Ischemia reperfusion injury of rat kidney relates more to tubular than to microcirculatory disturbances. *Renal Failure* 1996; 18(2): 211-223
42. Bonventre JV, Colvin RB. Adhesion molecules and renal disease. *Curr Opin Nephrol Hypertens* 1996; 5: 254-261
43. Bos A, Wever R, Roos D. Characterisation and quantification of the peroxidase in human monocytes. *Biochem Biophys Acta* 1978; 525: 37-44
44. Heinecke JW, Li W, Daehnke HL, Goldstein JA. Dityrosine, a specific marker of oxidation is synthesized by the myeloperoxidase-hydrogen peroxidase system of human neutrophils and macrophages. *J Biol Chem* 1993; 268: 4069-4077
45. Rabb H, Postler G. Leukocyte adhesion molecules in ischaemic renal injury. kidney specific paradigms? *Clin Exp Pharmacol Physiol* 1998; 25: 286-291

Received for publication: 3.12.99

Accepted in revised form: 26.5.00

Reactive Oxygen Species (ROS)-induced ROS Release: A New Phenomenon Accompanying Induction of the Mitochondrial Permeability Transition in Cardiac Myocytes

By Dmitry B. Zorov,^{*†} Charles R. Filburn,[‡] Lars-Oliver Klotz,[‡] Jay L. Zweier,[§] and Steven J. Sollott^{*}

From the ^{*}Laboratory of Cardiovascular Sciences and the [†]Laboratory of Biological Chemistry, Gerontology Research Center, Intramural Research Program, National Institute on Aging, National Institutes of Health, and the [‡]Department of Medicine, Division of Cardiology and the Electron Paramagnetic Resonance Center, Johns Hopkins Medical Institutions, Baltimore, Maryland 21224; and the [§]Department of Bioenergetics, A.N. Belozersky Institute of Physico-Chemical Biology, Moscow 119899, Russia

Abstract

We sought to understand the relationship between reactive oxygen species (ROS) and the mitochondrial permeability transition (MPT) in cardiac myocytes based on the observation of increased ROS production at sites of spontaneously deenergized mitochondria. We devised a new model enabling incremental ROS accumulation in individual mitochondria in isolated cardiac myocytes via photoactivation of tetramethylrhodamine derivatives, which also served to report the mitochondrial transmembrane potential, $\Delta\Psi$. This ROS accumulation reproducibly triggered abrupt (and sometimes reversible) mitochondrial depolarization. This phenomenon was ascribed to MPT induction because (a) bongkreikic acid prevented it and (b) mitochondria became permeable for calcein (~620 daltons) concurrently with depolarization. These photodynamically produced "triggering" ROS caused the MPT induction, as the ROS scavenger Trolox prevented it. The time required for triggering ROS to induce the MPT was dependent on intrinsic cellular ROS-scavenging redox mechanisms, particularly glutathione. MPT induction caused by triggering ROS coincided with a burst of mitochondrial ROS generation, as measured by dichlorofluorescein fluorescence, which we have termed mitochondrial "ROS-induced ROS release" (RIRR). This MPT induction/RIRR phenomenon in cardiac myocytes often occurred synchronously and reversibly among long chains of adjacent mitochondria demonstrating apparent cooperativity. The observed link between MPT and RIRR could be a fundamental phenomenon in mitochondrial and cell biology.

Key words: mitochondria • redox • heart • nitric oxide • Ca^{2+} sparks

Introduction

Beyond a fundamental role in energy metabolism, mitochondria also play key roles in maintenance of cellular redox potential (1), Ca^{2+} homeostasis (2), and apoptosis (3). A central event in apoptosis is now known to be a phenomenon called the mitochondrial permeability transition (MPT)¹

(for review see references 4 and 5). In addition, mitochondria are both a major source of reactive oxygen species (ROS; reference 6) and a target for their damaging effects (7). Understanding the interplay among these roles and ROS in both normal and pathological conditions has led to renewed interest in mitochondrial function and the MPT.

Observed originally in isolated liver mitochondria (8), the MPT is a proteinaceous pore or megachannel resulting in permeability to ions and solutes up to ~1,500 daltons and collapse of the mitochondrial membrane potential ($\Delta\Psi$) (2, 4). Many agents or conditions have been shown to cause pore opening in isolated mitochondria, most notably high Ca^{2+} loading and various treatments that cause oxidative stress (2). In addition, the MPT is regulated by $\Delta\Psi$,

Address correspondence to Steven J. Sollott, Laboratory of Cardiovascular Science, Intramural Research Program, Gerontology Research Center, Box 13, National Institute on Aging, 5600 Nathan Shock Dr., Baltimore, MD 21224-6825. Phone: 410-558-8657; Fax: 410-558-8150; E-mail: sollotts@grc.nia.nih.gov

¹Abbreviations used in this paper: BA, bongkreikic acid; EPR, electron paramagnetic resonance; ETC, electron transport chain; MPT, mitochondrial permeability transition; RIRR, ROS-induced ROS release; ROS, reactive oxygen species.

H⁺, Mg²⁺, adenine nucleotides, NAD(P)H, and the redox state of critical protein thiols (9, 10).

Mitochondria and the MPT play major roles in cell death. Agents that block the MPT (cyclosporin A, bongkreic acid [BA]) block apoptosis (3, 11). Various oxidants stimulate whereas antioxidants inhibit apoptosis, suggesting a role for ROS as initiators or downstream mediators of apoptosis (12). In addition, mitochondrial proteins (certain caspases, an apoptosis-inducing factor, and cytochrome *c*) that are released upon irreversible MPT activation play major roles in apoptosis (3).

A role for the MPT in normal cell function has also been proposed, especially in the context of Ca²⁺ homeostasis. Physiological stimuli can result in increases in mitochondrial Ca²⁺ (for review see reference 13), coupling energy demand to ATP production (14) via activation of rate-limiting steps in the respiratory chain (15). As sequential pulses of Ca²⁺ could summate and produce an overload of mitochondrial Ca²⁺, the MPT might serve a physiological function to counteract this accumulation by serving as a fast reversible Ca²⁺ release channel (9). While Hunter and Haworth (8) initially observed MPT reversibility in suspensions of isolated mitochondria, a physiologic role for the MPT in the regulation of mitochondrial Ca²⁺ homeostasis remains speculative.

Because mitochondria are themselves the major intracellular sources of ROS production, together with the fact that ROS exposure and altered redox state can lead to the MPT, we hypothesized that under certain circumstances this biological system could become self-amplifying and unstable. Thus, we sought to understand how these mechanisms are related and controlled in intact cells. Use of confocal microscopy enabled the recent demonstration of MPT gating in isolated individual mitochondria that was inhibited by catalase (16), supporting causation by ROS. This technique has also been used to show opening of the pore in hepatocytes exposed to MPT inducers (17). We addressed the role of ROS during MPT induction using isolated adult cardiac myocytes, taking advantage of the rigid, lattice-like distribution of mitochondria suitable for high precision confocal line-scan imaging. We present a model of controlled, photoexcitation-induced ROS production within individual mitochondria in these intact cells that triggers MPT induction in a reproducible and frequently reversible fashion. We have also identified a novel phenomenon resulting from this ROS-triggering of the MPT, which we have termed "ROS-induced ROS release" (RIRR).

Materials and Methods

Cardiac Myocyte Isolation. Single cardiac myocytes were isolated from adult rats (2–4 mo old) by a standard enzymatic technique (18). Cells were suspended in Hepes-buffered solution containing (in millimoles per liter) 137 NaCl, 4.9 KCl, 1.2 MgSO₄, 1.2 NaH₂PO₄, 15 glucose, 20 Hepes, and 1.0 CaCl₂, pH 7.4, and stored at room temperature until use.

Confocal Microscopy. Myocytes were loaded with dyes for >20 min on a microscope stage, incubated in Hepes-buffered so-

lution (same composition as the storage solution) at 23°C, and imaged with a LSM-410 inverted confocal microscope using a Plan-Neofluar 63×/1.4N.A. oil immersion lens (Carl Zeiss, Inc.). Time scans were recorded from mitochondria arrayed along individual myofibrils in a multichannel line-scan mode with excitation at both 488 nm (for 2, 7-dichlorodihydrofluorescein diacetate [DCF], diaminofluorescein diacetate [DAF]-2, and calcein-AM) and 568 nm (for TMRE, TMRM [tetramethylrhodamine, methyl and ethyl ester, respectively], and MitoTracker® Red CMXRos; Molecular Probes, Inc.), collecting simultaneous fluorescence emission at 515–540 nm and >590 nm, respectively. Each image consisted of 512–1,024 line scans obtained at 2–230 Hz, each line comprising 512 pixels spaced at 0.050-μm intervals. The confocal pinhole was set to obtain spatial resolutions of 0.4 μm in the horizontal plane and 1.0 μm in the axial dimension. Some protocols were performed using 351 nm excitation, collecting 400–435 nm fluorescence emission, using a Zeiss c-apo 63×/1.3N.A. water immersion lens. Experiments were carried out at 23°C. Image processing was done using MetaMorph® software (Universal Imaging).

Determination of Glutathione. Total glutathione (GSH) and glutathione disulfide (GSSG) were measured with the 5,5'-dithiobis(2-nitrobenzoic acid) (DTNB)-GSSG reductase recycling procedure according to Anderson (19) with minor modifications. Glutathione concentrations were calculated in relation to the 5-thio-2-nitrobenzoate (TNB) formation kinetics of identically processed GSH and GSSG standards. For determination of GSSG, the samples were treated with 2-vinylpyridine before addition to the reaction mix. Protein was determined from the centrifuged cell lysate before acid precipitation (BioRad Protein Assay Kit).

Electron Spin Resonance. Electron paramagnetic resonance (EPR) spectra were recorded in a quartz flat cell with a Bruker ER 300 spectrometer operating at X-band with a TM₁₁₀ cavity using a modulation frequency of 100 kHz, modulation amplitude of 0.5 G, microwave power of 20 mW, and microwave frequency of 9.785 GHz. Photoactivation of solutions of TMRM (100 μM) in Hepes-buffered medium containing 5-diethoxyphosphoryl-5-methyl-1-pyrroline-*N*-oxide (DEPMPO; 10 mM) or 5,5-dimethyl-1-pyrroline-*N*-oxide (DMPO; 100 mM) inside the EPR cuvette was produced by exposure to light from a 300 W halogen projector bulb passed through a 546 nm center/10 nm FWHM band pass filter (Corion). Temperature of the specimen was maintained at 23°C.

Materials. TMRE, TMRM, calcein-AM, MitoTracker Red CMXRos, and DCF were purchased from Molecular Probes, Inc.; diethylmaleate (DEM), *N*-ω-nitro-L-arginine methyl ester (L-NAME) and oligomycin were from Sigma-Aldrich; 5-nitroso-*N*-acetylpenicillamine (SNAP), DAF-2, Mn(III)tetrakis (1-methyl-4-pyridyl)porphyrin pentachloride (MnTMPyP), 1,2-bis(ω-amino-5-fluorophenoxy)ethane-*N,N,N',N'*-tetraacetic acid tetra (acetoxymethyl) ester (BAPTA-AM), Ru360, and 6-hydroxy-2,5,7,8-tetramethylchroman-2-carboxylic acid (Trolox) were from Calbiochem; and BA was from A.G. Scientific, Inc. All other chemicals were of the purest reagent grade available.

Results

Spontaneous ROS Production at the Sites of Deenergized Mitochondria. Mitochondria in freshly isolated adult rat cardiac myocytes are normally arrayed in a three-dimensional "lattice" of parallel rows surrounding the contractile myo-

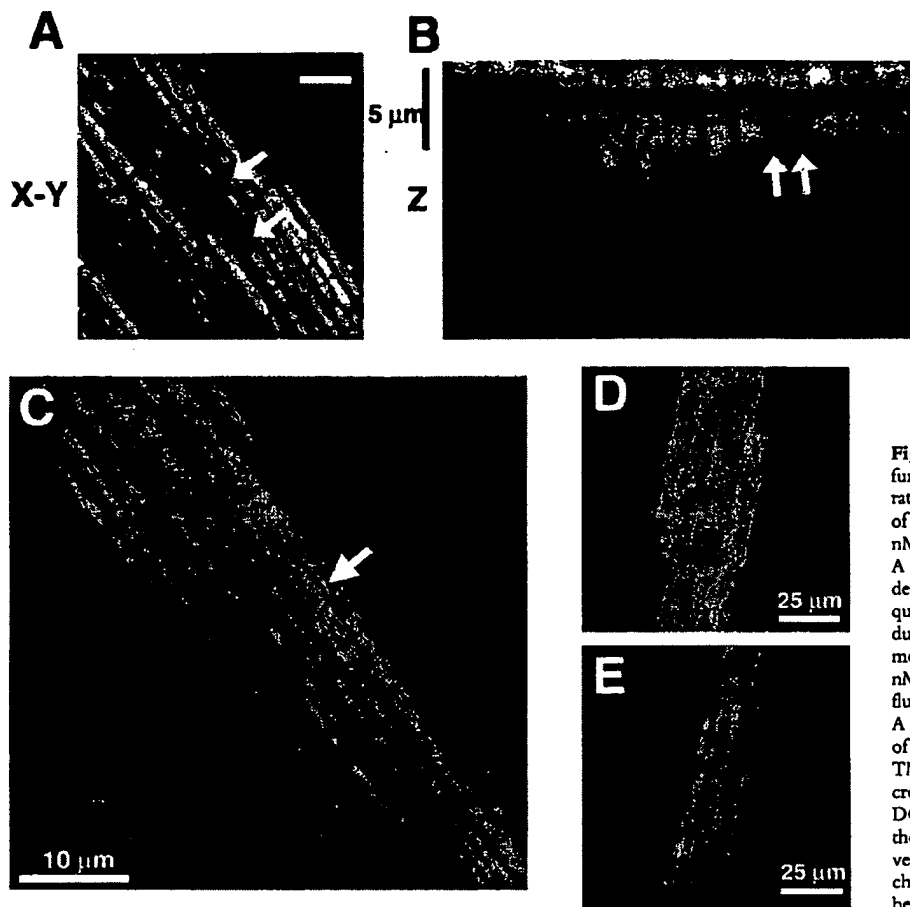


Figure 1. Spatial organization and function of mitochondria in isolated adult rat cardiac myocytes. (A) Confocal plane of a myocyte loaded with TMRM (125 nM; bar = 5 μ m). (B) z-section through A (1- μ m resolution). Arrows in A and B denote mitochondria lacking TMRM sequestration. (C) Spontaneous ROS production at sites of low mitochondrial membrane potential: red, TMRM (125 nM) fluorescence; green, DCF (10 μ M) fluorescence. (D) Exposure to antimycin A (25 μ M) produces widespread numbers of depolarized mitochondria (loss of red TMRM fluorescence) together with increased ROS production (increased green DCF fluorescence). (E) Pretreatment with the ROS scavenger Trolox (2 mM) prevents the antimycin A-induced mitochondrial depolarization seen in D (cell labeled with TMRM and DCF as in D).

filaments, as seen in cells loaded with the lipophilic cationic fluorophore TMRM accumulated by mitochondria in proportion to $\Delta\Psi$ (Fig. 1, A and B). Given the degree of TMRM concentration in mitochondria compared with all other cellular compartments, the extramitochondrial space appears black by contrast. Mitochondrial rows in the axial (or "z") dimension are sufficiently far apart (Fig. 1 B), so that confocal imaging with 1- μ m z-resolution would encompass a single mitochondrial thickness.

In TMRM-loaded cells, occasional discrete areas of the mitochondrial lattice lack fluorescence above background despite the (expected) presence of mitochondria (Fig. 1, A and B, arrows), suggesting that $\Delta\Psi$ has been locally dissipated. Hypothesizing that these deenergized mitochondria exhibit increased ROS production, these black "holes" in TMRM mitochondrial fluorescence were sought in cells dual-loaded with TMRM and the ROS-sensitive dye DCF. Fig. 1 C shows such a cell loaded with both TMRM (red) and DCF (green) in which a discrete area of two or three mitochondria have lost $\Delta\Psi$ (dark holes in red fluorescence; arrow) in precisely the same region in which increased DCF fluorescence is seen. This suggests that spontaneously deenergized mitochondria could produce significantly elevated levels of ROS, at least transiently.

The next series of experiments employs a novel method to study the relationship between mitochondrial $\Delta\Psi$ and ROS production in live cells.

ROS Triggers the Abrupt Loss of Mitochondrial $\Delta\Psi$ in Cardiac Myocytes. In the case of these spontaneously deenergized mitochondria, it was unclear whether local buildup of ROS caused or was the result of the loss of $\Delta\Psi$. Increasing endogenous ROS generation using the Complex III inhibitor antimycin A (25 μ M) produced widespread numbers of depolarized mitochondria with increased ROS production in cells loaded with both TMRM and DCF (Fig. 1 D). That this effect of antimycin A was prevented by the ROS scavenger Trolox (2 mM) provided further evidence that local ROS accumulation was likely involved in this loss of $\Delta\Psi$ (Fig. 1 E). As ROS are formed as a byproduct of photoexcitation, we set out to prove the causative role of ROS in this process by devising a laser excitation/confocal fluorescence imaging protocol using mitochondrially sequestered probes to follow $\Delta\Psi$ and simultaneously cause the incremental photoproduction and accumulation of ROS inside of specific mitochondria (Fig. 2 A). The line-scan (X-T) image in a TMRM-loaded cell, which displays how $\Delta\Psi$ varies with time in individual mitochondria by inspecting the fluorescence intensity along vertical columns

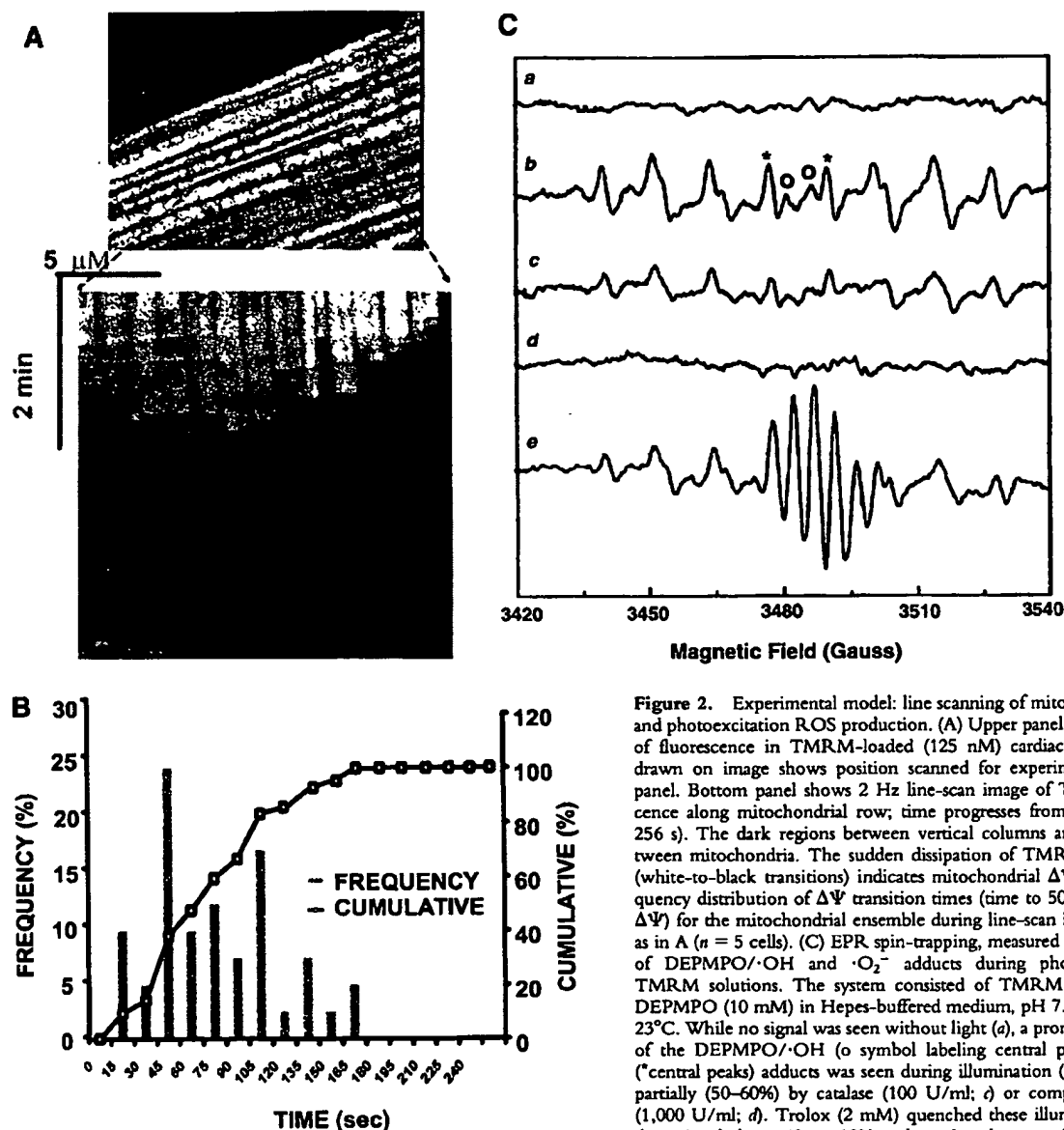


Figure 2. Experimental model: line scanning of mitochondrial arrays and photoexcitation ROS production. (A) Upper panel, confocal image of fluorescence in TMRM-loaded (125 nM) cardiac myocyte. Line drawn on image shows position scanned for experiment in bottom panel. Bottom panel shows 2 Hz line-scan image of TMRM fluorescence along mitochondrial row; time progresses from top (total scan 256 s). The dark regions between vertical columns are junctions between mitochondria. The sudden dissipation of TMRM fluorescence (white-to-black transitions) indicates mitochondrial $\Delta\Psi$ loss. (B) Frequency distribution of $\Delta\Psi$ transition times (time to 50% dissipation of $\Delta\Psi$) for the mitochondrial ensemble during line-scan imaging at 2 Hz as in A ($n = 5$ cells). (C) EPR spin-trapping, measured as the formation of DEPMPO/ $\cdot\text{OH}$ and $\cdot\text{O}_2^-$ adducts during photoactivation of TMRM solutions. The system consisted of TMRM (100 μM) and DEPMPO (10 mM) in HEPES-buffered medium, pH 7.4, maintained at 23°C. While no signal was seen without light (a), a prominent spectrum of the DEPMPO/ $\cdot\text{OH}$ (o symbol labeling central peaks) and $\cdot\text{O}_2^-$ ("central peaks") adducts was seen during illumination (b) and abolished partially (50–60%) by catalase (100 U/ml; c) or completely by SOD (1,000 U/ml; d). Trolox (2 mM) quenched these illumination-dependent signals by $\sim 60 \pm 10\%$ and produced a superimposed intense seven-line EPR signal of the Trolox-derived phenoxyl radical (e). Each spectrum is the sum of 24 1-min sequential acquisitions.

(time axis), shows a series of abrupt transitions (i.e., loss of fluorescence) in each mitochondrion, occurring at variable points during scanning (Fig. 2 A, bottom panel). This pattern of photoexcitation-induced $\Delta\Psi$ loss in TMRM-loaded cells is characterized by its mean occurrence time, which is typically between 60 and 90 s (Fig. 2 B). Photoexcitation of TMRM causes the production of both $\cdot\text{O}_2^-$ and $\cdot\text{OH}$ as measured by EPR spectroscopy (Fig. 2 C). Notably, Trolox is a potent scavenger of the ROS produced under these conditions.

ROS-induced $\Delta\Psi$ Loss Occurs Cooperatively and Reversibly. The typical pattern of ROS-induced $\Delta\Psi$ loss occurs synchronously, or "cooperatively," between mitochondrial

pairs along one sarcomere, with occasional higher order synchronization (Fig. 2 A). Infrequently, long-range synchronization between extended mitochondrial groups is observed (>30 mitochondria, over $\sim 35 \mu\text{m}$, < 500 ms; Fig. 3 A). Notably, this phenomenon remains synchronized during repeated episodes of $\Delta\Psi$ dissipation and, more interestingly, even during the spontaneous and abrupt recovery of TMRM fluorescence.

Clearly, large and abrupt changes in mitochondrial membrane permeability induced by ROS are responsible for these transitions. While these episodes of $\Delta\Psi$ loss often proceeded to the apparent complete loss of dye fluorescence, many examples were also observed of a step-wise

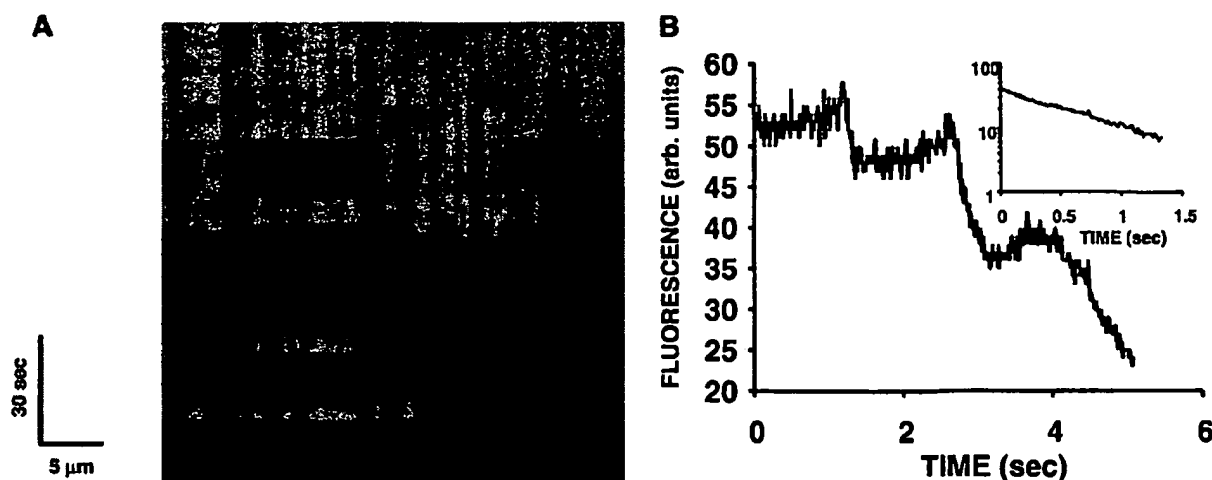


Figure 3. (A) Evidence of cooperativity and reversibility of $\Delta\Psi$ (TMRM) dissipation during 2 Hz line-scan imaging. (B) The abrupt dissipation phase of TMRM fluorescence during line-scan imaging can be described by first-order kinetics. In this example, the dissipation of $\Delta\Psi$ in a single mitochondrion occurs in step-wise fashion over several seconds. The inset shows all of the segments with negative slope (joined together; after background subtraction), fit by a single exponential model with $\tau_{1/2} = 0.54$ s.

progression by individual mitochondria (Fig. 3 B). This finding raises the question of whether this permeability phenomenon in general was the result of single or multiple conductance states. The inset in Fig. 3 B, using the data from this representative example, shows that each fluorescence segment (joined together) is well fit by a single exponential model. Indeed, an apparent single-state conductance behavior appears to be a general result, because first-order TMRM efflux kinetics described by the same rate constant (1.27 ± 0.12 s⁻¹) during MPT induction was consistently found in all of the cases examined ($n = 12$) regardless of step-wise or continuous progression.

RIRR in Single Mitochondria. Observing the spontaneous occurrence of high local ROS production at the sites of deenergized mitochondria (Fig. 1 C), we sought to discover whether the loss of $\Delta\Psi$ induced by laser scanning would also be accompanied by increased ROS production. In cells dual-labeled with TMRM and DCF (Fig. 4), line-scan imaging induced $\Delta\Psi$ loss, but in addition, there was an obvious "ROS burst" in each mitochondrion beginning at the moment of $\Delta\Psi$ loss. ROS production proceeded in two distinct phases: the initial, slow rise due to the accumulation of photoexcitation-related ROS production, i.e., "trigger ROS," followed by the ROS burst, occurring simultaneously with $\Delta\Psi$ dissipation, due to apparent mitochondrial ROS production (Fig. 4 C). We have called this the "ROS-induced ROS release" (RIRR) phenomenon.

The example in Fig. 4 D demonstrates coordinated flickering of $\Delta\Psi$ (i.e., reversible loss and transient recovery of $\Delta\Psi$ as in Fig. 3 A) and RIRR in a single mitochondrion. Notably, that the mitochondrial ROS burst phase profile evolves virtually as the mirror image of $\Delta\Psi$ is not a fluorescence artifact related to some interaction of TMRM and DCF or of their excitation/emission characteristics (i.e., an "inner filter" effect), because RIRR can be demonstrated

even in the absence of TMRM by performing laser line scanning using DCF itself as the photosensitizing species (at >10-fold the excitation intensity needed for the ordinary fluorescence measurements, confirming the accompanying $\Delta\Psi$ loss by finding the dissipation of the 351 nm-excited fluorescence from NAD(P)H, signifying its oxidation; not shown).

Thus, a source of ROS is able to trigger a mitochondrial burst of ROS production. The next step was to prove that the source of the ROS burst involved the diversion of electrons from the electron transport chain (ETC). The redox state of NAD(P)H (indicating the redox state of Complex I) was measured simultaneously with $\Delta\Psi$ during the usual line-scan imaging protocol (minimizing 351-nm exposure both by maximal attenuation of laser energy together with alternating scans with that for TMRM). The oxidation of NAD(P)H lags seconds behind the $\Delta\Psi$ loss (Fig. 4 E), which is compatible with the time course of the ROS burst (representing single-electron donation to oxygen) and the cessation of normal flow of respiratory chain electrons. Furthermore, the ROS burst magnitude upon MPT induction is successively decreased with increasing exposure to the Complex I inhibitor, rotenone (0.1 and 1 μ M), at concentrations not affecting TMRM sequestration (Fig. 4 F), indicating that the ROS burst derives from the ETC. Neither deferoxamine nor bathophenanthroline (each 200 μ M) had any effect in these experiments (not shown).

Photodynamic Triggering of RIRR Does Not Depend on a Specific Sensitizing Fluorophore. Thus far, the photoexcitation of rhodamines or DCF have been shown to initiate the RIRR process. Additional experiments in cells dual-loaded with the chemically distinct, $\Delta\Psi$ -sensitive dye MitoTracker® Red CMXRos, together with DCF, yield the identical pattern of $\Delta\Psi$ loss and RIRR compared with that observed with the rhodamines (Fig. 5).

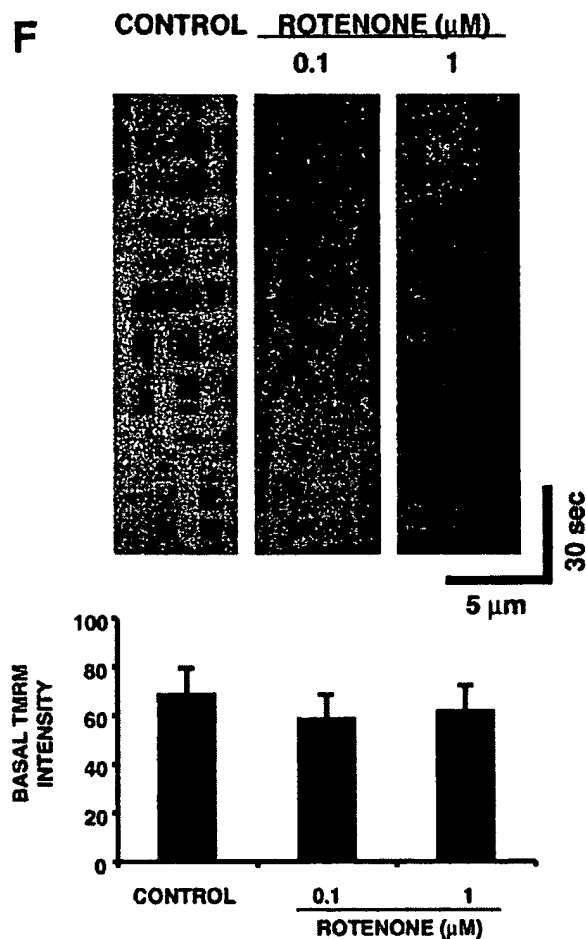
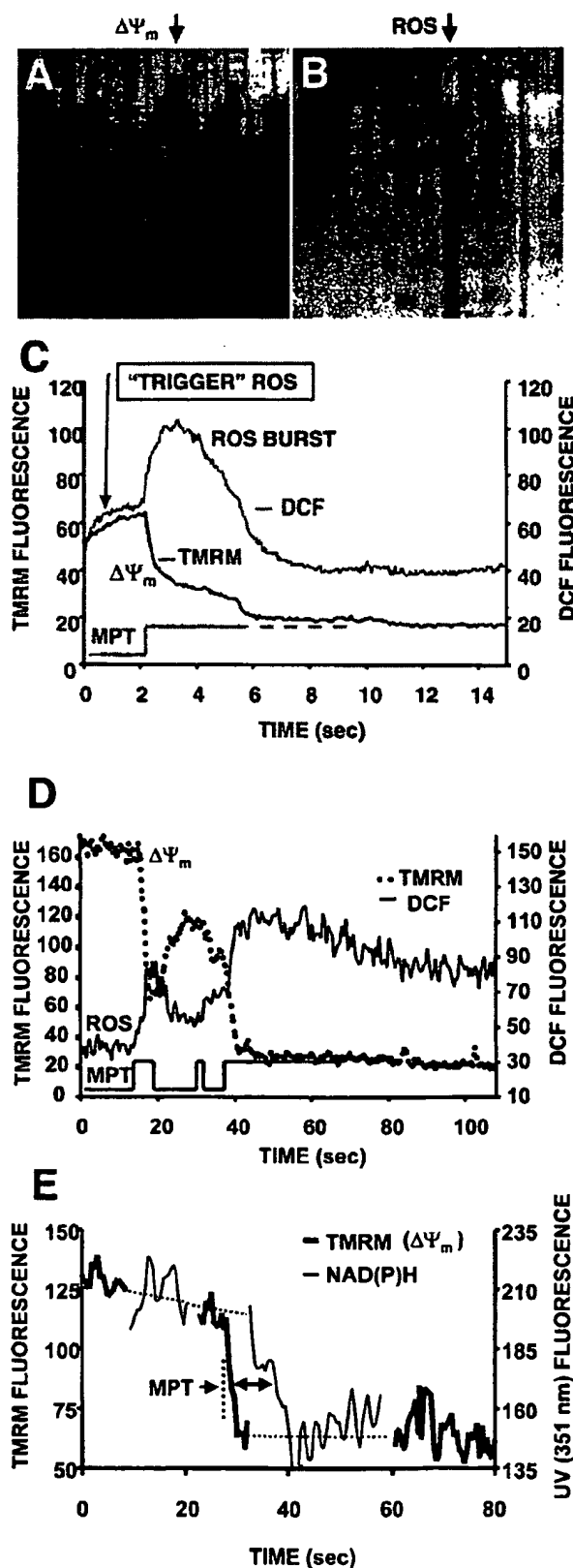


Figure 4. RIRR in single mitochondria. Representative cell that was dual-loaded with 125 nM TMRM (for $\Delta\Psi$) and 10 μM DCF (for ROS). (A) Typical pattern of $\Delta\Psi$ dissipation at 10 Hz line-scan imaging. (B) Generation of ROS, as indicated by the increase in DCF fluorescence (acquired simultaneously with A). (C) Temporal relationship between $\Delta\Psi$ and ROS production from the mitochondrial pair denoted by arrows in A and B. The trace at the bottom shows the hypothetical opening of the MPT pore. (D) Coordinated flickering of $\Delta\Psi$ and RIRR in a single mitochondrion at 2 Hz line-scan imaging. (E) Relationship between $\Delta\Psi$ and NAD(P) redox state during the MPT. $\Delta\Psi$ and the MPT are assessed by changes in the TMRM (125 nM) fluorescence and the intrinsic autofluorescence excited at 351 nm (index of NAD[P] redox state), respectively, during 2 Hz line-scan imaging. (F) Inhibition of mitochondrial electron transport at Complex I prevents the mitochondrial ROS burst after induction of the MPT. Cell loading with TMRM and DCF and line-scan imaging protocol, as in D, except for the exposure to rotenone (0.1 and 1 μM) as indicated. Representative regions (encompassing groups of about six mitochondria over three sarcomeres) from the respective 2 Hz line-scan protocols are shown from each experimental group (top panel).

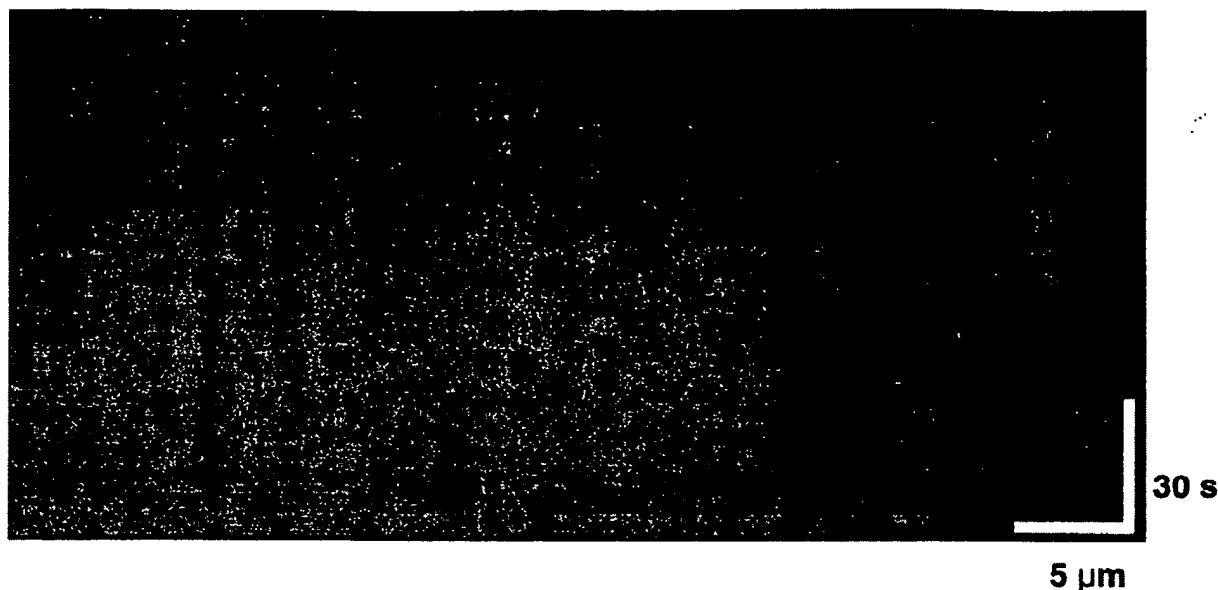


Figure 5. Triggering the RIRR process is not dependent on a sensitizing fluorophore. Cardiac myocyte dual-loaded with 400 nM MitoTracker Red CMXRos ($\Delta\Psi$, red signal) and 10 μM DCF (ROS, green signal); confocal line-scan imaging at 2 Hz.

RIRR Initiation Requires Simultaneous MPT Induction. Given the abruptness of $\Delta\Psi$ loss at the onset of RIRR, the most obvious candidate “pore” was the MPT, which allows nonspecific flux of molecules up to ~ 1.5 kD across the inner mitochondrial membrane. To test this possibility, cells were loaded with the acetoxymethylester derivative of calcein (a ~ 620 -dalton inert fluorescent marker), empirically resulting in a predominantly cytoplasmic compartmentalization. Using TMRM photoexcitation to induce RIRR in these cells, we observed that individual mitochondria accumulate calcein (as indicated by the increase of its mitochondria-localized fluorescence) at the moment that $\Delta\Psi$ loss occurs (Fig. 6 A).

We further confirmed that MPT induction not only occurred at the commencement of RIRR but was also required for its initiation altogether, by using the specific MPT inhibitor, BA (8). BA at low concentration (10 μM) partially inhibits the MPT and RIRR, while at high concentration (100 μM), MPT inhibition was virtually complete (Fig. 6, B and C). TMRM photoexcitation experiments using EPR demonstrated that BA (100 μM) has no significant ROS-scavenging activity (not shown). Exposure to cyclosporin A (ranging from 0.2 to 4 μM), however, had no effect on MPT induction (not shown). Although the MPT has been shown to be mediated by Ca^{2+} in other models, nevertheless, neither buffering intracellular Ca^{2+} with BAPTA-AM (15 μM) nor inhibiting the mitochondrial Ca^{2+} uniporter by Ru360 (6 μM) had any inhibitory effect in these experiments (not shown).

Scavenging Trigger ROS, or Exposure to Exogenous NO, Inhibits the MPT. To confirm that ROS triggered both MPT and ROS release, experiments were performed in the presence of 2 mM Trolox. Trolox treatment was found to

prevent $\Delta\Psi$ loss during laser line-scan imaging compared with control cells (Fig. 7 A). It is interesting to note that cells pretreated with the membrane-permeant superoxide scavenger Tiron (1–2 mM) or the superoxide dismutase (SOD) mimetics MnTBAP or MnTMPyP (500 μM each) failed to alter the ability to induce the MPT (not shown). Based on the fact that Trolox, but not the $\cdot\text{O}_2^-$ scavengers, prevented the MPT and RIRR, it is tempting to speculate that the important ROS species from the standpoint of MPT induction/RIRR is likely to be peroxide rather than $\cdot\text{O}_2^-$.

The oxidation of critical thiols, probably on the MPT itself, by ROS may be instrumental in MPT induction. Thus, S-nitrosylation of these critical thiols (i.e., via nitrosative stress) could alter their susceptibility to oxidative stress. In support of this notion, MPT induction was delayed by more than twofold in cells treated with 100 μM SNAP versus control (Fig. 7 A). Since the MPT was apparently stabilized rather than hastened by the SNAP treatment, it would seem that generation of peroxynitrite, a potent inducer of the MPT in isolated mitochondria, was minimal during the trigger stage.

Given the apparently protective role of exogenous NO against MPT induction in cardiac myocytes and the likelihood that endogenous production of NO in these cells could be playing important regulatory roles in excitation-contraction coupling (20, 21), we tested whether NO synthase inhibition would affect MPT induction. Pretreatment of cells with 1 mM L-NAME, which was associated with considerably increased variability of the times to MPT induction, nevertheless caused overall shorter times versus control (Fig. 7 A) and abolished spontaneous MPT reversal (not shown). The time course and localization of endoge-

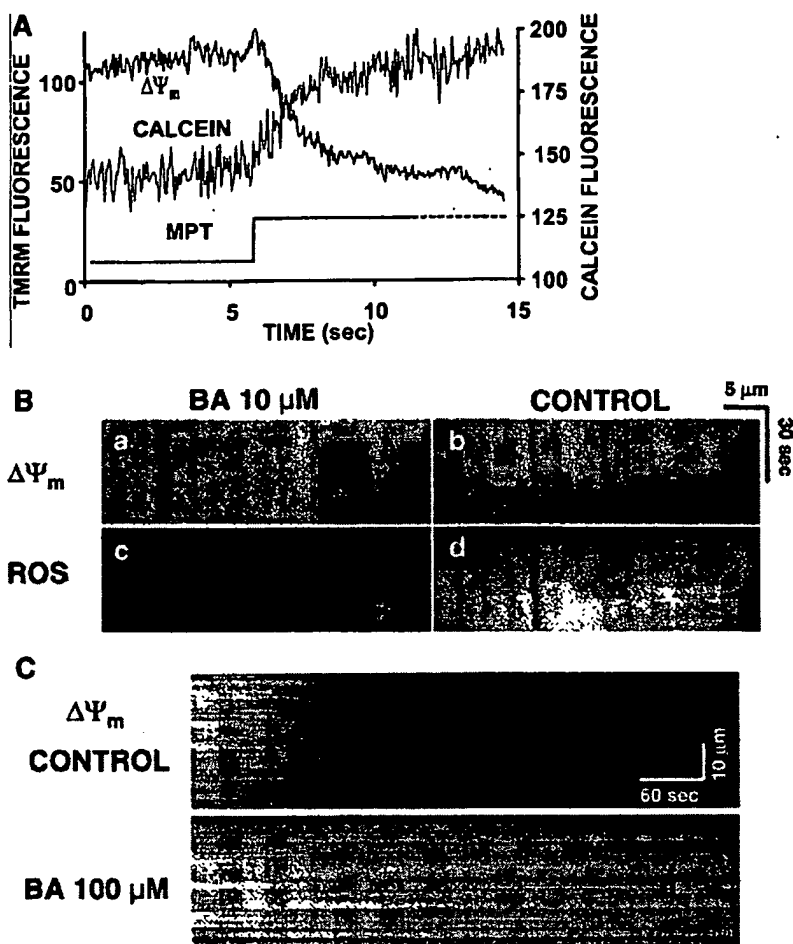


Figure 6. Demonstration of MPT induction by photoexcited trigger ROS. (A) Cells dual-loaded with TMRM ($\Delta\Psi$) and calcein-AM (the latter loaded under conditions that results in a cytosolic distribution initially in excess over that in mitochondria); line-scan imaging at 20 Hz. (B) 10 μ M BA partially inhibits the MPT ($\Delta\Psi$; a and b) and RIRR (ROS; c and d) versus control. Cells were dual-loaded with TMRM and DCF; line-scan imaging at 2 Hz. (C) 100 μ M BA completely inhibits the MPT versus control. Cells are loaded with 125 nM TMRM; line-scan at 2 Hz.

nous NO production in relationship to MPT induction was examined using cells loaded with DAF-2, which develops fluorescence upon reaction with NO. Fig. 7 B shows an increase of mitochondrial fluorescence in cells loaded with DAF-2 after MPT induction (suggesting that NO production has occurred in these areas) but with relatively slower kinetics compared with the ROS burst; the specificity of this phenomenon is demonstrated by the fact of its inhibition by L-NAME.

Altered MPT Characteristics due to Changes in Redox State of Soluble and Protein Thiols. The data so far suggest that when levels of triggering ROS accumulate past an apparent critical threshold, MPT induction occurs, precipitating the burst phase ROS generated by that particular mitochondrion. Assuming that MPT induction in these experiments resulted from the oxidation of critical protein thiols, and since glutathione is one of the primary redox buffer systems that defends protein thiols against oxidative stress, we examined how changes in this redox buffer induced by DEM exposure would affect MPT induction. Depleting cellular glutathione with 600 μ M DEM consistently shortened the MPT induction time by 50–60% (Fig. 8 A). At

higher concentrations, DEM is known to eliminate essential thiols (22) forming thioester adducts. Fig. 8 B shows a characteristic, unstable pattern of MPT flickering during scanning in a representative cell exposed to 5 mM DEM, with remarkably repetitive cycles of abrupt $\Delta\Psi$ loss and recovery that are clearly synchronized across large numbers of mitochondria.

Induction of Ca^{2+} Sparks after the MPT RIRR. This newly described RIRR phenomenon, though only seconds in duration, produces an apparently significant burst of local ROS that could have immediate consequences for the local cellular homeostasis. In particular, since oxidative and nitrosative stress can modulate the spontaneous activity of the ryanodine receptor (see reference 21), we examined the nature of Ca^{2+} spark activity in the “wake” of MPT induction. As shown in Fig. 9 in a representative cell dual-loaded with TMRM and the Ca^{2+} -sensitive dye fluo-3, there is frequently a period of significantly increased Ca^{2+} spark frequency at the z-lines (i.e., the site of the T tubule-sarcoplasmic reticulum junction) in the immediate vicinity of the mitochondrion shortly after MPT induction. Ordinarily, the spontaneous background (stochastic) event rate is about two

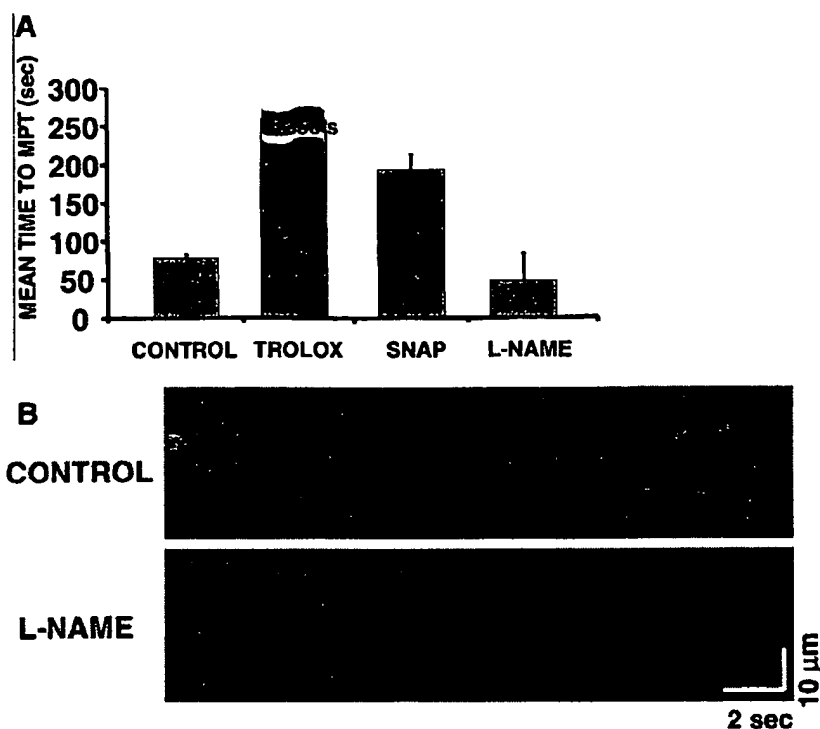


Figure 7. Scavenging the ROS trigger or exposure to exogenous NO inhibits the MPT. Cells loaded with 125 nM TMRM and confocal line-scan-imaged at 2 Hz. (A) Mean time to MPT induction in control versus pretreated cells as indicated: Trolox (2 mM); SNAP (100 μ M); L-NAME (1 mM). Data represent the average from 8–10 cells in each group. (B) Evidence of endogenous production of NO by mitochondria after MPT induction and inhibition by L-NAME (4 mM). Myocytes were loaded with 125 nM TMRM (red) and 10 mM DAF-2 (green) and line scanned at 100 Hz.

to three sparks per 100 μ m \cdot s. However, in proximity of the MPT (defined as within the sarcomere containing the involved mitochondria and within 3 s after MPT occurrence), the event rate approximately doubles to about five to six per 100 μ m \cdot s ($P < 0.05$; Fig. 9, inset). While ordinary background Ca^{2+} sparks are typically single events, the MPT-associated ones frequently occur as clusters, as seen in Fig. 9.

Discussion

We present a novel method to selectively expose arrays of mitochondria in isolated live adult cardiac myocytes to incremental doses of ROS by photoactivation of mitochondrial dyes while simultaneously recording functional mitochondrial parameters, including $\Delta\Psi$, ROS generation, NO production, permeability changes, and redox state.

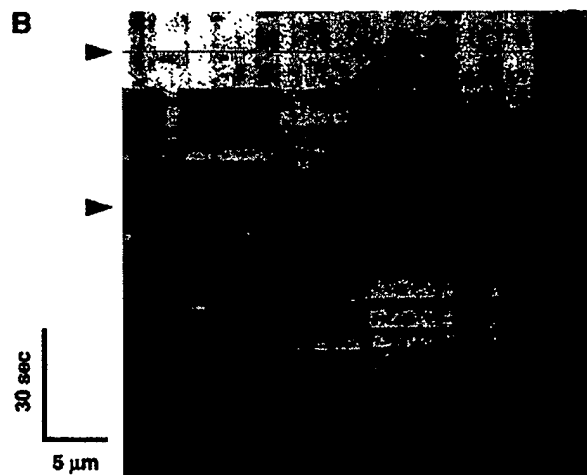
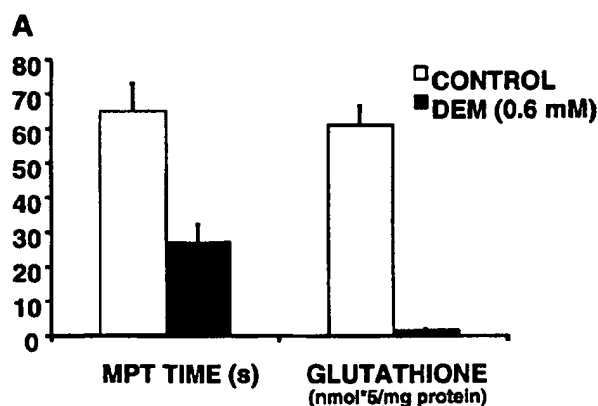


Figure 8. Altered MPT characteristics after modulation of the redox state of soluble and protein thiols. (A) Comparison of MPT times (during 2 Hz line-scan imaging in TMRM-loaded cells) and cellular glutathione content in control versus 600 μ M diethylmaleate-treated cells. (B) Development of apparent unstable MPT pore flickering during 2 Hz line-scan imaging in a representative TMRM-loaded (125 nM) cell exposed to 5 mM diethylmaleate. Arrows indicate movement artifacts.

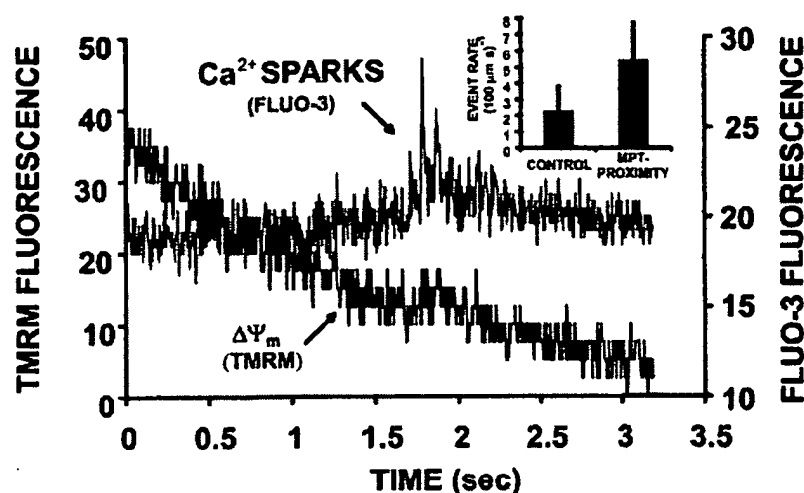


Figure 9. Induction of Ca^{2+} sparks after the MPT. Cell is dual-loaded with 125 nM TMRM ($\Delta\Psi$) and fluo-3 (Ca^{2+}) and line-scan imaged at 230 Hz. Representative example showing the dissipation of TMRM fluorescence from a single mitochondrion and a cluster of Ca^{2+} sparks in the immediate vicinity, within seconds of MPT induction. Inset: comparison of Ca^{2+} spark rate in proximity of MPT occurrence (i.e., within the sarcomere containing the involved mitochondria and within 3 s after MPT occurrence; $n = 90$ sparks) versus that at background ($n = 150$ sparks; $P < 0.05$).

This method of localized excitation causes generation of “triggering” ROS inside individual mitochondria, enabling us to demonstrate the induction of the MPT, and its spontaneous reversibility, in intact cells. The duration of exposure to the triggering ROS necessary to induce the MPT was dependent on the intrinsic ROS-scavenging ability of the cell, as MPT times were dependent upon the cellular glutathione content. We demonstrate that ROS specifically triggers the MPT, because ROS scavengers prevent it.

We term this new mitochondrial phenomenon “ROS-induced ROS release” (RIRR) by analogy to the phenomenon of “ Ca^{2+} -induced Ca^{2+} release” (23). Upon MPT induction, $\Delta\Psi$ rapidly dissipates, followed by a “burst phase” of ROS generated by that particular mitochondrion and lasting ~5–10 s (Fig. 4). Occasionally, contiguous mitochondria, in groups of at least 5–10, were observed to undergo synchronous cycles of both induction and reversal of the MPT (Fig. 3). These experiments also show that triggering ROS are not entirely sufficient for the development of burst phase ROS production by mitochondria. If the MPT is prevented with BA and $\Delta\Psi$ maintained indefinitely, then no burst phase occurs. Thus, it appears that trigger ROS induction of the MPT causes the mitochondrial ROS burst.

Photoinduction of the MPT RIRR process in mitochondria loaded with fluorescent probes is apparently due to the generation of photoproducts, probably originating from singlet oxygen ($^1\text{O}_2$) and $\cdot\text{O}_2^-$. $^1\text{O}_2$ is believed to be the primary ROS resulting from the energy transfer from the excited rhodamine molecule to oxygen (24), and this would be expected to induce lipid peroxidation (alkoxyl and peroxy radicals). $\cdot\text{O}_2^-$ is an effective oxidant itself but can also be transformed by dismutation into H_2O_2 , which, in the presence of Fe^{2+} , forms the strong oxidant $\cdot\text{OH}$ by the Fenton reaction (25). Indeed, we demonstrated by EPR that illumination of TMRM solutions produce $\cdot\text{O}_2^-$ and $\cdot\text{OH}$ signals that were suppressed by SOD or catalase, respectively, and scavenged by the α -tocopherol derivative

Trolox (Fig. 2 C). Furthermore, Trolox prevention of the MPT RIRR phenomenon argues for initiation by ROS.

As Trolox has a broad antioxidant capacity, we also performed experiments with other ROS scavengers with more selectivity. In contrast to the results with Trolox, the superoxide radical scavenger Tiron as well as the SOD mimetics MnTBAP and MnTMPyP were ineffective. This pointed to the likely importance of peroxide rather than $\cdot\text{O}_2^-$, and possibly the Fenton reaction, in our experiments. Not surprisingly, the impermeable antioxidant catalase (1,500 U/ml), which catalyzes the transformation of H_2O_2 into water and oxygen, was ineffective. In addition, the iron chelators deferoxamine and bathophenanthroline had no effect on the MPT induction, suggesting that Fenton chemistry may not be playing a significant role in induction of MPT RIRR. This suggests that peroxides (and possibly $^1\text{O}_2$) form the principal trigger ROS in our experiments. This is supported by the observation that catalase is effective in blocking $\Delta\Psi$ loss induced by excitation of TMRE-loaded, isolated mitochondria (16). However, it is possible that the lack of effect of deferoxamine might be due to its much higher affinity for Fe^{3+} compared with Fe^{2+} , which catalyzes the Fenton reaction, while bathophenanthroline is known to be poorly cell membrane permeable.

It would be reasonable to assume that these triggering ROS would eventually oxidize some critical protein targets, such as regulatory thiols (26), but that the cellular redox scavengers would tend to prevent this. Thus, it was important to establish that the soluble redox buffer capacity, principally GSH, would govern the characteristic delay between the trigger ROS onset and MPT induction/RIRR. This was confirmed using 0.6 mM DEM, which conjugates to nonprotein thiols (27) and caused both depletion of cellular GSH and the decrease in the time to MPT induction by 60% (Fig. 8 A).

Several independent lines of evidence lead to the conclusion that photoactivation-produced triggering ROS induces the MPT in cardiac mitochondria. First is the abrupt

collapse of $\Delta\Psi$ and its prevention by the ROS scavenger Trolox. Second, an otherwise membrane-impermeant fluorescent molecule, calcein (~ 620 daltons), originally present in the cytosol, enters mitochondria concurrently with the loss of $\Delta\Psi$ (Fig. 6 A). Third, inhibition of the transition by BA (Fig. 6 B), which inhibits the adenine nucleotide translocator (ANT) component of the pore and blocks the MPT (8).

Cyclosporin A ($0.2\text{--}4\ \mu\text{M}$) did not prevent the dissipation of $\Delta\Psi$ in our experiments. Although cyclosporin A is a powerful inhibitor of the MPT in isolated mitochondria, it is known to be ineffective in blocking it in some cell types and under different conditions. For example, in ischemia/reperfusion models with rat heart, the protective effect of cyclosporin A was observed over an extremely narrow concentration range (28). Also, mitochondrial signal peptides (29), butylated hydroxytoluene (30), and thyroxine (31) each induce mitochondrial permeability that is cyclosporin A insensitive.

Certain interesting MPT-related phenomena observed with this model provide mechanistic insights into the nature of the pore and of the communication between mitochondria. Although MPT induction was most typically observed as a synchronous event among mitochondria within a single sarcomere, certain higher levels of coordination were occasionally seen, involving mitochondria in several longitudinally adjacent sarcomeres (observed even beyond the length of 15 sarcomeres; Fig. 3 A). Given the distance and timing of this synchronization, it would seem that the signal coordinating such long-range MPT induction cannot plausibly be conveyed by a simple chemical-diffusive mechanism but rather must be transmitted along some electrical coupling ("cable") mechanism (32). Recently, the propagation of a mitochondrial "redox signal" was shown to occur both within single cardiomyocytes as well as from one cardiac cell to another, demonstrating both intra- and intercellular mitochondrial communications (33), but this is likely a different mechanism from that observed here.

One of the most important observations about the MPT from our experiments is that it can be spontaneously reversible. As with the pattern of synchronized pore openings, we observed synchronization of spontaneous MPT reversal among large mitochondrial groups (Fig. 3 A). This cyclical pattern of sequential induction and reversal of the MPT results in an apparent "flickering" mode of $\Delta\Psi$ that eventually becomes irreversible if the trigger does not cease. Reversibility of the MPT induced by photoactivation has also been observed in isolated heart mitochondria (16).

Our data also demonstrate that MPT induction can also occur in apparently halting, step-wise fashion, achieving intermediate stable levels without complete loss of the $\Delta\Psi$ -tracking dye fluorescence for several seconds at a time (Fig. 3 B). These observations raise the question of whether the MPT pore operates in a single conductance state or if there are multiple possible subconductance states. Studies on isolated mitochondria suggest that there are indeed different conductance states of the MPT (9, 10).

Our results in intact cells, however, suggest that the MPT pore most likely exhibits only a single open state and can flicker between the open and closed states. The regular structure of the cardiac myocyte and the confocal imaging conditions we used effectively limit the optical section to that of a single mitochondrion. Therefore, it is unlikely that separate and unrelated events from overlying/underlying planes of mitochondria (i.e., in the axial dimension) are "contaminating" the recording. As all of the $\Delta\Psi$ fluorescence decay segments during episodes of step-wise MPT progression (Fig. 3 B) can be described by the same first-order kinetic process (Fig. 3 B, inset), and, moreover, that all cells have the same rate constant of TMRM efflux during the MPT, the simplest explanation is that the MPT pore operates with a single open state conductance in the intact rat cardiac myocyte.

DEM at levels an order of magnitude higher than that needed to deplete glutathione (probably reacting with protein thiols [22]) yields a striking result: the MPT induction pattern becomes characteristically unstable with unusual repetitive cycles of abrupt $\Delta\Psi$ loss and recovery (Fig. 8). This suggests that the trigger ROS may target the same thiol moieties affected by this DEM exposure and possibly develops a certain dynamic "competition" between the formation of disulfide bonds and thioester adducts (of ethyl maleate) at the same critical target(s), each of which causes a protein conformational shift between the open and closed states (respectively) of the pore.

This concept that the competition of reactive species may determine the stability of the regulatory thiol redox state is further supported by the finding that pretreatment of cells with the spontaneous NO donor, SNAP, delayed MPT induction (Fig. 7). NO may interact with protein thiols via S-nitrosylation, a physiologically reversible modification that could alter the susceptibility to the SH/S-S transition, which is known to promote the MPT (4). In this case, NO could be regarded as a stabilizer of thiol groups against harsher oxidizing conditions (21). The overall role of NO in induction of the MPT and in apoptotic cell death is not at all clear, with seemingly contradictory data derived from studies on isolated mitochondria and different cell types (34–36). For example, NO has been shown to cause both induction of apoptosis through triggering the MPT (37, 38) as well as its inhibition at sites both upstream and downstream of cytochrome *c* release (39). Furthermore, NO \cdot has been shown to protect cardiomyocytes from oxidative damage induced by organic peroxides (40), whereas NO $^-$ is damaging in postischemic myocardial injury (41).

However, for cardiac cells, endogenous NO is likely to achieve micromolar levels in vivo, and, moreover, act in a beneficial manner as an essential modulator of excitation-contraction coupling (20, 21, 42) without causing apoptosis. The protection from MPT induction in cardiac mitochondria by SNAP demonstrated in our experiments supports this concept. Furthermore, our observation of a slow, L-NAME-sensitive rise of the fluorescence of the

NO-sensitive dye, DAF-2, inside mitochondria after induction of the MPT is compatible with a slow generation of NO in (or near) mitochondria after MPT induction (Fig. 7 B). Functionally, pretreatment of cardiac myocytes with L-NAME was associated with considerably increased variability of the times to MPT induction but overall with a tendency to shorter times (Fig. 7 A) and an absence of spontaneous MPT reversal versus control (not shown), suggesting that endogenous NO may contribute to some level of "protective" basal S-nitrosylation.

It would seem that there is a specific mechanistic link between MPT induction and RIRR, because other causes of rapid $\Delta\Psi$ loss (i.e., those not involving MPT induction) do not result in increased ROS production. In particular, exposure of cells to the mitochondrial uncoupler, carbonyl cyanide *p*-(trifluoromethoxy) phenylhydrazone (FCCP), which induces rapid $\Delta\Psi$ loss via induction of a large membrane proton leak, occurs without any rise of ROS production (not shown). Furthermore, as RIRR can be completely prevented by BA in spite of the prolonged exposure to the ROS trigger in this model, we concluded that MPT induction is obligatory for the ROS burst. It shows that ANT governs RIRR.

The mechanism(s) of the ROS burst accompanying the MPT remains unclear, although under ordinary conditions mitochondrial Complexes I and III are believed to be the major sources of ROS (43–45). Separate experiments presented here, (a) examining NAD(P)H oxidation and (b) using rotenone, indicate that the diversion of electrons from the respiratory chain provides the source of the ROS burst (Fig. 4, E and F). Given that trigger ROS cannot cause the ROS burst directly, it is tempting to speculate that occurrence of the MPT itself could change the properties of the phospholipid bilayer surrounding the major mitochondrial enzymes in the inner membrane, thus dramatically affecting their function. Indeed, MPT induction was found to alter the rigidity of the mitochondrial membrane, which could weaken protein–protein interactions necessary for proper function of the respiratory chain (46). If so, the ROS burst might be due to a block of the ETC caused by MPT induction.

The role of mitochondria in maintaining the cellular Ca^{2+} homeostasis is still under debate. In this connection, Bowser et al. (47) demonstrated that uncouplers or ETC inhibitors caused the progressive elevation of cytosolic $[\text{Ca}^{2+}]$ and the frequency of Ca^{2+} sparks. The latter represents the fundamental Ca^{2+} release process from the ryanodine receptor of the sarcoplasmic reticulum, which normally is triggered by Ca^{2+} influx through the adjacent sarcolemmal L-type Ca^{2+} channels and serves to couple electrical excitation to Ca^{2+} -mediated contraction in cardiac myocytes. In addition to this usual pathway, experiments here demonstrate that the ryanodine receptor also may be activated upon MPT induction (Fig. 9). Although it is possible that mitochondrial Ca^{2+} may contribute to Ca^{2+} spark formation (47), we also cannot exclude the possibility that such local Ca^{2+} release from sarcoplasmic reticulum may be driven by ROS generated in and released by

these adjacent mitochondria undergoing MPT induction (a "ROS-induced Ca^{2+} release" mechanism). Specifically, it has been demonstrated that the oxidation of free thiols on the cardiac ryanodine receptor can lead to its activation (21). A similar process of prooxidant-induced Ca^{2+} release has been discussed for mitochondria (48). At this point, we are unable to differentiate between the Ca^{2+} versus ROS induction models driving these Ca^{2+} sparks, because primary perturbations in mitochondrial Ca^{2+} efflux cannot readily be made without affecting underlying Ca^{2+} spark mechanisms, and paradigms involving scavenging ROS would prevent the induction of the MPT in the first place. Regardless of whether Ca^{2+} or ROS modulate this increase in Ca^{2+} spark frequency after MPT induction, this phenomenon could induce pathological disturbances in cardiac excitation and rhythm, for example, contributing to post-ischemic reperfusion arrhythmias.

We have identified a novel ROS-triggered phenomenon in mitochondria resulting from MPT induction, called "ROS-induced ROS release" in cardiac myocytes. Given the likely dramatic cellular consequences of ROS production seen in these experiments and its obligatory connection to the MPT, together with the fact that BA prevents both RIRR (this study) and apoptosis (11), it is tempting to speculate that these two phenomena are causally linked. Thus, the specific nature of the RIRR mechanism is probably fundamental, and we propose that it may be related to programmed mitochondrial destruction in cardiac myocytes as well as programmed cell death (apoptosis) in many cell types.

We wish to thank Dr. K.W. Fishbein for help solving complex technical problems and Dr. E.G. Lakatta for useful discussions.

This work was supported by the Intramural Research Program, National Institute on Aging (D.B. Zorov, C.R. Filburn, L.-O. Klotz, and S.J. Sollott); National Institutes of Health grants HL38324, HL52315, and HL63744 (J.L. Zweier); and Deutsche Forschungsgemeinschaft grant KL 1245/1-1 (L.-O. Klotz).

Submitted: 10 April 2000

Revised: 16 June 2000

Accepted: 24 July 2000

References

- Williamson, J.R. 1979. Mitochondrial function in heart. *Annu. Rev. Physiol.* 41:485–506.
- Gunter, T.E., and D.R. Pfeiffer. 1990. Mechanisms by which mitochondria transport calcium. *Am. J. Physiol.* 258:C755–786.
- Green, D.R., and J.C. Reed. 1998. Mitochondria and apoptosis. *Science* 281:1309–1312.
- Crompton, M. 1999. The mitochondrial permeability transition pore and its role in cell death. *Biochem. J.* 341:233–249.
- Zoratti, M., and I. Szabo. 1995. The mitochondrial permeability transition. *Biochim. Biophys. Acta* 1241:139–176.
- Boveris, A., N. Oshino, and B. Chance. 1973. The cellular production of hydrogen peroxide. *Biochem. J.* 128:617–630.
- Lenaz, G. 1998. Role of mitochondria in oxidative stress and ageing. *Biochim. Biophys. Acta* 1366:53–67.

8. Hunter, D.R., and R.A. Haworth. 1979. The Ca^{2+} -induced membrane transition in mitochondria. I. The protective mechanisms. *Arch. Biochem. Biophys.* 195:453–459.
9. Bernardi, P., and V. Petronilli. 1996. The permeability transition pore as a mitochondrial calcium release channel: a critical appraisal. *J. Bioenerg. Biomembr.* 28:131–138.
10. Ichas, F., and J.P. Mazat. 1998. From calcium signaling to cell death: two conformations for the mitochondrial permeability transition pore. Switching from low- to high-conductance state. *Biochim. Biophys. Acta.* 1366:33–50.
11. Zamzami, N., S.A. Susin, P. Marchetti, T. Hirsch, I. Gomez-Monterrey, M. Castedo, and G. Kroemer. 1996. Mitochondrial control of nuclear apoptosis. *J. Exp. Med.* 183:1533–1544.
12. Jacobson, M.D. 1996. Reactive oxygen species and programmed cell death. *Trends Biochem. Sci.* 21:83–86.
13. Duchen, M.R. 1999. Contributions of mitochondria to animal physiology: from homeostatic sensor to calcium signaling and cell death. *J. Physiol.* 516:1–17.
14. Robb-Gaspers, L.D., P. Burnett, G.A. Rutter, R.M. Denton, R. Rizzuto, and A.P. Thomas. 1998. Integrating cytosolic calcium signals into mitochondrial metabolic responses. *EMBO (Eur. Mol. Biol. Organ.) J.* 17:4987–5000.
15. Hansford, R.G. 1994. Physiological role of mitochondrial Ca^{2+} transport. *J. Bioenerg. Biomembr.* 26:495–508.
16. Huser, J., C.E. Rechenmacher, and L.A. Blatter. 1998. Imaging the permeability pore transition in single mitochondria. *Biophys. J.* 74:2129–2137.
17. Nieminen, A.L., A.K. Saylor, S.A. Tesfai, B. Herman, and J.J. Lemasters. 1995. Contribution of the mitochondrial permeability transition to lethal injury after exposure of hepatocytes to t-butylhydroperoxide. *Biochem. J.* 307:99–106.
18. Capogrossi, M.C., A.A. Kort, H.A. Spurgeon, and E.G. Lakatta. 1986. Single adult rabbit and rat cardiac myocytes retain the Ca^{2+} - and species-dependent systolic and diastolic contractile properties of intact muscle. *J. Gen. Physiol.* 88:589–613.
19. Anderson, M.E. 1985. Determination of glutathione and glutathione disulfide in biological samples. *Methods Enzymol.* 113:548–555.
20. Vila-Petroff, M.G., A. Younes, J. Egan, E.G. Lakatta, and S.J. Sollott. 1999. Activation of distinct cAMP-dependent and cGMP-dependent pathways by nitric oxide in cardiac myocytes. *Circ. Res.* 84:1020–1031.
21. Xu, L., J.P. Eu, G. Meissner, and J.S. Stamler. 1998. Activation of the cardiac calcium release channel (ryanodine receptor) by poly-S-nitrosylation. *Science.* 279:234–237.
22. Nishihata, T., L.J. Caldwell, and K. Sakai. 1988. Inhibitory effect of salicylate on 2,4-dinitrophenol and diethyl maleate in isolated rat intestinal epithelial cells. *Biochim. Biophys. Acta.* 970:7–18.
23. Fabiato, A., and F. Fabiato. 1975. Contractions induced by a calcium-triggered release of calcium from the sarcoplasmic reticulum of single skinned cardiac cells. *J. Physiol.* 249:469–495.
24. Shea, C.R., N. Chen, J. Wimberly, and T. Hasan. 1989. Rhodamine dyes as potential agents for photochemotherapy of cancer in human bladder carcinoma cells. *Cancer Res.* 49:3961–3965.
25. Khan, A.U., and T. Wilson. 1995. Reactive oxygen species as cellular messengers. *Chem. Biol.* 2:437–445.
26. Vercesi, A.E., A.J. Kowaltowski, M.T. Grijalba, A.R. Meinicke, and R.F. Castilho. 1997. The role of reactive oxygen species in mitochondrial permeability transition. *Biosci. Rep.* 17:43–52.
27. Plummer, J.L., B.R. Smith, H. Sies, and J.R. Bend. 1981. Chemical depletion of glutathione in vivo. *Methods Enzymol.* 77:50–59.
28. Griffiths, E.J., and A.P. Halestrap. 1993. Protection by cyclosporin A of ischemia/reperfusion-induced damage in isolated rat hearts. *J. Mol. Cell. Cardiol.* 25:1461–1469.
29. Sokolove, P.M., and K.W. Kinnally. 1996. A mitochondrial signal peptide from *Neurospora crassa* increases the permeability of isolated rat liver mitochondria. *Arch. Biochem. Biophys.* 336:69–76.
30. Kushnareva, Y.E., M.L. Campo, K.W. Kinnally, and P.M. Sokolove. 1999. Signal presequences increase mitochondrial permeability and open the multiple conductance channel. *Arch. Biochem. Biophys.* 366:107–115.
31. Malkevitch, N.V., V.I. Dedukhova, R.A. Simonian, V.P. Skulachev, and A.A. Starkov. 1997. Thyroxine induces cyclosporin A-insensitive, Ca^{2+} -dependent reversible permeability transition pore in rat liver mitochondria. *FEBS Lett.* 412:173–178.
32. Amchenkova, A.A., L.E. Bakeeva, Y.S. Chentsov, V.P. Skulachev, and D.B. Zorov. 1988. Coupling membranes as energy-transmitting cables. I. Filamentous mitochondria in fibroblasts and mitochondrial clusters in cardiomyocytes. *J. Cell Biol.* 107:481–495.
33. Romashko, D.N., E. Marban, and B. O'Rourke. 1998. Subcellular metabolic transients and mitochondrial redox waves in heart cells. *Proc. Natl. Acad. Sci. USA.* 95:1618–1623.
34. Balakirev, M.Yu, V.V. Khramtsov, and G. Zimmer. 1997. Modulation of the mitochondrial permeability transition by nitric oxide. *Eur. J. Biochem.* 246:710–718.
35. Wink, D.A., and J.B. Mitchell. 1998. Chemical biology of nitric oxide: insights into regulatory, cytotoxic, and cytoprotective mechanisms of nitric oxide. *Free Rad. Biol. Med.* 25:434–456.
36. Murphy, M.P. 1999. Nitric oxide and cell death. *Biochim. Biophys. Acta.* 1411:401–414.
37. Hortelano, S., B. Dallaporta, N. Zamzami, T. Hirsch, S.A. Susin, I. Marzo, L. Bosca, and G. Kroemer. 1997. Nitric oxide induces apoptosis via triggering mitochondrial permeability transition. *FEBS Lett.* 410:373–377.
38. Srivastava, R.K., S.J. Sollott, L. Khan, R. Hansford, E.G. Lakatta, and D.L. Longo. 1999. Bcl-2 and Bcl-X(L) block thapsigargin-induced nitric oxide generation, c-Jun NH(2)-terminal kinase activity, and apoptosis. *Mol. Cell. Biol.* 19:5659–5674.
39. Leist, M., B. Single, H. Naumann, E. Fava, B. Simon, S. Kuhnle, and P. Nicotera. 1999. Nitric oxide inhibits execution of apoptosis at two distinct ATP-dependent steps upstream and downstream of mitochondrial cytochrome c release. *Biochem. Biophys. Res. Commun.* 258:215–221.
40. Gorbunov, N.V., Y.Y. Tyurina, G. Salama, B.W. Day, H.G. Claycamp, G. Argyros, N.M. Elsayed, and V.E. Kagan. 1998. Nitric oxide protects cardiomyocytes against tert-butyl hydroperoxide-induced formation of alkoxyl and peroxy radicals and peroxidation of phosphatidylserine. *Biochem. Biophys. Res. Commun.* 244:647–651.
41. Ma, X.L., F. Gao, G.L. Liu, B.L. Lopez, T.A. Christopher, J.M. Fukuto, D.A. Wink, and M. Feelisch. 1999. Opposite effects of nitric oxide and nitroxyl on postischemic myocardial injury. *Proc. Natl. Acad. Sci. USA.* 96:14617–14622.
42. Pinsky, D.J., S. Patton, S. Mesaros, V. Brovkovich, E.

- Kubaszewski, S. Grunfeld, and T. Malinski. 1997. Mechanical transduction of nitric oxide synthesis in the beating heart. *Circ. Res.* 81:372–379.
43. Ricchelli, F., S. Gobbo, G. Moreno, and C. Salet. 1999. Changes of the fluidity of mitochondrial membranes induced by the permeability transition. *Biochemistry*. 38:9295–9300.
 44. Takeshige, K., and S. Minakami. 1979. NADH- and NADPH-dependent formation of superoxide anions by bovine heart submitochondrial particles and NADH-ubiquinone reductase preparation. *Biochem. J.* 180:129–135.
 45. Nohl, H., and W. Jordan. 1986. The mitochondrial site of superoxide formation. *Biochem. Biophys. Res. Commun.* 138: 533–539.
 46. Korshunov, S.S., O.V. Korkina, E.K. Ruuge, V.P. Skulachev, and A.A. Starkov. 1998. Fatty acids as natural uncouplers preventing generation of $\cdot\text{O}_2^-$ and H_2O_2 by mitochondria in the resting state. *FEBS Lett.* 435:215–218.
 47. Bowser, D.N., T. Minamikawa, P. Nagley, and D.A. Williams. 1998. Role of mitochondria in calcium regulation of spontaneously contracting cardiac muscle cells. *Biophys. J.* 75: 2004–2014.
 48. Richter, C. 1993. Pro-oxidants and mitochondrial Ca^{2+} : their relationship to apoptosis and oncogenesis. *FEBS Lett.* 325:104–107.